Reprocessing and Recycling of Spent Nuclear Fuel

Related titles

Geological repository systems for safe disposal of spent nuclear fuels and radioactive waste
(ISBN 978-1-84569-542-2)

Advanced separation techniques for nuclear fuel reprocessing and radioactive waste treatment
(ISBN 978-1-84569-501-9)

Handbook of advanced radioactive waste conditioning technologies
(ISBN 978-1-84569-626-9)

Woodhead Publishing Series in Energy: Number 79

Reprocessing and Recycling of Spent Nuclear Fuel

Edited by

Robin Taylor

AMSTERDAM • BOSTON • CAMBRIDGE • HEIDELBERG
LONDON • NEW YORK • OXFORD • PARIS • SAN DIEGO
SAN FRANCISCO • SINGAPORE • SYDNEY • TOKYO
Woodhead Publishing is an imprint of Elsevier

Woodhead Publishing is an imprint of Elsevier
80 High Street, Sawston, Cambridge, CB22 3HJ, UK
225 Wyman Street, Waltham, MA 02451, USA
Langford Lane, Kidlington, OX5 1GB, UK

British Library Cataloguing in Publication Data
A catalogue record for this book is available from the British Library

Library of Congress Control Number: 2014957596

ISBN 978-1-78242-212-9 (print)
ISBN 978-1-78242-217-4 (online)

Typeset by SPi Global
www.spi-global.com

Printed and bound in the United Kingdom

List of contributors

B. Boullis CEA, Saclay, France

S. Bourg CEA, Marcoule, France

Roger Cashmore UK Atomic Energy Authority, Oxfordshire, UK

Emory D. Collins Oak Ridge National Laboratory, Oak Ridge, TN, USA

Christian Ekberg Chalmers University of Technology, Göteborg, Sweden

Andreas Geist Karlsruhe Institute of Technology, Institut für Nukleare Entsorgung (INE), Karlsruhe, Germany

Jean-Paul Glatz European Commission, Karlsruhe, Germany

Ye Guoan China Institute of Atomic Energy, Beijing, China

Bruce Hanson University of Leeds, Leeds, UK

M.T. Harrison National Nuclear Laboratory, Central Laboratory, Sellafield, Seascale, UK

Masatoshi Iizuka Central Research Institute of Electric Power Industry, Tokyo, Japan

Yeong-il Kim Korea Atomic Energy Research Institute, Daejeon, South Korea

Ben Koppelman Science Policy Centre, The Royal Society, London, UK

Tadafumi Koyama Central Research Institute of Electric Power Industry, Tokyo, Japan

Hansoo Lee Korea Atomic Energy Research Institute, Daejeon, South Korea

R.G. Lewin National Nuclear Laboratory, Central Laboratory, Sellafield, Seascale, UK

Gregg J. Lumetta Pacific Northwest National Laboratory, Richland, WA, USA

Chris J. Maher National Nuclear Laboratory, Seascale, UK

R. Malmbeck European Commission, Karlsruhe, Germany

Manuel Miguirditchian DEN, Commissariat à l'Énergie Atomique et aux Énergies Alternatives, Marcoule, France

K. Minato Japan Atomic Energy Agency, Tokai-mura, Ibaraki-ken, Japan

Bruce J. Mincher Idaho National Laboratory, Idaho Falls, ID, USA

Giuseppe Modolo Forschungszentrum Jülich, Institute of Energy and Climate Research, Nuclear Waste Management (IEK-6), Jülich, Germany

Bruce A. Moyer Oak Ridge National Laboratory, Oak Ridge, TN, USA

Kenneth L. Nash Washington State University, Pullman, WA, USA

R. Natarajan Indira Gandhi Centre for Atomic Research, Kalpakkam, Tamilnadu, India

Mikael Nilsson University of California Irvine, Irvine, CA, USA

Ch. Poinssot CEA, Marcoule, France

Manuel A. Pouchon Paul Scherrer Institut, Laboratory for Nuclear Materials, Villigen, Switzerland

Mark J. Sarsfield National Nuclear Laboratory, Central Laboratory, Sellafield, Seascale, UK

Clint A. Sharrad Research Centre for Radwaste and Decommissioning, Dalton Nuclear Institute; Centre for Radiochemistry Research, School of Chemistry, and School of Chemical Engineering and Analytical Science, The University of Manchester, Manchester, UK

P. Souček European Commission, Karlsruhe, Germany

Yan Taihong China Institute of Atomic Energy, Beijing, China

T.A. Todd Idaho National Laboratory, Idaho Falls, ID, USA

Daniel M. Whittaker Research Centre for Radwaste and Decommissioning, Dalton Nuclear Institute, and Centre for Radiochemistry Research, School of Chemistry, The University of Manchester, Manchester, UK

L.G. Williams Imperial College, London, UK

Woodhead Publishing Series in Energy

1 **Generating power at high efficiency: Combined cycle technology for sustainable energy production**
Eric Jeffs
2 **Advanced separation techniques for nuclear fuel reprocessing and radioactive waste treatment**
Edited by Kenneth L. Nash and Gregg J. Lumetta
3 **Bioalcohol production: Biochemical conversion of lignocellulosic biomass**
Edited by Keith W. Waldron
4 **Understanding and mitigating ageing in nuclear power plants: Materials and operational aspects of plant life management (PLiM)**
Edited by Philip G. Tipping
5 **Advanced power plant materials, design and technology**
Edited by Dermot Roddy
6 **Stand-alone and hybrid wind energy systems: Technology, energy storage and applications**
Edited by John K. Kaldellis
7 **Biodiesel science and technology: From soil to oil**
Jan C. J. Bart, Natale Palmeri and Stefano Cavallaro
8 **Developments and innovation in carbon dioxide (CO_2) capture and storage technology Volume 1: Carbon dioxide (CO_2) capture, transport and industrial applications**
Edited by M. Mercedes Maroto-Valer
9 **Geological repository systems for safe disposal of spent nuclear fuels and radioactive waste**
Edited by Joonhong Ahn and Michael J. Apted
10 **Wind energy systems: Optimising design and construction for safe and reliable operation**
Edited by John D. Sørensen and Jens N. Sørensen
11 **Solid oxide fuel cell technology: Principles, performance and operations**
Kevin Huang and John Bannister Goodenough
12 **Handbook of advanced radioactive waste conditioning technologies**
Edited by Michael I. Ojovan
13 **Membranes for clean and renewable power applications**
Edited by Annarosa Gugliuzza and Angelo Basile
14 **Materials for energy efficiency and thermal comfort in buildings**
Edited by Matthew R. Hall
15 **Handbook of biofuels production: Processes and technologies**
Edited by Rafael Luque, Juan Campelo and James Clark
16 **Developments and innovation in carbon dioxide (CO_2) capture and storage technology Volume 2: Carbon dioxide (CO_2) storage and utilisation**
Edited by M. Mercedes Maroto-Valer

17 **Oxy-fuel combustion for power generation and carbon dioxide (CO_2) capture**
Edited by Ligang Zheng
18 **Small and micro combined heat and power (CHP) systems: Advanced design, performance, materials and applications**
Edited by Robert Beith
19 **Advances in clean hydrocarbon fuel processing: Science and technology**
Edited by M. Rashid Khan
20 **Modern gas turbine systems: High efficiency, low emission, fuel flexible power generation**
Edited by Peter Jansohn
21 **Concentrating solar power technology: Principles, developments and applications**
Edited by Keith Lovegrove and Wes Stein
22 **Nuclear corrosion science and engineering**
Edited by Damien Féron
23 **Power plant life management and performance improvement**
Edited by John E. Oakey
24 **Electrical drives for direct drive renewable energy systems**
Edited by Markus Mueller and Henk Polinder
25 **Advanced membrane science and technology for sustainable energy and environmental applications**
Edited by Angelo Basile and Suzana Pereira Nunes
26 **Irradiation embrittlement of reactor pressure vessels (RPVs) in nuclear power plants**
Edited by Naoki Soneda
27 **High temperature superconductors (HTS) for energy applications**
Edited by Ziad Melhem
28 **Infrastructure and methodologies for the justification of nuclear power programmes**
Edited by Agustín Alonso
29 **Waste to energy conversion technology**
Edited by Naomi B. Klinghoffer and Marco J. Castaldi
30 **Polymer electrolyte membrane and direct methanol fuel cell technology Volume 1: Fundamentals and performance of low temperature fuel cells**
Edited by Christoph Hartnig and Christina Roth
31 **Polymer electrolyte membrane and direct methanol fuel cell technology Volume 2: *In situ* characterization techniques for low temperature fuel cells**
Edited by Christoph Hartnig and Christina Roth
32 **Combined cycle systems for near-zero emission power generation**
Edited by Ashok D. Rao
33 **Modern earth buildings: Materials, engineering, construction and applications**
Edited by Matthew R. Hall, Rick Lindsay and Meror Krayenhoff
34 **Metropolitan sustainability: Understanding and improving the urban environment**
Edited by Frank Zeman
35 **Functional materials for sustainable energy applications**
Edited by John A. Kilner, Stephen J. Skinner, Stuart J. C. Irvine and Peter P. Edwards
36 **Nuclear decommissioning: Planning, execution and international experience**
Edited by Michele Laraia
37 **Nuclear fuel cycle science and engineering**
Edited by Ian Crossland
38 **Electricity transmission, distribution and storage systems**
Edited by Ziad Melhem

39 **Advances in biodiesel production: Processes and technologies**
Edited by Rafael Luque and Juan A. Melero
40 **Biomass combustion science, technology and engineering**
Edited by Lasse Rosendahl
41 **Ultra-supercritical coal power plants: Materials, technologies and optimisation**
Edited by Dongke Zhang
42 **Radionuclide behaviour in the natural environment: Science, implications and lessons for the nuclear industry**
Edited by Christophe Poinssot and Horst Geckeis
43 **Calcium and chemical looping technology for power generation and carbon dioxide (CO_2) capture: Solid oxygen- and CO_2-carriers**
Paul Fennell and E. J. Anthony
44 **Materials' ageing and degradation in light water reactors: Mechanisms, and management**
Edited by K. L. Murty
45 **Structural alloys for power plants: Operational challenges and high-temperature materials**
Edited by Amir Shirzadi and Susan Jackson
46 **Biolubricants: Science and technology**
Jan C. J. Bart, Emanuele Gucciardi and Stefano Cavallaro
47 **Advances in wind turbine blade design and materials**
Edited by Povl Brøndsted and Rogier P. L. Nijssen
48 **Radioactive waste management and contaminated site clean-up: Processes, technologies and international experience**
Edited by William E. Lee, Michael I. Ojovan, Carol M. Jantzen
49 **Probabilistic safety assessment for optimum nuclear power plant life management (PLiM): Theory and application of reliability analysis methods for major power plant components**
Gennadij V. Arkadov, Alexander F. Getman and Andrei N. Rodionov
50 **The coal handbook: Towards cleaner production Volume 1: Coal production**
Edited by Dave Osborne
51 **The coal handbook: Towards cleaner production Volume 2: Coal utilisation**
Edited by Dave Osborne
52 **The biogas handbook: Science, production and applications**
Edited by Arthur Wellinger, Jerry Murphy and David Baxter
53 **Advances in biorefineries: Biomass and waste supply chain exploitation**
Edited by Keith Waldron
54 **Geological storage of carbon dioxide (CO_2): Geoscience, technologies, environmental aspects and legal frameworks**
Edited by Jon Gluyas and Simon Mathias
55 **Handbook of membrane reactors Volume 1: Fundamental materials science, design and optimisation**
Edited by Angelo Basile
56 **Handbook of membrane reactors Volume 2: Reactor types and industrial applications**
Edited by Angelo Basile
57 **Alternative fuels and advanced vehicle technologies for improved environmental performance: Towards zero carbon transportation**
Edited by Richard Folkson
58 **Handbook of microalgal bioprocess engineering**
Christopher Lan and Bei Wang

59 **Fluidized bed technologies for near-zero emission combustion and gasification**
Edited by Fabrizio Scala
60 **Managing nuclear projects: A comprehensive management resource**
Edited by Jas Devgun
61 **Handbook of Process Integration (PI): Minimisation of energy and water use, waste and emissions**
Edited by Jiří J. Klemeš
62 **Coal power plant materials and life assessment**
Edited by Ahmed Shibli
63 **Advances in hydrogen production, storage and distribution**
Edited by Ahmed Basile and Adolfo Iulianelli
64 **Handbook of small modular nuclear reactors**
Edited by Mario D. Carelli and Dan T. Ingersoll
65 **Superconductors in the power grid: Materials and applications**
Edited by Christopher Rey
66 **Advances in thermal energy storage systems: Methods and applications**
Edited by Luisa F. Cabeza
67 **Advances in batteries for medium and large-scale energy storage**
Edited by Chris Menictas, Maria Skyllas-Kazacos and Tuti Mariana Lim
68 **Palladium membrane technology for hydrogen production, carbon capture and other applications**
Edited by Aggelos Doukelis, Kyriakos Panopoulos, Antonios Koumanakos and Emmanouil Kakaras
69 **Gasification for synthetic fuel production: Fundamentals, processes and applications**
Edited by Rafael Luque and James G. Speight
70 **Renewable heating and cooling: Technologies and applications**
Edited by Gerhard Stryi-Hipp
71 **Environmental remediation and restoration of contaminated nuclear and NORM sites**
Edited by Leo van Velzen
72 **Eco-friendly innovation in electricity networks**
Edited by Jean-Luc Bessede
73 **The 2011 Fukushima nuclear power plant accident: How and why it happened**
Yotaro Hatamura, Seiji Abe, Masao Fuchigami and Naoto Kasahara. Translated by Kenji Iino
74 **Lignocellulose biorefinery engineering: Principles and applications**
Hongzhang Chen
75 **Advances in membrane technologies for water treatment: Materials, processes and applications**
Edited by Angelo Basile, Alfredo Cassano and Navin Rastogi
76 **Membrane reactors for energy applications and basic chemical production**
Edited by Angelo Basile, Luisa Di Paola, Faisal Hai and Vincenzo Piemonte
77 **Pervaporation, vapour permeation and membrane distillation: Principles and applications**
Edited by Angelo Basile, Alberto Figoli and Mohamed Khayet
78 **Safe and secure transport and storage of radioactive materials**
Edited by Ken Sorenson
79 **Reprocessing and recycling of spent nuclear fuel**
Edited by Robin Taylor

Preface

In the twenty-first century the world will need increasing supplies of electricity to maintain economic growth, particularly with a growing global population and increasing industrialization in the developing nations. It is also becoming clear that a major effort will be needed to decarbonize our energy supplies by around 2050 if the more severe effects of global climate change are to be avoided. Against this background, there is a renewed interest in nuclear (fission) energy as it has the potential to provide large quantities of secure, low-carbon energy; although the events at Fukushima, following a magnitude 9.0 earthquake off the coast of Japan, have caused some countries to decide against new nuclear reactors or to plan an exit from the use of nuclear energy, Germany and Japan itself being obvious examples. However, elsewhere the growth in the use of nuclear energy is continuing, being planned, or under serious consideration; with the new generation of light water reactors expected to deliver new standards in safety and economics.

However, questions remain as to how to deal with the used nuclear fuel from past, present, and future generations of reactors. Essentially, two options exist: either dispose of the spent fuel after containment in a suitable waste form in a waste repository (the "open" or "once-through" fuel cycle option) or separate out the reusable components for recycling, disposing of the residual waste products only (the "closed" fuel cycle option). Many countries have adopted the open fuel cycle in which spent fuel is to be stored and then moved to a geological disposal facility (GDF), as soon as one is available. However, despite significant progress now being made in a few countries, especially Sweden and Finland, no country has yet opened a GDF for spent fuel disposal. Nor has any country yet implemented a fully closed fuel cycle, as this requires the deployment of fast neutron reactors that can utilize the full energy potential of uranium and plutonium fuels. "Partially" closed or "twice-through" fuel cycles in which plutonium (and some uranium) is recycled as mixed oxide fuel for thermal reactors have been implemented, to varying degrees of success, in a few countries; most notably France. The amount of spent fuel, therefore, being interim-stored rather than disposed of or reprocessed and recycled, is growing. Simple estimates suggest that, if nothing else is done, there could be over a million tonnes of spent fuel in interim storage worldwide by 2100. To put this in context, a GDF may hold a few tens of thousands of tonnes of spent fuel and a typical commercial-scale reprocessing plant will have a throughput of around 1000 ton/year.

Due to the increasingly urgent need to expand global supplies of low-carbon energy and, hence, renewed interest in nuclear energy, there are also concerns over sustainability including the security of supply of uranium in a "nuclear renaissance," safety of current systems, and proliferation risks across the civil nuclear fuel cycle. Moreover,

there is an increasing realization that GDF space will probably be a "scarce" resource and fuel cycles that minimize the impacts on the GDF may have significant benefits.

Against this backdrop, the option for closing the nuclear fuel cycle by introducing Generation IV fast reactor systems is being evaluated by a number of national and international programs as a potential solution to these issues that could be deployed around the middle of the twenty-first century.

To achieve the aim of a "fully" closed fuel cycle in which the energy potential of uranium and plutonium fuels are exploited in fast reactors and the plutonium inventory (and possibly also minor actinide inventory) is stabilized or even decreased will require actinide recycling. It should be stressed that even fully closed fuel cycles require a disposal facility for high-level wastes from reprocessing. However, closed cycles offer advantages for reducing the footprint of the GDF and the overall radiotoxic lifetime of the material being disposed (this requires the recycling of the minor actinides as well as plutonium—the so-called partitioning and transmutation or P&T scenario). While these latter factors do not necessarily benefit the safety case for the GDF, except against low probability (but high consequence) scenarios such as human intrusion and geological change, they may help in gaining public acceptance for radioactive waste disposal and siting of the GDF.

Arguments against closing the fuel cycle include concerns over safety and environmental impacts of fuel recycling plants; increased short-term proliferation risks from stockpiles of separated plutonium; the time scales to implementation; and the capital cost of providing complex infrastructure needed. Substantial R&D is also required to develop and demonstrate the technologies needed for a commercial fast reactor fuel cycle.

Obviously, closed fuel cycles need reprocessing and recycling capabilities in order to generate new nuclear fuels from used fuel. To date, commercial-scale reprocessing has been undertaken in a number of countries using the PUREX process. This produces separate pure uranium and plutonium oxide products using a hydrometallurgical process based on liquid-liquid extraction between aqueous and organic phases. The PUREX process has been an extraordinarily successful process for achieving these complex and potentially hazardous separations, but it is still used in a form that is only modestly changed since its initial development in the 1950s; essentially, as a technology to recover plutonium from low burn up fuels for nuclear weapons programs. It is unlikely to be an acceptable option for deployment in the mid-twenty-first century when economic, waste management, environmental impact, and nonproliferation demands will be far greater.

So the question arises that if we are to realize the benefits of nuclear energy while managing the wastes by closing the fuel cycle, what technologies are there that can realistically be deployed for reprocessing and recycling of spent nuclear fuels by the mid to late twenty-first century? Recognizing, as well, that 10-20 years may be needed to design, build, and commission new plants once the R&D phases are completed.

This book hopes to help address this question by providing a series of state-of-the-art reviews on many of the key technology developments, science, engineering, and technical issues related to the research and development of advanced reprocessing

options. The chapters are authored by a number of leading international experts in the reprocessing of spent nuclear fuels and partitioning of minor actinides. At the end of each chapter, authors have been encouraged to speculate on what they see as the future needs and directions for research in their field. The book is divided into four sections:

Part One, entitled "Introductory issues and future challenges," is intended to set out the context for advanced reprocessing R&D. Chapter 1 introduces the technologies and concepts. Chapter 2 looks more closely at the pros and cons of plutonium recycling with particular reference to the French nuclear fuel cycle. A quantitative methodology for evaluating the impacts of different nuclear fuel cycles is presented. These types of techniques and analyses are valuable tools to understand the case for closing the fuel cycle. Chapter 3 describes directions for advanced closed fuel cycle R&D, introducing themes that recur throughout the subsequent scientific review chapters. Finally, to frame R&D, an understanding of the wider issues is needed, and Chapter 4 provides a timely discussion on the safety and security of used nuclear fuel reprocessing operations. Such wider appreciation of the contextual issues described in these four introductory chapters will enable researchers to develop processes that address the concerns, real and perceived, that exist with regard to reprocessing and thus, in time, hopefully to remove some of the barriers to ultimate deployment.

Part Two covers "Advances in aqueous separation processes." Aqueous reprocessing is the dominant technology and is likely to remain so, at least under many closed fuel cycle scenarios. However, step changes in the conventional PUREX process and possibly new non-PUREX aqueous processes will undoubtedly be needed to enable any deployment by around 2050. Such step changes must mitigate the potential objections raised against reprocessing used fuel as well as enabling the processing of a wider range of spent fuel types (high plutonium content, nonoxide matrices, high burn ups, etc.). Furthermore, it is not sufficient to concentrate solely on the core separation process but the whole reprocessing and recycling system must be optimized to deliver the necessary improvements in performance. Therefore, this section starts with a chapter describing current and future dissolution technology in the headend plant area (Chapter 5). This is the essential stage to prepare used fuel for aqueous processing, one that must tackle some of the biggest challenges in recycling used fuels. The chemical engineering and process design of reprocessing plants are described in Chapter 6. Integrating successful lab-scale chemistry with chemical engineering and process design is a key step in efficiently transitioning new process concepts from R&D to industrial deployment. Chapters 7 and 8 then review two important aspects of the separation process chemistry—the design and application of organic ligands for solvent extraction and the effects of ionizing radiation on these ligands. Chapters 9–11 then take us into the core separation processes, covering two aspects particularly relevant to advanced recycling: (a) the reprocessing of fast reactor fuels and (b) the partitioning of the minor actinides from high-level wastes so that they can be burned (transmuted) in fast reactors. Recovering the minor actinides is extremely challenging due to the chemical similarity between the trivalent minor actinides and lanthanides. Nevertheless, much progress has been made internationally in this field and this is considered by two reviews of recent developments in Europe (Chapter 10) and in the United States (Chapter 11), where some really significant advances have been made.

Part Two concludes with three chapters describing how the separated actinide products in solution are converted to solid materials in the product finishing lines of a reprocessing plant. These solid materials are usually oxide powders suitable for processing into new nuclear fuels. The focus on these chapters is advanced methods of coconverting uranium and plutonium (or uranium, plutonium, and minor actinides) directly into mixed actinide oxides. Chapter 12 covers thermal denitration; Chapter 13 looks at the oxalate precipitation process; and Chapter 14 describes sol-gel and other routes. Development of more innovative product finishing routes such as these coconversion processes can provide better integration between reprocessing and fuel manufacturing, with potential gains in the overall economics, efficiency, and proliferation resistance of used fuel recycling.

Part Three, "Pyrochemical processes," looks at the progress being made internationally on the main alternative technology to aqueous-based reprocessing and recycling. There is a growing consensus of opinion that aqueous and pyroprocesses are not necessarily competing technologies but complementary, with each being better suited to particular nuclear fuel cycle scenarios. Chapter 15 gives an overview of international developments in the core pyrotechnology: metal electrorefining. Progress of international pyroprograms, including the United States and Russia, are then reviewed. This is followed up by three chapters looking in greater detail at the major advances made toward pyroprocessing in Korea (Chapter 16), at the European Joint Research Centre (Chapter 17), and in Japan (Chapter 18). As well as metal electrorefining, oxide electroreduction is covered as this is a necessary pretreatment if oxide fuels are to be reprocessed using pyrochemical methods. From these chapters, it is clear that the technical maturity of the pyroprocess is growing with significant efforts now being made to address the issues relevant to industrialization of the process and associated engineering.

The final section of the book, Part Four "Implementation of advanced closed fuel cycles," summarizes progress being made in some leading countries around the world toward deploying advanced closed nuclear fuel cycles later this century, or at least to have the *option* to do so. Regions covered are the United States (Chapter 19), China (Chapter 20), Korea (Chapter 21), and Japan (Chapter 22). Chapter 9 also includes a section looking at the Indian plans for closing the fuel cycle and Chapter 3 includes the French view on a roadmap toward deployment of advanced fuel cycles. Chapter 23 then considers how multinational or multilateral approaches could be developed to deliver internationalized fuel cycle services that enhance nonproliferation and security objectives while meeting world nuclear energy demands. With regard to removing some of the barriers to the future deployment of closed fuel cycles, this chapter and the Royal Society report on which it is based (Cashmore et al., 2011) summarize some important ideas for international nuclear fuel cycle development and growth. Lastly, up to this point, the book has concentrated on actinide recycling in the dominant (U, Pu) fuel cycle but, with increasing attention being paid once again to the role thorium might play in future nuclear power generation, the section, and book, ends with an overview of the recycling of thorium-based fuels in the thorium fuel cycle (Chapter 24). Similarities and differences with the (U, Pu) fuel cycle are apparent but, again, it is clear that R&D will still be required to optimize thorium fuel recycling.

From these chapters, it is clear that, while advanced reprocessing and recycling technologies can lead to acceptable options to close the nuclear fuel cycle by about 2050, their development and demonstration remains a major R&D challenge. Nevertheless, given the potential benefits of nuclear energy, it is a challenge worth addressing. There is clearly substantial progress being made internationally with both advanced aqueous and pyrochemical routes looking like realistic options, depending on the fuel cycle scenario envisioned by a particular country or region. Understanding wider concerns over safety, nonproliferation, economics, environmental impact, and public acceptability is vital to direct R&D that resolves the barriers to eventual deployment. The science base is fundamental to success but engineering and design are equally important in making real progress. Clearly, much of the R&D relies on highly specialized, rare facilities for handling radioactive materials and so international cooperation in R&D can enable faster progress, raising standards, while minimizing costs to collaborating nations.

To conclude, this book is aimed at researchers in the field of nuclear fuel reprocessing and actinide recycling; providing a mix of detailed reviews of specific chemical processes with overviews of some of the wider issues that influence the directions of R&D and, ultimately, the likelihood of implementation. Secondly, training and education of new scientists and engineers is of critical concern to the nuclear industry in many countries and, hopefully, this book will be a useful aid to the development of the next generation of researchers, experts, engineers, and managers that are needed for the safe, sustainable, and responsible use of nuclear energy in the twenty-first century.

Finally, in some parts, this book covers similar ground to the earlier book in the Energy Series from Woodhead Publishing, *Advanced separation techniques for nuclear fuel reprocessing and radioactive waste treatment*, edited by K.L. Nash and G.J. Lumetta. Additional details on some of the separation process chemistries covered herein can be found in this complementary and highly recommended title.

Robin Taylor
National Nuclear Laboratory, Central Laboratory,
Sellafield, Seascale, United Kingdom

Reference

Cashmore, R., Billowes, J., Bowen, W., Brown, C., Grimes, R., Howsley, R., Livens, F., Simpson, J., Styles, P., 2011. Fuel Cycle Stewardship in a Nuclear Renaissance. The Royal Society Science Policy Centre, London.

Introduction to the reprocessing and recycling of spent nuclear fuels

1

Kenneth L. Nash[1], *Mikael Nilsson*[2]
[1]Washington State University, Pullman, WA, USA; [2]University of California Irvine, Irvine, CA, USA

Acronyms

AGR	advanced gas-cooled reactor
AHA	acetohydroxamic acid
CEA	Commissariat à l'énergie atomique et aux énergies alternatives
COEX	coextraction process
CRIEPI	Central Research Institute of Electric Power Industry
HDBP	dibutyl phosphoric acid
HLLW	high-level liquid waste
HLW	high-level waste
IFR	integral fast reactor
IHM	initial heavy metal
LET	linear energy transfer
LMFBRs	liquid metal fast breeder reactors
LWR	light water reactor
MIBK	methyl(isobutyl) ketone
MOX	mixed oxide
OECD	The Organisation for Economic Cooperation and Development
PUREX	plutonium uranium reduction extraction
TBP	tri-*n*-butyl phosphate
THORP	thermal oxide reprocessing plant
UREX	uranium extraction
VVER	Voda Voda Energo Reactor

1.1 Introduction

1.1.1 Drivers for expansion of nuclear power/global climate/ base load generation

The Industrial Revolution began in the early to mid-nineteenth century, with the introduction of mechanization of work. Mankind's new machines (e.g., sawmills, steam engines) led to a general increase in prosperity and the development of the concept of leisure time; mechanization of repetitive tasks allowed human society to move away from a model for society based on the physical labor of humans and their domesticated draft animals. The combustion of fuel to produce heat engines enabled an

Reprocessing and Recycling of Spent Nuclear Fuel. http://dx.doi.org/10.1016/B978-1-78242-212-9.00001-0

expansion of free time that led in general terms to an increase of interest in how and why the universe works as it does. This evolution produced a continuous wave of increasingly sophisticated new machines that grew naturally out of mankind's increasing knowledge and curiosity. By the end of the twentieth century, men had walked on the moon and split the atom.

It is estimated that in the early 1800s the population of the planet passed the one billion mark. At the middle of the nineteenth century, about 95% of the power needed to sustain the pace of industrialization was derived from renewable sources, primarily hydromechanical power and the combustion of wood (Ristinen and Krushaar, 1999). The exploitation of this apparently inexhaustible resource at the scale needed to sustain the pace of progress led ultimately to the significant depletion of native forestland in the United States and in Europe. By the middle of the nineteenth century, the consumption of fossil fuels began with the serious exploitation of the much higher energy density of coal. Though adventitious petroleum products have been in use since 4000 BCE, modern exploitation of petroleum at a large scale can reasonably be traced to Edwin Drake's construction of the first petroleum drilling machine in Titusville, PA, in 1859 (Dickey, 1959). The introduction of liquid fuels enabled more options in transportation and led to the development of the automobile and increased mobility by the end of the nineteenth century. The exploitation of oil also arguably represents the first deliberate extraction of natural gas. Until the development of the Bunsen burner and the concept of a natural gas pipeline, methane was utilized primarily for the production of light. At each stage of evolution in fossil fuel consumption, the energy density of the fuel decreased (relative to coal), but utility and ease of distribution increased.

Meanwhile, global population and consumption of energy in all forms continued to grow. By the beginning of the twentieth century, global population was nearing 2 billion and power production in the developed world was more than 70% based on coal combustion. As a result of increasing consumption of power by man's machines, the workplace became a less hazardous environment and average life spans began to increase. Aside from the influence of two World Wars and the Great Depression during the twentieth century, average life expectancy tracks almost linearly with energy consumption (Figure 1.1). Jumping ahead to the twenty-first century, planetwide population passed 7 billion in October 2011. Today total consumption of power remains somewhere between 80% and 85% derived from fossil carbon combustion; low-carbon nuclear power represents about 9% of global energy consumption.

The cumulative effects of fossil carbon consumption and increased overall human knowledge led by the end of the twentieth century to a rise in concerns about the potential climatological impact of more than 150 years of reinjecting fossil carbon into the accessible environment. The report of a steep rise in atmospheric CO_2 concentration since the beginning of the industrial revolution (representing a roughly 25% increase) combined with the perception of increased frequency of more severe weather events led ultimately to increasing concerns that global climate change was being fueled (pun intended) by fossil fuel consumption. This observation led to increased activity related to the means of either (1) replacing energy derived from fossil carbon with less CO_2-intensive alternatives or (2) devising effective strategies for sequestration of CO_2.

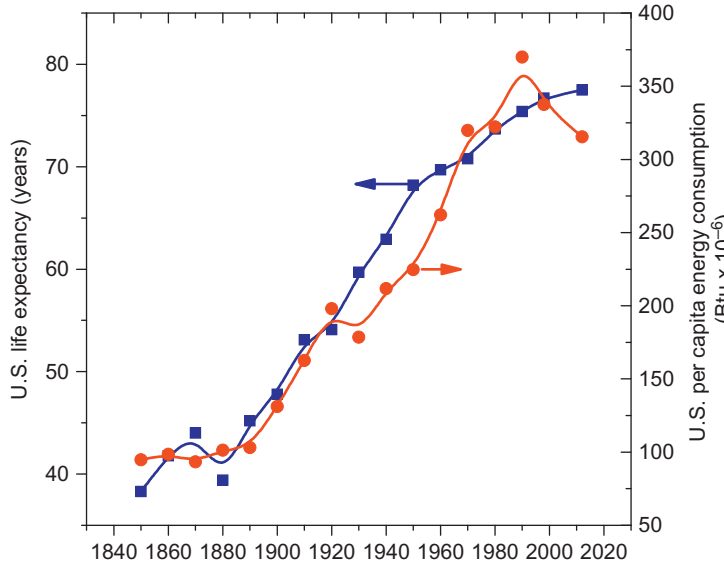

Figure 1.1 Average life expectancy (at birth) correlation with per capita energy consumption 1850-2010 (U.S. Life Expectancy, 1850-2011; U.S. Energy Consumption, 1775-2009; U.S. Population, 1810-2010; U.S. Census Bureau, 2013).

In response to option 1, renewable resources (wind and solar, primarily) and nuclear power became favored topics for consideration. Government tax incentives have supported (in the United States and elsewhere) a significant increase in wind and solar contributions to the overall energy production balance. This renewable energy has captured an increasing share of global energy production. Unfortunately, the pace of industrialization in underdeveloped countries has resulted in a large increase in consumption of energy and effectively little displacement of fossil carbon combustion (though natural gas is displacing coal[1]).

How large an impact on the livability of planet Earth the continued combustion of fossil carbon will have is in the province of climate modeling and mapping of the paleoclimate. In recent years, climatologists have almost universally agreed that continued injection of fossil carbon into the atmosphere will have deleterious effects, perhaps even in the near future. The development of alternative fuels that avoid the introduction of additional greenhouse gases into the atmosphere has spurred government subsidies supporting the creation of other power-production technologies that avoid fossil carbon combustion (in particular solar and wind technologies). Though

[1] Though both natural gas and coal combustion result in the transfer of fossil carbon from the subsurface into the accessible environment (predominantly in the form of CO_2), the per-kg emissions of CO_2 are approximately 50% lower for natural gas than coal. There are also no heavy-metal emissions associated with gas combustion while coal ash contains significant amounts of a variety of heavy metals and other mineral-derived toxins.

climate models cannot offer ironclad proof of a negative impact of continued reinjection of fossil carbon into the atmosphere, the increasing consensus is that severe climate impacts may/will result from continuing the domination of power production by fossil carbon.

A companion question is whether renewable energy sources/conservation strategies can be improved adequately to serve the energy needs of the 9 (or more) billion inhabitants of the planet that are expected by mid-century. Government subsidies and tax credits have spurred development of new wind and solar installations, principally in the developed world. Conservation efforts also have been stepped up and they are having an impact on the rate of power consumption increase, but a growing global population base and increasing demand for energy-consuming devices (computers, phones, automobiles, etc.) will ensure that demand will continue to grow. It will be challenging to overcome the reality that the wind does not always blow, nor does solar radiation always penetrate to where the solar receptors are located. Developing strategies for efficient storage are critically important for these options to respond adequately to demand cycles. In addition, the transition from electricity grids based on centralized generation (power plants) to distributed generation (e.g., rooftop solar collectors) will require considerable investment for electricity distribution. Fission energy represents an important opportunity to reduce the carbon emissions associated with power production.

Research and development activities for advanced nuclear power options and in some countries financial incentives for a generation of "new build" have been seen. At present, there are about 70 new nuclear power plants under construction globally, led to a significant degree by major construction activities in China, Russia, and India (World Nuclear Association, 2014). Unfortunately, a magnitude 9 earthquake and tsunami caused damage to four reactors at Fukushima, Japan, in March 2011. This natural disaster and subsequent nuclear reactor accident has led several countries to alter their new construction plans and, in fact, to consider eliminating fission-based power completely. Despite this complication, the plants under construction, and recognition that roughly 17% of the global population remain without electricity, appear poised to drive continued development of nuclear options. The major builds of new capacity ongoing in Russia and China particularly are perceived to represent a calculated campaign to develop potential nuclear construction and services commerce opportunities for these countries.

1.1.2 Nuclear fission with thermal and fast neutrons

Natural uranium is on average 99.3% ^{238}U/0.7% ^{235}U, with a very small percent of decay daughter ^{234}U. All uranium isotopes are radioactive ($t_{1/2}$ (^{238}U) = 4.5×10^9 years, $t_{1/2}$ (^{235}U) = 7.0×10^8 years, $t_{1/2}$ (^{234}U) = 1.6×10^5 years) though ^{238,235}U are primordial (Choppin et al., 2002a). In a neutron flux, each isotope has a moderate neutron capture cross section; for thermalized (0.025 eV kinetic energy) neutrons, capture by ^{234,238}U leads predominantly to the creation of the next heaviest isotope(s) of uranium, ^{235}U and ^{239}U; ^{239}U decays by β^- emission to produce first

^{239}Np then, after a second β^- decay, ^{239}Pu. The fissile isotopes ^{235}U and ^{239}Pu upon capture of a thermal neutron have, respectively, an 85% and 73% probability of undergoing fission, producing two large fragments, ionizing radiation and on average 2.5 excess neutrons that can enable a chain reaction (Choppin et al., 2002b). The remaining fraction loses its nuclear excitation energy to produce ^{236}U and ^{240}Pu, neither of which are fissile. With successive neutron capture reactions in a reactor, heavier isotopes (and elements) are produced. These isotopes are largely responsible for the buildup of transuranium elements in used reactor fuel; an additional neutron capture reaction by ^{240}Pu produces the fissile isotope ^{241}Pu that, with a higher overall capture cross section than ^{239}Pu, undergoes fission 73% of the time, each time it captures a thermal neutron.

In liquid metal fast breeder reactors (LMFBRs), the neutron spectrum is much harder (higher kinetic energy) due to the absence of a moderator. Under these conditions, overall capture cross sections are much lower than for thermal neutrons, but for many actinide isotopes the neutron capture cross-section ratio (n,γ vs. n,f) generally tends to favor fission: ^{235}U—77%, ^{238}U—13%, ^{239}Pu—77%, ^{240}Pu—41%, ^{241}Pu—82% (Choppin et al., 2002b). Per-event fission neutron yields are also typically higher in fast reactors. Among the most important activation products in discharged reactor fuel are the transuranium isotopes including (besides plutonium) ^{237}Np, ^{241,243,242m}Am, and ^{242,244,245,246}Cm. Several of these isotopes are comparatively long-lived and because they are α-emitting nuclides, they contribute significantly to the long-term radiotoxicity of used nuclear fuel. Americium-241 is particularly troublesome in aged nuclear fuel because it decays with a significant contribution to the penetrating radiation dose from a 60 keV γ-ray and its concentration actually increases in storage of intact fuel because of the significant presence of 14.3 year half-life ^{241}Pu parent nuclide. Lesser amounts of ^{241}Am are generated if plutonium is promptly recycled back to thermal reactors as mixed oxide (MOX) fuel.

Because of the general patterns of stability of the arrangements of neutrons and protons in nuclei, the process of fissioning an actinide nucleus produces a double humped, but more-or-less symmetrical distribution of heavy (average mass number about 140) and light (average mass number about 95) fission products. Because the average neutron/proton ratio for actinide nuclei is greater than 1.5 and that of fission products 1.2-1.4, the primary products of fission are neutron rich. As a result, fission products tend to undergo β^- decay and for some excited isotopes neutron emission. The average loss of mass in the process of fissioning a single actinide atom is the energetic equivalent of about 200 MeV of kinetic energy, most of which is carried to the matrix by the massive fission products. The fission products include isotopes of every element in the periodic table from gallium to holmium plus transuranium actinides; thus, the chemistry of all groups of the periodic table are represented in used nuclear fuel. Freshly discharged fuel is intensely radioactive and retains sufficient thermal heat (after removal from the reactor and the cessation of neutron capture reactions) to require active cooling for at least several years after removal from the reactor. The loss of the ability to cool discharged used fuel contributed to the severity of the accident at Fukushima.

1.1.3 Radiation, radiotoxicity indices, and thermal signature of fuel post removal from the reactor

In light water reactors (LWRs) powered by 3-5% enriched uranium, approximately one-third of the core must be replaced on an average 18 month cycle; the buildup of fission products (primarily lanthanides, which have a high thermal neutron capture cross section) makes control of reactor operation within recommended safe operation limits more difficult. Beyond 18 months of irradiation, degradation of the fuel matrix due to extensive fission product recoil damage is also a factor in determining the frequency of refueling. One day after discharge of fuel from the reactor, approximately 48,000 curies/kg of initial heavy metal (IHM) is present in spent fuel (Choppin et al., 2002c) decreasing to about 1000 curies after 1 year of cooling (33,000 MWd/t IHM burnup). During the first 20 years, average decay energy is about 700 keV, primarily β^- and γ radiation; after about 100 years, the dominant mode of decay is α-emission (from actinides) with a peak energy of about 5 MeV. At one day after discharge, radioactive decay heat is 193 W/kg (initial uranium), 76% from fission products (Choppin et al., 2002d); after one year in storage, the heat load decreases to 10.8 W/kg, 95% derived from fission product decay. After 1000 years in storage, the heat produced has dropped to 0.054 W/kg, 100% derived from actinides.

1.1.4 Motivation and options for managing risks presented by used nuclear fuel

Given the intensity and persistence of the radiation field of discharged irradiated nuclear fuel, it is clear that significant handling precautions are needed for reasons of safety and security. At the same time, it is clear that the thermal and penetrating radiation fields decrease to "manageable" levels after about 500 years, heat decreasing more rapidly than radiation. In a period up to about 200-300 years, intact nuclear fuel has been considered to be "self-protecting" from intrusion because of the intense gamma radiation field. This philosophy of using high radiation fields as a "guarantee" of fuel remaining where it is emplaced for an extended period of time was an important driver for adoption of the open (single pass, or once through) nuclear fuel cycle in the United States. In this approach, the used fuel is considered as the waste form to be deposited in a geological repository permanently with appropriate warnings announcing its presence with a "danger, keep out" type of warning.

The question of whether it is appropriate to dispose of fissile material, specifically isotopes of plutonium, in this manner is not addressed in this approach. Clearly, it is essential that this hazardous material be isolated from the accessible environment. It is equally clear that opportunities to someday develop a market in fissile material removed from a repository might not be a grand concept. A further argument against direct disposal could arise from consideration of the expense associated with the creation of a fissile fuel (plutonium) then treating it as an undesirable by-product. In a fossil-energy constrained world, the direct disposal option for operating a nuclear power cycle bears further consideration. Another possible motivation for considering processing of used nuclear fuel after some interval of storage is the presence of several

potentially valuable elements other than actinides that can be found in used fuel at concentrations higher than that found in many natural sources. A few fission products worthy of such consideration are selected lanthanides, xenon, platinum group metals, ^{137}Cs, and ^{90}Sr. Clearly, the decision whether or not to close the nuclear fuel cycle is complex and there is probably not a single correct solution that is applicable globally.

1.2 Options for spent fuel management (store, dispose, recycle)

1.2.1 Closed vs. open fuel cycles

The five essential features to be considered in the decision of whether or not to recycle nuclear fuel are discussed below.

1. *Protection of people from the effects of excess exposure to ionizing radiation*. Used nuclear fuel upon discharge from the reactor is intensely radioactive due initially to beta and gamma radiation from fission product decay. After a few hundred years the radiation field is dominated by decay of alpha-emitting transuranium actinide isotopes. At high-radiation dose levels, ionizing radiation is known to be harmful. The correlation between dose and effect is less clear at low-radiation dose levels. For the direct disposal option, long-term radiotoxicity is dominated by plutonium isotopes; thus, fuel must be isolated from the accessible environment for 10 decay half-lives of ^{239}Pu, about 250,000 years. Reprocessing with actinide transmutation shifts the radiotoxicity focus to fission products ^{90}Sr and ^{137}Cs, and the acute radiotoxicity threat is reduced to 300-400 years.

2. *Prevention of nuclear weapons proliferation*. By mass, about 1% of used fuel from conventional LWRs is plutonium isotopes, which could be isolated from the fuel using well-known chemistry. Though reactor-grade plutonium does not possess an optimum isotopic blend for nuclear weapons, separated plutonium reserves could be used to assemble crude fission devices; thus, it is essential to consider the ideal means by which such diversion could be hindered. An argument can be made for the continuous recycling of plutonium to maintain a persistent fission product gamma radiation "shield" to limit the probability of plutonium diversion to weapons production. Whether or not to develop actinide transmutation systems to consume the TRU elements for power production is a component of this discussion.

3. *Ensuring an adequate supply of nuclear fuel*. Best estimates are that terrestrial reserves of uranium might be adequate for current operational practices for around 300 years of continued operation (Uranium 2011: Resources, Production and Demand, 2012). A larger, but more dilute reserve exists in the world's oceans; uranium supplies could be extended by this means. Another alternative would be to develop fuel cycles based on the transmutation of thorium (terrestrial reserves estimated to be three to four times that of uranium) to produce fissile ^{233}U. With appropriate development of safeguards against weapons diversion, it is also conceivable that uranium-plutonium breeder reactor options could be developed to transform fertile ^{238}U into fissile ^{239}Pu.

4. *Expense of reprocessing*. Clearly, there must be a cost differential between direct disposal of used fuel after a single reactor cycle and the cost of treating that fuel to partition usable materials (fuel, minor actinides, and other potentially valuable by-products). Across the fuel cycle, the cost of reprocessing would be partially offset by reduced expenses for mining and enriching uranium. A further cost saving might be gained by reducing the need for repository space, as HLW volumes are decreased by about five times after reprocessing to isolate uranium and plutonium for recycling (Choppin et al., 2002e). Various analyses of these costs have produced different estimates of the net expense of reprocessing, partitioning, and transmutation of actinides. If plutonium and minor actinides are transmuted, consideration of an increased safety margin in repository design and execution should be (but is not always) incorporated into the analysis. A more challenging calculation would be to include the potential financial impact of increased climate upsets from continued/expanded use of fossil carbon as a primary energy source.

5. *The challenge of establishing the integrity of an engineered* (*repository*) *system for a time greater than that of all human civilization*. The oldest human engineered and built structures in existence today are probably the pyramids of Egypt, several thousand years old. Though a repository system would be located underground, thus in principle isolated from the accessible environment, there are no examples of durable man-made structures with longevity of greater than (the direct disposal minimum) 250,000 years. Actinide recycle and transmutation significantly reduces the time frame that the waste must remain intact and sequestered and effectively shortens the required intact life of a repository to less than perhaps 1000 years.

1.3 Technology overview

There are at present two options for developing reprocessing systems: the conventional approach based on aqueous solutions and the alternative concept of pyroelectrometallurgy (Nash et al., 2006). More than 60 years of research and process experience represent the foundation for aqueous methods. Pyrometallurgical approaches have been investigated and exercised on a smaller scale and primarily with an emphasis on research and development activities.

1.3.1 Aqueous options

Contemporary reprocessing technology begins with the dissolution of UO_2 fuel in concentrated nitric acid solutions followed by solvent-extraction processes designed to extract the target metallic species (mainly actinides). As presently configured, used fuel reprocessing is carried out using PUREX chemistry to extract uranium (95% of the heavy metal content) and plutonium (1% of the IHM content), and fission products and minor actinides are treated as wastes for disposal as high-level radioactive waste that is immobilized in a solid matrix, either glass or ceramic. Plutonium can be recycled to create MOX fuel by blending the plutonium with natural uranium.

In France (global leaders in commercial reprocessing) the recovered used uranium is stored for future use and plutonium converted to MOX fuel. MOX fuel can be recycled to conventional LWRs to extend the utilization of the mined uranium.

1.3.2 Dry (pyro) processing

Dry (or nonaqueous) methods, as the name implies, require that the process be performed under inert atmosphere and in the absence of aqueous media, as water and atmospheric oxygen may react violently with some of the chemicals used. Most processes that fall under this category use molten salts and/or liquid (molten) metals at temperatures above the melting point of the material. The benefit of pyroprocessing is that the chemicals used tolerate high radiation doses, which allows for treatment of used fuel without having to wait for an extended period of time to let the material decay to lower levels of activity. High levels of fissile material can also be tolerated without issues of criticality, as there is no moderator present (water moderates neutrons in aqueous processes). This makes pyroprocessing attractive for high burn up and short cooled fuels and for reprocessing of fuel from fast reactors.

There are still several different concepts of this type of process under development, unlike PUREX, which is the benchmark for aqueous reprocessing, and detailed descriptions of different types will be given in later chapters. One of the common processes is the molten salt electrorefining method used for example in the IFR (integral fast reactor) concept (IAEA Nuclear Energy Series, 2011). This process begins with chopping of the fuel pins and loading the pieces into a basket that is lowered into an electrorefining cell. The basket with the chopped up fuel is filled with cadmium chloride ($CdCl_2$) and comprises the anode. The electrorefining cell is filled with a molten salt, that is, electrolyte, such as a eutectic mixture of potassium chloride (KCl) and lithium chloride (LiCl) at high temperature. Two cathodes are lowered into the electrorefining cell, one solid cathode made of (for example) low carbon steel, and one liquid cathode consisting of liquid metal cadmium. An appropriate electrical potential is imposed across the circuit. At the anode the uranium, plutonium, minor actinides, and most fission products are dissolved and transported into the electrolyte. The metal cladding and hulls remain in the basket due to the difference in redox potential between the different elements. The cladding material, for example, zirconium, iron, as well as noble fission products, have a higher standard reduction potential than the actinides and other fission products (Koyama, 2011a). The uranium dissolved in the electrolyte is deposited on the solid cathode. The plutonium, the minor actinides, and some of the uranium are deposited in the molten cadmium cathode. The fission products remain in the molten salt. The actinides can be recovered in metallic form, as ingots. The salt can be purified by (for example) absorption of the fission products in a zeolite material to allow for the recycling of the salt back into the electrorefining cell. The salt waste product is processed into a ceramic waste form and the remaining waste is in metallic form. Although these processes have been studied for as long as aqueous processes, there is no plant at a scale comparable to commercial aqueous reprocessing in operation today. One of the challenges associated with pyroprocessing

is to create a continuous process, as the electrowinning is done batch-wise. This presents an obvious challenge for scale-up.

The pyroprocessing category also includes the fluoride volatility process that utilizes the difference in volatility and chemistry of uranium hexafluoride (UF_6) and plutonium hexafluoride (PuF_6) compared to other elements in the fuel. Although this process has advantages in terms of recovery and purity of the UF_6 product, there are challenges in the recovery of PuF_6 due to the instability of PuF_6 (IAEA Nuclear Energy Series, 2011).

1.4 Historical development of reprocessing

1.4.1 Nuclear weapons development

Nuclear fission was discovered in the late 1930s in Germany (Rhodes, 1986), shortly before the outbreak of World War II. The leap from discovery to consideration of the possible impact of creating weapons based on this discovery took only a very short time; in fact, it might arguably have predated the demonstration/discovery. The exigencies of wartime scientific discovery ultimately gave rise to the Manhattan Project, nuclear weapons, the end of World War II, and the Cold War. Though nuclear science advanced steadily throughout that period, nuclear technology dictated to a large degree the pace and direction of that progress. When President Eisenhower delivered his Atoms for Peace speech at the United Nations in December 1953 (Atoms for Peace Speech, 1953), it marked a transition toward a broader spectrum of potential applications of this new source of power. This shift led first to nuclear-powered submarines and ultimately to land-based nuclear power plants based on a scaled-up version of the submarine-designed water-cooled reactor.

1.4.2 $BiPO_4$/redox/butex/PUREX

The roots of nuclear fuel reprocessing also are found in that same realm of war and commercial technology. After Seaborg and coworkers discovered plutonium, it was quickly established as an alternative (more economical and potentially faster than uranium isotope enrichment) pathway to nuclear weapons that could be built around nuclear reactors and chemical processing (Seaborg and Loveland, 1990). Using precipitation methods first demonstrated at UC Berkeley/the Rad Lab, the bismuth phosphate process ($BiPO_4$) was scaled up from its first demonstration at the microgram scale to the kilogram scale (famously a factor of 10^9) without intermediate development of pilot-scale demonstrations. The $BiPO_4$ process suffered some important limitations: (1) it did not support the recycling of the limited supply of uranium that was available, (2) 2-3% of the desired plutonium product was lost to waste due to the inherent inefficiency of solid-liquid separations, and (3) it was a major generator of radioactive wastes (dealing with the phosphate from this process still represents one of the major challenges of the proposed cleanup of the Hanford site in Washington state; National Academy Press, 1996).

The inability to recycle uranium drove Hanford's transition to solvent-extraction-based processes. The first was the Redox process based on extraction of uranium and plutonium with separation of plutonium from uranium developed around manipulation of the redox chemistry of plutonium. As the methyl(isobutyl) ketone (MIBK) extractant is a relatively weak phase-transfer agent, the aqueous medium employed was based on aluminium nitrate ($Al(NO_3)_3$) as a salting-out agent. Wastes from this process represent the primary source of aluminum in Hanford tank wastes. In the United Kingdom, a cleaner option based on the polyether extractant "dibutyl cellosolve" used similar chemistry to partition U/Pu from nitric acid media. Arguably, the most enduring adjustment was the next one in which plutonium redox chemistry was still employed but the significantly more efficient extractant tri-*n*-butyl phosphate (TBP) enabled the PUREX process, which 60+ years later remains the industry standard. Decades of plant operation experience and continued research and development have steadily improved performance of the process.

1.4.3 Reprocessing of commercial fuels

In the 1950s, nuclear fission technology transitioned into a new source of electricity and commercial nuclear power plants were planned, built, and operated. In its earliest conception, civilian nuclear power was introduced with reprocessing of material as part of the plan. Used fuels from thermal reactors were to be reprocessed and the products, uranium and plutonium, recycled into new fuel. Furthermore, it was understood early on that recycling of the material would require a fleet of fast reactors to effectively utilize the uranium available from mining operations, that is, breeding and burning of plutonium.

The PUREX process rapidly took over from previous methods used (as discussed above) and in 1954 PUREX was put into operation at Aiken, South Carolina, albeit not for civilian purposes. In 1966 Nuclear Fuel Services, Inc., commissioned the first reprocessing plant in the Unite States for civilian fuel (Benedict et al., 1981). The plant was located in West Valley, New York, and operated with a capacity of 1 ton/day. The plant was closed in 1972 in preparation for upgrades to increase the capacity and to adhere to new federal regulations. However, as the political situation changed and emphasis on nonproliferation began to weigh heavily in the debate, President Carter announced in 1976 that reprocessing should not proceed in the United States. That same year Nuclear Fuel Services, Inc., announced that the West Valley plant would not be reopened (Tsoulfanidis, 2013). Since then no commercial fuel has been reprocessed in the United States. However, reprocessing on a commercial scale had at that point begun in countries outside of the United States and those activities have continued in several countries to the present day.

In France, the UP-1 plant in Marcoule was commissioned in 1958 for processing of defense waste. This plant used PUREX chemistry. The Windscale plant in the United Kingdom was commissioned in 1952 and initially used the Butex process (referring to the extractant used, dibutyl carbitol, i.e., Butex), but with the commissioning in 1964 of the larger Magnox reprocessing plant the site eventually switched to PUREX as this new technology was shown to be superior. The experience gained using the PUREX process allowed both France and the United Kingdom to construct and commission

larger-scale reprocessing plants for commercial use. In 1948 Russia, then part of the Union of Soviet Socialist Republics, began reprocessing, for defense purposes, at the Mayak plant in Chelyabinsk-65. In 1977, the RT-1 reprocessing facility was commissioned at the same site with the purpose to reprocess used fuel from VVER-440 reactors, as well as some other commercial, research, and naval reactor types. The plant was designed with a capacity of 400 ton/year, utilized the PUREX process, and produced material for MOX fuel. Japan started construction of their first reprocessing plant in 1971 at Tokai-Mura, which started operation in 1977. The plant had a capacity of 300 ton/year and provided the experience that would allow for the commercial plant in Rokkasho-mura to be constructed several decades later. Other countries have constructed and operated reprocessing plants larger than lab-scale. For example Belgium, in a consortium of 13 OECD member countries, operated a pilot-scale reprocessing plant in Dessel from 1957 to 1974 (Eurochemic—A Belgoprocess Project, n.d.); in Germany, the MILLI facility with a capacity of 1 kg fuel/day/extraction cycle allowed for the commissioning of the reprocessing plant in Karlsruhe, which operated until 1990.

1.5 Survey of modern PUREX-based reprocessing[2]

The bulk of used commercial nuclear fuel that has been reprocessed cumulatively to date has been done in France and the United Kingdom, where currently the largest reprocessing capacity exist. The La Hague site in France with its two reprocessing plants, UP-2 and UP-3, has a combined capacity of 1700 tHM/year. The UP-3 plant was built exclusively to reprocess foreign fuel from countries lacking this capability but with an inventory of used fuel. The Sellafield site in the United Kingdom operates two plants. The Magnox reprocessing plant operating since 1964 to reprocess fuel from the Magnox reactors, and the more recent THORP plant is dedicated to reprocess oxide fuel from LWRs and advanced gas-cooled reactors (AGRs). As the utilization of Magnox reactors ends, the Magnox reprocessing plant will become obsolete and is currently expected to end its operation around 2018. The THORP plant, where operations were initiated in 1994, is scheduled to end its operation in 2018 (Spent Fuel Management, n.d.). It has been indicated that the United Kingdom is still dedicated to have nuclear energy as part of its energy production portfolio, as new builds of nuclear power plants are planned. New build has been justified on the basis that the used fuel management scenario that will be adopted is an open cycle but alternative scenarios, even up to 75 GWe, are under consideration that would utilize closed cycles (HM Government, 2013).

A few other countries have active, or complete, reprocessing plants; the two largest outside of France and the United Kingdom being Russia and Japan. The Mayak plant in Russia is considering adding capacity for LWR reprocessing. The Rokkasho-mura

[2] As the future of the industrial adaptation of reprocessing technology and implementation of processes is uncertain, the information provided below should be regarded as a direction the field is heading at the time this text was prepared.

plant in Japan was recently completed and has a planned capacity for 800 tHM/year. Due to the political situation regarding nuclear energy in Japan, the Rokkasho-mura plant has not started full-scale operation, although small-scale test runs have been carried out successfully. India has operated a reprocessing plant in Kalpakkam for a number of years and is planning to expand the capacity at this site. China is operating a pilot-scale reprocessing plant in Lanzhou and is planning on increasing the capacity at this site to 400 tHM/year in 2017. Also in China, larger plants are planned either based on domestic technology or in collaboration with AREVA.

These plants for reprocessing and recycling of used nuclear fuel utilize the PUREX process as described above (and in greater detail in later chapters in this book). During decades of operation, a large amount of operational experience and insight has been gathered for the TBP-based PUREX process, both in the commercial fuel reprocessing and nuclear weapons industries. This, together with improvements in design of equipment and increased understanding of the principles of extraction, has led to improved PUREX-based processes. In addition, fear of proliferation has also been a driver for making adjustments to the operation of PUREX processes to avoid pure plutonium products. Of the adaptations, some worth mentioning are the COEX^{TM} process developed at CEA, France; the "Advanced PUREX" developed in the United Kingdom; and, although currently not considered for industrial application, the "UREX" process developed in the United States.

One common theme in these processes (aside from the fact that they extract metal ions from a nitric acid solution using a TBP/kerosene solvent) is that the plutonium product is "contaminated" with other elements making it less useful (i.e., less attractive) for possible diversion to nuclear weapon production. The COEX^{TM} process (Herbst et al., 2011) allows some uranium to remain in the plutonium stream, making the two main products of the COEX^{TM} process a pure uranium stream and a mixed U/Pu stream. The added benefit of this is that the U/Pu mixture may be treated to produce a MOX for MOX fabrication.

The "Advanced PUREX" and "UREX" processes instead rely on adjusting the process conditions so that the neptunium is routed with the plutonium in a Np/Pu product stream; a pure uranium stream is produced. Producing a pure uranium stream and a mixed Np/Pu product is a considerable challenge because the oxidation state of neptunium and plutonium are both prone to change as reducing or oxidizing agents are introduced. In these processes, Np/Pu partitioning away from uranium and fission products is accomplished by the addition of acetohydroxamic acid, AHA, to the aqueous feed. This reagent acts both to reduce Np(VI) to Np(V) and to complex Np(IV) and Pu(IV) in the aqueous phase, effectively holding them back allowing U(VI) to be extracted by TBP without Np/Pu contamination. A side effect of this is the coextraction of Tc (as TcO_4^-) together with uranium, which occurs at the elevated pH that this process requires compared to conventional PUREX. Without the pH adjustment, the AHA would be rendered inactive. As a result, these processes would potentially require a separate U/Tc separation strategy.

Although attempts have been made to replace TBP as the main extraction reagent, it is likely that PUREX and modern adaptations of PUREX will continue to play a major role in used nuclear fuel reprocessing, in large part due to the decades of

operational experience, predictability, and low cost of TBP. No other processes or extraction reagents have been studied as extensively as PUREX and TBP, although arguably there are still important discoveries to be made and there is always room for improvements.

1.6 Basic introduction to the chemistry

As much of what follows in the remaining chapters of this book will emphasize the technological aspects of nuclear energy and reprocessing, the following section will focus on laying the fundamental groundwork for the chemistry that enables and limits efficient use of nuclear power.

1.6.1 Key elements/isotopes of concern

The process of fissioning ^{235}U and ^{239}Pu in conventional reactors releases enough excess neutrons to sustain the fission chain reaction. The two possible outcomes for neutron capture by an actinide are fission and the production of heavier actinide isotopes. At least 400 primary fission products have been identified, implying the existence of about 200 exit channels for the fission reaction. The diverse mix of species present in irradiated fuel include kilograms per ton of lanthanides from lanthanum to gadolinium, ^{137}Cs, ^{90}Sr, long-lived ^{99}Tc and ^{129}I, significant amounts of noble metals (Rh, Pd, Ag), Xe, and transuranium elements including plutonium, americium, neptunium, and curium. If MOX fuel is utilized, heavier actinides (berkelium and californium) are produced. Plutonium isotopes are of particular concern as they represent a potential nuclear weapons proliferation risk; neptunium and americium are a concern for their role in establishing the long-term radiotoxicity of used fuel. Several of the lanthanides are strong neutron poisons, so they become important to remove in the pursuit of minor actinide transmutation systems.

1.6.2 Key process steps

When power reactor fuel is discharged from the reactor, it must first be cooled for some time (typically several years) to allow for reduction in the intensity of fission product beta and gamma radiation and coincidentally to reduce its thermal signature. After adequate thermal cooling, the fuel pins are chopped to breach the cladding material and expose the UO_2 matrix. Most of the fuel dissolves in hot concentrated nitric acid, which both neutralizes the basic oxide and oxidizes susceptible components (e.g., $U^{4+} \rightarrow UO_2^{2+}$). The dissolved components are separated from the undissolved residue of fuel cladding and selected fission products. In the current standard for aqueous processing, the dissolved fuel is typically contacted with one or more organic solutions to begin the separation process. Ideally, valuable components are recovered for recycle and reuse while waste is transformed to some sort of solid waste form for permanent emplacement in a geological repository.

1.6.3 Dissolution, aqueous separation, conversion, waste treatment

The dissolution of oxide fuel creates an aqueous solution that contains uranyl (UO_2^{2+}) as the major metal ion as well as significant amounts of the transuranium elements and fission products, as has been noted above. The solution is initially concentrated in nitric acid and also contains fines (suspended solids) and some other undissolved material. The solution is subjected to a clarification step in which the solution is either filtered or centrifuged to remove any solids. The nitric acid concentration is adjusted to a more moderate level ~2-4 M and routed to the separation stage (i.e., PUREX process). Before the aqueous phase is contacted with the organic phase, the plutonium oxidation state is adjusted to the tetravalent state, which is the most extractable state when using TBP in kerosene (the PUREX solvent); mainly, this is done by maintaining the HNO_3 concentration in the 2-4 M range. As the aqueous solution is contacted with the organic phase, U(VI) and Pu(IV) are extracted as their respective electroneutral nitrate complexes ($UO_2(NO_3)_2$, $Pu(NO_3)_4$) into the organic phase. This is called the codecontamination step and removes uranium and plutonium from most of the fission products and minor actinides.

The two phases are contacted, more or less vigorously, using some form of mechanical device. Industrial applications for aqueous separations have used pulse-columns, mixer-settlers, and centrifugal contactors to create an unstable emulsion in which metal ions partition between the organic and aqueous microenvironments. The emulsion is then allowed, or forced, to separate to restore a distinct biphasic system. The chemistry of aqueous and organic media is adjusted to achieve the desired selective partitioning of plutonium and uranium away from minor actinides and fission products. After the codecontamination step, the uranium and plutonium are mutually separated by reducing Pu(IV) to Pu(III) with either U(IV) or hydroxylamine (NH_3OH). Each product phase then goes through a cleaning process to produce pure uranium or pure plutonium product. The separation of uranium and plutonium, as well as the cleanup process are all based on solvent-extraction processes utilizing the same organic solvent but with adjustments in the aqueous phase and addition of redox reagents. Each operation is appropriately scaled with repeat stages that cumulatively achieve the desired degree of purity of products and/or reagents to be recycled. Additional stages translate into greater expense in operation and potentially in complexity, so maximizing efficiency in each operation is clearly desirable.

The final products are uranyl nitrate and plutonium nitrate solutions that are routed to conversion where plutonium nitrate is converted to PuO_2 by precipitation as an oxalate followed by calcination to a solid oxide. Uranium can be precipitated by addition of ammonium salts and partially reduced to form U_3O_8 or thermally denitrated, usually over a fluidized bed. The waste from the commercial PUREX process consists of an acidic aqueous raffinate with high levels of radioactive materials (HLLW); there are also significant volumes of lower-level waste streams and degraded organic solvent. Generally, the lower-level waste is concentrated as much as possible to produce a reduced volume of higher-level waste. The HLLW can be converted to a solid waste form by vitrification where in the waste stream is fed to a rotating kiln and components

of borosilicate glass are added. The mixture is melted in a furnace to produce an obsidian-like glass waste form that is poured into stainless steel containers, welded closed, and subsequently stored in high-level waste storage facilities. Ultimately, this HLW would be transported to a subsurface mined geologic repository for permanent emplacement.

1.6.4 Pyroprocessing alternatives

As mentioned previously, pyroprocesses require an absence of water and the steps involved in the process are all carried out under inert atmosphere and at high temperatures. The high concentration of salt and the elevated temperatures put great stress on containment materials. The effect of corrosion has been studied extensively and remains a significant challenge. The high temperatures and often high radiation fields increases the challenge for the design and use of sensors and probes to monitor the process continuously. The process may lend itself better to certain metallic fuels, as the dissolution of uranium metal alloys is accomplished more easily via pyrometallurgy than in strong acidic solutions. However, pyrochemical processes have been tested for oxide fuel as well. Pyroprocessing has traditionally been a batch-wise process, although technologies are under development and testing that will increase the throughput; for example, by continuously scraping off the uranium product from the cathode. Using moving cathodes and anode baskets to provide better mixing and to avoid stagnant interfaces between the salt eutectic and liquid metal have also been examined. Experiments have been carried out in Japan (by CRIEPI) using a system in which the liquid cadmium can be circulated, theoretically allowing for continuous recovery of plutonium and minor actinide metals (Koyama, 2011b). Researchers at CRIEPI have also tested a zeolite column that could be used to continuously clean the electrolyte salt from fission products by pumping the salt melt through the column and back to the electrorefiner (Koyama, 2011c).

An oftentimes cited benefit of pyroprocessing (relative to PUREX) is the comparative proliferation resistance of pyrometallurgy. One of the products from traditional PUREX is pure plutonium dioxide, while the plutonium produced from pyroprocessing will be contaminated with minor actinides, making it less attractive as potential weapons material.

1.6.5 Basic chemistry of separation processes

Designing a successful separation process for used nuclear fuel requires an understanding of a wide variety of physical and chemical concepts. The uniqueness of the process, in that it deals with large quantities of actinides (in particular transuranium elements), means that a significant amount of information is found in highly specialized books, periodicals, and technical reports. However, there are a number of common features across the periodic table; that is, methods that can be used in separation processes for strategic metals (e.g., copper refining) can be very successfully applied to processes for used nuclear fuel.

1.6.6 Redox, speciation, solvent extraction, ion exchange, holdback reagents, extractants

One of the unique features of plutonium chemistry, in fact, a key component of the PUREX process, is the accessibility of four different oxidation states that can be reached in solution under relatively gentle conditions. The reduction of Pu(IV) to Pu(III) makes the metal ion largely unextractable by TBP and immediate separation of U(VI) and Pu(III) is accomplished with this adjustment. The oxidation and reduction of other transuranics such as neptunium and americium have been investigated as potential routes to separation processes for Am/Cm separation or Np/Pu coextraction. The oxidation states of neptunium and particularly of americium are not as easy to adjust as those of plutonium; neptunium can be stabilized under process conditions in the IV, V, and VI oxidation states, and the relative stability of the V and VI states appears to change as nitric acid concentration increases. Without the application of strong oxidants, americium markedly prefers the trivalent state. The application of aggressive oxidants or strongly oxidizing electrical potentials often results in degradation of other chemicals in the process, thus rendering the separation significantly more challenging. This complexity is one of the reasons why aqueous separation processes for actinides other than uranium and plutonium have not been implemented at a scale larger than hot cell demonstrations. Most pyrochemical processes are based on differences in the redox chemistry of the metal ions of interest as the primary means of separating them from undesirable impurities. In typical nuclear applications of pyrometallurgy, once the chloride salts are formed the relative thermodynamic stabilities of the different metal halides also plays a role in the selective deposition at the cathode (IAEA Nuclear Energy Series, 2011).

In the main, aqueous processes for separation of metal ions rely on the formation of either water soluble or lipophilic coordination complexes. Multidentate chelating agents are designed for their specific affinity for target metal ions and against undesirable contaminants. Electrostatic and covalent bonding interactions and, in some instances, steric factors combine to produce the desired complex strength and selectivity. Redox chemistry can also play an important role for extraction of metal ions with multiple accessible oxidation states. Complexant design for such applications must balance three factors: complex strength, selectivity, and phase compatibility. Due to the high coordination numbers of actinides and the variety of valency states of the metal ions across the series, a detailed understanding of actinide chemistry is beneficial for predicting the outcome in a given separation process.

Cations, and especially hard cations like the actinides and lanthanides, are prone to forming hydrolysis products at relatively low pH. This can greatly affect a separation process and is one of the reasons why most aqueous separation processes proposed as a follow on to PUREX operate under acidic conditions. The PUREX process itself requires the nitric acid concentration to be relatively high. High nitric acid concentrations act to stabilize Pu(IV), to suppress hydrolysis, and to drive the phase transfer reaction. At very high concentrations, nitric acid competes with actinide nitrates and oxidizes components of the extractant phase.

One final concern that must always be considered in the handling of plutonium-rich solutions is the ever-present possibility of the accidental formation of a critical mass

(Choppin et al., 2002f). Solvent extraction systems are composed of excellent neutron moderators, so processing plants are necessarily designed in "criticality-safe" geometries. Neutron poisons (like gadolinium) can be added to minimize this risk (Choppin et al., 2002g). Unintended precipitation of plutonium-bearing solids or the formation of "third phases" at high metal loading demands vigilance and monitoring of ambient neutron fluxes.

Ever since the development of PUREX, several separation processes have been proposed (Nash and Lumetta, 2011). Some have been suggested as a substitute for PUREX (although no one process has yet achieved efficiency equivalent to PUREX). More have been developed for application to the waste stream exiting the PUREX process to accomplish further waste minimization or resource recovery. The R&D push for improvements in extraction processes have over the years resulted in a large variety of solvent-extraction reagents as well as holdback reagents that sometimes display separation factors of $1{:}10^5$ or more between metal ions that are considered very similar (e.g., Am(III)/Eu(III)). Details of many of these processes will be discussed in later chapters.

With very few exceptions, these separation systems are all based on solvent extraction. The maturity of solvent extraction into an industrial technique was in large part a result of the development of the PUREX process. Experiences that were gained using PUREX in industrial as well as laboratory studies have served as a springboard for the design of novel processes. PUREX is still used as a benchmark for how well a process performs. Some work has been done on ion exchange and extraction chromatography, in which selective ligands are sorbed to a solid support. These technologies can produce very high purity products and avoid the use of large volumes of organic solvents. However, there are limitations to using these techniques for solutions containing high concentrations of metal ions, and continuous operations are also a challenge as the columns need to be flushed or regenerated. Waste management can also be more complicated.

1.6.7 Impact of radiolysis

The high radiation fields that accompany used nuclear fuel, even after years of cooling, provide an interesting challenge to the chemical stability of solutions and solids. Organic solvents may degrade, aqueous solutions produce free radicals that affect the redox chemistry of metal ions, and the radiation may accelerate corrosion rates of pipes and equipment in the separation process. Overall, pyrochemistry has an advantage in that the chemicals used are simple ion pairs that are essentially unaffected by radiation. However, corrosion is still an issue and as the radiation fields can be higher in a pyrochemical process this makes R&D on materials a prime concern.

1.6.8 Basic radiation chemistry, impacts on reprocessing

From a radiation chemistry standpoint, there is more knowledge and understanding of the effects in aqueous processes (Mincher et al., 2009a,b,c). Arguably, the chemical components of aqueous separation systems are also more sensitive to radiation; thus,

pyrochemical processes will not be discussed further in this section. The effects of alpha, beta, and gamma radiation on water have been extensively studied since the early 1900s, essentially since the discovery of ionizing radiation (Choppin et al., 2002h). One of the most used techniques to measure dose by a chemical dosimeter is still the Fricke dosimeter developed in the 1920s that in its most common form utilizes the oxidation of Fe(II) to Fe(III) to estimate dose to water (in actuality, dose to a salt solution that, within reason, mimics human tissue). As the ionizing radiation passes through the solutions, a track of ion-electron pairs are formed. The electrons formed may have a high enough energy to cause secondary ionization and further damage to the solution. The result is that radicals and reactive species are formed close to the track and these species will rapidly react with molecules and ions in their vicinity. For low linear energy transfer (LET) radiation, beta, and gamma radiation, the ionization is sparsely distributed so that the reactive species are more likely to react with species that were originally present in the solution. High LET radiation, alpha particles, and FP from spontaneous fission, on the other hand deposit a large amount of energy in a short distance and the reactive species formed have a higher probability or reacting with other radiolysis products formed in their vicinity. The result when irradiating water is that low LET produces a higher relative amount of small products such as hydrogen atoms, hydrated electrons, and hydroxyl radicals while high LET produces higher relative amounts of larger products such as hydrogen peroxide (by recombination of two OH-radicals).

In a solvent-extraction system the radiolysis products in the aqueous phase may react with chemicals in the organic phase during the mixing stage and, to a lesser degree, in the settling stage. Radiation may also be directly deposited in organic solvents where a different suite of radicals and reactive species are expected to form in the tracks and further react with the chemicals in their vicinity. The effect of ionizing radiation on a solvent-extraction system is difficult to predict and a lot of information has been found by empirical studies; that is, investigating the degradation products formed after a certain dose has been deposited. Studies have also tracked the extraction efficiency of metal ions as a function of dose but this introduces uncertainties as some degradation products may be more efficient in extraction than the original molecule. A direct example is in the PUREX process, where TBP degrades by radiolysis to dibutyl phosphoric acid (HDBP). HDBP is a cation exchanging extractant and is a very efficient extracting reagent for tetravalent and trivalent metal ions; it also extracts hexavalent actinide ions (and Mo(VI)) in contact with reduced acid solutions. The result from extensive radiolysis of the PUREX solvent is that, as HDBP concentration increases with radiation dose, the plutonium extracted into the organic solvent will not be readily stripped and so is more difficult to separate from the uranium. Furthermore, fission products can be extracted into the organic phase causing serious process upsets. Finally, the introduction of degradation products and extensive dose to organic solvents can change the viscosity of the organic phase causing changes in the hydrodynamics of contactor equipment. In the PUREX process, HDBP increases the propensity of a third phase to form, which will cause process upsets and may be potentially hazardous from a criticality standpoint.

1.7 Prospects for the future

1.7.1 Education of the next generation of specialists

The foundations of nuclear science were established in the last decade of the nineteenth and the first decades of the twentieth century. Nuclear technology in the form of weapons and reactors advanced substantially during the middle decades of the twentieth century. During this period, many brilliant scientists and engineers were attracted to this field and major scientific and technological advances were made. In the United States and elsewhere, university-level investments in educational facilities saw sustained growth from the post-WWII era to the late 1970s. During the last two decades of the twentieth century, extremely unlikely (based on probabilistic risk analysis) reactor accidents occurred at Three Mile Island and again at Chernobyl and the academic community in the United States lost faith in nuclear science and technology as a discipline for study. Before the Three Mile Island accident, more than 100 nuclear and radiochemistry faculty members in the United States produced 25-30 new doctoral-level nuclear scientists and radiochemists per year. At the dawn of the twenty-first century, the number of faculty had declined by at least a factor of three and new PhD creation had dropped to an annual average of about 7 (National Academy Press, 2012). At the same time, nuclear engineering programs also decreased in numbers but less severe declines in the numbers of new graduates were seen, implying that the surviving programs had reacted to fill the void.

It is generally considered that nuclear engineering programs today are more-or-less in balance; nuclear chemical engineering, nuclear chemistry, and radiochemistry academic programs still remain underpopulated relative to perceived needs. During the first decade of the twenty-first century, the graduation rates for doctoral-level nuclear and radiochemists have improved somewhat but the rate is far below that required to replace an aging workforce. As nuclear science and technology is a demanding field, retraining of students from other disciplines for nuclear positions will produce a future workforce with reduced overall understanding and the need for a significant amount of on-the-job training, with that training coming from a vanishing mature workforce. Addressing this gap in knowledge and competency remains a serious concern, even though some advances have been achieved. The global situation does not differ appreciably from that of the United States—there is a greater need for experts than is being met.

For several reasons, the education of next generation experts must be viewed as a long-term challenge. Nine percent of global electricity production is based on this demanding technology, which produces waste by-products that must be either transmuted or sequestered for millennia; concerns about environmental quality and climate change virtually ensure that this option will gain increasing importance and likely expanded use. The depleted expertise base that has been discussed in the previous paragraph will recover slowly, given the comparatively small numbers of universities (and other institutions) engaged in graduate education in nuclear science and technology. The long half-lives of weapons-usable actinides will demand ongoing vigilance regarding diversion of this material to military applications. History has established

that, barring the intrusion of a global emergency (as happened during World War II, which sparked the Manhattan Project), developing new science and technology in this field requires decades of research and development. Each of these factors indicates the need for a long-term commitment and a strong talent base.

1.7.2 Preview of global perspectives to be discussed in the following chapters

In the following chapters, several authors will discuss the overall perspective on twenty-first century issues and approaches to the recycling of nuclear fuel, including the important issue of securing nuclear materials from possible diversion to weapons applications by countries or subnational groups. In subsequent sections, chapters will address aqueous recycling, pyrometallurgical reprocessing, and issues that are relevant concerns for any approach to nuclear materials reprocessing. Finally, authors will focus on the specific issues of each of the major regions participating in the advancement of nuclear energy technologies, including prospects for the thorium-uranium cycle.

It is clear that nuclear energy technology has an important role to play in a world that is challenged by (1) an increasingly unstable climate that demands low-carbon alternatives to coal-oil-gas, (2) significant development of underdeveloped countries toward modern economies, and (3) a projected 30% increase in global population during the next 40 years. The considerable promise of energy based on the fissioning of uranium-plutonium and thorium-uranium remains a globally underdeveloped resource that addresses all of these issues. Fuel supplies and responsible management of long-term radiotoxic by-products point toward the eventual operation of closed nuclear fuel cycles as the norm. Whether aqueous or pyrometallurgical (or both) options are pursued, more efficient exploitation of these resources appears to be in the best interest of all inhabitants of the planet. It is important that wise decisions are made and that the correct actions are pursued.

References

Atoms for Peace Speech, 1953. http://www.iaea.org/About/atomsforpeace_speech.html (accessed 19.04.14).

Benedict, M., Pigford, T.H., Levi, H.W., 1981. Nuclear Chemical Engineering, second ed. McGraw-Hill, New York, 469 pp.

Choppin, G.R., Liljenzin, J.O., Rydberg, J., 2002a. Radiochemistry and Nuclear Chemistry, third ed. Butterworth-Heinemann, Woburn, MA, pp. 104–105.

Choppin, G.R., Liljenzin, J.O., Rydberg, J., 2002b. Radiochemistry and Nuclear Chemistry, third ed. Butterworth-Heinemann, Woburn, MA, pp. 520–523.

Choppin, G.R., Liljenzin, J.O., Rydberg, J., 2002c. Radiochemistry and Nuclear Chemistry, third ed. Butterworth-Heinemann, Woburn, MA, pp. 594–595.

Choppin, G.R., Liljenzin, J.O., Rydberg, J., 2002d. Radiochemistry and Nuclear Chemistry, third ed. Butterworth-Heinemann, Woburn, MA, p. 598.

Choppin, G.R., Liljenzin, J.O., Rydberg, J., 2002e. Radiochemistry and Nuclear Chemistry, third ed. Butterworth-Heinemann, Woburn, MA, p. 632.

Choppin, G.R., Liljenzin, J.O., Rydberg, J., 2002f. Radiochemistry and Nuclear Chemistry, third ed. Butterworth-Heinemann, Woburn, MA, p. 530.
Choppin, G.R., Liljenzin, J.O., Rydberg, J., 2002g. Radiochemistry and Nuclear Chemistry, third ed. Butterworth-Heinemann, Woburn, MA, p. 528.
Choppin, G.R., Liljenzin, J.O., Rydberg, J., 2002h. Radiochemistry and Nuclear Chemistry, third ed. Butterworth-Heinemann, Woburn, MA, pp. 176–180.
Dickey, P.A., 1959. The first oil well. J. Pet. Technol. 9, 14–26.
Eurochemic—A Belgoprocess Project, n.d. http://www.eurochemic.be/eng/documents/Eurochemic-brochure.pdf (accessed 19.04.14).
Herbst, R.S., Baron, P., Nilsson, M., 2011. Standard and advanced separation: PUREX processes for nuclear fuel reprocessing. In: Nash, K.L., Lumetta, G.J. (Eds.), Advanced Separation Technologies for Nuclear Fuel Reprocessing and Radioactive Waste Treatment. Woodhead Publishing, Cambridge, pp. 168–172.
HM Government, 2013. Nuclear Energy Research and Development Roadmap: Future Pathways. Ref: BIS/13/632 (26 March, 2013). https://www.gov.uk/government/publications/nuclear-energy-research-and-development-roadmap-future-pathways (29.12.14).
IAEA Nuclear Energy Series, 2011. Report no. NF-T-4.2, Status of developments in the back end of the fast reactor fuel cycle. International Atomic Energy Agency, VIENNA, pp. 9–13.
Koyama, T., 2011a. Nuclear engineering for pyrochemical treatment of spent nuclear fuels. In: Nash, K.L., Lumetta, G.J. (Eds.), Advanced Separation Technologies for Nuclear Fuel Reprocessing and Radioactive Waste Treatment. Woodhead Publishing, Cambridge, pp. 272–273.
Koyama, T., 2011b. Nuclear engineering for pyrochemical treatment of spent nuclear fuels. In: Nash, K.L., Lumetta, G.J. (Eds.), Advanced Separation Technologies for Nuclear Fuel Reprocessing and Radioactive Waste Treatment. Woodhead Publishing, Cambridge, p. 288.
Koyama, T., 2011c. Nuclear engineering for pyrochemical treatment of spent nuclear fuels. In: Nash, K.L., Lumetta, G.J. (Eds.), Advanced Separation Technologies for Nuclear Fuel Reprocessing and Radioactive Waste Treatment. Woodhead Publishing, Cambridge, pp. 291–292.
Mincher, B.J., Modolo, G., Mezyk, S.P., 2009a. Review article: the effects of radiation chemistry on solvent extraction: 1. Conditions in acidic solution and a review of TBP radiolysis. Solvent Extr. Ion Exch. 27 (1), 1–25.
Mincher, B.J., Modolo, G., Mezyk, S.P., 2009b. Review article: the effects of radiation chemistry on solvent extraction: 2. A review of fission-product extraction. Solvent Extr. Ion Exch. 27 (3), 331–353.
Mincher, B.J., Modolo, G., Mezyk, S.P., 2009c. Review article: the effects of radiation chemistry on solvent extraction 3: A review of actinide and lanthanide extraction. Solvent Extr. Ion Exch. 27 (5–6), 579–606.
Nash, K.L., Lumetta, G.J. (Eds.), 2011. Advanced Separation Technologies for Nuclear Fuel Reprocessing and Radioactive Waste Treatment. Woodhead Publishing, Cambridge.
Nash, K.L., Madic, C., Mathur, J.N., Lacquement, J., 2006. Actinide separation science and technology. In: Katz, J.J., Morss, L.R., Edelstein, N., Fuger, J. (Eds.), The Chemistry of Actinides and Transactinide Elements, third ed. Springer, Dodrecht, pp. 2622–2798.
National Academy Press, 1996. Defense wastes. In: Nuclear Wastes—Technologies for Separation and Transmutation. National Academy Press, Washington, DC, pp. 87–98.

National Academy Press, 2012. Assuring a Future U.S.-Based Nuclear and Radiochemistry Expertise. National Research Council of the National Academies, National Academy Press, Washington, DC.

Rhodes, R., 1986. The Making of the Atomic Bomb. Simon and Schuster, New York, pp. 247–264.

Ristinen, R.A., Krushaar, J.J., 1999. Energy and the Environment. John Wiley and Sons, New York, pp. 2–4.

Seaborg, G.T., Loveland, W.D., 1990. The Elements Beyond Uranium. John Wiley and Sons, New York, pp. 11–17.

Spent Fuel Management, Sellafield Ltd., n.d. http://www.sellafieldsites.com/solution/spent-fuel-management/ (accessed 19.04.14).

Tsoulfanidis, N., 2013. The Nuclear Fuel Cycle. American Nuclear Society, La Grange Park, IL, pp. 242–243.

U.S. Census Bureau, 2013. Statistical Abstracts of the United States. https://www.census.gov/prod/www/statistical_abstract.html (accessed 19.04.14).

U.S. Energy Consumption, 1775-2009. http://www.eia.gov/todayinenergy/detail.cfm?id=10 (accessed 23.04.14).

U.S. Life Expectancy, 1850-2011. http://www.infoplease.com/ipa/A0005140.html (accessed 23.04.14).

U.S. Population, 1810-2010. http://geography.about.com/od/obtainpopulationdata/a/uspop.htm (accessed 23.04.14).

Uranium 2011: Resources, Production and Demand, 2012. A joint report by the OECD Nuclear Energy Agency and the International Atomic Energy Agency OECD, Paris, p. 122.

World Nuclear Association, 2014. World nuclear power reactors and uranium requirements. http://www.world-nuclear.org/info/Facts-and-Figures/World-Nuclear-Power-Reactors-and-Uranium-Requirements/(accessed 19.04.14).

Role of recycling in advanced nuclear fuel cycles

2

Ch. Poinssot[1], *B. Boullis*[2], *S. Bourg*[1]
[1]CEA, Marcoule, France; [2]CEA, Saclay, France

Acronyms

APM	Marcoule pilot plant
COEX	coextraction process
DIAMEX	diamide extraction
EXAm	extraction of americium
FNR	fast neutron reactor
FR	fast reactor
GANEX	grouped actinide extraction
GHG	greenhouse gas
HM	heavy metal
IAE	International Agency for Energy
IAEA	International Atomic Energy Agency
IPCC	International Panel for Climate Change
LWR	light water reactor
MOX	mixed oxide
OECD	Organisation for Economic Cooperation and Development
OTC	once-through cycle
PUREX	plutonium uranium reduction extraction
PWR	pressurized water reactor
SANEX	selective actinide extraction
TBP	tri-*n*-butylphosphate
TTC	twice-through cycle

2.1 Sustainability as a driving force for developing advanced fuel cycles

2.1.1 Sustainability as a key to face the global energy challenge

At the end of October 2011, humankind symbolically went over 7 billion people. Recent projections made under the auspices of the United Nations (UN) anticipate the population to be in the range of 9.6 billion by the year 2050 before reaching 10-12 billion around 2100 and stabilizing (UNO, 2013). Although the population is almost stabilized in the developed areas such as Western Europe and North America, it is still increasing in the developing and emerging countries in Africa and Asia. As human and economic development is clearly related to energy consumption, at least as

Reprocessing and Recycling of Spent Nuclear Fuel. http://dx.doi.org/10.1016/B978-1-78242-212-9.00002-2

long as it stands below a threshold of around 4000 kWh/person (Pasternark, 2000; Figure 2.1), this will clearly lead to a significant increase in total world energy consumption. Every international study performed under the auspices of the UN, the International Agency for Energy (IAE), or the Organisation for Economic Cooperation and Development (OECD) lead to the same conclusions. Although the figures could be slightly different, they all predict primary energy consumption will increase by roughly 50% by 2035, and electricity consumption will increase by 75-90% even in the case of a strong political shift toward the "green economy" (WEO, 2012). Meeting this increasing need is the first part of the energy challenge to be faced in the twenty-first century.

On the other hand, the current and drastic global climate change has now been clearly recognized and at least partially related to human activities (IPCC, 2013). This influence is first of all related to the very large amount of greenhouse gases (GHGs) that have been produced since the start of the industrial revolution in the nineteenth century: the concentration of carbon dioxide (CO_2) increased from 275 ppm to nearly 400 ppm in less than 150 years, whereas it had remained stable over the previous 10,000 years. Similar situations can be described for other GHGs like methane (CH_4) and nitrogen dioxide (NO_2). Simultaneously, the average surface temperature on Earth is estimated to have increased by nearly 1 °C on the same timescale, whereas the sea level has increased by roughly 20 cm. Simulations performed under the auspices of the IPCC and reported in the 2013 report evidenced that this evolution will go on as long as GHG emissions are not decreased. It could lead to a global surface

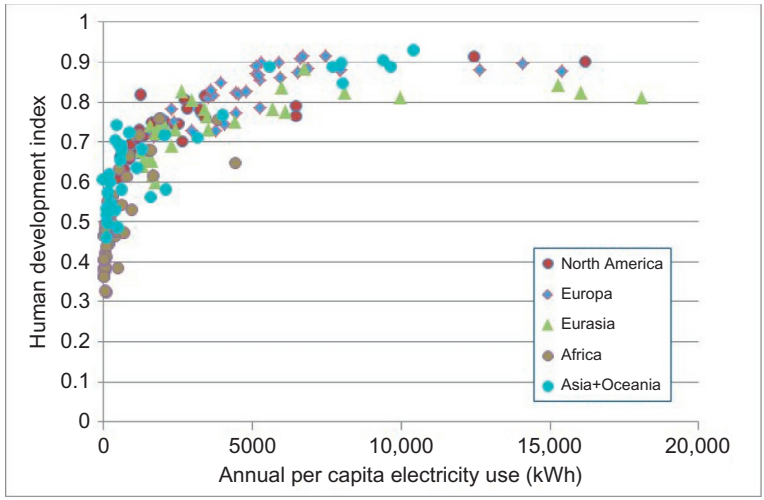

Figure 2.1 The United Nations' Human Development Index and electricity use for 2011. Population and electricity use data are taken for the electricity from the US Energy Information Administration, Independent Statistics & Analysis (http://www.eia.gov/) and Human Development Index from the United Nations Development Program (UNDP—http://hdr.undp.org/).

temperature increase ranging from 2 to 6 °C, depending on the scenario of GHG emissions. Decreasing GHG emissions is today a worldwide issue shared by every country, even though they do not all agree on the path to follow. Looking in detail at the origins of GHG, it quickly comes out that the main sources of emissions are related to energy production. Considering that fossil fuels represent 80% of the current world energy portfolio, it seems quite obvious that we will not be able to meet the requirement of decreasing GHG emissions without changing the global energy model and promoting low-carbon energies. This is far more drastic when considering the anticipated increase of the energy needs depicted previously. Consequently, this energy revolution toward carbon-free energy is anticipated to become a very strong driver in the evolution of the energy model. This corresponds to the second part of the energy challenge to be faced in the twenty-first century.

Therefore, in this early part of the twenty-first century, it is likely that for the first time in history, humankind has to face the global challenge of meeting our tremendous energy need while preserving our environment and promoting sustainable human development. This challenge can only be solved at the world level by addressing simultaneously three main issues: the energy transition toward new energy portfolios, the future of the Earth environment and climate, and the promotion of social and societal stability and equity. This approach is the so-called sustainable development.

Sustainable development was defined in 1987 by the Bruntland commission as development that "meets the needs of the present without compromising the ability of future generations to meet their own needs" (UNO, 1987). Clearly, such development has to be based on three "interdependent and mutually reinforcing pillars," which are economic, social, and environmental fields (see Figure 2.2).

2.1.2 About the meaning of sustainability for an energy source

To meet the requirements of sustainability, an energy source not only has to be relevant in terms of technical efficiency and economics, but also has to preserve the environment, to be widely accepted, and to promote the development of balanced and peaceful relationships within a given society (acceptance), between different

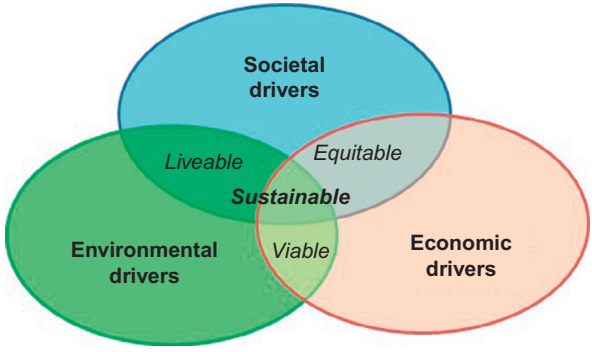

Figure 2.2 The three interdependent and mutually reinforcing pillars of sustainable development.

countries (international relations) and between different generations (intergenerational equity). This can be translated into several technical options.

With regard to the environment, the global environmental footprint of the energy sources has to be reduced as much as possible. Several key objectives have to be addressed:

- First, the GHG emissions have to be low to mitigate the impact of climate change and limit the temperature increase to a reasonable level.
- Second, the environmental footprint that describes the impact on the natural environment has to be as low as possible. This relates in particular to land-use requirements, atmospheric and aquatic pollution, and water withdrawal and consumption.
- Third, the natural resources used to produce the energy have to be preserved for future generations, which means that one should aim to save as much as possible by increasing global efficiency.

These objectives have to be understood in a global approach; that is, estimated by life cycle assessment approaches in order to consider not only instantaneous production but also the whole life cycle, in particular the construction, operation, and end-of-life cleaning and dismantling of the different facilities.

With regard to economics, the energy sources have to globally promote a viable development of the economy, which means an overall stability and predictability of the costs. This is related to several criteria:

- First, the cost of production has to be predictable over a very long time, which means it must be only slightly dependent on external parameters.
- Second, the subsequent energy price obviously has to be achievable in terms of cost of production, but it does not mean that it has to be the lowest possible cost. Indeed, current financial systems do not exhaustively consider the costs of externalities that should be theoretically included within a global assessment (for instance, the subsequent cost of global warming through a CO_2 price).
- Third, the energy portfolio also has to be a factor of international stability to reduce the risk of external perturbations on the economic system. The use of scarce and nondistributed resources should likely be limited.

With regard to social benefits, the energy sources should globally promote human development and the stability of society, which can be related to the following:

- The national energy portfolio should result from a large and consensual choice made by the society; that is, energy sources have to be accepted with their relative benefits and risks.
- The energy sources should not lead to significant risk on human health and societal stability. Hence, residual risk should be objectively assessed and reduced as much as is reasonably achievable.
- The energy sources should promote intra- and intergenerational equity and not be developed for the sole benefit of only part of the society.

These key criteria should be the initial driving forces for selecting the reference energy portfolio of a given country, considering that the solution for each country could be different based on the specific situation, resources, technology maturity level, or public opinion. It also represents the driving forces for improving the different energy

sources in the future. Therefore, it will be used in this chapter to define the relevant evolution of nuclear fuel cycles to improve their *sustainability footprint* on this whole set of criteria.

2.1.3 Role of nuclear energy in the future energy mix

Among the different energy sources, nuclear power already has one of the lowest GHG emissions (in the range of 6-100 g CO_{2eq}/kWh_e, e.g., Dones et al., 2007; Vattenfall, 2010) alongside the renewable energy technologies such as hydropower, solar, and wind energies. Furthermore, nuclear power has demonstrated over the past 30 years its capacity to produce base-load electricity at a relatively low, predictable, and stable cost due to the very low economic dependence on uranium prices. In addition, natural uranium resources are widely distributed on earth, unlike fossil fuels, and its mining is not subjected to high international stresses, as is the case for oil. Nuclear energy is, therefore, thought to have the potential to curtail the dependence on fossil fuels while promoting the energetic independence of the countries involved.

However, its relevance is questioned by public opinion after the Chernobyl and Fukushima accidents, in particular in Western Europe. These events have led people to be more sensitive to the health and environmental risks associated with nuclear energy and to question its relevance for energy production. Subsequently, one can anticipate that future energy systems, particularly nuclear, will only sustain and develop if they succeed in decreasing the residual risk down to a level that is thought to be acceptable by the population and to increase the understanding and acceptance of this energy source by a majority of citizens. This defines the third part of the energetic challenge to face: future energy systems will have to be accepted by the majority of the population.

2.2 Potential improvements of nuclear energy within the environmental field

The environmental footprint has to be understood across a complete set of environmental indicators that depict the influence of the process on the environment, due either to the withdrawal or to the release operations. Apart from GHG emissions, the environmental footprint of nuclear energy is little documented in the scientific literature, which concentrates mostly on the impact of renewable and fossil energies (e.g., Turconi et al., 2013). Life cycle analysis can help to better assess the footprint of nuclear energy. Thanks to a specially designed simulation tool entitled NELCAS, CEA has assessed the overall environmental footprint of the current French nuclear fuel cycle (twice-through cycle or TTC) considering data obtained over all the nuclear fuel cycle facilities and their whole lifetime (Poinssot et al., 2014). This footprint was compared with the footprints calculated for other energy sources. Figures were also derived for the once-through cycle (OTC). In the OTC, the spent uranium oxide (UO_x) fuel is directly considered as a waste for disposal. In opposition, in the TTC, the spent UO_x fuel coming from the first use in the reactor is reprocessed to recover both uranium and plutonium. The uranium is reenriched to be reused as

new UO*x* fuel and the plutonium is used to fabricate mixed uranium/plutonium oxide fuel (mixed oxide, MOX). Spent MOX and reenriched fuels are not reprocessed but stored for future use in fast reactors (FRs).

2.2.1 Optimizing the nuclear fuel cycle to reduce GHG emissions

As already described, nuclear energy is one of the energy forms with the lowest GHG emissions per kWh_e. These GHG emissions are mostly linked to ore mining activities, to the construction of the reactors (concrete penalties), and to the geological repository (Poinssot et al., 2014) (see Figure 2.3). With regard to this criterion, most of the potential benefits from the use of nuclear energy have already been achieved. Further potential improvements are only incremental and should be focused in four directions:

1. Feed the different fuel cycle plants with low GHG electricity (nuclear or renewable) to avoid any detrimental contribution to global GHG emissions, in particular the enrichment plant, which is quite energy intensive.
2. Limiting the extent of the mining and enrichment operations would lead to a substantial reduction in overall GHG emissions, as these operations represent roughly one-third of the total GHG emissions from the nuclear fuel cycle.
3. Optimize transportation and promote the use of efficient transport with low fossil fuel consumption, as this significantly contributes to overall GHG emissions (within mining and disposal operations).
4. Limit the volume of waste to be disposed of in underground repositories to reduce the GHG related to the construction and operation of the site (very close to an underground mine).

Even though such incremental improvements are achievable, they are second-order contributions and do not represent a key issue.

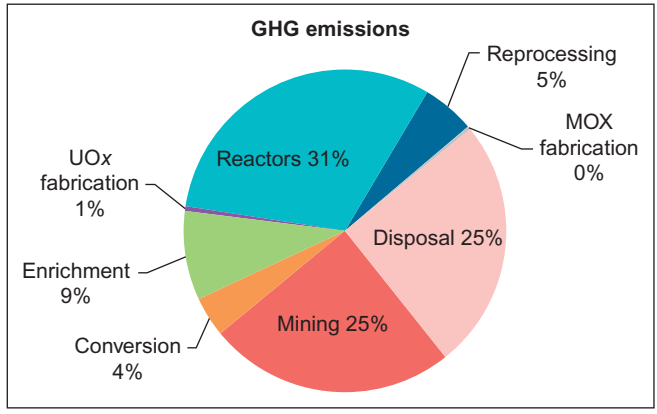

Figure 2.3 Estimates of the GHG emissions distribution over the different steps of the French nuclear fuel cycle based on a LCA approach with the NELCAS tool (Poinssot et al., 2014).

2.2.2 Decreasing the other environmental impacts

A set of environmental indicators are commonly assessed in the literature. They address air and water pollution, as well as their potential impact (acidification, eutrophication, and photochemical ozone), land-use, water withdrawal and consumption, and technological wastes. Three main conclusions come out of this study:

- First, the environmental footprint of nuclear energy is rather low for most of the indicators, as depicted by Figure 2.4, and in the same order of magnitude as the renewable energies.
- Second, for most of the indicators, the main contribution to the environmental footprint comes from the front end of the fuel cycle; that is, the ore mining, milling, and conversion operations (Figure 2.5).
- Third, recycling (TTC) has a beneficial influence on the environmental footprint (see Figure 2.6) as it leads to significant reductions in most of the environmental indicators compared to the OTC. This is due to decreasing the significant contributions from the front-end steps while the recycling operations have only a limited impact on most of the environmental indicators.

From this study, efforts directed toward improving the environmental footprint of the nuclear fuel cycle should lead to addressing these two main issues:

- First, upgrading and optimizing the processes that are used in the front end of the fuel cycle, in particular for separating and purifying the uranium ore. The contribution of these operations to the environmental footprint is significant and any modification in this area will influence the overall picture.
- Second, implementing the recycling of actinides that allows the reduction of the significance of the front end for the same electricity production and is, therefore, beneficial in terms of environmental footprint. It also allows a better conditioning of the ultimate waste and a reduction of the requirement for surface disposal as evidenced by Figure 2.7.

In addition, addressing the significance of the water withdrawal should also be an issue but this is primarily related to the cooling of reactors, which is beyond the scope of this chapter and book.

2.2.3 Preserving natural resources

Preserving the needs of future generations leads directly to addressing the issue of natural resource preservation. After irradiation, spent nuclear fuel that has been burned to produce electricity still contains ~96% of the uranium and plutonium that are potentially valuable materials for electricity production and could, therefore, be worth recycling in order to increase the sustainability of nuclear energy (see Figure 2.8).

For instance, in producing ~80% of its electricity through its nuclear reactor fleet (in the range of 410 TWh_e/year), France actually consumes ~60 ton of uranium (which is either fissioned or transformed to plutonium through neutron capture). A part of the plutonium is subsequently fissioned. However, if no recycling is implemented, such a fuel cycle requires the mining of ~9000 ton of natural uranium and the charging and discharging of ~1100 ton of spent fuel per year (see Figure 2.9) (HCTISN, 2010).

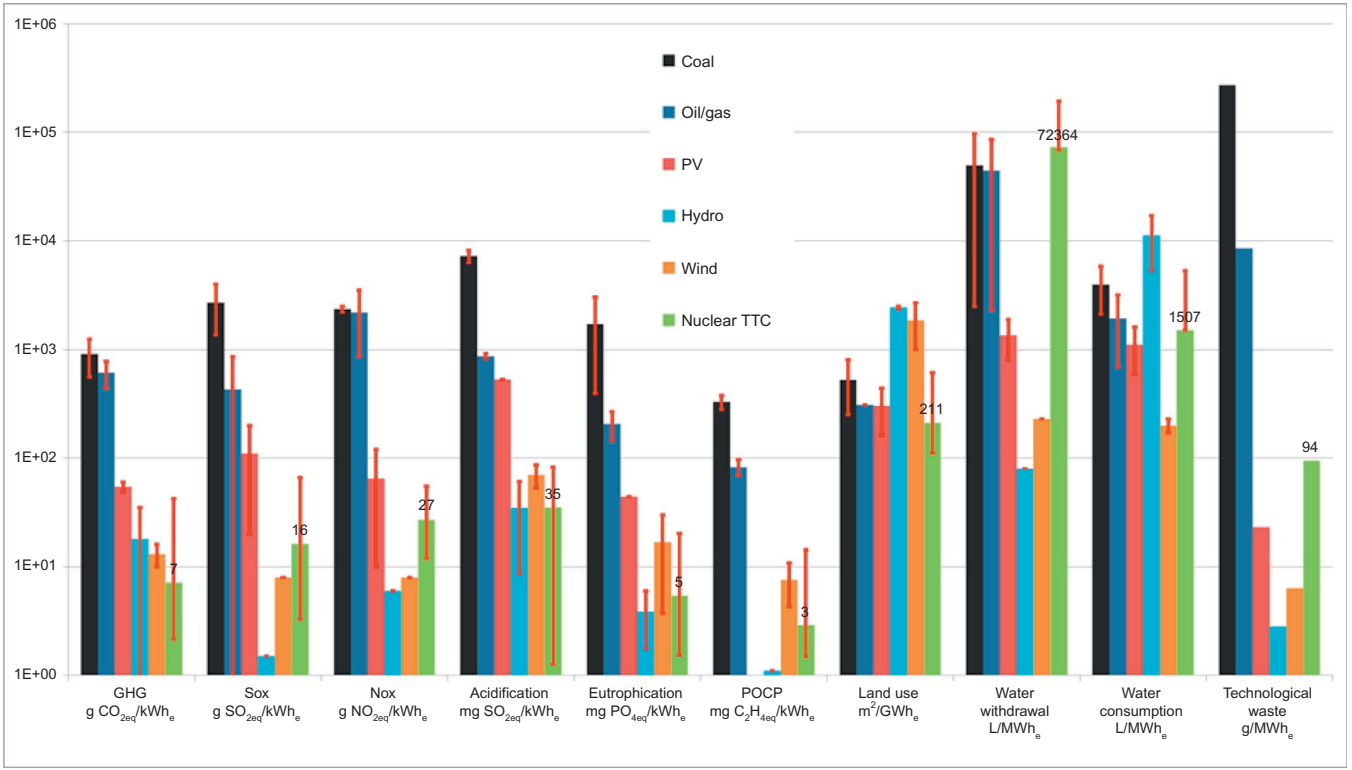

Figure 2.4 Comparison of the environmental footprint indicators for the different forms of energy. Nuclear (green) appears for many of them as a quite beneficial energy source (Poinssot et al., 2014).

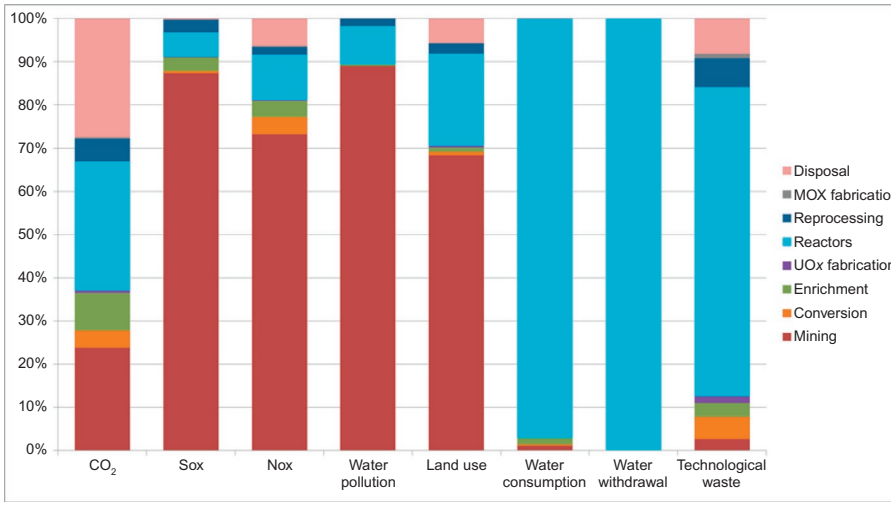

Figure 2.5 Contribution of the different fuel cycle steps on the main environmental footprint indicators. Ore mining and conversion represent for many of them the most important contributors (Poinssot et al., 2014).

This clearly illustrates that the efficiency of such a fuel cycle is relatively low, as only 0.6-0.7% of the resource is used to produce energy. Promoting long-term sustainability will require the improvement of this key indicator in order to preserve the uranium resource.

Since the beginning of the commercial use of nuclear energy, about 290,000 ton of spent fuel have been discharged and with the current development of nuclear energy, an additional 400,000 ton are expected to be generated worldwide between now and 2030 (source: World Nuclear Association). Moreover, one has to bear in mind that only ~30% of the worldwide inventory of discharged spent nuclear fuel has been reprocessed so far (90,000 ton). It means that the larger part has been stored (90% wet storage in pools), waiting for future disposition decisions (reprocessing or geological repository) (Fukuda et al., 2003). The accumulation of such a large amount of stored spent nuclear fuel is, hence, an increasing long-term burden and long-term risk that should be reduced, as evidenced by the problems created by the fuel storage pools on the Fukushima Daiichi site.

Thus, the question arises as to how we can better utilize natural uranium resources. Basically, the logical approach is both to increase the yield of consumption in reactors and to recycle the valuable materials from the spent fuel. Two successive steps can be identified in this direction, increasing in technological complexity:

- *The first and short-term step is to monorecycle uranium and plutonium* in the current reactors, which use thermal neutrons. Uranium and plutonium can easily be recovered from spent nuclear fuel thanks to efficient and economically viable industrial separation processes based on the PUREX process. They can be subsequently used to produce MOX fuels that

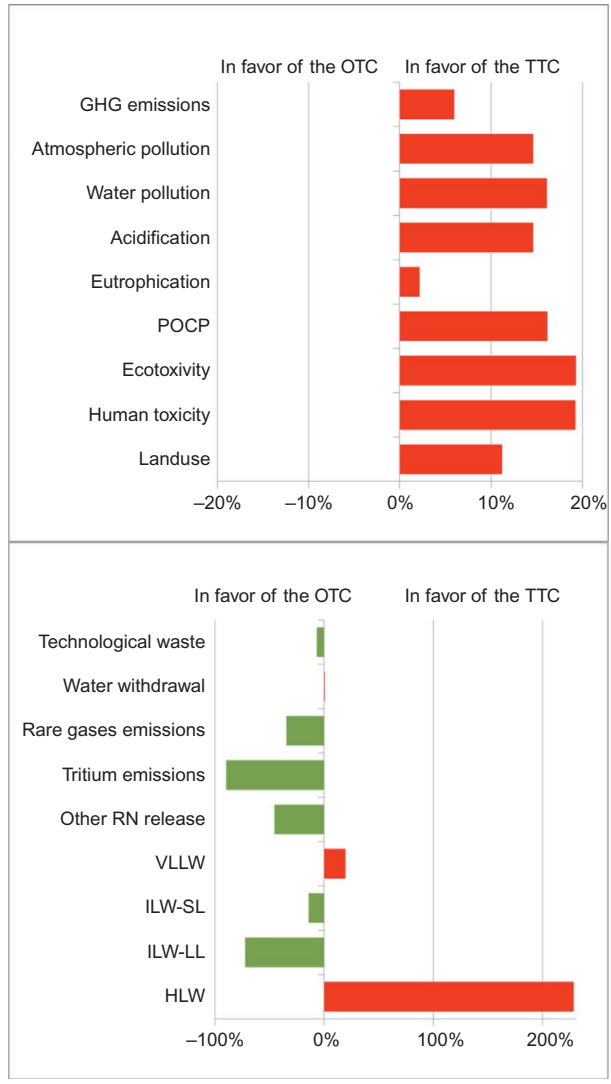

Figure 2.6 Influence of the mono-recycling of plutonium as implemented in France on the environmental footprint. The red bars indicate the % of evolution of the indicators when shifting from the current French TTC towards a hypothetical OTC (Poinssot et al., 2014).

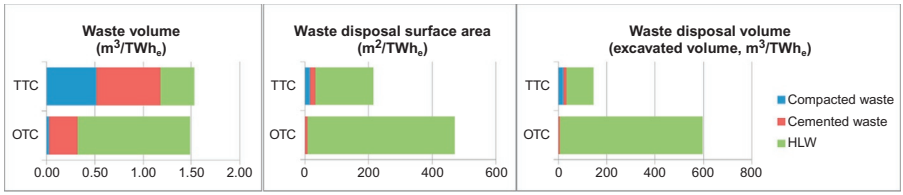

Figure 2.7 Comparison of the waste volume, waste disposal surface area and waste disposal excavated volume for the OTC and TTC. Recycling has a clear beneficial influence regarding the waste disposal surface area and excavated volume (Poinssot et al., 2014).

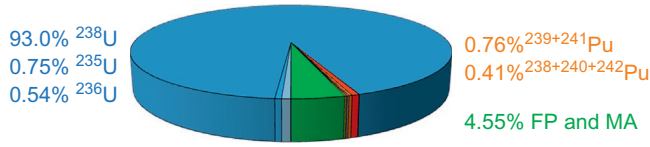

Figure 2.8 Relative composition of a 47.5 GWd/t UO*x* spent nuclear fuel after 4 years irradiation in PWRs. This clearly shows that spent nuclear fuel still contains a large amount of energetic valuable material as uranium and plutonium (Poinssot et al., 2012a,b).

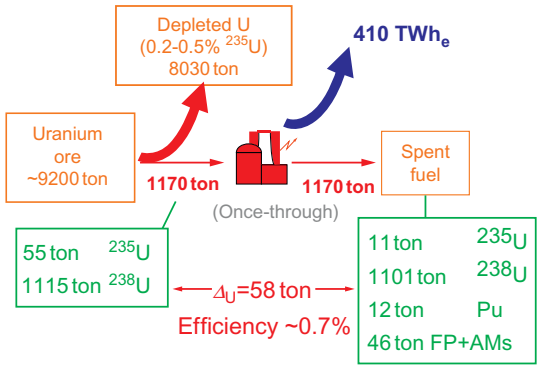

Figure 2.9 Global balance of uranium in a hypothetic once-through fuel cycle producing 410 TWh_e. The figures have been assessed by considering the French situation and assuming that no recycling is implemented. The current fluxes have therefore been corrected from the effect of the Pu and U recycling. The current mono-recycling of Pu and part of the reprocessed U allows saving 17% of the natural uranium resource (Poinssot et al., 2014).

can be used to feed the current reactors. France chose to implement such a strategy more than 20 years ago in the AREVA UP2 and UP3 reprocessing plants at La Hague and in the MELOX recycling plant at Marcoule. More than 26,000 tHM of spent uranium dioxide fuel have been treated, and the corresponding plutonium inventory has been recycled as MOX fuel. Twenty-two French pressurized water reactors (PWRs) are partially fed with this MOX fuel (over 40 reactors worldwide use MOX fuel). Over 6000 MOX fuel assemblies have been produced at MELOX. These treatment and recycling operations are today mature, efficient, safe, clean, and cost-effective technologies. Such a fuel cycle is referred to as the TTC. It already allows a saving of ~17% of natural uranium resources by comparison to an equivalent cycle without recycling (HCTISN, 2010).

- *The second and longer-term step is to multirecycle uranium and plutonium in fast neutron reactors* (*FNRs*). Indeed, plutonium and uranium recycling in thermal reactors is limited by the impossibility of fissioning even mass number plutonium isotopes and the limitation of ^{239}Pu formation from ^{238}U by neutron capture. At higher energy, neutrons are more efficient in fertilizing uranium by transforming ^{238}U to ^{239}Pu and favoring the fission of all the plutonium isotopes, subsequently reducing the amount of trans-plutonium minor-actinides, which are by-products produced by neutron capture on plutonium. For example, the ratio of fission to capture cross sections of ^{238}Pu, ^{240}Pu, and ^{242}Pu are, respectively, increased in fast neutron spectra by factors of 22, 250, and 36 in comparison to thermal spectra. FNRs are, therefore, able to efficiently consume natural uranium, with a yield anticipated to be higher than 80%, although it is around 0.7% in thermal reactors; that is, two orders of magnitude higher efficiency. Therefore, enriched uranium is not required and FNR can be fed with depleted uranium, the stockpile of which is very significant due to the tailings of former

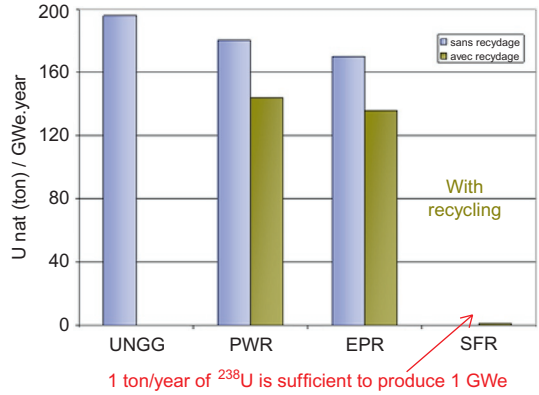

Figure 2.10 Evolution of the mass of uranium needed to produce 1 GWe annually for the natural uranium gas cooled reactor (UNGG—first generation), the classical pressurized water reactor (PWR—second generation), the European pressurized reactor (EPR—third generation) and the sodium fast reactor (SFR—fourth generation).

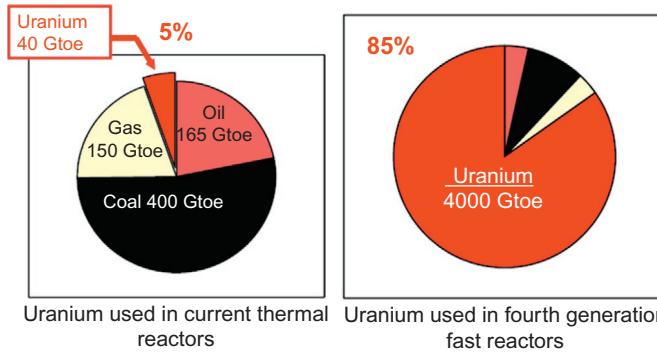

Figure 2.11 Comparison of the relative energy which can globally be produced by fossil and nuclear resource when considering (left) only the current thermal reactors and (right) the future fourth generation FRs. It clearly depicts the very significant amplification introduced by the FNRs (Boullis, 2011).

enrichment operations (about 250,000 ton in France, ANDRA, 2012). With regards to the fuel cycle, the main steps are rather similar to the TTC, except that it strongly decreases the need for additional natural uranium resources. The front end of the fuel cycle is, hence, going to be reduced proportionally. Ultimately, in a whole FR fleet, no additional mining and enrichment activities are required, and electricity can be produced from the existing depleted uranium and plutonium stockpiles for several thousands of years. Figure 2.10 presents the evolution of the amount of uranium that is needed to produce 1 GWe annually by various reactor types. It clearly illustrates the dramatic improvement brought about by the introduction of FRs in comparison with the current LWR fleet, even when considering the positive effect of plutonium monorecycling.

Recycling the actinides is, therefore, a key solution to improve the preservation of natural resources for future generations. It significantly improves the sustainability of nuclear energy and it can very strongly change the overall energy potential of the different energy resources worldwide as evidenced by Figure 2.11.

In this framework, the TTC can also be considered as a learning step for preparing for the fourth-generation reactors, regarding fuel cycle and recycling operations, and as a way to save 17% of natural uranium resources by comparison to the OTC without any recycling.

As a conclusion, nuclear energy already has a beneficial influence on the environment by comparison to other energies. In order to improve its environmental sustainability, actinide recycling has to be developed, first for the current thermal reactors with so-called monorecycling in the TTC and second in FNRs to improve the efficiency of the uranium resource consumption and to ultimately avoid the need of any additional mining of uranium ore.

2.3 Potential improvements within the societal field

Regular opinion polls have shown that a significant part of the public is reluctant with regard to the development of nuclear energy; the precise figure depending on each country (Foratom, 2012). More interesting, the main arguments against nuclear energy are as follows:

- Nuclear energy presents risks for health and the environment that are not acceptable.
- Nuclear energy can lead to the diversion of nuclear material and their use for military applications.
- Nuclear energy produces radioactive waste, the lifetime of which is so long that the practical meaning is not easily understandable for most of the people. Furthermore, no solution is thought to exist for such waste, meaning that radioactive wastes would last and could pollute almost forever.

From time to time, the opposition to nuclear energy is more or less significant depending on current events, but it has to be addressed as it can be a source of potential social instability. In fact, selecting a given source of energy production in a modern democracy cannot be imposed by a central government without considering the will of the population, as otherwise it could lead to the public strongly contesting decisions.

2.3.1 Increasing nuclear safety to limit the residual risk

The succession of events following the world's fifth largest earthquake (Tōhoku earthquake, Japan, March 2011) led to the Fukushima crisis reminding everyone that nuclear safety is never totally achievable and has to be continuously checked and improved. The existence of an independent and highly skilled safety authority (and technical experts) that regularly inspects any facilities partly answers the safety requirements. The existence of regular, objective, and exhaustive safety reassessment is also another path in the direction of a reinforced safety regime and allows assurance that any facility meets the most recent safety regulations and criteria. All these approaches are generic and relate more to the way society regulates and surveys nuclear activities than to technical issues.

With regard to processes more specifically involved all along the fuel cycle, future improvements should enhance the focus on safety and could be related to the following:

- The replacement of chemicals that can present risks of reactivity or are toxic for the environment or people. For instance, redox reactants are often highly reactive. Processes without any redox reactions could be more environmentally friendly.
- The simplification of separation processes to ease their industrial implementation and, in particular, limit the risk of malfunctions due to human error.
- The development of powerful and robust online monitoring techniques to ensure that the process is efficiently run without any bias.

These developments are generic directions and can lead to the optimization of the various chemical processes used all along the fuel cycle. They have to be accounted for while developing the processes for the different fuel cycle options.

2.3.2 Limiting proliferation risk: Toward the comanagement of uranium and plutonium

Recycling has long been thought to be a proliferation route for countries willing to develop nuclear weapons. Although it appears nowadays much easier to get fissile material from enrichment (as evidenced by recent developments in Iran for instance), resistance of the recycling processes toward proliferation is already ensured and could be further improved in two directions:

- Through international controls under the auspices of the IAEA; this allows the authorities to get a very precise image of the fissile material fluxes in the plants and ensures that no material has been diverted. It relies on highly accurate analytical techniques (online monitoring and remote video control). IAEA on-site labs are, hence, located at the recycling plants, as for instance the IAEA on-site lab at Rokkasho-Mura. Although very efficient techniques are already available, much room is still available for further improvements in online monitoring and analytical techniques.
- Through adaptation of the current recycling processes in order to avoid the existence of any separated plutonium flux all along the recycling plant. In particular, new processes that allow the comanagement of uranium and plutonium (such as the COEX^{TM}-type process for instance, Baron 2007) have been developed and are the new reference for any new recycling plant to be constructed.

2.3.3 Increasing public acceptability by decreasing the waste lifetime to a few centuries

A long-standing public misunderstanding still exists with regard to nuclear waste. They are thought to be a long-term burden for future generations without any practical solutions. Therefore, they are seen as one of the strongest drawbacks of nuclear energy when gauging public opinion. Several societal studies have been performed to understand in more detail the reason for such perceptions (for instance, D'Iribarne, 2005). They evidenced that people are worried both by underground disposal and the risk of

contaminating the "Earth-mother," and the lifetime of the waste, which is beyond human historical time frames and, therefore, approaches eternity. Quite surprisingly, chemical industry waste is much less feared, whereas the risk does not decay with time, perhaps because time is not mentioned?

In order to overcome this misleading situation, a very significant improvement could be brought about by the implementation of minor actinide recycling and transmutation. Indeed, minor actinides are demonstrated to be the main contributor to both long-term radiotoxicity of the ultimate waste after plutonium, which is anticipated to be already recycled in the advanced fuel cycle based on FNR, and long-term waste thermal power, which directly defines the repository surface area and volume.

Recycling and transmuting minor actinides would, hence, allow:

- Optimizing and saving the scarce repository resource by increasing the waste density. A gain of up to a factor of 6 of the surface repository area could thus be reached (Poinssot et al., 2012a,b).
- Decreasing the long-term radiotoxicity. In particular, minor actinides recycling would allow decreasing the waste lifetime to about 300 years instead of some tens of thousands or even hundreds of thousands of years, as evidenced by Figure 2.12.

This means that nuclear waste can be brought back within the timescales of human history, which should have a very positive influence on general public opinion and acceptance of nuclear energy and radioactive waste disposal. Technically, such an evolution requires two major improvements by comparison to the current situation:

- FNRs are needed to transmute the minor actinides, but this evolution is already mandatory to meet the need for preserving the uranium resource, as described above.
- Dedicated and efficient separation processes are needed to recover the minor actinides, either in a dedicated flux (so-called heterogeneous recycling) or grouped with the other actinides (so-called homogeneous recycling).

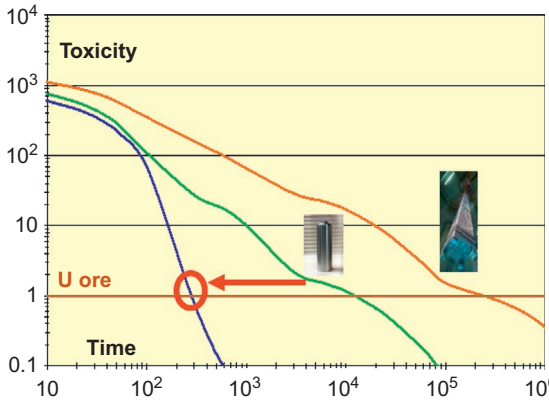

Figure 2.12 Evolution of the ultimate waste long-term toxicity as a function of time for three different types of fuel cycles: (orange) the OTC in which spent nuclear fuel is the ultimate waste, (green) the TTC in which spent nuclear fuel is once reprocessed once only, and (blue) the closed fuel cycle including the minor actinides recycling. This figure demonstrates that waste toxicity will be back to the initial uranium ore toxicity within 300 years only with the recycle of minor actinides (Poinssot et al., 2012a,b).

Both options have been studied, in particular in France and in European programs. They are described in detail in later chapters in this book.

2.4 Potential improvement with regard to fuel cycle economics

Nuclear fuel cycle activities are frequently questioned regarding their relative cost and impact on electricity cost. Various national assessments realized in France demonstrated that the cost of the recycling operations is a very limited part of the total cost of electricity, as evidenced by Figure 2.13.

Despite this limited overcost, nuclear electricity is demonstrated to be one of the cheapest sources of electricity, in the range of 40-50 €/MWh (Energie 2050 report, 2012). However, this very attractive feature does not account for the externalities that are currently not included in the economic models. In particular, the GHG penalty (the so-called CO_2 tax) will likely increase the relative cost of fossil fuels by comparison to renewable and nuclear energies.

Within this context, the improvement for the future should focus on the way to ease the inclusion of nuclear energy systems within economic models, which relates to three main directions:

- First, the costs of nuclear energy systems have to be stable and, therefore, predictable, which is a prerequisite to allow them to be accounted for by the economic system. Most of this statement relates to the investment cost, which represents roughly two-thirds of total electricity cost. This means that systems and processes have to be both robust enough not to be

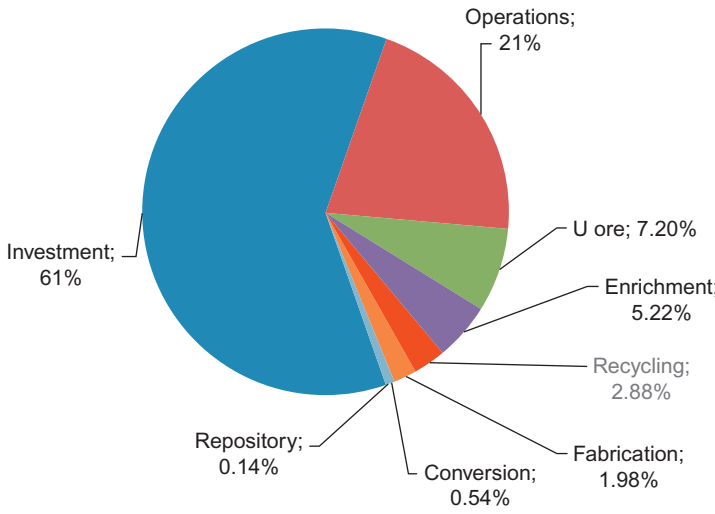

Figure 2.13 Relative contribution of the different contributions to the final cost of electricity in the French system. Treatment/recycling only represents 2.9% of the cost of electricity.

influenced by evolution in regulations, and flexible enough to accommodate these regulatory evolutions.
- Second, reduce the cost to the lowest level reasonably achievable. It means that simplification of the processes and facilities should be looked at to limit the cost, without compromising overall safety and efficiency.
- Third, investment should be eased by proposing a financial system that helps the industrial organizations cope with such huge investments. It is, hence, a financial and regulatory question rather than a technical one.

As for safety, improving economics is, therefore, mainly a general framework that has to be accounted for during the development of new processes rather than a driver for shifting toward any new types of fuel cycle.

2.5 Roadmap toward a sustainable advanced fuel cycle

The previous sections of this chapter describe where the environmental, societal, and economic drivers may lead nuclear fuel cycles. The aim of this final section is to synthesize the overall roadmap for future fuel cycles, which globally comes out as presented in Figure 2.14.

2.5.1 The twice-through cycle

The TTC requires implementation of separation and recycling processes for uranium and plutonium. It is a clear and efficient preliminary step toward a better use of the uranium natural resource: it already allows France to save 17% of uranium ore, which yearly represents 1100 ton saved. Such a fuel cycle requires dissolving the spent nuclear fuel to access the nuclear materials, and designing and running a very effective extraction process to partition the valuable elements, uranium and plutonium, from the ultimate waste, mainly fission products and minor actinides. The separation is

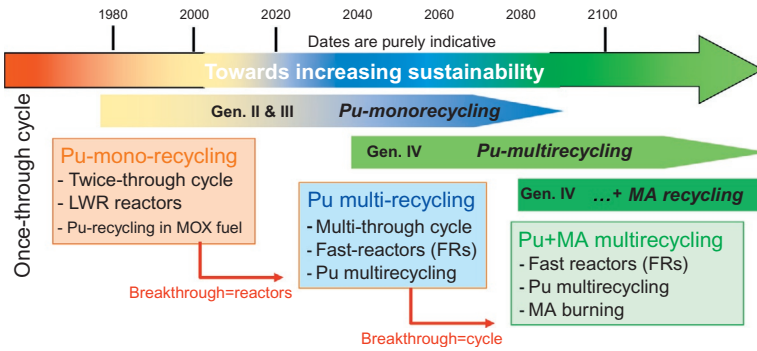

Figure 2.14 Roadmap of anticipated future fuel cycle in view of increasing the global sustainability of nuclear energy systems (Poinssot and Boullis, 2012).

currently performed by the PUREX process thanks to the selective extracting properties of the tri-butylphosphate (TBP) molecule. It is operated in countercurrent devices such as pulsed columns or mixer-settlers in order to allow a very efficient separation. For instance, in the La Hague plants, both recovery yields and purification levels are very high (in excess of 99.9% of uranium and plutonium recovered with decontamination factors of about 10^6 or more). A final conversion step allows the production of oxide powders thanks to the precipitation of intermediate oxalates. These powders are compatible with the specification of the fuel fabrication process (Figure 2.15).

Such a fuel cycle also allows the efficient conditioning of the ultimate waste (minor actinides and long-lived fission products) in a dedicated waste form, which has been tailored to ensure an optimized long-term confinement; that is, borosilicate nuclear glass. This matrix has been demonstrated to keep its confinement properties for more than 500,000 years in the geological repository environment. This fuel cycle also prevents any presence of plutonium in the ultimate waste.

This type of fuel cycle has been already implemented in several countries, including France, Russia, the United Kingdom, Japan, and, in the near-future, China. It is a mandatory step for paving the way to the fourth-generation fuel cycles where the recycling of actinides is mandatory.

2.5.2 Multirecycling of uranium and plutonium

In terms of the fuel cycle, the feasibility of multirecycling of uranium and plutonium has already been proven. The treatment of FR MOX fuels and the subsequent plutonium multirecycling have been demonstrated at the industrial scale in France; 27 ton of spent FR MOX fuel have been reprocessed in the APM (Marcoule pilot plant) and UP2-400 plants (La Hague) during the 1980s and 1990s. While further development is needed to refine the processing of MOX and FR fuels, there are no outstanding technological barriers.

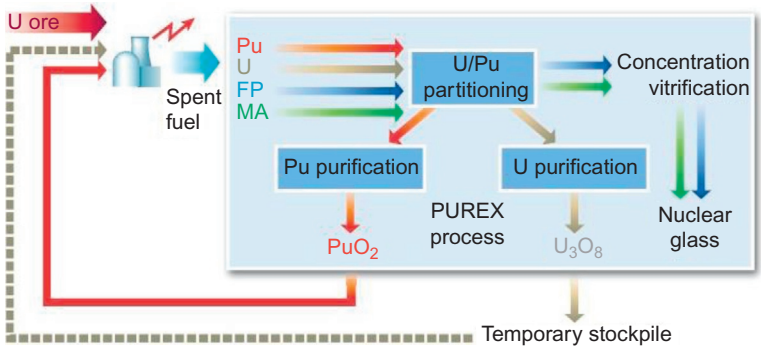

Figure 2.15 Schematic of the twice-through fuel cycle which is a preliminary step towards the fourth generation fuel cycle and allows saving 17% of uranium resource (Poinssot and Boullis, 2012).

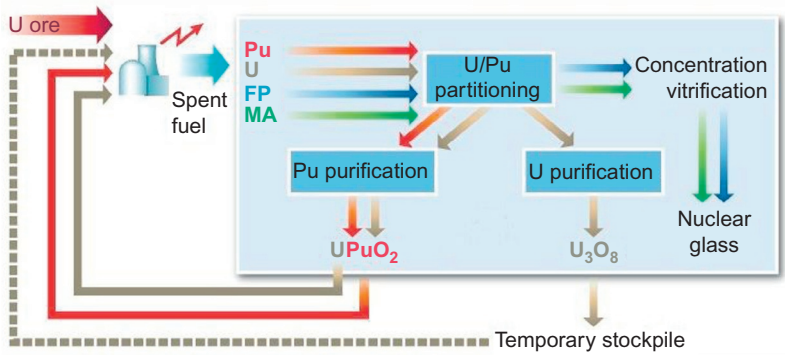

Figure 2.16 Schematic of the fuel-cycle for the future fuel cycles in which plutonium could be multi-recycled thanks to the use of FRs (Poinssot and Boullis, 2012).

For the separation processes, the same process as in the previous step can be implemented, PUREX or a modified COEX^{TM}-type process can be used as illustrated by Figure 2.16.

2.5.3 Multirecycling of the minor actinides

Minor actinide recycling has been widely studied in France since 1991 within the framework of two successive waste management Acts of the French Parliament and also in Europe in dedicated European projects (EUROPART, ACSEPT, and SACSESS projects, Bourg et al., 2013). Relevant processes have been developed and proven to be efficient at the lab-scale on real spent nuclear fuel solutions. Two main options are under consideration: either the homogeneous recycling of minor actinides in the whole reactor core at low concentrations or the heterogeneous recycling of minor actinides in dedicated targets or blanket at higher concentrations. It has to be mentioned that neptunium recycling is easily achievable through a simple modification of the PUREX process and is, therefore, not a key scientific issue.

2.5.3.1 Recycling of americium alone

As far as minor actinide recycling is considered, the French reference route is today the recycling of americium alone. A specific process, EXAm, has been developed to selectively recover americium from a PUREX raffinate, allowing its homogeneous or heterogeneous recycling (Rostaing et al., 2012). Alternative processes are under development in the field of European projects (Bourg and Geist, 2013) (Figure 2.17).

2.5.3.2 Multirecycling of all minor actinides

Ultimately, curium could also be recycled as is americium. It requires specific separation processes to recover it either in a dedicated flux (DIAMEX/SANEX processes on a PUREX raffinate) or in a global actinides flux (GANEX processes on spent fuel

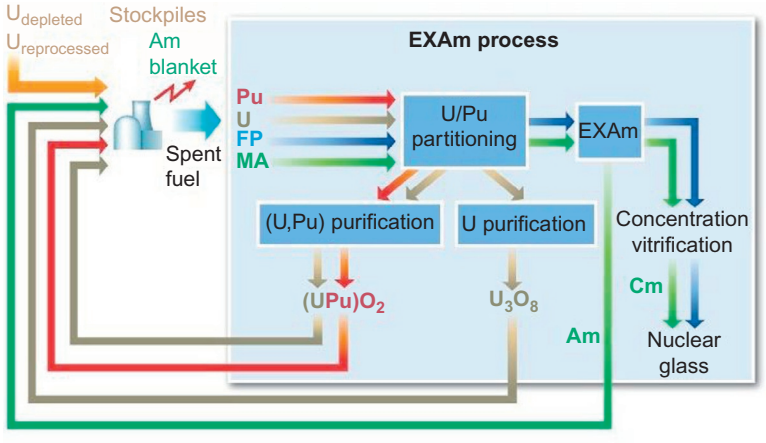

Figure 2.17 Schematic of a future fuel cycle which would allow the recycling of (i) U and Pu for improving the efficiency of the uranium ore consumption and (ii) Am for decreasing the lifetime and heat output of the ultimate waste (Poinssot and Boullis, 2012).

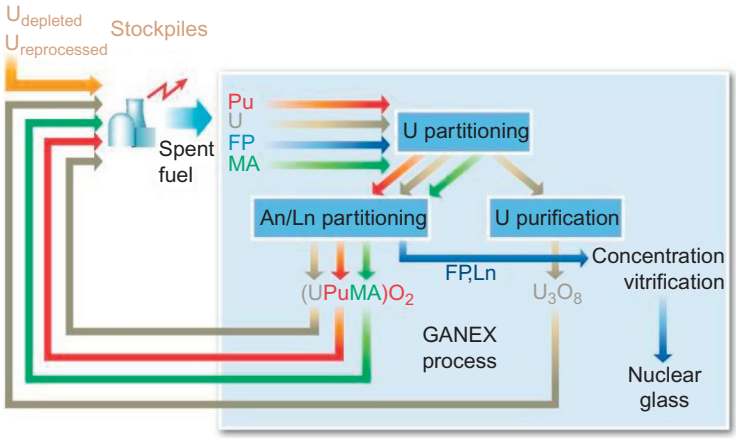

Figure 2.18 Schematic of a future fuel cycle in which both U, Pu and minor actinides would be recycled together thanks to a dedicated GANEX separation process (Poinssot et al., 2012a,b).

dissolution liquor) for the respective heterogeneous or homogeneous recycling (Miguirditchian et al., 2009; Bell et al., 2012) (Figure 2.18).

It may lead to an additional improvement of the residual radiotoxicity of the ultimate waste and, therefore, may improve the societal acceptance of nuclear energy. However, it requires handling curium all along the fuel cycle, which is a very demanding challenge due to the toxicity, heat power, and neutron emissions of curium. The associated cost would likely be higher and would have to be related to the potential societal benefit.

2.6 Conclusions

Actinide recycling is a key operation for future nuclear fuel cycles as (i) it is a mandatory step for the FNR-based fuel cycle, (ii) it is a prerequisite for improving the sustainability of any nuclear energy systems as addressed above, and (iii) it is a very efficient way to decrease the proliferation risk by decreasing the need for uranium enrichment, which is the most achievable proliferation route nowadays. Although the TTC is implemented in a limited number of countries, recycling is expected to expand in the next decades and the first steps will be the commercial start-up of the Rokkasho-Mura plant in Japan and the current preparation phase for the building of a new reprocessing plant in China (letter of intent AREVA/CNNC, 25 April 2013). Development of recycling processes is then anticipated to develop along a stepwise approach:

- Implementation of *plutonium monorecycling*, which allows for the development and the acquisition of the know-how about the treatment, recycling, and waste conditioning processes and buys time before multirecycling can be implemented.
- Implementation of *plutonium multirecycling*, which basically requires a shift toward FNRs but also the adaptation of the recycling processes to these new types of fuels.
- Implementation, if it is politically decided, of an additional and optional step that would allow the *recycling of the minor actinides* to decrease the toxicity and the thermal power of the ultimate waste. The first step would be the recycling of americium alone.

Recycling should progressively become the reference option for future sustainable fuel cycles. In this context, it is obvious that the recycling processes will have to evolve along three main objectives:

- To *adapt* to the future fuel cycles. This includes, in particular, the need for developing separation processes that are optimized for recycling MOX fuels coming either from LWR or FNR, which both present much higher plutonium content and a different microstructure. It also considers the need for adapting the waste conditioning processes to future waste composition.
- To *simplify* the processes in order to decrease the cost, reduce the operational risks and increase safety. For instance, reducing the number of required separation steps, and subsequently the number of workshops, would be a significant improvement in this direction.
- To *improve* the efficiency and robustness of the processes. This is a prerequisite for treating fuels with much higher plutonium content or for separating minor actinides that are difficult to handle. In particular, it should help to reduce the residual human error risk, which is a key asset for social acceptability.

As a conclusion, recycling is a cornerstone of any sustainable nuclear energy system and, therefore, a key asset for contributing toward mitigating global climate change while meeting global energy needs.

References

ANDRA, 2012. Inventaire national des matières et déchets radioactifs 2012: catalogue descriptif des familles. rajouter la référence complète, ANDRA report, reference DCOM-12-0120. downloadable on the www.andra.fr.

Baron, P., 2007. Process for reprocessing a spent nuclear fuel and of preparing a mixed uranium-plutonium oxide. Word Patent WO2007135178 A1.

Bell, K., et al., 2012. Progress towards the development of a new GANEX process. Procedia Chem. 7, 392.
Boullis, B., 2011. Future nuclear fuel cycles: toward sustainability, a French vision. In: Global 2011, Makuhari, Japan.
Bourg, S., Geist, A., 2013. SACSESS, a new FP7 EURATOM collaborative project on the safety of actinide separation processes. In: Global 2013, Salt Lake City, USA.
Bourg, S., et al., 2013. Overview of the main achievements of the FP7 EURATOM collaborative project ACSEPT. In: International Conference on Fast Reactors and Related Fuel Cycles: Safe Technologies and Sustainable Scenarios (FR13), Paris.
D'Iribarne, 2005. Les Français et les déchets nucléaires. La Documentation Française.
Dones, R., Bauer, C., Bollinger, R., Faist Emmenegger, M., Frischknecht, R., 2007. Life cycle inventory of energy systems in Switzerland and other UCTE countries. Data V2.0, Ecoinvent report no 5. PSI, Villigen.
FORATOM, 2012. What people really think about nuclear energy, January 2012.
Fukuda, K., Danker, W., Lee, J.S., Bonne, A., Crijns, M.J., 2003. IAEA overview of global spent fuel storage (IAEA-CN-102/60), 9 pp.
Haut Comité pour la Transparence et l'Information sur la Sûreté Nucléaire, HCTISN, report from the 12th July 2010. Avis sur la transparence et la gestion des matières et des déchets nucléaires produits aux différents stades du cycle du combustible, 57 pp.
IPCC, 2013. International Panel on Climate Change, Climate change 2013: the physical science basis, working group I contribution to the IPCC fifth assessment report (AR5), September 2013.
Miguirditchian, M., Roussel, H., Chareyre, L., Baron, P., 2009. GLOBAL 2009. American Nuclear Society, Paris.
Pasternark, A.D., 2000. Global energy futures and human development: a framework for analysis. US DOE, Lawrence Livermore National Laboratory, UCRL-ID-140773.
Poinssot, C., Boullis, B., 2012. Actinide recycling within closed fuel cycles. Nucl. Eng. Int. January 2012, 17–21.
Poinssot, C., Rostaing, C., Grandjean, S., Boullis, B., 2012a. Recycling the actinides, the cornerstone of any sustainable nuclear fuel cycles. Procedia Chem. 7, 349–357.
Poinssot, C., et al., 2012b. Main results of the French program on partitioning and transmutation of minor actinides. In: MRS Proceedings, vol. 1475.
Poinssot, C., Bourg, S., Ouvrier, N., Combernoux, N., Rostaing, C., Vargas-Gonzales, M., Bruno, J., 2014. Assessment of the environmental fooprint of nuclear energy systems. Comparison between close and open fuel cycles. Energy 69, 199–211.
Rostaing, C., Poinssot, C., Warin, D., Baron, P., Lorrain, B., 2012. Development and validation of the EXAm separation process for single Am recycling. Procedia Chem. 7, 367.
Turconi, R., Boldrin, A., Astrup, T., 2013. Life cycle assessment (LCA) of electricity generation technologies: overview, comparability and limitations. Renew. Sust. Energ. Rev. 28, 555–565.
United Nations, 1987. Report of the World Commission on Environment and Development. General Assembly Resolution 42/187, 11 December 1987. Retrieved: 12.04.07.
United Nations, 2013. World population prospects: the 2012 revision, highlights and advance tables, Department of Economic and Social Affairs, Population Division. Working paper no. ESA/P/WP.228.
Vattenfall, 2010. Nuclear Power certified Environmental Product Declaration EPD® of electricity from Forsmark Nuclear Power Plant. Sweden 2010. Energie 2050 report, 2012.
WEO, 2012. World Energy Outlook 2012. International Energy Agency, OECD, Paris, ISBN 978-92-64-18084-0.

Key challenges in advanced reprocessing of spent nuclear fuels

3

Jean-Paul Glatz, P. Souček, R. Malmbeck
European Commission, Karlsruhe, Germany

3.1 Rationale

To follow the sustainability goal of so-called Generation IV (GENIV) new reactor systems (http://www.gen-4.org/PDFs/GenIVRoadmap.pdf), the industrial reprocessing technologies in operation today have to be extended to include a full recycling of all actinides. The ongoing disputes worldwide on how to manage existing nuclear waste and delayed policy decisions lead to steadily increasing inventories of spent nuclear fuel, estimated at 250,000–300,000 ton worldwide. Ambitious new nuclear programs under development, especially in Asian countries, will drastically enhance this burden on future generations. Natural and societal analogs seem to indicate that nuclear waste can be safely stored in a geological repository for up to a few hundred thousand years; that is, the time when the radiotoxicity is reduced to a level typical for natural uranium mines. The European PAGIS study carried out in the late 1980s could demonstrate that even for the worst-case scenarios, the impact on the environment does not increase above that due to natural radiation (Cadelli et al., 1988). Nevertheless, for reasons including ethical and public acceptance issues, some favor a solution where the radiotoxicity impact can be reduced within a comprehensible period of time; that is, from a few hundred up to a few thousand years.

On the other hand, in recent years, the principle of intergenerational justice becomes more and more important in the context of climate change, where future generations will be adversely affected by our continued dependency on fossil fuels; this is obviously at least to some extent also applicable to nuclear power. It seems that the moral obligation to minimize any burden to future generations applies here also. Therefore, putting into practice this approach means that the reprocessing technologies already deployed for uranium and plutonium recycling have to be extended, and all options to recycle the long-lived waste constituents need to be thoroughly investigated. This can be achieved with a so-called partitioning and transmutation (P&T) scenario. Minor actinides (MAs) play a central role in this context and their recycling implies more complex, remote fuel cycle operations including fabrication, irradiation, and transport.

The industrial reprocessing flow sheets in operation today were initially developed to produce weapons grade plutonium. The separation efficiency and product qualification requirements defined by the operators of the reprocessing facilities were and still are very high. It seems that for sustainable new generation reactor systems a

Reprocessing and Recycling of Spent Nuclear Fuel. http://dx.doi.org/10.1016/B978-1-78242-212-9.00003-4

change from what could be named in this case a "clean fuel-dirty waste" concept to a "dirty fuel-clean waste" concept would be advantageous. Ultimately, recycling without separation of highly pure products but rather aiming at high recovery rates would fulfill these requirements and also improve fuel cycle economics.

According to the development objectives, the above-described P&T strategy should be inherent to the reactor systems under investigation in GENIV. To develop and implement clean waste technologies, a global actinide management strategy should be deployed. For this purpose, advanced fuel cycle processes involving a grouped recycling of all actinides and ultimate waste forms with a minimal content in actinides (<0.1%) are required.

3.2 Advanced actinide management options

Advanced actinide management, incorporating MA P&T, can be based on a heterogeneous or a homogeneous recycling concept.

3.2.1 Heterogeneous actinide recycling

The heterogeneous recycling option aims to recover the MAs americium and curium in a dedicated stream, separate from the recovery of major actinides uranium and plutonium, and recycle them in specific targets with a relatively high MA content (up to 20%), which are then irradiated preferentially in the periphery of the reactor core. In this case, individual treatment of actinides in the recycling process is being considered.

Today, concepts are already under investigation to include neptunium separation in a modified PUREX process. To achieve a complete extraction, a careful control of the Np(V)-(VI) redox reactions is required and recovery rates >99% are possible (Taylor et al., 2013).

Due to the high radioactivity of curium and specifically the arising neutron dose, a separation of americium from curium would make fuel fabrication much easier, in the sense that only americium would be recycled and curium would be left in storage for decay. However the separation of the two elements is extremely difficult because of their very similar chemical behavior. Column chromatography, displacement chromatography, and extraction using solvents with small differences in distribution coefficients between the two elements with an increased number of extraction stages in the extraction equipment are proposed solutions to achieve the goal. In 2010, a hot demonstration of the French ExAm process obtained a 99% recovery of americium (Montuir et al., 2012).

Another group of separation processes is based on an oxidation of americium to a higher oxidation state IV or VI. In the French SESAME process (Chartier et al., 1998), the americium is electrochemically oxidized to the IV or VI oxidation state, stabilized using a heteropolyanion, for instance, as a tungstosilicate or tungstophosphate complex, and then easily extracted by TBP. Recently, a new flow sheet concept has been

developed at INL (Mincher et al., 2012). In this case, a successful demonstration on the bench-scale resulted in 96% americium recovery with a few percent of remaining curium and the lanthanides in the separated product.

Major difficulties of these processes are the stability of Am(IV) or Am(VI) species and their respective complexes, which have to be guaranteed under irradiation, the generation of secondary solid wastes (heteropolyanions), and difficulties in developing a multistage process.

3.2.2 Homogeneous actinide recycling

The homogeneous recycling involves a grouped recycling of all actinides in a single stream, and irradiation at low concentration (up to 2%) of MAs in the whole fuel core.

In this case, a grouped actinide treatment, where all unnecessary separation and cleaning is avoided, can be pursued. At the same time, the process steps involved can be minimized and a general "simplicity" principle of nuclear operations can be applied in terms of improving proliferation resistance, investment, and operating costs. A first step in this direction is the French COEX process developed by AREVA and CEA as an evolution of the PUREX process. In this flow sheet, no uranium-plutonium separation is made, and both elements are coextracted and coprecipitated to produce a solid solution of (U, Pu)O_2, which can directly be used for MOX fabrication. An irradiation of coprecipitated fuel material (the COPIX program) took place in PHENIX during its last years of operation (Drain et al., 2008).

In the meantime, preliminary experiments are being done to include neptunium in the COEX concept; the fuel product would thus be (U, Pu, Np)O_2. It was then logical to go a step further and to develop a process where a grouped treatment of all actinides is envisioned. This is the case for the GANEX (Group ActiNide EXtraction) process,

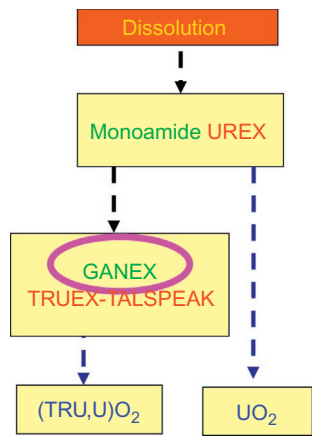

Figure 3.1 General scheme of the GANEX process.

first tested by CEA in the ATALANTE facility in Marcoule. A general scheme of the GANEX process is shown in Figure 3.1.

The GANEX concept foresees a first separation of uranium using a monoamide, to adjust the U/TRU ratio and to improve the hydrodynamics of the TRU extraction in the second extraction cycle before the coextraction and later the coconversion for fuel refabrication. Successful first laboratory-scale demonstrations using genuine irradiated fuel were carried out recently by CEA in the ATALANTE laboratory (Miguirditchian et al., 2009) for light water reactor (LWR) type fuel and by ITU in the framework of the European ACSEPT program for fast reactor (FR) type fuel (Brown et al., 2012).

Major issues to be solved in deploying a GANEX concept include the following:

- The possibility to extract actinides at oxidation states varying between III and VI.
- Capability to process fuels with plutonium contents ranging between 1 wt% (LWR) and 20 wt% (FR).
- Development of robust separation flow sheets, which can be operated using centrifugal contactors; that is, fast kinetics are mandatory.
- Avoiding plutonium precipitation (hydrolysis, oxalic acid).
- Use of CHON type molecules and avoid salt additions to minimize waste volumes.

3.2.3 Homogeneous actinide recycling using dry reprocessing

A similar concept can be applied to pyroreprocessing; here the metallic fuel alloy is anodically dissolved in a LiCl-KCl eutectic and the actinides are collected together onto aluminum cathodes as alloys, leaving lanthanides and other fission products in the salt phase. It is very likely that large-scale pyroprocessing by molten salt electrorefining will be operated as a batch process similar to the industrial aluminum fabrication process (Edwards et al., 1930). Simulating large-scale nuclear fuel processes, an experiment of 25 successive runs in the same salt bath was carried out at ITU to demonstrate the feasibility of a grouped actinide recovery, similar to GANEX but in this case only in one step, without U bulk separation. A total amount of more than 5 g of U61Pu22Zr10Am2Ln5 fuel was treated in this experiment and various process parameters were studied. The recovery rate of actinides was difficult to evaluate because new fuel was added in each run. Nevertheless, it was possible to determine a stable recovery rate better than 99.9%.

3.3 Advanced reprocessing options

Some of the other advanced reprocessing options under development can be characterized as fuel treatment processes within the headend of the recycle plant, specifically:

- the fluoride volatility process developed at Řež in the Czech Republic (Uhlir, 2000), where in a fluorinator the fuel particles are burned in fluorine gas to form uranium hexafluoride or
- the DUPIC process (direct use of pressurized water reactor spent fuel in CANDU), developed at KAERI in Korea to reuse LWR fuel in CANDU reactors (Yang et al., 2006).

The real core processes to achieve the separation of long-lived radionuclides can essentially be classified into two categories: hydrochemical (wet) and pyrochemical (dry). Both have advantages and disadvantages and should be applied in a complementary way. If a so-called double strata concept (as proposed for example in the OMEGA project) would be adapted, the well-established industrial reprocessing of commercial LWR fuel with recycling of uranium and plutonium based on PUREX extraction should be logically combined in this first stratum with an advanced aqueous partitioning scheme also based on liquid-liquid extraction to separate the long-lived radionuclides. In the second stratum, new generation reactors systems should preferably be combined with pyroreprocessing because most of the fuels under investigation for advanced reactor systems are more soluble in molten salts; additionally, shorter fuel cycles are possible due to a higher radiation resistance and a higher proliferation resistance is achievable due to reduced product purity.

Therefore, the decision on the partitioning process to be applied should depend on the boundary conditions, such as the type of fuel material to be treated, the maximum cooling time required, the possibility of combining irradiation and reprocessing in an integrated unit, and so on.

3.4 Lanthanides/actinides separation

In any case, whatever separation approach is selected, an efficient and selective recovery of the key elements from the spent nuclear waste is absolutely essential for a successful, sustainable fuel cycle concept. This necessitates that americium and curium can be selectively separated from lanthanide fission products—apart from the above-mentioned Am/Cm separation, certainly the most difficult and challenging task in advanced reprocessing of used nuclear fuel, due to the very similar chemical behavior of trivalent elements. There are three major reasons for separating actinides from lanthanides:

- Neutron poisoning: lanthanides (especially Sm, Gd, Eu) have very high neutron capture cross sections; for example, >250,000 barn for Gd-157.
- Material burden: in used LWR fuels, for instance, the lanthanide content is up to 50 times that of Am/Cm.
- Segregation: during fuel fabrication, lanthanides tend to form separate phases, which grow under thermal treatment; americium and curium would also concentrate in these phases.

3.4.1 Aqueous route

In the case of extraction, apart from the already described GANEX process, there are three alternative configurations of the selective actinide extraction (SANEX) process under investigation in Europe: the regular r-SANEX, the innovative i-SANEX, and the one-cycle 1c-SANEX variant. The bis-triazinyl pyridine (BTP) family of molecules, which was found in the late 1990s to have excellent selectivity toward trivalent actinide extraction (Kolarik et al., 1999), plays a central role in these developments.

Apart from the selectivity, another great advantage of this molecule is the ability to extract actinides directly from high acid solutions (e.g., ~2 M HNO_3). Variants of the molecule were developed to increase its stability against radiolysis and hydrolysis. Unfortunately, the extraction of metal ions by these derivates with larger alkyl chains is often slower and their solubility in organic diluents is reduced. The solubility issue can be addressed using a water soluble BTP molecule and thus exploit its selectivity in the back-extraction part of the process. Regarding kinetics, the modeling support provided, for instance, by the PAREX code (Sorel et al., 2011) is essential to optimize the flow sheet and adapt it to the extraction system used (centrifugal contactors, mixer-settlers, columns). Intensive research and development is still ongoing in the simulation and modeling area to search for the best compromise and an optimized MA extraction system.

3.4.2 Dry route

From the potential options proposed for dry core processes, selective precipitations do not appear to reach sufficient decontamination factors. It seems likely that only processes based on electrorefining or on liquid-liquid reductive extraction between a molten salt and a liquid metal are able to achieve the necessary separation efficiency between lanthanides and actinides.

Regarding electrorefining, the key parameter is the electrodeposition potential. Figure 3.2 summarizes the electrodeposition potentials of the major lanthanides and actinides for different types of electrodes.

Reactive electrodes, that is, electrodes alloying with the deposited material, have lower potentials and solid electrodes show a larger potential difference between lanthanides and actinides; therefore, reactive solid cathodes (in the present case aluminum) are the best choice for an electrode material. Considering a full process scheme (e.g., Figure 3.3), it might be useful to also investigate alternatives to aluminum used in the present case. Other reactive cathode materials such as copper, nickel, molybdenum, or others might be even better suited to such a scheme.

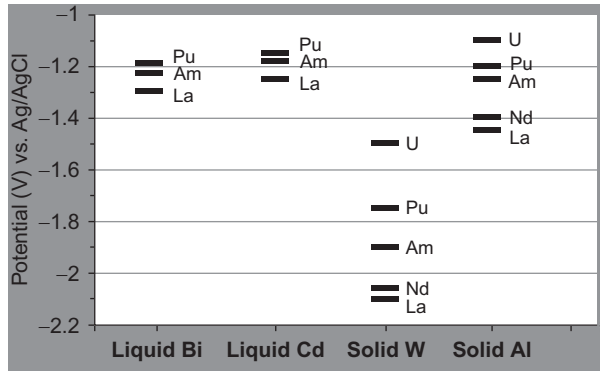

Figure 3.2 Reduction potentials of some actinides and lanthanides on different cathodic materials.

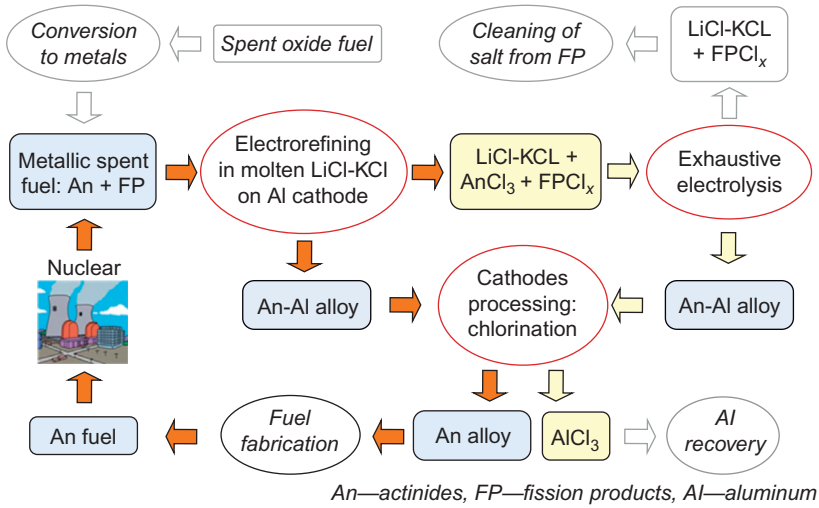

Figure 3.3 Process scheme for the electrorefining of metallic fuels using solid Al electrodes.

To close the fuel cycle, a recovery of deposited actinides (i.e., a separation from the electrode) is required. In the case of aluminum, chlorination is under investigation to separate and return the actinides to the fuel fabrication. A headend conversion of oxide fuels into metals has also been studied, and very promising results were obtained. A more or less complete reduction could be demonstrated for different fuel materials (both irradiated and un-irradiated) such as LWR UO_2 and MOX but also FR MOX. More data, especially on the fission product behavior, are required to have more reliable information for a realistic implementation. At the back end of the pyroprocess is the salt cleaning, allowing in the best case an efficient recycling back into the process and the conditioning of the remaining waste are still being studied. To avoid significant losses of actinides to the waste, an exhaustive actinide separation is needed at the end of operation of the salt bath (saturation in fission products), before consigning it for waste treatment.

Similar front- and back-end issues need to be solved in the French process developed at Marcoule, where the core process is a molten salt/liquid metal (LiF-AlF_3/Al-Cu) extraction. The potential of this technique for separating the actinides from the lanthanides has been demonstrated (Conocar et al., 2005). The fact that the process medium is a molten fluoride salt, should make it directly applicable to the reprocessing of fluoride-based fuel used in the molten salt reactor (MSR), one of the six GENIV systems. In the frame of the European SACSESS program (http://www.sacsess.eu/), electrorefining in molten fluoride is studied as an alternative to liquid-liquid extraction.

A common challenge for the dry reprocessing options is the selection of appropriate materials for construction of equipment; that is, materials that are able to withstand

over longer times the high temperature conditions in combination with very high radiation doses. Material improvements are needed in order to lessen the formation of dross and increase material recovery and throughput. Last but not least, appropriate safeguarding schemes have to be put in place for the different scenarios. Existing proven technology from the PUREX process could serve as the starting point for safeguards development for pyroprocessing.

3.5 Basic studies

3.5.1 Aqueous systems

Developing an extended extraction scheme for actinide recovery requires a good understanding of the processes involved, mainly the selectivity of the extractants, their stability and behavior in a strong radiation field, and interface phenomena (third-phase formation, red oil, etc.)

3.5.1.1 Understand extraction selectivity

To explain the great affinity of actinides for nitrogen-bearing molecules, numerous fundamental studies were carried out using a wide range of experimental methods and spectroscopic techniques. Lanthanide/actinide separations often depend upon a slightly stronger interaction of the trivalent actinides (compared to trivalent lanthanides) with ligands containing soft donor bases (sulfur, chloride, or nitrogen), or with amine extractants in contact with aqueous solutions containing high concentrations of chloride or thiocyanate. The formula, stability, and structure of the complexes containing Ln(III) and An(III) ions were determined both in aqueous solution and in various solvent media. It has been demonstrated that bonds between the nitrogen atoms of these ligands and Ln(III) and An(III) ions include some definite covalence, particularly visible in the fact that enthalpy is the driving force behind reactions. The covalence observed in bonds with the electron-donor nitrogen atoms of ligands seems higher for An(III) ions than for Ln(III) ions, which could be an indication of the greater affinity of these ligands for An(III). However, the difference is too small to really explain sometimes very large differences in the distribution factor. For BTP molecules, the affinity for An(III) ions can be more than a hundred times higher than for Ln(III) ions. Thus, more work will be needed to give a conclusive answer to this key question.

Additional support comes from theoretical studies in the fields of quantum chemistry and molecular mechanics, which have already provided greater insight into certain crucial aspects of reactions between the metal ions to be extracted and nitrogen-bearing ligands (Drew et al., 1998). In particular, the synergetic extraction mechanism of Ln(III) ions using a mixture of nitrogen-bearing ligand and carboxylic acid has been identified by computer calculations (Denecke et al., 2005). The calculated synergetic complex seems consistent with the experimental result. Better coordinated efforts between simulation and experiment could possibly contribute to a better understanding of extraction mechanisms (Drew et al., 2001).

3.5.1.2 Radiolytic and chemical stability

The radiolytic and chemical stability of extracting molecules as well as diluents is essential for the development of actinide separation processes. Several molecules suitable for process development were studied with respect to their stability versus radiation and nitric acid. The experience gained shows that most of these molecules have sufficient stability in nitric acid with the radiolytic stability being a much more critical issue.

Qualitative and quantitative characterizations of degradation fragments of the major extractants used in the SANEX process have been made. The influence of the integrated dose, dose rate, polarity of the diluents, pretreatment (particularly the influence of nitric acid), the structure, and the metal coordination were studied (Fermvik et al., 2009a; Fermvik et al., 2009b). A comparison of alpha and gamma irradiation must take into account that if actinides are extracted they are complexed and, thus, in direct contact with the extracting molecule (Magnusson et al., 2009).

These efforts should be pursued to achieve a knowledge level, where degradation mechanisms are sufficiently understood, to design molecules with increased stability that are of practicable use in industrial implementation.

3.5.1.3 Modeling of extraction systems

Molecular modeling developed at the ICSM Marcoule, mainly at the intermediate scales using a "coarse-graining" approach, allows determination of the thermodynamic properties in organic and aqueous phases of liquid-liquid extraction processes. The results show that the free energy related to ion transfer between phases (i.e., the extraction free energy), is different from the complexation free energy (van Hoof et al., 2011; Jairo Molina et al., 2011). This difference is the key to the selectivity of the separation process. It is expected that calculations validated by comparison with experimental results will lead to a global vision of the extraction processes; this route should be extensively explored.

3.5.2 Dry systems

Compared to aqueous techniques, the molten salt or dry techniques are far less developed. Also basic data, especially in the case of molten fluorides, are missing. Such data are mandatory to establish efficient process schemes. Similar to the aqueous route, modeling and simulation tools are being constantly improved and will become more and more relevant.

3.5.2.1 Basic data of actinides in molten salts

As the results in Figure 3.2 have shown, a precise knowledge of basic data is essential to select the most appropriate parameters for an efficient separation scheme. A large number of data were measured in recent years, essentially in molten chloride media. At ITU, comprehensive studies of actinides (uranium, plutonium, neptunium,

americium, curium), lanthanides, and some other important fission products were carried out involving thermochemical properties, derived from the electrochemical measurements and from basic thermodynamic data; for instance, in the case of neptunium (Masset et al., 2005).

In comparison to molten chloride salts, studies in molten fluorides are much less developed. Even if a substantial program of separation experiments was carried out in various salt mixtures, it is difficult to get relevant thermodynamic data, partly because reliable reference electrodes are not available.

3.5.2.2 *Modelling of molten salt systems*

As in the aqueous case, also for molten salt systems, the combination of spectroscopic techniques with molecular dynamics simulations seems to be a very promising approach to better understand and optimize separation schemes (Salanne et al., 2009). In contrast to experiments, fluorine media dominate the modeling efforts; for instance, to establish relationships between composition, structural order, entropy, and transport properties of multicomponent systems. Molecular dynamics simulations have enabled the calculation of self-diffusion coefficients of fluorine LiF-KF mixtures (Sarou-Kanian et al., 2009).

3.6 Scale-up

To bring the processes described above to industrial maturity, existing reprocessing technology as installed today in France (at La Hague), the United Kingdom (Sellafield), Russia (Mayak), Japan (Rokkasho), and four smaller plants in India with a total capacity of 5630 ton/year, gives a clear advantage to the aqueous route. For economic reasons as well as minimizing waste arising, one goal for an industrial advanced reprocessing plant should be to reuse the extractant as much as possible after solvent cleaning, in a similar fashion to the PUREX process.

An application of the alternative actinide management strategies proposed to achieve a sufficient radiotoxicity reduction at a technological scale represents a real challenge. Recovery rates should be on the order of 99.9% at large scale, which is difficult to reach as the neptunium example in PUREX shows (see paragraph 2.1, Taylor et al., 2013).

Over the last decades, significant progress in process optimization together with reducing losses and release to waste streams has been made. Back in 2005, the CEA carried out an intermediate-scale demonstration of the technical feasibility of the DIAMEX-SANEX process for americium and curium selective extraction (Pradel, 2006). The liquid-liquid extraction experiments were carried out with ~15 kg of irradiated nuclear fuel and showed the efficiency of the process for neptunium, americium, and curium with recovery rates higher than 99%. Today, research efforts are focused on concept optimization, increasing further the compactness of operations, simplifying, and developing variant routes.

In pyroreprocessing, large-scale experience has been gained over several decades in RIAR (Dimitrovgrad, Russia) and the Idaho National Laboratory. As regards P&T, the U.S. experience is more relevant because it is based on a metallic fuel cycle, where an extension to MA recycling can easily be implemented in contrast to the Russian process based on oxides, where the only option is precipitation of MA, which is not very selective.

Since 2009, in Japan, CRIEPI in collaboration with JAEA has carried out engineering-scale pyroprocessing tests (Koyama et al., 2012). Using the results of the study, the feasibility and costs of the pyroprocessing fuel cycle technology at a 40 tHM/year throughput was evaluated using a technology readiness level approach.

Also in Korea, KAERI has recently started large-scale demonstrations of pyroreprocessing in the integrated inactive demonstration facility (PRIDE) (Lee et al., 2011). The purpose of PRIDE is to test the process with respect to performance, remote operation of equipment, integration of unit processes, scale-up, process monitoring, argon environment system operation, and safeguards-related activities. All the above-mentioned efforts should be pursued in a well-coordinated manner to demonstrate the feasibility of pyroreprocessing at industrial scale.

3.7 Waste treatment

Following the example to date made with the PUREX process, further efforts have to be made to minimize waste arising from all the various advanced reprocessing schemes. For the aqueous schemes CHON-type solvents, having the highest possible chemical and radiation stability such that their recycling into the process is possible with minimum losses, should be used. The efficiency of the P&T concept defines the conditioning that will be required for the final waste form.

Regarding pyroprocesses, the fact that far less experience exists for the process itself also applies to the waste treatment. Whereas extensive expertise was developed over several decades for the final waste vitrification in the case of PUREX, several options are still under investigation for used molten salt or metallic phase conditioning at the back end of the pyroprocesses. Sodalites, zeolites, chloroapatite, and chlorospodiosite and their long-term stabilities also under final disposal conditions are under investigation.

Common to both options, the concepts should involve simple processes, with a minimum number of steps, such that secondary waste volumes are kept as low as possible.

3.8 The multidisciplinary aspect

P&T strategies rely on multidisciplinary concepts. The example of the METAPHIX experiment (Rondinella et al., 2009), carried out in collaboration between CRIEPI and ITU (see Figure 3.4), demonstrates the multidisciplinary character of such an

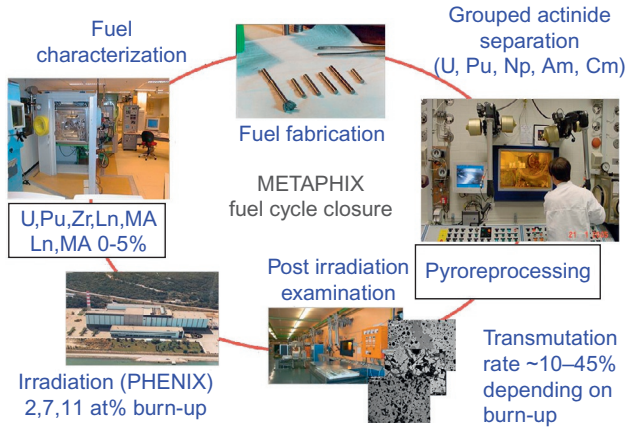

Figure 3.4 Closing the METAPHIX metallic fuel cycle (demonstration of MA recycling in a fast neutron spectrum).

undertaking. It involves fuel fabrication, material characterization for qualification purposes, irradiation (in the present case using the French PHENIX reactor), postirradiation examination to determine the transmutation rate and, of course, reprocessing, just to name the key disciplines. This example shows how important it is to have close links and efficient communications and interactions between the disciplines to achieve the best possible results.

References

Brown, J., McLachlan, F., Sarsfield, M., Taylor, R., Modolo, G., Wilden, A., 2012. Plutonium loading of prospective Grouped Actinide Extraction (GANEX) solvent systems based on diglycolamide extractants. Solvent Extr. Ion Exch. 30 (2), 127–141.

Cadelli, N., Cottone, G., Orlowski, S., Bertozzi, G., Girardi, F., Saltelli, A., 1988. PAGIS: performance assessment of geological isolation systems for radioactive waste. EUR report 11775 EN.

Chartier, D., Donnet, L., Adnet, J.M., 1998. Electrochemical oxidation of Am(III) with Lacunary heteropolyanions and silver nitrate. Radiochim. Acta 83, 129–134.

Conocar, O., Douyere, N., Lacquement, J., 2005. Extraction behavior of actinides and lanthanides in a molten fluoride/liquid aluminum system. J. Nucl. Mater. 344 (1–3), 136–141.

Denecke, M.A., Rossberg, A., Panak, P.J., Weigle, M., Schimmelpfennig, B., Geist, A., 2005. Characterization and comparison of Cm(III) and Eu(III) complexed with 2,6-di(5,6-dipropyl-1,2,4-triazin-3-yl)pyridine using EXAFS, TRFLS, and quantum-chemical methods. Inorg. Chem. 44, 8418–8425.

Drain, F., Emin, J.L., Vinoche, R., Baron, P., 2008. COEX process: crossbreeding between innovation and industrial experience. In: Proceedings from Waste Management 2008, Tucson, AZ, USA.

Drew, M., Hudson, M.J., Iveson, P.B., Russell, M.L., Madic, C., 1998. Theoretical and experimental structural studies of the extraction of actinides and lanthanides by tridentate

nitrogen ligands containing 1,2,4-triazines or 1,2,4-triazoles. In: Proceedings of the Fifth OECD/NEA Information Exchange Meeting on Actinide and Fission Product Partitioning and Transmutation, SCK-CEN, Mol, Belgium, 25-27 November 1998, pp. 487–489.

Drew, M.G., Guillaneux, D., Hudson, M.J., Iveson, P.B., Russell, M.L., Madic, C., 2001. Lanthanide(III) complexes of a highly efficient actinide(III) extracting agent—1,6-bis (5,6-dipropyl-1,2,4-triazin-3-yl)pyridine. Inorg. Chem. Commun. 4, 12–15.

Edwards, J.D., Frary, F.C., Jeffries, Z., all of ALCOA, 1930. The Aluminum Industry. I. Aluminum and its Production. McGraw-Hill, New York.

Fermvik, A., Ekberg, C., Englund, S., Foreman, M.R.S.J., Modolo, G., Retegan, T., Skarnemark, G., 2009a. Influence of dose rate on the radiolytic stability of a BTPB solvent for actinide(III)/lanthanide(III) separation. Radiochim. Acta 97 (6), 319–324.

Fermvik, A., Berthon, L., Ekberg, C., Englund, S., Retegana, T., Zorz, N., 2009b. Radiolysis of solvents containing C5-BTBP: identification of degradation products and their dependence on absorbed dose and dose rate. Dalton Trans. 38, 6421–6430.

Jairo Molina, J., Duvail, M., Dufrêche, J.-F., Guilbaud, P., 2011. Atomistic description of binary lanthanoid salt solutions: a coarse-graining approach. J. Phys. Chem. B 115 (15), 4329–4340.

Kolarik, Z., Müllich, U., Gassner, F., 1999. Selective extraction of Am(III) over Eu(III) by 2,6-ditriazolyl and 2.6-ditriazinylpyridines. Solvent Extr. Ion Exch. 17 (1), 23.

Koyama, T., Sakamura, M.I., Kato, T., Murakami, T., Glatz, J.-P., 2012. Development of pyro-processing fuel cycle technology for closing actinide cycle. Procedia Chem. 7, 772–778.

Lee, H., Hur, J.-M., Kim, J.-G., Ahn, D.-H., Cho, Y.-Z., Paek, S.-W., 2011. Korean pyrochemical process R&D activities. Energy Procedia 7, 391–395.

Magnusson, D., Christiansen, B., Malmbeck, R., Glatz, J.-P., 2009. Investigation of the radiolytic stability of a Cy-Me4BTBP based SANEX solvent. Radiochim. Acta 97 (9), 497–502.

Masset, P., et al., 2005. Thermochemical properties of lanthanides (Ln = La, Nd) and actinides (An = U, Np, Pu, Am) in the molten LiCl-KCl eutectic. J. Nucl. Mater. 344, 173–179.

Miguirditchian, M., Sorel, C., Camès, B., Bisel, I., Baron, P., Espinoux, D., Calor, J.-N., Viallesoubranne, C., Lorrain, B., Masson, M., 2009. HA demonstration in the Atalante facility of the GANEX 1st cycle for the selective extraction of uranium from HLW. In: Proceeding of the GLOBAL 2009, Paris, France, 6-11 September.

Mincher, B.J., Martin, L.R., Schmitt, N.C., 2012. Diamylamylphophonate solvent extraction of Am(VI) from nuclear fuel raffinate simulant solution. Solvent Extr. Ion Exch. 30, 445.

Montuir, M., et al., 2012. Sensitivity of americium and curium splitting flowsheet and running procedure. Procedia Chem. 7, 275–281.

Pradel, P., 2006. French fuel cycle strategy and partitioning and transmutation programme. In: OECD/NEA Proceedings 9th International Exchange Meeting on Partitioning and Transmutation, Nîmes, France.

Rondinella, V.V., Ohta, H., Papaioannou, D., Ogata, T., Nasyrow, R., Koyama, T., Glatz, J.-P., 2009. Characterization of metallic fuel for the transmutation of minor actinides in fast reactor. Trans. Am. Nucl. Soc. 101, 353–354.

Salanne, M., Simon, C., Groult, H., Lantelme, F., Goto, T., Barhoun, A., 2009. Transport in molten LiF-NaF-ZrF4 mixtures: a combined computational and experimental approach. J. Fluorine Chem. 130, 61–66.

Sarou-Kanian, V., Rollet, A.-L., Salanne, M., Simon, C., Bessadaa, C., Madden, P.A., 2009. Diffusion coefficients and local structure in basic molten fluorides: in situ NMR measurements and molecular dynamics simulations. Phys. Chem. Chem. Phys. 11, 11501–11506.

Sorel, C., Montuir, M., Balaguer, C., Baron, P., Dinh, B., Hérès, X., Pacary, V., Roussel, H., 2011. A powerful tool to model and simulate solvent extraction operations.

In: Proceedings of the 19th International Solvent Extraction Conference ISEC11, 3-7 October, Santiago, Chile.

Taylor, R.J., Gregson, C.R., Carrott, M.J., Mason, C., Sarsfield, M.J., 2013. Progress towards the full recovery of neptunium in an advanced PUREX process. Solvent Extr. Ion Exch. 31 (4), 442–462.

Uhlir, J., 2000. Pyrochemical reprocessing technology and molten salt transmutation reactor systems. In: OECD/NEA Workshop on Pyrochemical Separations, Avignon, France, 14-16 March 2000.

van Hoof, B., Markvoort, A.J., van Santen, R.A., Hilbers, P.A.J., 2011. The CUMULUS coarse graining method: transferable potentials for water and solutes. J. Phys. Chem. B 115 (33), 10001–10012.

Yang, M.S., et al., 2006. The status and prospect of the DUPIC fuel technology. Nucl. Eng. Technol. 38 (4), 359–374.

4 Safety and security issues in the reprocessing and recycling of spent nuclear fuels for advanced fuel cycles

L.G. Williams
Imperial College, London, UK

Acronyms

ALARP	as low as is reasonably practicable
BSL	basic safety level
BSO	basic safety objective
COEX	coextraction (of uranium and plutonium)
DBE	design basis event
DIAMEX-SANEX	diamide extraction-selective actinide extraction
EURATOM	European Atomic Energy Community
eV	electron volt
GANEX	grouped actinide extraction
GSR	general safety requirement (IAEA Standards)
HLW	high-level waste
HMNII	Her Majesty's Nuclear Installations Inspectorate
HSE	Health and Safety Executive
IAEA	International Atomic Energy Agency
ILW	intermediate-level waste
LLW	low-level waste
MAs	minor actinides
MeV	million electron volts
MOX	mixed oxide (fuel)
NIAct	Nuclear Installations Act
NISR	Nuclear Industries Security Regulations
NMAS	Nuclear Materials Accountancy System
NORMS	National Objectives, Requirements, and Model Standards
ONR	Office of Nuclear Regulation
P&T	partitioning and transmutation
PCmSC	precommissioning safety case
PCSC	preconstruction safety case
PDSC	predecommissioning safety case

Reprocessing and Recycling of Spent Nuclear Fuel. http://dx.doi.org/10.1016/B978-1-78242-212-9.00004-6

POSC	preoperational safety case
PSC	preliminary safety case
PSR	periodic safety review
PUREX	plutonium and uranium recovery by extraction
SAPs	safety assessment principles

4.1 Introduction

The safety and security of workers and the public and the protection of the environment from the adverse effects of ionizing radiation are of paramount importance when using nuclear energy. This chapter will explore how society and the environment are protected during the reprocessing and recycling of spent nuclear fuels. However, before getting into the detail of the measures that are taken to ensure that society and the environment are adequately protected, it is worth clarifying what is meant by the terms *nuclear safety, nuclear security, nuclear safeguards,* and *nuclear regulation.*

4.1.1 Nuclear safety

Nuclear safety is basically about protecting people and the environment from human error that can result in plant malfunctions during normal operations or in accidents. The International Atomic Energy Agency (IAEA) (International Atomic Energy Agency, 2007a) defines nuclear safety as

> *The achievement of proper operating conditions, prevention of accidents, or mitigation of accident consequences resulting in protection of workers, the public and the environment from undue radiation hazards.*

Human error can occur during design, construction, commissioning, operation, maintenance, and decommissioning of nuclear facilities, and hence, nuclear safety is an inherent part of all these activities.

4.1.2 Nuclear security

Nuclear security, on the other hand, is about protecting people and the environment from malicious acts by people who intend to steal nuclear materials for illicit purposes such as "dirty bombs," or who wish to sabotage nuclear facilities to cause a release of radioactivity. The IAEA define nuclear security as

> *The prevention and detection of, and response to, theft, sabotage, unauthorized access, illegal transfer or other malicious acts involving nuclear material, other radioactive substances or their associated facilities.*

Again malicious acts can be targeted at all stages from design through to decommissioning and can include cyber attacks.

4.1.3 Nuclear nonproliferation safeguards

Nuclear safeguards are about protecting people and the environment from the illicit development of nuclear weapons. Safeguards activities aim to prevent the proliferation of nuclear weapons from civil nuclear activities including reprocessing and recycling of spent nuclear fuel. As will be discussed later, safeguards measures are a matter of international jurisdiction and are implemented by the IAEA in conjunction with regional organizations such as EURATOM in the case of European Union countries. The IAEA (International Atomic Energy Agency, 2002) defines the technical objective as

> *the timely detection of diversion of significant quantities of nuclear material from peaceful nuclear activities to the manufacture of nuclear weapons or of other nuclear explosive devices or for purposes unknown, and deterrence of such diversion by the risk of early detection*

Safeguards are therefore all those activities that are necessary to account for and control nuclear materials that could potentially be used to produce nuclear weapons. Effective safeguards are important not only to international peace and security, but also to ensure that people and the environment are not exposed to ionizing radiation from the illicit use of a nuclear weapon.

4.1.4 Total protection

As shown schematically in Figure 4.1, workers, the public, and the environment are subject to potential hazards arising from plant malfunctions (nuclear safety), malicious acts (nuclear security), and terrorist attacks using nuclear weapons or other explosive devices, using materials or technologies diverted or stolen from civil

Figure 4.1 The importance of effective nuclear safety, security, and safeguards.

nuclear programs (safeguards). The effective application of nuclear safety, security, and safeguards is, therefore, essential to ensure that society will accept the use of nuclear energy. While national and international law places obligations on the users of nuclear materials, society expects the nuclear industry to be subject to very close scrutiny within a clear and robust regulation. Nuclear regulation is the means by which society can be assured that the users of nuclear energy are complying with their obligations and, hence, ensuring that people are safe, nuclear facilities are secure, and nuclear materials and technologies are not being stolen or diverted for illicit use.

4.2 Understanding the need for regulating the reprocessing and recycling of spent fuel

To understand why nuclear fuel reprocessing and recycling is subject to so much national and international oversight, it is necessary to understand why the use of nuclear energy is seen as being different from the use of other sources of energy. "Nuclear" is different because of public and political perceptions, and the high levels of energy that are locked in the atom that, when released by nuclear fission, presents some unique hazards that need to be managed.

4.2.1 Public and political perceptions

The awesome power of the atomic bomb and the subsequent public fear of radiation-induced cancer made the use of nuclear energy for electricity production a source of public and political concern. The issues surrounding the use of nuclear power are complex but in essence relate to four fundamental features:

- people's dread of cancer;
- the link between cancer and the exposure to ionizing radiations;
- the military roots of nuclear power; and
- national and international governance.

Cancer is such an emotive issue because of the variety of forms it can take, its life-threatening and debilitating effects, and the fact that there is often no cure. Although somewhere between 25% and 30% of the population will die from cancer, the fact that there is a link between cancer and exposure to ionizing radiation has not lessened the public view that the nuclear industry is uniquely dangerous even though the chances of being exposed to ionizing radiation from the activities of the nuclear industry are extremely low. The public seems to accept the risks associated with exposure to natural sources of radioactivity from cosmic rays, radon gas, radiation from rocks, and the natural radiation in their bodies. However, exposure to man-made sources of radiation is seen as more serious and a potential threat that needs to be justified and, whenever possible, minimized. The way the risks in relation to the health and safety of both the workers and the public can be minimized if not eliminated clearly needs to be explained.

Public and political views on nuclear power remain interlocked with the perceived links between the peaceful use of the energy for electricity production and its military roots. It is true that the civil nuclear energy programs in the United Kingdom, the United States, France, and Russia resulted from defense programs; however, throughout the 1960s and 1970s, the civil nuclear energy programs, particularly in the United Kingdom and the United States developed well beyond their military roots. Today, in the case of the United Kingdom and many other countries, nuclear power for electricity production is no longer dependent upon military technologies. This technological separation between the use of nuclear energy for electricity production and its use in nuclear weapons is, however, not recognized by all, and there are some who exploit this fear. Not because they believe nuclear power reactors can explode like nuclear bombs but because the infrastructure needed to sustain a nuclear power program can equally support a nuclear weapons program and lead to the proliferation of nuclear weapons.

The above societal concerns, at both national and international levels, have resulted in intense political interest in the nuclear industry. Given this intensity, politicians and the public require the nuclear industry to be subject to very close scrutiny within a clear and robust governance structure. Governance is provided via a range of international treaties and conventions relating to nuclear safety, nuclear security, nuclear insurance liabilities, and the nonproliferation of nuclear weapons. These treaties and conventions, which will be discussed later, are delivered at the national level through nuclear laws and regulations and nuclear specific regulatory bodies.

4.2.2 Nuclear and radiological hazards

No industrial activity, including the reprocessing and recycling of spent nuclear fuel, is immune from accidents; however, the political, public, and media responses to an accident involving nuclear installations or radioactive materials are usually more intense than for any other type of accident. "Nuclear" is perceived as "different" and, hence, accidents receive closer attention and can lead to calls for the cessation of the use of the technology as seen in the German response to the recent accident at Fukushima. Because of this perceived difference, the public and politicians expect the nuclear industry to go to extraordinary lengths to prevent accidents.

The main nuclear and radiological hazards associated with the reprocessing and recycling of spent fuel come from intense radioactivity of the fission products contained in the irradiated fuel rods, the radiotoxicity of nuclear materials such as plutonium and uranium, and the potential for an unconstrained neutron chain reaction (i.e., a criticality accident) in fissile materials such as uranium 235 and plutonium 239. Fission releases neutrons and intense gamma radiation from the fission products and a great deal of heat. For example, the fission of uranium 235 produces on average 2.42 neutrons. If these neutrons all went on to cause further fissions, in the next "generation" there would be 2.42 fissions (on average), producing 2.42^2 neutrons, which would go on to cause further fissions and the rate (and energy release) would increase exponentially. In fact, not all the neutrons released go on to cause further fissions. The neutron multiplication factor, k, is defined by,

$$k = \frac{\text{number of fissions in one generation}}{\text{number of fissions in preceding generation}}$$

If $k = 1$, the system is said to be critical, and energy is produced at a constant rate. If $k < 1$ (subcritical), the chain reaction would die away rapidly, whereas if $k > 1$ (supercritical), the chain reaction and energy released grow exponentially. Criticality can occur whenever fissile materials are present, depending upon such factors as the mass of material, its geometry or concentration, the presence of materials that can slow down neutrons, and in the case of uranium, the enrichment of the isotope of uranium 235.

The potential for criticality exists in various parts of the fuel cycle, namely enrichment facilities, nuclear fuel fabrication facilities that use enriched uranium or plutonium, spent fuel ponds because spent fuel contains residual levels of uranium 235 and plutonium, nuclear fuel reprocessing plants where uranium and plutonium are separated, and in fissile material stores.

The energy density stored in these fissile materials is so great that the fission of a single atom of a fissile material such as uranium 235 is about 2 million times greater than breaking the carbon-hydrogen bond in the combustion of coal, oil, or wood. The fission products that result from the breakup of the nucleus are neutron rich and so decay by the emission of β particles. The excess of neutrons in the fission products has both advantages and disadvantages. The disadvantage results from the fact that the radioactive decay of the fission products generates heat. Hence, spent fuel has to be cooled for long periods prior to reprocessing. Thus, even if the chain reaction in the core of a nuclear reactor is terminated, heat continues to be generated. This heat must be removed or the core will heat up with resultant damage to the nuclear fuel and possible release of radioactivity into the environment [as happened at Fukushima] (The National Diet of Japan, 2012).

The advantage is that the resulting daughter products tend to be in an excited state and usually decay to their ground state by γ emission. However, some excited daughter products can decay by neutron emission. These neutrons are known as delayed neutrons, in contrast to the prompt neutrons emitted at the instant of fission. The delay depends on the half-life of the fission product and typically varies between about 0.2 and 56 s (mean delay about 12 s). Only about 0.65% of the neutrons produced from fission are delayed neutrons; however, they play a major role in the control of nuclear reactors.

The materials either used in or produced by the use of nuclear energy are radioactive. Radioactivity produces radiation in the form of particles or waves. Ionizing radiation can cause biological damage to human cells and, hence, cause death or cancer. The principal forms of ionizing radiation are alpha and beta particles, neutrons, and gamma and X-rays, which have sufficient energy to strip electrons from atoms. Exposure to these ionizing radiations from either external or internal sources can have an adverse affect on human biology and hence human health.

Table 4.1 summarizes the properties of the main ionizing radiations that can cause us harm.

Because atoms consist mostly of empty space, uncharged particles such as neutrons can travel large distances before being stopped by collisions with the nucleus.

Table 4.1 Basic properties of ionizing radiation

Radiation	Mass (amu)	Charge	Range (in air)	Range (in tissue)
Alpha	4	+2	Up to 7.5 cm	0.05 mm
Beta	0.00055	−1	4 or 5 m	Several mm
Gamma/X	0	0	100 s of m	Through body
Neutron	1	0	100 s of m	Through body

However, charged particles (α and β) interact with electrons and lose energy by *ionization* (i.e., removal of electrons from the atom). Typical energies of particles emitted in radioactive decay are 1-10 MeV. The energy required to ionize an air molecule is about 30 eV. Therefore, a 1 MeV particle can ionize about 33,000 molecules before coming to rest. Although alpha and beta particles cause roughly the same total amount of ionization (assuming they have the same energy), the alpha particles, being heavier, move more slowly and so cause ionization over much shorter track lengths than the beta particles.

Radiation is harmful and unlike other harmful substances, human senses cannot detect it. Humans cannot feel, smell, or touch radiation, and this gives rise to fear of the unknown, especially as the effects of exposure to ionizing radiation may not occur for many years after exposure. For further information on radiation and the protection measures that can be taken, see Martin et al. (2012).

Where there is the potential for an industrial activity to cause harm, either to workers or the public, society demands that such activities be subject to regulation. The use of nuclear energy in general, and the reprocessing and recycling of spent fuel in particular, is covered by a legal framework at both international and national levels.

4.3 Legal framework governing the use of nuclear energy

The reprocessing and recycling of spent nuclear fuel has implications for nuclear safety (handling of radioactive and fissile materials), nuclear security (storage of plutonium and enriched uranium), and safeguards (diversion of fissile materials and sensitive proliferation technologies). In each of these areas, there are international conventions that provide for effective governance.

4.3.1 International framework

The development of nuclear power was originally based on national laws because of its initial links with military programs. However, the recognition by the international community that the use of nuclear energy had to be controlled because of its special nature led to the creation of the IAEA in the mid 1950s. As the peaceful use of nuclear energy was adopted by increasing numbers of countries, the need for an international legal framework became more apparent. The IAEA led the development of "nuclear law" (International Atomic Energy Agency, 2003, 2010a)

Nuclear law is designed and structured to reflect the special nature of the challenges associated with the use of nuclear energy. These challenges relate to the risks to the health and safety of people and to the adverse impact on the environment resulting from radioactive contamination.

Nuclear law is defined by the IAEA as

> *The body of special legal norms created to regulate the conduct of legal or natural persons engaged in activities related to fissionable materials, ionizing radiation and exposure to natural sources of radiation.*

This definition has four main parts. The first is that nuclear law is part of a country's general legislation. The second element relates to regulation and this is where the risks and benefits are considered. The third element is legal persons, which includes commercial, academic, governmental, or scientific entities or individuals. The fourth element focuses on radioactivity that is produced by nuclear fission as the defining feature justifying the special regime.

The primary objective of nuclear law is

> *To provide a legal framework for conducting activities related to nuclear energy and ionizing radiation in a manner which adequately protects individuals, property and the environment.*

The legal framework for the peaceful use of nuclear energy is provided by a number of international conventions and treaties that member states of the United Nations sign.

4.3.2 International conventions and treaties

International conventions and treaties are used as vehicles to obtain consistent international approaches to such things as nuclear liability, nuclear safety, nuclear security, nonproliferation, and mechanisms for obtaining cooperation in the event of accidents. The IAEA has played a major part in the development and administration of these conventions. To date, the key conventions relating to the peaceful uses of atomic energy are:

- The 1997 Vienna Convention on Civil Liability for Nuclear Damage and the 1997 Convention on Supplementary Compensation for Nuclear Damage—Explanatory Texts (International Atomic Energy Agency, 2007b).
- The Convention on the Physical Protection of Nuclear Material (International Atomic Energy Agency, 1980).
- The Convention on Early Notification of a Nuclear Accident (International Atomic Energy Agency, 1986a).
- The Convention on Assistance in the Case of a Nuclear Accident or Radiological Emergency (International Atomic Energy Agency, 1986b).
- The Convention on Nuclear Safety (International Atomic Energy Agency, 1994).
- Joint Convention on the Safety of Spent Fuel Management and on the Safety of Radioactive Waste Management (International Atomic Energy Agency, 1997).

- Code of Conduct on the Safety and Security of Radioactive Sources (International Atomic Energy Agency, 2004).
- Code of Conduct on the Safety of Research Reactors (International Atomic Energy Agency, 2006a).
- The Treaty on the Nonproliferation of Nuclear Weapons (NPT) (UN Treaty, 1968).

In relation to safeguards, the EURATOM Treaty (EURATOM Treaty, 2010) applies to countries within the European Union. Hence, within these countries, facilities used for reprocessing and recycling of spent nuclear fuel will be subject to international requirements (and regulation) from both the IAEA and EURATOM.

Many of the above treaties and conventions apply to reprocessing and the recycling of spent nuclear fuel. Their requirements provide the international legal framework to ensure that reprocessing and recycling of spent nuclear fuel can be carried out safely, facilities and nuclear materials are secure, and that fissile materials and sensitive technologies cannot be diverted to support illicit nuclear weapons programs. The principal treaties and conventions that have a direct impact on the safety and security of reprocessing and recycling of spent nuclear fuel are:

- The Treaty on the Nonproliferation of Nuclear Weapons (UN Treaty, 1968).
- EURATOM Treaty (EURATOM Treaty, 2010).
- Joint Convention on the Safety of Spent Fuel Management and on the Safety of Radioactive Waste Management (International Atomic Energy Agency, 1997).
- The Convention on the Physical Protection of Nuclear Material (International Atomic Energy Agency, 1980).

The Joint Convention does not specifically apply to reprocessing or recycling of spent nuclear fuel but the U.K. and French governments have included their reprocessing activities in their national reports to the "Convention Peer Review" meetings. However, reprocessing and recycling of spent nuclear fuel involve the handling, treatment, and storage of spent nuclear fuel (i.e., management) and the management of radioactive waste that arises from the process. Hence, the objectives of the Joint Convention, reproduced below, provide a sound basis for ensuring nuclear safety in reprocessing and spent nuclear fuel recycling activities.

Article 1: Objectives

The Objectives of the Convention are:

(i) to achieve and maintain a high level of safety worldwide in spent fuel and radioactive waste management, through the enhancement of national measures and international co-operation, including where appropriate, safety-related technical co-operation;

(ii) to ensure that during all stages of spent fuel and radioactive waste management, there are effective defenses against potential hazards so that individuals, society, and the environment are protected from harmful effects of ionizing radiation, now and in the future, in such a way that the needs and aspirations of the present generation are met without compromising the ability of future generations to meet their needs and aspirations;

(iii) to prevent accidents with radiological consequences and to mitigate their consequences should they occur during any stage of spent fuel and radioactive waste management.

The treaties and conventions are supported by the IAEA. The IAEA has played a major role in the design and development of the global nuclear safety regime. The IAEA:

- is an independent intergovernmental, science and technology-based organization, in the United Nations family, that serves as the global focal point for nuclear cooperation;
- assists its member states, in the context of social and economic goals, in planning for and using nuclear science and technology for various peaceful purposes, including the generation of electricity, and facilitates the transfer of such technology and knowledge in a sustainable manner to developing member states;
- develops nuclear safety standards and, based on these standards, promotes the achievement and maintenance of high levels of safety in applications of nuclear energy, as well as the protection of human health and the environment against ionizing radiation;
- verifies through its inspection system that states comply with their commitments, under the nonproliferation treaty and other nonproliferation agreements, to use nuclear material and facilities only for peaceful purposes.

4.3.3 IAEA Safety Standards Programme

At the heart of this global nuclear safety regime is the Safety Standards Programme (International Atomic Energy Agency, n.d.a). This program provides the global reference for the standards and expectations for the safety of nuclear facilities, including those for reprocessing and the recycling of spent nuclear fuel. The program is structured such that at the top there are the "Safety Fundamentals" that set out the high-level safety objectives and supporting safety principles for nuclear facilities and activities. Below the Safety Fundamentals come the "Safety Standards" that are grouped under the headings of "General Safety Requirements" and "Specific Safety Requirements." In each area, the standards comprise a "Requirements" document that sets out the detailed standards that must be met and "Guides" that provide information of how the requirements can be met.

The General Safety Requirements comprise:

Part 1. Governmental, Legal and Regulatory Framework for Safety
Part 2. Leadership and Management for Safety
Part 3. Radiation Protection and the Safety of Radiation Sources
Part 4. Safety Assessment for Facilities and Activities
Part 5. Predisposal Management of Radioactive Waste
Part 6. Decommissioning and Termination of Activities
Part 7. Emergency Preparedness and Response

The Specific Safety Requirements for facilities and activities and comprise:

Site Evaluation for Nuclear Installations
Safety of Nuclear Power Plants—Design and Construction
Safety of Nuclear Power Plants—Commissioning and Operation
Safety of Research Reactors
Safety of Nuclear Fuel Cycle Facilities
Safety of Radioactive Waste Disposal Facilities
Safety of Transport of Radioactive Material

As can be seen, there are specific standards and guides that cover fuel cycle activities and facilities.

4.3.4 National legal framework

The international nuclear framework sets out the fundamental principles and requirements that must be adopted by countries wishing to use nuclear energy for peaceful purposes. However, national governments are responsible for implementing these requirements in the areas of nuclear safety and nuclear security. The implementation will depend upon the national legal system. The approach in the United Kingdom is used here as an example of the regulatory environment and approach for nuclear operations such as reprocessing and recycling of spent nuclear fuel.

In the United Kingdom, nuclear safety legislation has developed over the years. The United Kingdom introduced the Nuclear Installations Act (NIAct) of 1959. This was subsequently amended in 1965 to take on broad new international treaties relating to nuclear liability and insurance and, although it has been amended on numerous occasions since then, to accommodate the licensing of BNFL and later the UKAEA. The 1965 (As Amended) Act (Nuclear Installations Act, 1965) has remained the vehicle for licensing all prescribed nuclear activities. The reprocessing and recycling of spent nuclear fuel are prescribed activities and, hence, any new facilities in the United Kingdom to undertake these activities will be covered by this Act of Parliament.

The NIAct gives the regulator considerable powers to control the use of nuclear energy and its safety in the United Kingdom.

4.3.4.1 Nuclear Installations Act

Section 1 of the NIAct is relevant to reprocessing and recycling of spent nuclear fuel. It addresses the control of certain nuclear installations and operations. In this section, it is made clear that:

> *. . . no person . . . shall use any site for the purpose of installing or operating:*
>
> **(a)** any nuclear reactor (other than such a reactor comprised in a means of transport whether by land, water or air): or
> **(b)** subject to subsection (2) of this section, any other installation of such class or description as may be prescribed, being an installation designed or adapted for –
>
> **I.** the production or use of atomic energy;
> **II.** the carrying out of any process which is preparatory or ancillary to the production or use of atomic energy and which involves or is capable of causing the emission of ionising radiation; or
> **III.** the storage, processing or disposal of nuclear fuel or bulk quantities of other radioactive matter, being matter which has been produced or irradiated in the course of production or use of nuclear fuel.
>
> Unless a licence so to do (in this Act referred to as a "nuclear site licence") has been granted in respect of that site by the Minister and is in for the time being in force.

When the NIAct came into force, the power to license nuclear installations was vested in ministers in the Ministry of Power. The NIAct also enabled the creation of a nuclear safety regulator that subsequently became known as Her Majesty's Nuclear Installations Inspectorate (HMNII). The minister in the Ministry of Power formally delegated the power to license nuclear installations to the head of NII, the chief inspector of nuclear installations. In 1975, the power to license nuclear installations was transferred to the Health and Safety Executive (HSE) and the executive formally delegated these licensing powers to HM Chief Inspector of Nuclear Installations. The responsibility for regulating nuclear security was subsequently transferred to HSE from the Department of Trade and Industry, and responsibility for regulating the transport of nuclear materials was transferred to HSE from the Department of Transport. To deliver a more integrated approach to nuclear regulation the government created the Office of Nuclear Regulation (ONR) as a Statutory Corporation in 2014. The Board of ONR, in line with previous practice, delegated the power to license nuclear installations to the chief inspector.

4.3.4.2 Nuclear industry security regulations

The security of nuclear installations is not covered by the NIAct because the primary focus of this Act is nuclear safety. As discussed above, the reprocessing and recycling of nuclear fuel will have nuclear security implications both in terms of the prevention of theft of fissile materials and in the prevention of sabotage to installations. The Nuclear Industries Security Regulations (NISR) (2003) were introduced to ensure that licensed nuclear sites, nuclear materials held at other premises or in transit, and the construction of new installations were subject to effective security protection. These regulations put obligations on a nuclear site licensee to produce and submit security plans for its activities (or proposed activities) that set out its security standards, procedures, and arrangements. The 2003 Regulations required the security plan to be approved by the regulator.

The original approach was somewhat prescriptive; however, new guidance has been issued by ONR. The National Objectives, Requirements, and Model Standards (NORMS) aim to provide a more goal-setting approach to nuclear security regulation. The duty holder is now required to propose and justify its nuclear security arrangements in order to meet ONR's nuclear security objectives.

4.4 Roles and responsibilities

The effective delivery of nuclear safety, nuclear security, and safeguards depends upon a whole range of "duty holders." These include governments that operate at the state and international level, regulators that operate mainly at the state level, operators or "licensees" that operate at the corporate level, and staff and others who undertake the day-to-day activities associated with nuclear and radioactive waste-related operations.

4.4.1 Nuclear safety

In the case of nuclear safety, the responsibilities for governments, regulators, and licensees are clear as set out in the IAEA document on Government, Legal, and Regulatory Framework for Safety (International Atomic Energy Agency, 2010b) and the IAEA's Fundamental Safety Principles (International Atomic Energy Agency, 2006b).

4.4.1.1 Government

Governments have the responsibility for putting in place a legal and governmental framework to establish the required laws, regulations, and standards that are necessary for the effective regulation of nuclear facilities and activities that give rise to radiation hazards. GSR1 Part 1 (International Atomic Energy Agency, 2010b) identifies a number of the key requirements for governments in relation to nuclear safety.

Governments, therefore, have a responsibility to put in place an effective legal framework for safety that includes the establishment of an independent regulatory body. In doing this, governments must ensure that the regulatory body

- has adequate legal authority, technical and managerial competence, and human and financial resources to fulfill its responsibilities; and
- is effectively independent of the licensee and of any other body that is responsible for the promotion of the use of nuclear energy, so that it is free from any undue pressure from interested parties.

4.4.1.2 The regulator

Once established, the regulatory body is responsible for setting the appropriate nuclear safety standards, licensing nuclear installations, and carrying out inspection and enforcement activities including permissioning activities on or related to a licensed nuclear site.

4.4.1.3 The licensee

The global framework for the effective delivery of nuclear safety makes it very clear that it is the licensee who is responsible for nuclear safety. Reference (International Atomic Energy Agency, 2010b) sets out the "requirements" that governments must deliver for the effective management of nuclear safety. Requirement 5 relates to nuclear safety responsibility:

> *Requirement 5: Prime responsibility for safety*
>
> *The government shall expressly assign the prime responsibility for safety to the person or organization responsible for a facility or an activity, and shall confer on the regulatory body the authority to require such persons or organizations to comply with stipulated regulatory requirements, as well as to demonstrate such compliance.*

Therefore, the prime responsibility for safety must rest with the person or organization responsible for facilities and activities that give rise to radiation risks.

The licensee retains the prime responsibility for nuclear safety throughout the lifetime of facilities and activities. This responsibility cannot be delegated to any other organization.

The licensee is therefore primarily responsible for inter alia:

- establishing, maintaining, and managing a corporate body with sufficient financial resource to undertake the required nuclear operations;
- establishing and maintaining the necessary competences to be the "controlling mind" of its operations or activities, and the "intelligent customer" for any services it contracts out to others;
- providing adequate training and information to its employees;
- establishing procedures and arrangements to maintain safety under all conditions;
- verifying appropriate design and the adequate quality of facilities and activities and of their associated equipment;
- ensuring the safe control of all radioactive material that is used, produced, stored, or transported; and
- ensuring the safe control of all radioactive waste that is generated.

4.4.2 Nuclear security

Nuclear security is not as straightforward as nuclear safety. This is because of the nature of nuclear security, which includes the detection and management of threats that originate outside the control of the licensee. Unlike nuclear safety, there are no international standards for nuclear security because of the aid such standards could give to those with malicious intent. The detection and management of security threats involve activities that are often considered to be "sensitive" and can include intelligence gathering, the exercise of police powers, trustworthiness, the vetting of persons working within (or associated with) a nuclear facility with access to nuclear or radioactive materials, or access to safety-related plant or equipment.

These sensitivities have resulted in governments being reluctant to open up nuclear security to international nuclear standards development. However, in the 1970s the IAEA recognized the need for some form of guidance on physical protection; this has been progressively updated, with the latest version being the IAEA document INFCIRC/225 (International Atomic Energy Agency, 2011). In 1987, the Convention on the Physical Protection of Nuclear Material (International Atomic Energy Agency, 1980) entered into force.

4.4.2.1 Government

Government has a responsibility to protect nuclear material that is within the scope of the Convention. The protection is required for nuclear materials that are within domestic use and storage or transport (both within national borders and when the material is on board a ship or aircraft under the jurisdiction of the state). The Convention does not prescribe how this responsibility should be delivered and, unlike in the case of nuclear safety, there are no legally binding requirements on roles and responsibilities. However, INFCIRC/225 does provide guidance to governments.

For states that are parties to the Convention, the government would be expected to establish a legal and regulatory framework and assign responsibilities. Neither the

Convention nor INFCIRC/225 use the term "regulatory body" that is used in terms of nuclear safety; however, the role of a regulatory body for nuclear security is vested in what is termed the "competent authority." The state would be expected to establish a competent authority with responsibility for the implementation of the legislation and provide it with adequate authority, competence, and financial and human resources to fulfill its assigned responsibilities. The competent authority would also be expected to have effective independence from those of any other body in charge of the promotion or utilization of nuclear energy.

4.4.2.2 The licensee

In the case of nuclear safety, the primary responsibility rests with the licensee; that is, the person in charge of day-to-day of activities on a site or in control of nuclear-related activities. The situation in relation to nuclear security is slightly different because government, usually via the regulator, holds some responsibilities in relation to threat assessment and definition. This is reflected in the IAEA guidance (International Atomic Energy Agency, 2011) on physical protection.

The licensee is typically responsible for:

- compliance with regulations and requirements established by the state or the regulator;
- cooperation with other organizations with security-related responsibilities such as off-site response forces;
- control of, and accountancy for, nuclear material at its facilities;
- reporting accounting discrepancies to the regulator;
- preparation of a security plan based upon state-defined threat assessments;
- maintenance of the physical protection system and contingency plans; and
- ensuring physical protection requirements are taken into account in the siting and design of new nuclear facilities.

4.4.3 Nuclear safeguards

As discussed above, the purpose of the international safeguards system is to prove to the international community with credible assurance that nuclear materials and related technologies are not being diverted from their peaceful uses into nuclear weapons programs. The IAEA has a statutory duty (International Atomic Energy Agency, n.d.c) to establish and administer the international safeguards system. The IAEA can conclude agreements with states or regional inspectorates for the application of safeguards. The IAEA's role in relation to safeguards is set out in INFCIRC/26 (International Atomic Energy Agency, 1961). This states that the IAEA is authorized

> *to establish and administer safeguards designed to ensure that special fissionable and other materials, services, equipment, facilities, and information made available by the Agency or at its request or under its supervision or control are not used in such a way as to further any military purpose; and to apply safeguards, at the request of the parties, to any bilateral or multilateral arrangement, or, at the request of a State, to any of that State's activities in the field of atomic energy.*

4.4.3.1 Government

Unlike nuclear safety or nuclear security, the IAEA has responsibilities for safeguards, additional to the responsibilities of states, regulators, and license holders (International Atomic Energy Agency, 1972)

Government has a responsibility to

- maintain a system of records of the material and facilities to which the safeguards agreement applies;
- submit routine and special reports on the facilities and materials under safeguards;
- allow inspections by the IAEA to account for material to which the safeguards agreement applies, and to detect diversion;
- provide design information on new facilities or changes to existing facilities as soon as the state authorities decide to construct, authorize construction, or to modify a facility; and
- set up a legal framework to enable the safeguards information required by the IAEA to be collected, this could be done via regulations that place duties on nuclear license holders or others to report their activities and furnish the necessary information.

4.4.3.2 The licensee

The responsibilities of nuclear licensees will vary depending upon the way in which a state implements its safeguards arrangements. In general, a nuclear license holder will have the responsibility to

- define and communicate the lines of responsibility and authority in relation to the state's nuclear materials accountancy system (NMAS);
- provide appropriate resources to enable the NMAS to be effectively implemented;
- ensure that those with responsibilities are adequately trained and have suitable qualifications and experience to undertake their duties; and
- ensure that the NMAS is successfully implemented.

4.5 Regulation

As stated earlier, society expects that all activities that have the potential to cause harm are subject to regulation. In the United Kingdom, any new advanced fuel cycle facility for reprocessing and recycling of spent nuclear fuel will be subject to regulation. Nuclear safety and nuclear security at nuclear installations and the transport of spent nuclear fuel and new nuclear fuels, such as mixed oxide (MOX) fuels produced from recycling, will be regulated by the ONR.

4.5.1 Licensing

Under the NIAct, no one can construct or operate a nuclear installation without a licence granted by ONR. The NIAct allows ONR to attach conditions to a nuclear site license as may be necessary or desirable in the interests of safety or with respect to the handing, treatment, or disposal of nuclear matter.

The current standard licence for a nuclear installation in the United Kingdom has some 36 conditions (Office of Nuclear Regulation, 2011). These conditions envelope all the requirements to effectively manage nuclear safety on a licensed nuclear site and cover such things as design, construction, commissioning, operation, maintenance, inspection and review, decommissioning, and the management of organizational change.

The United Kingdom's nuclear regulatory regime clearly puts the responsibility on the licensee to demonstrate that its activities are safe. Therefore, the licensee is required to show how it intends to comply with the conditions attached to the license. The licensee's arrangements are legal documents and, hence, form part of the criminal law. Failure by the licensee to comply with its arrangements is a breach of the criminal law and, hence, the licensee is liable to prosecution.

The licensing process operated by ONR is in effect a "permissioning regime"; that is, the duty holder is required to seek permission to undertake a nuclear safety related activity before that activity is undertaken. Permission is granted on the basis of the adequacy of the safety documentation (safety case) for the proposed activity.

4.5.2 Safety cases

The licence conditions give powers to the regulator to control activities by placing hold-points on the licensee's activities. Progress past a hold-point usually requires the licensee to produce a safety case that demonstrates that the licensee's proposed action will be safe. For major nuclear installations associated with reprocessing and recycling of spent nuclear fuel, the hold-points and associated safety cases could be

- Preliminary safety case (PSC)—demonstrates at the concept level that there are no fundamental flaws in the proposal.
- Preconstruction safety case (PCSC)—provides a detailed demonstration that the proposed plant will meet all the required nuclear safety standards and requirements. ONR are unlikely to allow construction to commence until it is satisfied that the arguments made in the PCSC have been substantiated.
- Precommissioning safety case (PCmSC)—provides a demonstration that the plant has been constructed to the required specification and there is a schedule of tests to demonstrate that all the systems are functioning as designed. ONR usually places two hold-points on the licensee, one to control inactive commissioning (i.e., testing of systems before any spent nuclear fuel is introduced); and the second to ensure that all the control and protection systems have been tested and the staff are ready to accept the introduction of spent nuclear fuel into the facility.
- Preoperational safety case (POSC)—provides a demonstration that the facility (spent fuel storage facility, reprocessing plant, or the associated MOX fuel production facility) has been designed, constructed, and commissioned properly and demonstrates the safe limits and conditions that are used to ensure the plant will be safe even under fault conditions. ONR usually would not allow a facility to go into routine operation until it is satisfied that the arguments made in the POSC have been substantiated during the active commissioning phase.
- Periodic safety review (PSR)—provides a demonstration every 10 years that the plant is safe to continue to operate for the next 10 years, including a check against changes in standards. ONR can prevent continued operation if the PSR has not demonstrated that it is safe to continue.
- Predecommissioning safety case (PDSC)—provides a demonstration that the plant can be decommissioned safely.

4.6 Standards and expectations

The above has shown that there is a comprehensive international and national legal framework for ensuring that nuclear activities, such as reprocessing and recycling of spent nuclear fuel are carried out safely, securely, and in a way that does not lead to the proliferation of nuclear weapons. The key to the delivery of nuclear safety (and in an indirect way nuclear security and safeguards) is the safety case. Safety cases are used to demonstrate that the design, construction, commissioning, and operation of the nuclear facilities meet the required safety goals and, hence, that the risks to the workers and the public are reduced so far as is reasonably practicable.

The facilities used to undertake the processes necessary to reprocess spent nuclear fuel and recycle the recovered uranium and plutonium to produce new fuel and manage the resultant radioactive wastes, including fission products and minor actinides (MAs), are required to meet specific nuclear safety standards. The safety cases must not only show what the appropriate standards are, and why they have been chosen, but also show how the design and subsequent construction, commissioning, and operation delivers the requirements of the standards.

The licensee must make the safety case and, hence, choose the appropriate standards that when met will reduce risks to as low as is reasonably practicable (ALARP). The IAEA safety standards program includes a number of documents that are relevant to reprocessing and recycling of spent nuclear fuel. The ONR has also published its safety assessment principles (SAPs) for Nuclear Facilities. The SAPs provide guidance to ONR Inspectors but they give a useful insight into what is required to demonstrate nuclear safety.

4.6.1 IAEA safety standards

There are no specific IAEA standards or guides for nuclear fuel reprocessing facilities but there are a number that are applicable to the various stages in the preprocessing and recycling process. Any advanced nuclear fuel cycle, by definition, will be a "closed" process. The safety requirements for the facilities used in the process are set out in the IAEA documents Safety Assessment for Facilities and Activities (International Atomic Energy Agency, 2009) and Safety of Nuclear Fuel Cycle Facilities (International Atomic Energy Agency, 2008a).

4.6.1.1 Storage of spent nuclear fuel

Spent nuclear fuel will need to be stored prior to reprocessing, and guidance on how the safety requirements can be met is given in Storage of Spent Nuclear Fuel (International Atomic Energy Agency, 2012). In advanced nuclear fuel cycles, it is likely that high burn up MOX fuels will be recycled and, hence, storage of this fuel prior to reprocessing will have a number of safety issues. Spent fuel storage can be either in ponds (wet storage) or in casks (dry storage). Each of these options has nuclear safety, nuclear security, and safeguards issues as set out in reference (International Atomic Energy Agency, 2012).

The facilities are required to be designed to provide protection against plant malfunctions (in the case of pond storage) and external events such as earthquakes, flooding, missiles, and aircraft crashes. The safety case for storage will need to take account of such things as the type of fuel, enrichment, plutonium content, criticality potential, burn up, heat generation, chemical characteristics of the cladding and storage medium, and the integrity of the fuel (failed, leaking). The licensee is also required to maintain records of the fuel for materials accounting and control. The length of storage prior to reprocessing may vary and, hence, the ability to retrieve the fuel is an essential part of the safety case for the storage facility.

4.6.1.2 Reprocessing facilities

The reprocessing of spent nuclear fuel presents numerous nuclear safety, nuclear security, and safeguards challenges. The general safety requirements for such facilities are covered in reference (International Atomic Energy Agency, 2008a), which gives a comprehensive description of what is required from the siting, design, construction, commissioning, and operation of fuel cycle facilities. In the case of a reprocessing plant, whether for the current generation based upon the PUREX process or for the advanced processes proposed for the future, the basic challenges are the same.

Reprocessing facilities must be designed to prevent and, when necessary, mitigate the consequences of plant malfunctions and human error. Defense in depth is a fundamental requirement to ensure risks are ALARP. These facilities must also be designed and operated to cope with internal hazards such as fire and external hazards arising from earthquakes, flooding, extreme temperatures, wind, and precipitation.

Reprocessing facilities typically comprise four main parts:

- Fuel receipt and storage (interim storage pending reprocessing);
- Headend (fuel shearing and dissolution);
- Chemical separation (separation of uranium, plutonium and fission products); and
- Finishing lines (production of uranium and plutonium oxide powders).

The nuclear safety, security, and safeguards challenges in the fuel receipt and storage part of the facility are dominated by

- mechanical handling;
- radiation protection (shielding during fuel transfer and interim storage);
- radiation protection (airborne release from failed fuel);
- criticality protection;
- heat removal from the interim storage pond;
- pond water chemistry;
- inventory control for safeguards; and
- control of access for security.

The nuclear safety, security, and safeguards challenges associated with the headend part of the facility, where the spent nuclear fuel is sheared and dissolved in nitric acid, are dominated by

- inventory control systems and accountancy;
- radiation protection (shielding for shear cave and dissolver cells);
- ventilation control in the shear cave and dissolver cells including off-gas treatment;
- criticality control in the dissolvers;
- process control of liquor volumes; and
- access control to operational areas.

Nuclear safety, security, and safeguards challenges in the chemical separation part of the plant where the uranium, plutonium, and fission product waste are separated are dominated by

- process control for chemical separation;
- criticality control;
- radiation protection (shielding for the main process fission product cells);
- radiation protection (ventilation control);
- inventory control; and
- access control to operational areas.

In the finishing lines where the uranium and plutonium bearing liquors are converted to uranium and plutonium oxides, nuclear safety, security, and safeguards challenges are dominated by

- process control;
- criticality control (for both uranium and plutonium lines);
- radiation protection (glove box for plutonium lines);
- radiation protection (ventilation);
- access control to operational areas and plutonium stores; and
- inventory control.

Nuclear safety, security, and safeguards throughout the facility are delivered by a combination of active, passive, and administrative controls.

4.6.1.3 Plutonium and reprocessed uranium storage

The plutonium and reprocessed uranium oxides (which are likely to be slightly enriched) will be put into interim storage pending being fed into the MOX fuel fabrication facility. The nuclear safety, security, and safeguards arrangements for these materials will be different because of their different hazard potentials.

Plutonium storage requires

- robust facilities that are designed to protect against plant malfunctions, human error, internal and external hazards, including aircraft crashes;
- containment (sealed canisters) because of the high radiological toxicity of plutonium;
- radiation protection (shielding) because of gamma radiation from americium build up;
- physical protection against external hazards and security threats;
- radiation protection (ventilation) with defense in depth to mitigate the consequences of canister failure;
- access control to store; and
- inventory control.

The storage of uranium dioxide powder is less onerous because of the lower levels of radiological toxicity and proliferation implications. However, reprocessed uranium is slightly enriched and requires safeguards controls. Storage facilities for reprocessed uranium will require

- buildings that are designed to provide a weatherproof environment;
- fire protection;
- criticality control;
- uranium containment (sealed drums);
- radiation protection (ventilation) with defense in depth to mitigate the consequences of drum failure;
- physical protection to control access to store; and
- inventory control.

4.6.1.4 Radioactive waste management

One of the main aims of reprocessing is to separate out the highly radioactive fission products that are considered to be radioactive waste. In addition, reprocessing also produces secondary radioactive wastes. All radioactive waste streams need to be effectively managed. While reference (International Atomic Energy Agency, 2008a) provides the requirements for the safety of fuel cycle facilities including facilities for the conditioning and storage of radioactive waste, the IAEA (International Atomic Energy Agency, 2013) gives more specific guidance on the safety case and safety assessment for radioactive waste management.

The main waste streams arising from reprocessing are

- Liquids
  - High-level waste (HLW) from the HA cycle
  - Low-level waste (LLW) from solvent recycle circuit and other waste solvents
- Gaseous
  - Kr-85 in dissolver off-gas—as Kr is chemically inert it is released to the environment.
  - I-129 in dissolver off-gas—removed by alkali scrubbing.
  - C-14 in dissolver off-gas as CO_2—removed by alkali scrubbing.
  - H-3—mostly as tritiated water vapor removed by scrubbing.
- Solids
  - Intermediate-level waste (ILW) such as contaminated fuel hulls.
  - LLW from various operations.

High-level radioactive waste results from the separation of the fission products from the spent fuel. In current reprocessing facilities, this waste stream is evaporated to reduce its volume and the fission products are vitrified in a glass matrix and sealed in a high-integrity stainless steel canister. These heat-generating canisters are stored on the surface for up to 50 years to allow the canisters to cool prior to disposal. As shown above, other waste streams arise from contaminated solvents used in the solvent-extraction process and the waste cladding and fuel assembly components. These ILW and LLW are conditioned, usually in a cement matrix in stainless steel drums, and stored pending disposal.

HLW and ILW wastes are highly radioactive and their processing and storage must be carried out in very thick-walled concrete cells to provide shielding from the intense radiation. The aim is to provide passive safety and, hence, for the heat-generating high-level vitrified wastes, cooling should be via natural convection. For ILW, passive safety is delivered through the waste containers and the robustness of the store. The key nuclear safety, security, and safeguards issues relating to radioactive waste are

- robust facilities to provide protection from plant malfunctions, human error, internal and external hazards including earthquakes, flooding, and aircraft crashes;
- retrievability of waste from store;
- radiation protection (shielding);
- radiation protection (ventilation);
- inventory control;
- access control to operational areas; and
- access control to storage areas.

The solid LLW can be disposed, after treatment, to surface or near-surface disposal facilities. The very low-level liquid wastes are discharged under authorization to the sea, and very low-level gaseous wastes are discharged to the atmosphere via tall stacks to enable dispersion.

4.6.1.5 MOX fuel fabrication

The main aim of reprocessing and recycling is to reuse the plutonium and uranium left in the spent fuel. Advanced fuel cycles will be based upon MOX fuels either for use in thermal reactors or in fast breeder reactors. Nuclear fuel fabrication is, therefore, an essential part of an advanced nuclear fuel cycle. As with other parts of the fuel cycle, MOX fabrication has nuclear safety, security, and safeguards issues. The IAEA (International Atomic Energy Authority, 2010) provides extensive guidance on the nuclear safety issues relating to MOX fabrication facilities.

The key nuclear safety, security, and safeguards issues relating to MOX fabrication are

- robust design to protect against plant malfunctions and human error;
- fire and explosion (hydrogen);
- earthquake and flooding;
- aircraft crash/missile impact;
- radiation protection (glove box operations);
- radiation protection (ventilation);
- radiation protection (shielding);
- criticality control;
- inventory control; and
- access control.

4.6.2 ONR SAPs

As shown above, the IAEA safety standards set out the nuclear safety requirements for reprocessing and nuclear fuel recycling facilities and they provide extensive guidance to designers, operators, and regulators on how the requirements can be delivered.

Although the standards have been produced for current nuclear fuel cycle facilities, there is no reason why they cannot be applied to advanced nuclear fuel cycles. The ONR SAPs (Office of Nuclear Regulation, 2008) are not standards, but they give an insight into what the regulator expects to see in a licensee's safety documentation. The SAPs have been benchmarked against the IAEA Safety Standards as they were in 2004. In relation to reprocessing and nuclear fuel recycling facilities it is likely that most of the SAPs would be applicable. In line with U.K. practice, any new facilities for reprocessing and recycling of spent nuclear fuel would need to demonstrate that the risk to the workers and the public are tolerable and ALARP.

4.6.2.1 Leadership

ONR would expect to see effective leadership in any organization that intended to design, construct, commission, and operate a nuclear facility such as those discussed in this book. Directors and their managers would be expected to focus their organization on achieving and sustaining high standards of safety. To do this, ONR would expect the organization to have sufficient suitably qualified and experienced staff to be the "controlling mind" for its operations and to be an "intelligent customer" capable of effectively managing its contractors in order to manage nuclear safety.

4.6.2.2 Safety case process

Safety cases are required to substantiate the licensee's arguments for permission to carry out specific nuclear safety-related activities throughout the life cycle of the facility, such as to undertake construction, commissioning, operation, modification, or decommissioning. ONR would expect the complexity of the safety case to be commensurate with the hazard; that is, the greater the hazard potential the more comprehensive the safety case should be to demonstrate that the risks are ALARP. The safety case should be a living document and be maintained throughout the life cycle of the facility. The safety case belongs to the licensee and it is produced for the licensee so that it can be assured at all times that the facility is safe. The safety case should not be produced for the regulator but to demonstrate to the regulator that the licensee's arguments are robust.

4.6.2.3 Siting

When siting a reprocessing and nuclear fuel recycling facility, the licensee should take account of the radiological risk the facility might have on the local population. The safety case should not only show that the risks from the facility are ALARP but, in the event of an emergency, it should also show that the local off-site population characteristics would enable an effective off-site emergency response. Account should also be taken of any natural or man-made external hazards, including the potential impact on neighboring hazardous installations associated with the proposed site.

4.6.2.4 Engineering principles

As seen in the IAEA standards, the ONR would expect a safety case for a new facility to demonstrate, whenever possible, the adoption of inherent safety. Also, the safety case should show that the sensitivity of the facility to potential faults has been minimized. It should also show that there are adequate levels of defense in depth against potentially significant faults to limit the consequences and reduce the risks to ALARP. ONR would expect to see the safety case address internal and external hazards with a clear definition of the design basis event (DBE) and a demonstration that a small change in the DBE will not lead to a disproportionate increase in radiological consequences. Many of the engineering principles relating to design, component manufacture, construction, commissioning, operation control and instrumentation, human factors, passively safe storage of nuclear materials, and nuclear materials accountancy are directly relevant to reprocessing and nuclear recycling facilities.

4.6.2.5 Numerical targets and legal limits

Any new reprocessing and nuclear fuel recycling facility would be expected to at least meet the risk target set out in the basic safety level (BSL) and strive to achieve the level of risk set out by the basic safety objective (BSO) if ALARP. Reference (Office of Nuclear Regulation, 2008) sets out the risk and radiation dose levels for workers and the public for the BSO, the BSL, and the legal limits. In essence, the targets for individual risk of death to a person on the site from accidents on-site would be

$$\text{BSL}: \ 1 \times 10^{-4} \text{ per annum}$$
$$\text{BSO}: \ 1 \times 10^{-6} \text{ per annum}$$

The same individual risks apply to a person off the site. In the event of a severe accident that went beyond the design basis, societal risk is used as the appropriate target. Societal risk is based upon accidents that can lead to the death (immediate or eventual) of 100 or more people. The targets for the total risk of 100 or more fatalities are

$$\text{BSL}: \ 1 \times 10^{-5} \text{ per annum}$$
$$\text{BSO}: \ 1 \times 10^{-7} \text{ per annum}$$

The safety case for any new reprocessing and nuclear fuel recycling facility would be required to demonstrate that total societal risk, including on-site and off-site fatalities are within the BSL and BSO target levels.

4.7 Advanced fuel cycle challenges

The strategy for the use of closed nuclear fuel cycles is aimed at the conservation of natural resources; for example, uranium, the utilization of plutonium as an energy source, the optimization of radioactive waste management including disposal,

improved fuel cycle economics, and proliferation resistance. The current reprocessing technology is some 60 years old. TBP is not a selective extractant, and it degrades due to radiolysis and acid hydrolysis and this gives it fairly rigid flow sheet conditions and the need for a solvent cleanup circuit. The PUREX process separates the bulk of the metals (U and Pu) from smaller quantities of fission products and MAs and, consequently, contactors are comparatively large. It does not separate long- and short-lived radionuclides; these are discarded together in the highly active liquid waste, which has an impact on radioactive waste disposal options.

Current research on partitioning is to find and develop processes suitable for separation of the heavier MAs (and possibly some long-lived fission products) on an industrial scale. Most of the research studies are concentrated on modified PUREX flow sheets, but some advanced fuel cycles are looking at reprocessing that does not involve the PUREX process and will use separation techniques with the potential to segregate radionuclides into "families" and that will produce a more sustainable approach to radioactive waste management that is more consistent with partitioning and transmutation (P&T). The objective of transmutation is to change the long-lived actinides into fission products and long-lived fission products into significantly shorter-lived nuclides. The goal is, therefore, to produce radioactive wastes that decay in a few hundred years compared with the current wastes that remain radioactive for tens of thousand years.

The adoption of a P&T approach, therefore, has several advantages:

- reduces the radiotoxic inventory of long-lived HLW;
- reduces the heat load of geological repositories; and
- reduces the intergenerational liabilities of nuclear power.

Some of the processes for advanced fuel cycles are discussed in references (OECD/NEA, 2006, 2012; International Atomic Energy Agency, 2008b; EPRI, 2010). Each is focused on specific objectives relating to more effective radioactive waste management, security, or nonproliferation goals. The DIAMEX-SANEX process (OECD/NEA, 2006) provides selective separation of long-lived radionuclides (with a focus on Am and Cm separation) from short-lived fission products. The COEX process (Drain et al., 2008) is based on coextraction and coprecipitation of uranium and plutonium (and usually neptunium) together, as well as a pure uranium stream (eliminating any separation of plutonium on its own). The GANEX (grouped extraction of actinides) process (Carrott et al., 2014) separates uranium and then recovers plutonium with the MAs from the high-level raffinate stream. The resultant uranium, plutonium, and MAs, together, can be made into MOX fuel for fast neutron reactors; the lanthanides and other fission products become waste. The DOUBLE STRATA process (OECD/NEA, 2001) is an extension of the mixed LWR + FR scheme. The goal is a 95% removal and transmutation of MAs, Tc-99 in HLW and I-129 from the PUREX process (Saito & Sawada, 2002). A reduction in these radionuclides will have an impact on the potential hazard from radioactive waste.

The successful exploitation of these advanced fuel cycles may not reduce the operational nuclear safety and nuclear security challenges but they have considerable implications for reducing proliferation threats and for the safe and secure disposal of radioactive waste.

4.7.1 Nuclear safety and security

Advanced nuclear fuel cycles would appear to have considerable advantages; however, these can only be realized if P&T can be made to work on an industrial scale. This will require the use of fast reactor technology that is as yet unproven at a commercial level. Another safety-related factor is the need for commercial-scale MOX fabrication facilities with higher levels of enrichment than current MOX facilities and possibly more use of remote fabrication technology to reduce worker doses.

4.7.2 Nuclear nonproliferation safeguards

At the operational stage, the safeguards implications for these new fuel cycles should not be any more onerous than the current arrangements for reprocessing and MOX fuel production plants. However, in the longer term these processes should enable a better utilization of uranium and plutonium than the current once through process that requires the disposal of spent fuel. They should also reduce the safeguards burden on disposal facilities and, hence, proliferation threats to future generations.

4.8 Conclusions

There is a comprehensive legal framework at both the international and national level to control the design, construction, commissioning, operation, and decommissioning of nuclear installations and to control the management of radioactive waste. These frameworks are designed to provide society with the confidence and the necessary levels of protection to enable the peaceful use of nuclear energy. Nuclear fuel cycle facilities are currently being designed, constructed, commissioned, operated, and decommissioned within this framework and at acceptable levels of risk to both workers and the public. However, this is as a result of considerable attention being paid to nuclear safety, nuclear security, and nonproliferation safeguards to ensure that these facilities are safe, secure, and that fissile materials and sensitive technologies are protected from diversion and theft.

The advanced nuclear fuel cycles under consideration could lead to more efficient reprocessing and recycling of nuclear fuel. There is no reason to believe that these new facilities will present technological challenges that will prevent them being licensed within the current nuclear safety or security approaches. However, the new processes have the potential to offer improvements in relation to radioactive waste management and reduce the safety, security, and safeguards burden on future generations.

References

Carrott, M., Bell, K., Brown, J., Geist, A., Gregson, C., Hères, X., Maher, C., Malmbeck, R., Mason, C., Modolo, G., Müllich, U., Sarsfield, M., Wilden, A., Taylor, R., 2014. Development of a new flowsheet for co-separating the transuranic actinides: the "EURO-GANEX" process. Solvent Extr. Ion Exch. 32, 447–467.

Drain, F., et al., 2008. COEX™ process: cross-breeding between innovation and industrial experience. In: WM'08, High Level and Spent Fuel Associated Technology Development and Deployment, Session 53. www.wmsym.org.

EPRI, 2010. Advanced Nuclear Fuel Cycles—Main Challenges and Strategic Choices, Palo Alto, CA, 1020307.

EURATOM, 2010. Summary of the EURATOM treaty. http://europa.eu/legislation_summaries/institutional_affairs/treaties/treaties_euratom_en.htm.

International Atomic Energy Agency, 1961. The agency's safeguards. In: INFCIRC/26, IAEA, Vienna.

International Atomic Energy Agency, 1972. The structure and content of agreements between the agency and states required in connection with the treaty on the non-proliferation of nuclear weapons. In: INFCIRC/153, IAEA, Vienna.

International Atomic Energy Agency, 1980. Convention on the physical protection of nuclear materials. In: INFCIRC/274/Rev1, IAEA, Vienna.

International Atomic Energy Agency, 1986a. Convention on early notification of a nuclear accident. In: INFCIRC/335, IAEA, Vienna.

International Atomic Energy Agency, 1986b. Convention on assistance in the case of a nuclear accident or radiological emergency. In: INFCIRC/336, IAEA, Vienna.

International Atomic Energy Agency, 1994. Convention on nuclear safety. In: INFCIRC/449, IAEA, Vienna.

International Atomic Energy Agency, 1997. Joint convention on the safety of spent fuel management and on the safety of radioactive waste management, INFCIRC/546, IAEA, Vienna.

International Atomic Energy Agency, 2002. IAEA safeguards glossary 2001 edition. In: International Nuclear Verification Series No. 3, IAEA, Vienna.

International Atomic Energy Agency, 2003. Handbook on Nuclear Law. IAEA, Vienna.

International Atomic Energy Agency, 2004. Code of Conduct on the Safety and Security of Radioactive Sources. IAEA, Vienna.

International Atomic Energy Agency, 2006a. Code of Conduct on the Safety of Research Reactors. IAEA, Vienna.

International Atomic Energy Agency, 2006b. Safety Fundamentals No. SF-1, Fundamental Safety Principles. IAEA, Vienna.

International Atomic Energy Agency, 2007a. IAEA Safety Glossary, Terminology Used in Nuclear Safety and Radiation Protection. IAEA, Vienna.

International Atomic Energy Agency, 2007b. The 1997 Vienna convention on civil liabilities for nuclear damage and the 1997 convention on supplementary compensation for nuclear damage—explanatory texts. In: IAEA International Law Series No. 3, IAEA, Vienna, ISBN 92-0-114106-8. www.iaea.org/books/IAEABooks/7594.

International Atomic Energy Agency, 2008a. Safety of nuclear fuel cycle facilities. In: Safety Requirements No. NS-R-5. IAEA, Vienna.

International Atomic Energy Agency, 2008b. Spent Fuel Reprocessing Options, IAEA-TECDOC-1587. IAEA, Vienna, ISBN 978-92-0-103808-1.

International Atomic Energy Agency, 2009. Safety assessment for facilities and activities. In: General Safety Requirement Part 4. IAEA, Vienna.

International Atomic Energy Agency, 2010a. Handbook on Nuclear Law—Implementing Legislation. IAEA, Vienna.

International Atomic Energy Agency, 2010b. Governmental, legal and regulatory framework for safety. In: General Safety Requirements Part 1, GRS Part 1. IAEA, Vienna.

International Atomic Energy Agency, 2011. Nuclear security recommendations on physical protection of nuclear material and facilities. In: Nuclear Security Series No. 13, INFCIRC/225/Revision 5, IAEA, Vienna.

International Atomic Energy Agency, 2012. Storage of spent nuclear fuel. In: Specific Safety Guide No. SSG-15. IAEA, Vienna.
International Atomic Energy Agency, 2013. The safety case and safety assessment for the predisposal management of radioactive waste. In: General Safety Guide No. GSG-3. IAEA, Vienna.
International Atomic Energy Agency. Safety standards brochure. http://www.iaea.org.
International Atomic Energy Agency. The safeguards system of the International Atomic Energy Agency. www.iaea.org/safeguards/documents/safeg-system.pdf.
International Atomic Energy Authority, 2010. Safety of uranium and plutonium mixed oxide fuel fabrication facilities. In: Specific Safety Guide No. SSG-7. IAEA, Vienna.
Martin, A., Harbison, S., Beach, K., Cole, P., 2012. An Introduction to Radiation Protection, sixth ed. Hodder Arnold, ISBN 978-1-4441-4607-3.
Nuclear Installations Act, 1965. http://www.opsi.gov.uk/RevisedStatutes/Acts/ukpga/1965/cukpga_19650057_en_1.
OECD/NEA, 2001. Trends in the Nuclear Fuel Cycle, Economic, Environmental and Social Aspects. OECD 2001.
OECD/NEA, 2006. Advanced Nuclear Fuel Cycles and Radioactive Waste Management. OECD 2006, NEA No. 5990.
OECD/NEA, 2012. Spent Nuclear Fuel Reprocessing Flowsheet. NEA/NSC/WPFC/DOC (2012)15. OECD 2012.
Office of Nuclear Regulation, 2008. Safety Assessment Principles for Nuclear Facilities, 2006 edition revision 1, www.hse.gov.uk/nuclear/saps.
Office of Nuclear Regulation, 2011. License Condition Handbook. www.onr.uk.
Saito, M., Sawada, T., 2002. Advanced Nuclear Energy Systems Towards Zero Release of Radioactive Waste. Pergamon, Prussia, PA, ISBN 0-08-0441734.
The National Diet of Japan, 2012. The official report of The Fukushima Nuclear Accident Independent Investigation Commission. The National Diet of Japan.
The Nuclear Industries Security Regulations, 2003. www.legislation.gov.uk/uksi/2003.
UN Treaty, July 1968. Multilateral: treaty on the non-proliferation of nuclear weapons. In: UN Treaty Series No. 10485.

Current headend technologies and future developments in the reprocessing of spent nuclear fuels

5

Chris J. Maher
National Nuclear Laboratory, Seascale, UK

Acronyms

AIROX	atomics international oxidation process
CANDU	Canadian deuterium reactor
CEPOD	catalyzed electrochemical plutonium oxide dissolution
DOG	dissolver off gas
DUPIC	direct use of PWR fuel in CANDU
GFR	gas fast reactor
HA	high active
HM	heavy metal
IAEA	International Atomic Energy Agency
IFCs	interfacial cruds
IFPs	insoluble fission products
IMF	inert matrix fuel
LFR	lead-cooled fast reactor
LWRs	light water reactors
MEO	mediated electrochemical oxidation
MOX	mixed oxide
NEA	Nuclear Energy Agency
OREOX	oxidation reduction oxidation process
OSPAR	convention for the protection of the marine environment of the north Atlantic
PWR	pressurized water reactor
SCWR	super critical water reactor
SFR	sodium fast reactor
SIMFUEL	unirradiated simulated fuel
THORP	Thermal Oxide Reprocessing Plant (at Sellafield, UK)
VHTR	very high temperature reactor
Volox	voloxidation

Reprocessing and Recycling of Spent Nuclear Fuel. http://dx.doi.org/10.1016/B978-1-78242-212-9.00005-8

5.1 Introduction

A key part of any reprocessing plant is headend; this is where spent fuel is received and a dissolved product solution of standard composition is produced. The headend currently produces three feeds for other parts of the reprocessing plant: the dissolver product, off-gases, and solid wastes. The position of the headend with the feeds and products are highlighted in Figure 5.1. As solid spent fuel is transformed into an aqueous solution, solids such as cladding and undissolved residues must be removed and dispatched to a waste treatment plant. During headend processing, gaseous and a portion of semivolatile fission products are evolved into the process ventilation system, which is decontaminated in a separate process step, the dissolver off-gas (DOG) treatment plant.

The reprocessing plant will have an overall process aim or specification that can be used to define the requirements for each part of a reprocessing plant. As the headend does not produce any final products, it must meet the requirements for the next process stages. The headend must provide feeds that allow the chemical separation plant, off-gas, and solid treatment plants to meet their objectives. An example of this is shown in Table 5.1. It is logical that any changes to the overall process aims could affect some or all of the final products. This in turn will affect the feed requirements to each process step. As the overall process aims for future reprocessing plants are continuously evolving as technology and regulatory constraints develop, the designs of future headend processes must adapt to these requirements.

A fundamental difference between the headend and any other part of the reprocessing plant is that spent fuel is received. Changes in fuel type or form can have a significant effect on the process steps needed to achieve the requirements for feeds to downstream processes. It is, therefore, highly important for developments in fuel

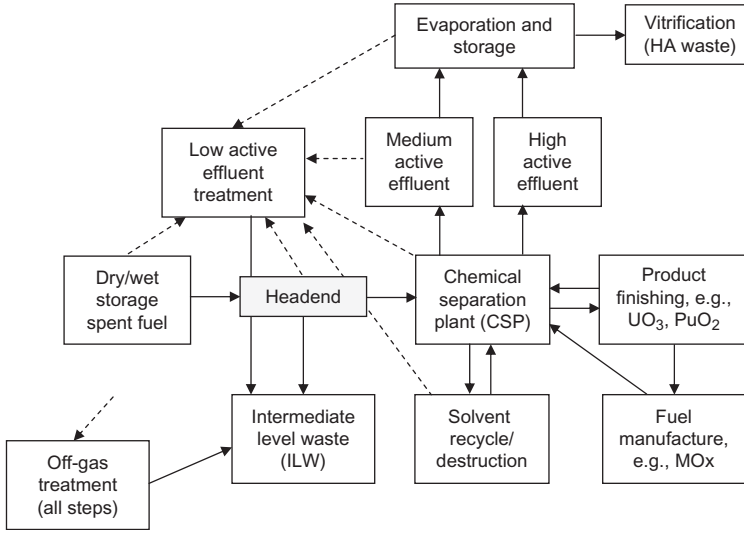

Figure 5.1 Position of the headend in the reprocessing plant.

Table 5.1 Key product requirements

Products	Requirements
Dissolver product	3-4 mol l^{-1} nitric acid Free from settling particulates Minimal organic species Minimal halides present
Off-gases	Minimal suspended spent fuel particulates Minimal quantities of nitric acid/nitrogen oxides
Solid wastes	Minimal undissolved spent fuel Minimal quantity of nitric acid

and reactor technology to be linked to headend development studies. For this reason, the concepts of future reactor and fuel types are summarized in Table 5.2 (GIF, 2002). The consequences of changes to fuel form or type will be the focus of discussion later in this chapter.

There are three other changes that may change the aims of a future reprocessing plant and that could greatly affect the process steps required in the headend. These are

- an increase in the percentage of transuranic actinides that need to be recovered;
- reduction in environmental discharge limits; and
- requirements to recover nonfuel components.

It is common that a small percentage of actinides, typically 0.05-0.5 wt%, is lost to the solid waste stream (NEA, 2012; IAEA, 2003). If there is a future requirement to recover >99.9% of the actinides, clearly improvements in chemical methods or engineering techniques will be needed. Another example is tritium (^{3}H), which is currently distributed between the off-gas, solid waste, and dissolver product streams (NEA, 2012). If a future requirement is to abate or recover tritium, then a significant change to the process steps is needed. Similarly, if there are components of the fuel that are valuable and these need to be recovered for reuse, headend processes must produce a product that is consistent with the recovery process. Examples of nonfuel components that may need to be recovered from the fuel are zirconium from cladding, nitrogen-15 from nitride fuel matrix, molybdenum from alloy, or inert matrix fuel (IMF).

5.2 Current practices

The headend plants that are currently operating use an engineering method of exposing the fuel prior to sending it to the dissolver to aid dissolution. For oxide fuel, following dissolution, hulls and insoluble fission products (IFPs) are removed from the dissolver liquor and then the liquor is conditioned to remove iodine and to convert plutonium to plutonium(IV). Accountancy and buffer storage tanks are also used. This layout is summarized for thermal oxide fuel reprocessing in Figure 5.2. Table 5.3 lists reprocessing plants that are currently operational.

Table 5.2 Summary of future generation IV reactor and fuel concepts (GIF, 2002)

Reactor	Fuel					Cladding	Spectrum, outlet temperature (°C)
	Oxide	Metal	Nitride	Carbide	Fuel description		
Gas fast reactor (GFR)			S	P	(U,Pu)C-SiC	Ceramic	Fast 850
Sodium fast reactor (SFR)		P			U-Pu-Zr	Steel	Fast 550
	P				$(U,Pu)O_2$	Steel	Fast 550
Lead-cooled fast reactor (LFR)		S	P		(U,Pu)N	Steel, ceramic or refractory alloy	Fast 550, Fast 800
Super critical water reactor (SCWR)	P				UO_2	Steel	Fast 550
					$(U,Pu)O_2$ dispersion	Steel	Thermal 550
Very high temperature reactor (VHTR)	P				TRISO U(OC) in graphite compacts; ZrC coating	ZrC coating and surrounding graphite	Thermal 1000

P—primary, S—secondary option.

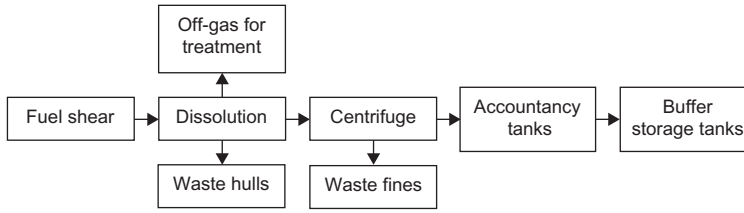

Figure 5.2 Overview of process steps in current generation oxide reprocessing plants.

Table 5.3 Civil reprocessing plants currently operational

Country	Site, name	Commissioning date	Throughput (tHM year^{-1})	Fuel type
UK	Sellafield, Magnox	1964	1500	Magnox
	Sellafield, THORP	1994	1000	LWR + AGR
France	La Hague, UP2-800	1990	800	LWR
	La Hague, UP3	1990	800	LWR
Russian	Mayak, BB, RT-1	1976	400	LWR
Japan	Rokkasho	2005	800	LWR
India	Tarapur	1982	100	PHWR
	Kalpakkam	1998	100	PHWR + FBR
	Tarapur	2011	100	PHWR

AGR, advanced gas cooled reactor; LWR, light water reactor; PHWR, pressurized heavy water reactor; FBR, fast breeder reactor.

5.2.1 Fuel conditioning

It is current practice to declad Magnox (uranium metal) fuel or shear (chop up) oxide fuel assemblies prior to dissolution. These operations remove or breach the cladding to allow good access of nitric acid for dissolution. Magnesium alloy is removed from Magnox fuel as it would dissolve in the dissolution step and this would increase the quantity of dissolved salts and so increase the amount of high active (HA) vitrified glass waste product. As oxide fuel cladding is zircaloy or stainless steel, these materials dissolve to a minimal extent so that they can be chopped up (sheared) and added to the dissolver without contributing significantly to the HA product volume. Fuel conditioning and addition of fuel to the dissolver is the most mechanically engineered part of the reprocessing plant.

Magnox fuel is decanned by feeding the element through a die where the outer heat sink fins are removed. At the start and end of this process the fuel endcaps are cropped with a rotating blade. In the second stage, cutter wheels slit the Magnox cladding along its length and the metal fuel rod is forced through a die allowing the cladding to be peeled away from the metal rod. The bare metal rod is then transferred into a container for movement to the dissolver. This process is illustrated in Figure 5.3.

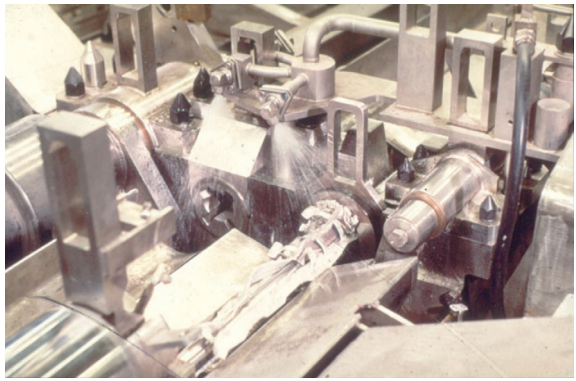

Figure 5.3 Illustration of Magnox decanning.

Oxide reprocessing plants are more modern compared to the Magnox reprocessing plant. This has led to an improvement in efficiency by integrating fuel conditioning and dissolution, hence reducing building and operating costs, thereby improving process efficiency. In THORP and other oxide reprocessing plants (e.g., UP2-800, UP3) fuel conditioning and addition of the fuel to the dissolver is carried out in a single step. This is achieved by chopping the fuel with a large hydrolytic shear; the cut fuel falls down a chute directly into the dissolver. Hydrolytic shears use a hydrolytic gag to hold the fuel securely and a hydrolytic cutting blade to shear the fuel (Asquith et al., 1988). Cuts at intervals of 5-10 cm are typical, which is suitable for leaching of the fuel from the hulls. Some reprocessing plants add the assembly endplates to the dissolver or, alternatively, they can be disposed of via a separate chute. This process is illustrated in Figure 5.4.

5.2.2 Dissolution

The dissolution of spent fuel is the first chemical step in current reprocessing plants. Spent fuel is dissolved in nitric acid as this is the medium of choice for solvent-extraction chemistry; nitric acid reduction chemistry also allows dissolution. Dissolution is carried out either in batch or continuous dissolvers. Dissolvers for oxide fuel use a basket to contain the cropped fuel and cladding pieces, which allows removal of the leached cladding hulls postdissolution. Dissolvers for bare metal rods do not need a basket, as there are not any insoluble cladding components that need to be removed.

5.2.2.1 Dissolvers

The Magnox reprocessing plant uses a continuous "kettle" dissolver, where fuel is dissolved in $\sim$3 mol l^{-1} nitric acid to give a final solution containing 300 g l^{-1} uranyl nitrate. The rate of addition of new fuel and top up nitric acid is controlled to prevent accumulation of fuel in the dissolver; these control the rate of liquor take off.

The THORP reprocessing plant uses three "kettle" batch dissolvers. Sheared fuel falls via a movable chute into one of the three dissolvers, which each contain a basket (Phillips, 1999). This is illustrated in Figure 5.5a. The dissolvers are used in sequence to allow continuous fuel shearing. This sequence allows one dissolver to have the fuel

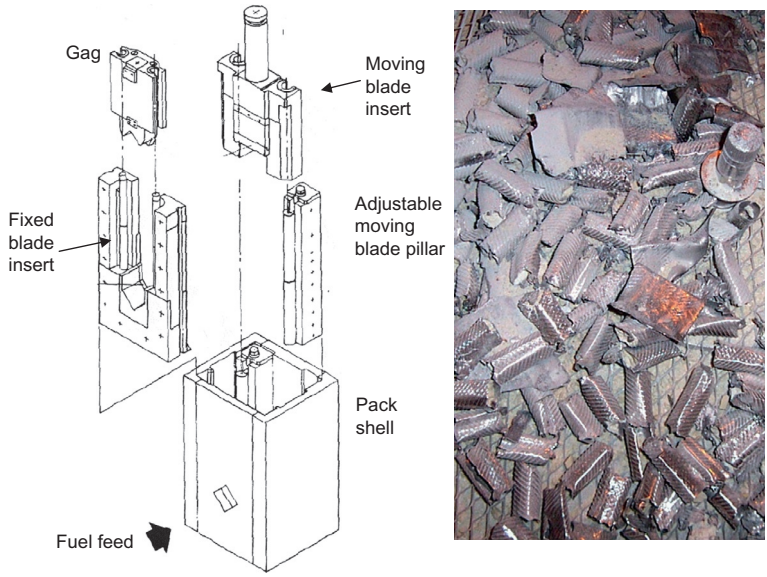

Figure 5.4 Left—illustration of the THORP hydrolytic shear; right—example sheared cross sections from an inactive dummy AGR fuel bundle.

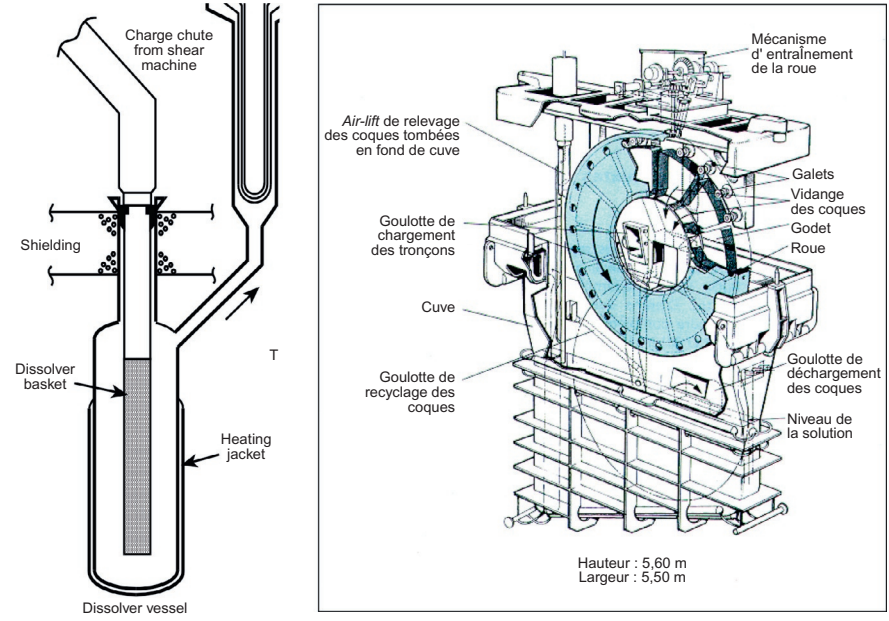

Figure 5.5 Schematic diagram of oxide (a) batch kettle dissolver and (b) continuous rotary wheel dissolver.
Courtesy of CEA.

added, the second is leaching fuel and conditioning the liquor, and the third is being emptied. The fuel is added to the dissolver initially containing ~8 mol l^{-1} nitric acid. The rate of addition of fuel is controlled to allow the vigorous dissolution of the finer crushed fuel to dissolve before the next addition. The dissolution consumes nitric acid resulting in a final solution composition of ~3 mol l^{-1} nitric acid and 250 g l^{-1} uranyl nitrate. Due to the relatively large amount of low-enriched fuel in the THORP dissolver, a neutron poison, gadolinium nitrate, is added to ensure criticality safety is maintained (Bierman et al., 1984).

The French reprocessing plants UP2-800 and UP3 operate a continuous rotary wheel dissolver, Figure 5.5b. These dissolvers have a rotating basket system that receives sheared fuel via a chute, allows dissolution, and empties the baskets in a single rotation of the wheel (Groenier, 1971; Parisot, 2008). A schematic diagram of the dissolver design is shown in Figure 5.5b. The continuous nature of the dissolver means fuel is dissolved in ~3 mol l^{-1} nitric acid to 250 g l^{-1} uranyl nitrate. The dimensions and relatively small amount of fuel in the dissolver means that a neutron poison is not required to maintain criticality safety.

5.2.2.2 *Factors controlling dissolution*

Nitric acid chemistry

It is key to understand the dissolution chemistry in nitric acid and, therefore, some background is provided. Nitric acid can be reduced to form a number of different species (see Figure 5.6) (Jones, 1973). Nitrogen dioxide, monoxide, and dinitrogen oxide are gaseous and so have limited solubilities in nitric acid. Nitrous acid has a limited vapor pressure but decomposes over time to nitrogen monoxide (Sakurai et al., 1988). The rate of decomposition of nitrous acid is determined by the liquor surface area and gaseous nitrogen oxide mass transfer (Fukasawa et al., 1991). The decomposition rate can, therefore, be greatly reduced by gas purges flowing over the liquor or sparges through the liquor.

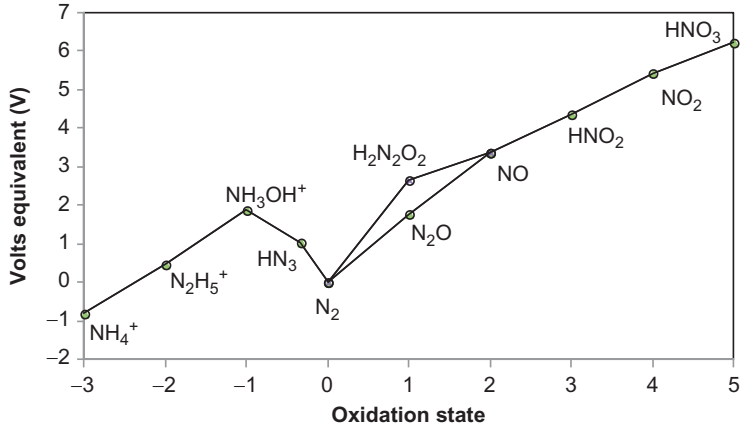

Figure 5.6 Nitric acid reduction chemistry (Jones, 1973).

The concentration of nitric acid (Sakurai et al., 1988), decomposition of nitrous acid and reaction kinetics (Takeuchi and Whillock, 2002) affect the ratio of the nitrogen oxides evolved during dissolution. There is a large variant of different fundamental (de Groot and Koper, 2004; Nakata et al., 2008a,b; Rima et al., 2010) and applied chemistry studies (Elcheikh et al., 1983; El-Egamy et al., 2004; Khalil and Elmanguch, 1987; El Haleem and El Aal, 2008) suggest that nitrous acid and other nitric acid reduction products are the key reactive species in dissolution (Parisot, 2008).

A second key factor in understanding dissolution is surface area. This is because dissolution is a heterogeneous reaction. There are several good examples of this. First, during the dissolution of pellets the changes in surface area follow an S-shape due to initial roughing of the pellets, which leads to an increase in surface area until a maximum is reached, followed by a decrease due to reduction in amount of material (Fukasawa and Ozawa, 1986; Hodgson, 1994). Second, during irradiation macroscopic cracking occurs and microscopic porosity develops (Parisot, 2008), again increasing the surface area available for dissolution. During the shearing of oxide fuel, pellets are crushed (Davis et al., 1979), which increases their surface area. Another significant factor that affects the leaching of fuel is the hulls, which lead to decreased rates of dissolution (Blanc, 1986; Taylor et al., 1963), for example, in a packed bed of the crushed material, and can result in incomplete dissolution for crimped endcaps due to gas locking.

Dissolution of uranium metal fuel

Uranium metal is a highly electropositive metal, with $E_0(U^{4+}/U) = -1.38\ V_{NHE}$ (Bard et al., 1985). Therefore, thermodynamically, dissolution can produce hydrogen; however, hydrogen is often not the kinetically favored reaction product under industrial dissolution conditions (Gresky, 1952). Strong exotherms can occur, which can result in large dissolvers requiring little heating or cooling to control the dissolver temperature. Industrially, dissolvers are often run to produce nitrogen oxides following Equation 5.1. The nitrogen oxides can be recovered either in the dissolver and condenser or in an acid recombination column to produce "fumeless" dissolution (Miles, 1955) according to Equation 5.2. Industrial dissolvers often utilize "fumeless" dissolution technology to varying degrees to minimize the nitrogen oxide burden on the off-gas treatment plant and facilitate the efficient use of nitric acid.

$$U_{(s)} + 5.5HNO_3 \rightarrow UO_2(NO_3)_{2(aq)} + 2.25NO_2 + 1.25NO + 2.75H_2O \tag{5.1}$$

$$U_{(s)} + 2\,HNO_3 + 1.5O_2 \rightarrow UO_2(NO_3)_{2(aq)} + H_2O \tag{5.2}$$

There have been numerous studies of dissolution of uranium metal in nitric acid, showing that surface area, nitric acid concentration, temperature, and the type of alloy are key factors in controlling the dissolution rate (Larsen, 1959; Swanson et al., 1985; Laue et al., 2004a,b; Schulz et al., 1962). Again, these experiments often observe an S-shaped dissolution profile, which is believed to be associated with a combination of the effects of surface area and autocatalytic mechanism, where an initial slow reaction

(with nitric acid) results in a product (nitrite or nitrous acid) that reacts with the fuel and generates more of itself, thereby accelerating both its own formation at the liquid/solid interface and interfacial dissolution simultaneously. This fits with general studies of nitric acid reduction chemistry where nitrate reduction is slow but nitric acid reduction products are more rapid oxidants (de Groot and Koper, 2004). Other workers have studied the sparging of solutions, or adding nitrous acid scavenging agents, which greatly slow the dissolution rate as only the nitrate reduction reaction can take place.

Dissolution of uranium-based oxide fuel

Two types of thermal oxide fuel are currently used in commercial reactors: low-enriched uranium oxide fuel and mixed uranium plutonium oxide (MOX) fuel. Current mixed uranium plutonium oxide fuels are manufactured by mechanical milling uranium dioxide and plutonium dioxide together (IAEA, 2003); this leads to a heterogeneous mix that contains a range of different plutonium contents (Oudinet et al., 2008).

The dissolution of uranium dioxide in nitric acid is known to be greatly affected by nitric acid concentration, temperature and surface area (Taylor et al., 1963). Like uranium metal, uranium dioxide dissolves via an autocatalytic mechanism and experiments lead to rate expressions that separate the nitrate and nitrous acid reaction rates (Carrott et al., 2012). Other process parameters, for example varying the ratio between dissolver liquor surface area and volume, sparging, and stirring have been shown to decrease the rate by depleting the nitrous acid concentration near the interface local to the dissolving solid and bulk solution concentration (Taylor et al., 1963; Shabbir and Robins, 1968, 1969). Results from this type of reaction make it possible to mathematically optimize the dissolution time for different dissolution conditions (Ikeda et al., 1995, 1999; Nishimura et al., 1995). Dissolution is, however, complicated by the presence of hulls, which can lead to a reduction to the dissolution rate by gas-locking or mass-transfer limitations (Blanc, 1986), which means industrial dissolvers are often optimized using more applied chemical engineering approaches. Dissolution experiments have led to expressions describing the rate in terms of nitrogen dioxide and monoxide concentration (Sakurai et al., 1988), as expressed in Equation 5.5. However, it is known that dinitrogen oxide is also produced (Croft and Tonkin, 1950). It must also be recognized that the proportion of nitrogen monoxide is dependent upon the amount of nitrous acid decomposition (Fukasawa et al., 1991; Nishimura et al., 1995) and the amount that is oxidized by oxygen to nitrogen dioxide (Jones, 1973).

$$UO_2 + 4HNO_3 \rightarrow UO_2(NO_3)_2 + 2NO_2 + 2H_2O \tag{5.3}$$

$$UO_2 + 2HNO_3 + 2HNO_2 \rightarrow UO_2(NO_3)_2 + 2NO + 2H_2O \tag{5.4}$$

$$3UO_2 + 4(2+x)HNO_3 \rightarrow 3UO_2(NO_3)_2 + 2(1-x)NO + 6xNO_2 + 2(2+x)H_2O$$

$$\text{where } 0 < x < 1 \text{ (Sakurai et al., 1988)} \tag{5.5}$$

The dissolution of MOX occurs via the same mechanism (Carrott et al., 2012), which is reasonable, but small plutonium-rich regions (Oudinet et al., 2008) lead to incomplete dissolution (Wurtz, 1987). This is expected, as the reaction between plutonium dioxide and nitric acid (or its reduction products) is thermodynamically much less favorable than the reaction of UO_2 (Madic et al., 1992). The decrease in solubility of MOX at 20-40 wt% plutonium has been demonstrated experimentally (Parisot, 2008; Vollath et al., 1985).

The presence of plutonium-rich particulates resulting from the industrial dissolution of MOX fuel is a criticality hazard that requires careful management. A great deal of work is necessary to justify the routing and control of these plutonium-rich particulates before industrial reprocessing is possible; for example, as justified and demonstrated in the French reprocessing plants at La Hague (Dancausse et al., 2008; Emin et al., 2005).

The formation and control of solids and precipitates in the headend

During the irradiation of oxide fuel, refractory-noble metal alloys form inclusions at grain boundaries; these are called ε-phase and contain molybdenum, technetium, rhenium, ruthenium, and palladium metals (Kleykamp, 1985). During dissolution, these particulates dissolve slowly and do not dissolve completely. The resulting particulate residues are termed IFPs.

As the burn up of fuel increases, the concentration of a large variety of fission product elements also increases. This leads to the formation of precipitates during dissolution, such as noble metal iodides or iodates (Sakurai et al., 1991) or zirconium molybdate (Magnaldo et al., 2007; Doucet et al., 2002; Usami et al., 2010). At even higher burn ups it is reasonable to expect that other precipitates will also form.

The formation of noble metal iodides and iodates is less of an issue, as smaller quantities of solids form. The solids are fine in nature and do not form on surfaces. During dissolver cycles the extent of formation is minimized, as iodine is removed from the dissolver solution; see below for further details.

Optimization of processing conditions in industrial dissolvers with the aim to achieve tolerable levels of zirconium molybdate formation are important as zirconium molybdate forms on surfaces in the dissolver, leading to the development of so-called cow pat deposits. The effects of temperature, nitric acid, molybdate and zirconium concentration are known to be key factors in the formation rate of zirconium molybdate (Magnaldo et al., 2007; Doucet et al., 2002; Usami et al., 2010). For industrial dissolvers, the preferred adjustable process parameter is temperature. In industrial dissolver cycles, the peak temperature is, therefore, often minimized to slow the formation rate of zirconium molybdate. At La Hague, parts of the reprocessing plant are leached with sodium carbonate to dissolve the zirconium molybdate and prevent chromic buildup (Rosse et al., 2012); a similar approach is employed in THORP, but using salt-free reagents (Jiang et al., 2005).

IFPs, together with fragments of cladding, precipitates (e.g., silver, palladium iodide, zirconium molybdate), and undissolved fuel (e.g., plutonium-rich particulates from MOX dissolution) form the dissolver insolubles.

5.2.3 Dissolver liquor conditioning

Current oxide reprocessing plants focus on three tasks during fuel conditioning: (i) removal of the majority of the iodine, (ii) conditioning plutonium to the tetravalent state, and (iii) removal of particulates. These three tasks are explained in the following three sections.

5.2.3.1 Iodine

Iodine is evolved into the off-gases in the headend to minimize accumulation in the organic phase in the solvent-extraction plant and to minimize aerial discharges through the reprocessing plant. It is typical that Magnox and thermal oxide fuel is cooled for a number of years prior to reprocessing, and this has the advantage that iodine-131 ($t_{½} = 8$ days), which has a high radiotoxicity, has decayed sufficiently to leave only the long-lived iodine-129 isotope ($t_{½} = 1.57 \times 10^7$ years).

During dissolution in nitric acid iodine is capable of existing in multiple oxidation states in equilibrium with each other (see Figure 5.7) (Sakurai et al., 1991, 1992, 1993, 1996; Boukis and Henrich, 1991). As elemental iodine has an appreciable vapor pressure it is evolved into the process off-gases; these act as a driving force to adjust the equilibrium to force the majority of the iodine to the off-gas system where it can be trapped or scrubbed from the gas stream. Solid silver or palladium iodides or iodates can form and are kinetically slow to dissolve as the solids "age" (Sakurai et al., 1991). Iodates can also be kinetically slow to equilibrate to iodine. The presence of iodine-containing solids or iodates can reduce the efficiency of iodine removal, resulting in a few percent of iodine remaining in the dissolver solution.

THORP batch dissolvers and the continuous dissolvers at La Hague employ different methods for maximizing the removal of iodine. The batch dissolvers can simply apply a sparge toward the end of the dissolver cycle, after dissolution is complete, removing the remaining fraction. For continuous dissolvers, the use of a sparge is not desirable as the dissolution rate is too slow to sequester the iodine that is produced. To achieve removal from continuous dissolver liquors a separate process step is used. The liquor flows through a column with a countercurrent air flow, transferring the majority of the iodine into the process off-gas stream (Wilson, 1996).

5.2.3.2 Plutonium(IV) conditioning

Plutonium can exist as a mixture of tetravalent and hexavalent oxidation states after dissolution. Continuous dissolution tends to produce a tetravalent product, whereas during the later stages of batch dissolution, when there is a low nitrous acid

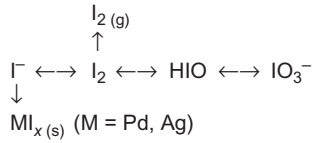

Figure 5.7 Multiple oxidation states of iodine in dissolver.

concentration, plutonium is partially oxidized to the hexavalent state (Wilson, 1996). As tetravalent plutonium is preferred for solvent-extraction processes, toward the end of the THORP batch dissolver cycle a mixture of air and nitrogen dioxide is sparged through the dissolver solution. This reduces the plutonium to the tetravalent state (see Equation 5.6) (Cleveland, 1970; Coleman, 1965). Radiolytic reduction (Rance et al., 2000) can also take place.

$$PuO_2(NO_3)_2 + HNO_2 + 2HNO_3 \rightarrow Pu(NO_3)_4 + H_2O \tag{5.6}$$

5.2.3.3 Removal of particulates

The removal of dissolver insolubles is carried out to minimize the accumulation of solids in downstream plants (Wilson, 1996). This is important as the solids are heat-generating due to their intense radioactivity. Also, irradiated MOX insolubles contain plutonium-rich particulates (Dancausse et al., 2008), which need to be removed and routed to a single location with high efficiency. Another important reason for removal of particulates is to minimize the formation of interfacial cruds (IFCs) in the first solvent-extraction cycle, which can lead to a reduction in solvent-extraction performance. The dissolver insolubles are removed by centrifugation. An example of an industrial centrifuge is shown in Figure 5.8 (Wilson, 1996). After a defined amount of liquor has been processed through the centrifuge, the bowls are washed and slurried solids are transferred to the waste plants for encapsulation.

5.2.4 Accountancy and buffer storage

Clarified dissolver product liquor is collected in tanks to allow accountancy checks by weighing the liquor and sending samples for analysis. This is the first point in a reprocessing plant where fuel accountancy can be implemented. Monitoring mass balances through the reprocessing plant is important to demonstrate control to regulators and international safeguards. Plant operators and international safeguards analyze samples to ensure that material is not diverted for other uses. The accountancy tanks or other separate tanks also act as buffer storage between the headend and chemical separation plants to ensure efficient continuous operation of the entire reprocessing plant.

5.3 Potential developments to meet future challenges

Future reprocessing plants may be required to process advanced fuels with very high burn ups. It may be necessary to achieve improved actinide recoveries (Carrott et al., 2012) and the recovery of other valuable materials, such as zirconium-based cladding. This may also need to be achieved against a much lower, near-zero discharge authorization limit (OSPAR, n.d.).

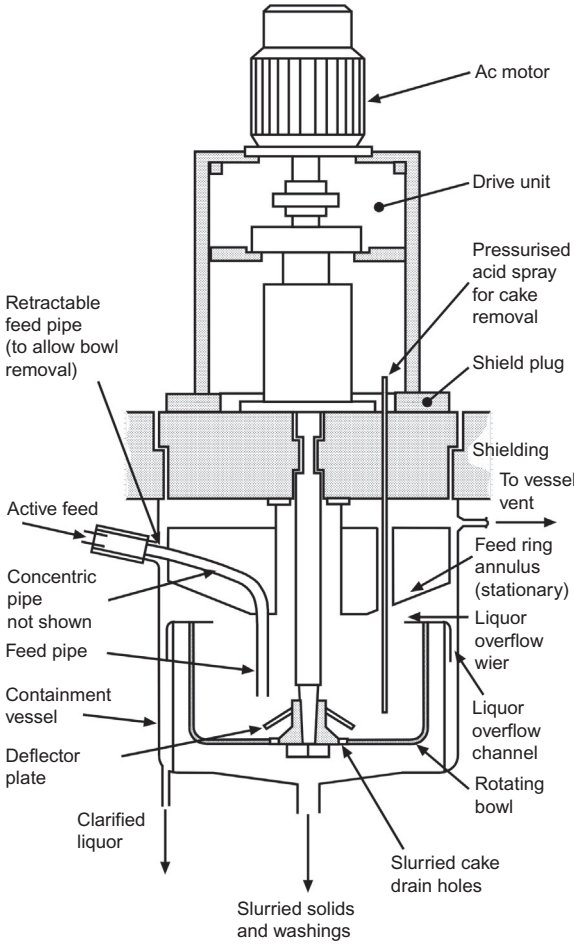

Figure 5.8 Industrial centrifuge used for clarification of the dissolver product.

The detailed justification of overall reprocessing plant specification is an often emotive subject, which needs to be studied and debated in depth in future years. Potential improvements are easy to discern

- An improvement in fuel recovery toward 99.99%
- Recovery of other valuable materials for reuse
- Reduction of radioactive discharges to near-zero
- Enhanced safety—improved management of conventional, radiological and criticality risks.

The improvement in actinide recovery could be of interest in reducing the long-lived radioactivity to high-level waste. This is of increased interest as development of solvent-extraction processes to recover uranium, neptunium, plutonium, americium, and curium reduces the radiotoxicity by more than five orders of magnitude in approximately 500 years (Carrott et al., 2012). The answer to requirements for

readily dissolvable fuels may well lie in improved process engineering but for harder to dissolve materials, such as MOX, improved dissolution technologies will be needed.

The recovery of fuel materials has the advantage of potentially reducing the volume and amount of waste, which will ultimately be stored in a geological disposal facility, and may make the material available for reuse. Examples of potential materials for recovery include zirconium from cladding or inert matrix materials, molybdenum from inert matrix or alloying, and nitrogen-15. Zirconium is an expensive metal that is considered a strategic resource (Collins et al., 2012). Isotopically purified molybdenum may be used to minimize the production of long-lived technetium-99. As the isotopic purification of the molybdenum is likely to be expensive, recovery and reuse of molybdenum is potentially required. The use of nitrogen-15 is important for nitride fuels, where it minimizes the quantities of carbon-14 produced (Matzke, 1986); again, recovery processes could be warranted.

In Europe the introduction of OSPAR, the convention for the protection of the marine environment of the northeast Atlantic, will require near-zero discharges of radioactive elements (OSPAR, n.d.). Current and future discharges of radionuclides into the environment will need to be set against the continued use of fossil fuels for energy production. The issue at the center of this evaluation is the definition of acceptable levels of radioactive discharges. A fundamental requirement will be that the risk due to radioactivity both locally and globally from nuclear fuel cycle operations is low. From these discussions it can be envisioned that there are several options to consider, these include

- Reduce risk of substantial failure
- Refine existing processes
- Abate tritium
- Abate noble gases

Existing abatement processes are discussed elsewhere; notably, carbon-14 (in the UK) (Wilson, 1996) and iodine-129 (in France) (Parisot, 2008) abatement. Improvements in abatement of these isotopes remain a possibility. This may be particularly warranted for short-cooled fuels, which contain iodine-131. The abatement of tritium is a potential future requirement along with other low-energy and radiotoxic isotopes. As tritium is currently distributed between dissolver liquor, off-gases, and solid waste streams this will require the use of technology before dissolution. There are currently no industrially viable processes for the abatement of krypton-85 and other noble gases, due to the inherently low radiotoxicity of noble gases and the difficulties associated with handling gases, also in passively safe storage. Infinite dispersal has, therefore, been considered the best practical method (NEA, 1980). If, in the future, noble gas abatement will be considered desirable, technology development will be necessary.

The implementation of new technologies is always subject to weighing the benefits against the disadvantages, which includes financial and risk analysis. Recent global events will lead to increased and more detailed analysis of hazards, greater scrutiny of facilities and processes, and expectations for improved safety in future sustainable nuclear fuel cycles.

5.3.1 Dissolution chemistry of alternative fuel types

5.3.1.1 Oxide fuels

Mixed uranium plutonium oxides are currently used in thermal reactors. Due to the maturity of mechanical oxide fabrication technology it is likely that MOX for future thermal and fast reactors will continue to be produced in this way for some time. The current MOX manufacturing technologies use milling techniques to intimately mix the uranium and plutonium. This, however, does not provide perfect homogenization at atomic length-scales and plutonium-rich heterogeneities remain (Oudinet et al., 2008). These heterogeneities lead to plutonium residues after dissolution (Wurtz, 1987). The percentage of residues is dependent on the quality of the manufacturing process, but typical residues postirradiation of thermal fuels (~5 wt% Pu) are 0.1-0.3% (NEA, 2012). Depending on the manufacturing and reactor conditions, fast reactor fuels can have lower solubilities (Matzke, 1986). For example, with 0.5 wt % plutonium residues for 20 wt% MOX, one kg of plutonium would be destined for waste per ton of heavy metal reprocessed. This is clearly unacceptable, from the perspectives of waste minimization, plant criticality control, and fissile material utilization. Future developments in dry manufacturing techniques could result in incremental improvements; however, it is expected that residues will continue to be an issue. The use of chemical precipitation techniques for manufacture of MOX could result in more homogeneous material that can wholly dissolve in nitric acid without leaving plutonium-rich residues (Lerch, 1972; Uriarte and Rainey, 1965). However, the dry manufacturing techniques are currently in use, and thus produced fuels will need to be dissolved for reprocessing.

If future fuel cycles include recycling of minor actinides (neptunium, americium, and curium), then the consequences of fuels containing elevated levels of these elements during dissolution will need to be assessed as well. However, there is significant opposition to recycling curium. Currently the recycling of americium-containing MOX seems a more likely development (Wallenius, 2010).

The dissolution rate of MOX decreases with increasing plutonium content (Parisot, 2008; Vollath et al., 1985; Ikeuchi et al., 2012), due to the unfavorable thermodynamics of plutonium dioxide dissolution, which has also been empirically explained in terms of kinetics (Uriarte and Rainey, 1965). Dissolution is slowed and ultimately halted by reducing the rates of initiation and of the rapid autocatalytic nitrous acid dissolution cycle. Figure 5.9 illustrates this phenomenon through an example of 8-h leaching experiments on MOX with increasing plutonium content, under otherwise identical conditions, in 5 and 10 mol l^{-1} nitric acid (Vollath et al., 1985).

5.3.1.2 Carbide fuels

Enriched uranium monocarbide and mixed uranium plutonium monocarbide have been used as protoype fast reactor fuels. Mixed uranium plutonium and minor actinide fuels are candidate fuels of the future (GIF, 2002; Matzke, 1986; Wallenius, 2010; EC, 2013). Carbide fuels have potential benefits over oxide fuels; for example, better neutron physics properties, which allow improved transmutation or breeding efficiency

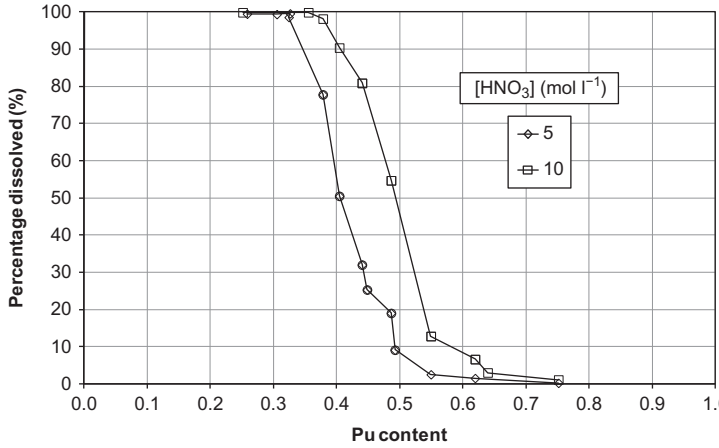

Figure 5.9 Extent of MOX dissolution for various plutonium contents (Vollath et al., 1985).

(Matzke, 1986; Wallenius, 2010). Actinide carbides react more energetically with many oxidants compared with oxides, placing a requirement to work in anaerobic conditions for finely divided material (Berthinier et al., 2011, 2013). This has implications for fuel shearing.

The primary issue for the reprocessing of carbide fuels is the dissolution in nitric acid, where a fraction of the carbon remains in solution as organic acids (Bradley and Ferris, 1962, 1964a,b; Ferris and Bradley, 1965) according to Equation 5.7. These organic acids are highly substituted with alcohol and carboxylic acid groups and include oxalic and mellitic acids (Choppin et al., 1983). These compounds decrease the extraction, backwashing, and phase-settling properties in solvent-extraction processes and, therefore, the soluble organic content must be destroyed. Dissolution followed by destruction is indeed an option. The dissolution rate of actinide carbides increases with surface area, nitric acid concentration and temperature (Ferris and Bradley, 1965). Recent studies have also demonstrated the role of nitrous acid in the dissolution mechanism (Maslennikov et al., 2007, 2009). Although not demonstrated, it is reasonable to assume that an autocatalytic mechanism initiated by nitrate reduction occurs. Experiments studying the off-gases during dissolution have shown that dinitrogen oxide is present to a larger extent during carbide than oxide fuel dissolution (Glatz et al., 1990). This suggests that nitrogen monoxide reduction plays a more significant role and probably reflects the more electronegative nature of carbides.

$$\mathrm{UC} + x\mathrm{HNO_3} \rightarrow \mathrm{UO_2(NO_3)_2} + \mathrm{aNO_2} + \mathrm{bNO} + \mathrm{cN_2O} + \mathrm{dN_2} + \mathrm{CO_2} + \mathrm{organics_{(aq)}} \tag{5.7}$$

The nitric acid consumption is much higher compared to oxides, as the carbon is at least partially oxidized. Like oxides, the dissolution rate is dependent upon nitric acid

concentration, with reaction product stoichiometry increasing from 4 to 10 as the initial nitric acid concentration is increased from 2 to 15.8 mol l^{-1} (Ferris and Bradley, 1964).

5.3.1.3 Nitride fuels

Like actinide carbides, nitrides are under consideration due to their potential improvements in reactor performance (Matzke, 1986; Wallenius, 2010). Nitrides are more reactive toward oxidation compared to oxide.

A key issue for the viability of nitrides is that natural nitrogen nitride fuels generate large quantities of carbon-14. This is illustrated in Table 5.4 (Matzke, 1986). For this reason nitrogen-15 is more likely to be used in the future, although the high cost of nitrogen-15 will mean that recovery for reuse may be necessary.

Studies of the dissolution of uranium nitride in nitric acid show rapid dissolution rates under nitric acid concentrations of industrial interest (Ferris, 1968; Sugihara and Imoto, 1969). The dissolution results in oxidation to uranyl and ammonium ions, according to Equation 5.8. The ammonium can then be oxidized further, as in Equation 5.9. The dissolution results in larger amounts of dinitrogen oxide (N_2O) and nitrogen (N_2) gases compared to oxide fuel, due to the oxidation of ammonium. The fact that ammonium is produced and oxidized by nitric acid means that its reduction products lead to the isotopic dilution of nitrogen-15, thereby complicating and reducing the viability of nitrogen-15 recovery (Hadibi-Olschewski et al., 1992). For this reason, the direct dissolution of nitrogen-15 nitrides in nitric acid is unlikely to be the first chemical treatment step for their reprocessing.

$$UN + 4HNO_3 \rightarrow UO_2(NO_3)_2 + NH_4NO_3 + NO \tag{5.8}$$

$$5NH_4^+ + 3NO_3^- \rightarrow 4N_2 + 2H^+ + 9H_2O \tag{5.9}$$

5.3.1.4 Alloys, composite materials, and inert matrix fuels

Alloyed, composite, and IMFs have been grouped together as they differ considerably from the materials described so far. These materials contain a substantial quantity of other elements with low neutron absorption properties; that is, they are "inert." These fuels include actinide-zirconium metal alloy fuel (sodium fast reactor, SFR),

Table 5.4 Comparison of ^{14}C production for 30 GWd tHM^{-1} fuel of various types (Matzke, 1986)

	MO_2	MC	$M^{14}N$	$M^{15}N$
^{14}C produced (GBq tHM^{-1} at ~30 GWd tHM^{-1})[a]	5.9	340	19,000	190

[a]Dependent upon neutron specimen, MO_2 based on 20 ppm C and 20 ppm N (natural isotopic composition), MC based on 1000 ppm N (natural isotopic composition), $M^{15}N$ assumes 99% ^{15}N.

silicon-actinide carbide composite ($(U_{0.8}Pu_{0.2})$C-SiC, Gas Cooled Fast Reactor, GCFR), "Triso"-type fuel (very high temperature reactor, VHTR), plutonium-zirconium nitride ($(Pu,Zr)^{15}N$, IMF), actinide oxide-molybdenum metal composite (e.g., $(Pu_{0.8}Am_{0.2})O_2$-Mo, IMF), and actinide oxide-magnesium oxide (PuO_2-MgO, IMF). They are either used as the major reactor fuel in reactors or as targets for transmutation to reduce the actinide content.

These fuel types are more problematic to reprocess as they either do not dissolve in nitric acid or dissolve to produce a product that contains additional metals that need to be recovered or cause concerns to the headend or solvent-extraction process chemistry. Some examples of these difficulties are described below:

- Actinide-zirconium metal alloy fuel does not readily dissolve in pure nitric acid (Laue et al., 2004a,b) and if dissolution is possible, zirconium-rich residues are an explosive hazard (Gens, 1958).
- GCFR and VHTR fuels are composites that include silicon carbide or carbon and refractory coatings, making fuel recovery difficult without intensive milling techniques prior to dissolution, for example (Goode and Flanary, 1967).
- Plutonium zirconium nitride IMF requires nitrogen-15 recovery. A two-step dissolution process has been proposed and is currently under testing. This involves hydrolysis to a hydrous oxide that allows recovery of the nitrogen-15 and then a second step to dissolve plutonium-rich oxides using aggressive reagents capable of doing this (EC, 2013).
- A similar approach for actinide oxide-magnesia or molybdenum metal composite materials has been proposed and is undergoing testing (EC, 2013). The first step is to dissolve the magnesia or molybdenum metal under cool dilute nitric acid. This is followed by the dissolution of the plutonium-rich oxides in a second, more aggressive step. It is hoped that this will allow the dissolved magnesium to be diverted away from the high-level wastes minimizing waste volumes. It is also hoped that the separate dissolution of molybdenum will allow the recovery of the isotopically enriched molybdenum for reuse (Bakker et al., 2004). This procedure also offers the potential to avoid the formation of solid molybdates, which are known to form when solutions are rich in actinides and molybdenum, for example (Schulz, 1960). These processes are shown schematically in Figure 5.10.

5.3.2 Fuel conditioning—potential benefits of fuel pretreatment

There are a number of reasons why future headend processes may deviate from the simple declad-leach and shear-leach process used today. These include

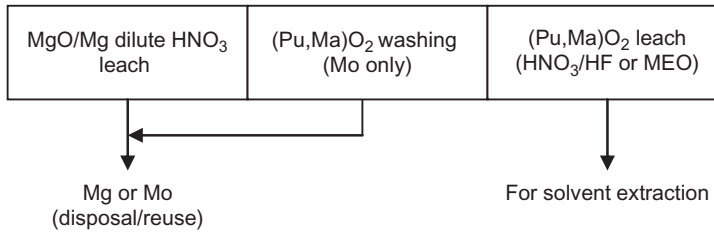

Figure 5.10 Two-step process to $(Pu_{0.8}An_{0.2})O_2$-MgO and PuO_2-Mo IMF.

- Mechanical processes that may be necessary to allow exposure of the fuel for dissolution.
- Chemical processes that may be necessary to prepare fuel before conditioning, for example, metal coolant debonding.
- Improved control for volatile fission products, for example, to allow tritium abatement.
- Simplification of dissolution process by preconverting material, for example, carbide to oxide.
- Recovery of fuel or cladding materials for reuse, for example, nitrogen-15 or molybdenum.

5.3.2.1 *Mechanical fuel preparation processes*

It is probable that fuels that are similar in design, such as GCFR actinide carbide with silicon carbide cladding, could be dismantled and sheared as a fuel preparation step. However, reactor fuels that are radically different from a rod or pellet in cladding are likely to require alternative techniques to prepare the fuel. Depending upon the design of the fuel, these processes could be very different from the current cladding stripping (Magnox metal fuel) and shearing (oxide fuel). Examples of fuels that are substantially different from conventional fuel types are (GIF, 2002)

- GCFR actinide carbide-silicon carbide composition fuel.
- VHTR fuel, which is a fuel microsphere surrounded by pyrolytic carbon and ceramic shells compacted into a rod or pebble.

Concepts to treat these fuels, including crushing and milling to breach the refractory components and allow access to the fuel for dissolution, have been developed (Goode and Flanary, 1967). Attempts to recover fuel from VHTR Triso-type fuels using the "grind-leach" process have shown a degree of success, with recoveries of 99.6% uranium. An example of this type of process is shown in Figure 5.11.

Currently, little work has been published about how to recover fuel from GCFR composite fuels. If the fuel is carbide pellets in silicon carbide cladding, recovery could be readily achievable; however, if actinide-silicon carbide, alloy, or composite are used, recovery could be more of a challenge to an aqueous headend.

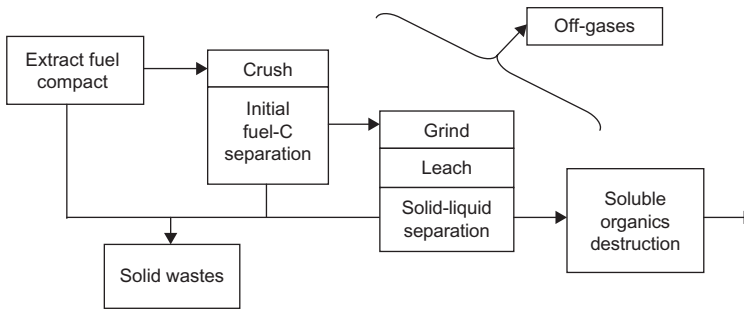

Figure 5.11 VHTR fuel "grind-leach" process.

The drive for process intensification to achieve higher throughputs in smaller plants or achieve improved fuel recoveries may also lead to consideration of replacing the shearing process with new innovative fuel preparation techniques (Bond et al., 1992).

5.3.2.2 Fuel pretreatment using high- and low-temperature processes

Oxides

High-temperature pretreatments that oxidize uranium dioxide to higher oxides have been under development for decades but not deployed in large-scale industrial reprocessing plants. These processes have been developed with different end purposes in mind:

- Volox—voloxidation, a method of removing volatile fission products from fuel to allow abatement and simplify the dissolution cycle (Goode, 1973).
- OREOX—oxidation reduction oxidation process is a development of the Volox process that uses alternate oxidation reduction processes to achieve higher efficiency of fission product removal (Strausberg et al., 1960).
- AIROX—atomics international reduction oxidation process is an OREOX process to allow pulverization of fuel in fuel rods with holes punched in them. This allows fuel and cladding separation before dissolution (Majumdar et al., 1992).
- DUPIC—direct use of PWR fuel in CANDU process is not strictly a headend to reprocessing; it is a pyrochemical method for fuel reprocessing. The concept allows the removal of some fission products prior to refabrication into fuel (Lee et al., 2012).

These processes essentially use the same chemistry, the oxidation of uranium dioxide to higher oxides, Equation 5.10, with the accompanying decrease in density ($\sim$11-8.4 g cm^{-3}), thus allowing fuel pulverization. During this process, depending upon the process conditions, various amounts of tritium, carbon-14, iodine-129, kryption-85, and semivolatiles, including caesium and ruthenium, are evolved. The fuel expansion process can also be used to break open cladding that has been punctured (AIROX process), thereby avoiding the need for a shear process, or the process could be carried out upon sheared fuel.

$$3UO_2 + O_2 - \text{via}\,(U_3O_7, U_4O_9) \rightarrow U_3O_8 \tag{5.10}$$

From experiments with unirradiated and irradiated materials, it is known that the presence of elements that cannot be oxidized in the solid state affects the process chemistry. Examples include the presence of plutonium (Rance and Beznosynk, 2005), thorium (Anderson et al., 1954), MOX or alkaline and rare earth elements (SIMFUEL or irradiated fuels) (Kang et al., 2007) with uranium. These reduce the material reactivity as there is a smaller percentage of uranium to provide the driving force for pulverization and release of fission products. The presence of high contents of these dopant elements can stabilize intermediate phases, increase temperature or oxidant conditions to achieve oxidation, and ultimately at high contents prevent oxidation (Thomas et al., 1993; McEachern et al., 1998).

Experiments oxidizing SIMFUEL with varying portions of simulated fission products show that the presence of >7% fission products (equivalent to ~70 GWd tHM^{-1}) greatly stabilizes the $(U,Fp)_4O_9$ phase[1] at 400 °C (Cobos et al., 1998). To achieve oxidation, an increase in temperature to 800 °C is needed.

During the oxidation of mixed uranium plutonium oxide, the material oxidizes to a plutonium-rich dioxide phase and a uranium-rich higher oxide phase, Equation 5.11 (Rance and Beznosynk, 2005). During this type of oxidation test, the solubility of plutonium in the M_3O_8 phase has been observed to be ~3% Pu HM^{-1}, which means that oxidation of most MOX will result in the formation of plutonium-rich oxide particulates. This reduces the proportion of the plutonium dissolved in nitric acid (Cadieux and Stone, 1980). However, at higher plutonium contents oxidation does not occur and experiments up to 900 °C have shown that unirradiated 20-25% Pu HM^{-1} MOX does not result in pulverization. Similar segregation is also observed for the oxidation of mixed uranium thorium oxide and, as thorium oxide does not dissolve readily in nitric acid (Anderson et al., 1954; Goode and Stacy, 1979), results in an increase in difficult to dissolve thorium oxide residues.

$$3(U, Pu)O_2 + xO_2 \rightarrow (1-x)MO_2 + xM_3O_8 \tag{5.11}$$

The oxidation of spent thermal and fast reactor fuels have been studied at the laboratory scale. These experiments have studied the effect of temperature, feed flow rate, and oxygen concentration upon the extent of fission product removal, for example (Goode, 1973). This type of experiment has shown that near-complete tritium removal is possible at moderate temperatures (480 °C) (Goode et al., 1980). Less complete removal of the noble gases and iodine-129 has been achieved (see Table 5.5).

Oxidation of fuel at higher temperatures, for example, greater than 700 °C, increases the amount of the so-called semivolatile elements that are released

Table 5.5 Effect of voloxidation conditions upon noble gas and iodine-129 removal (Goode, 1973)

			Volatilised (%)	
T (°C)	$[O_2]$ (%)	Gas flow (cfh)	^{85}Kr-^{133}Xe	^{131}I
450	75	0.2	19	~8
750	75	1.0	69	~99
450	25	0.2	73	~85
750	75	1.0	42	~90
450	75	1.0	36	~33
750	75	0.2	76	~95
450	25	1.0	11	~38
750	25	0.2	~99	~92

[1] Fp and M are used as chemical symbols to represent fission products (largely alkaline and rare earth elements) and general metals, respectively.

(Goode, 1973). Examples of fission products that are evolved in significant quantities are caesium-137, ruthenium-106, antimony-125, and niobium-105. Experiments underpinning the DUPIC cycle development show that oxidation at higher temperatures quantitatively increases the release and number of semivolatile elements (Bateman et al., 2006). These experiments also observe that control of the oxidation conditions can suppress the distillation of caesium and other elements by formation of less-volatile oxides. Oxidation of spent fuel and distillation of fission product elements under high-temperature conditions can be compared with studies of fuel distillation under severe reactor failure, such as Kundsen cell mass spectrometry studies (Capone et al., 1996).

The oxidation of irradiated fast reactor 20% Pu HM^{-1} MOX has also been demonstrated (Goode, 1973). These experiments have shown that despite the difficulties in the oxidation of unirradiated 20% Pu HM^{-1} MOX (Rance and Beznosynk, 2005), the oxidation of irradiated MOX is achievable. Removal efficiencies of noble gases of up to 98% at 750 °C has been demonstrated, which is excellent considering a portion of the noble gases are likely to be trapped in plutonium-rich oxides and not released. Comparing these results with irradiated uranium oxide experiments suggests good removal efficiencies of tritium, carbon-14, and iodine-129 will also be possible. This type of test clearly shows oxidation of 20% Pu HM^{-1} MOX is possible.

More recent advanced voloxidation studies have focused on the use of strong oxidants such as nitrogen dioxide and ozone (DelCul, 2010). These oxidants are capable of oxidizing uranium dioxide to trioxide, for example, Equation 5.12, and show promise that near-quantitative removal of tritium, carbon-14, noble gases, and iodine-129 are possible at temperatures lower than air or oxygen.

$$UO_2 + O_3 \rightarrow UO_3 + O_2 \tag{5.12}$$

Carbides and nitrides

The conversion of carbides and nitrides to oxides could be an important step to allow

- Carbides—removal of carbon that prevents the generation of organics during dissolution.
- Nitrides—evolution of nitrogen-15 predissolution for recovery.
- Carbides and nitrides—the removal of fission products for abatement.

These processes can be carried out with a variety of oxidants and temperatures. The conditions necessary tend to be more moderate compared to oxide due to the reactivity of the materials. However, the reactivity also leads to concerns over pyrophoricity of the materials, which means careful control to prevent ignition is a key consideration.

The oxidation of uranium carbide and nitrides with oxygen or air leads to the formation of triuranium octoxide. The accompanying density change is even greater than that for uranium dioxide oxidation, so although these reactions have not been studied in as much detail as the oxidation of uranium dioxide, the uranium dioxide oxidation literature can be used as a starting point. This leads to two conclusions:

- Efficient removal of volatile fission products should be achievable.
- Segregation of uranium and plutonium phases will lead to incomplete plutonium recovery during dissolution in nitric acid. The extreme case for carbide is illustrated in Equation 5.13.

$$(U, Pu)C + xO_2 \rightarrow yU_3O_8 + zPuO_2 + O_2 \quad (5.13)$$

However, there is a significant density change in the conversion of carbides or nitrides to dioxides, 13.6 or 14.3-11.0 g cm^{-3}, respectively. This density change is sufficient to cause pulverization of pellets. This could be used to as a pretreatment process to convert mixed uranium plutonium carbides or nitrides to oxides, with high plutonium solubility. This type of process has been demonstrated for unirradiated mixed uranium plutonium carbides using carbon dioxide (Murbach and Turner, 1963) and steam (Flanary et al., 1964). These processes proceed with two steps: oxidation to the dioxide and carbon followed by reaction of carbon. Of the two reactants, carbon dioxide is often preferred as water is prone to leave residual carbon and produces hydrogen as a product. However, the use of carbon dioxide or water as an oxidant for irradiated carbons would result in the abatement of very large quantities of carbon dioxide or water during the abatement of carbon-14 and tritium.

The conversion of mixed uranium plutonium nitride to solid-state mixed dioxide may provide a method of removing nitrogen-15 without reducing the plutonium solubility.

5.3.3 Developments in dissolution chemistry and technology

Whether or not pretreatment processes are used as a fuel preparation technology prior to dissolution it is likely that developments beyond the direct dissolution in nitric acid will need to be used. Examples of this include destruction of organics from direct dissolution of carbides and the dissolution of plutonium oxide (from IMF) or plutonium-rich oxides (MOX or voloxidized fuel). The dissolution of thorium oxide or thorium-containing fuels may also fall into this category. There is also likely to be interest in the multicycle leaching processes for composite fuels.

As the recovery of plutonium-rich oxide is likely to drive the development and use of enhanced dissolution technologies, the dissolution chemistry of pure plutonium oxide is a good starting place for any developments. It is widely reported there are three methods for the dissolution of plutonium dioxide:

- Use of strong complexants, the classic method is fluoride (Nikitina et al., 1997).
- Oxidative dissolution using cerium(IV) or silver(II) (Seaborg, 1990).
- Reductive dissolution using chromium(II) (Seaborg, 1990) or uranium(IV) (Inoue, 1988).

Large disadvantages of the use of mineral acids, such as hydrofluoric acid, are dissolver and downstream corrosion issues and addition of salts leading to increased HLW volumes. This will favor the use of catalytic processes, the most widely developed of which is the catalyzed dissolution of plutonium using cerium or silver as a mediator (Bourges et al., 1986). These processes use electrochemical or ozonolysis to regenerate the oxidant (mediator) making the processes low in salt content, or, if the mediator is recovered, salt-free. These oxidative processes are also relevant to the destruction of organics from the direct dissolution of carbides. Reductive dissolution using uranium(IV) would also be an elegant solution to the dissolution of MOX as uranium is already present; however, there has been little work on this topic.

The oxidative dissolution of plutonium dioxide is known to be possible at above $\sim$1.2 V_{NHE} (Madic et al., 1991) and with the use of cerium(IV) ($E_0 \approx 1.4$ V_{NHE}) in hot nitric acid (Seaborg, 1990) or silver(II) ($E_0 \approx 2.0$ V_{NHE}) at ambient temperatures (Rance et al., 2003) dissolutions are known to proceed rapidly. Silver is often preferred due to the high oxidation potential, rapid electron transfer rate (Fleischmann et al., 1971), and surprising stability against water oxidation due to nitrate complexation (Po et al., 1968). This type of process has been termed catalyzed electrochemical plutonium oxide dissolution (CEPOD) or, more generally, a mediated electrochemical oxidation (MEO) process. This process generates the mediator, for example silver(II) at an anode, Equation 5.14, and nitric acid is reduced at a cathode, Equation 5.15. The silver(II) dissolves the plutonium dioxide, Equation 5.16. The anode and cathode compartments are separated by a membrane that allows proton transfer and minimizes mixing of the anolyte and catholyte, which would cause reduction of the silver(II) by nitric acid reduction products. A schematic diagram of an industrial dissolver is shown in Figure 5.12. This process is known to be very rapid and little silver(II) is observed until bulk plutonium dioxide dissolution is achieved (Zundelevich, 1992). For this reason, dissolution is highly dependent upon the generation rate of silver(II), which is dependent upon electrochemical mass transfer limits. Dissolution of plutonium dioxide with ozone with silver mediation is also limited by mass transfer of ozone (Selbin and Usategui, 1961).

$$Ag^{+} \rightarrow Ag^{2+} + e^{-} \tag{5.14}$$

$$HNO_3 + H^{+} + e^{-} \rightarrow NO_2 + H_2O \tag{5.15}$$

$$PuO_{2(s)} + 2Ag^{2+} \rightarrow {PuO_2}^{2+}{}_{(aq)} + 2Ag^{+} \tag{5.16}$$

MEO-type processing using cerium or silver can be used to dissolve plutonium-rich oxides in dissolved spent MOX (Rance et al., 2003) or for the dissolution and organics

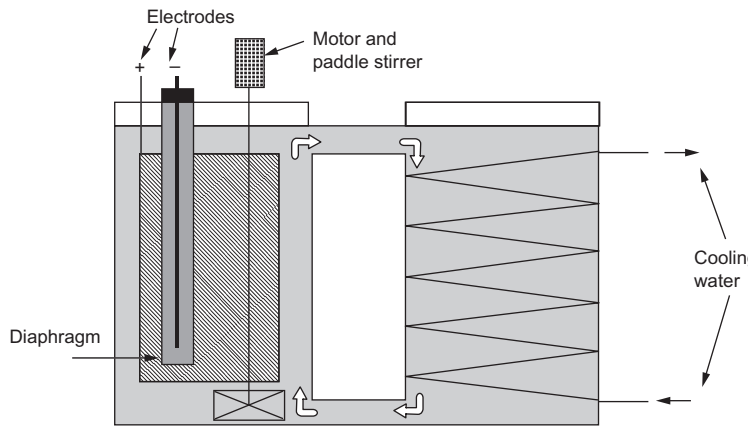

Figure 5.12 Industrial plutonium dioxide dissolver (Zundelevich, 1992).

destruction of spent carbides (Palamalai et al., 1991). The presence of a multitude of polyvalent metals leads to the oxidation of elements to high oxidation states. This can lead to side reactions or, in extreme cases, the catalytic consumption of the mediator (Rance et al., 2003). An example of this is ruthenium, which is oxidized to the volatile tetroxide and is distilled (Mousset et al., 2004). As a result, due to the quantity and radiotoxicity of ruthenium-106, suitably efficient abatement precautions must be made.

The application of mediated dissolution processes are likely to be used after direct nitric acid dissolution due to the ease and speed of direct dissolution. Mediated dissolution would ideally be used in the same dissolver so as to minimize the potential for accumulation of solids, by avoiding the movement of plutonium-rich solids. However, this approach leads to batch dissolver cycles. Multileach dissolver cycles continue to be in vogue despite their inherent disadvantages; for example, recent work with the select dissolution of inert matrices from IMF fuels (EC, 2013). Another similar example is the dissolution of thorium oxide containing fuels using nitric acid with organic complexants, followed by the destruction of the organic complexants. Innovations to integrate and simplify the process chemistry and engineering will be advantageous for efficient headend operations. An example may be the continuous dissolution of voloxidation product powder under cool conditions followed by continuous dissolution of plutonium-rich residues in a second dissolver or second part of the same dissolver. These developments will need to be mindful of the increasingly cautious nature of safety cases; for example, over the management of the accumulation of plutonium-rich particulates.

5.4 Summary and future developments

Headend is the first chemical treatment step in the reprocessing of spent nuclear fuel. Current practices use mechanical decladding and shearing followed by the direct dissolution of metal and oxide fuels in nitric acid. Changes to environmental discharge limits or the introduction of new fuel materials may require the introduction of additional process steps. Developments in fuel preparation, pretreatment, and dissolution technologies are expected. The significance of each part will depend upon evolution of reactor and fuel design for energy and actinide management (transmutation).

Radical changes in fuel design concepts from the rod or pellet in cladding could make exposure of fuel more difficult. Examples are adoption of Triso compacts or pebbles or actinide-silicon carbide composites; the refractory nature may require the use of intensive fuel preparation, such as grinding.

Fuel pretreatment as a method overcoming difficulties of direct dissolution in nitric acid may become attractive if environmental discharge limits are tightened, particularly if tritium abatement is required or if advanced fuels, such as carbides or nitrides, are to be reprocessed. These pre-treatment processes could allow the abatement of tritium, which cannot be abated when it is isotopically mixed with the dissolver liquor. The evolution of carbon-14, noble gases, and iodine-129 could also be achieved, giving other options for abatement and defining the dissolution and dissolver liquor

conditioning required. Pretreatment could also be a method to overcome the problem of dissolved organics from carbide fuels by conversion to an oxide and allow recovery of nitrogen-15 from nitride fuels for reuse.

The adaptation of new dissolution processing and technologies may also be required to receive pretreated fuel, new fuel types, achieve high-plutonium recoveries, or condition dissolved carbide fuel to remove organics generated from dissolution. These new processes could involve multileaching approaches; for example, to selectively dissolve inert matrices. The use of enhanced dissolution techniques using organic complexants or no or low salt mediated oxidative or reductive dissolution techniques could also be used to dissolve difficult materials or condition liquors.

Headend chemistry, engineering, and technology is expected to continue to be a demanding area of future reprocessing plants. As reactor fuel concepts develop and the required performance criteria for reprocessing plants become more clearly defined, the headend processes will be driven to become more innovative. It is, after all, the role of the headend to provide standardized dissolver product suitable for downstream separations processes, regardless of the different reactors and fuel types from which it originates.

References

Anderson, J.S., et al., 1954. The oxides of uranium. Part IV. The system UO_2-ThO_2-O. J. Chem. Soc. (Resumed), 3324–3331.

Asquith, R.W., Hudson, P.J., Astill, M., 1988. Shear elegance in the Thorp head end. Nucl. Eng. Int. 33, 37–40.

Bakker, K., et al., 2004. The use of molybdenum-based ceramic-metal (CerMet) fuel for the actinide management in LWRs. Nucl. Technol. 146 (3), 325–331.

Bard, A.J., Parsons, R., Jordan, J., 1985. Standard Potentials in Aqueous Solution (Monographs in Electroanalytical Chemistry & Electrochemistry). Marcel Dekker Inc, New York/Basel.

Bateman, K.J., et al., 2006. Effect of process variables during the head-end treatment of spent oxide fuel. United States Conference Paper, INL/CON-06-11605.

Berthinier, C., et al., 2011. Experimental study of uranium carbide pyrophoricity. Powder Technol. 208 (2), 312–317.

Berthinier, C., et al., 2013. Experimental kinetic study of oxidation of uranium monocarbide powders under controlled oxygen partial pressures below 230 degrees C. J. Nucl. Mater. 432 (1–3), 505–519.

Bierman, S.R., et al., 1984. Criticality experiments with low enriched UO_2 fuel rods in water containing dissolved gadolinium. United States of America Report, PNL-4976.

Blanc, M., 1986. Etude La Bibliographic relative A La Cinetique de dissolution de UO_2 dans L-acide nitrique. French Report, CEA-TR-2216.

Bond, W.D., Mailen, J.C., Michaels, G.E., 1992. Evaluation of methods for decladding LWR fuel for a pyroprocessing-based reprocessing plant. United States of America Report, ORNL/TM-12104.

Boukis, N., Henrich, E., 1991. 2-Step procedure for the iodine removal from nuclear fuel solutions. Radiochim. Acta 55 (1), 37–42.

Bourges, J., et al., 1986. Dissolution du bioxyde de plutonium en milieu nitrique par l'argent(II) electrogenere. J. Less-Common Met. 122, 303–311.

Bradley, M.J., Ferris, L.M., 1962. Hydrolysis of uranium carbides between 25 and 100 °C. 1. Uranium monocarbide. Inorg. Chem. 1 (3), 683–687.
Bradley, M.J., Ferris, L.M., 1964a. Hydrolysis of uranium carbides between 25 and 100 °C. 2. Uranium dicarbide, uranium metal-monocarbide mixtures and uranium monocarbide dicarbide mixtures. Inorg. Chem. 3 (2), 189–195.
Bradley, M.J., Ferris, L.M., 1964b. Hydrolysis of uranium carbides between 25 and 100 °C. 3. Uranium sesquicarbide and mixtures of sesquicarbide with monocarbide or dicarbide. Inorg. Chem. 3 (5), 730–734.
Cadieux, J.R., Stone, J.A., 1980. Voloxidation and dissolution of irradiated plutonium recycle fuels. United States of America Report, DP-MS-80-10.
Capone, F., et al., 1996. Mass spectrometric measurements of fission product effusion from irradiated light water reactor fuel. Nucl. Sci. Eng. 124 (3), 436–454.
Carrott, M.J., et al., 2012. The chemistry of (U,Pu)O_2 dissolution in nitric acid. Procedia Chem. 7, 92–97.
Choppin, G.R., Bokelund, H., Valkiers, S., 1983. Oxalate complexation in dissolved carbide systems. Radiochim. Acta 33 (4), 229–232.
Cleveland, J.M. (Ed.), 1970. The Chemistry of Plutonium. Americium Nuclear Society, LaGrange.
Cobos, J., et al., 1998. Phase characterisation of simulated high burn-up UO_2 fuel. J. Alloys Compd. 271–273, 610–615.
Coleman, G.H., 1965. The Radiochemistry of Plutonium. National Academy of Sciences, Washington, DC.
Collins, E.D., et al., 2012. Process development studies for zirconium recovery/recycle from used nuclear fuel cladding. Procedia Chem. 7, 72–76.
Croft, T.L.M., Tonkin, J.H., 1950. The dissolution of uranium in nitric acid. Review of the position in 21st June 1950. Great Britain Report, CF5057/8.
Dancausse, J.P., et al., 2008. CEA preliminary studies for industrial MOx reprocessing: from laboratory results to successful first industrial campaign on UP2-800 AREVA plant. In: Icone16: Proceeding of the 16th International Conference on Nuclear Engineering—2008, vol. 2. American Society of Mechanical Engineers, New York, pp. 51–54.
Davis, W.J., West, G.A., Stacy, R.G., 1979. Oxide particle size distribution from shearing irradiated and unirradiated LWR fuels in Zircaloy and stainless steel cladding: significance for risk assessment. United States of America Report, ORNL/NUREG-60.
de Groot, M.T., Koper, M.T.M., 2004. The influence of nitrate concentration and acidity on the electrocatalytic reduction of nitrate on platinum. J. Electroanal. Chem. 562 (1), 81–94.
DelCul, G.D., 2010. Advanced head end for the treatment of used LWR fuel. In: OECD Nuclear Energy Agency, 11th Information Exchange Meeting on Actinide and Fission Product Partitioning and Transmutation. Hyatt at Fisherman's Wharf, San Francisco, California, pp. 1–5 November 2010.
Doucet, F.J., et al., 2002. The formation of hydrated zirconium molybdate in simulated spent nuclear fuel reprocessing solutions. Phys. Chem. Chem. Phys. 4 (14), 3491–3499.
EC, 2013. ASGARD deliverable report 1.3.4—annual public report 2013.
El Haleem, S.M.A., El Aal, E.E.A., 2008. Thermometric behaviour of cobalt in HNO_3 solutions. J. Mater. Process. Technol. 204 (1–3), 139–146.
Elcheikh, F.M., et al., 1983. The role of intermediates in the kinetics of copper dissolution in nitric acid. Ann. Chim. 73 (1–2), 75–89.
El-Egamy, S.S., Ismail, K.M., Badawy, W.A., 2004. Corrosion behaviour of copper in acidic nitrate solutions. Corros. Prev. Control 51 (3), 89–97.

Emin, J.L., Zimmermann, A., Tribout-Maurizi, A., Dancausse, J.P., 2005. MOx reprocessing: the success of the first industrial campaign on UP2-800 COGEMA Plant. In: Global 2005.

Ferris, L.M., 1968. Reactions of uranium mononitride, thorium monocarbide and uranium monocarbide with nitric acid and other aqueous reagents. J. Inorg. Nucl. Chem. 30 (10), 2661–2669.

Ferris, L.M., Bradley, M.J., 1964. Off-gases from the reactions of uranium carbide with nitric acid at 90 °C. United States of America Report, ORNL-3719.

Ferris, L.M., Bradley, M.J., 1965. Reactions of uranium carbide with nitric acid. J. Am. Chem. Soc. 87 (8), 1710–1714.

Flanary, J.R., et al., 1964. Hot-cell studies of aqueous dissolution processes for irradiated carbide reactor fuels. United States of America Report, ORNL-3660.

Fleischmann, M., Pletcher, D., Rafinski, A., 1971. The kinetics of the silver (I)/silver (II) couple at a platinum electrode in perchloric and nitric acids. J. Appl. Electrochem. 1 (1), 1–7.

Fukasawa, T., Ozawa, Y., 1986. Relationship between dissolution rate of uranium dioxide pellets in nitric acid solutions and their porosity. J. Radioanal. Nucl. Chem. Lett. 106 (6), 345–356.

Fukasawa, T., Ozawa, Y., Kawamura, F., 1991. Generation and decomposition behavior of nitrous-acid during dissolution of UO_2 pellets by nitric acid. Nucl. Technol. 94 (1), 108–113.

Gens, T.A., 1958. Explosive reactions during reprocessing of reactor fuels containing uranium and zirconium or niobium. United States of America Report, ORNL CF-58-11-31.

GIF, 2002. A technology roadmap for generation IV nuclear energy systems. Available from GenIV International Forum website, www.gen-4.org.

Glatz, J.P., Bokelund, H., Zierfuss, S., 1990. Analysis of the off-gas from dissolution of nuclear oxide fuels and carbide fuels in nitric acid. Radiochim. Acta 51 (1), 17–22.

Goode, J.H., 1973. Voloxidation: removal of volatile fission products from spent LMFBR fuels. United States of America Report, ORNL-TM-3723.

Goode, J.H., Flanary, J.R., 1967. Hot cell evaluation of the grind-leach processes with irradiated pyrolytic carbon-coated sol–gel thoria-urania particles. United States of America Report, ORNL-TM-1880.

Goode, J.H., Stacy, R.G., 1979. Voloxidation and dissolution of irradiated $(Th,U)O_2$. United States of America Report, ORNL/TM-6643.

Goode, J.H., Stacy, R.G., Vaughen, V.C.A., 1980. Head-end reprocessing studies of H.B. Robinson-2 fuel: II. Parametric voloxidation studies. PBD, May 1980.

Gresky, A.T., 1952. Recovery of nitrogen oxides and rate gas fission products from the nitric acid dissolution of irradiated uranium. United States of America Report, ORNL-1208.

Groenier, W.S., 1971. Equipment for the dissolution of core material from sheared power reactor fuel. United States of America Report, ORNL-TM-3194.

Hadibi-Olschewski, N., et al., 1992. The fate of nitrogen upon reprocessing of nitride fuels. J. Nucl. Mater. 188, 244–248.

Hodgson, T.D., 1994. A model for fuel dissolution via fragmentation. In: RECOD.

IAEA, 2003. Status and advances in MOx fuel technology.

Ikeda, Y., et al., 1995. Kinetic study on dissolution of UO_2 powders in nitric acid. J. Nucl. Mater. 224 (3), 266–272.

Ikeda, Y., et al., 1999. Dissolution behavior of pulverized irradiated fuels in nitric acid solutions. J. Nucl. Sci. Technol. 36 (4), 358–363.

Ikeuchi, H., et al., 2012. Dissolution behavior of irradiated mixed-oxide fuels with different plutonium contents. Procedia Chem. 7, 77–83.

Inoue, A., 1988. Enhanced dissolution of PuO_2 in nitric acid using uranium(IV). J. Chem. Soc. Faraday Trans. I 84, 1195–1197.

Jiang, J., et al., 2005. A spectroscopic study of the dissolution of cesium phosphomolybdate and zirconium molybdate by ammonium carbamate. J. Solut. Chem. 34 (4), 443–468.

Jones, K., 1973. Nitrogen. In: first ed. Bailar, J.C., Emeléus, H.J., Nyholm, R., Trotman-Dickenson, A.F. (Eds.), Comprehensive Inorganic Chemistry: Ge, Sn, Pb, N, P, As, Sb, Bi, O, S, Se, Te, Po, F, Cl, Br, I, At, vol. 2. Pergamon Press, Oxford, pp. 147–388 (Chapter 19).

Kang, K.H., et al., 2007. Oxidation behavior of the simulated fuel with dissolved fission products in air at 573–873 K. Thermochim. Acta 455, 129–133.

Khalil, S.A., Elmanguch, M.A., 1987. The kinetics of zinc dissolution in nitric acid. Monatsh. Chem. 118 (4), 453–462.

Kleykamp, H., 1985. The chemical state of the fission products in oxide fuels. J. Nucl. Mater. 131 (2–3), 221–246.

Larsen, R.P., 1959. Dissolution of uranium metal and its alloys. Anal. Chem. 31 (4), 545–549.

Laue, C.A., Gates-Anderson, D., Fitch, T.E., 2004a. Dissolution of metallic uranium and its alloys—Part 1: review of analytical and process-scale metallic uranium dissolution. J. Radioanal. Nucl. Chem. 261 (3), 709–717.

Laue, C.A., Gates-Anderson, D., Fitch, T.E., 2004b. Dissolution of metallic uranium and its alloys—Part II: screening study results: identification of an effective non-thermal uranium dissolution method. J. Radioanal. Nucl. Chem. 262 (2), 517–524.

Lee, J.W., Park, G.I., Choi, Y., 2012. Fabrication of DUPIC fuel pellets using high burn-up spent PWR fuel. J. Nucl. Sci. Technol. 49 (11), 1092–1096.

Lerch, R.E., 1972. Dissolution of unirradiated mechanically blended, sol gel and coprecipitated mixed oxide fuel. United States of America Report, HEDL-TME-72-67.

Madic, C., Lecomte, M., Bourges, J., Koehly, G., Moulin, J.P., 1991. Mechanism of the rapid dissolution of PuO_2 under oxidizing conditions, and applications. In: Proceedings of Recod 1991, pp. 715–720.

Madic, C., Berger, P., Machuronmandard, X., 1992. Mechanisms of the rapid dissolution of plutonium dioxide in acidic media under oxidizing or reducing conditions. In: Transuranium Elements, pp. 457–468.

Magnaldo, A., Masson, M., Champion, R., 2007. Nucleation and crystal growth of zirconium molybdate hydrate in nitric acid. Chem. Eng. Sci. 62 (3), 766–774.

Majumdar, D., et al., 1992. Recycling of nuclear spent fuel with AIROX processing. United States of America Report, DOE/ID-10123.

Maslennikov, A., et al., 2007. Electrochemical behavior of UC in acidic media: preliminary results. J. Alloys Compd. 444, 550–553.

Maslennikov, A., et al., 2009. UC oxidation with HNO_2 in aqueous solutions of HNO_3 and $HClO_4$. Radiochim. Acta 97 (10), 571–580.

Matzke, H., 1986. Science of Advanced LMFBR Fuels. Elsevier Science, North-Holland.

McEachern, R.J., Doern, D.C., Wood, D.D., 1998. The effect of rare-earth fission products on the rate of U_3O_8 formation on UO_2. J. Nucl. Mater. 252, 145–149.

Miles, G.L., 1955. The Fumeless Dissolving of Uranium. UKAEA Atomic Energy Research Establishment, Harwell, UKAEA, AERE C/R 1804.

Mousset, F., Bedioui, F., Eysseric, C., 2004. Electroassisted elimination of ruthenium from dissolved RuO_2, xH_2O in nitric acid solution by using Ag(II) redox mediator: toward a new insight into the nuclear fuel reprocessing. Electrochem. Commun. 6 (4), 351–356.

Murbach, E.W., Turner, W.D., 1963. Oxidation of uranium carbide by carbon dioxide. Trans. Metall. Soc. AIME 227 (2), 488–491.

Nakata, K., et al., 2008a. Surface-enhanced infrared absorption spectroscopic studies of adsorbed nitrate, nitric oxide, and related compounds 2: nitrate ion adsorption at a platinum electrode. Langmuir 24 (8), 4358–4363.

Nakata, K., et al., 2008b. Surface-enhanced infrared absorption spectroscopic studies of adsorbed nitrate, nitric oxide, and related compounds 1: reduction of adsorbed NO on a platinum electrode. Langmuir 24 (8), 4352–4357.

NEA, 1980. Radiological Significance and management of tritium, carbon-14, krypton-85, iodine-129 arising from the nuclear fuel cycle: report. Nuclear Energy Agency, Organisation for Economic Co-operation and Development, Paris.

NEA, 2012. Spent nuclear fuel reprocessing flowsheet. Nuclear Energy Agency Report, NEA/NSC/WPFC/DOC(2012)15.

Nikitina, G.P., et al., 1997. Existing methods for dissolution of plutonium dioxide. 1. Dissolution in mineral acids and their mixtures. Radiochemistry 39 (1), 12–25.

Nishimura, K.U., Chikazawa, T., Hasegawa, A., Tanaka, T., Ikeda, U., Yasuike, Y., Takahima, Y., 1995. Effect of nitrous acid on dissolution of UO_2 powders in nitric acid optimal conditions for dissolving. J. Nucl. Sci. Technol. 32 (2), 157–159.

OSPAR. Radioactive substances. Available from: http://www.ospar.org/content/content.asp?menu=00220306000000_000000_000000. Oringallly access 11/08/2013.

Oudinet, G., et al., 2008. Characterization of plutonium distribution in MIMAS MOX by image analysis. J. Nucl. Mater. 375 (1), 86–94.

Palamalai, A., et al., 1991. Development of an electro-oxidative dissolution technique for fast reactor carbide fuels. Radiochim. Acta 55 (1), 29–35.

Parisot, J.F., 2008. Treatment and Recycling of Spent Nuclear Fuel. Actinide Partitioning—Application to Waste Management. CEA, Paris.

Phillips, C., 1999. The thermal oxide reprocessing plant at Sellafield: four years of successful treatment of irradiated nuclear fuel. In: Waste Management Conference, Tucson, AZ.

Po, H.N., Swinehart, J.H., Allen, T.L., 1968. Kinetics and mechanism of the oxidation of water by silver(II) in concentrated nitric acid solution. Inorg. Chem. 7 (2), 244–249.

Rance, P.J.W., Beznosynk, B., 2005. The oxidative pulverisation of mixed oxide fuel. In: Proceedings of GLOBAL 2005, Tsukuba, Japan, October 9–13, 2005, Paper No. 372.

Rance, P.J.W., Zilberman, B.Y., Akopov, G.A., 2000. Radiolysis of hexavalent plutonium in solutions of uranyl nitrate containing fission product simulants. In: Pillay, K.K.S., Kim, K.C. (Eds.), Plutonium Futures—The Science. American Institute of Physics, Melville, pp. 56–58.

Rance, P.J.W., Nikitina, G.P., Kirshyn, M.G., Koroleve, V.A., 2003. The effects of temperature, surface area and interfering species on the dissolution rate of plutonium dioxide by silver (II) in nitric acid. In: Global 2003: Atoms for Prosperity: Updating Eisenhower's Global Vision for Nuclear Energy, New Orleans, Louisiana, November 16–20, American Nuclear Society.

Rima, F.R., et al., 2010. Surface-enhanced infrared absorption spectroscopic studies of adsorbed nitrate, nitric oxide, and related compounds. 3. Formation and reduction of adsorbed nitrite at a platinum electrode. J. Phys. Chem. C 114 (13), 6011–6018.

Rosse, E., et al., 2012. Increase of the performances on the head facility. In: Atalante on Nuclear Chemistry for Sustainable Fuel Cycles, 2012 meeting held 3–7 September 2012, Montpellier, France.

Sakurai, T., et al., 1988. The composition of NOx generated in the dissolution of uranium dioxide. Nucl. Technol. 83 (1), 24–30.

Sakurai, T., et al., 1991. The interaction of iodine with insoluble residue in the dissolution of simulated spent fuel pelles. Nucl. Technol. 94 (1), 99–107.

Sakurai, T., et al., 1992. The iodine species and their behavior in the dissolution of spent fuel specimens. Nucl. Technol. 99 (1), 70–79.
Sakurai, T., et al., 1993. Thermochemical and experimental considerations of NOx composition and iodine species in the dissolution of spent PWR fuel specimens. J. Nucl. Sci. Technol. 30 (6), 533–541.
Sakurai, T., et al., 1996. Influence of NOx and HNO_2 on iodine quantity in spent-fuel solutions. Nucl. Technol. 116 (3), 319–326.
Schulz, W.W., 1960. Reprocessing uranium-molybdenum alloy fuels-dissolution in concentrated nitric acid. Technical report, original receipt date: 31 December 1960, 17 pp.
Schulz, W.W., Burns, R.E., Duke, E.M., 1962. Nitric acid dissolution of uranium-molybdenum alloy reactor fuels. Ind. Eng. Chem. Process. Des. Dev. 1 (2), 156–160.
Seaborg, G.T., 1990. Transuranium elements: a half century. United States of America Report, LBL-29445.
Selbin, J., Usategui, M., 1961. Higher oxidation states of silver. 1. Reaction of ozone with simple silver salts. J. Inorg. Nucl. Chem. 20 (1–2), 91–99.
Shabbir, M., Robins, R.G., 1968. Kinetics of dissolution of uranium dioxide in nitric acid 1. J. Appl. Chem. USSR 18 (5), 129–134.
Shabbir, M., Robins, R.G., 1969. Kinetics of dissolution of uranium dioxide in nitric acid 2. J. Appl. Chem. USSR 19 (2), 52–56.
Strausberg, S., et al., 1960. Low decontamination-processing of uranium dioxide by oxidation-reduction. Ind. Eng. Chem. 52 (1), 45–46.
Sugihara, S., Imoto, S., 1969. Hydrolysis of uranium nitrides. J. Nucl. Sci. Technol. 6 (5), 237–242.
Swanson, J.L., et al., 1985. Laboratory studies of shear/leach processing of zircaloy clad metallic uranium reactor fuel. PNL-5708.
Takeuchi, M., Whillock, G.O.H., 2002. Effect of NOx gases on corrosion of stainless steel in hot nitric acid solutions. Br. Corros. J. 37 (3), 199–205.
Taylor, R.F., Sharratt, E.W., de Chazal, L.E.M., Logsdale, D.H., 1963. Dissolution rates of uranium dioxide sintered pellets in nitric acid systems. J. Appl. Chem. 13, 32–40.
Thomas, L.E., Einziger, R.E., Buchanan, H.C., 1993. Effect of fission products on air-oxidation of LWR spent fuel. J. Nucl. Mater. 201, 310–319.
Uriarte, A.L., Rainey, R.H., 1965. Dissolution of high density UO_2, PuO_2 and UO_2-PuO_2 pellets in inorganic acids. United States of America Report, ORNL-3695.
Usami, T., et al., 2010. Formation of zirconium molybdate sludge from an irradiated fuel and its dissolution into mixture of nitric acid and hydrogen peroxide. J. Nucl. Mater. 402 (2–3), 130–135.
Vollath, D., et al., 1985. On the dissolution of $(U,Pu)O_2$ solid-solutions with different plutonium contents in boiling nitric acid. Nucl. Technol. 71 (1), 240–245.
Wallenius, J., 2010. Transmutation. In: First ACSEPT International Workshop, 31 March–2 April 2010, Hotel VIP Zurique, Lisbon, Portugal. Available from http://www.acsept.org/AIWOpdf/AIWO1-02-Wallenius.pdf accessed 27/11/2011.
Wilson, P.D. (Ed.), 1996. The Nuclear Fuel Cycle, from Ore to Waste. Oxford Science Publications, Oxford.
Wurtz, R., 1987. The solubility of irradiated MOx fuel elements in reprocessing. Atomwirtschaft-Atomtechnik 32 (4), 190–192.
Zundelevich, Y., 1992. The mediated electrochemical dissolution of plutonium oxide—kinetics and mechanism. J. Alloys Compd. 182 (1), 115–130.

Process engineering and design for spent nuclear fuel reprocessing and recycling plants

6

Bruce Hanson
University of Leeds, Leeds, UK

Acronyms

CAD (2-D/3-D)	computer-aided design (two-dimensional or three-dimensional versions)
CAM	computer-aided manufacturing
CFD	computational fluid dynamics
DNS	direct numerical simulation
LES	large eddy simulation
LWR	light water reactor
NASA	National Aeronautics and Space Administration
PUREX	plutonium uranium reduction extraction
THORP	thermal oxide reprocessing plant
TRL	technology readiness level

6.1 Introduction

In other chapters through this book we will see how various processes, such as solvent extraction and electrorefining, have been applied to spent nuclear fuel treatment. Many new developments and advances of these processes are currently being investigated in laboratories around the world and, if successful, will follow the path of previous technologies, such as the plutonium uranium reduction extraction (PUREX) process toward industrialization and commercial operations.

The common path for the transfer of these technologies from the laboratory to full-scale is through a handover from scientists to engineers; with the latter having a primary focus on the industrialization and application to a specific function. The key objective will be to scale the process up, economically, sometimes across several orders of magnitude, without loss of efficiency. In this context, engineering design is an attempt to take a laboratory system and scale it up to a working plant capable of being operated, consistently, on a daily basis by a team of trained personnel. It involves many trade-offs between efficiency, complexity, safety, and economy in order to arrive at an engineered solution.

In the early stages of development, engineers are usually involved in more of an advisory capacity, where they may provide a view on the applicability of a new process, so as to aid choice between competing options. As the R&D progresses and the fundamental

Reprocessing and Recycling of Spent Nuclear Fuel. http://dx.doi.org/10.1016/B978-1-78242-212-9.00006-X

science of the technology matures, it becomes increasingly more important to have a good view of the final application and means of deployment. At this stage it is common to have a multidisciplinary team of scientists and engineers working together on the development. This is typically the role of the nuclear process engineer. At some point the technology will be mature enough that the scientific development can be scaled back, as the majority of the issues will be related to the engineering. The focus will now shift to construction and the engineering team will become dominant, with other disciplines (mechanical, electrical, civil) being included.

Good practice should include testing of engineering solutions before full implementation. Risks and costs associated are huge, especially in nuclear applications, if the plant design is not correct. In the past, testing involved construction of pilot plant or demonstration facilities; however, advances in modeling techniques now allow testing of design options in different ways. For example three-dimensional computer-aided design (3-D CAD) modeling linked to virtual reality suites allow plant designs to be "walked through" before civil engineering is completed and 3-D prototyping can be used to test designs of complex equipment before construction.

Nuclear engineering has the added complication of dealing with radioactive materials. A normal approach is to extend the commissioning process and have staged testing of the plant, with uranium, plutonium, and then a full inventory of materials. Once the decision is made to move to fully active operations, there is no turning back as the plant is contaminated.

For the design process, there must be a test of the design options against the specific issues that affect nuclear plants. For example, if fissile materials are present in the inventory then the design must have a method to control criticality. Quite often these additional requirements put a heavy constraint on options available to engineers and lead to unique solutions.

In this chapter, we will explore,

- The principles of nuclear process engineering, the methodology we use to implement engineering design at different stages in the development of a technology, and the issues that need to be addressed;
- Plant design and engineering, in relation to the scale-up of a process;
- Solvent-extraction equipment and the advances being made to increase the effectiveness of their design and operation;
- The use of multiscale modeling and simulation, as a design aid;
- Current and future trends in design, with a move away from reliance on experimental testing.

6.2 Principles of nuclear process engineering

6.2.1 The design process

Initially, nuclear process design is not so very different from conventional process design. As the process develops and the design matures, the differences between a nuclear and a nonnuclear process plant become more obvious and significant, so the design process alters to accommodate these unique factors.

After the design has been completed and construction begins the differences are significant. For example, more testing is required on build quality than would normally be required for conventional chemical plant construction. In the United Kingdom, pipework that is welded need only be tested in 10% of the population, whereas in nuclear plants normal practice is for 90% radiography of welds to ensure quality. This means that 9 out of every 10 welds on a system have to be inspected for inclusions in the weld using radiography and the inspection recorded.

The most significant difference is in the commissioning of new nuclear plants. Once radioactive materials have been introduced into a plant, then any opportunity to modify and correct commissioning faults becomes very difficult.

In the United Kingdom, a design process has been developed that uses a stepwise approach and is integrated with assessments of cost, safety, and technical maturity. Figure 6.1 illustrates the overall process.

While cost and safety are specific to the local regulations and conditions, assessment of technical maturity, which directly relates to technical risk, is becoming more generic. Technical maturity is now commonly measured using a technology readiness level (TRL). This method was originally developed by National Aeronautics and Space Administration (NASA) and the U.S. Department of Defence for application in their space mission and submarine build programs. Figure 6.2 shows the TRL scale as applied by NASA. Typically, TRL 1 to 3 is classed as fundamental development and would normally be carried out in universities. TRL 4 to 6 is technology development and is the point at which scale-up would be tested. TRL 7 to 9 is technology proving and would be the preserve of industry.

6.2.1.1 Design strategy

This is the starting point for any design project. At this stage it is important to have as full an understanding as possible of the problem to be solved and to recognize the areas that are ill-defined or where data is missing. Typically, decisions on which process to use may be made on knowledge gained from TRLs up to 3. The output of this stage is referred to as a basis of design document and is the specification the engineers will use to commence design of the plant.

6.2.1.2 Concept design

This stage is the point at which the different process options are evaluated with the aim to choose and decide which option is the most appropriate for further design and development. An initial level of plant design is required for each option and so

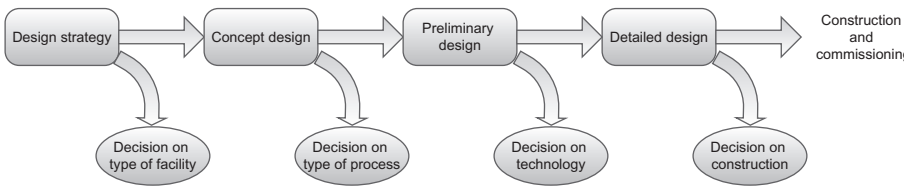

Figure 6.1 The design process as applied in the UK nuclear industry.

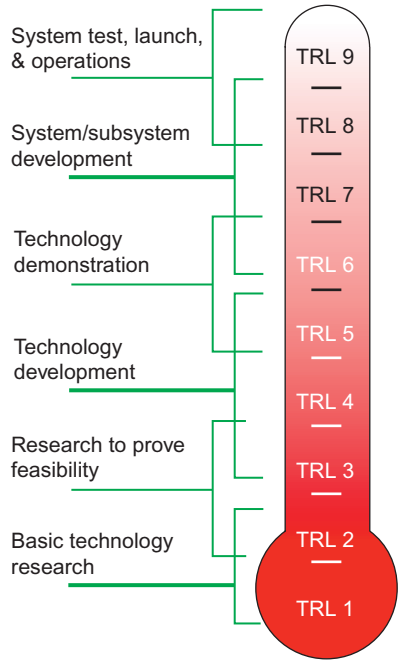

Figure 6.2 NASA's definition of technology readiness levels. Diagram courtesy of NASA.

technical maturity needs to be at TRL 4 to 6 levels, to allow the main technical risks to be addressed. The more information on scale-up available to the engineers designing the plant, the less risk is associated with the choice of preferred process(es). The output of this stage will usually be an initial design of the facility, with layout drawings, a process description, and an initial flow sheet.

6.2.1.3 Preliminary design

This stage is the point at which the engineer will begin to design specific equipment items and so will need a flow sheet to work from, where the separation factors and associated kinetics have been scientifically proven. Commencing equipment design means that mechanical and electrical engineering disciplines will become involved, so the preferred technology will need to be at a high enough maturity (TRL 6+) and pilot plant studies completed to allow correct specification for the design. This is the point at which nuclear issues, such as criticality control, will start to be addressed.

6.2.1.4 Detailed design

At this stage, the design of the plant has progressed far enough that multidisciplinary teams (process, mechanical, civil, and electric) of engineers will be working together. The flexibility to change a design still exists, but the level of detail in the work is such

that only proven technologies, with low technical risk, should be considered. Ideally, at this stage we would work with TRL 7 to 8.

6.2.2 Reliability and design life

One of the clear differences between nuclear and conventional process plant design is the issue of design life. For a conventional process plant designer there is always the option of replacement for failed plant items, should the needs of designing for the full lifetime of the plant become too constraining. In a nuclear reprocessing plant, replacement of failed items is most often far too costly and difficult, as the plant is contained within sealed cells and contaminated with highly radioactive material. Therefore, the nuclear process plant designer has to consider what principles will be adopted and these may vary throughout the plant. In summary, there are four options available:

- Design for life
- Build in redundancy
- Maintain
- Build in space for retrofit

6.2.2.1 Design for life

Most process plant equipment such as vessels and pipework will be designed to last the full lifetime of the plant. The most likely cause of failure will be loss of integrity due to corrosion from the presence of nitric acid. In the United Kingdom, for instance, reprocessing plants have been constructed using 304 L stainless steel, which typically contains 18.0-20.0% chromium and 8.0-12.0% nickel, and is commonly recommended for plants dealing with nitric acid. Even though it is a material of choice, 304 L can experience between 0.1 and 0.2 mm per year corrosion in nitric acid, depending on temperature (Winston, 2011; Kreysa and Schütze, 2008). Welds are a particular point of weakness, and corrosion rates of up to 0.27-0.54 mm per year can occur (Kreysa and Schütze, 2008). Over a plant lifetime of 20 years (not an uncommon target for reprocessing plants), the variation in wall thickness of vessels and pipes could be 2-10 mm from the effects of corrosion. This is difficult to predict, and with a wall thickness of about 5 mm (from a mechanical design perspective) adding a full lifetime, worst-case, corrosion allowance may lead to wall thicknesses up to 15 mm. The effect on material cost is obvious, but perhaps more important would be the effect on performance, especially if the vessel had a heat transfer function. For an evaporator with boiling acid on one side and condensing steam on the other, the main resistivity to heat transfer will be the metal wall of the vessel (304 L has a thermal conductivity of about 16 $Wm^{-1}\,K^{-1}$). In this situation, increasing the wall thickness from 5 to 15 mm may reduce overall heat transfer rates by up to 40% and so the designer may have to consider upgrading the construction material to a more resistant metal, such as Inconel, a nickel-chromium based alloy.

6.2.2.2 Build in redundancy

In some cases, even with high specification materials of construction, design for life cannot be guaranteed. In this case, the designer can consider installing redundant units that can be brought online in the event of a failure; for example, multiple tanks can be installed to store liquids, with an overall overcapacity to allow for failure. An example of built-in redundancy is the fans on the ventilation system for the thermal oxide reprocessing plant (THORP) reprocessing plant at the Sellafield nuclear site in the United Kingdom. It is necessary for the ventilation system to continuously operate under all conditions, but the fans themselves cannot be guaranteed to be failure-free, so if one fails there is a standby ready to operate.

6.2.2.3 Maintain

Failures for mechanical plant (bearings, gears, etc.) tend to be of the order of 10^6 hours, and so we would expect many years of operation before a failure will occur. However, this depends on the loads and operating conditions and, more importantly, is a statistical average; so failure could occur much earlier. In nuclear reprocessing plants, mechanical plant such as cranes and drive motors, are designed to be maintained and are situated in areas where they can be withdrawn into a clean area; for example, through a shield door for maintenance, or the area can be decontaminated to allow entry by personnel.

For process plant, maintenance is generally ruled out as vessels and pipework are fixed into sealed cells and need to be cut out, but in some cases maintenance is possible. For example process instruments can be installed into wells or sealed dip pipes in a process vessel so that they can be withdrawn and maintained (Figure 6.3).

6.2.2.4 Build in space for retrofit

In the United Kingdom, both full-scale reprocessing plants had space built-in to allow a retrofit of a replacement dissolver. In the Magnox reprocessing plant, originally commissioned in 1964, there have been two swapovers to new dissolvers, utilizing

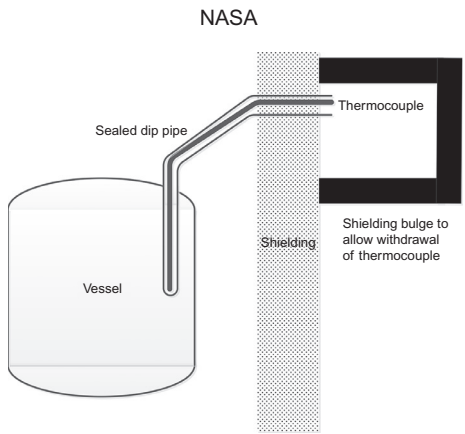

Figure 6.3 An example of an instrument engineered for maintenance in a nuclear plant.

a spare dissolver cell to construct a new dissolver. In THORP, a spare dissolver cell exists, but as yet, it has not been required. The advantage of this method is that there is no initial outlay for equipment and it leaves some latitude to build in new technological developments if they arise. The disadvantage is that the time to swap over can be lengthy and will inevitably involve breaking into a highly radioactive cell to connect the new plant.

6.2.3 Fissile material management

Nuclear fuel reprocessing plants will be dealing with fissile materials and so the design engineer must consider what methods can be adopted to manage criticality and what effect these measures will have on the plant design.

When considering criticality we will need an estimate of the effective neutron multiplication factor, k_{eff}. This is the net number of neutrons that are produced from a spontaneous fission. In a uranium system, ^{235}U will emit on average just over 2 neutrons per fission event. However, not all of these neutrons go on to be absorbed by another ^{235}U atom; the presence of moderators and neutron-absorbing materials will reduce the number and so $k_{\text{eff}} < 2$.

If $k_{\text{eff}} = 1$, then the criticality chain is sustained; this is what engineers will try to design for in a nuclear reactor. If $k_{\text{eff}} > 1$, then the system is super critical and an escalating chain reaction will ensue. To keep criticality under control, k_{eff} must be <1 and taking account of margins of error in its calculation, engineers will usually design the plant so that $k_{\text{eff}} \leq 0.95$ for a given system. During the detailed design phase, a full criticality assessment of vessels and pipework will be conducted to prove that this is so. Many methods exist that can be adopted to manage criticality and they fit into two categories: passive and active.

Passive methods will restrict the amount of material that can be present in the plant at any one time so that a fissile mass cannot accumulate. This can be either through a restriction on the volume or a dimension of the plant item; for example, volume of vessel or diameter for a pipe. This type of method is preferred as the control is ever present. However, the minimum fissile mass for ^{235}U is about 800 g and that for ^{239}Pu is about 500 g in water, so for a full-scale plant restricting the overall volume may not be feasible, as the throughput required is much greater than a fissile mass. Restricting the dimension of the plant item gives much more flexibility.

If we take a typical plant that is reprocessing uranium fuel with an initial ^{235}U enrichment of 4.5%w/w, using the PUREX process, then during dissolution we would expect to have a solution with about 300 g L^{-1} of uranium. The fissile concentration would then be 13.5 g L^{-1} (in this example we are assuming that there is no plutonium present and the only fissile material is uranium). An initial estimate of the maximum size for a subcritical sphere for this system would be 80 cm (Los Alamos National Laboratory). This means that we could not have any vessels with a volume greater than about 70 L. For a large reprocessing plant, this would not be a feasible option as we would expect to be producing 1500-2000 L per day.

Pipe diameters for this system would be 60 cm (Los Alamos National Laboratory), so transport of the liquid should not be a problem and we could design a long, thin tank. However, even then we will only be able to contain about 300 L for every meter

of vessel height. For a large reprocessing plant, we need a method to remove or relax the restrictions on the volume or dimensions of our equipment.

Maintaining a passive approach, we can install a fixed neutron poison into the system. Boron (^{10}B) and hafnium (most isotopes) are commonly used for this purpose and boronated steels are available. This approach can be very effective and can, in some cases, allow us up to 2-3 times the diameter.

Moving away from passive to active methods will have the greatest effect on design constraint, but at the cost of reduced certainty. Active methods will need to be backed up by a safety case that proves they are present at all times.

The first active method for criticality control is the use of soluble neutron poisons. Again boron (^{10}B) can be used and is the most common soluble neutron poison used in light water reactors (LWRs). However, for nuclear fuel reprocessing, gadolinium, in the form of a soluble nitrate ($Gd(NO_3)_3 \cdot xH_2O$), is used as it is more compatible with the PUREX process. The specific gadolinium isotope of interest is ^{157}Gd, which is about 15% in natural gadolinium. Present in quantities of a few grams per liter, gadolinium can be a very effective neutron poison and can allow engineers to design vessels that have virtually no restriction on their dimensions and still remain subcritical. In the headend of the United Kingdom's THORP reprocessing plant, the dissolvers and the vessels that receive the product liquor from dissolution have been designed taking account of gadolinium neutron poisoning and have diameters that far exceed that of an unpoisoned system.

The last method to consider is to manage and monitor the inventory of the system and prevent the input or accumulation of fissile mass in any area of the plant. This may be possible for a plant that is designed for operation in a batchwise fashion, but it would require rigorous control and any deviation from the standard process conditions could result in a criticality event.

One factor to consider for all systems is burn up credit, a form of inventory management. It is standard practice to design nuclear fuel reprocessing plants based on safety cases assuming worst-case scenarios. For criticality, this would be the reprocessing of unirradiated fuel. However, in reality, spent fuel, with a much lower enrichment, is the feed for a reprocessing plant and so design engineers and safety assessors may be able to take account of "burn up credit" (Brady-Raap et al.), which is the overall reduction in reactivity associated with the irradiation of fuel in a reactor and with cooling time. Before any burn up credit can be allowed into the design, the fuel fed to the reprocessing plant would need to have a fissile monitoring regime that proves its "burn up" and resulting reduction in fissile content.

6.2.4 Radiological and contaminant management

It is more the role of the civil engineer to design the building that houses process plant equipment; however, the type of building designed will have a significant influence on the technology options available to the nuclear process engineer.

Primary among the criteria that will drive the building design of a nuclear reprocessing plant will be containment of radiological materials and prevention of the spread of contamination. Ideally, the best way to contain radiological materials is within vessels and pipes in sealed cells. In almost all cases in a reprocessing plant there are areas where

this is not possible. One example is fuel dissolution, where spent fuel must be fed into a dissolver. In this case, vessel containment (i.e., the dissolver) must be broken to admit solids (i.e., the fuel) into the vessel. Breaking containment opens up the possibility for the spread of contamination into the surrounding environment. This would not be a problem if we did not expect to have to enter the cell until decommissioning, but this plant area will include mechanical equipment (fuel shear, cranes, and maneuvering equipment for the fuel assemblies) that can suffer breakdowns and may need to be maintained.

The main cause for the spread of contamination will be the movement of equipment or people from one plant area to another. Therefore, the building designer will zone the plant according to the level of radiological and contamination risk. Areas of high radioactivity and contamination will be sealed within cells with no entry allowed. Areas of no radioactivity or contamination will not need any access restrictions. In between these two extremes will be a gradual decrease in access for personnel.

For those areas where personnel can enter, even under special conditions, it is possible to have equipment that requires maintenance or could be replaced. One example of an area within this category in a nuclear reprocessing plant would be the uranium finishing area (conversion of nitrate solution to oxide powder), where the material being processed is uranium with very low levels of fission products. In this case it would be possible to advocate the use of centrifugal pumps and valves, albeit high-grade ones, as it would be possible to replace or maintain them in the event of a failure (Figure 6.4).

Contamination will often take the form of particulates or aerosols. Movement and spread of these can be controlled by the air flow through the plant (Figure 6.5). Small particles and droplets will be easily swept up by an airflow, if the velocity is sufficient,

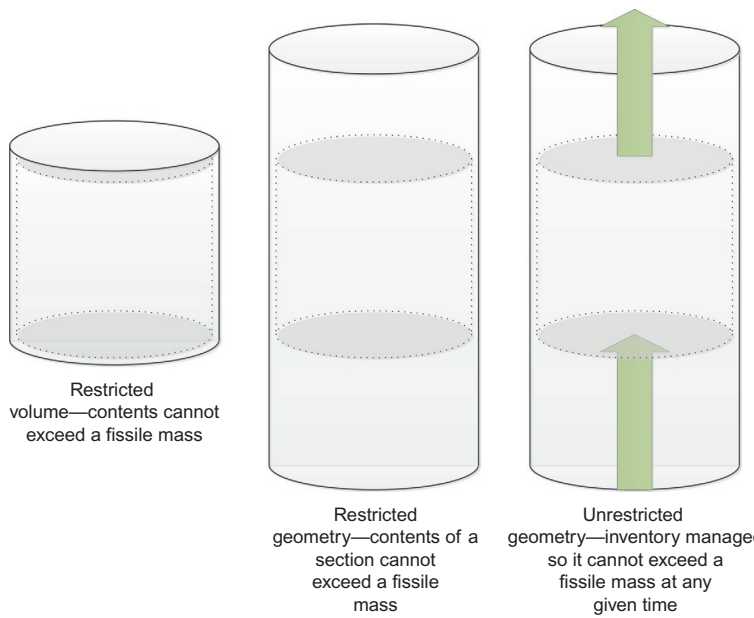

Figure 6.4 Fissile material management strategies based on control of geometry. Geometric constraints can be relaxed with the use of neutron poisons.

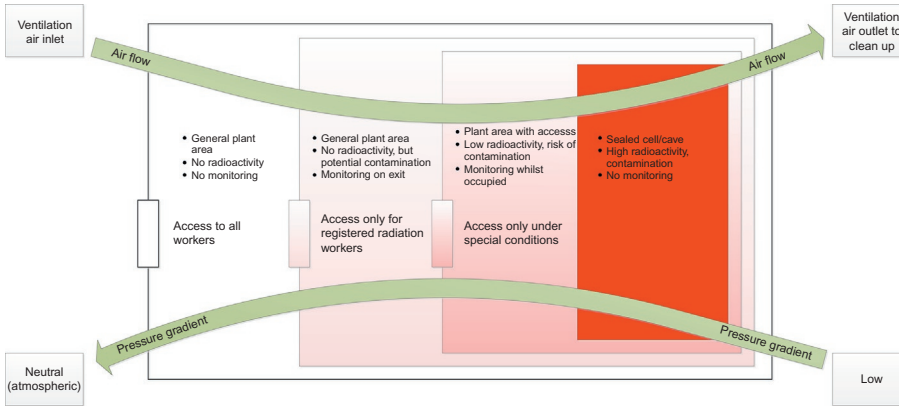

Figure 6.5 Ventilation philosophy for nuclear plants.

and so we can design our ventilation system to do this; typically, a 100 μm particle can be conveyed with an air velocity of a few meters per second. The flow of air through the building will always be from clean to dirty so as to prevent back flow of contamination. The final point for the air will be the sealed cells and after that the air will be scrubbed, filtered, and monitored prior to release.

Opposite to the direction of air flow will be the pressure gradient that will be set up across the plant, with the point of lowest pressure in the sealed cells. Careful design of equipment must be carried out to ensure that discharges to the vessel vent do not cause an imbalance in the ventilation system. For example, if we wish to operate a vessel under vacuum (such as an evaporator) we must ensure that we do not suck back contamination from an area of higher radioactivity into that vessel. As the overall driving force for the pressure gradient within the ventilation system will be the main fans, it is likely that the overall pressure drop will need to be limited to about 30 mBar. This creates a dilemma for the designer, as we wish to maximize velocity for efficient dust and aerosol entrainment, but the higher the velocity the higher the pressure across the system and so the designer will have to select an appropriate pipe size for each of the vessel vents to balance these.

The overall effect of these building constraints on the process design is that in some cases the obvious and more preferred choice for technology cannot be made as either the plant zone it must be placed into is incompatible (e.g., a fuel assembly shear in a sealed cell) or connection to the ventilation system is incompatible (e.g., the required pressure drop will be too large).

6.3 Plant design and engineering

6.3.1 Scale-up from laboratory to full-scale

The development of new chemical processes for reprocessing and recycling of spent nuclear fuel is primarily done at the laboratory-scale due to the difficulties in working with highly radioactive materials. However, industrial deployment of such new or

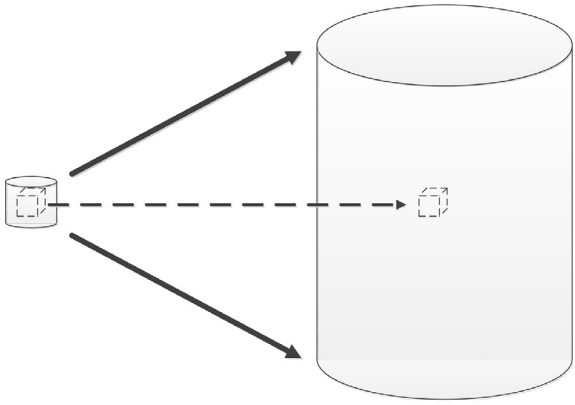

Figure 6.6 A comparison of scale.

improved processes requires a scaling-up from the laboratory-scale to full-scale. It is, therefore, very important to understand how chemical processes can vary as the engineers scale-up the design of the reprocessing plant; that is, are variations linear, exponential, or is there no variation with scale in the specific parameter?

Consider a volume of liquid within a small-scale vessel in a laboratory and compare that with the same volume of liquid at the center of a full-scale process vessel (Figure 6.6). If we look at three physical aspects of the liquid that may be important to the process (density, concentration, temperature), how will they be affected during scale-up?

The external forces acting on the two liquids will be different. For the full-scale process, our liquid in the center of the vessel will have the effect of pressure from the static head of the liquid above it (if this were water, each meter of liquid height would be equivalent to 0.1 bar of pressure). However, most liquids are incompressible, so the effect of pressure on density will be negligible (e.g., for water a 20 bar increase in pressure will increase density by <0.1%, ESDU report); in fact, most of its physical properties are unaffected by changes in pressure. Therefore, we can conclude that, with respect to the physical properties of the liquid, there are no scaling effects.

Now let us consider temperature. When conducting an experiment we will usually seek to control the temperature. Quite often the laboratory vessel will sit on a hot plate or within a water bath. The overall volume and dimensions (surface area to volume ratio) of a small vessel is such that the temperature of the liquid anywhere within the vessel will respond very quickly to changes at the edge of the vessel. For example, a vessel with 50 mm diameter and 50 mm height has a high surface area to volume ratio of 120. If we now scale-up to a large process vessel and consider the same liquid at the center, say to a vessel of 500 mm diameter and 500 mm height, the surface area to volume ratio decreases to 12. This means that our liquid in the center of the vessel will be slower to respond to temperature changes; as will the whole contents of the vessel.

If the liquid contents are static, then we will have to rely on conduction and natural convection to heat or cool the center. These two processes are not efficient mechanisms and there must be a temperature difference to drive any heat transfer.

We must have an understanding of the fundamental variation in order to extrapolate from small to large scales. Very often the jump from laboratory- to full-scale is so large that we will need to have one or more intermediate steps to prove our process. These are the pilot plant and demonstration stages.

Overall heat transfer from the surface to the liquid is given by

$$Q = U.A.\Delta T_1 \tag{6.1}$$

where Q is the overall heat transfer rate in watts, U is the overall heat transfer coefficient in watts per meter square per degree Celsius, A is the surface area in meter square, ΔT_1 is the temperature difference between the vessel surface and the bulk liquid in degree Celsius.

The heat required to increase the temperature (T) of the liquid by an amount ΔT is given by

$$W = \left(\rho \cdot V \cdot C_p \cdot \Delta T_2\right)/tT_1 \tag{6.2}$$

where W is the heat required to increase the temperature of the liquid in watts, ρ is the density of the liquid in kilogram per meter cube, V is the volume of the liquid in meter cube, C_p is the specific heat capacity of the liquid in Joule per kilogram per degree Celsius, ΔT_2 is the temperature increase in the bulk liquid in degree Celsius, t is the time taken for ΔT_2 to occur in seconds.

Assuming no other heat transfer mechanism exists, then $Q = W$ and we can rearrange Equations 6.1 and 6.2 to give us a function of ΔT_2 against surface area to volume ratio.

$$\frac{A}{V} = \left[\frac{r.C_p}{U.\Delta T_1}\right].\frac{\Delta T_2}{t} \tag{6.3}$$

We can see that if physical properties are unchanged ($\rho \cdot C_p$) and we can duplicate the equivalent heat transfer rate (U), then the temperature change in the vessel is directly proportional to the surface area to volume ratio. Reducing this from 120 to 12 will increase the time taken for our vessel contents to change temperature by a factor of ten. In reality, heat transfer rate will also be affected by an increase in scale; compounding the effect.

The result is that effects on a system in the laboratory are rapid, but on a full-scale plant take time. During that time it is possible that side effects may come into play that change the overall dynamics of the reaction and may allow for by-products to be created.

6.4 Advances in solvent-extraction equipment

6.4.1 The principles of solvent extraction

All liquid-liquid extraction systems are comprised of two sections: a mixing section and a separation section. Mixing breaks up one of the phases into small drops and disperses them in the other phase, called the dispersed phase and continuous phase, respectively.

In the mixing section the aim is to maximize the interfacial area available for mass transfer between the two phases. Separation of the dispersed phase from the continuous phase then needs to occur for the extraction to be complete. Usually, the kinetics of the extraction process is such that multiple stages are required to achieve the target separation required for reprocessing.

The process of liquid-liquid extraction relies on the optimization of efficient mixing with separation of the dispersed phase from the continuous phase. For a mixer-settler or pulsed column, this separation occurs due to a difference in the density of the phases, driven by gravity. The efficiency, or rate, at which the separation occurs is proportional to the size of the droplet and the density difference between the two phases. Hence, the degree of mixing allowed can be limited by the time required for dispersed droplets to settle and the two phases to separate.

The design of the mixing section is related to the overall mass transfer coefficient, which is defined within the Sherwood number.

$$Sh_c = \frac{k_{LC} d_p}{D_c} \tag{6.4}$$

where Sh_c is the Sherwood number for the continuous phase (dimensionless), k_{LC} is the overall liquid phase mass transfer coefficient for the continuous phase (meter per second), d_p is the droplet diameter (meter), D_c is the molecular diffusivity (meter square per second).

In general, the mass transfer coefficient in a stirred vessel can be approximated by $Sh_c = 6.6$ (Treybal, 1980). However, more detailed correlations have been developed that allow the engineer to calculate the mass transfer for a given mixer design (Skelland and Moeti, 1990).

$$Sh_c = \frac{k_{LC} d_{32}}{D_c} = 1.237 \times 10^{-5} (Sc)^{1/3} (Fr_C)^{5/12} (Eo)^{5/4} (\phi)^{-1/2} (Re)^{2/3} \left(\frac{D_i}{d_{32}}\right)^2 \left(\frac{d_{32}}{D_t}\right)^{1/2} \tag{6.5}$$

d_{32} = Sauter mean diameter, which is approximated to the droplet diameter (m), Sc is the Schmitt number, defined as diffusion of momentum/diffusion of mass, Fr_c = Froude number, defined as inertial forces/gravity forces, Eo = Eotvos number, defined as buoyancy force/surface tension force, φ = constant developed from experimental work, Re = Reynold's number, defined as inertia forces/viscous forces, D_i = impeller diameter (m), D_t = vessel/tank diameter (m).

From Equation 6.5 we can estimate mass transfer coefficients for some common extraction technologies. Agitated vessels (cf. mixer-settlers) have a k_{LC} of between 0.16 and 16 ms^{-1}, agitated columns have a k_{LC} of between 8 and 60 ms^{-1}, and packed columns have a k_{LC} of between 5 and 111 ms^{-1}. More efficient systems, such as rotating disks, have high k_{LC} values (20-260 ms^{-1}), but these involve rotating parts.

One of the first mixer-settlers to be used was developed by the UKAEA (United Kingdom Atomic Energy Agency) for the first-generation reprocessing plant at Windscale in the United Kingdom, operated in the 1950s (Lo et al., 1983). The units were a

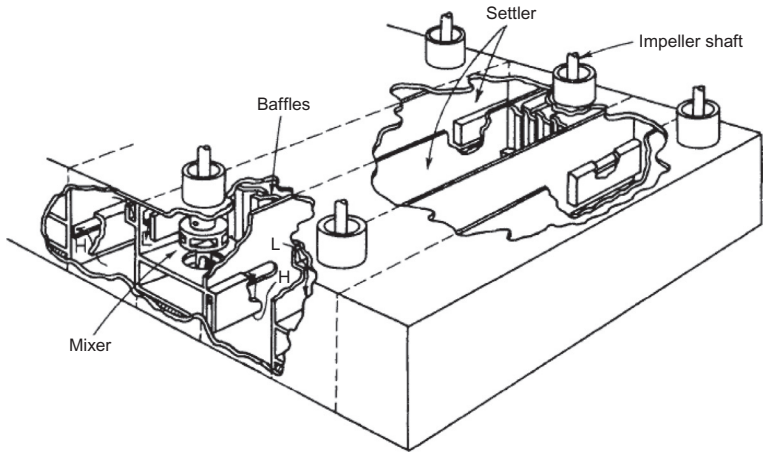

Figure 6.7 Simple box-type horizontal mixer settler used in the reprocessing of nuclear fuel (Perry, 2008).

simple box-type horizontal mixer and settler (Figure 6.7). Similar designs have been used in subsequent U.K. reprocessing plants, as well as plants in France and Japan.

In these designs, the volume of the mixer is determined by the residence time required to reach a reasonable degree of equilibrium (Treybal, 1980). Most often, the settler is many times larger than the mixer, as simple gravity settling is the only process at work and is the primary factor for determining overall equipment size. Mixing is carried out using a flat blade turbine, rotating at about 200 rpm (Treybal, 1980). The speed is limited so that the production of very fine droplets (haze) is minimized.

More recent reprocessing plants (e.g., British Nuclear Fuels Ltd. THORP, designed to reprocess oxide fuels from Advanced Gas Reactor and Light Water Reactor) replaced mixer-settlers in the primary separation area with pulsed columns. This was due to the increased fissile content of the spent fuel being reprocessed, which constrained the design of the solvent-extraction equipment to within certain parameters so that it remained subcritical. Also, the increased activity from fission products meant that solvent degradation would be too high if mixer settlers were used, due to the long residence times, especially in the settling section.

Pulsed columns consist of a vertical, cylindrical tube containing a set number of stationary, horizontal, perforated plates at equal distance from each other. The two immiscible liquids are added at the opposite ends (top and bottom) of the column, with the low-density liquid added at the bottom and the reverse for the heavy liquid. Gravity again provides the motive force, with the heavier phase falling to the bottom of the column while the lighter phase rises to the top (Figure 6.8). The pulsing action provides agitation to break up the light phase and disperse it, as well as forcing it upward. Plate spacing is designed to replicate the equivalent of a separation stage in a mixer-settler and the hole size in the plates, in conjunction with pulse frequency and amplitude, determines the droplet size. Due to the complexity of the system, it is difficult to define the mass transfer coefficient through a correlation similar to those that exist for

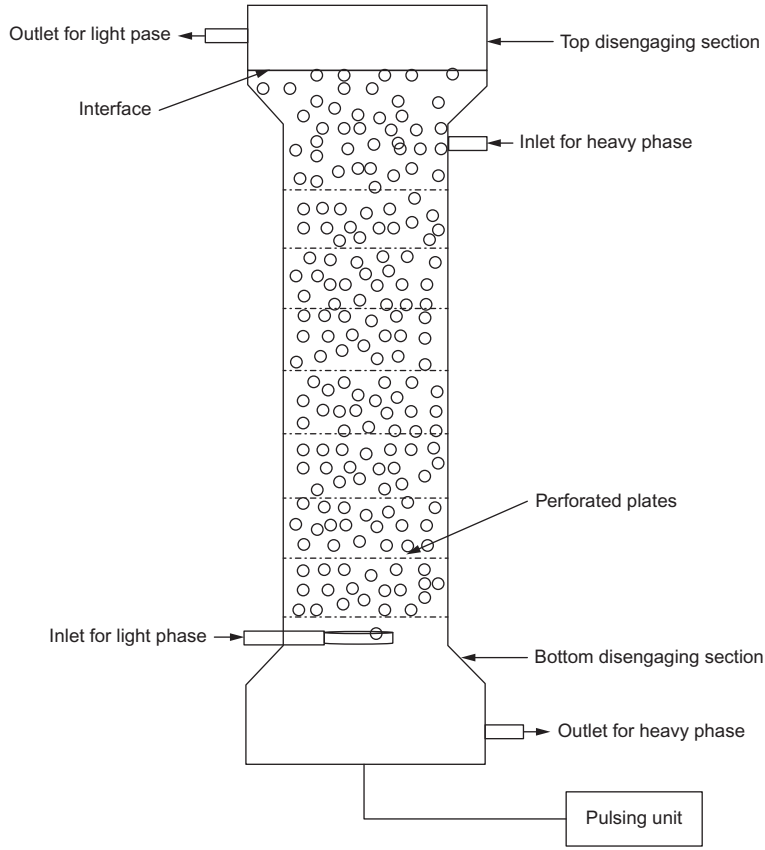

Figure 6.8 Diagram showing the internal workings of a pulsed column (Yadav and Patwardhan, 2008).

mixer-settlers. A recent review of a number of empirically derived correlations from experiments found little agreement on an overall correlation and so leave the engineer relying on proving any design via pilot plant trials (Yadav and Patwardhan, 2008).

6.4.2 Developments in conventional solvent-extraction systems

A number of different designs for mixer-settlers and column extractors have been used for many years in the metal extraction industry; examples include the IMI and Lurgi mixer-settlers and Rushton columns (Lo et al., 1983). In addition to liquid-liquid extraction technology development, the oil industry has been improving performance of gravity settlers for use on offshore oil rigs (American Petroleum Institute (API), 1990).

The most common advance in mixer-settler design, beyond the standard box-type used in spent fuel reprocessing plants, has been to decouple the dispersion and mass

transfer process. This has been achieved by having a two-stage mixer; with the first stage utilizing a high-efficient turbine to produce a fine dispersion, in a low residence time, followed by a lower speed mixing chamber sized to provide the correct residence time for mass transfer.

To advance separator design, the oil industry has developed the use of wave plates and coalescers installed in gravity settlers to enhance separation of oil and water. These devices encourage fine oil droplets to coalesce into larger droplets, which settle faster; so reducing the size for a given throughput (Figure 6.9). Close plate spacings are preferred, but significant savings in separator length (up to 75%) can be achieved with spacings of up to 22 mm (Schlieper et al.).

An example of the two advances in mixer-settler design (dual mixing zones and enhanced gravity settling) can be seen in the Krebs mixer-settler (Taylor); developed by Krebs in France in the 1970s, and subsequently installed in numerous uranium mining and copper facilities (Figure 6.10).

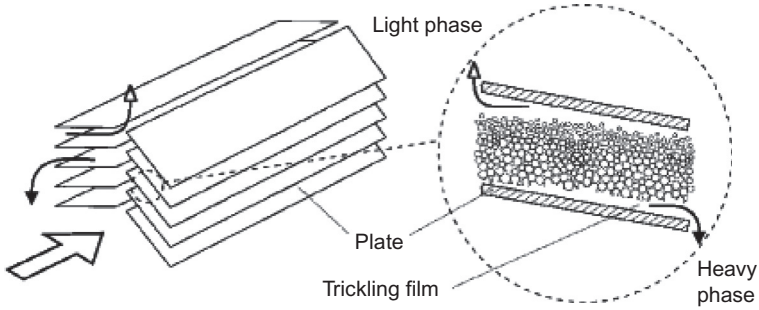

Figure 6.9 A typical wave plate coalescer used to enhance separation in a gravity settler (Schlieper et al.).

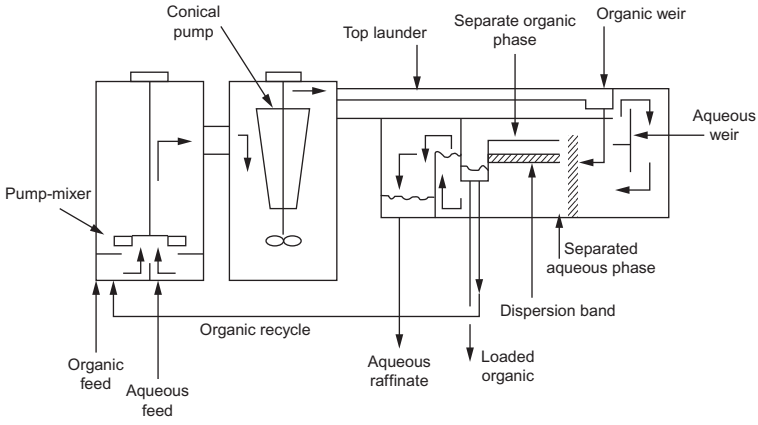

Figure 6.10 Side elevation of a Krebs mixer settler.

In this design, the first section is a pump-mix type agitator, similar to the conventional mixer-settler, but designed for less head generation because of the adjoining conical pump. Typically, the primary separation of the organic and aqueous phases is 90% complete at the discharge of the upper launder, which enables the phases to be directed separately to the main settler below, entering via a series of baffle plates to enhance coalescence. The organic and aqueous discharge weir boxes and weirs are similar to the conventional design.

Table 6.1 presents an economic comparison of the Krebs with the conventional mixer-settler taken from "Krebs and Solvent Extraction" by Roger Williams and Alain Sonntag presented at the ALTA Copper Hydrometallurgy Forum 1995. The reduced size and efficiency lead directly to a significant saving in cost.

For a nuclear application, the reduced solvent inventory (30-50% over a conventional design) would give advantages in reduced degradation.

6.4.3 Centrifugal contactors

In the 1930s, centrifugal countercurrent contactors were developed for liquid-liquid extraction processes. Compared to conventional liquid-liquid extraction technologies, centrifugal contactors have enhanced separation, as they are able to replace gravity with centripetal force, which radially separates the two phases and increases the separation velocities.

Centrifugal contactors can be classified into two groups: differential and staged contactors. In differential contactors, countercurrent flow of the two phases occurs within a single rotor, as the light phase is introduced at the periphery and the heavy phase at the axis. Centripetal force causes the two phases to travel in opposite

Table 6.1 An economic comparison of the Krebs with the conventional mixer-settler taken from 'Krebs and Solvent Extraction" by Roger Williams and Alain Sonntag presented at the ALTA Copper Hydrometallurgy Forum 1995

	Krebs	Conventional
Characteristics		
Typical a settler specific flow ($m^3/h/m^2$)	8-12	3-5
Relative solvent inventory	1	1.3-0.5
Organic entrainment losses ppm	30-100	30-100
Relative capital costs		
Equipment ex works	1	1-1.2 (depending on size)
Transportation/erection	1	1.3-1.5
Piping/cables	1	1.3
Civil work		
Outdoor	1	1.2
Indoor	1	1.8-2

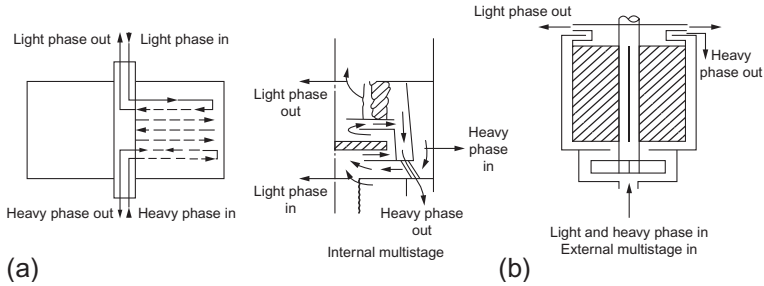

Figure 6.11 Operating principle of centrifugal extractors: (a) differential contact and (b) multistage contact (Lo et al., 1983).

directions. In staged contactors, both phases are introduced into a mixing section at the periphery. The mixed phases travel to a central section where centripetal force separates them. Countercurrent flow is achieved by a cascade of contactors. Figure 6.11 illustrates this diagrammatically.

Centrifugal contactors are used for a range of applications, such as antibiotic extraction in the pharmaceuticals industry, and have been used in reprocessing plants; for example, an 18-stage centrifugal mixer-settler, designed and developed at the Savannah River Laboratory successfully separated plutonium and uranium from radioactive fission products at the Savannah River site (Kishbaugh).

Table 6.2 classifies the existing designs in use today. The range of conditions for operating centrifugal contactors can vary quite significantly, depending on the solvent-aqueous system. Table 6.3 gives data on the operating parameters for some of the commonly used centrifugal contactors in industry (Figures 6.12 and 6.13).

Control of the hydrodynamics of centrifugal contactors is based on four parameters:

(1) *Pressure*: This is especially important in centrifugal contactors as this is the main means to control the interface between the two phases. Pressures on either side of the weirs are adjusted using control valves (PIC) on the outlets. A typical arrangement for a pressure control system is shown in Figure 6.14.

Table 6.2 Classifications of centrifugal contactors in use in industry (Lo et al., 1983)

Horizontal		Vertical		
Differential	***Multistage***	***Differential***	***Multistage***	***Single stage***
Podbielniak POD Quadronic		α-Laval UPV	Luwesta Robatel SGN	Robatel BXP Westfalia TA SRL & ANL MEAB SMCS-10

Table 6.3 Operating parameters for commonly used centrifugal contactors (Lo et al., 1983)

Extractor	System	Physical properties			Operating variables				Number of theoretical stages[d]	Efficiency (%)[a]
		P_h/P_i	h/l		rpm	$R = Q_h/Q_l$	Q_t (m^3/hi)	Flooding (%)		
Pod bieLniak										
B-10	Kerosene-NBA[b]-water	998/801	1/1	24	3000	0.5	5.1	73	6-6.5	24
D-I8	Keiosene-NBA-water	998/801	1/1	24	2000	0.5	11.1	58	5-5.5	15
A-I	Oil-aromatics-phenol[a]	1010/877	2/5	3	5000	3.5	0.01-0-02	33-66	5-7.7	28-43
9000	Broth-penicillin				2900	4.4	7.5		1.8	10.7
	B-pentacetate				2900	3.4	7.5		2.04	
					2900	2.4	7.5		2.21	14.0
9500	Some system				2900	3.5	7.5		2.04	
					2700	3.5	7.5		2.19	
					2500	3.5	7.5		2.30	
					2300	3.5	7.5		2.36	15.0
	Oil-aromatics-furfural				2000	4.0	12.0	90	3-6	24
A-l	IAA[c]-boric acid-water	998/810	1/5	6	5000	1-0.3	0.01-0,03	44-95	3.5-7.7	20-45
					3000	1.0	0.01!	44	2.3	13.5
					4075	1.0	0.01	44	2.8	16.5
					4600	1.0	0.01	44	2.96	17.5
UPV	Oil-aiomatics-phenol[a]	1010/910	2/8	2	1400	0.8-1.2	6	75	2-5.8	33-92

Continued

Table 6.3 Continued

Extractor	System	Physical properties			Operating variables				Number of theoretical stages[d]	Efficiency (%)[a]
		P_h/P_i	h/l		rpm	$R = Q_h/Q_l$	Q_t (m^3/hi)	Flooding (%)		
Robatel SGN										
LX-168N	Uranyl nitrate-30% TBP				1500	1-0.2	2.1-4.5		7	87
LX-324	Some system				3100	1.6	24-63		3.4-3.9	68-80
SRL single stage	Uranyl nitrate-Ultrasene				1790	0.5-1.5	6.4-12	33-96	0.92-0.99	92-99
ANL single stage	Uranyl nitrate-TBP/ dodacane				3500	0.3-4	0.8-1.6	50	0.97-1	97-100

Note that: ρ_h, ρ_l are the density of heavy and light phase in kilogram per meter cube; h/l is the heavy:light ratio; R is the ratio of total heavy phase flow, Q_h, and the light phase flow, Q_l, both in meter cube per hour; and Q_t is the total flow rate in meter cube per hour.

[a]Containing 1.7-5% water.

[b]Normal butyl amine.

[c]Isoamyl alcohol.

[d]Number of theoretical and actual stages.

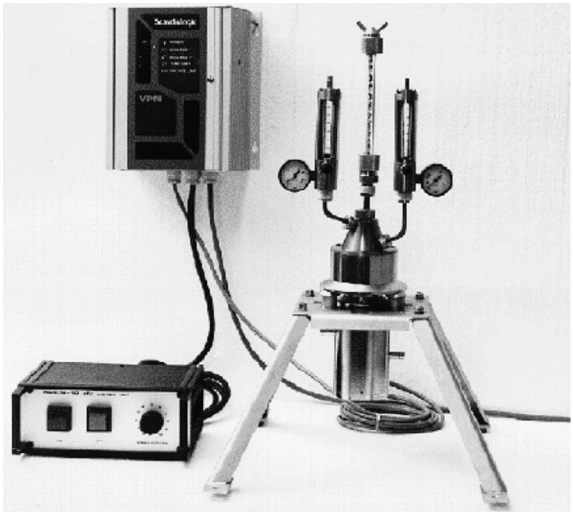

Figure 6.12 An experimental rig using a MEAB SMCS single stage contactor.
Photo courtesy of MEAB (http://www.meab-mx.se).

Figure 6.13 An industrial liquid-liquid extraction process using a counter cascade of Robatel BXP contactors
Photo courtesy of Rousselet Robotel (http://www.robatel.com).

(2) *Holdup*: In pressurized contactors this is directly proportional to the system parameters and can be estimated using the following equation:

$$\varnothing = 1 - \frac{2\pi b(P_{\text{li}} - P_{\text{lo}})}{\omega^2 \Delta\rho V_m} \tag{6.6}$$

where ϕ is the hold up, b is the contactor width in meters, P_{li} and P_{lo} are the pressure of the light phase at inlet and outlet in Pascal, respectively, ω is the speed of rotation in rpm, $\Delta\rho$ is the difference in density between heavy and light phase in kilogram per meter cube, V_m is the emulsion volume in meter cube.

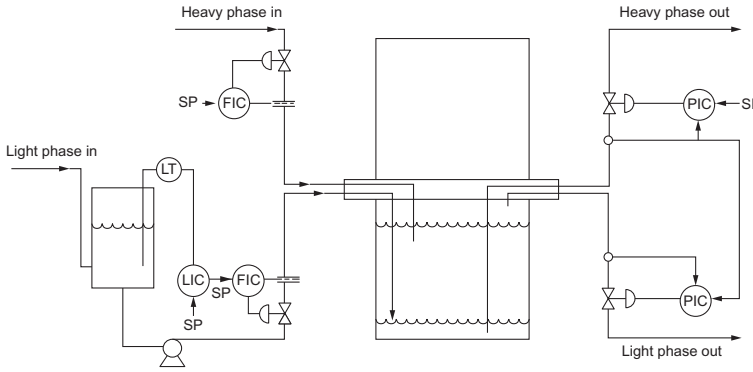

Figure 6.14 Pressure control system for a centrifugal contactor (Lo et al., 1983).

(3) *Flooding*: Operating the contactor above its capacity will lead to flooding. In most designs, capacity increases by increasing the diameter of the contactor and/or speed of rotation. This is different than mechanically agitated contactors, where increasing agitation (cf. speed of rotation) will lead to an increased chance of flooding.

(4) *Back mixing*: Generally, the extent of any back mixing in a centrifugal contactor cannot be predicted by applying dimensionless numbers, as would be the case for a mixer-settler (see Equation 6.5). This is due to the more complicated nature of the contactor; for example, driving velocities, differential pressures, and flow fields at different points within the contactor. Therefore, back mixing can only be measured for a specific system.

6.5 Multiscale modeling and simulation

With the advent of computer-aided design in the 1980s there began a shift away from direct incorporation of experimental results into plant designs toward the use of process models that were validated by experiment and informed the engineer to a much greater extent. As computers have become more powerful, software developers have been able to create codes that can be used across all the disciplines to model a system at the scale of their experiments (Figure 6.15). Nowadays, one of the goals of a good design is to integrate each of the different types of model as we move up the scale and across disciplines.

An example of modeling and its experimental validation is how it could be used to design the separation part of a reprocessing plant. At the atomic-scale, molecular modeling techniques such as density functional theory (DFM) or Lipinski's rule of five (a technique used in the pharmaceutical industry for molecular design) can be used to predict the bonding behavior of molecules and so predict the efficiency of ligands for separating actinides. These could lead to selection of ligands for experimental proving in the laboratory. Once separation factors have been determined, these can be fed back into process models that combine laboratory data with kinetics to design a flow sheet. The flow sheet is then proved using a contactor cascade, moving up to pilot-scale, to provide a design flow sheet; the starting point for a full plant design. Data from the laboratory trials and pilot plant trials feeds back into the process models to allow further refinement and so produce models that can then predict the behavior of the plant during operation.

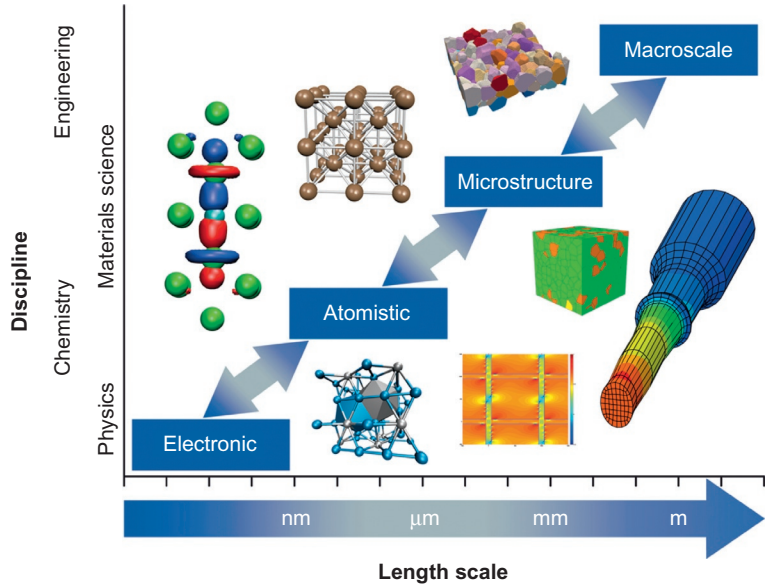

Figure 6.15 How modeling techniques can be used across the scale range in the design of a plant.
Taken from www.icams.de.

We can also consider how modeling at different scales can tell us how a liquid will behave when flowing down a pipe. Engineers are often predicting flow regimes in order to calculate the extent of heat and mass transfer or just pressure drops to ensure a liquid can be transferred using a particular pump. Most often, the flow regime in a pipe is approximated by the use of the Reynolds number, which is the ratio of inertial and viscous forces and is defined as

$$Re = \frac{u\rho L}{\mu} \tag{6.7}$$

where u is the fluid velocity in meters per second, ρ is the fluid density in kilo gram per meter cube, L is the characteristic length, which for a pipe is the diameter in meters, μ is the dynamic viscosity in kilogram per meter second.

For a system with a $Re < 2300$, we say the flow is laminar; that is, all velocities are streamlined with the direction of flow. Once the Re becomes >4000, we say the flow is turbulent and it will contain eddies. At values of Re between 2300 and 4000, the system is in transition and is impossible to predict. Engineers will try to ensure that their design is well within either laminar or turbulent regimes, as their means to predict pressure drop, heat, and mass transfer are derived for these. However, one major drawback is that Re is a bulk prediction and does not tell the engineer what is happening at the microscale, which for turbulent flows is important as the system behavior will be dependent on localized eddies. For systems with more than one phase (e.g., gas-liquid,

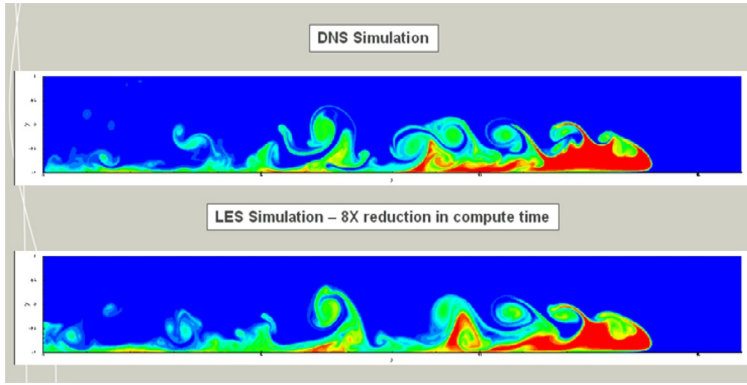

Figure 6.16 Prediction of turbulence in a pipe using CFD techniques.

liquid-liquid, or solid-liquid) this is also of importance as localized velocities may cause deposition or changes in droplet size, which go on to affect mass transfer.

Computational fluid dynamics (CFD) can be used to provide a more detailed analysis of a flow regime. For turbulence, the processes governing the conservation of mass, momentum, and energy in a viscous, Newtonian fluid are defined by the Navier-Stokes equations. These are a set of coupled partial differential equations, which could, in theory, be solved for a given system by using methods from calculus, but in practice, these equations are too difficult to solve analytically. CFD techniques have been developed that can be used to solve Navier-Stokes and have been converted into commercially available codes.

The most accurate method is direct numerical simulation (DNS), which is solely based on the physics of the system and is, in effect, a direct solution to the Navier-Stokes equations. Computationally this technique is very intensive, due to the huge numbers of solutions that need to be generated in order to obtain a simulation. However, if it is possible to use DNS, then a very accurate prediction of the turbulence in a pipe can be created. Large eddy simulation (LES) is an approximation of turbulence, which accounts only for large-scale motion. This is less computationally intensive and will resolve turbulence patterns within a pipe to the level at which solids deposition can be predicted. Figure 6.16 illustrates the different resolution levels of DNS and LES.

6.6 Current and future trends in design for nuclear fuel reprocessing plants

6.6.1 Computer-aided design

At the onset of computer-aided design (CAD) in the 1980s the focus was on the replacement of the traditional paper-based drawing office with a screen and keyboard-based system. CAD packages offered flexibility and increased speed for engineers and designers to create drawings on which to base construction.

As CAD software became more sophisticated, more and more detail could be included in the drawing, so that by the late 1990s CAD software had completely replaced traditional drawings and could show far more detail and information than any hand drawn document ever could.

Design was still based around 2-D representation and if the engineer wanted a 3-D view a physical, scale model of the plant would need to be constructed. These were expensive and time-consuming to produce and realistically could not be kept up to date with design changes.

In the last decade we have seen CAD systems that are moving beyond 2-D to include 3-D modules that allow engineers to "see" their system as they design it. Both of the major software suppliers (AutoCAD and Solidworks) market 3-D CAD versions of their product. These packages are still primarily screen-based, but can provide a multileveled view, whereby a complex plant such as a reactor (Figure 6.17) can be viewed with zoom in capability for individual items.

Already, there are numerous organizations that have 3-D immersion suites, where CAD software can be linked into visualization software and hardware to allow the engineer to literally walk around a plant while it is in the design stage. For nuclear plants the potential these capabilities offer is huge as, with the space management and constraints in a design for a remotely operated plant, it is very difficult for the engineer to optimize for layout and, when constructed, it may not be possible to see the plant in its final state.

6.6.2 Prototyping

The design process has been, or will soon be, revolutionized by the advent of 3-D design and virtual immersion suites; but the fabrication process is still effectively unchanged and based on casting or machining techniques. Although machining has

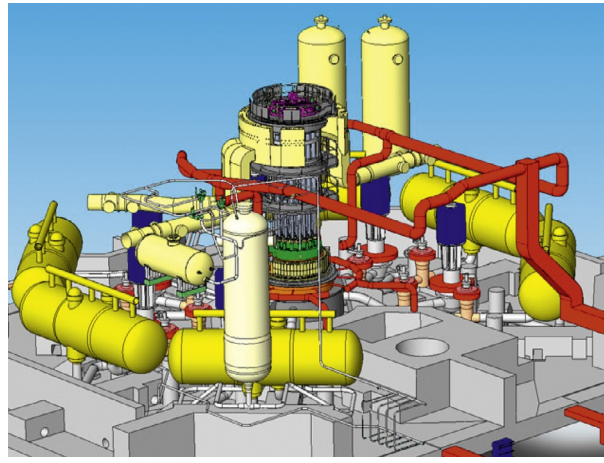

Figure 6.17 Screen shot from a 3D CAD representation of a PWR.

Figure 6.18 Evolution and optimization of component design using 3D prototyping. Left to right: simple cast item, cast with CAD machining and 3D metal printed. Each stage provides a reduction in material used with an increase in mechanical strength.

become far more accurate and efficient by computer-aided manufacturing (CAM) coupled to the CAD (CAD/CAM).

However, 3-D printing may offer the potential to revolutionize component fabrication in the way that 3-D software has revolutionized design. Already, there are economic and commercially available 3-D printers that can create objects of A4 and letter size out of polymers, and powdered metal printers are on the market that can produce metallic objects with similar strength and durability to objects fabricated from a metal block. These printed objects can be designed for optimum strength and materials usage, and the engineer can create components that could not be fabricated by existing casting or machining techniques. Figure 6.18 shows how a component designed for fabrication by traditional machining techniques can be optimized using 3-D printing, saving on material cost.

6.6.3 The future

As we move toward the next generation of reprocessing plants, nuclear engineering companies and fuel cycle service providers are likely to take a long view of plant development and design. Business planning using TRLs is now firmly embedded and a staged approach to design means that research and engineering are reviewed constantly before allowing progression. This reduces risks (technical and project) and overall leads to higher success rates for projects.

With the advent and maturity of molecular modeling techniques and improvements in laboratory capabilities we will see a closer coupling of experimental and theoretical design of chemical processes, providing more efficient separation for species of interest such as minor actinides. This will have a knock on effect of reducing plant and equipment sizes, allowing reprocessing to be more economical and improving safety from a reduction in inventory.

The use of advanced equipment designs with high-efficiency components will be possible, as 3-D design and process modeling will mean designs can be tested before construction. A link to 3-D prototyping will allow these new technologies to be manufactured at a fraction of the cost compared to traditional cast and machining manufacture.

In summary, the trends in advanced engineering design and modeling will lead to lower costs for reprocessing and for the closed fuel cycle as a whole.

References

American Petroleum Institute (API), 1990. Management of water discharges: design and operations of oil-water separators, first ed. American Petroleum Institute (API).

Brady-Raap M. C. et al. Nuclear Criticality Safety: A Subject of Growing International Importance. OECD NEA WPNCS Expert Group on Burn-up Credit Criticality Safety (BUC), available at https://www.oecd-nea.org/science/wpncs/Publications.

ESDU report 780404, ISBN 978 0 85679 244 1.

Kishbaugh, A.A., Development and Performance of Centrifugal Mixer-Settlers in the Reprocessing of Nuclear Fuel. USAEC Report-841, available at www.c-n-t-a.com/srs50_files/139kishbaugh.

Kreysa, G., Schütze, M., 2008. DECHEMA Corrosion Handbook (Revised and Extended 2nd Edition).

Lo, T.C., et al., 1983. Handbook of Solvent Extraction, third ed. Wiley, Hoboken, NJ. ISBN-13: 978-0894645464.

Los Alamos National Laboratory. Criticality safety in processing plants, available at library.lanl.gov/cgi-bin/getfile?00326164.p.

Perry, R.H., 2008. Chemical Engineers Handbook, eighth ed. McGraw-Hill, New York.

Schlieper, L., et al., 2004. Liquid-liquid phase separation in gravity settler with inclined plates. AIChE J. 50 (4), 802–811.

Skelland, A.H.P., Moeti, L.T., 1990. Mechanism of continuous-phase mass transfer in agitated liquid-liquid systems. Ind. Eng. Chem. Res. 29, 2258–2267.

Treybal, R., 1980. Mass Transfer Operations, third ed. McGraw-Hill, New York. ISBN 0-07-066615-6.

Winston, R.R., 2011. Uhlig's Corrosion Handbook, third ed.

Yadav, R.L., Patwardhan, A.W., 2008. Design aspects of pulsed sieve plate columns. Chem. Eng. J. 138, 389–415.

The use of organic extractants in solvent extraction processes in the partitioning of spent nuclear fuels

7

Clint A. Sharrad[1,2,3], *Daniel M. Whittaker*[1,2]
[1]Research Centre for Radwaste and Decommissioning, Dalton Nuclear Institute, The University of Manchester, Manchester, UK; [2]Centre for Radiochemistry Research, School of Chemistry, The University of Manchester, Manchester, UK; [3]School of Chemical Engineering and Analytical Science, The University of Manchester, Manchester, UK

Acronyms

ΔG	change in free energy
ΔH	change in enthalpy
ΔS	change in entropy
1c-SANEX	one cycle selective actinide extraction
An	actinide
BTBP	bis-triazinyl bipyridine
BTP	bis-triazinyl pyridine
BTPhen	bis-triazinyl phenanthroline
C2-BTBP	6,6′-bis(5,6-diethyl-1,2,4-triazin-3-yl)-2,2′-bipyridine
C5-BTBP	6,6′-bis(5,6-dipentyl-1,2,4-triazin-3-yl)-2,2′-bipyridine
C6-BTBP	6,6′-bis(5,6-dihexyl-1,2,4-triazin-3-yl)-2,2′-bipyridine
CEA	Atomic Energy and Alternative Energies Commission (*French: Commissariat à l'énergie atomique et aux énergies alternatives*)
CHON	carbon, hydrogen, oxygen, and nitrogen only
CMPO	octyl(phenyl)-*N*,*N*-diisobutylcarbomylmethylphosphineoxide
CyMe$_4$-BTBP	6,6′-bis(5,5,8,8-tetramethyl-5,6,7,8-tetrahydrobenzo(1,2,4)triazin-3-yl)-2,2′-bipyridine
CyMe$_4$-BTPhen	2,9-bis(5,5,8,8-tetramethyl-5,6,7,8-tetrahydrobenzo(1,2,4)triazin-3-yl)-1,10-phenanthroline
D	distribution coefficient
DIAMEX	diamide extraction
DMDBTDMA	dimethyl-dibutyl-tetradecyl malonamide
DMDOHEMA	*N*′*N*′-dimethyl-*N*,*N*′-dioctylhexylethoxymalonamide
DTPA	diethylene triamine pentaacetic acid
EI	electron ionization
ESI	electrospray ionization
Et,hemi-BTP	6-(5,6-diethyl-1,2,4-triazin-3-yl)-2,2′-bipyridine
EXAFS	extended X-ray absorption fine structure
HDEHP	bis(2-hexylethyl)hydrogenphosphate

Reprocessing and Recycling of Spent Nuclear Fuel. http://dx.doi.org/10.1016/B978-1-78242-212-9.00007-1

I	nuclear spin
***i*-SANEX**	innovative selective actinide extraction
Ln	lanthanide
MALDI	matrix-assisted laser desorption ionization
MBTP	2,6-bis(5,6-dimethyl-1,2,4-triazin-3-yl)pyridine
MeOH	methanol
Me,hemi-BTP	6-(5,6-dimethyl-1,2,4-triazin-3-yl)-2,2′-bipyridine
nIR	near infrared
NMR	nuclear magnetic resonance
OK	odorless kerosene
OTf	trifluoromethanesulfonate (*also known as* triflate)
^{i}PBTP	2,6-bis(5,6-di*iso*propyl-1,2,4-triazin-3-yl)pyridine
PBTP	2,6-bis(5,6-di-*n*-propyl-1,2,4-triazin-3-yl)pyridine
pH	$-\log_{10}[H^+]$
PUREX	plutonium and uranium extraction *or* plutonium and uranium reduction extraction
py	pyridine
QSAR	quantitative structure activity relationship
SF	separation factor
SNF	spent nuclear fuel
SX	solvent extraction
SANEX	selective actinide extraction
SO_3-BTP	2,6-bis(5,6-di(3-sulphophenyl)-1,2,4-triazin-3-yl)pyridine
TALSPEAK	trivalent actinide-lanthanide separation by phosphorous reagent extraction from aqueous komplexes
TBP	tri-*n*-butyl phosphate
thf	tetrahydrofuran
TODGA	*N,N,N′N′*-tetraoctyl diglycolamide
TPH	tetrahydrogenated propylene
TRLFS	time resolved laser-induced fluorescence spectroscopy
TRUEX	transuranium extraction
TRUSPEAK	transuranium separation by phosphorous reagent extraction from aqueous komplexes
UV	ultraviolet
XANES	X-ray absorption near-edge spectroscopy
XAS	X-ray absorption spectroscopy
XRD	X-ray diffraction

7.1 Introduction

Organic molecules that can selectively coordinate actinides (all or parts of the series) over the remaining fission and corrosion products in dissolved spent nuclear fuel are of great interest due to their applicability for partitioning actinides in the back end of the nuclear fuel cycle (Boyle et al., 1997; Sessler et al., 2006). As such, work has been continuing for many years into different ligand classes that can perform these separations.

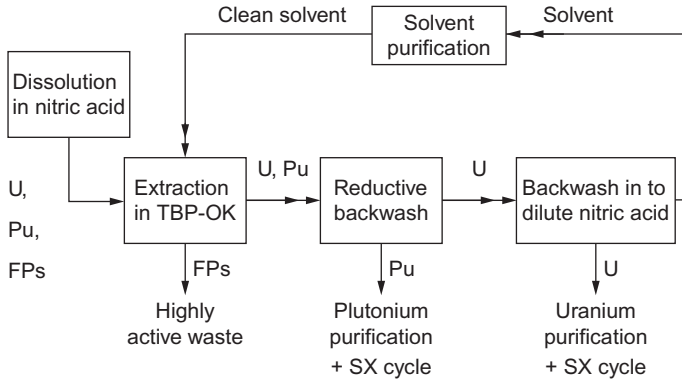

Figure 7.1 Generic flowsheet of the PUREX process.

TBP (tri-*n*-butyl phosphate, Figure 7.1) is the extractant used in the widely applied PUREX (plutonium uranium extraction or plutonium uranium reduction extraction) process for partitioning uranium and plutonium from the remaining constituents in spent nuclear fuel (SNF). Wider interest in partitioning all of the actinides (including the minor actinides) from SNF, in order to maximize nuclear fuel resources and minimize nuclear waste, has resulted in the investigation of many different ligand systems with a number of potential extractants showing significant promise in various process applications. In this context, a particular challenge is the separation of americium and curium from the lanthanide fission products as the chemical properties of these elements are highly similar under conditions likely to be encountered in a solvent-extraction process. Consequently, the partitioning of these elements by chemical means is considered to be extremely difficult (Marie et al., 2012).

The majority of extractants that are either currently applied or are being seriously considered for use, in solvent-extraction processes for the partitioning of SNF can be classified into two major categories: oxygen-only donor extractants and nitrogen donor extractants. Oxygen-only donor extractants tend to be used for the selective extraction of uranium and plutonium and/or the copartitioning of minor actinides and lanthanides from the remaining fission, activation, and corrosion products in SNF. Nitrogen donor extractants have generally been favored for the partitioning of the minor actinides, americium and curium, from the lanthanide fission products.

The initial identification of extractants that could be applied to SNF partitioning is typically performed by the determination of distribution coefficients and separation factors of relevant metals in specific oxidation states. These experiments are usually performed on small scales using radioisotopes at trace-level concentrations. The mode of action of these extractants (i.e., how extractants bind to selected metals and cross the phase boundary) at the ligand screening stage of process development is generally not understood. For example, even though PUREX has been in operation for the large-scale processing of SNF since the 1960s (Swanson, 1990), it was only in 1997 that the first direct spectroscopic evidence conclusively showing the manner in which TBP binds to uranium in the liquid phase was published (Den Auwer et al., 1997). Recently,

there have been considerable efforts devoted to understanding the manner in which proposed extractant molecules bind to metal ions found in dissolved SNF and consequently provide an improved understanding of the mechanism by which certain extractants are able to selectively partition radionuclides from a given mixture.

This chapter reviews results from some of the recent speciation studies of metal ion complexation, particularly actinide ions, by organic ligands currently used or proposed for use in solvent-extraction processes for the partitioning of spent nuclear fuels. These studies have utilized numerous spectroscopic and diffraction-based characterization techniques. There is a specific focus on the metal ion speciation of nitrogen-donor ligands that show promise for the separation of minor actinides from lanthanides, this exemplifying how understanding speciation can be used to improve extractant design. Hence, an established knowledge of what is occurring at the molecular level can lead to better process design and improved operational safety when conducting large-scale partitioning of spent nuclear fuel.

7.2 Overview of partitioning processes

7.2.1 PUREX process

The PUREX process (Figure 7.1) has been used for the separation of uranium and plutonium from spent nuclear fuel since the 1950s and 1960s (May et al., 1999). First, SNF is dissolved in aqueous HNO_3 creating uranium and plutonium nitrate complexes, and other aqueous nitrate complexes of the various metals present. NO_x is then added, which conditions the plutonium to form $Pu(NO_3)_4{\cdot}xH_2O$ (plutonium(IV)). All of the solids present (insoluble oxides, nitrates, metallic species, etc.) that may affect the separation are removed through chemical and physical means. Once a heavily laden aqueous phase containing uranium(VI) and plutonium(IV) nitrates has been formed it is contacted with an organic solution containing TBP (Figure 7.1) in a kerosene diluent such as OK (odorless kerosene) or TPH (tetrahydrogenated propylene) at a predetermined concentration (typically 20-30% v/v). This contacting and mixing enables the TBP to form a complex with the nitrate salts of uranium(VI) (as uranyl: $\{UO_2\}^{2+}$) and plutonium(IV) and sequester them into the organic phase. The plutonium(IV) in the organic phase is then reduced to plutonium(III) using a reducing agent, such as uranium(IV), allowing it to be selectively back-extracted leaving a uranium rich organic phase that is then backwashed into a dilute nitric acid aqueous phase in a subsequent process stage.

Along with uranium and plutonium, some neptunium and technetium are also extracted, an undesirable aspect of the process. These elements then have to be removed in later stages of the process. The uranium and plutonium species are then converted into the respective oxides ready for fabrication into fuel. The organic solution (TBP/OK) is used again in the process but any TBP/OK that has degraded, either by hydrolysis or by radiolysis, is removed in a solvent purification step. Purification takes the form of a basic wash that deprotonates the hydroxyl degradation products making them hydrophilic and so they move into the aqueous phase. Additionally, this

can be followed by an alumina wash to remove any remaining ligands, which could complex plutonium (Tripathi and Ramanujam, 2003). The exact species that exist in any one of the stages depends on the concentration of HNO_3 and the oxidation state of the element. However, it is known by EXAFS (extended X-ray absorption fine structure) and XANES (X-ray absorption near-edge spectroscopy) measurements that initial extraction across the phase boundary occurs via nitrate-bis-TBP complexes: $UO_2(NO_3)_2{\cdot}2TBP$ or $Pu(NO_3)_4{\cdot}2TBP$ (Den Auwer et al., 1997, 1998).

The distribution coefficients for uranium(VI) (as uranyl) and plutonium(IV) usually peak in the PUREX process at HNO_3 concentrations of around 2-6 mol/L. The process has been designed so that it can operate in acidic aqueous media to maximize the solubility of uranium and plutonium as the oxides and hydroxides formed by hydrolysis at pH >1 are highly insoluble. The necessity for redox control of the species in solution is a slight drawback in reprocessing, as it requires extra preparation stages before extraction can commence. The generation of less stable oxidation states such as plutonium(III) is also undesirable, as stabilization in solution is required to stop catalytic oxidation by HNO_2 that is produced by the radiolytic decomposition of HNO_3.

Another drawback of the PUREX process is the use of a phosphorus-containing extraction agent. This can lead to nonincinerable wastes being generated making the management of any radionuclide contaminated organic waste problematic (Thiollet and Musikas, 1989). In comparison, if only carbon, hydrogen, oxygen, and nitrogen were present in the extraction media (an approach that has been termed the *CHON principle*) then the waste organics could be incinerated and any remaining contaminated residual materials converted to an encapsulated or immobilized waste form for final disposal.

7.2.2 DIAMEX process

The DIAMEX (diamide extraction) process is currently being developed by the French CEA (Atomic Energy and Alternative Energies Commission). The process utilizes diamides to extract the minor actinides and lanthanides out of the waste stream from PUREX processing posturanium and plutonium removal, leaving only the fission products (apart from the lanthanides) and corrosion products behind (Courson et al., 2000). Example diamides used in the process include DMDOHEMA (*N*′*N*′-dimethyl-*N*,*N*′-dioctylhexylethoxymalonamide, Figure 7.2) or analogous diamides like DMDBTDMA (*N*,*N*′-dimethyl-*N*,*N*′-dibutyl-tetradecylmalonamide). The flow sheet in Figure 7.3 demonstrates the stages used in the process. First, the highly active raffinate from PUREX processing is contacted with the hydrophobic diamide, partitioning the minor actinides and lanthanides into the organic phase and leaving the remaining fission products in the aqueous (now waste) stream. Concurrently, the addition of oxalic acid prevents the extraction of zirconium and molybdenum into the organic phase with the minor actinides and lanthanides. The organic phase is then stripped of the minor actinides and lanthanides and the organic phase recycled similarly to the PUREX process.

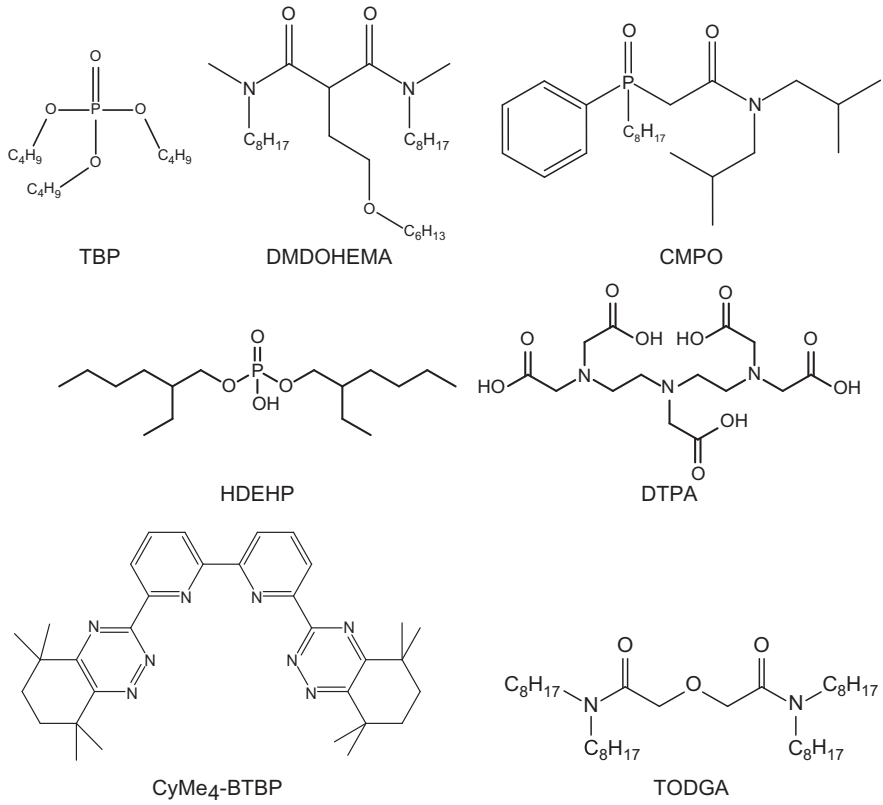

Figure 7.2 Structural diagrams of molecules used in various solvent extraction processes.

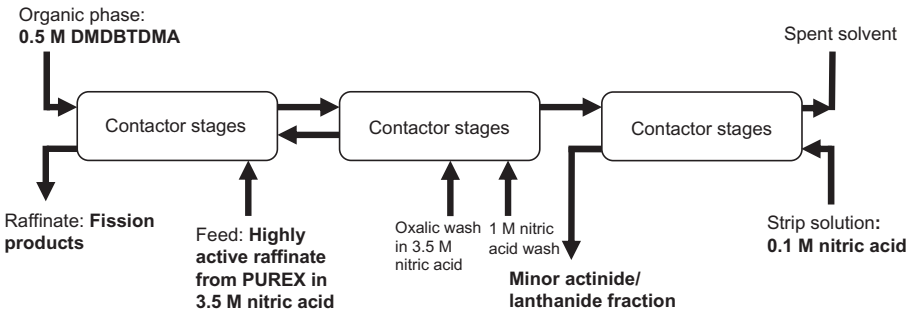

Figure 7.3 Flowsheet of the DIAMEX process used in tests for feasibility studies.

This process, unlike PUREX, only uses molecules containing C, H, O, and N and, as such, is likely to generate less problematic secondary wastes by allowing potentially simpler organic waste management options (Thiollet and Musikas, 1989). The product solution from DIAMEX processing still contains lanthanides, which will

lead to difficulties in the transmutation of the problematic minor actinides. The process also fully extracts the fission products technetium, palladium, and (partially) ruthenium (Thiollet and Musikas, 1989). This is not ideal, but is acknowledged as requiring further optimization before being applied for plant-scale partitioning. Usually the DIAMEX process is followed by the selective actinide extraction (SANEX) process (see Section 7.2.5) to separate the minor actinides from the lanthanides. Further details on the development of both DIAMEX and SANEX processes are given in Chapter 10.

7.2.3 TRUEX process

The TRUEX (transuranium extraction) process has previously been used in the United States as an addition to the PUREX process. It utilizes a mixture of CMPO (Figure 7.2) and TBP to selectively remove the actinides (uranium, plutonium, and the minor actinides) and technetium from PUREX waste solutions with very high efficiencies (99.97% of activity removed) (Law et al., 1996). However, testing resulted in iron (a corrosion product) also being extracted alongside the actinides as well as some mercury (a fission product), which could pose problems downstream. The mercury was removed from the strip solution by use of carbonate washing and the iron through use of another "wash" procedure. The flow sheet is similar to that of the DIAMEX process (Figure 7.3) with a sodium carbonate washing stage instead of oxalic acid.

The TRUEX process shows significant promise for the reprocessing and partitioning of the actinides from the fission products (Law et al., 1996). However, extractant degradation and mercury/iron partitioning have been highlighted as problem areas despite the sodium carbonate wash (Law et al., 1996).

7.2.4 TALSPEAK process

The TALSPEAK (trivalent actinide-lanthanide separation by phosphorus reagent extraction from aqueous komplexes) process has been in development in the United States since the late 1960s for use in the separation of the minor actinides from the lanthanides (Nilsson and Nash, 2007). The process utilizes an acidic organophosphorus reagent in an organic phase and a polyaminocarboxylic acid in a buffered aqueous phase. In contrast to the PUREX, and most other processes, the actinide elements are held back in the aqueous phase while the lanthanide elements are extracted. The process has been shown to work, but the role of each component is yet to be definitively established. The optimum buffer (identified as L-lactic acid/L-lactate) may have multiple roles during extraction, including kinetics and phase modification. The organophosphorus reagent (HDEHP—bis(2-hexylethyl)hydrogenphosphate, Figure 7.2) acts as an extractant. The hold back reagent (DTPA—diethylenetriaminepentaacetic acid, Figure 7.2) has multiple equilibria and kinetics with the variety of elements present in the aqueous phase. DTPA also undergoes radiolysis quite readily, which is a considerable problem if TALSPEAK is to be considered as part of a strategy for partitioning (Kolarik and Kuhn, 1974).

These issues are all under review and there have been several recent modifications to the process, including combining TALSPEAK and TRUEX processes to create the TRUSPEAK (transuranium separation by phosphorous reagent extraction from aqueous komplexes) process (Lumetta et al., 2010). However, the main issue with the process is the necessity to use a buffer to maintain a pH of ~3.5 (Lumetta et al., 2010; Leggett et al., 2010). In industrial application, high acid concentrations ($[H^+] > 1$ M) are routinely employed to ensure solubility of metal ions. As such, implementation of this process would lead to the possibility of the hydrolysis and subsequent precipitation of many actinide species (plutonium in particular), therefore creating a serious maloperation concern. It is also difficult to control pH with sufficient precision at this required acid concentration under process conditions.

7.2.5 SANEX process

The SANEX process is a post-PUREX process designed to separate the trivalent actinides from the lanthanides. After PUREX processing, the highly active raffinate undergoes a DIAMEX-style process to isolate only the trivalent actinides and lanthanides in an aqueous phase (no other fission or corrosion products). This aqueous phase is then contacted with an organic phase containing an organic molecule capable of separating the actinides from the lanthanides (Figure 7.4). The system has been, and is still being, developed over many years and thus far has resulted in the design and synthesis of the BTBP (bis-triazinyl-bipyridine) molecular backbone and other analogues. The $CyMe_4$-BTBP molecule (2,9-bis(5,5,8,8-tetramethyl-5,6,7,8-tetrahydro-1,2,4-benzotriazin-3-yl)-2,2′-bypyridine, Figure 7.2) is currently considered the most effective ligand for use in this system. The molecule has been designed to have excellent radio- and hydrolytic stability through the removal of all benzylic hydrogen positions while retaining high selectivity for actinides over lanthanides. The SANEX process is only viable if other complimentary partitioning processes (i.e., PUREX and DIAMEX) are undertaken. This leads to a very high number of overall stages being necessary to implement the SANEX process. There are other issues associated with the kinetics of the extraction and the potential need for phase modifiers to increase the rate of extraction. However, these issues can be overcome by

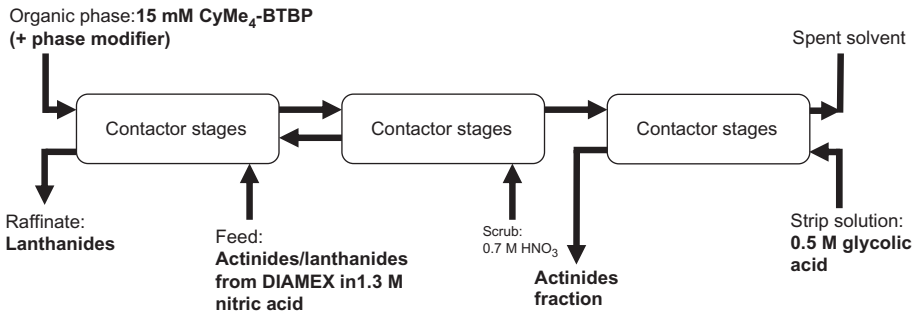

Figure 7.4 Flowsheet of the SANEX process used in testing (Magnusson et al., 2009).

variation of the organic molecule and/or organic phase used to perform the extraction, as investigated by Distler et al. (2012). This, coupled with the other processes, promises to be an excellent method of isolating all the minor actinides from the SNF.

7.2.6 i-*SANEX process*

Another process that is receiving attention is the *i*-SANEX (*i*nnovative-selective actinide extraction) process. This is similar to the SANEX process with a variation in the methodology of the extraction, more akin to the TALSPEAK process discussed above. The *i*-SANEX process is a relatively new process that builds on the knowledge gained in the development of the SANEX processes. The process is similar to the TALSPEAK process except it uses a selective hydrophilic BTP-based (bis-triazinylpyridine) stripping reagent and TODGA (tetraoctyldiglycolamide, Figure 7.2) as the organic phase extractant for the lanthanide ions. The current reference molecule for the process is 2,6-bis(5,6-di(3-sulphophenyl)-1,2,4-triazin-3-yl)pyridine (SO_3-BTP). Additionally, the process does not require buffering like the TALSPEAK process and is operational at pH <1. A potential flow sheet for this process has been developed and is presented in Figure 7.5. As there is no need to perform DIAMEX processing before the *i*-SANEX process, the number of stages needed in order to achieve complete partitioning is decreased. This means the size of the plant footprint could be decreased; the process could be even further improved by optimization. However, the use of the SO_3-BTP molecule means the process deviates from the CHON principle—an undesirable facet.

7.2.7 *Process summary*

Each of the processes covered has a variety of strengths and weaknesses that are summarized in Table 7.1. It is noted that there are new or modified separations processes regularly being developed; for instance, the 1c-SANEX (one cycle SANEX) process developed by Magnusson et al. (2013) and Wilden et al. (2013). This process is a simplified combination of the DIAMEX and SANEX processes whereby Am^{3+} and Cm^{3+} are isolated directly from a PUREX raffinate. It utilizes both TODGA and $CyMe_4$-BTBP,

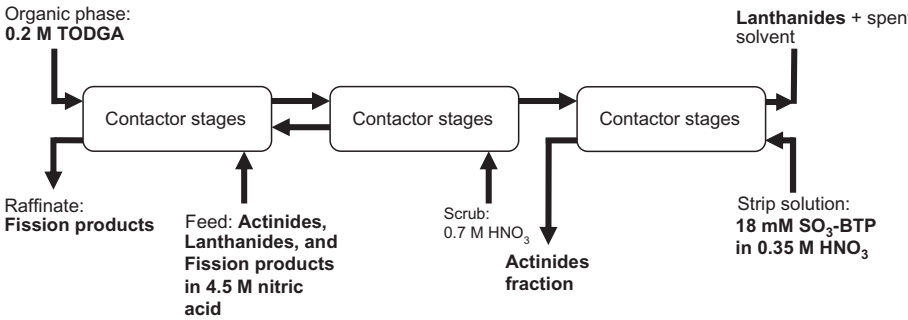

Figure 7.5 Proposed flowsheet for the *i*-SANEX process.

Table 7.1 Some major points of the processes developed for nuclear waste reprocessing

	PUREX	DIAMEX	TRUEX	TALSPEAK	SANEX[a]	*i*-SANEX[a]
Extractant(s)	TBP	Diamide	CMPO/TBP	HDEHP/DTPA/lactate	$CyMe_4$-BTBP	SO_3-BTP/TODGA
Separate An/Ln?	No	No	No	Yes	Yes	Yes
CHON?	No	Yes	No	No	Yes	No
Can be used on raffinate?	Yes	Yes	Yes	Yes	Yes	Yes
Depends on other process?	No	Yes—PUREX	No	No	Yes—PUREX + DIAMEX	Yes—PUREX
Limitations	• Only isolates U/Pu	• An/Ln containing product	-	• pH control	• Kinetics	-
Major advantages	• Very well understood • Plant in operation	• Simple ligands	• 99.97% activity removal	• Can be combined with other systems	• Radiolytic stability • Very good SF	• Fast kinetics • High flow rate • Fever stages needed
Major disadvantages	• Extracts Np • TBP degradation • Requires redox control of Pu	• Extracts Zr, Mo, Ru	• Extracts Fe, Hg	• pH buffering	• Slow kinetics	• Sulfur present in SO_3-BTP

[a]In development.

where the TODGA acts as a phase modifier and a coextractant. Both molecules extract the later lanthanides more efficiently than the early lanthanides, leading to an increase in overall extraction of the later lanthanides. Addition of scrub sections to the flow sheet remove undesirably extracted elements (i.e., palladium, molybdenum, and zirconium) to ultimately yield the required product solution.

7.3 Overview of speciation techniques

7.3.1 Introduction to speciation techniques

Numerous techniques and methods have been applied in order to understand how extractant molecules bind to metal ions relevant to spent nuclear fuel processing streams. Many of these techniques have limitations that may not necessarily allow for the direct probing of speciation in process-like conditions. In addition, having access to these techniques for studying radionuclide behavior can be problematic due to the availability of appropriate infrastructure combined with the safety concerns of working with radioactive materials. Despite these problems, there is still a significant body of work in this area. The following provides a brief summary of the main techniques that are currently used to probe metal ion speciation with extractant ligands and how these tend to be applied in investigating the speciation of partitioning processes.

7.3.2 X-ray diffraction

Single crystal X-ray diffraction (XRD) is probably the most commonly used technique for probing metal speciation with extractant molecules or analogues thereof. This technique provides definitive evidence on the structure of the complexes isolated giving information on the number and types of ligand in the metal coordination sphere and provides details on the bonding found in the complex including bond lengths and angles. This technique requires the growth of single crystals of the formed compound/s, which is inherently avoided during solvent-extraction processes (as this represents a maloperation concern). Therefore, for the vast majority of structures obtained that are considered relevant to SNF reprocessing, the crystalline samples, from which these structures were determined, were synthesized in conditions that would not be encountered in a process environment. For example, the use of volatile and/or highly flammable diluents (e.g., dichloromethane and ethanol, respectively) is commonly undertaken to promote the crystallization process but would never be considered for use in plant-scale separations of spent nuclear fuel. The extractants themselves and their complexes may not be amenable to crystallization under any synthetic conditions. For example, TBP has no reported structures in the Cambridge Structural Database (Thomas et al., 2010). Consequently, many researchers have used different analogues of TBP that more readily crystallize in order to use XRD to understand the nature of trialkylphosphate binding to various metal ions. This approach has also been applied to other classes of extractants. The main drawback of single crystal XRD is the

structure observed from a solid-state sample may not necessarily correlate to what is obtained in solution, particularly in solvent-extraction conditions. Also, attempting to obtain appropriate crystals from samples that contain high specific activity radionuclides and subsequently analysis by XRD can be extremely difficult both because generally a relatively large quantity of material (>1 mg) is required to isolate crystals and the physical form of any crystals obtained can deteriorate very quickly due to radiation effects.

7.3.3 UV-visible-nIR spectrophotometry

Solution-state UV-visible-nIR spectrophotometry is typically used in this field in a methodology where multiple spectra are obtained over various metal ion:extractant ratios in order to assess the number of extractant ligands that can bind to the metal ion being studied. Studies for which metal-based absorptions are weak (e.g., the f-f transitions of lanthanide(III) ions) will normally probe the more intense ligand-based transitions, such as those found for many of the N-donor extractants proposed for minor actinide/lanthanide separations, as metal is added to ligand solution. Metal-based transitions can also be probed if the absorptions are of an appropriate intensity and do not overlap with ligand-based transitions. This approach tends to be used for studying transuranic behavior during which the actinide d-f and f-f transitions occur in the visible near-infrared region of the spectrum (Griffiths et al., 2013; Reilly et al., 2012; Tian et al., 2005). Solutions for analysis can be prepared by a titration approach into a single phase or by solvent extraction with the phase of interest isolated and studied. The changes in spectral profiles with changes in concentration of metal, extractant, or other components can be fitted to obtain stability constants associated with identified complexation equilibria, and subsequently be used to determine thermodynamic parameters ΔG, ΔH, and ΔS.

7.3.4 Luminescence spectroscopy

Luminescence spectroscopy, in particular time-resolved laser fluorescence spectroscopy (TRLFS), complements UV-visible-nIR spectrophotometry in that it can be used to obtain similar information and parameters. However, only a relatively small number of elements in certain oxidation states exhibit fluorescence of sufficient intensity that they can be studied. The technique is most effectively used to probe complexation behavior of inorganic ligands in aqueous solution as under these conditions luminescence-quenching mechanisms are avoided and minimized as much as possible. Nonetheless, considerable information on the coordination environment can still be obtained by luminescence spectroscopy with organic ligands in organic solvents.

The position and intensity of metal-based transitions observed by luminescence spectroscopy are typically highly dependent on the coordination environment and are commonly used to distinguish metal complex species with different numbers of coordinating extractant ligands. The lifetimes of transitions observed by luminescence spectroscopy provides the ability to quantify the number of bound molecules with O-H oscillators (e.g., H_2O, CH_3OH) through use of the Horrocks equation (Equation 7.1; Holz et al., 1991).

Horrocks equation, where q *is the number of bound* H_2O *(or MeOH) molecules,* A *is a proportionality constant specific to the luminescent metal ion, and* τ *is the fluorescence lifetime (Tedeschi et al., 2000).*

$$q = A\left(\frac{1}{\tau_{H_2O}} - \frac{1}{\tau_{D_2O}}\right) \tag{7.1}$$

The most common metal ions studied by luminescence spectroscopy to understand their behavior with extractant molecules are curium(III) and europium(III) because of their excellent fluorescence properties. This method is, therefore, ideally utilized for investigating speciation relevant to minor actinide/lanthanide partitioning. A particular practical advantage of luminescence spectroscopy is that only relatively small concentrations are necessary (~1 μM) to obtain a usable signal from highly fluorescent systems such as those containing curium(III). This is of particular benefit when handling high specific activity radionuclides in order to minimize any dose exposure concerns.

7.3.5 Mass spectrometry

Mass spectrometry is used to determine the molecular mass of species present within typically solution samples. The sample is vaporized and then ionized by a number of different possible techniques including electron ionization (EI), electrospray ionization (ESI), chemical ionization (CI), or matrix-assisted laser desorption ionization (MALDI). After ionization, the charged particles are accelerated by an electric field, deflected by a magnetic field, and ultimately detected. Detection is based on the mass/charge ratio of the particles. Ideally, for the purposes of speciation the ionization process should be relatively soft so the molecule remains intact allowing the molecular ion species to be directly detected.

7.3.6 Nuclear magnetic resonance spectroscopy

Nuclear magnetic resonance (NMR) spectroscopy is most commonly used to identify organic molecules and/or metal complexes of these organic molecules in solution. Nuclei with spin I (e.g., ^1H and ^{13}C have $I = ½$) each generate a magnetic field giving a magnetic moment that is proportional to the spin and will have $2I + 1$ possible states or orientations. Usually, these states are degenerate but upon application of an external magnetic field, like those used in a NMR spectrometer, they will occupy different energy levels. The magnitude of this energy difference is dependent on the strength of the applied magnetic field. Radiofrequency radiation can be absorbed by the nucleus causing the spin to "flip" from in line to opposing the external field. The spin relaxes back to its ground state, and it is this absorption-relaxation resonance process that is monitored to provide a NMR spectrum. The resonance frequency of a given nucleus is influenced by electrons in the vicinity of this nucleus. The independent

spins of the electrons causes the nucleus to be shielded, thus requiring increased field strength to absorb at its transition frequency. Conversely, if electrons are drawn away from a given nucleus it becomes deshielded resulting in a lower frequency resonance. The position, or chemical shift, of this resonance is, therefore, highly dependent on the surrounding atoms. The spin of a given nucleus can also couple to the spin of adjacent nuclei providing further information on the surroundings of the nuclei studied.

The application of NMR for speciation studies relevant to partitioning most commonly uses ^{1}H NMR to probe hydrocarbon-based extractants in a single solution phase and fundamentally prove whether certain metal ions are able to coordinate to extractant molecules. This information can be obtained by a change in the NMR spectrum from the "free" ligand to when the metal ion is present in solution. Titrations can also be performed, similar to those described for UV-visible spectrophotometry, to indicate the stoichiometry of extractant molecule binding to metal ions and may be used to determine stability constants for complexation. A major drawback in the application of NMR to probe extraction behavior is that the use of solvents that are likely to be used in extractions may not be feasible for NMR studies.

7.3.7 X-ray absorption spectroscopy

X-ray absorption spectroscopy (XAS) is an element-specific technique that provides information on the local coordination environment, similar to X-ray diffraction, and electronic structure of the metal ion investigated, but in any phase including solutions. This makes XAS the ideal technique to probe the solution structure of metals in extraction or extraction-like conditions. The main disadvantage of XAS is that it is an averaging technique and cannot conclusively determine if multiple species of a single metal are present in a sample and, if so, in what composition.

XAS requires a tunable and intense X-ray source that is only provided at synchrotron radiation facilities. The X-rays of a monochromated energy excite a core electron from the metal at a particular edge (K-, L-, or M-), which is typically from the L_{III}-edge corresponding to the 2p orbital of the likes of the lanthanides and actinides as this provides the most information on the coordination environment of these elements. Useful information from an X-ray absorption spectrum (see Figure 7.6) is obtained at energies beyond the ionization potential and can be considered in two major regions: the X-ray absorption near-edge structure (XANES) region, which is approximately 5–150 eV after the ionization potential, and the extended X-ray absorption fine structure (EXAFS), which is beyond 150 eV past the ionization potential. The XANES region provides information on the valence state of the element, coordination geometry, and some indication of the coordination environment. The EXAFS region shows how the excited electron interacts with the neighboring atoms and can be fitted using the EXAFS equation to determine the atomic environment surrounding the metal. Generally, fits of the EXAFS region provide the most powerful information on metal speciation in solutions.

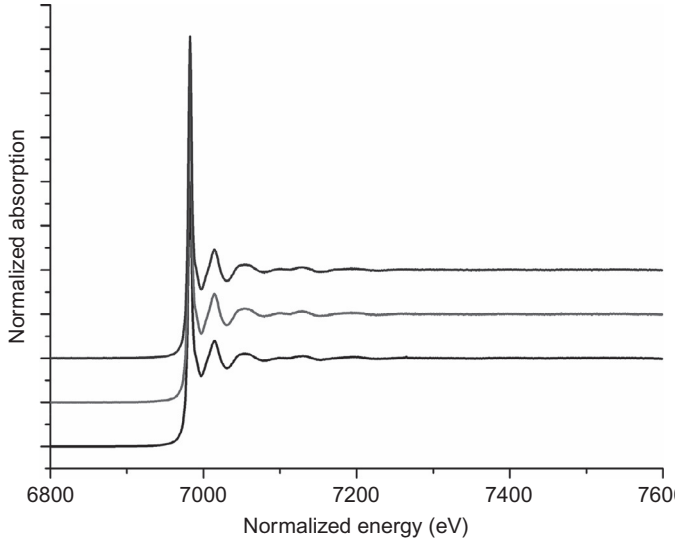

Figure 7.6 Stacked plot of example X-ray absorption spectra.

7.3.8 Summary and comment

The determination of metal speciation in extraction conditions is rarely achieved by the use of a single technique. A multiple technique approach is usually required to provide conclusive information on metal ion speciation relevant to the partitioning of SNF in order to overcome the inherent weaknesses and disadvantages of each applied technique. However, some of these techniques have not been readily accessible for researchers in this area, either because of the facilities required (e.g., synchrotron radiation for XAS) and/or providing such facilities where high specific activity radionuclides (e.g., americium, curium) can be safely handled. Therefore, the majority of speciation investigations with extractants have tended to involve inactive or low-activity studies using techniques that most research laboratories have access to (e.g., XRD). Recently though, there have been considerable efforts to develop networks that provide access to facilities that have not been previously accessible to many research groups and provide infrastructure to study highly radioactive materials, including the transuranic actinides, through projects such as TALISMAN and ACTINET (Bourg et al., 2012).

7.4 Review of speciation studies

Historically, the development of the majority of partitioning processes has been achieved with only limited knowledge, if not no understanding, of the speciation that underpins the separation. Developments in minor actinide/lanthanide partitioning, particularly in SANEX separations, over the last 20 years have shown how speciation

studies can be applied to not only understand the process being proposed, but also to amend and improve the process by designing alternative extractants for screening.

7.4.1 Bistrazinylpyridines (BTPs)

The ligands that have been shown to express the best performance in a SANEX-type process have come from a large body of previous work into neutral N-donor complexing agents. Kolarik et al. identified this in 1999 with his work on BTPs (bis-triazinyl pyridines; Figure 7.7) and similar molecules while using them for selective actinide extraction (Kolarik et al., 1999a). Initially two classes of molecules, 2,6-bistriazolyl- and 2,6-bistriazinylpyridines, were identified as potential extractants for minor actinide/lanthanide separations. However, only the BTPs were shown to extract the nitrate forms of the actinides in reasonable quantities, which is required for partitioning under process conditions.

Once this particular class of molecules as potential extractants for minor actinide/lanthanide partitioning had been identified, further work on improving the partitioning ability of the ligands was performed. Kolarik and coworkers identified that branching at the α-position of the substituent at the 5,6-positions on the triazinyl rings decreased extraction efficiency. However, they did contend that a CH_2 spacing group between the branches and the triazinyl ring lessened this negative effect (Kolarik et al., 1999b).

The next stage of development of the BTPs was to investigate the acid and hydrolytic stability of the molecules (Hill et al., 2002a). Further testing revealed that the α-CH_2 position on the triazinyl rings undergoes a variety of reactions as shown in Figure 7.8. This is unfavorable as it decreases the D_{Am} (by ~50%) obtained during the separation and can lead to precipitation of the extractant. This was suppressed by use of solvents such as tetrachloroethane and nitrobenzene; however, these are unsuitable in a process environment due to volatility concerns.

In contrast to the work of Kolarik et al. (1999b), Hill and coworkers identified that substitution at the α-position of the triazinyl ring, changing the solvent to *n*-octanol, and adding a phase transfer catalyst improved the acid stability of the molecules during extraction testing (Hill et al., 2002b). A phase transfer catalyst is a molecule that can improve the transfer kinetics of a species of interest across a phase boundary. For example, TODGA (0.005 mol/L) is used in the 1c-SANEX process as a phase transfer catalyst (where $CyMe_4$-BTBP is the kinetically slow but selective actinide extractant). The substituted BTP, ^{i}PBTP (2,6-bis(5,6-di*iso*propyl-1,2,4-triazin-3-yl)pyridine;

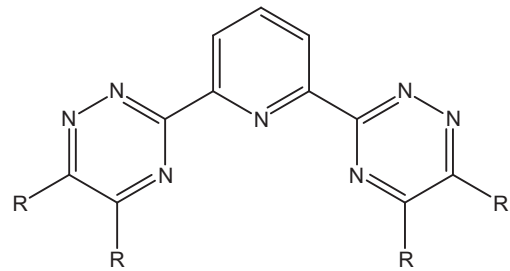

Figure 7.7 Generic structure of the BTP molecule.

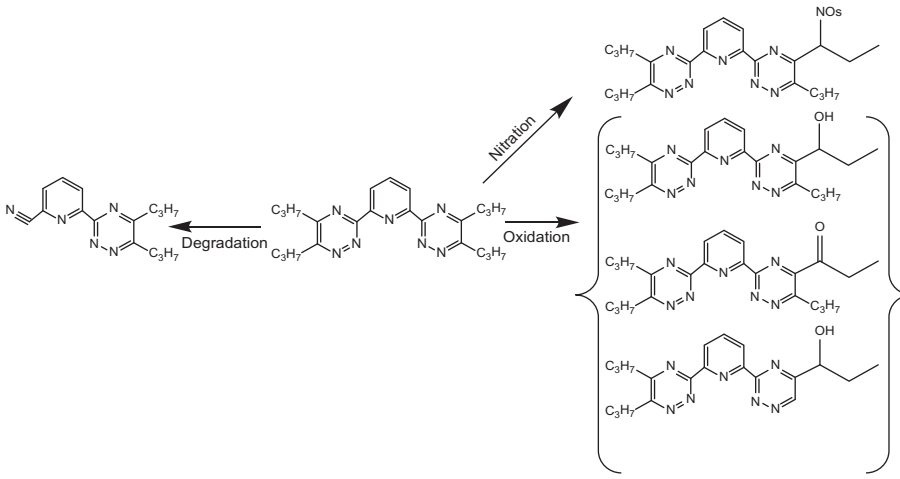

Figure 7.8 Acidic hydrolysis pathways of PBTP (Hill et al., 2002b).

Figure 7.9), demonstrated greater acid stability, yet slower back extraction kinetics compared to BTPs where the α-position was not substituted. It was also recognized that ^{i}PBTP underwent radiolysis during subsequent testing and this was acknowledged as an area for further research (Hill et al., 2002b).

Subsequent development with the BTP molecules came from Hudson et al. (2006). They demonstrated that not only does substitution of the α-CH_2 positions on the triazinyl residues increase the acid stability but that the addition of delocalized π-systems can decrease the probability of radiolytic degradation. Using knowledge gained from a TBP analogue in aromatic solvents and its increased radiolytic stability they annulated the side chains of the BTPs to increase their stability (e.g., $CyMe_4$-BTBP or $ArCyMe_4$-BTBP; Figure 7.9) (Batey, 1992).

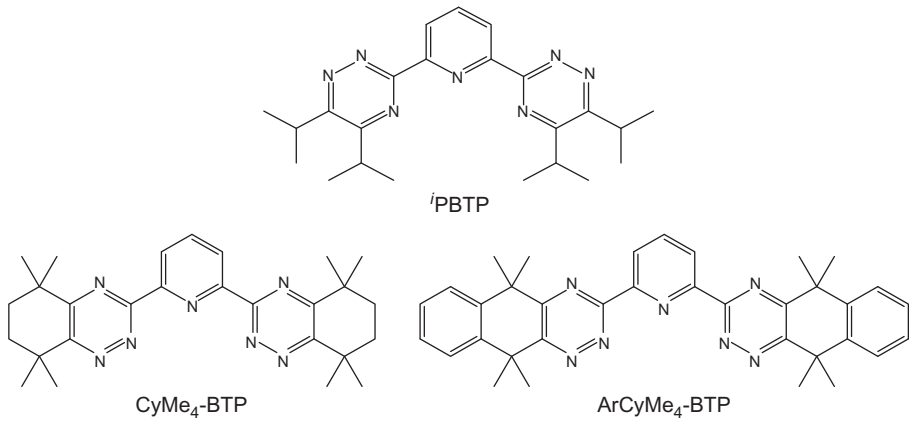

Figure 7.9 Structural diagrams of various molecules of the BTP family.

Irradiation tests of the extractants displayed in Figure 7.9 demonstrated that annulation of the periphery does increase the radiolytic stability quite effectively with the $ArCyMe_4$-BTP molecule not degrading cf. RBTP (e.g. Figure 7.13), where D values decreased ~50%.

Drew et al. in 2004 published a QSAR (quantitative structure activity relationship) study of N-heterocyclic donor molecules (Drew et al., 2004). Based on tri-dentate N-donor systems, the model used molecular properties to predict the SF of untested molecules and to guide the experimentation and design process (Drew et al., 2004). The molecular descriptors used were quite exhaustive. They covered a wide range of variables between the molecules, which were generated by testing 36 different molecules and then were used to predict the SF of 11 previously untested varieties. Before this could be achieved, the structure of the ligand and complex was determined computationally. In all cases, results indicated a conformational shift upon coordination, where rotation of the triazinyl units occurs; this has been confirmed experimentally by multiple groups (Figure 7.10).

The study demonstrated that QSAR, a technique usually used in the pharmaceutical industry, can be useful for understanding molecular properties where large-scale synthesis and testing of molecules is not practically possible. The use of QSARs still requires further work before it can be used quantitatively but it does firmly demonstrate that selectivity is a facet of multiple properties and not just a single asset of a molecule.

7.4.1.1 Lanthanide speciation

Drew et al. in 2001 published solid-state structures of metal complexes determined with PBTP by single crystal XRD (Drew et al., 2001). It was found, when crystallized from ethanol, that three of the PBTP molecules coordinated to the lanthanide(III) ion to form $[Ln(PBTP)_3]^{3+}$ (where Ln = samarium to lutetium; Figure 7.11). The BTP-based molecule coordinates in a tridentate manner through the central pyridine nitrogen and through a nitrogen in each of the triazinyl units.

Further work and a comparison of the mode of action in solid and solution states of the PBTP and methyl analogue, MBTP (2,6-bis(5,6-dimethyl-1,2,4-triazin-3-yl)-pyridine), was performed by Iveson et al. (2001). They demonstrated that both 1:3 and 1:2 cerium(III):L (L = extractant ligand) species can exist in anhydrous

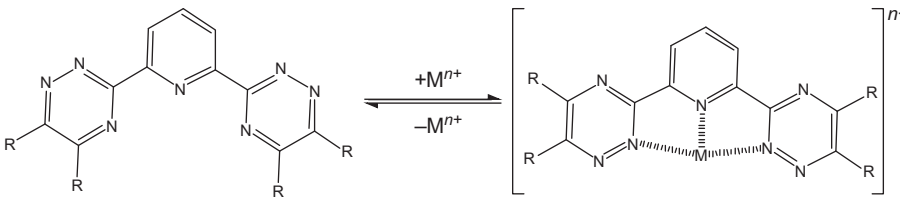

Figure 7.10 Molecular depiction of the isomerization upon complexation of the BTP molecules (Drew et al., 2001).

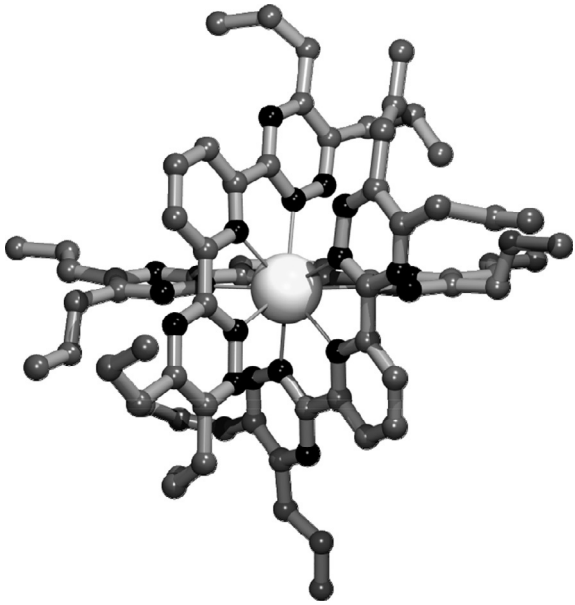

Figure 7.11 Depiction of the crystal structure of the common lanthanide complex cation species with PBTP, [Ln $(PBTP)_3^{3+}$] (Ln = samarium to lutetium) (Iveson et al., 2001). Hydrogen atoms have been omitted for clarity.

pyridine. This was proven through ^{1}H NMR studies using cerium iodide as the source of cerium(III).

Various analogues of the BTP ligand have been synthesized and their behavior with the lanthanide series has been investigated. A number of different complex stoichiometries have been isolated in the solid state and have been observed in solution showing that the assumption that all BTP-type molecules bind to lanthanide(III) ions forming just 1:3 or 1:2 lanthanide(III):BTP complexes cannot be made. Examples include complex species containing two lanthanide(III) ions where each ion is coordinated by a single BTP-type molecule (6-(5,6-dimethyl-1,2,4-triazin-3-yl)-2,2′-bipyridine; also known as Me,hemi-BTP) and the lanthanide(III) ions are bridged by coordinating nitrate anions (Figure 7.12; Hudson et al., 2003). For the Me,hemi-BTP ligand, isolation of this charge neutral species seems to be favored for the early (and larger) lanthanide(III) ions. The latter (and smaller) lanthanides seem to have a preference of

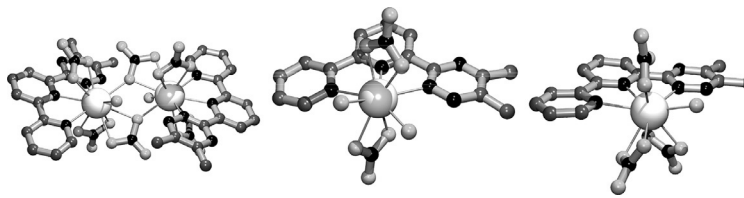

Figure 7.12 Depiction of the crystal structures of $[La_2(Me,hemi\text{-}BTP)_2(H_2O)_2(NO_3)_6]$ (left), $[Er(Me,hemi\text{-}BTP)(H_2O)_2(NO_3)_2]^+$ (center) and $[Pr(Me,hemi\text{-}BTP)(H_2O)(NO_3)_3]$ (right) (Hudson et al., 2003). Hydrogen atoms have been removed for clarity.

forming 1:1 lanthanide(III):Me,hemi-BTP complex cations of the general formula $[M(Me,hemi\text{-}BTP)(H_2O)_2(NO_3)_2]$ (Figure 7.12; Hudson et al., 2003). Only a Pr(III) complex with Me,hemi-BTP from the lanthanides studied gave evidence for the formation of a charge neutral monometallic species of the formula $[Pr(Me,hemi\text{-}BTP)(H_2O)(NO_3)_3]$ (Figure 7.12; Hudson et al., 2003).

These lanthanide(III) studies show that water and nitrate coordination may very well have a role in the selective extraction of metal species into the organic phase with BTP-type ligands. Solution studies of both Me,hemi-BTP and Et,hemi-BTP (6-(5,6-diethyl-1,2,4-triazin-3-yl)-2,2′-bipyridine) in the presence of lanthanide(III) do not provide any evidence for the formation of the 1:3 lanthanide(III):BTP-type complexes for these systems. Therefore, water and/or nitrate coordination must be occurring in solution with these ligands. Even though these alternative BTP molecules do not form the common 1:3 lanthanide(III):BTP complex, the separation factors for americium over europium obtained with these ligands can be as high as 30 depending on the aqueous acid concentration. Therefore, it could be possible that different nitrogen-donor ligands can still effectively separate minor actinides from lanthanides but achieve this by different molecular processes.

7.4.1.2 Actinide speciation

Iveson et al. studied the solution behavior of uranium(III) with methyl-substituted BTP (MBTP) in pyridine by ^{1}H NMR spectroscopy and the only complex species with MTBP that was detected in solution was $[U(MBTP)_3]^{3+}$, irrespective of the amount of MBTP present (Iveson et al., 2001). This is in contrast with the analogous cerium(III) studies, where both 1:2 and 1:3 Ce:MBTP complexes were observed in similar solution conditions (Iveson et al., 2001). Competition studies where stoichiometric amounts of uranium(III) and cerium(III) were present in pyridine with up to 3 molar equivalents of MBTP showed the only complex species to form was $[U(MBTP)_3]^{3+}$ with no evidence for the formation of any cerium(III) complex with MBTP, thereby demonstrating the greater affinity that BTP molecules generally have for actinides over lanthanides. Uranium(III) was used as an analogue for americium/curium(III) for its relative ease of manipulation and lower radiotoxicity relative to americium/curium(III) and is of a similar size to cerium(III) so any differences in binding affinity between these metal ions to the BTP molecules is likely to be due to the nature of the bonding rather than a size mismatch between the ionic radii and the binding cavity of the BTP molecules. A crystal structure for the uranium(III) complex with the propyl analogue, PBTP, was obtained and is similar to that depicted in Figure 7.11 but with shorter M-N bond distances for the uranium(III) complex compared to that of the analogous cerium(III) structure with PBTP (Iveson et al., 2001). The shortened metal-nitrogen bonds of the uranium(III) complex are believed to be due to the greater covalency within the actinide coordination sphere owing to the "soft" nature of the neutral nitrogen-donor ligands with some possible π-back bonding from the uranium to nitrogen atoms (Iveson et al., 2001; Kaltosoyannis and Scott, 1998). It is believed the same effect is the reason these ligands can ultimately separate minor actinides from lanthanides.

Studies into the speciation of minor actinide/lanthanide extractions with PTBP in TPH:1-octanol (7:3) media gave further insight into the selectivity of this extractant (Denecke et al., 2005). EXAFS measurements of curium(III) and europium(III) extracted from nitric solutions into the organic phase showed that the coordination environments for both curium(III) and europium(III) complexes were identical with no differences identified between the M-N distances observed for the formed complexes, which was confirmed by computational modeling (Denecke et al., 2005), unlike for the uranium(III) analogue (Iveson et al., 2001). This shows that uranium (III) is not necessarily the best indicator for understanding minor actinide behavior, particularly with respect to bonding to nitrogen-donor ligands. The extracted species for both curium(III) and europium(III) were identified as the commonly found 1:3 metal:BTP complex cations showing that charged species are present in the organic phase upon extraction. Luminescence measurements, specifically TRLFS, showed that the $[Cm(PBTP)_3]^{3+}$ complex is more thermodynamically stable than the europium(III) analogue. The $[Cm(PBTP)_3]^{3+}$ complex was the only curium(III) complex observed in these luminescence experiments over curium:PBTP molar ratios varying from 8.3 to 624, in contrast to the analogous europium(III) experiments, which needed >300 molar equivalents of PTBP to form the 1:3 europium:PBTP complex. This is postulated to be the source of the relatively large SF found for minor actinide over lanthanides using PBTP in extraction studies ($SF_{Am/Eu} = 143$) (Kolarik et al., 1999a).

Investigations of the complexation of plutonium(III) and americium(III) have been performed with PBTP by extraction from an acidic nitrate aqueous phase into a kerosene/1-octanol (70:30 vol.) organic phase (Banik et al., 2010). The use of both UV-visible-nIR spectrophotometry and EXAFS proved that the 1:3 actinide:PBTP complex, $[An(PBTP)_3]^{3+}$, is the most stable stoichiometry for these actinide(III) complex species and provides further confirmation that charged complex species do form in the organic phase when actinide(III) is extracted by BTP extractant molecules, in contrast to the PUREX process where charge neutral uranium(VI) and plutonium(IV) species are extracted into the organic phase.

It is generally accepted that the major reason why nitrogen donor ligands like BTP have greater affinity for the minor actinides over the lanthanides is due to the "soft" nature of nitrogen donors over, for example, oxygen donors combined with a small, but significant, level of covalency exhibited in actinide coordination environments over the purely ionic lanthanide coordination sphere. However, there has been very little experimental evidence that definitively proves this until recently. ^{15}N NMR spectroscopic studies of the americium(III) complex with nitrogen-15 labeled PBTP, $[Am(PTBP)_3]^{3+}$, by Adam et al. have shown for the first time the influence of covalency in the americium-nitrogen bonds for these complexes, which is not observed in the analogous lanthanide complexes of PTBP (Adam et al., 2013). This is evident from comparison of the ^{15}N chemical shifts of lanthanide(III) and americium(III) complexes with PBTP (Table 7.2). Substantial upfield shifts of ~300 ppm were observed for the coordinated nitrogen atoms in the americium(III) complex compared to those observed for the lanthanide(III) complexes. In contrast, the chemical shifts for the noncoordinating nitrogen atoms for the americium(III) and lanthanide(III) complexes were all similar. The ^{15}N chemical shift of the coordinating triazinyl nitrogen atoms in

Table 7.2 ^{15}N NMR chemical shifts (ppm) of $[M(PBTP)_3]^{3+}$ species (relative to NH_4Cl) (Adam et al., 2013)

Metal(III) ion	Nitrogen atom			
	Pyridine group (coordinating)	Triazinyl groups (coordinating)	Triazinyl groups (noncoordinating)	
None	303	347	398	289
Samarium	226	261	383	293
Europium	–	–	354	284
Lutetium	269	309	386	293
Americium	−26	-18	418	289

the americium(III) complex also exhibited temperature dependence, indicating the americium(III) ion is weakly paramagnetic (Adam et al., 2013). These ^{15}N NMR observations for the $[Am(PTBP)]^{3+}$ complex can be explained by unpaired electron spin density from the americium(III) ion being delocalized along the relatively covalent nature of the americium-nitrogen bond. This does not occur for the lanthanide(III) complexes as the purely ionic nature of the lanthanide coordination sphere does not allow delocalization of any unpaired electron from the lanthanide(III) ion, if present (Adam et al., 2013). Further research challenges in this area include proving whether this explanation is correct and attempting to quantify the level of covalency observed in such actinide complexes. By doing so, this could effectively inform the essential design requirements for tailoring extractant ligands for particular partitioning needs.

7.4.2 Bistrazinylbipyridines and bistriazinylphenanthrolines

The next major step in the development of these extractants came in the form of C2-BTBP (6,6′-bis(5,6-diethyl-1,2,4-triazin-3-yl)-2,2′-bipyridine; Figure 7.13) (Drew et al., 2005). This molecule gave higher $SF_{Am/Eu}$ (160 ± 16) values than those for the BTP molecules, postulated to be due to the extra N-donor in the system.

Foreman et al. reported some ^1H NMR titrations and structural parameters of C5/C6-BTBP (6,6′-bis(5,6-di-X-yl-1,2,4-triazin-3-yl)-2,2′-bipyridine where X = pent/hex,

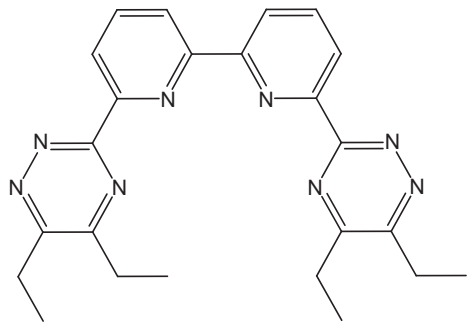

Figure 7.13 Structural diagram of C2-BTBP.

respectively) and a new variant $CyMe_4$-BTBP (Figure 7.2) with a range of lanthanide ions. For $CyMe_4$-BTBP, the benzylic protons were substituted with methyl groups preventing hydrogen abstraction, and thereby molecular degradation from occurring (Foreman et al., 2006). Despite an extensive synthesis, the acidic/radiolytic stability of $CyMe_4$-BTBP far surpasses that of the alkyl-BTBPs and, as such, represents a candidate extractant for minor actinide partitioning. The free ligands were also characterized by XRD and found to exist, in the solid state, in a different conformation to the complex form. Similar to the BTP molecules, the triazinyl residues rotate to coordinate a metal center. In addition, rotation about the bipyridine bond occurs in order for the BTBP to coordinate to the metal in a tetravalent manner (Figure 7.14).

Lewis et al. have further modified $CyMe_4$-BTBP to fix the bipyridine backbone in place in the form of a phenanthroline moiety, called $CyMe_4$-BTPhen (Figure 7.15; Lewis et al., 2011).

By locking the bipyridine backbone to stop the isomerism displayed in Figure 7.14, it was also hoped an increase in the rate of extraction would occur by forcing the extractant into a better conformation for complexation, although rotation of the triazinyl rings is still possible. Extraction work with $CyMe_4$-BTPhen has provided very encouraging results; namely, the extraction (coordination) kinetics are orders of magnitude better with the preorganization (Lewis et al., 2013).

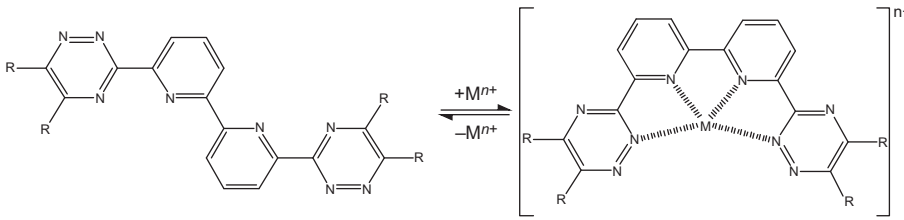

Figure 7.14 Depiction of the isomerization possible with alkyl-substituted(R) BTBP molecules.

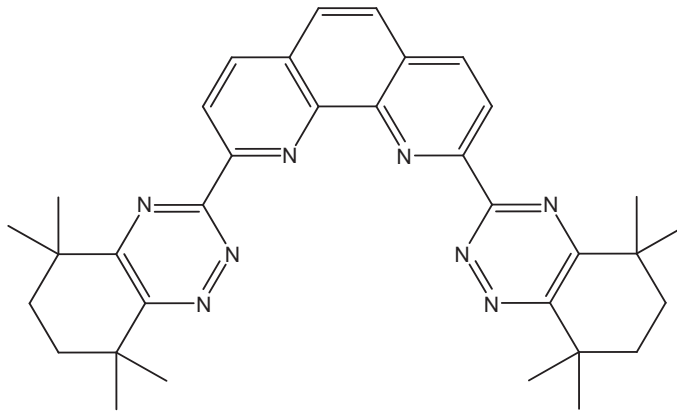

Figure 7.15 Structural diagram of $CyMe_4$-BTPhen (Lewis et al., 2013).

The evolution of the triazinyl-containing ligands has provided highly selective extractants, which are capable of partitioning the minor actinides over the lanthanides, corrosion, and fission products. It is clear to see how the acid and radiation stability have been introduced to the ligands and that it enables them to be used for the separation of HAR with no loss of efficiency over multiple tests. Selected data are provided in Table 7.3, demonstrating the evolution of the ligands and showing the general increase in minor actinide/lanthanide separation factors with the progression from BTP- to BTBP-based extractants. The test conditions for which the data are reported are different for each molecule but the overall trend is clearly observable. However, the metal species that form with many of these extractant ligands have not been clearly established, particularly under process conditions. An improved understanding of metal speciation with these extractants should be obtained in order to confidently predict extractant behavior in process environments.

Table 7.3 Separations data (*D* and SF) for selected extractants developed for minor actinide/lanthanide partitioning (TPH = tetrahydrogenated propylene)

Species	Acid/ radiolytically stable?	D	SF	Org. phase	References
PBTP	No	Am: 45.3 Eu: 0.316	$\frac{Am}{Eu}$: 143	TPH: 2-ethyl-1-hexanol 4:1	Kolarik et al. (1999a)
^{i}PBTP	No	Am: 85 Eu: 21	$\frac{Am}{Eu}$: 4	TPH: 2-ethyl-1-hexanol 4:1	Kolarik et al. (1999b)
C2-BTBP	No	Am: 650 ± 33 Eu: 4.1 ± 0.21	$\frac{Am}{Eu}$: 160 ± 16	1,1,2,2-Tetrachloroethane	Drew et al. (2005)
C5-BTBP	No	Am: ~1000 Eu: ~8	$\frac{Am}{Eu}$: ~160	1,1,2,2-Tetrachloroethane	Nilsson et al. (2006)
$CyMe_4$-BTBP	Yes	Very dependent on organic phase	$\frac{Am}{Eu}$: 101 $\frac{Pu}{Eu}$: 363 $\frac{U}{Eu}$: 91 $\frac{Np}{Eu}$: 28	Cyclohexanone	Aneheim et al. (2010)
$CyMe_4$-BTPhen	Yes	Am: >1000 Eu: <10	$\frac{Am}{Eu}$: 68-1000	*n*-Octanol	Foreman et al. (2006)

7.4.2.1 Lanthanide speciation

For lanthanide(III) complexes with both $CyMe_4$-BTPhen and $CyMe_4$-BTBP, the majority of the complex cations structurally characterized are of a 1:2 lanthanide (III):nitrogen-donor ligand stoichiometry with the two ligands binding the lanthanide ion through four nitrogen atoms (Whittaker et al., 2013). This binding motif creates a cavity that is filled with either a H_2O or a NO_3^- species creating a nona- or deca-coordinated complex, respectively (Figure 7.16). The nitrate-coordinated complexes are dicationic while the water-coordinated complexes are tricationic species. Thereby, indicating the possibility that charged complex species may be generated when metal ions cross the phase boundary in extractions using these tetradentate triazinyl-containing extractants in a similar manner observed for the BTP extractants (Whittaker et al., 2013). In PUREX extractions, it is accepted that only charge neutral complex species cross the phase boundary. As the lanthanide series is traversed, the lanthanide bond distances for these structures do decrease in accordance with the lanthanide contraction. The lanthanide(III) ion sits outside both of the planes created by

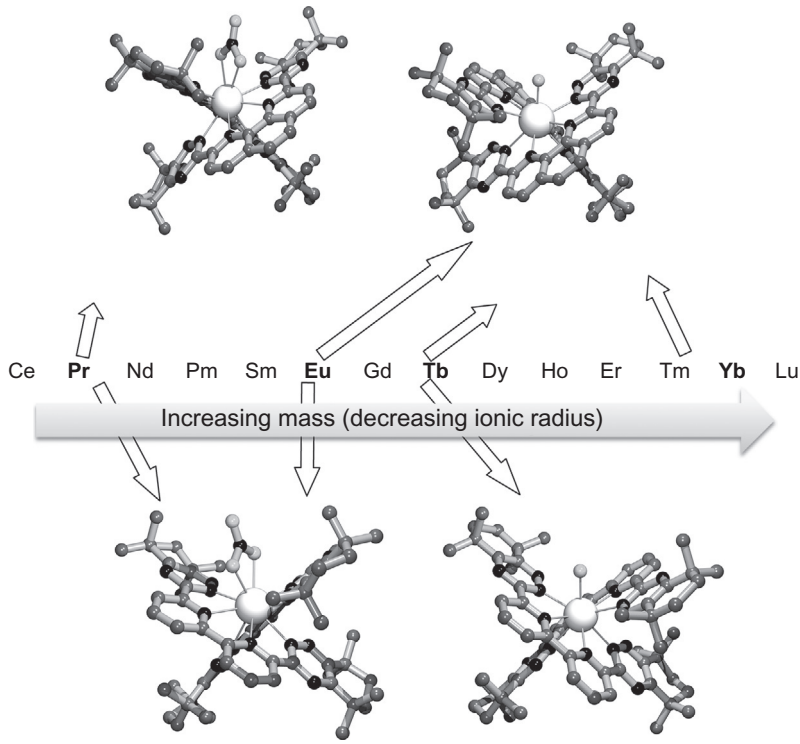

Figure 7.16 Depictions of the crystal structures of various lanthanide(III) complexes with $CyMe_4$-BTPhen (top) and $CyMe_4$-BTBP (bottom). Top left $[Ln(CyMe_4\text{-}BTPhen)_2(NO_3)]^{2+}$; top right $[Ln(CyMe_4\text{-}BTPhen)_2(H_2O)]^{3+}$; bottom left $[Ln(CyMe_4\text{-}BTBP)_2(NO_3)]^{2+}$; bottom right $[Ln(CyMe_4\text{-}BTBP)_2(H_2O)]^{3+}$. Hydrogen atoms, solvent molecules, anionic species, and disorder are removed for clarity (Whittaker et al., 2013).

the four coordinating nitrogen atoms for each of the nitrogen donor ligands in all structures, indicating the sizes of the lanthanide ions do not provide the best fit with the binding cavity of the BTBP/BTPhen ligands. The early lanthanides tend to prefer coordination to nitrate in the remaining coordination sites, whereas the latter lanthanides seem to prefer water coordination at this position.

While the 1:2 metal:extractant stoichiometry has been observed in the solid and solution states for the BTBP and BTP complexes, there are also examples of 1:1 metal:extractant species with the BTBP class of extractants where the coordination sphere is completed by coordinating anions giving charge neutral complexes. The ligand C2-BTBP (Figure 7.13) formed a europium(III) complex, which was identified as 12-coordinate with four nitrogen-donors from the lone BTBP ligand and three bidentate nitrate anions (Figure 7.17; Drew et al., 2005). The europium(III) ion sits in plane with the bipyridine and triazinyl residues of the molecule, indicating minimal steric distortion upon complexation.

Further work performed by Foreman et al. with C2-BTBP yielded solid-state structures of most of the lanthanide series (Foreman et al., 2006). Most of the structures are isostructural to that presented in Figure 7.17 where only one BTBP ligand is coordinated to the lanthanide ion with the remaining coordination sites occupied by either three nitrate ions forming a charge neutral complex or a combination of nitrate anions and water molecules. Similar charge neutral species have been identified for lanthanide (III) complexes with $CyMe_4$-BTBP (Whittaker et al., 2013). Despite the fact that structural characterization of the majority of the lanthanide series with the C2-BTBP ligand had predominantly yielded complexes of a 1:1 lanthanide(III):C2-BTBP stoichiometry (Foreman et al., 2006; Drew et al., 2005), a substantial body of work on lanthanide(III) behavior with $CyMe_4$-BTPhen and $CyMe_4$-BTBP from a number of different research groups have yielded predominantly 1:2 lanthanide(III): $CyMe_4$-BTPhen/$CyMe_4$-BTBP structures (Lewis et al., 2011; Whittaker et al., 2013; Lundberg et al., 2013). This demonstrates that even though the binding moiety of the nitrogen donor extractant ligands are essentially of the same structure, subtle changes in the ligand periphery can cause substantial changes in speciation upon metal ion complexation.

The solution behavior of C5-BTBP with lanthanide(III) in a mixture of dichloromethane and acetonitrile has been probed by ^{1}H NMR spectroscopy (Foreman et al., 2006). This provided evidence that multiple species were present in solution under most of the conditions studied. At low metal-to-ligand (<0.5) ratios, a 1:2 lanthanide

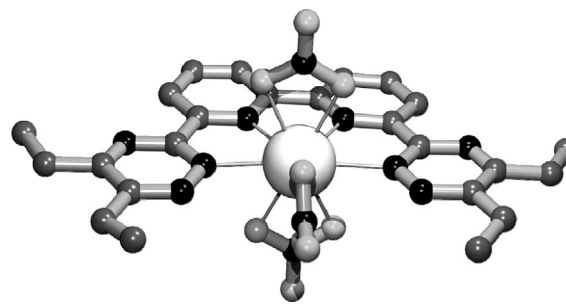

Figure 7.17 Depiction of the crystal structure of [Eu(C2-BTBP)$(NO_3)_3$] (Foreman et al., 2006). Hydrogen atoms have been omitted for clarity.

(III):C5-BTBP species was predominant but at ratios greater than this (>0.5), a 1:1 lanthanide(III):C5-BTBP species was the majority complex species. Similar observations have been reported by Hudson et al. with $CyMe_4$-BTBP where the 1:2 lanthanide(III):$CyMe_4$-BTBP complex was seen by NMR experiments with gadolinium(III) (Hudson et al., 2006).

Solution studies of lanthanide behavior with $CyMe_4$-BTBP and $CyMe_4$-BTPhen probed by UV-visible spectrophotometric titrations in methanol show little difference across the lanthanide series (Figure 7.18; Whittaker et al., 2013). The spectra show that the initial addition of lanthanide(III) gives complexation that proceeds through a 1:2 lanthanide(III):$CyMe_4$-BTBP/$CyMe_4$-BTPhen species. However, further additions of lanthanide(III), to give a stoichiometric excess of lanthanide(III), indicate the possibility that a small quantity of the 1:1 lanthanide(III):$CyMe_4$-BTBP/$CyMe_4$-BTPhen species can form, which is likely to be in equilibrium with the 1:2 lanthanide(III):$CyMe_4$-BTBP/$CyMe_4$-BTPhen complex. This mixed speciation has been observed previously with the lanthanides and the BTBP-type ligands in the solid-state and in solution experiments (Bremer et al., 2014; Hubscher-Bruder et al., 2010). Stability constants relating to these complexation equilibria for many BTP- and BTBP-type ligands for most of the lanthanide series have been determined and are summarized in Table 7.4.

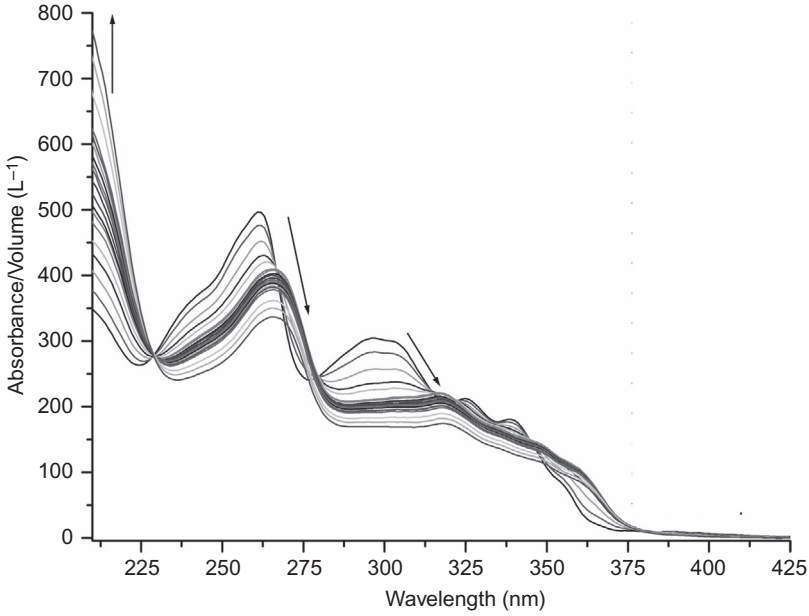

Figure 7.18 UV-visible absorption spectrum of the titration of $Pr(NO_3)_3$ against $CyMe_4$-BTPhen. Initial ligand concentration was 20 μM. Each subsequent profile represents ~0.1 eq. of $Ln(NO_3)_3$ being added to the solution until ~2.5 eq. was added when it was increased to 0.5 eq. until 3.5 eq. All performed in MeOH (Whittaker et al., 2013).

Table 7.4 Overall stability constants determined from UV-visible spectrophotometric titrations in MeOH

Extractant (L)	M:L	Log β							
		La^{3+}	Pr^{3+}	Nd^{3+}	Eu^{3+}	Gd^{3+}	Tb^{3+}	Er^{3+}	Yb^{3+}
C5-BTBP	1:1	4.8 ± 0.3	–	5.0 ± 0.1	5.7 ± 0.3	4.15 ± 0.06	–	7.4 ± 0.3	8.0 ± 0.2
	1:2	10.0 ± 0.3	–	10.8 ± 0.1	11.3 ± 0.2	10.2 ± 0.3	–	13.4 ± 0.2	13.9 ± 0.4
$CyMe_4$-BTBP	1:1	4.4 ± 0.2	–	–	6.5 ± 0.2	–	–	–	5.9 ± 0.1
	1:2	8.8 ± 0.1	10.32 ± 0.03[a]	–	11.9 ± 0.5[a]	–	11.54 ± 0.11[a]	–	–
$CyMe_4$-BTPhen	1:1	–	–	–		–	–	–	–
	1:2	–	11.43 ± 0.11[a]	–	12.6 ± 0.5[a]	–	12.04 ± 0.06[a]	–	–

[a]Whittaker et al. (2013) and Gans et al. (1996).
MeOH, $I = 10$ mM, Et_4NNO_3: Data from Hubscher-Bruder et al. (2010), unless otherwise stated.

The log β values determined by UV-visible spectrophotometry (Table 7.4) generally show that the lanthanide(III) complexes of $CyMe_4$-BTPhen are approximately an order of magnitude more stable than those for the analogous complexes of $CyMe_4$-BTBP and C5-BTBP. This is most likely due to the phenanthroline moiety in $CyMe_4$-BTPhen fixing the molecule in a position that is preformed for metal ion binding with the exception of rotation about the triazinyl rings, thereby minimizing the loss of entropy on metal ion complexation. The values for the 1:2 europium(III):$CyMe_4$-BTBP and 1:2 europium(III):$CyMe_4$-BTPhen stability constants are similar to those determined by luminescence spectroscopy($\log \beta = 11.3 \pm 0.3$ and 11.6 ± 0.4, respectively), albeit using $Eu(ClO_4)_3$ instead of $Eu(NO_3)_3$, confirming that these stability constant determinations are reasonably robust (Bremer et al., 2014).

Luminescence spectroscopy is a useful tool for identifying the complete coordination environment for the 1:2 metal:ligand complexes that have been identified between the lanthanide ions and the $CyMe_4$-BTBP/$CyMe_4$-BTPhen. Typical coordination numbers for the lanthanide ions are between 6 and 10 depending on the denticity and size of the ligands. The $CyMe_4$-BTBP/$CyMe_4$-BTPhen ligands coordinate with four N-donor atoms. So in 1:2 lanthanide(III): $CyMe_4$-BTBP/$CyMe_4$-BTPhen complexes, eight coordination sites are occupied by the N-donor ligands, leaving space for small molecules/ions to also bind to the lanthanide ion. Luminescence spectroscopy can determine the number of bound O—H oscillators, like H_2O or MeOH, to the lanthanide ion through use of the Horrocks equation (Equation 7.1). Luminescence spectroscopy can, therefore, enable the identification of the entire lanthanide(III) coordination sphere in solutions where tetradentate ligands are present. By comparing the lifetimes of the fluorescence of an emissive species in nondeuterated and deuterated solvents, it is possible to determine the number of coordinated H_2O or MeOH molecules in the emissive species (see Figure 7.19; Whittaker et al., 2013). For the europium(III) complexes with both $CyMe_4$-BTBP and $CyMe_4$-BTPhen as the nitrate salts dissolved in methanol, the lifetimes determined give an average number of coordinated water/methanol molecules as $\sim$0.3 (Whittaker et al., 2013). Thus, demonstrating that under these conditions the nitrate anion is the predominant ligand to complete the coordination sphere of the 1:2 lanthanide(III): $CyMe_4$-BTBP/$CyMe_4$-BTPhen complexes in solution.

X-ray absorption spectra were obtained for europium(III) and terbium(III) species formed by extraction from an acidic aqueous phase into an organic phase containing an excess of either $CyMe_4$-BTBP or $CyMe_4$-BTPhen in cyclohexanone (Whittaker et al., 2013). Spectra were also obtained for the various lanthanide(III) complexes isolated as crystalline solids where structures were obtained by XRD. Little difference was observed between the XAS profiles of the extracted species and those of the 1:2 lanthanide(III):$CyMe_4$-BTBP/$CyMe_4$-BTPhen complexes isolated in crystalline form. Fitting of the EXAFS region (see Figure 7.20) of the spectra for the extracted samples showed that the majority species in the bulk organic phase was indeed the relevant 1:2 lanthanide(III):$CyMe_4$-BTBP/$CyMe_4$-BTPhen complex. The interatomic distances of the complexes in extracted solutions, obtained by fits of the EXAFS, generally correlated well with those obtained by XRD for the crystallized samples. XAS of these species was unable to determine conclusively whether nitrate or water was

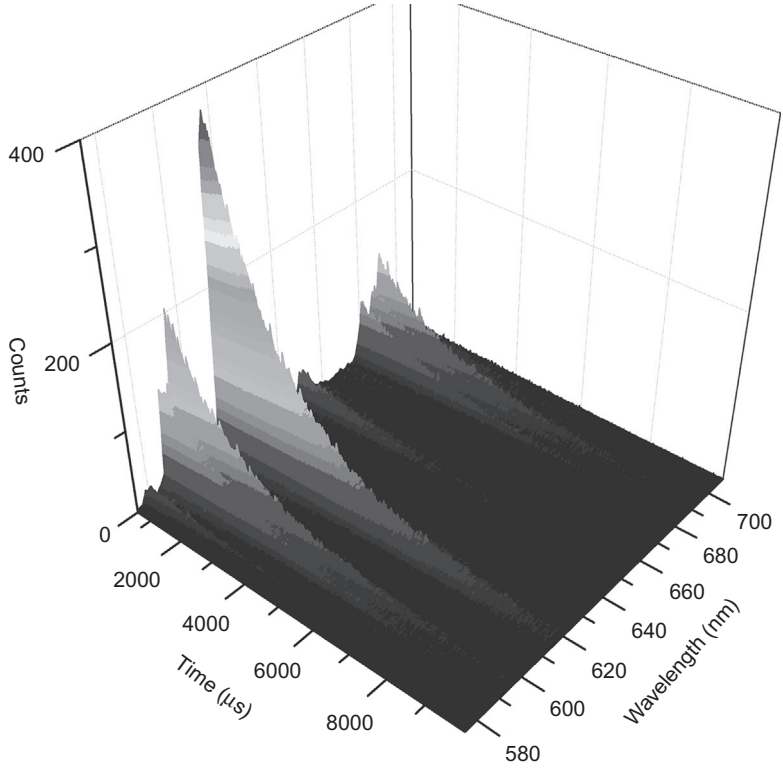

Figure 7.19 Time resolved emission spectrum of $[Eu(CyMe_4\text{-}BTBPn)_2(X)]^{n+}$ following excitation at 320 nm (Whittaker et al., 2013).

completing the coordination sphere in these complexes, but in any case cationic complex species are obtained in the bulk organic phase in extraction-like conditions.

7.4.2.2 Actinide speciation

The most important oxidation state of uranium for partitioning is uranium(VI) as the linear dioxo-cation, uranyl ($\{UO_2\}^{2+}$). In this form, there are five equatorial sites available for coordination. The $CyMe_4$-BTBP and $CyMe_4$-BTPhen ligands contain four nitrogen donor atoms, leaving a fifth, sterically hindered, site on the uranyl ion available for the binding of another species. Even though these ligands have been developed for minor actinide/lanthanide separations, understanding their behavior with uranium is still useful for the development of alternative partitioning processes where, for example, uranium may be routed with the minor actinides.

In 2008, Ephritikhine et al. published the first 5f complexes of the $CyMe_4$-BTBP molecule (Berthet et al., 2008a). By mixing the uranyl starting materials $UO_2(OTf)_2$, $UO_2I_2(thf)_3$, or $UO_2I(thf)_{2.7}$ (OTf^- = trifluouromethanesulfonate or triflate; thf = tetrahydrofuran) with $CyMe_4$-BTBP they managed to form multiple structures

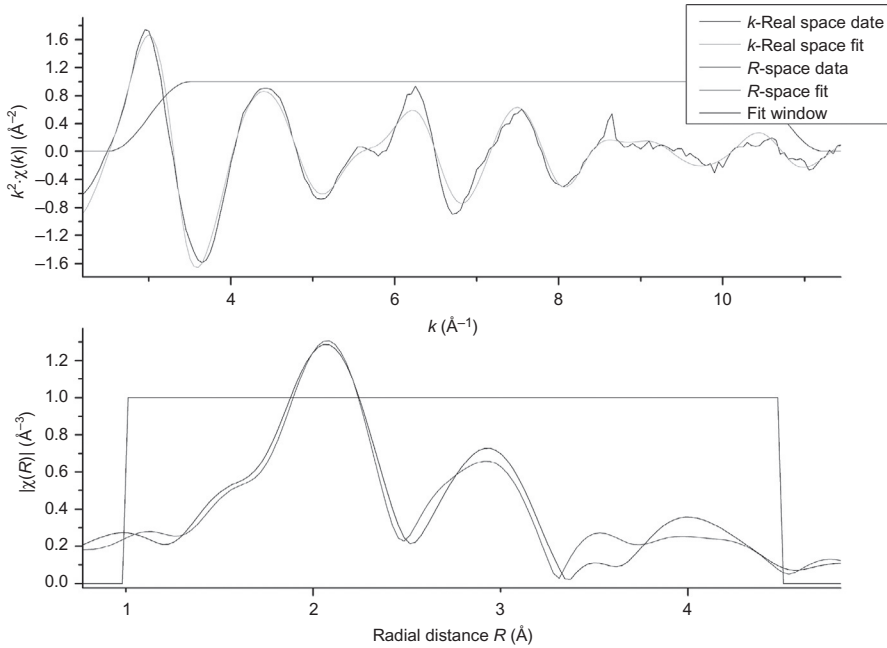

Figure 7.20 Eu L_{III}-edge EXAFS spectrum in *k* space (upper plot) and its Fourier transform in *R* space (lower plot) of the extraction of europium(III) into cyclohexanone with $CyMe_4$-BTPhen (Whittaker et al., 2013). The data are fitted to the model complex $[Eu(CyMe_4\text{-}BTPhen)_2(NO_3)]^{2+}$.

containing the ligand and gain some understanding of the thermodynamics of complexation. In solutions with pyridine or CH_3CN the complexation produced $[UO_2(CyMe_4\text{-}BTBP)(X_2)]$ (where $X = OTf^-$ or I^- depending on whether $[UO_2(OTf)_2]$ or $[UO_2I_2(thf)_3]$ were used). However, this species displays an equilibrium (with $[UO_2X_2(py)_3]$ and $CyMe_4$-BTBP) in neat pyridine solution thereby allowing calculation of some thermodynamic parameters. The equilibrium was only visible with pyridine, a coordinating solvent in great excess that is unlikely to be used in partitioning processes. The crystal structures of a large range of complexes were reported, all being essentially the same except for the identity of the species on the fifth site, which was pyridine, ethoxide, or iodide (Berthet et al., 2008a). Where OTf^- was the anion, pyridine or ethoxide occupy the fifth site, but in the case where UO_2I_2 was used as the reactant, one iodide anion binds to the fifth site (Figure 7.21; Berthet et al., 2008a). All of the structures display the expected pentagonal bipyramidal coordination environment of the uranyl ion.

They also characterized a bis(uranyl) species with the $CyMe_4$-BTBP ligand system, formed by mixing the ligand with a uranium(V) starting material, $UO_2I(THF)_{2.7}$, and allowing the mixture to crystallize. However, it would appear that the uranium center is oxidized to the more redox-stable $\{UO_2\}^{2+}$ species. The structure obtained (Figure 7.21) shows the ligands are essentially planar with the uranium

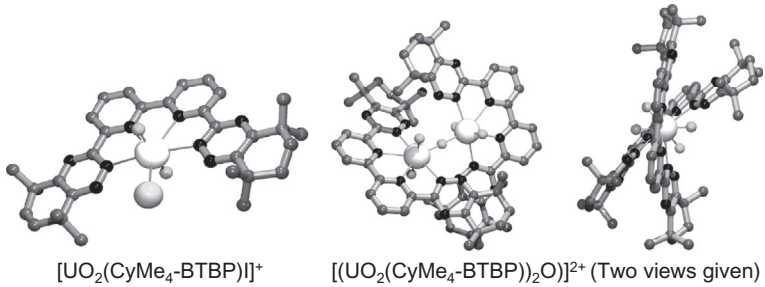

Figure 7.21 Depiction of the crystal structures of various uranium complexes with $CyMe_4$-BTBP of the complex cation (Berthet et al., 2008). Hydrogen atoms have been omitted for clarity.

atoms both being in the respective planes of the BTBP moieties and being staggered with respect to each other (Figure 7.21). The two uranyl centers are bridged by an oxygen ion of unknown oxidation state. The source of the oxygen ion, in this case, is not known either, as all of these structures were formed in anhydrous solvents. The species does show the variety of complexes that can form with $CyMe_4$-BTBP. These conditions are very different than what is expected in process conditions.

A novel mixed-valent species, $[U(CyMe_4\text{-}BTBP)_2(O)(UO_2)(NO_3)_3(OTf)]$ (Figure 7.22), was also crystallized (Berthet et al., 2008b). It was serendipitously synthesized by simple mixing of $U(OTf)_4$, $[UO_2(NO_3)_2{\cdot}CH_3CN]$, and $CyMe_4$-BTBP. The uranium(IV) ion is coordinated by two $CyMe_4$-BTBP molecules and a bridging oxo anion. The oxo anion is also coordinated to a uranyl unit, which itself is

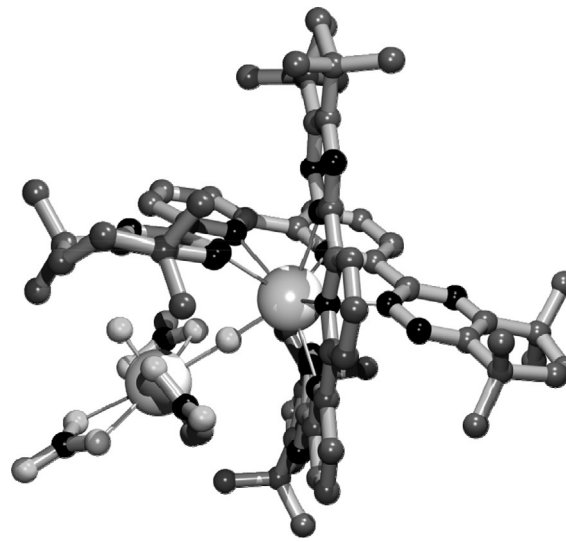

Figure 7.22 Depiction of the crystal structure of $[U(CyMe_4\text{-}BTBP)_2(O)(UO_2)(NO_3)_3(OTf)]$ (Berthet et al., 2008b). Hydrogen atoms have been omitted for clarity.

coordinated to three bidentate nitrate anions, one of which is axially bound to the uranyl moiety, a rare example of such coordination.

Ephritikhine et al. have also published multiple uranium(V) (as $\{UO_2\}^+$) structures of $CyMe_4$-BTBP (Berthet et al., 2009); however, as the uranium(V) oxidation state is quite unstable, it is, therefore, of little relevance to the more process-specific chemistry that is being considered for partitioning spent nuclear fuel. Even though much of these uranium studies were performed in conditions that are not necessarily relevant to partitioning processes, this work does show how metal ion speciation with these extractant ligands can be very complicated with the potential formation of multiple species with multiple stoichiometries, particularly with the actinides.

The major interest with regard to the deployment of the nitrogen-donor extractants $CyMe_4$-BTBP and $CyMe_4$-BTPhen is with minor actinide/lanthanide separations and, in order to understand the reasons why these ligands are able to deliver relatively high separation factors for minor actinides over lanthanides, the speciation of these ligands with americium(III) and curium(III) needs to be understood. Recent work by Bremer et al. has shown how curium(III) behaves in solution with $CyMe_4$-BTBP and $CyMe_4$-BTPhen using luminescence spectroscopy (TRLFS specifically) (Bremer et al., 2014). Studies have shown that the kinetics of complex formation for curium (III) upon the addition of two molar equivalents of either $CyMe_4$-BTBP or $CyMe_4$-BTPhen in wet methanol acidified with perchloric acid are relatively slow with formation of the 1:2 curium(III):$CyMe_4$-BTBP/$CyMe_4$-BTPhen complex, taking up to 24 h to reach equilibrium. In a solvent-extraction process environment, slow transfer kinetics, which can be influenced by complexation kinetics, may prove a serious hindrance toward developing such systems for large-scale partitioning. The fluorescence spectra of the curium(III) complexation with $CyMe_4$-BTPhen (Figure 7.23) show the slow conversion of "free" curium(III), indicated by the peak at ~599 nm, to the 1:2 curium(III):$CyMe_4$-BTPhen complex, shown by the peak at ~619 nm, via the intermediate 1:1 curium(III):$CyMe_4$-BTPhen species, which is assigned the transition at ~607 nm (Bremer et al., 2014). Despite the slow complexation kinetics, stability constants for the curium(III) and europium(III) complexes were obtained by comparing fluorescence intensities over various curium(III):ligand ratios using a batchwise approach. The stability constants (Table 7.5) clearly show the nitrogen donor ligands have a greater affinity for curium(III) over europium(III) and correlate to the curium(III)/europium(III) separation factors obtained in biphasic separations experiments (Bremer et al., 2014). This suggests that, in this system, the ability to partition curium(III) over europium (III) in liquid-liquid extractions is mainly driven by the thermodynamic binding affinities of these nitrogen-donor ligands for the metal ions present.

In extraction conditions where nitrate is present, curium(III) again shows a preference to form the 1:2 curium(III):ligand complex with both $CyMe_4$-BTBP and $CyMe_4$-BTPhen in the organic phase of 1-octanol as determined by fluorescence studies (Bremer et al., 2014). Subtle shifts were observed in the emission band for the extracted curium(III) species with different nitrate concentrations in the aqueous phase, providing strong evidence that nitrate is coordinating to the curium(III) ion to give the complex $[Cm(CyMe_4\text{-}BTPhen)_2(NO_3)]^{2+}$ or $[Cm(CyMe_4\text{-}BTBP)_2(NO_3)]^{2+}$. The analogous lanthanide(III) speciation studies also show the formation of these

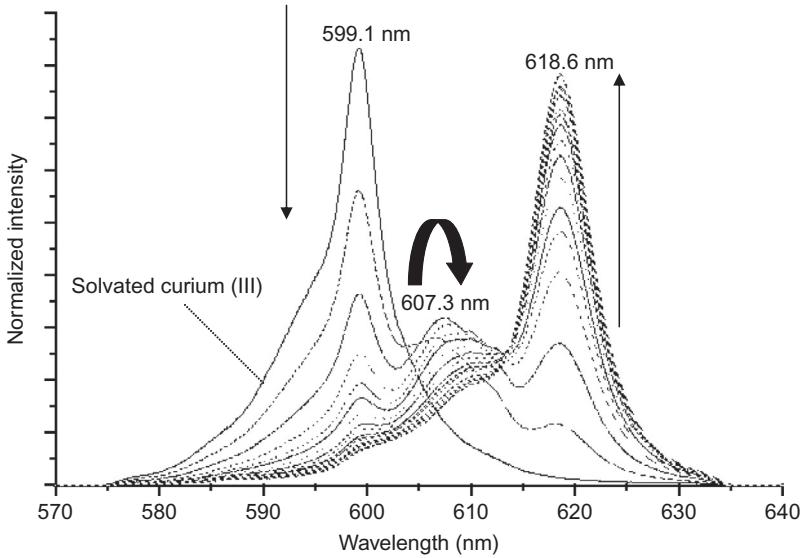

Figure 7.23 Normalized fluorescence spectra of curium(III) with 2 eq. of $CyMe_4$-BTPhen in methanol with 3.3% water taken at intermittent time intervals over ~1 h after the addition of the ligand ($[HClO_4] = 91.2$ mM) (Bremer et al., 2014).

Table 7.5 Overall stability constants for 1:2 M:L complexes with curium(III) and europium(III) as determined by TRLFS (in methanol with 3.3 mol% water) (Bremer et al., 2014)

Extractant (L)	Log β	
	Eu^{3+}	Cm^{3+}
$CyMe_4$-BTBP	11.3 ± 0.3	12.4 ± 0.3
$CyMe_4$-BTPhen	11.6 ± 0.4	13.8 ± 0.2

cationic metal complex species in the bulk organic phase. Therefore, it is likely that the source of the ability for these nitrogen donor ligands to partition minor actinides over lanthanides is due to preferred thermodynamic affinities rather than forming alternative species (e.g., cationic vs. charge neutral complexes), which are then selectively extracted.

7.5 Conclusions and outlook

The development of the triazinyl-based extractants for a SANEX process has been performed in conjunction with speciation studies for the first time in the development of SNF partitioning. This has shown how the development of future solvent-extraction

processes for the reprocessing of spent fuel or partitioning of minor actinides is likely to proceed with speciation studies complementing process flow sheet development. Also, with a greater emphasis on safety in the nuclear industry than there ever has been previously, it is essential that a science-based understanding of how novel extractants and their complexes behave in process conditions is obtained. The continued development of research infrastructure that will allow the studies of highly radioactive species makes this goal achievable. There is still much information on the mechanism of many partitioning processes, including minor actinide/lanthanide separations, that is currently not established and development of novel techniques for application in nuclear environments needs to continue. One such area is understanding speciation at the interfacial region where the development of microfocus techniques such as those for XAS can be applied. The speciation at the interfacial region may not necessarily be the same as that for the bulk organic phase and understanding how extractants behave in this crucial region of separations may very well lead to significant advances in extractant design and process optimization.

References

Adam, C., Kaden, P., Beele, B.B., Müllich, U., Trumm, S., Geist, A., Panak, P.J., Denecke, M. A., 2013. Dalton Trans. 42, 14068.

Aneheim, E., Ekberg, C., Fermvik, A., Foreman, M.R.S.J., Retegan, T., Skarnemark, G., 2010. Solv. Extr. Ion Exch. 28, 437.

Banik, N.L., Shimmelpfennig, B., Marquardt, C.M., Brendebach, B., Geist, A., Denecke, M.A., 2010. Dalton Trans. 39, 5117.

Batey, W., 1992. Science and Practice of Liquid-Liquid Extraction, vol. 2 Clarendon Press, Oxford, p. 139.

Berthet, J.-C., Thuery, P., Foreman, M.R.S.J., Ephritikhine, M., 2008a. Radiochim. Acta 96, 189.

Berthet, J.-C., Thuery, P., Dognon, J.-P., Guillaneux, D., Ephritikhine, M., 2008b. Inorg. Chem. 47, 6850.

Berthet, J.-C., Siffredi, G., Thierry, P., Ephritikhine, M., 2009. Dalton Trans. 3478.

Bourg, S., Poinssot, C., Geist, A., Cassayre, L., Rhodes, C., Ekberg, C., 2012. Procedia Chem. 7, 166. 2013 Bourg, S., . TALISMAN: Transnational Access to Large Infrastructure for a Safe Management of ActiNide [online]. Available at: http://www.talisman-project.eu. Accessed 28 August 2014.

Boyle, N.C., Nicholson, G.P., Piper, T.J., Taylor, D.M., Williams, D.R., Williams, G., 1997. Appl. Radiat. Isot. 48, 183.

Bremer, A., Whittaker, D.M., Sharrad, C.A., Geist, A., Panak, P.J., 2014. Dalton Trans. 43, 2684.

Courson, O., Malmbeck, R., Pagliosa, G., Romer, K., Satmark, B., Glatz, J.-P., 2000. Radiochim. Acta 88, 885.

Den Auwer, C., Lecouteux, C., Charbonnel, M.C., Madic, C., Guillaumont, R., 1997. Polyhedron 16, 2233.

Den Auwer, C., Charbonnel, M.C., Presson, M.T., Madic, C., Guillaumont, R., 1998. Polyhedron 17, 4507.

Denecke, M.A., Rossberg, A., Panak, P.J., Weigl, M., Schimmelpfennig, B., Geist, A., 2005. Inorg. Chem. 44, 8418.

Distler, P., Spendlikova, I., John, J., Harwood, L.M., Hudson, M.J., Lewis, F.W., 2012. Radiochim. Acta 100, 747.
Drew, M.G.B., Guillaneux, D., Hudson, M.J., Iveson, P.B., Russell, M.L., Madic, C., 2001. Inorg. Chem. Commun. 4, 12.
Drew, M.G.B., Hudson, M.J., Youngs, T.G.A., Alloys, J., 2004. Compt. Rendus Geosci. 374, 408.
Drew, M.G.B., Foreman, M.R.S.J., Hill, C., Hudson, M.J., Madic, C., 2005. Inorg. Chem. Commun. 8, 239.
Foreman, M.R.S.J., Hudson, M.J., Drew, M.G.B., Hill, C., Madic, C., 2006. Dalton Trans. 1645.
Gans, P., Sabatini, A., Vacca, A., 1996. Talanta 43, 1739, Data previously published in Reference Lundberg et al. (2013) refined using Hyperquad 2008.
Griffiths, T.L., Martin, L.R., Zalupski, P.R., Rawcliffe, J., Sarsfield, M.J., Evans, N.D.M., Sharrad, C.A., 2013. Inorg. Chem. 52, 3728.
Hill, C., Guillaneux, D., Berthon, L., Madic, C., 2002a. J. Nucl. Sci. Technol. 39, 309.
Hill, C., Berthon, P., Bros, P., Dancausse, J.-P., Guillaneux, D., 2002b. Sanex-BTP Process Development Studies. In: Proc of the 7th Intern. Exch. Meeting on Actinide and Fiss. Prod. Part., Jeju, Korea, October 14-16, 2002.
Holz, R.C., Chang, C.A., Horrocks Jr., W.DeW., 1991. Inorg. Chem. 30, 3270.
Hubscher-Bruder, V., Haddaoui, J., Bouhroum, S., Arnaud-Neu, F., 2010. Inorg. Chem. 49, 1363.
Hudson, M.J., Drew, M.G.B., Foreman, M.R.StJ., Hill, C., Huet, N., Madic, C., Youngs, T.G.A., 2003. Dalton Trans. 1675.
Hudson, M.J., Boucher, C.E., Brackers, D., Desreux, J.F., Drew, M.G.B., Foreman, M.R.S.J., Harwood, L.M., Hill, C., Madic, C., Marken, F., Youngs, T.G.A., 2006. New J. Chem. 30, 1171.
Iveson, P.B., Riviers, C., Guillaneux, D., Nierlich, M., Thuery, P., Ephritikhine, M., Madic, C., 2001. Chem. Commun. 1512.
Kaltosoyannis, N., Scott, P., 1998. Chem. Commun. 1665.
Kolarik, Z., Kuhn, W., 1974. In: *Proceedings of the International Solvent Extraction Conference*, ISEC 74, 3. Society of Chemical Industry, Lyon, p. 2593.
Kolarik, Z., Mullich, U., Gassner, F., 1999a. Solv. Extr. Ion Exch. 17, 23.
Kolarik, Z., Mullich, U., Gassner, F., 1999b. Solv. Extr. Ion Exch. 17, 1155.
J. D. Law, K. N. Brewer, R. S. Herbst and T. A. Todd, *Demonstration of the TRUEX Process for Partitioning of Actinides from Actual ICPP Tank Waste Using Centrifugal Contactors in a Shielded Cell Facility*, Idaho, National Engineering and Environmental Laboratory Report INEL-96/0353, Idaho Falls, ID, 1996.
Leggett, C.J., Liu, G., Jensen, M.P., 2010. Solv. Extr. Ion Exch. 28, 313.
Lewis, F.W., Harwood, L.M., Hudson, M.J., Drew, M.G.B., Modolo, G., Wilden, A., Sypula, M., Vu, T.-H., Simonin, J.-P., 2011. J. Am. Chem. Soc. 133, 13093.
Lewis, F.W., Harwood, L.M., Hudson, M.J., Drew, M.G.B., Hubscher-Bruder, V., Videva, V., Arnaud-Neu, F., Stamberg, K., Vyas, S., 2013. Inorg. Chem. 52, 4993.
G. J. Lumetta, S. I. Sinkov, D. Neiner, T. G. Levitskaia, J. C. Braley, J. C. Carter, M. G. Warner, J. W. Pittman and B. M. Rapko, *Sigma Team for Minor Actinide Separation: PNNL FY 2010 Status Report*, Technical Report No. PNNL-19655, 2010.
Lundberg, D., Persson, I., Ekberg, C., 2013. Dalton Trans. 3767.
Magnusson, D., Christiansen, B., Glatz, J.-P., Malmbeck, R., Modolo, G., 2009. D. Serrano-Purroy and C. Sorel. Radiochim. Acta 97, 155.
Magnusson, D., Geist, A., Wilden, A., Modolo, G., 2013. Solv. Extr. Ion Exch. 31, 1.
Marie, C., Hiscox, B., Nash, K.L., 2012. Dalton Trans. 41, 1054.

May, I., Taylor, R.J., Denniss, I.S., Wallwork, A.L., 1999. Czech. J. Phys. 49, 597.
Nilsson, M., Nash, K.L., 2007. Solv. Extr. Ion Exch. 25, 665.
Nilsson, M., Andersson, S., Drouet, F., Ekberg, C., Foreman, M., Hudson, M., Liljenzin, J.-O., Magnusson, D., Skarnemark, G., 2006. Solv. Extr. Ion Exch. 24, 299.
Reilly, S.D., Gaunt, A.J., Scott, B.L., Modolo, G., Iqbal, M., Verboom, W., Sarsfield, M.J., 2012. Chem. Commun. 48, 9732.
Sessler, J.L., Melfi, P.J., Pantos, G.D., 2006. Coord. Chem. Rev. 250, 816.
Swanson, J.L., 1990. Purex process flowsheets. In: Schulz, W.W., Burger, L.L., Navratil, J.D. (Eds.), In: Science and Technology of Tributyl Phosphate, vol. III. CRC Press, Boca Raton, pp. 55–80.
Tedeschi, C., Picard, C., Azéma, J., Donnadieu, B., Tisnès, P., 2000. New J. Chem. 24, 735.
Thiollet, G., Musikas, C., 1989. Solv. Extr. Ion Exch. 7, 813.
Thomas, I.R., Bruno, I.J., Cole, J.C., Macrae, C.F., Pidcock, E., Wood, P.A., 2010. J. Appl. Cryst. 43, 362.
Tian, G., Xu, J., Rao, L., 2005. Angew. Chem. Int. Ed. 44, 6200–6203.
Tripathi, S.C., Ramanujam, A., 2003. Sep. Sci. Technol. 38, 2307.
Whittaker, D.M., Griffiths, T.L., Helliwell, M., Swinburne, A.N., Natrajan, L.S., Lewis, F.W., Harwood, L.M., Parry, S.A., Sharrad, C.A., 2013. Inorg. Chem. 52, 3429.
Wilden, A., Modolo, G., Schreinemachers, C., Sadowski, F., Lange, S., Sypula, M., Magnusson, D., Geist, A., Lewis, F.W., Harwood, L.M., Hudson, M.J., 2013. Solv. Extr. Ion Exch. 31, 519.

Radiation chemistry in the reprocessing and recycling of spent nuclear fuels

8

Bruce J. Mincher
Idaho National Laboratory, Idaho Falls, ID, USA

Acronyms

BATP	bis annulated triazinylbipyridine
BTBP	bistriazinylbipyridine
BTP	bistriazinylpyridine
CHON	carbon hydrogen oxygen nitrogen
CMPO	octylphenyl-*N*,*N*-diisiobutylcarbamoylmethyl phosphine oxide
DHoEPA	di(hexoxyethyl)phosphoric acid
DIAMEX	diamide extraction
DIDPA	diisodecylphosphoric acid
DMDOHEMA	dimethyl dioctyl hexylethoxymalonamide
HDBP	dibutylphosphoric acid
H2DBP	monobutylphosphoric acid
HDEHP	bis-(2-ethylhexyl)phosphoric acid
H2MEHP	mono-2-ethylhexylphosphoric acid
LET	linear energy transfer
MIDPA	monoisodecylphosphoric acid
PUREX	plutonium uranium redox extraction
TALSPEAK	trivalent actinide lanthanide separation by phosphorous reagent extraction from aqueous komplexes
TBP	tributylphosphate
TRUEX	transuranium extraction

8.1 Introduction to radiation chemistry

Current concepts for closure of the nuclear fuel cycle involve the dissolution of used nuclear fuel and the use of complex organic ligands designed for highly selective solvent extraction-based separations. Current proposals envision at least three separations: (1) recovery of the redox active actinides: uranium, neptunium, and/or plutonium; (2) group separation of the remaining trivalent actinides and lanthanides; and (3) separation of trivalent actinides from trivalent lanthanides. The last step is especially challenging given the similar chemistry of the trivalent f-elements, and research is underway worldwide to develop a partitioning scheme to separate americium and/or

Reprocessing and Recycling of Spent Nuclear Fuel. http://dx.doi.org/10.1016/B978-1-78242-212-9.00008-3

curium from the lanthanide fission products. A large number of complexing agents have been evaluated for application in one or more of these steps.

In the majority of proposals, the first step to recover uranium, neptunium, and/or plutonium is based on the conventional PUREX (plutonium uranium redox extraction) process with tributylphosphate (TBP) extraction. This separation has been successfully employed for decades and was thoroughly reviewed by Schulz and Navratil (1984). Other organophosphorous reagents such as octylphenyl-*N*, *N*-diisobutylcarbamoylmethylphosphine oxide (CMPO) have been proposed for the group actinide/lanthanide extraction in the TRUEX (transuranium extraction) process (Schulz and Horwitz, 1988) and bis-(2-ethylhexyl)phosphoric acid (HDEHP) for the actinide/lanthanide separations in the TALSPEAK (trivalent actinide lanthanide separation by phosphorous reagent extraction from aqueous komplexes) process (Nilsson and Nash, 2007).

However, in an effort to simplify waste disposal options for spent solvents, reagents observing the CHON principle (i.e., those containing only carbon, hydrogen, oxygen, and nitrogen) have also been proposed for these separations (Madic and Hudson, 1998). The advantage of such reagents is that they are completely incinerable (Musikas, 1988). For example, malonamides (Spjuth et al., 2000) such as dimethyl dioctyl hexylethoxymalonamide (DMDOHEMA) have been proposed in the DIAMEX (diamide extraction) process (Serrano-Purroy et al., 2005). Alternately, tetraalkyldiamides such as tetraoctyldiglycolamide (TODGA) (Sasaki et al., 2001) have also been investigated as group f-element extraction ligands for process application (Modolo et al., 2007). In processes observing the CHON principle, the final actinide/lanthanide separation corresponding to TALSPEAK is called SANEX (selective actinide extraction) (Magnusson et al., 2009a) and uses one of several bistriazinyl bipyridine (BTBP) N-donor ligands to selectively complex the actinides (Geist et al., 2006).

Additional options have been considered; however, these are currently the most important molecules and processes undergoing research for application. Regardless of any other considerations, all the reagents proposed must have exceptional stability under the extreme radiolysis conditions resulting from the radioactive decay of the fission products (low linear energy transfer (LET) β/γ radiation) and actinides (high LET α radiation) present in dissolved nuclear fuel.

8.1.1 Reactive species in γ-irradiated solution

The interaction of ionizing radiation with a solution containing solutes results mainly in the interaction of photons and energetic particles with the diluent. Diluent molecules are ionized or excited, and some excited molecules decay into neutral radical species (Spinks and Woods, 1990). These reactive species have lifetimes measured in microseconds, but may diffuse into the bulk solution to react with solutes of interest, including solvent extraction ligands. Ligand reactions often result in deleterious effects such as loss in ligand concentration or production of decomposition products that may also be complexing agents that interfere with desired separations.

The radiation chemistry of aqueous and organic solutions is understood well enough to make certain predictions about which radicals are of interest in solvent extraction systems.

Among the main transient reactive species produced are the oxidizing hydroxyl ($^{\bullet}OH$), nitrite ($^{\bullet}NO_2$), and nitrate ($^{\bullet}NO_3$) radicals from water and nitric acid radiolysis, the reducing solvated electron (e^-_{sol} or e^-_{aq}) and $^{\bullet}H$ atoms from water and organic diluent radiolysis, and various carbon-centered radicals produced from the organic diluent. Longer lived molecular products such as H_2O_2 and HNO_2 may also be important reactive species in some systems. Important radiolysis products are given in Equations 8.1–8.3 (Buxton et al., 1988; Jiang et al., 1994; Spinks and Woods, 1990):

$$^{\bullet}H_2O - \gamma \rightarrow [0.28]^{\bullet}OH + [0.27]e^- + [0.05]^{\bullet}H + [0.07]H_2O_2 + [0.27]H_3O^+ + [0.05]H_2 \quad (8.1)$$

$$HNO_3 - \gamma \rightarrow {}^{\bullet}H + e^-_{aq} + {}^{\bullet}NO_3 + {}^{\bullet}NO_2 + HNO_2 \quad (8.2)$$

$$CH_3(CH_2)_nCH_3 - \gamma \rightarrow e^-_{sol} + {}^{\bullet}\left[CH_3(CH_2)_nCH_3\right]^+ + {}^{\bullet}CH_2(CH_2)_nCH_3 + {}^{\bullet}CH_3 + {}^{\bullet}H + H_2 \quad (8.3)$$

The bracketed numbers in Equation 8.1 are the yields (G-values in μmol J^{-1}) for the products of water radiolysis in neutral, β/γ-irradiated solution, at about 1×10^{-7} s after the initial event (Buxton et al., 1988). The equations are not meant to be balanced; rather, they are lists showing the most important products. The radical products of Equation 8.1 may then react with each other to recreate water (geminate recombination), react with each other to form other molecular products (radical addition reactions), or diffuse into the bulk solution to react with solutes such as solvent extraction ligands. These yields may be altered in any given solution by scavenging reactions that remove the corresponding radicals from further consideration with regard to their reactions with solvent extraction ligands. In the presence of air and nitric acid, for example, the reducing radicals are rapidly scavenged by dissolved oxygen, hydronium ion, and nitrate ion to produce less reactive species and a mainly oxidizing system is expected for reactions in the aqueous phase (Buxton et al., 1988; Buxton et al., 1988; Gordon et al., 1964):

$$e^-_{aq} + H^+ \rightarrow {}^{\bullet}H, \quad k = 2.3 \times 10^{10} M^{-1} s^{-1} \quad (8.4)$$

$$e^-_{aq} + O_2 \rightarrow {}^{\bullet}O_2{}^-, \quad k = 1.9 \times 10^{10} M^{-1} s^{-1} \quad (8.5)$$

$$e^-_{aq} + NO_3{}^- \rightarrow {}^{\bullet}NO_3^{-2}, \quad k = 9.7 \times 10^{9} M^{-1} s^{-1} \quad (8.6)$$

$$H^{\bullet} + O_2 \rightarrow {}^{\bullet}HO_2, \quad k = 2.1 \times 10^{10} M^{-1} s^{-1} \quad (8.7)$$

These reactions occur in competition with potential ligand reactions. The k-values in Equations 8.4–8.7 are the aqueous bimolecular rate constants for the reactions shown

and these high values indicate that they are very fast, essentially limited only by the rate of diffusion in the irradiated solution. Thus, even if its rate constant for reaction with a ligand is fast, in molar amounts of nitric acid the reaction of the e_{aq}^- with millimolar amounts of ligand is not expected to be competitive. Reactions of the $^\bullet$H atom with ligands may occur in competition with the millimolar amounts of dissolved oxygen in air-saturated solution, depending on the ligand concentration and its rate constant for the reaction.

In the near absence of the reducing species in irradiated, aerated, and acidic solution, the most important reactive transient species generated by water radiolysis is the oxidizing $^\bullet$OH radical. It reacts with fairly fast rate constants with nearly all organic compounds. In the presence of nitric acid, the oxidizing $^\bullet NO_3$ and $^\bullet NO_2$ radicals are also produced. In general, the reactivity of these species with solvent extraction ligands occurs in the order $^\bullet OH > {}^\bullet NO_3 > {}^\bullet NO_2$. The typical reactions of these species with organic compounds are $^\bullet$H atom abstraction, radical addition, and electron transfer, as shown for the $^\bullet$OH radical reacting with a generic organic compound RH in Equations 8.8–8.10:

$$HR + {}^\bullet OH \rightarrow {}^\bullet R + HOH \tag{8.8}$$

$$HR + {}^\bullet OH \rightarrow {}^\bullet HROH \tag{8.9}$$

$$HR + {}^\bullet OH \rightarrow {}^\bullet HR^+ + OH^- \tag{8.10}$$

Reactions such as these that create organic radical species may result in continued decomposition of the original compound.

In the organic phase shown in Equation 8.3, once the solvated electron (e_{sol}^-) is eliminated, the main products of alkane diluent radiolysis are various neutral and cationic carbon-centered radicals. Neutral carbon-centered radicals may react by radical addition to create higher molecular weight organic species or nitrated derivatives of the original organic species, including nitration of the diluents:

$$^\bullet HR + {}^\bullet CH_3 \rightarrow HRCH_3 \tag{8.11}$$

$$^\bullet HR + {}^\bullet NO_2 \rightarrow HRNO_2 \tag{8.12}$$

Reactions of the neutral $^\bullet$OH and $^\bullet NO_3$ radicals might also be expected in the organic phase after diffusion of these species across the phase boundary. To the knowledge of this author, no work has been done to examine rates of transfer of these species across the phase boundary. In unpublished work, this author and coworkers have measured the rate constants for the reaction of $^\bullet NO_3$ radical in organic solution with a number of solutes and found that, in general, the reactions are slower than in aqueous solution. This may be a viscosity effect. The radical cation product of alkane radiolysis shown in Equation 8.3 has the further possibility to react with organic compounds by electron transfer:

$$HR + {}^\bullet\left[CH_3(CH_2)_nCH_3\right]^+ \rightarrow {}^\bullet HR^+ + CH_3(CH_2)_nCH_3 \tag{8.13}$$

The reactions of all these transient species in irradiated solution are discussed in more detail by Mincher and Mezyk (2009) and Mincher et al. (2009a).

In addition to the transient radicals, longer-lived molecular reactive species are produced by radiolysis, including especially H_2O_2 from water radiolysis (Equation 8.1) and HNO_2 from nitric acid radiolysis (Equation 8.2). Both act as redox reagents and may affect the oxidation state of metal ions in the irradiated solution. This has importance to solvent extraction where maintenance of desired oxidation states determines solvent extraction distribution ratios. Examples of redox speciation changes include the oxidation of iron and the reduction of cerium, both used to advantage in aqueous dosimetry (Klassen et al., 1999; ISO/ASTM 2006):

$$H_2O_2 + Fe^{2+} \rightarrow Fe^{3+} + OH^- + {}^{\bullet}OH \tag{8.14}$$

$$H_2O_2 + 2Ce^{4+} \rightarrow 2Ce^{3+} + 2H^+ + O_2 \tag{8.15}$$

Similarly, radiolytically produced HNO_2 reduces NpVI to NpV according to Equation 8.16 (Siddal and Dukes 1959; Mincher et al., 2013a):

$$NpO_2^{2+} + HNO_2 + H_2O \rightarrow NpO_2{}^+ + 3H^+ + NO_3{}^- \tag{8.16}$$

Further, HNO_2 is a powerful nitrating agent. It is capable of nitrating especially aromatic ligands via the nitrous acid catalyzed mechanism, shown in Equations 8.17–8.20 (Turney and Wright, 1959; Schramm and Westheimer, 1948):

$$HNO_2 + H^+ \rightarrow NO^+ + H_2O \tag{8.17}$$

$$ArH + NO^+ \rightarrow ArHNO^+ \tag{8.18}$$

$$ArHNO^+ \rightarrow ArNO + H^+ \tag{8.19}$$

$$ArNO^+ + HNO_3 \rightarrow ArNO_2 + HNO_2 \tag{8.20}$$

The aromatic compound (ArH) undergoes electrophilic substitution by the nitroso ion in Equations 8.18 and 8.19, following which it is oxidized to a nitro-substituted product in Equation 8.20, which also regenerates HNO_2.

8.1.2 Reactive species in α-irradiated solution

Higher yields (*G*-values) of the molecular products and lower yields of radical products are expected for α-radiolysis, due to the higher linear energy transfer (LET) of the α-particle. For example, as shown in Equation 8.21, the yield of H_2O_2 for α radiation has increased, while the yields of ${}^{\bullet}OH$ radical, e_{aq}^-, and ${}^{\bullet}H$ atom have decreased (LaVerne, 2004):

$$\begin{aligned} H_2O - \alpha \rightarrow {} & [0.05]{}^{\bullet}OH + [0.03]e^- + [0.01]{}^{\bullet}H + [0.10]H_2O_2 + [0.03]H_3O^+ \\ & + [0.12]H_2 + [0.01]{}^{\bullet}HO_2 \end{aligned} \tag{8.21}$$

The higher LET of the α-particle (156 eV nm^{-1} for a 5 MeV He ion; < 1 eV nm^{-1} for β/γ radiation) results in the deposition of larger amounts of energy in a smaller volume of solution (Spinks and Woods, 1990). The resulting high yields of radicals and ions then undergo geminate recombination or radical addition reactions to generate molecular species before they can diffuse into the bulk solution to react with ligands. The addition reaction of $^{\bullet}OH$ radicals to produce H_2O_2 is shown in Equation 8.22 (Spinks and Woods, 1990):

$$^{\bullet}OH + {}^{\bullet}OH \rightarrow H_2O_2, \quad k = 5.5 \times 10^9 M^{-1}s^{-1} \tag{8.22}$$

As the fast radical reactions become less important for α-radiolysis, the slower reactions of the produced molecular species become competitive. The effects of α-irradiation are often attributed to the radiolytic generation of H_2O_2.

Thus, although radiation chemistry in multispecies systems is a complicated mix of competing reactions, the reactive species produced and their main reactions are understood. The species that are most important in a given system will depend not only on the yields of these reactive species, but also on their kinetics of reaction with the ligands of interest. These transient species react in a competitive environment where they may be scavenged by oxygen, acidity, or even the diluent, limiting their ability to react with solutes of interest. Based on the discussion above, in the biphasic, aerated, and acidic conditions of the solvent extraction process, the reactive species of greatest interest are the strongly oxidizing $^{\bullet}OH$ and $^{\bullet}NO_3$ radicals, and to a lesser extent $^{\bullet}NO_2$ radical; all produced by aqueous nitric acid radiolysis, the neutral and cationic carbon-centered radicals produced in the irradiated organic phase, and the molecular products H_2O_2 and HNO_2.

8.1.3 On the utility of the *G*-value as a metric in describing ligand degradation

The most common metric used in the literature to describe the yield (negative or positive concentration change with absorbed dose) is the *G*-value (μmol J^{-1}). For the generation of products in a neat irradiated solution such as pure water in Equation 8.1, the *G*-value is an appropriate metric. However, the *G*-value is inadequate when describing the radiolysis-induced concentration change of a solute because it is a rate, rather than a rate constant (Mincher and Curry, 2000). Some *G*-values for the radiolysis of neat solvent extraction ligands have been reported, such as those for neat TBP given by Wilkinson and Williams (1961) or neat HDEHP given by Wagner and Towle (1958) and Kuzin et al. (1969); however, these values have limited utility with regard to the decomposition rates or products of ligands in a diluent. Except for reactions with zero-order kinetics, the *G*-value is concentration dependent and varies as the solute concentration changes during irradiation. To account for the nonconstant *G*-value, initial *G*-values (G_0) have sometimes been reported. These are by nature imprecise as they rely on a limited subset of data collected early in the irradiation, often prior to the establishment of equilibrium conditions.

Better metrics are easily recommended, including the slope of the line obtained for zero-order plots of concentration versus absorbed dose curves, and the exponential constant for pseudo first-order plots of concentration versus absorbed dose. These are the most common systems. However, as *G*-values have usually been reported in the literature, often in the absence of solute concentrations or other solution characteristics that might influence them, there is no choice but to refer to them in this review. Given their dependence on system conditions, it should be kept in mind that they are of limited utility and may be misleading when reported in the absence of these conditions. Reporting them here has been minimized as much as practicable.

8.2 Examples of radiation chemical effects on solvent extraction ligands

8.2.1 Tributylphosphate

The most common ligand used in fuel cycle solvent extraction is tributylphosphate (TBP). The compound is used on a process scale in the PUREX (plutonium uranium reduction extraction) process (Lanham and Runion, 1949) and is also added as a phase modifier to improve the solubility of other ligands and to mitigate third-phase formation in other processes such as TRUEX (transuranium extraction). In addition to being one of the most important fuel cycle compounds, its radiation chemistry has long been studied and its reactions are illustrative of those to be expected for many other ligands.

It has long been recognized that a major product of TBP radiolysis with adverse effects on solvent extraction is dibutylphosphoric acid (HDBP); its reported yield (G_{HDBP}) varies, probably depending on experimental conditions. Only those measured in the presence of the diluent and the aqueous phase are pertinent to the process, and only a few studies have measured HDBP yields in the presence of both its alkane diluents and the acidic aqueous phases. Values reported for G_{HDBP} in irradiated 30% TBP alkane solution in contact with nitric acid range from 0.11 (Becker et al., 1983) to 0.06 μmol J^{-1} (Nowak, 1977), illustrating the problems associated with this metric. The *G*-value has been reported to be constant with dose rate but to vary with solution conditions (Adamov et al., 1990).

HDBP is produced from TBP by multiple radiolytic mechanisms. Several authors have reported that HDBP is produced by dissociative electron capture (Haase et al., 1973; Zaitsev and Khaikin, 1994; Jin et al., 1999); however, this mechanism is not important under solvent extraction process conditions because electrons are scavenged by acidity, dissolved oxygen, and nitrate anion (Equations 8.4–8.6). In the irradiated process, TBP decomposition is most likely initiated by $^{\bullet}H$ atom abstraction from one of the butyl chains, mainly by reaction with $^{\bullet}OH$ or $^{\bullet}NO_3$ radicals in analogy with Equation 8.8, or with $^{\bullet}H$ atoms in competition with Equation 8.7. In this case, $^{\bullet}H$ atom reactions may be important despite the fast reaction with dissolved O_2 shown in Equation 8.7, as TBP is used at the very high concentration of ~1 M in the process. The $^{\bullet}H$ atom abstraction reaction using the $^{\bullet}OH$ radical as the example is shown below:

$$(C_4H_9O)_3PO + {}^{\bullet}OH \rightarrow {}^{\bullet}(C_4H_8O)(C_4H_9O)_2PO + HOH \quad (8.23)$$

The rate constants for the reactions of TBP with $^{\bullet}H$, $^{\bullet}OH$, $^{\bullet}NO_3$, and $^{\bullet}NO_2$ radicals are 1.8×10^8, 5×10^9, 4.3×10^6, and $< 2 \times 10^5$ M^{-1} s^{-1}, respectively (Mincher et al., 2008). Following production of the neutral, carbon-centered radical, there are three possible mechanisms for decay to HDBP. They are direct radical decay (Burr, 1958), hydrolysis (von Sonntag et al., 1972), or reaction with oxygen (Khaikin, 1988) shown in Equations 8.24–8.26, respectively.

$$^{\bullet}(C_4H_8O)(C_4H_9O)_2PO \rightarrow {}^{\bullet}C_4H_8{}^{+} + (C_4H_9O)_2OPO^{-} \quad (8.24)$$

$$^{\bullet}(C_4H_8O)(C_4H_9O)_2PO + H_2O \rightarrow {}^{\bullet}C_4H_8OH + (C_4H_9O)_2OPO^{-} + H^{+} \quad (8.25)$$

$$^{\bullet}(C_4H_8O)(C_4H_9O)_2PO + O_2 \rightarrow {}^{\bullet}OO(C_4H_8O)(C_4H_9O)_2PO \quad (8.26)$$

The peroxyl radical product of Equation 8.26 is a common product of the reaction of many carbon-centered radicals in the presence of dissolved O_2, and the reaction occurs with rate constants in the range of $\sim 5 \times 10^9$ M^{-1} s^{-1} (Alfassi, 1997). It was postulated to decompose to HDBP (Khaikin, 1988):

$$^{\bullet}OO(C_4H_8O)(C_4H_9O)_2PO \rightarrow {}^{\bullet}O_2{}^{-} + (C_4H_8O)(C_4H_9O)_2PO^{+} \quad (8.27)$$

$$(C_4H_8O)(C_4H_9O)_2PO^{+} + H_2O \rightarrow (C_4H_9O)_2OPO^{-} + C_3H_7CHO + 2H^{+} \quad (8.28)$$

It should be noted that Wilkinson and Williams (1961) suggested the possibility that the TBP radical cation, produced by TBP ionization, also decays to HDBP. The numerous reactions described above all lead to the production of HDBP and probably occur competitively.

Produced HDBP degrades by similar mechanisms, with rate constants for the reactions with $^{\bullet}H$, $^{\bullet}OH$, $^{\bullet}NO_3$, and $^{\bullet}NO_2$ radicals reported to be 1.1×10^8, 4.4×10^9, 2.9×10^6, and $< 2 \times 10^5$ M^{-1} s^{-1}, respectively (Mincher et al., 2008). These are slightly slower than the corresponding reactions for TBP, probably reflecting the reduced number of sites available for $^{\bullet}H$ atom abstraction reactions for HDBP. The products of HDBP radiolysis are monobutylphosphoric acid (H_2DBP) and eventually phosphate anions.

In the process, TBP would be irradiated not only as the free ligand but also as the metal complex. The kinetics of the reactions of the metal complex with radiolytically produced reactive species may be different than for the free ligands. The presence of uranium and/or plutonium in irradiated solution has been reported to increase (Nowak et al., 1979; Kulikov et al., 1983) or, in contrast, to decrease (Williams and Wilkinson, 1957; Burger and McClanahan, 1958; Becker et al., 1983) the yield of HDBP. Further investigation of this effect will be necessary before the radiation chemistry of PUREX extraction systems is to be modeled.

Additional radiolysis products of TBP when irradiated in the presence of nitric acid include nitrated, methylated, and/or hydroxylated phosphates, often of higher

molecular weight (Adamov et al., 1990; Tripathi et al., 2001; He et al., 2004). High molecular weight products were found to include those with alkane groups heavier than butyl, TBP dimers, and various acidic organophosphorous compounds (Lasage et al., 1997; Lamouroux et al., 2001). These species are all potential metal complexing agents, and the neutral ones are not removed by the alkaline wash used to remove HDBP in the process.

8.2.2 The amidic compounds CMPO, DMDOHEMA, and TODGA

In addition to TBP, a number of compounds are under investigation in various fuel cycle proposals that act as stronger but less selective complexing agents for the lanthanides and actinides. The most important of these are octylphenyl-*N*,*N*-diisobutylcarbamoylmethyl phosphine oxide (CMPO), dimethyl dioctyl hexylethoxymalonamide (DMDOHEMA), and *N*,*N*,*N*′,*N*′-tetraoctyl-3-oxapentane-1,5-diamide (TODGA, also known as tetraoctyldiglycolamide). Each contains an amidic functional group, which lends some similarity to their radiation chemistry. For each, irradiation of an alkane solution containing the ligand in the presence of aqueous nitric acid results in the preferred rupture of the amidic C—N bond. The resulting major products are the corresponding amine and carboxylic acids (Nash et al., 1988; Berthon et al., 2001; Mincher et al., 2009a,b, Groenewold et al., 2012). This is shown for DMDOHEMA in Figure 8.1.

Values for the degradation yields of CMPO, DMDOHEMA, and TODGA when irradiated as components of their process formulations have been reported. For example, $-G_{CMPO}$ in the TRUEX formulation 0.2 M CMPO/1.2 M TBP/dodecane irradiated in the presence of nitric acid was reported to be independent of the acid concentration over the range 1.25-5.0 M at 0.12 μmol J^{-1} (Nash et al., 1989). More recently, a value of 0.18 μmol J^{-1} was reported for 0.1 M CMPO/dodecane irradiated in the absence of TBP and either in the absence of the aqueous phase or in the presence of 0.1 M HNO_3 (Mincher et al., 2013b). However, in that work the $-G_{CMPO}$ was reported to decrease with increasing nitric acid concentration, reaching a value of 0.02 μmol J^{-1} at 5 M HNO_3. The presence of dissolved oxygen also provided radioprotection. The degradation of CMPO exposed to α-radiolysis was lower (Mincher et al., 2014).

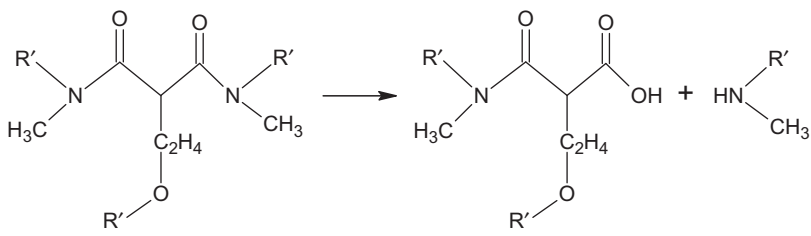

Figure 8.1 The radiolytic decomposition of DMDOHEMA into an acidamide and an amine in the presence of the acidic aqueous phase.

For the SANEX formulation of 0.65 M DMDOHEMA/dialkylphosphoric acid irradiated in the presence of 0.5-3.0 M HNO_3, a $-G_{DMDOHEMA} \sim 0.5$ μmol J^{-1} was reported (Berthon et al., 2004, Bisel et al., 2007). Values for TODGA decomposition were reported to be even higher. Sugo et al. (2007a) measured dose constants of 1.7×10^{-6} Gy^{-1} for 0.5 M TODGA and 2.9×10^{-6} Gy^{-1} for 0.1 M TODGA irradiated in dodecane in the absence of an aqueous phase. These dose constants (analogous to rate constants) may be converted to *G*-values (analogous to rates) (Mincher and Curry, 2000) and, when corrected for solution density, correspond to 0.22 and 0.65 μmol J^{-1}, respectively. Generally, one would expect the rate of TODGA decomposition to increase with TODGA concentration; however, Sugo et al. (2007a) attributed this contrasting result to the increase in the dodecane concentration, and suggested that electron transfer reactions with the dodecane radical cation were responsible for TODGA degradation. This is consistent with the lower ionization potential of TODGA as compared to dodecane. The apparent higher stability of CMPO is likely due to the presence of the aromatic functional group, which would facilitate intramolecular energy transfer to mitigate bond rupture. Increased stability has been shown for other benzyl substituted amides (Sugo et al., 2007b).

Using DMDOHEMA as the example, radiolytic degradation of the amides to amine and carboxylic acids is shown in Figure 8.1. Initiation of the sequence is likely due to an $^{\bullet}H$ atom abstraction by reaction with radiolytically produced free radicals as was shown in Equations 8.8 and 8.23, or by electron transfer reactions with radiolytically produced radical cations such as in Equation 8.13. Bond rupture follows, preferably forming the amine in the presence of nitric acid. Oxidation of the balance of the molecule produces a carboxylic acid; in the case of DMDOHEMA, the acid is an acidamide. Decarboxylation of the acidamide may also produce a monoamide. These products have been identified in mass spectrometric work (Berthon et al., 2001; 2004).

Among additional products of irradiated amides are numerous dealkylation products such as phenyl-*N*,*N*-diisobutylcarbamoylmethyl phosphine oxide (Mincher et al., 2013b) and octylphenyl monoisobutylcarbamoylmethylphosphine oxide (Nash et al., 1988; Mincher et al., 2013b) from CMPO and loss of the alkyl chain containing the ether linkage for DMDOHEMA (Berthon et al., 2001; 2004).

The acidic products of amide degradation have been implicated in adversely affecting the ability to strip the loaded organic phase. For CMPO, the products octylphenylphosphinyl acetic acid and octylphenylphosphinic acid have been shown to interfere with americium stripping by preventing back extraction into aqueous solutions of dilute acid (Chiarizia and Horwitz, 1986; Nash et al., 1989). Similar results have been reported for the acidic products of DMDOHEMA radiolysis (Berthon et al., 2001; Berthon et al., 2004). The generation of these products necessitates additional process steps to wash the irradiated solvent, similar to the conventional use of alkaline aqueous contacts to remove HDBP from irradiated TBP solutions.

8.2.3 Bis(2-ethylhexyl)phosphoric acid

Acidic organophosphorus compounds are of interest in solvent extraction radiation chemistry not only because they are degradation products of neutral compounds such as TBP and CMPO but also because compounds such as bis(2-ethylhexyl)phosphoric

acid (HDEHP) have been used as extractants. This compound is a component of the process that has become known as TALSPEAK for actinide/lanthanide extraction (Nilsson and Nash, 2007).

The mode of degradation of HDEHP by dealkylation is analogous to that for TBP, with the main product being mono(2-ethylhexyl)phosphoric acid (H_2MEHP) (Schulz, 1968; Tachimori, 1979a). Ether linkages were shown once again to be especially susceptible to radiolytic rupture, as reported above for TBP and DMDOHEMA, and also widely reported for the crown ethers (see, for example, Draye et al., 1993). This reaction may be initiated by dissociative electron capture, $^{\bullet}H$ atom abstraction, or direct radiolysis:

$$[C_4H_9(C_2H_5)CHCH_2O]_2POOH \rightarrow C_4H_9(C_2H_5)CHC^{\bullet}H_2 + {}^{\bullet}O[C_4H_9(C_2H_5)CHCH_2O]POOH \quad (8.29)$$

Rearrangement of the carbon-centered radical product of Equation 8.29 produces the 1-methyl-1-ethylpentyl radical, which has been identified in electron spin resonance studies (Tachimori and Ito, 1979). Acquisition of an $^{\bullet}H$ atom by the second product of Equation 8.29 gives H_2MEHP. Continued irradiation would be expected to eventually create phosphoric acid, also in analogy with TBP.

Irradiation of HDEHP solutions results in variable changes in solvent extraction performance, although generally these cannot be accounted for merely by the change in HDEHP concentration. Metal extraction distribution ratios may increase (Tachimori et al., 1978) or decrease (Schulz, 1968), apparently depending on the mole ratio of HDEHP to H_2MEHP (Tachimori, 1979b) and pH (Tachimori, 1978). Tachimori (1979b) added H_2MEHP to HDEHP solutions and found that a mole ratio of HDEHP:H_2MEHP of two gave the highest americium distribution ratios. Tachimori and Nakamura (1979) reported that although the magnitude of the distribution ratios changed with absorbed dose, the separation factor $\alpha_{Nd/Am}$ was unchanged for extractions using solutions of 0.5 M HDEHP in normal paraffinic hydrocarbon prepared using irradiated HDEHP.

In contrast to work with CMPO (Mincher et al., 2013b), the presence of the aqueous phase appears to increase radiolytic degradation of HDEHP (Schulz, 1968; Tachimori, 1979b). The loss in extraction efficiency for americium was more severe for irradiation in the presence of the nitric acid aqueous phase for the analogous compounds diisodecylphosphoric acid (DIDPA) and di(hexoxyethyl)phosphoric acid (DHoEPA) (Tachimori et al., 1979). Degradation of the ether was especially severe. The products of radiolysis included monoisododecylphosphoric acid (MIDPA) from DIDPA and monohexoxyethylphosphoric acid from DHoEPA, in analogy with the production of H_2MEHP from HDEHP.

8.2.4 Bistriazinylpyridines and their derivatives

The bistriazinylpyridines (BTPs) are sensitive to hydrolytic and radiolytic degradation, and a great deal of research has been conducted to improve their stability for nuclear solvent extraction applications, making them among the first nuclear solvent extraction ligands to undergo design changes with radiation stability in mind.

Kolarik (2008) and Ekberg et al. (2008) have reviewed the history of their development. Kolarik et al. (1999) reported that solutions containing BTPs with non-branched side chains (*n*Bu-, *n*Pr-, and Et-BTP) changed color rapidly upon contact with an acidic aqueous phase, suggesting degradation of the solvent due to acid hydrolysis. The degradation of *n*Pr-BTP appears to be initiated by attack on the α-CH_2 group of the propyl chain of the triazinyl ring. The lability of hydrogen atoms at this position was demonstrated in electrospray mass spectrometry work by Retegan et al. (2009) and the isopropyl derivative (*i*Pr-BTP) was more resistant (Hill et al., 2005).

The radiolytic degradation of the BTPs has received extensive investigation. Nilsson et al. (2006a) investigated the γ-radiolytic stability of Et-BTP in hexanol solution in the absence of an aqueous phase. Postirradiation americium distribution ratios decreased with increasing absorbed dose, falling below unity at <5 kGy; attributed to BTP degradation. Hill et al. (2002) reported that the degradation products of *i*Pr-BTP irradiated with or without the aqueous phase were heavier than the original BTP. These products were likely produced by addition reactions between BTP radicals and the α-hydroxy octyl radical, produced by diluent radiolysis. The addition of cyclic rings to BTPs to produce the BATPs increased stability toward radiolysis, probably also by protection of the α-CH_2 group; however, absorbed doses in excess of 100 kGy still substantially decreased the extraction of americium (Hill et al., 2005; Hudson et al., 2006).

The inclusion of a second pyridine ring into the BTP molecule to produce a bis-triazinylbipyridine (BTBP) moderated extraction efficiency to facilitate stripping (Geist et al., 2006). When a solvent formulation containing 0.01 M 6,6′-bis(5,5,8,8-tetramethyl-5,6,7,8-tetrahydrobenzo[1,2,4]-triazin-3-yl)-[2,2′]-bipyridine ($CyMe_4$-BTBP) (Figure 8.2) was irradiated to the rather low maximum absorbed dose of 12-14 kGy in cyclohexanone or hexanol, there was no decrease in performance, although the related compound 6,6′-bis(5,6-dipentyl-[1,2,4]-triazin-3-yl)-[2,2′]-bipyridine (C5-BTBP) (Figure 8.2), which has *n*-pentane alkyl groups rather than cyclic alkyl groups, exhibited a significant decrease in the extraction efficiency over a similar absorbed dose range (Retegan et al., 2007). This further illustrates the importance of protecting the α-CH_2 groups. Similarly, a solution of 0.005 M C5-BTBP in cyclohexanone exhibited an 80% decrease in D_{Am} at an absorbed dose of only 17 kGy when irradiated by Nilsson et al. (2006b).

The Ekberg group has investigated the radiolysis and hydrolysis of C5-BTBP in detail in a series of papers (Nilsson et al., 2006b; Retegan et al., 2007; Fermvik et al., 2009ab, 2011, 2012). Mass spectrometric analysis identified radiolysis products including derivatives resulting from the addition of hydroxyl or keto groups at the α-CH_2 position of the BTBP alkyl chains (Figure 8.2), similar to those reported above for hydrolysis. The ingrowth of products with increased oxygen donor functionality probably explains why the extraction of americium is frequently reported to be more adversely affected than the extraction of europium, resulting in a decreased actinide/lanthanide separation factor (Nilsson et al., 2006b; Retegan et al., 2007; Fermvik et al., 2009a). Further, it must also be noted that C5-BTBP was not stable

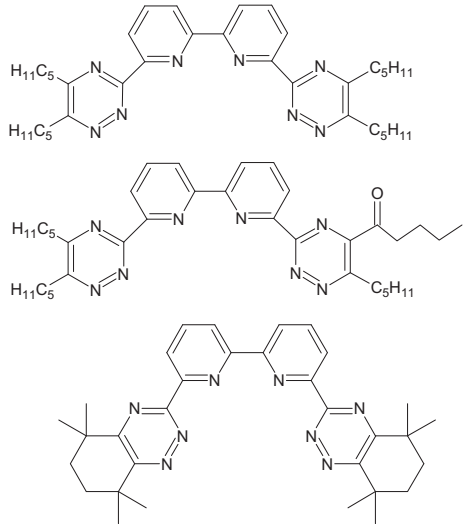

Figure 8.2 The structures of C5-BTBP (top), the keto derivative of C5-BTBP produced by hydrolysis and radiolysis, and $CyMe_4$-BTBP showing protection of the vulnerable α-CH_2 groups.

over time even in the absence of radiation. The products of C5-BTBP aging were also due to hydroxyl and keto formation at the α-hydroxy position. Other products that were identified by mass spectrometry included dealkylation derivatives and products related to the decomposition of a triazinyl ring (Fermvik et al., 2009a).

Because C5-BTBP was not sufficiently stable for use in a process, Fermvik (2011) performed similar studies on $CyMe_4$-BTBP, which is protected at the vulnerable α-CH_2 positions. The D_{Am} was predictable based merely on the decrease in the BTBP concentration, suggesting that in the absence of vulnerable α-CH_2 positions oxygenated degradation products that complex metals were not produced. Mass spectrometric analysis confirmed this supposition. A product corresponding to loss of a triazinyl ring was identified, as was also previously found for C5-BTBP. Diluent radical addition products were identified, as reported above for *i*Pr-BTP (Hill et al., 2002).

When $CyMe_4$-BTBP was irradiated as a component of the SANEX (selective actinide extraction) process (0.015 M $CyMe_4$-BTBP/0.25 M DMDOHEMA in *n*-octanol), in contact with an equal volume of americium-spiked 1 M HNO_3, Magnusson et al. (2009b) reported that γ-irradiation effects were more severe than for α, resulting in a loss of 35% of extraction efficiency within 100 kGy, in agreement with Hill et al. (2005). By 1200 kGy-γ, 70% of extraction efficiency was lost (Magnusson et al., 2009b). The finding that α-irradiation effects are less severe than those of γ is consistent with the high LET of α-particles. As was discussed above, lower degradation rates due to α-irradiation have been reported for CMPO (Mincher et al., 2014) and DMDOHEMA (Cames et al., 2010).

8.2.5 Examples of radiation chemical effects on metal ion oxidation states

As strongly oxidizing and reducing species are generated by radiolysis, it is expected that the valence state of metal ions in solution may be affected. As mentioned previously, the irradiated, acidic, and aerated solution encountered in fuel cycle separations is overwhelmingly oxidative. In nitric acid solutions containing NpV, low absorbed doses result in its oxidation to NpVI, presumably by reaction mainly with $^{\bullet}OH$ radical (Mincher et al., 2013a):

$$NpO_2^{+} + {}^{\bullet}OH \rightarrow NpO_2^{2+} + OH^{-} \tag{8.30}$$

The rate constant for this oxidation was reported to be relatively fast at about $5 \times 10^8\ M^{-1}\ s^{-1}$ (Shilov et al., 1982). However, after continued irradiation, produced nitrous acid then begins to reduce NpVI to NpV. That the reducing agent was radiolytically produced HNO_2 was demonstrated by the decrease in the reduction rate as the produced HNO_2 was consumed following termination of the irradiation. Depending on the concentration of the oxidizing nitric acid, equilibrium was reached between the two oxidation states. A kinetic model, based on the water radiolysis reactions and literature rate constants successfully reproduced this chemistry for 4 M HNO_3 solution (Mincher et al., 2013a). Vladimirova (1995) had published an earlier, more complicated model that involved NpIV reactions and a radiation dose rate dependency. However, no NpIV production or dose rate dependency was found in the experimental work of Mincher et al. (2013a).

Plutonium also has multiple simultaneous oxidation states in aqueous nitric acid, and the mix is also affected by acid concentration and radiation. The radiolysis products H_2O_2 and HNO_2 are reducing agents with respect to plutonium; upon accumulation of millimolar amounts of HNO_2, Pu(VI) is reduced to Pu(IV), and possibly even to Pu(III) (Miner and Seed, 1967). Pentavalent plutonium, if produced, would not be measured in nitric acid solution due to rapid disproportionation. Also like neptunium, the rate of reduction decreases with increasing nitric acid concentration (Vladimirova et al., 1976; Pikaev et al., 1997). Vladimirova et al. (1981) proposed an autocatalytic reduction, requiring reactions between various plutonium valence states with an overall result that PuVI was reduced to PuIV. In some experiments, oxidation of PuIV initially occurred, followed by the reduction of PuVI at higher absorbed doses, similar to that reported for neptunium above.

In continued work, Vladimirova (1990) modeled experimental results that claimed that PuVI was reduced in nitric acid solution only above certain plutonium concentrations; for example, > 5 mM in irradiated 3 M HNO_3 and > 10 mM in 6 M HNO_3. The reduction rate was increased in the presence of uranium. At low plutonium concentrations, PuIV was instead oxidized. These findings were attributed to a mechanism in which PuIV was produced by the reaction of PuV and PuIII at low plutonium concentration and by PuV disproportionation at higher plutonium concentrations. However, it must be pointed out that the $^{\bullet}OH$ radical reactions with plutonium were ignored in this model. Based on analogy with the corresponding reactions

for neptunium (Mincher et al., 2013a), these ignored rate constants may be fast. Therefore, the rate constants for the reactions that Vladimirova (1990) calculated using sensitivity analysis are questionable. Clearly, a great deal of additional research is needed.

High valence states of americium are also reduced by radiolysis. In the earliest work with AmV and AmVI, it was shown that the reduction rate of these oxidation states was faster for high specific activity ^{241}Am than for longer-lived ^{243}Am and was zero order with respect to the concentration of the high valence state. The rates had a first-order dependence on the total americium concentration, indicating that reduction occurred due to the radiolysis products of americium decay (Hall and Markin, 1957). Asprey and Stephanou (1950) suggested that the reducing species was H_2O_2, a reasonable suggestion given the high H_2O_2 yields associated with α-radiolysis (Equation 8.21). The reaction of H_2O_2 with AmVI is

$$2AmO_2^{2+} + H_2O_2 \rightarrow 2AmO_2^{+} + 2H^{+} + O_2 \tag{8.31}$$

It can be seen that the rate of this reaction will be dependent on acidity, and Woods et al. (1974) reported a rate constant of 3.8×10^4 M^{-1} s^{-1} in 1 M $HClO_4$ at 25 °C and 5.1×10^4 M^{-1} s^{-1} at 0.1 M $HClO_4$. The rate of reaction with AmV is comparable at 5.3×10^4 M^{-1} s^{-1} at the same temperature in 0.1 M $HClO_4$ (Zaitsev et al., 1960). Other acid concentrations were not investigated for AmV. However, AmV is known to be more stable than AmVI. Therefore, other reducing agents are implicated.

8.3 Conclusions and commentary

It has been shown that the radiolytic degradation of solvent extraction ligands proceeds in a mainly oxidative fashion, due to the radical scavenging reactions that take place in irradiated, acidic, and aerated solution. Among the most common reactions are •H atom abstractions to produce carbon-centered radicals, which may add O_2 to initiate further oxidation via peroxyl radical decomposition, or undergo C—C bond rupture to cause dealkylation. Carbon radicals may also undergo additional reactions to produce higher molecular weight products from the starting molecule. The rupture of C—O bonds, especially, is to be expected. Electron transfer reactions from radical cations also occur. The products of these reactions are often more deleterious to the solvent extraction than is the loss in ligand concentration itself.

The study of solvent extraction and radiation chemistry are both mature fields, but they are fields that have developed somewhat independently. This has resulted in a situation where the knowledge base of radiation chemistry has not always been taken advantage of, and the effects of radiation chemistry on solvent extraction have often been evaluated mainly in an indirect way; that is, through the measurement of changes in distribution ratios on irradiated samples. However, as was shown here, the techniques for developing a mechanistic understanding of the effects of radiation chemistry on solvent extraction are available, and are beginning to be exploited.

Those techniques include steady-state radiolysis, employing γ-ray and α-emitter sources that, when combined with mass spectrometric product analyses, provide the information necessary to understand the degradation pathways of ligands.

Pulse radiolysis has been used for decades to measure the kinetics of the radiolytically produced radical reactions with solutes, and can be as readily applied to solvent-extraction ligands to elucidate mechanisms and thus to understand possible scavenging reactions that would protect those ligands. In the future, the study of the radiolytic degradation of solvent extraction ligands will likely rely more heavily on pulse radiolytic determination of rate constants, and new techniques will also be developed for making these measurements in the organic phase. Collections of rate constants for the reactions of a selected ligand with the major radical species expected under process conditions, in combination with radiolysis product identification, will be used to model degradation reactions. This will provide predictive capabilities for process modifications. A key component of such models will include measurements of the rates of transfer of radicals across the phase boundary, important work that is yet to be performed.

References

Adamov, V.M., Andreev, V.I., Belyaev, B.N., Markov, G.S., Polyakov, M.S., Ritari, A.E., Shil'nikov, A.Yu., 1990. Identification of decomposition products of extraction systems based on tri-*n*-butyl phosphate in aliphatic hydrocarbon. Kerntechnik 55, 133–137.

Alfassi, Z.B., 1997. Formation of peroxyl radicals in solution. In: Alfassi, Z.B. (Ed.), Peroxyl Radicals. John Wiley and Sons, New York, pp. 1–18.

Asprey, L.B., Stephanou, S.E., 1950. The autoreduction of Am(VI) and Am(V) in dilute acid, Report AECU-924.

Becker, R., Stieglitz, L., Bautz, H., 1983. Untersuchung der strahlenchemischen TBP-Zersetzung unter den Bedingungen des PUREX-prozesses, Report KfK3639.

Berthon, L., Journet, S., Lalia, V., Morel, J.M., Zorz, N., Berthon, C., Amekraz, B., 2004. Use of chromatographic techniques to study a degraded solvent for minor actinides partitioning: qualitative and quantitative analysis. In: Atalante-2004, Nimes, France.

Berthon, L., Morel, J.M., Zorz, N., Nicol, C., Virelizier, H., Madic, C., 2001. DIAMEX process for minor actinide partitioning: hydrolytic and radiolytic degradations of malonamide extractants. Sep. Sci. Technol. 36, 709–728.

Bisel, I., Cames, B., Faucon, M., Rudloff, D., Saucerotte, B., 2007. DIAMEX SANEX solvent behavior under continuous degradation and regeneration operation. In: Global-2007, Boise, ID, USA.

Burger, L.L., McClanahan, E.D., 1958. Tributyl phosphate and its diluent systems. Ind. Eng. Chem. 50, 153–156.

Burr, J.G., 1958. The radiolysis of tributylphosphate. Rad. Res. 8, 214–221.

Buxton, G.V., Greenstock, C.L., Helman, W.P., Ross, A.B., 1988. Critical review of rate constants for reactions of hydrated electrons, hydrogen atoms and hydroxyl radicals (OH/O-) in aqueous solution. J. Phys. Chem. Ref. Data 17, 513–886.

Cames, B., Bisel, I., Baron, P., Hill, C., Rudloff, D., Saucerotte, B., 2010. DIAMEX solvent behavior under continuous degradation and regeneration operations. In: Wai, C.M., Mincher, B.J. (Eds.), Nuclear Energy and the Environment. In: ACS Symposium Series, 1046, American Chemical Society, Washington, DC, pp. 255–269.

Chiarizia, R., Horwitz, E.P., 1986. Hydrolytic and radiolytic degradation of octyl(phenyl)-N, N-diisobutylcarbamoylmethylphosphine oxide and related compounds. Sol. Extr. Ion Exch. 4, 677–723.

Draye, M., Chomel, R., Doutreluingne, P., Guy, A., Foos, J., Lemaire, M., 1993. Radiolytic products study of dicyclohexano-18-crown-6, a selective extractant for nuclear fuel reprocessing. J. Radioanal. Nucl. Chem. Lett. 175, 55–62.

Ekberg, C., Fermvik, A., Retegan, T., Skarnemark, G., Foreman, M.R.S., Hudson, M.J., Englund, S., Nilsson, M., 2008. An overview and historical look back at the solvent extraction using nitrogen donor ligands to extract and separate An(III) from Ln(III). Radiochim. Acta 96, 225–233.

Elliot, A.J., 1989. A pulse radiolysis study of the temperature dependence of reactions involving H, OH and $e^-_{(aq)}$ in aqueous solution. Radiat. Phys. Chem. 34, 753–758.

Fermvik, A., 2011. Radiolytic degradation of BTBP type molecules for treatment of used nuclear fuel by solvent extraction (University dissertation), Chalmers University of Technology, Gothenburg, Sweden.

Fermvik, A., Aneheim, E., Grüner, B., Hájková, Z., Kvíčalová, M., Ekberg, C., 2012. Radiolysis of C5-BTBP in cyclohexanone irradiated in the absence and presence of an aqueous phase. Radiochim. Acta 100, 273–282.

Fermvik, A., Gruner, B., Kvicalova, M., Ekberg, C., 2011. Semi-quantitative and quantitative studies on the gamma radiolysis of C5-BTBP. Radiochim. Acta 99, 113–119.

Fermvik, A., Berthon, L., Ekberg, C., Englund, S., Retegan, T., Zorz, N., 2009a. Radiolysis of solvents containing C5-BTBP: identification of degradation products and their dependence on absorbed dose and dose rate. Dalton Trans. 6421–6430.

Fermvik, A., Ekberg, C., Englund, S., Foreman, M.R.St.J., Modolo, G., Retegan, T., Skarnemark, G., 2009b. Influence of dose rate on the radiolytic stability of a BTBP solvent for actinide(III)/lanthanide(III) separation. Radiochim. Acta 97, 319–324.

Geist, A., Hill, C., Modolo, G., Foreman, M.R.S., 2006. 6,6'-Bis(5,5,8,8-tetramethyl-5,6,7, 8-tetrahydro-benzo[1,2,4]triazin-3-yl)[2,2']bipyridine, an effective extracting agent for the separation of americium(III) and curium(III) from the lanthanides. Solvent Extr. Ion Exch. 24, 463–483.

Groenewold, G.S., Elias, G., Mincher, B.J., Mezyk, S.P., LaVerne, J.A., 2012. Characterization of CMPO and its radiolysis products by direct infusion ESI-MS. Talanta 99, 909–917.

Haase, K.D., Schulte-Frohlinde, D., Kouřím, P., Vacek, K., 1973. Low-temperature radiolysis of organic phosphates studied by electron spin resonance. Int. J. Radiat. Phys. Chem. 5, 351–360.

Hall, G.R., Markin, T.L., 1957. The self-reduction of americium(V) and (VI) and the disproportionation of americium(V) in aqueous solution. J. Inorg. Nucl. Chem. 4, 296–303.

He, H., Lin, M., Muroya, Y., Kudo, H., Katsumura, Y., 2004. Laser photolysis study on the reaction of the nitrate radical with tributylphosphate and its analogues—comparison with sulfate radical. Phys. Chem. Chem. Phys. 6, 1264–1268.

Hill, C., Berthon, L., Madic, C., 2005. Study of the stability of BTP extractants under radiolysis. In: Global-2005, Tsukuba, Japan.

Hill, C., Berthon, L., Bros, P., Dancausse, J.-P., Guillaneux, D., 2002. SANEX-BTP process development studies. In: 7th International Exchange Meeting on Actinide and Fission Product Partitioning, Jeju, Korea.

Hudson, M.J., Boucher, C.E., Braekers, D., Desreux, J.F., Drew, M.G.B., Foreman, M.R.St.J., Harwood, L.M., Hill, C., Madic, C., Marken, F., Youngs, T.G.A., 2006. New bis(triazinyl) pyridines for selective extraction of americium(III). New J. Chem. 30, 1171–1183.

ISO/ASTM, 2006. Standard practice for use of a ceric-cerous sulfate dosimetry system, report 51205:2002(E) of the ASTM International, West Conshohocken, PA, USA.

Jiang, P.-Y., Nagaishi, R., Yotsuyunagi, T., Katsumura, Y., Ishigure, K., 1994. γ-Radiolysis study of concentrated nitric acid solutions. J. Chem. Faraday Trans. 90, 93–95.

Jin, H., Wu, J., Zhang, X., Fand, X., Yao, S., Zuo, Z., Lin, N., 1999. The examination of TBP excited state by pulse radiolysis. Radiat. Phys. Chem. 54, 245–251.

Khaikin, G.I., 1988. Reactions of trialkylphosphates with hydroxyl radicals and hydrated electrons. High Energy Chem. 32, 287–289.

Klassen, N.V., Shortt, K.R., Seuntjens, J., Ross, C.K., 1999. Fricke dosimetry: the difference between $G(Fe^{3+})$ for ^{60}Co γ-rays and high-energy x-rays. Phys. Med. Biol. 44, 1609–1624.

Kolarik, Z., 2008. Complexation and separation of lanthanides(III) and actinides(III) by heterocyclic N-donors in solutions. Chem. Rev. 108, 4208–4252.

Kolarik, Z., Müllich, U., Gassner, F., 1999. Selective extraction of Am(III) over Eu(III) by 2,6-ditriazolyl- and 2,6-ditriazinepyridines. Solvent Extr. Ion Exch. 17, 23–32.

Kulikov, I.A., Kermanova, N.V., Vladimirova, M.V., 1983. Radiolysis of TBP in the presence of plutonium and uranium. Sov. Radiochem. 24, 310–316.

Kuzin, I.A., Semushin, A.M., Romanovskii, V.N., 1969. Stability of di(2-ethylhexyl) hydrogen phosphate against radiation. High Energy Chem. 3, 248–249.

Lamouroux, C., Virelizier, H., Moulin, C., Jankowski, C.K., 2001. Application of gas chromatography-tandem mass spectrometry to the analysis of inhibition of dimerisation of tributylphosphate under radiolysis. Identification of isomeric tributylphosphate-alkylbenzene inhibitor coupling products. J. Chrom. 917, 275–290.

Lanham, W.B., Runion, T.C., 1949. PUREX process for plutonium and uranium recovery. Report ORNL 479.

Lasage, D., Virelizier, H., Jankowski, C.K., Tabet, J.C., 1997. Identification of minor products obtained during radiolysis of tributylphosphate (TBP). Spectroscopy 13, 275–290.

LaVerne, J.A., 2004. Radiation chemical effects of heavy ions. In: Mozumder, A., Hatano, Y. (Eds.), Charged Particle and Photon Interactions with Matter. Marcel Dekker, New York, pp. 403–429.

Madic, C., Hudson, M.J., 1998. High level liquid waste partitioning by means of completely incinerable extractants, final report, European Commission contract no. F12W-CT91-0112, EUR 18038.

Magnusson, D., Christiansen, B., Foreman, M.R.S., Geist, A., Malmbeck, R., Modolo, G., Serrano-Purroy, D., Sorel, C., 2009a. Demonstration of a SANEX process in centrifugal contactors using the $CyMe_4$-BTBP molecule on a genuine fuel solution. Solvent Extr. Ion Exch. 27, 97–106.

Magnusson, D., Christiansen, B., Malmbeck, R., Glatz, J.-P., 2009b. Investigation of radiolytic stability of a CyMe4-BTBP based SANEX solvent. Radiochim. Acta 97, 497–502.

Mincher, B.J., Mezyk, S.P., Elias, G., Groenewold, G.S., LaVerne, J.A., Nilsson, M., Pearson, J., Schmitt, N.C., Tillotson, R.D., Olson, L.G., 2014. The radiation chemistry of CMPO: part 2. Alpha radiolysis. Solvent Extr. Ion Exch. 32, 167–178.

Mincher, B.J., Precek, M., Mezyk, S.P., Elias, G., Martin, L.R., Paulenova, A., 2013a. The redox chemistry of neptunium in γ-irradiated aqueous nitric acid. Radiochim. Acta 101, 259–265.

Mincher, B.J., Mezyk, S.P., Elias, G., Groenewold, G.S., Riddle, C.R., Olson, L.G., 2013b. The radiation chemistry of CMPO: part 1. Gamma radiolysis. Solvent Extr. Ion Exch. 31, 715–730.

Mincher, B.J., Mezyk, S.P., 2009. Radiation chemical effects on radiochemistry: a review of examples important to nuclear power. Radiochim. Acta 97, 519–534.

Mincher, B.J., Modolo, G., Mezyk, S.P., 2009a. Review article: The effects of radiation chemistry on solvent extraction: 1. Conditions in acidic solution and a review of TBP radiolysis. Solvent Extr. Ion Exch. 27, 1–25.

Mincher, B.J., Modolo, G., Mezyk, S.P., 2009b. Review article: the effects of radiation chemistry on solvent extraction: 3. Solvent Extr. Ion Exch. 27, 579–606.
Mincher, B.J., Mezyk, S.P., Martin, L.R., 2008. A pulse radiolysis investigation of the reactions of tributyl phosphate with the radical products of aqueous nitric acid radiolysis. J. Phys. Chem. A 112, 6275–6280.
Mincher, B.J., Curry, R.D., 2000. Considerations for choice of a kinetic fig. of merit in process radiation chemistry for waste treatment. Appl. Radiat. Isot. 52, 189–193.
Miner, F.J., Seed, J.R., 1967. Radiation chemistry of plutonium nitrate solutions. Chem. Rev. 67, 299–315.
Modolo, G., Asp, H., Schreinemachers, C., Vijgen, H., 2007. Development of a TODGA based process for partitioning of actinides from a PUREX raffinate part 1: batch extraction optimization studies and stability tests. Solvent Extr. Ion Exch. 25, 703–721.
Musikas, C., 1988. Potentiality of nonorganophosphorous extractants in chemical separations of actinides. Solvent Extr. Ion Exch. 23, 1211–1226.
Nash, K.L., Rickert, P.G., Horwitz, E.P., 1989. Degradation of TRUEX-dodecane process solvent. Solvent Extr. Ion Exch. 7, 65–675.
Nash, K.L., Gatrone, R.C., Clark, G.A., Rickert, P.G., Horwitz, E.P., 1988. Hydrolytic and radiolytic degradation of OϕD(iB)CMPO: continuing studies. Sep. Sci. Technol. 23, 1355–1372.
Nilsson, M., Nash, K.L., 2007. Review article: a review of the development and operational characteristics of the TALSPEAK process. Solvent Extr. Ion Exch. 25, 665–701.
Nilsson, M., Andersson, S., Ekberg, C., Foreman, M.R.S., Hudson, M.J., Skarnemark, G., 2006a. Inhibiting radiolysis of BTP molecules by addition of nitrobenzene. Radiochim. Acta 94, 103–106.
Nilsson, M., Andersson, S., Drouet, F., Ekberg, C., Foreman, M., Hudson, M., Liljenzin, J.-O., Magnusson, D., Skarnemark, G., 2006b. Extraction properties of 6,6'-bis-(5,6-dipentyl-[1,2,4]triazin-3-yl)-[2,2']bipyridine. Solvent Extr. Ion Exch. 24, 299–318.
Nowak, Z., Nowak, M., Seydel, A., 1979. The radiolysis of TBP-dodecane-HNO_3 systems. Radiochem. Radioanal. Lett. 38, 343–354.
Nowak, Z., 1977. Radiolytic degradation of extractant-diluent systems used in the PUREX process. Nuklionika 22, 155–172.
Pikaev, A.K., Shilov, V.P., Gogolev, A.V., 1997. Radiation chemistry of aqueous solutions of actinides. Russ. Chem. Rev. 66, 763–788.
Retegan, T., Berthon, L., Ekberg, C., Fermvik, A., Skarnemark, G., Zorz, N., 2009. Electrospray ionization mass spectrometry investigation of BTBP lanthanide(III) and actinide(III) complexes. Solvent Extr. Ion Exch. 27, 663–682.
Retegan, T., Ekberg, C., Englund, S., Fermvik, A., Foreman, M.R.S., Skarnemark, G., 2007. The behaviour of organic solvents containing C5-BTBP and $CyMe_4$-BTBP at low irradiation doses. Radiochim. Acta 95, 637–642.
Sasaki, Y., Sugo, Y., Suzuki, S., Tachimori, S., 2001. The novel extractants, diglycolamides for the extraction of lanthanides and actinides in HNO_3-*n*-dodecane system. Solvent Extr. Ion Exch. 19, 91–103.
Schramm, R.M., Westheimer, F.H., 1948. The mechanism of the nitration of anisole. J. Am. Chem. Soc. 70, 1782–1784.
Schulz, W.W., 1968. Effects of some synergistic and antagonistic agents on HDEHP extraction of strontium, Pacific Northwest Laboratory report BNWL.
Schulz, W.W., Horwitz, E.P., 1988. The TRUEX process and the management of liquid TRU waste. Solvent Extr. Ion Exch. 23, 1191–1210.
Schulz, W.W., Navratil, J.D., 1984. Science and Technology of Tributyl Phosphate. CRC Press, Boca Raton.

Serrano-Purroy, D., Baron, P., Christiansen, B., Malmbeck, R., Sorel, C., Glatz, J.P., 2005. Recovery of minor actinides using the DIAMEX process. Radiochim. Acta 93, 351–355.

Shilov, V.P., Fedoseev, A.M., Pikaev, A.K., 1982. Study of reactivity of neptunium ions toward OH radicals in perchloric-acid solutions by pulse-radiolysis method. Bull. Acad. Sci. USSR Div. Chem. Sci. 31, 832–834.

Siddall, T.H., Dukes, E.K., 1959. Kinetics of HNO_2 catalyzed oxidation of Np(V) by aqueous solutions of nitric acid. J. Am. Chem. Soc. 81, 790–794.

Spinks, J.W.T., Woods, R.J., 1990. An Introduction to Radiation Chemistry, third ed. John Wiley and Sons, New York.

Spjuth, L., Liljenzin, J.O., Hudson, M.J., Drew, M.G.B., Iverson, P.B., Madic, C., 2000. Comparison of extraction behaviour and basicity of some substituted malonamides. Solvent Extr. Ion Exch. 18, 1–23.

Sugo, Y., Izumi, Y., Yoshida, Y., Nishijima, S., Sasaski, Y., Kimura, T., Sekine, T., Kudo, H., 2007a. Influence of diluent on radiolysis of amides in organic solution. Radiat. Phys. Chem. 76, 794–800.

Sugo, Y., Sasaki, Y., Kimura, T., Sekine, T., 2007b. Attempts to improve radiolytic stability of amidic extractants, In: Global-2007, Boise, ID, USA.

Tachimori, S., 1979a. Mass spectrometric study of the radiolysis of di-(2-ethylhexyl)phosphoric acid. J. Radioanal. Chem. 49, 179–184.

Tachimori, S., 1979b. Synergistic extraction of americium with MEHPA-DEHPA mixed solvent from nitric acid solution. J. Radioanal. Chem. 49, 31–35.

Tachimori, S., 1978. Effects of radiolysis of di(2-ethylhexyl)phosphoric acid upon the extraction of strontium(II). J. Radioanal. Chem. 44, 25–35.

Tachimori, S., Ito, Y., 1979. Radiation damage of organic extractant in partitioning of high-level waste, (I) Radiolysis of di(2-ethylhexyl)phosphoric acid by irradiation with cobalt-60 gamma-rays. J. Nucl. Sci. Technol. 16, 49–56.

Tachimori, S., Nakamura, H., 1979. Radiation effects on the separation of lanthanides and transplutonides by the TALSPEAK-type extraction. J. Radioanal. Nucl. Chem. 52, 343–354.

Tachimori, S., Nakamura, H., Sato, A., 1979. A study of radiation effects of americium(III) with acidic organophosphates. J. Radioanal. Chem. 50, 143–151.

Tachimori, S., Krooss, B., Nakamura, H., 1978. Effect of radiolysis products of di-(2-ethylhexyl) phosphoric acid upon the extraction of lanthanides. J. Radioanal. Chem. 43, 53–63.

Tripathi, S.C., Ramanujam, A., Gupta, K.K., Bindu, P., 2001. Studies on the identification of harmful radiolytic products of 30% TBP-*n*-dodecane-HNO_3 by gas-liquid chromatography. II. Formation and characterization of high molecular weight organophosphates. Sep. Sci. Technol. 36, 2863–2883.

Turney, T.A., Wright, G.A., 1959. Nitrous acid and nitrosation. Chem. Rev. 59, 497–513.

Vladimirova, M.V., Kulikov, I.A., Ryabova, A.A., Milovanova, A.S., 1976. Radiation chemistry of aqueous solutions of Pu and Np. Radiokhimiya 18, 172–177.

Vladimirova, M.V., Kulikov, I.A., Sosnovskii, O.A., 1981. Reduction of PuO_2^{2+} in γ radiolysis in aqueous HNO_3. Sov. At. Energ. 51, 475–478.

Vladimirova, M.V., 1990. Radiation chemistry of actinides. J. Radioanal. Nucl. Chem. 143, 445–454.

Vladimirova, M.V., 1995. Mathematical modeling of the radiation chemical behavior of Np in nitric acid. Equilibrium states. Radiokhimiya 37, 410–416.

Von Sonntag, C., Ansorge, G., Sugimori, A., Omori, T., Koltzenburg, G., Schulte-Frohlinde, D., 1972. Alkyl phosphate cleavage of aliphatic phosphates induced by hydrated electrons and OH radicals. Z. Naturforschung. Teil. B 27, 471–472.

Wagner, R.M., Towle, L.H., 1958. Radiation stability of organic liquids. Stanford Research Institute report AECU-4053.

Williams, T.F., Wilkinson, R.W., 1957. The radiolysis of tri-n-butyl phosphate and allied systems, A.E.R.E. report C/R 2179.

Wilkinson, R.W., Williams, T.F., 1961. The radiolysis of tri-n-alkyl phosphates. J. Chem. Soc. 4098–4107,

Woods Sr., M., Cain, A., Sullivan, J.C., 1974. A kinetic study of the reduction of americium(VI) by hydrogen peroxide in aqueous perchlorate media. J. Inorg. Nucl. Chem. 36, 2605–2607.

Zaitsev, A.A., Kosyakov, V.N., Rykov, A.G., Sobolev, Yu.P., Yakovlev, G.N., 1960. Kinetics of americium(V) reduction by hydrogen peroxide. Radiokhimiya 2, 348–350.

Zaitsev, V.D., Khaikin, G.I., 1994. Precursors of dibutylphosphoric acid upon radiolysis of tributylphosphate. High Energy Chem. 28, 269–272.

Reprocessing of spent fast reactor nuclear fuels

9

R. Natarajan
Indira Gandhi Centre for Atomic Research, Kalpakkam, Tamilnadu, India

Acronyms

AHA	acetohydroxamic acid
CE	centrifugal extractor
CFD	computational fluid dynamics
DBP	dibutyl phosphate
DF	decontamination factor
DFR	Dounreay fast reactor
DFRP	demonstration fast reactor fuel reprocessing plant
DiBiOP	di-isobutyl isooctyl phosphate
FBTR	fast breeder test reactor
FBR	fast breeder reactor
FR	fast reactor
FRFR	fast reactor fuel reprocessing
FRP	fuel reprocessing plant
FRSF	fast reactor spent fuel
FS	ferrous sulfamate
HAN	hydroxylamine nitrate
HDBP	dibutyl phosphoric acid
H_2MBP	monobutyl phosphoric acid
HNP	heavy normal paraffin
LOC	limiting organic concentration
LWR	light water reactor
PFBR	prototype fast breeder reactor
PFR	prototype fast reactor
RTD	residence time distribution
TAP	tri-*n*-amyl phosphate
TBP	tri-*n*-butyl phosphate
THP	tri-*n*-hexyl phosphate
TiAP	tri-isoamyl phosphate
TiBP	tri-isobutyl phosphate
TR	thermal reactor
TRFR	thermal reactor fuel reprocessing
TRSF	thermal reactor spent fuel

Reprocessing and Recycling of Spent Nuclear Fuel. http://dx.doi.org/10.1016/B978-1-78242-212-9.00009-5

9.1 Introduction

The fully closed nuclear fuel cycle is arguably the most attractive nuclear energy option for meeting the global needs for increased power generation capacities, both in terms of sustainability and economics, and for meeting the requirements of addressing greenhouse gas emissions. Spent nuclear fuel reprocessing is the vital activity that closes the fuel cycle, with reprocessing plants designed to recover and recycle both the uranium and the plutonium from the spent fuel. The recovered plutonium is used more efficiently in fast reactors (FRs) than in thermal reactors (TRs) and it can also be recycled more than 10 times in FRs compared to a maximum of 2 or 3 times in TRs without losing its utility as a fuel. Accordingly, plutonium utilization in FRs (or "plutonium multirecycling") is being pursued in many countries such as Russia, India, and France.

In the reprocessing of fast reactor spent fuel (FRSF), although plutonium concentrations are higher than thermal uranium oxide or mixed oxide fuels, the chemistry involved is not very different from that of thermal reactor fuel reprocessing (TRFR). However, due to the higher specific radioactivity associated with spent FR fuels and the solution chemistry of plutonium, modifications are required in the reprocessing flow sheet. These aspects along with other challenges involved in the design of fast reactor fuel reprocessing (FRFR) are enumerated in the following sections.

9.2 Differences between thermal and fast reactor spent fuel reprocessing

Cooling of spent nuclear fuel, prior to reprocessing, offers substantial advantages as both the levels of radioactivity and decay heating involved are markedly lower. Spent fuel storage to give cooling periods of not less than 5 years is a general norm, though in reality it is usually well beyond that period. Such storage is well demonstrated internationally as large storage facilities, which are either wet or dry, have been in operation for over 50 years in many countries. However, in countries such as India, where the natural uranium resources are limited and the required rate of energy growth is high, the fuel has to be recycled as quickly as possible. Less than 2 years is the targeted cooling period as this would reduce the inventory of plutonium locked up in the system. Accordingly, the radioactivity of the spent fuel to be processed in the FRFR plant will be at least an order of magnitude higher than that seen in TRFR plants, as will the associated decay heating.

Reprocessing aims for quantitative recovery of uranium and plutonium from the spent reactor fuel in the required form together with extraction and storage of the fission products. The objective is also to separate fissile materials to enable conversion into new fuel elements for reactors. The product purities required from the two types of reprocessing plants (thermal and fast) are decided by the in-reactor neutron absorption characteristics of the impurities in the fuel and the radioactivity associated with the impurities, which could result in personnel exposures during the downstream conversion and fuel fabrication operations. As the neutron absorption cross sections of

Table 9.1 Typical product specifications for fast reactor fuel reprocessing plants

Product	Gross βγ activity due to fission products (Bq/g)	Separation between U and Pu
Uranium	$<10^4$	<0.4 μgPu/gU
Plutonium	$<10^6$	Uranium is not an impurity (potential to be producing Pu/U mixed product)

most of the nuclides are higher in the thermal spectrum than in the fast spectrum, there can be a relaxation in the contamination levels of many of the nuclides for the FR fuels. As the processes of conversion and fabrication operations are similar for both types of reactor fuels, the radioactivity levels of both types of the products should be the same, unless greater levels of shielding are to be used in downstream plants.

For FRSF, due to plutonium content being more than an order of magnitude greater compared with TRSF, the decontamination factor (DF) required for plutonium-uranium separation is higher. However, there can be some relaxation in levels of the allowable concentrations of uranium in the plutonium product. This is because the core will contain a mixture of uranium and plutonium. Thus, this would call for limits on the band of concentration in the product in order to optimize the process conditions for making acceptable powders in the fuel fabrication plant. However, in reactors where there is a uranium blanket, the specification of the uranium product would be almost the same (with tight control over the concentration limits of alpha emitting nuclides, particularly plutonium) as the major quantity of the reprocessed uranium product would be required for blanket fuel manufacture without glove box-type operations (depending on the source of the uranium). There can be variation between different reprocessing plants depending upon the burn up, cooling period, and the fabrication technology. Typical optimized minimum product specifications for FRFR plants with around 10% atom burn up and an approximately 2-year cooling period are given in Table 9.1.

9.3 Adaptation of the PUREX process for high plutonium bearing spent fuels

Nuclear fuel reprocessing has been carried out since the early 1950s on a commercial scale almost exclusively by solvent extraction based on the *p*lutonium-*ur*anium *ex*traction or PUREX process. The experience, both in terms of performance and safety, has been highly satisfactory (International Atomic Energy Agency, 2006). The time-tested PUREX process is, therefore, also deployed for FRFR. A simplified process flow sheet is given in Figure 9.1. The major process steps in reprocessing using PUREX process are

- Headend treatment
- Solvent extraction
- Reconversion
- Vitrification

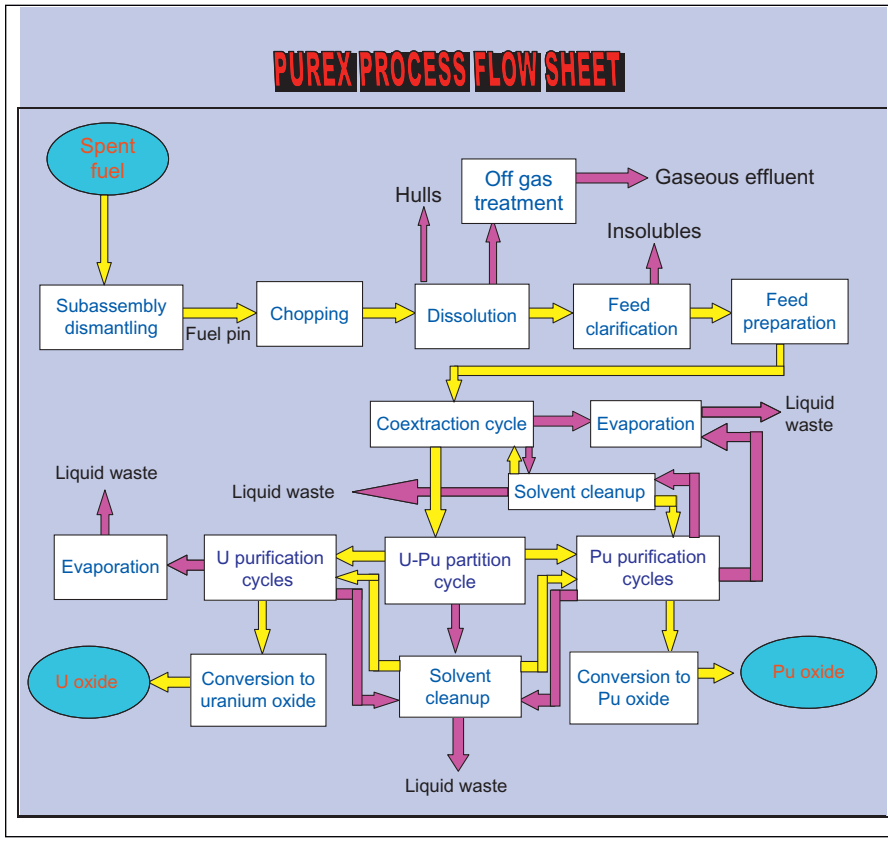

Figure 9.1 Schematic PUREX process flow sheet for thermal or fast reactor reprocessing (yellow (light gray in print version) arrows indicate product streams and pink (dark gray in print version) arrows indicate waste streams).

The activities involved in all these process steps are generally similar for the reprocessing of both thermal and FR fuels but with some exceptions in the first two steps, namely, headend treatment and solvent extraction. Only the major differences in these two steps are discussed in detail in the following sections.

9.3.1 Headend treatment

In this step, the fuel is declad or chopped and then dissolved in nitric acid, and the resulting solution is filtered to remove the undissolved particles and clad fines. Conditioning of the resulting solution is then carried out so that the dissolved fuel solution is at the required acidity and the valency states of uranium and plutonium are suitable for the subsequent solvent-extraction process.

9.3.1.1 Chopping

Chemical decladding is not an appropriate choice for FRSF reprocessing because the cladding is stainless steel, which is difficult to dissolve with conventional chemical reagents. The mechanical chopping of fuel, which is widely adopted for TR fuels, will be different for FRFR. This is because, as the fuel pins are slender in dimension, they would be crimped at the ends if bundled chopping were carried out. In thermal oxide reprocessing plants, where the bundle pin chopping is practiced, the crimping is not a serious issue as the fuel pins are larger in diameter. As this will result in slower or incomplete dissolution, either single pin chopping or multipin chopping of a linear array of pins is preferred for FR fuels. The presence of spacer wire around the fuel pins also poses challenges during chopping.

9.3.1.2 Dissolution

Dissolution is the most difficult step in FRFR containing high concentrations of plutonium. Generally, 6 mol/L nitric acid will be adequate for dissolution of most of the spent fuels from light water reactors (LWRs), while more aggressive conditions would be required for dissolving spent FR fuels.

In 1980, Ryan and Bray (1980) gave an account of the problem of dissolving plutonium oxide from a thermodynamic standpoint. Their work showed that pure PuO_2 is not only kinetically difficult to dissolve in nitric acid, but also thermodynamically impossible in nitric acid solutions below about 4 mol/L. Fluoride ions were used based on their ability to complex Pu(IV) in strong acidic solutions where fluoride acts to increase both the rate of PuO_2 dissolution and its thermodynamic solubility (Scott Barney, 1977). The formation of the Pu(IV) fluoride complex influences the dissolution process. Hence, the fluoride concentration often must exceed the final dissolved plutonium concentration.

Subsequently, based on the studies to eliminate corrosive reagents like HF, a method based on cerium(IV) (Horner et al., 1977) was developed. This is attractive because it avoids the usage of corrosive fluoride ions. Also, it was found to be superior to other strong oxidants, including ozone, permanganate, persulfate, and Ce(III). During dissolution, Ce(IV) gets reduced to Ce(III) which can be reoxidized *in situ* by electrolysis. The main disadvantage of this method is the increased consumption of Ce(IV) by the other oxidizable FPs such as ruthenium (Harmon, 1975).

Ryan and Bray proposed a concept to dissolve PuO_2 and PuO_2^{2+} ions by using electrical energy (Ryan et al., 1990). They named it CEPOD (catalyzed electrolytic plutonium oxide dissolution). In this process, PuO_2 is dissolved in an anolyte containing small (catalytic) amounts of elements that form kinetically fast, strongly oxidizing ions. The oxidizing ions are regenerated at the anode; they act in a catalytic manner, carrying electrons from the solid PuO_2 surface to the anode of the electrochemical cell.

Important conclusions that can be drawn from the published literature (Clark and Gens, 1961; Burch, 1982; Cleveland, 1964; Vaughen and Goode, 1979;

Bourges et al., 1986; Veleckis and Hoh, 1991; Woltermann et al., 1973) for the design of processes for the efficient dissolution of plutonium-rich oxide fuels follow:

- Initial dissolution rates depend on nitric acid concentration and solution temperature (Taylor et al., 1963).
- Plutonium-lean spent fuels (less than 5% or so) can be dissolved in a similar manner to UO_2 in nitric acid (Steward and Gray, 1994).
- Spent fuel with plutonium content above 35% of the total heavy metal content needs aggressive conditions for dissolution (Uriarte and Rainey, 1965).
- Irradiation renders the fuel more brittle proportionate to the burn up due to the gaseous fission products, decay heat, and neutron flux (Finney et al., 1969). Therefore, when agitated physically, small fragments of fuel particles are released out of the chopped fuel pin into the acid medium, which dissolve faster than the fuel particles inside the chopped pin. Thus, irradiation enhances dissolution rate.
- Irradiation also leads to the formation of certain alloys in the spent fuel comprised of the noble metals and actinides leading to high undissolved residues (Campbell et al., 1984).
- Voloxidation, in general, enhances dissolution rate, but also increases the amount of plutonium left in the undissolved residue (Vaughen and Goode, 1972).

When plutonium-rich mixed carbide fuel was considered for the fast breeder test reactor (FBTR) in India, it was thought that the 70% plutonium-rich FRSF cannot be dissolved in pure nitric acid to produce a solution suitable for solvent extraction. However, the CORAL (Indian pilot-scale reprocessing plant) operating experience has revealed that reflux heating in boiling concentrated nitric acid without any oxidizing or reducing agent could not only dissolve the fuel completely but also sufficiently remove the carbon present from the carbide matrix (thus avoiding formation of organics that can potentially interfere in subsequent solvent-extraction steps) (Natarajan and Raj, 2007). Also, dissolution of this fuel does not require fluoride, even though it contains as much as 70% plutonium. Thus, the experience of reprocessing mixed carbide fuels is entirely different from that of oxides. Very limited experience is available for metal matrices.

The issue of criticality control in the dissolver also becomes more onerous in FRFR due to the presence of higher amounts of plutonium, making it more challenging to design the dissolver. However, the treatment of off-gases from the dissolution process is similar to that of thermal spectrum spent fuel.

9.3.1.3 Feed clarification

Under conditions of boiling nitric acid, all the fuel material dissolves leaving a small quantity of fine residues that mainly consists of noble metal alloys with small quantities of plutonium (Kolarik, 1991a; Vondra and Crouse, 1979). The quantity of this undissolved material depends upon the nature of the fuel, burn up, and plutonium content. However, these residues generally increase with burn up and plutonium content. Typically, this quantity can be as high as 0.74% in FR fuels (Anderson et al., 1994).

While processing the mixed (U,Pu) carbide fuel discharged from FBTR in CORAL, the dissolver solution contained some black particles, which could be carbon-based compounds but the plutonium content in the undissolved solids was very low. The dissolver solution needed to be treated for removal of these fine particles before being fed to the solvent-extraction process. While, feed clarification in thermal reactor spent fuels is required for removing the clad fines, it is required for the removal for undissolved fuel particles in FRSF. It has been found from operating experience that filtration reduces the maintenance requirement of downstream solvent-extraction equipment such as centrifugal extractors (CEs).

9.3.1.4 Conditioning

Conditioning is done to adjust the acidity to a suitable concentration that enables high recovery of uranium and plutonium and optimum fission product decontamination in the first solvent-extraction step. Because dissolution requires a high acidity of around 6 mol/L, and because 3-4 mol/L is normally used in solvent extraction for FR fuels containing higher concentrations of plutonium, the acidity of the dissolver solution has to be adjusted to the required value.

Under the highly oxidizing conditions of dissolution, plutonium exists mostly in the VI valency state but, to ensure high recovery, plutonium must be converted to the IV valency state, as the distribution coefficient of Pu(IV) is higher. Because plutonium also exists in III and VI oxidation states, conversion of all plutonium to the IV valency has to be done prior to solvent extraction. This is carried out either chemically or electrolytically. Sparging with NO_2 gas is the most common practice for this conversion. The earlier practice of using $NaNO_2$ for *in situ* generation of NO_2 for conditioning is avoided in most of the recent plants as that increases the quantities of solid wastes. The following reactions are involved in the conversion (Flagg, 1961):

$$PuO_2^{2+} + NO_2^- + 2H^+ \rightarrow Pu^{4+} + NO_3^- + H_2O$$

$$Pu^{3+} + NO_2^- + 2H^+ \rightarrow Pu^{4+} + NO + H_2O$$

$$6Pu^{3+} + 2NO_2{}^- + 8H^+ \rightarrow 6Pu^{4+} + N_2 + 4H_2O$$

The same conversion can be carried out electrochemically, which involves the following reactions:

$$Pu^{3+} \rightarrow Pu^{4+} + e^-, \quad E = -0.914\,V$$

$$Pu^{6+} + 2e^- \rightarrow Pu^{4+}, \quad E = 1.054\,V$$

Though studies have shown that electrolytic conditioning is possible, this has not been introduced in any of the commercial-scale plants so far.

9.3.2 Solvent-extraction step

The solvent-extraction step consists of two stages: (a) purification of uranium and plutonium from the fission products and (b) the separation of uranium and plutonium from one another. In both these stages, there are differences between TRFR and FRFR.

9.3.2.1 Purification stage

The difference in the design of this step is primarily due to the increased radioactivity of the feed solution and the increased plutonium concentration.

Increased radioactivity of the feed solution

Even though the concentration of fission products are higher at 10-15% in FRs compared to 0.6-5% in thermal reactor spent fuels, which is due to the increase in the burn up, most of the fission products are easily removed in the purification step except a few elements such as cerium, europium, ruthenium, and zirconium. Table 9.2 gives the DFs required for these fission products for the two types of spent fuels.

The increased requirement in FR reprocessing arises from the shorter cooling period and the difference in the fission product distribution, which depends on the type of fissile nuclide (whether it is ^{235}U or ^{239}Pu) and also on neutron energy (thermal or fast). For example, ^{106}Ru yield is around six times higher (Figure 9.2) (JEFF-3.1, 2006; Koning et al., 2006) in a fast spectrum. As the thermal reactor spent fuels are taken up for reprocessing well beyond 5 years, ^{95}Zr with 65 days half-life does not pose any problem as a contaminant in the products of TRFR plants, while the same is not the case with FRSFs for the specific case of a 2-year cooling period. In addition to the fission products, the activation products, particularly ^{54}Mn and ^{60}Co, in the stainless steel clad, which gets leached during the dissolution, also need decontamination. TR fuels do not have this problem because zircaloy is used as the clad.

As cerium and europium have very low distribution ratios under the PUREX process conditions, the required additional DFs in reprocessing FRSFs can be easily achieved by modifying the scrubbing conditions. Because zirconium and ruthenium

Table 9.2 Typical decontamination factors for selected fission and activation products required for thermal reactor and fast reactor reprocessing

Nuclide	Thermal reactor spent fuel DF	Fast reactor spent fuel DF
^{144}Ce	$\sim 10^4$	$\sim 10^6$
^{155}Eu	$\sim 10^3$	$\sim 10^4$
^{106}Ru	$\sim 10^4$	$\sim 10^6$
^{95}Zr	-	$\sim 10^4$
^{60}Co	-	$\sim 10^5$
^{54}Mn	-	$\sim 10^4$

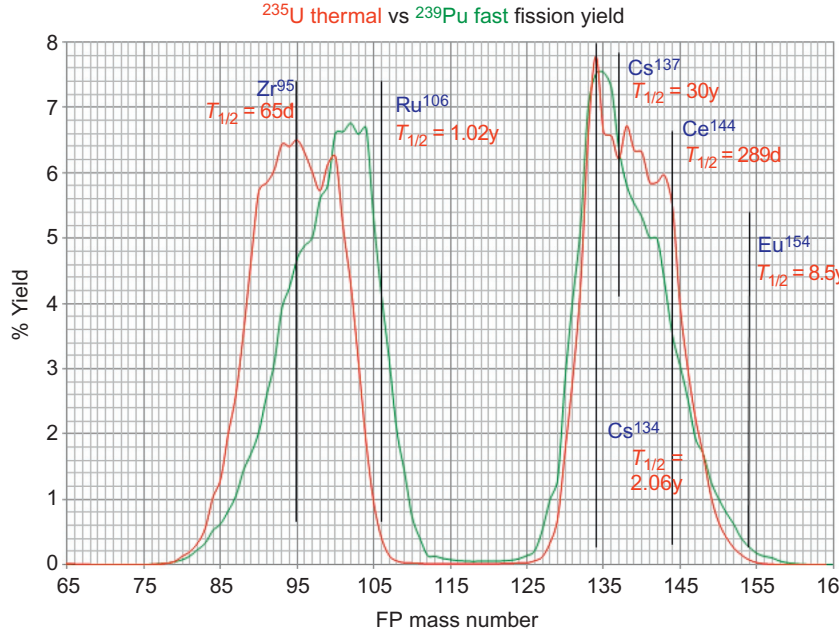

Figure 9.2 Fission yield data for ^{235}U and ^{239}Pu nuclides.

have more complex process chemistry, they must be studied in detail and the flow sheet requires modifications to obtain the additional DFs. Hence, the issues connected with these nuclides are discussed in the following sections in greater detail.

Decontamination of zirconium

^{95}Zr has a half-life of 65 days and is in transient equilibrium with ^{95}Nb (half-life of 35 days). As the thermal reactor spent fuels are reprocessed after relatively long cooling periods, obtaining the required DF for zirconium is not difficult. However, for FR fuels with only a 2-year cooling period and higher concentrations of zirconium in the feed, the process flow sheet will require modifications to improve zirconium decontamination. This problem is compounded by the fact that as the plutonium concentrations are high the acid profile in the primary extraction section needs to be higher than in thermal reactor spent fuel reprocessing flow sheets, which favors zirconium extraction. Hence, the scrub section must be suitably modified to obtain the required zirconium DF.

Also the degradation products of tri-*n*-butyl phosphate (TBP), such as dibutyl phosphate (DBP), extract zirconium leading to a reduction in DFs. One way to overcome this problem is to reduce the concentration of such degradation products by using short residence time contactors. Complexing with fluoride ions is another method that has been successfully exploited (Breschet and Miquel, 1971; Chesne and Germain, 1992) to improve the decontamination. It has also been reported (Jones, 1987) that at lower

acidities and elevated temperatures, zirconium undergoes hydrolysis leading to the formation of species of the type $Zr(OH)_x(NO_3)_{4-x}$, which tend to polymerize and severely affect the distribution reactions. Niobium, ^{95}Nb, which is in transient equilibrium with ^{95}Zr, although normally inextractable has been found to extract in the presence of silica (Hyder et al., 1979).

Decontamination of ruthenium

In typical FR fuels, about 95% of ruthenium activity would be due to ^{106}Ru and the remainder due to ^{103}Ru. As the half-life of ^{106}Ru is 368 days, the DF required for ruthenium is high even for fuels with less than 5 years of cooling. A significant quantity of ruthenium has been found (Ramanujam et al., 1978) to be present as undissolved residue in the dissolver. Ruthenium behavior in the PUREX process has been extensively studied (Pruett, 1984; Swain et al., 2013). Ruthenium has been found to exist in several forms and the interconversion between forms is very slow. Higher acidity and temperature are found to improve the DFs of ruthenium. Also, fast extraction and slow scrubbing are recommended for getting higher decontamination, due to slower extraction kinetics. PUREX reprocessing plant experience has indicated that DFs of 10^2-10^4 can normally be achieved (Fletcher and Scargill, 1965). When it comes to the reprocessing of high burn up FRSFs, ruthenium will be a major issue as the DFs required will be one to two orders of magnitude greater, especially for short cooled fuels.

Thus, based on the above analysis, a dual scrub flow sheet with the required acid profile has been proposed and demonstrated at the laboratory scale to meet the necessary DFs for zirconium and ruthenium (Natarajan, 2011). In this flow sheet, extraction is carried out at moderate acidities (optimized for plutonium recovery), with scrubbing sections at lower acidity for zirconium removal and higher acidity for ruthenium removal.

Increased concentrations of plutonium

The plutonium concentration in thermal reactor spent fuel is 0.3-1.5% of the total heavy metal (uranium and plutonium) while in FRSF it is around 25-30%. Due to this higher concentration of plutonium in FRSF, there are challenges due to formation of third-phase during solvent extraction. This arises due to the limited solubility of the plutonium-TBP complex in the diluent, the organic phase separates into two when the plutonium concentration exceeds certain values. Apart from causing difficulties in the operation of the extraction unit, this phenomenon introduces safety-related issues such as nuclear criticality due to the potential accumulation of plutonium in the third phase.

Several studies (Kolarik, 1991b; Srinivasan et al., 1986; Nakashima and Kolarik, 1983; Wilson and Smith, 1987; Manson et al., 1987; Vasudeva Rao, 1994; Vasudeva Rao and Kolarik, 1996) have been carried out on the solubility limits of plutonium (IV) in TBP. The limiting organic concentration (LOC) of Pu(IV) is found to increase with temperature, acidity, and concentration of other extractable species. Also, the LOC increases with increased branching of the alkyl group or decreasing chain length of the diluent or the presence of an aromatic or polar solvent. Based on the above studies, under the process conditions prevailing in FRFR, a limit of 45 g/L of plutonium is kept as the safety limit, with an upper limit of 30 g/L under normal operating

conditions. This value is strongly dependent on temperature, uranium concentration, acidity, and percentage of TBP (Kolarik, 1991c).

In addition to the above parameters, it should also be noted that choice of appropriate extraction equipment is necessary. Because the extraction reactions are fast, CEs, which have low residence times, are chosen for the purification cycle of FRSFs to reduce the radiation damage to the solvent. Also, these units can be designed for criticality safety with a single parameter "ever-safe geometry" as the dimension of a stage would be within 50 mm.

9.3.2.2 Separation of uranium and plutonium

In the separation section, conventionally plutonium is separated from uranium by reducing it from the extractable Pu(IV) to the inextractable Pu(III) state with hydrazine-stabilized uranous nitrate as the reducing agent. Due to various side reactions, the uranous consumption is generally 10-15 times the stoichiometric requirement. This is not a serious problem in TRFR as the concentration of plutonium is low. But in FRFR with significant concentrations of plutonium present, optimal use of uranous is required to reduce the uranium load in the plant. To meet this challenge, a flow sheet with multiple uranous streams has been postulated and tested in IGCAR, which demonstrated that the stoichiometric requirement of U(IV) can be reduced to around two to four times. The typical flow sheet is given in Figure 9.3.

It is found that technetium decreases the effectiveness of the uranous nitrate reduction process by catalytically destroying hydrazine, which is used as the scavenger for NO_2. Process flow sheets have been developed (Miles, 1993) to remove the coextracted technetium from the loaded organic prior to partitioning; this has been

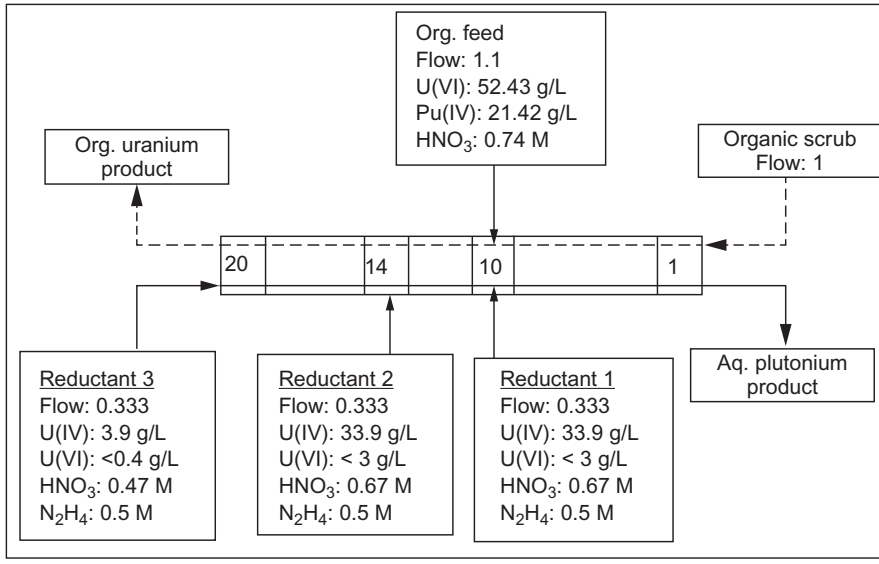

Figure 9.3 Typical U-Pu separation flowsheet with optimal U(IV) requirement.

incorporated (Fournier et al., 1992) in the UP3 plant in France. This typically involves a separate scrub with 5-6 mol/L HNO_3 which improves technetium removal. Though uranous-based reduction is the popular method of separating uranium and plutonium, there are other options that are being contemplated such as the hydroxylamine nitrate (HAN)-based process and the electrolytic reduction process.

Partitioning using HAN

HAN was adopted as the plutonium reductant in the PUREX second cycle during the early 1970s (Malvyn McKibben and Bercaw, 1971). HAN also destroys nitrite, but the reaction is slower at lower acidity (Scott Barney, 1971). HAN had been shown to reduce not only plutonium (IV), but also iron (III). The relevant stoichiometric reactions are given below:

$$2NH_3OH^+ + 4Pu^{4+} \rightarrow 4Pu^{3+} + H_2O + N_2O + 6H^+$$

$$2NH_3OH^+ + 4Fe^{3+} \rightarrow 4Fe^{2+} + H_2O + N_2O + 6H^+$$

The above reactions are slower than the corresponding reactions of ferrous sulfamate (FS) which was also employed as a reducing agent in U/Pu partitioning (Malvyn McKibben et al., 1983), but they are much faster at lower acidity (Scott Barney, 1976). This suggests that it is possible to use a mixture of FS-HAN, with much lower FS concentration, instead of FS alone in the first cycle. Hence, the use of HAN along with FS has been tried in the Savannah River plant in the United States to reduce the quantity of FS, and it has been reported that up to 50% reduction has been achieved.

The disadvantage with HAN is that it decomposes at higher acidities and so lower acidities are required for partitioning. Hence, the reduction has to be carried out at lower acidity, which also is favorable from the reaction kinetics point of view. However, handling Pu(IV) under low-acid conditions is complicated as Pu(IV) can polymerize at lower acidity, which, if not avoided, can lead to unwanted problems in the flow sheet.

Partitioning by electrolytic reduction

To avoid the external addition of uranous nitrate, *in situ* generation by electrolytic means has gained importance. In this process, U(VI) and Pu(IV) in the loaded organic phase are stripped when it is contacted with a solution containing low concentrations of nitric acid and hydrazine. Pu(IV) will be stripped to a greater extent compared to U(VI) because of its lower distribution ratio. In the settler where electrolytic reduction takes place, U(VI) is reduced to U(IV) at the cathode to a greater extent because of its lower E^O value, but also Pu(IV) is reduced to Pu(III) to some extent. As the solution moves from stage to stage, the reduction of Pu(IV) continues by the production of U(IV) in those stages. This significantly reduces the requirement for external uranous nitrate feed.

The process has been studied and implemented both in mixer-settler (Pandey and Koganti, 2004) as well as in pulsed column (Salunke et al., 2005) types of equipment. Under the conditions prevailing in the equipment, hydrazine gets converted to HN_3 as well as NH_4NO_3, which poses safety issues as both are explosive. Electroreduction without adding hydrazine has been attempted at lower acidities (Schmieder and Petrich, 1989).

Partitioning by complexation

Complexation of Pu(IV) in a hydrophilic complex, rather than reduction to inextractable Pu(III), has been proposed as an alternate approach for the partitioning of plutonium from uranium (Birkett et al., 2005). A major advantage of complexant-based stripping is that there is no need for the addition of a stabilizing agent such as hydrazine. The organic ligand acetohydroxamic acid (AHA) has recently been developed for this purpose (Taylor et al., 1998). AHA forms aqueous phase complexes of higher stability with Pu(IV) than with U(VI), which remains in the organic phase complexed by TBP. But the drawback of AHA is that it can also undergo hydrolysis, slowly leading to the formation of hydroxylamine, which reduces Pu(IV) to Pu(III), and acetic acid, which would interfere with the subsequent purification of the plutonium product (Carrott et al., 2007). Nevertheless, solvent-extraction flow sheets using AHA to separate plutonium from uranium have been successfully tested (Govindan et al., 2008a; Kumar and Koganti, 2008) even up to FR concentrations of plutonium (Eddie Birkett et al., 2007).

9.3.3 Auxiliary process steps

In addition to the above main process-related issues, there are a few steps in the auxiliary process, such as in the treatment of solvent for recycling and in the waste evaporation cycles, which require careful consideration in the design of the FRFR flow sheet.

9.3.3.1 Solvent recycling

Both solvent and diluent get degraded during the solvent-extraction process. At one time, due to this phenomenon, there was a question over whether the PUREX process would be applicable for FRFR. A brief description of the degradation process, its impact, and possible remedial measures are described below.

9.3.3.2 Solvent degradation

Problems related to solvent degradation are well known in the PUREX process, but in FRFR the problems are more severe due to the very high radiation field, the presence of elevated concentrations of plutonium, which would increase solvent degradation by alpha radiolysis, and the higher acid conditions, which would degrade the solvent by acid hydrolysis. On contact with nitric acid, TBP is degraded by hydrolysis or dealkylation. The reactions involved are

$$(C_4H_9)_3PO_4 + H_2O \rightarrow H(C_4H_9)_2PO_4 + (C_4H_9)OH$$

$$H(C_4H_9)_2PO_4 + H_2O \rightarrow H_2C_4H_9PO_4 + (C_4H_9)OH$$

$$H_2C_4H_9PO_4 + H_2O \rightarrow H_3PO_4 + (C_4H_9)OH$$

The rates of the above reactions increase with both the concentration of nitric acid and the temperature (Burger, 1955; Moffat and Thompson, 1961). In hydrolysis, the primary products are butyl alcohol and dibutylphosphoric acid (HDBP), monobutyl

phosphoric acid (H_2MBP), and phosphoric acid (H_3PO_4). In dealkylation, the initial products will be butyl nitrate and HDBP:

$$(C_4H_9)_3PO_4 + HNO_3 \rightarrow H(C_4H_9)_2PO_4 + (C_4H_9)NO_3$$

The butyl nitrate subsequently slowly hydrolyzes to form butyl alcohol. Butyl alcohol and butyl nitrate are volatile and enter the off-gas system and, unless captured, would be vented through the stack. It is also known that butyl alcohol under certain conditions can lead to the formation of butyl nitrate, which could lead to explosion. Under normal design conditions even though it is formed and could accumulate in some low-temperature region of the off-gas system, the quantities are too small to be of any consequence.

The solvent also contains extracted metal ions that can accelerate the degradation of TBP by nitric acid; zirconium, which is present as a fission product, greatly accelerates the degradation of TBP to HDBP (Schulz et al., 1984a).

Radiation degradation of the TBP-diluent-HNO_3 system depends on many factors, including the presence of uranium and oxygen (Stieglitz et al., 1968; Novak et al., 1977; Nowak et al., 1979; Kulikov et al., 1983). The significance of radiation degradation relative to that by nitric acid depends on many factors peculiar to each PUREX plant design (Schulz et al., 1984b).

Extensive investigations have been carried out on solvent degradation, and a number of excellent reviews have been published (Naylor, 1967a; Blake, 1968; Healy, 1961; Mailen and Tallent, 1984a). The degradation products (Markov et al., 1993) of TBP, namely, DBP, MBP, and H_3PO_4, form complexes with zirconium, niobium, ruthenium, and plutonium that lead to reduced recoveries of uranium and plutonium and lower the DFs. The degradation products are found to cause emulsions, interfacial cruds, and precipitates (Stieglitz and Baker, 1982), which lead to difficulties in the smooth operation of extraction equipment. Because the concentrations of Pu(IV) and Zr(IV) are higher, the degradation products of TBP in FRFR are increased and the removal of these degradation products needs additional attention.

9.3.3.3 Diluent degradation

The impacts of diluent degradation are more related to the recycle of the solvent rather than deleterious effects on the process operation, as with the degradation of the TBP extractant. The principal diluent degradation products positively identified are as follows (Tallent et al., 1984, 1985):

- Aliphatic nitro compounds, which result from nitration by nitric acid or nitrous acid.
- Aliphatic carboxylic acids, resulting from oxidation reactions of nitric acid and nitrous acid.
- Aliphatic nitroso compounds, produced by the action of nitrous acid on secondary nitro compounds.
- Ketones and aldehydes, which may be intermediates in the oxidation reactions that lead to carboxylic acid formation.

It is considered prudent to choose a diluent that has a lower tendency to form secondary degradation products. Note that diluents such as hydrogenated propylene

tetramer and odorless kerosene are a special category of diluent found to have a reduced tendency for third-phase formation (Plaue et al., 2006).

9.3.3.4 Remedial measures

One approach for reducing the rate of degradation is to reduce the time of contact in solvent extraction by the proper choice of equipment. Even then, due to higher acidities it is possible that degradation will occur. This can be addressed by providing suitable solvent-treatment procedures.

Several methods of solvent cleanup or "washing" have been investigated and deployed at plant scale (Naylor, 1968) to treat the spent solvent. Solvent wash aims at reducing the radioactivity of the solvent, recovering residual plutonium and uranium, and removing degradation products; thus, enabling the treated solvent to be recycled and, thereby, reducing the requirement for fresh TBP and organic waste volume generation.

Some of the important techniques are (a) washing with Na_2CO_3 (Naylor, 1967b), (b) washing with hydrazine or hydrazine carbonate (Goldacker et al., 1976a) or hydrazine oxalate (Tallent and Mailen, 1982), (c) washing with hydroxylamine salts, (d) washing with tetra methyl ammonium hydroxide, (e) washing with ammonium carbonate (Govindan et al., 2008b), (f) use of solid sorbents, and (g) vacuum distillation.

The most common solvent wash reagent utilized in the past has been sodium carbonate solution, but PUREX plants have reported occasional failure of solvent treatment due to formation of emulsions (Orth and Olcott, 1963). This is primarily due to the secondary long chain degradation products as well as other complexants that are not removed by any basic solvent-treatment system. Moreover, the solid waste produced due to this treatment is significant; typically, for every ton of fuel processed there may be as much as 100 kg of $NaNO_3$ generated (Goldacker et al., 1976b; Tallent, 1982). Recovery of U/Pu from the $NaCO_3$ wash has been reported to be very difficult and requires drastic conditions such as boiling with 1 mol/L $UO_2(NO_3)_2$ in 6 mol/L HNO_3.

Hydrazine and its salts have advantages (Mailen and Tallent, 1984b), as they can be converted into gaseous products. Alternative approaches, based on the use of hydrazine or hydrazine carbonate or hydrazine oxalate, have been reported. Though these reagents reduce the quantity of solid waste substantially, the main disadvantage of these reagents is instability even at room temperature and difficulty in preparation and storage. Moreover, there are potential hazards including the possibility of reaction with nitric or nitrous acids (Cotton and Wilkinson, 1972), giving rise to sudden release of gases. Hydrazine carbonate is being tested for the recycle of the lean solvent that is generated in FBTR fuel reprocessing in the CORAL facility in India. This step is preceded by washing with oxalic acid to remove and recover plutonium from the lean solvent. Initial results (Natarajan et al., unpublished result.) are very encouraging.

In the case of hydrazine oxalate, apart from the potential hazards of hydrazine salts, it also has the drawback of loss of plutonium in the filtrate during the preconcentration step due to oxalate complex formation. This complex cannot be destroyed easily.

The use of tetra methyl ammonium hydroxide as an alternative solvent wash has also been reported in the literature (Naohito et al., 1989) but the costs of tetra methyl ammonium hydroxide are considered to be a disadvantage.

In the reprocessing of TR fuels, with low plutonium content, low burn up, and low acidity compared with FBR fuels, there is less solvent degradation. Hence, solvent washing with ammonium carbonate or hydrazine carbonate has been found to be a suitable option that avoids crud formation during washing as compared to Na_2CO_3.

Solid sorbents such as silica gel treated with NaOH or PbO_2, hydrous titanium oxide, activated alumina, and macroreticular resins such as Amberlyst A-26 have also been explored for the cleanup of the solvent (Healy, 1961).

Another purification step developed (Ginisty and Guillaume, 1990) in France and successfully implemented in the UP3 plant at La Hague involves evaporation and distillation. This is designed to take care of diluent-solvent secondary degradation products. Evaporation removes the heavy polymers while distillation, which is carried out under vacuum, removes the lighter ones. In the regular plant operation, a small fraction of the lean solvent is treated continuously and the purified solvent is mixed with the bulk. This method consists of washing the solvent with suitable reagent, vacuum dehydration, vacuum distillation, and vacuum fractionation of the distillate to get diluent and TBP fractions.

9.3.3.5 Waste volume reduction

The FRFR separation flow sheet uses lower concentrations of heavy metals to avoid the risk of third-phase formation. Consequently, higher volume reduction factors are required to concentrate the high active raffinate wastes. These volume reduction factors call for killing the acid so that the acidity of the concentrate is lower than 6 mol/L. The most widely used acid killing agent is formaldehyde, which reacts with nitric acid as per the following reaction:

$$HCHO + 4HNO_3 \rightarrow CO_2 + 3H_2O + 4NO_2$$

This reaction has an incubation period at lower temperatures, which can lead to a sudden release of energy. As the reaction is instantaneous at higher temperatures (e.g., 90 °C), the acid killing is carried out generally in the waste concentrators while evaporation is taking place. It is found that there is severe frothing during evaporation of waste solutions, leading to lower DFs (with respect to radioactivity) of condensates. As frothing is a function of salt concentration, design of the concentrators should take into consideration this factor as the FRFR raffinates generally would have higher salt strengths. Published literature in this area is very limited.

Furthermore, as TBP undergoes degradation it can form explosive alkyl nitrates such as butyl nitrate, which decomposes rapidly under certain conditions. It is observed that a mixture of TBP and nitric acid when heated, under certain conditions, changes color from amber to red due to the formation of nitrated organics. This compound is called “red oil.” It is observed that this could generate heat and large

amounts of detonable vapor and is a matter of serious concern in the safety of the plant. Three red-oil incidents have happened in the plants in the United States and in Russia (IAEA, 1998). Based on large amounts of data collected (Colvin, 1956; Rudsill and Crooks, 2000; Cowan, 1994) on the red-oil formation, it is found that the risk of red-oil runaway reaction is extremely low at temperatures below 130 °C and so the temperature of the evaporator is always kept below this limit during all operating conditions.

9.4 Additional considerations in the design of fast reactor fuel reprocessing plants

9.4.1 Additional considerations in the selection of material of construction

In FRFR, where the dissolution of high plutonium bearing refractory fuels require highly oxidizing conditions (Palamalai, 1988), titanium alloys and zirconium are appropriate materials of construction for these applications (Kamachi Mudali et al., 1993). Though zircaloy is being used in the UP-3 and Rokkasho reprocessing plants in France and Japan and titanium in the Tokai Mura reprocessing plant in Japan, austenitic stainless steel is still used in other thermal reactor reprocessing plants such as in THORP in the United Kingdom.

Based on a review of past experience, zircaloy appears to be the most suitable choice of construction material for dissolvers, acid, uranium, and plutonium concentrators and waste evaporators for realizing the design life of reprocessing plants; while in the rest of the plant 304 L, stainless steel would be adequate.

9.4.2 Additional considerations for auxiliary systems

Additional considerations in the design of plants for FRFR arise from the presence of high concentrations of plutonium. Hence, even in the first extraction cycle itself, plutonium concentration is high along with high γ-active fission products, unlike in TRFR. Thus, preventing the spread of α-contamination due to handling higher plutonium should be inherently built-in the design. This requires special design considerations to enable the maintenance of master-slave manipulators. Similar considerations would be required while taking out other systems or materials either on removal for maintenance or for replacement.

Another major challenge in the design of these reprocessing plants is nuclear safety. In order to prevent any criticality accident that may cause a sudden burst of intense neutron and gamma radiation dose to operating personnel, it is necessary to prevent the accumulation of fissionable material to a critical mass by suitable design features. Online monitoring of the inventory of plutonium in process vessels is an additional challenge in the FR reprocessing plants.

9.5 Status of fast reactor spent fuel reprocessing

FR fuels with high plutonium contents have been reprocessed in France, the United Kingdom, India, Germany, Japan, and Russia. Large-scale reprocessing of spent fuel discharged from the FRs, Rapsodie and Phoenix, in France, have been carried out either separately or by mixing with thermal reactor spent fuels. The United Kingdom has reprocessed spent Dounreay fast reactor (DFR, UK) and prototype fast reactor (PFR) fuel in a dedicated reprocessing plant. Japan has carried out the reprocessing of Monju reactor fuel at the Tokai Mura reprocessing plant. Russia has reprocessed their FR fuel through molten salt electrolysis in RIAR, a pyrochemical reprocessing facility in Russia. Germany has reprocessed the KNK-II (an experimental German FR) spent fuel in their MILLI, a German reprocessing facility. Except in RIAR, which adopted the nonaqueous molten salt-based process, the basic chemistry involved in all other reprocessing facilities is essentially the same. Some of the important experiences reported in the literature are given in the following sections.

9.5.1 French experience

The RAPSODIE (French experimental FR) fuel containing 30% plutonium was reprocessed in the AT1 workshop at La Hague (1 kg/day) from 1969 until 1979. A total of more than one ton of mixed oxide spent fuel with burn up as high as 120 GWd/te and a cooling period as low as 1.5 months was processed here. Part of the product from this plant was used for the core of the PHENIX FR in France. From commissioning in 1963, the Marcoule pilot facility (SAP) in France reprocessed 11 ton of fuels, most of which were from fast breeder reactors. Some plutonium assemblies were reprocessed and recycled as many as three times. Around 8 ton of PHENIX fuel has been reprocessed in the TRFR facility, UP2 plant at La Hague, after dissolution in the presence of gadolinium as a soluble neutron poison by mixing with thermal fuels from LWRs.

The process operational data (Bourgeois et al., 1984) demonstrated that the PUREX process can be used for reprocessing FR fuels with low cooling times and high plutonium content. Some important results based on this operation are summarized below.

The level of contamination in hulls (the cladding left in the dissolver after fuel is dissolved) was high, with ruthenium as the main contaminant (2.78×10^{11} Bq/kg), which was around 97% of the fission product activity in the hull. The activation products accounted for 17% of the aggregate activity. Plutonium contamination was around 150 mg/kg. The main problems were high levels of radioactivity and decay heat. The characterization of dissolution residues was difficult and they were even found to reach the pulse columns in the extraction section of the solvent-extraction plant.

The fission product DFs obtained were not strongly dependent on the feed activity ($1.11 \times 10^{11} - 8.88 \times 10^{11}$ Bq/L). Partitioning in mixer-settlers by electrolysis or with HAN with some addition of U(IV) was found to be satisfactory, with plutonium contamination in uranium being 0.25 μg/g of uranium at the output of the second cycle. The third uranium cycle facilitated reaching a plutonium contamination level of less

than 0.04 μg/g in the final uranium oxide product. Uranium contamination in the partitioned plutonium stream was around 2 mg/g of plutonium.

Between 50% and 80% of neptunium was extracted in the first solvent-extraction cycle. Depending on the partitioning method, neptunium followed either uranium (~85% if U(IV) was used) or plutonium (90-100% if HAN was used). After the first cycle coextraction, ruthenium/rhodium was found to be the main contaminant. Two more purification cycles for uranium and one more for plutonium yielded the required product qualities. The β-γ activity of uranium was 1.85×10^3 Bq/g, while that of plutonium was $2.96 \times 10^3 - 1.67 \times 10^4$ Bq/g.

Based on these results, the following recommendations for future plants were made:

- Use of salt-free processes for solvent extraction with HAN for partitioning and solvent treatment with hydrazine carbonate.
- Incorporation of a second plutonium cycle to obtain a concentrated product with the use of HAN for stripping as no plutonium concentrator (evaporator) was envisioned.

9.5.2 United Kingdom experience

The first discharge from the DFR (UK demonstration FR) was reprocessed in 1961 at the reprocessing plant at Dounreay (Allardice et al., 1984). It handled 10 ton of DFR core and 22 ton of DFR breeder (blanket) fuel. The DFR core was 75% enriched U-Mo alloy, while the breeder was natural uranium metal slugs. Plant refurbishments were made during 1973-1979 to enable reprocessing of PFR fuel. The refurbished plant was designed to handle 120-day cooled core fuel (17-25% Pu MOX) with a decay heat of 3 kW per subassembly. The plant processed 16 subassemblies totaling 200 kg of plutonium (1.2 te of uranium + plutonium) in 1980. By 1984 it had processed more than 5.5 ton of mixed oxide fuel containing more than 1.1 ton of plutonium. The peak burn up of fuel handled was 8.3 atom% (approximately 83 GWd/te burn up) with a cooling time of 136 days. This plant reprocessed PFR fuel from 1980 to 1996 and was shut down in 1996 due to dissolver failure.

The plant used a laser system for dismantling subassemblies and a mechanical chopper. The dissolver was of the batch type. Insolubles from the dissolution were characterized and typically found to contain noble metal alloys with ^{106}Ru contribution to the decay heat as high as 1 W/g. These insolubles contained up to 1% uranium and plutonium and a high-speed centrifuge clarifier was used for removing these solids prior to solvent extraction.

The solvent-extraction process consisted of three cycles based on 20% TBP. Due to several constraints in the layout, because the plant was installed in existing cells, sulfuric acid was used as a complexant, as neither ferrous sulfamate nor hydroxylamine reductant could be used for partitioning. The process exploited the higher formation constant of plutonium sulfate, which is two orders of magnitude higher than uranium sulfate, for the separation (Gourisse et al., 1971). This was accomplished by a mixture of sulfuric acid and nitric acid. Operating experience showed no detectable corrosion of stainless steel. In the third cycle, the plutonium product stream of 20-40 g/L concentration was purified before being concentrated by evaporation to 300 g/L and

transported to the fuel fabrication plant at Sellafield. Plutonium recoveries achieved were >99.8% and fission product DFs of $>10^7$ were achieved. Typical DFs achieved were 4×10^4, 50, and 5, respectively, in I, II, and III cycles.

9.5.3 Japanese experience

MOX fuel with 18% PuO_2, irradiated up to 40 GWd/te in the JOYO reactor (Japan) and cooled for 1.2-2.3 years, was reprocessed in the chemical processing facility (CPF) at Tokai (Ohuchi et al., 1984). The dissolution was carried out in 3.5 mol/L nitric acid below boiling point. The dissolution could be completed in 4 h. The undissolved residues were ~0.6% of the core fuel with the major constituents being molybdenum and ruthenium. A typical solvent-extraction feed contained 200 g/L uranium and 15.9 g/L plutonium, with fission product activity of 2.7×10^{11} Bq/L. Separate 16-stage mixer-settler batteries were used for coextraction and costripping. During the runs, interfacial cruds were observed.

9.5.4 German experience

Several kilograms of spent fuel discharged from KNK-II (a German experimental FR) were reprocessed in the MILLI facility (pilot plant for reprocessing FR fuels). Core and axial blanket fuels (maximum burn up of 100 GWd/te and mean burn up of 74 GWd/te, cooled to 10 months) was dissolved and subjected to the coextraction and partitioning cycle. Plutonium content was 30% in the core and the core and axial blankets were reprocessed together. The performance data (Bleyl et al., 1984) for two typical runs are given in Table 9.3.

It was found that the β-γ activity of the extractant in the second run was almost the same as that in the first run, despite the higher feed activity. Uranium/plutonium were separated using U(IV), which required 5.2 times the stoichiometric requirement. A separation factor of 2×10^5 was obtained for plutonium in the uranium product and 650 for the uranium in plutonium product. Electrochemical methods for partitioning were also tried with similar results.

Table 9.3 Typical results from reprocessing campaigns in the MILLI facility, Germany

Run	Burnup (GWd/te)	Cooling time (months)	Feed composition
1	11.7	25	[U]: 22 g/L; [Pu]: 27.5 g/L; $[H^+]$: 3.6 mol/L; fluoride: 0.02 mol/L FP composition: ^{144}Ce: 7.03×10^{10} Bq/L; ^{137}Cs: 2.44×10^{10} Bq/L; ^{106}Ru: 5.18×10^{09} Bq/L; ^{95}Zr: 3.33×10^{08} Bq/L
2	74	10	[U]: 167 g/L; Pu: 25 g/L; $[H^+]$: 4.6 mol/L FP composition: total $\gamma \approx 8.141 \times 10^{11}$ Bq/L

9.5.5 Russian experience

In Russia, the RT-1 (Russian reprocessing plant) facility, with a design capacity of 400 te/a, was constructed at the MAYAK reprocessing plant at Chelyabinsk-65 (now Ozersk). This is based on the PUREX process and has reprocessed spent fuels from VVER-210 and VVER-440 power reactors (nuclear power plants in Russia). In this plant, spent fuel from the FRs BN-600 and BN-350 (FRs in Russia) has also been reprocessed (Bibilashvili and Reshetnikov, 1993). In 1975, it was decided to construct a second reprocessing facility, RT-2, at Krasnoyarsk, with a capacity of 1000 te/a to reprocess fuel from VVER-1000s and other reactors. The operating experience of FR fuels in this plant is reasonably well documented (World Nuclear Association, 2014).

9.5.6 Indian experience

From 2003, spent mixed carbide fuels from the Indian FBTR having a composition of $(Pu_{0.7},U_{0.3})C$ and $(Pu_{0.55},U_{0.45})C$ are being reprocessed (Venkataraman et al., 2007; Subbarao et al., 2009) in the pilot plant facility, CORAL, which was set up for validating the process and equipment developed in India. This facility is designed to enable evaluation of the process flow sheet, equipment, and systems for the reprocessing of FR fuels that are rich in plutonium. Several batches of irradiated fuel pins with varying burn ups of 25, 50, 100, and 155 GWd/te and cooling times from 2 years to 6 years, have been reprocessed in this facility. The spent fuels reprocessed in this facility had a concentration of ~70% plutonium; the highest so far using the PUREX process anywhere in the world. Table 9.4 gives the gross activity of dissolver solutions that have been processed in this facility. These dissolver solutions are obtained by dissolving spent fuels with different burn up and cooling time.

Optimized flow sheet conditions were established from the laboratory studies and the resulting flow sheet parameters such as feed acidity, aqueous to organic ratios, and so forth, were tested using 16 stages of CEs; 10 stages for extraction and 6 stages for scrubbing (Koganti et al., 2009). During the course of the campaigns, modifications in CEs were carried out inside the hot cell, which improved the performance of the solvent-extraction cycles.

CEs are important for the success of FRFR plants as they offer several advantages compared to other conventional solvent-extraction equipment, such as lower holdups, residence times, and solvent inventories. They also provide high mass transfer

Table 9.4 Total fission product activity (Bq/kg of Pu + U) in dissolver solutions

Burn up(GWd/te)	25	50	100	155
Cooling period (years)	7.5	4	2.5	2
γ	1.07×10^{11}	3.9×10^{11}	6.37×10^{11}	3.17×10^{12}
β	2.1×10^{11}	7.3×10^{11}	1.57×10^{12}	3.94×10^{12}

efficiencies. Annular CEs have been successfully deployed in the CORAL facility. Based on this experience, higher-capacity models have been designed based on R&D activities in India. To understand the operation of a central extractor (CE) and to improve the design, computational fluid dynamics (CFD) simulation has been performed to understand the flow patterns inside mixer and settler regions in the annular CE (Vedantam et al., 2006a, 2012; Tamhane et al., 2012a). Also, hydrodynamic experiments were conducted for CEs of different bowl size to understand their operating range, axial mixing behavior, flooding throughput, and drop size distribution (Kumar and Kamachi Mudali, 2013; Joshi et al., 2013; Kumar et al., 2014; Kadam et al., 2008, 2009; Vedantam et al., 2006b; Tamhane et al., 2012b,c). These efforts have led to improved and reliable CE operations in the CORAL plant.

Fission product DFs are found not to have a strong bearing on the feed solution radioactivity. Typical DFs for some of the important fission products such as ^{106}Ru and ^{137}Cs are $>10^3$ in the first extraction cycle. The recoveries were found to be more than 99.8% for plutonium and 99.9% for uranium. Typical hull losses for plutonium have been found to be less than 0.008% (for the hulls from the 100 GWd/te burn up campaign).

9.6 Recent developments in aqueous processes for spent fast reactor fuel reprocessing

Recently, in some countries, there has been a resurgence of interest in R&D for reprocessing FR or Generation IV reactor fuels with promising processes for plutonium and minor actinide separations under development (International Atomic Energy Agency, 2011; Nuclear Energy Agency, 2012). Some of these are briefly described below.

9.6.1 France

9.6.1.1 The COEX™ process

The COEX™ process, developed by CEA, France, was first reported by Drain et al. (2008). This process is primarily aimed at modifying the PUREX process to enhance proliferation resistance. This is accomplished by ensuring that there is no separation of plutonium from uranium in the process. Coconversion of the purified plutonium and uranium mixture to solid form is carried out to give a product suitable for manufacture into mixed oxide fuel, either for thermal or FRs.

In this patented process, the major modification is in the operational parameters of the separation step of the PUREX process. After the first solvent-extraction cycle, some uranium is allowed to go with the plutonium stream while the majority of uranium is removed separately. The plutonium stream containing uranium is further purified and conditioned for conversion to a mixed oxide by oxalate coprecipitation and calcination.

The extensive industrial operating experience obtained at the La Hague reprocessing plants enabled formulation and optimization of this process. It has been demonstrated at laboratory scale that for plutonium contents up to 50% in the mixed oxide, the solid is a single phase. Hence, the coprecipitated product is acceptable for reactor fuel manufacture. It has also been reported that neptunium, a troublesome actinide element in spent fuel reprocessing, can be diverted to this mixed oxide stream; thus, if desired, neptunium can be incorporated into MOX fuel elements for burning in FRs.

Even though this process is attractive from the nonproliferation point of view, for a typical commercial FR based on fuel with around 25% plutonium, the coprecipitation process will be at least four times larger than the conventional PUREX systems. As these processes have to be carried out in plutonium glove boxes, they are likely to involve significant increases in manual operations and plant footprint.

9.6.1.2 Process development with alternate solvents

Though many countries are pursuing various alternate (non-PUREX) aqueous processes for the reprocessing of thermal reactor spent fuels, France has demonstrated the amide-based processes, such as the DIAMEX-SANEX process (Baron et al., 2001), with spent fuel. This process uses an amidic solvent that has less environmental issues compared with TBP, as there is no phosphorus atom, making it completely incinerable. These processes are basically designed for the removal of minor actinides (americium and curium) from the shorter-lived fission products with the aim of burning these minor actinides in FRs. The DIAMEX-SANEX process can be added on to the PUREX process for the recovery of the actinides from the high active PUREX waste stream. With the separation of the minor actinides from the shorter-lived fission products, the time period for storage of the high active wastes is reduced. This process can also be integrated with the COEX process to address both the nonproliferation and long-term waste storage issues.

The GANEX process (Miguirditchian et al., 2009) is an adapted version of the DIAMEX-SANEX process (Heres et al., 2007) for the separation of neptunium and plutonium along with the americium and curium, so that they can be prepared as fuel elements for burning in FRs.

9.6.2 Russia

Trialkyl phosphates with optimized hydrocarbon chains such as tri-isoamyl phosphate (TiAP) and di-isobutyl isooctyl phosphate (DiBiOP) have been tested as alternate extractants in the reprocessing of BR-10 and BOR-60 FRSF in Russia (Nikiforov et al., 1989). It has been seen that the LOC for plutonium is much higher than that of TBP because as much as 120 gPu/L can be loaded in the 36% TiAP-dodecane system compared to around 75 gPu/L for TBP-dodecane system.

Typical operating results with this process are the core and axial blanket of the fuel were reprocessed together. The core had U 20% + Pu 80% with a burn up of 100 GWd/te

burn up and was cooled between 3 months and 2 years. After dissolution and clarification, the solution concentration was around 165 gU/L, 23 gPu/L, 4.3 mol/L HNO_3, with an activity up to 1000 Ci/L. The extractants used were 30% TBP, 30% TiAP, and 40% DiBiOP. The organic could be loaded up to 82 ± 5 g/L of heavy metals.

Extraction studies were carried out with 25 L/h capacity CE banks. Coextraction was carried out in 10 extraction stages followed by a dual scrub section of 11 mol/L acid (3 stages) and 0.5 mol/L acid (3 stages). Reductive stripping or partitioning using U(IV) was carried out in 16 stages; uranium stripping in 8 stages. The lean solvent was washed with carbonate in three stages.

The fission product DF for uranium was $1.5\text{-}1.6 \times 10^5$ for TiAP, while it was $1.2\text{-}1.5 \times 10^5$ for DiBiOP; for plutonium, the DF for the both the solvents are of the same order: 4×10^4. The uranium purification factor from plutonium is of the order of 1.5×10^5. These factors were similar to those obtained in mixer-settler experiments, indicating that the contact time is not the controlling factor on flow sheet performance.

9.6.3 India

Considering the potential advantages of higher homologues of TBP, tri-*n*-amyl phosphate (TAP) and tri-*n*-hexyl phosphate (THP) were studied as potential alternate solvents (Suresh et al., 1994). The distribution ratios for uranium and plutonium were compared with TBP, which indicated that with increasing chain length the distribution ratio increases. This is attributed to the marginal increase in the basicity of the P═O bond due to the increase in the carbon chain length in the presence of an oxygen atom between the phosphorous and the alkyl chain.

Experiments were also conducted to understand the effects of branching for which tri-isobutyl phosphate (TiBP) and TiAP were considered. While TiAP showed increased distribution coefficients compared to TAP, the opposite behavior was observed with TBP and TiBP. Steric hindrance of the complexing compound is the reason for the reduced extraction behavior of TiBP compared to TBP (because the branching of the carbon atom is immediately next to the carbonyl carbon, unlike in TiAP where it is at the third carbon from the oxygen).

Third-phase studies were conducted with thorium in TBP, TiBP, TAP, and TiAP. It was observed that the limiting concentration for the formation of third-phase increased when increasing the chain length of the alkyl group of the extractant. Similarly, third-phase formation was not observed with THP. The increased loading with higher chain length solvents may be due to the organophilic character of the metal solvate leading to the increased solubility with the diluent. Branching is not found to increase the solubility.

TAP has been tested (Suresh et al., 2009a) with U(VI) under extraction conditions in a 16-stage mixer-settler. With 1.1 mol/L TAP in HNP diluent, with feed conditions of 267 gU/L at 3.5 mol/L acidity, the organic could be loaded with a concentration of 75.9 gU/L with a raffinate U(VI) concentration of <1 mgU/L. The loaded organic, with U(VI) concentrations as high as 93.5 g/L, could be stripped in the 16-stage mixer-settler with 0.01 mol/L acid with a strip product U(VI) concentration of 90.8 g/L. The lean organic retained 0.4 g/L U(VI) under these conditions. This run indicates that TAP is a promising alternate solvent. The chemical and radiation

behavior of TAP have also been studied (Venkatesan et al., 2009), which indicates that the properties are comparable to that of TBP. An important advantage of TAP is that its aqueous solubility is 19 mg/L compared to 390 mg/L under typical experimental conditions (Suresh et al., 2009b).

9.7 Future development and deployment of the closed fuel cycle in India

PUREX process-based reprocessing plants have been in operation in India since the late 1950s. Based on the operating experience of these plants and associated R&D, the pilot plant "CORAL" was designed and has been operating in Kalpakkam since 2003 with objectives to establish the process and standardize the equipment for FRFR. Several reprocessing campaigns of spent FBTR mixed carbide fuel with a peak burnup of 155 GWd/te and a cooling period of 2 years and more have been successfully carried out in this pilot plant. This has validated the process flow sheet for reprocessing the plutonium-rich FR fuels with high burnups and short cooling periods.

A demonstration fast reactor reprocessing plant (DFRP) is under construction at Kalpakkam for reprocessing the FBTR spent fuel as well as to demonstrate the reprocessing of prototype fast breeder reactor (PFBR) spent fuel. Another reprocessing plant to close the fuel cycle of PFBR is designed and construction has already started. This plant (FRP) will be capable of reprocessing the fuel arising from two more FBRs, which are planned to be constructed adjacent to the PFBR subsequently.

R&D on removal of minor actinides is also being pursued in India. A plant has been constructed in Tarapore to treat the high active liquid waste from the reprocessing of thermal reactor spent fuels. The process flow sheet for partitioning has been demonstrated at Kalpakkam with the wastes generated in CORAL. Based on these studies, a pilot plant will be installed in the fuel reprocessing plant (FRP).

9.8 Conclusion

This chapter has described the status of FR aqueous fuel reprocessing technology and relevant international experience. The TBP-based PUREX process is adaptable for deployment in the reprocessing of these fuels based on the experience of various plants worldwide. The challenges associated with the design and operation of these plants also have been outlined in this chapter. Development work related to alternate solvents and diluents would need to reach a greater level of maturity before they can be considered for plant-level deployment. The incentive for this development is the possibility of avoiding the risk of third-phase formation due to high plutonium loading in the solvent phase. Another area of development required is in the removal of dissolved organic from the aqueous phases that are evaporated. This is to ensure that no explosion occurs due to "red-oil" formation. In conclusion, it appears that the PUREX process will remain unchallenged for many more years to come in the field of spent fuel reprocessing, even if FR fuel cycles are to be introduced.

References

Allardice, R.H., Hickey, H.B., Smith, G.E.I., Walker, B.J., Ward, M.D., 1984. Proceedings of Fuel Reprocessing and Waste Management, Wyoming, August 2, p. 214.

Anderson, B., Frew, J.D., Pugh, O., Thompson, P.J., 1994. Reprocessing the fuel from the prototype fast reactor (PFR) Nucl. Eng. 35, 129.

Baron, P., Heres, X., Lecomte, M., Masson, M., 2001. Separation of the minor actinides: the DIAMEX-SANEX concept. In: Proceedings of the International Conference on Future Nuclear Systems, GLOBAL'01, Paris, France, September 9–13.

Bibilashvili, Yu.K., Reshetnikov, F.G., 1993. Russia's nuclear fuel cycle: an industrial perspective. IAEA Bulletin 3, IAEA, Vienna, pp. 28–33.

Birkett, J.E., Carrott, M.J., Fox, O.D., Jones, C.J., Maher, C.J., Roube, C.V., Taylor, R.J., Woodhead, D.A., 2005. Recent developments in the purex process for nuclear fuel reprocessing: complexant based stripping for uranium-plutonium separation. Chimia 59, 898–904.

Blake Jr., C.A., 1968. Solvent stability in nuclear fuel processing: evaluation of the literature, calculation of radiation dose, and effects of iodine and plutonium. USAEC report ORNL-4212.

Bleyl, H.J., Oscsenfeld, W., Schmieder, H., Haug, H.O., Ertel, D., Stieglitz, I., 1984. Proceedings of the Fuel Reprocessing an Waste Management, Wyoming, p. 2462.

Bourgeois, M., Le Bouhellec, J., Eymerry, R., Viala, M., 1984. Proceedings of Fuel Reprocessing and Waste Management, ANS International Topical Meeting on Fuel Reprocessing and Waste Management; Jackson Hole, WY (USA); 26–29 August 1984. American Nuclear Society, LaGrange Park, IL, USA, pp. 201–213.

Bourges, J., Madic, C., Koehly, G., Lecomte, M., 1986. Dissolution of PuO_2 in HNO_3 medium with electro generated Ag(II). J. Less-Common Met. 122, 303–311.

Breschet, C., Miquel, P., 1971. In: Proceedings of the ISEC 1971, The Hague, vol. I. Society of Chemical Industry, London, p. 565.

Burch, W.D., 1982. Advanced concepts under development in the US breeder-fuel-reprocessing program. CONF-811154–1, DE82 003965. Oak Ridge National Laboratory. http://www.iaea.org/inis/collection/NCLCollectionStore/_Public/13/691/13691682.pdf?origin=publication_detail.

Burger, L.L., 1955. The chemistry of tributyl phosphate, a review. USAEC report HW-40920, Hanford Works.

Campbell, D.O., Mailen, J.C., Fellows, R.L., 1984. Dissolution behavior of FFTF fuel. CONF-840802-19, DE85 001854, 26–29 August 1984. Oak Ridge National Laboratory.

Carrott, M.J., Fox, O.D., Maher, C.J., Mason, C., Taylor, R.J., Sinkov, S.I., Choppin, G.R., 2007. Solvent extraction behaviour of plutonium (IV) ions in the presence of simple hydroxamic acids. Solvent Extr. Ion Exch. 25 (6), 723–746.

Chesne, A., Germain, M., 1992. Solvent Extraction 1990. Elsevier B.V, p. 539.

Clark, W.E., Gens, T.A., Oct 1961. A study of dissolution of reactor fuels containing Zr in a Ti vessel. ORNL-3118.

Cleveland, J.M., 1964. Dissolution of refractory PuO_2. J. Inorg. Nucl. Chem. 26, 1470–1471.

Colvin Jr., T.J., 1956. Nitric acid recovery units permissible steam pressure in reboilers. DPST-56-243, EI. Du Pont de Nemours and Company.

Cotton, F.A., Wilkinson, G., 1972. Advanced Inorganic Chemistry, third ed. Wiley Interscience, New York, p. 353.

Cowan, M.L., 1994. Uncontrolled TBP-nitric acid BIO risk analysis. EPD-SSS-94010, Westinghouse Savannah River Company.

Drain, F., Ermin, J.L., Vinoche, R., Baron, P., 2008. In: COEX Process: Cross Breeding Between Innovation and Industrial Experience, Session 53 – Abstract 8220, wm'08, Phoenix, Arizona, February 2008.

Eddie Birkett, J., Carrott, M.J., Danny Fox, O., Jones, C.J., Maher, C.J., Roube, C.V., Taylor, R. J., Woodhead, D.A., 2007. Controlling neptunium and plutonium within single cycle solvent extraction flowsheets for advanced fuel cycles. J. Nucl. Sci. Technol. 44 (3), 337–343.

Finney, B.C., Hannaford, B.A., West, G.A., Watson, C.D., 1969. Shear-leach process. ORNL-3984.

Flagg, J.F., 1961. Chemical Processing of Reactor Fuels. Nuclear Science and Technology, vol. 1. Academic Press, New York.

Fletcher, J.M., Scargill, D., 1965. In: Solv. Ext. Chem. of Metals, Int. Conf., Harwell, England. MacMillan, London.

Fournier, W., Hugelmann, D., Dalverny, E., 1992. Solvent Extraction 1990, Pt A. Elsevier B.V, p. 747.

Ginisty, C., Guillaume, B., 1990. Solvent distillation studies for a purex reprocessing plant. Sep. Sci. Technol. 25, 1941.

Goldacker, H., Schieder, H., Steingrunn, F., Stieglitz, L., 1976. A newly developed solvent wash process in nuclear fuel reprocessing decreasing the waste volume. Kerntechnik 18, 426.

Gourisse, D., Bathellier, A., Alanchard, J.C., 1971. In: Proceedings of ISEC'71, vol. I. Society of Chemical Industry, London, p. 147.

Govindan, P., Sukumar, S., Subba Rao, R.V., 2008a. Partitioning of uranium and plutonium by acetohydroxamic acid. Desalination 232 (1–3), 166–171.

Govindan, P., Dhamodharan, K., Vijayan, K.S., Subba Rao, R.V., Venkataraman, M., Natarajan, R., 2008b. Wash solution suitable for use in continuous reprocessing of nuclear fuel and a system thereof. Patent Application, PCT International Application No. PCT/IN2008/00516.

Harmon, H.D., 1975. Dissolution of PuO_2 with cerium(IV) and fluoride promoters. Savannah River Laboratory report DP-1371.

Healy, T.V., 1961. Fuel Reprocessing Solvent Tributyl Phosphate: Its Degradation, Clean-Up and Disposal, vol. 1. IAEA, Vienna, pp. 201–214; Symposium on the management of radioactive wastes from the nuclear fuel cycle; Vienna, Austria; 22–26 Mar 1976; IAEA-SM–207/23.

Heres, X., Ameil, E., Martinez, I., Baron, P., Hill, C., 2007. Extractant separation in DIAMEX-SANEX process. In: International Conference; 7th, Advanced Nuclear Fuel Cycles and Systems; 2; GLOBAL 2007, p. 699.

Horner, D., Crouse, D.J., Mailen, J.C., 1977. Cerium-promoted dissolution of PuO_2 and PuO_2-UO_2 in nitric acid. ORNL/TM-4716.

Hyder, M.L., Perkins, W.C., Thompson, M.C., Burney, G.A., Russel, E.R., Holcomb, H.P., London, L.F., 1979. USAWC report DP-1500.

IAEA, 1998. The radiological accident in the reprocessing plant at TOMSK. STI/PUB/1060.

International Atomic Energy Agency, 2006. Management of spent fuel from nuclear power reactors. In: Proceedings of an International Conference held in Vienna, 19-22 June 2006; Proceedings Series.

International Atomic Energy Agency, 2011. Status of developments in the back end of the fast reactor fuel cycle. IAEA-NF-T-4.2, International Atomic Energy Agency, Vienna. http://www-pub.iaea.org/MTCD/publications/PDF/Pub1493_web.pdf.

JEFF-3.1, Joint evaluated fission and fusion file, incident-neutron data, http://www-nds.iaea.org/exfor/endf00.htm, 2 October 2006.

Jones, C.J., 1987. Comprehensive Coordination Chemistry, vol. 6. Pergamon Press, Oxford, p. 881.

Joshi, J.B., Tamhane, T., Patra, J., Balamurugan, M., Pandey, N.K., Kumar, S., Kamachi Mudali, U., Natarajan, R., Patil, R., 2013. Design of liquid-liquid settlers: capacity and solvent characterization using dimensionless dispersion number. Ind. Eng. Chem. Res.

Kadam, B.D., Joshi, J.B., Koganti, S.B., Patil, R.N., 2008. Hydrodynamic and mass transfer characteristics of annular centrifugal extractors. Chem. Eng. Res. Des. 86, 233–244.

Kadam, B.D., Joshi, J.B., Koganti, S.B., Patil, R.N., 2009. Dispersed phase hold-up, effective interfacial area and Sauter mean drop diameter in annular centrifugal extractors. Chem. Eng. Res. Des. 87, 1379–1389.

Kamachi Mudali, U., Dayal, R.K., Gnanamoorthy, J.B., 1993. Corrosion studies on materials of construction for spent nuclear fuel reprocessing plant equipment. J. Nucl. Mater. 203, 73.

Koganti, S.B., Ravisankar, A., Natarajan, R., 2009. In: Proceedings of National Seminar on Solvent Extraction Chement-2009, 23–24 June, Kalpakkam.

Kolarik, Z., 1991a. In: Handbook on the Physics and Chemistry of the Actinides, vol. 6. Elsevier, p. 181.

Kolarik, Z., 1991b. In: Handbook on the Physics and Chemistry of the Actinides, vol. 6. Elsevier, p. 511.

Koning, A., Forrest, R., Kellett, M., Mills, R., Henriksson, H., Rugama, Y., 2006. The JEFF-3.1 nuclear data library. JEFF report 21, OECD/NEA, Paris, France. ISBN 92-64-02314-3.

Kulikov, A., Kermonova, N.V., Vladimorova, M.V., 1983. Radiolysis of TBP in the presence of plutonium and uranium. Sov. Radiochem. 25, 310.

Kumar, S., Kamachi Mudali, U., 2013. Experimental measurements of drop size distributions in 30 mm diameter annular centrifugal contactor with 30%TBP-nitric acid biphasic system. Int. J. Nucl. Energy. 2013. http://dx.doi.org/10.1155/2013/402505.

Kumar, S., Koganti, S.B., 2008. Next generation Purex flowsheets with acetohydroxamic acid as complexant for FBR and thermal-fuel reprocessing, in solvent extraction: fundamentals to industrial applications. In: Moyer, B.A. (Ed.), Proceedings ISEC 2008 International Solvent Extraction Conference. Can. Inst. Min. Metall. Pet., Montreal, Canada, pp. 635–640.

Kumar, S., Singh Shekhawat, R., Singh, A., Balamurugan, M., Priyadarshini, N., Sampath, M., Kamachi Mudali, U., 2014. Characterization of submicron size entrainment in the aqueous product stream of a 40 mm diameter centrifugal extractor for 30% TBP/nitric acid biphasic system. Int. J. Nucl. Sci. Technol. 8 (8), 49–60. http://dx.doi.org/10.1504/IJNEST.2014.057903.

Mailen, J.C., Tallent, O.K., 1984a. Improved Purex solvent scrubbing methods. In: International Topical Meeting on Fuel Reprocessing and Waste Management, August 26–29, 1984, Jackson Hole, Wyoming, CONF-840S02-10.

Mailen, J., Tallent, O.K., 1984b. In: Proceedings of the ANS International Topical Meeting of Fuel Reprocessing and Waste Management, Jackson, vol. I, p. 431.

Malvyn McKibben, J., Bercaw, J.E., 1971. Hydroxylamine nitrate as a plutonium reductant in the purex solvent extraction process. DP-1248, E. I. du Pont de Nemours and Co., Savannah River Plant.

Malvyn McKibben, J., Chostner, D.F., Orebaugh, E.G., 1983. Plutonium-uranium separation in the purex process using mixtures of hydroxylamine nitrate-ferrous sulfamate. USDOE report DP-1656, E. I. du Pont de Nemours & Co., Savannah River Plant, Aiken, SC.

Manson, C., Thompson, R., Tolchard, A.C., 1987. I.Ch.E. Symp. Series 75.

Markov, G.S., Moshkov, M.M., Shcherbakov, V.A., 1993. Proc. ISEC 93, York, vol. 3, p. 1531.

Miguirditchian, M., Roussel, H., Chareyre, L., Baron, P., Espinoux, D., Calor, J.N., Viallesoubranne, C., Lorrain, B., Masson, M., 2009. HA demonstration in the Atalante facility of the Ganex 2nd cycle for the grouped TRU extraction. In: Proceedings of the GLOBAL 2009, Paris, France, 6–11 September.

Miles, J.H., 1993. A flowsheet for the removal of technetium from TPB/OK streams. Nucl. Eng. 34, 27.

Moffat, J., Thompson, R.D., 1961. Basic studies of chemical stability in extraction systems. I. The effect of zirconium nitrate and nitric acid upon the chemical stability *o*-tributyl phosphate. IDO-14543, Idaho Chemical Processing Plant.

Nakashima, T., Kolarik, Z., 1983. The formation of a third phase in the simultaneous extraction of actinide(IV) and uranyl nitrates by tributyl phosphate in dodecane. Solvent Extr. Ion Exch. 1, 497.

Naohito, U., Fumio, K., Hideo, Y., 1989. Alternative solvent wash process using tetramethylammonium hydroxide solution as salt-free wash reagent. J. Nucl. Sci. Technol. 26 (2), 270–277.

Natarajan, R., 2011. Studies to improve the separation and purification of uranium and plutonium in the solvent extraction of fast reactor fuels. PhD Thesis. Sathyabama University.

Natarajan, R., Raj, B., 2007. Fast reactor fuel reprocessing technology in India. J. Nucl. Sci. Technol. 44 (3), 393–397.

Natarajan, R., Vijayakumar, V., Subbarao, R.V. Unpublished result.

Naylor, A., 1967a. Fission product chemistry in relation to TBP processes, in reprocessing of fuel from present and future power reactors. Kjeller-report KR-126, S. 101.

Naylor, A., 1967b. Kjeller report KR-126, p. 120.

Naylor, A., 1968. Kjeller report ORNL-4212.

Nikiforov, A.S., Zakharkin, B.S., Renard, Eh.V., Rozen, A.M., Smetanin, Eh.Ya., 1989. In: Proceedings of the International Conference on Actinides – 89, Tashket, USSR, September 24-29, 1989, p. 20.

Novak, Z., Novak, M., Zaydel, A., 1977. Research on the effect of salts of uranium, zirconium and ruthenium on radiolysis of the tributyl phosphate-dodecane-HNO systems. ORNL-tr-4879, In: Translation of Paper from 4th Symp. on Study into Irradiated Fuel Reprocessing, Karlovy Vary, Cz.

Nowak, Z., Nowak, M., Seydel, A., 1979. The radiolysis of TBP-dodecane-HNO_3 systems. Radiochem. Radioanal. Lett. 38 (5–6), 343–353.

Nuclear Energy Agency, 2012. Spent nuclear fuel reprocessing flowsheet; A report by the WPFC Expert Group on Chemical Partitioning of the NEA Nuclear Science Committee; Nuclear Science, NEA/NSC/WPFC/DOC(2012)15, June 2012, http://www.oecd-nea.org/science/docs/2012/nsc-wpfc-doc2012-15.pdf

Ohuchi, J., Horie, M., Kashihara, H., Yamamoto, M., 1984. Reprocessing experiments on FBR spent fuels in CPF. In: Proceedings of the Fuel Reprocessing and Waste Management (2), pp. 243–256.

Orth, D.A., Olcott, T.W., 1963. PUREX process performance versus solvent exposure and treatment. Nucl. Sci. Eng. 17, 593.

Palamalai, A., 1988. Development of an electro-oxidative dissolution technique for reprocessing of fast breeder reactor ceramic fuel materials. PhD Thesis. Madras University, Chennai, India.

Pandey, N.K., Koganti, S.B., 2004. Simulation of electro-mixer-settler for the partitioning of uranium and plutonium in PUREX process. Indian J. Chem. Technol. 11 (July), 535–547.

Plaue, J., Gelis, A., Czerwinski, K., 2006. Plutonium third phase formation in the 30% TBP/HNO_3/hydrogenated polypropylene tetramer. Solvent Extr. Ion Exch. 24, 271–282.

Pruett, D.J., 1984. In: Science and Technology of Tributyl Phosphate, vol. III. CRC Press Inc., Boca Raton, p. 81.

Ramanujam, A., Ramakrishna, V.V., Patil, S.K., 1978. The effect of temperature on the extraction of plutonium(IV) by tri-*n*-butyl phosphate. J. Inorg. Nucl. Chem. 40, 1167.

Rudsill, T.S., Crooks, W.J., 2000. Initiation temperature of runaway TBP/nitric acid reactions. WSRC-TR-2000-00427-RO, Westinghouse Savannah River Company.

Ryan, J.L., Bray, L.A., 1980. Dissolution of plutonium dioxide — a critical review. In: Navratil, J.D., Schultz, W.W. (Eds.), Actinide Separations.ACS Symposium Series, 17th ACS National Meeting, Honolulu, HI, p. 499.

Ryan, J.L., Bray, L.A., Wheelwright, E.J., Bryan, G.H., July 1990. Catalyzed electrolytic plutonium oxide dissolution (CEPOD): the past seventeen years and future potential. PNL-SA-18018, DE91 004066.

Salunke, S.U., Vincent, T., Patil, A.R., October 2005. BARC Newsletter (261), 107–110.

Schmieder, H., Petrich, G., 1989. A concept for an improved Purex process. Radiochim. Acta 40, 181–192.

Schulz, W.W., Burger, L.L., Navratil, J.D., Bender, K.P. (Eds.), 1984. In: Science and Technology of Tributyl Phosphate, vol. III. CRC Press Inc., Boca Raton.

Scott Barney, G., June 1971. The reaction of hydroxylamine. Nitrous acid. ARH-SA-97.

Scott Barney, G., 1976. A kinetic study of the reaction of plutonium(IV) with hydroxylamine. J. Inorg. Nucl. Chem. 38, 1677–1681.

Scott Barney, G., 1977. The kinetics of plutonium oxide dissolution in nitric/hydrofluoric acid mixtures. J. Inorg. Nucl. Chem. 39 (9), 1665–1669.

Srinivasan, T.G., Ahmed, M.K., Shakila, A.M., Dhamodaran, R., Vasudeva Rao, P.R., Mathews, C.K., 1986. Radiochim. Acta 40, 151.

Steward, S.A., Gray, W.J., Jan 1994. Comparison of U dissolution rates from spent fuel and uranium dioxide. UCRL-JC-115355, Lawrence Livermore National Laboratory.

Stieglitz, L., Baker, R., 1982. In: Nuklear Entsorgung, vol. 2. Verlag Chemie, Weinheim, p. 333.

Stieglitz, L., Ochenfeld, W., Schmieder, H., 1968. The influence of the radiolysis of tributyl phosphate on the plutonium yield in the purex process for high plutonium content. KfK 691, KarlsruheKarlsruhe Nuclear Research Center.

Subbarao, R.V., Venkatarakan, M., Natarajan, R., Raj, B., 2009. Operating experience of Fast Reactor Spent Fuel Reprocessing Facility. CORAL, Paper 9126, In: Proceedings of Global 2009, Paris, France, September 6–11, 2009.

Suresh, A., Srinivasan, T.G., Vasudeva Rao, P.R., 1994. Extraction of U (VI), Pu (IV) and Th (IV) by some trialkyl phosphates. Solvent Extr. Ion Exch. 12 (4), 727–744.

Suresh, A., Sreenivasan, N.L., Robert Selvan, B., Antony, M.P., Srinivasan, T.G., Koganti, S.B., Vasudeva Rao, P.R., 2009a. Nucl. Technol. 167 (August), 333.

Suresh, A., Srinivasan, T.G., Vasudeva Rao, P.R., 2009b. Solvent Extr. Ion Exch. 27 (2), 258.

Swain, P., Annapoorani, S., Srinivasan, R., Mallika, C., Kamachi Mudali, U., Natarajan, R., 2013. Separation of ruthenium from simulated nuclear waste in nitric acid medium using N-paraffin hydrocarbon. Sep. Sci. Technol. 49 (1), 112–120. http://dx.doi.org/10.1080/01496395.2013.815629.

Tallent, O.K., et al., 1982. Method for cleaning solution used in nuclear fuel reprocessing. US Patent 4358426, 423/10, November 1982.

Tallent, O.K., Mailen, J.C., 1982. An alternative solvent cleanup method using a hydrazine oxalate wash reagent. Nucl. Technol. 59, 51.

Tallent, O.K., Mailen, J.C., Pannel, K.D., 1984. Purex diluent degradation. USDOE report ORNL/TM-8814.

Tallent, O.K., Mailen, J.C., Dodson, K.E., 1985. PUREX diluent chemical degradation. Nucl. Technol. 71, 417–425.

Tamhane, T.V., Joshi, J.B., Kamachi Mudali, U., Natarajan, R., Patil, R.N., 2012a. Axial mixing in annular centrifugal extractors. Chem. Eng. J. 207–208, 462–472.
Tamhane, T.V., Joshia, J.B., Mudali, Kamachi, Natarajan, R., Patil, R.N., 2012b. Measurement of drop size characteristics in annular centrifugal extractors using phase Doppler particle analyzer (PDPA). Chem. Eng. Res. Des. 90, 985–997.
Taylor, R.F., et al., 1963. Dissolution rate of uranium dioxide sintered pellets in nitric acid systems. J. Appl. Chem. 13, 32–40.
Taylor, R.J., May, I., Wallwork, A.L., Denniss, I.S., Hill, N.J., Galkin, B.Ya., Zilberman, B.Ya, Fedorov, Yu.S, 1998. The applications of formo- and aceto- hydroxamic acids in nuclear fuel reprocessing. J. Alloys Compd. 271-273, 534–537.
Uriarte, A.L., Rainey, R.H., April 1965. ORNL-3695.
Vasudeva Rao, P.R., 1994. IANCAS Bull. 10 (2), 16.
Vasudeva Rao, P.R., Kolarik, Z., 1996. Solvent Extr. Ion Exch. 14 (6), 955–993.
Vaughen, V.C.A., Goode, J.H., June 1972. Fuel reprocessing tests with short cooled LMFBR type fuel rods. CONF-720607-16, Chemical Technology Division, ORNL.
Vaughen, V.C.A., Goode, J.H., Oct 1979. Dissolution of irradiated MOX fuels. CONF-791086-4, Chemical Technology Division, ORNL.
Vedantam, S., Joshi, J.B., Koganti, S.B., 2006a. CFD simulation of RTD and mixing in the annular region of a Taylor-Couette contactor. Ind. Eng. Chem. Res. 45, 6360–6367.
Vedantam, S., Joshi, J.B., Koganti, S.B., 2006b. Three-phase CFD simulation of stratified two-fluid Taylor Couette flow. Can. J. Chem. Eng. 84, 279–286.
Vedantam, S., Wardle, K.E., Tamhane, T.V., Ranade, V.V., Joshi, J.B., 2012. CFD simulation of annular centrifugal extractors. Int. J. Chem. Eng. 2012, 1–31. Review article, Article ID 759397, http://dx.doi.org/10.1155/2012/759397.
Veleckis, E., Hoh, J.C., March 1991. Dissolution characteristics of mixed UO_2 powders in J-13 water under saturated conditions. ANL-91/8, DE91 010968, Chemical Technology Division, Argonne National Laboratory.
Venkataraman, M., Natarajan, R., Raj, Baldev, 2007. CORAL: a stepping stone for establishing the Indian Fast reactor Fuel Reprocessing Technology. In: Proceedings of Global 2007, Boise, Idaho, pp. 208–216.
Venkatesan, K.A., Robert Selvan, B., Antony, M.P., Srinivasan, T.G., Vasudeva Rao, P.R., 2009. Solvent Extr. Ion Exch. 27 (2), 258.
Vondra, B.L., Crouse, D.J., 1979. Proc. AIChE Symposia Series 191, vol. 75. p. 207.
Wilson, P.D., Smith, J.K., 1987. I.Ch.E. Symp. Series 103, 67.
Woltermann, H.A., Ulrick, T.L., Antion, D., March 1973. Dissolution of high fired plutonium oxide. MLM-2010, TID-4500, UC-4, Monsanto Research Corporation, Ohio, USA.
World Nuclear Association, 2014. Processing of Used Nuclear Fuel. http://www.world-nuclear.org/info/Nuclear-Fuel-Cycle/Fuel-Recycling/Processing-of-Used-Nuclear-Fuel/.

Minor actinide separations in the reprocessing of spent nuclear fuels: recent advances in Europe

10

Giuseppe Modolo[1], *Andreas Geist*[2], *Manuel Miguirditchian*[3]
[1]Forschungszentrum Jülich, Institute of Energy and Climate Research, Nuclear Waste Management (IEK-6), Jülich, Germany; [2]Karlsruhe Institute of Technology, Institut für Nukleare Entsorgung (INE), Karlsruhe, Germany; [3]DEN, Commissariat à l'Énergie Atomique et aux Énergies Alternatives, Marcoule, France

Acronyms

ACSEPT	actinide recycling by separation and transmutation
BTBP	bis-triazinyl-bipyridine
BTP	bis-triazinyl-pyridine
CDTA	cyclohexanediaminetetraacetic acid
DEHiBA	*N*,*N*-di-(ethyl-2-hexyl)isobutyramide
DF	decontamination factor
DIAMEX	diamide extraction
DIDPA	di-*iso*-decylphosphoric acid
DMDBTDMA	*N*,*N*′-dimethyl-*N*,*N*′-dibutyl-tetradecyl-malonamide
DMDOHEMA	*N*,*N*′-dimethyl-*N*,*N*′-dioctyl-2-(2-hexyloxyethyl)-malonamide
DTPA	diethylenetriaminepentaacetic acid
EXAm	extraction of americium
GANEX	grouped actinide extraction
GEN-IV	Generation IV
HAC	high active concentrate
HAR	high active raffinate
HDEHP	di(2-ethylhexyl) phosphoric acid
HEDTA	*N*-(2-hydroxyethyl)ethylenediaminotriacetic acid
HLLW	high-level liquid waste
IAEA	International Atomic Energy Agency
MA	minor actinides (Np, Am, and Cm)
OECD/NEA	Organisation for Economic Cooperation and Development-Nuclear EnergyAgency
P&T	partitioning and transmutation
PUREX	plutonium uranium reduction extraction
SACSESS	safety of actinide separation processes
SANEX	selective actinide extraction
TBP	tri-*n*-butylphosphate, extractant of the PUREX process

Reprocessing and Recycling of Spent Nuclear Fuel. http://dx.doi.org/10.1016/B978-1-78242-212-9.00010-1

TEDGA	*N*,*N*,*N*′,*N*′-tetraethyl diglycolamide
TPH	hydrogenated tetrapropene
TODGA	*N*,*N*,*N*′,*N*′-tetraoctyl diglycolamide
TRU	transuranium elements

10.1 Introduction

Currently, about 10,500 t of used nuclear fuel are discharged every year from nuclear power reactors worldwide (IAEA, 2008). After a typical burn up of 40 GWd/t, the used fuel contains the major fertile uranium (95% U-238) component, residual fissile uranium (0.8% U-235), the mainly short-lived fission products (3-4%), and a significant amount of the higher actinides (approximately 1%) neptunium (Np), plutonium (Pu), americium (Am), and curium (Cm). It is these higher actinides that are mainly responsible for the long-term radiotoxicity of the used fuel. At present, two management options are considered worldwide: the open fuel cycle, where the used fuel is directly sent to long-term storage in a deep geological repository, and the closed fuel cycle including reprocessing. The latter can recover the residual uranium and plutonium for reuse in MOX fuel and condition the wastes into suitable forms (e.g., vitrified glass) for disposal.

The protection of the biosphere from highly radiotoxic used nuclear fuel constituents over very long timescales is extremely important. Both the used nuclear fuel (direct disposal) and the highly active waste from reprocessing (in a closed cycle) need to be stored for a very long time (over 100,000 years) in a well-shielded, leach-resistant deep geological repository.

The final disposal of the vitrified high active wastes from the reprocessing of spent nuclear fuel in an underground repository is a complex problem mainly related to the fact that these wastes contain long-lived radionuclides with high radiotoxicity, and this remains the case for a very long period of time, that is, thousands to millions of years. A possible solution to this problem is not to incorporate these long-lived radionuclides into the vitrified waste. After separation (partitioning) before the vitrification step, the long-lived radionuclides could be partially transmuted into short- or medium-lived or stable nuclides by nuclear means. This is the so-called partitioning and transmutation strategy (P&T) under study in several countries (OECD-NEA, 1999, 2006, 2011). The benefits of "advanced fuel cycle" schemes including P&T in terms of waste management can be summarized as follows (OECD-NEA, 2011):

- Reducing the capacity needs for geological repositories by reducing the volumes and the heat of high-level wastes to be disposed of.
- Reducing the repository long-term risk by reducing long-term radiotoxic inventories.
- Reducing uncertainties in repository performance, especially for disruptive scenarios (e.g., human intrusion).
- Improving public acceptance of geological disposal.

Up to now, hydrometallurgical (i.e., solvent extraction) processes have been the reference technology for nuclear fuel processing at commercial scale for more than 60 years, and the reasons for this are multiple. Solvent-extraction processes are able

to provide extremely high separation factors, considering both recovery and purification yields, without generating excessive amounts of secondary waste, which is very important in the nuclear industry.

In hydrometallurgical processing, after dissolution of irradiated fuel in hot nitric acid, target solutes such as actinide ions are extracted into an organic phase that is immiscible with the aqueous phase. Extraction is promoted by a reaction between the actinide ions to be extracted and a selective extracting agent present in the organic phase. As the resulting complexes are soluble in the organic phase, the actinide ions are transferred from the aqueous to the organic phase, separating them from other solutes such as fission products. By reversing the complex formation reaction, an aqueous product solution containing actinide ions only is generated while the organic phase is recycled.

Plutonium, the main contributor to the long-term radiotoxicity, can already be recovered today by the PUREX (plutonium uranium reduction extraction) process, as commercially operated in France, the United Kingdom, Russia, and Japan (IAEA, 2008). Among the long-lived radionuclides to additionally remove from the high active raffinate (HAR) (i.e., the aqueous raffinate or concentrate issuing from the first cycle of the PUREX process), those belonging to the so-called minor actinides (MAs), neptunium, americium, and curium are the most important to eliminate. It has been shown in many studies that the radiotoxic inventory can be reduced by a factor of up to 10 if all plutonium is recycled and fissioned. Reduction factors higher than 100 can be obtained if, in addition, the MAs are recycled. The recovery of Np can certainly be done by the PUREX process (see Section 10.3). This is not the case for americium and curium, which exist in the +III oxidation state in the spent fuel aqueous dissolution liquor. These trivalent MAs possess very low affinities for tri-*n*-butylphosphate (TBP), the extractant used in the PUREX process, and thus require additional processes for their separation. The chemical similarity of trivalent actinides (An(III)) and lanthanides (Ln(III)) combined with the unfavorable mass ratio necessitate very demanding and complex process steps. The high neutron-capture cross sections of the lanthanides would hinder an efficient transmutation of the trivalent MAs, and, therefore, the two groups of elements have to be separated. The separation of trivalent 4f and 5f elements has consequently become a challenging but key issue in the technical feasibility demonstration and success of the P&T strategy (Hill, 2010).

10.1.1 Scope

Several review papers covering a broad spectrum of R&D issues related to partitioning of MAs have been published during the last decade. This complementary report provides an overview of important developments in the field of MA separation processes achieved in Europe. Most of the processes reported in this chapter have been developed within the scope of European collaborative projects from the third to the seventh European Union (EU) Framework Programmes (see Section 10.2). Neptunium recovery from used fuel has not been considered in most European projects because, in a partitioning strategy, this element could be separated simply using an improved PUREX process, which will be separately discussed in Section 10.3. The challenges,

the key separation chemistry involved, and the strategies adopted for the process demonstrations are then introduced in Section 10.4. Significant scientific and technical progress has been made in European collaborative research that has resulted in the development and demonstration of several new processes, as described in the following sections: DIAMEX (diamide extraction) (Section 10.5), SANEX (selective actinide extraction) (Section 10.6), GANEX (Section 10.7), and EXAm (extraction of americium) (Section 10.8). Section 10.9 will conclude with a perspective of the likely future trends.

10.2 Overview of European partitioning projects within the Framework Programmes FP3 to FP7

In Europe, research for the design of hydrometallurgical processes for the partitioning of trivalent MAs was primarily triggered by two French waste management acts (1991 and 2006). These acts enabled organization of the French research program on P&T of long-lived radionuclides that includes preparing the construction of both an industrial MA partitioning facility and an actinide-burner reactor by 2025, under the aegis of the French Commissariat à l'Énergie Atomique et aux Énergies Alternatives (CEA) (Rouyer, 1992; Warin, 2007).

At the European level, several research programs dedicated to hydrometallurgical separation of MAs have been funded by the European Commission (EC) within the Framework Programmes FP3 to FP7.

European research over the last two decades, that is, in the NEWPART (Madic et al., 2000), PARTNEW (Madic et al., 2001, 2004), and EUROPART (Madic and Ouvrier, 2008) programs, has resulted in the development of multicycle processes (e.g., DIAMEX+SANEX) and recently within the FP7 project ACSEPT (actinide recycling by separation and transmutation) (Bourg et al., 2011) the development of innovative processes with reduced numbers of cycles (innovative-SANEX, 1-cycle-SANEX) has also been envisioned.

In FP3, a joint research program (Madic and Hudson, 1998) was carried out between the CEA (France) and the University of Reading (United Kingdom), related to the investigation of new chemical systems for the separation of long-lived radionuclides, based on solvent-extraction techniques. Among the long-lived radionuclides concerned, it was decided to focus exclusively on the MAs. To ensure that the separation processes applied will generate a minimum of secondary solid wastes, it was decided that all the chemical reagents used in these new processes, and particularly the extractants, should be totally destructible into gases, easily releasable into the environment at their "end of life." Hence, all the substances investigated only contained atoms of carbon (C), hydrogen (H), oxygen (O), and nitrogen (N). This molecular engineering strategy has been dubbed the *CHON principle*. These choices demanded completely incinerable extractants to perform the separations from high-level liquid waste (HLLW) solutions to be processed, without any decrease in the nitric acid concentration of the feed, in order to prevent major drawbacks, like

precipitate formation. At that time it was considered impossible to separate An(III) ions from the fission products, including Ln(III), from HLLW in a single step. Thus, faced with the difficulty of the problem, it was decided to perform this separation in a two-step approach using two extraction cycles. The first step aimed to separate the mixture of An(III) + Ln(III) from most of the fission products other than lanthanides, from the HLLW that comes from the PUREX process. The second step concerned the separation of the group of An(III) (Am + Cm) from Ln(III). Considering the very high Ln/An mass ratio of 20:1, this separation should preferably be performed by selective extraction of An(III). At that time, it was considered necessary to develop a consecutive third step to separate americium from curium. The SESAME (process for Am/Cm separation by the selective extraction of Am(VI) by TBP by electrolysis techniques) process (Madic et al., 2002b) was developed, based on the oxidation of americium to oxidation state (VI) prior to its selective extraction (by, e.g., TBP), but this was not the subject of research within the Partitioning FP3 project.

Nonselective diamide-based extractants, with the formula $(RR'NCO)_2CHR''$, were selected for the first cycle (Musikas, 1988). A first version of the DIAMEX process, based on the use of dimethyl-dibutyl-tetradecyl-malonamide (DMDBTDMA), was designed and successfully tested on genuine HLLW. For the An(III)/Ln(III) separation cycle (the so-called SANEX process), the potential of synergistic mixtures of nitrogen polydendate ligands and long-chain-substituted carboxylic acids were investigated. The initial mixture considered, tripyridyltriazine (TPTZ) + α-bromodecanoic acid, achieved this separation, but presented a number of drawbacks including (i) partial transfer of TPTZ from organic to aqueous phases; (ii) the nonincinerable character of α-bromodecanoic acid; and (iii) the relatively high pH required to perform An(III)/Ln(III) separations.

The research in this hydrometallurgical domain was continued during the European fourth framework program (FP4) NEWPART project, where eight laboratories were involved, and the target elements to be separated from the waste were the trivalent americium and curium (without modification of the oxidation state). The target waste to be used as a feed in the processes to be developed was the acidic (3-4 mol/L HNO_3) HAR or HLLW generated during the reprocessing of spent nuclear fuel by the PUREX process. In order to minimize the amount of solid secondary waste, the proposed aim for the process design was to develop molecules (extractants, organic diluent, water-soluble reagents) which fulfill the above-mentioned CHON principle. An exception was made for the S-donor bearing ligands (e.g., dithiophosphinic acids), which are highly selective extractants for actinides(III). The work program thus had been defined in continuity with the work performed in the third FP by CEA and the University of Reading. It consisted of the further development of the DIAMEX and SANEX processes for An(III)/Ln(III) separations, and for both parts of the work, fundamental and process development research were carried out.

The aim of the research carried out within PARTNEW, a research project cofinanced by the EC in the framework of the FP5 program, was to study and define efficient solvent-extraction hydrometallurgical processes for the partitioning of the trivalent americium and curium ions from the HAR and for the mutual Am(III)/Cm (III) separation. The research done within PARTNEW followed on the previous

research projects mentioned above. Eleven laboratories were involved in the consortium. Within the DIAMEX domain of research, several new bis-malonamides with interesting extraction properties were prepared. Several DIAMEX processes were developed and tested, some of them with synthetic spiked and some with genuine feed solutions. The highlight of PARTNEW was the successful development and "hot" implementation of a DIAMEX process for the treatment of a high active concentrate (HAC), the industrial product before the vitrification step. In addition, a new DIAMEX process was developed that used the *N*,*N*,*N*′,*N*′-tetraoctyl-diglycolamide (TODGA).

Within the SANEX domain, numerous polydentate nitrogen and sulfur-bearing ligands were prepared, and the basic understanding of the reactions between An(III) and Ln(III) and these ligands was improved with the aid of thermodynamic, kinetic, and structural studies together with molecular modeling. Several SANEX processes were developed and tested, and those based on BTP (bis-triazinyl-pyridine) ligands were tested on genuine feed solutions. Although interesting results were obtained, unfortunately the chemical stability of the *i*-Pr-BTP used was not sufficient to enable a robust SANEX process to be proposed for industrial process development.

Due to the high decay heat and neutron emission of curium, any dry or wet fabrication process will require remote handling and continuous cooling in neutron-shielded hot cells. As it will be difficult to fabricate curium containing targets or fuel, it was considered necessary to define an additional Am(III)/Cm(III) separation process. The separation of adjacent trivalent actinides represents an even more challenging task than the An(III)/Ln(III) separation. Two Am(III)/Cm(III) separation processes were developed and tested in PARTNEW. They were based on the use of (1) the malonamide DMDOHEMA ($SF_{Am/Cm} = 1.6$) and (2) a synergistic system composed of an aromatic dithiophosphinic acid + trisethylhexylphosphate ($SF_{Am/Cm}$ around 8).

The FP5 project CALIXPART (Arnaud-Neu et al., 2004) was also related to the partitioning of MA using calixarenes, cavitands, podants, and others, on which several chemical binding groups were grafted. Some of them showed interesting actinide(III) extraction and An(III)/Ln(III) separation properties. However, none of them were further developed for process applications using genuine PUREX raffinate solutions.

The purpose of the hydrochemistry part of the FP6 integrated project EUROPART (Madic and Ouvrier, 2008), was to focus on selective extractants for removal of MAs from high active liquid wastes. Research and development objectives were to synthesize and test new ligands; to select the most promising compounds and then to optimize the relevant processes via two different routes:

- The first route was the direct selective extraction of MAs (Am, Cm) in one cycle from a PUREX raffinate or in an alternative two-cycle process from a first-cycle product containing trivalent lanthanides and actinides. This work was built on the previously acquired knowledge, and the synthesis of new extracting molecules such as polyamides, polydentate nitrogen, or sulfur-bearing extractants, calixarenes, and cosans, continuing the research performed within the PARTNEW and CALIXPART FP5 programs.
- The second route was the group separation of actinides (Pu, Np, Am, Cm) after a first uranium separation, either by liquid-liquid extraction or by solid extraction. The extracting

molecules for the actinide group separation were directly derived from those studied for the one- or two-cycle selective extraction of MAs. Several process concepts were studied, including the use of mixtures of extractants, bi-topic extractants (new concept of extractant molecules with two different complexing or chelating groups)- and chromatographic techniques.

Within EUROPART, more than 100 new ligands were synthesized and their complexing and extraction properties were assessed in screening tests according to a precise extraction protocol. Only a few ligands successfully passed the screening tests, thus fulfilling the requirements for further process development (i.e., solubility in suitable organic diluents, high extraction and separation performance, extraction reversibility, good radiochemical stability, etc.). Basic and process development studies were also carried out on several separation systems developed in former FP5 projects (CALIXPART, PARTNEW). For the coextraction of An(III) and Ln(III) from PUREX raffinates, five systems were studied besides the reference DIAMEX solvent, consisting of dimethyl-dioctyl-hexylethoxy-malonamide (DMDOHEMA), dissolved in hydrogenated tetrapropene (TPH). Among these five systems, only the "TODGA/TBP" mixture was selected to prove the scientific feasibility of the coextraction of An(III) and Ln(III) from PUREX raffinates, and highly active tests have been successfully carried out on genuine feed solutions (Magnusson et al., 2009b).

For the separation of An(III) from Ln(III) in DIAMEX product solutions, two SANEX systems based on $CyMe_4$-BTBP were studied in the EUROPART project. In both systems the solvent contained an additional extracting agent to improve kinetics, either TODGA or DMDOHEMA. A spiked SANEX process test was performed with the $CyMe_4$-BTBP+TODGA solvent (Modolo et al., 2013). A flow sheet was designed for a hot SANEX test using a $CyMe_4$-BTBP+DMDOHEMA solvent (Magnusson et al., 2009c); the corresponding hot test (Magnusson et al., 2009a) was performed shortly after the EUROPART project was finished.

For the actinide group separation (with actinide ions in oxidation states III to VI) directly from spent fuel dissolution solutions, no system had been developed up to a highly active test: the "TODGA/TBP" mixture dissolved in TPH, which was also selected for actinide group separation, was investigated in batch tests on genuine PUREX HAR only, and not on spent nuclear fuel (or target) dissolution liquors. No efficient bitopic ligand, fulfilling all the requirements for process development, could be designed in spite of all the efforts applied, even considering covalently bonded CMPO-COSAN and CMPO-TODGA compounds as "bitopic" ligands.

As EUROPART and the earlier FP4 and FP5 integrated projects—NEWPART and PARTNEW—have shown, the separation of the MAs from PUREX raffinate or concentrate is very challenging. By the end of EUROPART, some partitioning processes had been demonstrated to be "technically" feasible on the laboratory scale, with some actual demonstrations performed with irradiated spent fuel at the CEA or at the European Commission's Joint Research Centre, Institute for Transuranium Elements (ITU) hot laboratories. These multicycle processes made use of different extractants for every single process and, by this point in European development programs, one of the most promising options for the removal of An(III) was considered to be the DIAMEX-SANEX concept (Miguirditchian et al., 2007; Bourg et al., 2011).

There are, however, significant challenges to face in optimizing these processes and proving the viability of the technology at the industrial scale in the context of an advanced fuel cycle. Furthermore, the integration of these new separation processes with Generation IV (GenIV) reactor fuel cycles has yet to be demonstrated. In most of the GenIV systems the comanagement of all the actinides (U, Np, Pu, Am, Cm, etc.) through recycling is foreseen. Different routes for the treatment and recycling of actinides are still open, specifically (a) the homogeneous recycling in mixed fuels via a prior-grouped separation and (b) their heterogeneous recycling in targets or core blankets via the selective separation of MAs (Am, Cm) from fission products. In addition, various forms of fuels are still being considered according to the reactor type: most likely oxides, carbides, and nitrides or even metallic fuels are options.

Within the hydrometallurgical domain of the FP7 ACSEPT collaborative project (Bourg et al., 2011), the development of new extracting agents and innovative separation processes with a reduced number of cycles was envisioned. A schematic representation of the processes studied is shown in Figure 10.1. A new approach, which was also studied within the ACSEPT project, is the GANEX (grouped actinide extraction) concept (Figure 10.1, left) addressing the simultaneous partitioning of all transuranium (TRU) elements for their homogeneous recycling in advanced GenIV reactor systems. In the GANEX concept developed by CEA (France), bulk uranium is removed in the GANEX first cycle (e.g., using a monoamide extractant) (Miguirditchian et al., 2009b), followed by the TRU group separation in the GANEX second cycle (Miguirditchian et al., 2009a). Other approaches have also been

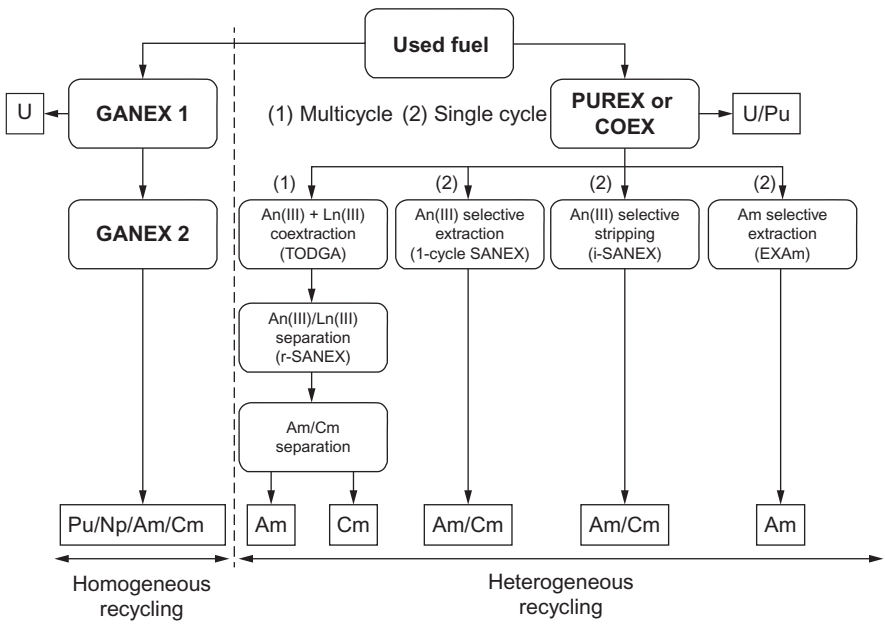

Figure 10.1 European hydrometallurgical partitioning process strategy for the homogeneous and heterogeneous recycling of actinides from used fuel.

proposed in the frame of the ACSEPT program (Aneheim et al., 2013; Bell et al., 2012) (cf. "*Overview and status of GANEX process*") and are described in more detail in Section 10.5. Single-cycle processes (Figure 10.1, right) are advantageous in comparison to multicycle processes as they would make the advanced reprocessing of nuclear waste easier and more economical. Consequently, in France, the americium-selective extraction process "EXAm™" (Rostaing et al., 2012) was recently presented by the CEA (cf. Section 10.8) as a solution to separate americium alone from PUREX HLLW in one cycle.

Finally, two new advanced concepts based on the PUREX-SANEX process route have been studied in Europe: the innovative-SANEX concept and the 1-cycle-SANEX concept (Wilden et al., 2012). In the 1-cycle-SANEX concept, the direct and selective extraction of trivalent actinides from PUREX raffinate by a highly selective extractant system is required. This is a complicated task since the PUREX raffinate includes a wide range of elements with varying concentrations (Wilden et al., 2011). In the innovative-SANEX process, An(III) and Ln(III) are coextracted from a PUREX raffinate and the An(III) ions are separated from Ln(III) in a selective stripping step, for example, using a hydrophilic polyaminocarboxylic acid such as diethylenetriaminepentaacetic acid (DTPA) (Nilsson and Nash, 2007). The most important developments of this kind of process based on selective stripping include the reversed TALSPEAK (trivalent actinide-lanthanide separation by phosphorus reagent extraction from aqueous complexes) process developed in the United States, di-*iso*-decylphosphoric acid (DIDPA) and SETFICS (solvent extraction for trivalent F-elements intragroup separation in CMPO-complexant system) processes developed in Japan, and the DIAMEX-SANEX process (France). The TODGA-SANEX process was developed by the CEA and a hot demonstration was carried out within the ACSEPT project (Hérès et al., 2009). However, a common feature of these processes is the complicated and precise pH control required during the important An(III) stripping step. Within the ACSEPT project, the new hydrophilic complexing agent SO_3-Ph-BTP was recently introduced for the An(III) selective stripping step (Geist et al., 2012). This molecule combines the high selectivity of the well-known BTP family (bis-triazinyl-1,2,4-pyridines) of extracting agents with high solubility in aqueous phases. Ln(III)/An(III) separation factors in the range of 1000 were achieved. The selective stripping of An(III) now becomes possible, even at relatively high nitric acid concentrations of up to 1 mol/L HNO_3. More details can be found in Section 10.6.

10.3 Neptunium

A significant amount of neptunium (300-700 g/t_{HM} at burn ups of 30-50 GWd/t_{HM}) is produced during reactor operation due to neutron absorption on ^{238}U and ^{235}U isotopes and subsequent decays to ^{237}Np (Yoshida et al., 2011). The management of the highly radiotoxic alpha-emitting ^{237}Np with a half-life of 2.14 million years is still an issue and matter of concern within advanced fuel cycles including P&T (OECD-NEA, 1999). The current practice in spent fuel reprocessing is to treat it as a waste, as all the neptunium is routed to the liquid high-level waste for vitrification. The chemical

and redox behavior of neptunium under conditions relevant to reprocessing of spent nuclear fuel (PUREX process) is very complex and has been the scope of many studies (Birkett et al., 2007; Herbst and Baron, 2011; Bernier et al., 2012; Precek and Paulenova, 2010).

Neptunium is present in the feed solution to the separation process as a mixture of Np(V) and Np(VI) according to the following redox equilibrium:

$$2NpO_2^+ + 3H^+ + NO_3^- \rightleftarrows 2NpO_2^{2+} + HNO_2 + H_2O \quad (10.1)$$

In the hexavalent form, it is extracted together with uranium and plutonium by TBP, in the extraction part of the PUREX process. In contrast, Np(V) has a very low extractability into the PUREX solvent (typically 30% TBP in kerosene-type diluent). The oxidation state of neptunium ions in the process solution, however, varies significantly depending on the chemical environment. According to Equation 10.1, HNO_2 reduces Np(VI) to Np(V). On the other hand, at low nitrous acid concentration, which coexists in nitric acid solution of high concentrations, it accelerates the oxidation of Np(V) to Np(VI). Hence, the role of HNO_2 is twofold (thermodynamic and kinetic). In addition, during the extraction operation the equilibrium is shifted to the right, because Np(VI) and HNO_2 are well extracted by TBP.

In the current operating conditions at the reprocessing sites in La Hague, France, and Thorp, United Kingdom, around 25-30% of neptunium is left in the PUREX raffinate and the remaining fraction follows the uranium and plutonium in the solvent product. During the further uranium and plutonium purification steps, neptunium is separated again and routed back to the high-level wastes for vitrification (Taylor et al., 2013).

Many studies have been carried out to develop an advanced PUREX process, with the aim of improving the neptunium extraction efficiency by carefully controlling the Np(V)/Np(VI) equilibrium. Very promising results showing full neptunium recovery in advanced PUREX process flow sheet trials have been obtained at different sites across the world and were recently summarized by Taylor et al. (2013).

Of particular importance are the advanced flow sheets trialed at the CEA Marcoule in France, the Japan Atomic Energy Agency (JAEA), the China Institute of Atomic Energy (CIAE), and at National Nuclear Laboratory (NNL) at Sellafield, United Kingdom, which are summarized in Table 10.1. It has been shown that an increase of the nitric acid concentration in the PUREX feed solution should lead to a high neptunium extraction yield (>99%), thanks to an increase in Np(V) oxidation kinetics (Equation 10.1).

An alternative scenario is that neptunium is routed to the PUREX high-level raffinate waste stream with the other MAs. A considerable amount of work has been performed to develop methods for the partitioning of the actinides (including neptunium) from high active liquid waste streams (e.g., HLLW). Several partitioning processes based on solvent extraction (not TBP system) have been proposed (OECD-NEA, 1999).

The well-known TRUEX process for the recovery of all actinides from various types of nuclear waste solutions is based on *n*-octyl(phenyl)-*N*,*N*-diisobutyl-carbamoyl methylphosphine oxide (CMPO) extraction (Horwitz et al., 1982; Kolarik and Horwitz, 1988). Because Np(V) is inextractable with CMPO, it must be either oxidized to Np(VI) or reduced to Np(IV) with special REDOX chemicals.

Table 10.1 Summary of conditions and results from improved PUREX flow sheet trials reported in the literature

Laboratory reference	U (g/L) Pu (g/L) Np (mg/L)	Process equipment test scale	$[HNO_3]$ (mol/L)	Np recovery (%)
CEA (Dinh et al., 2008)	U + Pu = 250 Np: not quoted	Pulsed column pilot scale hot test	4.5	>99.6
CIAE (Zhang et al., 2013)	220 2 40	Mixer-settler lab simulant test	4.5	99
JAEA (Nakahara et al., 2012)	126 23 184	Centrifugal contactor hot test	5.5	>98.99
NNL (Taylor et al., 2013)	250 0 150	Centrifugal contactor lab simulant test	4.5	>99

Adapted from data reported in Taylor et al. (2013).

Solvent extraction with DIDPA was applied in Japan to the partitioning of all actinides from HLLW (Morita et al., 1996). Even Np(V) in the sample solution is extracted by DIDPA. The addition of H_2O_2 enhances the rate of the extraction of Np(V) (Morita and Kubota, 1988; Yoshida et al., 2011).

The trialkyl phosphine oxide (TRPO) process was developed at Tsinghua University in China during the 1990s for the recovery of neptunium, plutonium, and trivalent actinides from HLLW. In the TRPO process, the oxidation state of neptunium is adjusted to the tetravalent state by electrolytic reduction (Zhu and Song, 1992; Chen et al., 2007).

Further details about the extraction of neptunium with other extracting agents can be found in different review articles (Mathur et al., 2001; Nash et al., 2006; Tachimori and Morita, 2010).

10.4 Trivalent actinide separation: challenges, key separations chemistry, and strategies to be adopted

The separation of trivalent actinides from the HAR (i.e., the aqueous raffinate or concentrate from the PUREX process) is challenging due to the presence of nitric acid, fission products (one-third of them being lanthanides), and corrosion/activation products that can interfere with actinide extraction.

TBP extracts tetravalent and hexavalent actinide ions from nitric acid solutions, while trivalent and pentavalent actinide ions are practically inextractable and remain in the PUREX raffinate. Thus, uranium (as UO_2^{2+}), plutonium (as Pu^{4+}), and neptunium (if oxidized to NpO_2^{2+}, cf. Section 10.3) can be separated by the PUREX process involving TBP as extracting agent. However, this is not the case for americium and

curium, which are present as trivalent ions in the fuel dissolution solution. Even though Am(III) can be oxidized to higher oxidation states to make it extractable by TBP, this requires strong oxidants (Runde and Mincher, 2011). Oxidation of Cm (III) to higher oxidation states is virtually impossible in aqueous systems.

The separation of Am(III) and Cm(III) from the PUREX raffinate requires developing new processes and, hence, new extracting agents.

So-called DIAMEX processes were developed in France, utilizing alkylated malonamide extracting agents. More recently, alkylated diglycolamides (DGAs) have started replacing the malonamides (cf. Section 10.6).

Malonamides and DGAs coextract the lanthanide ions with Am(III) and Cm(III), due to the chemically similar behavior of trivalent actinides and lanthanides; indeed, it is well known that oxygen donor extracting agents do not discriminate trivalent actinides from lanthanides of the same cationic size (Peppard et al., 1957). Considering some lanthanides have large cross sections for neutron capture, their presence in transmutation fuels would impact transmutation efficiency. This requires separation of Am (III) and Cm(III) from the lanthanides(III).

The chemical similarity of trivalent actinides (An) and lanthanides (Ln) combined with the unfavorable mass ratio necessitates very demanding and complex process steps. This is due to the fact that both groups of elements are highly hydrated in an aqueous solution, with very similar ionic radii. Both are classed as “hard acids” in Pearson’s theory of hard and soft acids and bases and, thus, they react preferentially with hard bases, such as ligands involving oxygen atoms, by way of electrostatic interactions (Pearson, 1963). On the other hand, ligands involving electron-donor atoms less hard than oxygen (e.g., nitrogen or sulfur) are known to make An(III)-Ln(III) separation possible; this being the chief challenge posed by recovery of americium, and curium, from a PUREX raffinate.

Bearing in mind that the americium and curium inventory within the PUREX raffinate is low in comparison to the other constituents (HNO_3, FPs), the direct selective An(III) extraction would be the preferred but also the most challenging route, because the feed contains many other competing cationic species. This requires a highly selective extracting agent, which currently does not exist. However, the substantial developments made under successive EU projects have brought us significantly closer to this goal; see the 1-cycle-SANEX process described in Wilden et al. (2013).

Early work on actinide(III)/lanthanide(III) separation carried out in Europe focused on the selective extraction of actinides (SANEX process) from the DIAMEX product solution (i.e., from actinides(III) and lanthanides(III) in nitric acid solutions). Triggered by studies showing the potential of nitrogen and sulfur donor extracting agents (Musikas et al., 1980, 1983), the first European projects were commenced in the early 1990s (Kolarik et al., 1996; Madic and Hudson, 1998). These were followed by ever-larger European research projects, NEWPART, PARTNEW, EUROPART, ACSEPT, and the current project, SACSESS (safety of actinide separation processes; as described in the earlier section).

Much progress was made but no breakthrough was achieved until the development of new aromatic dithiophosphinic acids (Modolo and Odoj, 1998) (Figure 10.2 left) and alkylated BTP (Kolarik et al., 1999b) (Figure 10.2 right) in the late 1990s.

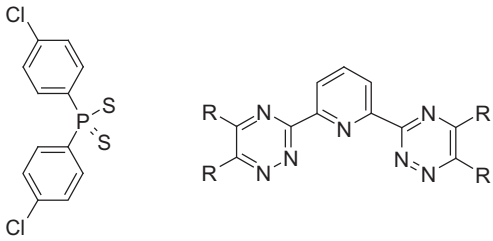

Figure 10.2 Earlier SANEX extracting agents: aromatic dithiophosphinic acids and alkylated BTP.

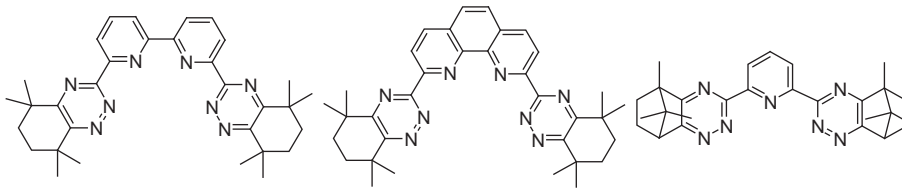

Figure 10.3 Current SANEX extracting agents: $CyMe_4$-BTBP, $CyMe_4$-BTPhen, and CA-BTP.

These were the first extracting agents to extract actinides(III) selectively over lanthanides(III) from highly acidic nitric acid solutions. From there a long journey led to the current class of bis-triazinyl-bipyridine (Foreman et al., 2006; Geist et al., 2006) (BTBP, Figure 10.3 left), bis-triazinyl phenanthroline (Lewis et al., 2011a, 2013) (BTPhen, Figure 10.3 middle), and CA-BTP (Trumm et al., 2011) (Figure 10.3 right) extracting agents (Ekberg et al., 2008; Lewis et al., 2011b; Panak and Geist, 2013) (cf. Section 10.6).

There are significant differences between the aromatic dithiophosphinic acids and the BT(B)P molecules:

1. Different donor atoms coordinating the metal ions to be extracted, namely sulfur versus nitrogen.
2. BT(B)P are CHON molecules while the dithiophosphinic acids are not.
3. BT(B)P are neutral (or solvating) extracting agents; whereas dithiophosphinic acids are acidic (i.e., cation exchanging) extracting agents; see the following equations. Solvating extracting agents coextract the metal ion(s) of interest, M^{n+}_{aq}, together with its anion(s), A^{-}_{aq}, (Equation 10.2) whereas acidic extracting agents exchange acidic protons for the metal ion to be extracted (Equation 10.3).

$$M^{n+}_{aq} + nA^{-}_{aq} + mL_{org} \rightleftarrows (MA_nL_m)_{org} \tag{10.2}$$

$$M^{n+}_{aq} + nHL_{org} \rightleftarrows (ML_n)_{org} + nH^{+}_{aq} \tag{10.3}$$

From a practical point of view, this means that extraction is performed at intermediate nitric acid concentration; back-extraction requires higher (acidic extracting agents) or lower (neutral extracting agents) nitric acid concentration. Note that TBP, malonamides, and DGAs are solvating extracting agents.

Current development aims at simplifying the DIAMEX + SANEX + Am(III)/Cm (III) separation scheme by reducing the number of process cycles; options being as follows:

(a) The 1-cycle-SANEX process omits the DIAMEX process; Am(III) and Cm(III) are directly extracted from the PUREX raffinate (Wilden et al., 2013).

(b) The innovative-SANEX process merges DIAMEX and SANEX into one process. This concept is based on the TALSPEAK process (Weaver and Kappelmann, 1964). Hydrophilic complexing agents selective for actinides(III) over lanthanides(III) such as DTPA or *N*-(2-hydroxyethyl)-ethylenediaminotriacetic acid (HEDTA) (Hérès et al., 2009) or water-soluble BTP (Geist et al., 2013b) are used to strip actinides(III) from a DIAMEX solvent loaded with actinides(III) and lanthanides(III).

Finally, as explained above, Am(III) and Cm(III) may need to be separated. Most extracting agents have a low Am(III)/Cm(III) selectivity (typical separation factors are ~1.6), requiring processes with a large number of stages. Using an aromatic dithiophosphinic acid system with a separation factor $SF_{Am/Cm}$ of approximately 8, a more compact process has been developed (Modolo et al., 2010).

A further step in simplification is the French EXAm™ process (Bollesteros et al., 2012; Rostaing et al., 2012), separating only Am(III) from the PUREX raffinate (cf. Section 10.8).

10.5 Overview and status of DIAMEX processes

10.5.1 An(III) + Ln(III) coextraction using malonamide-based solvents

The acronym DIAMEX stands for diamide extraction and is used for many different processes, using a diamide-based solvent. During the 1980s, the family of malonamides was developed for the extraction of An(III) + Ln(III) nitrates from HLLW solutions (Musikas, 1987, 1988; Musikas and Hubert, 1987; Nigond et al., 1994).

From the multitude of synthesized compounds, DMDBTDMA (Figure 10.4) was found to have the most promising properties for use in liquid-liquid extraction processes. A huge improvement over the formerly used phosphorus-based extractants was the complete combustibility of the solvent, containing only carbon, hydrogen, oxygen, and nitrogen (CHON principle) (Madic and Hudson, 1998).

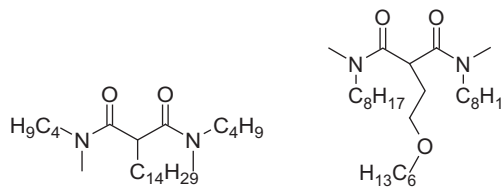

Figure 10.4 Structures of DMDBTDMA (left) and DMDOHEMA (right).

The DIAMEX process was successfully tested using real waste solution for the first time in 1993 in the CEA's Fontenay-aux-Roses research center (Madic et al., 1994), and it was also further developed within European collaborative projects (third, fourth, and fifth Framework Programmes).

In the NEWPART project (Madic et al., 2002a), 26 different malonamides were synthesized and tested for their suitability for An(III) extraction. In addition, intensive studies were conducted on hydrolysis and radiolysis stability. Laboratory studies have been undertaken at the CEA Marcoule plant to optimize the structure of the malonamide from the standpoint of its affinity for trivalent elements, its loading capacity, and the ease of managing its degradation compounds (Hill, 2010). Molecular optimizations ultimately led to a new DIAMEX reference molecule: the *N*,*N*′-dimethyl-*N*,*N*′-dioctyl-2-hexylethoxy-malonamide (DMDOHEMA, Figure 10.4) (Baron et al., 1997).

Its suitability for use in the process was demonstrated in a range of hot tests using genuine fuel solutions, both at CEA in Marcoule and at the ITU in Karlsruhe. The flow sheet of the DIAMEX process tested in a hot cell using a set of centrifugal contactors at the ATALANTE facility in CEA Marcoule is presented in Figure 10.5.

In the feed and in the scrubbing solutions, two complexing agents were added to prevent the coextraction of some fission products: (i) Zr(IV) and Mo(VI) were not extracted due to the presence of oxalic acid, and (ii) Pd(II) was not extracted owing to the presence of HEDTA.

In the framework of the 1991 French act, the technical feasibility of this DIAMEX process was demonstrated in 2005 at CEA Marcoule by performing a hot test in pulsed columns and mixer-settlers from a genuine PUREX raffinate (Figure 10.6); four meter-high pulsed columns were used in order to be representative of industrial contactors. The extraction and scrubbing steps were carried out in three pulsed columns while the stripping of both actinides and lanthanides was performed in mixer-settlers. Annular centrifugal contactors with immersed stirring rotors (ECRAN) were also used for the solvent treatment step. After 33 h, the americium and curium recovery yields

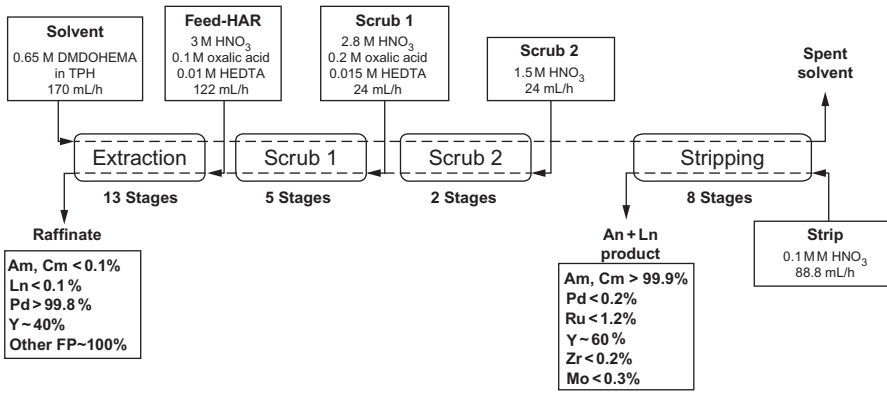

Figure 10.5 DIAMEX process flow sheet tested at the ATALANTE facility at CEA Marcoule in 2000 with genuine HAR.
Adapted from Madic et al. (2007).

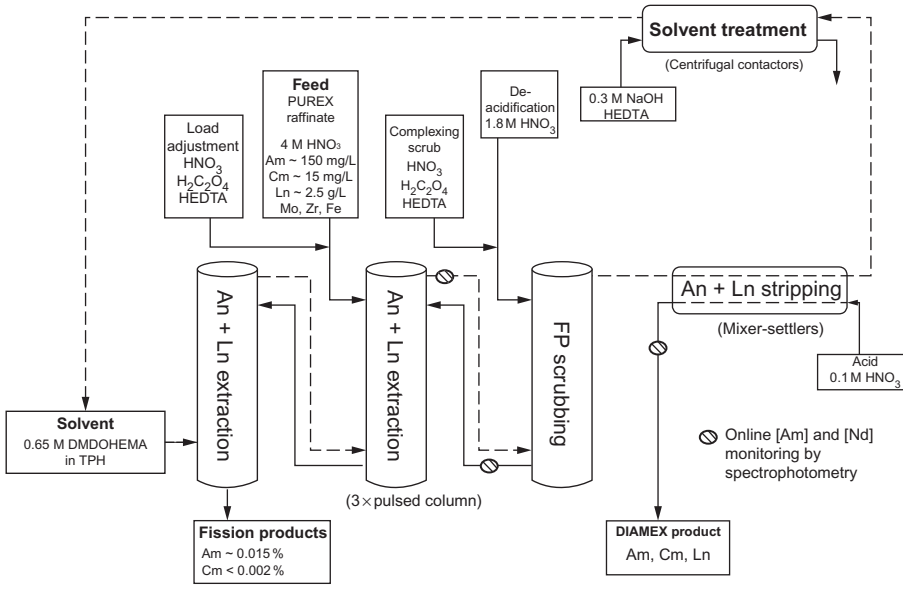

Figure 10.6 Flow sheet and main results from the DIAMEX demonstration test carried out in November 2005 in the CBP line at CEA Marcoule (Sorel et al., 2008).

exceeded 99.9% with losses of actinides in the raffinate and in the solvent lower than 0.1%. Good decontamination factors (DFs) of actinides were obtained with respect to fission and corrosion products ($DF_{Zr} = 889$, $DF_{Mo} = 108$, $DF_{Fe} = 10$), which confirmed the potential of the DMDOHEMA solvent for separation of trivalent actinides and lanthanides from fission products even in continuous contactors such as pulsed columns (Sorel et al., 2008).

Currently, during reprocessing with the PUREX process, the HAR is concentrated by evaporation and then denitrated for subsequent vitrification. The volume of the evaporator product, which is known as HAC, is reduced by a factor of 15 compared to HAR. As a result, the high active process flows to be processed are also reduced in volume, as is the size of the processing unit required. In the PARTNEW project, three partners (ITU, CEA, and FZJ) collaborated on the development of a DIAMEX process for separating An(III) from HAC (Serrano-Purroy et al., 2005c).

As a result of the very high metal concentrations in HAC, the question arose as to how the coextraction of certain transition metals (Zr, Mo, Pd, etc.) together with the trivalent actinides and lanthanides could be avoided. The first step was the production of a genuine starting solution by small-scale PUREX reprocessing of MOX fuel (1.4 kg; 30 GWd/t burn up). The spent fuel was dissolved in a 7 mol/L HNO_3 aqueous solution, then uranium and plutonium were extracted by a PUREX process. The HAR produced had a volume of 4.064 L; the HAR was then concentrated and denitrated to generate the HAC of 0.442 L volume, which was used for the active DIAMEX test. A final concentration factor of about 10 and an acidity of 4 mol/L were reached.

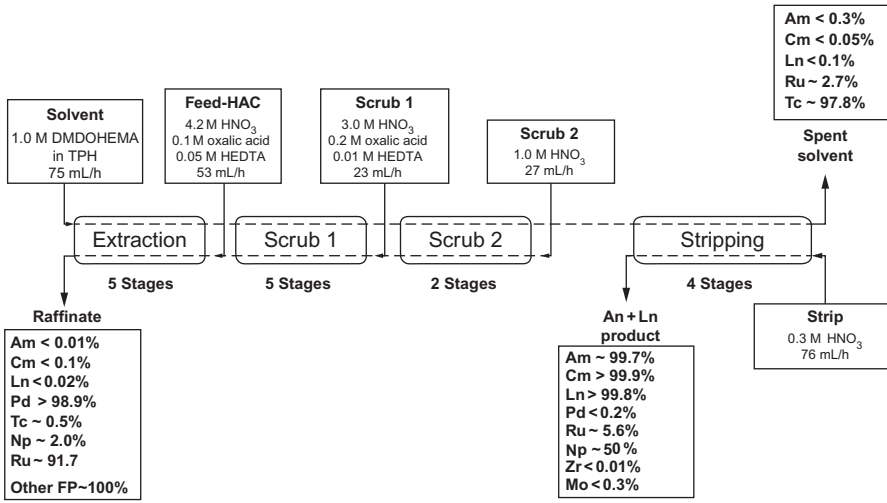

Figure 10.7 DIAMEX flow sheet tested at ITU on genuine HAC (Serrano-Purroy et al., 2005a).

In the experiment a precipitate mainly composed of strontium, zirconium, molybdenum, tin, and barium was formed. MA precipitation was not significant (<0.001%). In batch-extraction experiments, the thermodynamic distribution data were determined for the DIAMEX process and a 16-stage flow sheet was generated with the aid of computer code calculations (Modolo et al., 2007b; Serrano-Purroy et al., 2005a). To minimize the risks during a hot test (third-phase formation, precipitation, etc.), a cold DIAMEX test was first performed at FZJ, using a centrifugal contactor battery. More than 99% of the An(III) together with the Ln(III) were recovered and very high DFs for most of the fission products were achieved. Based on the positive results of the spiked test, a hot DIAMEX experiment was successfully performed in the hot cell facility at ITU using a genuine fuel solution (Figure 10.7). The results obtained were excellent: 99.9% of An(III) and Ln(III) were recovered in this test. Most fission products were not extracted, the exception being technetium, which had a DF = 217; yttrium, DF = 85; and ruthenium, DF = 1.1. Even better results should be achieved by process optimization; for example, by increasing the number of stages in the stripping section. The findings are discussed in detail in Serrano-Purroy et al. (2005a).

10.5.2 An(III) + Ln(III) coextraction using TODGA-based solvents

In the early 1990s, Stephan et al. (1991) reported on the extraction of different metals using multidentate ligands such as DGA. The DGA substance class also satisfies the CHON principle, and during the late 1990s, Japanese scientists recognized that these ligands are particularly suitable for extracting An(III) from acidic waste solutions (Sasaki et al., 2001).

Different DGAs were synthesized and TODGA (Figure 10.8) was found to have the best properties in terms of extraction, solubility in aliphatic solvents, and process

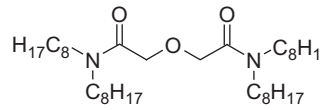

Figure 10.8 Chemical structure of TODGA.

stability. The tri-dentate TODGA extractant exhibits even higher affinity for trivalent actinides and lanthanides than the reference diamide DMDOHEMA, and it was realized that it could, therefore, be an interesting alternative to the diamide-based processes (Sasaki and Choppin, 1998; Sasaki et al., 2001; Tachimori et al., 2002).

However, TODGA has a tendency for third-phase formation in aliphatic solvents such as *n*-dodecane, particularly at high HNO_3 concentrations (Nave et al., 2004; Yaita et al., 2004).

Numerous basic studies with TODGA and related compounds can be found in the literature nowadays. Around 2001, almost no information existed on process development studies or process demonstrations and this motivated Modolo and coworkers to develop a continuous reversible partitioning process, which was successfully tested for the first time in 2003 in centrifugal contactors at Forschungszentrum Jülich (Modolo et al., 2003).

Following this, Modolo and coworkers optimized the partitioning process and suggested a new continuous process in which the extractant was a mixture of 0.2 mol/L TODGA and 0.5 mol/L TBP in TPH (Modolo et al., 2007a). The addition of TBP not only improved the hydrodynamic properties but also increased the loading capacity of the extractant and reduced the tendency for third-phase formation. In 2006, Forschungszentrum Jülich performed two tests in centrifugal extractors in cooperation with the ITU and CEA Marcoule (Modolo et al., 2008).

Based on encouraging results from the spiked tests, a hot process test was run at the end of 2006 in ITU's centrifugal contactor battery with almost identical results (Figure 10.9) (Magnusson et al., 2009b). Very high feed DFs were obtained for americium and curium (DF ~40,000) and the recovery of these elements was higher than 99.99%. Only yttrium and a small part of ruthenium were routed to the product fraction together with the lanthanides and the MA. The collected actinide/lanthanide fraction had an acidity of 0.13 mol/L HNO_3 and could be used for a subsequent An (III)/Ln(III) separation process. The acidity can be easily adjusted to cope with the requirements of the subsequent process. The main objective (>99.9% actinide separation) and a high fission product DF were achieved. The results were comparable to those obtained for the DIAMEX processes developed in France and within European projects (Serrano-Purroy et al., 2005b).

Finally, TBP was replaced by 1-octanol, making the TODGA solvent CHON compliant. A solvent consisting of 0.2 mol/L TODGA + 5 vol.% 1-octanol in kerosene was shown to have good performance with respect to loading and third-phase formation (Geist and Modolo, 2009). This solvent is currently the subject of further process development. A comprehensive review of the chemistry and process development studies using DGAs was recently published by Ansari et al. (2011).

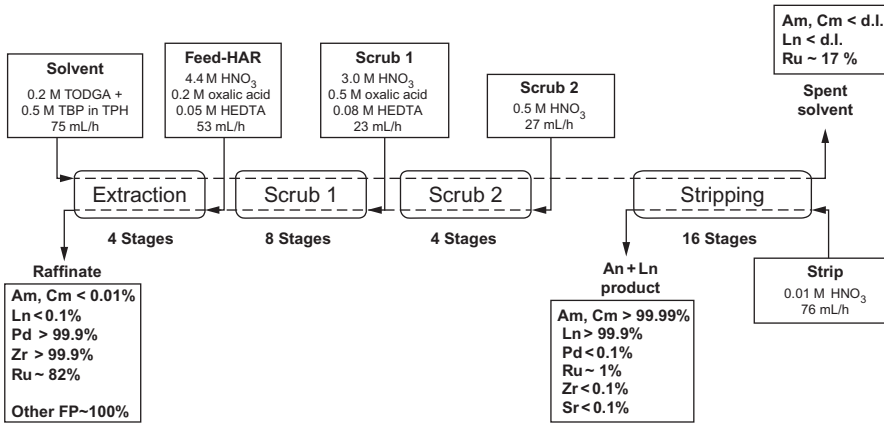

Figure 10.9 Flow sheet and main results of the hot TODGA-based process test carried out at ITU in 2006 (Magnusson et al., 2009b).

10.6 Overview and status of SANEX process development including SANEX variants

In the framework of earlier European research projects, several SANEX processes have been developed and demonstrated. These have been reviewed previously (Hill, 2010). Unfortunately, most of them had not much potential, as the chemical and radiolytic stability of the extracting agents was not good. In the last 5 years, however, several SANEX processes using the $CyMe_4$-BTBP extracting agent (Foreman et al., 2006) have been developed and demonstrated in Europe that seem more promising for an industrial application. $CyMe_4$-BTBP was the first SANEX extracting agent to combine favorable thermodynamics (i.e., high selectivity for actinides(III) over lanthanides(III) and suitable distribution ratios under extraction and stripping conditions) (Geist et al., 2006) with good chemical and radiolytic stability (Retegan et al., 2007; Fermvik et al., 2009; Magnusson et al., 2009d; Aneheim et al., 2011). Drawbacks are its low solubility (Ekberg et al., 2010), loading capacity (Magnusson et al., 2009d), and comparatively slow kinetics (Geist et al., 2013a). More recently developed extracting agents such as $CyMe_4$-BTPhen (Lewis et al., 2011a, 2013; Bremer et al., 2014) and CA-BTP (Trumm et al., 2011) address these issues; however, these extracting agents so far have not been used in a process.

The "classic" SANEX process extracts Am(III) and Cm(III) from a DIAMEX product solution, routing the lanthanides to the raffinate. Recently, new SANEX processes have been developed and tested, integrating the DIAMEX and the SANEX cycles into one process.

One way would be to simply skip the DIAMEX process and try to extract only Am (III) and Cm(III) directly from the PUREX raffinate. The late Charles Madic, coordinator of European partitioning projects from NEWPART to EUROPART, always

said that this would be his dream. No one seriously thought about making this dream come true until scientists at Jülich developed and tested the 1-cycle-SANEX process.

Another way is based on the established TALSPEAK process (Weaver and Kappelmann, 1964; Persson et al., 1984), coextracting Am(III), Cm(III), and lanthanides(III) into a DIAMEX-type solvent and selectively stripping Am(III) and Cm(III) from the loaded solvent using selective water-soluble masking agents. Such processes, called innovative-SANEX, were developed at the CEA and later in the ACSEPT project.

A description of several SANEX, 1-cycle-SANEX, and innovative-SANEX processes follows.

10.6.1 SANEX: Am(III)+Cm(III) extraction from DIAMEX product

In 1999, Kolarik introduced *n*-Pr-BTP (Figure 10.2 right, R = *n*-C_3H_7) as a highly efficient SANEX extracting agent (Kolarik et al., 1999a,b). Shortly afterwards the CEA ran a SANEX process test in a 16-stage laboratory-scale mixer-settler unit using *n*-Pr-BTP (Madic et al., 2000; Hill et al., 1999, 2000; Rat and Hérès, 2000). The feed solution contained 126 mg/L ^{241}Am(III), 1 mg/L ^{244}Cm(III), and inactive metal ions (Fe(III), Y(III), Ru(III), Pd(II), La(III)-Gd(III)) in 1 mol/L HNO_3; the organic phase was a solution of 40 mmol/L *n*-Pr-BTP in kerosene/1-octanol (70:30 vol.); stripping phase was 0.05 mol/L HNO_3. Promising results were achieved: <0.2% of Am(III) and Cm(III) were lost to the raffinate. The Am(III)+Cm(III) product solution contained <1% of the initial lanthanide mass. Further tests were run at the ITU in a 16-stage centrifugal contactor setup (Madic et al., 2000) and at the CEA using a 32-stage centrifugal contactor cascade (Madic et al., 2004). However, these tests indicated a low chemical and radiation stability of *n*-Pr-BTP (Hill et al., 2000; Rat and Hérès, 2000).

The isopropyl analogue, *i*-Pr-BTP (Figure 10.2 right, R = *i*-C_3H_7), was shown to have better chemical stability than *n*-Pr-BTP (Hill et al., 2002). Hence, the CEA designed a countercurrent lab-scale separation process with a solvent consisting of 10 mmol/L *i*-Pr-BTP+0.5 mol/L DMDOHEMA (added as a phase transfer catalyst to accelerate kinetics) in 1-octanol. A genuine high active feed solution was used. Two process tests were run in their 32-stage centrifugal contactor cascade, one test without and one test with solvent recycling. In the first test (without solvent recycling), >99.9% Am(III) and >99.8% Cm(III) were recovered together with <1% lanthanides(III). In the second test (with solvent recycling), the extraction performance of the solvent decreased by 40% after two cycles (Hill et al., 2004). Despite its good stability in nitric acid, *i*-Pr-BTP was degraded by alpha radiolysis.

Around the same time, the ALINA (actinide(iii)-lanthanide intergroup separation in acidic medium) process was developed at Jülich, using a synergistic mixture of bis(chlorophenyl)dithiophosphinic acid (Figure 10.2 left) and tri-*n*-octylphosphine oxide (TOPO) (Modolo and Odoj, 1999). The ALINA process (Modolo et al., 2002) was run using miniature centrifugal contactors; eight stages for extraction, eight stages for scrubbing, and eight stages for stripping. The solvent was 0.5 mol/L bis(chlorophenyl)dithiophosphinic acid and 0.15 mol/L TOPO in *tert*-butylbenzene/*iso*-octane (80:20). The feed solution contained 5.5 g/L lanthanides(III) in 0.5 mol/L HNO_3 and was spiked with ^{241}Am(III) and ^{244}Cm(III); the scrub solution was 1 mol/L

HNO_3 and the strip solution was 1.5 mol/L HNO_3. Flow rates were in the range of 50 mL/h for all solutions except the scrub solution, the flow rate of which was 12 mL/h. Less than 0.1% of Am(III) and 22% of Cm(III) was lost to the raffinate. The product solution contained 99.9% Am(III), ≈80% Cm(III), <0.01% of the lanthanides(III), and <0.1% of Y(III). Despite the fact that the test was not optimized for Cm(III) recovery, very good results were achieved.

Two SANEX processes based on selective extraction into a solvent containing the "next generation" nitrogen-donor ligand, $CyMe_4$-BTBP, were subsequently developed and tested, a spiked (Modolo et al., 2013) and a hot test (Magnusson et al., 2009a) being undertaken.

The flow sheet for the spiked test consisted of 12 extraction stages, 4 scrubbing stages, and 4 stripping stages. The solvent consisted of 15 mmol/L $CyMe_4$-BTBP +5 mmol/L TODGA in 1-octanol. The feed solution contained lanthanides(III) in nominal concentrations and Am(III)+Cm(III) spikes in 1.3 mol/L HNO_3. Scrub solution was 0.7 mol/L HNO_3; strip solution was a 0.5 mol/L glycolate solution set to pH 4. All flow rates were 10 mL/h. 0.08% of Am(III) and 0.3% of Cm(III) were lost to the raffinate; 0.04% of Am(III) remained in the solvent after stripping. The product solution, hence, contained approximately 99.9% of Am(III) and 99.7% of Cm(III). It was contaminated with approximately 0.1% of the lanthanide inventory and 3% of Y(III).

The flow sheet (Magnusson et al., 2009c) for the hot test (Magnusson et al., 2009a) was modified slightly to allow the whole process to be run in 1 day using the 16-stage centrifugal contactor setup at JRC-ITU (see Figure 10.10). Nine stages were used for extraction and three for scrubbing, and feed solution acidity was increased to 2 mol/L. The feed solution was a hot product solution originating from a TODGA-DIAMEX process test performed earlier (Magnusson et al., 2009b). A further difference between the spiked and the hot test was the choice of solvent, 0.25 mol/L DMDOHEMA being used (rather than 5 mmol/L TODGA) to accelerate kinetics. As shown in Figure 10.10, only 0.01% of Am(III) and 0.09% of Cm(III) went to the raffinate;

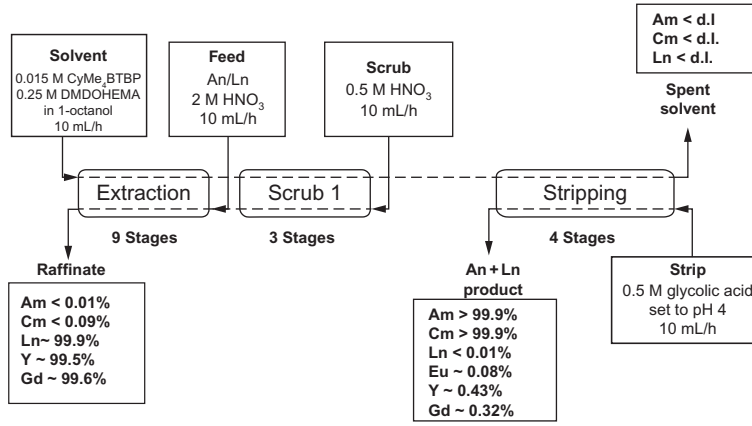

Figure 10.10 Flow sheet and main results of the hot SANEX $CyMe_4$-BTBP/DMDOHEMA process test carried out at ITU (Karlsruhe, Germany) in 2008 (Magnusson et al., 2009a).

no Am(III) or Cm(III) was found in the solvent after stripping. The product solution contained >99.9% of Am(III) and Cm(III), <0.01% of the lighter lanthanides, and 0.1-0.4% of Y(III), Eu(III), and Gd(III).

The better performance of the hot test compared to the spiked test was mainly due to the more efficient centrifugal contactors (Robatel BXP-012) used for the former process test (Magnusson et al., 2009a).

The SXProcess computer code used to calculate the flow sheet for the hot $CyMe_4$-BTBP+DMDOHEMA SANEX test has since been further developed and improved (Magnusson and Malmbeck, 2012; Magnusson et al., 2013a,b). It was also used to calculate the flow sheets for the 1-cycle-SANEX and SO_3-Ph-BTP innovative-SANEX processes (see below).

10.6.2 1-Cycle-SANEX: Am(III)+Cm(III) extraction from PUREX raffinate

The direct extraction of Am(III)+Cm(III) from the PUREX raffinate could lead to a simplification of the overall An(III) recycling strategy; ideally, the DIAMEX process could simply be eliminated. However, this is an obvious challenge: the extracting agent must have sufficient affinity for the target actinide ions at elevated nitric acid concentration (3-4 mol/L) and selectivity over all fission and corrosion products present in the fuel dissolution solution.

Although, for example, $CyMe_4$-BTBP extracts actinides(III) selectively over lanthanides(III) from 3 to 4 mol/L HNO_3, the coextraction of iron, nickel, zirconium, and palladium (Aneheim et al., 2013) has hampered the development of such a process so far. Nevertheless, a 1-cycle-SANEX system was developed at Jülich (Wilden et al., 2011). A solvent consisting of $CyMe_4$-BTBP+TODGA was used (similar to the solvent used in the spiked $CyMe_4$-BTBP r-SANEX process (Modolo et al., 2013); cyclohexanediaminetetraacetic acid (CDTA) was added to the feed to mask zirconium and molybdenum (Sypula et al., 2012). Palladium was coextracted and selectively stripped by L-cysteine before actinides(III) were stripped by a glycolate solution. Based on equilibrium distribution ratios and kinetic data, a flow sheet was designed (Magnusson et al., 2013c) using the SX Process code (Magnusson and Malmbeck, 2012; Magnusson et al., 2013a,b).

Based on this flow sheet, a continuous process test was performed in a 16+16 stage lab-scale centrifugal contactor setup (Wilden et al., 2013). Figure 10.11 shows the flow sheet and the main results. As the centrifugal contactor setup available at Jülich has only 16 stages, the test was divided into two parts, extraction/scrubbing and palladium scrubbing/stripping. These were run on two consecutive days.

The results of this spiked test were very encouraging. The raffinate contained 0.03% of the Am(III) inventory and 0.2% of the Cm(III) inventory. The Pd(II) fraction was very pure, containing only ≈0.01% of Am(III), ≈3% of both Eu(III) and Gd(III), 6% of Y(III), and 10% of the Ag(I) inventory. Other elements were found to be below 1%. The product solution contained ≥99.8% of Am(III) and ≥99.4% of Cm(III). It was contaminated by 9% of Y(III) and <1% of Pd(II). Very low concentrations of Ln(III) (<1%) were found in the Am(III)+Cm(III) product solution.

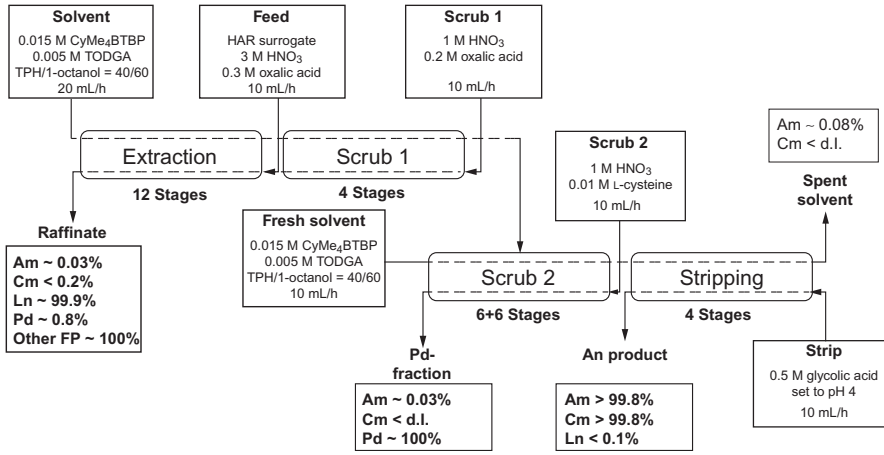

Figure 10.11 Flow sheet and main results of the 1-cycle-SANEX process test (Wilden et al., 2013) carried out at Forschungszentrum Jülich (Jülich, Germany) in 2011.

Due to $CyMe_4$-BTBP's rather slow extraction kinetics (Geist et al., 2013a; Lewis et al., 2011a) a comparatively low feed flow rate of 10 mL/h had to be used (same as in the $CyMe_4$-BTBP r-SANEX process tests, Magnusson et al., 2009a; Modolo et al., 2013).

10.6.2.1 Innovative-SANEX: selective back-extraction of Am(III) + Cm(III) from DIAMEX solvent

Another way of simplifying the overall flow sheet for separating actinides(III) is their selective stripping from a loaded DIAMEX solvent. The concept is similar to a reverse TALSPEAK process (Weaver and Kappelmann, 1964; Persson et al., 1984). Actinide (III) and lanthanide(III) ions are separated from the remaining fission and corrosion products by, for example, DMDOHEMA or TODGA; an aqueous solution containing DTPA or HEDTA is then used to strip actinides(III) from the solvent. Finally, lanthanide(III) ions (and fission products retained in the solvent) are back washed in a final strip section.

The original TALSPEAK chemistry uses an acidic extracting agent (Nilsson and Nash, 2007). Thus, the trivalent lanthanides remain in the organic phase in the actinide (III) strip section, which is operated at very low acidity (pH 2-4). Indeed, this low acidity is required because DTPA and HEDTA are not efficient at higher acidity. This, in turn, requires measures to keep lanthanides in the organic phase if solvating extracting agents are used; either a second acidic extracting agent is added to the solvent (Hérès et al., 2008) or nitrate salt is added to the actinide(III) stripping solution (Hérès et al., 2009; Sypula et al., 2011).

Spiked (Hérès et al., 2009) and hot (Poinssot et al., 2010) innovative-SANEX processes were demonstrated at the CEA, using a TODGA+TBP solvent to coextract An(III) and Ln(III) and a solution containing DTPA, malonic acid, and $NaNO_3$ for stripping An(III). The hot test flow sheet is shown in Figure 10.12. The extraction-scrubbing

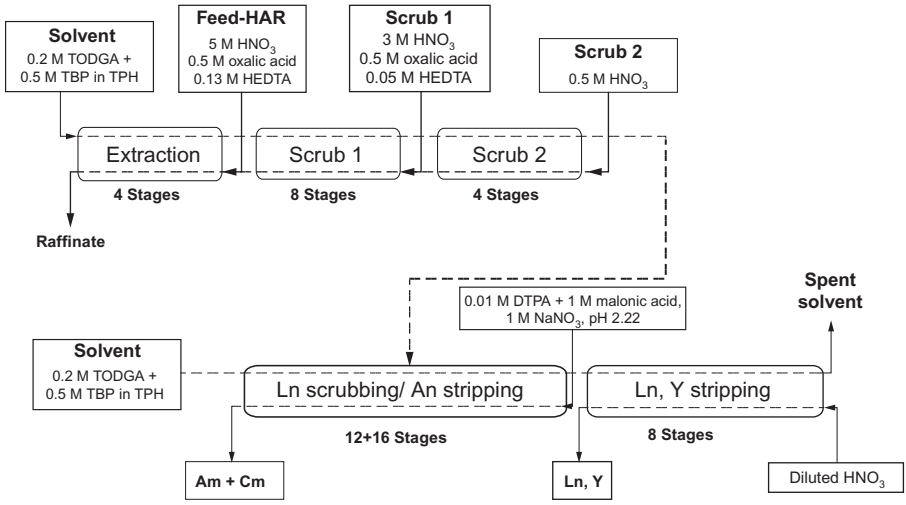

Figure 10.12 Flow sheet for the hot innovative-SANEX process test performed at the CEA (Poinssot et al., 2010).

section (stages 1-16) is similar to that of a hot TODGA-DIAMEX process (Magnusson et al., 2009b) (see Figure 10.9). An(III) is selectively stripped in 16 stages from the loaded solvent using a DTPA solution of pH 2.2 and containing 1 mol/L $NaNO_3$ to keep Ln(III) in the organic phase; fresh solvent is used to reextract the fraction of lanthanides costripped with An(III). Finally, Ln(III) are stripped in eight stages into dilute HNO_3. Very good results were obtained in this hot test; recovery yields of An(III) >99.9% with high DFs toward Ln(III) (less than 5% mass of lanthanides compared to the total amount of the actinides in the actinide product).

The hydrophilic complexing agent SO_3-Ph-BTP (Figure 10.13) was recently introduced for the actinide(III) selective stripping step (Geist et al., 2012). When coextracting Am(III) and Eu(III) from nitric acid into TODGA, adding SO_3-Ph-BTP to the aqueous phase suppresses Am(III) extraction while Eu(III) is extracted. Separation factors in the range of 1000 are achieved. The selective stripping of An(III) now becomes possible, even at relatively high nitric acid concentrations of up to 1 mol/L HNO_3.

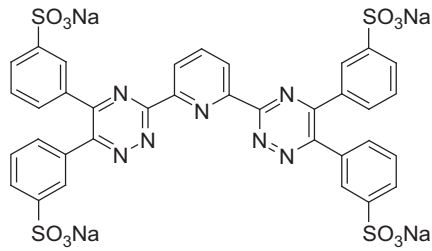

Figure 10.13 Structure of 2,6-bis(5,6-di(sulfophenyl)-1,2,4-triazin-3-yl)pyridine (SO_3-Ph-BTP).

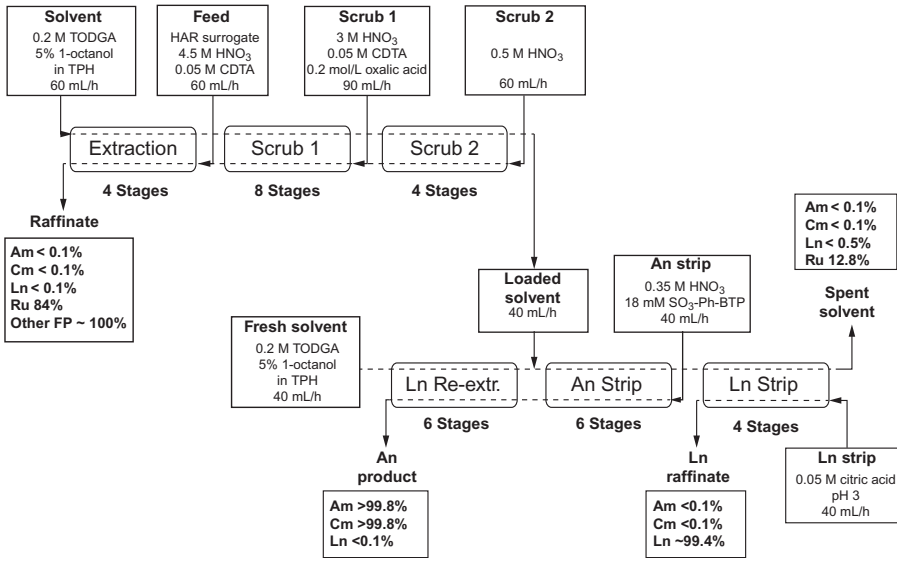

Figure 10.14 Flow sheet and main results for the SO_3-Ph-BTP innovative-SANEX process test carried out at Forschungszentrum Jülich (Jülich, Germany) in 2012 (Modolo et al., 2014).

This means that nitric acid at a suitable (process level) concentration can be used to keep lanthanides in the organic phase; nitrate salt or an acidic extractant are not required for this purpose.

Later, an innovative-SANEX process was designed using an organic phase comprising TODGA in TPH + 5 v/v% 1-octanol and an aqueous phase containing SO_3-Ph-BTP for the selective strip. This process (Figure 10.14) consists of four main steps:

Step 1: Coextraction of An(III) and Ln(III): four stages.
Step 2: Back-extraction of coextracted molybdenum, strontium, and HNO_3 using two scrubbing solutions: eight stages of Scrub 1 and four stages of Scrub 2.
Step 3: Six stages for the selective back-extraction of An(III) using the selective aqueous complexing agent SO_3-Ph-BTP at high acidity (0.35 mol/L HNO_3) with an additional six stages for Ln(III) reextraction.
Step 4: Stripping of lanthanides and residual elements from the solvent using a citric-acid-buffered solution at pH 3: four stages.

Once again the extract-scrub sections are similar to those of the TODGA-DIAMEX test shown in Figure 10.9. TBP (which is a non-CHON compound) was replaced by 5 v/v% 1-octanol (Geist and Modolo, 2009) to suppress third-phase formation. Finally, after optimization studies, a solvent consisting of 0.2 mol/L TODGA + 5% 1-octanol in TPH was chosen.

The results of the SO_3-Ph-BTP innovative-SANEX process (Geist et al., 2013b; Modolo et al., 2014) show that Am(III) + Cm(III) and Ln(III) were quantitatively extracted (>99.9%) and very high feed/raffinate DFs were achieved with $DF > 10^3$.

To limit the coextraction of zirconium and palladium 0.05 mol/L CDTA was added to the feed (Sypula et al., 2012). The Scrub 1 and Scrub 2 steps proved to be very efficient for the back-extraction of molybdenum, zirconium, and strontium; the collected organic phase (stage 16) contained only 0.07% molybdenum, 0.07% zirconium, and 0.27% strontium of the initial amounts. The behavior of ruthenium was very similar to that in earlier TODGA tests with 16% being coextracted. The results from the selective back-extraction of An(III) show that six stages were sufficient for An(III) stripping and only four stages were needed for complete Ln(III) stripping with citric acid solution. Less than 0.1% of Am(III), Cm(III), and Eu(III) were found in the spent solvent after stripping. As expected, the spent solvent was contaminated with 12.8% ruthenium, thus requiring further investigation, either to avoid the extraction of ruthenium using special complexing agents or to regenerate the solvent by specific washing steps. The Am(III)+Cm(III) product was very pure and only contaminated with 0.34% strontium, 0.44% ruthenium, and <0.1% Ln(III). Over 99.8% of the Am (III) and Cm(III) were recovered in the actinide product fraction.

10.6.2.2 Comparison of SANEX processes

From the above discussion it is clear that much effort has been put into development of the SANEX process for MA recovery. However, given the complexities of the later SANEX flow sheets the question arises as to whether a 1-cycle-SANEX or an innovative-SANEX process is really a simplification over a combination of a DIAMEX and a SANEX process. To answer this question, the SO_3-Ph-BTP *innovative*-SANEX test (Figure 10.14) and the 1-cycle-SANEX test (Figure 10.11) are compared to a combination of TODGA-DIAMEX (Figure 10.9) and SANEX (Figure 10.10) tests with respect to efficiency (i.e., DFs, number of stages, flow rates) and use of chemicals.

Some of the major performance indicators are compared in Table 10.2. Most importantly, Am(III) losses to raffinate solutions are <0.1% in all of the process schemes.

Table 10.2 Efficiency of the different processes

	TODGA-DIAMEX +SANEX	1-Cycle SANEX	*Innovative*-SANEX
Stages	32+16	32	32
Feed flow rate, Q_{feed} (mL/h)	60 (DIAMEX) 10 (SANEX)	10	60 (aqueous feed) 40 (organic feed)
Am(III) in raffinate	<0.02%[a]	0.04%[b]	<0.1%[c]
Eu(III) in product	0.08%[d]	0.4%	0.09%
CHON	Yes	No (cysteine)	No (SO_3-Ph-BTP)

[a]Sum of Am(III) in DIAMEX and SANEX raffinates.
[b]Sum of Am(III) in raffinate and in Pd(II) raffinate.
[c]Sum of Am(III) in raffinate and in Ln(III) raffinate.
[d]Eu(III) in SANEX product.

Furthermore, the final product solutions contain less than 1% of Eu(III) (representing Ln (III)) in all cases, indicating that very pure An(III) products are generated.

The numbers of required stages cannot be compared directly because feed flow rates were different (60 mL/h for the TODGA process, 10 mL/h for the SANEX and 1-cycle-SANEX processes, 40 mL/h for the innovative-SANEX process). A qualitative comparison is nevertheless made: fewer stages can be used in the DIAMEX processes if flow rates are lowered to match those of the consecutive SANEX process (i.e., 10 mL/h). A further reduction is possible by changing the DIAMEX strip solution from 0.01 mol/L HNO_3 to a solution containing a complexing agent. For a feed flow rate of 10 mL/h, the total number of stages (TODGA-DIAMEX + SANEX) would probably be similar to that used in the 1-cycle-SANEX test. Comparing the 1-cycle-SANEX and *innovative*-SANEX tests, the latter requires less stages at a given flow rate. This makes the SO_3-Ph-BTP *innovative*-SANEX process the most compact option.

Regarding the use of chemicals, both the TODGA-DIAMEX and the SANEX processes use only compounds consisting of C, H, O, and N atoms. These can be destroyed to gaseous products, which is advantageous with respect to the generation of secondary waste. Both the 1-cycle-SANEX process and the SO_3-Ph-BTP innovative-SANEX process use sulfur compounds (L-cysteine to strip Pd(II) or SO_3-Ph-BTP to strip An(III)). These compounds (or their degradation products) are a source of solid waste.

On the other hand, the combination of a DIAMEX and a SANEX process requires two different solvents, involving two different solvent handling and regeneration systems. This increases the size of a plant and may produce more waste than does only one solvent regeneration cycle.

10.7 Overview and status of GANEX process development

The GANEX process (group actinide extraction) was first developed by the CEA for the hydrometallurgical reprocessing of GenIV spent nuclear fuels and the homogenous recycling of actinides. It is composed of two extraction cycles following the dissolution of the spent fuel in nitric acid. Uranium(VI) is first selectively extracted from the dissolution solution before the group separation of transuranic elements (Np, Pu, Am, Cm), which occurs in the second cycle prior to the coconversion step. The preliminary separation of uranium in the first cycle is required in order to recover uranium at a high purity. This can then be used to adjust the ratio of U/TRU before the coconversion of the actinides and to handle the excess of uranium due to the reprocessing of fuels discharged both from light water and fast reactors in the future. Additionally, the separation of the major constituent of the spent fuels is helpful for the hydrodynamics of the second extraction cycle by reducing the heavy metal masses and liquor volumes to be processed.

10.7.1 GANEX first cycle: uranium selective separation

The selective separation of uranium is operated by solvent extraction using *N*,*N*-dialkylamide extractants. DEHiBA (*N*,*N*-di-(ethyl-2-hexyl)isobutyramide) was selected from the possible *N*,*N*-dialkylamides because it showed a good compromise

between quantitative extraction of uranium and high U(VI)/Pu(IV) selectivity ($SF_{U(VI)/Pu(IV)}$ ~80 at 3 mol/L HNO_3). DEHiBA can selectively extract uranium (VI) without addition of any reducing or complexing agents for plutonium(IV), thus avoiding its coextraction in the process. Batch distribution data were acquired and these allowed the modeling of extraction equilibria with DEHiBA and the calculation of flow sheets using the PAREX code (Miguirditchian et al., 2008). A flow sheet was tested in 28 laboratory-scale mixer-settlers on a genuine spent fuel solution containing 176 g/L of uranium and 2.5 g/L of plutonium in the CEA Atalante facility in 2008. Hydrazinium nitrate was added in the scrubbing solution to reduce Tc(VII) and Np (VI) and facilitate stripping them from the solvent. The results show that the goals of uranium recovery yield and DFs were reached. The losses of uranium to the raffinate and the solvent were lower than 0.002% and 0.003%, respectively, corresponding to a recovery yield of uranium higher than 99.99%. The DFs versus neptunium, technetium, and plutonium were high enough with the help of hydrazinium nitrate in the scrubbing section and β-γ isotopes (^{137}Cs, ^{106}Ru, etc.) were very well decontaminated, thus confirming the great selectivity of this molecule for uranium versus fission products (Miguirditchian et al., 2009b).

This GANEX first-cycle process was also tested as part of the ACSEPT project in 2012 in the hot cell facility of ITU in order to remove bulk uranium and prepare the feed for the so-called EURO-GANEX test (group actinide separation). In order to simulate future GenIV spent fuels, the feed was prepared by dissolving a mixture of carbide and nitride fast reactor fuel pieces in 6 mol/L HNO_3, after a thermal treatment for oxidation. After adjustment of the nitric acid concentration, it contained 5 mol/L HNO_3, 103 g/L of uranium, and 22.7 g/L of plutonium. A new flow sheet was designed by CEA, see Figure 10.15, taking the much more plutonium-rich feed

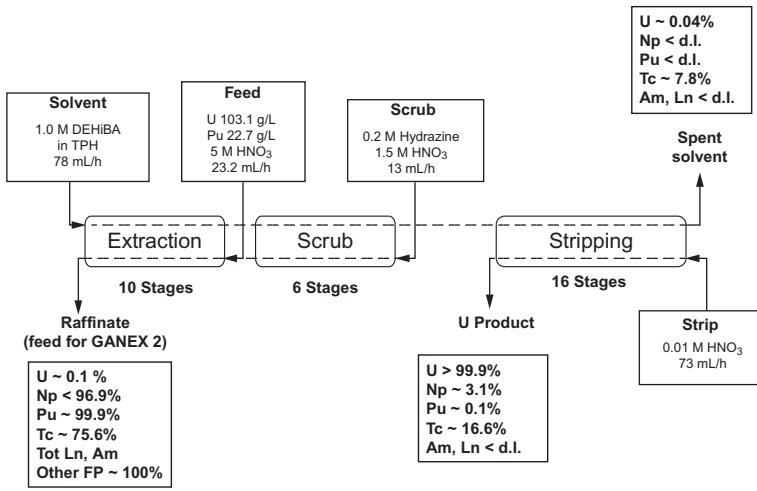

Figure 10.15 Flow sheet and main results of the ITU GANEX first-cycle hot test (ITU Hot Cells Facility, 2012).

into account, as well as the shorter holdup times of the 16-stage centrifugal contactor system (mass transfer kinetics of uranium and technetium with DEHiBA were incorporated into the PAREX code). Due to the limited number of centrifugal contactors, the experiment was run in two steps; one step for extraction and scrubbing, with the loaded organic phase being collected for uranium stripping in the second step. The results confirmed the excellent properties of DEHiBA for the uranium selective separation even from plutonium-rich solutions and in short residence time contactors. 99.9% of uranium was recovered with only 0.1% left in the raffinate with the other actinides (96.9% of Np, 99.9% of Pu, and 100% of Am) and the fission products (Malmbeck et al., 2014). Uranium was efficiently separated with DFs versus plutonium, neptunium, and technetium equal to 282, 20, and 5, respectively. While these values are lower than those measured after the CEA test in mixer-settlers, differences could be explained by a higher content of plutonium and shorter residence time in the scrubbing section of the contactors in the ACSEPT-ITU test.

10.7.2 GANEX second cycle: TRU group separation

The group separation of TRU (Np, Pu, Am, and Cm) was first developed in Europe by the CEA by adapting the DIAMEX-SANEX process (Miguirditchian et al., 2007), initially developed for the partitioning of trivalent MAs (americium and curium) to the global management of neptunium and plutonium along with americium and curium. A mixture of a malonamide (DMDOHEMA) and an alkylphosphoric acid (HDEHP) diluted in TPH allows a quantitative extraction of all actinides from concentrated nitric acid solution without adjusting the neptunium valence. Molybdenum and technetium, coextracted with actinides by the HDEHP-DMDOHEMA solvent, are then selectively stripped by a citric acid solution at pH around 2-3, prior to the selective actinide stripping using a mixture of HEDTA and citric acid at pH 3. Hydroxyurea is also added in this stripping solution to reduce Np(VI) and ease its stripping with the other actinides, while the lanthanides and other extractable fission products (Zr, Fe) remain extracted by HDEHP in the organic phase. Eventually, lanthanides, zirconium, and iron are stripped from the solvent using a mixture of two water-soluble complexing agents: TEDGA (tetraethyl diglycolamide) and oxalic acid diluted in HNO_3. A model was developed from batch experiments in order to describe the extraction of actinides and the main fission products (Ln, Mo, Tc, Zr, Fe) in each step of this process and to support the development of flow sheets. The flow sheet, depicted in Figure 10.16 was tested in 48 stages of lab-scale mixer-settlers in a hot cell of the Atalante facility in 2008 on the HAR produced from the GANEX first-cycle test. Neptunium, plutonium, americium, and curium were recovered together in the actinide product and the losses of transuranic elements to the other aqueous outputs and solvent raffinate were estimated to total less than 0.5% (neptunium essentially) at the end of the test, corresponding to a recovery yield of actinides higher than 99.5% (Miguirditchian et al., 2009a). The DFs for fission products were quite high except for middle series lanthanides (especially neodymium, samarium, and europium), which were less efficiently separated than expected (5% of lanthanides were found in the actinide product at the end of the test). This rather poor Ln/An separation

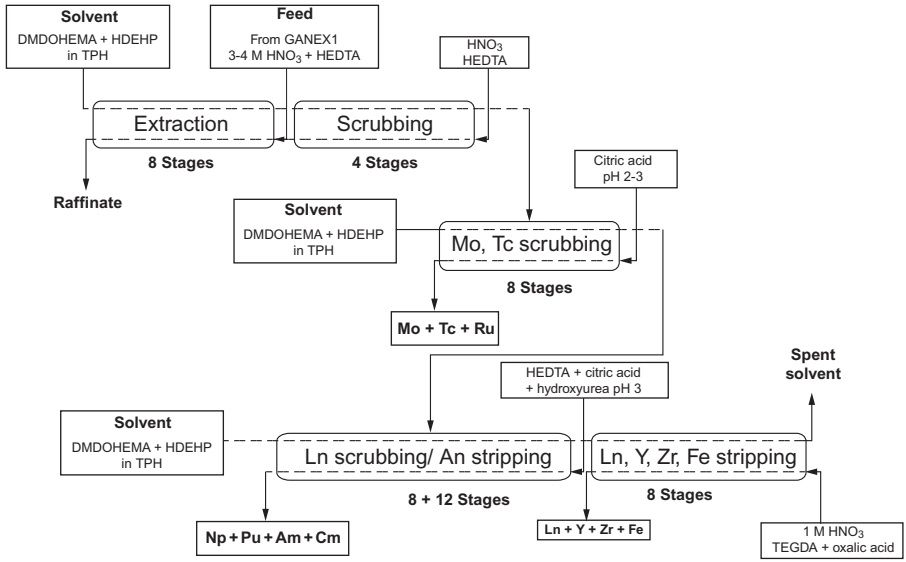

Figure 10.16 Flow sheet of the CEA GANEX-2 hot test (Bordier et al., 2008).

was due to an accumulation of lanthanides in the actinide stripping section caused by an underestimation of lanthanide, zirconium, and iron concentrations in the feed solution, which led to losses of lanthanides in the actinide product. However, it was possible to simulate this accumulation with the simulation code and thus to extrapolate the separation performance to higher values by correcting the organic cationic concentrations or the feed flow rate. Recoveries and DFs are given in Table 10.3.

Alternative second cycle GANEX processes have been developed in Europe through the ACSEPT program. Chalmers University (Sweden) proposed to use a mixture of $CyMe_4$-BTBP and TBP diluted in cyclohexanone to extract actinides (Np, Pu, Am, Cm) from nitric acid after a preliminary extraction of bulk uranium (Aneheim et al., 2010, 2011, 2013). This solvent has the advantage that it can selectively extract the actinides from the fission products and, in particular, the lanthanides thanks to the well-known An(III)/Ln(III) selectivity of the BTBP molecule. It is indeed possible to extract neptunium, plutonium, americium, and curium as well as low quantities of U(VI) from highly acidic solutions with a high selectivity versus lanthanides and to recover actinides altogether after stripping at low acidity (glycolic acid at pH 4) in this so-called CHALMEX process.

However, some fission or activation products (e.g., Ag, Pd, Cd, Mo, Zr, Tc, and Ni) are also strongly extracted by the $CyMe_4$BTBP+TBP solvent and masking agents such as bimet (for Pd), mannitol (for Mo and Zr), or glucolactone (for Mo) have to be added in different scrubbing sections to partially prevent these extractions (Aneheim et al., 2013). Moreover, cyclohexanone selected as the diluent to improve extraction kinetics has several drawbacks such as high solubility in water and the

Table 10.3 Main results of the CEA GANEX-2 hot test (Bordier et al., 2008).

Element	% in raffinate	% in TRU product	DF	% in solvent
Np	<0.46	98.9 > Np < 99.4	–	<0.6
Pu	<0.041	≈99.95	–	<0.005
Am	0.016	≈99.97	–	<0.008
Cm	0.004	≈99.99	–	<0.0002
La	<1	<3	>36	–
Ce	<3	<2	>62	0.06
Pr	<1	<3	>37	0.06
Nd	<1	6	16	–
Sm	<2	18	5.5	–
Eu	<10	8	13	0.06
Pd	57	44	2.6	–
Tc	9	<0.1	>1335	–
Ru	82	<3.5	75	–
Fe	<3	32.5	3.6	–
Zr	<2	<1.4	>86	–
Mo	<3	<1.8	72	–

potential for exothermic reaction with concentrated nitric acid, which would be too hazardous to manage in an industrial process.

The UK NNL also worked on the group actinide extraction in the framework of the ACSEPT project and proposed another route based on the TODGA solvent. TODGA is an efficient extracting agent for trivalent and tetravalent actinides (Sasaki et al., 2001) but can lead to plutonium precipitates under high plutonium loading conditions. DMDOHEMA was thus added to TODGA to prevent demixing in the organic phase, which allowed the use of this solvent for future GenIV fuels reprocessing (i.e., plutonium-rich solutions, > 10 g/L of plutonium in organic phase). Neptunium, plutonium, americium, and curium are extracted along with lanthanides by the solvent (0.2 mol/L TODGA + 0.5 mol/L DMDOHEMA in Exxsol D80) from the highly acidic raffinate obtained in the first step of the process (Bell et al., 2012). Process development studies showed that neptunium can be quantitatively extracted into the organic phase by increasing the feed acidity in order to facilitate Np(V) disproportionation to Np(IV) and Np(VI) (Carrot et al., 2013). CDTA is added to the feed to mask zirconium and palladium (Sypula et al., 2012) and an acid scrub is needed to scrub strontium at 0.5 mol/L HNO_3.

Actinides are then selectively stripped using a mixture of AHA (acetohydroxamic acid) and SO_3-Ph-BTP in 0.5 mol/L HNO_3. AHA is added to strip Pu(IV), Np(IV), and Np(VI) (Taylor et al., 1998; Carrott et al., 2007; Bernier et al., 2012) while the SO_3-Ph-BTP (Figure 10.13) is used to strip americium and curium selectively from

lanthanides at high nitric acidity (0.5 mol/L) (Geist et al., 2012). Lanthanides are then stripped in the last step using 0.5 mol/L glycolic acid at pH 4 or 0.01 mol/L HNO_3.

Several spiked tests were first performed at NNL in 32 stages of centrifugal contactors, and these showed that it is possible to separate actinides as a group with this process even though rather high losses of neptunium (30%) to the raffinate were found and a small fraction of europium (7%, used as a marker for lanthanide behavior) was measured in the actinide product (Carrott et al., 2014).

This process was then selected as the reference route for the EURO-GANEX process and tested in HA conditions at ITU at the end of the ACSEPT project. A flow sheet (Figure 10.17) was produced for the hot test and adapted to the 16-stage centrifugal contactor setup in the hot cell facility in ITU. The experiment was split over two consecutive days; 16 stages for extraction and scrubbing on the first day and 16 stages redeployed for back-extraction on the second day. To prepare the feed solution, the raffinate from the first GANEX cycle was adjusted to 10 g/L of plutonium and the acidity increased to 5.9 mol/L. Twelve extraction stages in combination with the higher acidity were chosen to optimize Np(V) disproportionation and efficiency of extraction. Selective back-extraction of actinides was then achieved by a mixture of water-soluble SO_3-Ph-BTP in combination with AHA at an acidity of 0.5 mol/L in six stages. Six stages were used for reextraction of lanthanides and four stages for back-extraction of lanthanides using 0.01 mol/L HNO_3 (Malmbeck et al., 2014).

The results reported in Figure 10.17 show that 99.9% of the TRU (Pu, Np, and Am) have been recovered as a group with a high selectivity (<0.1% of lanthanides in the actinide product), which confirms the scientific feasibility of this system for the group actinide extraction.

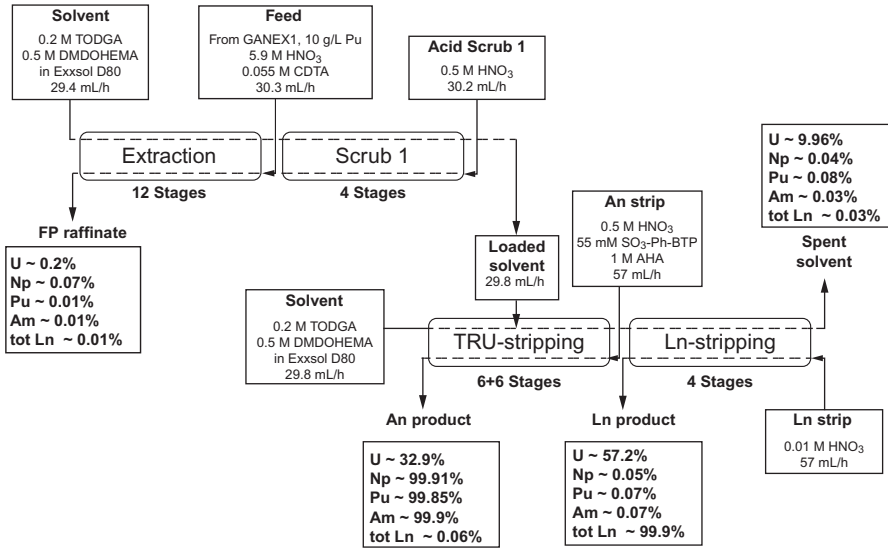

Figure 10.17 Flow sheet and main results of the Euro-GANEX hot test (ITU Hot Cell Facility, 2012).

10.8 Overview and status of EXAm process development

Americium is the main contributor to the long-term radiotoxicity and to the heat generation of glasses used for HLW conditioning. To decrease these impacts and to avoid the difficult recycling of curium, the CEA has developed the EXAm process for the separation and the recovery of a pure americium product directly from PUREX raffinate. The principle of the EXAm process is based on the DIAMEX-SANEX process and uses the same mixture of HDEHP and DMDOHEMA as the solvent. A water-soluble complexing agent, TEDGA, is added in the feed solution (PUREX raffinate) and in the scrubbing section to increase Am/Cm and Am/heavy lanthanides selectivity, by utilizing the preferential complexation of curium and heavy lanthanides by this DGA. Americium and light lanthanides (La, Ce, Pr, Nd) are thus selectively extracted by the EXAm solvent from high nitric acid media, leaving curium, zirconium, and heavy lanthanides (Sm, Eu, Gd) in the raffinate. After the molybdenum stripping step (molybdenum is coextracted with americium but can be selectively stripped with citric acid at pH 3), americium is separated from the light lanthanides by selective stripping using HEDTA and citric acid at pH 3 (or DTPA and malonic acid at pH 2.5) before the lanthanide-iron stripping using TEDGA and oxalic acid.

Many experimental data were acquired mainly at the extraction-scrubbing step (Am/Cm separation) and were used for the development of a phenomenological model implemented in the PAREX process simulation code. The EXAm flow sheet (see Figure 10.18) was tested in 2010 on a genuine PUREX raffinate in the ATALANTE hot cells. The contactor setup consisted of 68 stages of laboratory-scale mixer-settlers:

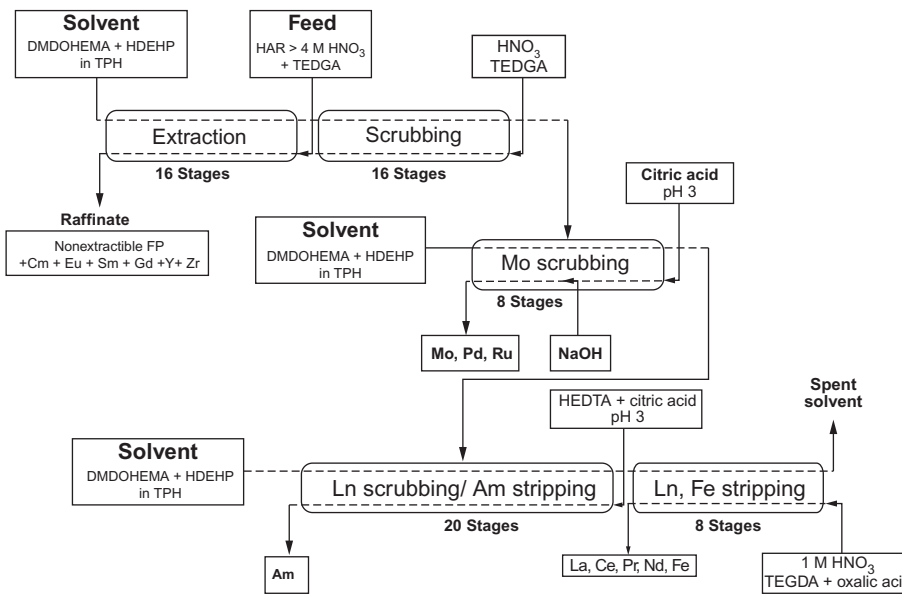

Figure 10.18 Flow sheet of the EXAm CEA hot test (Bordier et al., 2008).

16 stages for americium extraction, 16 for curium scrubbing, 8 stages for molybdenum stripping, 20 stages for americium stripping, and 8 stages for lanthanide and iron stripping.

At the steady state, the americium recovery rate was 98.3% with a DF of americium from curium of 505. More than 99% of americium initially in the feed solution was extracted into the organic phase after the extraction-scrubbing section but 0.7% of americium was lost in the molybdenum stripping step, which still needs to be improved. The americium output was also decontaminated versus lanthanides as only 2.2% of neodymium (in mass/Am mass in the product) was found with americium.

The results from this test have demonstrated the scientific feasibility of separating a pure americium product from a genuine PUREX raffinate for the first time (Bollesteros et al., 2012; Miguirditchian et al., 2013).

Other EXAm routes are currently being studied for americium-selective extraction in the context of the new European program SACSESS. Several processes are proposed, mostly based on the use of TODGA solvent (with 5% 1-octanol) and consist of coextraction of americium, curium, and lanthanides followed by selective americium stripping. In this case, curium and lanthanide would remain extracted by TODGA in the organic phase while americium would be stripped by a water-soluble selective complexing agent efficient at moderate acidity (0.1-1 mol/L HNO_3). It is anticipated that a EURO-EXAm process will be selected during the SACSESS project and will be tested in HA conditions in ITU hot cells before the end of the project in 2016.

10.9 Future trends

The separation processes described in this chapter are based on solvent-extraction studies that benefit from the experience gained over the last 20 years in European international collaborative projects. Research on partitioning in the EU is at such an advanced stage that serious consideration is being given to the industrialization of some hydrometallurgical separation processes; most notably in France, which has an ambitious R&D program on partitioning and transmutation. Nevertheless, after more than two decades of research in this area, separating MAs (americium and curium) from the PUREX raffinate still poses a challenge.

Several aqueous partitioning processes were selected and developed up to the demonstration level on the laboratory scale using genuine fuel solutions. As shown, the scientific feasibility of these processes involving new extracting or complexing organic molecules and new diluents was demonstrated. It is important to improve the mechanistic understanding of the chemical and physical reactions involved in the solvent-extraction processes (thermodynamics and kinetics) and the diverse safety issues involved in the chemical processes under operational as well as malfunctioning conditions. An increased focus on kinetics, in particular, is needed to understand the scope for process intensification, including the appropriate choice of extraction equipment. Overall, a better understanding of the chemical systems involved is needed to enhance the potential for future process operations at the industrial scale.

This knowledge is important to develop multiscale models to be used in a simulation code, which is an indispensable tool for design and safe operation of such processes.

Last but not least, the long-term operation of the solvent accounting for degradation by hydrolysis and radiolysis reactions must be demonstrated before industrial deployment can be considered. The washing of the solvent to enable solvent recycling and the management of spent solvent, including the secondary wastes generated, also need to be studied.

Acknowledgements

The authors would like to acknowledge the financial support of the European Commission in the projects: NEWPART (FI4I-CT96-0010), PARTNEW (FIKW-CT2000-00087), EUROPART (F16W-CT-2003-508854), ACSEPT (FP7-CP-2007-211267), SACSESS—Contract No. FP7-Fission-2012-323 282.

This work is dedicated to the memory of Charles Madic for his strong scientific support during the coordination of the European projects.

References

Aneheim, E., Ekberg, C., Fermvik, A., Foreman, M.R.S., Retegan, T., Skarnemark, G., 2010. A TBP/BTBP-based GANEX separation process. Part 1: feasibility. Solvent Extr. Ion Exch. 28, 437–458.

Aneheim, E., Ekberg, C., Fermvik, A., Foreman, M.R.S., Gruner, B., Hajkova, Z., Kvicalova, M., 2011. A TBP/BTBP-based GANEX separation process—part 2: ageing, hydrolytic, and radiolytic stability. Solvent Extr. Ion Exch. 29, 157–175.

Aneheim, E., Ekberg, C., Foreman, M.R.S., 2013. A TBP/BTBP-based GANEX separation process—part 3: fission product handling. Solvent Extr. Ion Exch. 31, 237–252.

Ansari, S.A., Pathak, P., Mohapatra, P.K., Manchanda, V.K., 2011. Chemistry of diglycolamides: promising extractants for actinide partitioning. Chem. Rev. 112, 1751–1772.

Arnaud-Neu, F., Böhmer, V., Casensky, B., Casnati, A., Desreux, J.F., Gruner, B., Grüttner, C., DE Mendoza, J., Pina, G., Selucky, P., Verboom, W., Wipff, G., 2004. CALIXPART—selective extraction of minor actinides from high active liquid waste by organised matrices. (CALIXPART FIKW-CT2000-00088). Final Technical Report no. 6466, 31-3-2004, available at: http://cordis.europa.eu/publication/rcn/6466_en.html.

Baron, P., Charbonnel, M.C., Nicol, C., Berthon, L., 1997. State of advancement of DIAMEX process. In: Proceeings of GLOBAL'97 (International Conference on Future Nuclear Systems), Yokohama (Japan).

Bell, K., Carpentier, C., Carrott, M., Geist, A., Gregson, C., Hérès, X., Magnusson, D., Malmbeck, R., Mclachlan, F., Modolo, G., Müllich, U., Sypula, M., Taylor, R., Wilden, A., 2012. Progress towards the development of a new GANEX process. Proc. Chem. 7, 392–397.

Bernier, G., Miguirditchian, M., Ameil, E., Sorel, C., Balaguer, C., Espinoux, D., Costenoble, S., Esseyric, C., 2012. Hot test in mixer settlers of alpha barrier with AHA in PUREX process. Proc. Chem. 7, 160–165.

Birkett, J.E., Carrott, M.J., Fox, O.D., Jones, C.J., Maher, C.J., Roube, C.V., Taylor, R.J., Woodhead, D.A., 2007. Controlling neptunium and plutonium within single cycle solvent extraction flowsheets for advanced fuel cycles. J. Nucl. Sci. Technol. 44, 337–343.

Bollesteros, M.-J., Calor, J.-N., Costenoble, S., Montuir, M., Pacary, V., Sorel, C., Burdet, F., Espinoux, D., Hérès, X., Eysseric, C., 2012. Implementation of americium separation from a PUREX raffinate. Proc. Chem. 7, 178–183.

Bordier, G., Warin, D., Masson, M., 2008. The Atalante facility at CEA/Marcoule: towards GenIV systems fuel cycle, ATALANTE 2008 Montpellier (France). May 19–22, 2008.

Bourg, S., Hill, C., Caravaca, C., Rhodes, C., Ekberg, C., Taylor, R., Geist, A., Modolo, G., Cassayre, L., Malmbeck, R., Harrison, M., De Angelis, G., Espartero, A., Bouvet, S., Ouvrier, N., 2011. ACSEPT—partitioning technologies and actinide science: towards pilot facilities in Europe. Nucl. Eng. Des. 241, 3427–3435.

Bremer, A., Whittaker, D.M., Sharrad, C.A., Geist, A., Panak, P.J., 2014. Complexation of Cm (III) and Eu(III) with CyMe4-BTPhen and CyMe4-BTBP studied by time resolved laser fluorescence spectroscopy. Dalton Trans. 43, 2684–2694.

Carrot, M.J., Gregson, C.R., Taylor, R.J., 2013. Neptunium extraction and stability in the GANEX solvent: 0.2 M TODGA/0.5 M DMDOHEMA/kerosene. Solvent Extr. Ion Exch. 31, 463–482.

Carrott, M.J., Fox, O.D., Maher, C.J., Mason, C., Taylor, R.J., Sinkov, S.I., Choppin, G.R., 2007. Solvent extraction behavior of plutonium (IV) ions in the presence of simple hydroxamic acids. Solvent Extr. Ion Exch. 25, 723–745.

Carrott, M., Bell, K., Brown, J., Geist, A., Gregson, C., Hérès, X., Maher, C., Malmbeck, R., Mason, C., Modolo, G., Müllich, U., Sarsfield, M., Wilden, A., Taylor, R., 2014. Spiked demonstration of a new flowsheet for co-separating the transuranic actinides: the "EURO-GANEX" process. Solvent Extr. and Ion Exch. 32 (5), 447–467.

Chen, J., Wang, J., Jing, S., 2007. A pilot test of partitioning for the simulated highly saline high level waste. In: Proceedings of the International Conference on GLOBAL 2007 (Advanced Nuclear Fuel Cycles and Systems), Boise, Idaho, USA, 9–13 September 2007.

Dinh, B., Moisy, P., Baron, P., Calor, J.-N., Espinoux, D., Lorrain, B., Benchikouhne-Ranchoux, M., 2008. Modified PUREX first-cycle extraction for neptunium recovery. In: Moyer, B.A. (Ed.), Proceedings of the International Solvent Extraction Conference (ISEC 2008), Tucson, Arizona, USA, 15–19 September.

Ekberg, C., Fermvik, A., Retegan, T., Skarnemark, G., Foreman, M.R.S., Hudson, M.J., Englund, S., Nilsson, M., 2008. An overview and historical look back at the solvent extraction using nitrogen donor ligands to extract and separate An(III) from Ln(III). Radiochim. Acta 96, 225–233.

Ekberg, C., Aneheim, E., Fermvik, A., Foreman, M., Löfström-Engdahl, E., Retegan, T., Spendlikova, I., 2010. Thermodynamics of dissolution for bis(triazine)-bipyridine-class ligands in different diluents and its reflection on extraction. J. Chem. Eng. Data 55, 5133–5137.

Fermvik, A., Ekberg, C., Englund, S., Foreman, M.R.S.J., Modolo, G., Retegan, T., Skarnemark, G., 2009. Influence of dose rate on the radiolytic stability of a BTBP solvent for actinide(III)/lanthanide(III) separation. Radiochim. Acta 97, 319–324.

Foreman, M.R.S., Hudson, M.J., Drew, M.G.B., Hill, C., Madic, C., 2006. Complexes formed between the quadridentate, heterocyclic molecules 6,6'-bis-(5,6-dialkyl-1,2,4-triazin-3-yl)-2,2'-bipyridine (BTBP) and lanthanides(III): implications for the partitioning of actinides(III) and lanthanides(III). Dalton Trans. 1645–1653.

Geist, A., Modolo, G., 2009. TODGA process development: an improved solvent formulation. In: Proceedings of the International Conference GLOBAL 2009 (The Nuclear Fuel Cycle: Sustainable Options & Industrial Perspectives), Paris, 6–11 September.

Geist, A., Hill, C., Modolo, G., Foreman, M.R.S.J., Weigl, M., Gompper, K., Hudson, M.J., Madic, C., 2006. 6,6'-bis (5,5,8,8-tetramethyl-5,6,7,8-tetrahydro-benzo[1,2,4]triazin-3-yl) [2,2']bipyridine, an effective extracting agent for the separation of americium(III) and curium(III) from the lanthanides. Solvent Extr. Ion Exch. 24, 463–483.

Geist, A., Müllich, U., Magnusson, D., Kaden, P., Modolo, G., Wilden, A., Zevaco, T., 2012. Actinide(III)/lanthanide(III) separation via selective aqueous complexation of actinides (III) using a hydrophilic 2,6-bis(1,2,4-triazin-3-yl)-pyridine in nitric acid. Solvent Extr. Ion Exch. 30, 433–444.

Geist, A., Magnusson, D., Müllich, U., 2013a. A kinetic study on the extraction of Am(III) into CyMe4-BTBP. In: Actinide and Fission Product Partitioning and Transmutation, 12th Information Exchange Meeting, Prague, Czech Republic, 24–27 September 2012. OECD-NEA.

Geist, A., Modolo, G., Wilden, A., Kaufholz, P., 2013b. Minor actinide separation: simplification of the DIAMEX-SANEX strategy by means of novel SANEX processes. In: Proceedings of the International Conference on GLOBAL 2013 (Nuclear Energy at a Crossroads), Salt Lake City, USA, 29 September–3 October.

Herbst, R.S., Baron, P., 2011. Standard and advanced separation: PUREX processes for nuclear fuel reprocessing. In: Nash, K.L., Lumetta, G.J. (Eds.), Advanced Separation Techniques for Nuclear Fuel Reprocessing and Radioactive Waste Treatment. Woodhouse Publishing Ltd., United Kingdom.

Hérès, X., Baron, P., Hill, C., Ameil, E., Martinez, I., Rivalier, P., 2008. The separation of extractants implemented in the DIAMEX-SANEX process. In: Proceedings of the International Conference ATALANTE 2008 (Nuclear Fuel Cycles for a Sustainable Future), Montpellier, France, 19–23 May.

Hérès, X., Sorel, C., Miguirditchian, M., Camès, B., Hill, C., Bisel, I., Espinoux, D., Eysseric, C., Baron, P., Lorrain, B., 2009. Results of recent counter-current tests on An (III)/Ln(III) separation using TODGA extractant. In: Proceedings of the International Conference on GLOBAL 2009 (The Nuclear Fuel Cycle: Sustainable Options & Industrial Perspectives), Paris, France, 6–11 September.

Hill, C., 2010. Overview of recent advances in An(III)/Ln(III) separation by solvent extraction. In: Moyer, B.A. (Ed.), Ion Exchange and Solvent Extraction. CRC Press, Boca Raton, London, New York.

Hill, C., Heres, X., Calor, J.-N., Guillaneux, D., Mauborgne, B., Rat, B., Rivalier, P., Baron, P., 1999. Trivalent actinides/lanthanides separation using bis-triazinyl-pyridines. In: Proceedings of the International Conference on Future Nuclear Systems (GLOBAL 1999), Jackson Hole, Wyoming, USA, 29/8–3/9.

Hill, C., Guillaneux, D., Hérès, X., Boubals, N., Ramain, L., 2000. SANEX-BTP process development studies. In: Proceedings of the International Conference on ATALANTE 2000 (Scientific Research on the Back-end of the Nuclear Fuel Cycle for the 21st Century), Avignon, France, 24–26 October.

Hill, C., Guillaneux, D., Berthon, L., Madic, C., 2002. SANEX-BTP process development studies. J. Nucl. Sci. Technol. (Suppl. 3), 309–312.

Hill, C., Berthon, C., Guillaneux, D., Dancausse, J.P., Madic, C., 2004. SANEX-BTP process development: from bench to hot test demonstration. In: Proceedings of the International Conference on ATALANTE 2004 (Advances for Future Nuclear Fuel Cycles), Nîmes, France, 21–24 June.

Horwitz, E.P., Kalina, D.G., Kaplan, L., Mason, G.W., Diamond, H., 1982. Selected alkyl(phenyl)-*N*,*N*-dialkylcarbamoylmethylphosphine oxides as extractants for Am(III) from nitric acid media. Sep. Sci. Technol. 17, 1261–1279.

IAEA, 2008. Spent fuel reprocessing options. IAEA-TECDOC-1587. International Atomic Energy Agency, Vienna.

ITU Hot Cells Facility, 2012. https://ec.europa.eu/jrc/en/institutes/itu

Kolarik, Z., Horwitz, E.P., 1988. Extraction of neptunium and plutonium nitrates with *n*-octyl (phenyl)-*N*, *N*-diisobutyl-carbamoylmethylphosphine oxide. Solvent Extr. Ion Exch. 6, 247–263.

Kolarik, Z., Schuler, R., Müllich, U., 1996. Partition of high-level radioactive waste. EUR 16958, European Commission, Luxembourg.

Kolarik, Z., Müllich, U., Gassner, F., 1999a. Extraction of Am(III) and Eu(III) nitrates by 2,6-di-(5,6-dipropyl-1,2,4-triazin-3-yl)pyridines. Solvent Extr. Ion Exch. 17, 1155–1170.

Kolarik, Z., Müllich, U., Gassner, F., 1999b. Selective extraction of Am(III) over Eu(III) by 2,6-ditriazolyl- and 2,6-ditriazinylpyridines. Solvent Extr. Ion Exch. 17, 23–32.

Lewis, F.W., Harwood, L.M., Hudson, M.J., Drew, M.G.B., Desreux, J.F., Vidick, G., Bouslimani, N., Modolo, G., Wilden, A., Sypula, M., Vu, T.H., Simonin, J.P., 2011a. Highly efficient separation of actinides from lanthanides by a phenanthroline-derived bis-triazine ligand. J. Am. Chem. Soc. 133, 13093–13102.

Lewis, F.W., Hudson, M.J., Harwood, L.M., 2011b. Development of highly selective ligands for separations of actinides from lanthanides in the nuclear fuel cycle. Synlett 18, 2609–2632.

Lewis, F.W., Harwood, L.M., Hudson, M.J., Drew, M.G.B., Hubscher-Bruder, V., Videva, V., Arnaud-Neu, F., Stamberg, K., Vyas, S., 2013. BTBPs versus BTPhens: some reasons for their differences in properties concerning the partitioning of minor actinides and the advantages of BTPhens. Inorg. Chem. 52, 4993–5005.

Madic, C., Hudson, M.J., 1998. High-level liquid waste partitioning by means of completely incinerable extractants. EUR 18038, European Commission, Luxembourg.

Madic, C., Ouvrier, N., 2008. EUROPART: EUROpean research program for the PARTitioning of minor actinides from high active wastes arising from the reprocessing of spent nuclear fuels. Radiochim. Acta 96, 183–185.

Madic, C., Blanc, P., Condamines, N., Baron, P., Berthon, L., Nicol, C., Pozo, C., Lecomte, M., Philippe, M., Masson, M., Hequet, C., Hudson, M.J., 1994. Actinide partitioning from HLLW using the DIAMEX process. In: RECOD '94 (4th International Conference on Nuclear Fuel Reprocessing and Waste Management), London, UK.

Madic, C., Hudson, M.J., Liljenzin, J.-O., Glatz, J.-P., Nannicini, R., Facchini, A., Kolarik, Z., Odoj, R., 2000. New partitioning techniques for minor actinides. Final report. EUR 19149, European Commission, Luxembourg.

Madic, C., Lecomte, M., Testard, F., Hudson, M.J., Liljenzin, J.O., Sätmark, B., Ferrando, A., Facchini, A., Geist, A., Modolo, G., Espartero, A., De Mendoza, J., 2001. PARTNEW. A European research programme for the partitioning of minor actinides from high level liquid wastes. In: Proceedings of the International Conference on GLOBAL 2001 (Back End of the Fuel Cycle: From Research to Solutions), Paris, France, 9–13 September.

Madic, C., Hudson, M.J., Liljenzin, J.-O., Glatz, J.-P., Nannicini, R., Facchini, A., Kolarik, Z., Odoj, R., 2002a. Recent achievements in the development of partitioning processes of minor actinides from nuclear wastes obtained in the frame of the NEWPART European programme (1996–1999). Prog. Nucl. Energy 40, 523–526.

Madic, C., Lecomte, M., Baron, P., Boullis, B., 2002b. Separation of long-lived radionuclides from high active nuclear waste. C. R. Phys. 3, 797–811.

Madic, C., Testard, F., Hudson, M.J., Liljenzin, J.-O., Christiansen, B., Ferrando, M., Facchini, A., Geist, A., Modolo, G., Espartero, A.G., de Mendoza, J., 2004. PARTNEW—new solvent extraction processes for minor actinides. Final report. CEA-R-6066Commissariat à l'Énergie Atomique, France.

Madic, C., Boullis, B., Baron, P., Testard, R., Hudson, M.J., Lijenzin, J.O., Christiansen, B., Ferrando, M., Facchini, A., Geist, A., Modolo, G., Espartero, A.G., De Mendoza, J., 2007. Futuristic back-end of the nuclear fuel cycle with the partitioning of minor actinides. J. Alloys Compd. 444, 23–27.

Magnusson, D., Malmbeck, R., 2012. Development of a solvent extraction model for process tests in short residence time centrifugal contactors. Solvent Extr. Ion Exch. 30, 115–126.

Magnusson, D., Christiansen, B., Foreman, M.R.S., Geist, A., Glatz, J.P., Malmbeck, R., Modolo, G., Serrano-Purroy, D., Sorel, C., 2009a. Demonstration of a SANEX process in centrifugal contactors using the CyMe4-BTBP molecule on a genuine fuel solution. Solvent Extr. Ion Exch. 27, 97–106.

Magnusson, D., Christiansen, B., Glatz, J.P., Malmbeck, R., Modolo, G., Serrano-Purroy, D., Sorel, C., 2009b. Demonstration of a TODGA based extraction process for the partitioning of minor actinides from a PUREX raffinate. Part III: centrifugal contactor run using genuine fuel solution. Solvent Extr. Ion Exch. 27, 26–35.

Magnusson, D., Christiansen, B., Glatz, J.P., Malmbeck, R., Modolo, G., Serrano-Purroy, D., Sorel, C., 2009c. Towards an optimized flow sheet for a SANEX demonstration process using centrifugal contactors. Radiochim. Acta 97, 155–159.

Magnusson, D., Christiansen, B., Malmbeck, R., Glatz, J.P., 2009d. Investigation of the radiolytic stability of a CyMe4-BTBP based SANEX solvent. Radiochim. Acta 97, 497–502.

Magnusson, D., Geist, A., Malmbeck, R., 2013a. SX process—a code for solvent extraction processes in centrifugal contactors simulation. Chem. Eng. Sci. 99, 292–297.

Magnusson, D., Geist, A., Malmbeck, R., Müllich, U., 2013b. Study of the mass transfer behavior in a centrifugal contactor and verification of the solvent extraction model for the SX Process program. Solvent Extr. Ion Exch. 31, 578–589.

Magnusson, D., Geist, A., Wilden, A., Modolo, G., 2013c. Direct selective extraction of actinides (III) from PUREX raffinate using a mixture of CyMe4-BTBP and TODGA as 1-cycle SANEX solvent part II: flow sheet design for a counter-current centrifugal contactor demonstration process. Solvent Extr. Ion Exch. 31, 1–11.

Malmbeck, R., Carrott, M., Christiansen, B., Geist, A., Hérès, X., Magnusson, D., Modolo, G., Sorel, C., Taylor, R., Wilden, A., 2014. EURO-GANEX, a process for the co-separation of TRU. In: Sustainable Nuclear Energy Conference, Manchester, UK, 9–11 April 2014.

Mathur, J.N., Murali, M.S., Nash, K.L., 2001. Actinide partitioning—a review. Solvent Extr. Ion Exch. 19, 357–390.

Miguirditchian, M., Chareyre, L., Hérès, X., Hill, C., Baron, P., Masson, M., 2007. GANEX: adaptation of the DIAMEX-SANEX process for the group actinide separation. In: Proceedings of the International Conference on GLOBAL 2007 (Advanced Nuclear Fuel Cycles and Systems), Boise, Idaho, USA, 9–13 September 2007.

Miguirditchian, M., Sorel, C., Camès, B., Bisel, I., Baron, P., 2008. Extraction of uranium(VI) by *N*,*N*-di-(ethyl-2-hexyl)isobutyramide (DEHiBA): from the batch experimental data to the counter-current process. In: Moyer, B.A. (Ed.), Proceedings of the International Solvent Extraction Conference (ISEC 2008), Tucson, Arizona, USA, 15–19 September 2008.

Miguirditchian, M., Roussel, H., Chareyre, L., Baron, P., Espinoux, D., Calor, J.-N., Viallesoubranne, C., Lorrain, B., Masson, M., 2009a. HA demonstration in the Atalante facility of the GANEX 2nd cycle for the grouped TRU extraction. In: Proceedings of the International Conference on GLOBAL 2009 (The Nuclear Fuel Cycle: Sustainable Options & Industrial Perspectives), Paris, France, 6–11 September.

Miguirditchian, M., Sorel, C., Camès, B., Bisel, I., Baron, P., Espinoux, D., Calor, J.-N., Viallesoubranne, C., Lorrain, B., Masson, M., 2009b. HA demonstration in the Atalante facility of the GANEX 1st cycle for the selective extraction of uranium from HLW.

In: Proceedings of the International Conference on GLOBAL 2009 (The Nuclear Fuel Cycle: Sustainable Options & Industrial Perspectives), Paris, France, 6–11 September.
Miguirditchian, M., Rostaing, C., Poinssot, C., Baron, P., Charbonnel, M.C., Hérès, X., Warin, D., Boullis, B., 2013. Selective recovery of americium alone from PUREX or COEX(TM) raffinate by the EXAm process. In: Proceedings of the FR'13 Conference, Paris, France, 4–7 March 2013.
Modolo, G., Odoj, R., 1998. The separation of trivalent actinides from lanthanides by dithiophosphinic acids from HNO_3 acid medium. J. Alloys Compd. 271–273, 248–251.
Modolo, G., Odoj, R., 1999. Synergistic selective extraction of actinides(III) over lanthanides from nitric acid using new aromatic diorganyldithiophosphinic acids and neutral organophosphorus compounds. Solvent Extr. Ion Exch. 17, 33–53.
Modolo, G., Seekamp, S., Nabet, S., 2002. Development of an extraction process for separation of actinoids (III)/lanthanoids (III) with the aid of dithiophosphinic acids. Chem. Ing. Tech. 74, 261–265.
Modolo, G., Vijgen, H., Schreinemachers, C., Baron, P., Dinh, B., 2003. TODGA process development for partitioning of actinides(III) from PUREX raffinate. In: Proceedings of the International Conference on GLOBAL 2003 (Atoms for Prosperity: Updating Eisenhower's Global Vision for Nuclear Energy). New Orleans, USA, 16–20 November 2003.
Modolo, G., Asp, H., Schreinemachers, C., Vijgen, H., 2007a. Development of a TODGA based process for partitioning of actinides from a PUREX raffinate. Part I: batch extraction optimization studies and stability tests. Solvent Extr. Ion Exch. 25, 703–721.
Modolo, G., Vijgen, H., Serrano-Purroy, D., Christiansen, B., Malmbeck, R., Sorel, C., Baron, P., 2007b. DIAMEX counter-current extraction process for recovery of trivalent actinides from simulated high active concentrate. Sep. Sci. Technol. 42, 439–452.
Modolo, G., Asp, H., Vijgen, H., Malmbeck, R., Magnusson, D., Sorel, C., 2008. Demonstration of a TODGA-based continuous counter-current extraction process for the partitioning of actinides from a simulated PUREX raffinate, part II: centrifugal contactor runs. Solvent Extr. Ion Exch. 26, 62–76.
Modolo, G., Kluxen, P., Geist, A., 2010. Demonstration of the LUCA process for the separation of americium(III) from curium(III), californium(III), and lanthanides(III) in acidic solution using a synergistic mixture of bis(chlorophenyl)dithiophosphinic acid and tris(2-ethylhexyl)phosphate. Radiochim. Acta 98, 193–201.
Modolo, G., Wilden, A., Daniels, H., Geist, A., Magnusson, D., Malmbeck, R., 2013. Development and demonstration of a new SANEX partitioning process for selective actinide (III)/lanthanide(III) separation using a mixture of CyMe4-BTBP and TODGA. Radiochim. Acta 101, 155–162.
Modolo, G., Wilden, A., Kaufholz, P., Bosbach, D., Geist, A., 2014. Development and demonstration of innovative partitioning processes (i-SANEX and 1-cycle SANEX) for actinide partitioning. Prog. Nucl. Energy 72, 107–114.
Morita, Y., Kubota, M., 1988. Extraction of neptunium with di-isodecyl phosphoric acid from nitric acid solution containing hydrogen peroxide. Solvent Extr. Ion Exch. 6, 233–246.
Morita, Y., Glatz, J.P., Kubota, M., Koch, L., Pagliosa, G., Roemer, K., Nicholl, A., 1996. Actinide partitioning from HLW in a continuous DIDPA extraction process by means of centrifugal extractors. Solvent Extr. Ion Exch. 14, 385–400.
Musikas, C., 1987. Solvent extraction for the chemical separations of the 5f elements. Inorg. Chim. Acta 140, 197–206.
Musikas, C., 1988. Potentiality of nonorganophosphorus extractant in chemical separations of actinides. Sep. Sci. Technol. 23, 1211–1226.

Musikas, C., Hubert, H., 1987. Extraction by *N*,*N*'-tetraalkylmalonamides II. Extraction of metallic ions. Solvent Extr. Ion Exch. 5, 877–893.

Musikas, C., Le Marois, G., Fitoussi, R., Cuillerdier, C., 1980. Properties and use of nitrogen and sulfur donors in actinide separations. In: Navratil, J.D., Schulz, W.W. (Eds.), ACS Symposium Series, vol. 117. ACS, Washington, DC.

Musikas, C., Vitorge, P., Pattee, D., 1983. Progress in trivalent actinide lanthanide group separations. Proceedings of the International Solvent Extraction Conference (ISEC 1983), Denver, Colorado, USA, 26 August–2 September.

Nakahara, M., Nakajima, Y., Koizumi, T., 2012. Extraction behavior of fission products with tri-*n*-butyl phosphate by countercurrent multistage extraction in a uranium, plutonium, and neptunium co-recovery system. Ind. Eng. Chem. Res. 51, 13245–13250.

Nash, K.L., Madic, C., Mathur, J.N., Lacquement, J., 2006. Actinide separation science and technology. In: Morss, L.R., Edelstein, N.M., Fuger, J., Katz, J.J. (Eds.), The Chemistry of Actinide and Transactinide Elements, third ed. Springer, Dordrecht, The Netherlands.

Nave, S., Modolo, G., Madic, C., Testard, F., 2004. Aggregation properties of *N*,*N*,*N*′,*N*′-tetraoctyl-3-oxapentanediamide (TODGA) in *n*-dodecane. Solvent Extr. Ion Exch. 22, 527–551.

Nigond, L., Musikas, C., Cuillerdier, C., 1994. Extraction by *N*,*N*,*N*',*N*'-tetraalkyl-2-alkyl propane-1,3-diamides. II. U(VI) and Pu(IV). Solvent Extr. Ion Exch. 12, 297–323.

Nilsson, M., Nash, K.L., 2007. Review article: a review of the development and operational characteristics of the TALSPEAK process. Solvent Extr. Ion Exch. 25, 665–701.

OECD-NEA, 1999. Actinide and fission product partitioning and transmutation: status and assessment report. OECD, Nuclear Energy Agency (NEA), Paris.

OECD-NEA, 2006. Advanced nuclear fuel cycles and radioactive waste management. NEA No. 5990OECD, Nuclear Energy Agency (NEA), Paris.

OECD-NEA, 2011. Potential benefits and impacts of advanced nuclear fuel cycles with actinide partitioning and transmutation. NEA No. 6894, OECD, Nuclear Energy Agency (NEA), Paris.

Panak, P.J., Geist, A., 2013. Complexation and extraction of trivalent actinides and lanthanides by triazinylpyridine N-donor ligands. Chem. Rev. 113, 1199–1236.

Pearson, R.G., 1963. Hard and soft acids and bases. J. Am. Chem. Soc. 85, 3533–3539.

Peppard, D.F., Mason, G.W., Maier, J.L., Driscoll, W.J., 1957. Fractional extraction of the lanthanides as their di-alkyl orthophosphates. J. Inorg. Nucl. Chem. 4, 334–343.

Persson, G., Svantesson, I., Wingefors, S., Liljenzin, J.-O., 1984. Hot test of a TALSPEAK procedure for separation of actinides and lanthanides using recirculating DTPA-lactic acid solutions. Solvent Extr. Ion Exch. 2, 89–113.

Poinssot, C., Warin, D., Rostaing, C., 2010. Recent achievements towards the recycling of minor actinides for the improvement of future nuclear fuel cycles. In: European Nuclear Conference, Barcelona, 30 May–2 June.

Precek, M., Paulenova, A., 2010. Kinetics of reduction of hexavalent neptunium by nitrous acid in solutions of nitric acid. J. Radioanal. Nucl. Chem. 286, 771–776.

Rat, B., Hérès, X., 2000. Modelling and achievement of a SANEX process flowsheet for trivalent actinides/lanthanides separation using BTP extractant (bis-1,2,4-triazinyl-pyridine). In: Proceedings of the International Conference ATALANTE 2000 (Scientific Research on the Back-end of the Nuclear Fuel Cycle for the 21st Century), Avignon, France, 24–26 October.

Retegan, T., Ekberg, C., Englund, S., Fermvik, A., Foreman, M.R.S., Skarnemark, G., 2007. The behaviour of organic solvents containing C5-BTBP and CyMe4-BTBP at low irradiation doses. Radiochim. Acta 95, 637–642.

Rostaing, C., Poinssot, C., Warin, D., Baron, P., Lorrain, B., 2012. Development and validation of the EXAm separation process for single Am recycling. Proc. Chem. 7, 367–373.

Rouyer, H., 1992. Separation and transmutation of actinides: the SPIN programme. General introduction. Revue Genérale Nucléaire 5, 407–413.

Runde, W.H., Mincher, B.J., 2011. Higher oxidation states of americium: preparation, characterization and use for separations. Chem. Rev. 111, 5723–5741.

Sasaki, Y., Choppin, G.R., 1998. Extraction of Np(V) by *N*,*N*'-dimethyl-*N*,*N*'-dihexyl-3-oxapentanediamide. Radiochim. Acta 80, 85–88.

Sasaki, Y., Sugo, Y., Suzuki, S., Tachimori, S., 2001. The novel extractants, diglycolamides, for the extraction of lanthanides and actinides in HNO_3/*n*-dodecane system. Solvent Extr. Ion Exch. 19, 91–103.

Serrano-Purroy, D., Baron, P., Christiansen, B., Glatz, J.-P., Madic, C., Malmbeck, R., Modolo, G., 2005a. First demonstration of a centrifugal solvent extraction process for minor actinides from a concentrated spent fuel solution. Sep. Purif. Technol. 45, 157–162.

Serrano-Purroy, D., Baron, P., Christiansen, B., Malmbeck, R., Sorel, C., Glatz, J.P., 2005b. Recovery of minor actinides from HLLW using the DIAMEX process. Radiochim. Acta 93, 351–355.

Serrano-Purroy, D., Christiansen, B., Glatz, J.P., Malmbeck, R., Modolo, G., 2005c. Towards a DIAMEX process using high active concentrate. Production of genuine solutions. Radiochim. Acta 93, 357–361.

Sorel, C., Montuir, M., Espinoux, D., Lorrain, B., Baron, P., 2008. Technical feasibility of the DIAMEX process. In: Moyer, B.A. (Ed.), Proceedings of the International Solvent Extraction Conference (ISEC 2008), Tucson, USA, 15–19 September 2008.

Stephan, H., Gloe, K., Beger, J., Mühl, P., 1991. Liquid-liquid extraction of metal ions with amido podands. Solvent Extr. Ion Exch. 9, 459–469.

Sypula, M., Wilden, A., Modolo, G., Geist, A., 2011. Innovative SANEX process for actinide (III) separation from PUREX raffinate using TODGA-based solvents. In: Proceedings of the International Solvent Extraction Conference (ISEC 2011), Santiago, Chile, 3–7 October.

Sypula, M., Wilden, A., Schreinemachers, C., Malmbeck, R., Geist, A., Taylor, R., Modolo, G., 2012. Use of polyaminocarboxylic acids as hydrophilic masking agents for fission products in actinide partitioning processes. Solvent Extr. Ion Exch. 30, 748–764.

Tachimori, S., Morita, Y., 2010. Overview of solvent extraction chemistry for reprocessing. In: Moyer, B.A. (Ed.), Ion Exchange and Solvent Extraction. CRC Press, Boca Raton, London, New York.

Tachimori, S., Sasaki, Y., Suzuki, S.-I., 2002. Modification of TODGA-*n*-dodecane solvent with a monoamide for high loading of lanthanides(III) and actinides(III). Solvent Extr. Ion Exch. 20, 687–699.

Taylor, R.J., May, I., Koltunov, V.S., Baranov, S.M., Marchenko, V.I., Mezhov, E.A., Pastuschak, V.G., Zhuravleva, G.I., Savilova, O.A., 1998. Kinetic and solvent extraction studies of the selective reduction of Np(VI) by new salt-free reducing agents. Radiochim. Acta 81, 149–156.

Taylor, R.J., Gregson, C.R., Carrott, M.J., Mason, C., Sarsfield, M.J., 2013. Progress towards the full recovery of neptunium in an advanced PUREX process. Solvent Extr. Ion Exch. 31, 442–462.

Trumm, S., Geist, A., Panak, P.J., Fanghänel, T., 2011. An improved hydrolytically-stable bis-triazinyl-pyridine (BTP) for selective actinide extraction. Solvent Extr. Ion Exch. 29, 213–229.

Warin, D., 2007. Status of the French research program on partitioning and transmutation. J. Nucl. Sci. Technol. 44, 410–414.

Weaver, B., Kappelmann, F.A., 1964. TALSPEAK: a new method of separating americium and curium from the lanthanides by extraction from an aqueous solution of an aminopolyacetic acid complex with a monoacidic organophosphate or phosphonate. USAEC report ORNL-3559, Oak Ridge National Laboratory, USA.

Wilden, A., Schreinemachers, C., Sypula, M., Modolo, G., 2011. Direct selective extraction of actinides (III) from PUREX raffinate using a mixture of CyMe4-BTBP and TODGA as 1-cycle SANEX solvent. Solvent Extr. Ion Exch. 29, 190–212.

Wilden, A., Modolo, G., Sypula, M., Geist, A., Magnusson, D., 2012. The recovery of An(III) in an innovative-SANEX process using a TODGA-based solvent and selective stripping with a hydrophilic BTP. Proc. Chem. 7, 418–424.

Wilden, A., Modolo, G., Schreinemachers, C., Sadowski, F., Lange, S., Sypula, M., Magnusson, D., Geist, A., Lewis, F.W., Harwood, L.M., Hudson, M.J., 2013. Direct selective extraction of actinides (III) from PUREX raffinate using a mixture of CyMe4-BTBP and TODGA as 1-cycle SANEX solvent part III: demonstration of a laboratory-scale counter-current centrifugal contactor process. Solvent Extr. Ion Exch. 31, 519–537.

Yaita, T., Herlinger, A.W., Thiyagarajan, P., Jensen, M.P., 2004. Influence of extractant aggregation on the extraction of trivalent f-element cations by a tetraalkyldiglycolamide. Solvent Extr. Ion Exch. 22, 553–571.

Yoshida, Z., Johnson, S.G., Kimura, T., Krsul, J.R., 2011. Neptunium. In: Morss, L.R., Edelstein, N.M., Fuger, J. (Eds.), The Chemistry of the Actinide and Transactinide Elements. Springer, Dordrecht, The Netherlands (Chapter 6).

Zhang, H., Ye, G.-A., Li, L., Zheng, W.-F., Cong, H.-F., Xiao, S.-T., Yang, H., Lan, T., 2013. Simulation of the neptunium behavior during the first solvent extraction cycle in the PUREX process. J. Radioanal. Nucl. Chem. 295, 883–888.

Zhu, Y., Song, C., 1992. In: Morss, L.R., Fuger, J. (Eds.), Transuranium Elements, A Half Century. American Chemical Society Books, Washington, DC, USA (Chapter 32).

Minor actinide separation in the reprocessing of spent nuclear fuels: recent advances in the United States

11

Bruce A. Moyer[1], *Gregg J. Lumetta*[2], *Bruce J. Mincher*[3]
[1]Oak Ridge National Laboratory, Oak Ridge, TN, USA; [2]Pacific Northwest National Laboratory, Richland, WA, USA; [3]Idaho National Laboratory, Idaho Falls, ID, USA

Acronyms

ALSEP	actinide-lanthanide separation process concept
An	actinide
CDTA	*trans*-1,2-diaminocyclohexane-*N*,*N*,*N*′,*N*′-tetraacetic acid
CMPO	octyl(phenyl)-*N*,*N*-diisobutylcarbamoylmethylphosphine oxide (TRUEX extractant)
DAAP	diamylamylphosphonate
DGA	diglycolamide
DIAMEX	diamide extraction process
DTPA	diethylenetriaminepentaacetic acid, actinide-selective complexant used in TALSPEAK aqueous phase
FCRD	Fuel Cycle Research and Development
FP	fission product
HDEHP	bis(2-ethylhexyl)phosphoric acid, extractant for An(III) and Ln(III) in TALSPEAK process
HEDTA	*N*-(2-hydroxyethyl)ethylenediamine-*N*,*N*′,*N*′-triacetic acid, actinide-selective complexant used in Advanced TALSPEAK aqueous phase
HEH[EHP]	2-ethylhexylphosphonic acid mono-2-ethylhexyl ester, extractant for An(III) and Ln(III) in Advanced TALSPEAK and ALSEP processes
Ln	lanthanide
MA	minor actinide
OECD	Organization for Economic Cooperation and Development
P&T	partitioning and transmutation
STMAS	Sigma Team for Minor Actinide Separations
T2EHDGA	*N*,*N*,*N*′,*N*′-tetra(2-ethylhexyl)diglycolamide, extractant for An(III) and Ln(III) in ALSEP
TALSPEAK	trivalent actinide-lanthanide separations by phosphorus-reagent extraction from aqueous complexes
TBP	tri-*n*-butyl phosphate

Reprocessing and Recycling of Spent Nuclear Fuel. http://dx.doi.org/10.1016/B978-1-78242-212-9.00011-3

TEDGA	*N*,*N*,*N*′,*N*′-tetraethyldiglycolamide
TRUEX	transuranic extraction
UREX+	uranium extraction plus, a suite of actinide and fission-product separations
USDOE	U.S. Department of Energy

11.1 Introduction

Neptunium, americium, and curium constitute the so-called minor actinides (MAs), which represent only about a tenth of a percent of the total heavy metal mass in used light-water nuclear reactor fuel. In contrast to their relatively minor mass percentage, due to their radiotoxicity and heat generation, their role is major in terms of formulating strategies for used fuel recycle or in designing repositories. With the general motivation of finding more effective methods for used fuel recycle, the separation of MAs is being pursued in various fundamental-to-applied research programs in the United States. In particular, a concentration of effort has been focused within the Sigma Team for Minor Actinide Separation (STMAS) formed in 2009 within the U.S. Department of Energy (USDOE) Fuel Cycle Research and Development (FCRD) program. The STMAS serves within the framework of the Nuclear Energy Research and Development Roadmap (USDOE, 2010a) and, in particular, it supports the goal of developing sustainable nuclear fuel cycles (USDOE, 2010b). Accordingly, the overarching goal of the STMAS is to provide the scientific basis for more efficient separation methods, especially for americium and curium, in order to greatly improve the overall benefit of fuel recycle. The specific aim of the STMAS is the development of a robust, more efficient actinide/lanthanide (An/Ln) separation process. The possibility of separating americium from curium has also been examined. While the first years of the STMAS emphasized research on the applicable science behind germinating technology concepts, the scope of the program has advanced to include the development and testing of functional separations systems, leading to bench-scale demonstration.

The above aims are being pursued mainly within the paradigm of aqueous reprocessing of used oxide nuclear fuel dissolved in nitric acid. Given that an array of previously matured separation technologies for MA separations had been brought successfully through demonstrations in the context of the UREX+ (uranium extraction plus) suite of processes (Regalbuto, 2011; Gelis et al., 2009; Laidler, 2008), the present challenge deals primarily with the question of the efficiency and economy with which these separations can be achieved with the aim of developing a manageable and affordable fuel cycle. The magnitude of this problem will require unprecedented simplification and compaction of separations processes, preferably eliminating and combining steps. It is anticipated that this will entail new chemistry and likely altogether new separation agents.

This chapter examines two major approaches being undertaken within the STMAS, first discussing the need for recycle of the MAs and the available chemical principles by which separation strategies can be developed. The first approach being pursued in the STMAS relies on aqueous complexation chemistry using nitrogen-donor polycarboxylic acid chelating agents to generate the selectivity for trivalent americium and

curium versus the trivalent lanthanides between the aqueous phase and a nonselective solvent system. The second approach entails developing the chemistry of the V and VI oxidation states of americium to achieve a separation from trivalent lanthanides and curium via solvent extraction. Although other approaches are being pursued, both in the STMAS and elsewhere, this chapter will focus on the above-mentioned examples to provide more detailed treatments of these significant advances. The conclusion of the chapter will look forward to future developments.

11.2 Significance of minor actinide separation

As recognized widely by the national and international scientific community (Salvatores and Palmiotti, 2011; Tachimori and Morita, 2010; Hill, 2010; Boullis, 2008; Arm et al., 2008; Todd and Wigeland, 2006; Nash et al., 2006), the major benefit of MA separation in general lies in the reduced heat load on a repository, effectively increasing repository capacity. At the same time, the recycle of the recovered MAs provides additional energy utilization of the used nuclear fuel, in part offsetting the cost of performing the separation. In addition, process simplification resulting from separations research serves the interest of accountability and therefore nonproliferation. International arguments have also stressed the reduced long-term radiotoxicity of the waste stored in geologic repositories, though long-lived fission products (FPs) like ^{99}Tc, ^{129}I, and ^{135}Cs are still likely to require long-term geologic storage.

From a technical perspective, the specific requirements for MA separations depend on the nature of the future fuel cycle that will ultimately be implemented, involving such system choices as reactor type, fuel type, and waste disposition. A systems-option study of these myriad choices is in progress within FCRD and will inform R&D planning in the coming years (USDOE, 2010b). In its Partitioning and Transmutation (P&T) Exchange Meetings (OECD, 2010, 2012), the Organization for Economic Cooperation and Development (OECD) has been engaging the general question of MA separation and transmutation for several decades from multiple perspectives. A recent review summarizes the current situation, pointing to the need for research on numerous aspects of advanced fuel cycles, including MA separations (Salvatores and Palmiotti, 2011). While specific needs for MA separations are in the process of being more clearly defined, it is taken for present purposes that separations research will play a critical enabling role, primarily within the full-recycle option as opposed to a once-through open cycle (USDOE, 2010b).

Benefits of a full-recycle option with separation and recycle (P&T) of MAs include increased repository capacity (performance), decreased long-term radiotoxicity, and reduced risk from low-probability/high consequence scenarios such as geologic events and human intrusion (Salvatores and Palmiotti, 2011; Wigeland et al., 2006). With no separations whatsoever, as is the case with the once-through option, Figure 11.1 shows that the heat load on a geologic repository out to 2000 years is dominated by ^{241}Am ($t_{1/2} = 433$ years) after the FPs have decayed sufficiently (75 years) (Wigeland et al., 2006). Given that heat loading directly determines the storage capacity of a repository,

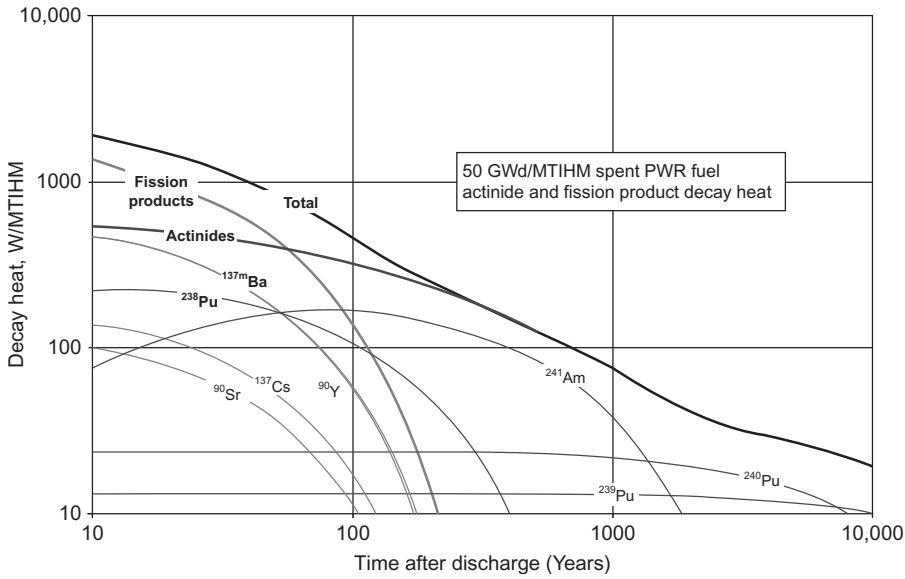

Figure 11.1 Decay heat for used fuel discharged after being irradiated for 50 GWd/MTIHM (Wigeland et al., 2006).
Reprinted with permission. Copyright 2006 by the American Nuclear Society, La Grange Park, IL.

removal of ^{241}Am alone has clear benefit for increasing storage capacity, reducing repository size, or permitting a lower repository operating temperature. Estimates of such benefits have been given for the case of the controversial Yucca Mountain project (Wigeland et al., 2006), which can be used as an illustrative example. Accordingly, a 4.3-5.4-fold increase in waste loading would be expected for 90-99.9% removal of americium, assuming equal removal efficiency of plutonium. A maximum 225-fold increase in waste loading would be expected upon removal of 99.9% of the plutonium, americium, and curium, along with the FPs cesium and strontium. Similar benefits for other repositories may also be expected depending on the geology and repository design. Repository benefits of MA separation and transmutation also include decreased overall repository radiotoxicity and decreased radiotoxicity lifetime, goals that also promote public acceptance of nuclear energy (Carelli et al., 2011). While decreased radiotoxicity of the repository is itself thought to have limited impact on repository performance, substantial reduction of risk is recognized in terms of disruptive events due, for example, to geologic phenomena and human intrusion (Salvatores and Palmiotti, 2011).

As described in Section 11.1, the need to develop an efficient An/Ln separation stands out as most urgent. This separation is important because the lanthanides are strong thermal neutron absorbers and thus cannot be recycled in light-water reactor fuel, though fast reactors are expected to be more tolerant. A further separation of americium from curium has been viewed as a necessary process option (Laidler, 2008), as curium presents difficulties in fuel fabrication due to the greater shielding

requirements, though this is not a universally agreed upon opinion (Arm et al., 2008). Given that an effective chemistry already exists for manipulating neptunium in contemporary solvent-extraction systems employing tri-*n*-butyl phosphate (TBP), the need for neptunium separations research seems relatively less urgent than the need for americium and curium separations research. By contrast, An/Ln or Am/Cm separations have been especially difficult because the chemistry of their common trivalent oxidation states is very similar. Although we can point to significant progress, a fully satisfactory solution has not yet been found (Hill, 2010, 2011).

A clear need to simplify separations in fuel recycle is universally recognized. Although the successful demonstrations of UREX+ (Regalbuto, 2011; Gelis et al., 2009; Laidler, 2008) increased overall confidence in our ability to reprocess used light-water reactor fuel at a commercial scale to meet a variety of potential U.S. advanced fuel cycle objectives, the level of complexity and projected cost of deploying multiple process steps was unprecedented. Whether to separate the MAs in the first place and what types of streams containing the MAs are best suited to fuel fabrication or waste disposal must be a result of a comprehensive fuel cycle systems analysis. While such guidance is being formulated, a chemical toolbox approach has been undertaken by STMAS under the philosophy that the chemical understanding in the context of potential separation methods will be available for exploitation as systems goals are more clearly defined.

11.3 General approaches to minor actinide separation

As shown in Figure 11.2 and discussed in detail in subsequent sections of this chapter, two distinct strategies for americium separation may be pursued based on either the competitive complexation (Tachimori and Morita, 2010; Hill, 2010) or the higher oxidation states of americium (Runde and Mincher, 2011). Complexation presents

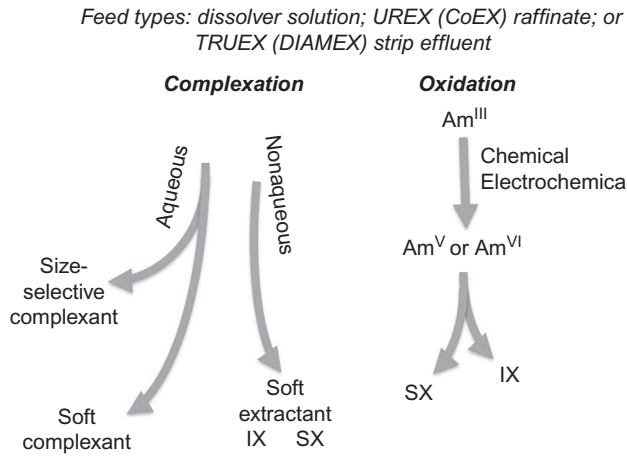

Figure 11.2 Strategies for achieving selectivity in two-phase separation systems.

particular challenges in that the trivalent 4f and 5f elements have very similar bonding characteristics, dominated by electrostatics. For Am(III)/Cm(III) separations, the ionic radii differ very slightly, and these fall within the much wider size range of the lanthanides (Shannon, 1976), making An(III)/Ln(III) discrimination difficult. Regarding the second strategy, the higher oxidation states of americium that can be exploited require aggressive oxidizing conditions. The oxidation potentials greatly exceed the potentials for oxidation of water, and americium(V) and americium(VI) are thus thermodynamically unstable once formed (Runde and Mincher, 2011). Indeed, both americium(V) and americium(VI) both spontaneously return to americium(III), the lifetime of americium(V) being on the order of days, while that for americium(VI) being only minutes in aqueous solutions. The auto-reduction rates are highly dependent on conditions and, for americium(VI), a holding oxidant will likely be required to perform a separation.

Both complexation and oxidation strategies can be used in either phase of a separation system. For example, by use of the extractant bis(2-ethylhexyl)phosphoric acid (HDEHP), which is not selective for actinide(III) vs lanthanide(III), and addition of the actinide(III)-selective complexant diethylenetriaminepentaacetic acid (DTPA) to the aqueous phase, the lanthanide(III) ions are render significantly more extractable than actinide(III) ions (see Section 11.4). This principle can be made to operate in an extraction of lanthanide(III) ions away from americium(III) or in stripping extracted americium(III) from coextracted lanthanide(III). Alternatively, the actinide-selective complexant can be the extractant. One could employ the same ideas in the use of inorganic ion exchangers. For example, an inorganic exchanger with affinity for both actinide(III) and lanthanide(III) ions could be used in the presence of an appropriate aqueous-phase complexant that has an affinity for An(III) versus Ln(III), such that only the lanthanide(III) are removed from the feed stream. Alternatively, the complexant could be added to the eluent after the combined uptake of americium(III) and lanthanide(III) to selectively desorb the americium(III). To succeed overall, complexation strategies must be highly sensitive, taking advantage of subtle effects due to very small differences in ionic radii or interaction with f-orbitals. Manipulation of the americium oxidation state is, in principle, a powerful approach for a selective americium separation, either in the context of solvent extraction or ion exchange, but the very high oxidation potentials required for oxidation of americium(III) to americium(V) and americium(VI) (Runde and Mincher, 2011) present a formidable challenge. Indeed, if this were not such a challenge, the two aims of the STMAS likely would have been preempted long ago.

11.4 Advanced TALSPEAK

The trivalent actinide-lanthanide separations by phosphorus-reagent extraction from aqueous complexes (TALSPEAK) process was first described in the 1960s (Weaver and Kappelmann, 1968), and the key features of this process have recently been reviewed (Nilsson and Nash, 2007). In the TALSPEAK process, a mixture of trivalent lanthanides and actinides is dissolved in a lactate-buffered aqueous phase, and DTPA (Table 11.1) is added. The DTPA preferentially binds the actinide ions, presumably

Table 11.1 Chemical structures of the extractants, aqueous-phase actinide complexants, and buffers used in the TALSPEAK and advanced TALSPEAK processes

	TALSPEAK	Advanced TALSPEAK
Extractant	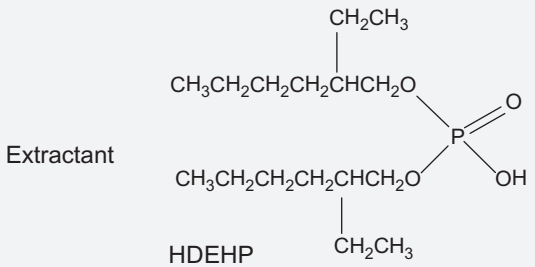	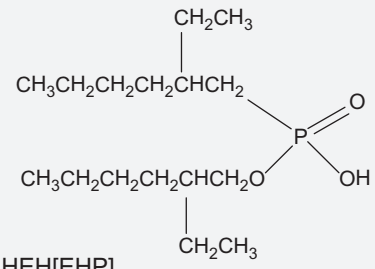
Actinide complexant	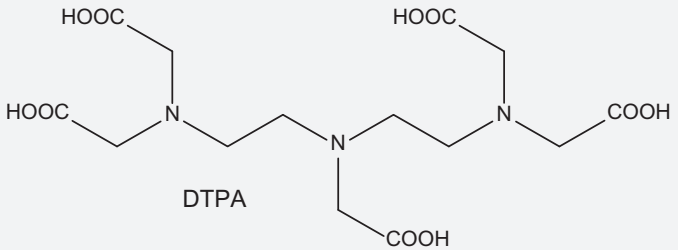	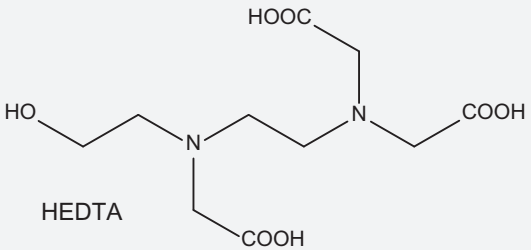
Buffer	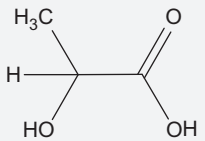	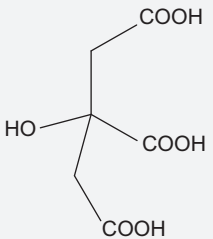

because the slightly softer Lewis acidic character of the actinides favors binding to the soft-donor amine groups (Pearson, 1963). This aqueous phase is then contacted with an organic phase containing HDEHP (Table 11.1), which binds the lanthanide ions and thereby transfers them to the organic phase. The DTPA-complexed actinide ions remain in the aqueous phase. The process can be operated in a slightly different mode in which the lanthanides and actinides are coextracted from an aqueous phase that does not contain DTPA, and then the actinides are selectively stripped into a lactate-buffered DTPA solution. This latter approach is referred to as "reverse TALSPEAK."

The TALSPEAK process has been demonstrated at a laboratory scale using solutions derived from irradiated commercial nuclear fuel (Regalbuto, 2011). However, industrial implementation of the process is complicated by its high sensitivity to the solution pH and relatively slow kinetics (Nilsson and Nash, 2007). The latter can be mitigated somewhat by using a high concentration of lactate in the aqueous buffer. For example, Figure 11.3a presents data that show the distribution of americium into 1 mol/L HDEHP in odorless kerosene reaches equilibrium more quickly as the lactate concentration is increased (Svantesson et al., 1979). Although effective, the high concentration of lactate is undesirable in terms of downstream processing because this material must ultimately be managed as process waste. The severe pH dependence is not easily mitigated in the traditional TALSPEAK process. Figure 11.3b presents the pH dependence of the neodymium and americium distribution ratios for extraction from 0.05 mol/L

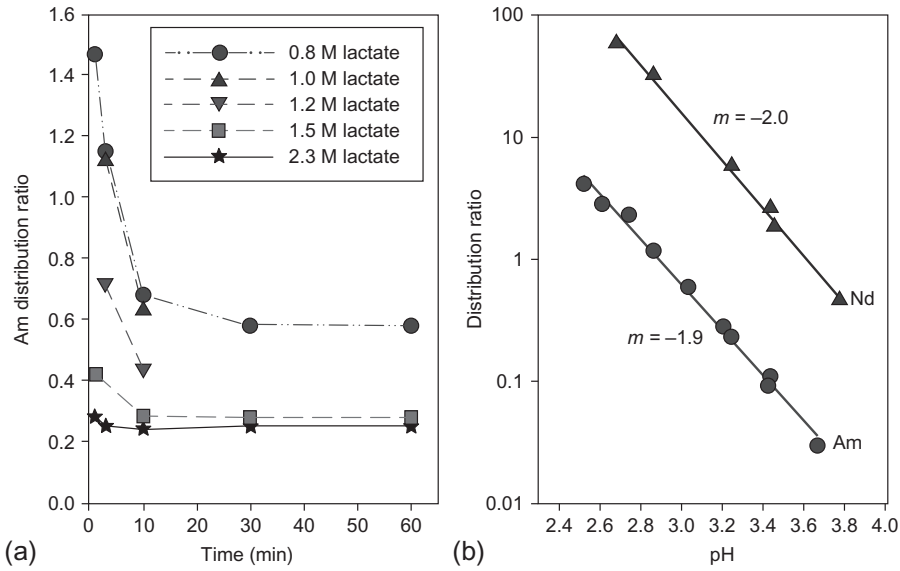

Figure 11.3 Distribution ratios for neodymium and americium for extraction from 0.05 mol/L DTPA into 1 mol/L HDEHP in odorless kerosene: (a) influence of the lactate concentration on the extraction kinetics at pH 3.4 and (b) pH dependence for 1.5 mol/L lactate system. Data taken from Svantesson et al. (1979).

DTPA/1.5 mol/L lactic acid into an organic phase consisting of 1 mol/L HDEHP in odorless kerosene (Svantesson et al., 1979). As can be seen from this plot, the pH of the system should be kept between about 3.2 and 3.4 to give reasonable extraction of neodymium while maintaining americium distribution ratios below 1. Maintaining this tight pH regime would be difficult in a shielded industrial radiochemical facility.

Recently, it has been suggested that the HDEHP extractant be replaced by the related extractant 2-ethylhexylphosphonic acid mono-2-ethylhexyl ester (HEH[EHP]; Table 11.1) (Braley et al., 2012). Because HEH[EHP] is a weaker extractant than HDEHP, the DTPA actinide complexant must be replaced with a weaker complexant; otherwise, the lanthanide distribution ratios are too low. *N*-(2-Hydroxyethyl) ethylenediamine-*N*,*N*′,*N*′-triacetic acid (HEDTA; Table 11.1) provides a suitable balance between complexing the trivalent actinides and allowing the extraction of the lanthanides by HEH[EHP]. Finally, in this modified system, the lactate buffer is replaced with a citrate buffer. This new actinide separation system is termed the "Advanced TALSPEAK" concept, and the development of this concept to date suggests that it overcomes the major shortcomings of the traditional TALSPEAK process. In particular, the pH dependence is much less in the Advanced TALSPEAK system compared with the traditional TALSPEAK system.

Figure 11.4 presents the pH dependence of the distribution ratios for americium and selected lanthanides for extraction from 0.11 mol/L HEDTA/0.2 mol/L citric acid into

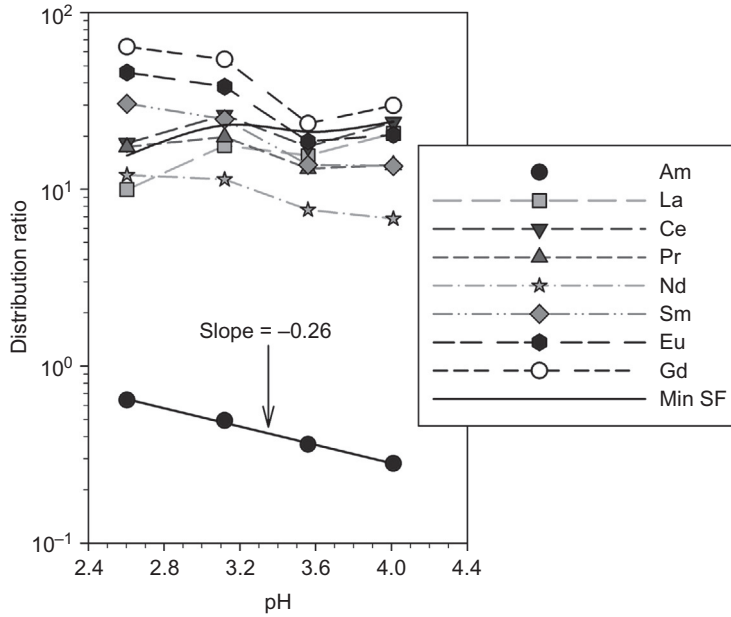

Figure 11.4 Americium and lanthanide distribution ratios for the Advanced TALSPEAK system: organic solvent, 1 mol/L HEH[EHP] in *n*-dodecane; aqueous phase, 0.11 mol/L HEDTA in 0.2 mol/L citrate buffer (Lumetta et al., 2014a).

an organic phase consisting of 1 mol/L HEH[EHP] in *n*-dodecane. Comparison of the data in Figure 11.4 to that in Figure 11.3b clearly shows the advantage of the Advanced TALSPEAK system. Whereas the slopes of the distribution ratio versus pH lines for the traditional TALSPEAK system are about −2 (Figure 11.3b), that for the Advanced TALSPEAK system is only about −0.3 (Figure 11.4). This shallower slope with Advanced TALSPEAK provides for a much wider pH operating range for Advanced TALSPEAK compared with traditional TALSPEAK.

11.5 Actinide-lanthanide separation process concept

A major disadvantage with both the TALSPEAK and Advanced TALSPEAK approaches is that a separate solvent-extraction process is needed upstream to separate the lanthanides and actinides together as a group from the high-level waste raffinate arising from the primary fuel reprocessing step. This can be done with, for example, the transuranic extraction (TRUEX) process (Horwitz et al., 1985) or the diamide extraction (DIAMEX) process (Courson et al., 2000; Malmbeck et al., 2000). To reduce the complexity of MA separations, a number of attempts have been made at combining extractants to produce a single solvent-extraction process that can separate the MAs from acidic high-level waste raffinate, including their separation from the lanthanides (Lumetta et al., 2010a).

An early example of this approach was the combination of the TRUEX extractant octyl(phenyl)-*N*,*N*-diisobutylcarbamoylmethylphosphine oxide (CMPO) with HDEHP (Dhami et al., 2001; Lumetta et al., 2013a). It was hypothesized that under highly acidic conditions (molar concentrations of nitric acid), the chemistry of CMPO would dominate, and the MAs and the lanthanides would be extracted together. Furthermore, it was assumed that switching the aqueous chemistry to a carboxylate-buffered solution of a polyaminocarboxylate complexant would result in a selective stripping of the MAs, akin to the reverse TALSPEAK approach. The combination of CMPO and HDEHP proved to be problematic because interactions between the two extractants in the organic phase reduced the effectiveness of the coextraction of the MAs and lanthanides from nitric acid and limited the separation factors that could be achieved (Lumetta et al., 2010b, 2011, 2013a). These problems were reduced by replacing HDEHP with HEH[EHP]. The interaction between HEH[EHP] and CMPO is weaker than that between HDEHP and CMPO. But the HEH[EHP]/CMPO interaction still adversely affects the effectiveness of this extraction system, especially at nitric acid concentrations greater than 2 mol/L (Braley et al., 2013).

A new combined system is under investigation that combines a diglycolamide (DGA) extractant with HEH[EHP]. The interaction between the DGA extractant and HEH[EHP] is very weak, resulting in a system that closely fulfills the original intent; that is, the chemistry of the DGA dominates at molar concentrations of nitric acid, allowing the MAs to be extracted along with the lanthanides. When the aqueous-phase chemistry is switched to a buffered (pH 3-4) polyaminocarboxylate solution, the MAs are selectively stripped from the solvent, separating them from the lanthanides. This approach has been termed the actinide-lanthanide separation (ALSEP) process

concept (Lumetta et al., 2014b; Gelis and Lumetta, 2014; Guelis, 2013). The currently preferred formulation of the ALSEP solvent consists of 0.05 mol/L *N,N,N′,N′*-tetra(2-ethylhexyl)diglycolamide (T2EHDGA) plus 0.75 mol/L HEH[EHP] dissolved in *n*-dodecane (this will hereafter be referred to as the ALSEP solvent). Figure 11.5 presents the chemical structures of the chemical components used in ALSEP.

The ALSEP solvent effectively extracts americium at nitric acid concentrations greater than 1 mol/L (Figure 11.6a). The heavier lanthanides samarium, europium, and gadolinium, are also efficiently extracted into the ALSEP solvent under these conditions. The neodymium distribution ratios for extraction from nitric acid closely parallel those of americium, but are slightly lower. The light lanthanides are less strongly extracted by the ALSEP solvent. This is especially true for lanthanum. The distribution ratios for this element remain below 1 mol/L up to a nitric acid

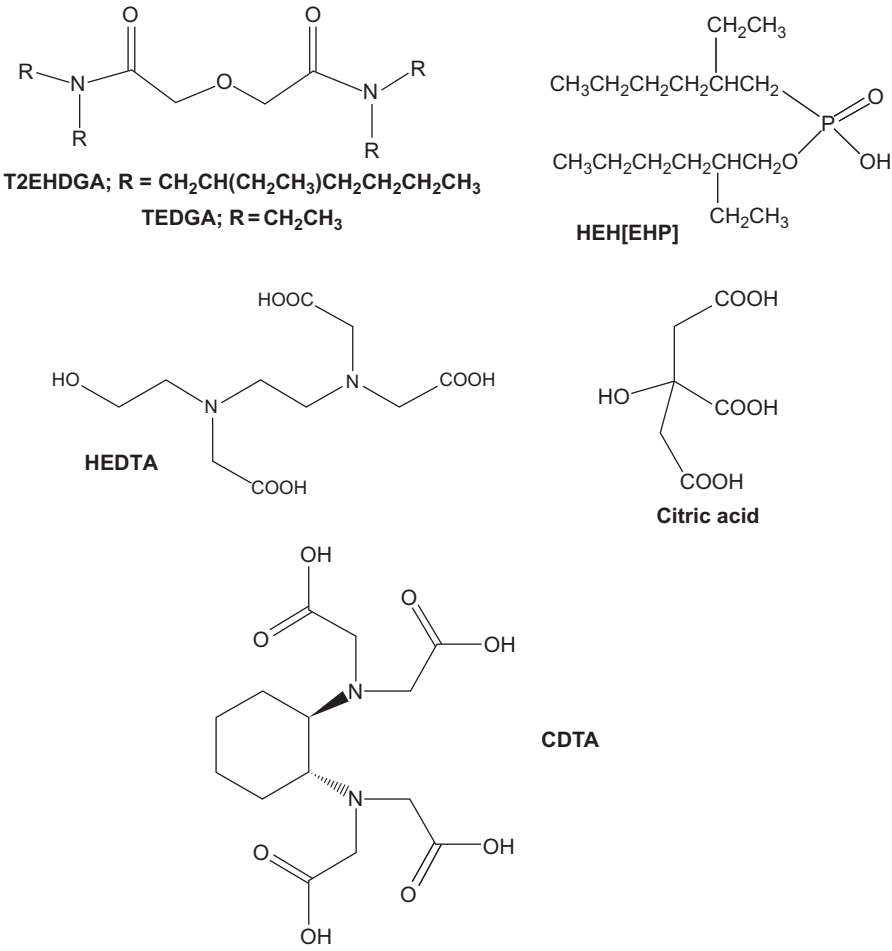

Figure 11.5 Structures of the chemicals used in the ALSEP concept.

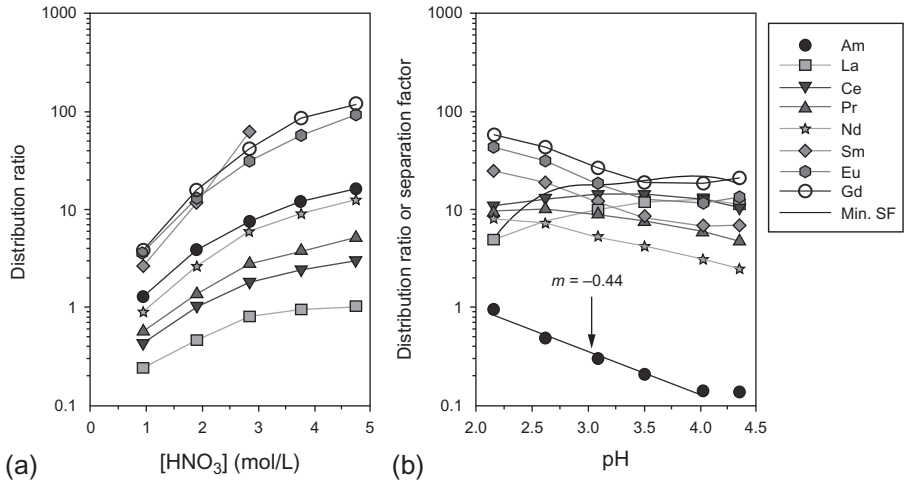

Figure 11.6 Americium and lanthanide distribution ratios for the ALSEP system: organic solvent, 0.05 mol/L T2EHDGA plus 0.75 mol/L HEH[EHP] in *n*-dodecane; aqueous phase, (a) various concentrations of HNO_3, (b) 0.125 mol/L HEDTA in 0.2 mol/L citrate buffer (Lumetta et al., 2014a).

concentration of approximately 5 mol/L. These results suggest that americium can be separated from lanthanum in irradiated fuel during the ALSEP extraction step, which would reduce the metal loading in the organic phase and improve the efficiency of the downstream stripping steps.

Figure 11.6b presents the americium and lanthanide distribution ratios under the conditions used for selectively stripping the MAs. In this case, the aqueous phase consists of 0.125 mol/L HEDTA in 0.2 mol/L citrate buffer. The distribution ratios for the lanthanides remain above 1 for the entire pH range examined (2.1-4.4). The americium distribution ratios decrease with increasing pH. The slope of the logarithm of the americium distribution ratio versus the pH plot (slope approximately −0.4) is slightly more negative than that observed for the Advanced TALSPEAK system (slope approximately −0.3; Figure 11.4), but is still substantially closer to zero than that for the traditional TALSPEAK process (slope approximately −2; Figure 11.3). The minimum separation factors (defined as the distribution ratio for the most poorly extracting lanthanide, neodymium, divided by that for americium) are relatively insensitive to the pH in the range 2.6-4.0, with the minimum separation factors being about 20.

The ALSEP chemistry is complicated by the extraction of zirconium and molybdenum. The latter element must be removed from the loaded organic phase before the MAs are stripped with HEDTA; otherwise it will contaminate the MA product. Contacting the metal-loaded ALSEP solvent with 0.2 mol/L citrate at pH 3.3-4.0 removes the molybdenum from the solvent. This citrate scrub also serves to precondition the solvent for the MA stripping step by removing any residual nitric acid in the solvent. Zirconium is somewhat more difficult to control. Two approaches have been

proposed to manage zirconium in ALSEP. The first approach involves adding *trans*-1,2-diaminocyclohexane-*N*,*N*,*N*′,*N*′-tetraacetic acid (CDTA; Figure 11.5) to the feed solution. The CDTA suppresses zirconium extraction so that it goes directly to the high-level waste raffinate. However, in some experiments, the extraction of ruthenium was enhanced by the presence of CDTA. An alternative approach to manage zirconium is to allow it to extract into the ALSEP solvent and then strip it from the solvent with an aqueous oxalic acid solution after the MAs have been recovered, and after the lanthanides have been stripped. The lanthanides can be removed by contacting the ALSEP solvent with a nitric acid solution containing *N*,*N*,*N*′,*N*′-tetraethyldiglycolamide (TEDGA, Figure 11.5) (Lumetta et al., 2013b).

In summary, Advanced TALSPEAK and ALSEP are promising methods for separating the MAs from high-level waste raffinate arising from reprocessing of nuclear fuel. Both of these methods use HEH[EHP] as the extractant together with a weaker aqueous complexant, which leads to systems that are less sensitive to pH than analogous systems that use HDEHP as extractant. Key aspects of the process chemistry for both systems have been addressed, but some challenges remain, especially regarding the fate of transition metal FPs such as molybdenum, zirconium, and ruthenium. With the Advanced TALSPEAK system, separation from the transition metal FPs occurs in the upstream process used to isolate the combined Ln/MA stream (e.g., during the TRUEX or DIAMEX process). In the case of ALSEP, the flow of the transition metals must be controlled within the ALSEP solvent-extraction cycle.

11.6 Exploiting high oxidation states of americium

The valence state of americium in aqueous solution is almost ubiquitously trivalent (Am^{3+}), resembling that of most of the lanthanides. However, higher americium oxidation states (IV, V, and VI) are available, and they have occasionally been exploited for analytical separations (Runde and Mincher, 2011). Tetravalent americium rapidly disproportionates and is only observed in the presence of strongly complexing ligands such as phosphate, fluoride, polytungstate, or carbonate. In its (IV) oxidation state, americium forms hydrated or complexed high charge-density Am^{4+} ions, while in the (V) and (VI) oxidation states, the bare cations hydrolyze to form the linear *trans*-dioxo americyl cations, AmO_2^+ and AmO_2^{2+}, in analogy with uranium, neptunium, and plutonium. For separations to be conducted from nitric acid solution, it is these latter, more stable oxidation states that are of potential utility. Such ions with either much higher (AmO_2^{2+}) or much lower (AmO_2^+) charge density than trivalent ions (Ln^{3+} and Am^{3+}) offer alternative options for separations chemistry.

Values of about 1.7 and 1.75 V are typically reported for the electrode potentials for the couples Am(III)/Am(VI) and Am(III)/Am(V), respectively, in acidic solution (Runde and Mincher, 2011). The use of strong oxidizing agents is thus required to produce these valences under the conditions envisioned for fuel cycle separations. The first reported preparation of americium(VI) was by Asprey et al. (1950, 1951). They used an excess of solid ammonium peroxydisulfate $(NH_4)_2S_2O_8$, added to

0.2 mol/L nitric, perchloric, or sulfuric acid solutions containing 0.002-0.035 mol/L americium(III). At 85 °C, the pink americium(III) color was replaced by straw yellow, and a sharp spectral absorbance peak was reported at 992 nm, with another minor peak at 666 nm. No evidence of americium(III) or americium(V) absorbance was reported in these preparations. The separations potential inherent in the ability to perform americium valence-state adjustments was recognized immediately. Precipitation of the trivalent elements away from soluble americium(VI) was commonly employed. Many salts, including the fluorides of lanthanides, americium(III), and curium(III), exhibit low solubilities and can be scavenged on lanthanide precipitates. The salts of higher oxidation states of americium have higher solubility and stay in solution when the trivalent species are precipitated. An early example was provided by Stephanou and Penneman (1952), in which americium was oxidized in the presence of curium by treating 0.1-0.3 mol/L HNO_3 solutions with solid ammonium peroxydisulfate and heating at 85 °C for 1-2 h. Following oxidation, the solution was made 3-4 mol/L in HF to precipitate CmF_3 on La carrier, leaving oxidized americium in solution.

In theory, the above procedures should yield nearly quantitative americium(VI), as any produced americium(V) is easy to oxidize further. The reduction potential for the Am(V)/Am(VI) couple is reported to be 1.6 V (Runde and Mincher, 2011). However, depending on parameters such as acidity, peroxydisulfate concentration, and duration of heating, significant amounts of americium(V) may also be produced (Burns et al., 2012). Mixtures of all three oxidation states are even possible. The generation of large amounts of americium(V) is probably due to reduction of the produced americium(VI).

Peroxydisulfate decomposes in solution to produce two strong oxidizing agents, the sulfate radical anion ($SO_4^{\bullet -}$) and the hydroxyl radical ($OH^{\bullet}$) (Behrman and Edwards, 1980):

$$S_2O_8^{2-} \rightarrow 2SO_4^{\bullet -} \tag{11.1}$$

$$S_2O_8^{2-} + H_2O \rightarrow SO_4^{\bullet -} + HSO_4^{-} + OH^{\bullet} \tag{11.2}$$

In acidic solution the peroxydisulfate anion protonates, initiating a series of reactions ultimately producing H_2O_2:

$$H^+ + S_2O_8^{2-} \rightarrow HS_2O_8^- \tag{11.3}$$

$$HS_2O_8^- \rightarrow SO_4 + HSO_4^- \tag{11.4}$$

$$SO_4 + H_2O \rightarrow H_2SO_5 \tag{11.5}$$

$$H_2SO_5 + H_2O \rightarrow H_2O_2 + H_2SO_4 \tag{11.6}$$

Hydrogen peroxide is an effective reducing agent for oxidized americium. Thus, the use of peroxydisulfate as an americium(VI) reagent is limited to low-acid concentrations. Lengthy high-temperature oxidations would also have a tendency to reduce americium(VI) to americium(V), which is more stable in acidic solution (Schulz,

1976). Ammonium peroxydisulfate alone is thus not always a reliable reagent for the production of americium(VI). For example, Ward and Welch (1954) reported that the yield of americium(VI) was only 80% in 0.2 mol/L HNO_3 under similar conditions to those used successfully by others. In fact, recently Burns et al. (2012) have shown the quantitative production of americium(V) in 0.01 mol/L HNO_3, using peroxydisulfate. This group is currently investigating the separation of americium(V) from curium(III) on titanate ion exchange materials following peroxydisulfate oxidation.

To achieve more reliable yields of americium(VI) with peroxydisulfate, Ward and Welch (1954) recommended the addition of silver nitrate to ensure quantitative oxidation. When Ag^+ is added, the Ag^{2+} ion is generated according to Equation 11.7, which acts as a one-electron transfer agent capable of oxidizing substrates,

$$Ag^+ + S_2O_8^{2-} \rightarrow Ag^{2+} + SO_4^{2-} + SO_4^{\bullet -} \tag{11.7}$$

The use of silver-catalyzed $S_2O_8^{2-}$ oxidation rapidly became the standard method for the production of americium(VI) for the analytical-scale separation of americium from the lanthanides and curium (Holcomb, 1954; Moore, 1971; Hindman, 1986).

Despite its success in analytical applications, peroxydisulfate suffers from two main drawbacks for use in the fuel cycle. The first has already been mentioned; it cannot be used in highly acidic solution. The second is the production of sulfate anion (Equations 11.6–11.7), which interferes with waste vitrification and is an undesirable constituent of the final waste form (Moyer et al., 2013). However, the TBP solvent extraction of americium(VI) from nitric acid solutions following silver/peroxydisulfate oxidation is possible, as reported by Kamoshida and Fukusawa (1996), who used neat TBP to achieve an americium distribution ratio (D_{Am}) of ~4 following oxidation in 0.1 mol/L HNO_3 and adjustment of the acidity to 1.0 mol/L. In continued work, the extraction of silver/peroxydisulfate-oxidized americium from diluted dissolved nuclear fuel was demonstrated, after previous extraction of uranium, plutonium, and neptunium (Kamoshida et al., 1999).

An alternative oxidizing agent that has been a major focus of fuel cycle research is sodium bismuthate ($NaBiO_3$). This reagent is a stable, convenient, off-the-shelf compound, only sparingly soluble in nitric acid. The reduction potential for the Bi(III)/Bi(V) redox couple has been reported to be 2.0 V, which is comparable to that of the peroxydisulfate system (Ford-Smith and Habeeb,1973). As a reagent that is slow to dissolve, bismuthate has the advantage that it acts as its own holding oxidant, as bismuth(V) ions are continually introduced to the system when in the presence of the solid, helping to counteract the tendency of americium(VI) to auto-reduce (Mincher et al., 2008).

The earliest report of the use of sodium bismuthate to oxidize americium(III) was that by Hara and Suzuki (1977), who prepared a form of americium that did not precipitate at nitric acid concentrations as high as 2 mol/L. This report was followed by one in which bismuthate was used as the oxidizing agent to study the stability of oxidized americium (Hara and Suzuki, 1979). Renewed investigation of sodium bismuthate did not occur until the last few years, mainly in work at Idaho National Laboratory, where it has been investigated for potential fuel cycle applications using

several ligands (Mincher et al., 2008, 2011; Martin et al., 2009). The current ligand of choice is diamylamylphosphonate (DAAP), which was chosen for investigation due to its utility in U(VI) extraction (Siddall, 1959; Mason and Griffin, 1980; Brahmmananda Rao et al., 2007). It was demonstrated that a 1-mol/L DAAP/dodecane solution could be used to extract bismuthate-oxidized americium across a wide range of acid concentrations, with maximum D_{Am} obtained at ~6.5 mol/L HNO_3. Typical results for americium extractions from a first-cycle UREX raffinate simulant solution adjusted across a range of acid concentrations are shown in Figure 11.7, where it can be seen that europium and curium were not oxidized and not extracted. At 6.5 mol/L HNO_3, Am/Eu and Am/Cm separation factors ($\alpha_{Am/Eu} = D_{Am}/D_{Eu}$ and $\alpha_{Am/Cm} = D_{Am}/D_{Cm}$) of ~50 and ~70 were obtained, respectively. It can also be seen that at nitric acid concentrations of <4 mol/L, americium behavior is similar to that of europium, suggesting that it was not oxidized, possibly due to the lower concentration of dissolved bismuthate at that acidity. It has since been shown that this pattern of decreasing extractive capability with decreasing acid concentration is common to the trivalent metals, including the other lanthanides, curium(III), and bismuth(III) (Mincher et al., 2012).

Among other fuel dissolution constituents of concern, the only lanthanide that is oxidized and extracted is cerium, as Ce^{4+}. However, americium is readily reduced, even by the organic phase itself, and thus it is easy to selectively strip (Mincher et al., 2012). Among nonlanthanide constituents, only ruthenium, which is oxidized by bismuthate, and zirconium were extracted. The occasionally problematic elements

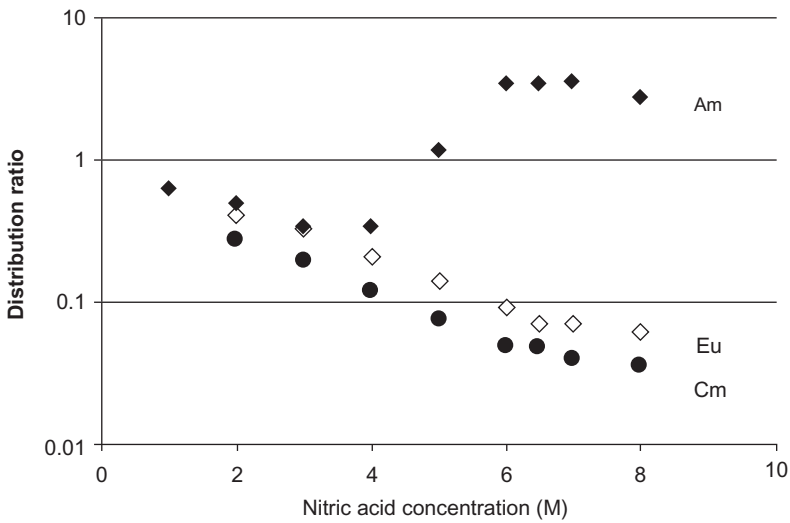

Figure 11.7 The 1 mol/L DAAP solvent extraction of americium (closed diamonds), europium (open diamonds), and curium (closed circles) versus nitric acid concentration for extractions from bismuthate-treated raffinate simulant.
Data replotted from Mincher et al. (2012) and Mincher et al. (2014).

palladium, technetium, and molybdenum were not extracted at acid concentrations of interest for americium extraction (Mincher et al., 2014).

The D_{Am} values achieved during DAAP extraction depend on the oxidation yield of americium(VI). Pentavalent and trivalent americium do not get extracted. The initial oxidation yield can be measured by UV/Vis spectroscopy and depends on the amount of solid bismuthate used, temperature, and duration of oxidative treatment (Mincher et al., 2008, 2011), as well as the americium and acid concentrations (Mincher et al., 2012). Given 40-60 mg/mL bismuthate in >4 mol/L HNO_3 with a 2 h oxidation at ambient temperature, yields of >85% can be expected for tracer americium concentrations, with higher yields at higher americium concentrations. The UV/Vis absorbance spectrum of a bismuthate-oxidized 0.1 mol/L HNO_3 solution, containing americium(III) (503 nm, $\varepsilon = 386.7$ L/mol cm) (Mincher et al., 2008); americium(V) (513 nm, $\varepsilon = 39.7$ L/mol cm) (Mincher et al., 2011); and americium(VI) (666 nm, $\varepsilon = 27.9$ L/mol cm) (Mincher et al., 2008), is shown in Figure 11.8. The total americium concentration was 4×10^{-5} mol/L. The americium(VI) content of this solution is 68%.

The persistence of americium(VI) after oxidation is also important, as hexavalent americium must have a lifetime sufficient to allow the extraction. Small amounts of trace-reducing agents will decrease the yield and persistence of americium(VI). The use of high-purity reagents is important, as is preequilibration of the organic phase with bismuthate-containing acid. Contact with the organic phase begins to reduce americium(VI), and contact times must be short to prevent reduction and back-extraction of americium. In the research cited here, 10-s contact times were used, with longer contacts giving lower distribution ratios for both TBP (Mincher et al., 2008) and DAAP extraction (Mincher et al., 2012).

In the absence of reducing agents in nitric acid solution, the higher oxidation states of americium undergo auto-reduction. Auto-reduction is zero-order with respect to the

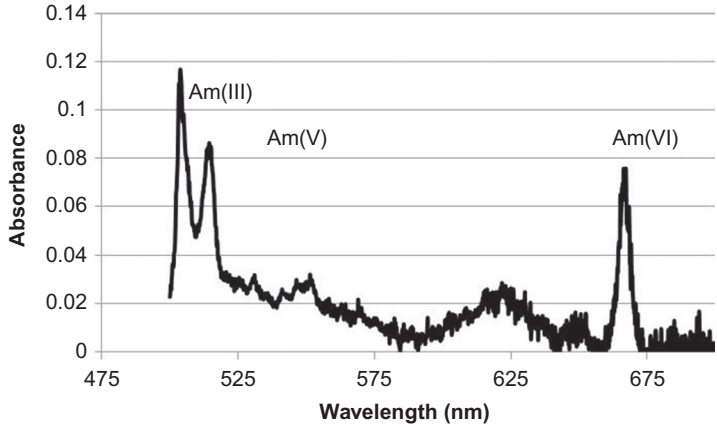

Figure 11.8 The UV/Vis absorbance spectrum of a 0.1 mol/L HNO_3 solution containing a mixture of Am(III) (503 nm), Am(V) (513 nm), and Am(VI) (666 nm) measured in a 100-cm liquid waveguide capillary cell.

concentration of high-valence americium, but pseudo-first-order with respect to the total americium concentration, suggesting that reduction is caused by reaction with the radiolysis products of americium decay (Asprey and Stephanou, 1950). Thus, for tracer experiments, ^{243}Am(VI) will be more stable than higher specific activity ^{241}Am(VI). More importantly from a fuel cycle perspective, the additive radiation dose rate during processing will contribute to americium reduction. The radiolytically produced reducing-radical species are scavenged in the aerated, irradiated acidic solvent-extraction system and are unlikely to be responsible for the reduction of americium (Mincher et al., 2009). However, especially for α-irradiated systems, molecular species such as H_2O_2 and HNO_2 are produced from irradiated water and nitric acid, respectively. These species accumulate with absorbed dose, as demonstrated for the reduction of neptunium(VI) by radiolytically produced HNO_2 (Mincher et al., 2013). The kinetics of the reduction of americium(VI) by H_2O_2 was reported by Woods et al. (1974) and found to depend on the nitric acid concentration. While americium(VI) has a half-life of minutes in nitric acid solution, americium(V) is found to be far more stable, persisting for hours (Schulz, 1976; Mincher et al., 2011). The presence of residual bismuth(V) mitigates the fast reduction of americium. However, once the bismuth has been reduced, onset of americium(VI) reduction can be expected (Mincher et al., 2008).

While bismuthate oxidation has the advantages described above, a significant objection is the need to filter undissolved solids from the aqueous phase prior to the process solvent-extraction contact. Also, the oxidation kinetics are slow. Cross-flow filtration has been demonstrated at Idaho National Laboratory during a nonradioactive test in which 2 L of 2.3 mM cerium was oxidized using 30 g/L sodium bismuthate in a stirred batch reactor for 1 h. The color change due to the oxidation of cerium(III) to cerium(IV) was visually discernible. This slurry was then easily filtered using a cross-flow filter with a cross-membrane pressure of 20 psig and a flow rate of 0.6 Lpm. The bismuthate-free, cerium(IV)-yellow permeate was then introduced into a 5-cm centrifugal contactor for a 1-stage contact with 0.25 mol/L DAAP/dodecane, and the resulting D_{CeIV} value was 167, in good agreement with batch contacts at this DAAP concentration. However, only 70% total cerium was extracted, indicating that cerium (IV) was reduced in the stainless steel filter. Americium(VI) would thus also be reduced, and filtration and extraction would need to be performed using more inert materials. A radioactive test is currently in design (Law et al., 2014).

Alternative oxidizing agents are also being investigated. Researchers at Pacific Northwest National Laboratory have shown that the Cu(III) salt $Na_5[Cu(HIO_6)_2]$ is able to oxidize 2 mM americium to americium(VI), with the estimated reduction potential of the Cu(II)/Cu(III) couple being ~2.4 V (Bratsch, 1989). The oxidation yield was 98-99% at nitric acid concentrations $\leq$3 mol/L, with an auto-reduction rate of $<$1%/h. These preliminary results are encouraging.

The potential electrochemical oxidation of americium is also being pursued. Previous literature has investigated the oxidation of americium only in very strongly complexing solutions in order to stabilize the americium(IV) product of single electron transfer. For example, Yanir et al. (1969) reported the preparation of americium (IV) in 12 mol/L phosphoric acid using a 1-h electrolysis with a two-compartment cell

and a platinum anode. At lower acid concentrations of about 5 mol/L, preparation of americium(VI) was claimed. Similarly, Myasoedov and coworkers (1973) successfully reproduced the work of Yanir et al. (1969) and reported long half-lives for the reduction of americium(IV) and americium(VI), depending on the phosphoric acid and americium concentrations. However, attempts to oxidize americium(III) in nitric acid until now have not been successful, possibly because americium(IV) does not exist long enough to oxidize to americium(V) or americium(VI).

Currently, catalytic oxidation using ruthenium-containing phosphonate complexes anchored to indium-tin oxide carbon electrodes is being studied at the University of North Carolina at Chapel Hill. This research is based on reports that ruthenium complexes can be used to catalytically oxidize water (Jurss et al., 2010). In preliminary work, manganese is being used as a surrogate for americium, because the metals have some similarities in their electrochemical behavior. The one-electron oxidation of americium(III) to americium(IV) (2.6 V) and Mn(IV) to Mn(V) (4.3 V) both occur at very positive potentials. Therefore, in order to access the higher valences, multielectron redox reactions must occur if the difficult one-electron transfer step is to be bypassed. It has been shown in preliminary results that bulk electrolysis has generated permanganate (Mn(VII)) (Dares, 2014). The system has not yet been tested on americium.

11.7 Conclusions

In addressing the need for nuclear fuel recycle as part of the goal toward developing sustainable nuclear energy, research on MA separation in the United States and other countries faces many challenges, both scientifically and technologically. The technological challenges depend on the nature of the fuel cycle envisioned in any given country and stem generally from the need to reduce the heat load on geologic repositories, reduce waste radiotoxicity, and recover energy value. Presently, full recycle of actinides from used nuclear fuel does not exist in any country, nor are the technological requirements well defined. In the United States, a systems options study is taking place and can be expected to provide a basis for identifying the most desirable systems, from which technology gaps in MA separation can be recognized and prioritized. In view of this evolving framework, the Sigma Team for MA Separations in the USDOE nuclear energy program will continue to employ a "toolbox" approach to developing potentially useful separations chemistry and technology concepts, focusing on separation of trivalent actinides from lanthanides. Progress on MA separations in the United States has been made along two lines, one exploiting the higher oxidation states of americium and one exploiting differences between the complex stabilities of An(III) versus Ln(III). One example of each of these lines of investigation has been described in detail in this chapter. Widely recognized scientific challenges of separating trivalent f-elements include discriminating small differences in ionic radii and covalency, or surmounting the difficulties in oxidizing americium and holding it in the V or VI states long enough to achieve a separation.

The development of the ALSEP concept has led to successful nonselective extraction of actinides and lanthanides using a combination of neutral extractant and cation

exchanger followed by a selective strip of the trivalent actinides using a polyaminocarboxylate-type aqueous complexant. A candidate solvent system has been identified, and conditions are being optimized to deal with FPs such as zirconium, molybdenum, and ruthenium, improve stripping kinetics, and increase contactor stage efficiency, thus moving toward a bench-scale multistage countercurrent test with simulated high-level waste feed. An optional americium-selective strip from curium is possible. Alternative extractants and aqueous-phase complexants are also under development.

Significant progress has been made in generating americium(V) and americium (VI) species in nitric acid solution and effecting selective separations from lanthanides and curium. Most of the results so far have been obtained using sodium bismuthate as an oxidant, but more attractive oxidants are being tested with positive results. Testing of tandem oxidation and extraction concepts is in progress to demonstrate the feasibility of generating americium(VI) and carrying out a fast extraction using a corrosion-resistant centrifugal contactor.

In the long term, effecting trivalent actinide separation from lanthanides represents a daunting challenge for science and technology. Indeed, it has been an active research topic for half a century. To accelerate progress will require better tools for research as well as engineering. Computational techniques are becoming more powerful and available to researchers, enabling prediction of properties, design of new separation agents, and understanding of observed behaviors. Spectroscopic tools exploiting intense photon and neutron sources provide powerful experimental methods to characterize f-element bonding and structure. Advances in engineering are also needed, for example, in the design of more efficient contactors for solvent extraction to overcome kinetic and hydraulic limitations prevalent in many extraction systems. As fuel recycle requirements are refined in the coming years, continuing progress in MA separation will likely be able to provide effective process options that are simpler, more effective, and economical than current methodologies.

Acknowledgement

This research was sponsored by the Fuel Cycle Research and Development Program, Office of Nuclear Energy, U.S. Department of Energy.

References

Arm, S.T., Phillips, C., Dobson, A., 2008. Industrial application of GNEP solvent-extraction processes. In: Moyer, B.A. (Ed.), Proceedings of ISEC 2008 International Solvent Extraction Conference; Tucson, AZ, September 15–19, 2008. In: Solvent Extraction: Fundamentals to Industrial Applications, vol. 1. The Canadian Institute of Mining, Metallurgy and Petroleum, Montreal, pp. 709–714.

Asprey, L.B., Stephanou, S.E., 1950. The autoreduction of Am(VI) and Am(V) in dilute acid. United States Atomic Energy Commission report AECU-924, Los Alamos Scientific Laboratory, Los Alamos.

Asprey, L.B., Stephanou, S.E., Penneman, R.A., 1950. A new valence state of americium, Am (VI). J. Am. Chem. Soc. 72, 1425–1426.

Asprey, L.B., Stephanou, S.E., Penneman, R.A., 1951. Hexavalent americium. J. Am. Chem. Soc. 73, 5715–5717.

Behrman, E.J., Edwards, J.O., 1980. The thermal decomposition of peroxydisulfate ions. Rev. Inorg. Chem. 2, 179–206.

Boullis, B., 2008. Future nuclear fuel cycles: prospects and challenges. In: Moyer, B.A. (Ed.),. Proceedings of ISEC 2008 International Solvent Extraction Conference; Tucson, AZ, Sept. 15–19, 2008. In: Solvent Extraction: Fundamentals to Industrial Applications, vol. 1. The Canadian Institute of Mining, Metallurgy and Petroleum, Montreal, pp. 29–41.

Brahmmananda Rao, C.V.S., Srinivasan, T.G., Vasudeva Rao, P.R., 2007. Studies on the extraction of actinides by diamylamyl phosphonate. Solvent Extr. Ion Exch. 25, 771–789.

Braley, J.C., Grimes, T.S., Nash, K.L., 2012. Alternatives to HDEHP and DTPA for simplified TALSPEAK separations. Ind. Eng. Chem. Res. 51, 629–638.

Braley, J.C., Lumetta, G.J., Carter, J.C., 2013. Combining CMPO and HEH[EHP] for separating trivalent lanthanides from the transuranic elements. Solvent Extr. Ion Exch. 31 (6), 567–577.

Bratsch, S.G., 1989. Standard electrode potentials and temperature coefficients in water at 298.15 K. J. Phys. Chem. Ref. Data 18, 1–21.

Burns, J.D., Shehee, T.C., Clearfield, A., Hobbs, D.T., 2012. Separation of americium from curium by oxidation and ion exchange. Anal. Chem. 84, 6930–6932.

Carelli, M., Franceschini, F., Lahoda, E., Petrovic, B., 2011. A comprehensive approach to deal with the nuclear waste problem. In: Proceedings of the WM2011 Conference. American Nuclear Society, Phoenix, AZ, Paper 11452.

Courson, O., Lebrun, M., Malmbeck, R., Pagliosa, G., Römer, K., Sätmark, B., Glatz, J.-P., 2000. Partitioning of minor actinides from HLLW using the DIAMEX process. Part 1—demonstration of extraction performances and hydraulic behavior of the solvent in a continuous process. Radiochim. Acta 88 (12), 857–863.

Dares, C., 2014. University of North Carolina, Chapel Hill, personal communication.

Dhami, P.S., Chitnis, R.R., Gopalakrishnan, V., Wattal, P.K., Ramanujam, A., Bauri, A.K., 2001. Studies on the partitioning of actinides from high level waste using a mixture of HDEHP and CMPO as extractant. Sep. Sci. Technol. 36, 325–335.

Ford-Smith, M.H., Habeeb, J.J., 1973. Kinetics of oxidation-reduction reactions between elements of group V and VII. Part 1. Bismuth(V) with halide ions and other reductants. Dalton Trans. 461–464.

Gelis, A.V., Lumetta, G.J., 2014. Actinide lanthanide separation process—ALSEP. Ind. Eng. Chem. Res. 53 (4), 1624–1631.

Gelis, A.V., Vandegrift, G.F., Bakel, A., Bowers, D.L., Hebden, A.S., Pereira, C., Regalbuto, M., 2009. Extraction behaviour of actinides and lanthanides in TALSPEAK, TRUEX and NPEX processes of UREX+. Radiochim. Acta 97, 231–232.

Guelis, A.V., 2013. Actinide and Lanthanide Separation Process (ALSEP). US Patent 8354085, January 15, 2013.

Hara, M., Suzuki, S., 1977. Oxidation of americium(III) with sodium bismuthate. J. Radioanal. Chem. 36, 95–104.

Hara, M., Suzuki, S., 1979. The chemistry of americium. IV. The stability of Am(V) and Am (VI) in nitric acid solutions and in solutions containing ozone gas, fluoride, or phosphate ions. Bull. Chem. Soc. Jpn. 52, 1041–1045.

Hill, C., 2010. Overview of recent advances in An(III)/Ln(III) separation by solvent extraction. In: Moyer, B.A. (Ed.), In: Ion Exchange and Solvent Extraction, vol. 19. Taylor and Francis, Philadelphia (Chapter 3).

Hill, C., 2011. Development of highly selective compounds for solvent extraction processes: partitioning and transmutations of long-lived radionuclides from spent nuclear fuels. In: Nash, K.L., Lumetta, G.J. (Eds.), Advanced Separation Techniques for Nuclear Fuel Reprocessing and Radioactive Waste Treatment. Woodhead Publishing, Oxford, pp. 311–362.

Hindman, F.D., 1986. Actinide separations for α spectrometry using neodymium fluoride coprecipitation. Anal. Chem. 58, 1238–1241.

Holcomb, H.P., 1954. Separation of americium from curium with calcium fluoride. Anal. Chem. 36, 2329–2332.

Horwitz, E.P., Kalina, D.G., Diamond, H., Vandegrift, G.F., Schulz, W.W., 1985. The TRUEX process—a process for the extraction of the transuranic elements from nitric acid wastes utilizing modified PUREX solvent. Solvent Extr. Ion Exch. 3, 75–109.

Jurss, J.W., Concepcion, J.C., Norris, M.R., Templeton, J.L., Meyer, T.J., 2010. Surface catalysis of water oxidation by the blue ruthenium dimer. Inorg. Chem. 49, 3980–3982.

Kamoshida, M., Fukusawa, T., 1996. Solvent extraction of americium(VI) by tri-*n*-butyl phosphate. J. Nucl. Sci. Technol. 33, 403–408.

Kamoshida, M., Fukusawa, T., Kawamura, F., 1999. Preparation of hexavalent americium in nitric acid solution. J. Nucl. Sci. Technol. 26, 535–539.

Laidler, J.J., 2008. An overview of spent-fuel processing in the Global Nuclear-Energy Partnership. In: Moyer, B.A. (Ed.),. Proceedings of ISEC 2008 International Solvent Extraction Conference; Tucson, AZ, Sept. 15–19, 2008. In: Solvent Extraction: Fundamentals to Industrial Applications, 1. The Canadian Institute of Mining, Metallurgy and Petroleum, Montreal, pp. 695–701.

Law, J.D., Mincher, B.J., Garn, T., Greenhalgh, M., Schmitt, N., Rutledge, V., 2014. Development and testing of an americium/lanthanide separation flowsheet using sodium bismuthate. In: Proceedings of ICAPP 2014, Charlotte, North Carolina, United States, Paper No. 14040.

Lumetta, G.J., Gelis, A.V., Vandegrift, G.F., 2010a. Solvent systems combining neutral and acidic extractants for separating trivalent lanthanides from the transuranic elements. Solvent Extr. Ion Exch. 29, 287–312.

Lumetta, G.J., Carter, J.C., Gelis, A.V., Vandegrift, G.F., 2010b. Combining octyl(phenyl)-*N*,*N*-diisobutyl-carbamoylmethylphosphine oxide and bis-(2-ethylhexyl)phosphoric acid extractants for recovering transuranic elements from irradiated nuclear fuel. In: Wai, C. M., Mincher, B.J. (Eds.), Nuclear Energy and the Environment. American Chemical Society, Washington, DC, pp. 107–118.

Lumetta, G.J., Neiner, D., Sinkov, S.I., Carter, J.C., Braley, J.C., Latesky, S.L., Gelis, A.V., Vandegrift, G.F., 2011. Combining neutral and acidic extractants for recovering transuranic elements from nuclear fuel. In: XIX International Solvent Extraction Conference, Santiago, Chile. Gecamin Ltda, Santiago, Chile, Paper No. 68.

Lumetta, G.J., Gelis, A.V., Braley, J.C., Carter, J.C., Pittman, J.W., Warner, M.G., Vandegrift, G.F., 2013a. The TRUSPEAK concept: combining CMPO and HDEHP for separating trivalent lanthanides from the transuranic elements. Solvent Extr. Ion Exch. 31, 223–236.

Lumetta, G.J., Carter, J.C., Niver, C.M., Guelis, A.V., 2013b. Zirconium and fission product management in the ALSEP process. In: Global 2013, Salt Lake City, UT, September 29–October 3, 2013. American Nuclear Society, Salt Lake City, UT, pp. 912–916.

Lumetta, G.J., Casella, A.J., Rapko, B.M., Levitskaia, T.G., Pence, N.K., Carter, J.C., Niver, C. M., Smoot, M.R., 2014a. An advanced TALSPEAK concept using 2-ethylhexylphosphonic acid mono-2-ethylhexyl ester as extractant. Solvent Extr. Ion Exch., published on-line, November 11, 2014, http://dx.doi.org/10.1080/07366299.2014.985920.

Lumetta, G.J., Gelis, A.V., Carter, J.C., Niver, C.M., Smoot, M.R., 2014b. The actinide-lanthanide separation concept. Solvent Extr. Ion Exch. published on-line February 21, 2014, http://dx.doi.org/10.1080/07366299.2014.895638.

Malmbeck, R., Courson, O., Pagliosa, G., Römer, K., Sätmark, B., Glatz, J.-P., Baron, P., 2000. Partitioning of minor actinides from HLLW using the DIAMEX process. Part 2—"Hot" continuous counter-current experiment. Radiochim. Acta 88 (12), 865–871.

Martin, L.R., Mincher, B.J., Schmitt, N.C., 2009. Extraction of americium(VI) by a neutral phosphonate ligand. J. Radioanal. Nucl. Chem. 282, 523–526.

Mason, G.W., Griffin, H.E., 1980. Demonstration of the potential for designing extractants with preselected extraction properties: possible application to reactor fuel processing. In: Navratil, J. (Ed.), Actinide Separations. American Chemical Society, Washington, DC (Chapter 7).

Mincher, B.J., Martin, L.R., Schmitt, N.C., 2008. Tributylphosphate extraction behavior of bismuthate-oxidized americium. Inorg. Chem. 47, 6984–6989.

Mincher, B.J., Modolo, G., Mezyk, S.P., 2009. Review article: The effects of radiation chemistry on solvent extraction: 1. Conditions in acidic solution and a review of TBP radiolysis. Solvent Extr. Ion Exch. 27, 1–25.

Mincher, B.J., Schmitt, N.C., Case, M.E., 2011. A TRUEX-based separation of americium form the lanthanides. Solvent Extr. Ion Exch. 29, 247–259.

Mincher, B.J., Martin, L.R., Schmitt, N.C., 2012. Diamylamylphosphonate solvent extraction of Am(VI) from nuclear fuel raffinate simulant solution. Solvent Extr. Ion Exch. 30, 445–456.

Mincher, B.J., Precek, M., Mezyk, S.P., Elias, G., Martin, L.R., Paulenova, A., 2013. The redox chemistry of neptunium in γ-irradiated aqueous nitric acid. Radiochim. Acta 101, 259–265.

Mincher, B.J., Schmitt, N.C., Tillotson, R.D., Elias, G., White, B.M., Law, J.D., 2014. Characterizing diamylamylphosphonate (DAAP) as an americium ligand for nuclear fuel cycle applications. Solvent Extr. Ion Exch. 32, 153–166.

Moore, F.L., 1971. New method for separation of americium from curium and associated elements in the zirconium phosphate-nitric acid system. Anal. Chem. 43, 487–489.

Moyer, B.A., Custelcean, R., Hay, B.P., Sessler, J.L., Bowman-James, K., Day, V.W., Kang, S.-O., 2013. A case for molecular recognition in nuclear separations: sulfate separation from nuclear wastes. Inorg. Chem. 52, 3473–3490.

Myasoedov, B.F., Mikhailov, V.M., Lebedev, I.A., Koiro, O.E., Frenkel, V.Ya., 1973. Preparation and stability of Am/IV/ and Am/V/in phosphoric acid solutions. Radiochem. Radioanal. Lett. 14, 17–24.

Nash, K.L., Madic, C., Mathur, J.N., Lacquement, J., 2006. Actinide separation science and technology. In: Morss, L.R., Edelstein, N.M., Fuger, J., Katz, J.J. (Eds.), third ed., In: The Chemistry of the Actinide and Transactinide Elements, vol. 4. Springer, Dordrecht, pp. 2622–2798 (Chapter 22).

Nilsson, M., Nash, K.L., 2007. Review article: A review of the development and operational characteristics of the TALSPEAK process. Solvent Extr. Ion Exch. 25, 665–701.

OECD Nuclear Energy Agency, 2010. In: Actinide and Fission Product Partitioning and Transmutation. Tenth Information Exchange Meeting; Mito Japan, October 6–10, 2008; NEA No. 6420. Organisation for Economic Cooperation and Development, Paris, France. ISBN: 978-92-64-99097-5.

OECD Nuclear Energy Agency, 2012. Actinide and Fission Product Partitioning and Transmutation. Eleventh Information Exchange Meeting; San Francisco, CA, United States, November 1–4, 2010; NEA No. 6996. Organisation for Economic Cooperation and Development, Paris, France, ISBN: 978-92-64-99174-3.

Pearson, R.G., 1963. Hard and soft acids and bases. J. Am. Chem. Soc. 85, 3533–3539.
Regalbuto, M., 2011. Alternative separation and extraction: UREX+ processes for actinide and targeted fission product recovery. In: Nash, K.L., Lumetta, G.J. (Eds.), Advanced Separation Techniques for Nuclear Fuel Reprocessing and Radioactive Waste Treatment. Woodhead Publishing, Oxford, pp. 176–200.
Runde, W.H., Mincher, B.J., 2011. The higher oxidation states of americium: preparation, characterization and use for separations. Chem. Rev. 111 (9), 5723–5741.
Salvatores, M., Palmiotti, G., 2011. Radioactive waste partitioning and transmutation within advanced fuel cycles: achievements and challenges. Progr. Part. Nucl. Phys. 66, 144–166.
Schulz, W.W., 1976. The chemistry of americium. In: ERDA Critical Review Series, TID 26971, ERDA Technical Information Center, Oak Ridge, TN.
Shannon, R.D., 1976. Revised effective ionic radii and systematic studies of interatomic distances in halides and chalcogenides. Acta Crystallogr. A32, 751–767.
Siddall III, T.H., 1959. Triakyl phosphates and dialkylphosphates in uranium and thorium extraction. Ind. Eng. Chem. 51, 41–44.
Stephanou, S.E., Penneman, R.A., 1952. Observations on curium valence states; a rapid separation of americium and curium. J. Am. Chem. Soc. 74, 3701–3702.
Svantesson, I., Hangström, I., Persson, G., Liljenzin, J.O., 1979. Separation of smericium and neodymium by selective stripping and subsequent extraction with HDEHP using DTPA–lactic acid solution in a closed loop. Radiochem. Radioanal. Lett. 37, 215–222.
Tachimori, S., Morita, Y., 2010. Overview of solvent extraction chemistry for reprocessing. In: Moyer, B.A. (Ed.), In: Ion Exchange and Solvent Extraction, Taylor and Francis, Philadelphia (Chapter 1).
Todd, T.A., Wigeland, R.A., 2006. Advanced separation technologies for processing spent nuclear fuel and the potential benefits to a geologic repository. In: Lumetta, G.J., Nash, K.L., Clark, S.B., Friese, J.I. (Eds.), In: Separations for the nuclear fuel cycle in the 21st century, vol. 933. American Chemical Society, Washington, DC, pp. 41–55.
USDOE, 2010a. Nuclear energy research and development roadmap. Report to congress, US Dept. of Energy, Office of Nuclear Energy, Washington, DC.
USDOE, 2010b. Research objective 3 implementation plan: developing sustainable fuel cycle options. FCRD-TIO-2011-000025, DOE Office of Nuclear Energy, Washington, DC.
Ward, M., Welch, G.A., 1954. The oxidation of americium to the sexavalent state. J. Chem. Soc., 4038.
Weaver, B., Kappelmann, F.A., 1968. Preferential extraction of lanthanides over trivalent actinides by monoacidic organophosphates from carboxylic acids and from mixtures of carboxylic acids and aminopolyacetic acids. J. Inorg. Nucl. Chem. 30, 263–272.
Wigeland, R.A., Bauer, T.H., Fanning, T.H., Morris, E.E., 2006. Separations and transmutation criteria to improve utilization of a geologic repository. Nucl. Technol. 154, 95–106.
Woods Sr., M., Cain, A., Sullivan, J.C., 1974. A kinetic study of the reduction of americium(VI) by hydrogen peroxide in aqueous perchlorate media. J. Inorg. Nucl. Chem. 36, 2605–2607.
Yanir, E., Givon, M., Marcus, Y., 1969. Higher oxidation states of americium in phosphate solutions. Inorg. Nucl. Chem. Lett. 5, 369–372.

Advanced thermal denitration conversion processes for aqueous-based reprocessing and recycling of spent nuclear fuels

12

Emory D. Collins
Oak Ridge National Laboratory, Oak Ridge, TN, USA

Acronyms

ADU	ammonium diuranate (process)
ASTM	American Society for Testing and Materials
MDD	modified direct denitration (process)
MH	microwave heating
MOX	mixed oxide
NOx	nitrogen oxide
ORNL	Oak Ridge National Laboratory
RD&D	research, development, and demonstration
UNH	uranyl nitrate hexahydrate

12.1 Introduction

The aqueous nitrate solutions of uranium and plutonium resulting from the reprocessing of spent nuclear fuels must be denitrated and converted to oxide particles with good ceramic properties for fabrication of recycle fuels. Several processes are suitable for this purpose, including those that utilize precipitation: filtration-calcination, such as the ammonium diuranate (ADU) process; the plutonium oxalate precipitation process using plutonium in either the trivalent or the tetravalent state; the uranium or plutonium peroxide precipitation process; or the ammonium-uranium carbonate process. Also, the use of direct thermal denitration processes is possible and is the subject of this chapter.

12.2 History and concepts for improvement

Thermal denitration has been used for many years in the processing and recovery of uranium from mining ores in the United States. Simple thermal denitration was used in large-scale operations to convert aqueous uranyl nitrate hexahydrate (UNH) solution to a solid oxide (uranium trioxide: UO_3) interim product, usually for subsequent conversion to uranium fluorides UF_4 or UF_6 (Haas, 1988). The conversion of UNH to UO_3 is a two-step process in which the aqueous solution is first evaporated and

Reprocessing and Recycling of Spent Nuclear Fuel. http://dx.doi.org/10.1016/B978-1-78242-212-9.00012-5

concentrated to eliminate most of the water and produce a syrupy liquid, followed by calcination and decomposition (denitration) to produce a solid caked oxide product. In the calcination step, decomposition of the UNH begins at temperatures less than 300 °C and is completed by 400-500 °C. These operations have been performed in heated pots, fluidized beds, and stirred troughs, either in batch or in continuous mode. In European refineries, the denitration and conversion is accomplished by means of the addition of ammonia to the UNH solution to precipitate ADU, which is then filtered, dried, and calcined to form uranium trioxide powder.

The use of direct thermal denitration eliminates multiple precipitation-filtration-calcination steps and enables the use of less-complicated process equipment (Lerch and Norman, 1984). Direct thermal denitration, however, does not provide any separation of impurity metals and relies on previous chemical separations to provide the required product purity. Although direct thermal denitration offers significant process simplification, the process has not been used widely due to the formation of a "mastic" phase during melting and decomposition of the metal salts, leading to poor handling characteristics and poor ceramic properties of the product oxide.

Since the 1980s, research, development, and demonstration (RD&D) studies in Japan and the United States have focused on direct thermal denitration processes to prepare uranium oxide and mixed oxides (MOXs) for recycle nuclear fuel fabrication (Koizumi et al., 1983; Haas et al., 1981). The RD&D studies have been aimed at the use of more uniform heating equipment or the addition of modifier agents to avoid the mastic phase formation and to enable suitable product quality. A major breakthrough in this area occurred when Haas et al. (1981) discovered that, by introducing ammonium nitrate into a uranium solution, the mastic phase is eliminated by the formation and denitration of double salts of ammonium-uranium nitrate. The process is called *modified direct denitration* (MDD).

Current reprocessing and recycle fuel fabrication operations rely on the production of separated uranium oxide and plutonium oxide and the use of ball-milling methods to produce a suitable MOX for use in recycle fuels. Separated plutonium is viewed as a safeguards concern that increases the "attractiveness level" (Bathke et al., 2009) for diversion of the fissile material to weapons of mass destruction. Therefore, coprocessing and co-conversion methods are being developed in several countries for use in future reprocessing and recycle fuel fabrication plants. A microwave heating (MH) process has been developed and demonstrated in Japan for codenitration of uranium-plutonium solutions without formation of the mastic phase to produce a homogeneous MOX.

Both the Japanese MH process and the U.S. MDD process are suitable for codenitration. Description of these processes is the focus of this chapter.

12.3 Process chemistry

Thermal denitration of uranium and plutonium, either individually or from mixed uranium-plutonium, is believed to be represented by the following approximate calcination reactions:

$$UO_2(NO_3)_2 \cdot 6H_2O \rightarrow UO_3 + 1.86NO_2 + 0.14NO + 0.57O_2 + 6H_2O \qquad (12.1)$$

$$Pu(NO_3)_4 \cdot 5H_2O \rightarrow PuO_2 + 3.4NO_2 + 0.6NO + 1.3O_2 + 5H_2O \quad (12.2)$$

The denitration begins at a temperature <300 °C and is completed at 350-400 °C. The reaction can be performed in a batch mode, as in the Japanese MH process, or in a continuous mode, as in the U.S. MDD process.

The Japanese MH process proceeds through a sequence of four steps as the temperature is increased (Numao et al., 2007):

1. The mixed uranium-plutonium nitrate solution is concentrated at 120 °C, the azeotropic temperature of nitric acid and water.
2. Decomposition (denitration) of the fused salt occurs between 120 and 250 °C, during which nitrogen oxide (NO*x*) gases are generated, recovered by scrubbing of the off-gas, and subsequently recycled.
3. Above 250 °C, residual moisture evaporates and NO*x* evolves from the decomposition of uranium.
4. The denitration is completed at about 350 °C, and the temperature begins to drop as the UO_3 begins to decompose to U_3O_8. The temperature at that point in the process is detected by means of an infrared thermometer, and the MH is stopped to prevent excessive decomposition of the UO_3 product.

The reaction sequence occurs in a time frame of 30-40 min per batch. Slower heating was found to result in localized heating and temperature increase, creating a product powder that is less active and less suitable for MOX fuel fabrication (Numao et al., 2007).

The process chemistry of the MDD process was studied by Notz and Haas (1981) for the denitration of the ammonium-uranium nitrate double salt, which proceeds through a sequence of reactions (Equations 12.3–12.5) as illustrated by the results of a thermogravimetric analysis shown in Figure 12.1.

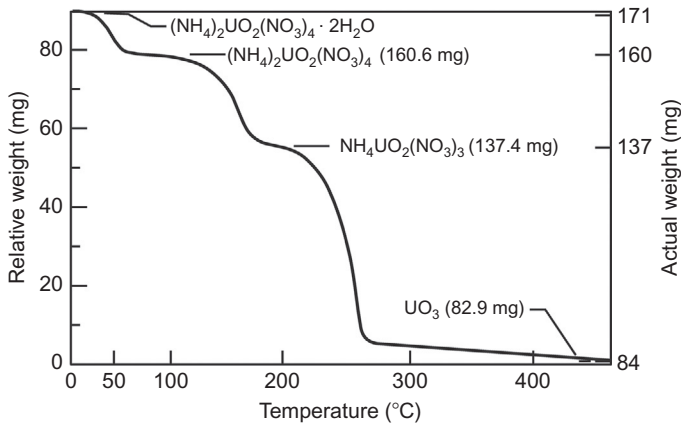

Figure 12.1 Thermogravimetric analysis of $(NH_4)_2UO_2(NO_3)_4 \cdot 2H_2O$ (initial sample weight, 171 mg).

The thermal decomposition proceeds in three distinct steps:

1. Dehydration at ~40 °C:

$$(NH_4)_2UO_2(NO_3)_4 \cdot 2H_2O \rightarrow (NH_4)_2UO_2(NO_3)_4 + 2H_2O \tag{12.3}$$

2. Loss of 1 mole of ammonium nitrate (NH_4NO_3) at ~170 °C

$$(NH_4)_2UO_2(NO_3)_4 \rightarrow NH_4UO_2(NO_3)_3 + N_2O + 2H_2O \tag{12.4}$$

3. Conversion to UO_3 at ~270 °C:

$$NH_4UO_2(NO_3)_3 \rightarrow UO_3 + (N_2O_5) + N_2O + 2H_2O \tag{12.5}$$

The decomposition products for the latter two reactions were inferred on the basis that NH_4NO_3 decomposes under controlled conditions to H_2O and N_2O, which is a standard method for the preparation of N_2O. However, a differential thermal analysis, shown in Figure 12.2, and effluent gas analysis, shown in Table 12.1, indicated that a combination of several other reactions, which are known to occur for decomposition of NH_4NO_3, are involved. Some are exothermic, but the overall effect is endothermic with a large endotherm occurring immediately after the exotherm, as indicated in Figure 12.2.

12.4 Process equipment and operation

The Japanese MH process equipment is centered on multiple-batch MH units, each contained in a glove box. Each batch of uranium-plutonium solution is loaded into a 50 cm diameter, 6 cm deep round denitration dish, which is constructed of Si_3N_4; a ceramic material that transmits the microwave energy uniformly from the surface to the bottom

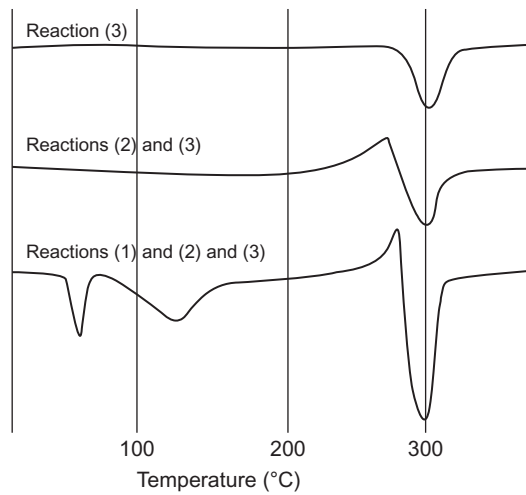

Figure 12.2 Differential thermal analyses. Upward deflection = exothermic effect; downward deflection = endothermic effect.

Table 12.1 Effluent gas analysis

Mass no.	Species	Relative quantity				
		Temperature of maximum rate (°C)				
		320	185	280	185	290
		Decomposition products				
		$UO_2(NO_3)_2$	NH_4NO_3	$NH_4UO_2(NO_3)_3$	$(NH_4)_2UO_2$	$(NO_3)_4$
14	N^+	m	t	M	m	M
15	NH^+		M	m	M	M
16	NH_2^+	m	M	m	M	m
17	NH_3^+		M	m	M	
18	H_2O^+	m	M	M	m	M
28	N_2^+	m		m		m
30	NO^+	M		M		M
32	O_2^+	m		M		M
44	N_2O^+		m	M	m	M
46	NO_2^+	M		M		M

Abbreviations: m, minor component; t, trace component; M, major component.

of the solution. In addition, the denitration dish is slowly rotated on a turntable inside the glove box to heat the solution uniformly. Active tests have been made of full-size production units at the Rokkasho Reprocessing Plant (Numao et al., 2007).

Uranium nitrate solution and plutonium nitrate solution are received from the chemical purification facility and are blended at a mass ratio of 1:1 U:Pu for codenitration and conversion to UO_3-PuO_2. The denitrated powder has a porous structure due to foam formation by evolution of NOx gas during boiling. Bulk density of the product is typically about 2 g/cm^3. Accessory equipment includes a microwave generation and wave guide transmission to each glove box, plus process off-gas treatment for recovery and recycle of nitric acid. The capacity of the MH system at Rokkasho is 108 kg (U + Pu) per day (Numao et al., 2007).

The MDD process equipment is centered on one or more rotary kilns, such as the development unit illustrated in Figure 12.3.

Each kiln is basically a straight length of stainless steel tubing with a diameter selected for the capacity of oxide production needed. Typically, the kiln is mounted on steel wheels and rotates within a tube furnace, which surrounds about one-third or more of the pipe length. Feed solution is introduced at one end of the rotary pipe kiln, which is angled downward to enable the decomposing salt and solid oxide powder to move by a combination of gravity and tube rotation to the end of the kiln, where the oxide product is collected. One or more solid stainless steel rods are located within the kiln and roll freely to act as "breaker bars" to crush lumps or to remove solid oxide from the tube wall. An air purge gas enters the kiln at the powder discharge end and

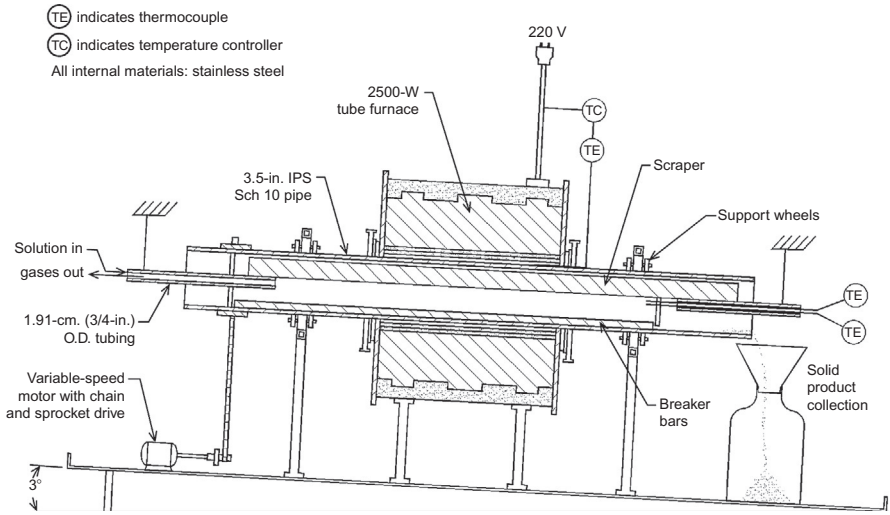

Figure 12.3 Rotary kiln cross section.

flows countercurrently through the kiln to remove the water, acid, and NO*x* gases that are formed. The off-gases leave the kiln at the liquid feed end and are routed to a scrubber and condenser system for recovery and recycle of nitric acid and for removal of entrained oxide.

Most of the development work has been done with uranium in rotary kilns measuring up to 16 cm in diameter and has progressed to demonstration at the multi-kilogram-per-hour scale. More recently, small-scale units (Figure 12.4) have been built and installed in a glove box to permit testing of the process for denitration of ammonium-uranium-plutonium nitrate solutions and co-conversion to MOX powder at a rate of ~100 g/h.

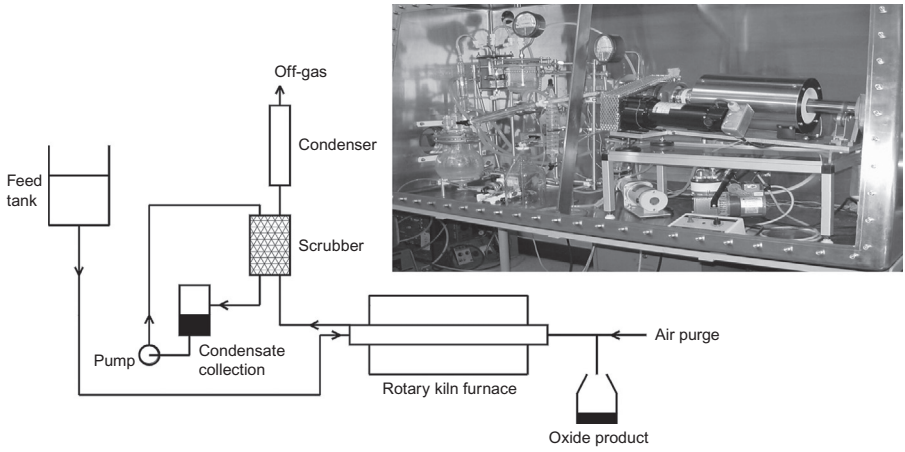

Figure 12.4 The U.S. MDD process and small-scale experimental equipment.

Coprocessed uranium-plutonium nitrate solution is mixed with ammonia gas or ammonium nitrate solution to provide the desired ratio of NH_4^+ to heavy metal, typically 2:1. The resulting ammonium-heavy metal double salt solution is fed to the rotary kiln at the rate needed for the production capacity. Inside the kiln, the solution goes through the sequence of (i) evaporation of water and nitric acid, (ii) denitration of the fused double salt, and (iii) formation of mixed uranium-plutonium powder. With the tube furnace operating at a typical temperature of 650 °C, measurements of the temperature profile and decomposition gas concentrations within the kiln have indicated that the denitration is completed within a short distance from the liquid feed entry point.

12.5 Conversion of UO_3 to UO_2

Thermal denitration of uranium produces a UO_3 product; codenitration of mixed uranium and plutonium produces a mixed UO_3-PuO_2 product. Subsequently, a separate calcination and reduction step is required to convert the UO_3 to UO_2 or the UO_3-PuO_2 to a single-phase $(U,Pu)O_2$ solid solution.

The UO_3 can be converted to UO_2 by means of the following calcination and reduction reactions:

$$3UO_3 \rightarrow U_3O_8 + 0.5O_2 \tag{12.6}$$

$$U_3O_8 + 2H_2 \rightarrow 3UO_2 + 2H_2O \tag{12.7}$$

The calcination occurs at temperatures up to ~700 °C. The reduction reaction occurs at a temperature of 700-800 °C in a period of 4 h. Alternatively, by heating in a reducing atmosphere, uranium trioxide (UO_3) can be directly converted to uranium dioxide (UO_2).

For the Japanese MH process at the Rokkasho plant, the dry MOX product from the denitration dish is crushed and placed into a rotary calcination furnace. Then, the calcined powder is transferred to a rotary reduction furnace, where it is treated with 95% N_2-5% H_2 to convert the powder to the final MOX form $(U,Pu)O_2$ (Numao et al., 2007).

The oxide powder produced in the MDD rotary kiln leaves the kiln in an agglomerated form, which requires screening through a 40-mesh sieve before calcination and reduction. Although not extensively developed, the calcination-reduction process and equipment would likely be similar to the process and equipment used for the MH process at Rokkasho. X-ray diffraction examination of MDD MOX has determined that the oxides in the MOX form a solid solution during reduction (Walker et al., 2007).

12.6 Product characteristics

Table 12.2 shows the endothermic heat of decomposition and typical UO_2 product characteristics from direct thermal denitration in comparison with those from the MDD process.

Table 12.2 Comparison of typical oxide product characteristics produced by MDD and direct denitration

	Direct thermal denitration	Modified direct denitration
Heat of decomposition, ΔH (kcal/gmol U)	110	26
Characteristics		
Surface area (m^2/g)	0.1-1.6	8-12
Average particle size (μm)	43	~2.5 μm
Bulk density (g/cm^3)	1.6-2.5	0.7-0.9
Appearance	Hard glass slag-like chunks	Fine granular solids
Sinterability (%)	~70	>90

Much less heat is required to decompose and denitrate the ammonium-uranium double salt in the MDD process, and the MDD oxide product has greater surface area, better sinterability, and smaller average particle size. In appearance, the MDD oxide product is in the form of fine granular agglomerates; the oxide produced by direct thermal denitration is in the form of hard glass-like chunks. These characteristics show that significant improvements in product quality are achieved in the MDD process.

In Table 12.3, key physical properties of MDD-produced UO_2 are compared with those of industrial grades of UO_2 produced by the ADU process. The physical properties of MOX produced by the MH process and the MDD process and the U.S. ASTM (American Society for Testing and Materials) standards for UO_2 and PuO_2 are also shown for comparison. The ADU process is already industrially deployed and produces UO_2 suitable for fuel fabrication (Haas, 1988). The properties shown for MH- and MDD-produced MOX also indicate suitability for fuel fabrication.

Table 12.3 Comparison of UO_2 and coconverted MOX physical properties

Source	Density (g/mL)		Surface area (m^2/g)	Mean particle size (μm)
	Bulk	Tap		
ADU UO_2 (Source #1)	2.36	3.21	4.81	5.52
ADU UO_2 (Source #2)	2.3	2.65	3.11	2.40
MDD UO_2	1.0	1.3	6.90	3.43
MH (UO_2-PuO_2)	2.2	3.7	4.5	Milled
MDD (92U-7.4Pu-0.4Np)O_2	~1	1.4	7.5	5.36
Prior to reduction of UO_3	~1	1.3	10.6	5.51
UO_2 (ASTM C 757-79)	–	–	>2.5	<10
PuO_2 (ASTM C 753-81)	–	–	>2.5	~10

Further tests of oxide powder rheology have been made to compare the product-handling characteristics of the MDD-produced UO_2 with the industrial-grade UO_2 products produced by the ADU process. The results indicated that:

- the MDD powder requires less energy to transport because it has less particle-to-particle friction during flow;
- the MDD powder agglomerates have a larger amount of interparticle void space and are more compressible; and
- the MDD powder is finer, more densely packed, and less permeable.

Thus, based on these analyses, the product-handling characteristics appear to be improved by the MDD process.

Mailen et al. (1982) conducted tests with MDD-produced mixed uranium-plutonium oxide having a plutonium content of 22.4 wt%, which is typical of MOX fuel recycled to fast breeder reactors. Part of the MOX product from these tests was shipped to Pacific Northwest National Laboratory for determination of fuel fabrication characteristics. The results are shown in Table 12.4. Sintered densities of >93% of theoretical were obtained.

Microstructure analyses made at Oak Ridge National Laboratory (ORNL) showed that the sintered pellets were free of significant porosity. Additional sintered pellets were used in dissolution tests at ORNL; the results showed that the pellets were completely dissolved in ~15 h by refluxing in nitric acid (initially 7 M). Periodic samples were taken and showed that the dissolution rate was linear over the 15-h period, indicating the homogeneity of the MOX pellets.

Table 12.4 Fabrication properties for MDD-produced MOX powder tests performed at Pacific Northwest National Laboratory

MOX powder		
Tap density (g/cm^3)	1.23	
Surface area (m^2/g)	9.2	
Calcined powder		
Calcining conditions		
Temperature (°C)	600	
Time (h)	4	
Weight loss (%)	13.6	
Tap density (g/cm^3)	1.22	
Surface area (m^2/g)	10.2	
Pellet properties[a]		
Forming pressure (MPa)	269	296
Green density (g/cm^3)	5.39	5.50
Sintered density (% of theoretical)[b]	93.9	93.5

[a]After being calcined, the powder was preslugged to 4.7 g/cm^3 and was granulated through a 14-mesh screen. 35.4 wt% of the granules were −14+20 mesh. The remaining particles were less than 20 mesh in size.
[b]Sintered at 1700 °C in 4% H_2-Ar for 4 h.

12.7 Co-conversion process comparisons

In comparison with precipitation and gelation processes, the MH and MDD advanced direct denitration processes require less-complicated process steps and equipment and do not require precise feed solution concentrations. For example, the one-step denitration replaces the multiple precipitation, filtration, and drying steps. In addition, less liquid waste and recycled product are generated. However, the advanced direct denitration processes do not remove any impurities, whereas coprecipitation has some impurity removal capability. Production of UO_2-PuO_2 MOX by means of oxalate coprecipitation requires a prereduction (of U^{6+} to U^{4+}), whereas the MH and MDD processes require a postcalcination reduction of UO_3 to UO_2.

The attributes of the MH and MDD processes are compared in the following list:

- The MH process has greater technical maturity.
- The MH process does not require addition of the ammonium nitrate denitration modifier and corresponding safety evaluation.
- The MH process is an automated multiple-batch process, whereas MDD is operated continuously in a rotary calciner.
- Both processes use simple one-step denitration but produce UO_3, which requires an additional calcination-reduction process.
- The MDD oxide powder does not require crushing and milling as does the MH product. The MDD product requires only screening through a 20-40 mesh sieve to deagglomerate larger agglomerates.
- The MH product is 50% plutonium and requires a ball-milling step with UO_2 to be down-blended to recycle fuel concentrations, whereas the MDD product may be able to use liquid blending of uranium and plutonium nitrate solutions to meet the precise recycle fuel concentrations.

12.8 Future trends

The MH process has been fully demonstrated at the Japanese Tokai Reprocessing Facility and is being deployed at full industrial scale in the Rokkasho Reprocessing Plant. The MH process product has been tested for production of both light water reactor recycle fuel and fast breeder recycle fuel (Numao et al., 2007).

The MDD process has been demonstrated at industrial scale for UO_2 production, but MOX production has only been tested at the engineering scale in research and development studies. As indicated in Table 12.3, the MDD process has been used to accomplish co-conversion of uranium-plutonium-neptunium nitrate. Moreover, in companion tests (Walker et al., 2007; Felker et al., 2008), co-conversion of uranium-plutonium-neptunium-americium nitrate was successfully demonstrated.

Variations of the MDD process using different modifiers are used industrially for other applications. For example, at the French LaHague reprocessing plant, a similar process and similar equipment are used for codenitration and c-conversion of fission-product nitrate solutions to a solid oxide form prior to incorporation into vitrified high-level waste (Brueziere et al., 2013).

Because of its promising simplicity, the MDD process will likely be the focus of continued RD&D in the United States. Variations of the process are of interest in other countries.

References

Bathke, C., Ebbinghaus, B., Sleaford, B., Wallace, R., Collins, B., Hase, K., Robel, M., Jarvinen, G., Bradley, K., Ireland, J., Johnson, M., Prichard, A., Smith, B., 2009. An assessment of the attractiveness of material associated with a MOX fuel cycle from a safeguards perspective. In: Proceedings of 50th Annual Meeting of INMM.

Brueziere, J., Chauvin, E., Piroux, J., 2013. World first in high level waste vitrification—a review of French vitrification industrial achievements. In: Proceedings of Global 2013 International Conference.

Felker, L., Vedder, R., Walker, E., Collins, E., 2008. Product conversion: the link between separations and fuel fabrication. In: Proceedings of Atalante 2008 International Conference.

Haas, P., 1988. A comparison of processes for the conversion of uranyl nitrate into ceramic-grade UO_2. Nucl. Technol. 81, 383–406.

Haas, P., Arthur, R., Stines, W., 1981. Development of thermal denitration to prepare uranium oxides and mixed oxides for nuclear fuel fabrication. ORNL-5735, Oak Ridge National Laboratory, Oak Ridge, TN.

Koizumi, M., Katsuyuki, O., Isagawa, H., Akiyama, H., Todokoro, A., 1983. Development of a process for the co-conversion of Pu-U nitrate mixed solutions to mixed-oxide powder using a microwave heating method. Nucl. Technol. 61, 55–70.

Lerch, R., Norman, R., 1984. Nuclear fuel conversion and fabrication chemistry. Radiochim. Acta 36, 75–88.

Mailen, J., Pruett, D., McTaggart, D., 1982. Direct thermal denitration to prepare mixed oxides for nuclear fuel fabrication. ORNL/TM-8197, Oak Ridge National Laboratory, Oak Ridge, TN.

Notz, K., Haas, P., 1981. Properties and thermal decomposition of the double salts of uranyl nitrate-ammonium nitrate. ORNL/TM-7820, Oak Ridge National Laboratory, Oak Ridge, TN.

Numao, T., Nakayashiki, H., Arai, N., Miura, S., Nakamura, H., Tanaka, I., 2007. Results of active test of uranium-plutonium co-denitration Facility at Rokkasho Reprocessing Plant. In: Proceedings of Global 2007 International Conference.

Walker, E., Vedder, R., Felker, L., Marschman, S., 2007. Application of modified direct denitration to support the ORNL coupled-end-to-end demonstration in production of mixed oxides suitable for pellet fabrication. In: Proceedings of Global 2007 International Conference.

The coprecipitation and conversion of mixed actinide oxalates for aqueous-based reprocessing of spent nuclear fuels

13

Mark J. Sarsfield
National Nuclear Laboratory, Central Laboratory, Sellafield, Seascale, UK

Acronyms

CEA	Commissariat à l'énergie atomique et aux énergies alternatives
COEX™	coprecipitation of uranium and plutonium
EXAFS	extended X-ray absorption fine structure
MA	minor actinide
MOx	mixed oxide fuel
P&T	partitioning and transmutation
PUREX	plutonium uranium redox extraction
PXRD	powder X-ray diffraction
SSA	specific surface area
TD	theoretical density
UMACS	uranium minor actinides conventional sintering
XANES	X-ray absorption near edge structure

13.1 Introduction

To enhance the sustainability of the nuclear fuel cycle, and fully utilize the fissionable material from spent nuclear fuel, the recovered plutonium can be fabricated into mixed uranium and plutonium oxide fuel (MOx) and irradiated in a nuclear reactor to generate more energy. In addition, minor actinides (e.g., MA = Np, Am, Cm) can be included in the fuel or as targets to be transmuted into shorter-lived isotopes and reduce the radiotoxicity and heat loading of long-term waste storage locations (Salvatores and Palmiotti, 2011).

Industrial reprocessing of spent nuclear fuel currently involves the separation of uranium and plutonium from waste fission products by hydrometallurgical methods (plutonium uranium redox extraction, PUREX process) (Wilson, 1996). The output streams are metal nitrates in nitric acid solution that require conversion to a final form that is suitable for either storage or fabrication into new fuel. For plutonium this "finishing process" involves precipitation as solid plutonium oxalate, and has been

Reprocessing and Recycling of Spent Nuclear Fuel. http://dx.doi.org/10.1016/B978-1-78242-212-9.00013-7

the technology of choice with over 50 years of industrial experience. The oxalate product is then converted to the dioxide (PuO_2) by decomposition at temperatures >400°C.

For MOx fuel fabrication, the plutonium dioxide product is intimately mixed with uranium dioxide and milled to provide material of suitable consistency for efficient pressing and sintering to produce ceramic fuel. This methodology provides a fuel that is as homogeneous as possible in order to avoid hot spots during irradiation and to make the fuel easier to dissolve during reprocessing; difficulties that can arise as a result of localized plutonium-rich areas. Achieving this through powder mixing methods requires rigorous process control and falls short of complete homogeneity (Oudinet et al., 2008). At the same time, the amount of milling and mixing of finely divided powders increases the risk of spreading contamination making alpha glove boxes and associated equipment difficult to maintain. Similarly for the transmutation of MAs, simple dust-free processes are preferred to convert the nitric acid streams into either a homogeneous U,Pu,MA containing MOx fuel or U,MA blanket/target fuel (Salvatores and Palmiotti, 2011; Somers, 2011). The high neutron and gamma radiation fields make manufacturing MA fuels particularly challenging.

A novel method for solving some of these problems is to have the two (or more) actinides in the same oxalate precursor material ensuring complete homogeneity at the molecular level by coprecipitation. This chapter summarizes the developments made in this area and the challenges to be faced in application at an industrial-process scale. A discussion on the current industrial-scale plutonium oxalate precipitation will introduce the chemistry and equipment involved in the process. This is followed by current oxalate coprecipitation knowledge and how it is applied to actinide finishing processes. Finally, there will be a discussion of how the technology is being implemented for MOx and transmutation target fuels.

13.2 Plutonium oxalate precipitation and decomposition

From the early days of plutonium production at the Hanford plant in the 1940s and 1950s, precipitation of plutonium using oxalic acid has provided a simple and effective way to isolate plutonium in a pure form (Sukumar et al., 2013).

Plutonium can be precipitated as Pu(IV) oxalate, $Pu(C_2O_4)_2 \cdot 6H_2O$, which has been characterized by powder X-ray diffraction (PXRD) (Jenkins et al., 1965a) and shown to be isostructural with the $U(C_2O_4)_2 \cdot 6H_2O$ (Duvieubourg-Garea et al., 2008) and Np $(C_2O_4)_2 \cdot 6H_2O$ (Harmon and Reas, 1957) analogues. Alternatively, Pu(IV) can be reduced to Pu(III) and precipitated as $Pu_2(C_2O_4)_3 \cdot 9\text{-}10H_2O$ (Jenkins et al., 1965b; Runde et al., 2009), which is isostructural with $Ln_2(C_2O_4)_3 \cdot 10H_2O$; (Ln = La, Ce, Pr, Nd (Gelman and Moskvin, 1958)). Much of the research performed on actinide oxalates relates to these two plutonium materials because of their usefulness in producing PuO_2 as a final form for storage and use in MOx fuel (Wilson, 1996), or for use in radioisotope heating units in space power systems (Hayashi et al., 2013).

The oxalate ligands bond to plutonium centers in a bidentate fashion through two oxygen atoms. For $Pu(C_2O_4)_2 \cdot 6H_2O$, the overall crystal structure is triclinic and isostructural to $U(C_2O_4)_2 \cdot 6H_2O$ (Duvieubourg-Garea et al., 2008), which contains uranium atoms surrounded by four oxalates bonding through two oxygens each making the metal center

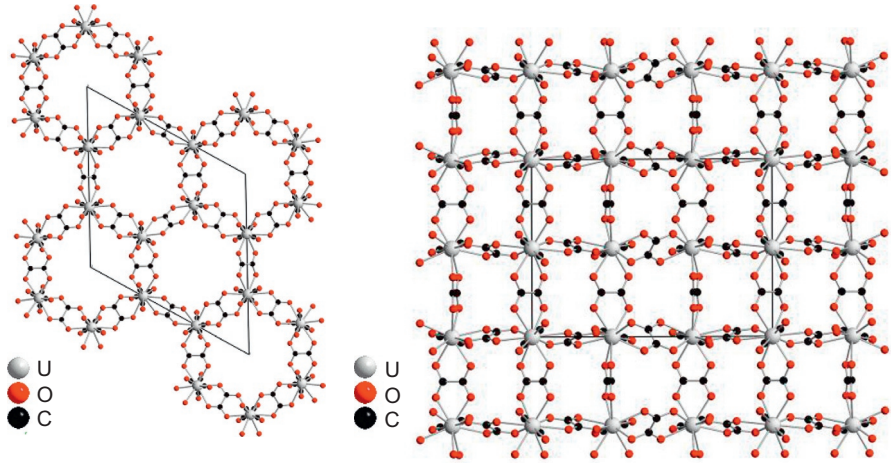

Figure 13.1 Crystal structure within $U(C_2O_4)_2 \cdot 6H_2O$ (Runde et al., 2009) showing (left) the layer of $[U(C_2O_4)]_6$ rings; (right) the side view of the layers (gray spheres, uranium; red spheres, oxygen; black spheres, carbon). Interstitial waters have been removed for clarity.

8 coordinate. Each oxalate is also bonded to another uranium atom to make a layer of connected six-membered rings (Figure 13.1 left). Each layer is also connected above and below via a bridging oxalate group resulting in a polymeric 3-D layered structure (Figure 13.1 right). The solvated water molecules lie between these layers.

For $Pu_2(C_2O_4)_3 \cdot 9\text{-}10H_2O$, the PXRD structure was determined as monoclinic and assumed to be the same as the crystallographically determined $Ln_2(C_2O_4)_3 \cdot 10H_2O$; Ln = La, Ce, Pr, Nd, Er, Eu-Dy (Ollendorff and Weige, 1969; Michaelides et al., 1988; Kalinina et al., 2003; Trombe and Jaud, 2003), Am (Weigel and TerMeer, 1967). Recent single-crystal studies have confirmed the structure as $Pu_2(C_2O_4)_3(\text{-}H_2O)_3 \cdot 6H_2O$ (Runde et al., 2009), which is the same as the lanthanide oxalates (Hansson, 1970) with three bidentate oxalates and three water molecules bonded to the metal in the inner coordination sphere. The additional waters in the lanthanide structures are in the outer coordination sphere and between the metal oxalate layers. The oxalates are bonded to neighboring plutonium atoms forming a two-dimensional layer of $[Pu(C_2O_4)]_6$ connected rings (Figure 13.2).

There are a number of structures proposed with varying levels of hydration and these demonstrate the flexibility of the structures toward inclusion of small molecules within the layers, particularly important when considering the countercations incorporated within coprecipitated actinide complexes, which will be discussed later in this chapter.

The precipitation mechanism of plutonium oxalates is dependent on a number of factors that can influence the particle morphology and size distribution of the final plutonium dioxide product. These include temperature of precipitation, nitric acid concentration, oxalate concentration, stirring speeds, order of mixing, and residence time before filtering (through Ostwald ripening, Kahlweit, 1975).

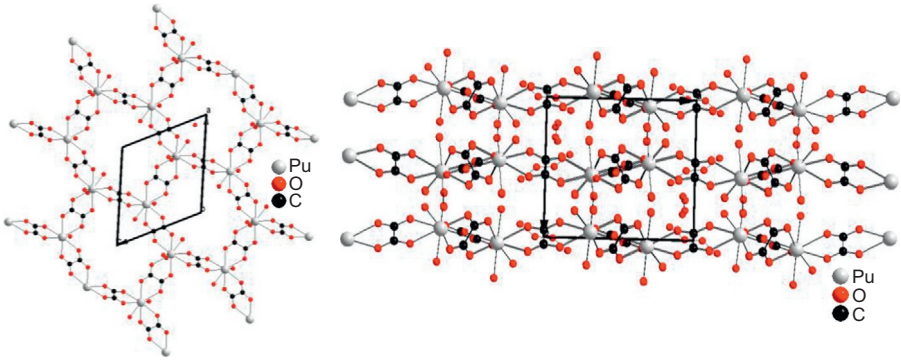

Figure 13.2 Crystal structure within $Pu_2(C_2O_4)_3(H_2O)_3 \cdot 6H_2O$ (Runde et al., 2009) showing (left) the layer of $[Pu(C_2O_4)]_6$ rings; (right) the side view of the layers (gray spheres, plutonium; red spheres, oxygen; black spheres, carbon). Interstitial waters have been removed for clarity.

The precipitation mechanism includes nucleation, dependent on the supersaturation of the system and growth of the plutonium oxalate crystals. The classical theory of crystal precipitation is based on these two processes. Nucleation can be described by the terms:

$$R_N = A_N \exp\left[-\frac{B_N}{(\ln S)^2}\right]$$

where R_N is the rate of nucleation; A_N and B_N are the rate constants specific to the system in question that are determined by experiment; S is the supersaturation and is further defined as the ratio of the activities of each species in solution divided by the solubility product at equilibrium:

$$S = 5\sqrt{\left(\frac{a_{Pu^{3+}}^2 \times a_{C_2O_4^{2-}}^3}{K_{SP}}\right)} \quad \text{for } Pu_2(C_2O_4)_3$$

$$S = 3\sqrt{\left(\frac{a_{Pu^{4+}} \times a_{C_2O_4^{2-}}^2}{K_{SP}}\right)} \quad \text{for } Pu(C_2O_4)_2$$

Once nucleation has occurred, the growth rate (G in m/s) of the crystal is expressed as

$$\frac{\partial n(L,t)}{\partial t} + G(t)\,\frac{\partial n(L,t)}{\partial L} = 0$$

where $n(L,t)$ is the number particle size distribution and $G(t)$ represents the linear growth rate (Randolph and Larson, 1988).

From both the nucleation and growth terms, it is clear to see that concentration differences within the reactor vessel can have a profound effect on the local supersaturation and growth rate values leading to changes in the particle size distribution.

For more details, the interested reader is directed to the work of Bertrand-Andrieu and references therein (Bertrand et al., 2012; Bertrand-Andrieu et al., 2004).

On an industrial scale, $Pu(C_2O_4)_2 \cdot 6H_2O$ is the target oxalate, and high throughput is desired with a precipitate that has a large enough particle size to ensure efficient filtering. The many precipitation variables are controlled by using a continuous precipitation process that involves a simple vessel with an overflow spout that pours onto a rotary vacuum table where it is filtered, washed, and scraped into a rotary calcination tube (Figure 13.3). Within the calcination tube the material is dried and then decomposed into the dioxide (calcined) coming out of the process and into cans used to store the product. This continuous process allows 10s kg/day throughput levels in a criticality safe manner.

The decomposition of plutonium oxalates has been a subject of study for over 50 years as it exhibits a complex mechanism with potential operational safety and quality implications. A more detailed review of the work in this area is provided in Orr et al. (submitted) but is summarized here to highlight some of the potential issues that may affect the coconversion of mixed actinide oxalates to oxide products.

The decomposition mechanism follows different paths for different plutonium oxidation states and different reaction atmospheres. Early studies of the decomposition reaction gave conflicting results (Glasner, 1964; Jenkins and Waterman, 1964; Karelin et al., 1990; Kartushova et al., 1957; Kozlova et al., 1984; Myers et al., 2003; Nissen, 1980; Rao et al., 1963; Sali et al., 2005; Subramanian and Subramanian, 2012; Vigier et al., 2007; Waterbury et al., 1961) but more recent studies have clarified the situation somewhat using a combination of complimentary analytical techniques.

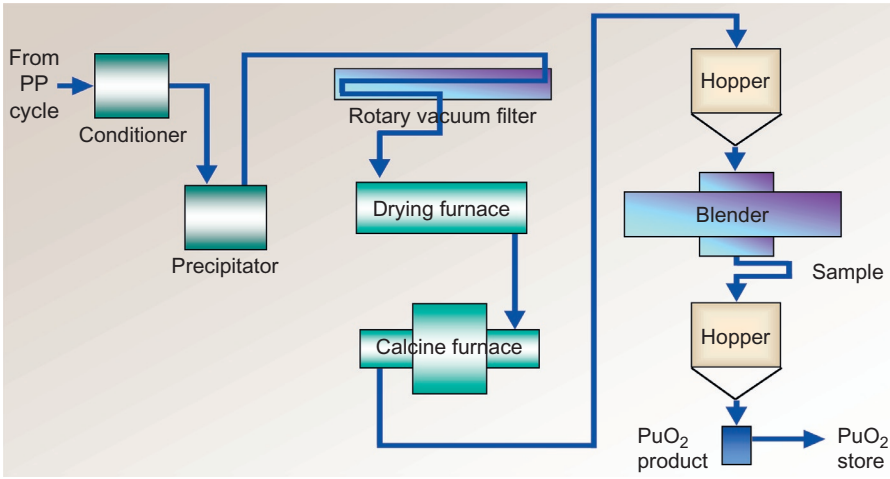

Figure 13.3 Schematic of the plutonium finishing process as used at the industrial scale.

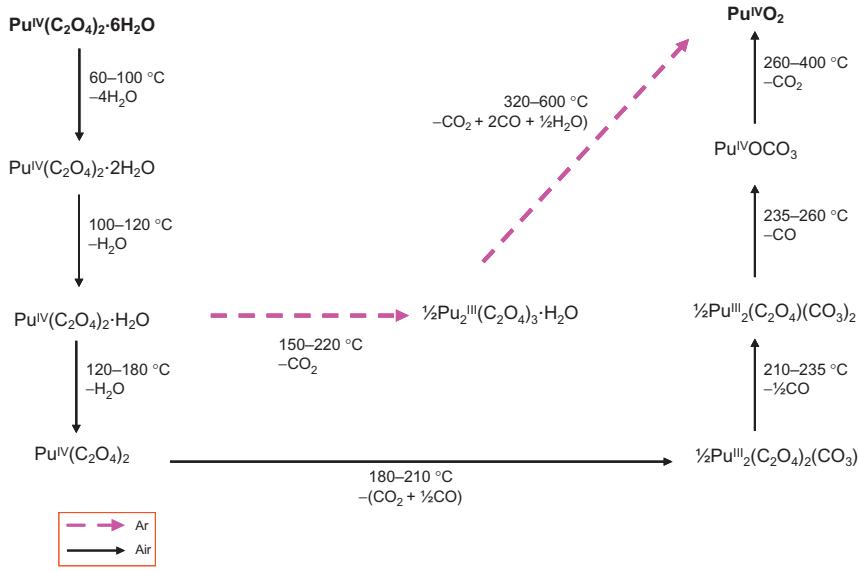

Figure 13.4 Decomposition mechanism for $Pu(C_2O_4)_2 \cdot 6H_2O$ in air and in an argon atmosphere (Vigier et al., 2007).
Reproduced from Orr et al. (submitted).

For $Pu(C_2O_4)_2 \cdot 6H_2O$ there are a number of dehydration steps followed by oxalate decomposition either directly to the dioxide or via a series of mixed oxalate-carbonate complexes (Figure 13.4). Samples of the oxalate heated in a thermogravimetric analyzer (TGA) under either flowing argon or static air were isolated at particular temperature points in the process and analyzed by solid-state electron absorption spectroscopy (EAS) and infrared (IR) spectroscopy (Vigier et al., 2007). Changes in the amount of hydration between ambient temperature and 200 °C could not be confirmed because of the tendency to readily rehydrate, but distinct water losses are identifiable from the weight loss of the TGA curves. Successive replacement of oxalate by carbonate groups was indicated by IR spectroscopy that also identified CO_2 occluded or sorbed within the solid. EAS showed that in static air, oxalate decomposition starts when dehydration is complete and confirmed that full reduction from Pu(IV) to Pu(III) occurs as the oxalate-carbonate complexes are formed. This reduction process is believed to be attributed to the oxidation of CO to CO_2 by the anhydrous plutonium oxalate. Decomposition under argon followed a different path in that the intermediate carbonate compounds were not observed, although reduction to Pu(III) was confirmed by EAS. Releases of CO and CO_2 are thought to be distinctly sequential with the decomposition to PuO_2 complete by ~400°C in air and ~600 °C in argon (Figure 13.4).

The fact that reduction occurs demonstrates that the reaction progression is heavily influenced by the immediate atmosphere around the solid and that physical effects such as gas flow rates, temperature gradients, and thickness of the solid bed can have

a marked influence on the efficiency of the decomposition process, particularly the amount of carbon impurities in the product. For example, the disproportionation of carbon monoxide (Boudouard reaction) results in the depositing of carbon within the product and the amount will be dependent on the kinetics and thermodynamics of CO oxidation by O_2 and C oxidation by CO_2 and O_2. Thus, under inert atmospheres and low temperatures, more carbon is found as an impurity in the PuO_2 product. It is also important to note that carbon monoxide in high concentrations can cause a deflagration risk (Hustad and Sonju, 1988) within operating vessels and so understanding when and how much is released is vital for underpinning safety cases.

For the decomposition of $Pu_2(C_2O_4)_3(H_2O)_3 \cdot 6H_2O$, a similar study was performed with direct comparison to neodymium and cerium as potential surrogates for plutonium (Almeida et al., 2012). Samples of the oxalate were heated at 2 °C/min under air or argon. The initial hydration number was different in each case, this being attributed to the drying of the furnace under vacuum prior to heating in argon. There are two or three discreet dehydration stages to get to the anhydrous Pu(III) oxalate from which complete decomposition to PuO_2 occurs under both air and argon atmospheres (Figure 13.5). Loss of waters is an endothermic process while oxalate decomposition is strongly exothermic, especially in air due to Pu(III) to Pu(IV) oxidation and, therefore, is accelerated by an oxidizing atmosphere (complete at <450 °C in air cf. 700 °C in argon) (Almeida et al., 2012). It was also concluded that cerium rather than neodymium is the more appropriate simulant for plutonium oxalate decomposition studies.

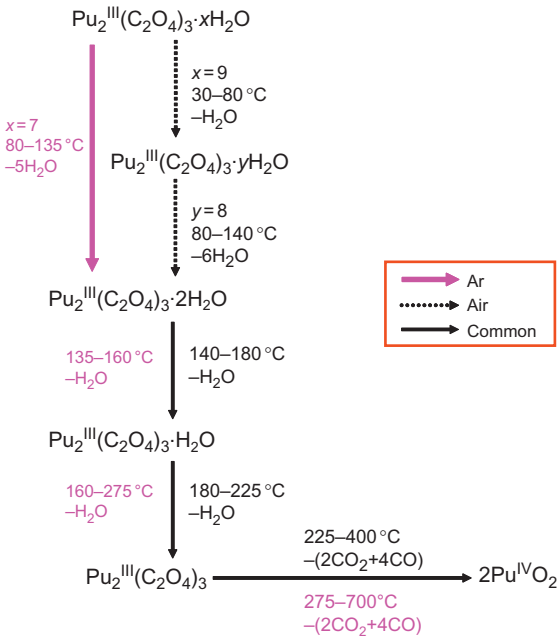

Figure 13.5 Decomposition mechanism for $Pu_2(C_2O_4)_3(H_2O)_3 \cdot 6H_2O$ in air and in an argon atmosphere (Almeida et al., 2012). Reproduced from Orr et al. (submitted).

Production of PuO_2 for fuel manufacture is required to have a low carbon content because of the potential detrimental effects on the sintering and densification of pellets (Cina, 1963). From the information gathered on the oxalate decomposition mechanism, it would appear logical to perform the calcination processes at high temperatures (>700 °C) in air to ensure low carbon impurities. However, other factors need to be considered that generally require a compromise of conditions.

One significant factor is the specific surface area (SSA) of the final oxide material. Higher surface area is often considered more reactive when it comes to making ceramic pellets. The oxalate precipitation conditions can determine the particle size and shape (Burney and Smith, 1984) and this morphology is generally retained upon conversion to the oxide, albeit with a ~20% volume reduction. Calculation of the SSA for the average PuO_2 particle size distribution assuming a theoretical perfect sphere is $<1\ m^2/g$, and yet the SSA can range from above 40 to 1 m^2/g depending on the calcination temperature (Haschke and Ricketts, 1995a; Machuron-Mandard and Madic, 1996; Moseley and Wing, 1965; Dias and Chackraburtty, 1971). High SSA is believed to occur at low calcination temperatures because of the fracturing of the particles along a particular crystal plane as gases such as H_2O, CO, and CO_2 escape the particle. This appears to result in a "puff pastry"-like structure with large porosity. Low SSA material is believed to form at higher calcination temperatures because of a closing of the pores and repairing of the particle structure. A review of the dependence of temperature and residence time of the calciner versus SSA has been made by Daniel (2012). The review culminated in an empirical equation describing the approximate dependence of SSA on calcination temperature (T) and calcination time (t) between 250 and 1100 °C.

$$\mathrm{SSA} = A + \left\{B.\mathrm{e}^{-0.5\left(\frac{T-C}{D}\right)^2}\right\} + \left\{E.\mathrm{e}^{-0.5\left(\frac{t-F}{G}\right)^2}\right\} + \left\{H.\mathrm{e}^{-0.5\left(\frac{T-C}{D}\right)^2+\left(\frac{t-F}{G}\right)^2}\right\}$$

$A = 2.5080$, $B = 42.241$, $C = 310.99$, $D = 184.85$, $E = -0.39178$, $F = 2.5971$, $G = 0.64387$, and $H = 29.805$.

Other reports suggest that the calcinations atmosphere could also influence the SSA and Vigier found that PuO_2 calcined at 650 °C under air gave 11 m^2/g, while under argon the SSA was 20 m^2/g; although the latter had high (1% w/w) carbon within the final material (Vigier et al., 2007). Also, Crowder reported that the batch size, or powder depth, was statistically the most significant influence on the SSA (Crowder et al., 2012).

Further analysis by Orr et al. (submitted) showed that removing the materials decomposed below 400 °C allowed a simplification of the empirical fit to the data given the inherent uncertainty in the conditions used to generate the material from one study to the next.

$$\mathrm{SSA}_{\mathrm{fit}} = \exp\left(-5.227 \times 10^{-3} T + (5.635 \pm 0.755)\right)$$

The best fit and 95% confidence interval are overlaid on the experimental data as the solid and dashed lines, respectively, in Figure 13.6.

Importantly for actinide coprecipitation and calcination processes, the decomposition of the oxalate in an oxidizing atmosphere is in most cases not an option and this

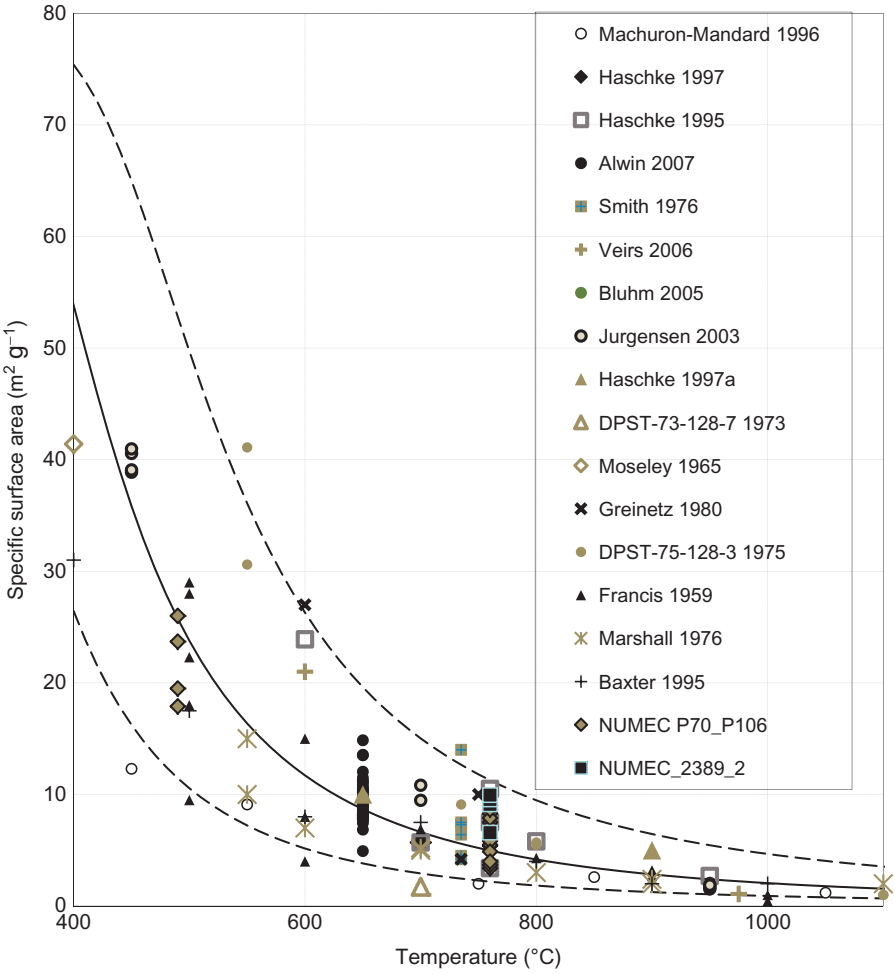

Figure 13.6 Best fit to experimental data showing the specific surface area of plutonium dioxide against the temperature at which the plutonium oxalate was calcined assuming an exponential function. *Note*: The best fit is shown by the solid line and the 95% confidence interval by the dashed line (Moseley and Wing, 1965; Marshall et al., 1976; Francis and Sowden, 1959; Baxter, 1995; SRNL, 1973, 1975; Puechl, 1963a,b,c, 1962, 1964; Puechl and Garber, 1961; Puechl et al., 1961; Greinetz and Neal, 1980; Haschke et al., 1997; Jurgensen et al., 2003; Bluhm et al., 2005; Veirs, 2006; Smith et al., 1976; Alwin et al., 2007; Livingston and Duffey, 2001; Caldwell, 1961; Caldwell and Menis, 1961; Haschke and Ricketts, 1995b, 1997; Stakebake and Robinson, 1983; Nicholson, 1965; German and Munir, 1979; Subramanian et al., 1963).
Reproduced from Orr et al. (submitted).

must be considered from the viewpoint of total carbon impurity in the solid and the desired SSA of the final product. Often, the presence of U(IV) in coprecipitated actinides requires calcination under inert atmosphere and, thus, higher temperatures are required to remove residual carbon, the levels of which must be balanced against the SSA required for fabrication into new fuel.

13.3 Coprecipitation of mixed oxalates

It is worth pointing out some of the attributes of coprecipitation that will be important for the eventual conversion to the final oxides:

- The compounds must be reproducible and properly controlled to give a homogeneous mix of the two (or more) metal ions.
- It should be possible to decompose any counterions (e.g., cations) within the oxalate structure such that the final oxide is free of impurities.
- It must be possible to decompose the oxalates in a safe way without possible deflagration events.
- There needs to be some consideration of the increased throughput of precipitation required compared to current plutonium finishing processes as the amount of solids for MOx fuel could increase to anywhere between a factor of 2 and 10.
- Oxidation state control will be important particularly for U^{IV} because autocatalytic oxidation (Koltunov, 1974; Dvoeglazov et al., 2005) back to U^{VI} will undoubtedly change the final oxalate product.

There are many reports of mixed metal oxalates containing actinides now published but most since 2005. To understand which structures are of most interest, and why, the following section will categorize the crystal structures and draw some general trends from the published research to date.

13.3.1 Crystal structures of the mixed M^{III}/M^{IV} oxalates

As already seen in the structures of $U(C_2O_4)_2{\cdot}6H_2O$ and $Pu_2(C_2O_4)_3(H_2O)_3{\cdot}6H_2O$ there is a propensity for metal oxalates to form layers or double layers and the number of possible structural types increases when monovalent cations are introduced that often occupy the gaps between these layers. The numbering convention for different families of tertiary systems can be categorized by the ratio of counter-cation/metal ion/oxalate. For example $M[Ln(H_2O)_2(C_2O_4)_2]{\cdot}H_2O$; Ln = La, M = K, NH_4 (Bataille et al., 2000) and $NH_4[Ln(H_2O)_x(C_2O_4)_2]{\cdot}yH_2O$; Ln = La, $x = 2$, $y = 1$; Ln = Gd, $x = 1$, $y = 0$s (Trombe et al., 2001) are of the 112 class and all have a 2-D layered structure.

The earliest reports of mixed uranium lanthanide oxalate structures in the 1990s were of the 124 structure $(M^{I})[Ln^{III}U^{IV}(C_2O_4)_4]{\cdot}8H_2O$; Ln = La, Ce, Pr, Nd Tb; M = K (Chadha et al., 1991); NH_4 (Mudher et al., 1997). The purpose of the experiments was to assess structural variations in the K_2UO_4 system, but instead thermal decomposition of the oxalates resulted in a mixed phase system including $K_2U_2O_7$

and a cubic (Ln,U)$O_{2\pm x}$. This interesting result gave an early indication that homogeneous mixed M^{III}/U^{IV} oxides could be made from coprecipitated oxalates.

These early mixed oxalates were characterized by PXRD and other analytical methods, but their exact structures were not solved mainly because the insolubility of the oxalates made it very difficult to grow single crystals suitable for crystallography. This was overcome by the use of slow diffusion of metal ions through silica gel impregnated with oxalic acid or diffusion through membranes separating compartments containing oxalic acid and actinide nitrate solutions (Tamain et al., 2012). The first structurally characterized mixed metal oxalate containing an actinide was $(NH_4)_2[U_2(C_2O_4)_5]\cdot 0.7H_2O$, part of the 225 class of oxalates (Chapelet-Arab et al., 2005a). Substituting Ln^{III} for a U^{IV} site readily occurs with a concomitant increase in the number of monovalent cations and water molecules that can be accommodated in the hexagonal tunnels running down the [001] direction, although unlike the 112 family of metal oxalates, a 3-D structure is formed with oxalate ions bridging the layers resulting in a hexagonal honeycomb structure. Compounds with different monovalent cations were made: $(N_2H_5)_{2.6}U_{1.4}Ln_{0.6}(C_2O_4)_5\cdot xH_2O$ (Ln = Nd, Sm), $Na_{2.56}U_{1.44}Nd_{0.56}(C_2O_4)_{5.7}\cdot 6H_2O$, and $Na_3UCe(C_2O_4)_5\cdot 10.4H_2O$, all with hexagonal tunnels throughout the structure (Chapelet-Arab et al., 2005a). The incorporation of the hydrazinium cation ($H_5N_2^+$) is notable as this is generally present in processing solutions as a nitrite (NO_2^-) scavenger to stabilize U^{IV} in nitric acid solution and can be decomposed to leave no metal impurities in the final product. These early compounds demonstrated that up to 50% of a M^{III} ion could be incorporated into the U^{IV} oxalate structure.

By taking the converse approach of substituting Ln^{III} sites with U^{IV} ions and concomitant removal of cations, a 112 family of oxalate compounds was prepared with a higher Ln^{III} to U^{IV} ratio ranging from 75% to 50% Ln^{III} incorporation in $(N_2H_5)_x[Ln_xU_{1-x}(C_2O_4)_2]\cdot nH_2O$ (Ln = Nd, Gd; $x = 0.75$) and $(Na)_x[Ln_xU_{1-x}(C_2O_4)_2]\cdot nH_2O$ (Ln = Nd, $x = 0.5$; Ln = Gd, $x = 0.65$) (Chapelet-Arab et al., 2005b). These compounds were of the triclinic space group rather than the hexagonal or orthorhombic space group as seen with the 225 oxalate family; however, the six-membered rings remain present and the interstitial layers are occupied by waters and monovalent cations. It is clear from these structures that changing the monovalent cation can lead to a significant change in the Ln^{III}:U^{IV} ratio.

A third series of compounds supports the importance of the role of the monovalent cation. While still in the 112 family of compounds $(NH_4)_xLn_xU_{x-1}(C_2O_4)_2(H_2O)]\cdot(4-x)H_2O$ (Ln = Y, Pr, Nd, Sm, Gd, Tb; $x = 0.40$-0.75)s containing ammonium cations has a very different structure than the 112 family containing H_5N_2 or Na countercations (Chapelet-Arab et al., 2006). All six compounds made are of the tetragonal space group and the structures consist of a 2-D framework of layers composed of four-membered rings joined by metal oxalate linkages rather than six-membered rings observed for all previous structures. The structure is related to the 112 $Na[Y(C_2O_4)_2(H_2O)]\cdot 3H_2O$ compound (Bataille and Louër, 1999). The difference in ring size is not fully understood; however, the 45-75% M^{III} loading makes this an attractive structure to target for high plutonium fuels.

It was also not clear from these studies whether the single crystals obtained would actually be representative of a powder product obtained in a continuous process. Thus bulk powder production and analysis of products from varying Ln^{III}/U^{IV} nitrate solution ratios treated with oxalic acid were required to establish whether the mixed metal content can be controlled and whether the oxalate products are a single phase or a mixture, for example, of trigonal and tetragonal 112 compounds. The influence of monovalent cation on the structures also needed to be confirmed.

More recently, the first crystallographic characterization of the mixed U^{IV}/Pu^{III} oxalates has been reported (Tamain et al., 2013). Interestingly, two crystallographic forms of the mixed oxalate were produced with NH_4^+ as the countercation. Using a three-compartment diffusion cell containing oxalic acid, ammonium nitrate and the actinide solutions each separated by a compressed glass fiber membrane, single crystals were grown of suitable quality for X-ray diffraction. Crystals related to the tetragonal 112 class of mixed oxalates $(NH_4)_{0.5}[Pu_{0.5}U_{0.5}(C_2O_4)_2(H_2O)]\cdot nH_2O$ were formed in the oxalic acid-rich compartment. In the same diffusion experiment, crystals of the hexagonal 225 class of mixed oxalates $(NH_4)_{2.7}Pu_{0.7}U_{1.3}(C_2O_4)_5\cdot nH_2O$ were formed in the actinide-rich solution (Tamain et al., 2012, 2013).

The tetragonal structure $(NH_4)_{0.5}[Pu_{0.5}U_{0.5}(C_2O_4)_2(H_2O)]\cdot nH_2O$ is directly related to the $(NH_4)_xLn_xU_{x-1}(C_2O_4)_2(H_2O)]\cdot(4-x)H_2O$ [Ln = Y, Pr, Nd, Sm, Gd, Tb; $x = 0.40$-0.75] (Chapelet-Arab et al., 2006) with each actinide ion coordinated to nine oxygens in a monocapped square antiprism of $(U,Pu)O_9$ with eight of the oxygens from four symmetrically related bidentate oxalate anions and capped with the oxygen atom of a water molecule (Figure 13.7). This tetragonal structure is also similar to that of $[U(C_2O_4)_2]\cdot H_2O\cdot$dma (dma = dimethylamine) containing neutral dma molecules within the interlayer structure rather than monovalent cations (Duvieubourg-Garea et al., 2008).

The hexagonal $(NH_4)_{2.7}Pu_{0.7}U_{1.3}(C_2O_4)_5\cdot nH_2O$ structure is comprised of six-membered rings in a three-dimensional honeycomb array (Figure 13.8). Each actinide

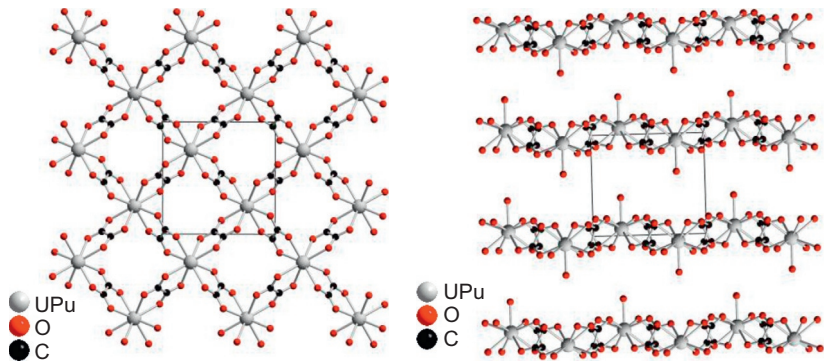

Figure 13.7 Crystal structure of tetragonal $(NH_4)_{0.5}[Pu_{0.5}U_{0.5}(C_2O_4)_2(H_2O)]\cdot nH_2O$ showing (left) the four-membered ring tunnels through the structure and (right) the two-dimensional layers (gray spheres, uranium/plutonium; red spheres, oxygen; black spheres, carbon) (Tamain et al., 2013).

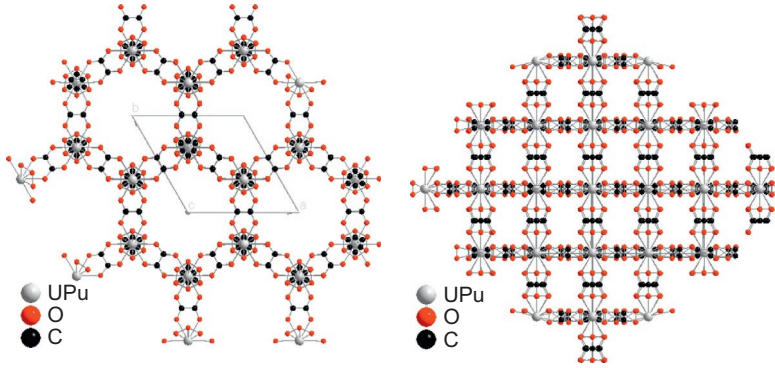

Figure 13.8 Crystal structure of hexagonal $(NH_4)_{2.7}Pu_{0.7}U_{1.3}(C_2O_4)_5 \cdot nH_2O$ showing (left) the hexagonal tunnels through the structure and (right) the three-dimensional structure with bridging oxalate groups between layers (gray spheres, uranium/plutonium; red spheres, oxygen; black spheres, carbon) (Tamain et al., 2012).

ion is 10 coordinate surrounded by 5 bidentate oxalate anions, 2 of which bridge the six-membered ring layers. The crystal morphology is one of hexagonal tubes that may not be conducive to high-density pellet pressing (Tamain et al., 2012, 2013).

This confirms that it is possible to access the tetragonal structure, which may be preferred because of the high plutonium loading and the tetragonal plate morphology of the crystals that may require less processing when converting to the oxide and pressing into ceramic mixed oxide pellets. It seems that the hexagonal structure is the kinetically stable form and will be preferentially made during bulk oxalate powder processing unless some radical change to the production method is made.

13.3.2 Bulk powder studies of the mixed M^{III}/M^{IV} oxalates

Later studies on bulk powder properties of M/Nd/U oxalates demonstrated that near quantitative recovery of just the single solid solution of the hexagonal phase $(M)_{2+x}[U_{2-x}Nd_x(C_2O_4)_5] \cdot nH_2O$ was produced when the ratio of metal nitrates in the feed (Nd/(U + Nd)) was between 0% and 50% (Arab-Chapelet et al., 2008). Beyond 50%, a mixture of the mixed oxalate and single $Nd_2(C_2O_4)_3 \cdot 10H_2O$ phases were formed. When Sm is substituted for Nd the situation is more complex. From 0% to 10% Sm there is a mixture of two oxalate phases $U(C_2O_4)_2 \cdot 6H_2O$ and the U^{IV}-Sm^{III} 225 hexagonal mixed oxalate. Between 10% and 30% Sm there is a single hexagonal 225 phase but between 30% and 50% Sm there is a mixture of the hexagonal 225 phase and the tetragonal 112 phase. For 50-70% Sm a single tetragonal 112 phase is formed and at higher Sm levels (70-100%) a mixture of the tetragonal 112 and $Sm_2(C_2O_4)_3 \cdot 10H_2O$ were formed (Arab-Chapelet et al., 2008).

A study into the influence of the monovalent cation has been performed for the 225 family of oxalates using Th^{IV} and Nd^{III} metal ions of the general formula $(M)_{2+x}[Th_{2-x}Nd_x(C_2O_4)_5] \cdot nH_2O$ (M = Li, Na, K, Rb, Cs, NH_4) (Gil-Martin et al., 2012a,b). Variation in the Nd/(Nd + Th) ratio of the feed gave a single phase of the

oxalate between 5% and 50% depending on the cation radius. A small solid-solution window 40-50% Nd/(Nd+Th) was observed for the smallest cation Li^+ while for Cs^+ a solid solution is obtainable for a wide range of 10-50% Nd/(Nd+Th). Above and below these windows mixed phases or single metal oxalate phases were formed. This study also gave confidence that the bulk PXRD patterns were consistent with the single-crystal data for the hexagonal 225 family of mixed oxalates.

Building on the single-crystal characterization work for the mixed Ln^{III}/U^{IV} systems, a number of experiments were performed with varying actinides in the M^{III} and M^{IV} positions. A summary of the crystallographic results are provided in Table 13.1. For a ratio of $An^{III}/(U^{IV}+An^{III})$, close to 10% the mixed oxalate adopts a 225 hexagonal structure regardless of the An^{III} used (Arab-Chapelet et al., 2007). For a 50:50 ratio with M^{IV}:Pu^{III}, the larger Th^{IV} and U^{IV} ions gave the 225 hexagonal $(H_5N_2)_{2+x}[An^{IV}_{2-x}An^{III}_{x}(C_2O_4)_5]\cdot nH_2O$ structure, while the smaller Np^{IV} and Pu^{IV} gave the 112 tetragonal $(H_5N_2)_{1-x}[An^{III}_{1-x}An^{IV}_{x}(C_2O_4)_2\cdot H_2O]\cdot nH_2O$ (Arab-Chapelet et al., 2007). Solid-state UV-visible spectroscopy confirmed that quantitative coprecipitation of the An^{III} and An^{IV} occurred without modification of the initial metal ions ratio or of the oxidation states (Arab-Chapelet et al., 2008).

Extending this study to the incorporation of An^{III} into the U^{IV} 225 structure was performed for americium and curium in shielded hot cells to protect operators from high gamma and neutron radiation doses. Using a 10% $An^{III}/(U^{IV}+An^{III})$ ratio, both americium and curium were successfully incorporated into the hexagonal 225 structure as demonstrated by PXRD analysis (Grandjean et al., 2009).

13.4 Decomposition of coprecipitated oxalates to the oxides

The synthesis of a range of mixed U^{IV}/Pu^{III} oxalate powders containing varying amounts of Pu/(Pu+U) (7-70%Pu) were made by mixing a solution of U^{IV} and Pu^{III} stabilized by hydrazinium nitrate with a concentrated solution of oxalic acid (in a slight molar excess) (Arab-Chapelet et al., 2007; Grandjean et al., 2005, 2009). The powders were all shown by PXRD analysis to be of the 225 hexagonal class of structure $(H_5N_2)_{2+x}[U^{IV}_{2-x}Pu^{III}_{x}(C_2O_4)_5]\cdot nH_2O$ (Arab-Chapelet et al., 2007). There is little information on the decomposition of the mixed oxalates. One report showing the TGA trace during decomposition under argon confirms that the mixed metal oxalate $(H_5N_2)_{2.55}[U^{IV}_{1.45}Pu^{III}_{0.55}(C_2O_4)_5]\cdot nH_2O$ is converted to $U_{0.725}Pu_{0.275}O_2$ (a U/Pu ratio of 2.64:1) at temperatures above 700 °C (Arab-Chapelet et al., 2007). There does not appear to be any steep or sudden losses of material during the TGA run due to $H_5N_2^+$ decomposition, which is to be expected in an argon atmosphere but may be more exothermic in an oxygen atmosphere. There is no discussion on the residual carbon left in the material, which may be considerable under these inert atmosphere conditions.

For this material to be beneficial from a MOx production viewpoint it must be demonstrated that the uranium and plutonium are homogenously mixed in the final oxide. There are a few reports on the characterization of the $(U,Pu)O_2$ samples produced

Table 13.1 A summary of the crystal structure information of relevance to oxalate coprecipitation

Method[a,b]	Molecular formula	M(III)	M(IV)	Cation	No. H_2O	System symmetry	Space group	References
SCXRD	$(NH_4)_2[U_2(C_2O_4)_5]\cdot 0.7H_2O$	–	U	NH_4	0.7	Hexagonal	$P6_3/mmc$	Chapelet-Arab et al. (2005a)
PXRD	$(N_2H_5)_{2.6}[Nd_{0.6}U_{1.4}(C_2O_4)_5]\cdot xH_2O$	Nd	U	N_2H_5	x	Hexagonal	$P6_3/mmc$	Chapelet-Arab et al. (2005a)
PXRD	$(N_2H_5)_{2.6}[Sm_{0.6}U_{1.4}(C_2O_4)_5]\cdot xH_2O$	Sm	U	N_2H_5	x	Hexagonal	$P6_3/mmc$	Chapelet-Arab et al. (2005a)
SCXRD	$Na_{2.56}[Nd_{0.56}U_{1.44}(C_2O_4)_5]\cdot 7.6H_2O$	Nd	U	Na	7.6	Orthorhombic	$Pbcn$	Chapelet-Arab et al. (2005a)
SCXRD	$Na_3[CeU(C_2O_4)_4]\cdot 10.4H_2O$	–	U/Ce	Na	10.4	Monoclinic	$C2/c$	Chapelet-Arab et al. (2005a)
SCXRD	$(N_2H_5)[Nd(C_2O_4)_2]\cdot 4H_2O$	Nd	–	N_2H_5	4	Trigonal	$P-1$	Chapelet-Arab et al. (2005b)
SCXRD	$(N_2H_5)[Gd(C_2O_4)_2]\cdot 4.5H_2O$	Gd	–	N_2H_5	4.5	Trigonal	$P-1$	Chapelet-Arab et al. (2005b)
SCXRD	$(N_2H_5)_{0.75}[Nd_{0.75}U_{0.25}(C_2O_4)_2]\cdot 4.5H_2O$	Nd	U	N_2H_5	4.5	Trigonal	$P-1$	Chapelet-Arab et al. (2005b)
SCXRD	$(N_2H_5)_{0.75}[Gd_{0.75}U_{0.25}(C_2O_4)_2]\cdot 4H_2O$	Gd	U	N_2H_5	4	Trigonal	$P-1$	Chapelet-Arab et al. (2005b)
SCXRD	$(N_2H_5)_{0.65}[Nd_{0.65}U_{0.35}(C_2O_4)_2]\cdot 3H_2O$	Nd	U	Na	3	Trigonal	$P-1$	Chapelet-Arab et al. (2005b)
SCXRD	$(N_2H_5)_{0.65}[Gd_{0.65}U_{0.35}(C_2O_4)_2]\cdot 4H_2O$	Gd	U	Na	4.5	Trigonal	$P-1$	Chapelet-Arab et al. (2005b)
SCXRD	$Na[Y(C_2O_4)_2(H_2O)]\cdot 3H_2O$	Y	–	Na	4	Monoclinic	Pc	Chapelet-Arab et al. (2006)

Continued

Table 13.1 Continued

Method	Molecular formula	M(III)	M(IV)	Cation	No. H_2O	System symmetry	Space group	References
SCXRD	$(NH_4)_{0.53}[Y_{0.53}U_{0.47}(C_2O_4)_2(H_2O)]\cdot 3.47H_2O$	Y	U	NH_4	3.47	Tetragonal	*P*4/*n*	Chapelet-Arab et al. (2006)
SCXRD	$(NH_4)_{0.58}[Pr_{0.58}U_{0.42}(C_2O_4)_2(H_2O)]$ $3.42H_2O$	Pr	U	NH_4	3.42	Tetragonal	*P*4/*n*	Chapelet-Arab et al. (2006)
SCXRD	$(NH_4)_{0.40}[Nd_{0.40}U_{0.60}(C_2O_4)_2(H_2O)]\cdot 3.60H_2O$	Nd	U	NH_4	3.6	Tetragonal	*P*4/*n*	Chapelet-Arab et al. (2006)
SCXRD	$(NH_4)_{0.45}[Sm_{0.45}U_{0.55}(C_2O_4)_2(H_2O)]$ $3.55H_2O$	Sm	U	NH_4	3.55	Tetragonal	*P*4/*n*	Chapelet-Arab et al. (2006)
SCXRD	$(NH_4)_{0.75}[Gd_{0.75}U_{0.25}(C_2O_4)_2(H_2O)]\cdot 3.25H_2O$	Gd	U	NH_4	3.25	Tetragonal	*P*4/*n*	Chapelet-Arab et al. (2006)
SCXRD	$(NH_4)_{0.48}[Tb_{0.48}U_{0.52}(C_2O_4)_2(H_2O)]\cdot 3.52H_2O$	Tb	U	NH_4	3.52	Tetragonal	*P*4/*n*	Chapelet-Arab et al. (2006)
SCXRD	$(NH_4)_{0.50}[Pu_{0.50}U_{0.50}(C_2O_4)_2(H_2O)]\cdot xH_2O$	Pu	U	NH_4	x	Tetragonal	*P*4/*n*	Tamain et al. (2013)
SCXRD	$(NH_4)_{2.7}[Pu_{0.7}U_{1.3}(C_2O_4)_5]\cdot xH_2O$	Pu	U	NH_4	x	Hexagonal	*P*6/*mmm*	Tamain et al. (2013)
PXRD	$(N_2H_5)_{2.5}[Pu_{0.5}Th_{0.5}(C_2O_4)_5]\cdot xH_2O$	Pu	Th	"N_2H_5"	~4	Hexagonal	"*P*6/*mmm*"	Arab-Chapelet et al. (2008)

Continued

Table 13.1 **Continued**

Method[a]	Molecular formula	M(III)	M(IV)	Cation	No. H_2O	System symmetry	Space group	References
PXRD	$(N_2H_5)_{2.5}[Pu_{0.5}U_{0.5}(C_2O_4)_5]\cdot xH_2O$	Pu	U	"N_2H_5"	~4	Hexagonal	"*P6/mmm*"	Arab-Chapelet et al. (2008)
PXRD	$(N_2H_5)_{2.5}[Am_{0.5}U_{0.5}(C_2O_4)_5]\cdot xH_2O$	Am	U	"N_2H_5"	~4	Hexagonal	"*P6/mmm*"	Arab-Chapelet et al. (2008)
PXRD	$(N_2H_5)_{0.5}[Pu_{0.5}Np_{0.5}(C_2O_4)_2(H_2O)]\cdot xH_2O$	Pu	Np	"N_2H_5"	~4	Tetragonal	"*P4/n*"	Arab-Chapelet et al. (2008)
PXRD	$(N_2H_5)_{0.5}[Pu_{0.5}Pu_{0.5}(C_2O_4)_2(H_2O)]\cdot xH_2O$	Pu	Pu	"N_2H_5"	~4	Tetragonal	"*P4/n*"	Arab-Chapelet et al. (2008)
PXRD	$(N_2H_5)_{2.5}[Cm_{0.1}U_{0.9}(C_2O_4)_5]\cdot xH_2O$	Cm	U	"N_2H_5"	~4	Hexagonal	"*P6/mmm*"	Grandjean et al. (2009)
PXRD	$(N_2H_5)_{2.5}[Am_{0.1}U_{0.9}(C_2O_4)_5]\cdot xH_2O$	Am	U	"N_2H_5"	~4	Hexagonal	"*P6/mmm*"	Grandjean et al. (2009)

[a]Powder X-ray diffractometry.
[b]Single-crystal X-ray diffractometry.

from coprecipitation of the metal oxalates. A PXRD and X-ray absorption spectroscopy study were used to examine the bulk and localized structure respectively of $(U_{1-y},Pu_y)O_2$ ($y = 0.07$-0.5) (Martin et al., 2007). The lattice parameter (a) was used to demonstrate a solid solution by showing a linear change in a with variation in y according to Vegard's law. Indeed, a linear correlation was observed, although later studies (Grandjean et al., 2009) showed a deviation from linearity once the value of y exceeded 0.5, with the formation of a biphasic mixed oxide. To assess the local structure XANES and EXAFS were used. Initial results suggested some discrepancies for samples with $y < 0.5$ that were attributed to a disordered hyperstoichiometric structure $(U_{1-y},Pu_y)O_{2+x}$ (Martin et al., 2007). Later repeat studies demonstrated that by careful production of the samples, calcined at 900 °C in flowing argon, no hyperstoichiometric structure was observed and the material was deemed to be a true ideal solid solution of $(U_{1-y},Pu_y)O_2$ (Grandjean et al., 2009).

Other mixed oxalates have been successfully converted to oxides for the hexagonal 225 class of compounds with U^{IV}/Am^{III} and U^{IV}/Cm^{III} in $(H_5N_2)_{2+x}[U^{IV}_{2-x}An^{III}_x(C_2O_4)_5]\cdot nH_2O$, where $x = 0.1$ (Grandjean et al., 2009). The oxides have the expected fcc pattern for $UCmO_2$ and $UAmO_2$. There are no significant changes in morphology upon conversion, although the particles illustrated appear quite amorphous possibly as a result of self-irradiation.

13.5 Developments in the application of the coprecipitation process

One of the main applications for the oxalate coprecipitation process is the pivotal role played in the COEX™ process, which is an evolutionary change to the traditional PUREX process used for the reprocessing of spent nuclear fuel (Bordier et al.,

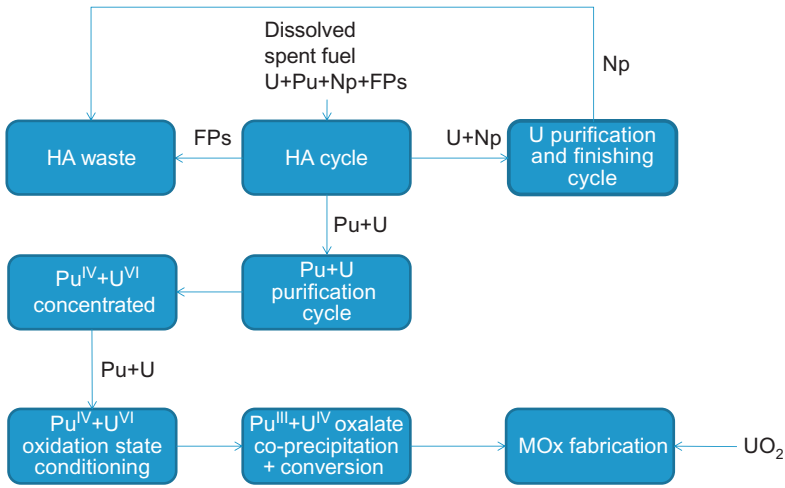

Figure 13.9 Overview of the COEX™ process (Drain et al., 2008).

2008). The COEX™ process is developed to avoid the separation of pure plutonium during any step of the reprocessing and recycling process and to avoid the storage of large quantities of solid plutonium oxide (Figure 13.9). Rather than completely separating the uranium and plutonium into individual product streams, some of the uranium is allowed to follow the plutonium through to the oxalate precipitation finishing process.

One potential problem with this process is the reduction of uranium and plutonium to the U^{IV} and Pu^{III} oxidation states. The current solution to this problem is to add U^{IV} to the process from an external source (Drain et al., 2008). Such a source of U^{IV} is currently supplied to both the oxide reprocessing plants at Sellafield and La Hague by the catalytic reduction of U^{VI} by H_2. A by-product from this strategy is the presence of U^{VI} that needs to be separated from the U^{IV} and Pu^{III} mix during coprecipitation (Drain et al., 2008). Possibly a more elegant and proliferation resistant method would be to convert the U^{VI} and Pu^{IV} to U^{IV} and Pu^{III} *in situ* by chemical or electrochemical reduction methods.

The COEX™ process takes advantage of the 225 class of mixed oxalates to produce a master blend that is combined with UO_2 to make the composition of choice and results in a homogeneous pellet with uranium and plutonium mixed at the molecular level. Another possible disadvantage that has been touched on is the hexagonal particle morphologies that derived from the 225 class of mixed oxalates, which may require additional milling to achieve consistent results. A move to the 112 tetragonal platelet particles could provide advantages in this area.

Another topic not discussed in the literature that may or may not be problematic is the removal of any residual carbon from the final oxide produced under an inert atmosphere and whether this presents difficulties in achieving high-density pellets.

Other areas where developments are taking place include novel oxalate precipitation methods to cope with potentially higher (at least double) throughputs of material within a COEX™ plant in a criticality safe manner. For example, the use of pulsed columns is being considered for the precipitation of metal oxalates that form emulsions in a recirculating inert organic phase (hydrogenated tetra propylene). The metal nitrate and oxalic acid are fed into the column at different stages and when the aqueous droplets meet then the precipitation reaction takes place. The precipitate falls to the bottom of the column under gravity to a separated aqueous phase (below where the pulse is applied), which is circulated to a decanting/filtering system. Process modeling from the drop-scale to bulk-process scale has also been reported (Chartona et al., 2013; Borda et al., 2011; Lalleman et al., 2012).

A very encouraging recent development has seen the utilization of the 225 hexagonal material $(H_5N_2)_{2+x}[U^{IV}_{2-x}Am^{III}_x(C_2O_4)_5]\cdot nH_2O$ in a much simplified pelleting process for the creation of americium-bearing blanket fuels for transmutation targets (Kumar et al., 2011). Previous methods used a dry powder mixing process named uranium MAs conventional sintering (UMACS) developed by CEA and AREVA NC (Magesvaran et al., 2012; Horlait et al., 2013; Kulyako et al., 2011; Grate et al., 2011; Claparede et al., 2011; Reboul et al., 2011; Sivakumar et al., 2012a,b) that is designed to carefully control the oxygen potential of the atmosphere during heat treatment processes and avoid undue americium volatilization. For the more common reactive sintering methods employed for UO_2 or MOx fuel, reducing conditions are

acceptable but generally produce low-density material <92% TD (theoretical density) when americium is present. Unfortunately, if the temperature is high enough and the conditions reducing enough (to avoid UO_2 oxidation) it is possible to reduce the americium to the metal form, which has a high vapor pressure under normal sintering conditions (Ohmura et al., 2011).

The UMACS process can achieve high TDs (>94%) by using a two-stage heating process. UO_2 and AmO_2 powders are mixed and pelletized to give a green pellet of ~49% TD that is then sintered under a controlled atmosphere to provide a solid solution of $U_{1-x}Am_xO_{2\pm\delta}$ at a temperature of 1873 K and an oxygen potential of $-414\ kJ\ mol^{-1}$. These conditions are sufficient to avoid significant volatilization of americium (Kulyako et al., 2011) but are not sufficient to obtain high-density pellets. The pellets are then ground to a fine reactive powder and pelletized again before a second heat treatment reaching higher sintering temperatures, resulting in pellets of the desired high (>94% TD) density (Kulyako et al., 2011) (Figure 13.10). It is because at the second stage of heating the solid solution retards the volatility of americium

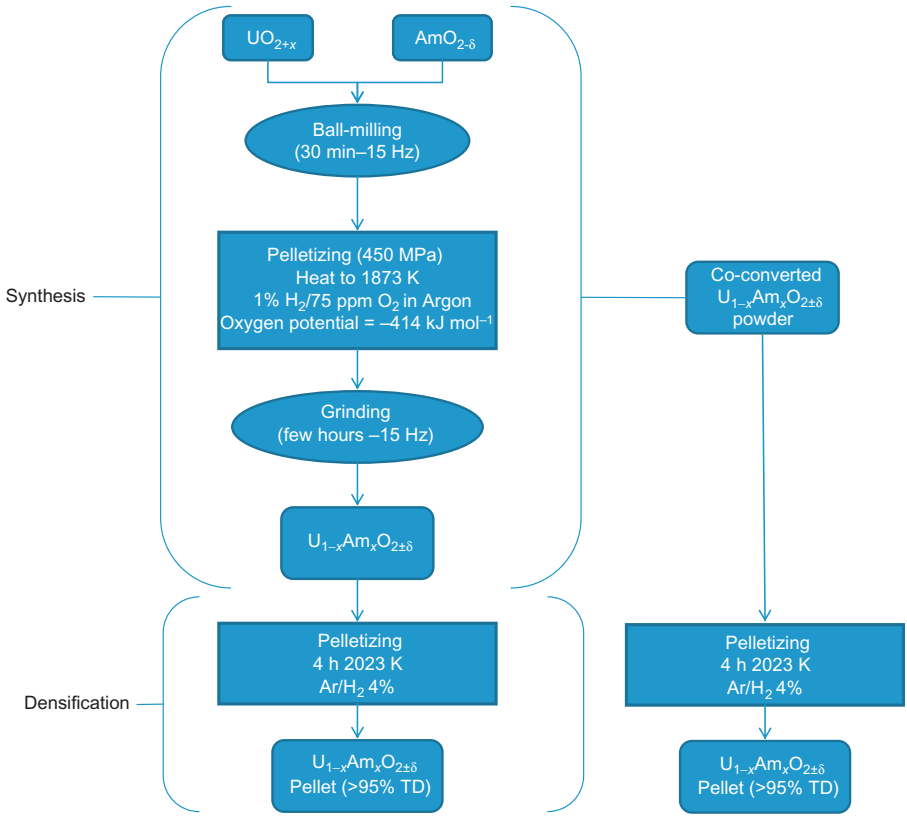

Figure 13.10 Process for making americium-bearing blanket fuels by (left) the UMACS process and (right) powder generated from coprecipitation.

and this allows higher temperatures to be achieved safely. Unfortunately, the long grinding stage can potentially produce large amounts of undesirable radioactive dusts.

Dual benefits of control of the particle morphology and homogeneous mixing of americium and uranium at the molecular level are realized by simple mixing of respective metal nitrate solutions followed by calcining the mixed oxalate precursor to the mixed oxide. A solid solution of $U_{1-x}Am_xO_{2\pm\delta}$ can thus be obtained (Figure 13.10). Dense pellets of >95% TD were produced with a homogeneous composition and microstructure, and limited residual porosity. Residual carbon from the calcinations of the oxalate precursor (~2700 ppm) did not appear to be an issue with a final carbon content of ~400 ppm in the densified pellet. It was also noted that the sintering temperature was 100 K lower than that used in the UMACS process because of the higher reactivity of the coconverted powders (Kumar et al., 2011).

This much simpler process has the potential to open the door to americium transmutation in fast reactor systems reducing the heat load and, therefore, the overall volumes of geological waste repositories.

13.6 Summary

The use of oxalate chemistry to produce a homogeneous mixed metal actinide oxide suitable for fabrication into pellets for new nuclear fuel or partitioning and transmutation (P&T) targets is demonstrated at the laboratory scale. The two- and three-dimensional structures of the 225 and 112 class of mixed oxalates are capable of accommodating both An^{III} and An^{IV} ions into the crystal lattice sites distributing the metals homogeneously through the material. A desired An^{III}:An^{IV} ratio can easily be achieved by mixing the two metal nitrates in the appropriate ratios. Thermal decomposition of the materials in an inert atmosphere can provide the mixed metal oxides needed for pelletizing. While limited information is as yet available regarding the applications to traditional (U+Pu) MOx as part of the COEX™ process or MA-bearing MOx fuel for P&T, the oxalate coprecipitation strategy has already been proven beneficial for MA-bearing (Am+U) blanket fuel targets.

Future considerations for oxalate coprecipitation may include the following:

- Assessing whether the $(H_5N_2)_{2+x}[U^{IV}_{2-x}Pu^{III}_x(C_2O_4)_5]\cdot nH_2O$ 225 hexagonal particle morphology is acceptable for direct MOx production without the need for milling, or whether there are sufficient benefits in accessing the $(NH_4)_{0.5}[Pu_{0.5}U_{0.5}(C_2O_4)_2(H_2O)]\cdot nH_2O$ 112 tetragonal structures with platelet morphology.
- Understanding if the potential hazards of decomposing metal oxalates containing the hydrazinium cation can be controlled through process design or if a suitable alternative cation (e.g., ammonium ion) can be substituted.
- Understanding the effects of residual carbon on the final pellet quality.
- Oxidation state control of U^{IV} within the COEX™ process without using an external source of U^{IV}.
- Implementing an industrial-scale precipitation process that can deal with the higher throughputs required for the COEX™ process while maintaining criticality safety margins.

References

Almeida, L.D., Grandjean, S., Vigier, N., Patisson, F., 2012. Insights into the thermal decomposition of lanthanide(III) and actinide(III) oxalates—from neodymium and cerium to plutonium. Eur. J. Inorg. Chem. 2012, 4986–4999.

Alwin, J.L., Coriz, F., Danis, J.A., Bluhm, B.K., Wayne, D.W., Gray, D.W., Ramsey, K.B., Costa, D.A., Bluhm, E.A., Nixon, A.E., 2007. Plutonium oxide polishing for MOX fuel fabrication. J. Alloys Compd. 444-445, 565–568.

Arab-Chapelet, B., Grandjean, S., Nowogrocki, G., Abraham, F., 2007. Synthesis of new mixed actinides oxalates as precursors of actinides oxide solid solutions. J. Alloys Compd. 444, 387–390.

Arab-Chapelet, B., Grandjean, S., Nowogrocki, G., Abraham, F., 2008. Synthesis and characterization of mixed An(IV)An(III) oxalates (An(IV) = Th, Np, U or Pu and An(III) = Pu or Am). J. Nucl. Mater. 373 (1-3), 259–268.

Bataille, T., Louër, D., 1999. Yttrium sodium oxalate tetrahydrate, $[Y(H_2O)]Na(C_2O_4)_2 \cdot 3H_2O$. Acta Crystallogr. C 55, 1760–1762.

Bataille, T., Louër, M., Auffrédic, J.-P., Louër, D., 2000. Crystal structure and thermal behavior of $La(H_2O)_2M(C_2O_4)_2 \cdot H_2O$ (M_5K, NH_4) studied by powder X-ray diffraction. J. Solid State Chem. 150, 81–95.

Baxter, N.W., 1995. BNFL report.

Bertrand, M., Plasari, E., Lebaigue, O., Baron, P., Lamarque, N., Ducros, F., 2012. Hybrid LES multi-zonal modelling of the uranium oxalate precipitation. Chem. Eng. Sci. 77, 95–104.

Bertrand-Andrieu, M., Plasari, E., Baron, P., 2004. Determination of nucleation and crystal growth kinetics in hostile environment—application to the tetravalent uranium oxalate $U(C_2O_4)_2 \cdot 6H_2O$. Can. J. Chem. Eng. 82, 930.

Bluhm, E.A., Abney, K.D., Balkey, S., Brock, J.C., Coriz, F., Dyke, J., Garcia, D.J., Griego, B., Martinez, B.T., Martinez, D., Martinez, J.R., 2005. Plutonium oxide polishing for MOX fuel production. Separ. Sci. Technol. 40, 281–296.

Borda, G., Brackx, E., Boisset, L., Duhamet, J., Ode, D., 2011. Use of a pulsed column contactor as a continuous oxalate precipitation reactor. Nucl. Eng. Des. 241, 809–814.

Bordier, G., Warin, D., Masson, M., 2008. The Atalante facility at CEA/Marcoule: towards GenIV systems fuel cycle. In: Atalante, Montpellier, France.

Burney, G.A., Smith, P.K., 1984. Controlled PuO_2 Particle Size from Pu(III) Oxalate Precipitation. E. I. du Pont de Nemours & Co., Aiken.

Caldwell, C.S., 1961. Development of Plutonium Bearing Fuel Materials. Nuclear Materials and Equipment Corporation.

Chadha, A.K., Mudher, K.D.S., Krishnan, I.L., Jayadevan, N.C., 1991. X-ray and thermal studies on $KLnU(C_2O_4)_4 \cdot 8H_2O$ (Ln = La, Ce, Pr, Nd and Tb). Thermochim. Acta 191, 323–331.

Chapelet-Arab, B., Nowogrocki, G., Abraham, F., Grandjean, S., 2005a. U(IV)/Ln(III) unexpected mixed site in polymetallic oxalato complexes. Part I. Substitution of Ln(III) for U(IV) from the new oxalate $(NH_4)_2[U_2(C_2O_4)_5 \cdot 0.7H_2O]$. J. Solid State Chem. 178 (10), 3046–3054.

Chapelet-Arab, B., Nowogrocki, G., Abraham, F., Grandjean, S., 2005b. U(IV)/Ln(III) unexpected mixed in polymetallic oxalato complexes. Part II. Substitution of U(IV) for Ln(III) in the new oxalates $(N_2H_5)[Ln(C_2O_4)_2 \cdot nH_2O]$ (Ln = Nd, Gd). J. Solid State Chem. 178 (10), 3055–3065.

Chapelet-Arab, B., Duvieubourg, L., Nowogrocki, G., Abraham, F., Grandjean, S., 2006. U(IV)/Ln(III) mixed site in polymetallic oxalato complexes. Part III: structure of

Na[Yb(C_2O_4)$_2$(H_2O)]·3H_2O and the derived quadratic series (NH_4)$_{1-x}$[Ln_{1-x} U_x(C_2O_4)$_2$(H_2O)]·3+$x$$H_2O$, Ln = Y, Pr-Sm, Gd, Tb. J. Solid State Chem. 179 (12), 4029–4036.

Chartona, S., Kacema, A., Amokranea, A., Borda, G., Puel, F., Klein, J.-P., 2013. Actinides oxalate precipitation in emulsion modeling: from the drop scale to the industrial process. Chem. Eng. Res. Des. 91, 660–669.

Cina, B., 1963. Some decomposition effects in PuO_2 on sintering. J. Nucl. Mater. 9, 85.

Claparede, L., Clavier, N., Dacheux, N., Moisy, P., Podor, R., Ravaux, J., 2011. Influence of crystallization state and microstructure on the chemical durability of cerium-neodymium mixed oxides. Inorg. Chem. 50 (18), 9059–9072.

Crowder, M.L., Pierce, R.A., Scogin, J.H., Daniel, W.E., King, W.D., 2012. Small-Scale Testing of Plutonium(IV) Oxalate Precipitation and Calcination to Plutonium Oxide to Support the MO_X Feed Mission. Savannah River National Laboratory, Aiken.

Daniel, W.E., 2012. Literature Review of PuO_2 Calcination Time and Temperature Data for Specific Surface Area. Savannah River National Laboratory, Aiken.

Dias, R.M.A., Chackraburtty, D.M., 1971. Evaluation of crystallinity and surface area measurements of plutonium dioxide samples. J. Appl. Crystallogr. 4, 74–75.

Drain, F., Emin, J.L., Vinoche, R., Baron, P., 2008. COEX^{TM} process: cross breading between innovation and industrial experience. In: Waste Management Conference Proceedings.

Duvieubourg-Garea, L., Vigier, N., Abraham, F., Grandjean, S., 2008. Adaptable coordination of U(IV) in the 2D-(4,4) uranium oxalate network: from 8 to 10 coordinations in the uranium (IV) oxalate hydrates. J. Solid State Chem. 181 (8), 1899–1908.

Dvoeglazov, K.N., Marchenko, V.I., Koltunov, V.S., 2005. Oxidation of U(IV) in HNO_3 solutions containing urea and Tc(VII). Radiochemistry 47, 61.

Francis, K.E., Sowden, R.G., 1959. BNFL report.

Gelman, A.D., Moskvin, A.I., 1958. An investigation of oxalate and carbonate complexes of plutonium(IV) in water solutions by the solubility method. Dokl. Akad. Nauk SSSR 118 (3), 493–496.

German, R.M., Munir, Z.A., 1979. Surface area reduction during isothermal sintering. J. Am. Ceram. Soc. 59, 379.

Gil-Martin, A., Arab-Chapelet, B., Rivenet, M., Grandjean, S., Abraham, F., 2012a. Influence of the monovalent M cation on the M^{2+x}[$Th_{2-x}Nd_x$(C_2O_4)$_5$]·$n$$H_2O$ solid solution domain. In: Poinssot, C. (Ed.), Atalante 2012 International Conference on Nuclear Chemistry for Sustainable Fuel Cycles, pp. 33–38.

Gil-Martin, A., Arab-Chapelet, B., Rivenet, M., Grandjean, S., Abraham, F., 2012b. Influence of the monovalent M cation on the M^{2+x}[$Th_{2-x}Nd_x$(C_2O_4)$_5$]·$n$$H_2O$ solid solution domain. Proc. Chem. 7, 33.

Glasner, A., 1964. Remarks on the thermal decomposition of plutonium(IV) oxalates. J. Inorg. Nucl. Chem. 26 (8), 1475–1476.

Grandjean, S., Beres, A., Rousselle, J., Maillard, C., 2005. Vol. World Patent WO 2005/119699.

Grandjean, S., Arab-Chapelet, B., Robisson, A.C., Abraham, F., Martin, P., Dancausse, J.P., Herlet, N., Leorier, C., 2009. Structure of mixed U(IV)-An(III) precursors synthesized by co-conversion methods (where An = Pu, Am or Cm). J. Nucl. Mater. 385 (1), 204–207.

Grate, J.W., O'Hara, M.J., Farawila, A.F., Douglas, M., Haney, M.M., Petersen, S.L., Maiti, T. C., Aardahl, C.L., 2011. Extraction chromatographic methods in the sample preparation sequence for thermal ionization mass spectrometric analysis of plutonium isotopes. Anal. Chem. 83 (23), 9086–9091.

Greinetz, R.M., Neal, D.H., 1980. Plutonium(III) Oxalate Precipitation and Calcination Process for Plutonium Nitrate to Oxide Conversion. Rockwell International, Energy Systems Group.

Hansson, E., 1970. Structural studies on the rare earth carboxylates 5. The crystal and molecular structure of neodymium (iii) oxalate 10.5-hydrate. Acta Chem. Scand. 24, 2969.
Harmon, K.M., Reas, W.H., 1957. Conversion chemistry of plutonium nitrate. In: Symposium on the Reprocessing of Irradiated Fuels; Brussels, Belgium, p. 332.
Haschke, J.M., Ricketts, T.E., 1995a. Plutonium Dioxide Storage: Conditions for Preparation and Handling. Los Alamos National Laboratory, New Mexico.
Haschke, J.M., Ricketts, T.E., 1995b. PuO_2 Storage: Conditions for Preparation and Handling. Los Alamos National Laboratory.
Haschke, J.M., Ricketts, T.E., 1997. Adsorption of water on plutonium dioxide. J. Alloys Compd. 252, 148.
Haschke, J.M., Venetz, T., Szempruch, R., McCZard, J.W., 1997. White Paper on Possible Inclusion of Mixed Plutonium-Uranium Oxides in DOE-STD-3013-96. Los Alamos National Laboratory.
Hayashi, H., Hagiya, H., Kim, S.-Y., Morita, Y., Akabori, M., Minato, K., 2013. Separation and recovery of Cm from Cm-Pu mixed oxide samples containing Am impurity. J. Radioanal. Nucl. Chem. 296 (3), 1275–1286.
Horlait, D., Lebreton, F., Delahaye, T., Blanchart, P., 2013. Dilatometric study of $U_{1-x}Am_xO_{2+/-\delta}$ sintering: determination of activation energy. J. Am. Ceram. Soc. 96 (11), 3410–3416.
Hustad, J.E., Sonju, O.K., 1988. Experimental studies of lower flammability limits of gases and mixtures of gases at elevated temperatures. Combust. Flame 71, 283.
Jenkins, I.L., Waterman, M.J., 1964. The thermal decomposition of hydrated plutonium(IV) oxalates. J. Inorg. Nucl. Chem. 26 (1), 131–137.
Jenkins, I.L., Moore, F.H., Waterman, M.J., 1965a. X-ray powder crystallographic data on plutonium and their oxalates. 2. Plutonium(4) oxalate dihydrate uranium(4) oxalate hexahydrate, uranium(4) oxalate dihydrate and thorium oxalate dihydrate. J. Inorg. Nucl. Chem. 27 (1), 81.
Jenkins, I.L., Moore, F.H., Waterman, M.J., 1965b. X-ray powder crystallographic data on plutonium and other oxalates—I: the oxalates of plutonium(III) and plutonium(VI) and their isomorphs. J. Inorg. Nucl. Chem. 27 (1), 77–80.
Jurgensen, A.R., Missimer, D.M., Rutherford, R.L., 2003. Surface Area (BET) and TGA-MS Analysis of Calcined Neptunium Oxide (U). Westinghouse Savannah River Company, Aiken.
Kahlweit, M., 1975. Ostwald ripening of precipitates. Adv. Colloid Interf. Sci. 5, 1.
Kalinina, I.V., Guschin, A.L., Samsonenko, D.G., Gerasimenko, A.V., Sokolov, M.N., Fredin, V.P., 2003. Hexaaquatrioxalatodierbium(III) tetrahydrate: $[\{Er(H_2O)_3\}_2(C_2O_4)_3]\cdot 4H_2O$. Acta Crystallogr. E 59, 784.
Karelin, A.I., Krot, N.N., Kozlova, R.D., Lobas, V.A., Matukha, V.A., 1990. Thermal decomposition of Np(IV) and Pu(III, IV) oxalates. J. Radioanal. Nucl. Chem. 143, 241–252.
Kartushova, R.E., Rudenko, T.I., Fomin, V.V., 1957. Thermal decomposition of tetravalent and trivalent plutonium oxalates. Soviet J. Atom. Energy 5, 831–835.
Koltunov, V.S., 1974. Kinetika reaktsii aktinoidov (Kinetics of Actinide Reactions). Atomizdat, Moscow, p. 58.
Kozlova, R.D., Karelin, A.I., Lobas, O.P., Matyukha, V.A., 1984. Thermal decomposition of plutonium(IV) oxalate. Sov. Radiochem. 26 (2), 165–171.
Kulyako, Y.M., Trofimov, T.I., Il'in, E.G., Myasoedov, B.F., 2011. New approaches to processing and fabrication of oxide nuclear fuels. Russ. J. Gen. Chem. 81 (9), 1960–1965.
Kumar, R., Yadav, J.R., Rao, D.D., 2011. Separation and determination of Am-241 in urine samples from radiation workers using PC88-A and alpha spectrometry. J. Radioanal. Nucl. Chem. 289 (2), 451–454.

Lalleman, S., Bertrand, M., Gaillard, J.-P., Plasari, E., 2012. Scale-up study of agglomeration during oxalic precipitation in nuclear industry. Proc. Chem. 7, 493–498.

Livingston, R.P., Duffey, J.M., 2001. Effects of Plutonium Dioxide Moisture Content and Calcination Temperature on the Headspace Gas Composition of Sealed Containers. Westinghouse Savannah River Company, Aiken.

Machuron-Mandard, X., Madic, C., 1996. Plutonium dioxide particle properties as a function of calcination temperature. J. Alloys Compd. 235 (2), 216–224.

Magesvaran, P., Kumar, K.S., Kumar, T., Gayen, J.K., Shreekumar, B., Dey, P.K., 2012. Direct spectrophotometric analysis of low level Pu(III) in Pu(IV) nitrate of Pu precipitation process feed solution. J. Radioanal. Nucl. Chem. 294 (2), 329–331.

Marshall, A., Holburt, G.A., Shoebottom, A.S., 1976. BNFL report.

Martin, P., Grandjean, S., Valot, C., Carlot, G., Ripert, M., Blanc, P., Hennig, C., 2007. XAS study of $(U_{1-y}Pu_y)O_2$ solid solutions. J. Alloys Compd. 444, 410–414.

Michaelides, A., Skoulika, S., Aubry, A., 1988. Crystal growth and structure of $La_2(C_2O_4)_3$ $9.5H_2O$. Mater. Res. Bull. 23, 579.

Moseley, J.D., Wing, R.O., 1965. Properties of plutonium dioxide. Rocky Flats.

Mudher, K.D.S., Krishnan, K., Chadha, A.K., Venugopal, V., 1997. Thermal and X-ray studies on mixed metal oxalates—$(NH_4)LnIIIUIV(C_2O_4)_4 \cdot 8H_2O$ (Ln = La, Ce, Pr, Nd Tb). Thermochim. Acta 297 (1–2), 169–175.

Myers, W.K., Ruggiero, C.E., Reilly, S.D., Neu, M.P., 2003. Evaluation of ovotransferrin-matrix metal-affinity metalloprotein chromatography for Pu(IV) separations. Radiochim. Acta 91 (12), 697–704.

Nicholson, D., 1965. Variation of surface area during the thermal decomposition of solids. Trans. Faraday Soc. 61, 990.

Nissen, D.A., 1980. The thermal decomposition of plutonium(IV) oxalate hexahydrate. J. Therm. Anal. 18 (1), 99–109.

Ohmura, H., Mizuguchi, K., Kanamura, S., Ohsato, T., Fujita, R., Omori, T., Utsunomiya, K., 2011. Development of hybrid reprocessing technology based on solvent extraction and pyro-chemical electrolysis. Prog. Nucl. Energy 53 (7), 940–943.

Ollendorff, W., Weige, F., 1969. The crystal structure of some lanthanide oxalate decahydrates, $Ln_2(C_2O_4)_3 \cdot 10H_2O$, with Ln = La, Ce, Pr, and Nd. Inorg. Nucl. Chem. Lett. 5, 263.

Orr, R.M., Sims, H.E., Taylor, R.J., submitted. A review of plutonium oxalate decomposition reactions and effects of temperature on surface area of plutonium dioxide. J. Nucl. Mater.

Oudinet, G., Munoz-Viallard, I., Aufore, L., Gotta, M.-J., Becker, J.M., Chiarelli, G., Castelli, R., 2008. Characterization of plutonium distribution in MIMAS MOX by image analysis. J. Nucl. Mater. 375, 86–94.

Puechl, K.H., 1962. Development of Plutonium-Bearing Fuel Materials. Nuclear Materials and Equipment Corporation.

Puechl, K.H., 1963. Development of Plutonium-Bearing Fuel Materials. Nuclear Materials and Equipment Corporation.

Puechl, K.H., 1964. Development of Plutonium-Bearing Fuel Materials. Nuclear Materials and Equipment Corporation.

Puechl, K.H., Garber, N.M.J., 1961. Development of Plutonium-Bearing Fuel Materials. Nuclear Materials and Equipment Corporation.

Randolph, A.D., Larson, M.A., 1988. Theory of Particulate Processes, second ed. Academic Press, New York.

Rao, G.S., Subramanian, M.S., Welch, G.A., 1963. Thermal decomposition of plutonium oxalates. J. Inorg. Nucl. Chem. 25 (10), 1293–1295.

Reboul, S.H., Best, D.R., Stone, M.E., Click, D.R., 2011. Partitioning of gadolinium in the chemical processing cell (CPC) of the Defense Waste Processing Facility (DWPF). In: Abstracts of Papers of the American Chemical Society, vol. 242.

Runde, W., Brodnax, L.F., Goff, G., Bean, A.C., Scott, B.L., 2009. Directed synthesis of crystalline plutonium(III) and (IV) oxalates: accessing redox-controlled separations in acidic solutions. Inorg. Chem. 48 (13), 5967–5972.

Sali, S.K., Noronha, D.M., Mhatre, H.R., Mahajan, M.A., Chander, K., Aggarwal, S.K., Venugopal, V., 2005. A novel methodology for processing of plutonium-bearing waste as ammonium plutonium(III)-oxalate. Nucl. Technol. 151 (3), 289–296.

Salvatores, M., Palmiotti, G., 2011. Radioactive waste partitioning and transmutation within advanced fuel cycles: achievements and challenges. Prog. Part. Nucl. Phys. 66, 144–166.

Sivakumar, P., Meenakshi, S., Rao, R.V.S., 2012a. Partitioning of plutonium and uranium in aqueous medium using hydroxyurea as reducing agent. J. Radioanal. Nucl. Chem. 292 (2), 603–608.

Sivakumar, P., Meenakshi, S., Rao, R.V.S., 2012b. Purification and recovery of plutonium from uranium oxide obtained in the fast reactor fuel reprocessing plant using hydroxyurea as reductant. J. Radioanal. Nucl. Chem. 291 (3), 763–767.

Smith, P.K., Burney, G.A., Rankin, D.T., Bickford, D.F., Sisson, J.R.D., 1976. Effect of Oxalate Precipitation on PuO_2 Microstructures. Savannah River Laboratory, Aiken.

Somers, J., 2011. Minor actinide bearing fuels: fabrication and irradiation experience in Europe. Energy Proc. 7, 169–176.

SRNL, 1973. Savannah River Laboratory monthly report, ^{238}Pu fuel form processes.

SRNL, 1975. Savannah River Laboratory monthly report: Pu-238 fuel form process, DuPont.

Stakebake, J.L., Robinson, H.N., 1983. Effects of water vapor on the surface chemistry of calcined plutonium peroxide as determined by nitrogen adsorption. J. Colloid Interface Sci. 95, 37.

Subramanian, K., Subramanian, M.V., 2012. Development of radio analytical method for in-vitro monitoring of Pu in urine matrix. Desalin. Water Treat. 38 (1-3), 121–125.

Subramanian, M.S., Singh, R.N., Sharma, H.D., 1963. Thermal decomposition of plutonium oxalates. J. Inorg. Nucl. Chem. 25, 1293.

Sukumar, S., Sharma, P.K., Govindan, P., Rao, R.V.S., 2013. Purification of uranium product from plutonium contamination using acetohydroxamic acid (AHA) based process. J. Radioanal. Nucl. Chem. 295 (1), 191–196.

Tamain, C., Arab-Chapelet, B., Rivenet, M., Abraham, F., Grandjean, S., 2012. Single crystal synthesis methods dedicated to structural investigations of very low solubility mixed-actinide oxalate coordination polymers. Cryst. Growth Des. 12 (11), 5447–5455.

Tamain, C., Chapelet, B.A., Rivenet, M., Abraham, F., Caraballo, R., Grandjean, S., 2013. Crystal growth and first crystallographic characterization of mixed uranium(IV)-plutonium(III) oxalates. Inorg. Chem. 52 (9), 4941–4949.

Trombe, J.-C., Jaud, J., 2003. SCXRD of $Nd_2(C_2O_4)_3 \cdot 10H_2O$. J. Chem. Crystallogr. 33, 19.

Trombe, J.-C., Thomas, P., Brouca-Cabarrecq, C., 2001. Synthesis, crystal structure of Gd $(H_2O)(C_2O_4)_2 \cdot NH_4$ and of $La(C_2O_4)_2 \cdot NH_4$. Characterization of the $Ln(H_2O)(C_2O_4)_2 \cdot NH_4$ (with Ln-Eu-Yb). Solid State Sci. 3, 309–319.

Veirs, D.K., 2006. Gas generation from water adsorbed onto pure plutonium dioxide powder. In: Materials Research Society Symposium, vol. 893.

Vigier, N., Grandjean, S., Arab-Chapelet, B., Abraham, F., 2007. Reaction mechanisms of the thermal conversion of Pu(IV) oxalate into plutonium oxide. J. Alloys Compd. 444, 594–597.

Waterbury, G., Douglass, R.M., Metz, C.F., 1961. Thermogravimetric behaviour of plutonium metal, nitrate, sulfate, and oxalate. Anal. Chem. 33 (8), 1018.
Weigel, F., TerMeer, N., 1967. The unit cells of some americium (III)—salts with organic anions. Inorg. Nucl. Chem. Lett. 3, 403.
Wilson, P.D., 1996. The Nuclear Fuel Cycle: From Ore to Wastes. Oxford University Press, Oxford, NY.

Gelation and other innovative conversion processes for aqueous-based reprocessing and recycling of spent nuclear fuels

14

Manuel A. Pouchon
Paul Scherrer Institut, Laboratory for Nuclear Materials, Villigen, Switzerland

Acronyms

BISO	bistructural-isotropic fuel (see TRISO)
DCC	direct coagulation casting (sol-gel based method to produce arbitrary shapes)
HMTA	hexamethylenetetramine (also called hexamine)
HMUR	mixture of hexamethylenetetramine (HMTA) and urea in 1:1 proportion
INRAM	infiltration of highly radioactive materials
KFA	Kernforschungs anlage (former name of "Forschungszentrum Jülich," Germany)
ORNL	Oak Ridge National Laboratory (United States)
PSI	Paul Scherrer Institut (Switzerland)
SGMP	sol-gel microsphere pelletization process (process to gain pellets from gelled particles)
SNAM	Società Nazionale Metanodoti (Italy)
Sphere-pac	particle fuel composed of fuel beads gained in a gelation process
TRISO	tristructural-isotropic fuel (concept where the central fuel kernel is surrounded by several layers of pyrolytic carbide and silicon carbide)
Vipac, Vibropack	particle fuel composed of small fuel fragments gained from the electrode in a pyroprocess
(V)HTR	gas-cooled (very) high-temperature reactor

14.1 Motivation

Fuel production in a closed nuclear fuel cycle implies a considerable presence of minor actinides and, therefore, the production of fuels in shielded hot cells with remote manipulation. In this environment the conventional, powder-based, fuel production presents major disadvantages as it requires powder handling with unavoidable dust production. Mechanical processes like milling and grinding also result in dust, which can be handled in an open process, but which is much more difficult to treat in a hot cell. Furthermore, the mechanical manipulation devices used are also subject

Reprocessing and Recycling of Spent Nuclear Fuel. http://dx.doi.org/10.1016/B978-1-78242-212-9.00014-9

to regular maintenance and, sometimes, costly replacement. These challenges are the main driving force to look for alternative production methods and in some cases for alternative fuel forms. Processes that remain aqueous up to the final product and minimize dust generation appear to be an attractive alternative. In this chapter, different aqueous production methods are, therefore, introduced.

14.2 History and overview

Early thoughts about alternative ways of producing nuclear fuel go back to the late 1950s, when at the Hanford/Pacific Northwest Laboratory (USA) (Hauth, 1959) direct use of small fuel particles promised a much simplified production method, implying less powder handling and maintenance effort. The concept was first developed using products from a pyrochemical process, as described in Hauth (1959), which was generally known as the vipac or vibropac concept. Later the process was modified at the Oak Ridge National Laboratory (ORNL) for products from aqueous reprocessing, this being commonly referred to as sphere-pac. Both concepts have been developed to a high technical readiness, with production and fuel performance studies, up to in-reactor experiments and postirradiation examinations. Today the vipac concept is mainly pursued by the Russian Federation, whereas the sphere-pac concept is being explored in the United States and Europe. After a decline of interest in closing the fuel cycle as a consequence of the Chernobyl accident in the 1980s, today there is a revitalized interest in these processes and fuel forms as part of the development of a more sustainable closed fuel cycle that enables enhanced resource usage with the potential for reduction in long-lived and heat generating radioactive wastes.

14.3 Fuel concepts

14.3.1 Sphere-pac

Two particle fuel concepts, the sphere-pac and vibropac (vipac), have been researched in the past and are still under active development. The vibropac is the first choice when coming from a pyroreprocessing route. Sphere-pac can directly be employed when coming from an aqueous route, and it represents the simplest usage of spheres produced in a sol-gel process. After having been treated thermally, the sintered sol-gel spheres are directly filled into the fuel pin, with no further modification. Besides its simplicity, this concept also offers the advantage that a single fuel sphere is small and if not stored in a compact form with more spheres, does not heat to very high temperatures even for high curium contents. This applies for the production process up to the thermal treatment of the spheres, where the spheres could be stored in flat beds, before they are filled into the pins. The sphere-pac fuel form, a packing of two or more size fractions of these fuel spheres is, however, very different from the classical pellet and questions arise about the fuel performance. The main issues here are the heat

transfer and fuel restructuring. These questions have initiated large international research programs, which are partially summarized in Pouchon et al. (2012a,b).

14.3.2 BISO and TRISO

A classical application of fuel beads being produced by the gelation technique are the kernels of the bistructural-isotropic fuel (BISO) and tristructural-isotropic fuel (TRISO) concepts, which were employed for the high-temperature gas-cooled reactors in the past (HTR) and potentially in the future for very high-temperature reactors (VHTRs). This is part of the Generation IV initiative, aiming for gas temperatures of around 1270 K. In order to get excellent fission gas retention behavior, the kernels are coated with several layers, ensuring microencapsulation. The names come from the two (bi-) or three (tri-) different materials classes being used for the coating. As an actual new development, TRISO particles are also considered as accident tolerant fuel for use in light-water reactors, with the potential of retaining the fission gases even under the most severe accident conditions (Terrani et al., 2012).

14.3.3 Composite fuels

Fuel kernels have also been investigated in the frame of composite fuel concepts, such as cermet or cercer, where "cer" stands for the ceramic nature of a dispersed phase and "met" for a metallic matrix; also, cercers have been investigated with a fuel ceramic being dispersed into a ceramic matrix (Meyer, 2012). In case of a cermet, an actual example can be found in reference (Hunt et al., 2014) concerning fuel for space reactors. Cermet is a heterogeneous concept, as two different materials are used; cercers can be heterogeneous with two different ceramics, or homogeneous with the same ceramic. The idea is a division of functions. On one hand there is a fuel-carrying container, where the material often contains the heavy metal in a solid solution, and that shows tolerant irradiation behavior. This phase is formed into small particles, representing a dispersion. On the other hand, there is the matrix containing the dispersed ceramic phase, which serves as an inactive container and a thermally conducting medium, transferring the heat toward the cladding wall in the case of a classical pin design. By choosing a balanced size and distribution density of the dispersoids, both aspects, the particle internal temperature gradient and the radiation damage of the conducting containing phase, can be optimized.

14.3.4 Pellet

Even though the classical pellet production has some disadvantages, such as the final machining of the pellet, the pellet as an end form is so well established that there is a large interest in maintaining it. Therefore, some modified production methods are studied that try to minimize the known disadvantages. This can be a simplified pelleting process (Suzuki, 2008) or the compaction of sol-gel derived fuel particles into a pellet, also called the sol-gel microsphere pelletization process (SGMP) (Ganguly et al., 1985, 1989; Ganguly and Hegde, 1997; Nästren et al., 2013). A very innovative

approach here is direct coagulation casting (DCC), which promises direct production of the precise pellet shape by an aqueous route, without the need of grinding. This technique is described in Section 14.10 below. Another approach is the hybrid method of a pellet being produced by the powder method, and then being infiltrated with an actinide containing liquid. This process is called INRAM (infiltration of highly radioactive materials) and was invented at the Institute for Transuranium Elements (Germany) (Richter et al., 1997).

14.4 Sol-gel techniques

The idea behind the sol-gel techniques is a simple, dustless process for forming dense fuel kernels that can then be utilized in a sphere-pac concept, in fuel kernels for high-temperature gas-cooled reactors (HTR), or compacted to classical pellets.

The starting phase is a true colloidal suspension: a sol. This is destabilized leading to an aggregation and the formation of a rigid network: a gel. A gel is an intermediate phase between solid and liquid and only with drying and a thermal treatment the final dense ceramic phase can be obtained. The term sol-gel is widely used for virtually all chemical processes from solutions to ceramics. The starting solution can be metallo-organic, polymeric, or ionic solutions. The chemistry in the sol-gel process then dictates the physical characteristics, such as the structure and density distribution of the network in the gel product. There are three principle classes of networks, these are a simple *particle network* (*a*), where the surface chemistry controls the suspension properties or the single particles, the *aggregate network* (*b*) with a clustering of aggregates, a collection of macromolecules, with a nonuniform density distribution. Here the solution is prepared in a way that a solid phase precipitates out with tiny particle sizes and there is a continuous aggregation of these particles, forming a rigid network. The third class is a *polymer network* (*c*) with a rather low uniform density distribution formed by cross-linking polymers. The desired metal atom of the targeted ceramic is contained in the inorganic polymers, which are formed by metal-oxygen bonds. Figure 14.1 gives a qualitative representation of the three classes. For a more in-depth description, see Ring (1996). An overview of early nuclear related activities using these techniques is provided in Sol-Gel Processes for Ceramic Nuclear Fuels (1968) and De Leone (1968).

14.5 Water extraction process (ORNL process)

14.5.1 Introduction

This technique has been suggested by researchers at the ORNL in the United States (Haas et al., 1968; McBride et al., 1972). Compared to other sol-gel processes, the solvent extraction avoids the contamination of the resulting kernels with organics and, therefore, enables the omission of an additional process step (i.e., the cleaning procedure), with a consequent reduction in liquid radioactive waste. The major disadvantage of this process, the slow dehydration process, will become obvious in the next section; this issue makes industrial implementation difficult.

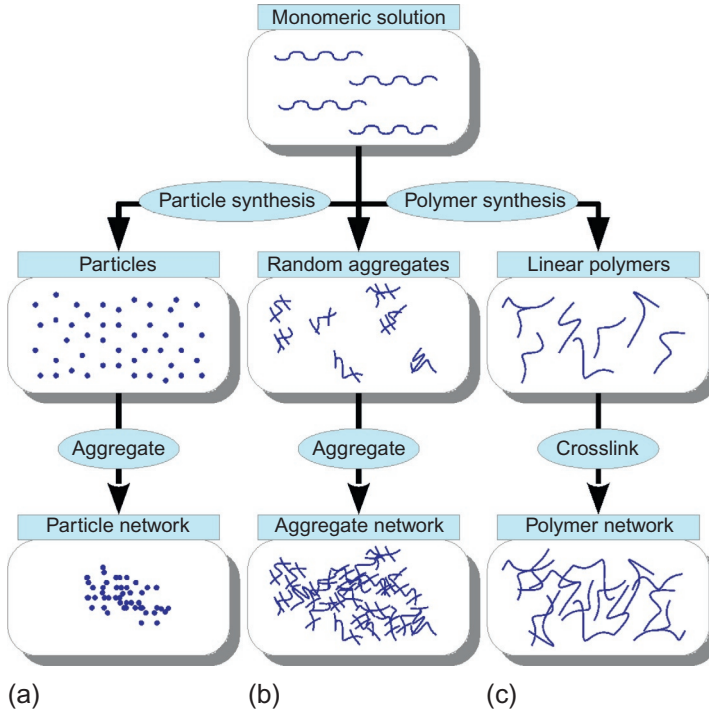

Figure 14.1 Schematic representation of the sol-gel routes for the different sol classes. (a) The particle network, (b) the aggregate network, and (c) the polymer network. After Ring (1996, p. 341).

14.5.2 The process

Dioxides of the actinides of interest, such as thorium, uranium, plutonium, and neptunium, are highly insoluble; this can be changed by having nitrates as counterions. For the preparation of sols the tetravalent nitrates $Th(NO_3)_4$, $U(NO_3)_4$, $Pu(NO_3)_4$, and $Np(NO_3)_4$ are used as starting solutions. Among these, $U(NO_3)_4$ is not stable, as U(IV) is oxidized to U(VI) in air and nitrate solutions. In the case of thorium, the oxide sol ThO_2 is prepared by precipitation of the hydroxide $Th(OH)_4$ with an ammonia addition. In order to provide NO_3^- counterions for stabilization of the suspension, the precipitation step is followed by the addition of small quantities of $Th(NO_3)_4$ and a boiling step. Similar processes are used for the production of UO_2 and PuO_2 sols (Sood, 2011). The sol is therefore surface chemistry driven and is a particle network, corresponding to Figure 14.1a.

Solvent extraction (instead of precipitation) is then used to produce gels, whereby 70-80% of the nitrate is removed, followed by digestion (Ostwald ripening of the precipitate) at 370 K for 10 min (Sood, 2011). Countercurrent flow within a 2-ethyl-1-hexanol tapered column for 10-15 min leads to the desired dehydration. Fluidized

droplets travel down the column as they become denser. The gelled particles are removed from the bottom of the column. The main drawbacks of this technique are the need for U(IV), which is not stable, and the lengthy dehydration process.

14.6 External gelation

14.6.1 Introduction

The external gelation process was originally developed in Italy (Brambilla et al., 1970), where it was known as the *SNAM-process* (Società Nazionale Metanodoti), and in Germany (Ringel and Zimmer, 1979), where it was referred to as the *KFA-process* (Kernforschungs anlage Jülich). The main purpose of the process is the conversion of uranyl nitrate solution into microspeheres without the need for reducing U(VI) to U(IV), compared to the solvent extraction technique, making the procedure more stable.

14.6.2 The process

Given the fact that uranyl nitrate $UO_2(NO_3)_2$ in contact with ammonia results in a very fragile gel, not being usable for further processing, water-soluble organic polymers are added to the uranyl nitrate solution for stabilization and to obtain a broth. Employed candidate polymers are

- hydroxypropyl methylcellulose (methocel): semisynthetic, inert, viscoelastic polymer with the molecular formula $C_{17}H_{32}O_{11}$
- polyvinyl alcohol (PVA): water-soluble synthetic polymer with the molecular formula $(C_2H_4O)_x$
- dextran: complex, branched glucan composed of chains of varying lengths, with the molecular formula $(C_6H_{10}O_5)_x$

In order to adjust the properties additionally, the following modifiers are used:

- tetrahydrofurfuryl alcohol (THFA): molecular formula $C_5H_{10}O_2$
- formamide: molecular formula CH_2O
- urea: molecular formula CH_4N_2O
- ammonium nitrate: molecular formula $(NH_4)(NO_3)$
- dioxane: molecular formula $C_4H_8O_2$

Therefore, this gelation corresponds to case (c) in Figure 14.1, based on the polymeric network. In the SNAM process a mixture of these components was found to be most efficient. Then the solution is dropped though a nozzle, first passing a curtain of ammonia gas, providing a hard outer shell to the droplet, consequently stabilizing the spherical shape before impact, and then falling into a bath of ammonium hydroxide (typically 4 mol/L NH_4OH). The polymer provides a stable framework to the hydrated UO_3 gel. In order to get mixed oxides (MOXs) with plutonium and/or thorium, colloidal solutions can be added to the broth.

$$2UO_2(NO_3)_{1.5}(OH)_{0.5}(aq) + 5NH_4OH(aq) \rightarrow (NH_4)_2U_2O_7(s) + 3NH_4NO_3(aq) + 3H_2O \quad (14.1)$$

The gelation, and therefore the protonation, is initiated by a pH shift. In the case of external gelation, this shift is driven by the external addition of a base, in this case ammonium hydroxide:

$$UO_2(NO_3)_2 + NH_4OH \rightarrow UO_3 \cdot xH_2O \cdot yNH_3 + NH_4NO_3 \quad (14.2)$$

In the KFA process, the chemistry has been refined for the production of ThO_2 and (U, Th)O_2 kernels. Avoiding the usage of any organic polymer, the thorium nitrate is neutralized with ammonia to get a suspension of $Th(OH)_4$ and then boiled to get a ThO_2 suspension. Compared to the SNAM process, the heavy metal concentration reached three times higher values (2.0 versus 0.7 mol/L), making the resulting sol highly viscous, such that the addition of polymers can be avoided. Figure 14.2 shows a generalized flowchart of the process, with the ammonia gas surface hardening and the successive entire gelation in ammonium hydroxide.

14.6.3 Programs

The external gelation, especially the KFA process, is the reference production route for the TRISO particles in the HTR fuel, such as employed in the German pebble bed reactor AVR (Arbeitsgemeinschaft Versuchsreaktor Jülich) and the follow up thorium reactor THTR-300 (Thorium-Hoch-Temperatur-Reaktor) in Hamm, Germany. The process has also been used for the Japanese, American, South African, and the Chinese high temperature reactor programs. Besides these applications, the production of minor actinide-containing fuels as transmutation targets has also been addressed. One successful approach is the production of porous beads by internal gelation that can then be infiltrated with a minor actinide-containing solution. In Nästren et al. (2013), 6% americium content fuels are reported. The particles are then compacted into pellets.

14.7 Internal gelation

14.7.1 Introduction

The internal gelation process was initially developed at KEMA (Keuring van Elektrotechnische Materialen te Arnhem) laboratories in the Netherlands, partly under a contract with the Dragon Project for ThO_2 spheres (Kanij et al., 1968), and for UO_2 spheres (Kanij et al., 1974) (van der Brugghen et al., 1970). Contrary to the external gelation process, the pH shift is driven from the decomposition of an agent in the feed solution, acting as an internal donor of ammonia. It allows the preparation of oxide spheres of ThO_2, containing up to 15% UO_2, with a size range of 100-700 μm.

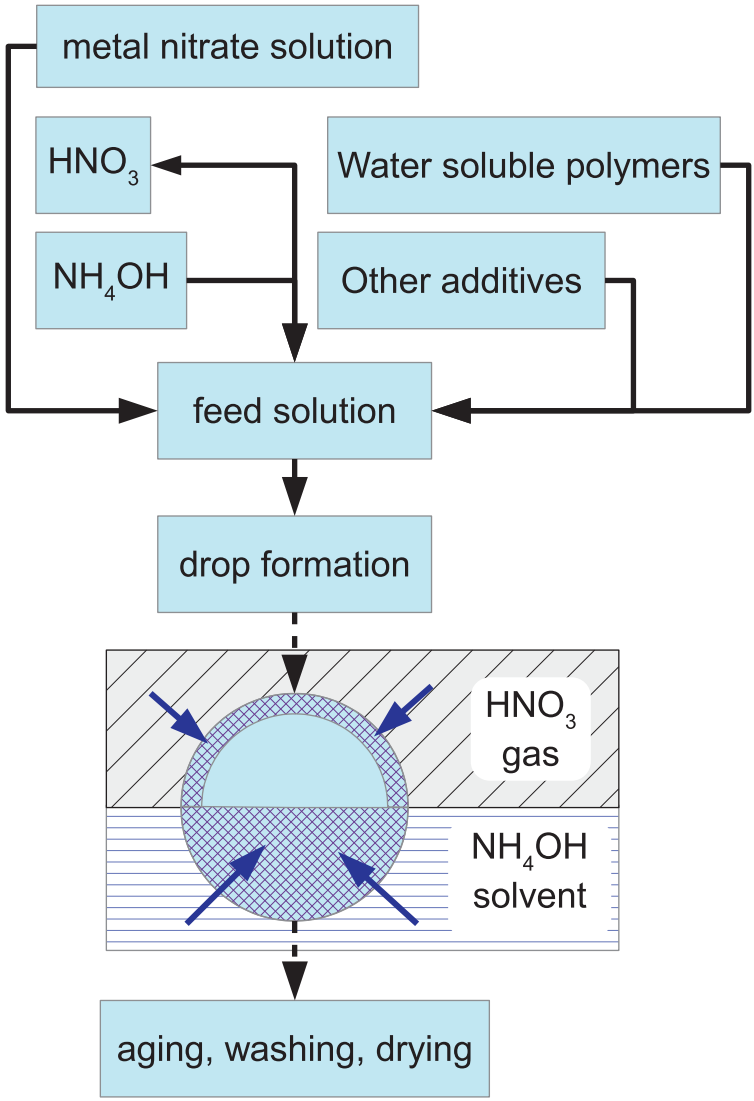

Figure 14.2 Generalized flowchart of the external gelation process up to the drying process.

14.7.2 The process

The usage of gel-forming additives is omitted. The gelation is instead launched by an internal reagent, the organic compound hexamethylenetetramine, also called hexamine or HMTA (Hexamine), which is acting as a homogeneous precipitating agent. HMTA causes rapid precipitation of U(VI). Therefore, in order to prevent a premature

process the organic compound urea ($CO(NH_2)_2$) is added to complex the uranyl ions (Equation 14.3):

$$2CO(NH_2)_2 + UO_2{}^{2+} \leftrightarrow UO_2\left[CO(NH_2)_2\right]_2{}^{2+} \tag{14.3}$$

Therefore, the initial broth is composed of acid deficient uranyl-nitrate solution (ADUN) and a mixture of HMTA and urea, also known as HMUR. At increasing temperature, HMTA decomposes and releases ammonia. In order to prevent this reaction at preparation time, the solutions are cooled to temperatures around 273 K.

At increasing temperatures, the initial ADUM-urea complex (Equation 14.3) weakens. Then the metal ion gets hydrolyzed and releases a hydrogen ion

$$UO_2{}^{2+} + H_2O \leftrightarrow UO_2(OH)^+ + H^+ \tag{14.4}$$

followed by the HMTA protonation with the consumption of this hydrogen ion, this can be denoted by

$$(CH_2)_6N_4 + H^+ \leftrightarrow \left[(CH_2)_6N_4H\right]^+ \tag{14.5}$$

Finally, the decomposition of HMTA occurs:

$$\left[(CH_2)_6N_4H\right]^+ + 3H^+ + 6H_2O \rightarrow 4NH_4{}^+ + 6CH_2O \tag{14.6}$$

With this release of ammonia, the formation of the UO_3H_2O gel is launched:

$$2UO_2(OH)_{0.5}(NO_3)_{1.5} + 3NH_4OH \rightarrow 2UO_3H_2O + 3NH_4NO_3 \tag{14.7}$$

Therefore, the process is driven by a temperature increase, which classically is introduced by immersion into a hot immiscible liquid, such as silicon oil. This approach has the disadvantage of creating an additional waste flow, as the silicon oil gets contaminated. On the other hand, the gelled particles get contaminated by the silicon oil. This requires a sophisticated recycling technique for the silicon oil and an additional cleaning step for the fuel particles with an organic solvent, creating yet another waste stream.

An alternative approach is microwave heating, which was already suggested in the early 1980s (Bonek et al., 1982) and further developed in that period (Ledergerber, 1985) (Yamagishi et al., 1994). The elimination of a fluid heat carrier promises a reduction in liquid waste, as there is no need for the spheres to contact a liquid for heating and, therefore, no liquid is contaminated; plus, the spheres do not have to be cleaned from this immiscible liquid, the silicon oil. In recent work the process has been revisited, developing it to a reliable procedure (Pouchon, n.d.-a; Cabanes-Sempere et al., 2012), where the issues associated with including minor actinide-containing fuel have been addressed (Pouchon, n.d.-b). Other approaches

address the droplet formation allowing a larger range of particle sizes to be produced, using microfluid channels, for example, Ye et al. (2013). A similar technique is proposed in Couland et al. (2012) where the immiscible liquid is tetrachloroethylene (C_2Cl_4), replacing the classical silicon oil. Figure 14.3 shows the scheme for the classical process using hot silicone oil to reach the temperature step for the gelation;

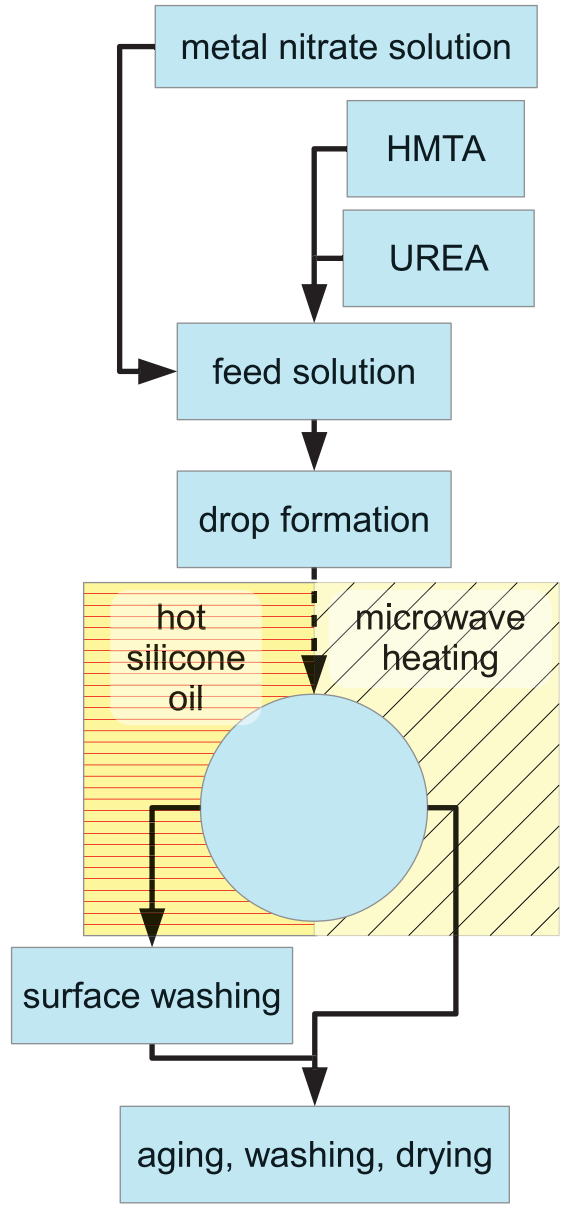

Figure 14.3 Generalized flowchart of the internal gelation process up to the drying process.

at the same time, the flowchart also shows the simplified method that uses microwave heating, where the surface washing procedure, necessary to remove the silicone oil, can be omitted.

14.7.3 Programs

The internal gelation process is the most employed route for fabrication of fuel particles for the sphere-pac concept; a concept where the pellet is replaced by an arrangement of spherical fuel particles, being directly filled into the fuel pin. An overview of the conducted programs can be found in Pouchon et al. (2012b). It was generally used as fast reactor fuel with two size fractions, but was also tested as light-water reactor fuel with three size fractions to reach high smear densities (up to 90%). Beside oxide, carbide and nitride matrices were also produced, which was simply achieved by adding carbon black to the feed solution and performing a carbothermic reduction under either an argon or nitrogen atmosphere. In most of the programs, UO_2 was produced and often irradiated and postirradiation examined. However, MOXs, inert matrix fuels (e.g., yttria stabilized zirconia-based fuel with plutonium as the fissile component), and many more compositions, were produced and tested. The internal gelation is a very versatile method where almost all metals could be coprecipitated. Products directly fabricated by internal gelation with the highest minor actinide content are reported in Hellwig et al. (2006) and Morihira et al. (2005), where 20% plutonium and 5% neptunium (at% in metal) was processed into a sphere-pac fuel and tested.

14.8 Total gelation

14.8.1 Introduction

In the frame of the Chinese high-temperature program and fuel production for the HTR 10, a new, combined technique has been developed using both the external and the internal gelation approaches. The process is, therefore, called total gelation of uranium (Fu et al., 2004).

14.8.2 The process

A sol is prepared according to the external gelation process, by mixing a uranyl nitrate solution with urea, PVA, and THFA. However, HMTA is added to the sol resulting in an internal gelation by the ammonia being released by the HMTA, and by the external ammonia. The metal concentration can at the same time also be increased, resulting in a lower shrinking of the final product when undergoing the thermal treatment. This promises to give a better shape conservation, or very symmetric spheres. Vacuum drying is applied, resulting in an open porosity for the later thermal treatment. The spheres are then calcined and sintered at about 900 K and above 1900 K, respectively, resulting in 98% dense spheres.

14.9 Weak acid resin process

14.9.1 Introduction

The *w*eak *a*cid *r*esin (WAR) process was developed in the early 1970s in the United States at ORNL (Haas; Weber et al., 1977; Notz et al., 1978) and later also at the Commissariat à l'énergie atomique et aux énergies alternatives (CEA), France (Moreau et al., 1977). Recently the process has gained interest again in the production of minor actinide-containing fuel kernels (Picart et al., 2010). In the latter reference, a production example of kernels with americium is given. Americium and curium are the more difficult elements to handle in production, whereas neptunium-containing fuels are easier to realize. Therefore, americium-containing products represent a significant step forward.

14.9.2 Process

The process consists of two steps. First, the carboxylic resin is loaded and then the fully loaded resin is thermally converted into an oxide or into carbide phases depending on temperature and atmosphere. The loading represents hereby the more difficult part, as the actinide cation-containing solution must meet precise pH conditions enabling hydrolysis. The actinide metal content must also be adjusted to fit the desired product stoichiometry (Picart et al., 2010).

Ionic exchange between the proton of a carboxylic resin and a metallic cation is only possible at low acidity. The loading reaction in case of uranium is (Notz et al., 1978b)

$$2\mathrm{RCOOH} + \mathrm{UO_2^{2+}} \leftrightarrow \mathrm{UO_2(RCOO)_2} + 2\mathrm{H^+} \tag{14.8}$$

For carboxylate resins, an alkaline pH is normally required to drive the reaction to the right. One disadvantage of the process is the low conversion rate, depending on the actinides being loaded, which makes a recycling process necessary.

14.10 Direct coagulation casting

14.10.1 Introduction

DCC offers the option to produce special, almost arbitrary shaped pellets, offering new pin designs with potentially higher burn up. The method is mainly known for the production of complex zirconia parts, such as turbine rotors. The parts can be directly produced with high precision, so that no grinding is necessary as a final shaping step. In the perspective of having a dustless production method, this technique has been investigated for nuclear fuel (Streit et al., 2003).

14.10.2 Process

Direct coagulation is a colloidal-forming technique based on the time-delayed reactions that alter an electrostatically stabilized ceramic suspension (Balzer and Gauckler, 2003; Streit et al., 2002; Gauckler et al., 1999). This consolidation is performed by changing pH or ionic strength catalyzed by enzymatic reactions (ETH—NONMET—Colloidal Forming Techniques). Such a reaction can be the hydrolysis of urea in the presence of the enzyme urease, in solution buffered to pH 9 (Zimmer, 2000; Lippard, 1995):

$$CO(NH_2)_2 + H_2O \rightarrow NH_3 + CO(NH_2)OH \tag{14.9}$$

$$CO(NH_2)OH + H_2O \rightarrow NH_3 + H_2CO_3 \tag{14.10}$$

It is, however, known that enzymes can be inactivated or destroyed, when being irradiated (Kopp et al., 1966). Therefore, the applicability of the process for the production of highly radioactive nuclear fuel can be questioned. These findings are also reported in Streit et al. (2002). The chemistry has, however, a high potential for optimization, making the process so fast that the inactivation of the enzymes would be after solidification.

14.11 Conclusions

Experience with sol-gel techniques has been gained within the framework of high temperature and fast reactor programs. The external and internal gelation techniques, especially, were applied in large production programs with irradiation experiments. They have proven to be very stable and effective production methods. The two main applications have been the production of microencapsulated fuel kernels, for the high temperature fuels (BISO and TRISO), and the idea of having a dustless and simple production method for the (re)fabrication of highly active fuel; these have been the main motivations for these aqueous production routes. The latter aspect has, however, only partially been satisfied, as only a few minor actinide-containing targets have been produced and tested. All of the approaches still bear a large optimization potential, and especially the need to prove the applicability for high contents of minor actinides, facing problems like decay heating and change in chemistry due to radiolysis. These aspects will have to be covered in greater detail in future programs. The next section emphasizes the actual state of affairs and an outlook to potential further developments.

14.12 Present state and outlook

The aqueous production techniques have mainly been developed in the 1950s-1970s, as closing of the fuel cycle was of large interest at these times, and nuclear energy was regarded as the future technology with the need of large fissile material resources,

including breeding through the introduction of fast reactors. With the Three Mile Island accident in the United States (1979) and later the Chernobyl accident in Ukraine (1985), the technology development was slowed down, at least in the western world. Recently, with the Generation IV initiative, the fuel cycle has gained interest again and is the subject of numerous American and European (FP7 ACSEPT Project; FP7 ASGARD Project; FP7 PELGRIMM Project) projects. Here, the different gelation techniques have received renewed interest with particular emphasis placed on the internal gelation process for the sphere-pac concept. Some techniques like the WAR project have also gained renewed attention, with some successful production of minor actinide-containing samples.

The two most experienced gelation techniques are the internal and external gelation methods. Important experience with the production of minor actinide-containing fuel has been gained with neptunium containing fuel particles being produced by the internal gelation route (Hellwig et al., 2006b), and americium containing particles where the minor actinide was infiltrated into porous particles from external gelation (Nästren et al., 2013), similar to the aforementioned INRAM process. However, much more experience in conversion of minor actinide-containing solutions to fuels is required in the development of processes for advanced closed fuel cycles. Presently, americium containing sphere-pac, also produced by the infiltration method (Somers and Fernandez, 2006), is being irradiated in the "sphere irradiation" study in the framework of the European projects FAIRFUELS and PELGRIMM (FP7 FairFuels Project; FP7 PELGRIMM Project). The direct production of a minor actinide containing sphere-pac is also addressed by the Swiss projects PINE (Pouchon, n.d.-a) and MeAWaT (Pouchon, n.d.-b) for waste minimization. Additionally, addressing minimization of the influence of radiolysis and decay heating on product formation is necessary. The latter two aspects are addressed by the application of an instantaneous preparation of the feed solutions, not allowing the mixing time to affect the gelation process. In a current development, the elapsed time of the solution from mixing to dripping into the anticipated spheres is reduced into the subsecond regime. This way, cooling of the source solutions can be omitted. Even the internal gelation with a metal solution being heated up to 50 °C has been successfully tested (Tian et al., 2014). Besides an increased versatility of the process, because any self-heating solution can be treated, this development also signifies an important simplification of the fabrication units.

Acknowledgements

The compilation of this chapter and part of the newly reported developments has been facilitated by the Swiss CCEM.ch program MeAWaT (Pouchon, n.d.-b) and the European FP7 programs ASGARD (Contract No. 295825) (FP7 ASGARD Project) and PELGRIMM (Contract No. 295664) (FP7 PELGRIMM Project).

References

Balzer, B., Gauckler, L., 2003. 5.5 novel colloidal forming technique direct coagulation casting. In: Somiya, S., Aldinger, F., Claussen, N., Spriggs, R.M., Uchino, K., Koumoto, K., Kaneno, K. (Eds.), In: Handbook of Advanced Ceramics, vol. I. Elsevier, Amsterdam, pp. 435–458.

Bonek, E., Knotik, K., Leichter, P., Magerl, G., Rohrecker, L., 1982. Microwave hardening of free-falling radioactive droplets, Conference Proceedings of 12th European Microwave Conference 82, Helsinki, Finland, 13–17 September 1982, pp. 610–614. http://dx.doi.org/10.1109/EUMA.1982.333128.

Brambilla, G., Gerontopoulos, P., Neri, D., 1970. SNAM process for preparation of ceramic nuclear fuel microspheres—laboratory studies. Energ. Nucl. 17 (4), 217–224.

Cabanes-Sempere, M., Cozzo, C., Vaucher, S., Catalá-Civera, J.M., Pouchon, M.A., 2012. Innovative production of nuclear fuel by microwave internal gelation: heat transfer model of falling droplets. Prog. Nucl. Energy 57, 111–116.

Couland, M., Fourcaudot, S., Jovani Abril, R., Fernandez-Carretero, A., Somers, J., 2012. Novel production route of yttria-stabilized zirconia fuel kernels and pellets for nuclear fuel applications. J. Am. Ceram. Soc. 95 (1), 133–137.

De Leone, R. (Ed.), 1968. I Processi Sol-Gel per la Produzione di Combustibili Ceramici, Simposio nuceare di Torino, ottobre 2-3, 1967, Via Belisario 15, Roma.

ETH—NONMET—Colloidal Forming Techniques. Available: http://www.nonmet.mat.ethz.ch/research/Colloidal_Chemistry_Ceramic_Processing/Colloidal_Forming_Techniques (accessed 24.03.14) (Online).

FP7 ACSEPT Project (Actinide reCycling by SEParation and Transmutation), EC-GA No. 211267. Available: http://www.acsept.org/ (accessed: 04.05.14) (Online).

FP7 ASGARD Project (Advanced fuelS for Generation IV reActors: Reprocessing and Dissolution), EC-GA No. 295825. Available: http://asgardproject.eu/ (accessed: 04.05.14) (Online).

FP7 FairFuels Project (FAbrication, Irradiation and Reprocessing of FUELS and targets for transmutation), EC-GA No. 232624. Available: http://www.fp7-fairfuels.eu/ (accessed 04.05.14) (Online).

FP7 PELGRIMM Project (PELlets versus GRanulates: Irradiation, Manufacturing & Modelling), EC-GA No. 295664. Available: http://www.pelgrimm.eu/ (accessed: 04.05.14) (Online).

Fu, X., Liang, T., Tang, Y., Xu, Z., Tang, C., 2004. Preparation of UO_2 kernel for HTR-10 fuel element. J. Nucl. Sci. Technol. 41 (9), 943–948.

Ganguly, C., Hegde, P.V., 1997. Sol-gel microsphere pelletisation process for fabrication of (U, Pu)O_2, (U, Pu)C and (U, Pu)N fuel pellets for the prototype fast breeder reactor in India. J. Sol-Gel Sci. Technol. 9 (3), 285–294.

Ganguly, C., Langen, H., Zimmer, E., Merz, E.R., 1985. Sol-gel microsphere pelletization process of high-density ThO_2-2%UO_2 fuel for advanced pressurized heavy water reactors. Nucl. Technol. 73, 84–95.

Ganguly, C., Basak, U., Vaidya, V.N., Sood, D.D., Roy, P.R., 1989. Sol-gel microsphere pelletisation of UO_2 and UO_2-PuO_2 pellets of PHWR fuel specifications using internal gelation process. In: Proceedings of the Second International Conference on CANDU Fuel, Pembroke, Ontario, Canada, October 1-5, 1989, pp. 108–124.

Gauckler, L.J., Graule, T., Baader, F., 1999. Ceramic forming using enzyme catalyzed reactions. Mater. Chem. Phys. 61 (1), 78–102.

Haas, P.A. Loading a cation exchange resin with uranyl ions. US 3800023 A.

Haas, P.A., Haws, C.C.J., Kitts, F.G., Ryon, A.D., 1968. Engineering Development of Sol-Gel Processes at the Oak Ridge National Laboratory. Oak Ridge National Lab, Tennessee (ORNL-TM-1978; CONF-671008-4).

Hauth, J.J., 1959. Vibration-Compacted Ceramic Fuel Elements, HW-60346. General Electric Co. Hanford Atomic Products Operation, Richland, WA.

Hellwig, C., Bakker, K., Ozawa, T., Nakamura, M., Ingold, F., Nordström, L.Å., Kihara, Y., 2006. FUJI: a comparative irradiation test with pellet, sphere-pac, and vipac fuels. Nucl. Sci. Eng. 153 (3), 233–244.

Hexamine. Available: http://ull.chemistry.uakron.edu/erd/Chemicals/8000/6553.html (accessed 27.02.14) (Online).

Hunt, R.D., Hickman, R.R., Ladd-Lively, J.L., Anderson, K.K., Collins, R.T., Collins, J.L., 2014. Production of small uranium dioxide microspheres for cermet nuclear fuel using the internal gelation process. Ann. Nucl. Energy 69, 139–143.

Kanij, J.B.W., Noothout, A.J., Van der Plas, T., Hermans, M.E.H., 1968. Sol-gel development at K.E.M.A. In: De Leone, R. (Ed.), I Processi Sol-Gel per la Produzione di Combustibili Ceramici, Simposio nuceare di Torino, ottobre 2-3, 1967. Comitato Nationale Energia Nucleare, Via Belisario 15, Roma, pp. 139–160.

Kanij, J.B.W., Noothout, A.J., Votocik, O., 1974. The KEMA-U(IV)-process for the production of UO_2 microspheres. In: Proceedings of the IAEA Conference on Sol-Gel Processes for Fuel Fabrication, Vienna, May 21-24, 1973, pp. 185–195 (IAEA-TECDOC-161).

Kopp, P.M., Read, J.F., Charlesby, A., 1966. Comparison of the effect of alpha- and gamma-radiation on an enzyme. Nature 211 (5052), 959–960.

Ledergerber, G., 1985. "Internal gelation using microwaves" IAEA-TECDOC, advanced fuel technology and performance, Proceedings of an Advisory Group Meeting, Würenlingen, Switzerland, 4–6 December 1984, 352, 165–174.

Lippard, S.J., 1995. At last—the crystal structure of urease. Science 268 (5213), 996–997.

McBride, J.P., McCorkle, K.H., Finney, B.C., Pattison, W.L., 1972. Cusp process for preparing concentrated, crystalline Urania sols by solvent-extraction. Nucl. Technol. 13 (2), 148–158.

Meyer, M.K., 2012. 3.10—composite fuel (cermet, cercer). In: Konings, R.J.M. (Ed.), Comprehensive Nuclear Materials. Elsevier, Oxford, pp. 257–273.

Moreau, C., Ballagny, A., Bujas, R., Holder, J., Ranc, R., Soulhier, R., 1977. Fabrication et performances du combustible français pour réacteurs à haute température (IAEA-CN-36/270). In: Nuclear Power and Its Fuel Cycle, Salzburg, May 2-13, 1977, vol. 3, pp. 411-431.

Morihira, M., Nakamura, M., Ozawa, T., Kihara, Y., Hellwig, C., Ingold, F., Nordström, L.Å., Pouchon, M.A., Bakker, K., Thesingh, H.G., Thijssen, P.J.M., 2005. Final Report of the FUJI Project concerning the Research and Development of Advanced Sphere-Pac Fuel Among JNC, PSI and NRG, JNC TY8400 2005-006 (振動充填燃料開発に関するスイスPSI・オランダNRGとの共同研究 (FUJI プロジェクト) 最終報告書). Japan Nuclear Cycle Development Institute (JNC), Tokai-mura, Ibaraki, Japan.

Nästren, C., Staicu, D., Somers, J., Fernandez, A., 2013. Synthesis of (Zr, Y, Am)O_{2-x} transmutation targets. J. Nucl. Mater. 433 (1-3), 314–318.

Notz, K.J., Haas, P.A., Shaffer, J.H., 1978. The preparation of HTGR fissile fuel kernels by uranium-loading of ion exchange resins. Radiochim. Acta 25 (3-4), 153–160.

Picart, S., Mokhtari, H., Ramière, I., Jobelin, I., 2010. Preparation of minor actinides targets or blankets by means of ionic exchange resin. IOP Conf. Ser. Mater. Sci. Eng. 9 (1), 012025.

Pouchon, M.A., n.d.-a. CCEM Project PINE (Platform for Innovative Nuclear FuEls). Available: http://www.ccem.ch/science/pine (accessed 04.05.14) (Online).

Pouchon, M.A., n.d.-b. CCEM.ch Project MeAWaT (MEthods of Advanced WAste Treatment). Available: http://www.ccem.ch/meawat (accessed 04.05.14) (Online).

Pouchon, M.A., Nordström, L.-Å., Hellwig, C., 2012a. Modeling of sphere-pac fuel. In: Konings, R.J.M. (Ed.), Comprehensive Nuclear Materials. Elsevier, Oxford, pp. 789–817.

Pouchon, M.A., Ledergerber, G., Ingold, F., Bakker, K., 2012b. Sphere-pac and VIPAC fuel. In: Konings, R.J.M. (Ed.), Comprehensive Nuclear Materials. Elsevier, Oxford, pp. 275–312.

Richter, K., Fernandez, A., Somers, J., 1997. Infiltration of highly radioactive materials: a novel approach to the fabrication of targets for the transmutation and incineration of actinides. J. Nucl. Mater. 249 (2-3), 121–127.

Ring, T.A., 1996. 8.6 sol-gel synthesis. In: Ring, T.A. (Ed.), Fundamentals of Ceramic Powder Processing and Synthesis. Academic Press, San Diego, CA, pp. 340–355.

Ringel, H.D., Zimmer, E., 1979. External gelation of thorium process for preparation of ThO_2 and (Th, U)O_2 fuel kernels. Nucl. Technol. 45 (3), 287–298.

Sol-Gel Processes for Ceramic Nuclear Fuels. Panel Proceedings Series. Proceedings of a Panel Held in Vienna, 6-10 May 1968, International Atomic Energy Agency, Vienna, Austria, July 1968 (STI/PUB-207; CONF-680532).

Somers, J., Fernandez, A., 2006. Inert matrix kernels for actinide incineration in high temperature reactors. Prog. Nucl. Energy 48 (3), 259–267.

Sood, D.D., 2011. The role sol-gel process for nuclear fuels—an overview. J. Sol-Gel Sci. Technol. 59 (3), 404–416.

Streit, M., Ingold, F., Gauckler, L.J., Ottaviani, J.-P., 2002. (Pu,Zr)N annular fuel pellets shaped by direct coagulation casting. In: Journal of Nuclear Science and Technology: Proceedings of Actinide 2001 International Conference, Hayama, Japan, supplement 3, pp. 741–744.

Streit, M., Ingold, F., Pouchon, M., Gauckler, L.J., Ottaviani, J.-P., 2003. Zirconium nitride as inert matrix for fast systems. J. Nucl. Mater. 319, 51–58.

Suzuki, M., 2008. Development of FR fuel cycle in Japan(3)—current state on unified technology of denitration conversion and granulation for simplified pellet fuel fabrication based on microwave heating. In: Proceedings of the 2008 International Congress on Advances in Nuclear Power Plants (ICAPP '08), Anaheim, California, June 8-12, 2008, pp. 2036–2045.

Terrani, K.A., Snead, L.L., Gehin, J.C., 2012. Microencapsulated fuel technology for commercial light water and advanced reactor application. J. Nucl. Mater. 427 (1-3), 209–224.

Tian, W., Pouchon, M.A., Qin, Z., 2014. Cooling less internal gelation for the production of nuclear fuel. J. Sol-Gel Sci. Technol. Submitted for publication.

van der Brugghen, F.W., Noothout, A.J., Hermans, M.E.A., Kanij, J.B.W., Votocek, O., 1970. A U(VI)-process for microspheres production. In: Proceedings of the Symposium on Sol-Gel Processes and Reactor Fuel Cycles, Gatlinburg, TN, May 4-7, 1970, pp. 253–263.

Weber, G.W., Beatty, R.L., Tennery, V.J., 1977. Processing and composition control of weak-acid resin-derived fuel microspheres. Nucl. Technol. 35 (2), 217–226.

Yamagishi, S., Hasegawa, A., Ogawa, T., 1994. Development of Rapid Gelation Apparatus with Microwave Heating. JAERITech 94-010.

Ye, B., Miao, J.-L., Li, J.-L., Zhao, Z.-C., Chang, Z., Serra, C.A., 2013. Fabrication of size-controlled CeO_2 microparticles by a microfluidic sol-gel process as an analog preparation of ceramic nuclear fuel particles. J. Nucl. Sci. Technol. 50 (8), 774–780.

Zimmer, M., 2000. Molecular mechanics evaluation of the proposed mechanisms for the degradation of urea by urease. J. Biomol. Struct. Dyn. 17 (5), 787–797.

International developments in electrorefining technologies for pyrochemical processing of spent nuclear fuels

15

R.G. Lewin, M.T. Harrison
National Nuclear Laboratory, Central Laboratory, Sellafield, Seascale, UK

Acronyms

ACP	advanced spent fuel conditioning process
ACSEPT	actinide recycling by separation and transmutation
An	actinide
ANL	Argonne National Laboratory (-W: West, -E: East)
CEA	Commissariat à l'Energie Atomique
CEFR	Chinese Experimental Fast Reactor
CIAE	China Institute of Atomic Energy
CRIEPI	Central Research Institute of Electric Power Industry
DEOX	declad and oxidize
DER	direct electrochemical reduction
DF	decontamination factor
DOVITA	dry oxide vibropacking integrated transmutation of actinides
DPV	differential pulse voltammetry
EBR II	Experimental Breeder Reactor II
ENEA	Italian National Agency for New Technologies, Energy and Sustainable Economic Development
ER	electrorefining
FBR	fast breeder reactor
FP	fission product
FR	fast reactor
GWe	gigawatt electric
HLLW	high-level liquid waste
IAEA	International Atomic Energy Agency
IFR	integral fast reactor
IGCAR	Indira Gandhi Centre for Atomic Research
INERI	International Nuclear Energy Research Initiative
INL	Idaho National Laboratory
ITU	Institute for TransUranium Elements
JAEA	Japan Atomic Energy Agency
KAERI	Korean Atomic Energy Research Institute
LCC	liquid cadmium cathode

Reprocessing and Recycling of Spent Nuclear Fuel. http://dx.doi.org/10.1016/B978-1-78242-212-9.00015-0

LKE	lithium potassium eutectic (salt)
Ln	lanthanide
LWR	light water reactor
MA	minor actinide
MOX	mixed oxide
MSR	molten salt reactor
MWe	megawatt electric
NEA	Nuclear Energy Agency
NM	noble metal
NPV	normal pulse voltammetry
OECD	Organisation for Economic Co-operation and Development
P&T	partitioning and transmutation
PFBR	prototype fast breeder reactor
PRIDE	pyroprocess inactive integrated demonstration
PWR	pressurized water reactor
R&D	research and development
REEs	rare earth elements (lanthanides)
RIAR	Russian Institute of Atomic Reactors
ROK	Republic of Korea
SF	separation factor
tHM	tons heavy metal
TRU	transuranium (elements)
USDOE	U.S. Department of Energy

15.1 Introduction

Increasingly, it is being recognized that the use of nuclear energy will be required to achieve a satisfactory security of supply for electricity for many nations and, as a consequence, the demand for economically viable, safe, and proliferation-resistant nuclear fuel cycle solutions will be sought. One essential component of these objectives is the effective management of spent nuclear fuel. A review by the International Atomic Energy Agency (IAEA) (Lovasic, 2008) estimated that, in 2010, the cumulative waste arising from the world's nuclear energy production would be in the region of 340,000 tons heavy metal (tHM), rising to an estimated value of 445,000 tHM in 2020. Development of advanced fuel cycle strategies necessitate the development of both reactor systems and complementary and compatible fuel cycles.

The quest for pyrochemical alternatives to aqueous reprocessing started in the United States and Russia around the late 1950s, with the metal electrorefining (ER), oxide electrowinning, and fluoride volatility processes winning greatest acceptance internationally. Electrorefining now has wide international interest, with research and development (R&D) being performed in the United States, the Republic of Korea (ROK), Japan, India, and Europe; while oxide electrowinning is favored in Russia with R&D also being performed in Japan and India. R&D on fluoride volatility now takes place predominantly in Russia and the Czech Republic.

Advantages of pyrochemical processes, for Generation IV fuel cycles, are claimed to include

- Good integration of reactor operation and fuel processing;
- High resistance of molten salt and liquid metal solvents to radiation damage that is especially valuable for short-cooled and high-burn up fuels such as the fast breeder reactor (FBR) type;
- Higher fissile mass limits in salt as compared to aqueous solution or as metal;
- Low quantities of wastes arising;
- Inherent actinide (An) partitioning with good nonproliferation characteristics and well suited to future fast neutron cycles where low decontamination factors (DFS) are acceptable;
- Simplicity and compactness of equipment;
- Low off-gas flows and simplified noble fission gas recovery;
- Compatible with inert matrix fuel chemistries and the dissolution and processing of fuels of high plutonium content; and
- Suited to high minor actinide (MA) concentrations found in fuels of some accelerator-driven system and critical burner reactor partitioning and transmutation (P&T) cycles.

This chapter sets out to provide a state-of-the-art review of nonaqueous reprocessing options for spent nuclear fuel. Particular emphasis has been placed on one of the numerous options discussed: pyrochemical reprocessing using LiCl-KCl (LKE) molten salt, which represents the pyrochemical technology option receiving the greatest international development funding.

15.2 Molten salt technologies

Pyrochemical techniques form a powerful range of chemical, electrochemical and physical treatments for separations of nuclear materials. They include the following:

- Oxidation/reduction with selective extraction between metal and salt phases
- Electrowinning
- Electrorefining
- Electroslag refining in molten salts
- Precipitation, coprecipitation, and fractional crystallization from melts
- Selective absorption of species in molten media (e.g., ion exchange, zeolite occlusion)
- Chemical transport (e.g., conversion to unstable compounds)
- Vapor phase transport (e.g., fluoride volatility with gas/solid reactions)
- Physical methods including melting, alloying, zone refining, transport by differential solubility, volatilization, vacuum distillation, sintering, and hot pressing

A short summary of the most relevant technologies related to advanced fuel cycles is provided in Sections 15.2.1–15.2.3.

15.2.1 Molten salt reactors

The molten salt reactors (MSR) concept was first developed in the United States in the 1960s as a backup option to the FBR (http://www.world-nuclear.org/info/Nuclear-Fuel-Cycle/Power-Reactors/Generation-IV-Nuclear-Reactors/, December 2010.DE07003/06/48/29.). MSRs are one of the Generation IV reactor systems that do not have a solid phase

fuel but comprise a molten fluoride-based salt in which fuel is dissolved. A wide range of fuels is possible, which include thorium. Fertile ^{232}Th can be introduced to the system where it can be converted to fissile ^{233}U, the main reactor fuel (http://www.world-nuclear.org/info/Nuclear-Fuel-Cycle/Power-Reactors/Generation-IV-Nuclear-Reactors/, December 2010.DE07003/06/48/29) (Research Agenda, 2012).

Molten salt flows through a neutron-moderating graphite core to produce heat. The heated salt is then passed to a complex set of heat exchangers that raise high-pressure steam to drive conventional steam turbines.

Removing fission products (FPs) from the salt system is required to sustain the fission process, which can be undertaken by processing a small purge stream of the salt diverted to a stand-alone separation unit, then returning the "clean" salt to the reactor. Pyrochemical processes to cleanup and recycle the fuel are considered ideal for this system. A general schematic of the cleanup is shown in Figure 15.1 (Generation IV International Forum, 2011).

15.2.2 Liquid-liquid extraction

In the CEA's (Commissariat à l'Energie Atomique) pyrochemical R&D program, an innovative fluoride process has been developed that allows a grouped separation of the actinides with sufficient decontamination of FPs. Previous lab-scale studies had demonstrated an effective immobilization of up to 15 wt% fluoride salt in a glass-ceramic matrix compatible with existing industrial-scale nuclear waste vitrification processes (Grandjean, 2005). These results led to the development of a novel reference process (Lacquement et al., 2005; Boussier, 2006; Mendez et al., 2012a), which is shown in Figure 15.2 (Mendez et al., 2012b), with the current areas of experimental investigation indicated by the red circles.

The process has, at its core, two different liquid-liquid extractions, which are shown schematically in Figure 15.3. The first consists of the reductive extraction of actinides from spent fuel dissolved in a molten fluoride salt into liquid metallic aluminum, that is,

$$AnF_{3\,(\text{salt phase})} + Al_{(\text{metal})} = AlF_{3(\text{salt phase})} + An_{(\text{metal})}$$

The aluminum acts as both the reductant and solvent for the actinides, resulting in an aluminum-actinide alloy. In order to remove the actinides from this alloy, it is then necessary to perform a liquid-liquid oxidative back-extraction using a molten chloride salt containing $AlCl_3$, that is,

$$An_{(\text{metal solvent})} + AlCl_{3\,(\text{salt phase})} = AnCl_{3\,(\text{salt phase})} + Al_{(\text{metal solvent})}$$

The first stage has been demonstrated by using various LiF-AlF_3 eutectics at ~830 °C, and the latter using LiCl-$CaCl_2$ (30-70 mol%)-$AlCl_3$ at 700 °C, providing a complete assessment of the core of the CEA's reference pyrochemical process (Mendez et al., 2012a). Recent studies have shown that the reductive extraction efficiency decreases with an increase of the AlF_3 content of the salt and that uranium is the most difficult element to be back-extracted (plutonium and americium recovery is almost quantitative) (Mendez et al., 2012a).

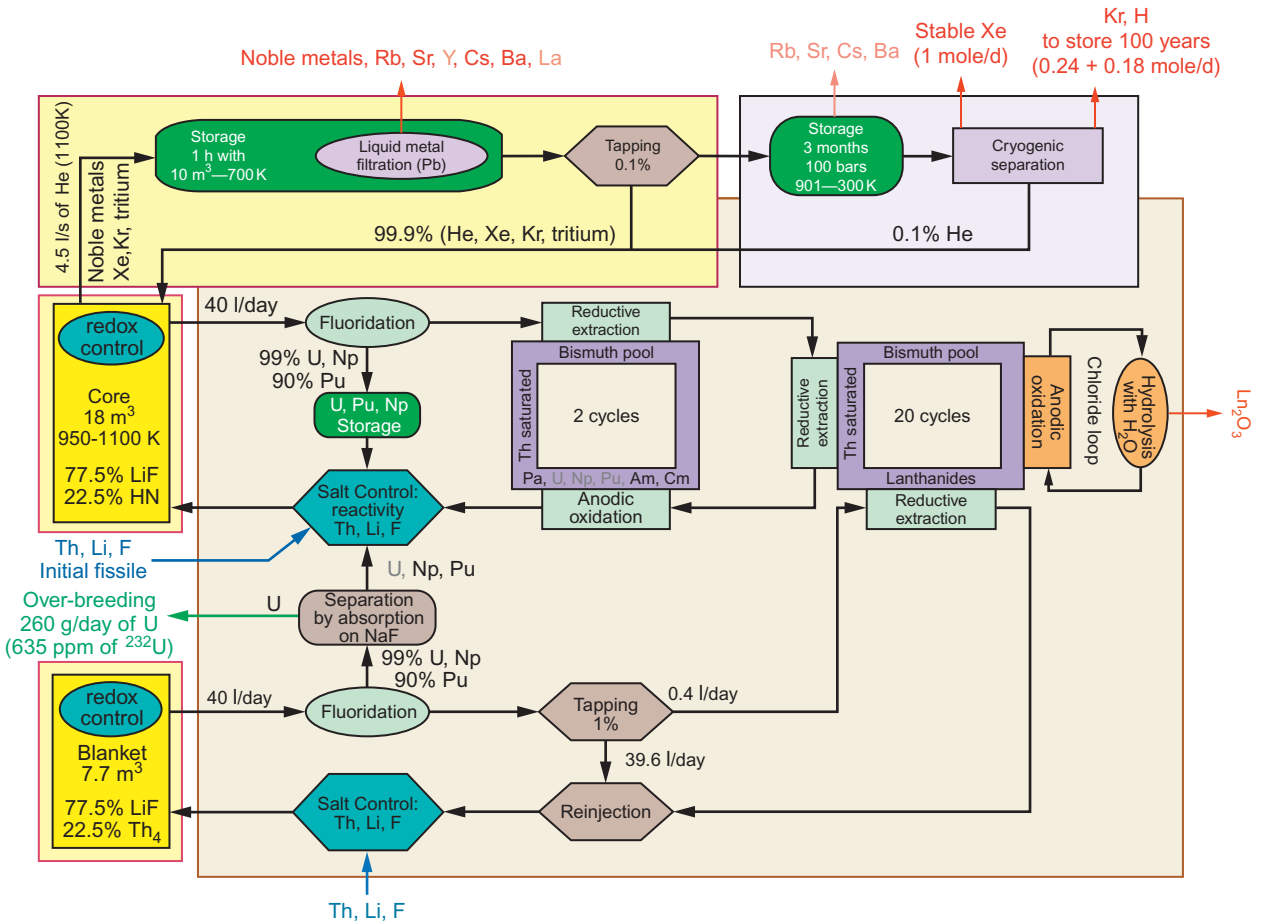

Figure 15.1 Fuel salt management scheme for a MSR (Generation IV International Forum, 2011).

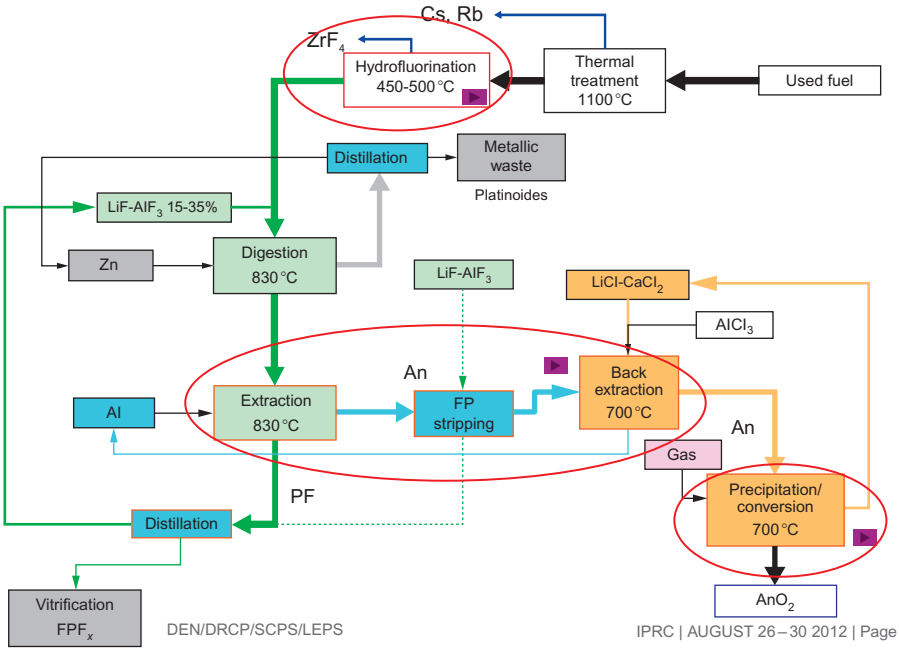

Figure 15.2 CEA's liquid-liquid extraction process flow sheet indicating current areas of investigation (Mendez et al., 2012b).

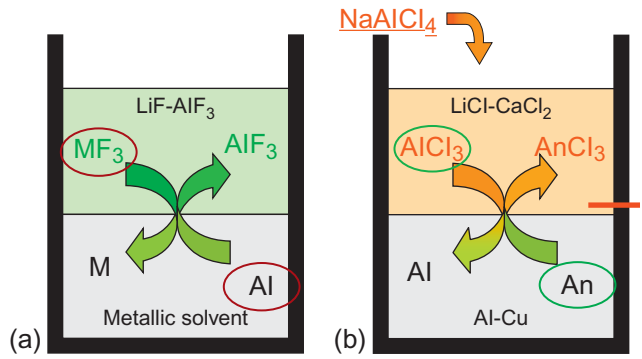

Figure 15.3 Schematic of the two main CEA extraction processes: (a) reductive extraction and (b) oxidative back-extraction (Mendez et al., 2012b).

The other stages of the process that are currently being studied are the headend steps and conversion of the back-extracted $AnCl_3$ into oxides for the refabrication of nuclear fuel. The former consists of a hydrofluorination of the oxide spent fuel, which is carried out between 300 and 500 °C for several hours using HF generated in situ. It has been shown that the lanthanide oxides all convert to fluorides, whereas the transition metals all remain as oxides. For the latter, the technique of wet argon

sparging has been shown to be effective, producing a mixture of UO_2 and PuO_2, although further investigations are needed.

In terms of future perspectives, a few of the unit operations in Figure 15.2 need to be demonstrated and tested using genuine spent fuel and an alternative headend process that does not use HF is under investigation. Furthermore, the waste treatment aspects of the process have not been well studied. Distillation is the only method that has been investigated for cleaning and removing the FPs from the LiF-AlF_3, and the process was far from optimized (Bourg et al., 2012).

15.2.3 Electrodeposition-based processes

15.2.3.1 Electrowinning (RIAR process)

The Russian Institute of Atomic Reactors (RIAR) has developed processes for dry recycle of oxide fuels (Bychkov et al., 1993, 1997; Kormilitzyn et al., 2000; Organisation for Economic Co-operation, 2004) based on the following:

- Pyroprocessing of spent oxide fuel to produce a dense recycled granulated fuel particle product and waste treatment.
- Manufacturing of fuel pins by the vibropac method.
- Remote automated equipment for reprocessing and fuel manufacturing.

Electrochemically, uranium and plutonium oxides behave like metals. During salt dissolution, they form complex oxygen ions MeO_2^{n+}, which are reduced at the cathode to oxides. At higher temperatures (>400 °C), UO_2 and PuO_2 have poor conductivity in comparison to the melt, which creates a flat front of crystallization with compact cathode deposits. In molten alkali chlorides, the stable oxidation states of uranium are U(III), U(IV), and U(VI). The highest states of plutonium oxidation, Pu(V) and Pu (VI), are stable only for particular oxidation-reduction potentials of the system. For electrocodeposition of UO_2 and PuO_2, the melt must be treated with a chlorine-oxygen sparge to create the required PuO_2^{2+} ion concentration. Plutonium can be converted from all oxidation states to oxide by change of the oxidation-reduction potential. This process is called *precipitative crystallization*. Under oxidizing conditions, uranium stays in the melt and plutonium can be preferentially precipitated. UO_2^{2+} and PuO_2^{2+} are reduced at positive potentials in comparison to FPs; therefore, purification of UO_2 and PuO_2 occurs during electrodeposition. Various size chlorator-electrolyzers have been tested for fuel processing, which differ only in crucible volume. Pyrolitic graphite is used as working materials for bath, anode, cathode, and gas tubes. Further equipment is used for crushing cathodic deposits, removal of salts, drying, and classification. RIAR has demonstrated electrodeposition of UO_2, electrocodeposition of UO_2-PuO_2, and precipitation of PuO_2 using uranium and mixed oxide (MOX) fuels.

An indicative electrowinning process described in Figure 15.4 was developed within the DOVITA (dry oxide vibropacking integrated transmutation of actinides) program (National Programmes in Chemical Partitioning—A Status Report et al., 2010; Organisation for Economic Co-operation, 2004) and comprises the following typical unit operations: decladding, dissolution, electrodeposition, crystallization, salt cleanup, and product processing prior to vibropac (NEA-OECD, 2012; DOE Nuclear

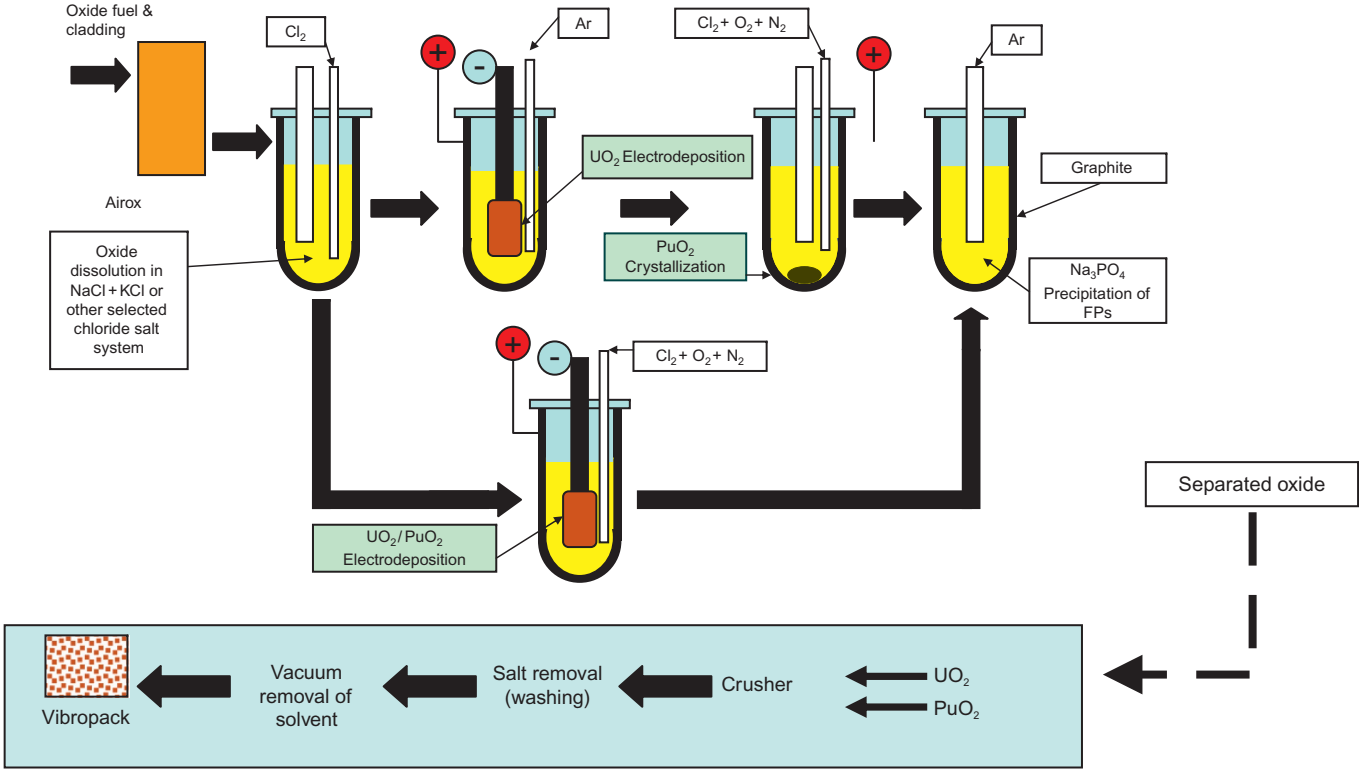

Figure 15.4 Oxide electrowinning from spent oxide fuel.

Energy Research Advisory Committee and the Generation IV International Forum, 2002), as shown in Figure 15.4. A second UO_2 electrodeposition process can also be performed after PuO_2 crystallization, if required. Figure 15.4 shows a number of representative unit operations. It should be noted that these take place in one single reactor vessel made of pyrolytic graphite.

15.2.3.2 Electrorefining process

Today, there are a number of organizations working to develop various technology elements for the pyrochemical electrorefining process. However, at this point in time, there is no generally agreed process flow sheet or agreed key steps in the process. It must, therefore, be stated that the following process steps are to be considered generic, and comprise unit operations that have been investigated by several organizations. An overview of these is provided in Figure 15.5. This process is discussed in much greater detail in Section 15.3.

The process steps in the metal electrorefining process for the integral fast reactor (FR) fuel cycle may be summarized as follows:

- Fuel receipt and dismantling
- Fuel decladding/hulls separation
- Oxide reduction (if processing oxide fuels)
- Electrorefining
  - Anodic dissolution of spent fuel
  - Cathodic deposition of actinides onto/into solid or liquid electrodes
- Cathode processing
  - Solid electrode-salt removal by volatilization
  - Liquid electrode (cathode) actinide separation by distillation
  - Actinide metal casting/blending for store or recycle
- Anode processing
  - Removal of sludge
  - Removal of hulls
- Salt cleaning and recycle
  - Actinide strip
  - Reductive extraction of FPs

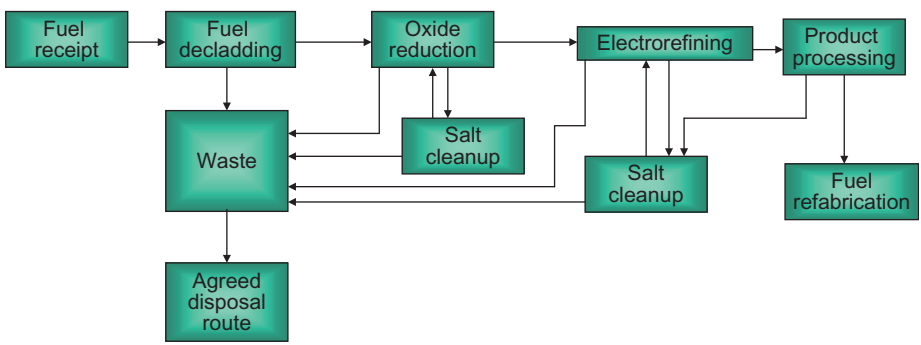

Figure 15.5 Schematic representation of the ER process.

  - Phosphate precipitation of FPs
  - Zeolite polish
  - Recycle or sentence to waste
- Actinide recovery through cathode reprocessing
- Wastes
  - Recovery of FPs from reductive extraction by distillation
  - Oxidation and immobilization of FPs within a glass-sodalite ceramic waste form
  - Immobilization of phosphate waste in glass or glass ceramic
  - Immobilization of noble metal (NM) FP anode sludges and cladding hulls as a stainless steel-zirconium metal waste form by melting (~1600 °C)

It should be noted that the above example is generic and describes process options for spent metal and oxide fuels. In the case of oxide fuels, a reduction step is necessary before electrorefining. A detailed analysis of all the different unit operations for both metal and oxide fuels is provided in Section 15.3.

The main separation step is performed in the electrorefining unit operation, although some decontamination is likely in earlier process steps. Electrorefining of irradiated metallic fuel is performed in LiCl-KCl salt. Batches of fuel are anodically dissolved and uranium is electrotransported to a solid iron cathode, where it deposits in purified form. Plutonium, MA, and reactive FPs convert to chlorides and accumulate in the salt. FPs that are unreactive generally accumulate as metallic solids in the anode baskets (anode sludge). When a number of fuel batches have been treated, the plutonium is recovered as a Pu-U-MA alloy in an LCC with a "pounder" for interfacial agitation to maximize transuranium (TRU) electrodeposition and prevent growth of pure uranium from the cathode-salt interface.

15.3 Status of electrorefining

15.3.1 Introduction

The term electrorefining (ER) is used here to collectively describe all the unit reprocessing operations associated with the core actinide separation step, and does not include headend fuel preparation and subsequent waste treatment processes. Today, there are several international research institutes and organizations developing this process for the future recycling of spent nuclear fuel. A full description of the electrorefiner unit operations can be found in Section 15.3.3.

15.3.2 Fuel preparation

Fuel preparation for an ER flow sheet is not expected to be significantly different than that already used throughout the nuclear industry. Fuel pins would be chopped by conventional methods to produce short segments, typically 2.5-5.0 cm.

For metallic FR fuel, the fuel segments and metallic fines produced in the chopping process are collected and transferred directly to a basket that serves as the anode in the electrorefining process.

Oxide fuels have to be reduced to a metallic feed prior to electrorefining. Hence, the fuel cladding has to be removed. This can be achieved using conventional mechanical methods, although the majority of the proposed ER flow sheets use a high-temperature pretreatment process such as voloxidation or declad and oxidize (DEOX) (see Section 15.4.6.1) (NEA-OECD, 2012; DOE Nuclear Energy Research Advisory Committee and the Generation IV International Forum, 2002; Westphal et al., 2007).

Note, however, that it has been found that after the DEOX process, sufficient amounts of spent fuel still remain in the cladding hulls to classify them as HLW. In order to significantly reduce the TRU elements being sent into the waste streams, Seoul National University (SNU) has proposed a hull electrorefining stage as part of their PyroGreen process. The PyroGreen process (NEA-OECD, 2012) uses Korean Atomic Energy Research Institute (KAERI)'s pyroprocessing flow sheet but with three additional stages to significantly reduce the amount of TRUs in the waste: hull electrorefining, salt purification, and technetium/iodine target fabrication for transmutation.

15.3.2.1 Hull electrorefining

Multistage hull electrorefining is employed in the PyroGreen process for the recovery of zirconium, uranium, and TRU from the waste stream, with the actinides recycled back to the main process stream. Both the cladding hulls containing residual fuel from the DEOX stage and the uranium and NM remaining at the anode of the electrorefiner (see Section 15.3.3) are fed into the process, which is shown schematically in Figure 15.6. Literature results have shown that hull electrorefining can yield a very high DF to produce high-purity zirconium, free from significant radioactive contamination (Goto et al., 2009).

15.3.3 Oxide reduction

For an electrorefining pyrochemical process to be applied to a spent oxide fuel, the oxide must first be reduced into its metallic form. To date, this has been done by either contact with lithium metal or direct electrochemical reduction (DER). This provides the metal feed for the electrorefiner. These two approaches are discussed below.

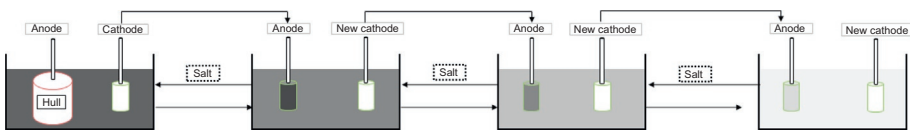

Figure 15.6 Schematic of multistage countercurrent hull electrorefining.

15.3.3.1 Oxide reduction using lithium metal

The reduction of UO_2 and PuO_2 by lithium metal is described by Usami et al., (2002). Lithium metal is dissolved in LiCl salt at 650 °C. LiCl is then contacted with the actinide oxide. The oxides are reduced to metal and lithium is converted to Li_2O. UO_2 was converted to a porous solid metal, whereas the PuO_2 was converted to a molten metal product. The concentration of Li_2O influenced the extent of reduction. Americium oxide, present in the PuO_2, could be reduced at Li_2O concentrations of 1.8 wt%. However, at 8.8 wt%, little reduction was observed.

Reduction of actinides can be achieved by contacting lithium metal with metal oxide as described; however, this process necessitates the recovery of lithium metal from the Li_2O formed. Additional process steps, while feasible, are not particularly favored when the process is to be remotely operated. DER has less unit operations and has thus become the preferred technique to convert actinide oxides to metal.

15.3.3.2 Direct electrochemical reduction

Oxide reduction is simple in principle: spent metal oxide fuel is introduced into a cathode basket and loaded into a cell containing an electrolyte of, usually, LiCl containing ~1 wt% Li_2O. An appropriate potential is applied to the cathode, sufficient to reduce the oxide to metal without breaking down the salt to produce lithium metal. Oxygen is transported through the electrolyte, as oxide ions, to the anode, where they are removed as oxygen, carbon monoxide, or carbon dioxide (i.e., when the anode is a carbonaceous material). A general schematic is shown in Figure 15.7.

Considerable research has been invested in this technology, and key areas include the following:

- Oxide form—Particle size and oxidation state, UO_2 versus U_3O_8
- Oxide ion concentration in the salt
- Basket materials of construction
- Anode materials
- Scale-up for industrialization

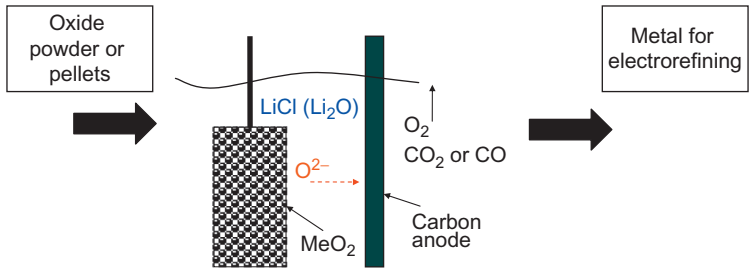

Figure 15.7 Schematic arrangement of a direct electrochemical reduction process.

15.3.4 Electrorefining

Electrorefining of irradiated metallic fuel is currently a batch process performed in a LiCl-KCl salt. Batches of fuel are anodically dissolved with the uranium electrotransported to a solid iron, steel, or graphite cathode where it deposits in purified form. Plutonium, MAs, and reactive FPs convert to chlorides and accumulate in the salt. FPs that are unreactive, NMs and residual oxide from the reduction step, generally accumulate as metallic or oxide solids in the anode baskets to form an anode sludge. When a number of fuel batches have been treated and the TRU concentration has reached a suitable value, plutonium and MAs are recovered from the salt as a Pu-U-MA alloy in an LCC. A "pounder" is used to create interfacial agitation at the liquid cadmium surface to maximize TRU electrodeposition and prevent growth of pure uranium from the cathode-salt interface. Recovery of the actinides from the deposition process is completed using a cathode processor.

Considerable laboratory-scale R&D has been completed over the last two decades to establish a broad range of data to underpin scale-up and industrialization; for example, DFs for voloxidation, separation factors (SFs) for solid and liquid metal cathodes, cathode deposition efficiencies and actinide recovery from product. The Institute for Transuranium Elements (ITU) have studied both solid and liquid cathode systems and are now looking at aluminum, which behaves more like a gel rather than a solid or liquid, and is reported to have improved actinide selectivity (Malmbeck et al., 2011). Studies of anodic processes at Idaho National Laboratory (INL) have led to the conclusion that diffusion of reactants from a metal alloy fuel, and thus anodic dissolution, is the rate-controlling step in the ER (Benedict et al., 2007; Simpson, 2012). The dissolution process is, under normal conditions, performed using a constant current; however, studies have also shown that the anode voltage becomes more positive with time, which can lead to increased zirconium metal dissolution. An inverse relationship between uranium dissolution and zirconium metal retention was found during these studies (Li and Simpson, 2005; Li et al., 2005; Simpson, 2012).

Engineering-scale development has continued to progress as greater emphasis is placed on industrialization and some highly innovative approaches to electrorefiner design have been taken. INL continue to develop their Mark IV and V electrorefiner designs and modes of operation to improve anodic dissolution and cathodic deposition and actinide recovery. KAERI are developing a number of innovative approaches to support a continuous industrial process, namely:

- The separation of electrorefining into electrorefining and electrowinning of uranium and uranium plus TRUs, respectively.
- A process that comprises a "nonstick" graphitic cathode, thus producing a self-scraping graphite cathode system.
- A mechanical product transfer system (Kim et al., 2012; Lee et al., 2007).

CRIEPI (Central Research Institute of Electric Power Industry) have designed a system in which anode baskets are located in the center while the cathode is formed by the inner wall of the vessel. The dendrites are removed by scraping and collection in a basket located at the bottom of the vessel (Koyama et al., 2009; Shirai et al., 2000).

Deposition of uranium and the TRUs to a liquid cathode has been demonstrated at laboratory scale and engineering scale in the INL Mark IV ER, recovering >4 kg of TRU material (Benedict et al., 2007). Management of the liquid cathode is a major concern. Migration of the molten metal throughout the electrolyser, due to its high vapor pressure (Simpson, 2012) is problematic, together with poor elemental selectivity, although this may support the argument for increased proliferation resistance due to product impurity levels. Uncontrolled growth of metal dendrites from the liquid metal surface has also been observed when the liquid metal has reached its saturation limit for uranium and TRUs. Agitation of the metal surface to submerge growing dendrites using a ceramic "pounder" has been the main approach to minimizing dendritic growth.

INL have performed work to demonstrate that the performance of the anode is rate limiting in the electrorefining process and work is ongoing to improve electrochemical dissolution. Further studies will be necessary to develop a better understanding of the system for both metal and oxide spent nuclear fuel, because these arrive in an anode basket with and without cladding material, respectively. The performance characteristics will, therefore, necessarily be different.

Anodic "sludge" will be produced as part of the anodic process. This will comprise cladding material, NMs, and fuel fragments from metal fuels and NMs and residual oxide from the reduction step, in the case of an oxide fuel. Metal fuel sludge will be sent to the cathode processor to remove the salt and consolidate the product as a metal ingot prior to disposal. Oxide fuel sludge will have a NM/oxide separation and recycle step to maximize overall actinide recovery.

15.3.5 Product processing

15.3.5.1 Cathode processing

Cathode processing is a high-temperature distillation process performed under vacuum. It comprises a process vessel, induction furnace, crucible, and condenser/collector. It was originally developed for purifying and consolidating both solid cathode uranium product and liquid cathode TRU products.

The solid cathode product removed from an ER comprises metal uranium dendrites containing a large volume of entrained salt. Using the processor, salt is vaporized and condensed under vacuum, while the metal dendrites melt and coalesce in the process vessel to form a product in the form of a metal ingot. In the case of an LCC containing uranium and TRUs, this again, is heated under vacuum; the cadmium is distilled, condensed, and collected for reuse while the uranium and TRU product remain as a solid metal ingot in the process vessel. In both cases, the separated salt is returned to the ER unit.

15.3.5.2 Anode processing

At the anode, fuel fines and NMs, including cladding hulls or inert matrix material (zirconium), are retained with the anode after electrorefining. These materials are removed from the anode baskets and loaded into a vacuum distillation unit to remove any adherent salt. The metals are melted and consolidated in the process to produce a

metal waste form suitable for disposal in a high-level waste repository (Simpson and Law, 2003). Work has been completed to understand and characterize the metal waste form (Simpson, 2012).

15.3.6 Salt cleanup

15.3.6.1 Actinide recovery

In order to meet the sustainability requirements of advanced nuclear fuel cycles and minimize the inventory of long-lived radionuclides being sent to waste, it is necessary to maximize the amount of actinides recovered in any pyrochemical separation process. Hence, following the main electrorefining separation stage(s), any residual actinides present in the LiCl-KCl salt must be removed prior to it being sent for FP cleanup and recycle. A number of different options for this process are currently being investigated worldwide:

- Exhaustive electrolysis on a solid (aluminum) cathode (Souček et al., 2010, 2011).
- Exhaustive electrolysis on a liquid (cadmium) cathode plus oxidation of lanthanides (Song et al., 2010).
- Multistage reductive extraction using bismuth (Kinoshita et al., 1999).
- Hydrometallurgical chromatography.
- Chemical reduction/oxidation (Simpson et al., 2012).

Exhaustive electrolysis: Solid cathode

This process, shown schematically in Figure 15.8, is a group-selective electrolysis using a chlorine gas-producing inert anode with actinides deposited on a solid aluminum cathode forming An—Al alloys (Souček et al., 2010). It is currently being investigated by ITU, Germany, where proof-of-principle experiments have been undertaken. Most notably, a chlorine gas-producing inert anode has been designed

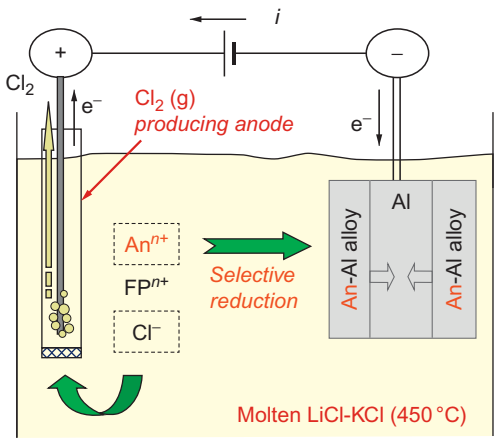

Figure 15.8 Schematic of the exhaustive electrolysis process.

and successfully tested, although management of Cl_2 and scale-up are still significant issues for this process.

Note efficient recovery of actinides from the An-Al alloys formed by exhaustive electrolysis is key for establishing the feasibility of the overall process. However, the An-Al alloys will be similar to those produced in an electrorefining process using solid aluminum cathodes; hence, the same process for actinide recovery can be used (i.e., chlorination) (Souček et al., 2011). The chlorination method is based on the different volatilities of $AnCl_3$ and $AlCl_3$ and comprises four main steps, which are shown schematically in Figure 15.9:

- Vacuum distillation for removal of salt adhered on the electrodes after the electrochemical separation process.
- Chlorination of the entire deposit (An—Al alloys) by chlorine gas.
- Sublimation of the resulting $AlCl_3$ by heating under inert atmosphere.
- Conversion of the nonvolatile $AnCl_3$ into metals via reduction.

Exhaustive electrolysis: Liquid cathode

The residual actinide recovery process, which combines electrolysis using an LCC and chlorination of lanthanide FP, is being developed by KAERI (Song et al., 2010). The first stage is the LCC electrolysis that collects all of the residual actinides and some of the lanthanide FP to form a Cd—An—Ln alloy. In the second stage, $CdCl_2$ is added to the cadmium alloy, whereupon the lanthanide elements are selectively chlorinated and redissolve back into the LiCl-KCl salt. The actinides are then recovered from the cadmium using a distillation process, which is the same as that used in the main actinide separation process. Indeed, one advantage of this process is that it uses the same compact LCC equipment developed for the core separation stage. Again, proof-of-principle experiments have been demonstrated at laboratory scale (Song et al., 2010).

Multistage reductive extraction using bismuth

The multistage extraction process proposed by Kinoshita of CREIPI in Japan (Kinoshita et al., 1999) was investigated for the treatment of salt containing actinides, lanthanides, and alkaline earth FP. It comprises the sequential addition

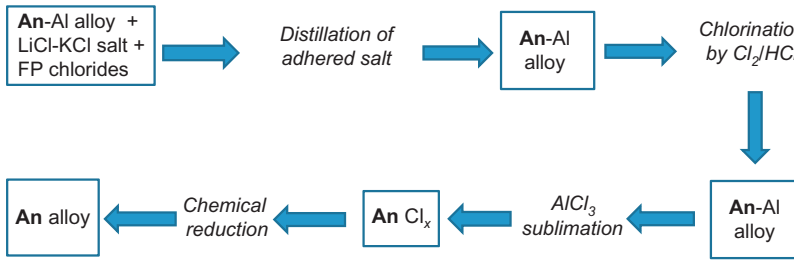

Figure 15.9 Schematic of the process for recovery of the actinides from an An-Al alloy.

of bismuth-lithium alloy at ~500 °C, with the actinides preferentially extracted into the liquid metal phase, separated from the lanthanides by the difference in distribution coefficients between LiCl—KCl and bismuth. Multiple-batch experiments have been performed with five additions of Bi-Li, which gave > 99% of the actinides extracted into the bismuth phase. In addition, a countercurrent extraction method using the same principle was simulated, which indicated potentially higher An—Ln separation efficiencies.

Chemical reduction/oxidation

Using a similar principle to the above, Simpson et al. of INL have recently proposed selective precipitation as a means of removing residual actinides from waste LiCl—KCl salt (Simpson et al., 2012). Both chemical reduction using lithium and oxidation using Li_2O additions were proposed, as these processes are suitable for scale-up and avoid the issues of chlorine evolution inherent with electrolysis. The main concerns, however, were the lack of selectivity between actinide and lanthanide ions and product recovery.

Preliminary results using surrogates for the actinides confirmed the drawback of low selectivity for specific species, but lithium metal reduction performed better in this respect. Furthermore, the thermodynamic proximity of plutonium and the lanthanides is expected to lead to some loss of plutonium into the waste stream or substantial carryover of lanthanides into the reduced product.

15.4 International programs

Pyrochemical R&D and engineering studies for nuclear process applications are underway in the Czech Republic, the European Union (EU), France, Italy, Japan, the ROK, the Russian Federation, the United Kingdom and the United States. Further countries involved with such work, now or previously, include Belgium, Spain, China, India, and the Netherlands. Many of the studies are scientific and small-scale, technical assessments/design studies, although a limited number are larger-scale demonstrations. For example, the electrowinning process at RIAR, Dimitrovgrad, which has been used to treat and reprocess irradiated fuels.

Major worldwide studies include the Argonne National Lab (ANL) integral fast reactor (IFR) recycle process in the United States, where metallic fuel was electrorefined in a LKE molten salt with separated products recycled as FR fuel. CRIEPI in Japan participated as a major collaborator in the IFR program until program termination in 1995. More recently, electrometallurgical treatment has been used to condition FR fuel at INL (before February 2005, this site was known as ANL-West) in the United States for storage and disposal. The former Soviet Union and now Russian program at RIAR has successfully tested the electrowinning process on 7000 kg of unirradiated fuel and 40 kg of BN-350 and BOR-60 irradiated oxide fuel (Bychkov, 2008).

Japan continues its R&D program building on its fundamental scientific studies, again with a focus on industrialization. Integrated facilities have been constructed and an electrorefiner developed to improve throughput. Pyrochemical processes, post Fukushima, are considered as potential options for treating legacy materials from the Fukushima incident.

The ROK has a major research program. All facets of the electrorefining program are being investigated at laboratory scale and many at engineering scale. A strong focus has been placed on industrialization, and a large-scale integrated facility named PRIDE (pyroprocess inactive integrated demonstration) is planned for operations in 2017. The ROK and the United States are collaborating under the International Nuclear Energy Research Initiative (INERI) program.

India is undertaking a wide range of pyrochemical R&D activities. Several pyrochemical technology options are being evaluated at laboratory or small scales. Early fuels for treatment will be oxide fuels from FRs. However, in the longer term, fuels are likely to be metal fuels, as they provide an improved plutonium breeding ratio over oxide and carbide fuels, which is an essential component of the 3-stage plan for the nuclear fuel cycle in India.

Within Europe, relatively small-scale R&D is being performed. The major contributors are CEA, ITU, and the Nuclear Research Institute Rež (Czech Republic). The R&D is focused on two reference scenarios: liquid-liquid extraction in molten fluoride and electrorefining in LKE onto solid aluminum cathodes. Studies have also included oxide reduction, to link a light water reactor (LWR) oxide fuel cycle to a metal-fueled FR recycle scenario; the "double strata" concept.

The United States and the Russian Federation have pyrochemical demonstration plants for metal fuel conditioning and oxide fuel recycling at INL and RIAR, respectively. They prove process viability even though an industrial-scale plant and associated cost level have not yet been shown.

Sections 15.4.1–15.4.7 provide a more detailed discussion with respect to the current status of nonaqueous reprocessing on an international basis. Note the level of detail does vary, but is, nevertheless, representative of the current status of that region.

15.4.1 India

Nuclear energy is expanding in India with a 3-stage approach to closing the fuel cycle, transitioning over time from thermal to FRs and, ultimately, implementation of the thorium fuel cycle. In the medium term, it is expected that the use of metal fuels, designed for their high breeding ratio, will be used in FRs. The exact choice of fuel has not yet been established, although the fuel selected is expected to have a burn up in the region of 200 GWd/t. The fuel cycle will also be short-cooled (<1 yr) to minimize out-of-pile inventory (Kutty et al., 2009).

During the early phase of development, the fast breeder test reactor at Kalpakkam has been used to test fuel pins. However, with a 500 MWe prototype fast breeder reactor (PFBR) at an advanced stage of construction, together with four more expected to be built by 2020, facilities to test metal fuel will become available (Reddy et al., 2010). These facilities will be sited at Kalpakkam, together with an FR fuel cycle facility that will include reprocessing, fuel fabrication, and waste management plants (Kutty et al., 2009).

Initial fuels for the PFBRs will be based on MOX. However, the use of oxide fuel will reduce such that, after 2020, metal fuel will be the primary fuel of use. A well-defined roadmap for the development of the metal fuel cycle has been established (Reddy et al., 2010), which in this case includes pyrochemical processing using the LiCl and LKE molten salt systems. A general flow sheet for the treatment of metal fuel is shown in Figure 15.6. R&D on all aspects of the fuel cycle for metal fuels is currently in progress (Reddy et al., 2010; Nagarajan, 2010; Nagarajan et al., 2011).

The R&D (Kutty et al., 2009; Reddy et al., 2010; Nagarajan, 2010; Nagarajan et al., 2011; Sri Maha Vishnu et al., 2012; Ghosh et al., 2009, 2011; Vandarkuzhali et al., 2012) at IGCAR (Indira Gandhi Centre for Atomic Research) in the area of molten salts is comprehensive and includes studies with respect to electrowinning of actinide oxides, separation processes linked to fluoride-based systems relevant to MSRs, and recycling fuel by dissolution in tin as well as electrorefining of metal fuel. In the area of electrorefining, the work comprises research in the areas of the following:

- Reduction
- Electrorefining-electrochemical studies on anodes and cathodes
- Analytical studies
- Materials development
- Development of waste forms

Active facilities have been designed and built at both laboratory and engineering scale. Laboratory-based studies are defined as those performed at gram scale and have included electrorefining experiments on uranium and uranium-bearing alloys, plutonium and plutonium alloys, including distillation of salt and cadmium together with product and metal consolidation.

Reduction studies include calciothermic reduction of metal fluorides and the DER of oxide. DER is covered in greater detail in Sections 15.3.3.2 and 15.4.6.2; however, in this case the system comprises a UO_2 (pellet) working electrode, platinum counter electrode, and platinum reference electrode in a LiCl—Li_2O salt, with the Li_2O concentration being between 2 and 3 wt% (Nagarajan, 2010). Consumption of the platinum anode has been problematic and further work is being performed on different anode materials; for example, tantalum, molybdenum, and graphite to improve the anode characteristics. Reduction of the oxide to metal was also found to be limited to the surface of the oxide pellet when reduction was performed in either $CaCl_2$ or LiCl salt systems. Propagation of the reduction through the oxide matrix has been proposed (Sri Maha Vishnu et al., 2012).

Reduction, in principle, also extends to the salt cleanup process where a liquid Li/Cd metal alloy is used to "drawdown" dissolved actinide species from the salt into the liquid metal as an alloy. This has been developed to an engineering-scale unit operation that is discussed later in this section.

Electrorefining studies have considered the reduction of U^{3+} at bulk cadmium and cadmium films and shown a 200 mV underpotential deposition of uranium at cadmium surfaces. Semistable uranium and UCd_{11} were also identified after the deposition of uranium at a bulk cadmium surface. The underpotential deposition of uranium and other species is a well-recognized phenomenon that allows group capture of the

actinides. However, other FPs are also reduced, which means the process is difficult to control and optimize. Anodic dissolution studies on U—Zr have shown that the alloy dissolves to form U^{3+} and $Zr^{2+/}Zr^{4+}$ and that zirconium oxidation to the +2 and +4 states is a two-stage diffusion-controlled process (Reddy et al., 2010; Nagarajan, 2010; Ghosh et al., 2011). The presence of zirconium metal influences the oxidation state of the zirconium ions in solution (Ghosh et al., 2009). Cathode studies have covered different electrode materials, including stainless steel and cadmium as well as aluminum (Vandarkuzhali et al., 2012), which in other studies have been claimed to have better selectivity for actinides. The PRAGAMAN code is being developed to model the electrorefining process. It is based on the thermodynamic equilibria between the actinides and FPs and will solve nonlinear equations under different electrorefining conditions.

Three electroanalytical techniques have been developed to quantify species in solution. Normal pulse voltammetry (NPV), differential pulse voltammetry (DPV), and square wave voltammetry have been used on an LKE salt containing 1 wt% UCl_3, 0.7 wt% $EuCl_3$, 1 wt% $CeCl_3$, and $LaCl_3$, respectively. Separate peaks for the different species were readily identified, and the presence of lanthanides did not influence the estimation of uranium concentration in solution. NPV and DPV gave a linear dependence of concentration across all species.

Larger-scale development, using facilities that can handle materials in the region of 1-3 kg of uranium or uranium alloys, is ongoing and being performed on the following:

- Chopping of fuel pins.
- Electrorefining, including salt transfer systems.
- Salt cleanup.
- Distillation.
- Development of manipulators.

Electrorefining comprised 1 kg of uranium metal in a rotating perforated stainless steel anode basket of cruciform geometry and a stainless steel cathode rod that appears to rotate between two vertical parallel rods. It is assumed these retain the dendritic deposit within a confined and predetermined volume. Electrolysis was galvanostatically controlled with the cathodic potential being ~ -1.5 to -1.6 V versus an Ag/AgCl reference electrode. The current efficiency for deposition was $\sim$60% with the deposit containing about 25 wt% occluded salt.

As of 2010, there were plans to clean up salt by transferring several liters of contaminated salt and Li-Cd alloy to a mixing vessel with “clean salt” and “spent” cadmium alloy returning to receipt tanks. This is a significant step in both engineering and scale-up, as the ability to move salt and liquid metal safely and effectively is a cornerstone to industrialization.

A distillation unit capable of consolidating 500 cm^3 of dendritic material has been designed and built. An MgO container is housed within a graphite crucible that acts as a susceptor for an induction heating process, and deposits are heated and melted at 1473 K. The chamber operates at 0.01 torr and salt vapor is cooled, condensed, and collected in a chamber above the hot zone.

15.4.2 China

According to Chen et al. (2009), the capacity for nuclear power is expected to be 40 GWe by 2020, with a predicted rise to a maximum of 350 GWe by 2050. The predicted expansion, however, has been evaluated in three bands with expansion being low, medium, or high. This has led to the following ranges:

- 40-60 GWe by 2020.
- 82-180 GWe by 2035.
- 150-350 GWe by 2050.

Clearly, as the reactor fleet develops, the type of fuel, composition, burn up, and overall fuel cycle will have to be developed in a complementary way to ensure a sustainable future, using resources in the best way possible. In the case of China, aqueous reprocessing is being developed to manage spent fuel emerging from the pressurized water reactor (PWR) fleet and those reactors using oxide fuel. Parallel R&D is also being performed on FR fuel cycle scenarios. The Chinese Experimental Fast Reactor (CEFR), based on the BN-800 reactor, was started in 2010 and connected to the grid in 2011 with its fuel cycle designed to use electrometallurgical reprocessing. As the next step in the China Institute of Atomic Energy (CIAE) program, a Chinese Demonstration FR, 1000 MWe prototype reactor (CDFR-1000) based on the CEFR, is being considered for construction in 2017 and commissioning in 2023, with the ultimate objective to have metal fuel in a closed cycle. The CDFR-1000 is then expected to be followed by a 1200 MWe China Demonstration FBR comprising a U—Pu—Zr metal fuel with a burn up of 120 GWd/t (http://www.world-nuclear.org/info/inf63.htmlDE07003/06/48/30).

In addition to those FRs using solid fuel systems, the Chinese Academy of Sciences launched a thorium MSR program. A 5 MWe system is apparently under construction with planned operation in 2015 and is claimed to be the world's largest national effort on thorium breeding MSRs. The U.S. Department of Energy (USDOE) is collaborating with the Chinese Academy of Sciences (http://www.world-nuclear.org/info/inf63.htmlDE07003/06/48/30).

According to Guoan (Guoan et al., 2012), pyrochemical R&D studying the measurement of basic parameters has been started at CIAE. These include studies on the electrochemistry of uranium and rare earth elements (REEs) in chloride and fluoride melts, dissolution processes, purification/recycle, and process control.

15.4.3 Japan

In 1999, the Japan Atomic Energy Agency (JAEA) initiated a feasibility study on FR fuel cycle systems to meet targets on economics, environmental impact, and nonproliferation. It was concluded that the most promising system was aqueous reprocessing of oxide fuel, with an alternative option being a pyrochemical reprocessing system to treat metal fuel (National Programmes in Chemical Partitioning—A Status Report et al., 2010). Programs of work to evaluate and develop both these approaches have taken place and pyroreprocessing has been included as a "subconcept" of FR cycle

technology (FaCT)—a project for the commercialization of the FBR fuel cycle for the twenty-first century (Koyama et al., 2012).

CRIEPI is taking part in the feasibility study and the OMEGA (options making extra gain from actinides) long-term R&D P&T program. Their focus is on pyroprocessing metal FR fuel and partitioning of TRUs from aqueous high-level liquid waste (HLLW) (Inoue et al., 2011) to get 99.99999% recovery of uranium and plutonium and 99.5% recovery of MAs (Inoue et al., 2011). Oxide reduction is included in the study to provide an option to treat oxide fuels using pyrochemical techniques. Their studies started in 1986 to determine basic properties to underpin process chemistry and engineering (Koyama et al., 2012).

CRIEPI has, in collaboration with a number of other organizations (ANL, USDOE, ITU, United Kingdom Atomic Energy Authority (UKAEA), Kyoto University, and the University of Missouri) (National Programmes in Chemical Partitioning—A Status Report et al., 2010), performed laboratory-scale active and inactive testing on LKE with solid and liquid electrode systems to establish thermodynamic properties (Sakamura et al., 1998; Uozumi et al., 2001; Masset et al., 2005), including SFs and distribution coefficients related to electrorefining. Experimental work on UO_2 and other TRU oxides, including MOX pellets, has demonstrated the feasibility of oxide reduction using lithium metal (Usami et al., 2000) or DER (Iizuka et al., 2006). Work on reductive extraction to reduce the lanthanide concentration in molten salt containing actinides, after electrorefining, has also been undertaken.

CRIEPI and JAEA have collaborated to demonstrate the electrorefining of uranium, plutonium, and neptunium using solid and liquid electrode systems (Iizuka et al., 2001) and developed an integrated facility comprising lithium reduction, electrorefining, and distillation unit operations (National Programmes in Chemical Partitioning—A Status Report et al., 2010). Tests have been successfully completed on UO_2 and PuO_2 and testing of MOX fuel started in 2010.

JAEA have undertaken small-scale studies on electrorefining and oxide electrowinning, and performed active studies on nitride systems (fuels for the transmutation of long lived MA in the double-strata concept) determining redox potentials for uranium, neptunium, and plutonium systems and investigating the possible recovery of ^{15}N.

An integrated test equivalent to 1 tHM/yr has been designed and built and comprises the following main process elements: oxide reduction, electrorefining, product processing (solid and liquid cathodes), a six-stage countercurrent reduction extraction contactor, and fuel casting. Uranium testing is being performed to verify system integrity and reliability (Koyama et al., 2012).

15.4.3.1 Electrorefining: Underpinning and integrated technology

CRIEPI is adopting a two-stage approach: (i) laboratory-scale electrorefining tests to develop an understanding of the process chemistry and (ii) an engineering-scale system to establish an understanding of scale-up issues (Koyama et al., 2012; Inoue et al., 2011), including a strong focus on process integration.

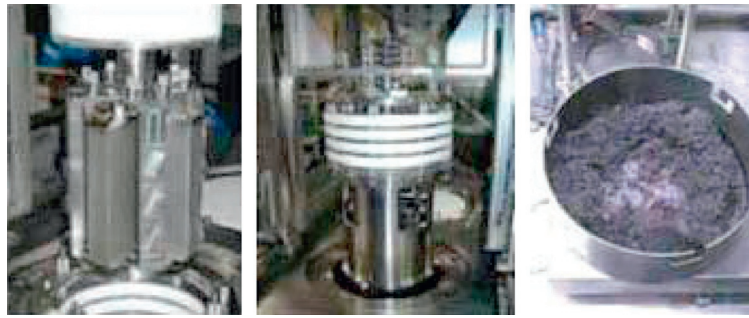

Figure 15.10 Engineering-scale electrorefiner at Toshiba (Inoue et al., 2011).

Laboratory-scale deposition trials onto solid and liquid cathodes using nonirradiated metal fuel simulants, uranium, plutonium, zirconium, and MA have been performed for CRIEPI at ITU (Koyama et al., 2009), while deposition at liquid cadmium electrodes using plutonium and americium have been completed at JAEA (Uozumi et al., 2004). Intermetallic compounds, (U,Pu)Cd_6 and (U,Pu)Cd_{11}, were identified and americium concentration was seen to increase with increasing plutonium content. Metal fuel, U—Pu—Zr, with and without MAs or REEs have been irradiated in PHENIX and subsequently electrorefined, successfully, to recover the actinides (Koyama et al., 2012). Separation of the actinides from the lanthanides agreed well with data from nonirradiated experiments and the behavior of NMs was similar to that of zirconium.

A uranium-active engineering-scale ER has been set up at Toshiba, Figure 15.10. The anode baskets are located in the center while the cathode is formed by the inner wall of the vessel. Dendrites are removed by scraping and collection in a basket located at the bottom of the vessel (Shirai et al., 2000; Uozumi et al., 2004). Simulant metal fuel, U/Zr, in stainless steel cladding has been used for the test.

15.4.3.2 Reductive extraction

Reductive extraction is the process in which lithium metal, dissolved in either cadmium or bismuth, is exposed to a molten salt containing less electropositive elements like TRUs or FPs. In theory, lithium will react with the least electropositive elements, the TRUs, leaving the most electropositive elements as soluble products in the salt.

A multistage reductive extraction process has been demonstrated on simulant aqueous HLLW, after the HLLW was converted sequentially to an oxide and then chlorinated to form the corresponding chloride. 99.5% of the plutonium and neptunium were recovered together with 99.4% of the americium from salt, which contained 10 times the concentration of FPs (Kinoshita et al., 1999). Uranium was removed by electrochemical deposition onto a solid cathode prior to reductive extraction.

Validation of the overall process using HLLW from MOX reprocessing was completed; however, the technical feasibility of a three-stage, engineering-scale countercurrent reductive extractor has yet to be established (Inoue et al., 2011).

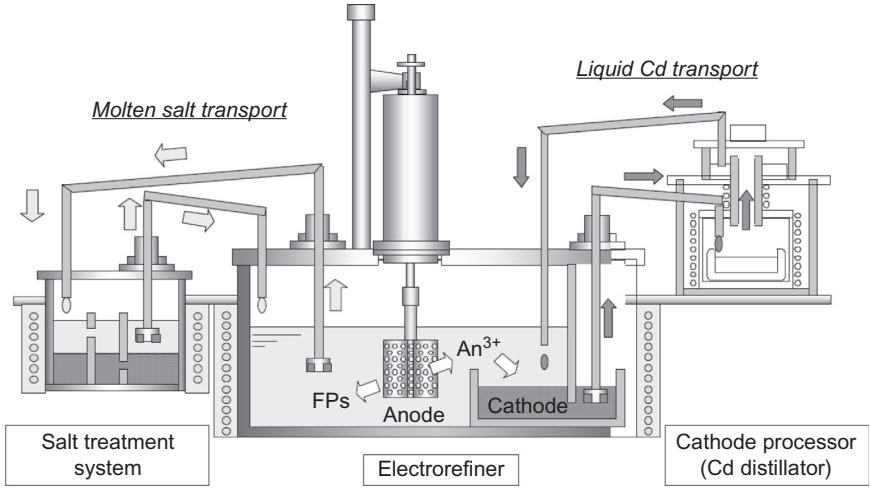

Figure 15.11 Concept molten salt/liquid cadmium industrial transport system for a pyrochemical process (Koyama et al., 2007).

15.4.3.3 Salt and cadmium pumping

The ability to transfer salt and liquid metal is one of the main challenges in the path toward industrialization (Koyama et al., 2007). Molten salt and liquid cadmium pumping to a distillation and electrorefining unit has been demonstrated. Centrifugal pumps transport cadmium to a distillation unit and salt to a salt treatment system. A schematic describing the concept for the transfer system is shown in Figure 15.11. The whole assembly is located in an argon-filled glove box of dimensions 7 m × 3 m × 5 m height (Inoue et al., 2011). Cadmium has been lifted to a height of 1.7 m.

15.4.3.4 System integration

Process integration of unit operations is a major challenge and progress has been made in addressing this issue. UO_2 has been reduced to uranium metal in order to prepare a simulated metal fuel U-Zr, which is seen as a key process step linking LWR oxide fuels to the metal FBR fuel cycle. Sequential operations starting from the reduction step and finishing with injection casting have been implemented, and repeated recycling of the U-zirconium fuel is in progress to simulate the closed metal fuel cycle (Koyama et al., 2012). Electrorefining, product transfer, distillation, and injection casting have been successfully operated; however, challenges still remain with the electroreduction step.

15.4.4 Russian Federation

Pyroprocessing in Russia has a long history, with early investigations in the 1960s leading to the demonstration of fluoride volatility reprocessing technology in the 1970s, a pilot facility for pyrochemical MOX fuel production starting in the late

1970s, and finishing in the 1990s. Following this, DOVITA, a dry technologies oxide-based reprocessing and fuel processing program, including vibropac pin production to close the fuel cycle for an FR and initially designed for MA partitioning for transmutation (National Programmes in Chemical Partitioning—A Status Report et al., 2010), was proposed by RIAR. The processes adopted for this program included the reprocessing of neptunium, uranium, and plutonium oxide fuel and the recycling of americium, curium, and uranium oxide transmutation targets, described as homogeneous and Heterogeneous processing operations, respectively (see Figure 15.12). DOVITA started in 1992 (Kormalitsyn et al., 2008), which was followed by the DOVITA-2, again designed for MA partitioning for transmutation by an FR. DOVITA-2 expands the range of fuels to include nitrides and metals and various melts to be considered for processing in a reactor island concept (colocation of reactor and reprocessing facilities). Techniques include electrochemical deposition on solid and liquid cathodes, anodic dissolution, and oxide precipitation in a range of melts including chlorides, fluorides, molybdates, and ionic liquids.

The processing of oxide is based on simple principles. Fuel would be irradiated and partially recycled by decladding, crushing, and vacuum reprocessing, followed by vibropacking to produce a fuel element, which may be returned to the reactor. Every second cycle, the fuel is fully reprocessed using the electrowinning process described in Section 15.2.3.1, to separate actinides, MAs, FPs, and REEs. Americium and

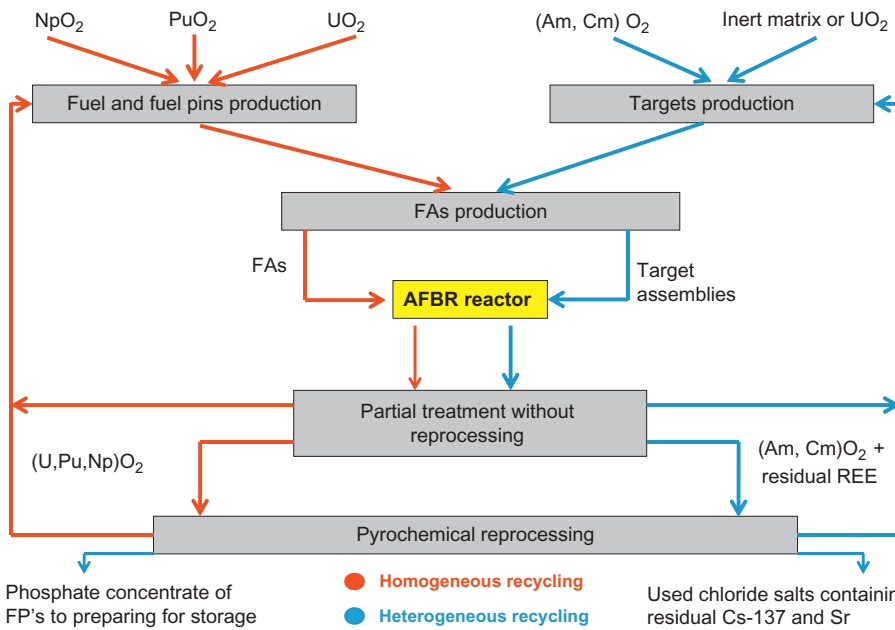

Figure 15.12 DOVITA fuel cycle (Bychkov et al., 2006). *Note*: FAs, REEs, and FPs are fuel assemblies, rare earth elements, and fission products respectively.

curium separation from REEs is achieved using a liquid metal cathode (National Programmes in Chemical Partitioning—A Status Report et al., 2010).

R&D appears to be at an advanced stage, with key process steps and equipment for oxide fuel reprocessing tested using ~7 tons of nonirradiated oxide fuel and 40 kg of BN-350 and BOR-60 irradiated fuels (Bychkov, 2008). A considerable amount of research has been performed to establish fundamental data to underpin the future technology development toward industrialization, with a major emphasis on spent fuel partitioning (Kormalitsyn et al., 2008; Bychkov et al., 2006).

15.4.5 Republic of Korea

The ROK operates 20 nuclear power plants. Spent fuel from these plants amounted to ~8000 tons in 2005, with the total accumulated waste expected to reach 20,000 tons by 2020. In 2005, KAERI proposed a long-term plan; the Korean innovative environmentally friendly proliferation resistant system for the twenty-first century (KIEP-21) (National Programmes in Chemical Partitioning—A Status Report et al., 2010), which comprises:

- Direct use of PWR spent fuel in Canadian deuterium uranium (CANDU) reactors.
- The advanced spent fuel conditioning process (ACP).

The ACP (National Programmes in Chemical Partitioning—A Status Report et al., 2010; You et al., 2007) is a process that contains many of the recognized pyrochemical process steps for the LKE system, which are typically decladding (voloxidation), oxide reduction, electrorefining, product processing to condition the metal actinides product, salt cleanup, and waste treatment.

However, in the KAERI process there are two additional process steps: cathode processing, which sits between the reduction and electrorefining unit operations, and electrowinning of TRU products after electrorefining. The overall pyroprocess is shown schematically in Figure 15.13.

Following reduction, the reduced oxide is treated using a cathode processor designed to remove salt and separate any unreduced oxide from the metal. Using this process, minimal LiCl salt and unwanted oxide will be transferred to the electrorefining stage.

KAERI has developed a number of innovative concepts aiming to improve the throughput of an industrial-scale electrorefiner (Kim et al., 2012). One such concept is the separation of the uranium deposition from the TRU recovery. Uranium is recovered on to a solid cathode in the normal manner, while the TRUs are electrochemically deposited onto a liquid cathode in a separate electrowinning process vessel. A second concept is the recovery of uranium onto a self-scraping graphite cathode, created by a spontaneous deposit release through the formation of a uranium graphite intercalation compound (Lee et al., 2007), instead of more conventional rotating mechanical scrapers. Using this arrangement, uranium metal is easily released from the surface, dropping into a collection vessel in the bottom of the electrorefining unit. A third concept uses a bucket transfer mechanism to move the collection bucket from the bottom of the electrorefiner to the top, allowing the continual recovery of dendritic material.

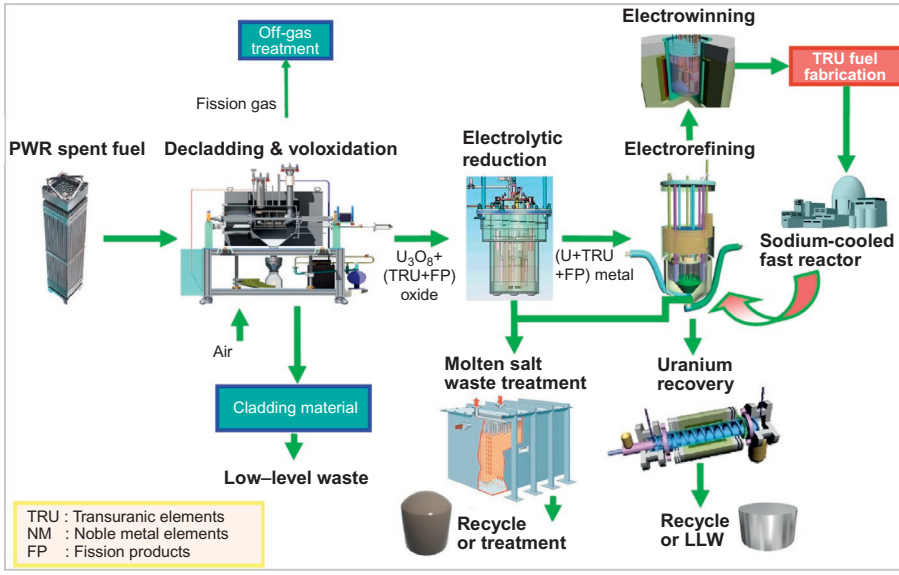

Figure 15.13 Schematic representation of the KAERI pyrochemical process (Lee, 2010).

This latter arrangement has been demonstrated and, together with the graphite cathodes, has shown a significant increase of electrorefiner throughput. These advances are expected to deliver a continuous, high-throughput, uranium, recovery unit operation well-suited to industrial application. A continuous electrorefining system (CERS) comprising a uranium chlorinator, electrorefiner, and salt distiller have also been described (Song et al., 2010).

Having recovered the uranium dendritic deposit, the vast majority of the entrained salt is removed by vacuum distillation, leaving clean dendritic uranium. A throughput of 28.5 kg uranium per day has been achieved. This product is melted in an induction furnace under vacuum by heating the product to 1300 °C in a zirconia-coated graphite crucible and poured into molds to demonstrate the basic principles of metal fuel fabrication.

After a defined quantity of uranium has been recovered in the electrorefining unit, the build up of TRUs in the salt is sufficient to permit the recovery of these onto a liquid metal cathode in an electrowinning electrolyser. Using lab-scale electrowinning units, the data and performance characteristics of the system components have been obtained and further development to improve performance is planned (Song et al., 2010). Following TRU recovery, the cadmium is removed from the TRUs by distillation. Data for distillation at temperatures between 500 and 565 °C and pressure of 0.5-10 torr demonstrated evaporation rates increased with increasing temperature and decreasing pressure.

To ensure minimum losses of actinides from the system, salt from the electrowinning step is sent for further actinide recovery using a combination of reduction of

uranium plus TRUs (and some REEs) onto a liquid cathode followed by REE oxidation using $CdCl_2$. Less than 0.01 wt% of the uranium and TRUs remained in the salt.

KAERI aims to minimize waste generation by recycling salt for reuse using innovative cleaning technologies; for example, melt crystallization or more conventional oxidative precipitation followed by distillation. Eighty to ninety percent of the salt could be recovered using the former process, compared with ~99% for the latter.

By using a new inorganic composite of silicone, aluminum, and phosphorus oxide, a solid final waste form with a much lower waste volume, compared to zeolite, can be produced. A composite of transition metal oxides and phosphates has also been developed to improve the processing conditions for treating separated REEs.

The main goals of KAERI are to increase throughput and minimize waste for the pyrochemical process. New and innovative technologies are being developed to support this, with bench- and laboratory-scale tests underpinning the design and build of a 10 te/yr nonactive engineering-scale integrated process facility—PRIDE.

15.4.6 United States

Since the 1940s, the United States has undertaken R&D in several areas of pyrochemical processing that included fluoride volatility, oxide electrowinning, oxidative reductive extraction, and electrorefining. The main focus of this section, however, is to review the nonaqueous technology currently being developed for treating spent nuclear fuel; effectively, the work being performed at the Idaho National Laboratory INL and the ANL.

R&D in the area has focused on two main areas: the treatment of spent fuel from the Experimental Breeder Reactor II (EBR II) and the development of advanced technology to help close the nuclear fuel cycle (Simpson, 2012).

Between 1984 and 1995 a pyrochemical process based on LKE molten salt technology was developed as part of the IFR program—a program to treat and recycle spent fuel from the EBR II. The pyroprocessing equipment was housed in the fuel cycle facility at INL (then known as ANL-West) (Benedict et al., 2007; Simpson, 2012; Simpson and Law, 2010), which operated until the program was stopped in 1994.

After closure of the IFR program in 1994, fuel fabrication was no longer necessary and the IFR program was converted to a spent fuel treatment program to treat the 25 tHM from EBR-II. The fuel cycle facility at INL (then ANL-West) was modified to demonstrate the technology at engineering scale, becoming the fuel conditioning facility that, from 1996 to 1999, successfully demonstrated the feasibility of pyrochemical processing by treating more than 1 tHM of driver and blanket fuels. Since 2000, the Idaho facility has continued to process EBR-II spent fuel in addition to that from the fast flux test facility. A total of 4.62 tHM had been treated as of January 2012, leaving 21.13 tHM remaining. Plans to move from a demonstration facility to production operations have not materialized, and the current focus is to recover uranium from driver fuel only. Treatment to remove the sodium bond from blanket fuel prior to disposal remains a future option (Simpson, 2012).

Generally, pyrochemical processing aims for technical simplicity with low DFs incorporating MA recycle while facilitating economical remote fabrication of "low DF" metallic fuel by casting. Pyrochemical processing technology still remains at laboratory-scale and engineering-scale demonstration, although the continuous R&D performed at INL and ANL has led to the acquisition of considerable knowledge, know-how, and technical understanding. INL remains, internationally, the largest-scale active electrorefining facility.

Use of pyrochemical technology to treat spent oxide fuel has also been considered; however, in this case, a pretreatment step to reduce the oxide to metal is necessary. Chemical reduction using lithium metal and DER are the main candidate processes, although DER appears to be the preferred technique at the time this is written. A tail end step of reoxidation would also be required prior to oxide fuel fabrication.

A summary of the current status of the INL pyrochemical program and the associated unit operations is given below. These are treated in the order one would expect to see in a process flow diagram.

15.4.6.1 Headend

Chopping/DEOX

INL is currently considering two process options for the headend unit operation—chopping or oxidation (DEOX) for metal and oxide fuels, respectively.

Chopping of fuel elements is very much the norm for metal fuel and represents conventional headend processing to reprocess spent nuclear fuel. It is, therefore, not discussed in any significant detail in this text, other than to compare physical aspects of the process to that of DEOX, which is a specially designed technology dedicated to pyrochemical processing of oxide fuel.

The DEOX process was originally developed by collaborative research between KAERI and INL as part of the International Nuclear Energy Research Initiative (INERI) program (NEA-OECD, 2012; Westphal et al., 2007). Oxide fuel is heated to 1200 °C in air, with the evolution of volatile and semivolatile FPs and the oxidation of UO_2 to U_3O_8. This conversion is accompanied by a volume increase, as the U_3O_8 is less dense than UO_2, which ruptures the cladding and results in separation of the pulverized fuel from the hulls.

The relative merits of treating oxide fuel elements by chopping or DEOX in terms of particle size, fuel cladding separation, and volatile FP release have been discussed by Westphal et al., (2007). Particle morphology is also relevant to downstream processes, namely, oxide reduction. According to Karell and Gourishankar (1998), the oxide reduction rate can be increased by a factor of three for crushed versus uncrushed oxide.

DEOX is expected to reduce the contamination on the inner surface of cladding from spent fuel compared to chopping, thus reducing the additional decontamination burden needed to meet regulatory waste disposition criteria. Using DEOX also removes the need for cladding material to be introduced into the reduction and electrorefining unit operations, preventing the chemical reactions between lithium and cladding oxide, the reaction of UO_2 with zircalloy, and the additional carryover of

LiCl into the LKE eutectic salt. DEOX also offers the potential to remove and trap significant quantities of volatile and semivolatile species in a single unit operation, possibly simplifying the overall flow sheet and assisting waste management.

15.4.6.2 Direct electrochemical reduction

Electrorefining of spent nuclear fuel requires a metal feed. Therefore, reprocessing oxide fuel necessitates a reduction of oxide to metal before any further pyrochemical treatment. An electrolytic reduction process is being developed at INL as part of an integrated process for the treatment of spent oxide nuclear fuel (Herrmann et al., 2007). A detailed description of the overall process has been given in Section 15.2 and a typical apparatus is shown in Figure 15.14.

Early reduction processes used lithium metal, where lithium reacts with the spent fuel oxide to form lithium oxide, soluble in LiCl salt, with the counterreaction being the reduction of oxide to metal. Using lithium metal is not ideal; managing the chemistry is challenging, the process tends to be performed in batches, and requires the recovery of lithium metal for the reduction of the next batch of oxide fuel. Workers have tried to couple the lithium metal recovery with the reduction of oxide to produce a semicontinuous process. However, over the last decade or so, DER of metal oxide has received considerable attention and some interesting research has been performed.

ANL has investigated the DER of oxides of uranium (Barnes and Willit, 2007). Reduction of UO_2 and U_3O_8 were found to behave differently. Numerous tests on UO_2

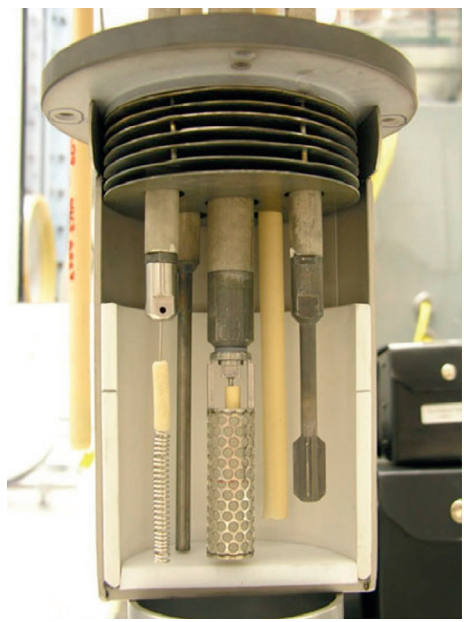

Figure 15.14 Sectional view of DER cell at INL.
From Benedict et al. (2007).

demonstrated that >99% reduction could be achieved at ~75% efficiency, while a reduction of ~93% was achieved for U_3O_8. The difference in the reduction processes has yet to be fully explained. During the reduction of UO_2, the concentration of O^{2-} was routinely found to reduce gradually throughout the reduction process from ~1.5 to 0.6 wt%, while with U_3O_8 the concentration decreases rapidly to ~0.4 wt%. This is thought to be due to the reaction of Li_2O with U_3O_8 to form Li_2UO_4 (Barnes and Willit, 2007).

Herrmann et al. (2006) electrochemically reduced 26-year cooled Belgium reactor 3 (BR3) UO_2 fuel. It was concluded that uranium and transuranic oxides had comparable reduction efficiencies of 99.7%, 97.8%, 98.8%, and 90.2% for uranium, plutonium, neptunium, and americium, respectively. Cesium, barium, strontium, and iodine accumulated in the salt phase with REE and NM remaining with the reduced UO_2 phase. The REEs were found to have only partially reduced. The effect of FP accumulation in the salt was inconclusive and no comment was made with respect to the impact of particle size distribution. Similar work was reported by Herrmann et al. (2005); additionally, the reduction of zirconium was observed to be similar to that of the REE oxides.

Lab-scale work to assess the performance of U_3O_8 versus UO_2 and the behavior of cathode containment materials was also performed by Herrmann et al. (2007) in collaboration with KAERI as part of the INERI program. These tests were performed in the hot fuel dissolution apparatus located in the hot fuel examination facility at INL. Oxide fuel from the Belgium reactor BR3 was oxidized by heating in air to in excess of 450 °C to produce U_3O_8. Results indicated that there was no significant difference in reduction performance for U_3O_8 when compared to the reduction work completed by Herrmann et al. (2006) on UO_2. Different oxide containment vessels were tested and the authors noted the loss of the porous MgO vessel. The loss of porous magnesia baskets was highlighted as one of the major challenges in using ceramic materials in remotely operated pyrochemical processes.

15.4.6.3 Electrorefining

This is a key unit operation that, potentially, has two feed streams: spent metal fuel and a metal feed produced by the DER of spent oxide fuel. In the case of the former, uranium and TRUs are electrochemically separated from the cladding material, sodium bond, FPs, REEs, and NMs. A more detailed description of oxide reduction is given in Section 15.3.3.

INL has developed two high throughput electrorefining (HTER) units, which are known as the Mark IV and Mark V units, designed to process driver and blanket fuels, respectively (see Figure 15.15).

These electrorefiners are cylindrical steel vessels with a height and internal diameter of one meter and have four ~25 cm ports to provide access for the anode and cathode assemblies. Essentially, the ER units are similar with the Mark IV having a 33 cm layer of LKE on top of a 15 cm layer of molten cadmium, in comparison to the Mark V, which comprises a single 42 cm layer of LKE (Davies and Li, 2007).

The Mark IV electrochemical reactor was the first concept for a production-scale unit. The anode design includes four rectangular baskets, arranged in a cruciform geometry. The cathode is a solid steel rod (Westphal et al., 2009).

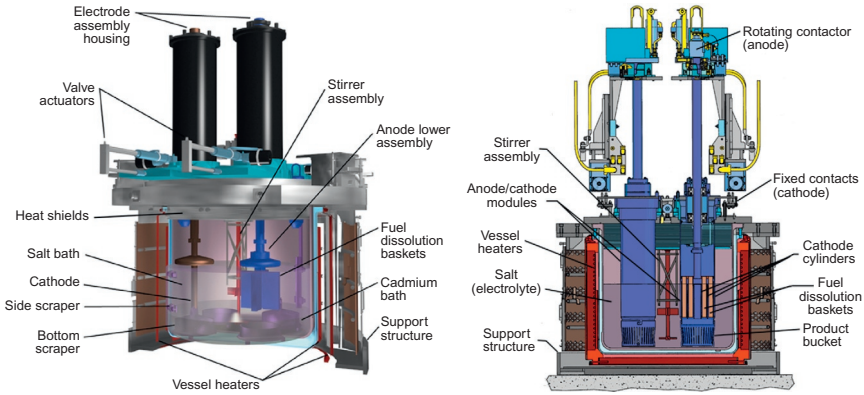

Figure 15.15 Mark IV (left) and Mark V (right) INL electrorefining units. From Simpson (2012).

In the Mark V ER, the anode and cathode are vertically colocated in a single module and called the anode-cathode module (ACM). The ACM comprises nine curved anode baskets, positioned between cathode cylinders (Figure 15.15). During electrorefining, the baskets are rotated and scrapers shear uranium dendrites off the cathode cylinder. Deposits fall into a product collector located below the ACM.

The Mark IV design is complex and has met with some interesting challenges (Simpson, 2012). Early tests indicated poor current efficiency ~50%, which was attributed to the recovery of uranium from the cadmium that had fallen from the solid cathode. Current efficiencies of ~70% were achieved when the anode baskets were rotated. Uranium was also found to enter the cadmium pool electrochemically (Li, 2008), adding further complexity to the ER operation. The incorporation of a cadmium pool has led to the condensation of cadmium at various locations within the electrorefiner. Although this might largely be expected due to the high vapor pressure of the cadmium system, it has created electrical short circuits. The operating protocol, which includes electrochemical stripping (current reversal), has improved overall performance, alleviating anode stalling caused by buildup of the cathode deposit (Westphal et al., 2009; Brunsvold et al., 2000).

Modifications have been made to the design to improve reliability, but also include larger anode baskets to improve throughput and reference electrodes to provide better process monitoring (Benedict et al., 2007).

Anodic dissolution has been identified as a rate-limiting step in the electrorefiner (Benedict et al., 2007; Li and Simpson, 2005; Li et al., 2005). An inverse relationship between uranium dissolution and the retention of NM, including zirconium, was also found. Increasing uranium dissolution beyond 98% resulted in significant NM loss (Li and Simpson, 2005). Li (Li et al., 2005) reported that in excess of 99% uranium dissolution could be achieved although ~88% zirconium and ~25% of other NM products were lost from the anode. This was believed to be due to fine particulate matter not being retained in the anode basket and falling through the mesh into the cadmium

pool. Zirconium dissolution was found to be preventable by using an "interrupting current" technique (Li and Simpson, 2005).

In 2007, an engineering-scale LCC system was used to successfully recover >4 kg of transuranic materials (Benedict et al., 2007), and tests were performed over a range of U^{3+} concentrations to establish provisional bounding conditions. The recovery of transuranic materials will improve the useful lifetime of the salt, prevent any breech of criticality limits for plutonium, and minimize the amount of actinide sentenced to the final waste form.

15.4.6.4 Product processing

INL has developed and operated cathode processor equipment with electrorefined uranium products from irradiated FR fuels. This is a batch-type operation that utilizes a high-temperature vacuum retort and a heavy-metal-melting furnace. It was originally developed for purifying and consolidating both solid cathode uranium product and liquid cathode TRU products. The main equipment components are process vessel, induction furnace, crucible, and condenser/collector. The equipment is capable of reaching 1673 K and, therefore, capable of melting uranium, some U-Zr alloys, and INL metal waste alloys. A uranium cathode of ~40 kg batch size has been successfully processed. In processing LCCs, the batch size is restricted to a single cathode. To maintain criticality safety, a mass limitation of ~25 kg is imposed. As of 2007, the cathode processor had processed >300 batches, a cadmium distillation rate of 0.41 g/min/cm^2 achieved, and >99 wt% cadmium recovered for recycle. Salt, recovered from cathode processing, has been returned to the electrorefiner over a period of time and analysis has shown that impurities from the product processing unit operation have not been detected.

Historically, graphite crucibles coated with zirconia have been used to minimize the reaction of uranium and the crucible material. However, the coating can react with uranium metal to form the oxide. Oxide can be reduced and recycled back into the process, although this is inefficient; the process is labor intensive and has the potential to limit throughput. Different crucibles are being developed, which include niobium coated with hafnium nitride. Experimental work has provided promising results (Benedict et al., 2007).

15.4.6.5 Process integration

An integrated efficiency test between element chopper, Mark IV electrorefiner, cathode processor, and casting furnace was performed at an engineering scale (50 kgHM) by Li et al. (Li et al., 2007). The total mass balance was found to be 101.28%, indicating slightly more output than input, while 99.3% of the uranium was electrochemically dissolved in comparison to the 98.4% collected in the casting furnace. The behavior of zirconium was found to be complex, with results indicating that there was significant loss to the cadmium pool. A problem with material holdup was also identified.

15.4.6.6 Cross-cutting activities

Reference electrode development

Reference electrode systems have been developed to provide real-time data with respect to electrodes in an operating electrorefiner. These were based on Ag/AgCl in the salt of choice and held in a ceramic or glass housing. Housing materials investigated included vycor glass, quartz, mullite, zirconia, and alumina. Original reference electrodes were complex constructions requiring multiple ceramic-glass or ceramic-metal joints to be made under inert conditions.

A simplified approach has used commercially available mullite tubes and ceramic material. Using these components and materials to provide electrode location, structural and internal atmosphere integrity, a robust, easily constructed, and reliable reference electrode has been fabricated, which is shown in Figure 15.16.

Online monitoring

Square wave voltammetry and NPV techniques are under investigation (Johnson and Dunzik-Gougar, 2006) as online monitoring techniques. These are being developed to measure the ratio of Pu/U in solution to control the electrorefiner operations. Knowledge of this ratio is a fundamental parameter that determines the point at which uranium recovery on a solid mandrel stops and recovery of uranium and TRUs in an LCC starts.

Modeling

Process modeling has been developed to enhance the fundamental understanding of physicochemical processes and to predict the mass and inventory composition based on the input and output streams during the ER process (Simpson, 2012; Hoover et al., 2009, 2010, 2011).

A project, in collaboration with the University of Idaho, the Seoul National University, and KAERI, as part of the US-ROK INERI program, to develop a kinetic model of the Mark IV electrorefiner was started in 2007 (Hoover et al., 2009, 2010, 2011). The model was able to track uranium and zirconium dissolution and produced data consistent with experimental results. Increasing the concentration of uranium in the salt was

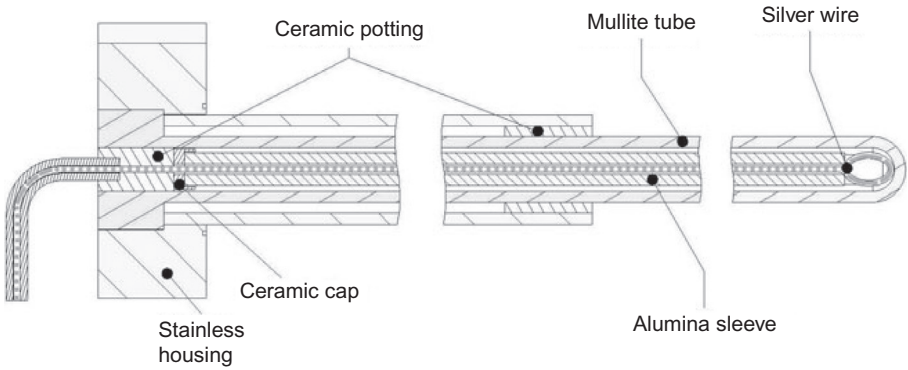

Figure 15.16 Reference electrode developed at INL (Davies and Li, 2007).

also shown to be detrimental in that uranium and zirconium dissolution are retarded and enhanced, respectively. Potential mapping of the electrode also indicated the remote parts of the electrode have small potential gradients and little ionic movement.

15.4.7 Europe

The recently completed European Seventh Framework Program (FP7) project ACSEPT (actinide recycling by separation and transmutation) comprised 34 partners gathered together to address chemical separation development challenges for Generation IV fuel cycle initiatives in both aqueous and pyrochemical technologies. From a pyrochemical perspective, four main areas were studied: fuel dissolution, core process (separations), salt treatment for recycle, and waste conditioning.

To date, a significant amount of data has been gathered with respect to dissolution in chloride media and, therefore, ACSEPT has included significant work on dissolution in fluoride systems. The core process has two reference technologies (Mendez et al., 2012a,b; Bourg et al., 2011, 2012), liquid-liquid extraction in molten fluoride and electrorefining in LKE onto solid aluminum cathodes. Progress has been made on actinide recovery from aluminum, and exhaustive electrolysis has been investigated as a salt treatment process to recover actinides from the salt before decontamination, using zeolite or phosphate/carbonate precipitation. Sodalite was shown to have poor characteristics and properties for long-term storage of actinides and FPs. In molten fluoride systems, distillation of the reference salt was seen to provide effective decontamination for salt recycle. Cross-cutting activities included engineering and system studies, online monitoring, and corrosion studies (Bourg et al., 2011, 2012).

Outside the collaborative European frameworks, NRI, in the Czech Republic, continues to develop the fluoride volatility method as a "front-end" technology for the MSR and electroseparation methods for online reprocessing of the circulating MSR fuel (Uhlír et al., 2007; Uhlíř et al., 2012). In France, the CEA R&D molten salt program for reprocessing Generation IV spent fuels is focused on liquid-liquid extraction in fluoride media (Lacquement et al., 2007, 2009). ITU continues their studies of actinide and lanthanide separation onto an aluminum cathode and oxide reduction using spent nuclear fuel in collaboration with CRIEPI (Malmbeck et al., 2011). Recovery of actinides from aluminum is also reported (Cassayre et al., 2011). ENEA (Italian National Agency for New Technologies, Energy and Sustainable Economic Development) continues to develop waste forms from zeolite (De Angelis et al., 2009, 2012). REFINE (reduction of spent fuel vital in a closed loop nuclear energy cycle) is a coordinated U.K. research program delivering the materials science required for sustainable spent fuel reduction in a closed loop nuclear energy cycle (REFINE research consortium). This builds on a significant U.K. (British Nuclear Fuels) molten salt program in the early 2000s, which focused on engineering and fundamental science using state-of-the-art specialist equipment. This included a fully inerted argon glove box designed for alpha active programs, and a molten salt dynamics rig, designed and built as a one-of-a-kind test facility, with three pumping options and replaceable test sections for process flow characterization, to provide data and test capability for pumping molten salt. The molten salt dynamics rig is an integral part of the current REFINE program.

15.5 Future directions and outlook

Globally, nuclear energy will form part of the non-greenhouse gas generating energy mix; however, the safe and economic management of spent nuclear fuel will have to be demonstrated. Current forecasts show the generation of spent nuclear fuel outstripping available reprocessing capacity, and different international fuel cycle approaches are being considered. Development of advanced fuel cycle strategies necessitate the development of both reactor systems and complementary and compatible fuel cycles. Nonaqueous reprocessing techniques for treating high fissile, high burn up, short-cooled metal, oxide, carbide, nitride, or inert matrix fuels offer potential solutions.

This chapter has provided a state-of-the-art review of nonaqueous reprocessing technologies that are being considered for advanced fuel cycle initiatives. Based on the number of institutes and development programs underway, particularly in the ROK, electrorefining in LKE appears to represent the single technology option receiving greatest international development interest. Therefore, particular emphasis has been placed, in this study, on the pyrochemical reprocessing of metal and oxide nuclear fuels using LKE molten salt.

As industrialization of the process is a major focus, improvement in electrochemical reduction, electrorefiner, and electrowinning performance is essential. Analytical techniques to underpin process operation and control, criticality, and safeguards are vital, together with the movement and management of molten salts with maintenance-free pumping technology being ideal for remote applications.

Clearly, electrorefining technology still requires significant development before reaching a mature status. A substantial amount of R&D is being performed internationally, and some ambitious development targets have been set to demonstrate an integrated process at 1-10 tHM/annum throughput. Meeting such targets is a challenge from both a technical and financial viewpoint. International alliances and research programs, for example, KAERI and INL under the INERI program, the EU seventh framework SACSESS (safety of actinide separation processes) program, or the OECD (Organisation for Economic Co-operation and Development) expert working groups on P&T have been formed to help generate, share, and disseminate knowledge and information in order to maximize the technical return on any financial investment. Given the scale of the challenge, future new joint international R&D projects will inevitably be required to support the different national strategies.

Acknowledgement

The preparation of this review was supported by the UK National Nuclear Laboratory and the UK Government Department of Energy and Climate Change.

References

Barnes, L.A., Willit, J.L., 2007. Direct electrolytic reduction of UO_2 vs. U_3O_8. In: Global 2007, Boise, Idaho, September 9-13, pp. 763–765.

Benedict, R.W., Solbrig, C., Westphal, B., Johnson, T.A., Li, S.X., Marsden, K., Goff, K.M., Benedict, R.W., Solbrig, C., Westphal, B., Johnson, T.A., Li, S.X., Marsden, K., Goff, K.M., 2007. Pyroprocessing Progress at Idaho National Laboratory. In: Global 2007, Boise, Idaho, September 9-13.

Bourg, S., Hill, C., Caravaca, C., Rhodes, C., Ekberg, C., Taylor, R., Geist, A., Modolo, G., Cassayre, L., Malmbeck, R., Harrison, M., de Angelis, G., Espartero, A., Bouvet, S., Ouvrier, N., 2011. ACSEPT—partitioning technologies and actinide science: towards pilot facilities in Europe. Nucl. Eng. Des. 241, 3427–3435.

Bourg, S., Poinssot, C., Geist, A., Cassayre, L., Cassayre, L., Rhodes, C., Ekberg, C., 2012. Advanced reprocessing developments in Europe Status on European projects ACSEPT and ACTINET-I3. Proc. Chem. 7, 166–171.

Boussier, H., 2006. Waste minimisation study on pyrochemical reprocessing processes. In: 2006 International Pyroprocessing Research Conference, August 8-10, 2006, Idaho Falls, Idaho (USA).

Brunsvold, A.R., Roach, P.D., Westphal, B.R., 2000. Design and development of a cathode processor for electrometallurgical treatment of spent nuclear fuel. In: Proceedings of the ICONE 8, International Conference on Nuclear Engineering, Baltimore, MD, USA, April 2-6, 2000.

Bychkov, A., 2008. In: International Workshop for Asian Nuclear Prospect, Kobe, Japan, October 19-22.

Bychkov, A.V., Vavilov, S.K., Porodnov, P.T., Skiba, O.V., 1993. Pyroelectrochemical reprocessing of irradiated uranium-plutonium oxide fuel for fast reactors. In: Proceedings International Conference, Global 1993, vol. 2, pp. 1351–1356.

Bychkov, A.V., Vavilov, S.K., Skiba, O.V., Porodnov, P.T., Pravdin, A.K., Popkov, G.P., Suzuki, K., Shoji, Y., Kobayashi, T., 1997. Pyroelectrochemical reprocessing of irradiated FBR MOX fuel. Experiment on high burn-up fuel of the BOR-60 reactor. In: Proceedings International Conference, Global 1997, vol. 2, pp. 912–917.

Bychkov, A.V., Skiba, O.V., Kormalitsyn, M.V., 2006. Partitioning of fissile and radiotoxic materials from spent nuclear fuel. In: 9th Information Exchange Meeting on Actinide and Fission Product Partitioning and Transmutation, Nimes, France, 25-29 September.

Cassayre, L., Souček, P., Mendes, E., Malmbeck, R., Nourry, C., Eloirdi, R., Glatz, J.-P., 2011. Recovery of actinides from actinide-aluminium alloys by chlorination: part I. J. Nucl. Mater. 414, 12–18.

Chen, J., Liu, X., Wang, J., 2009. Develop advanced nuclear fuel cycle in China, nuclear fuel cycle: sustainable options & industrial perspectives. In: Global 2009, Paris, France, p. 9030.

Davies, K., Li, S.X., 2007. Simplified reference electrode for electrorefining of spent nuclear fuel in high temperature molten salt. In: Global 2007, Boise, Idaho, September 9-13, 2007, pp. 1099–1103.

De Angelis, G., Bardez-Giboire, I., Mariani, M., Capone, M., Chartier, M., Macerata, E., 2009. Synthesis and characterization of sodalite as matrix for conditioning chloride spent salts from pyroprocesses. Mat. Res. Soc. Symp. Proc. 1193, 73–78.

De Angelis, G., Fedeli, C., Manniello, A., Da Ros, M., Giacobbo, F., Macerata, E., Mariani, M., 2012. Conditioning of chloride salt wastes from pyroprocesses through the pressureless consolidation. Proc. Chem. 7, 746–753.

U.S.DOE Nuclear Energy Research Advisory Committee and the Generation IV International Forum, 2002. A Technology Roadmap for Generation IV Nuclear Energy Systems, GIF-002-00.

Generation IV International Forum. Proliferation resistance and physical protection of the Six Generation IV Nuclear Energy Systems. The Proliferation Resistance and Physical

Protection Evaluation Methodology Working Group and the System Steering Committees of the Generation IV International Forum, July 15, 2011. GIF/PRPPWG/2011/002.

Ghosh, S., Vandarkuzhali, S., Venkatesh, P., Seenivasan, G., Subramanian, T., Reddy, B.P., Nagarajan, K., 2009. Electrochemical studies on the redox behaviour of zirconium in molten LiCl-KCl eutectic. J. Electroanal. Chem. 627, 15–27.

Ghosh, S., Vandarkuzhali, S., Gogoi, N., Venkatesh, P., Seenivasan, G., Reddy, B.P., Nagarajan, K., 2011. Anodic dissolution of U, Zr and U-Zr alloy and convolution voltammetry of $Zr^{4+}|Zr^{2+}$ couple in molten LiCl-KCl eutectic. Electrochim. Acta 56, 8204–8218.

Goto, T., Nohira, T., Hagiwara, R., Ito, Y., 2009. Selected topics of molten fluorides in the field of nuclear engineering. J. Fluor. Chem. 130, 102–107.

Grandjean, A., 2005. Feasibility of immobilising fluorinated pyrochemical reprocessing salts in a glass-ceramic matrix. In: Materials Research Society Symposium Proceedings, vol. 848, Symposium FF, Paper FF9-32.

Guoan, Y., Hui, H., Rushan, L., Wenbin, Z., 2012. R&D activities on actinide separation in China, ATALANTE 2012. Proc. Chem. 7, 215–221.

Herrmann, S.D., Li, S.X., Simpson, M.F., 2005. Electrolytic Reduction of Spent Oxide Fuel—Bench-Scale Test Results. In: Global 2005, Tsukuba, Japan, October 9-13, 2005p. 488.

Herrmann, S.D., LI, S.X., Simpson, M.F., Phongikaroon, S., 2006. Electrolytic reduction of spent nuclear oxide fuel as part of an integral process to separate and recover actinides from fission products. Sep. Sci. Technol. 41 (10), 1965–1983.

Herrmann, S.D., Li, S.X., Sell, D.A., Westphal, B.R., 2007. Electrolytic reduction of spent nuclear oxide fuel—effects of fuel form and cathode containment materials on bench-scale operations. In: Boise, Idaho, September 9-13, 2007.

Hoover, R.O., Phongikaroon, S., Li, S., Simpson, M., Yoo, T.S., 2009. A computational model of the Mark-IV electrorefiner: phase I—fuel basket/salt interface. J. Eng. Gas Turbines Power 131, 054503.

Hoover, R.O., Phongikaroon, S., Simpson, M.F., Li, S.X., Yoo, T.S., 2010. Development of computational models for the Mark-IV electrorefiner—effect of uranium, plutonium, and zirconium dissolution at the fuel basket/salt interface. Nucl. Technol. 171 (3), 276–284.

Hoover, R.O., Phongikaroon, S., Simpson, M.F., Yoo, T.S., 2011. Computational model of the Mark-IV electrorefiner—2D potential and current distributions. Nucl. Technol. 173, 176–182.

Iizuka, M., Uozumi, K., Inoue, T., Iwai, T., Shirai, O., Arai, Y., 2001. Behavior of plutonium and americium at liquid cadmium cathode in molten LiCl-KCl electrolyte. J. Nucl. Mater. 299, 32–42.

Iizuka, M., Sakamura, Y., Inoue, T., 2006. Electrochemical reduction of $(U\text{-}40Pu\text{-}5\ Np)_2$ in molten LiCl electrolyte. J. Nucl. Mater. 359, 102–113.

Inoue, T., Koyama, T., Arai, Y., 2011. State of the art of pyroprocessing technology in Japan. Energy Proc. 7, 405–413.

Johnson, C.W., Dunzik-Gougar, M.L., 2006. On-line monitoring of actinide concentrations in molten salt electrolyte. In: ANS 2006 Winter Meeting.

Karell, E.J., Gourishankar, K.V., 1998. Electrometallurgical treatment of oxide spent fuel—engineering-scale development. In: Proceedings of the DOE Spent Nuclear Fuel and Fissile Materials Management, Charleston, SC, vol. 2 pp. 681–688.

Kim, J.-G., Lee, S.-J., Park, S.-B., Hwang, S.-C., Lee, H., 2012. High-throughput electrorefining system with graphite cathodes and a bucket-type deposit retriever, ATALANTE 2012. Proc. Chem. 7, 754–757.

Kinoshita, K., Inoue, T., Fusselman, S.P., Grimmett, D.L., Roy, J.J., Gay, R.L., Krueger, C.L., Nabelek, C.R., Storvick, T.S., 1999. Separation of uranium and transuranic elements from rare earth elements by means of multistage extraction in LiCl-KCl/Bi system. J. Nucl. Sci. Technol. 36, 189–197.

Kormalitsyn, M.V., Bychkov, A.V., Skiba, O.V., Osipenko, A.G., 2008. The RIAR-DOVITA-2 P&T programme—results of the year 15 R&D activities. In: 10th Information Exchange Meeting on Actinide and Fission Product Partitioning and Transmutation, MITO, Japan, 6-10 October, 2008.

Kormilitzyn, M.V., Vavilov, S.K., Bychkov, A.V., Skiba, O.V., Chistyakov, V.M., Tselichshev, I.V., 2000. Pyroelectrochemical reprocessing of irradiated MOX fast reactor fuel testing of the reprocessing process with direct MOX fuel production. In: Proceedings International Conference, Atalante 2000, 6-12, Avignon, France, October 24-26.

Koyama, T., Hijikata, T., Yokoo, T., Inoue, T., 2007. Development of engineering technology basis for industrialization of pyrometallurgical reprocessing. In: Global 2007, Boise, Idaho, September 9-13, pp. 1038–1043.

Koyama, T., Sakamura, Y., Ogata, T., Kobayashi, H., 2009. Pyroprocess and metal fuel development for closing actinide fuel cycle with reduced waste burden. In: Global 2009, Paris, France, September 6-11, p. 9247.

Koyama, T., Sakamura, Y., Iizuka, M., Kato, T., Murakami, T., Glatz, J.-P., 2012. Development of pyro-processing fuel cycle technology for closing actinide cycle. Proc. Chem. 7, 772–778.

Kutty, K.V.G., Rao, P.R.V., Raj, B., 2009. Current status of the development of the fast reactor fuel cycle in India. In: Global 2009, Paris, September 6-11, p. 9547.

Lacquement, J., Bourg, S., Boussier, H., Conocar, O., Laplace, A., Lecomte, M., Boullis, B., Duhamet, J., Grandjean, A., Brossard, P., Warin, D., 2005. Progress of the R&D programme on pyrochemistry at CEA. In: Proceedings of International Conferences, Global 2005, Tsukuba, Japan, Paper No. 153, 2005.

Lacquement, J., Boussier, H., Laplace, A., Conocar, O., Grandjean, A., 2007. Potentialities of fluoride-bases salts for specific nuclear reprocessing: overview of the R&D program at CEA. J. Fluor. Chem. 130, 18–21.

Lacquement, J., Boussier, H., Laplace, A., Conocar, O., Grandjean, A., 2009. Potentialities of fluoride-based salts for specific nuclear reprocessing: overview of the R&D program at CEA. J. Fluor. Chem. 130, 18–21.

Lee, H.S., 2010. Pyroprocessing technology development at KAERI. In: International Pyroprocessing Research Conference (IPRC) 2010.

Lee, J.H., Kang, Y.H., Hwang, S.C., Park, S.B., Shim, J.B., Lee, H.S., Kim, E.H., Park, S.W., 2007. Conceptual design of a high throughput electrorefining of uranium by using a graphite cathode. In: Global 2007, Boise, Idaho, September 9-13, pp. 1845–1849.

Li, S.X., 2008. Experimental observations on the roles of cadmium pool in Mark-IV electrorefiner. J. Nucl. Technol. 162 (2), 144–152.

Li, S.X., Simpson, M.F., 2005. Anodic process of electrorefining spent nuclear fuel in molten LiCl-KCl-UCl_3/Cd system. J. Mineral Metallurg. Process. 22, 4.

Li, S.X., Johnson, T.A., Westphal, B.R., Goff, K.M., Benedict, R.W., 2005. Electrorefining experience for pyrochemical processing of spent EBR-II driver fuel. In: Proceedings of GLOBAL 2005, Tsukuba, Japan, October 9-13, p. 487.

Li, S.X., Vaden, D., Westphal, B.R., Fredrickson, G.L., Benedict, R.W., Johnson, T.A., 2007. Integrated efficiency test for pyrochemical fuel cycles. In: Global 2007, Boise, Idaho, September 9-13, 2007, pp. 766–771.

Lovasic, Z., 2008. Spent Fuel Reprocessing Options, IAEA Report, IAEA–TECDOC-1587, ISBN 978-92-0-103808-1.

Malmbeck, R., Nourry, C., Ougier, M., Souček, P., Glatz, J.P., Kato, T., Koyama, T., 2011. Advanced fuel cycle options. Energy Proc. 7, 93–102.

Masset, P., Konings, R.J.M., Malmbeck, R., Serp, J., Glatz, J.-P., 2005. Thermochemical properties of lantanides (Ln = La, Nd) and actinides (An = U, Np, Pu, Am) in the molten LiCl-KCl eutectic. J. Nucl. Mater. 344, 173–179.

Mendez, E., Conocar, O., Laplace, A., Douyere, N., Miguirditchian, M., 2012a. Assessment of the complete core of the reference pyrochemical process, developed by the CEA. Proc. Chem. 7, 791–797.

Mendez, E., Boussier, H., Laplace, A., Vigier, J.F., Miguirditchian, M., 2012b. Development status on the Pyrochemistry R&D program at CEA. In: 2012 International Pyroprocessing Research Conference, Fontana, WI, USA. August 27-29.

Nagarajan, K., 2010. In: First ACSEPT International Workshop, 31 March-2 April 2010, Lisbon, Portugal.

Nagarajan, K., Reddy, B.P., Ghosh, S., Ravisankar, G., Mohandas, K.S., Kamachi Mudali, U., Kutty, K.V.G., Viswanathan, K.V.K., Anand Babu, C., Kalyanasundaram, P., Rao, P.R.V., Raj, B., 2011. Development of pyrochemical reprocessing for spent metal fuels. Energy Proc. 7, 431–436.

National Programmes in Chemical Partitioning—A Status Report, NEA No. 5425, OECD 2010, 45-56.

NEA-OECD, 2012. "Spent Nuclear Fuel Reprocessing Flowsheet" A Report by the WPFC Expert Group on Chemical Partitioning of the NEA Nuclear Science Committee, NEA/NSC/WPFC/DOC(2012)15, June 2012.

Organisation for Economic Co-operation and Development, 2004. Pyrochemical separations in nuclear applications, a status report by the Pyrochemistry Expert Group, OECD/NEA 2004, NEA No. 5427.

Reddy, B.P., Nagarajan, K., Rao, P.R.V., Raj, B., 2010. Current status of pyroprocess development at IGCAR, Kalpakkam, India. In: IPRC, Dimitrovgrad, Russia, November 29-December 3.

REFINE research consortium: http://www.refine.eng.ed.ac.uk, http://gow.epsrc.ac.uk/NGBOViewGrant.aspx?GrantRef=EP/J000779/1.

Strategic Research Agenda, 2012. Sustainable Nuclear Energy Technology Platform, Strategic Research Agenda—Annex, January 2012.

Sakamura, Y., Hijikata, T., Kinoshita, K., Inoue, T., Storvick, T.S., Krueger, C.L., Roy, J.J., Grimmett, D.L., Fusselman, S.P., Gay, R.L., 1998. Measurement of standard potentials of actinides (U, Np, Pu, Am) in LiCl-KCl eutectic salt and separation of actinides from rare earths by electrorefining. J. Alloys Compd. 271-273, 592–596.

Shirai, O., Iizuka, M., Iwai, T., Suzuki, Y., Arai, Y., 2000. Recovery of neptunium by electrolysis of NpN in LiCl-KCl eutectic melts. J. Nucl. Sci. Eng. 37 (8), 676–681.

Simpson, M.F., 2012. Developments of spent nuclear fuel pyroprocessing technology at Idaho National Laboratory, March 2012, INL/EXT-12-25124.DE07003/06/09/05.

Simpson, M.F., Law, J.D., 2010. Nuclear fuel reprocessing, INL/EXT-10-17753.DE07003/06/09/03.

Simpson, M.F., Yoo, T.-S., Shaltry, M., Phongikaroon, S., LaBrier, D., Lineberry, M., 2012. Selective precipitation of rare earth chlorides from LiCl-KCl. In: 2012 International Pyroprocessing Research Conference, Fontana, WI, USA, August 27-29.

Song, K.-C., Lee, H., Hur, J.-M., Kim, J.-G., Ahn, D.-H., Cho, Y.-Z., 2010. Status of pyroprocessing technology development in Korea. Nucl. Eng. Technol. 42, 131–144.

Souček, P., Malmbeck, R., Mendes, E., Nourry, C., Glatz, J.-P., 2010. Exhaustive electrolysis for recovery of actinides from molten LiCl-KCl using solid aluminium cathodes. J. Radioanal. Nucl. Chem. 286, 823–828.

Souček, P., Malmbeck, R., Nourry, C., Glatz, J.-P., 2011. Pyrochemical reprocessing of spent fuel by electrochemical techniques using solid aluminium cathodes. Energy Proc. 7, 396–404.

Sri Maha Vishnu, D., Sanil, N., Murugesan, N., Shakila, L., Ramesh, C., Mohandas, K.S., Nagarajan, K., 2012. Determination of the extent of reduction of dense UO_2 cathodes from direct electrochemical reduction studies in molten chloride medium. J. Nucl. Mater. 427, 200–208.

Uhlír, J., Marecek, M., Tulá'ková, R., Chuchvalcová Bímová, K., 2007. Development of fluoride reprocessing technologies devoted to molten-salt reactor systems. In: Global 2007, Boise, Idaho, September 9-13, 2007, pp. 1490–1496.

Uhlíř, J., Mareček, M., Škarohlíd, Jan, 2012. Current progress in R&D of fluoride volatility method. Proc. Chem. 7, 110–115.

Uozumi, K., Kinoshita, K., Inoue, T., Fusselman, S.P., Grimmett, D.L., Roy, J.J., Storvick, T.S., Krueger, C.L., Nabalek, C.R., 2001. Pyrometallurgical partitioning of uranium and transuranic elements from rare earth elements by electrorefining and reductive extraction. J. Nucl. Sci. Technol. 38 (1), 36–44.

Uozumi, K., Iizuka, M., Kato, T., Inoue, T., Shirai, O., Iwai, T., Arai, Y., 2004. Electrochemical behaviors of uranium and plutonium at simultaneous recoveries into liquid cadmium cathodes. J. Nucl. Mater. 325, 34–43.

Usami, T., Kurata, T., Inoue, T., Jenkins, J., Sims, H., Beetham, S., Brown, D., 2000. Pyrometallurgical reduction of unirradiated TRU oxides by lithium in a lithium chloride medium. In: Proceedings Of OECD/NEA Workshop on Pyrochemical Separations, Avignon, France, 14-15 March 2000.

Usami, T., Kurata, M., Inoue, T., Sims, H.E., Beetham, S.A., Jenkins, J.A., 2002. Pyrochemical reduction of uranium dioxide and plutonium dioxide by lithium metal. J. Nucl. Mater. 300 (1), 15–26.

Vandarkuzhali, S., Gogoi, N., Ghosh, S., Reddy, B.P., Nagarajan, K., 2012. Electrochemical behaviour of $LaCl_3$ at tungsten and aluminium cathodes in LiCl-KCl eutectic melt. Electrochim. Acta 59, 245–255.

Westphal, B.R., Bateman, K.J., Herrmann, S.D., 2007. Top ten reasons for DEOX as a front end to pyroprocessing. In: ANS Winter Meeting.

Westphal, B.R., Vaden, D., Li, S.X., Fredrickson, G.L., Mariani, R.D., Westphal, B.R., Vaden, D., Li, S.X., Fredrickson, G.L., Mariani, R.D., 2009. Fate of noble metals during the pyroprocessing of spent nuclear fuel. In: Global 2009, Paris, France, September 6-11, p. 9309.

You, G.-S., Choung, W.-M., Ku, J.-H., Cho, I.-J., Kook, D.-H., Kwon, K.-C., Lee, E.-P., Yoon, J.-S., Park, S.-W., Lee, W.-K., 2007. Development of an ACP facility. In: Global 2007, Boise, Idaho, September 9-13, 2007.

Oxide electroreduction and other processes for pyrochemical processing of spent nuclear fuels: Developments in Korea

16

Hansoo Lee
Korea Atomic Energy Research Institute, Daejeon, South Korea

Acronyms

ACPF	advanced spent fuel conditioning process facility
ANL	Argonne National Laboratory
CANDU	Canadian deuterium uranium reactors
DDP	Dimitrovgrad dry process
DFDF	DUPIC fuel development facility
DUPIC	direct use of spent pressurized water reactor fuel in the Canadian deuterium uranium reactors
EBR	experimental breeder reactor
IFR	integral fast reactor
KAERI	Korea Atomic Energy Research Institute
PRIDE	pyroprocessing integrated inactive demonstration facility
PUREX	plutonium uranium redox extraction
REEs	rare-earth elements
TRU	transuranic

16.1 Introduction

Pyro from the Greek means fire, and this implies pyroprocessing is a high-temperature operation. The pyroprocess is generally called a metallurgical or electrochemical process as it produces metal from ore at high temperature. In the 1960s, Argonne National Laboratory (ANL) in the United States started the integral fast reactor (IFR) program, which applied the pyroprocess as a spent fuel treatment process (Till and Chang, 2011). Because the fast reactor in the IFR concept used metal fuel, the pyroprocess is considered an appropriate process to treat the spent fuel from fast reactors.

At the outset, the pyroprocess to handle the spent fuel was pyrometallurgy that liquefies metal followed by extraction of desired elements from the metal mixture at high temperature. This was realized later to be unsuitable for large-scale use so it was replaced by electrochemical processing at high temperature to improve process efficiency.

Reprocessing and Recycling of Spent Nuclear Fuel. http://dx.doi.org/10.1016/B978-1-78242-212-9.00016-2

There are two methods to treat spent nuclear fuel: an aqueous process and a dry process. An aqueous process, of which the plutonium uranium redox extraction (PUREX) process is representative, uses nitric acid to dissolve spent oxide fuel and applies organic reagents to recover target materials in aqueous and organic phases. On the contrary, the dry pyrochemical process uses molten salt so it is able to handle metal fuel directly.

Recently, research institutes worldwide have been interested in pyroprocessing as a potential option for the closed fuel cycle. Fast reactors in Russia and France use oxide fuel, while experimental breeder reactors (EBRs) in the United States use metal fuel. The metal fuel is considered more efficient with respect to heat conductivity, breeding ratio, and so forth, and is considered as a potential fuel for a fast reactor in the future. This use of metal fuel drives the interest in pyroprocessing technology development to handle and recover metal fuel in the fuel cycle. The attractiveness of its intrinsic proliferation resistance is another interesting factor.

In the United States, through the IFR program, spent metal fuel was treated by pyroprocessing (Till and Chang, 2011). Indeed, from 1964 to 1969, approximately 30,000 fuel pins were processed by the melt refining process. The averaged throughput was 100 kg/month. The electrorefining process replaced melt refining, as melt refining was not able to control noble fission product composition in high burn up spent fuel. The electrorefining process can also increase the plutonium and uranium ratio to some extent for refreshing core fuel. After termination of the IFR program in 1994, about 4400 kg of EBR-II driver and blanket spent fuels were treated from 1996 to 2010 by pyroprocessing.

Apart from the US concept of pyroprocessing, Research Institute of Atomic Reactors (RIAR) in Russia developed the Dimitrovgrad dry process (DDP). The DDP, which uses molten salt as an electrolyte, starts with oxide spent fuel and produces oxide fuel for fast reactors. The product from the DDP with vipac technology supplies mixed oxide (MOX) fuel for the Russian fast reactor. Although Japan has developed aqueous processes and constructed a reprocessing plant at Rokashomura, currently waiting for permission to operate, there have been studies on pyroprocessing as a supplementary process. There has been research and development of a process similar to the US concept and engineering-scale experiments were conducted recently. France and India have also studied pyroprocessing as an alternative process. France, in the context of European Commission research projects, have studied liquid aluminum as a cathode for recovering a mixture of transuranic (TRU). Compared with liquid cadmium, liquid aluminum is a favorable material to recover TRU from mixtures of TRU and rare-earth element (REE), due to higher selectivity between the two groups, but higher temperatures are needed to recover the TRU from the Al-TRU mixture. India has a 1-5 kg capacity laboratory for electrochemical processes and is planning construction of the pyrochemical reprocessing research and development (PRRD) facility, which is to be commissioned in 2015. China is also interested in pyroprocessing. Based on their long-term plan, China will construct a pyroprocessing plant by 2030. Korea started pyroprocessing in 1997. Before developing pyroprocessing as a potential spent fuel treatment technology, Korea focused on the development of direct use of spent pressurized water reactor fuel in the Canadian deuterium

uranium reactor (DUPIC) technology, which has higher proliferation resistance than other recycling technologies as there is no chemical or metallurgical separation of fission products from spent oxide fuel. There are pressurized water reactor (PWR) and Canadian deuterium uranium (CANDU) reactors together in Korea, and this enables DUPIC to be developed as a candidate technology for addressing spent fuel management. However, for reasons described later, most activities of the DUPIC program, except the headend process, were halted. Now, Korea is one of the most active countries working on the deployment of pyroprocessing technology for spent fuel treatment.

16.2 Overview of DUPIC process

16.2.1 Background

In 1991, a joint project called DUPIC was launched between ROK, Canada, and the United States (Yang et al., 2006). The purpose of this project was to resolve spent fuel accumulation issues from PWRs and enhance energy resource efficiency by reusing PWR fuels in CANDU reactors. Because no separations on the spent fuel are made, DUPIC can be considered as a highly proliferation resistant recycling process, attractive to countries concerned about proliferation risks of nuclear fuel cycle separations. DUPIC fuel from PWR fuel was fabricated and tested, from which technical data for its appropriate use in CANDU reactors was produced. However, because adoption of CANDU fuel normally takes place in areas without shielding and DUPIC fuel contains high heat and radioactivity, modifications to the construction of existing CANDU reactor buildings were needed to handle DUPIC fuels by remote operations. This led to remarkable cost increases of CANDU reactors with respect to building reconstruction and also the need for new licensing processes from regulatory bodies. Consequently, nuclear power plants were reluctant to accept DUPIC fuel, although it has obvious benefits of reusing PWR fuel as a resource and reducing spent fuel waste. Currently, a part of this DUPIC program remains in order to facilitate handling of PWR fuel in the headend area of the pyroprocess. Developed technologies in the DUPIC program such as decladding, voloxidation, and granulation technologies, are applicable to fuel fabrication for advanced spent fuel conditioning process facility (ACPF) in which oxide reduction is being undertaken.

16.2.2 Progress

The principle of DUPIC is reuse of PWR spent fuel without any chemical separation. The PWR spent fuel is pulverized by an oxidation and reduction process alternately. Then, pelletization and sintering processes fabricate the pulverized powder into pellets. The flow sheet of the DUPIC process is shown in Figure 16.1 (Song et al., 2008). The oxide PWR fuel is disassembled, followed by decladding. Then, it is treated by an oxidation and reduction of oxide fuel (OREOX) process in which oxidation at 450 °C in air and reduction at 700 °C in 4% H_2/Ar processes take place three times,

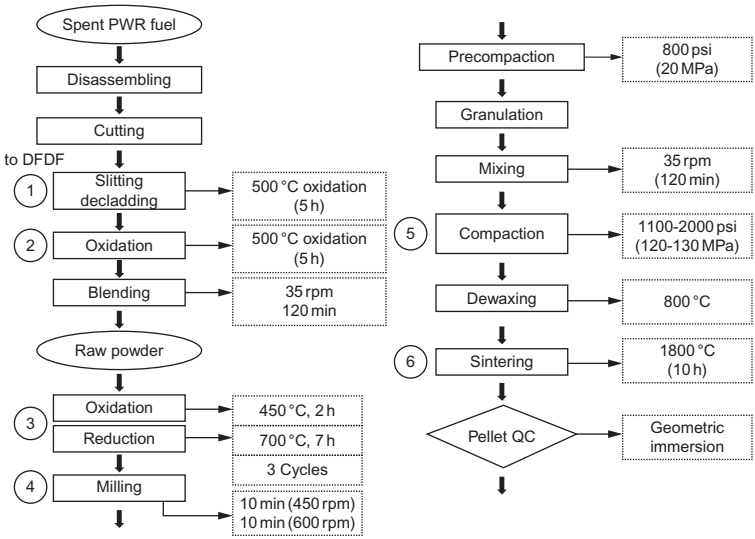

Figure 16.1 Qualified process flow sheet of the DUPIC fuel fabrication.

alternately, to produce suitable powder for DUPIC fuel manufacture. This powder is granulated, mixed, compacted, dewaxed, and sintered, consequently yielding the DUPIC pellets.

The pellet was irradiated in HANARO, a research reactor at Korea Atomic Energy Research Institute (KAERI), and postirradiation effects were examined (Yang et al., 2006). Good results showed the applicability of DUPIC fuel in a CANDU reactor. The optical microstructures of irradiated fuel pellets shown in Figure 16.2 (Yang et al., 2006) indicated the irradiation test of DUPIC fuel at HANARO and DUPIC fuel in National Research Universal (NRU) reactor in Canada were under the same conditions as CANDU, and not much different.

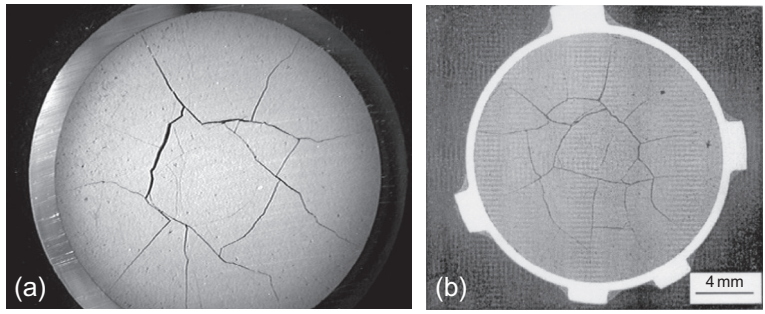

Figure 16.2 View of irradiated fuel pellets: (a) DUPIC fuel irradiated at Hanaro and (b) DUPIC fuel irradiated in NRU, Canada.

A part of DUPIC technology is used as the pretreatment technology of pyroprocessing. Remote operations such as disassembling, decladding, and slitting technologies are useful to handle spent oxide fuel from PWRs. The voloxidation process is also applied for removing volatile elements. Destructive analysis and nondestructive assay for oxide fuel are directly employed for nuclide distribution analysis in oxide fuel.

16.3 Role of pyroprocessing in the fuel cycle; advantages and disadvantages of pyroprocessing

The advanced fuel cycle addresses the issues associated with managing spent fuel. The main idea is to recover groups of elements according to their characteristics. Uranium, which comprises about 92% of the spent fuel, is recovered for reuse in fast reactors. This enhances uranium utilization efficiency. Recovering and also reusing the TRU elements in fast reactors allows burning of long-lived actinides with the effect that the overall radiotoxicity of the waste can be reduced by a factor of 1000 (OECD/NEA, 2009; Warin, 2011). Cesium and strontium in spent fuel are major elements that emit heat in the short term after fuel is removed from the reactor. Recovering these elements reduces the heat load from the spent fuel, resulting in a dramatic reduction of repository footprint (Wigeland et al., 2006; Ko and Kim, 2009).

Pyroprocessing is able to recover TRU elements together; this is due to the thermodynamic characteristics in the molten salt system, in which the TRU elements have quite similar deposition potentials in the liquid cadmium cathode. Pyroprocessing can then be used to supply the recycled fuel for the fast reactor. Aqueous processes can also recover groups of elements but, in the case of metal fuels, pyroprocessing is arguably a more appropriate technology. Because the molten salt in pyroprocessing is known to be stable under a strong radioactive environment, pyroprocessing is able to handle short-cooled spent fuel with high heat and high radioactivity (Hannum et al., 1997; Inoue and Koch, 2008). The environment of high heat and radioactivity increases intrinsic barriers to human intrusion. Consequently, pyroprocessing needs a facility comprising hot cells, implying consequent application of better containment and surveillance concepts with a strengthened physical barrier (Borrelli, 2013). The inseparable product mixture of U, TRU, and other fission products significantly increases intrinsic proliferation resistance (see Table 16.1).

Regarding technical maturity, pyroprocessing is immature with technology still to be developed for commercialization. In contrast, aqueous processing using the PUREX process is a commercial operation, which means the technology is mature. However, compared with pyroprocessing, aqueous processes require a longer cooling time at the storage pool to reduce heat and radioactivity of spent fuel to prevent excessive organics degradation.

Table 16.1 PWR spent fuel composition (4.5 wt% enriched U, 55 GWd/tU burn up, 10 years cooling)

Group	Elements	wt%
U	U	92.9
FP	Cs, Sr	0.53
	I, Tc	0.16
	Other FPs	5.01
TRU	Pu	1.16
	MA	0.2

16.4 Fundamentals of molten salts separations

The principle behind exploiting electrochemistry for separation is using the differences in Gibbs free energy of formation. Table 16.2 shows Gibbs free energy of formation for various elements (Till and Chang, 2011; Koyama et al., 2012).

The benefits of using molten salt instead of aqueous electrolyte are higher operating temperature, insensitivity to radioactivity, and higher conductivity. These enable stable operations under high radioactivity and temperature conditions. If liquid cadmium is used as a cathode, then the deposition potential of actinides lies in a narrow band so that the separation of actinides is most unlikely. This induces high intrinsic proliferation resistance as well.

Table 16.2 Gibbs free energy of formation

Element	Standard Gibbs free energy (kcal/g-equiv.)
KCl	86.7
LiCl	82.5
$LaCl_3$	70.2
$CeCl_3$	68.6
$NdCl_3$	67.9
YCl_3	65.1
$AmCl_3$	64.3
$CmCl_3$	64.0
$PuCl_3$	62.4
$NpCl_3$	58.1
UCl_3	55.2
$ZrCl_4$	46.6
$CdCl_2$	32.3
$FeCl_2$	29.2
$MoCl_4$	16.8

The principle of electrochemistry is applying an appropriate voltage to dissolve metal at the anode in the electrolyte and deposit the metal simultaneously at the cathode. The required equilibrium potential is expressed by the Nernst equation (Bard and Faulkner, 2001).

$$E = -\frac{\Delta G}{zF} = -\frac{\Delta G^{\circ}}{zF} - \frac{RT}{zF}\ln a = E^{\circ} - \frac{RT}{zF}\ln a \tag{16.1}$$

To proceed with the reaction, an overvoltage is necessary. This overvoltage is associated with current, which can be expressed by the Butler-Volmer equation.

$$i = i_0\left\{\exp\left((1-\alpha)\frac{zF}{RT}\eta\right) - \exp\left(-\alpha\frac{zF}{RT}\eta\right)\right\} \tag{16.2}$$

The operation of electrochemical reaction can be in galvanostatic or potentiostatic modes. For each case, reaction kinetics can be simulated based on the model with proper assumptions (Bard and Faulkner, 2001). In galvanostatic mode, when a planar electrode and unstirred condition in the electrolyte are assumed, the relation of transition time, τ, and diffusivity of solute in the solution is expressed as follows:

$$\frac{i\tau^{1/2}}{C_o} = \frac{nFAD^{1/2}\pi^{1/2}}{2} \tag{16.3}$$

where i is constant current, τ is transition time in which the surface concentration at the surface drops from C_o to zero, n is stoichiometric number of electrons, F is the Faraday constant, A is the surface area of the electrode, and D is the diffusivity.

In potentiostatic mode, under the same assumptions of a planar electrode and unstirred solution, the current density i and diffusivity of solute in the solution is expressed as follows:

$$i(t) = \frac{nFAD^{1/2}C_o}{\pi^{1/2}t^{1/2}} \tag{16.4}$$

This information provides the operational voltage and current for the electrochemical reaction, from which parameter values pertinent to the design of an electrochemical reactor can be induced.

16.5 Introduction to the pyrochemical process

16.5.1 Background

Korea has increased the share of nuclear power in the total energy supply since the country industrialized. This is due to lack of natural resources as indicated by the fact that 97% of the country's energy is imported. Growth of nuclear power plants

inevitably led to a rise in spent fuel management issues. In order to address spent fuel issues, KAERI has developed pyroprocessing technology. Aqueous processing, in which class the PUREX process is representative, is considered to be a less proliferation-resistant process; so, for this reason, Korea is trying to develop a proliferation-resistant fuel cycle using the pyroprocess.

16.5.2 Flow sheet

The pyroprocessing flow sheet is shown in Figure 16.3. Pyrochemical processes are used to group-recover actinides using electrochemical processing. As the metal phase is requisite to flow electric current, an upfront oxide-reduction process is necessary to convert spent oxide fuel to metal. Detailed descriptions on the processes are published elsewhere (Lee et al., 2013a).

In the headend stage, separation of oxide spent fuel from the assembly is followed by a voloxidation process that changes the physical form of oxide spent fuel to powder, and volatile elements including iodine and cesium are released. The powder produced by the voloxidation process is compacted to a pellet, which is transferred to the following oxide-reduction process.

Strontium and residual cesium are removed from spent metal fuel in the oxide-reduction process. Uranium is recovered mainly in the electrorefining process, which employs a solid cathode. The rest of the dissolved elements in the salt such as residual U, TRU, and REE are recovered in an electrowinning process with the liquid metal cathode. Salts in oxide-reduction and electrowinning processes are recycled after purification of contaminated salt by appropriate methods.

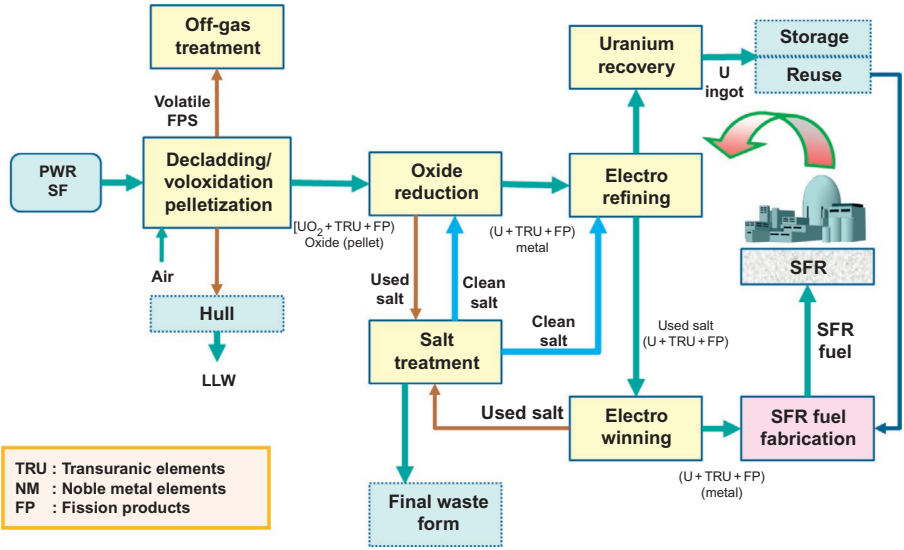

Figure 16.3 Pyroprocessing flow sheet developed by KAERI.

16.5.3 History

In 1997, KAERI started to study pyroprocessing. In the beginning, the oxide-reduction process was studied. Similar to ANL, liquid metal extraction was tested to reduce the oxide fuel. Laboratory-scale experiments were successfully conducted. However, the operational conditions and procedures were inadequate to scale-up, so that the metal-reduction process was switched to an electrochemical process. The next trial was an integrated oxide-reduction system in which a magnesia crucible encompassed a cathode rod, oxide powder produced after voloxidation, and the Li_2O reducing agent. The benefit of using this integrated oxide-reduction system is direct loading of oxide powder after voloxidation at the cathode. Moreover, magnesia is a nonconducting material used to separate the anode and cathode electrically, while being porous so the ion can be freely transferred through the magnesia crucible from the salt. However, magnesia crucibles have less mechanical integrity and sometimes the crucible was broken and the process was difficult to operate remotely. After trials, a stainless steel screen was used to accommodate the oxide pellet at the cathode.

The electrorefining system has been tested with various cathodes to recover uranium dendrites efficiently. Graphite was chosen as a potential cathode because the graphite shell peels off as uranium dendrites grow on the surface of the cathode. This reduces the work related to recovery of dendrites by cutting them off from the cathode surface, and it increases current efficiency, which can be lowered if reverse current is applied to eliminate residual dendrite tips.

Electrowinning process development started recently, beginning in 2007. Though actual actinides are not authorized to be used in experiments, simulated material is effectively used to investigate electrochemical reactions. A residual actinide recovery system was developed to control the REE concentrations after the electrowinning process, as the maximum RE concentrations are confined by the requirements for fast reactor fuel composition.

16.6 Headend and oxide-reduction process

16.6.1 Headend process

The headend stage includes disassembling, cutting of fuel rods, decladding, and feed material fabrication. The goals of technology development for the headend process are enhancement of the fuel material recovery and increase of fission product removal from the cladding material. Mechanical decladding is relatively easier than the oxidative method. Roller straightener, hammering, agitation using a ball mill, and slitting methods are the various potential mechanical decladding methods. Mechanical decladding efficiency with fuel burn up is shown in Figure 16.4. Decladding efficiency is high; up to 58 GWd/tU burn up. However, it is significantly reduced as burn up increases. Mechanical decladding followed by the oxidative method showed more than 99% recovery of fuel material. The efficiency of oxidative decladding depends on fuel burn up, oxidation conditions, and chopped fuel length. Figure 16.5 shows that

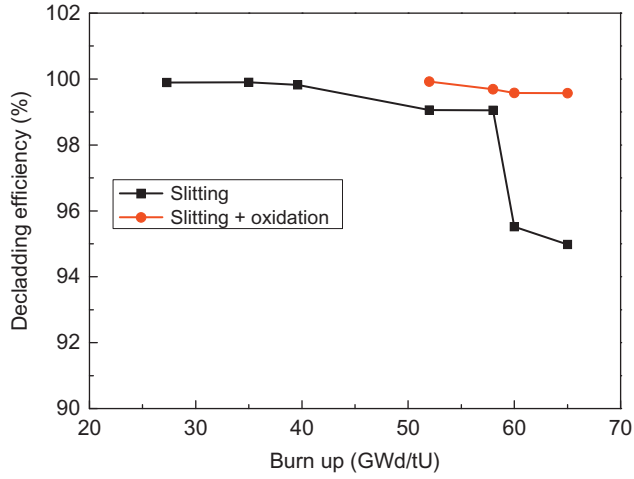

Figure 16.4 Decladding efficiency according to variation of burn up. (Fuel: PWR oxide fuel with 3.5-4.5% enrichment; cladding material: all Zircaloy-4 except Zirlo for 65 GWd/tU.)

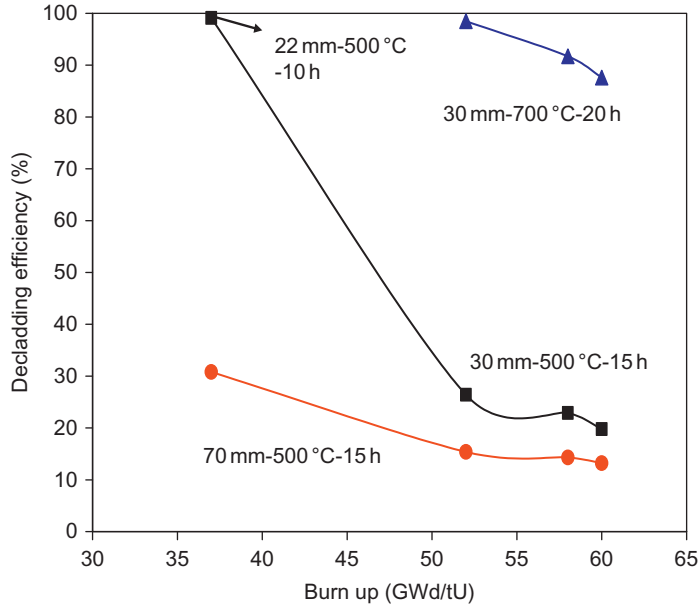

Figure 16.5 Oxidative decladding efficiency according to variation of rod cut length and burn up. (Fuel: PWR oxide fuel with 3.5-4.5% enrichment; cladding material: Zircaloy-4.)

decladding efficiency depends on burn up and chopped fuel lengths (Park et al., 2009). High temperatures, vacuum, and shorter chopped fuel lengths enhance decladding efficiencies. The product of oxidative decladding is U_3O_8 powder.

The feed material for the following process is fabricated by granulation or pelletization. For granule production, U_3O_8 powder is treated in the rotary voloxidizer at a temperature of 1150-1200 °C in an argon atmosphere. The recovery rate is about 89% for granules larger than 1 mm, while 98% for granules larger than 0.5 mm. Porous pellets with true densities of 60-70% can be fabricated by conventional compaction followed by sintering (Lee et al., 2012b).

16.6.2 Oxide reduction

Oxide reduction converts the oxide materials from the headend process to a metal feed ready for the following electrochemical process. The anode is normally platinum, while the cathode uses a stainless steel mesh basket encompassing the oxide material. The salt is LiCl containing Li_2O, and the reaction takes place at 650 °C. The reactions at the cathode are

$$\begin{aligned} &Li^+ + e^- \rightarrow Li \\ &UO_x + 2x\,Li \rightarrow U + xO^{2-} + 2x\,Li^+ \\ &UO_x + 2x\,e^- \rightarrow U + xO^{2-} \end{aligned} \tag{16.5}$$

At the anode, the reaction is

$$xO^{2-} \rightarrow \frac{x}{2}O_2 + 2x\,e^- \tag{16.6}$$

The lithium facilitates the electroreduction rate of UO_2, as verified by cyclic voltammetry and chronopotentiometry (Park et al., 2008a,b; Jeong et al., 2010; Hur et al., 2010).

Li^+ ion concentration is a key factor for the platinum anode corrosion and reduction reaction. When Li^+ ion concentrations are low, a platinum spallation process occurs, resulting in platinum loss (Jeong et al., 2009). If the Li^+ ion concentration is high, the backward reaction in Equation 16.5 is favored, impeding the material reduction rate (Usami et al., 2002). The optimum Li_2O concentration is known to be about 1%. For monitoring the reaction, the O^{2-} ion concentration can be measured by *in situ* square wave voltammetry (Choi et al., 2012). Li_2O concentrations less than ~0.8% are compared through the measurements of square wave voltammetry and acid titration, and the results are very close together.

Investigations of reaction rate kinetics are necessary to design the reduction reactor efficiently. Oxygen is evolved as a gas at the anode and oxide ion is dissolved into the salt at the cathode. The rate determining resistance in the overall reaction is on the gas evolution side rather than the oxide ion dissolution reaction. This has been verified experimentally (Choi et al., 2011) in Figure 16.6, showing that, after a threshold point, decreasing cathode to anode ratio increases the current density. This indicates that

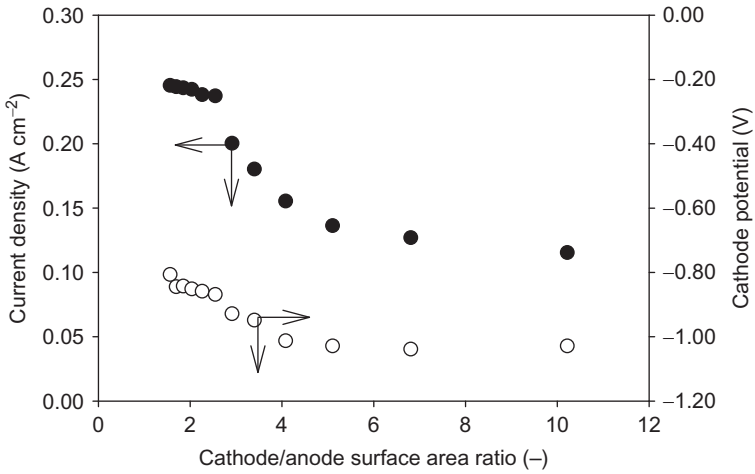

Figure 16.6 Effect of the cathode/anode surface area ratios on the current density and the cathode potential.

attention should be paid to anode surface area in the reactor design. Another issue at the anode is guiding oxygen evolution by a shroud. Without a shroud, evolved oxygen is present in the cover gas; consequently, oxygen is released to the argon cell when the reactor flange is open. The shroud also protects against lithium reaction with the anode material, which causes corrosion of the anode. If a nonporous shroud is applied at the anode, then the reaction is occurring at the tip of the anode, which leads to the corresponding oxygen evolution reaction area to be small. The porous shroud is much better from this perspective (Choi et al., 2014).

Unlike uranium oxide, some rare earth oxides are not completely reduced by lithium; however, unreduced rare earth oxide can be handled by further electrochemical processing (Park et al., 2012). The unreduced rare earth oxides can react with UCl_3, which is a chemical constituent in the salt of the electrorefining reactor, to give rare earth chlorides and uranium oxide. Rare earth chlorides in the salt are routed to the electrowinning process, where most of them are removed, and eventually become part of the waste product. Uranium oxide produced by the reaction of unreduced REE and UCl_3 is recovered from the electrorefining salt and is recycled to be a part of oxide fuel material in a headend process or abandoned as a waste.

The oxide feed form, as fabricated from the prior process, was tested to investigate the impact on reduction rate (Choi et al., 2013) in Table 16.3. Cylindrical pellets, crushed lumps and particles, and granules were tested. Lower densities and smaller size are favorable for higher reduction rates; however, mechanical integrity should also be considered when choosing the feed form.

After the reaction, the reduced cathode product includes salt. This salt should be removed before being transferred to the following process; that is, distillation at 900 °C under 1 torr vacuum is applied to remove the salt. More than 99% of the salt is recovered. This salt contains strontium and residual cesium, which emit high heat in

Table 16.3 Comparison of conversion rate of various UO_2 forms after electrolytic reduction in 1 wt% Li_2O-LiCl at 650 °C

Type (pictures)	Density (%)	Size[a] (mm)	Conversion rate to metal U (%)[b]				
			Run 1	Run 2	Run 3	Run 4	Run 5
Cylindrical pellet	55	ϕ 6, 8 (H)	Not used	Not used	100 ± 0.3	Not used	97.0 ± 2.7
	60	ϕ 9, 8 (H)	Not used	Not used	86.0 ± 3.5	68.0 ± 4.5	Not used
	70	ϕ 8, 8 (H)	Not used	Not used	96.4 ± 0.5	96.0 ± 3.9	Not used
	80	ϕ 8, 7 (H)	Not used	87.4 ± 6.0	95.5 ± 0.5	90.0 ± 4.1	Not used
	>95	ϕ 10, 12 (H)	46.0 ± 4.0	Not used	Not used	12.0 ± 5.6	Not used
Crushed particles of type P-95%	>95	1-5	97.0 ± 4.0	Not used	Not used	Not used	95.0 ± 3.2
Granule	40	ϕ 1-5	Not used	100 ± 0.5	Not used	Not used	Not used

[a]The sizes were measured in ambient atmosphere.
[b]In each run, the different UO_2 forms were loaded in a cathode basket and their electrolytic reduction was simultaneously performed.

the short term. The salt is transferred to a waste salt treatment system where the salt is recycled by purification, and the residual materials are abandoned as solid waste.

16.7 Transuranic separations

16.7.1 Electrorefining

The role of the electrorefiner is to recover most of the uranium from metallic spent fuel transferred from the preceding oxide-reduction process. The solid cathode is used for uranium deposition, while the anode uses a metal basket for containing the metallic fuel. These electrodes are immersed in LiCl-KCl eutectic salt maintained at 500 °C. At the anode, elements including U, TRU, and REE dissolve. The residual elements such as zirconium and others remain at the anode, which is treated as waste at the end of the electrorefining. These remaining elements are fine particles that may be suspended in the salt. This requires that the basket be finely porous in order to retain the particles inside the basket. So, the respective reactions at the cathode and anode are

$$U^{3+} + 3e^- \rightarrow U \tag{16.7}$$

$$U, TRU, REE \rightarrow U^{3+}, TRU^{3+}, REE^{3+} + 3e^- \tag{16.8}$$

The graphite cathode is used for recovery of uranium dendrites, at which the graphite peels off as the uranium dendrites grow on the graphite surface (Kang et al., 2006; Lee et al., 2008). This eliminates the conventional scraping process for recovering uranium dendrites from the solid cathode, resulting in an increase of the throughput.

The rate-determining step in the overall reaction has been experimentally explored and found to be anodic dissolution (Li, 2002). Interfacial charge transfer coupled with diffusion resists the anode dissolution reaction, implying increased anode area should be considered to overcome the weakness of a rate-determining step (Lee et al., in press). However, in reality the anode area effect is not a significant issue, as the overall reaction in electrorefining takes place in constant current mode. This means the reaction is proportional to the applied current and the rate-determining step affects only an increase in the overpotential that relates to the product purity. As the reaction proceeds, the potential increases gradually under the constant current due to a decrease of concentration of target material in the salt. As the potential increases, the element next to the target material is recovered together with the target material, leading to increasing product impurity.

UCl_3 is a precursor in the electrorefining reaction, which allows uranium and other elements to be dissolved in the salt and deposit on the cathode. If the UCl_3 concentration is too low, then TRU in the metal at the anode is able to codeposit on the cathode. More than 6% of UCl_3 is required to restrict the deposition of elements other than uranium (Lee et al., 2006). The uranium purity is crucial because, if the uranium product is contaminated, then it can be classified into a higher-level waste category. The dependencies of applied voltage and initial UCl_3 concentration on the composition of recovered metal are shown in Figure 16.7.

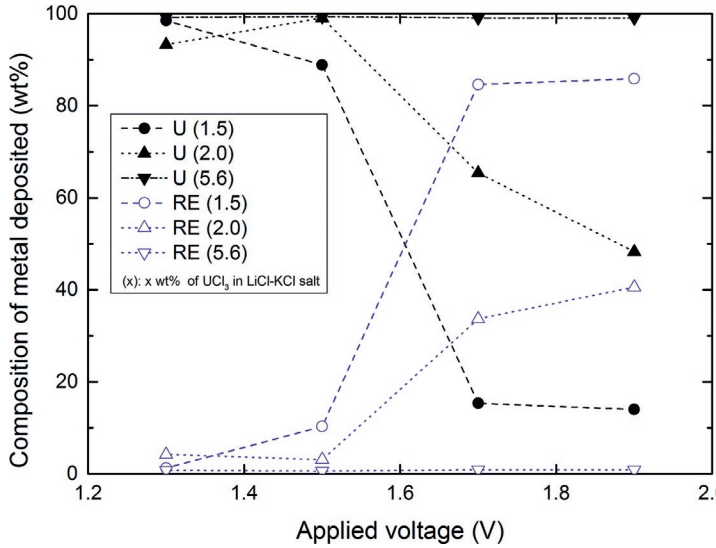

Figure 16.7 Dependencies of the applied voltage and initial UCl_3 concentration in the LiCl-KCl salt on the composition of the metal deposited at 500 °C.

The uranium product contains LiCl-KCl eutectic salt entrapped in dendrites. The salt is recycled to the electrorefiner after distillation. The distillation behavior of mixtures of uranium and rare earth chlorides were investigated. The vapor pressure of rare earth chlorides is lower than LiCl and KCl; however, it was found that the rare earth chloride is covaporized with LiCl-KCl eutectic salt (Park et al., 2011). Prior to distillation, liquid separation by moderate heating is favored for removal of liquid salt from the solid dendrites in regard to reduction of the distillation burden and faster processing rates (Kwon et al., 2011).

The distilled uranium dendrite is cast in a furnace into ingot form for safe and easy interim storage. An initial charge of molten metal in the crucible, followed by the addition of solid dendrite into the molten metal, facilitates smooth processing (Jang et al., 2013).

The salt containing residual U, TRU, and rare earth elements then moves to the electrowinning process, where all the elements are recovered together.

16.7.2 Electrowinning

The LiCl-KCl eutectic salt transferred to electrowinning from the electrorefining process contains residual U, TRU, and REE. These elements can be recovered together by using the liquid cadmium cathode. The anode can use uranium for compensating element depletion in the salt, or an inert cathode at which Cl_2 gas evolves as the electrochemical reaction proceeds. Various materials were tested for an inert anode. Molybdenum corroded but graphite or glassy carbon were found to be suitable materials (Paek et al., 2013). However, if the anode is a rod, of which the surface area is

relatively small, then the overall reaction rate can be reduced as the rate-determining step is Cl_2 evolution at the anode. This suggests that the surface area of the anode should be relatively large. Another issue in anode design is a shroud to guide evolved Cl_2 gas. If a nonconducting material is used, then ions for transfer are concentrated at the bottom tip of the anode, which increases nonuniform potential distribution around the anode leading to decrease of the current efficiency. To resolve these issues, a graphite tube with a silicon carbide shroud is introduced to the electrowinning reactor, showing enhanced results by increasing the anode area and allowing salt transport through the shroud (Kim et al., 2013).

While the electrowinning reaction proceeds, uranium deposits faster than TRU and REE, so that deposited uranium on the surface of cadmium at the cathode grows to run off from the cadmium cathode crucible. This process was hampered by introducing a mesh-type stirrer. The rotating mesh-type stirrer moves down into the cadmium cathode, pushing uranium dendrites into the liquid cadmium. This mesh functions not only to restrict uranium growth out of the crucible but also to increase the uranium content in cadmium. The uranium solubility in cadmium is 2.35%, but this pushing of uranium into cadmium increases the uranium content up to 5% (Paek et al., 2010).

The U:TRU:REE elemental ratio in the salt from the electrorefining process is approximately 1:3:4. If these elements are recovered all together, the composition is not compatible with fuel requirements for the fast reactor. The maximum allowable REE concentration is reported to be 5% (Ohta et al., 2009). In order to adjust the REE concentration in the product, oxidation of REE by $CdCl_2$ injection has been tested (Shim et al., 2009). Once all elements are deposited in cadmium, the injection of $CdCl_2$ oxidizes the REE selectively. The product is rare earth chlorides that redissolve into the salt. Oxidation of the REE is more favorable than oxidation of TRU or uranium. Accordingly, REE becomes richer in the salt, while poorer in cadmium as the oxidation reaction proceeds.

Finally, the product with adjusted composition of U-TRU-REE is distilled to remove cadmium and transferred to the fast reactor fuel fabrication process.

16.8 Waste treatment

There are two salt wastes; one is from the oxide-reduction process containing cesium and strontium, and the other is the waste containing REE from the electrowinning process.

Cesium and strontium are characterized by high heat emission so that not only the purpose of salt recovery but also separation of heat-emitting elements is necessary to satisfy fuel cycle objectives. Crystallization is used to recover pure salt from LiCl salt containing cesium and strontium (Cho et al., 2010). Crystallization uses the difference of solubilities of elements in liquid and solid phases. This method is preferred compared with ion exchange methods to remove Group I and II elements, because ion exchange needs exchange media, which increases the waste volume.

Oxidation is used to remove REEs from the LiCl-KCl salt used in the electrowinning process (Cho et al., 2009). The oxide-conversion efficiency is 99%. In order to

enhance operating conditions such as lower operating temperature and faster oxidation reaction rate, phosphate precipitation is used (Cho et al., 2013). In this case, Li_3PO_4 and K_3PO_4 are used as oxidants together. REEs react with phosphate ions to produce rare earth phosphates that are subject to precipitation, while both lithium and potassium ions in the oxidants remain in the salt. Consequently, the eutectic ratio of lithium and potassium is preserved in the salt.

After oxidation, the sediment involves eutectic salt and REE precipitates, in particular, containing 80% eutectic salt and 20% rare earth oxides. In order to reduce waste volume and increase the amount of recycled salt, the sediment is treated by distillation (Eun et al., 2012). The salt recovery rate by precipitation followed by vacuum treatment is 99%.

The separated cesium and strontium in LiCl salt concentrates need to be solidified for production of the final waste form. SAP (SiO_2-Al_2O-P_2O_5) was investigated as a stabilizer (Park et al., 2008a,b). SAP functions well by resolving the difficulty of solidification of chloride salt. The stabilized solid is mixed with borosilicate glass and heat treatment so that the final solid matrix satisfies conditions for final disposal by having low leachability. The precipitated REEs are mixed with ZIT (zinc titanate: Zn_2TiO_4) producing a ceramic for waste disposal (Ahn et al., 2011).

16.9 Facilities for engineering-scale development of the Korean pyroprocess

DUPIC fuel development facility (DFDF) illustrated in Figure 16.8 is the hot cell facility for DUPIC fuel handling. It has 10 operating windows and operates under an air environment. It was constructed in 1999 and has been in operation since 2006 for DUPIC fuel pellets/rod fabrication using PWR spent fuel including qualification of DUPIC fuel fabrication. The high-power irradiation test on DUPIC fuel manufactured at DFDF was carried out at the HANARO research reactor (Jung et al., 2001; Ryu et al., 2008). From 2007, DFDF has been used for the improvement of key technologies for DUPIC such as fabrication of DUPIC fuel using high burn up PWR spent fuel. More recently, DFDF functions as a headend process for pyroprocessing. Disassembly and rod cutting activities are carried out at post irradiation examination facility (PIEF), and decladding, mixing, voloxidation, and fuel fabrication for the oxide-reduction process are conducted in DFDF.

Figure 16.8 Views of DFDF: (left) the exterior view of DFDF; (right) spent fuel rod in manipulator.

ACPF was constructed in 2005 for testing oxide reduction of spent fuel. In the beginning, the cathodic part of the oxide-reduction reactor used an integrated unit of magnesia crucible containing uranium oxide powder and cathode. This integrated unit was immersed in the salt. The reduction reaction was successfully demonstrated; however, a magnesia crucible was too weak to be remotely handled. The design of the oxide-reduction reactor was consequently changed. ACPF is now under refurbishment for accommodating an argon chamber in the hot cell.

Instead of using spent fuel, an integrated inactive test facility is needed to test integrity of all pyroprocessing unit processes, process flow monitoring, equipment remote operability, and process information tracking. (*Inactive* test here means no use of irradiated fuel.) Instead, uranium and surrogate materials will be in use as feed material. For these purposes, the pyroprocessing integrated inactive demonstration facility (PRIDE) was constructed in 2012. It has 17 windows and 17 sets of manipulators. The PRIDE environment is under argon, and an argon purification process is installed to keep the environmental conditions such as moisture and oxygen contents below specified limits. There is a large transfer lock system to transfer equipment into the cell and to return the broken parts back to a workshop. A small transfer lock is located at the end of the cell. Samples or small equipment are transferred through the small transfer lock. Two gravity tubes are placed at both ends of the cell. Tools and simple devices will be introduced through the gravity tubes. Views of PRIDE are shown in Figure 16.9.

Safety analyses have been carried out on the PRIDE with process with radiological, criticality, structural, environmental, and industrial safety issues evaluated and reviewed (You et al., 2011). The dose-rate assessment considering use of uranium and simulated materials turned out to be far below the regulation limit.

The remote operability of the facility system and equipment are crucial to operate the facility properly. Conventional master-slave manipulators with 15 kg payload are used in the operation of unit equipment and material transportation. However, finer actions for operations and more complex motions are envisioned to operate the complicated equipment so that a bridge-transported bilateral master-slave manipulator (BDSM) was developed (Lee et al., 2012a, 2013b). This manipulator, capable of handling 25 kg/arm, was successfully installed, showing good performance in meeting the desired actions.

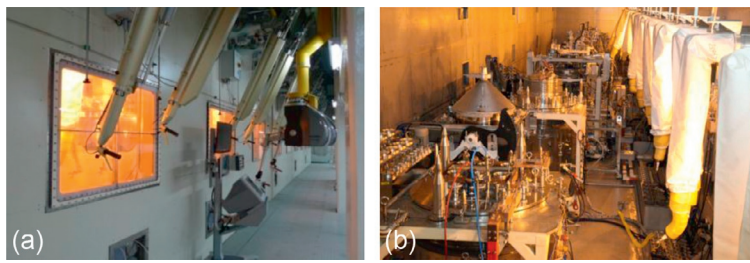

Figure 16.9 Views of PRIDE: (a) exterior view of PRIDE and (b) interior view of PRIDE.

Because the PRIDE cell was planned to be constructed in a pre-existing building used for another purpose, the cell space was limited to accommodate all unit equipment. The oxide-reduction, electrorefining, electrowinning, and waste salt treatment processes are in an argon cell placed on the second floor. Fuel fabrication, uranium ingot casting equipment, and waste solidification processes in glove boxes are located on the first floor. The design information verification by IAEA was achieved in 2012. After completing the blank test, which comprises assembling and disassembling equipment by remote operation, temperature testing, electric current checking, and an electronic devices check, a salt was recently introduced. The purpose of the salt test is investigation of individual equipment operability, evaporated salt vapor effects on moving parts, salt transportation, process losses in individual unit processes, holdup information, and electronic signal transmittances. The salt test was continued through 2014, followed by uranium testing in 2015. Surrogate materials will be tested subsequently. Operation of PRIDE will provide utility operational experience, equipment design improvement, material measurement, online/offline monitoring, material flow checks, testing of other innovative concepts for unit processes, and personnel training, which includes not only process operation, but also maintenance of equipment and apparatus.

16.10 Future trends

Pyroprocessing research and development must be continued to develop the range of interrelated technologies needed. Laboratory-scale testing has been successfully verified and the technologies for engineering-scale deployment are now under development. PRIDE, using "inactive" materials, will contribute toward technology development with this perspective. For actinide-related experiments, a US-ROK joint fuel cycle study is in progress. Combination of these two activities, scale-up technology and actinide-related technology development, will increase the technical maturity of pyroprocessing in the future.

The direction of technology developments is to increase process efficiency and throughput, to enhance economic viability and proliferation resistance. The reactor design related to electrochemistry will thus be studied. The effects of actinides or impurities of REE will be carried out to explore the product quality and generated waste volume. Handling of high-temperature salts and reactions with corrosive materials will be explored. Various innovative concepts will be examined to increase throughput, remote operability, and safety.

In particular, for increasing transparency of pyroprocessing technology, cooperation with IAEA is needed in terms of safeguards development. The development of safeguards technology is essential to ensure proliferation resistance. NDA and DA technologies, online and offline monitoring for tracking special nuclear materials will be stringently deployed.

Conceptual designs for pyroprocessing incorporating advanced technologies and advanced safeguards concepts will be needed to evaluate economic viability and proliferation perspectives. Reflecting the political strategy will also be an important issue. It is obvious that application of a closed fuel cycle can be a promising option to resolve

spent fuel management issues by reducing repository footprint and decay periods of disposed products as well. In this regard, worldwide discussions on closed fuel cycle strategies will energize technology development by clarifying the benefits of closing the fuel cycle and making a consensus between stakeholders and the public regarding the closed fuel cycle option.

References

Ahn, B.G., Park, H.S., Kim, I.T., Cho, Y.Z., Lee, H., 2011. Immobilization of lantanide oxides waste from pyrochemical process. Energy Procedia 7, 529–533.

Bard, A.J., Faulkner, L.R., 2001. Electrochemical Methods. John Wiley & Sons, Inc., New York.

Borrelli, R.A., 2013. Use of curium spontaneous fission neutrons for safeguardability of remotely-handled nuclear facilities: fuel fabrication in pyroprocessing. Nucl. Eng. Des. 260, 64–77.

Cho, Y.Z., Park, G.H., Yang, H.C., Han, D.S., Lee, H., Kim, I.T., 2009. Minimization of eutectic salt waste from pyroprocessing by oxidative precipitation of lanthanides. J. Nucl. Sci. Technol. 46, 1004–1011.

Cho, Y.Z., Park, G.H., Lee, H., Kim, I.T., Han, D.S., 2010. Concentration of cesium and strontium elements involved in a LiCl waste salt by a melt crystallization process. Nucl. Technol. 171, 325–334.

Cho, Y.Z., Lee, T.K., Eun, H.C., Choi, J.H., Kim, I.T., Park, G.I., 2013. Purification of used eutectic (LiCl-KCl) salt electrolyte from pyroprocessing. J. Nucl. Mater. 437, 47–54.

Choi, E.Y., Hur, J.M., Choi, I.K., Kwon, S.G., Kang, D.S., Hong, S.S., Shin, H.S., Yoo, M.A., Jeong, S.M., 2011. Electrochemical reduction of porous 17 kg uranium oxide pellets by selection of an optimal cathode/anode surface area ratio. J. Nucl. Mater. 418, 87–92.

Choi, E.Y., Choi, I.K., Na, S.H., Hur, J.M., Kang, D.S., Shin, H.S., Jeong, S.M., 2012. In situ electrochemical measurement of O^{2-} concentration in molten salt Li_2O/LiCl during uranium oxide reduction process. Electrochem. Solid Lett. 15, E11–E13.

Choi, E.Y., Kim, J.K., Im, H.S., Choi, I.K., Na, S.H., Lee, J.W., Jeong, S.M., Hur, J.M., 2013. Effect of the UO_2 for on the electrochemical reduction rate in a LiCl-Li_2O molten salt. J. Nucl. Mater. 437, 178–187.

Choi, E.Y., Won, C.Y., Cha, J.S., Park, W., Im, H.S., Hong, S.S., Hur, J.M., 2014. Electrochemical reduction of UO_2 in LiCl-Li_2O molten salt using porous and nonporous anode shroud. J. Nucl. Mater. 444, 261–269.

Eun, H.C., Cho, Y.Z., Son, S.M., Lee, T.K., Yang, H.C., Kim, I.T., Lee, H., 2012. Recycling of LiCl-KCl eutectic based salt wastes containing radioactive rare earth oxychlorides of oxides. J. Nucl. Mater. 420, 548–553.

Hannum, W.H., Wade, D.C., McFarlane, H.F., Hill, R.N., 1997. Nonproliferation and safeguards aspects of the IFR. Prog. Nucl. Energy 31, 203–217.

Hur, J.M., Jeong, S.M., Lee, H., Lee, H., 2010. Underpotential deposition of Li in a molten LiCl-Li_2O electrolyte for the electrochemical reduction of U from uranium oxide. Electrochem. Commun. 12, 706–709.

Inoue, T., Koch, L., 2008. Development of pyroprocessing and its future direction. Nucl. Eng. Technol. 40, 183–190.

Jang, J.H., Kang, H.S., Lee, Y.S., Lee, H., Kim, J.G., 2013. Development of continuous ingot casting process for uranium dendrites in pyroprocess. J. Radioanal. Nucl. Chem. 295, 1743–1751.

Jeong, S.M., Shin, H.S., Cho, S.H., Hur, J.M., Lee, H., 2009. Electrochemical behavior of a platinum anode for reduction of uranium oxide in a LiCl molten salt. Electrochim. Acta 54, 6335–6340.

Jeong, S.M., Shin, H.S., Hong, S.S., Hur, J.M., Do, J.B., Lee, H., 2010. Electrochemical reduction behavior of U_3O_8 powder in a LiCl molten salt. Electrochim. Acta 55, 1749–1755.

Jung, I.H., Song, K.C., Kang, K.H., Yoo, B.O., Hung, Y.H., Park, H.S., Yang, M.S., 2001. Characterization of irradiated simulated DUPIC fuel. Met. Mater. Int. 7, 513–518.

Kang, Y.H., Lee, J.H., Hwang, S.C., Shim, J.B., Kim, E.H., Park, S.W., 2006. Electrodeposition characteristics of uranium by using a graphite cathode. Carbon 44, 3142–3145.

Kim, T.J., Kim, G.Y., Yoon, D., Ahn, D.H., Paek, S., 2013. Development of an anode structure consisting of graphite tubes and a SiC shroud for the electrowinning process in molten salt. J. Radioanal. Nucl. Chem. 295, 1855–1859.

Ko, W.I., Kim, E., 2009. Implications of the new national energy basic plan for nuclear waste management in Korea. Energy Policy 37, 3484–3488.

Koyama,T., Kobayashi, T., Iizuka, M., Ogata, T., 2012. Evaluation of technology feasibility for commercialization of pyroprocessing fuel cycle facility. Presented material at 3rd International Conference on Asian Nuclear Prospects.

Kwon, S.W., Park, K.M., Ahn, H.G., Lee, H., Kim, J.G., 2011. Separation of adhered salt from uranium deposits generated in electrorefiner. J. Radioanal. Nucl. Chem. 288, 789–793.

Lee, S.J., Park, S.B., Lee, J.H., Kim, J.G. Fundamental electrochemistry of uranium dissolution in LiCl-KCl fused salt. J. Nucl. Mater., in press.

Lee, J.H., Kang, Y.H., Hwang, S.C., Shim, J.B., Ahn, B.G., Kim, E.H., Park, S.W., 2006. Electrodeposition characteristics of uranium in molten LiCl-KCl eutectic and its salt distillation behavior. J. Nucl. Sci. Technol. 43, 263–269.

Lee, J.H., Kang, Y.H., Hwang, C., Shim, J.B., Kim, E.H., 2008. Application of graphite as a cathode material for electrorefining of uranium. Nucl. Technol. 162, 135–143.

Lee, J.K., Lee, H.J., Park, B.S., Kim, K., 2012a. Bridge-transported bilateral master-slave servo manipulator system for remote manipulation in spent nuclear fuel processing plant. J. Field Rob. 29, 138–160.

Lee, J.W., Kim, Y.H., Cho, K.H., Park, G.I., Lee, H.S., 2012b. Effects of thermal pretreatment conditions on the densification behavior of U_3O_8 green pellet. In: The Proceedings of the International Korea-Japan Seminar on Ceramics, EXCO, Daegu, Korea, November 21-24.

Lee, H., Park, G.I., Lee, J.W., Kang, K.H., Hur, J.M., Kim, J.K., Paek, S., Kim, I.T., Cho, I.J., 2013a. Current status of pyroprocessing development at KAERI. Sci. Technol. Nucl. Install. 2013, 1–11.

Lee, H.J., Lee, J.K., Park, B.S., Kim, K., Ko, W.L., Cho, I.J., 2013b. Development of a remote handling system in an integrated pyroprocessing facility. Int. J. Adv. Rob. Syst. 10, 1–14.

Li, S.X., 2002. Anodic process of electrorefining spent nuclear fuel in molten LiCl-KCl-UCl_3. In: Proceeding of the 201st Meeting of the Electrochemical Society, Philadelphia, PA, May 12-17, 2002 (Paper No. 1449).

OECD/NEA, 2009. Nuclear fuel cycle transition scenario studies, status report, ISBN 978-92-64-99068-5.

Ohta,H., Ogata, T., Papaioannou, D., Koyama, T., Kurata, M., Glatz, J.-P., Rondinella, V.V., 2009. Development of minor actinide-containing metal fuels. Presentation Material, FR2009, Kyoto, Japan, December 9.

Paek, S., Kim, S.H., Yoon, D., Lee, H., Ahn, D.H., 2010. Performance of the mesh-type liquid cadmium cathode structure for the electrodeposition of uranium from the molten salt. Radiochim. Acta 98, 779–783.

Paek, S., Kim, S.H., Yoon, D., Kim, T.J., Ahn, D.H., Lee, H., 2013. Electrochemical study on various types of anode materials in LiCl-KCl eutectic salt used in electrowinning process. J. Radioanal. Nucl. Chem. 295, 439–444.

Park, B.H., Lee, L.W., Seo, C.S., 2008a. Electrolytic reduction behavior of U_3O_8 in a molten LiCl-Li_2O salt. Chem. Eng. Sci. 63, 3485–3492.

Park, H.S., Kim, I.T., Cho, Y.Z., Yang, H.C., Lee, H., 2008b. Stabilization/solidification of radioactive salt waste by using $x$$SiO_2$-$y$$Al_2O_3$-$z$$P_2O_5$(SAP) material as molten salt state. Environ. Sci. Technol. 42, 9357–9362.

Park, G.I., Kim, K.W., Lee, D.Y., Lee, J.W., Park, J.J., Song, K.C., 2009. Effect of spent PWR fuel burn-up on oxidative decladding efficiency. In: Proceedings of Global 2009, Paris, France, September 6-11, pp. 139–142.

Park, S.B., Cho, D.W., Woo, M.S., Hwang, S.C., Kang, Y.H., Kim, J.G., Lee, H., 2011. Investigation of the evaporation of rare earth chlorides in a LiCl-KCl molten salt. J. Radioanal. Nucl. Chem. 287, 603–608.

Park, B.H., Choi, I.K., Hur, J.M., 2012. Study on the reduction of rare earth oxides by lithium metal in a molten LiCl salt for a pyrochemical processing of spent fuels. J. Chem. Eng. Jpn. 45, 1–5.

Ryu, H.J., Jung, I.H., Park, C.J., Kang, K.H., Lee, J.W., Choi, Y., Park, G.I., Song, K.C., 2008. Post-irradiation examination results of DUPIC fuel pellets irradiated in HANARO. In: 2008 Water Reactor Fuel Performance Meeting, Seoul, Korea, October 19-23. (Paper No. 8087).

Shim, J.B., Han, K.S., Kim, S.H., Paek, S.W., Kwon, S.W., Kim, J.G., Kim, K.R., Chung, H., Lee, H., Ahn, D.H., 2009. Effects of $CdCl_2$ on the residual actinide recovery (RAR) system of a spent LiCl-KCl salt. In: Proceedings of Global 2009, Paris, France, pp. 1207–1213.

Song, K.C., et al., 2008. Fractional release behavior of volatile and semi-volatile fission products during a voloxidation and OREOX treatment of spent PWR fuel. Nucl. Technol. 162, 158–168.

Till, C.E., Chang, Y.L., 2011. Plentiful energy—the story of the integral fact reactor, ISBN: 978-1466384606.

Usami, T., Kato, T., Murata, M., Inoue, T., Sims, H.E., Beetham, S.A., Jenkins, J.A., 2002. Lithium reduction of americium dioxide to generate americium metal. J. Nucl. Mater. 304, 50–55.

Warin, D., 2011. Advanced aqueous partitioning: progress and prospects for recycling process. Presentation Material WM2011, Phoenix, USA.

Wigeland, R., Bauer, T.H., Fanning, T.H., Morris, E.E., 2006. Separations and transmutation critical to improve utilization of geologic repository. Nucl. Technol. 154, 95–106.

Yang, M.S., Choi, H., Jeong, C.J., Song, K.C., Lee, J.W., Park, G.I., Kim, H.D., Ko, W.I., Park, J.J., Kim, K.H., Lee, H.H., Park, J.H., 2006. The status and prospect of DUPIC fuel technology. Nucl. Eng. Technol. 38, 359–374.

You, G.S., Cho, I.J., Chung, W.M., Lee, E.P., Hong, D.H., Lee, W.K., Ku, J.H., 2011. Concept and safety studies of an integrated pyroprocess facility. Nucl. Eng. Des. 241, 415–424.

Pyrochemical processes for recovery of actinides from spent nuclear fuels

17

P. Souček, R. Malmbeck
European Commission, Karlsruhe, Germany

Acronyms

ACSEPT	Actinide Recycling by Separation and Transmutation (project)
ADS	accelerator driven system
BOR 60	fast experimental reactor operated in Research Institute of Atomic Reactors, Russia
CP	chronopotentiometry
CV	cyclic voltammetry
DDP	Dimitrovgrad dry process
DOE	U.S. Department of Energy
EBR-II	Experimental Breeder Reactor-II
EC/ EURATOM	European Commission/European Atomic Energy Community
EMF	electromotive force measurements
EUROPART	European Research Programme for the Partitioning of Actinides (project)
FBR	fast breeder reactor
FP	fission products
ICP-MS	inductively coupled plasma mass spectrometry
IFR	integral fast reactor concept
ITU	Institute for Transuranium Elements
MA	minor actinides (Np, Am, Cm)
METAPHIX	experimental fast reactor metal fuel based on U-Pu-Zr matrix containing minor actinides and rare earths
MOX	mixed oxide fuel
OCP	open circuit potentials measurements
OECD	Organisation for Economic Cooperation and Development
OMEGA	Options Making Extra Gain from Actinides (project)
P&T	partitioning and transmutation
PYROREP	Pyrometallurgical Processing Research Programme (project)
SEM-EDX	scanning electron microscopy-energy-dispersive X-ray spectroscopy
SW	square-wave voltammetry

Reprocessing and Recycling of Spent Nuclear Fuel. http://dx.doi.org/10.1016/B978-1-78242-212-9.00017-4

17.1 Pyrochemical reprocessing of spent nuclear fuels

Major objectives for future advanced nuclear energy systems are effective fuel utilization for sustainability as well as waste minimization through recycling of all actinides (DOE, 2002). Waste minimization is also the overall goal of partitioning and transmutation (P&T) strategies (Magill et al., 2003), which are being developed as an alternative waste management option to direct geological disposal of spent nuclear fuels (OECD, 1999). P&T schemes specifically aim to reduce the long-term radiotoxicity of spent fuel by "burning" plutonium, minor actinides (i.e., neptunium, americium, and curium) and long-lived fission products in dedicated reactors. For any successful sustainable fuel cycle concept, an efficient and selective recovery of the key elements from spent nuclear fuel is absolutely essential. Regardless of whether transmutation of actinides is to be pursued by a heterogeneous accelerator driven system (ADS) or fast reactor concept, or as integrated waste burning with a homogenous recycling of all actinides, the fuels used in advanced systems are likely to be significantly different than the commercial fuels of today due to, for example, fuel matrix, plutonium and minor actinide content, burn up, and so on. Because of the fuel type and the very high burn up needed, traditional hydrometallurgical reprocessing such as is used today might not be the most appropriate method. The main reasons are the limited solubility of some fuel materials in acidic aqueous solutions and the limited radiation stability of the organic solvents used in the extraction processes. Therefore, different pyrometallurgical (nonaqueous) separation techniques are under development based on high-temperature molten salts as the solvent (OECD, 2012).

As a molten salt is a very radiation-resistant solvent, the fuel cooling times before reprocessing can be significantly shortened. Cooling times of a few months seem feasible, which can be compared to five years or longer needed for (conventional) aqueous reprocessing. A pyroprocess can also be made fairly compact compared to conventional reprocessing and integrated concepts are thus foreseen in which the irradiation and recycling/reprocessing are combined in the same facility. Further advantages of using a molten salt are the reduced criticality hazard and the more proliferation-resistant process due to the relatively impure product fractions. However, pyrochemical processes also have a number of drawbacks. Molten salts and liquid metals are aggressive media; the high melting points and the corresponding high operating temperatures require resistant construction materials. A highly pure atmosphere is normally needed, which implies rather sophisticated technology at the industrial scale. In addition, technological and process wastes, such as waste salt, require novel treatments.

Pyrochemistry is often based on electrochemical methods, such as electrolysis or electrorefining, or on reductive extraction. For metallic fuels, electrochemical methods are particularly well-suited due to the high conductivity of both the fuel and the solvent. Purification and recycling of uranium and plutonium from the irradiated fuel is done by electrorefining in molten LiCl-KCl salt and is currently the most advanced pyroprocess (Laidler et al., 1997). It is used in the metal fuel fast breeder reactor cycle, which has attracted global attention as one of the most promising energy

sources for the next-generation systems. This technique was originally developed at the Argonne National Laboratory for the integral fast reactor (IFR) concept, which included on-site processing and recycling of irradiated metallic EBR-II fuel (McFarlane and Lineberry, 1997). In Japan, this concept was further developed for the OMEGA double-strata P&T scenario (Inoue and Tanaka, 1997; Koyama et al., 2011). The proposed concept, based on deployment of fast reactors with a closed fuel cycle, is shown in Figure 17.1. The spent metal fuel is processed to recover uranium, plutonium, and MA (pyrometallurgical processing); the recovered actinides are used to fabricate a metal fuel (injection casting), which is irradiated in the fast breeder reactor (metal fuel FBR).

In the following text, some of the important present pyrochemical activities worldwide are discussed. The METAPHIX experiment (Ohta et al., 2011) is an experimental demonstration project on a closed nuclear metal fuel cycle. The program includes fabrication, irradiation at the Phenix reactor (Marcoule, France), postirradiation examination, and finally pyrometallurgical reprocessing of the fuel. The pyroprocessing stage is composed of molten salt chemical/electrochemical techniques (electrorefining, electroreduction, and pyropartitioning) using the METAPHIX fuel before and after irradiation.

The Russian DDP (Dimitrovgrad dry process) process has been developed up to a semi-industrial scale. After initial chlorination of the oxide fuel in a molten chloride salt, the separation process is based on electrodeposition of UO_2 or on codeposition of UO_2 and PuO_2 for production of MOX fuels by the vibropacking technique and subsequent irradiation in the BOR 60 fast reactor. Selective precipitation of PuO_2 in this process is optional. This process has been successfully demonstrated on irradiated fuels (Kormilitsyn et al., 2003).

Dry methods open up possibilities to also treat refractory fuel materials, such as ceramic (oxide) or ceramic/metal-based fuels and targets. The key is the molten salt-based electroreduction process (Kurata et al., 2004; Sakamura et al., 2009) in which an oxide fuel is converted (reduced) to metallic form. The metallic fuel is then subsequently treated by electrorefining.

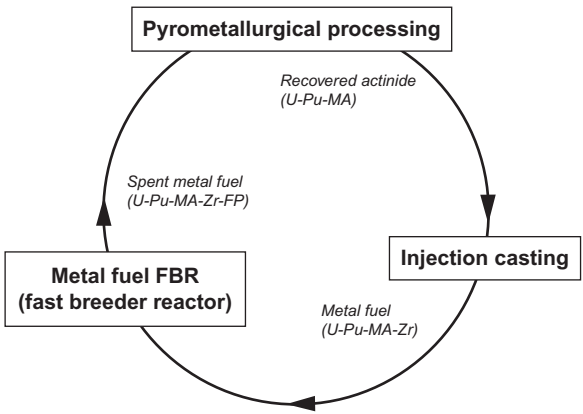

Figure 17.1 Concept of the metal fuel fast breeder reactor cycle. MA: minor actinide (Np, Am and Cm), FP: fission products.
Glatz et al. (2013).

Pyrochemical processing of nuclear fuels and targets, using established and new technologies, is under continuous development today (OECD, 2004). Several countries have domestic programs, for example, France (Mendes et al., 2012a), Japan (Inoue et al., 2011), Korea (Lee et al., 2011), India (Nagarajan et al., 2011), and China (Guoan et al., 2012). Also, in Europe, several research collaborations have been launched over the last decade (Bourg et al., 2011; Madic and Hudson, 2004).

17.2 Electrochemical studies of actinides in molten salts

17.2.1 Basic studies in molten salt systems

An accurate knowledge of the thermodynamic and electrochemical properties of actinides, lanthanides, and other fission products dissolved in a suitable carrier molten salt (e.g., LiCl-KCl or LiF-CaF_2 eutectics) is crucial for the development of pyrochemical separation processes. The separation between actinides and fission products is enabled by the difference in the Gibbs free energies of formation of the respective halides, according to media used for their dissolution. This can be directly translated to the terms of electromotive forces of the corresponding electrochemical cell reactions and, thus, to the differences of electrode potentials needed to deposit the metals onto an inert (e.g., W, Mo, Au, Pt) or reactive (e.g., Cd, Bi, Al, Ni) cathode. The following data have the greatest importance: (i) standard, apparent, and deposition electrode potentials and reaction mechanisms describing general electrochemical behavior; (ii) activity coefficients, enthalpies, and entropies of formation as thermodynamic quantities; and (iii) diffusion coefficients for evaluation of kinetic aspects.

In order to obtain correct and accurate results, it is necessary to have access to suitable equipment that maintains the required experimental conditions; to have methods that enable preparation of the high purity chemicals required; and to correctly use relevant techniques for the determination of experimental quantities. These three topics are discussed in the following sections.

17.2.1.1 Experimental equipment for studies in molten salt media

Pyrochemical research requires a particularly pure inert atmosphere in order to protect the highly hygroscopic materials used (chloride and fluoride salts, pure metals) from unwanted reactions with moisture, oxygen, nitrogen, and others. The electrochemical reactor can possibly be placed directly in a laboratory with normal atmosphere if sufficient argon flow to the reactor is provided, the reactor is gastight, and additional in situ purification of the chemicals used is possible. However, typically the storage and handling of all chemicals as well as the electrochemical experiments are carried out in a glove box under a purified argon atmosphere (the atmospheric content of water and oxygen should be less than 5 ppm). A photograph of a glove box installed at the ITU (Karlsruhe, Germany) and equipped for work with molten salt is shown in Figure 17.2.

High-temperature furnaces, electrolysers, and reactors must be used for the studies of molten salt media as the typical temperature range needed is 400-1000 °C. Construction materials resistant for the used chemicals at the given conditions are typically stainless steel or quartz for chlorides and nickel-based alloys for fluorides.

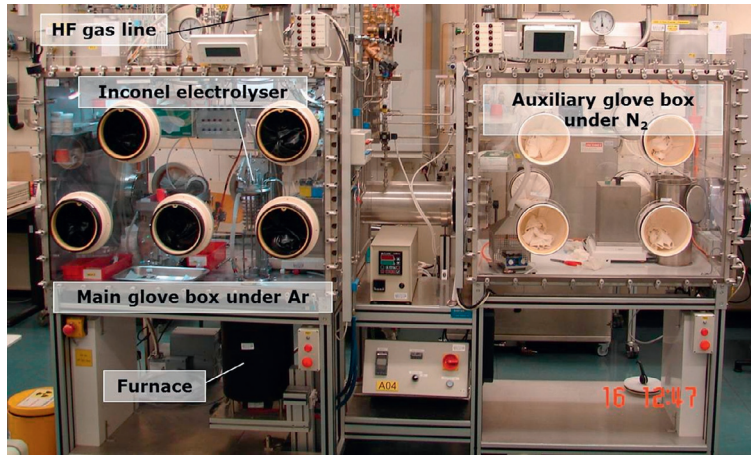

Figure 17.2 Glove box equipped for work with molten fluoride media installed at the ITU (Karlsruhe, Germany).

For molten salt containers, alumina or magnesia is used for chloride-based media and boron nitride or glassy carbon for fluorides.

A three-electrode setup consisting of working, reference, and counter electrodes is required for the electrochemical measurements. A typical electrochemical cell used for molten chlorides is a working electrode consisting of a metallic wire, auxiliary electrode made of molybdenum wire bent into a spiral shape, and a reference electrode based on silver-silver chloride (1-10 wt.%) red-ox couple. A scheme and photograph of the set-up as used in ITU is shown in Figure 17.3. The situation is more complex for molten fluorides, as under many working conditions it is very difficult to design a

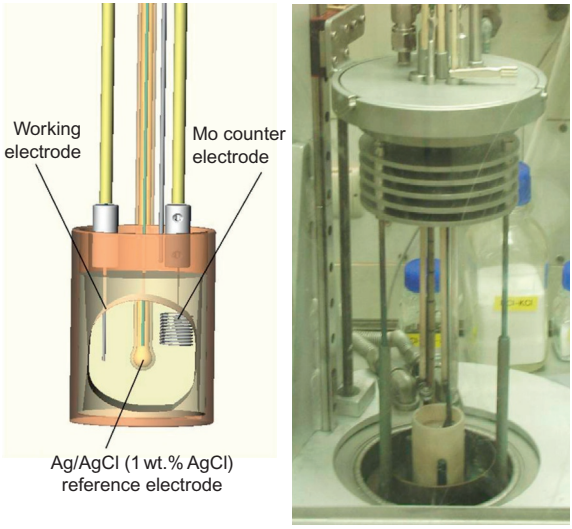

Figure 17.3 Scheme (left) and photo (right) of a three-electrode set-up for electrochemical measurements in molten chloride media used at ITU.

suitable and stable reference electrode, except for lower-melting fluoride mixtures (e.g., LiF-NaF-KF or LiF-BeF_2 eutectics). Therefore, platinum wire is typically used as a semireference electrode based on the $Pt/PtO_x/O^{2-}$ redox system. Detailed information of the setup and equipment needed can be found in the literature, for example, Masset et al. (2005b) for molten chloride and Massot et al. (2002) and Souček et al. (2003) for high- and low-melting fluoride media.

17.2.1.2 Chemicals and melt preparation

All chemicals have to be moisture free, either purified by the producer and delivered in a sealed package under argon atmosphere (typically chlorides) or they must be purified in situ. Typical examples are heating under vacuum up to the melting point of the given mixture or chemical treatment, for example, bubbling of HF through the molten salts (fluorides).

Preparation of melt depends on the available input materials, because actinides, especially transuranium elements, are rare and highly radioactive materials that are not commercially available. They are typically stored as oxides and need a conversion into the halide form before use. However, some actinides can be found as metals or alloyed with zirconium. In this case, the actinide-based bath can be prepared in a setup consisting of a crucible containing a metallic pool (usually bismuth or cadmium) and a carrier salt phase. The actinide metal/alloy is added to the metallic pool and oxidized by adding the corresponding metal halide (e.g., $BiCl_3$) to the salt phase as described in Equation 17.1

$$\mathrm{An}^{0}_{\text{Bi-phase}} + \mathrm{Bi}^{3+}_{\text{salt-phase}} \rightarrow \mathrm{An}^{3+}_{\text{salt-phase}} + \mathrm{Bi}^{0}_{\text{Bi-pool}} \tag{17.1}$$

Care must be taken that substoichiometric amounts (compared to the actinide) of the metal halide are added in order to avoid residual metal ion impurities in the bath. The reaction rate can be increased by applying a higher temperature; specifically, 550 °C is recommended for LiCl-KCl eutectic carrier salt.

If available only as oxide, halidation of actinides oxides in a molten carrier salt by $Cl_2(g)$, HF(g), or other halidation agents can be used for preparation of the salt bath. A particular chlorination process as carried out in ITU to prepare plutonium, neptunium, and americium containing LiCl-KCl carrier salt from respective actinide oxides is summarized in the following text. A glove box equipped with a chlorine gas line and an off-gas treatment system (wash bottles containing 4 and 8 M KOH solutions) was specially designed for the chlorinations. The bath containing actinide oxide is prepared in a glassy carbon crucible placed on the bottom of a quartz reactor, which is inserted in a vertical oven. $Cl_2(g)$ is bubbled directly to the melt with a flow rate of 15 ml/min using a quartz tube guided through the lid of the reactor. After about 2-4 h of bubbling, the reactor is sealed and left overnight to complete the reaction. If needed, the complete procedure is repeated twice. As the oxygen released from actinide oxides reacts with carbon from the crucible, this procedure is referred to as a "carbochlorination" process. The final product can be checked for purity (e.g., by electrochemical measurements). If needed, the impurities (likely consisting of actinide oxychlorides)

can be removed by complete reduction using Li-Bi alloy (35 mol.% Li) followed by reoxidation of the reduced actinide metal by $BiCl_3$.

The reactions are described by the following schemes for tetra- and tri-valent actinides (Equations 17.2 and 17.3):

$$2\,AnO_2 + 3Cl_2 + 2C \rightarrow 2AnCl_3 + 3CO_2 \tag{17.2}$$

$$2\,An_2O_3 + 6Cl_2 + 3C \rightarrow 4AnCl_3 + 3CO_2 \tag{17.3}$$

All actinides, plutonium, neptunium, and americium were successfully chlorinated at a temperature of 650 °C during the bubbling of Cl_2 and 450-500 °C during the period of reaction completion with the reactor isolated.

17.2.1.3 Experimental techniques

The determination of the above-mentioned electrochemical properties of actinides in molten salts relies on transient electrochemical techniques; for example, cyclic voltammetry (CV), chronopotentiometry (CP), and square-wave voltammetry (SW) and equilibrium techniques such as electromotive force measurements (EMF) or open circuit potentials measurements (OCP). In Table 17.1, the methods, conditions, and the relevant equations typically used for the determination of the most important electrochemical properties are summarized. In the selected references, practical application of the methods for studies of actinides in molten salt media can be found.

17.2.2 Electrochemical properties of actinides in molten chloride salts

The electrochemical and thermodynamic properties of actinides and lanthanides have been extensively studied worldwide with the main focus on the carrier salt composed of LiCl-KCl eutectic mixture, which has been selected as the main candidate for pyrochemical recovery of actinides from spent nuclear fuel. The selected experimental data collected mainly within projects PYROREP (Boussier et al., 2003), EUROPART (Madic and Hudson, 2004), and ACSEPT (Bourg et al., 2011) of the EC/EURATOM fifth to seventh framework programs are summarized in Table 17.2.

For development of an electrochemical separation process, the choice of cathode material onto which the actinides are deposited is crucial. The use of reactive electrodes is very advantageous, as the actinide metals are stabilized by the formation of alloys with the cathode material, and undesired side-reactions of the deposit (Serp et al., 2006) can be prevented. According to the available activity coefficients of actinides and lanthanides (particularly plutonium, uranium, and cerium) in different reactive metals, aluminum has been identified as the reactive electrode material enabling the highest separation factor of actinides from lanthanides (Conocar et al., 2006). The formation of An-Al and FP-Al alloys has been studied in molten LiCl-KCl in order to determine the deposition potentials (the potential point from which

Table 17.1 Methods, conditions, and the relevant equations typically used for the determination of the most important electrochemical properties

Quantity/ feature	Method	Equation	Conditions, validity, notes	References
Reaction mechanism	CV, SW	No equation, the evaluation is based on analysis of the curves (shapes of the peaks)		Masset et al. (2005b), Serp et al. (2006)
Reversibility	CV	$I_p \approx v^{1/2}$ and $\Delta E = E_{p,a} - E_{p,c} \approx 2.3RT/nF$	Linear dependency	Nourry et al. (2012)
	SW	$I_p \approx f^{1/2}$	Linear dependency	Nourry et al. (2012), Serp et al. (2006)
Number of exchanged electrons	CV	$\lvert E_p - E_{p/2} \rvert = 2.2RT/nF$	Reversible soluble-soluble transition	Serp et al. (2006)
		$\lvert E_p - E_{p/2} \rvert = 0.77RT/nF$	Reversible insoluble-soluble transition	Masset et al. (2005a)
	SW	$W_{1/2} = 3.52RT/nF$	Reversible systems	Nourry et al. (2012), Serp et al. (2006)
	All below listed methods for apparent standard potential can be used for the determination of the number of exchanged electrons using the slope of the lines E vs. $\ln X_{An(ox)}$ and/or E vs. $\left(\tau^{1/2} - t^{1/2}\right)/\tau^{1/2}$			Masset et al. (2005a), Cassayre et al. (2007b)
Apparent standard potential	EMF +OCP	$E^{eq.}_{An(ox)/An^0} = E^{*0}_{An(ox)/An^0} + \frac{RT}{nF} \ln X_{An(ox)}$	Insoluble-soluble transition	Cassayre et al. (2007b)
	CP	$E = E^{0*}_{An(ox)/An^0} + \frac{RT}{nF} \ln X_{An(ox)} + \frac{RT}{nF} \ln \left(\frac{\tau^{1/2} - t^{1/2}}{\tau^{1/2}}\right)$	Reversible insoluble-soluble transition	Masset et al. (2005b)
	CV	$E_{p,c} = E^{0*}_{An(ox)/An^0} + \frac{RT}{nF} \ln X_{An(ox)} - 0.854\frac{RT}{nF}$	Reversible insoluble/soluble transition	Masset et al. (2005a)
		$E^{0*}_{An(ox)/An^0} = \left(\frac{E_{p,a} + E_{p,c}}{2}\right) - \frac{RT}{nF} \ln \left(\frac{\sqrt{D_{An(red)}}}{\sqrt{D_{An(ox)}}}\right)$	Reversible soluble/soluble transition	Masset et al. (2005a)

Diffusion coefficient	CP	$i\sqrt{\tau} = 0.5nFc_{An^{n+}}S\sqrt{\pi D_{An^{n+}}}$	Not dependent on the reversibility	Cassayre et al. (2007b), Masset et al. (2005b)
	CV	$I_p = 0.446(nF)^{3/2}(RT)^{-1/2}c_{An^{n+}}S(vD_{An^{n+}})^{1/2}$	Reversible soluble-soluble transition	Masset et al. (2005a), Serp et al. (2006)
		$I_p = 0.61(nF)^{3/2}(RT)^{-1/2}c_{An^{n+}}S(vD_{An^{n+}})^{1/2}$	Reversible insoluble-soluble transition	
		$I_p = 0.496nFSc_{An^{n+}}(vD_{An^{n+}})^{1/2}(\alpha n_\alpha F/RT)^{1/2}$	Diffusion controlled totally irreversible system	Bard and Faulkner (2000)
		αn_α from $\lvert E_p - E_{p/2}\rvert = 1.857RT/\alpha n_\alpha F$		
Activity coefficient	CP, CV, EMF	$E^{*0}_{An(ox)/An^0} = E^0_{An(ox)/An^0} + \frac{RT}{nF}\ln\gamma_{An(ox)}$	$E^0_{An(ox)/An^0}$ is calculated from the available thermodynamic data	Cassayre et al. (2007b), Serp et al. (2006)
		$RT\ln\gamma_{An(ox)} = nFE^{*0}_{An(ox)/An^0} - nFE^0_{An(ox)/An^0}$		
		$= \Delta G^\infty_f - \Delta G^0_{f,SC}$		

List of variables:
R universal gas constant (J mol^{-1} K^{-1}), $E^0_{An(ox)/An^0}$ standard electrode potential (V);
F Faraday constant (C), $E^{0*}_{An(ox)/An^0}$ apparent standard potential (V);
T absolute temperature (K), $E^{eq.}_{An(ox)/An^0}$ equilibrium potential for a pure metal/metal halide (V);
X molar fraction of the specie, $E_{p,c}$, $E_{p,a}$ cathodic, anodic peak potential for CV (V);
S electrode surface (cm^2), $E_{p/2}$ half-peak potential for CV (V);
f frequency for SW (Hz), $W_{1/2}$ half width of the peak for SW (V);
n number of exchanged electrons, $c_{An^{n+}}$ concentration of dissolved An (mol cm^{-3});
t elapsed time for CP (s), $\gamma_{An(ox)}$ activity coefficient;
τ transition time for CP(s), $D_{An^{n+}}$ diffusion coefficient (cm^2 s^{-1});
I_p peak current of wave/peak, ΔG^∞_f Gibbs free energy of formation at infinite dilution (J);
v potential scan rate (V s^{-1}), $\Delta G^0_{f,SC}$ Gibbs free energy of formation in the supercooled state (J).

Table 17.2 Apparent standards potentials, diffusion coefficients, free Gibbs energies of formation, and activity coefficients of selected $AnCl_x$ and FPs in the molten LiCl-KCl eutectic at 773 K

Element	Red-ox couple	E°[a] [V *vs* Cl_2/Cl^-]	D [$cm^2/s]\cdot10^{-5}$	ΔG^{∞}_{MClx} (kJ mol^{-1})	$\gamma \cdot 10^3$	References
Th	Th(IV)/Th	−2.559	4.47	−987.62	0.68	Cassayre et al. (2007b)
U	U(III)/U	−2.509	3.10	−726.20	1.39	Masset et al. (2005a)
	U(IV)/UCl_3	−1.428	2.20	−137.80	14.8	
Np	Np(III)/Np	−2.682	3.15	−776.44	0.079	Masset et al. (2007)
	Np(IV)/Np(III)	−0.724	2.79	−69.87	8.45	
Pu	Pu(III)/Pu	−2.770	1.6[a]	−801.9	12.0	Serp et al. (2004)
Am	Am(III)/Am(II)	−2.676	3.20	−816.6	5.1	Serp et al. (2006)
	Am(II)/Am	−2.893	1.65	−558.3	56	
Cm	Cm(III)/Cm	−2.861	1.26	−809.8	—	Osipenko et al. (2011)
Ce	Ce(III)/Ce	−3.054	1.54	−850.11	5.05	Castrillejo et al. (2003), Madic et al. (2007)
La	La(III)/La	−3.095	1.63	−896.003	6.64	Castrillejo et al. (2003), Madic et al. (2007)
Nd	Nd(III)/Nd	−3.079	1.61	−891.371	0.38	Castrillejo et al. (2003), Madic et al. (2007)
Pr	Pr(III)/Pr	−3.060	1.59	−885.87	5.53	Castrillejo et al. (2003), Castrillejo et al. (2005)
Sm	Sm(III)/Sm(II)	−2.00	1.35	−193.340	0.358	Cordoba and Caravaca (2004), Madic et al. (2007)
Eu	Eu(III)/Eu(II)	−0.800	0.20	−77.200	2.178	Madic et al. (2007)
Gd	Gd(III)/Gd	−2.9993	0.95	−868.29	0.150	Caravaca et al. (2007)

[a]Temperature 733 K.

Table 17.3 Deposition potentials of selected An and FPs on solid aluminum cathode in molten LiCl-KCl eutectic

Element M^{3+}/M^0(Al)	Temperature (°C)	Deposition potential [V vs. Cl^2/Cl^-]	Concentration (wt.%)	References
U	450	−2.25	1.58	Souček et al. (2009a), Cassayre et al. (2008)
Np	450	−2.38	3.20	Souček et al. (2009a), Souček et al. (2009b)
Pu	450	−2.43	1.65	Mendes et al. (2012b), Souček et al. (2009a)
Am	450	−2.48	0.46	Souček (2008)
Nd	460	−2.63	0.50	Conocar et al. (2006)
Gd	460	−2.64	1.58	Caravaca and Cordoba (2006)
La	460	−2.68	0.84	Serp et al. (2005)

the reduction starts in the real-studied system). The obtained values with original references are summarized in Table 17.3.

17.2.3 *Electrochemical properties of actinides in molten fluoride salts*

In comparison to molten chloride salts, studies in molten fluoride are less developed. Even though a lot of experiments were carried out in various salts (e.g., LiF-NaF, LiF-NaF-KF, LiF-CaF_2), thermodynamic data could not be unequivocally determined. This is mainly due to the lack of an invariable reference electrode. The diffusion coefficients collected for different fluoride melts and calculated deposition coefficients for selected actinides and lanthanides are summarized in Table 17.4.

17.3 Electrorefining process using solid aluminum electrodes

Within the EC/EURATOM framework programs, two pyrochemical processes have been selected as reference nonaqueous technologies for recovery of the actinides from spent nuclear fuel to enable a concentration of effort on the most promising options from the viewpoint of development of the advanced nuclear fuel cycle in Europe. These are (i) electrorefining of actinides onto solid aluminum cathodes in molten

Table 17.4 Diffusion coefficients and calculated deposition potentials of selected An and FPs in molten LiF-CaF_2 eutectic mixture

Element	Compound	Temperature (K)	D [cm^2/s]·10^{-5}	E_{dep} [V *vs* F_2/F^-]	References
Th	Th(IV)/Th	1113	5.0	−4.57	Chamelot et al. (2007, 2010)
U	U(III)/U	1083	2.2	−4.53	Hamel et al. (2007)
	U(IV)/U(III)[b]	993	1.25	−3.81	
Pu	Pu(III)/Pu	810	n/a	−4.7	Hamel (2005)
Am	Am(II)/Am	780	n/a	−4.80	Lacquement et al. (2009)
Ce	Ce(III)/Ce	1093	2.2-5.4	n/a	Chandra et al. (2011)
Nd	Nd(III)/Nd	1083	1.1-1.3	−4.98	Hamel et al. (2004)
Pr	Pr(III)/Pr	900	n/a	−5.2	Straka et al. (2011)
Sm	Sm(III)/Sm(II)	1103	2.96	−5.15	Chamelot et al. (2007), Massot et al. (2005)
Eu	Eu(III)/Eu(II)	1073	3.18	−3.53[a]	Massot et al. (2009)
Gd	Gd(III)/Gd	1106	1.56	−4.93	Chamelot et al. (2007), Nourry et al. (2008)

[a]Experimentally determined formal standard potential.
[b]In molten LiF-NaF eutectic mixture.

chloride media and (ii) liquid-liquid reductive extraction in molten fluoride media. The following section describes the principles and main achievements of the electrorefining process.

17.3.1 Principle of the process

Results of the electrochemical studies described in Section 17.2.2 led to the development of the electrorefining process for group-selective recovery of actinides from nuclear fuel using reactive solid aluminum cathodes. In this process, electroseparation of actinides from fission products is carried out in LiCl-KCl eutectic molten salt at $T = 450$ °C by applying a constant current between the metallic fuel contained in a tantalum basket and an aluminum cathode. During the electrolysis, actinide cations arising from the anodic oxidation of the fuel are electrotransported and deposited onto the aluminum cathode, where they form An-Al alloys.

Alkali, alkaline earth metal, and rare earth fission products are also dissolved into the melt during the process, but they are not reduced thanks to the controlled deposition potential. The selectivity of this process is maintained by controlling the cathodic polarization above a cutoff potential for codeposition of fission products. Theoretically, zirconium and more noble metal FP should not be oxidized and remain in the anodic basket. However, in practice, the extent of their cooxidation depends on the portion of recovered actinides. According to Westphal et al. (2009), the oxidized noble metals probably will be partly codeposited with actinides and partly remain on the electrolyser hardware. The principle of the electrorefining process is illustrated in Figure 17.4.

17.3.2 Group selective recovery of actinides by electrorefining

A group selective separation of actinides from lanthanides was demonstrated by electrorefining of both nonirradiated and irradiated An-Ln-Zr fuel produced at the ITU (METAPHIX-1 fuel, composition U_{61}-Pu_{22}-Am_2-$Nd_{3.5}$-$Gd_{0.5}$-$Y_{0.5}$-$Ce_{0.5}$-Zr_{10}) (Ohta et al., 2011). During the experiments, pieces of metallic alloy were loaded into a tantalum anode basket and immersed into the molten salt, which already contained dissolved actinide and lanthanide ions. A constant current was then applied between the basket and an aluminum cathode. The metallic alloy was anodically dissolved feeding An^{3+} and Ln^{3+} to the salt, while only actinides were collected onto the aluminum foils, plates, and rods as An-Al alloys. Destructive (ICP-MS) and nondestructive (calorimetry; neutron coincidence counting; gamma spectrometry; X-ray fluorescence) analyses were used to monitor the concentration of actinides and lanthanides both in the salt and in the deposits; SEM-EDX analysis and optical

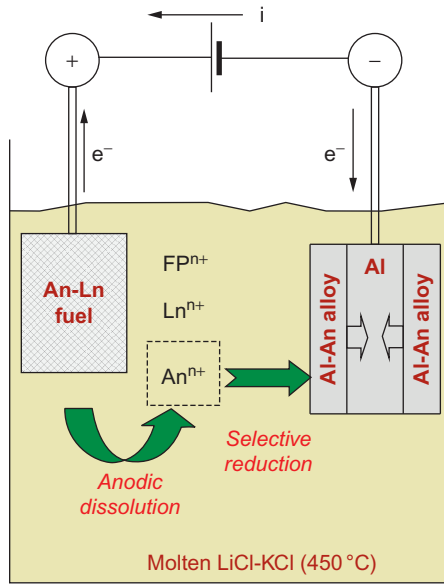

Figure 17.4 Principle of the electrorefining process of metallic An-Ln fuel using solid aluminum cathodes.

microscopy was used for characterization of the morphology and composition of the deposits.

The experiments with nonirradiated fuel were focused mainly on confirmation of the selectivity of the process and capacity of aluminum to take up actinides. More than 20 electrolyses were carried out with 24 g of metallic alloy. Homogeneous and compact deposits were obtained at the aluminum foil cathodes containing mainly uranium, plutonium, and americium. The excellent separation of actinides from lanthanides was shown, as the deposit was composed of more than 99.9 wt.% actinides. Even when comparing only americium to lanthanide content in the deposit, a very efficient separation was achieved (Souček et al., 2009a). Compositions of the selected deposits during electrorefining of METAPHIX-1 fuel are shown in Table 17.5 together with the concentrations of actinides and fission products dissolved in the melt at the beginning of each run.

17.3.3 High capacity of solid aluminum for recovery of actinides

Several experiments were carried out to characterize An-Al alloys formed by electrodeposition of individual actinides or their mixtures from LiCl-KCl-based melts and on the capacity of solid aluminum to take up actinides (Cassayre et al., 2007a; Souček et al., 2008). The theoretical maximum loading of actinides in an aluminum cathode is dependent on the alloy composition; for the most typical alloy compositions of $AnAl_3$, this value is 2.94 g of actinides in 1 g of aluminum. Electrorefining of U-Pu-Zr alloy (71-19-10 wt.%, respectively) was carried out to examine the maximum possible loading of the solid aluminum electrodes. The highest actinide content in aluminum was achieved for potentiostatic electrolysis, with 2.3 g of actinide loaded into 1 g of aluminum. The average value for all experiments was 1.9 g of actinides. An example of the almost fully loaded aluminum cathode prepared by the electrorefining process is shown in Figure 17.5.

Although the experiments with thin aluminum plates showed a very high capacity of aluminum to take up actinides, the maximum actinide content is limited by the intermetallic diffusion of actinides and aluminum through the solid alloy phase. With

Table 17.5 Total masses of actinides (An = U, Pu, Am) and fission products including Zr (FP = Y, Ce, Nd, Gd) in the deposits and their concentration in melt for selected runs during electrorefining of nonirradiated METAPHIX-1 fuel

	Run					
	1	2	3	4	5	6
An in dep. (mg)	1017	768	265	437	330	310
FP+Zr in dep. (mg)	2.12	0.31	0.08	0.24	0.34	0.29
An in melt (wt.%)	1.63	1.30	1.27	0.51	0.71	1.66
FP+Zr in melt (wt.%)	0.50	0.55	0.79	0.81	2.66	2.37

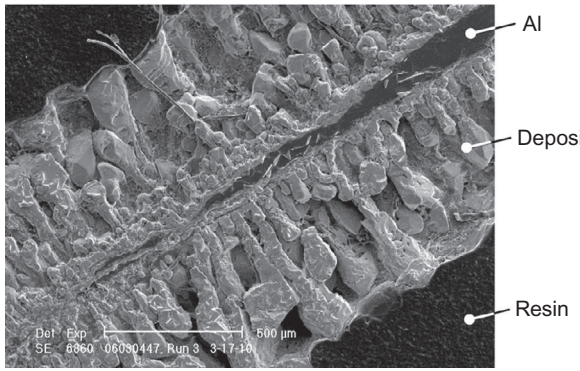

Figure 17.5 SEM micrograph of an almost fully loaded aluminum electrode after electrorefining of U-Pu-Zr alloy fuel in LiCl-KCl salt. The deposit is composed of $(U,Pu)Al_3$ alloy.

increasing thickness of the alloy, the deposition of actinides as An-Al alloy is more difficult, and the cathodic potential is shifted toward the deposition potential of lanthanides. The final point for the process is reached when the potential becomes too negative to allow the selective separation and the current could not be decreased to keep the desired process rate.

17.3.4 Experiments with irradiated An-Zr metallic fuel

Therefore, the experiments with the irradiated METAPHIX-1 fuel were aimed not only toward verification of the separation abilities in a complex mixture of actinides and fission products, but also to study the diffusion of actinides in solid aluminum. Aluminum plates and rods were used as cathodes. The plate cathodes were 1 mm thick and 3 mm wide, the rods had diameter 0.3 cm, and the active surface was in the range 0.9-1.2 cm^2. One hundred-thirty grams of LiCl-KCl salt originating from previous experiments was used, containing 6.15 wt.% of actinides and 0.17 wt.% of lanthanides. All experiments (five runs with aluminum plates, two runs with rod cathodes) were galvanostatic, using different constant current densities in a range 10-40 mA/cm^2. Each run was stopped after the An-Al intermetallic diffusion became too slow to enable alloy formation at the given current; that is, when the uranium metal deposition potential was reached. In all cases, a uniform, dense, and well-adherent metallic-shiny deposit was obtained. The thickness of the An-Al alloy layer on the electrode surface was determined for each current density using optical microscope photographs of the electrode cross sections taken inside the hot cell. Figure 17.6(left) shows resulting deposits from the run carried out at a current density of 28 mA/cm^2; this represents an average value of the applied conditions. The layer of the An-Al alloy is 0.48 mm thick. In addition, the alloy layer on the electrode surface is shown in Figure 17.6(right).

The diffusion coefficient of actinides in aluminum was calculated using the equation for solid-state diffusion; knowing how the thicknesses of the alloy layers depend on the time of electrodeposition and assuming formation of a uniform $AnAl_3$ alloy. The diffusion coefficient of actinides in aluminum was estimated to be

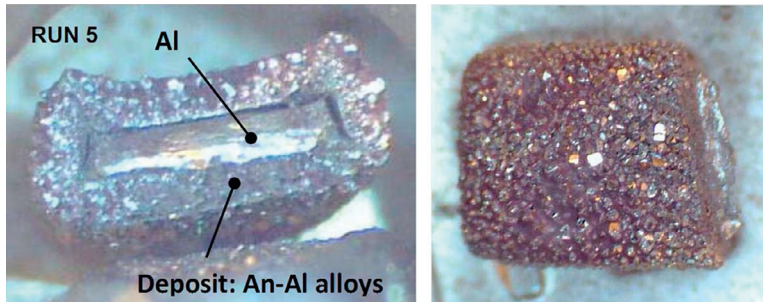

Figure 17.6 Optical microscopy pictures of an aluminum cathode with An-Al alloy deposit after electrorefining of irradiated METAPHIX fuel (left: transverse cut, right: surface of the electrode).

$1.5 \cdot 10^{-7}$ cm^2/s, that is, two orders of magnitude lower than the diffusion coefficients of actinides dissolved in molten salt media.

During the experiments, salt samples were regularly taken and analyzed by ICP-MS, as well as samples of the deposits. The analyses showed high current efficiencies for the process (84-96%) and confirmed the excellent ability of the process for recovery of the actinides. Even though the experiment was not focused on the selective actinide deposition and the potential was allowed to drop to the value of uranium metal deposition, high separation factors from lanthanides were achieved, especially for the lower current density runs.

17.4 Summary and future trends

Pyrochemical methods and technologies are currently under development in several countries around the world and are seen as an important complement to traditional recycling technologies, particularly in the treatment of refractory fuels and targets in advanced nuclear fuel cycles. The oxide electroreduction process is a key process in this respect, enabling oxide fuel materials to be routed into pyrochemical reprocessing schemes already based on metallic fuels.

The molten chloride system has been especially well-investigated and most of the basic electrochemical data are nowadays available. For reprocessing of metallic fuels, a scheme has been developed utilizing the homogenous recycling of all actinides based on the well-established electrorefining process. It takes advantage of the specific alloying behavior of actinides onto reactive solid aluminum cathodes. An efficient and selective separation of actinides has been demonstrated using unirradiated as well as irradiated fuel materials. However, a particular problem of these pyrochemical processes relates to management of process wastes, especially chloride-based salts, that require special treatment.

The molten fluoride systems are less developed and are inherently more difficult to study because of the aggressive solvent and lack of a suitable reference electrode.

Nevertheless, reprocessing schemes based on reductive extraction (Mendes et al., 2012a) or fluoride volatility (Kani et al., 2009; Uhlíř and Mareček, 2009) have been proposed, which look promising. The processes deploying molten fluoride media play an essential role in development of the molten salt reactor fuel cycle, where liquid fuel consisting of molten fluoride salt will be processed (Delpech et al., 2009; Rosenthal et al., 1971; Uhlíř, 2005).

References

Bard, A.J., Faulkner, L.R., 2000. Electrochemical Methods, Fundamentals and Applications. John Wiley & Sons, New York.

Bourg, S., Hill, C., Caravaca, C., Rhodes, C., Ekberg, C., Taylor, R., Geist, A., Modolo, G., Cassayre, L., Malmbeck, R., Harrison, M., De Angelis, G., Espartero, A.G., Bouvet, S., Ouvrier, N., 2011. ACSEPT—partitioning technologies and actinide science: towards pilot facilities in Europe. Nucl. Eng. Des. 241, 3427–3435.

Boussier, H., Malmbeck, R., Marucci, G., 2003. The European pyrometallurgical processing research program PYROREP: main issues. In: Proceedings of Global 2003, November 16-20, New Orleans, Louisiana, USA, pp. 966–975.

Caravaca, C., Cordoba, G., 2006. Formation of Al-Gd alloy films by molten salt electrochemical process. In: Proceedings of EUCHEM 2006, September 16-22, Hammamet, Tunisia.

Caravaca, C., de Córdoba, G., Tomás, M.J., Rosado, M., 2007. Electrochemical behaviour of gadolinium ion in molten LiCl-KCl eutectic. J. Nucl. Mater. 360, 25–31.

Cassayre, L., Malmbeck, R., Masset, P., Rebizant, J., Serp, J., Soucek, P., Glatz, J.P., 2007a. Investigation of electrorefining of metallic alloy fuel onto solid Al cathodes. J. Nucl. Mater. 360, 49–57.

Cassayre, L., Serp, J., Soucek, P., Malmbeck, R., Rebizant, J., Glatz, J.P., 2007b. Electrochemistry of thorium in LiCl-KCl eutectic melts. Electrochim. Acta 52, 7432–7437.

Cassayre, L., Caravaca, C., Jardin, R., Malmbeck, R., Masset, P., Mendes, E., Serp, J., Souček, P., Glatz, J.-P., 2008. On the formation of U-Al alloys in the molten LiCl-KCl eutectic. J. Nucl. Mater. 378, 79–85.

Castrillejo, Y., Bermejo, M.R., Barrado, E., Martínez, A.M., Díaz Arocas, P., 2003. Solubilization of rare earth oxides in the eutectic LiCl-KCl mixture at 450 °C and in the equimolar $CaCl_2$-NaCl melt at 550 °C. J. Electroanal. Chem. 545, 141–157.

Castrillejo, Y., Bermejo, M.R., Díaz Arocas, P., Martínez, A.M., Barrado, E., 2005. Electrochemical behaviour of praseodymium (III) in molten chlorides. J. Electroanal. Chem. 575, 61–74.

Chamelot, P., Massot, L., Hamel, C., Nourry, C., Taxil, P., 2007. Feasibility of the electrochemical way in molten fluorides for separating thorium and lanthanides and extracting lanthanides from the solvent. J. Nucl. Mater. 360, 64–74.

Chamelot, P., Massot, L., Cassayre, L., Taxil, P., 2010. Electrochemical behaviour of thorium (IV) in molten LiF-CaF_2 medium on inert and reactive electrodes. Electrochim. Acta 55, 4758–4764.

Chandra, M., Vandarkuzhali, S., Ghosh, S., Gogoi, N., Venkatesh, P., Seenivasan, G., Reddy, B. P., Nagarajan, K., 2011. Redox behaviour of cerium (III) in LiF-CaF_2 eutectic melt. Electrochim. Acta 58, 150–156.

Conocar, O., Douyere, N., Glatz, J.-P., Lacquement, J., Malmbeck, R., Serp, J., 2006. Promising pyrochemical actinide/lanthanide separation processes using aluminum. Nucl. Sci. Eng. 153, 253–261.

Cordoba, G., Caravaca, C., 2004. An electrochemical study of samarium ions in the molten eutectic LiCl+KCl. J. Electroanal. Chem. 572, 145–151.

Delpech, S., Merle-Lucotte, E., Heuer, D., Allibert, M., Ghetta, V., Le-Brun, C., Doligez, X., Picard, G., 2009. Reactor physics and reprocessing scheme for innovative molten salt reactor system. J. Fluorine Chem. 130, 11–17.

DOE, 2002. A technology roadmap for generation IV nuclear energy systems. In: U.S. DOE, Nuclear Energy Research Advisory Committee at the Generation IV International Forum. http://www.gen-4.org/PDFs/GenIVRoadmap.pdf.

Glatz, J.-P., Malmbeck, R., Souček, P., Claux, B., Meier, R., Ougier, M., Murakami, T., 2013. Chapter 26—Development of pyrochemical separation processes for recovery of actinides from spent nuclear fuel in molten LiCl-KCl. In: Groult, H., Lantelme, F. (Eds.), Molten Salts Chemistry. Elsevier, Oxford.

Guoan, Y., Hui, H., Rushan, L., Wenbin, Z., 2012. R&D activities on actinide separation in China. Procedia Chem. 7, 215–221.

Hamel, C., 2005. Separation Actinides-Lanthanides (Neodyme) Par Extraction Electrolytique En Milieux Fluorures Fondus, thesis at l'Universite Paul Sabatier, Toulouse, France.

Hamel, C., Chamelot, P., Taxil, P., 2004. Neodymium(III) cathodic processes in molten fluorides. Electrochim. Acta 49, 4467–4476.

Hamel, C., Chamelot, P., Laplace, A., Walle, E., Dugne, O., Taxil, P., 2007. Reduction process of uranium(IV) and uranium(III) in molten fluorides. Electrochim. Acta 52, 3995–4003.

Inoue, T., Tanaka, H., 1997. Recycling of actinides produced in LWR and FBR fuel cycles by applying pyrometallurgical process. In: Proceedings of Global 1997, October 5-10, Yokohama, Japan, pp. 646–652.

Inoue, T., Koyama, T., Arai, Y., 2011. State of the art of pyroprocessing technology in Japan. Energy Procedia 7, 405–413.

Kani, Y., Sasahira, A., Hoshino, K., Kawamura, F., 2009. New reprocessing system for spent nuclear reactor fuel using fluoride volatility method. J. Fluorine Chem. 130, 74–82.

Kormilitsyn, M.V., Bychkov, A.V. Ishunin, V.S., 2003. Pyroelectrochemical reprocessing of irradiated fuel of fast reactors. VI. Generalization of experience on BOR-60 spent nuclear fuel reprocessing using approaches "UO_2 to UO_2" "MOX to PuO_2" and "MOX to MOX". In: Proceedings of Global 2003, November 16 – 20, New Orleans, Louisiana, U.S.A., pp. 782–783.

Koyama, T., Ogata, T., Myochin, M., Arai, Y., 2011. Japanese programs in development of pyro-processing fuel cycle technology for sustainable energy supply with reduced burdens. In: Proceedings of Global 2011, December 11-16, Makuhari, Japan, Paper No. 452983.

Kurata, M., Tadashi, I., Serp, J., Ougier, M., Glatz, J.-P., 2004. Electro-chemical reduction of MOX in LiCl. J. Nucl. Mater. 328, 97–102.

Lacquement, J., Boussier, H., Laplace, A., Conocar, O., Grandjean, A., 2009. Potentialities of fluoride-based salts for specific nuclear reprocessing: overview of the R&D program at CEA. J. Fluorine Chem. 130, 18–21.

Laidler, J.J., Battles, J.E., Miller, W.E., Ackerman, J.P., Carls, E.L., 1997. Development of pyroprocessing technology. Progr. Nucl. Energy 31, 131–140.

Lee, H., Hur, J.-M., Kim, J.-G., Ahn, D.-H., Cho, Y.-Z., Paek, S.-W., 2011. Korean pyrochemical process R&D activities. Energy Procedia 7, 391–395.

Madic, C., Hudson, M.J., 2004. European EUROPART integrated project on actinide partitioning. In: Proceedings of 8th IEM on Actinide and Fission Product Partitioning and Transmutation 2004, 9-11 November, Las Vegas, Nevada, USA, pp. 393–394.

Madic, C., Bourg, S., Caravaca, C., De Angelis, G., Harrison, M., Malmbeck, R., Uhlíř, J., 2007. EUROPART Final Activity Report. CEA, France.

Magill, J., Berthou, V., Haas, D., Galy, J., Schenkel, R., Wiese, H.-W., Heusener, G., Tommasi, J., Youinou, G., 2003. Impact limits of partitioning and transmutation scenarios on radiotoxicity of actinides in radioactive waste. Nucl. Energy 42, 263–277.

Masset, P., Bottomley, D., Konings, R., Malmbeck, R., Rodrigues, A., Serp, J., Glatz, J.-P., 2005a. Electrochemistry of uranium in molten LiCl-KCl eutectic. J. Electrochem. Soc. 152, A1109–A1115.

Masset, P., Konings, R.J.M., Malmbeck, R., Serp, J., Glatz, J.-P., 2005b. Thermochemical properties of lanthanides (Ln = La, Nd) and actinides (An = U, Np, Pu, Am) in the molten LiCl-KCl eutectic. J. Nucl. Mater. 344, 173–179.

Masset, P., Apostolidis, C., Konings, R.J.M., Malmbeck, R., Rebizant, J., Serp, J.R.M., Glatz, J.-P., 2007. Electrochemical behaviour of neptunium in the molten LiCl-KCl eutectic. J. Electroanal. Chem. 603, 166–174.

Massot, L., Chamelot, P., Bouyer, F., Taxil, P., 2002. Electrodeposition of carbon films from molten alkaline fluoride media. Electrochim. Acta 47, 1949–1957.

Massot, L., Chamelot, P., Taxil, P., 2005. Cathodic behaviour of samarium(III) in LiF-CaF_2 media on molybdenum and nickel electrodes. Electrochim. Acta 50, 5510–5517.

Massot, L., Chamelot, P., Cassayre, L., Taxil, P., 2009. Electrochemical study of the Eu(III)/Eu(II) system in molten fluoride media. Electrochim. Acta 54, 6361–6366.

Mcfarlane, H.F., Lineberry, M.J., 1997. The IFR fuel cycle demonstration. Progr. Nucl. Energy 31, 155–173.

Mendes, E., Conocar, O., Laplace, A., Douyere, N., Miguirditchian, M., 2012a. Assessment of the complete core of the reference pyrochemical process, developed by the CEA. Procedia Chem. 7, 791–797.

Mendes, E., Malmbeck, R., Nourry, C., Souček, P., Glatz, J.P., 2012b. On the electrochemical formation of Pu-Al alloys in molten LiCl-KCl. J. Nucl. Mater. 420, 424–429.

Nagarajan, K., Prabhakara Reddy, B., Ghosh, S., Ravisankar, G., Mohandas, K.S., Kamachi Mudali, U., Kutty, K.V.G., Kasi Viswanathan, K.V., Anand Babu, C., Kalyanasundaram, P., Vasudeva Rao, P.R., Raj, B., 2011. Development of pyrochemical reprocessing for spent metal fuels. Energy Procedia 7, 431–436.

Nourry, C., Massot, L., Chamelot, P., Taxil, P., 2008. Data acquisition in thermodynamic and electrochemical reduction in a Gd(III)/Gd system in LiF-CaF_2 media. Electrochim. Acta 53, 2650–2655.

Nourry, C., Souček, P., Massot, L., Malmbeck, R., Chamelot, P., Glatz, J.-P., 2012. Electrochemistry of uranium in molten LiF-CaF_2. J. Nucl. Mater. 430, 59–63.

OECD, 1999. Actinide and Fission Product Partitioning and Transmutation—Status and Assessment report. OECD-NEA. http://www.oecd-nea.org/trw/docs/neastatus99/.

OECD, 2004. Pyrochemical Separations in Nuclear Applications—A Status Report. OECD-NEA. ISBN 92-64-02071-3 NEA No. 5427.

OECD, 2012. Spent Nuclear Fuel Reprocessing Flowsheet. OECD-NEA. NEA/NSC/WPFC/DOC(2012)15, June 2012, www.oecd-nea.org.

Ohta, H., Ogata, T., Papaioannou, D., Kurata, M., Koyama, T., Glatz, J.-P., Rondinella, V.V., 2011. Development of fast reactor metal fuels containing minor actinides. J. Nucl. Sci. Technol. 48, 654–661.

Osipenko, A., Maershin, A., Smolenski, V., Novoselova, A., Kormilitsyn, M., Bychkov, A., 2011. Electrochemical behaviour of curium(III) ions in fused 3LiCl-2KCl eutectic. J. Electroanal. Chem. 651, 67–71.

Rosenthal, M.W., Haubenreich, P.N., Mcneese, L.E., 1971. Recent progress in Molten-Salt reactor development. At. Energy Rev. 9, 601.

Sakamura, Y., Iizuka, M., Inoue, T., 2009. Development of oxide reduction process to bridge oxide fuel cycle and metal fuel cycle. In: Proceedings of Global 2009, September 6-11, Paris, France, paper 9176.

Serp, J., Konings, R.J.M., Malmbeck, R., Rebizant, J., Scheppler, C., Glatz, J.P., 2004. Electrochemical behaviour of plutonium ion in LiCl-KCl eutectic melts. J. Electroanal. Chem. 561, 143–148.

Serp, J., Allibert, M., Le Terrier, A., Malmbeck, R., Ougier, M., Rebizant, J., Glatz, J.-P., 2005. Electroseparation of actinides from lanthanides on solid aluminum electrode in LiCl-KCl eutectic melts. J. Electrochem. Soc. 152, C167–C172.

Serp, J., Chamelot, P., Fourcaudot, S., Konings, R.J.M., Malmbeck, R., Pernel, C., Poignet, J.C., Rebizant, J., Glatz, J.P., 2006. Electrochemical behaviour of americium ions in LiCl-KCl eutectic melt. Electrochim. Acta 51, 4024–4032.

Souček, P., 2008. Study of electroseparation process for spent nuclear fuel reprocessing using a reactive aluminium electrode in molten LiCl-KCl, thesis at Institute of Chemical Technology, Prague, Czech Republic.

Souček, P., Lisý, F., Zvejšková, R., 2003. Electroseparation studies of uranium and selected lanthanides in molten LiF-NaF-KF. In: Proceedings of Global 2003, November 16-20, New Orleans, Louisiana, USA, pp. 1582–1590.

Souček, P., Cassayre, L., Malmbeck, R., Mendes, E., Jardin, R., Glatz, J.-P., 2008. Electrorefining of U-Pu-Zr-alloy fuel onto solid aluminium cathodes in molten LiCl-KCl. Radiochim. Acta 96, 315–322.

Souček, P., Malmbeck, R., Mendes, E., Nourry, C., Glatz, J.-P., 2009a. Recovery of actinides from spent nuclear fuel by pyrochemical reprocessing. In: Proceedings of Global 2009, September 6-11, Paris, France, pp. 1156–1165.

Souček, P., Malmbeck, R., Mendes, E., Nourry, C., Sedmidubsky, D., Glatz, J.P., 2009b. Study of thermodynamic properties of Np-Al alloys in molten LiCl-KCl eutectic. J. Nucl. Mater. 394, 26–33.

Straka, M., Korenko, M., Szatmáry, L., 2011. Electrochemistry of praseodymium in LiF-CaF_2. J. Radioanal. Nucl. Chem. 289, 591–593.

Uhlíř, J., 2005. Chapter 24—Fluoride technologies application within the Molten-Salt Reactors fuel cycle. In: Groult, H., Nakajima, T. (Eds.), Fluorinated Materials for Energy Conversion. Elsevier Science, Amsterdam.

Uhlíř, J., Mareček, M., 2009. Fluoride volatility method for reprocessing of LWR and FR fuels. J. Fluorine Chem. 130, 89–93.

Westphal, B.R., Vaden, D., Li, S.X., Fredrickson, G.L., Mariani, R.D., 2009. Fate of noble metals during the pyroprocessing of spent nuclear fuel. In: Proceedings of Global 2009, September 6-11, Paris, France, pp. 1291–1297.

18 Pyrochemical fuel cycle technologies for processing of spent nuclear fuels: Developments in Japan

Tadafumi Koyama, Masatoshi Iizuka
Central Research Institute of Electric Power Industry, Tokyo, Japan

Acronyms

AEM	alkaline earth metals
AM	alkali metals
ANL	Argonne National Laboratory
CRIEPI	Central Research Institute of Electric Power Industry
DF	decontamination factor
EBR-II	Experimental Breeder Reactor-II
EPMA	electron probe microanalyzer
FBR	fast breeder reactor
FCF	fuel conditioning facility
FEM	finite element model
FP	fission product
HLLW	high-level liquid waste
HM	heavy metal
IFR	integral fast reactor
INL	Idaho National Laboratory
JAEA	Japan Atomic Energy Agency
JRC-ITU	Joint Research Centre—Institute of TransUranium Elements
LCC	liquid cadmium cathode
LWR	light water reactor
MA	minor actinide
MOX	mixed oxide
NM	noble metal
NPP	nuclear power plant
PUREX	plutonium uranium reduction extraction
PWR	pressurized water reactor
RE	rare earth
SEM-EDX	scanning electron microscope/energy dispersive X-ray
SF	separation factor
SS	stainless steel

Reprocessing and Recycling of Spent Nuclear Fuel. http://dx.doi.org/10.1016/B978-1-78242-212-9.00018-6

TEPCO Tokyo Electric Power Company
TMI Three Mile Island
TRU transuranium or transuranic
XRD X-ray diffraction

18.1 Introduction

The study of pyrochemical fuel cycle technology started in Japan around the 1950s; however, most of the activities were terminated in the 1970s because the government had started construction of the pilot-scale Tokai plant using aqueous reprocessing technology. Based on the domestic experience on the Tokai plant and French experience on the UP3 reprocessing plant at La Hague, Japanese utilities determined to deploy a PUREX reprocessing plant, Rokkasho, as a first commercial facility. It was constructed in 1993-2001, and is still in the hot testing phase in 2014 due to initial troubles with the glass melter, and new regulations after major earthquakes. In the course of this elongated introduction of the commercial plant, construction costs were drastically increased from the original estimate. On the other hand, government started to develop FBR cycle technology for the utilization of plutonium to be produced by Rokkasho reprocessing. Fast breeder reactors were successfully built one after another; that is, the experimental reactor Joyo and prototype reactor Monju. As for the reprocessing facility for fast reactor fuels, a small hot cell for PUREX testing per pin was constructed and successfully operated. However, the construction of an engineering-scale hot cell was suspended; not only due to the increase of construction costs of the cell itself but also because of the predicted increases in the costs of the future FBR fuel cycle based on the scale-up experience with PUREX plants. Hence, technology innovation capable of significant cost reductions was expected. Under the circumstances, pyrochemical reprocessing technology for metal fuel, termed *pyroprocess,* developed for the Integral Fast Reactor (IFR) concept, as proposed by Argonne National Laboratory (ANL) in USA, became the focus of R&D at the Central Research Institute of Electric Power Industry (CRIEPI) on behalf of the electric utilities in Japan.

As well as the participation in the IFR program of ANL, CRIEPI has been carrying out its own program consisting of basic data measurement, simulation code development, engineering technology development, and so on, in order to address the technology gaps between the output of the IFR program and the readiness of commercial fuel cycle technology. For implementation of the own program, CRIEPI has been carrying out collaborating studies with many domestic organizations having knowledge of spent fuel reprocessing; for example, Japan Atomic Energy Research Institute, Power Reactor and Nuclear Fuel Development Corporation (later integrated into JAEA), Toshiba Corporation, Kawasaki Heavy Industry, Hitachi Ltd., and several universities. After the termination of the IFR project, demonstration tests with irradiated materials have been carried out through a joint program between CRIEPI and Joint Research Centre-Institute for Transuranium Elements (JRC-ITU). Such extensive activities at CRIEPI have renewed the focus on the advantages possessed by the pyroprocess; for example, nuclear proliferation resistance, waste burden

reduction, and MA recovery, in addition to fuel cycle cost reduction. Hence, several other organizations within Japan have started studies into various types of pyrochemical reprocessing technologies; for example, JAEA has studied electrowinning technology for oxide spent fuel, Hitachi has studied the fluoride volatility process for spent oxide fuel, and so on.

In order to select the reference technologies for the commercialization of an FBR fuel cycle in the mid-twenty-first century from pyrochemical technologies and modified aqueous technologies, the Japanese government and utilities jointly carried out a feasibility study consisting of technology evaluation and cost evaluation. In 2006, they selected two reference technologies; the "main concept" was an advanced aqueous reprocessing technology for mixed oxide (MOX) fuel, which had been developed by JAEA, while the "subconcept" was the pyroprocess for metal fuel, which had been studied mainly by CRIEPI. They recognized the potential advantages of a metal fuel cycle over a MOX fuel cycle in the core performance aspects such as breeding ratio and fuel cycle cost, but pointed out the less experience in industrial-scale operation (MEXT, 2006). Hence, development of the pyroprocess has continued with a focuses on the engineering technology development and demonstration with irradiated fuels.

In this chapter, key results of the developments and basic studies will be summarized along with theoretical works such as simulation model developments. The goal is to provide a comprehensive understanding of pyrochemical fuel cycle technologies as well as the state of-the-art in Japanese technology development.

18.2 Role of pyrochemical processing in the Japanese fuel cycle scenario; synergy of aqueous reprocessing and pyroreprocessing

As mentioned above, in Japan, because the reprocessing facility for light water reactor UO_2 fuel by PUREX has long been operated and MOX fuel has been manufactured at the pilot scale, the combination of MOX fuel and aqueous reprocessing technology was recognized as the reference commercial FBR fuel cycle technology. However, if reduction of the waste burden by minor actinide (MA: neptunium, americium, and curium) transmutation as well as a high plutonium breeding ratio are required for the fast reactor in the future, it will be hard for the combination of MOX fuel and aqueous reprocessing to realize an economic fuel cycle because of unsolved technological difficulties. For instance, the fabrication of MOX fuel containing MA (strong radiation source) requires very complicated remote operation, and the recovery of MA requires complex separations among MAs and between MA and lanthanides.

Therefore, whether it occurs at the beginning or middle of FBR deployment, it will be reasonable to assume a shift in the FBR fuel cycle technology to the metallic fuel cycle, which can realize the economic reactor core with high plutonium breeding and high MA transmutation ratios and uses remote fuel fabrication technology known as *injection casting*. The separation characteristics of TRU from lanthanide elements by pyrochemical processing are well-known; the technology development will be

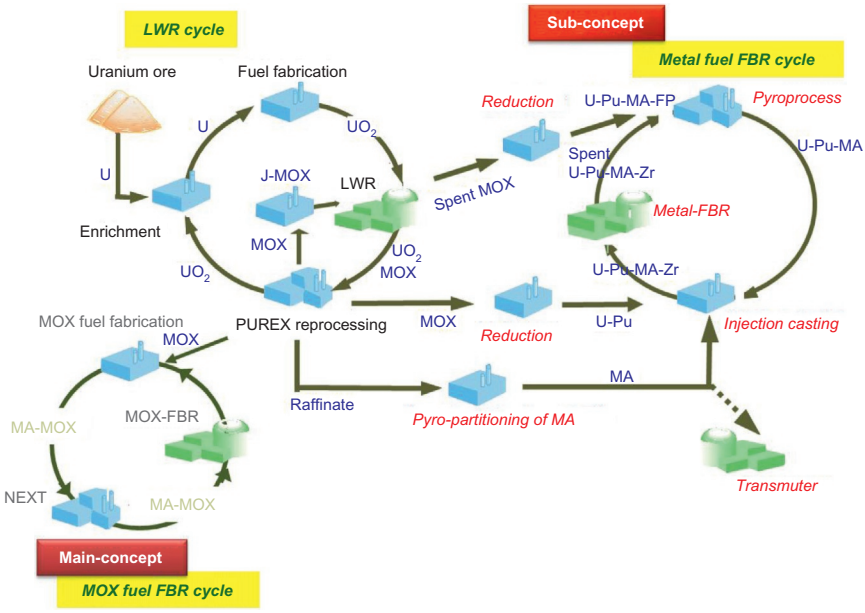

Figure 18.1 Proposed future fuel cycle scenario in Japan.

discussed in this chapter. The scenario implies the coexistence of oxide fuel aqueous-based reprocessing and metallic fuel reprocessing by pyroprocessing for a certain period. It is expected to be required in the future that the shift will be carried out flexibly, maintaining economic rationality.

By using the advantages of pyroreprocessing technology, which is applicable to various fuels, CRIEPI has proposed the fuel cycle scenario given in Figure 18.1, which has increased flexibility in the future nuclear fuel cycle deployment. In this scenario, partitioning and transmutation (P&T) of the long-lived nuclides in high-level waste from aqueous reprocessing of light water reactor fuel is also realized by applying pyrochemistry to the HLLW. Hence, all actinide elements generated in the LWR fuel cycle will be burnt in fast reactors or transmuters, thus realizing a closed actinide cycle.

On the other hand, after the Fukushima accident, pyrochemistry has been considered for an additional role in the treatment of damaged fuel debris because it is almost impossible to dissolve corium, $(U,Zr)O_2$ with nitric acid.

18.3 Pyroreprocessing process development

A typical process flow sheet for pyroreprocessing for metallic and oxide fuels is shown in Figure 18.2 (Koyama, 2011). In order to process either the LWR spent fuels or the MOX products from the PUREX fuel reprocessing plant, these materials are

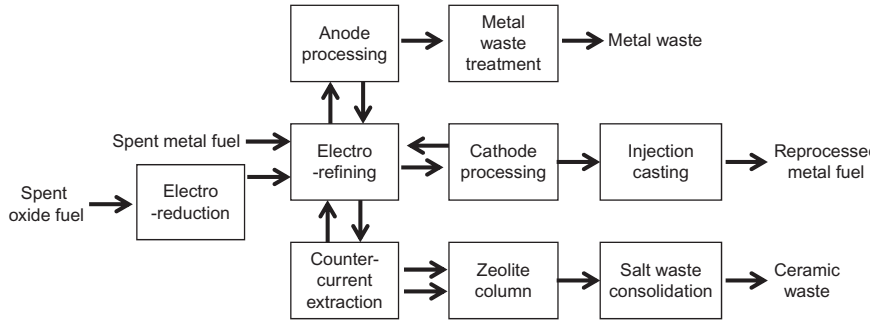

Figure 18.2 Process flow sheet of the pyro-reprocessing for metallic and oxide fuels.

transformed to metals using the electrolytic reduction technique. Spent metallic fuel dismantled from a fast reactor is disassembled and irradiated fuel pins are mechanically chopped into 5-10 mm lengths. The chopped fuel pins are then sent to the molten salt electrorefining step, where the actinides are decontaminated from the fission products (FPs) and recovered in LiCl-KCl eutectic melt at 773 K. The electrolytic reduction product is also fed to the electrorefining step. In the electrorefining step, two kinds of cathodes are used to obtain different streams of products. One is a solid cathode made of iron, where uranium is selectively collected due to its higher standard electrode potential compared with other actinide elements. The other cathode is a liquid cadmium cathode (LCC), where TRUs are collected together with uranium taking advantage of low activity coefficient and subsequent chemical stabilization of these elements in liquid cadmium. The cathode products taken out from the electrorefining apparatus are accompanied by the solvents (chlorides and cadmium metal). In the high-temperature distillation step, called *cathode processing,* those solvents are distilled off, and the cathode products are consolidated into dense metal ingots at the same time. The products of the cathode-processing step are adequately blended with other product and supplementary zirconium to make the fuel composition, and then sent to the injection casting step to fabricate the recycled fuel slug.

As described above, the main part of the pyroreprocessing flow sheet is very simple and the number of the required steps is much smaller than the PUREX process. Because water, which is an excellent moderator of neutrons, does not exist in the process as a solvent, restrictions in the apparatus design from the viewpoint of criticality are less severe. The dimension of the process equipment per its capacity would be consequently smaller. The elimination of organic solvents that are degraded by irradiation is advantageous not only from the standpoint of process waste reduction, but also in acceptability for high burn up spent fuel such as LWR-MOX, fast reactor fuels, MA-containing fuels, and fuels with short cooling times. The injection-casting step does not need minute manipulations and it has been already demonstrated to be adaptable to remote operations required for handling of highly active materials. All these characteristics indicate the excellent economical potential of pyroreprocessing due to a remarkable reduction in the plant volume.

Another feature of the pyroreprocessing is that its economic advantage is not diminished even in a small-scale operation as pyroprocessing is primarily a sequence of batch processes. This feature greatly increases the value of pyroprocessing during an introductory period of fast reactor cycle technologies where a superior flexibility should be needed toward stepwise deployment and expeditious improvement in the process equipment design and operational conditions.

Further, plutonium is always recovered with uranium, MAs, and a small amount of lanthanide FPs into the LCC product. Such low decontamination properties of products from the pyroreprocessing could be an advantage from the viewpoint of proliferation resistance. It is also an important feature that MAs inevitably accompany plutonium throughout the pyroprocess, as it indicates attainment of "self-confinement" of MAs in the metallic fast reactor cycle conjointly with the excellent suitability of the metallic fuel for transmutation (see Section 18.4).

Regarding the major steps in the process flow sheet, fundamental feasibility has been demonstrated through a large number of experimental studies using actinides and various simulants. Especially for the core steps from the disassembly of spent fuel to the cathode processing, a lot of operational experiences with prototype or practical-scale equipment have been already accumulated in the fuel conditioning facility (FCF) at the Idaho National Laboratory (INL) by reprocessing of actual spent metallic fuels from Experimental Breeder Reactor-II (EBR-II) (Goff et al., 2007; Goff and Simpson, 2009; Li et al., 2007).

However, there still remains a vast area of technical challenges to be solved before the practical use of pyroreprocessing technologies. In this section, we present current achievements in the research and development activities on such areas, while studies on waste treatment processes are reviewed later in a separate section (see Section 18.5).

18.3.1 Flow sheet development, experiments, and computational analysis

18.3.1.1 Demonstration of the electrolytic reduction process

The principle of the electrolytic reduction process is schematically shown in Figure 18.3 (Sakamura et al., 2009). In this process, oxide fuels are loaded at the cathode in a molten chloride bath that dissolves oxide ions (O^{2-}). The reactions at the cathode and anode are as follows:

$$\text{Cathode}: MO_2 + 4e^- \rightarrow M + 2O^{2-} \tag{18.1}$$

$$\text{Anode}: 2O^{2-} \rightarrow O_2 + 4e^- \tag{18.2}$$

where M denotes actinides such as uranium and plutonium. The oxygen is electrochemically ionized and the actinide metal remains at the cathode. The ionized O^{2-} is transported through the molten chloride bath and discharges at the anode to form O_2 gas. When a carbon anode is employed, CO_2 or CO is evolved instead of O_2.

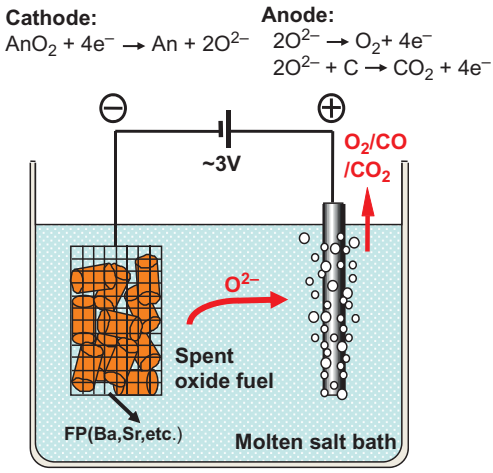

Figure 18.3 Schematic diagram of electrolytic reduction process.

The distinctive feature of the process is that the actinides never dissolve into the salt. The advantages of the electrolytic reduction process are as follows. No reductant is needed and the by-product is only oxygen or carbon oxide gas. The O^{2-} concentration in the salt is almost constant and can be maintained at a low value, which is effective for reducing transuranic oxides (Usami et al., 2002). The amount of salt used in the process may be small because O^{2-} does not accumulate in the salt bath.

Three kinds of molten chloride melts (i.e., LiCl, $CaCl_2$, and LiCl-KCl eutectic mixture) were investigated for their suitability as an electrolytic reduction bath. In $CaCl_2$, the reduced uranium metal cohered due to the high operating temperature (>800 °C) and a dense metal skin that covered the UO_2 surface, which prevented the reduction from progressing inside (Sakamura et al., 2006). When LiCl-KCl was used at 650 °C, the reduction rate of UO_2 was quite slow because the removal of reduction product O^{2-} from the cathode was retarded due to low Li_2O solubility in this melt (Sakamura et al., 2005b). Finally, it was verified that LiCl is a more suitable solvent for reducing oxide fuels, where UO_2 a1nd MOX were easily reduced into metal at 650 °C.

The effect of coexistence of alkali and alkaline earth FPs (AM, AEM), which accumulate gradually in the salt bath during a long-term operation, was also investigated (Sakamura et al., 2008). In the LiCl-CsCl system, the Li_2O solubility decreased with increasing CsCl composition; this caused the low UO_2 reduction rate. On the other hand, the presence of $SrCl_2$ and $BaCl_2$ did not have appreciable effect.

An electrolytic reduction test using MOX containing neptunium $(U_{0.55}Pu_{0.40}Np_{0.05})O_2$ was performed in LiCl-0.72 mol% Li_2O at 650 °C to gain a better understanding of the fundamental behavior of transuranium elements (Iizuka et al., 2006). Figure 18.4 shows the MOX before and after the reduction. Complete reduction of the MOX was suggested by the weight change through the reduction and SEM-EDX observations. The reduced metal cohered to form a coral-like structure. The chemical composition of the reduction products was homogeneous and

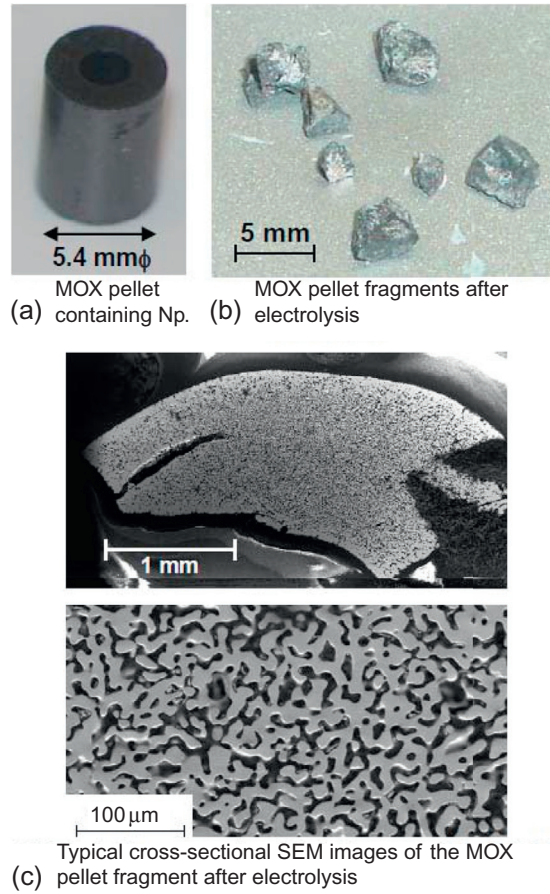

Figure 18.4 MOX pellet ($(0.55U\text{-}0.40Pu\text{-}0.05Np)O_2$) before and after electrolytic reduction in LiCl at 923 K.

identical to that of the initial MOX, indicating that the reduction was not selective among the actinides. Although the concentrations of plutonium and americium (the decay product of Pu^{241}) in the LiCl salt bath increased through the tests, their absolute values were very small.

From the results of laboratory-scale experiments, it was clarified that the oxide reduction rate is controlled by the transportation of O^{2-} from the inside of the cathode to the bulk salt. In order to find optimum conditions with improved reduction rates, engineering-scale UO_2 reduction tests in a LiCl salt bath were conducted using various types of cathode basket and oxide material. Adoption of a cathode design using perforated thin baskets, which decreased the thickness of the UO_2 powder layer, brought an improvement in the reduction rate (Sakamura et al., 2009). In addition, preparing porous UO_2 pellets was of great advantage in the reduction process (Figure 18.5). It was demonstrated that 100 g of UO_2 could be completely reduced to metal within 10 h with a current efficiency of 60-80% (Sakamura and Omori, 2010). Larger-scale tests have been performed using a cell design with a diaphragm made from MgO between

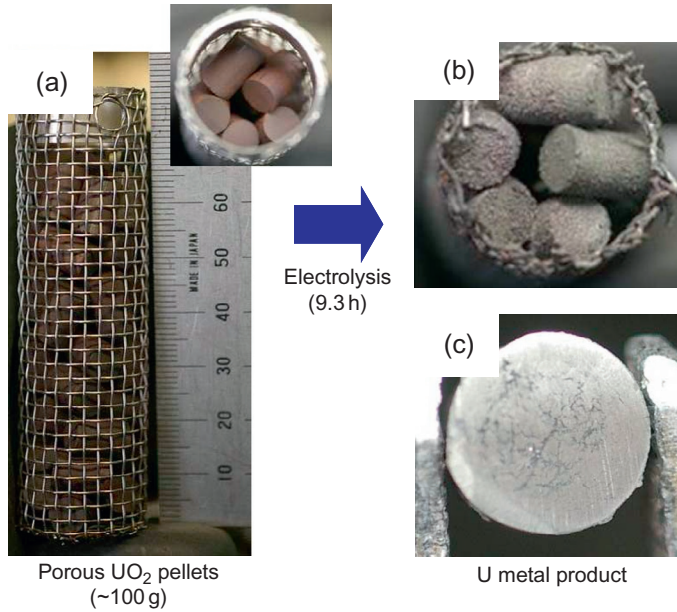

Figure 18.5 Electrolytic reduction test for porous UO_2 pellets: (a) Cathode basket charged with 103.6 g of UO_2 pellets, (b) inside of cathode basket after reduction, (c) Polished cross section of reduced UO_2 pellet.

the anode and cathode to restrain the back reactions, which are caused by metallic lithium and O_2 gas and decrease the current efficiency (Iizuka et al., 2013c). This modification, combining high reduction current and excellent current efficiency, achieved almost complete reduction of approximately 1 kg of UO_2 within about 8 h.

Electrorefining tests using the reduction products obtained from the porous UO_2 pellet were performed in a LiCl-KCl-UCl_3 electrolyte at 500 °C (Sakamura et al., 2009). In this test, 97% of the uranium metal in the reduction product was anodically dissolved into the electrolyte with a current efficiency of 88% and dendritic uranium metal was successfully collected on the stainless steel cathode.

18.3.1.2 Development of the electrorefining process for TRU recovery

Molten salt electrorefining, schematically shown in Figure 18.6, is a major step in pyrometallurgical reprocessing, in which the actinide elements in chopped spent metal fuel are recovered and decontaminated from fission products (FPs). To recover the material for the fabrication of recycled fuel, uranium is deposited on a solid cathode (Tomczuk et al., 1992; Koyama et al., 1997b). This process utilizes the difference between the free-energy changes of metal chlorides. The constituents in the spent metal fuel that tend to form their chlorides more easily than zirconium are

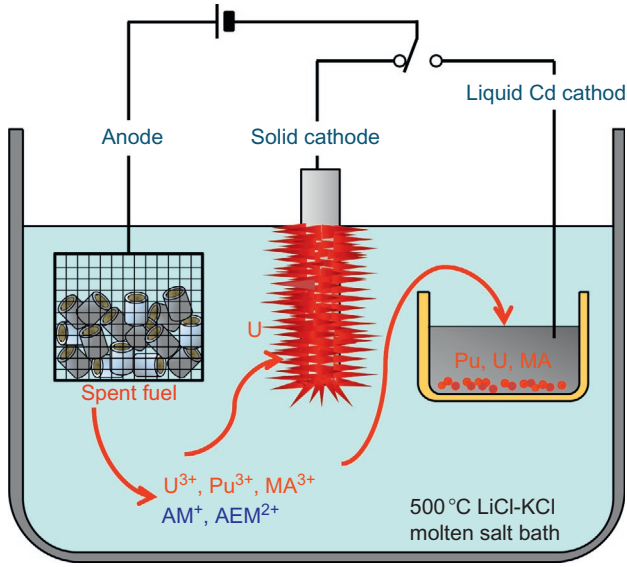

Figure 18.6 Schematic diagram of electrorefining process.

electrochemically dissolved at an anode. At a cathode, uranium, the most easily reduced element among the dissolved materials, is preferentially reduced and collected. Other actinides, such as plutonium and americium, are recovered in a liquid cadmium cathode (LCC) because they are thermodynamically stabilized in liquid cadmium owing to their low activity coefficients (Iizuka et al., 2001). The main reaction schemes of the electrorefining process are described as follows:

$$\text{Anode}: \quad \mathrm{U_{in\ spent\ fuel}} \rightarrow \mathrm{U^{3+}} + 3\mathrm{e^-} \tag{18.3}$$

$$\mathrm{Pu_{in\ spent\ fuel}} \rightarrow \mathrm{Pu^{3+}} + 3\mathrm{e^-} \tag{18.4}$$

$$\text{Cathode (solid)}: \quad \mathrm{U^{3+}} + 3\mathrm{e^-} \rightarrow \mathrm{U} \tag{18.5}$$

$$\text{Cathode (liquid cadmium)}: \mathrm{U^{3+}} + 3\mathrm{e^-} \rightarrow \mathrm{U_{in\ Cd}} \tag{18.6}$$

$$\mathrm{Pu^{3+}} + 3\mathrm{e^-} + 6\mathrm{Cd} \rightarrow \mathrm{PuCd_6} \tag{18.7}$$

Solubility of actinide elements in liquid cadmium at 773 K is generally limited to a few wt% (Johnson, 1960). Beyond the solubility, these elements form solid phases in cadmium (uranium metal, intermetallic compounds of TRU, and cadmium). Especially, dendritic uranium deposit formed at the surface of LCC causes significant problems. It grows in uncontrollable length and direction and easily leads to mechanical and electrical problems in the electrorefiner. Furthermore, the extended surface of the dendrite does not function as an LCC any longer but as a solid cathode instead, where

only uranium is collected in preference to TRUs. These problems are revealed clearly under conditions where the uranium deposits tend to remain at the molten salt/liquid cadmium interface; for example, at uranium content beyond its solubility in LCC or at high uranium collection rate per unit LCC surface area (current density) (i.e., at high cathodic current density). Many experiments and equipment design studies have been carried out to determine conditions that enable both avoidance of growth of the solid phases and collection of actinides at as high a recovery rate into LCC as possible.

At ANL, a "dendrite breaker" (Steindler et al., 1992) and a "pounder" (Battles et al., 1993) were devised to push the uranium dendrite down into the cadmium phase. In contrast, CRIEPI tried to optimize the stirring operation (Koyama et al., 1997c) to collect actinides at high cathodic current density beyond its solubility in liquid cadmium. In the laboratory-scale electrorefiner for plutonium experiments, a LCC equipped with a paddle-shaped stirrer rotating at the interface between the molten salt/liquid cadmium phases was employed, as seen in Figure 18.7 (Uozumi et al., 2004). The Pu/U ratio in the molten salt electrolyte was noted as an important parameter because the partial cathodic current density of uranium reduction, corresponding to its deposition rate, was considered to have the most significant impact on the solid-phase growth. At the Pu/U ratio of 4.4 in LiCl-KCl, these elements were collected together at a constant proportion into a LCC up to 12 wt% in total. No trace of remarkable solid-phase growth on the surface of the LCC was found, indicating smooth recovery of plutonium and uranium throughout the electrorefining. Similar experiments were repeated under various conditions. It was finally concluded that plutonium

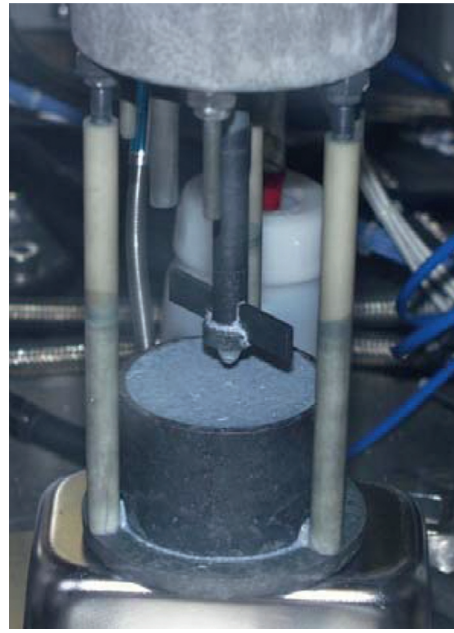

Figure 18.7 Liquid Cd cathode equipped with a paddle-shaped stirrer.

and uranium can be collected together in the LCC at Pu/U ratios of more than 2-3 in the molten salt bath. The largest cathodic current density achieved for simultaneous recovery of plutonium and uranium beyond their solubility in liquid cadmium was 156 mA/cm^2 (Kato et al., 2003). Based on this result, the maximum recovery rate of actinides into a LCC for practical use, whose dimension is assumed to be 30 cm in diameter, can be estimated to be approximately 320 g/h.

To investigate the anodic behavior of a U-Pu-Zr ternary fuel alloy and the cathodic behavior of MAs (Np, Am, Cm) at a LCC, small-scale electrorefining experiments using unirradiated alloys 71U-19Pu-10Zr and 67U-19Pu-10Zr-2MA (1.2 Np,0.6Am,0.2Cm)-2RE(1.4Nd,0.2Ce,0.2Gd,0.2Y) by wt%, were carried out (Koyama et al., 2002; Kinoshita et al., 2005). These alloys were originally fabricated at JRC-ITU for a transmutation test (see Section 18.4.3). Plutonium and uranium were simultaneously recovered into the LCC with codeposition of small amounts of MAs, zirconium, and REs. The separation factors (SFs) of uranium, neptunium, americium, curium, and cerium against plutonium, derived from the composition of recovered deposits and the salt bath, were similar to the values obtained from the equilibrium distribution experiment in the LiCl-KCl/Cd system. These results demonstrated that it is feasible to recover all actinides separated from RE fission products by electrorefining using LCC. The anodic dissolution of the alloys progressed from the outside, leaving a dense layer containing salt and zirconium metal around the alloy surface. More than 99.9% of both uranium and plutonium elements were dissolved from the alloys and about 55% of zirconium remained.

SFs of element M (M: U, Am, La, Ce, Pr, Nd) against plutonium, defined as [M/Pu in molten salt]/[M/Pu in Cd alloy (cathode)], were evaluated for LCC products beyond saturation with deposited elements (Kato et al., 2006). After annealing the LCC product in the salt bath, the evaluated SFs were close to literature values determined in the equilibrated system (see Section 18.6), although there were small discrepancies due to formation of the MCd_{11}-type solid phase of different composition from the liquid cadmium phase. For the LCC product samples without annealing, evaluated SFs (La: 91, Ce: 23, Pr: 16, Nd: 16) showed somewhat larger differences from the literature values. These differences were considered to be caused by the concentration gradient at the salt/LCC interface formed by the diffusion-limited electrochemical transfer of the actinide and lanthanide elements. This result indicates a necessity to account for kinetic considerations in the quantitative discussion on the behavior and performance of the LCC.

18.3.1.3 Development of electrorefining simulation codes

The material transport in the electrorefining process is quite a complicated phenomenon and influenced by a great number of parameters. Therefore, it is necessary for improvement in performance of the electrorefining step to develop and use an analysis code founded on the accumulated knowledge about this process. For this purpose, a simulation code TRAIL was developed (Figure 18.8), which introduced a simple kinetic treatment based on a diffusion layer model into the calculation of the material transport in the electrorefining process (Kobayashi and Tokiwai, 1993). Assuming a

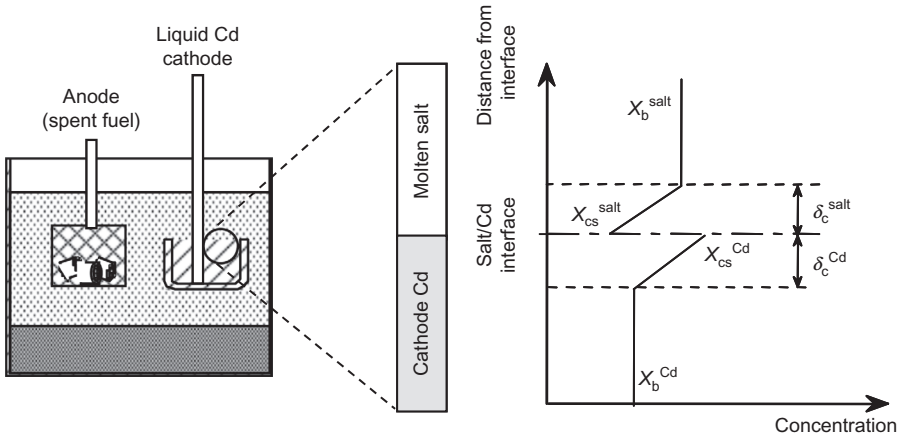

Figure 18.8 Diffusion layer model used in TRAIL (example for molten salt/LCC interface).

local equilibrium at the electrolyte/electrode interfaces and a linear concentration gradient of the species in the vicinity of the electrode, the following Equations 18.8–18.10 are used for each electrode reaction (at the molten salt electrolyte/LCC interface under a constant electrorefining current, for example):

$$E_c = E_0^X + \frac{RT}{Z_X F} \ln\left(\frac{\gamma_X^{salt} X_{cs}^{salt}}{\gamma_X^{Cd} X_{Cs}^{Cd}}\right) \tag{18.8}$$

where E_c (V) is the cathode potential, E_0^X is the standard potential of element X, R is the gas constant (8.314 J/mol K), T (K) is the temperature, Z_X is the number of equivalents per mole of X in the salt, F is Faraday constant (96,485 C/mol), γ_X^{salt} is the activity coefficient of X in the salt, X_{cs}^{salt} (mol/cm^3) is the concentration of X at the salt side of the salt/LCC interface, γ_X^{Cd} is the activity coefficient of X in liquid cadmium, X_{cs}^{Cd} is the concentration of X at the cadmium side of the salt/LCC interface, and

$$i_X^c = Z_X F D_X^{Cd} \frac{X_{cs}^{Cd} - X_b^{Cd}}{\delta_c^{Cd}} = Z_X F D_X^{salt} \frac{X_b^{salt} - X_{cs}^{salt}}{\delta_c^{salt}} \tag{18.9}$$

where i_X^c (A/cm^2) is the anodic current density carried by X, D_X^{Cd} (cm^2/s) is the diffusion coefficient of X in liquid cadmium, X_b^{Cd} (mol/cm^3) is the concentration of X in bulk liquid cadmium, δ_c^{Cd} (cm) is the thickness of diffusion layer in liquid cadmium, D_X^{salt} (cm^2/s) is the diffusion coefficient of X in the salt, X_b^{salt} (mol/cm^3) is the concentration of X in bulk salt, δ_c^{salt} (cm) is the thickness of diffusion layer in the salt, and

$$i_{total} = \sum_X i_X^c \tag{18.10}$$

where i_{total} (A/cm^2) is the total cathodic current density.

If the cathode potential E_c is given, the concentration of element X on both sides of the cathode surface (X_{cs}^{salt}, X_{cs}^{Cd}) and the current density by each element can be calculated by

solving Equations 18.8 and 18.9 under the boundary conditions (X_b^{salt}, X_b^{Cd}). Then the current density for each element can be calculated by Equation 18.9. This procedure is iterated by testing different values of E_c until the sum of the calculated current components given by Equation 18.10 agrees with the applied total anodic current.

The evaluations by this code finely reproduced the change of molten salt bath composition during solid cathode operation and the transition of the LCC composition, indicating its validity.

An excess increase of cell voltage in an electrorefiner causes a local overpotential and possibly leads to unexpected reactions and electrochemical corrosion. In the electrorefiner design, therefore, reduction of the cell resistance by optimization of electrode shape and arrangement is an important problem for minimization of the cell voltage, maximization of the electrolytic current, and leveling of the current/potential distribution. To evaluate the current/potential distribution in the electrorefiner, the effect of polarization on the electrochemical potential at the electrode surface should be taken into consideration. In evaluation of the secondary current/potential distribution in the electrorefiner using the DEVON code (Kobayashi et al., 1995), calculation of the current/potential distribution by solving the Laplace equation using the FEM method and estimation of the polarization effect based on the diffusion-layer model are repeated alternately until they converge to constant states. The calculation on the relation between cell resistance/amplitude of polarization and uranium concentration in the molten salt bath are in good agreement with the experimental result, demonstrating the utility of this code in the electrorefiner design.

The electrorefining experiments using unirradiated U-Pu-Zr alloy pins (Koyama et al., 2002; Kinoshita et al., 2005) showed that anodic dissolution of plutonium and uranium proceeded in the radial direction in preference to zirconium and that a porous zirconium layer was left at the surface of the anode residue. The anode potential was abruptly increased at a certain point to a level suggesting that zirconium in the alloy was involved in the anodic dissolution, although a large amount of uranium and plutonium remained inside the residue. On the other hand, the observation of anode residue after the engineering-scale electrorefining tests using U-Zr alloy pins revealed that an intermediate layer containing 50-67 at%-Zr, corresponding to the δ-phase in the U-Zr binary phase diagram, was formed between the porous zirconium layer at the surface and undissolved U-Zr layer (Iizuka et al., 2010).

To improve the performance of the whole pyrometallurgical process, it is highly important to quantitatively understand and precisely predict the relation between the conditions of the electrorefining operation and the anodic behavior of metallic fuel. However, the TRAIL code cannot model the spent metallic fuel anode, which is essentially a composite of solid phases changing its structure, dimension, and composition of every moment. Therefore, the complex anodic dissolution of metallic fuel (U-Zr or U-Pu-Zr alloys) was modeled (Iizuka and Moriyama, 2010) on the basis of the findings from a number of past electrorefining tests.

In this model, a multilayered structure consisting of the undissolved fuel alloy, an intermediate layer that has the δ phase composition, and a porous zirconium layer is formed according to anodic dissolution of the actinides (Figure 18.9). The succeeding anodic reaction and its location are determined from the limiting diffusion rate of dissolved actinides in those layers in addition to a diffusion layer formed in the

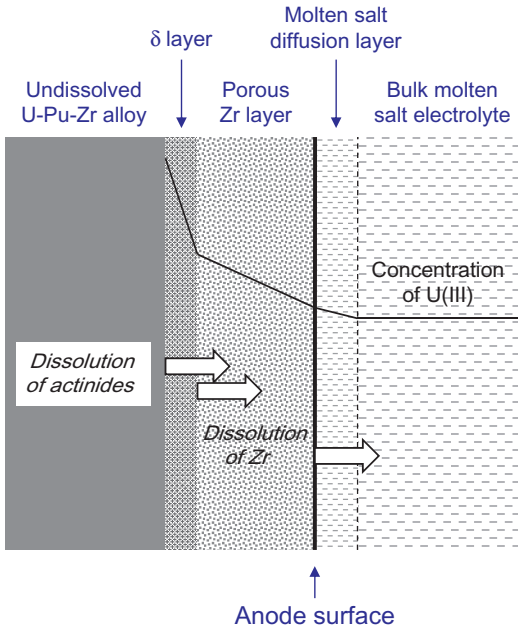

Figure 18.9 Schematic view of anode model with multi-diffusion layers.

electrolyte at the surface of the anode. To calculate the anode potential based on the local equilibrium of uranium at the surface of the anode residue, an exponential distribution of uranium activity in the porous zirconium layer was assumed.

Simulation of the previous engineering-scale U-Zr electrorefining tests (Iizuka et al., 2009) using the model showed that the calculated dissolution ratios of uranium and zirconium, which are directly affected by the multilayer formation, were in agreement with the experimental result when the alloy pin is chopped sufficiently short. The growth of the thick δ layer found in some parts of the anode residue samples was also explained by simulating the local anode behavior at lower anodic current density than the average value.

The laboratory-scale electrorefining tests with the unclad U-Pu-Zr ternary alloy were also simulated. The characteristic change of the anode potential during these tests was reproduced in the calculation by fitting the parameters used in the definition of the uranium activity in the porous zirconium layer (Figure 18.10). Small disagreements found between the experimental and calculation results, such as the gradual increase in the actual anode potential, would be attributed to the distribution of the porous zirconium layer thickness at the surface of the anode or the slight decrease in the amount of uranium dissolved in solid α-phase zirconium.

18.3.1.4 Development of an actinide recovery process from anode residues

In the electrorefining step for spent metallic fuel, one of the most important points is to maximize the anodic dissolution rate and minimize the remaining amounts of the actinides in the anode residue. Because zirconium in the metallic fuel has a high standard redox potential relatively close to that of uranium, it is inevitable that some of the

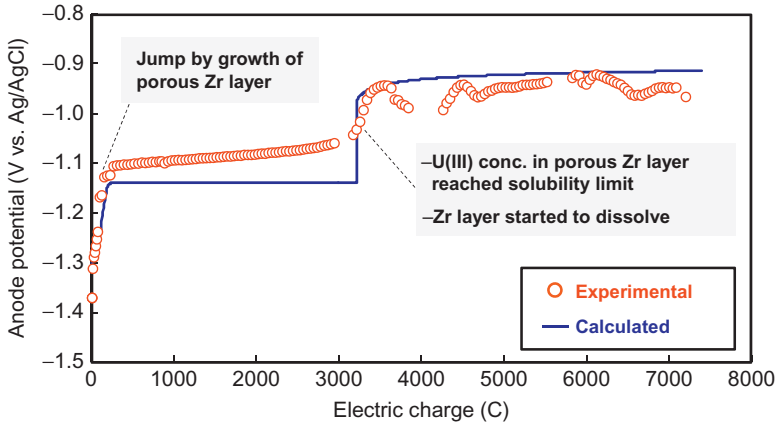

Figure 18.10 Change in anode potential during electrorefining test using U-Pu-Zr ternary alloy calculated using multi-diffusion layer model.

zirconium is dissolved when a very low remaining concentration of the actinides is required or when a large anodic current density is imposed to obtain a high dissolution rate (Iizuka et al., 2009, 2010).

Some of the anodically dissolved zirconium is rereduced and accumulates in the electrorefiner. The recovery of zirconium from the electrorefiner vessel requires a significant amount of time. The remaining zirconium is electrotransported with uranium to the cathode and increases the operational temperature at the cathode-processing step, where the electrolyte accompanying the cathode product is removed by high-temperature distillation. From these viewpoints, it is clearly desirable to leave as much zirconium as possible in the anode residue at the end of anodic dissolution. However, it is expected that a low ratio of remaining uranium and a high recovery rate of the actinides cannot coexist under such restrictions.

CRIEPI proposed a new treatment process called *anode processing* for the anode residue that is added after the electrorefining step to achieve a high recovery rate and percentage recovery of the actinides in the pyrometallurgical reprocessing flow sheet (Figure 18.11) (Iizuka et al., 2013a). Anode processing consists of two steps: (i) oxidation of the remaining actinides in the anode residue into the molten chloride solvent by the addition of cadmium chloride ($CdCl_2$), and (ii) removal of the accompanying chloride by high-temperature distillation. After these steps, the anode residue is melted and consolidated as a metallic waste for disposal. Finally, the chloride containing the recovered actinides is recycled to the electrorefining step.

The oxidation of the remaining uranium by $CdCl_2$ was studied using anode residue from previous electrorefining experiments with U-Zr alloys. The reaction between uranium and $CdCl_2$ was completed in about two days with a satisfactory chlorine balance among the species in the molten chloride solvent (Figure 18.12). A high uranium oxidation rate was attained by appropriately controlling the rate of $CdCl_2$ addition.

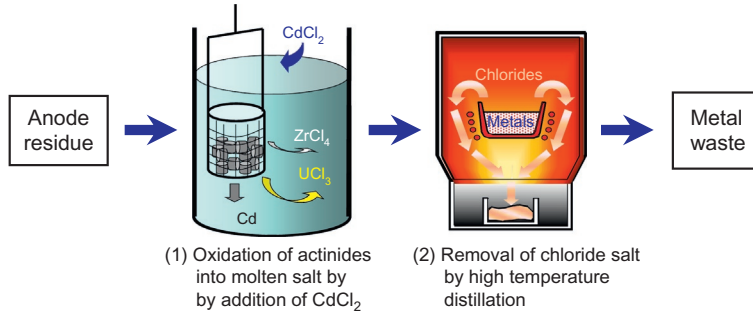

Figure 18.11 Anode processing proposed by CRIEPI for recovery of residual actinides in anode residue from the electrorefining process.

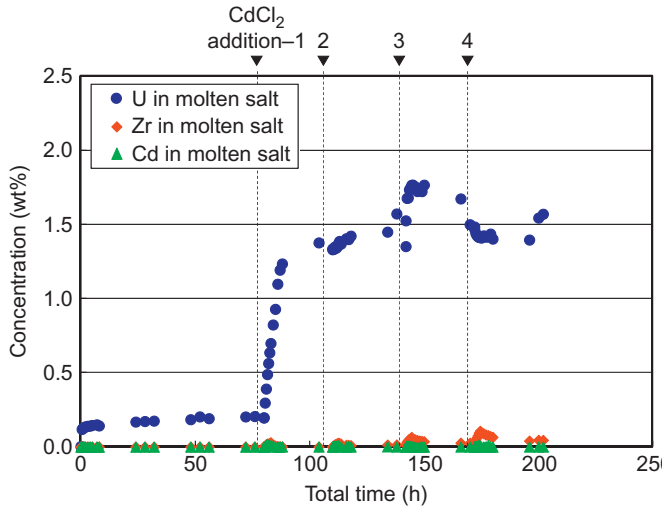

Figure 18.12 Change in U/Zr/Cd concentrations in molten salt solvent during oxidation of U remaining in anode residue by addition of $CdCl_2$.

The analytical results indicated that essentially all the noble metal fission products were held in the anode residue throughout the proposed treatment process.

Processing the anode residue after the oxidation of uranium, high-temperature distillation tests were carried out at 1473 K and a pressure of approximately 300 Pa to remove the accompanying salt. The chloride content in the anode residue was lowered to 1-2.5% by the distillation operation. Although the anode residue was heated to 1673-1773 K at a pressure of about 50 kPa after the distillation, it was not melted completely. The concentration of remaining uranium after the electrorefining and the above treatment process was evaluated to be 0.04-0.20%. This value is considered to be satisfactorily low considering the target uranium recovery of 99.5% in the previous pyrometallurgical reprocessing facility design study.

18.3.1.5 Design of high-performance equipment

As the largest portion (70-90 wt%) of the spent metal fuel is occupied by uranium, the recovery rate of uranium at the solid cathode is a very important factor for evaluating the feasibility of the electrorefining process. An electrorefiner equipped with a concentrically configured anode/solid cathode module of 30 cm diameter and a mechanism for scraping off cathode deposits was developed to increase the uranium recovery rate (Figure 18.13). Stalling of the anode and scraper rotation due to the interference by the cathode deposits was completely diminished by the modifications in the design of the anode basket and scraper mechanism. Under the condition that the dissolution of zirconium from the spent metal fuels take place simultaneously with uranium for obtaining maximum throughput, a current of 400-450 A was maintained until 82% of about 7 kg of uranium, initially loaded to the anode, was recovered. The uranium recovery rate for the same duration reached 789 g U/h per electrode (Iizuka et al., 2009).

In handling operations, it is time-consuming to move the LCC in and out of the electrorefiner for each batch operation because the risk of the ceramic crucible breaking due to thermal shock needs to be avoided. Employing transport technologies for high-temperature liquids (see Section 18.6.3), an engineering-scale electrorefiner with a semicontinuous LCC was designed and fabricated (Koyama et al., 2007, 2011). The masses of the molten salt electrolyte and cathode cadmium used in this electrorefiner were about 190 kg and 50 kg, respectively. The integrated tests to demonstrate the recovery of plutonium through electrorefining and distillation were carried out using gadolinium as a simulant. The obtained throughput corresponding to 215 g-HM/h was high enough to demonstrate the feasibility of the novel electrorefiner (Koyama et al., 2009). Finally, the above-mentioned high-throughput anode/cathode module and the semicontinuous LCC were incorporated into a prototypic electrorefiner as shown in Figure 18.14.

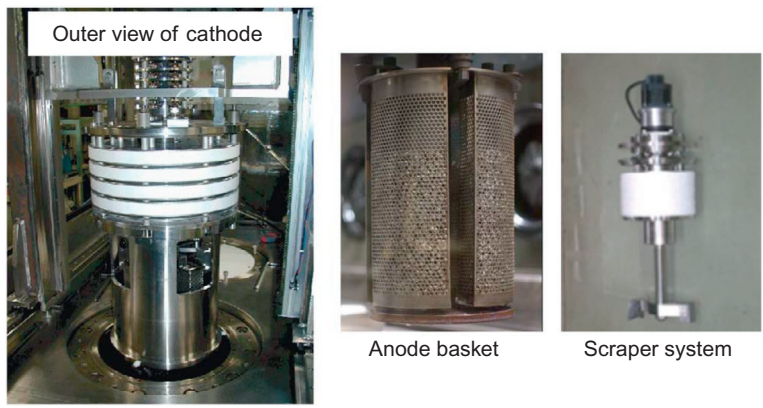

Figure 18.13 Electrorefiner equipped with concentrically configured anode/solid cathode module and scraper system for cathode deposit.

Figure 18.14 Engineering-scale electrorefiner with high-throughput anode/cathode module and the semi-continuous LCC.

18.3.1.6 Reduction of actinide losses in pyrochemical processes

In order to develop a process flow sheet appropriate for evaluation of industrial applicability, pyrochemical process steps such as reduction, electrorefining, and distillation have been tested in sequential mode using unirradiated plutonium fuels as a part of the joint studies between CRIEPI and JAEA (Kitawaki et al., 2011). MOX fuels were reduced to metal form by the electroreduction, and the reduction products were charged in the electrorefiner to recover uranium and Pu-U as cathode deposits. The deposits were heated to separate the accompanying cadmium and salt and to obtain consolidated uranium or U-Pu alloy. As shown in Figure 18.15, the obtained mass balance for plutonium and americium is satisfactory to demonstrate the feasibility of the process in sequential mode. Imbalance was observed for uranium, because UCl_3 in the electrorefining electrolyte reacted with oxygen impurity to form precipitates. However, it was also demonstrated that the material balance of uranium can be recovered by the addition of $ZrCl_4$ (Sakamura et al., 2005a), which reacts with the precipitated UO_2 by rechlorinating it back into the electrolyte. The recovered plutonium was supplied for fabrication of U-Pu-Zr alloy for future experiments with metallic fuels.

18.3.2 Small-scale demonstration with irradiated fuels

In the framework of the collaboration program between CRIEPI and JRC-ITU, pyroreprocessing experiments using various types of irradiated fuels have been performed. In the following section, an outline and major results of these activities are

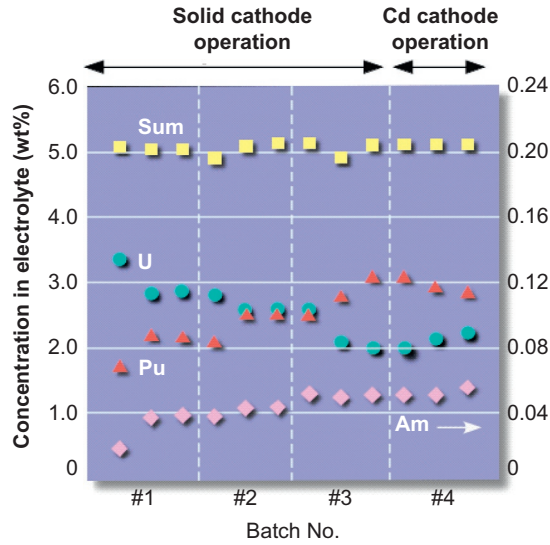

Figure 18.15 Mass balance of U, Pu and Am in electrorefiner during sequential test of pyro-reprocessing.

presented. A detailed description of the hot cell facility dedicated to the pyroreprocessing studies and the metallic fuels irradiated at Phénix (METAPHIX) are given in Section 18.4.3.

18.3.2.1 Electrolytic reduction of irradiated MOX fuels

The recovery of TRUs from spent oxide fuels and their introduction to the metallic fuel cycle leads to reduction of the environmental burden of radioactive wastes. To demonstrate the feasibility of this proposal, electroreduction of irradiated commercial MOX fuel and SuperFact fast reactor fuel were carried out (JRC-ITU, 2010; Kato et al., 2011).

The burn up of the commercial MOX fuel used in this work was 44 GWd/t-U and the plutonium content was 3.6 wt% HM. After decladding, the fuel fragments were put in a steel mesh basket and electrochemically reduced in LiCl-1 wt% Li_2O melt at 923 K. Three runs were conducted at a scale of 5 g fuel per batch. In the first and second runs, the current was applied to achieve complete reduction, while it was stopped before complete reduction of the loaded fuel in the third run. Figures 18.16(a) and (b) show the cross section of the reduced fuels in the third and first runs, respectively. Arrangement of shiny metal and dark oxide parts observed in Figure 18.16(a) indicates the reduction proceeded from outer to center in the basket as well as in the respective fuel fragments. Because only the metallic part was observed on the cross section of all the cut fragments in Figure 18.16(b), most parts of the fuel appeared to be reduced. The reduction yield determined by means of the gas burette technique was about 95%.

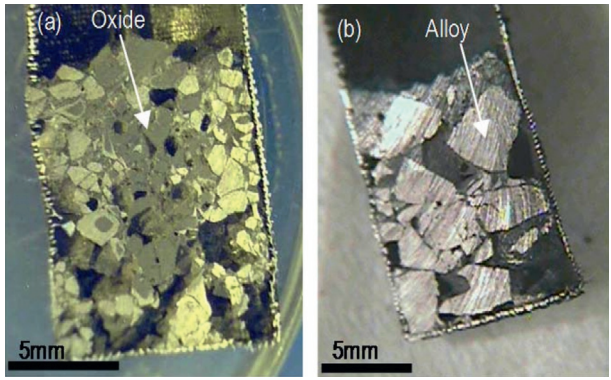

Figure 18.16 Cross section of irradiated LWR MOX fuel after electrolytic reduction: (a) current was stopped before complete reduction, (b) current was applied to achieve complete reduction.

Nearly all of the actinides and noble metals remained in the reduced fuel. Alkali metals, alkali earth metals, and tellurium, selenium, and europium moved out of the fuel and dissolved in the salt bath. It was considered that some portion of lanthanides also moved out of the fuel in the form of complex oxides with Li_2O: MLi_2O_3 (M: lanthanides), as dissolution ratios of these elements into the molten salt bath were in reverse order of solubility of their oxides (Gourishankar et al., 1997; Kato et al., 2009). The amounts of lanthanides in the salt bath were, however, much smaller than these decreases in concentrations from the cathode. This discrepancy was explained by the precipitation of once-dissolved oxides at the bottom of the crucible used in the experiment. In fact, TRUs and rare earths were found in the samples taken from the bottom part of the salt bath in much more highly enriched conditions compared to U^{235}.

The reduced MOX fuel was electrorefined in a LiCl-KCl-UCl_3 melt at 773 K. Dendritic uranium deposited successfully on to a solid cathode and TRUs were recovered into a liquid cadmium cathode. The separation of TRUs from REs was consistent with the previously available thermodynamic data.

The electroreduction test using about 0.4 g of SuperFact fuel, which was a test fuel used for neptunium transmutation and irradiated up to 6.5% burn up (approximately 62 GWd/t-HM) in the Phénix reactor (Babelot and Chauvin, 2009), was also performed in LiCl-1 wt% Li_2O melt at 923 K. The composition of this fuel was 57 wt% of uranium, 23 wt% of plutonium, 1.5 wt% of neptunium, 2.2 wt% of Am + Cm, and 5.1 wt% of fission products (FPs). The gas burette analysis showed that the reduction yield achieved in this test was 97%, indicating that the majority of uranium, neptunium, and plutonium in the fuel was successfully reduced to metal forms.

18.3.2.2 Electrorefining of irradiated metallic fast reactor fuels

Electrorefining experiments using metallic fuels irradiated at Phénix are in progress under the collaborative program between CRIEPI and JRC-ITU to clarify their characteristics in the anodic dissolution and establish knowledge on the behavior of actinides and fission products during the electrorefining process. The latest results of the

small-scale electrorefining tests using the irradiated U-Pu-Zr ternary alloy fuels are summarized in this section (Murakami et al., 2014).

A high dissolution ratio of actinides (U: 98.9%, Pu: 99.8%, Np: 99.0%, Am: 98.9%) was achieved even under conditions aiming to restrain codissolution of zirconium. In the molten LiCl-KCl bath, the concentration of uranium decreased while those of TRUs increased with the progress of the electrorefining step as only solid cathodes were used. The material mass balance of actinide elements was excellent throughout the experiments.

The concentration of alkali and alkaline earth elements in the molten salt bath increased dramatically in the initial stage of the electrorefining to reach a plateau. This result indicated that the dissolution of AM and AEM occurred chemically and independently of the progress of the anodic dissolution according to the following reactions:

$$3\mathrm{AM} + \mathrm{U}^{3+} \rightarrow 3\mathrm{AM}^{+} + \mathrm{U} \qquad (\mathrm{AM}: \mathrm{Cs\ or\ Na}) \tag{18.11}$$

$$3\mathrm{AEM} + 2\mathrm{U}^{3+} \rightarrow 3\mathrm{AEM}^{+} + 2\mathrm{U} \quad (\mathrm{AEM}: \mathrm{Ba\ or\ Sr}) \tag{18.12}$$

It was also suggested that some alkalis and alkaline earths, dissolved in the bonding sodium in the metallic fuels pins, were transported to the upper gas plenum area together with sodium during the irradiation (Ohta et al., 2009a,b, 2011). A favorable material mass balance was obtained also for rare earth FPs. The major part of these elements dissolved and accumulated in the molten salt bath, although 0.5-1.5% of them remained in the anode residue, probably in the form of alloys with noble metal FPs (Keiser and Mariani, 1999; Mariani et al., 2011, 2012). About 82.5% of zirconium remained in the anode residue, while the rest was found in the cathode deposits or at the bottom of the crucible. Most of the noble metal FPs remained in the anode residue.

SEM-EDX analyses showed that the anode residue was composed of three distinct concentric areas of different zirconium content, which had been formed according to the thermal gradient in the fuel during irradiation as seen in Figure 18.17 (Murakami et al., 2014). These three areas were the central part (porous zirconium structure of γ phase, ~27 wt% Zr), the intermediate part (aggregated zirconium particles of $\gamma + \zeta$ phase, ~2 wt% Zr), and the outer part (porous zirconium structure of $\delta + \zeta$ phase, ~14 wt% Zr). In each area, noble metal fission products were retained in the structures of zirconium in a similar fashion as observed in the anode residues obtained in the tests using unirradiated alloys (Iizuka et al., 2009).

18.3.3 Scale-up demonstration with uranium sim-fuels

18.3.3.1 Engineering-scale fuel cycle tests using simulated oxide/metal fuels

As pyrometallurgical reprocessing is primarily a sequence of batch processes, its economic advantage is not compromised by small-scale facilities that process several tons of heavy metals (HMs) per year only. Then, in the case of pyrometallurgical reprocessing, the critical step on the way to practical use would be a demonstration using

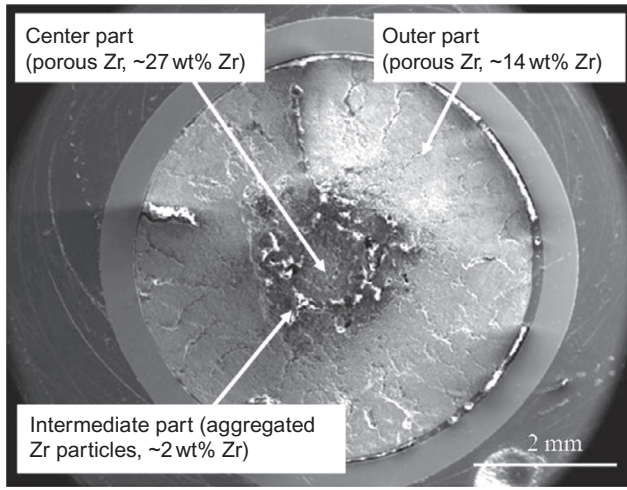

Figure 18.17 Cross section of anode residue after electrorefining of irradiated U-Pu-Zr ternary fuel.

irradiated materials and process equipment of several tens of kilograms capacity. As a preliminary stage for the demonstration, a fuel cycle test using uranium and simulants with process equipment of 1 t-HM/y throughput (Figure 18.18) was carried out (Iizuka et al., 2013b) to obtain the following knowledge and to demonstrate the major steps in the pyrometallurgical reprocessing from an engineering viewpoint.

1. Establishment of equipment design for long-term and hot cell operation with stable performance
2. Quantitative influence of the impurities on the behavior of sensitive materials such as molten chlorides and active metals on the material balance during repeated engineering-scale operations.
3. Design of the handling and transfer systems for intermediate solid products between the various process equipment used in hot cell operations.

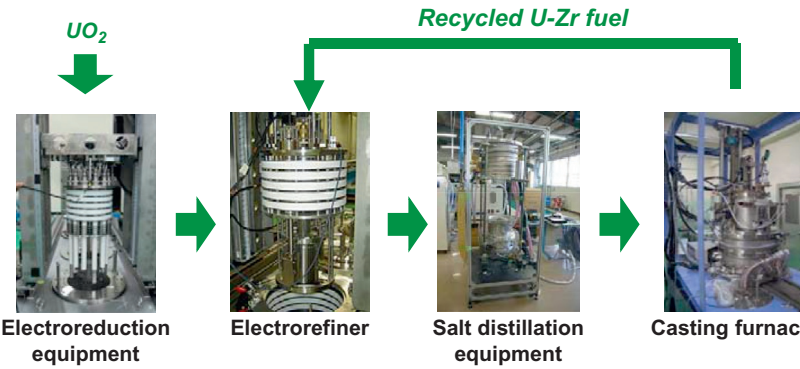

Figure 18.18 Fuel cycle test using U and simulants with process equipment of 1 t HM/y throughput.

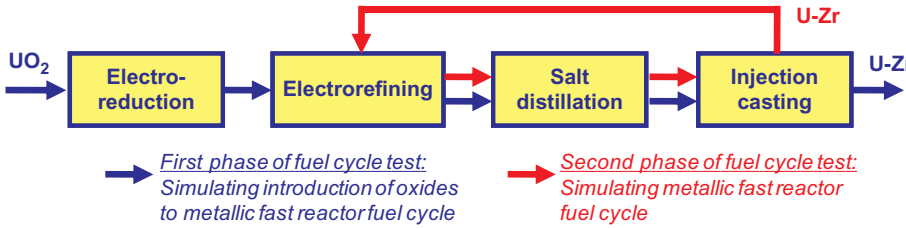

Figure 18.19 Scheme of first and second phases of fuel cycle test using uranium and simulants.

These cycle tests were performed in two phases (Figure 18.19). The first phase simulated the introduction of spent oxide fuel into the metallic fuel cycle by sequential operation of the electroreduction of UO_2, the electrorefining of the reduction product, the salt distillation from the electrorefining product, and the injection casting of U-Zr alloy using the recovered uranium metal. In the second phase, the cycle tests, including the electrorefining, salt distillation, and injection casting steps, were repeated three times, simulating the metallic fuel itself. In the second and third cycles, simulant fission products (cerium and ruthenium) were added at the injection-casting step to study their behavior and distribution during the cycle tests. The U-Zr alloy rods manufactured in the injection-casting step using the electrorefining product were cut into small pieces, and supplied again for the electrorefining step of the following cycle.

The electroreduction equipment contains about 10 l of LiCl-Li_2O electrolyte, and 6 kg-UO_2 can be loaded into the cathode at maximum capacity. The electrorefiner has a capacity of about 30 liters of LiCl-KCl electrolyte. A cylindrical cathode is located at the center, surrounded by four anode baskets in which up to 5 kg of the electroreduction product or chopped U-Zr alloy pins are loaded. The uranium cathode product is removed using scraper blades and collected in the container below the electrodes (Figure 18.20). The accompanying electrolyte to the electrorefining cathode product is separated and the remaining metal is consolidated by high-temperature distillation.

Figure 18.20 Cathode deposit obtained by electrorefining operation in fuel cycle test using uranium and simulants.

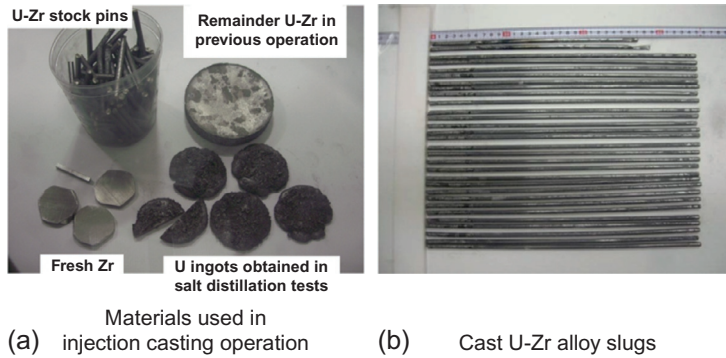

Figure 18.21 Loaded materials and U-Zr alloy rod product from injection casting operation in fuel cycle test using uranium and simulants.

The consolidated metal product is sent to the injection-casting furnace with a capacity of about 6 kg/batch. Thirty slugs of approximately 300 mm in length and 6 mm in outer diameter can be casted in one operation (Figure 18.21). The casting operation is automated. The fabricated U-Zr pins are chopped and brought back to the electrorefining step to simulate the metal fast reactor fuel cycle. Besides these items of process equipment, the product treatment equipment and self-propelled in-cell transfer system have been installed. The former heats the electroreduction/electrorefining cathode products to 773-923 K to melt the adhering electrolytes and transfers them from one container to the other. The latter is remotely controlled to move both the electrodes in the electroreduction/electrorefining equipment and also the equipment itself for replacement or maintenance.

During the first phase of the fuel cycle tests, it was demonstrated that the simulated metallic fuel (U-Zr alloy rods) was successfully fabricated at the engineering scale using UO_2 as the starting material. The electrorefining, product transfer, salt distillation, and injection-casting equipment operated satisfactorily, and their performance was sufficiently high. The material balance of uranium was excellent and the change of the total amount of uranium in the whole process accounted for, at the start of the electroreduction test and after the completion of the injection casting test, was no more than 1.12%.

The second phase of the fuel cycle tests was also successfully completed with satisfactory performance of each item of process equipment. The material balance of uranium, zirconium, and ruthenium was essentially satisfactory and no influence of the three-time repetition of the fuel cycle tests on performance was found from this viewpoint. Changes in the total amount of uranium accounted for during each cycle were evaluated to be 3-4%, which may be somewhat large to be applied directly to the material accountancy in the future engineering-scale demonstration using irradiated fuels. Because the most important origin of the discrepancy is considered to be the inhomogeneity of the anode residue and cathode products, this problem would be solved by obtaining more representative samples from these materials by performing the anode

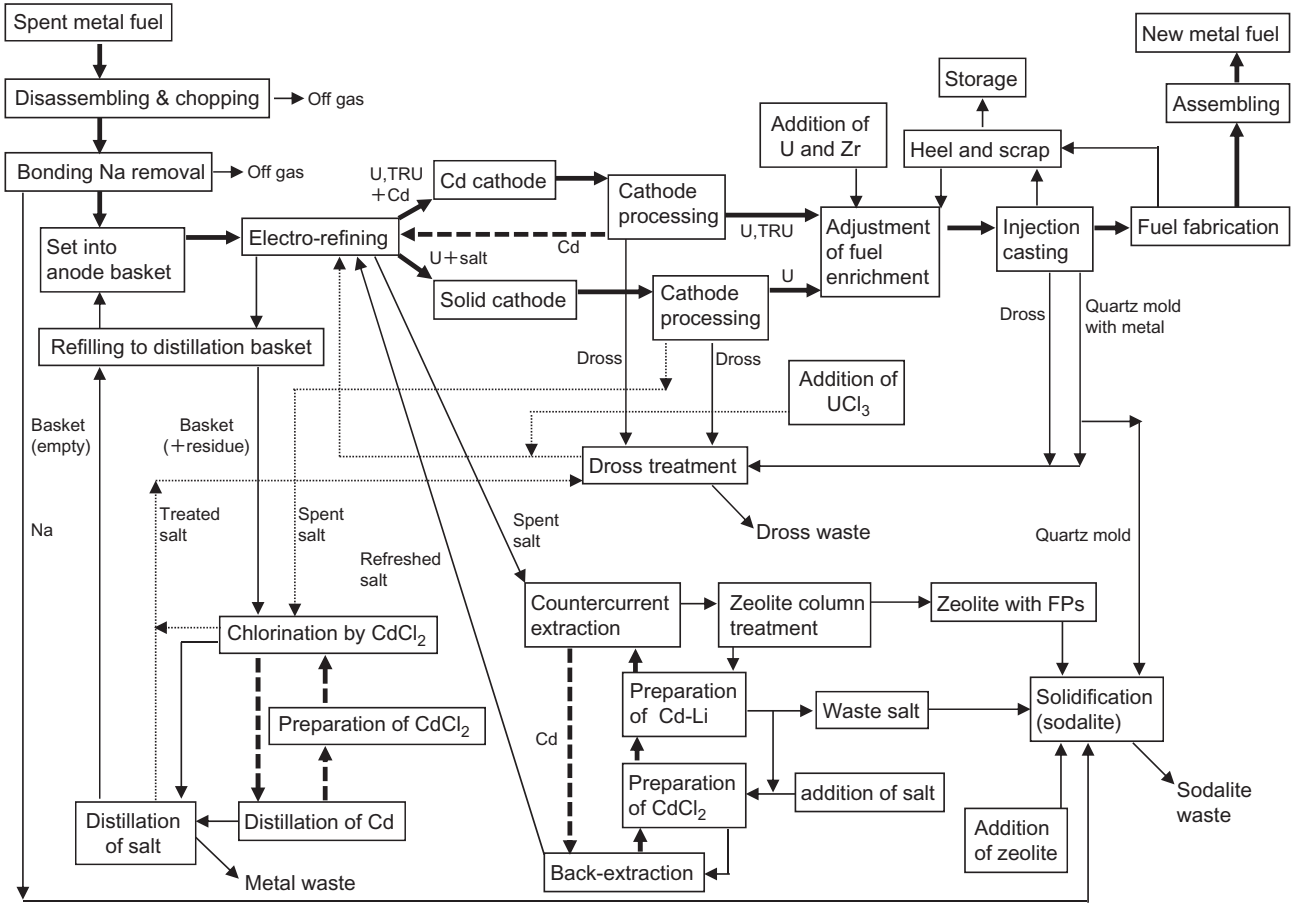

Figure 18.22 Revised process flow sheet of pyrometallurgical reprocessing plant for metallic fast reactor fuel.

residue treatment including metal waste consolidation (Iizuka et al., 2013a) and the cathode processing for all the cathode products.

18.3.4 Conceptual studies on a fuel cycle facility

With recent technological progress, including the process and engineering development introduced in this chapter, the process flow sheet of a pyrometallurgical reprocessing plant for metallic fast reactor fuel was revised as seen in Figure 18.22 (Kinoshita et al., 2012). Major points of modification are a decrease in the quantity of electrorefining equipment derived from the improvement of its performance through the engineering studies, the application of anode processing, a decrease in the amount of ceramic waste coming from the optimization of composition of zeolite material used in the spent salt treatment process (preconversion from $Na_{12}[(AlO_2)_{12}(SiO_2)_{12}]$ to $Na_{4.3}Li_{7.7}[(AlO_2)_{12}(SiO_2)_{12}]$ in aqueous solution), and so on.

The material balance calculated based on the revised process flow sheet showed that losses of actinide elements during pyrometallurgical reprocessing are small, as shown in Table 18.1, and that the recovery ratio of each actinide is estimated to be higher than 99%.

On the basis of the above evaluation studies, the conceptual design of a pyroprocessing fuel cycle facility for 40 tHM/y throughput of metal fuel was carried out. In addition to detailed design of each apparatus, safety issues such as loss of the cooling system were incorporated in the design. As shown in the bird's eye view in Figure 18.23, the designed facility has a size of 50 mW × 103 mL × 34 mH, and consists of four floors. Hot cells for fuel fabrication apparatus and waste treatment apparatus were installed on the basement floor. Hot cells for the reprocessing apparatuses, such as two electrorefiners and six cathode processors, were installed on the first floor along with in-cell transport equipment and stock areas, while a six-staged contactor and two zeolite columns were installed on the second floor. Utilities were located on the third floor. Based on this design, capital cost of this facility was roughly estimated, and a relatively low fuel cycle cost was obtained: 500,000 yen/kg-HM for reprocessing and 280,000 yen/kg-HM for fuel fabrication. As the construction cost of the metal fuel FBRs is expected to be the same as that of the oxide fuel FBRs, which is reported to be about 1.9 yen/kWh, the total cost of electricity from the metal fuel

Table 18.1 Evaluated loss and recovery ratio of actinide elements based on revised process flow sheet (in %)

	Loss in zeolite & waste salt	Loss in casting mold	Recovery ratio
U	0.00	0.17	99.83
Pu	0.09	0.13	99.76
Np	0.05	0.13	99.83
Am, Cm	0.37	0.13	99.50

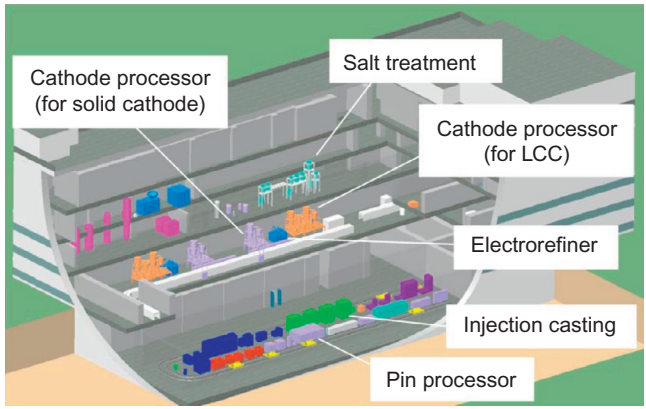

Figure 18.23 Pyro-processing fuel cycle facility for 40 tHM/y throughput of metallic fuel.

FBRs and its fuel cycle facility is expected to be about 2.7 yen/kWh, which shows better potential than the other energy sources.

18.4 Pyropartitioning process development

To complete the link between the current LWR fuel cycle and the metallic fast reactor fuel cycle, and to show the practicality of confinement and transmutation of long-lived MAs in the total fuel cycle concept shown in Figure 18.1, technological demonstrations in the following two areas have to be made along with establishment of the metallic fuel cycle technology:

- Pyropartitioning process for HLLW.
- Behavior of MAs throughout the metallic fuel cycle, including transmutation in the reactor.

In this section, major achievements and current status of activities in these areas are described.

18.4.1 Flow sheet development using simulating materials

18.4.1.1 Introduction

The schematic flowchart of the pyropartitioning process proposed by CRIEPI is shown in Figure 18.24 (Uozumi et al., 2011a). In the first step, most of the elements in the HLLW, which mainly exist as nitrate forms, are converted to oxide forms by calcination under air in the denitration step. Then, the denitrated product is converted to chlorides by reaction with chlorine gas and carbon in a molten LiCl-KCl eutectic salt bath in the chlorination step. After the chlorination, pyrometallurgical methods such as reductive extraction in a molten salt/liquid metal system and/or electrolysis in molten salt are applied to recover actinide elements with sufficient separation from fission products (FPs). The actinide elements are selectively recovered from the

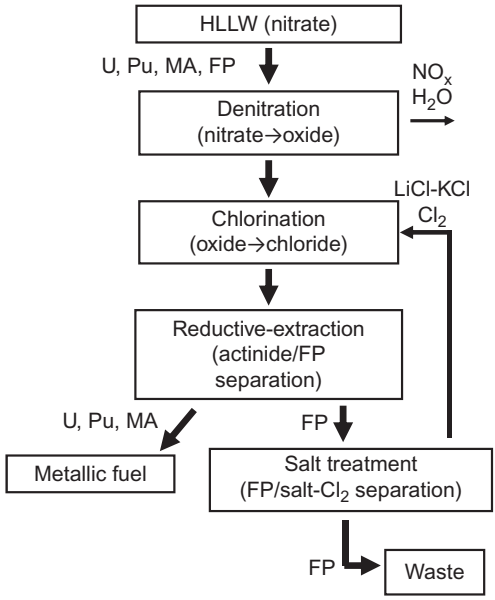

Figure 18.24 Schematic flow chart of pyropartitioning process.

molten salt in their metallic state. The FPs remaining in the molten salt, that is, RE, AM, and AEM FPs, are removed by electrolysis using a liquid lead cathode or by absorption on zeolite, and finally stabilized as a vitrified glass waste or a glass-bonded sodalite waste, respectively (Nabeshima et al., 1996; Sakamura et al., 1997; Tsukada and Takahashi, 2008). The recovered actinides are made into U-Pu-Zr-MA-RE metallic fuel and sent to fast reactors for energy production and transmutation of MAs.

Two fundamental criteria were given to the pyropartitioning process development (Inoue and Tanaka, 1997). One is a recovery ratio of more than 99% for each MA in the HLLW. Another is lanthanide FPs/MAs mass ratio of less than one in the recovered product. Because the mass of lanthanide FPs in the HLLW is approximately 10 times larger than that of the MAs, the second criterion indicates that the decontamination factor of lanthanide FPs from MAs should be larger than 10.

In the following sections, demonstration studies on the pyropartitioning process using simulating materials including actinide elements are summarized.

18.4.1.2 Denitration and chlorination

A successive test of denitration and chlorination was performed using simulating HLLW containing uranium (Kurata et al., 2000). The simulating HLLW solution was heated at 500 °C for an hour to decompose the nitrate compounds. Almost all of the uranium and some FP elements, such as AEM, lanthanides, zirconium, and palladium, were recovered as a water-insoluble residue after the denitration. Then, the denitration product was heated to 700 °C together with LiCl-KCl eutectic salt in a graphite crucible, which was placed in a quartz vessel. The conversion of denitration product to chlorides was performed by introducing pure chlorine gas into the molten

salt for 10 h. Samples taken from the salt phase after the chlorination contained less than 0.1% of water-insoluble species, indicating that uranium and FP elements such as RE and AEM were converted to water-soluble species, which were regarded as chlorides, by the chlorination. Probably due to direct introduction of chlorine gas into the molten salt and an operating temperature of 700 °C, 5% of uranium evaporated in the form of UCl_4 during the chlorination.

18.4.1.3 Separation of uranium and TRUs by electrolysis and reductive extraction

A demonstration test to separate uranium and TRUs from simulant chlorination product salt by electrolysis in molten salt and the reductive extraction in molten salt/liquid bismuth system was performed (Uozumi et al., 2001). The amounts of the actinides and FPs in the stimulant chlorination product salt were the same as those in HLLW generated by aqueous reprocessing of 100 grams of spent oxide fuel. The mass ratio of TRUs to rare-earth elements was 0.10 in the initial condition and changed to 2.0 in the recovered product. The remaining ratio of each actinide element in the salt after the tests was less than 1%, although recovery ratios evaluated from the chemical analyses of the products were slightly less than 100% due to analytical error.

18.4.1.4 Removal of simulating FPs from waste salt by electrolysis

In order to recycle the LiCl-KCl salt after the actinide separation, recovery of the remaining FPs, such as lanthanides, alkaline earths, and alkali metals, by electrolysis was proposed. Several electrolysis tests were performed using solid iron, liquid lead, and liquid cadmium cathodes. It was concluded that the liquid lead cathode is most suitable to separate alkaline-earth elements from the LiCl-KCl salt. Almost all of the FP elements separated to the liquid lead phase were oxidized by introducing air at 800 °C, and successfully extracted into the molten slag phase as shown in Table 18.2 (Sakamura et al., 1997).

Table 18.2 Change in amount of simulating FPs in liquid Pb cathode before and after oxidation by introduction of air under contact with molten slag

Element	Content in Pb cathode (g)	
	Before oxidation	After oxidation
Li	0.034	<0.002
Na	0.298	<0.001
K	0.072	<0.001
Cs	18.0	<0.002
Sr	0.796	<0.002
Bo	7.75	<0.002
Eu	1.09	<0.002

18.4.2 Small-scale demonstration with actual HLLW

18.4.2.1 Preparation of HLLW

For the demonstration of the pyropartitioning process, a series of tests for recovery of TRUs from real HLLW through denitration, chlorination, and reductive extraction was performed under a joint research program between CRIEPI and JRC-ITU (Uozumi et al., 2011a). The HLLW was prepared mainly from the raffinate generated by PUREX reprocessing of a MOX fuel irradiated in a PWR. Approximately 520 g of the prepared HLLW, which contained roughly 8400 μg/g of uranium, 600 μg/g of TRUs, and 2000 μg/g of FPs, including 870 μg/g of rare earth FPs, was used.

18.4.2.2 Denitration and chlorination

The denitration was performed in an air atmosphere hot cell. After heating the HLLW at 90-120 °C for concentration, it was dried at 100-140 °C. Then, the dried material was calcined at approximately 500 °C for 88 h under air flow. Almost all the denitrated material, which is shown in Figure 18.25, was recovered from the crucible (Uozumi et al., 2011a). The mass of the calcined material agreed with the theoretical value estimated from the initial HLLW composition. Only 0.3% of ruthenium in the initial HLLW was detected as evaporated material. The chlorination step was performed in an argon atmosphere hot cell (see Section 18.4.3 for details). A schematic view of the experimental setup is given in Figure 18.26. The entire denitration product was loaded in a graphite crucible filled with LiCl-KCl eutectic salt. The graphite crucible was placed in a quartz reactor and heated to 650 °C in the furnace. After melting the salt, pure chlorine gas was introduced to the reactor. The chlorination was conducted for a total of 32.2 h. The chemical analysis of the chlorination product samples showed that almost all the actinide elements, lanthanides, AM, and AEM FPs were converted to their chloride forms. No actinide element was detected in the evaporated part during denitration and chlorination steps. Most parts of technetium and noble metal FPs were not vaporized and remained in the chlorination product, while some other FPs such as zirconium and molybdenum evaporated during the chlorination as expected.

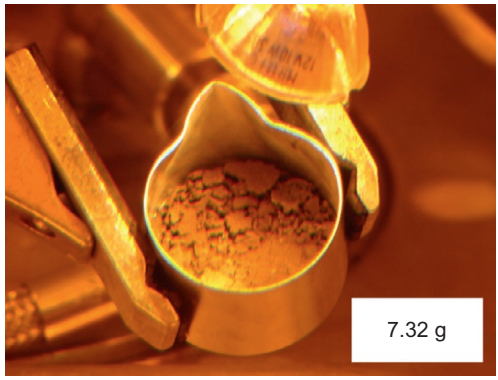

Figure 18.25 Recovered material after denitration in small-scale demonstration of pyropartitioning using actual HLLW.

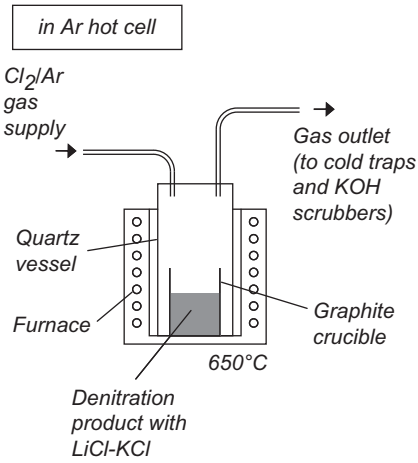

Figure 18.26 Schematic view of experimental apparatus for chlorination test using denitration product from actual HLLW.

18.4.2.3 Separation of uranium and TRUs by reductive extraction

The following reductive-extraction step was also performed in the argon atmosphere hot cell. Together with a part of the chlorination product, cadmium metal was put in an MgO crucible and heated to 500 °C. By addition of Cd-Li alloy as a reductant, the elements in the salt phase were reduced and extracted into the cadmium phase. The concentrations of actinide elements in the salt phase were gradually decreased with the addition of Cd-Li alloy, and finally, almost all of them were recovered into the cadmium phase as shown in Figure 18.27 (Uozumi et al., 2011a). Slightly poor mass balance of uranium is considered to be attributed to the formation of UO_2 caused by the impurities in the argon atmosphere such as oxygen and moisture.

18.4.2.4 Summary

Throughout the above demonstration test, the actinides completely reacted as expected and the loss of TRUs was negligible in the denitration, chlorination, and reductive-extraction steps. The separation behavior of the actinides from FPs was quite similar to the previous results obtained using unirradiated material. These results indicate that the predicted reaction in each step will be complete, and that actinide elements will be satisfactorily separated from FPs and successfully recovered in the actual separation system.

18.4.3 METAPHIX-PYRO project

18.4.3.1 Background and objectives of the METAPHIX project

To demonstrate the transformation of MAs in a metallic fast reactor fuel cycle, an integrated and systematic research program is necessary that consists of extensive areas of R&D such as fuel characterization and irradiation, analyses of reactor core design

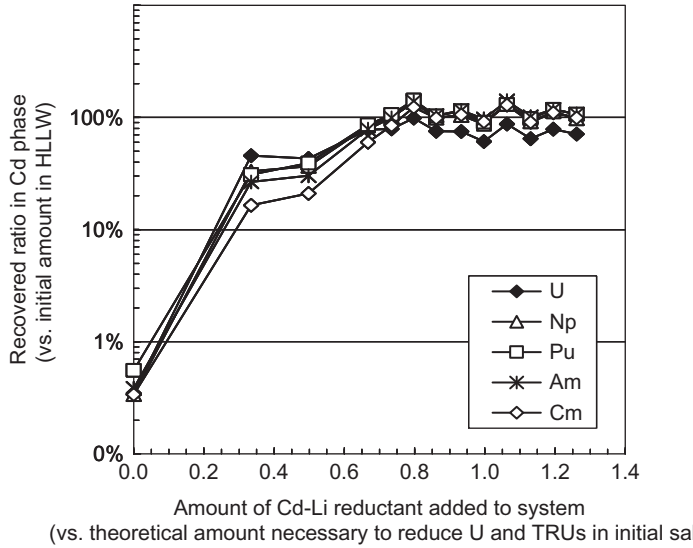

Figure 18.27 Recovered ratio of actinide elements into liquid Cd phase through pyropartitioning test using actual HLLW.

from the viewpoints of safety and introduction scenario for transmutation systems, development of reprocessing technologies for the irradiated MA-containing fuels, and so on. For this purpose, the so-called METAPHIX project was started in 1988 as a part of a collaboration program between CRIEPI and JRC-ITU to obtain basic data demonstrating the fundamental concepts related to the MA partition and transmutation scenario based on the metal fueled fast reactor and pyrochemical technologies. Such data includes behaviors of MAs and FPs in the fuel alloys under irradiation and during pyrochemical processing. This project consisted of MA-containing metal fuel alloys characterizations at JRC-ITU and irradiation of these alloys at the Phénix reactor.

18.4.3.2 Fabrication and irradiation of METAPHIX fuels

On the basis of the results of various characterization (miscibility, phase structure, phase transition temperature, and so on) experiments on U-Pu-Zr-MA-rare earth (RE) alloys and expected decontamination performance of the pyropartitioning process, three types of MA-containing alloys: U-19Pu-10Zr-2MA-2RE, U-19Pu-10Zr-5MA-5RE, and U-19Pu-10Zr-5MA (in wt%) were selected (Kurata et al., 1997; Ohta et al., 2011). Here, MA is a mixture of neptunium, americium, and curium, and RE is a mixture of yttrium, neodymium, cerium, and gadolinium. Compositions of MA and RE were decided based on the spent LWR fuel composition calculated using the ORIGEN-II code. The MA metals were obtained through chemical reduction of each oxide with metal reductant, such as neodymium or thorium, followed by vaporization/deposition treatment. Arc melting and gravity casting techniques were used for the fabrication of reference (U-19Pu-10Zr) and MA-containing alloy rods

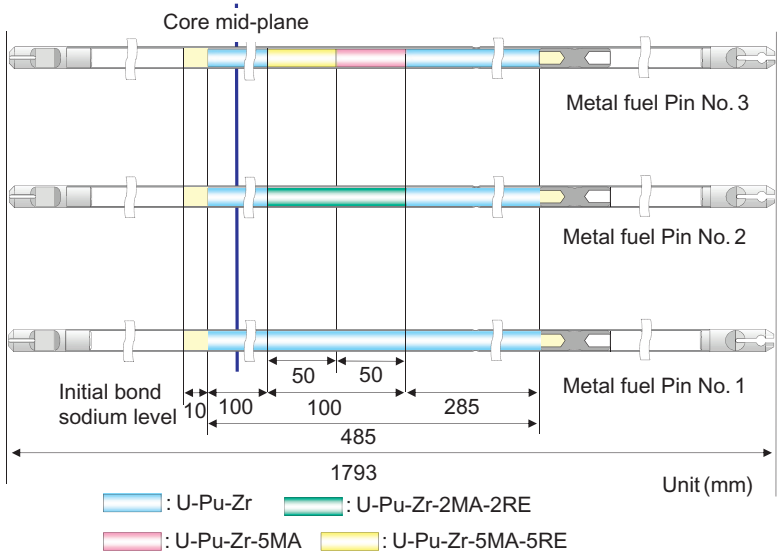

Figure 18.28 Schematic view of configuration of METAPHIX fuel pins.

of the above-mentioned compositions (Ohta et al., 2013). The cast alloy rods with a diameter of 4.9 mm were cut into lengths of 20-50 mm and then inserted in the cladding tubes with sodium metal. The cladding material is austenitic steel, CW15-15Ti (Seran et al., 1992; Maillard et al., 1994). The MA-containing alloys were sandwiched by U-19Pu-10Zr rods, 100 mm and 285 mm length; thus, the total length of the fuel stack was 485 mm, as shown in Figure 18.28. These three pins with different compositions are loaded in the same irradiation capsule. Three capsules of an identical configuration were fabricated and charged in the Phénix core to achieve three different burn ups of ~2.5 at% (METAPHIX-1), ~7 at% (METAPHIX-2), and ~10 at% (METAPHIX-3), respectively. Irradiation was started at the end of 2003 and successfully completed by May 2008 with the support of CEA (France). After the irradiation, all the METAPHIX samples have been transferred to JRC-ITU (Germany).

18.4.3.3 Postirradiation examination of METAPHIX

Nondestructive tests (measurement of outer diameter distribution of cladding tubes and observation using X-ray transmission) have been completed for METAPHIX-1, -2, and -3. No significant damage on the fuel pins has occurred during the irradiation, up to the highest burn up of ~10 at%. It was shown that MA or RE addition made no difference to the change of cladding diameter during irradiation and the swelling behavior of fuel alloys (Ohta et al., 2011). Pin-puncture tests METAPHIX-1 and -2 showed that MA addition to metal fuel has no influence on the FP gas release ratio and that a significant amount of helium formed by alpha-decay of MAs was released (Ohta et al., 2012).

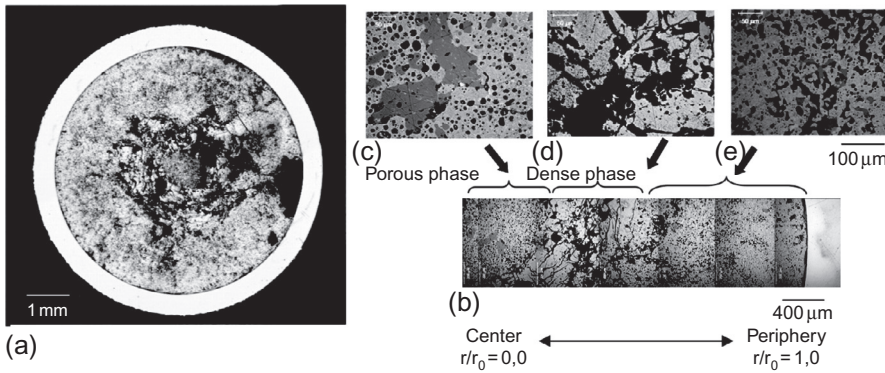

Figure 18.29 Optical metallography of METAPHIX-1 (U-19Pu-10Zr-5MA-5RE) after irradiation: (a) cross-sectional overview, (b) fuel morphology along the radius and magnified images at (c) central zone, (d) intermediate zone and (e) outer zone.

Observations of the cross section of the fuel alloys using an optical microscope have been completed for METAPHIX-1 (Figure 18.29) and -2 (Ohta et al., 2011), while other surface analyses such as SEM/EDX and EPMA are underway. These analyses showed radial phase distributions similar to that seen in ternary alloys, and MA-rich or RE-rich segregated phases formed during irradiation of METAPHIX alloys. According to destructive analysis for METAPHIX-1 (Ohta et al., 2013) and -2, the change in the isotopic composition of MAs indicated the expected progress of transmutation.

18.4.3.4 Pyrochemical examination using irradiated METAPHIX samples

An argon atmosphere and lead-shielded hot cell dedicated to pyrochemical studies using irradiated materials was designed, fabricated, and installed in the CRIEPI-ITU collaboration (Figure 18.30). After being put into hot operation in 2004, a

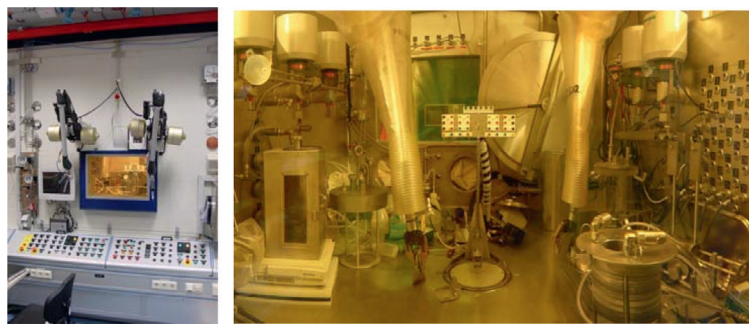

Figure 18.30 Ar-atmosphere iron-shielded hot cell dedicated to pyroprocessing studies using irradiated materials installed in JRC-ITU under collaboration with CRIEPI.

substantial number of experiments, including pyropartitioning of real high-level liquid waste (Uozumi et al., 2011a), electroreduction of irradiated LWR-MOX fuel (Kato et al., 2011), and electrorefining of METAPHIX-1 and -2, have been satisfactorily performed in this hot cell without any serious technical problems.

Up to 2014, two runs of the electrorefining test using about 4 grams of irradiated MA-containing METAPHIX alloy (U-19wt%Pu-10wt%Zr-2wt%MA-2wt%RE, 2.5 wt%-b.u.) have been performed. In the first run, uranium was selectively collected to a solid cathode by potentiostatic electrotransport. High dissolution ratios of actinides (>99% for U, Np, Pu, >98% for Am, Cm) were achieved, while the majority of zirconium was left in the anode residue by keeping the anode potential sufficiently high. In the second run, all the actinide elements in the electrorefiner were simultaneously recovered into a liquid cadmium cathode by galvanostatic electrotransport. Separation factors of actinide and lanthanide fission product elements at the liquid cadmium cathode at the end of the test agreed with the values that were evaluated from equilibrium distribution of unirradiated materials. These results successfully demonstrated that MAs, as well as uranium and plutonium, can be recovered from irradiated metallic fuels by the electrorefining method, being governed satisfactorily by the well-established principles and basic properties of actinides in molten salt media.

18.5 Waste management

18.5.1 Salt treatment process development

In the electrorefiner, AM and AEM FPs in the molten salt gradually build up during processing of the spent fuels. In order to limit the decay heat content and the contamination of the cathode products, the molten salt in the electrorefiner has to be treated to decontaminate AM and AEM FPs, converting them into a stable waste form. As shown in Figure 18.2, Japanese developments in this process mainly focused on the countercurrent extraction process and zeolite column process followed by the salt waste consolidation process to form aluminosilicate ceramic waste, because of the potential feasibility of industrialization. In this section, recent developments on these processes will be described.

18.5.1.1 Countercurrent extraction

In the countercurrent extraction process, feed salt from the electrorefiner comes in contact with liquid cadmium at approximately 450 °C to extract actinides into liquid cadmium (as a liquid metal solvent), see Figure 18.31. The treated salt (raffinate) is additionally decontaminated during the zeolite column process by ion exchange with structural elements of zeolite or by occlusion of chloride molecules in the three-dimensional cage structures of zeolite, and the decontaminated salt comes in contact with the cadmium (extract) from the first stage of the countercurrent extraction, stripping actinides from the molten salt to be recycled in the electrorefiner. The number

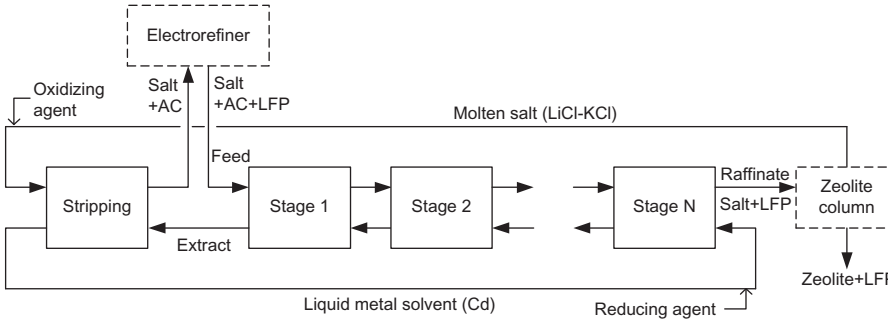

Figure 18.31 Counter current extraction process flows sheet.
Koyama (2011).

(N) of stages necessary depends on the separation requirements and distribution characteristics.

The countercurrent contactor is another important piece of equipment used to recover actinides from the salt in electrorefiners with separating lanthanide FPs. CRIEPI has developed a countercurrent contactor that requires a rotation speed of only approximately 300 rpm with the aim of increasing long-term integrity. As radiation damage on molten salt and liquid metal are negligible compared with that of organic solvents used in aqueous reprocessing, the flow rate of the countercurrent contactor can be decreased. Using the material balance calculated for commercial throughput, the required flow rate was sufficiently slow to complete the reduction reaction without strong mixing. The large density difference between molten salt (1.7 g/cm^3) and liquid cadmium (7.8 g/cm^3) eases the phase separation problem. On the basis of this consideration, a six-stage countercurrent contactor was developed and installed in an argon glove box, as shown in Figure 18.32. The contactor was connected to two separate tanks used for salt supply, cadmium supply, salt recovery, and cadmium recovery,

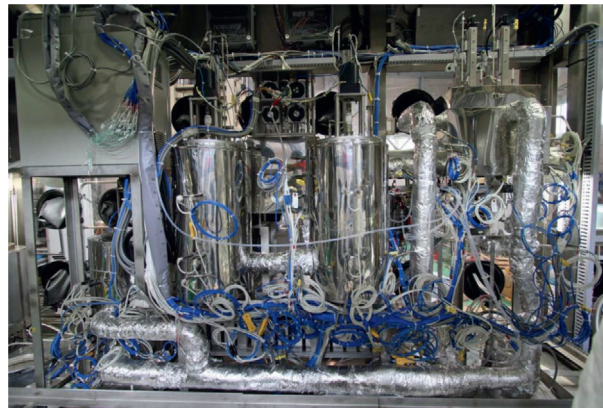

Figure 18.32 Mark-II centrifugal contactor test apparatus developed by CRIEPI.

respectively. Each stage of the contactor has a capacity of 300 ml molten salt and 300 ml liquid cadmium. Molten salt and liquid cadmium were supplied from the tanks at a constant rate of 10-50 ml/min. Extraction tests were carried out using molten salt and liquid cadmium at 450 °C. Three rare earth elements, cerium, gadolinium, and yttrium, were used as substitutes for uranium, transuranic elements, and rare earth FPs, respectively. In a three-stage countercurrent extraction test, a high recovery ratio of close to 100% with efficient separation was achieved (Kinoshita et al., 2007; Kinoshita and Tsukada, 2008).

18.5.1.2 Zeolite column adsorption

Because the treated salt from the countercurrent contactor still contains most of the less-noble metals, decontamination of these FPs from the salt is important to decrease the waste volume through recycling LiCl-KCl. The ion exchange behavior of zeolite with various cations was studied for efficient removal of FPs from the spent molten salt (Lexa and Johnson, 2001). The anhydrous form of zeolite 4A presented as $Na_{12}[(AlO_2)_{12}(SiO_2)_{12}]$ has a cage structure in which Al^{3+} bonds to four oxygen atoms and is, thus, negatively charged. Therefore, cations such as Na^+ must be present to compensate the charge in the framework structure. With a molten salt such as LiCl-KCl eutectic, the Na^+ in the zeolite can exchange with other cations such as Li^+ and K^+ in the molten salt. If FP elements exist as cations in the salt, the FP cations may also be exchanged with the cations in the zeolite according to their affinities to the zeolite. Furthermore, the zeolite 4 Å has cavities whose entrance diameters are approximately 4 Å and some FPs are expected to be absorbed in the cavities together with Cl^-; that is, as the forms of chlorides. The absorption behavior of FP elements on zeolite 4 Å has been studied, and complex absorption isotherms for FP elements were estimated (Tsukada and Takahashi, 2008).

The next step is to design an efficient and remotely applicable zeolite column for industrialized use (Uozumi et al., 2011b). The first model of the zeolite column had an inner diameter (ID) of 11.1 mm and was 300 mm in length; it used LiCl-KCl containing CsCl as a simulating FP. The column contained zeolite 4 Å in powder form (<75 μm). The sintered stainless steel (SS) filters of mesh size of 10 μm were sealed at both the upper and lower ends of the columns. The column was connected to a molten salt reservoir and the salt was pushed by pressured argon gas up to 0.5 MPa so that the salt passed through the column in an upward direction. The effluent salt after the column treatment was collected in aluminum crucibles placed on a turntable. The whole system was heated to 450-500 °C under an argon atmosphere. The changes in mole fractions of lithium, sodium, potassium, and cesium among these alkaline elements in the treated salt are shown in Figure 18.33. The abscissa denotes the amount of salt passed through the columns (in grams) divided by the amount of zeolite in the columns (in grams). The velocity of the molten salt in the column ranged between 1.3 and 1.6 cm/min under the driving pressure of up to 0.3 MPa. Absorption of cesium was demonstrated by the low cesium concentration in the treated salt. However, absorption capacity for cesium seemed to be saturated at the abscissa value of around three, which was earlier than that for lithium. The result was translated to a decontamination factor value (DF), which is defined as Equation 18.13.

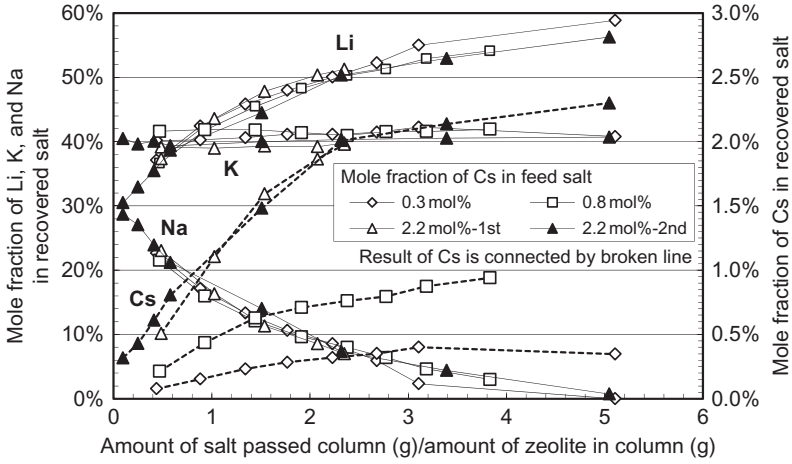

Figure 18.33 Mole fraction change in LiCl-KCl-CsCl salt after zeolite column treatment.

$$\mathrm{DF} = \frac{[\text{mole fraction of cesium in the feed salt}]}{[\text{mole fraction of cesium in the treated salt}]} \tag{18.13}$$

The change of DF values for Cs was described as shown in Figure 18.34. The obtained DF was about six at the beginning, and decreased to around one at the abscissa value of around three.

Consequently, an engineering-scale model of the zeolite column was designed and installed in an argon glove box. As shown in Figure 18.35, the apparatus is equipped

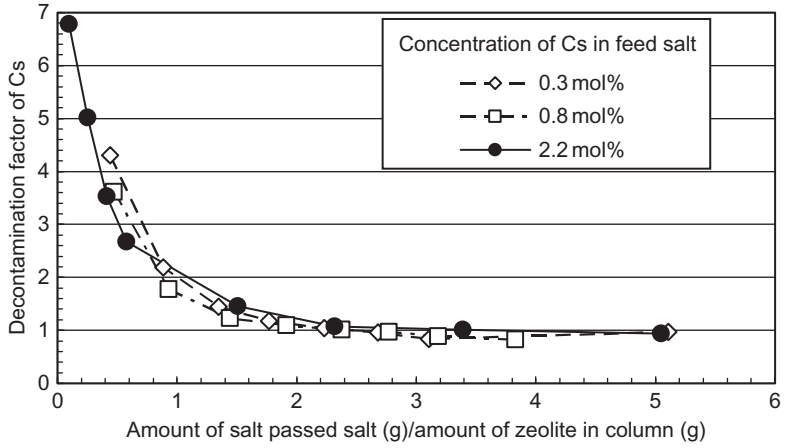

Figure 18.34 Decontamination factor of cesium in molten salt treated by column filled with zeolite 4A powder.

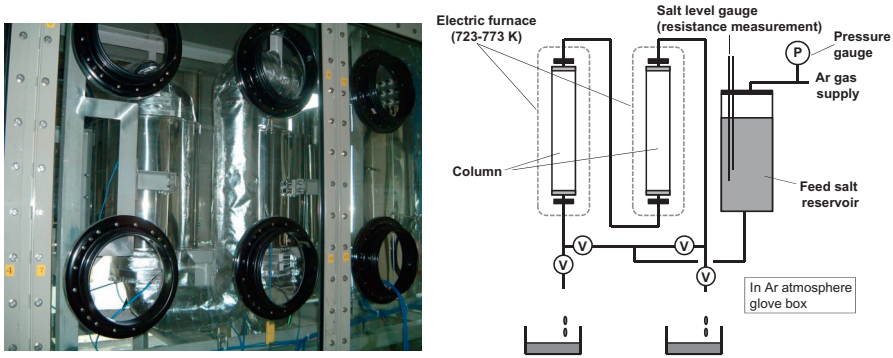

Figure 18.35 Engineering-scale zeolite column apparatus.

with two columns (35 mm in maximum inner diameter and 300 mm in length) and a feed salt tank, in which up to 11 kg of salt can be loaded. The maximum pressure to drive the molten salt to go through the columns is 0.8 MPa. Two columns are connected in series and the direction of molten salt passing through the columns (i.e., up-flow or down-flow in the columns) is varied by using the valve operations. The effluent salt from the second column is collected in SS cups, which are put on a turntable placed on an electric balance in order to measure the change of the effluent salt composition and flow rate of the molten salt. Experiments to demonstrate the decontamination of simulating FPs in the molten salt using the engineering-scale apparatus are now underway. Functional data on the salt velocity-driving pressure relationship were obtained.

18.5.1.3 Salt waste consolidation into ceramic form

A natural analogue for an acceptable salt waste form, *sodalite*, $Na_6[(AlO_2)_6(SiO_2)_6]\cdot 2NaCl$, was found from naturally occurring minerals that contain chlorine in a stable configuration, through the joint study between ANL and CRIEPI. An artificial synthesis method for sodalite containing LiCl-KCl was invented by Koyama (1994) as

$$3Na_2CO_3 + 6Al_2O_3 + 6SiO_2 + 2(\text{LiCl-KCl}) \rightarrow Na_6\left[(AlO_2)_6(SiO_2)_6\right]\cdot 2(\text{LiCl-KCl}) + 3CO_2 \quad (18.14)$$

This was later modified as

$$6NaAlO_2 + 6SiO_2 + 2(\text{LiCl-KCl}) \rightarrow Na_6\left[(AlO_2)_6(SiO_2)_6\right]\cdot 2(\text{LiCl-KCl}) \quad (18.15)$$

which does not generate a gaseous product; therefore, it is easier to accelerate the solid-solid reaction by pressing the raw materials. Using simulated waste salt, synthetic conditions such as maximum temperature and duration of heating were optimized and sodalite pellets with an acceptable leach rate were obtained (Koyama et al., 1997a). Actually, 8 h of heating at 850 °C was the best condition to form single-phase sodalite, because with further heating sodalite decomposed to volatile chloride vapors and the aluminosilicate, nepheline ($Na_3KAl_4Si_4O_{16}$), while unreacted phases remained with shorter heating times. However, the expected content of FP elements in this product was only around 2-3 wt% because the concentration of FP elements in the treated salt from the extraction step was less than 10 mol% of LiCl-KCl. Compared with the content of FPs in traditional boron silicate glass waste form, around 15 wt%, the content of FPs in sodalite was relatively low. Hence, an additional process to separate or concentrate FPs from molten salt was studied by CRIEPI, such as the precipitation process that adds chemicals like phosphate or sulphate to the molten salt, but recovery of precipitates from molten salt seemed hard to industrialize. Meanwhile, ANL has found the transformation of ion-exchanged zeolite 4 Å into sodalite structure at high temperature (Lewis and Johnson, 1997). Based on this invention, ANL and INL developed the monolithic ceramic waste form, glass-bonded sodalite, fabricated under relatively low pressures and high temperatures by Battisti et al. (2002) and Bateman and Capson (2004). Additionally, the experiments carried out by INL used only the salt without concentrating the FP contents, because the current program at the INL does not cover the zeolite column process. While agreeing with the glass-bonded zeolite as a candidate for the disposal waste form, CRIEPI has started studying intensively the optimization of conditions to fabricate a glass-bonded sodalite using FP-concentrated salt based on the experience gained in synthesizing single-phase sodalite.

Hence, effects of the maximum temperature, the heating duration, the glass ratio in the initial material, and the weight load on the fabrication of the glass-bonded sodalite were studied using the type-Å zeolite granules immersed in molten LiCl-KCl salt containing cesium, strontium, neodymium, and iodine for simulating the zeolite discharged from the columns. After removing the adhered salt by filtration using a SS mesh, the zeolite was pulverized and mixed with additional pulverized fresh zeolite, the glass material, and this mixture was used as the initial material in each test (the weight ratio of the mixture was salt/zeolite/glass equal to 1/9/3.3). Based on the reported procedure of temperatures by Battisti et al. (2002) and Bateman et al. (2002), the standard heating condition and the range of condition change were determined as in Table 18.3 and Figure 18.36 with consideration of the conversion temperature of sodalite (770 °C) and the collapse temperature of sodalite (1000 °C); as well as, the softening temperature of the borosilicate glass (820 °C). The product was a monolith of 27 mm in diameter and 14 mm in height, with an apparent density of 1.66 g/cm^3. No significant cracks or cavities at the cross section of the product were found. According to the chemical analysis, the volatilized contents of cesium, strontium, and neodymium were less than 0.05%. On the other hand, the vaporized content of iodine was 1.79% and higher than

Table 18.3 Fabrication test conditions

Fabrication parameter	Test conditions	
	Standard condition	Varied condition
(1) Maximum temperature	915 °C	770, 820, 1000 °C
(2) Duration a max. temp.	5 h	10, 20 h
(3) Glass ratio of material	25 wt%	13, 33 wt%
(4) Weight load	70 g/cm^2	2, 36, 200 g/cm^2

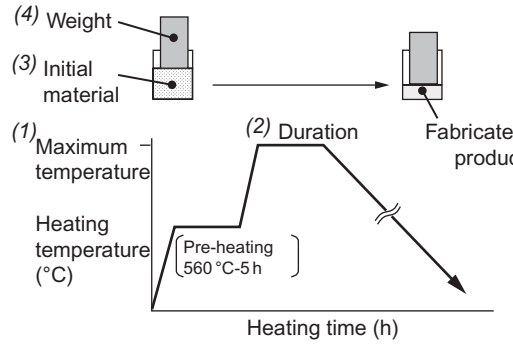

Figure 18.36 Fabrication test conditions.

chlorine according to the difference in melting point (i.e., 1324 °C for potassium iodine and 1407 °C for potassium chloride). Most of the vaporized salt adhered to the cover of the heating vessel, and was analyzed to contain sodium, potassium, and chlorine as the main components. The total amount of the free salt was 0.74 mg per gram of the product, and it included sodium and chlorine as the main components.

Figure 18.37 shows the effect of the maximum temperature on the mass ratios of the volatilized salt, the free salt in the product, and the apparent density of the product. Increasing the maximum temperature, the volatilized salt and the free salt content were increased remarkably beyond 820 °C; suggesting the decomposition of sodalite structure as described in the direct synthesis reaction of Equation 18.15.

In the same way, effects of the duration time at the maximum temperature, the glass ratios of the initial material, and the weight load during heating on the mass ratios of the volatilized salt, the free salt in the product and the apparent density of the product were tested (Fujihata et al., 2013). The obtained results suggested that the maximum temperature should be kept at around 820 °C for reduction of the volatilized salt ratio and the load value of the weight of 200 g/cm^2, but other parameters agreed with the standard condition.

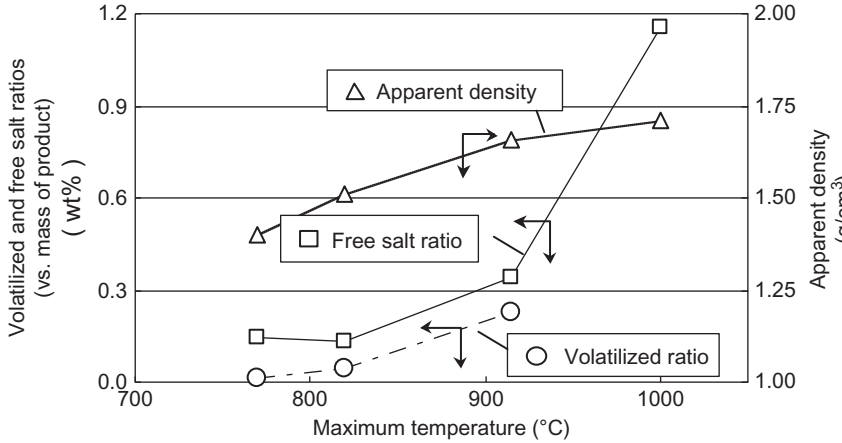

Figure 18.37 Influence of maximum temperature on mass ratios of volatilized salt, free salt in product, and apparent density of product.

18.5.2 Metal waste treatment process and waste form development

As for the treatment of metal waste originating from the anode residue of the electrorefiner, stable characteristics of noble metal FPs alloyed with zirconium and austenitic stainless steel cladding have been reported (Ebert, 2005). However, ferritic steel base cladding is a reference candidate for metal FBR fuel in Japan. Therefore, appropriate alloying composition and conditions for metal waste form with ferritic steel have been studied. Hence, ferritic SS and NM were melted together in an induction-heating furnace to alloy the metal waste, which was then subjected to surface analysis and leaching behavior measurements (Uozumi et al., 2011b). Molybdenum, ruthenium, rhodium, palladium, and rhenium (a surrogate for ^{99}Tc) were chosen as the representative NM FPs. Major parameters were zirconium content (2-60 wt%), NM/Zr ratio (1-5 vs. the average value in the spent metallic fuel), melting temperature (1500-1700 °C), the pressure during the process, and the material for the crucible containing the melted metals.

By observing the microstructure and homogeneity of the fabricated alloys, temperatures of more than 1600 °C, zirconium content between 5 and 20 wt%, and argon pressure of more than 4 kPa, were found to be appropriate conditions to obtain excellent metal waste ingots. XRD analysis of the SS-Zr-NM alloys indicated the existence of the ferrite (Fe-Cr) phase and some unidentified phases, which are considered to be intermetallic compounds consisting of iron, zirconium, and NMs. These phases were also determined by SEM/EPMA analysis as shown in Figure 18.38, and it was found that the zirconium content in the ferrite phase was very low and zirconium distributed unevenly in the intermetallic phases. Ruthenium, rhodium, and palladium were also

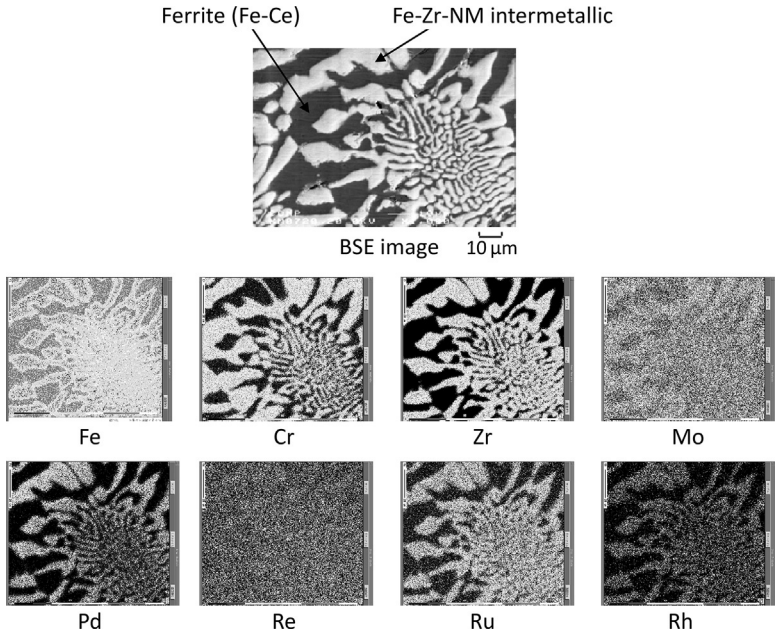

Figure 18.38 Section view and element distribution of metal waste sample (SS-10 wt% Zr-4 wt%NM).

heavily concentrated in the intermetallic phases. On the other hand, molybdenum and rhenium distributed more evenly throughout the samples, and they rather preferred to be in the ferrite phase at higher concentration. It was concluded that the NM/Zr ratio in the SS-Zr-NM alloy should not be far larger than that in the spent fuel. The normalized leaching rates of the major constituents from the metal waste samples prepared in those tests are shown in Figure 18.39. Though the data considerably scattered, the normalized elemental mass loss (NL) values were much lower than those for simulated waste glass, which ranged from 9 to 23 g/m^2 for silicon and from 10 to 30 g/m^2 for

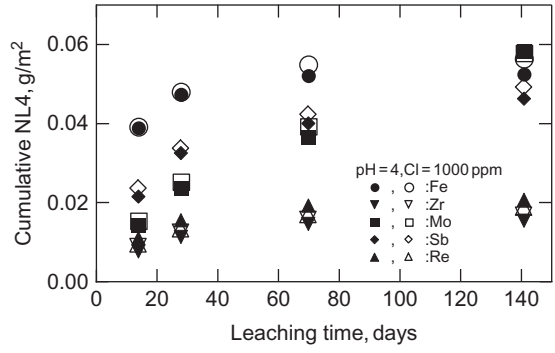

Figure 18.39 Cumulative normalized leaching rates from metal waste.

boron, respectively. These data indicate the excellent potential of the SS-Zr-NM alloys as a stable waste form.

18.6 Basic studies

18.6.1 Measurement of basic properties

The basics of pyrochemistry, standard potentials, thermodynamic properties, and kinetic properties have been assessed. Due to a lack of basic properties necessary for understanding the process chemistry, a substantial number of basic properties have been measured since the early stage of the program.

18.6.1.1 Thermodynamic and electrochemical properties

Figure 18.40 shows the typical configuration of the electrochemical cell used for measuring electrochemical properties of actinide elements and lanthanide elements. As a material for the working electrode, tungsten, or tantalum is selected according to the chemical reactivity of the element. Table 18.4 shows the most reliable standard potentials and reduction potentials of relevant elements in LiCl-KCl at 450 °C, as measured by Japanese researchers.

In addition to the electrochemical potentials, equilibrium distribution factors are important basic data for predicting separation behavior in a molten salt/liquid metal extraction process. In a liquid chloride salt and cadmium metal system, equilibria between the elements is achieved by redox reactions between cations in the salt and metal atoms in the cadmium. The chlorine anions remain in the salt and are not oxidized. Thus, the equilibrium between two cations can be represented as an exchange reaction between the pair of elements

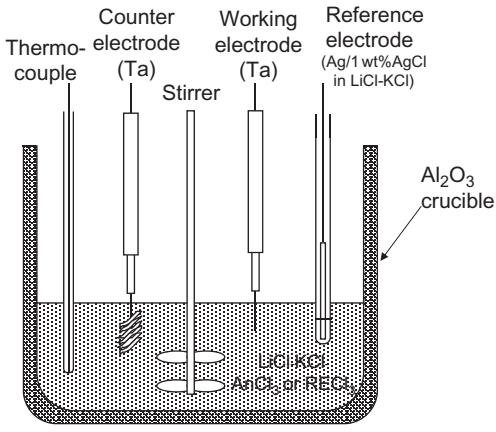

Figure 18.40 Electrochemical cell for standard potential measurement.

Table 18.4 Electrochemical potential of relevant elements measured by (a) Sakamura et al. (1995), (b) Sakamura et al. (1998), (c) Sakamura et al. (2001), and (d) Hayashi (2013)

Inert electrode	Standard potential V vs Cl_2/Cl^-	Cd electrode	Reduction potential* V vs Cl_2/Cl^-
U(lll)/U(0)	−2.468[a]	U(III)/U-Cd	−2.557[a]
Np(lll)/Np(0)	−2.674[b]	Np(III)/Np-Cd	−2.560[b]
Pu(lll)/Pu(0)	−2.773[c]	Pu(III)/Pu-Cd	−2.564[c]
Am(ll)/Am(0)	−2.827[c]	Am(III)/Am-Cd	−2.576[c]
Cm(lll)/Cm(0)	−2.805[d]	Cm(III)/Cm-Cd	−2.566[d]
Gd(lll)/Gd(0)	−2.990[b]	Gd(III)/Gd-Cd	−2.665[b]
Pr(lll)/Pr(0)	−3.040[b]	Pr(III)/Pr-Cd	−2.631[b]
Nd(lll)/Nd(0)	−3.047[a]	Nd(III)/Nd-Cd	−2.633[a]
Ce(lll)/Ce(0)	−3.056[a]	Ce(III)/Ce-Cd	−2.636[a]
Y(lll)/Y(0)	−3.068[a]	Y(III)/Y-Cd	−2.753[a]
La(lll)/La(0)	−3.103[c]	La(III)/La-Cd	−2.661[c]

*The reduction potentials of elements in LiCl-KCl eutectic salt into liquid cadmium alloy were derived when the concentration of the elements in the salt and in the liquid cadmium are the same (0.001 mol fraction).

$$n\mathrm{UCl_3} + 3\mathrm{M} = n\mathrm{U} + 3\mathrm{MCl}_n \tag{18.16}$$

The equilibrium constant, Ke, for the reaction is

$$\mathrm{Ke} = \left(\frac{[\mathrm{MCl}_n]}{[\mathrm{M}]}\right)^3 \left(\frac{[\mathrm{U}]}{[\mathrm{UCl_3}]}\right)^n = \exp\left(\frac{-[\mathrm{DG^o(MCl}_n) - \mathrm{DG^o(UCl_3)}]}{RT}\right) \tag{18.17}$$

where [M], [MCl_n], ΔG^o, R, and T denote activity of M in the cadmium phase, activity of M in the salt phase, standard free energy of formation, gas constant and temperature in Kelvin, respectively.

Here the distribution coefficient of an element, M, in a molten salt and liquid metal system is defined as

$$D_\mathrm{M} = \frac{Y_\mathrm{M}}{X_\mathrm{M}} \tag{18.18}$$

where Y_M and X_M denote mole fraction of M in salt, and atom fraction of M in metal, respectively.

The separation factor of element M relative to uranium is defined as

$$\mathrm{SF_M} = \frac{D_\mathrm{M}}{D_\mathrm{U}} \tag{18.19}$$

Table 18.5 Measured separation factors of actinides and lanthanides in molten salt/liquid cadmium system (uranium-base)

Element	Koyama et al. (1992) 500 °C	Kato et al. (2011) 500 °C	Koyama et al. (2008) 510 °C
Np	2.1	2.4	—
U	1	1	1
Pu	1.9	2.1	2.0
Am	3.1	3.0	3.4
Cm	3.5	3.7	3.8
La	—	78	—
Ce	45	37	—
Nd	39	39	—

According to the thermodynamic relationship described in Equation 18.17, the separation factor of trivalent elements, that is most of the actinides and lanthanides, is described as

$$SF_M = Ke\left(\frac{\gamma_M}{\gamma_{MCl_n}}\right)\left(\frac{\gamma_{UCl_3}}{\gamma_U}\right) \tag{18.20}$$

where γ denotes the activity coefficient.

Table 18.5 shows the separation factors of the actinide and lanthanide elements obtained in various studies carried out by Japanese researchers. The data agreed well with each other, and suggests the possibility to separate americium and curium from other lanthanides.

18.6.1.2 Diffusion coefficients in molten salts

As described in Section 18.3.1, it is necessary to acquire reliable kinetic data such as diffusion coefficients of the actinides and major FPs in the molten salt and in liquid cadmium, in addition to the thermodynamic and electrochemical properties, to understand and predict the behavior of these elements in the pyroreprocessing flow sheet using simulation codes. Chronopotentiometry is one of the electrochemical techniques that has been frequently used to determine the diffusion coefficient of species in electrolytes. In this method, a change of potential at a working electrode, where the species of interest is involved in an electrochemical reaction, is measured at a constant current. The diffusion coefficient can be calculated from a transition time, which is a period between the beginning of the reaction and a rapid change of the potential, indicating depletion of the species in the vicinity of the working electrode, using the Sand equation (Sand, 1901)

$$\frac{i\tau^{1/2}}{C} = \frac{nFAD^{1/2}\pi^{1/2}}{2} \tag{18.21}$$

where i is the current passed through the electrode (A), τ transition time (s), C is bulk concentration of the reactant (mol/cm^3), n is the number of the electrons involved in the reaction, F is Faraday's constant (C/equiv.), A is the surface area of the working electrode (cm^2), and D is the diffusion coefficient of the reactant (cm^2/s). In this method, however, it is always difficult to define the surface area of the working electrode exactly in the molten salt due to (i) wetting between the electrode and the salt, and (ii) lack of suitable insulator materials that have enough thermal strength and comparable thermal expansion coefficients to the electrode materials (Lantelme et al., 1984). When active metal is produced at the electrode, it becomes more difficult to use an insulating material due to the chemical reactions between the metal and the insulator. Thus, a novel method was devised to minimize the error in defining the effective surface area of the working electrode without any insulator material in the molten salt (Iizuka, 1998).

When the concentration of a reactant in a solution, the current passed through the working electrode, and the temperature of the system are kept constant, the transition time should be a function of the surface area of the working electrode alone:

$$\tau^{1/2} = f(A) = \frac{nFCD^{1/2}\pi^{1/2}}{2i}A \tag{18.22}$$

Under such conditions, the change of the square root of the transition time is proportional to the change of the surface area of the working electrode:

$$d\tau^{1/2} = \frac{nFCD^{1/2}\pi^{1/2}}{2i}dA \tag{18.23}$$

Then, the diffusion coefficient can he determined from the slope of the $\tau^{1/2}$-A plot obtained by changing the surface area of the working electrode in an adequate way, even if the absolute value of the surface area cannot be defined:

$$D^{1/2} = \frac{2i}{nFC\pi^{1/2}}\left(\frac{\mathrm{d}\tau^{1/2}}{\mathrm{d}A}\right) \tag{18.24}$$

Some chronopotentiograms for LiCl-KCl-$CeCl_3$ with variable surface areas of the working electrode (W) are shown in Figure 18.41. It can be seen the transition time decreased as the electrode was raised with longer spacers. This tendency was plotted in Figure 18.42 for the case of LiCl-KCl-$CeCl_3$ at 775 K as an example. The $\tau^{1/2}$-A plot in this figure shows a good linearity as expected above. Finally, the diffusion coefficient was calculated from the slope of this plot using Equation 18.24. The results were formulated as follows, including the temperature dependence:

$$\log D_{\mathrm{Cd}} = -2.69\ (\pm 0.145) - \frac{1670\ (\pm 108)}{T} \qquad \left(D_{\mathrm{Ce}} : \mathrm{cm}^2/\mathrm{s}\right) \tag{18.25}$$

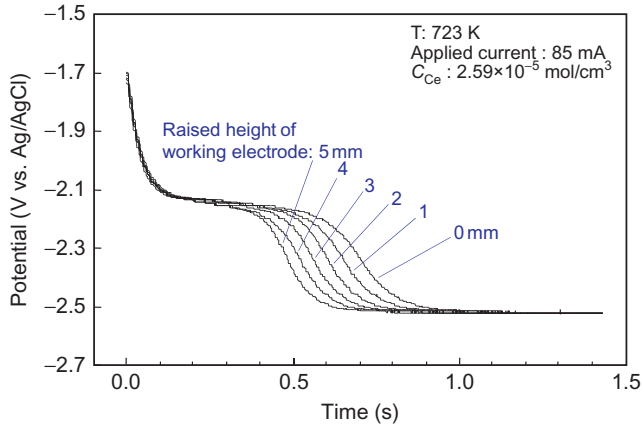

Figure 18.41 Chronopotentiograms for LiCl-KCl-$CeCl_3$ solutions with various surface areas of working electrodes.

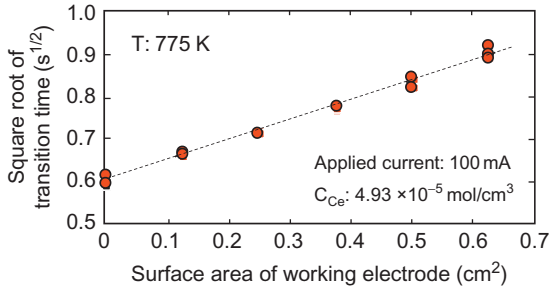

Figure 18.42 Relation between square root of transition time and surface area of working electrode for cerium.

$$\log D_{\mathrm{Gd}} = -2.78\ (\pm 0.128) - \frac{1670\ (\pm 94.3)}{T} \qquad \left(D_{\mathrm{Gd}} : \mathrm{cm}^2/\mathrm{s}\right) \tag{18.26}$$

The dependence of the diffusion coefficient of lanthanide ions on their ionic radii shown in Figure 18.43 arouses a scientific interest in an envisioned correlation between the structure of the complex ion MCl_6^{3-} and kinetic properties in the LiCl-KCl melt; although the diffusion data for other lanthanides and computational studies for the structure and the transport process in molten salts are needed for more quantitative discussions.

18.6.1.3 Diffusion coefficients in liquid metal

Conventionally, a capillary method was used to measure a diffusion coefficient of a solute in liquid metals; however, this method requires highly sophisticated experimental techniques to obtain reliable and reproducible results. Hence, CRIEPI proposed a

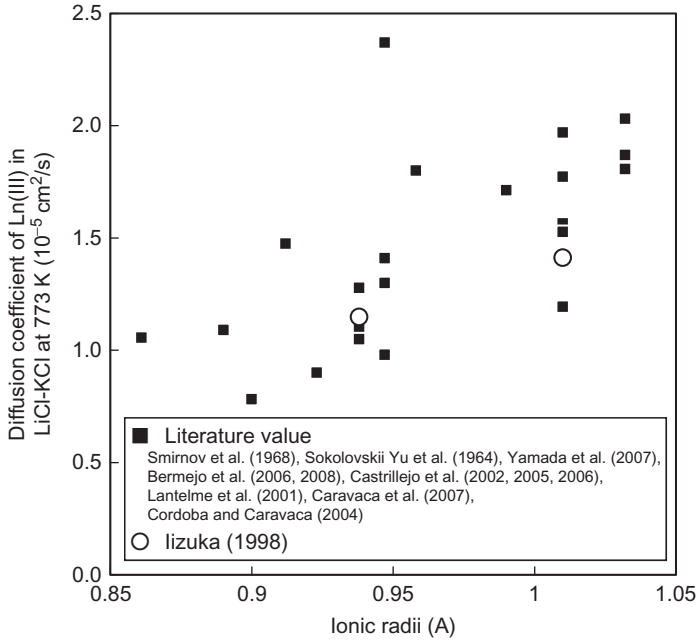

Figure 18.43 Relation between diffusion coefficient in LiCl-KCl at 773 K and ionic radii of trivalent lanthanide ions.

novel method to measure the diffusion coefficient in liquid metal by an electrochemical method (Murakami and Koyama, 2011). When a constant anodic current is applied to a liquid metal electrode, an element (M: actinides, rare earths) dissolved in liquid metal is oxidized to form M^{3+} in LiCl-KCl-MCl_3 melts:

$$\mathrm{M\,(in\,liquid\,Cd)} \rightarrow \mathrm{M^{3+}} + 3\mathrm{e^-} \tag{18.27}$$

During the chronopotentiometry, the concentration of M at the surface of the liquid metal electrode (C_M) decreases continuously. After C_M reaches zero, the electrode potential steeply shifts positive toward the liquid metal dissolution potential. When the transition time (τ) is defined as the time until C_M drops to zero, the diffusion coefficient of M in the liquid metal (D_M) is calculated according to the following equation:

$$2I\tau^{1/2} = 3\pi^{1/2}FAD_M{}^{1/2}C^*{}_M \tag{18.28}$$

where I, F, A, and $C^*{}_M$ are respectively the applied anodic current, Faraday constant, electrode surface area, and initial concentration of M in the liquid metal. Diffusion

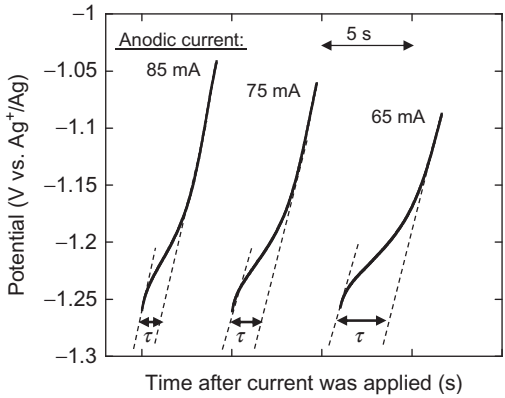

Figure 18.44 Typical chronopotentiograms of the liquid Cd electrode containing U in LiCl-KCl-1.6 wt% UCl_3 melts at 773 K.

coefficients of major actinides and lanthanides in liquid cadmium have been measured. As shown in Figure 18.44, each chronopotentiogram for reduction of uranium into the liquid cadmium electrode shows a potential plateau at around −1.23 V corresponding to the oxidation of uranium dissolved in liquid cadmium and a steep potential shift toward positive potentials after the uranium concentration near the surface of the liquid cadmium electrode reached zero at $t=\tau$ (transition time). The chronopotentiometry was terminated before the potential would reach the cadmium metal dissolution potential to avoid any losses of liquid cadmium. With the plot of $\tau^{1/2}$ against $C^*_U I-^1$, it was confirmed that $\tau^{1/2}$ changed linearly with respect to $C^*_U I^{-1}$. Therefore, according to Equation 18.28, the diffusion coefficient of uranium in liquid cadmium was evaluated to be 1.9×10^{-5} cm^2 s^{-1} at 773 K. Diffusion coefficients of other elements have been measured in the same way, and are presented in Table 18.6.

18.6.2 Material developments

18.6.2.1 Development of coating material for the cathode-processing crucible

Before the electrorefining cathode products are sent to the fuel fabrication step, the electrolyte adhering to them has to be removed and the products need to be consolidated in the form of a homogeneous ingot for storage and adjustment of fuel composition. This treatment, called *cathode processing,* is carried out by high-temperature distillation at a reduced pressure.

One of the most difficult problems to be solved toward the practical use of the cathode-processing equipment is the development of a container material compatible with both the high-temperature chlorides and chemically active alloy melt. The results of large-scale high-temperature distillation tests using a solid cathode product for the treatment of spent metallic fuels from EBR-II were reported by INL (Westphal et al., 2008).

Table 18.6 The diffusion coefficient (D) at various temperature and the activation energy (E_a) in liquid cadmium at 773 K determined by chronopotentiometric method

	U	Pu	La	Pr	Nd	Gd	Y	Sc
$D \times 10^6$ ($cm^2\ s-^1$)	17 (738 K) 19 (773 K) 23 (823 K)	6.8 (723 K) 9.3 (773 K) 10 (823 K)	1.9 (723 K) 2.5 (773 K) 3.4 (823 K)	3.2 (723 K) 3.8 (773 K) 4.3 (823 K)	2.7 (743 K) 3.4 (773 K) 3.9 (823 K)	3.2 (723 K) 3.9 (773 K) 4.3 (823 K)	6.8 (743 K) 8.2 (773 K) 9.3 (823 K)	6.5 (737 K) 7.7 (773 K) 8.0 (823 K)
E_a (kJ mol^{-1})	17	19	28	15	22	15	19	12

In these tests, a zirconia-based castable crucible (78 wt% zirconia, 20 wt% aluminum, and 2 wt% carbon) was used normally at 1473 K as a lining material for the graphite secondary container. This material was durable against repeated use for at least four to six times, although the loss of uranium of a few percent inevitably occurred owing to chemical reaction with the crucible material. However, higher operating temperatures would be required for the cathode processor to adapt to the actual electrorefining situation; this is because the solid cathode product obtained near the end of each anode batch tends to contain more zirconium, which increases the melting point of U-Zr alloy, compared with that recovered at the beginning (Iizuka et al., 2010). This means that cathode-processing crucible materials durable against more severe conditions still need to be developed. For this purpose, small-scale high-temperature distillation experiments were performed using U-Zr cathode products with a variety of U/Zr ratios (Iizuka et al., 2009) at temperatures of 1273-1573 K for salt vaporization and 1573-1673 K for metal consolidation.

The surface of a commercially available ZrO_2 crucible turned brown and peeled off during the experiment, probably due to a reaction between ZrO_2 and the U-Zr alloy melt or between UCl_3 and Y_2O_3, which was a stabilizing agent contained in the ZrO_2 crucible at a concentration of 5 mol%. Considering the above-mentioned result by INL, the temperature in this experiment (up to 1673 K) may have been too high to expect compatibility with the U-Zr alloy melt. The commercial ZrO_2 coating material had a difficulty of an interaction with the graphite substrate rather than that with the U-Zr alloy melt, and the U-Zr ingot after distillation could not be removed without breaking the crucible. A zirconia coating material originally developed in this study by mixing zirconia beads (25-106 μm) and powder (40 nm) (Figure 18.45) showed superior performance in restraining reaction between alloy melt and graphite crucible and also in easy release of U-Zr ingot from the crucible as shown in Figures 18.46 and 18.47. Although it was evaluated that about 2.72% of uranium contained in the initially loaded cathode product reacted with this coating material, the resultant UO_2 remaining in the coated layer has no influence on final material mass balance of the pyrometallurgical process because it can be converted

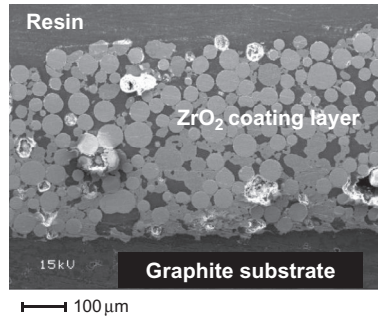

Figure 18.45 Cross-sectional view of newly developed ZrO_2 coating applied on graphite substrate.

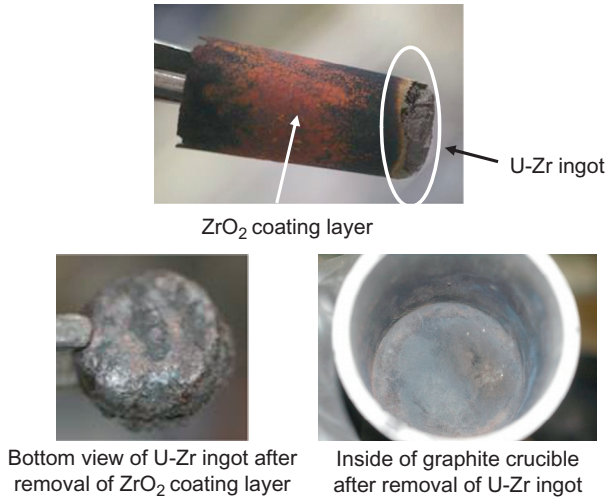

Figure 18.46 U-Zr distillation product ingot and graphite crucible after removal of originally developed ZrO_2 coating layer.

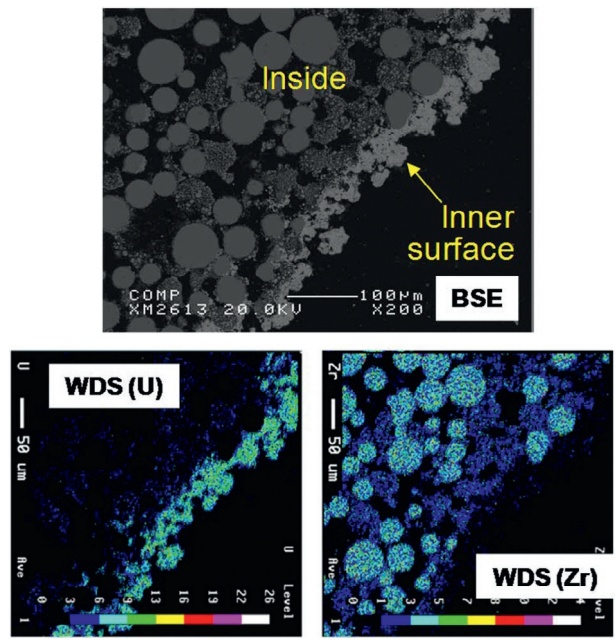

Figure 18.47 Cross-sectional BSE and WDS views of coating layer developed using ZrO_2 beads and powder the distillation experiment.

to its chloride by reaction with zirconium and $ZrCl_4$ (Sakamura et al., 2005a). Although a tungsten crucible double-coated with the commercial ZrO_2 coating material and ZrN also showed an easy separation between the U-Zr ingot and the crucible substrate, no further advantages over the simple originally developed ZrO_2 coating could be found.

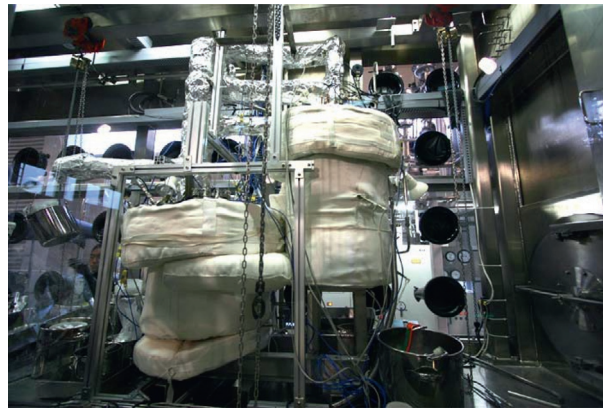

Figure 18.48 Molten salt transport test rig installed in Ar atmosphere glove box.

18.6.3 Technological developments for safe and efficient pyrochemical process operations

18.6.3.1 Molten salt and liquid metal transport

Because pyrometallurgical reprocessing is conducted in a molten salt/liquid metal system, the transport of these high-temperature melts is an essential technology for their practical use. The transport technologies for high-temperature liquids (molten salt and liquid cadmium) enhance the interoperation of the processes between the electroreduction cell, electrorefiner, countercurrent contactor, and/or cathode processor by decreasing the time required for freezing and remelting. Although the success of large-capacity centrifugal pumps for molten salt reactor systems has been reported (Rosenthal, 1972), the development of small transport systems applicable to pyrochemical processing has not been reported in detail. A molten salt transport test and liquid metal transport test have been carried out at CRIEPI, as shown in Figure 18.48, to develop transport technologies suitable for pyrochemical treatment (Hijikata and Koyama, 2009a,b). The applicability of a high-temperature centrifugal pump, suction pump, and valves was tested at 500 °C, and the controllability of the flow rate in a practical range of several L/min was demonstrated. The durability of the high-temperature centrifugal pump was demonstrated by repeating its operation about 500 times during a total of 700 h of operation of the molten salt test loop (Hijikata and Koyama, 2009a).

18.7 Applications to processing damaged core (corium) for Fukushima remediation

During the accident in Fukushima Dai-ichi NPP, almost certainly core melting occurred and a large amount of "fuel debris" (mixture of melted fuel, cladding, structural material, and so on) was generated in the reactor pressure vessel and the pressure containment vessel. Because the total amount of the fuel debris and its detailed characteristics

are not clarified at present, the scheme and methods for the fuel debris management has not been determined. According to "the Mid-and-Long-Term Roadmap towards the Decommissioning of TEPCO's Fukushima Daiichi Nuclear Power Station Units 1-4" issued by the Japanese government, processing and/or disposal methods for fuel debris are planned to be determined in parallel to removal of it from reactor cores. Currently, the technical and economic feasibility of various options for fuel debris management are under study to provide the basis for reasonable decision making.

The chemical analyses of the corium samples obtained from the TMI-2 damaged core, which mainly consist of $(U,Zr)O_2$, have shown that it is hard to dissolve them into nitric acid (Akers et al., 1986). This result suggests that it is unpromising to adopt conventional aqueous process for fuel debris treatment and that approaches other than the PUREX process should be investigated for their feasibility and expected performance in stabilization of the fuel debris. On the basis of extensive knowledge and experience obtained in the research and development of pyroprocessing technology, CRIEPI proposes a flow sheet in which actinides are separated for storage and FPs are packed into stable waste forms (Figure 18.49). In this flow sheet, the actinides in the fuel debris are reduced to metals by electroreduction at the beginning. ANL reported that a synthetic corium, containing $(U,Zr)O_2$, zirconium, iron, and chromium, was completely reduced by reacting it with lithium metal in molten LiCl (Karell et al., 1997). This result indicates an excellent feasibility of applying the headend process in the proposed flow sheet. The reduction product is sent to the electrorefining step to separate uranium, plutonium, and MAs for storage. As plutonium and MAs are recovered using the liquid cadmium cathode, they are inevitably accompanied with a small amount of lanthanide FPs such as neodymium and cerium due to their thermodynamic properties. Zirconium and noble metal FPs remain at the anode after the electrorefining step. They are to be processed as a metal waste form, which has been developed for pyrometallurgical reprocessing. According to the evaluation of core materials and FP inventory after the TMI-2 accident (Akers et al., 1990), heat-generating FPs such as cesium and strontium, which tend to accumulate in molten salt solvents used in pyrochemical processes, are expected to have been remarkably decreased from the corium due to the core melting at high temperature and long-term leaching into injected and circulated cooling water. Under such a condition, the molten salt solvents can be used for a prolonged duration because the majority of FPs accumulated in the molten salt solvents is lanthanides and they can be easily

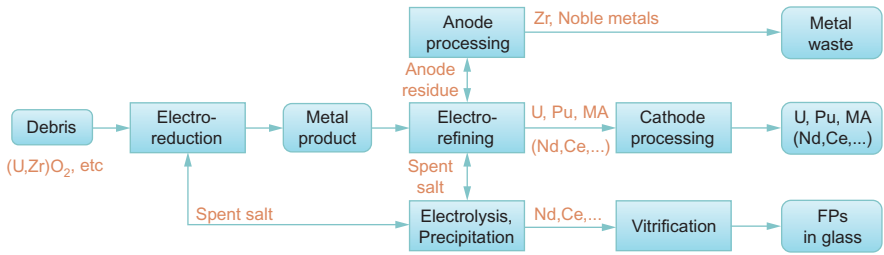

Figure 18.49 Proposed flow sheet for fuel debris treatment by application of pyro-processing technology.

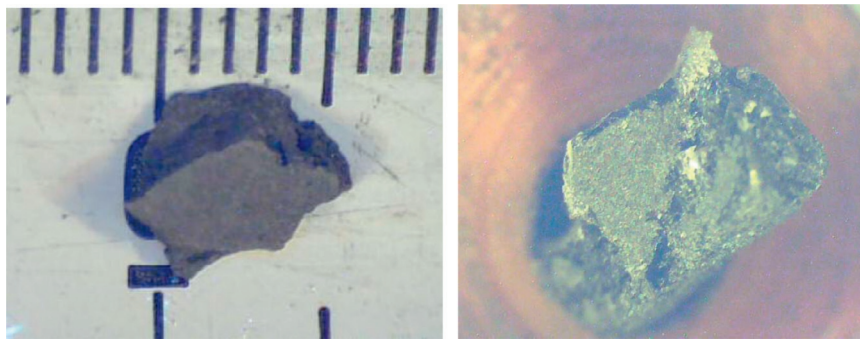

Figure 18.50 Section view of TMI-2 corium samples before (left) and after (right) electrolytic reduction in LiCl-Li_2O at 923 K.

removed and finally vitrified into the conventional glass waste form. CRIEPI and JAEA jointly conducted a feasibility study of pyrochemical processes as effective options for fuel debris treatment. Up to the present, behavior of ZrO_2 and simulated corium (U,Zr)O_2 during the electroreduction in LiCl-Li_2O electrolyte was investigated, and it has been shown that uranium can be reduced to metal at least partially (Kitawaki et al., 2013). Concerning the behavior of zirconium, it was found that ZrO_2 favorably reacts with Li_2O in the electrolyte to form complex oxides such as Li_2ZrO_3, and these products are hardly reduced to zirconium metal (Sakamura et al., 2012). In addition, studies on the pyrochemical treatment using TMI-2 corium samples are in progress as a joint program between CRIEPI and JRC-ITU (Iizuka et al., 2013). Figure 18.50 shows the electroreduced sample of TMI-2 corium, suggesting the possibility of complete reduction of actinides. Definition of adequate reducing conditions based on detailed analysis of the samples is now underway.

References

Akers, D.W., et al., 1986. TMI-2 core debris grab samples—examination and analysis Part 1,2. GEND-INF-075.

Akers, D.W., McCardell, R.K., Russel, M.L., Worku, G., 1990. TMI-2 core materials and fission product inventory. Nucl. Eng. Des. 118, 451–461.

Babelot, J.-F., Chauvin, N., 2009. Joint CEA/ITU synthesis report of the experiment SUPERFACT 1. JRC-ITU-TN-99/03.

Bateman, K.J., Capson, D.D., 2004. A finite difference model used to predict the consolidation of a ceramic waste form produced from the electrometallurgical treatment of spent nuclear fuel. ANL-NT-209.

Bateman, K.J., Rigg, R.H., Wiest, J.D., 2002. Hot isostatic pressing of ceramic waste from spent nuclear fuel. ANL/ENT/CP-105871.

Battisti, T.J., et al., 2002. Ceramic waste form production and development at ANL-West. In: Proc. 5th Top1. Mtg. DOE Owned Spent Nuclear Fuel and Fissile Materials Management, Charleston, SC, USA, September 17-20, 2002, Argonne National Lab.

Battles, J.E., Myles, K.M., Laidler, J.J., Green, D.W., 1993. Argonne National Laboratory Chemical Technology Division Annual Technical Report 1992, ANL-93/17.

Bermejo, M.R., Gomez, J., Medina, J., Martinez, A.M., Castrillejo, Y., 2006. The electrochemistry of gadolinium in the eutectic LiCl-KCl on W and Al electrodes. J. Electroanal. Chem. 588, 253–266.

Bermejo, M.R., Gomez, J., Martinez, A.M., Barrado, E., Castrillejo, Y., 2008. Electrochemistry of terbium in the eutectic LiCl-KCl. Electrochim. Acta 53, 5106–5112.

Caravaca, C., Cordoba, G., Tomas, M.J., Rosado, M., 2007. Electrochemical behavior of gadolinium ion in molten LiCl-KCl eutectic. J. Nucl. Mater. 360, 25–31.

Castrillejo, Y., Bermejo, M.R., Pardo, R., Martinez, A.M., 2002. Use of electrochemical techniques for the study of solubilization processes of cerium-oxide compounds and recovery of the metal from molten chlorides. J. Electroanal. Chem. 522, 124–140.

Castrillejo, Y., Bermejo, M.R., Barrado, A.I., Pardo, R., Barrado, E., Martinez, A.M., 2005. Electrochemical behavior of dysprosium in the eutectic LiCl-KCl at W and Al electrodes. Electrochim. Acta 50, 2047–2057.

Castrillejo, Y., Bermejo, M.R., Barrado, E., Martinez, A.M., 2006. Electrochemical behavior of erbium in the eutectic LiCl-KCl at W and Al electrodes. Electrochim. Acta 51, 1941–1951.

Cordoba, G., Caravaca, C., 2004. An electrochemical study of samarium ions in the molten eutectic LiCl+KCl. J. Electroanal. Chem. 572, 145–151.

Ebert, W.L., 2005. Testing to evaluate the suitability of waste forms developed for electrometallurgically treated spent sodium-bonded nuclear fuel for disposal in the Yucca Mountain repository. ANL-05/43.

Fujihata, K., Uozumi, K., Tsukada, T., 2013. Parameter survey on heating conditions for glass-bonded sodalite ceramic waste fabrication from type-A zeolite containing simulating FPs. In: Proceedings of GLOBAL2013, Salt Lake City, September 2013.

Goff, K.M., Simpson, M., 2009. Dry processing of used nuclear fuel. In: Proceedings of GLOBAL 2009, Paris, France.

Goff, K.M., Benedict, R.W., Howden, K.L., Teske, G.M., Johnson, T.A., 2007. Pyrochemical treatment of spent nuclear fuel. In: Proceedings of GLOBAL 2005, Tsukuba, Japan.

Gourishankar, K.V., Johnson, G.K., Johnson, I., 1997. Thermodynamics of mixed oxide compounds, $Li_2O{\bullet}Ln_2O_3$ (Ln = Nd or Ce). Metall. Mater. Trans. B 28, 1103–1110.

Hayashi, H., Takano, M., Otobe, H., Koyama, T., 2013. Syntheses and thermal analyses of curium trichloride. J. Radioanal. Nucl. Chem. 297 (1), 139–144.

Hijikata, T., Koyama, T., 2009a. Development of high-temperature transport technologies for liquid cadmium in pyrometallurgical. J. Eng. Gas Turbines Power 131, 042902-1-8.

Hijikata, T., Koyama, T., 2009b. Development of high-temperature molten salt transport technology for pyrometallurgical reprocessing. J. Power Energy Syst. 3 (1), 170–181.

Iizuka, M., 1998. Diffusion coefficients of cerium and gadolinium in molten LiCl-KCl. J. Electrochem. Soc. 145, 84–88.

Iizuka, M., Moriyama, H., 2010. Analysis of anodic behavior of metallic fast reactor fuel using a multi diffusion layer model. J. Nucl. Sci. Technol. 47, 1140–1154.

Iizuka, M., Uozumi, K., Inoue, T., Iwai, T., Shirai, O., Arai, Y., 2001. Behavior of plutonium and americium at liquid cadmium cathode in molten LiCl-KCl electrolyte. J. Nucl. Mater. 299, 32–42.

Iizuka, M., Sakamura, Y., Inoue, T., 2006. Electrochemical reduction of $(U\text{-}40Pu\text{-}5\ Np)_2$ in molten LiCl electrolyte. J. Nucl. Mater. 359, 102–113.

Iizuka, M., Omori, M., Ogata, T., Tsukada, T., 2009. Development of an innovative electrorefiner for high uranium recovery rate from metal fast reactor. J. Nucl. Sci. Technol. 46, 699–716.

Iizuka, M., Omori, T., Tsukada, T., 2010. Behavior of U-Zr alloy containing simulated fission products during anodic dissolution in molten chloride electrolyte. J. Nucl. Sci. Technol. 47, 244–254.

Iizuka, M., Akagi, M., Omori, T., 2013a. Development of treatment process for anode residue from molten salt electrorefining of spent metallic fast reactor fuel. Nucl. Technol. 181, 507–525.

Iizuka, M., Kinoshita, K., Sakamura, Y., Ogata, T., Koyama, T., 2013b. Performance of pyro-process equipment of semi-industrial design and material balance in repeated engineering-scale fuel cycle tests using simulated oxide/metal fuels. Nucl. Technol. 184, 107–120.

Iizuka, M., Koyama, T., Sakamura, Y., Uozumi, K., Fujihata, K., Kato, T., Murakami, T., Tsukada, T., Glatz, J., 2013c. Development of pyro-process technology at CRIEPI for curving out the future of nuclear fuel cycle. In: Proceedings of GLOBAL2013, Salt Lake City, USA.

Inoue, T., Tanaka, H., 1997. Recycling of actinides produced in LWR and FBR fuel cycle by applying pyrometallurgical process. In: Proceedings of GLOBAL '97, Yokohama, Japan.

Johnson, I., 1960. Solubilities in liquid metals, argonne national laboratory report ANL-HMF-SL-1747.

JRC-ITU, 2010. JRC-ITU Annual Report 2009, pp. 34-35.

Karell, E.J., Gourishankar, K.V., Johnson, G.K., 1997. Electrometallurgical treatment of TMI-2 fuel debris. ANL/CMT/CP-92022.

Kato, T., Uozumi, K., Inoue, T., Shirai, O., Iwai, T., Arai, Y., 2003. Recovery of plutonium and uranium into liquid cadmium cathodes at high current densities. In: Proceedings of GLOBAL 2003, New Orleans, LA, USA.

Kato, T., Inoue, T., Iwai, T., Arai, Y., 2006. Separation behaviors of actinides from rare-earths in molten salt electrorefining using saturated liquid cadmium cathode. J. Nucl. Mater. 357, 105–114.

Kato, T., Sakamura, Y., Iwai, T., Arai, Y., 2009. Solubility of Pu and rare-earths in LiCl-Li_2O melt. Radiochim. Acta 97, 183–186.

Kato, T., Murakami, T., Uozumi, K., Koyama, T., Ougier, M., Rodrigues, A., Winckel, S.V., Malmbeck, R., Glatz, J.-P., 2011. Actinides recovery from irradiated MOX fuel by pyro-chemical reprocessing. In: Proceedings of GLOBAL 2011, Makuhari, Japan.

Keiser Jr., D.D., Mariani, R.D., 1999. Zr-rich layers electrodeposited onto stainless steel cladding during the electrorefining of EBR-II fuel. J. Nucl. Mater. 270, 279–289.

Kinoshita, K., Tsukada, T., 2008. Counter-current test in LiCl-KCl and liquid Cd system for pyropartitioning and pyro-reprocessing. In: Proceedings of 10th P&T Meeting of OECD/NEA, Mito, Japan.

Kinoshita, K., Koyama, T., Inoue, T., Ougier, M., Glatz, J.-P., 2005. Separation of actinides from rare earth elements by means of molten salt electrorefining with anodic dissolution of U-Pu-Zr alloy fuel. J. Phys. Chem. Solids 66, 619–624.

Kinoshita, K., Tsukada, T., Ogata, T., 2007. Signal-stage extraction test with continuous flow of Molten LiCl-KCl salt and liquid Cd for pyro-reprocessing of metal FBR fuel. J. Nucl. Sci. Technol. 44 (12), 1557–1564.

Kinoshita, K., Koyama, T., Kobayashi, T., Ogata, T., Iizuka, M., Hijikata, T., Sakamura, Y., Uozumi, K., Murakami, T., 2012. Material balance evaluation and plant design of pyro-reprocessing for metal fuel. CRIEPI Report L11009 (in Japanese).

Kitawaki, S., Nakayoshi, A., Fukushima, M., Sakamura, Y., Murakami, T., Akiyama, N., 2011. Electrorefining test of U-Pu-Zr alloy fuel prepared pyrometallurgically from MOX. In: Proceedings of GLOBAL 2011, Makuhari, Japan.

Kitawaki, S., Nakayoshi, A., Sakamura, Y., Akiyama, N., 2013. Electrochemical reduction behavior of U Zr mixed oxide. In: 2012 Annual Meeting Atom Energy Soc Japan, Higashi-Osaka, Japan, in Japanese.

Kobayashi, T., Tokiwai, M., 1993. Development of TRAIL, a simulation code for the molten salt electrorefining of spent nuclear fuel. J. Alloys Comp. 197, 7–16.

Kobayashi, T., Fujita, R., Fujie, M., Koyama, T., 1995. Polarization effects in the molten salt electrorefining of spent nuclear fuel. J. Nucl. Sci. Technol. 32, 653–663.

Koyama, T., 1994. Method to synthesize dense crystallized sodalite pellet for immobilizing halide salt radioactive waste. United States Patent, Patent Number: 5340506, Date of Filed: September 11, 1992, Date of Patent August 23.

Koyama, T., 2011. Chapter 10: Nuclear technology for pyrochemical treatment of spent nuclear fuels. In: Nash, K.L., Lumetta, G.J. (Eds.), Advanced separation techniques for nuclear fuel reprocessing and radioactive waste treatment. In: Woodhead Energy Series No. 2, Woodhead.

Koyama, T., Johnson, T.R., Fischer, D.F., 1992. Distribution of actinides in molten chloride salt/cadmium metal systems. J. Alloys Comp. 189, 37.

Koyama, T., Matsubara, C., Sawa, T., 1997a. Waste form development for immobilization of radioactive halide salt generated from pyrometallurgical reprocessing. In: Proceedings of GLOBAL'97, Yokohama, October 1997.

Koyama, T., Iizuka, M., Shoji, Y., Fujita, R., Tanaka, H., Kobayashi, T., Tokiwai, M., 1997b. An experimental study of molten salt electrorefining of uranium using solid iron cathode and liquid cadmium cathode for development of pyrometallurgical reprocessing. J. Nucl. Sci. Technol. 44, 384–393.

Koyama, T., Iizuka, M., Kondo, N., Fujita, R., Tanaka, H., 1997c. Electrodeposition of uranium in stirred liquid cadmium cathode. J. Nucl. Mater. 247, 227–231.

Koyama, T., Kinoshita, K., Inoue, T., Ougier, M., Malmbeck, R., Glatz, J.-P., Koch, L., 2002. Study of molten salt electrorefining of U-Pu-Zr alloy fuel. J. Nucl. Sci. Technol. (Suppl. 3), 765–768.

Koyama, T., Hijikata, T., Yokoo, T., Inoue, T., 2007. Development of engineering technology basis for industrialization of pyrometallurgical reprocessing. In: Proceedings of Global 2007, Boise, Idaho, pp. 1038–1043.

Koyama, T., Kinoshita, K., Ougier, M., Glatz, J.-P., 2008. Distribution of actinides including Cm in molten chloride salt and liquid cadmium. Radiochim. Acta 96, 311–313.

Koyama, T., Sakamura, Y., Ogata, T., Kobayashi, H., 2009. Pyroprocess and metal fuel development for closing actinide fuel cycle with reduced waste burden. In: Proceedings of GLOBAL 2009, Paris, France.

Koyama, T., Ogata, T., Myochin, M., Arai, Y., 2011. Japanese programs in development of pyro-processing fuel cycle technology for sustainable energy supply with reduced burdens. In: Proceedings of GLOBAL 2011, Makuhari, Japan.

Kurata, M., Sasahara, A., Inoue, T., Betti, M., Babelot, J.-F., Spirlet, J.-C., Koch, L., 1997. Fabrication of U-Pu-Zr metallic fuel containing minor actinides. In: Proceedings of GLOBAL '97, Yokohama, Japan.

Kurata, M., Kinoshita, K., Hijikata, T., Inoue, T., 2000. Conversion of simulated high-level liquid waste to chloride for the pretreatment of pyrometallurgical partitioning process. J. Nucl. Sci. Technol. 37, 682–690.

Lantelme, F., Inman, D., Lovering, D.G., 1984. Electrochemistry—I. In: Gale, R.J., Lovering, D.O. (Eds.), In: Molten Salt Techniques, vol. 2. Plenum Press, New York.

Lantelme, F., Cartailler, T., Berghoute, Y., Hamdani, M., 2001. Physicochemical properties of lanthanide and yttrium solutions in fused salts and alloy formation with nickel. J. Electrochem. Soc. 148, C604–C613.

Lexa, D., Johnson, I., 2001. Occlusion and ion exchange in the molten (lithium chloride-potassium chloride-alkali metal chloride) salt+zeolite 4A system with alkali metal chlorides of sodium, rubidium, and cesium. Metall. Mater. Trans. B 32B, 429.

Lewis, M.A., Johnson, T.R., 1990. A study of the thermodynamic and reducing properties of lithium in cadmium at 773 K. J. Electrochem. Soc. 137, 1414–1416.

Li, S.X., Vaden, D., Westphal, B.R., Fredrickson, G.L., Benedict, R.W., Johnson, T.A., 2007. Integrated efficiency test for pyrochemical fuel cycle. In: Proceedings of GLOBAL 2007, Boise, USA.

Maillard, A., Touron, H., Seran, J.-L., Chalony, A., 1994. Swelling and irradiation creep of neutron-irradiated 316Ti and 15-15Ti steels. ASTM Spec. Technol. Publ. 1175, 824–837.

Mariani, R.D., Porter, D.L., O'Holleran, T.P., Hayes, S.L., Kennedy, J.R., 2011. Lanthanides in metallic nuclear fuels: their behavior and methods for their control. J. Nucl. Mater. 419, 263–271.

Mariani, R.D., Porter, D.L., Hayes, S.L., Kennedy, J.R., 2012. Metallic fuels: the EBR-II legacy and recent advances. Proc. Chem. 7, 513–520.

MEXT, 2006. R&D direction of Fast Breeder Fuel Cycle Technology. The Ministry of Education, Culture, Sports, Science and Technology [in Japanese].

Murakami, T., Koyama, T., 2011. Application of electrochemical method to measure diffusion coefficient in liquid metal. J. Electrochem. Soc. 158 (8), 147–153.

Murakami, T., Kato, T., Rodrigues, A., Ougier, M., Iizuka, M., Koyama, T., Glatz, J.-P., 2014. Anodic dissolution of irradiated metallic fuels in LiCl-KCl melt. J. Nucl. Mater. 452, 517–525.

Nabeshima, M., Shimizu, T., Sakamura, Y., Sakata, M., Inoue, T., 1996. Transfer kinetics of metals from molten fission product chloride to liquid lead cathode during electrolysis in pyrometallurgical treatment of highly radioactive waste. J. Nucl. Sci. Technol. 33, 245–249.

Ohta, H., Ogata, T., Yokoo, T., Ougier, M., Glatz, J.-P., Fontaine, B., Breton, L., 2009a. Low-burnup irradiation behavior of fast reactor metal fuels containing minor actinides. Nucl. Technol. 165, 96–110.

Ohta, H., Papaioannou, D., Ogata, T., Yokoo, T., Koyama, T., Rondinella, V.V., Glatz, J.-P., 2009b. Postirradiation examinations of fast reactor metal fuels containing minor actinides -fission gas release and metallography of ~2.5 at.% burnup fuels. In: Proceedings of GLOBAL 2009, Paris, France.

Ohta, H., Ogata, T., Papaioannou, D., Kurata, M., Koyama, T., Glatz, J.-P., Rondinella, V.V., 2011. Development of fast reactor metal fuels containing minor actinides. J. Nucl. Sci. Technol. 48, 654–661.

Ohta, H., Ogata, T., Papaioannou, D., Nasyrow, R., Rondinella, V.V., 2012. Evaluation of gas release behavior of minor actinide-containing metal fuel. In: Proceedings of NFSM 2012, Chicago, IL, USA.

Ohta, H., Ogata, T., Winckel, S.V., Papaioannou, D., Rondinella, V.V., 2013. Minor actinide transmutation performance in fast reactor metal fuel. In: Proceedings of FR13, Paris, France.

Rosenthal, M.W., 1972. The development status of molten salt breeder reactors ORNL-4812.

Sakamura, Y., 2008. Effect of alkali and alkaline earth chloride addition on electrochemical reduction of UO_2 in molten LiCl. In: Proceedings of 8th Int. Conf. Molten Salt Chem. Technol. (MS8), Kobe, Japan.

Sakamura, Y., Omori, T., 2010. Electrolytic reduction and electrorefining of uranium to develop pyrochemical reprocessing of oxide fuels. Nucl. Technol. 171, 266–275.

Sakamura, Y., Inoue, T., Storvick, T.S., Grantham, L.F., 1995. Development of pyropartitioning process–separation of transuranium elements from rare earth elements in molten chlorides

solution: electrorefining experiments and estimation by using the thermodynamic properties. In: Proceedings of GLOBAL '95, Verseilles, France, 2, 1185.
Sakamura, Y., Inoue, T., Shimizu, T., Kobayashi, K., 1997. Development of pyrometallurgical partitioning technology for TRUs in high level radioactive wastes-vitrification process for salt wastes. In: Proceedings of GLOBAL '97, Yokohama, Japan.
Sakamura, Y., Hijikata, T., Kinoshita, K., Inoue, T., Storvick, T.S., Krueger, C.L., Roy, J.J., Grimmett, D.L., Fusselman, S.P., Gay, R.L., 1998. Measurement of standard potential of actinides (U, Np, Pu, Am) in LiCl-KCl eutectic salt and separation of actinides from rare earths by electrorefining. J. Alloys Comp. 271–273, 592.
Sakamura, Y., Shirai, O., Iwai, T., Suzuki, Y., 2001. Distribution behavior of plutonium and americium in LiCl-KCl eutectic/liquid cadmium systems. J. Alloys Comp. 321, 76–83.
Sakamura, Y., Inoue, T., Iwai, T., Moriyama, H., 2005a. Chlorination of UO_2, PuO_2 and rare earth oxides using $ZrCl_4$ in LiCl-KCl eutectic melt. J. Nucl. Mater. 340, 39–51.
Sakamura, Y., Kurata, M., Inoue, T., 2005b. Electrochemical reduction of UO_2 in molten LiCl or LiCl-KCl eutectic. In: Proceedings of 7th Int Symp Molten Salts Chem Technol (MS7), Toulouse, France.
Sakamura, Y., Kurata, M., Inoue, T., 2006. Electrochemical reduction of UO_2 in molten $CaCl_2$ or LiCl. J. Electrochem. Soc. 153, D31–D39.
Sakamura, Y., Omori, T., Inoue, T., 2008. Application of electrochemical reduction to produce metal fuel material from actinide oxides. Nucl. Technol. 162, 169–178.
Sakamura, Y., Iizuka, M., Inoue, T., 2009. Development of oxide reduction process to bridge oxide fuel cycle and metal fuel cycle. In: Proceedings of GLOBAL 2009, Paris, France.
Sakamura, Y., Iizuka, M., Kitawaki, S., Nakayoshi, A., Kofuji, H., 2012. Behavior of ZrO_2 in LiCl-Li_2O melt. In: 2012 Fall Meeting Atom Energy Soc Japan, Higashi-Hiroshima, Japan. (in Japanese).
Sand, H.J.S., 1901. On the concentration at the electrodes in a solution, with special reference to the liberation of hydrogen by electrolysis of a mixture of copper sulphate and sulphuric acid. Philos. Mag. 1, 45–79.
Seran, J.-L., Levy, V., Dubuisson, P., Gilbon, D., Maillard, A., Fissolo, A., Touron, H., Cauvin, R., Chalony, A., Le Boulbin, E., 1992. Behavior under neutron irradiation of the 15-15Ti and EM10 steels used as standard materials of the phenix fuel subassembly. ASTM Spec. Technol. Publ. 1125, 1209–1233.
Smirnov, M.V., Krasnov Yu, N., Komarov, V.E., Alekseev, V.N., 1968. Diffusion coefficients of trivalent lanthanum in molten LiCl-KCl and LiCl-KCl + LiF mixtures. Trans. Inst. Electrochem. Urals Acad. Sci. (Engl. Transl.) 6, 47.
Sokolovskii Yu, S., Smirnov, M.V., Skiba, O.V., 1964. Tr Inst Elektrokhim, Akad Nauk SSSR, Ural'sk. Filial 5, 41.
Steindler, M.J., Nelson, P.A., Battles, J.E., Green, D.W., 1992. Chemical Technology Division Annual Technical Report, 1991, Argonne National Laboratory Report ANL-92/15.
Tomczuk, Z., Ackerman, J.P., Wolson, R.D., Miller, W.E., 1992. Uranium transport to solid electrodes in pyrochemical reprocessing of nuclear fuel. J. Electrochem. Soc. 139, 3523–3528.
Tsukada, T., Takahashi, K., 2008. Absorption characteristics of fission product elements on zeolite. Nucl. Technol. 162, 229–243.
Uozumi, K., Kinoshita, K., Inoue, T., Fusselman, S.P., Grimmett, D.L., Roy, J.J., Storvick, T.S., Krueger, C.L., Nabelek, C.R., 2001. Pyrometallurgical partitioning of uranium and transuranic elements from rare earth elements by electrorefining and reductive extraction. J. Nucl. Sci. Technol. 38, 36–44.

Uozumi, K., Iizuka, M., Kato, T., Inoue, T., Shirai, O., Iwai, T., Arai, Y., 2004. Electrochemical behaviors of uranium and plutonium at simultaneous recoveries into liquid cadmium cathodes. J. Nucl. Mater. 325, 34–43.

Uozumi, K., Iizuka, M., Kinoshita, K., Tsukada, T., Koyama, T., 2011a. Development of salt and metal waste treatment technology for pyroprocess in CRIEPI. In: Proceedings of GLOBAL2011, Makuhari, Chiba.

Uozumi, K., Iizuka, M., Kurata, M., Inoue, T., Koyama, T., Ougier, M., Malmbeck, R., Glatz, J.-P., 2011b. Recovery of transuranium elements from real high-level liquid waste by pyropartitioning process. J. Nucl. Sci. Technol. 48, 303–314.

Usami, T., Kato, T., Kurata, M., Inoue, T., Sims, H.E., Beetham, S.A., Jenkins, J.A., 2002. Lithium reduction of americium dioxide to generate americium metal. J. Nucl. Mater. 304, 50–55.

Westphal, B.R., Marsden, K.C., Price, J.C., Laug, D.V., 2008. On the development of a distillation process for the electrometallurgical treatment of irradiated spent nuclear fuel. Nucl. Eng. Technol. 40, 163–174.

Yamada, D., Murai, T., Moritani, K., Sasaki, T., Takagi, I., Moriyama, H., Kinoshita, K., Yamana, H., 2007. Diffusion behavior of actinide and lanthanide elements in molten salt for reductive extraction. J. Alloys Comp. 444–445, 557–560.

Development of closed nuclear fuel cycles in the United States

19

T.A. Todd
Idaho National Laboratory, Idaho Falls, ID, USA

Acronyms

An	actinide
AMUSE	Argonne Model for Universal Solvent Extraction
ALSEP	actinide-lanthanide separation process concept
DAAP	diamylamylphosphonate
FCT	fuel cycle technologies program
GANEX	group actinide extraction concept
GNEP	Global Nuclear Energy Partnership
HDEHP	bis(2-ethylhexyl)phosphoric acid, extractant for An(III) and Ln(III) in TALSPEAK process
HEDTA	*N*-(2-hydroxyethyl)ethylenediamine-*N*,*N*′,*N*′-triacetic acid, actinide-selective complexant used in Advanced TALSPEAK aqueous phase
HEH[EHP]	2-Ethylhexylphosphonic acid mono-2-ethylhexyl ester, extractant for An(III) and Ln(III) in Advanced TALSPEAK and ALSEP processes
Ln	lanthanide
MPACT	material protection, accountability, and control technologies
MT	metric ton
PUREX	plutonium uranium reduction extraction process
SANEX	selective actinide extraction concept
STMAS	Sigma Team for Minor Actinide Separations
TALSPEAK	Trivalent actinide-lanthanide separations by phosphorus-reagent extraction from aqueous komplexes
TBP	tri-*n*-butyl phosphate
TRU	transuranium element (typically referring to Np, Pu, Am, Cm in used nuclear fuel)
TRUEX	transuranic extraction process
T2EHDGA	*N*,*N*,*N*′,*N*′-tetra(2-ethylhexyl)diglycolamide, extractant for An(III) and Ln(III) in ALSEP
UREX	uranium extraction process
USDOE	U.S. Department of Energy

19.1 Introduction

The United States has approximately 100 operating nuclear reactors, and the used fuel from each reactor is temporarily stored at each reactor site. On-site storage includes both wet and dry storage facilities, with the majority of the fuel (approximately

Reprocessing and Recycling of Spent Nuclear Fuel. http://dx.doi.org/10.1016/B978-1-78242-212-9.00019-8

three-quarters of the fuel as of 2011) in wet storage; however, the percentage of fuel in dry storage is rapidly increasing. The current U.S. Department of Energy (USDOE) approach to the nuclear fuel cycle is to open a geologic repository around mid-century, and directly dispose of the used fuel inventory in the repository (http://www.energy.gov/downloads/strategy-management-and-disposal-used-nuclear-fuel-and-high-level-radioactive-waste, January 2013). This fuel amounts to nearly 70,000 metric tons of used nuclear fuel as of 2014. The fuel generated beyond approximately 2014 will be stored, either on-site or in consolidated storage facilities, until a future decision is made on a long-term approach to managing used nuclear fuel. To support this future decision, research is being performed on a number of fuel cycle options, including closed fuel cycles. It is generally recognized that partitioning and transmutation in fast spectrum reactors have significant potential benefit in terms of resource utilization and waste management. Fuel cycles that continually recycle U/Pu or U/TRU are currently the focus of research efforts in the United States. It should be noted that each nation or region will have their own set of constraints and drivers, so an approach that is ideal for one nation or region may or may not be for a different nation or region.

19.2 Future fuel cycle development requirements

The requirements for fuel cycle performance are dependent on a number of factors that vary depending on the objectives of the fuel cycle. For example, the amount of TRU losses that can be tolerated in waste streams depends on the ultimate waste form and the geology that the waste will be placed in. It is very important to look at the performance of the entire fuel cycle, not just a portion of the fuel cycle, to determine performance requirements. To focus on the TRU losses in separation processes, for example, without considering losses in fuel fabrication could lead to inaccurate analyses. The consideration of integrated processes is also important. One cannot determine requirements for the separations processes without first knowing the specifications for fuel fabrication (which drive separation purity requirements) and the limitations of waste forms and repository performance (which drive extent of recovery requirements). In the United States, the separations and waste form research activities are integrated into a single program, and while the fuels development program is separate, there are several activities to integrate development results between the two programs. A critical factor for fuel development is the amount of rare earth elements that the fuel can safely accommodate to avoid high neutron cross sections and to avoid fuel cladding chemical interaction, which could lead to early fuel failure. For metal transmutation fuels, the current estimate of the amount of rare earth elements in the fuel range from about 1% to 5%. Future testing of transmutation fuels is needed to further refine this number, as it could impact the choice of the separation processes used.

A wide range of estimates exist for the needed recovery of TRU elements. Early in the U.S. Global Nuclear Energy Partnership (GNEP) program, recoveries of the TRU elements of greater than 99.9% were targeted (Wigeland et al., 2014). This value was

largely arbitrary, and could be achieved by many of the separation processes tested at laboratory scale; however, TRU losses in the undissolved solids and in the fuel fabrication processes far exceed the 0.1% losses in the separation process. Therefore, losses in the separation process could reasonably be expected to be more, on the order of 0.5% to 1.0%, without having a significant impact on the overall fuel cycle performance. To date, a sensitivity analysis has not been performed to determine the effects of separation process losses on the overall fuel cycle performance. The U.S. Fuel Cycle Technologies (FCT) program will perform an initial sensitivity analysis in 2014, following the completion of the Nuclear Fuel Cycle Evaluation and Screening report (Wigeland et al., 2014). This study will evaluate separation recoveries in the range of 90%, 95%, 99%, and 99.9%, to determine at what recovery level fuel cycle performance is significantly altered. Another key development requirement is the need to assess and address technical maturity. Assessing technical maturity can be very useful in identifying areas that are less mature and need more development effort. This approach is helpful in identifying research needs and prioritizing research to address the less-mature aspects of a technology.

19.3 U.S. Fuel Cycle Technologies program

The U.S. Fuel Cycle Technologies program is managed under the USDOEs Office of Nuclear Energy. The various programs (or "campaigns") are organized by function, as shown in Figure 19.1; advanced fuels development, separations and waste form development, fuel cycle options/systems analysis and integration, material protection,

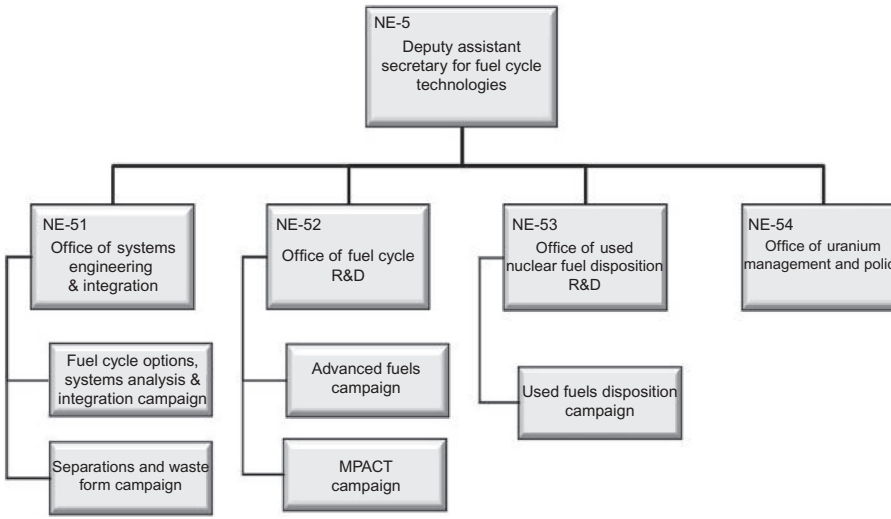

Figure 19.1 USDOE office of nuclear energy fuel cycle technologies program.

accountability and control technologies, and used fuel disposition. The objectives, goals, and time lines for development of future fuel cycles is described in the USDOE Office of Nuclear Energy Research and Development Roadmap (http://energy.gov/sites/prod/files/NuclearEnergy_Roadmap_Final.pdf, April 2010), which was issued in 2010. A revision of the roadmap is underway, but has not been published at the time this is written. The primary objectives laid out in the roadmap are (1) Develop Technologies and Other Solutions That Can Improve the Reliability, Sustain the Safety, and Extend the Life of Current Reactors; (2) Develop Improvements in the Affordability of New Reactors to Enable Nuclear Energy to Help Meet the Administration's Energy Security and Climate Change Goals; (3) Develop Sustainable Nuclear Fuel Cycles; and (4) Understand and Minimize the Risks of Nuclear Proliferation and Terrorism. The development of reprocessing and recycling technologies falls under Objective 3: Develop Sustainable Nuclear Fuel Cycles. The roadmap lays out a strategy for developing new technologies to enable implementation in mid-century, if the decision is made to close the fuel cycle. Because of the very long time frames to develop, design, build, and startup large nuclear facilities, it is imperative that we are actively evaluating new technologies now, with testing and down selection in the near future to support this schedule.

The general U.S. approach to advanced fuel cycles is to utilize aqueous processes to reprocess/recycle light water reactor oxide-based fuels. The reasons for this include the long historical experience and technical maturity, the high throughput of aqueous processing facilities (the United States currently generates about 2000 MT of used nuclear fuel per year), and the compatibility of the fuel matrix with aqueous processing. For a closed fuel cycle with fast reactors, the United States leans toward the use of metal fuel. It should be pointed out that no decision on future fuel cycle reactor types, fuels, or fuel cycles has been made by the USDOE, but these are the areas currently of most interest for research and development. The primary method for recycling fast reactor metal fuel in the United States is the electrochemical (or pyroprocessing) approach. The reasons supporting this approach include lower throughput and purity requirements needed for fast reactor recycle, the fact that the process begins with metal feed and produces metal product for recycling, and that the process has advantages in terms of radiation stability and criticality control.

The primary research area for advanced aqueous processing in the U.S. program is the separation of minor actinides (neptunium, americium, curium) from the used fuel. Separation of uranium and plutonium are industrially established technologies, and recent trends to coprocess uranium with the plutonium product to reduce material attractiveness require only minor adjustments to the current industrial process. Historically, in the PUREX process, neptunium was not recovered and routed to the high-level waste fraction. This is straightforward, as neptunium primarily exists in the pentavalent state and will not extract in tri-*n*-butyl phosphate (TBP). There are a number of ways to manage neptunium in advanced closed fuel cycles, including extracting the neptunium with the uranium and plutonium or leaving the neptunium in a PUREX or UREX type process raffinate to be removed with the remaining TRU elements in a subsequent step. In the first approach, the key to removing the neptunium is to change its oxidation state to one that is extractable by TBP (either IV or

VI) and ensure that the valance state can be maintained during the separation process (Gregson et al., 2012; Sarsfield et al., 2009). This is one of the preferred methods of managing neptunium in the U.S. approach, but the option to separate neptunium with the other minor actinides still exists. Due to similar chemistry, it is appealing to be able to remove the neptunium with the other tetra and hexavalent metals. The current U.S. program has not been actively investigating neptunium extraction; instead, it has chosen to model various approaches using the Argonne Model for Universal Solvent Extraction (AMUSE) code to assess the efficacy of various neptunium management approaches (Wigeland et al., 2014). Specific flow sheets to address neptunium separation with uranium and plutonium are now being developed.

The separation of the trivalent minor actinides from the lanthanides has been the primary focus of the U.S. separations program now for the past five years. The Sigma Team for Minor Actinide Separations (STMAS), a multidiscipline, multilaboratory collaboration among U.S. national laboratories and universities, has been investigating multiple approaches for separating the trivalent actinides. This work is described in Chapter 11 of this book in detail, so only a brief overview will be provided in this chapter. The STMAS was conceived to formulate a program that encouraged collaboration and teamwork, while maintaining individual researcher interests and creativity. A number of leading scientists from U.S. national laboratories and one university were selected as the core team, and collaborations beyond this team with several other universities and research institutes soon followed. Until the formation of the STMAS, the U.S. approach to An(III) separations was the TRUEX process followed by the TALSPEAK process, which had been demonstrated at lab scale a number of times in the mid-2000s (Weaver and Kappelmann, 1968; Horwitz et al., 1885; Gelis et al., 2009). While demonstrated in short lab-scale tests with actual used nuclear fuel, the TALSPEAK process posed a number of chemistry and engineering challenges, as well as the cost and complexity of operating two separate solvent-extraction processes with different solvents. The goals of the STMAS were to develop simplified separation approaches, with more robust operational parameters, so that both the chemistry and engineering of the process could be well characterized and understood.

The two primary focus areas investigated under the STMAS, are enhanced selectivity of An(III) over Ln(III) by selective complexation and the utilization of the higher valence states of americium (primarily V and VI) to selectively extract americium from Ln(III) and Cm(III). In the area of advanced complexation, new approaches such as the "Advanced TALSPEAK" process, which utilizes a weaker organic extractant 2-ethylhexylphosphonic acid mono-2-ethylhexyl ester or HEH [EHP], along with a weaker aqueous soluble complexant *N*-(2-hydroxyethyl)ethylenediamine-*N*,*N*′,*N*′-triacetic acid or HEDTA in a citrate buffer to selectively extract the lanthanides from the trivalent actinides (Braley et al., 2012). In the Advanced TALSPEAK process, the distribution coefficients for Ln(III) and An(III) are much flatter across the pH range of interest (~2.8-3.5). In addition, the chemistry of the citrate buffer appears to be more predictable and less complex in comparison to the lactate buffer in the TALSPEAK process. Attempting to further simplify the separation of the trivalent actinides from lanthanides has led to the development of the actinide-lanthanide separations (ALSEP) concept, which effectively combines the two step

TRUEX-TALSPEAK functions into a single process (Gelis and Lumetta, 2014). The ALSEP process utilizes a solvent containing *N*,*N*,*N*′,*N*′-tetra(2-ethylhexyl)diglycolamide (T2EHDGA) plus HEH[EHP] dissolved in *n*-dodecane. The ALSEP solvent extracts both trivalent actinides and lanthanides (except for lanthanum and possibly cerium), and then uses an aqueous soluble complexant, HEDTA, in a citrate buffer to selective strip the actinides from the lanthanides.

The approach to exploit higher oxidation states of americium has been demonstrated using diamylamylphosphonate (DAAP) as the extractant in a solution where americium has been oxidized to Am(VI) using sodium bismuthate (Mincher et al., 2012). The challenge for this process is to effectively oxidize americium to the hexavalent state and be able to stabilize it in that valence state, long enough to perform the extraction process. A major focus of the program has been to search for alternative oxidation/stabilization agents for americium.

Another area of great importance to the understanding of these solvent extraction approaches is the radiation chemistry of the solvents and the systems, particularly the stability of the solvent due to radiolysis and hydrolysis, as well as the effect of radiation and free radical formation on the valence states of multivalent cations (such as neptunium and possibly americium, if oxidized). Developing a fundamental scientific understanding of the chemistry of separations processes, including the radiation chemistry, thermodynamics, and kinetics of the systems, is an integral part of the U.S. Separations and Waste Form Campaign research effort.

In the area of electrochemical processing of fuel, the primary effort in the U.S. Fuel Cycle Technologies program is part of a collaboration between the United States and the Republic of Korea to demonstrate at the kilogram scale the electroreduction of oxide fuel and the electrorefining of the resultant metal to recover uranium and U/TRU fractions. This research program is planning to process a large number of sequential kg-scale batches of fuel in an integrated process. This demonstration is currently scheduled for the 2016-2017 time frame. Additional research in the U.S. domestic electrochemistry program focuses on the recovery of U/TRU on nonalloying metal cathodes. As described in an earlier chapter, recovery of uranium from spent Experimental Breeder Reactor-II fuel has been ongoing at the Idaho National Laboratory for about two decades, processing over 4 tons of driver and blanket fuels.

19.4 Future trends

Only a decade ago, many approaches to the partitioning of trivalent actinides from lanthanides were still based on two-step processes with TALSPEAK-type chemistry, utilizing bis(2-ethylhexyl)phosphonic acid (HDEHP) as an extractant. There is a very common trend between U.S. and European research programs to simplify and combine processes to a single-process approach (after a process to remove uranium or uranium, plutonium (and possibly neptunium)). There are a number of similarities to the SANEX and GANEX approaches studied in Europe with the ALSEP process chemistry. Most notable is the trend that many approaches are converging toward

the use of diglycolamide extractants and aqueous soluble complexants to selectively strip An(III) or americium. While these approaches were arrived at somewhat independently (with a healthy awareness of published literature), the collaboration between international research programs is increasing. The U.S. Separations and Waste Form program is planning to perform laboratory-scale flow sheet tests in the near future with simulant feeds and eventually used nuclear fuel, and these tests will most likely involve international support or participation. While the United States appears to be the only group actively investigating higher oxidation states of americium, there is a common interest in processes that separate americium without curium, to potentially simplify the transmutation fuel fabrication process. French and European research programs have made significant progress in americium extraction processes based on selective complexation.

In the area of electrochemical processing, there is much common interest in the general approach, but less convergence on the specific technologies. The European Union programs are investigating solid alloying cathodes for the recovery of U/TRU. There are many similarities in approaches by the Republic of Korea and Japan with the U.S. approach, but each has unique aspects aimed at addressing issues of importance for each country.

The U.S. Fuel Cycle Technologies program objectives are to develop technical options to support future decisions by the U.S. government on nuclear fuel cycles. Currently, the focus of the U.S. program is the near-term storage and disposal of existing light-water reactor fuel. The long-term research and development focus is the development of separation technologies, transmutation fuels, and advanced waste forms, for a closed fuel cycle. The overall time line, according to the current Nuclear Energy R&D Roadmap is to deploy advanced fuel cycles, if selected, by about 2050. In support of this long-term goal, the separations program is researching advanced separation technologies leading to laboratory-scale testing of these technologies with simulated feeds in the 2016-2017 time frame and with actual used fuel in the 2017-2020 time frame. Longer-term activities include scale-up testing at the engineering scale with simulated and eventually actual fuel, approximately in the mid-2020s time frame. This testing will provide data that will be used to evaluate the technical and economic viability of advanced closed fuel cycles in support of future nuclear energy policy decisions by the U.S. government. For this reason, a primary driver for the separations and waste form program is to develop technologies that have robust operational conditions and are as simple as possible to make them industrially useable and cost effective.

References

Braley, J.C., Grimes, T.S., Nash, K.L., 2012. Ind. Eng. Chem. Res. 51, 629–638.

Gelis, A.V., Lumetta, G.J., 2014. Ind. Eng. Chem. Res. 53 (4), 1624–1631.

Gelis, A.V., Vandegrift, G.F., Bakel, A., Bowers, D.L., Hebden, A.S., Pereira, C., Regalbuto, M., 2009. Radiochem. Acta 97, 231–232.

Gregson, C., Boxall, C., Carrott, M., Edwards, S., Sarsfield, M., Taylor, R., Woodhead, D., 2012. Procedia Chem. 7, 398–403. http://dx.doi.org/10.1016/j.proche.2012.10.062.

Horwitz, E.P., Kalina, D.G., Diamond, H., Vandegrift, G.F., Schulz, W.W., 1885. Solvent Extr. Ion Exch. 3, 75–109.
Mincher, B.J., Martin, L.R., Schmitt, N.C., 2012. Solvent Extr. Ion Exch. 30, 445–456.
Sarsfield, M., Sims, H., Taylor, R., 2009. Solvent Extr. Ion Exch. 27 (5-6), 638–662.
Weaver, B., Kappelmann, F.A., 1968. J. Inorg. Nucl. Chem. 30, 263–272.
Wigeland, et al., 2014. Nuclear Fuel Cycle Evaluation and Screening Final Report, INL/EXT-14-31465. Idaho National Laboratory.

Development of closed nuclear fuel cycles in China

20

Ye Guoan, Yan Taihong
China Institute of Atomic Energy, Beijing, China

Acronyms

ADS	accelerator driven system
AHA	acetohydroxamic acid
APOR	advanced process based on organic reagents
BTP	bis-triazinyl-pyridine
CDFR	China demonstration fast reactor
CEFR	China experimental fast reactor
CIAE	China Institute of Atomic Energy
CMPO	octyl(phenyl)-*N*,*N*-dibutyl carbamoylmethyl phosphine oxide
DHOA	*N*,*N*-dihexyloctamide
DHU	dihydroxyurea
DIAMEX	diamide extraction
DIDPA	diisodecylphosphoric acid
DMHAN	*N*,*N*-dimethylhydroxylamine
FBR or FR	fast breeder reactor or fast reactor
FP	fission product
HEU	highly enriched uranium
HLLW	high-level liquid waste
HSC	hydroxyl-semicarbazide
HU	hydroxyurea
LEU	low enriched uranium
MA	minor actinides
MH	methylhydrazine
MOX	mixed oxide
MSR	molten salt reactor
NPP	nuclear power plant
PUREX	plutonium uranium extraction
PWR	pressurized water reactor
R&D	research and development
RPP	reprocessing pilot plant
TBP	tributyl phosphate
TRPO	trialkylphosphineoxide
TODGA	*N*,*N*,*N*′,*N*′-tetraoctyldiglycolamide
TRU	transuranic

Reprocessing and Recycling of Spent Nuclear Fuel. http://dx.doi.org/10.1016/B978-1-78242-212-9.00020-4

20.1 Introduction

With the development of China's economy, the domestic energy demand is expected to grow; before 2020 being predicted to reach an installed capacity for electricity production of about 58 GWe (National Energy Administration, 2013). Therefore, it has been concluded that nuclear energy is an important option in the Chinese energy mix. In accordance with *The Medium and Long-Term Nuclear Power Development Planning (2007-2020)* (National Development and Reform Commission, 2007), China is expanding its civil nuclear power programs to meet its energy needs. China's nuclear power installed capacity, including that in operation and under construction, is predicted to be higher than 80 GW by 2020. In order to realize the sustainable development of Chinese nuclear energy, a three-stage strategic plan has been devised:

- In the first stage, natural uranium would be used in thermal reactors; thermal reactors are the main type of nuclear power provision.
- Plutonium extracted from the spent fuel of these thermal reactors by reprocessing would drive fast reactors in the second stage. The second stage is mainly to develop fast reactors and realize the transition from thermal reactors to fast reactors.
- The final stage is the development of fission-fusion systems.

Without a doubt, the success of the sustainable development of fissile energy is based on the establishment of an efficient closed fuel cycle approach with recycling of both fissile and fertile components of the spent fuel to appropriate reactor systems (OECD/Nuclear Energy Agency, 2013; International Atomic Energy Agency, 2013). Spent fuel reprocessing is the vital link in the closed fuel cycle, especially for the transition from an advanced thermal reactor to a fast reactor-based fuel cycle. Reprocessing used nuclear fuel improves fuel utilization by extracting additional energy from the recycled uranium and plutonium. Recycling the plutonium into future fast reactors or high-conversion thermal reactors could achieve a significant improvement in resource utilization. Reprocessing also reduces the radiological hazard from spent fuel, resulting in an improvement in repository performance in scenarios in which the repository may be disturbed. To date, the PUREX process has been the only commercially used process for the recovery of plutonium and uranium from commercial used fuel in the world. For the advanced reprocessing of future used fuels, the objective is not only to recover plutonium and uranium, but also to manage all minor actinides and fission products (Wigeland et al., 2006; Polyakov et al., 2000). In this regard, many studies have already been made exploring new reprocessing technologies and new separation methods (Nash and Lumetta, 2011a).

The objective of this chapter is to give a brief overview on the status and the future prospects of reprocessing and recycling of spent nuclear fuel in China, in the context of China's nuclear power and nuclear fuel cycle deployment. Recent research and development of spent nuclear fuel reprocessing in China is described. Some processes for the minor actinides separations are also described. Finally, prospects for further development and future trends in managing the back end of the nuclear fuel cycle in China are also discussed.

20.2 Recycling strategy for spent nuclear fuel

20.2.1 Nuclear power deployment

In the future, nuclear power will play a bigger role in improving China's energy structure, coping with climate change, and controlling air pollution. Up to December 2013, 17 nuclear reactor units were under commercial operation and an additional 28 units were under construction. Total installed capacity reached 14833.79 MWe, accounting for about 2.11% of total electricity supply (as shown in Figure 20.1) (China Committee of Nuclear Power Operators, 2014).

Significant research and development (R&D) programs have been pursued worldwide, bringing the knowledge on fast reactor technology to a high level of maturity. In China, the national program on fast reactors is a part of the ambitious objective to reach a nuclear electricity ratio of more than 20% by 2050 (Zhang, 2013; Xu, 2008). The first step of this program is acquisition of the necessary experience through the operation of the China experimental fast reactor (CEFR), which was connected to the grid in 2011. Currently, the construction of the demonstration reactor CFR-600 is planned by 2025-2030, which will act as bridge to the commercial fast reactor by 2040-2050.

20.2.2 Development of the closed fuel cycle

In order to match nuclear power development with consideration for the domestic condition and the reality of the Chinese nuclear industry, it is necessary to set up a complete nuclear fuel cycle system (Ye, 2011). The principles applying to China's nuclear fuel development are the following: a combination of opening up from abroad and domestic orientation of fuel supply; and adopting the reprocessing option for spent fuel from NPPs and abiding by the state regulations on radiation protection and environmental protection to ensure the safety of nuclear facilities and personnel. For spent

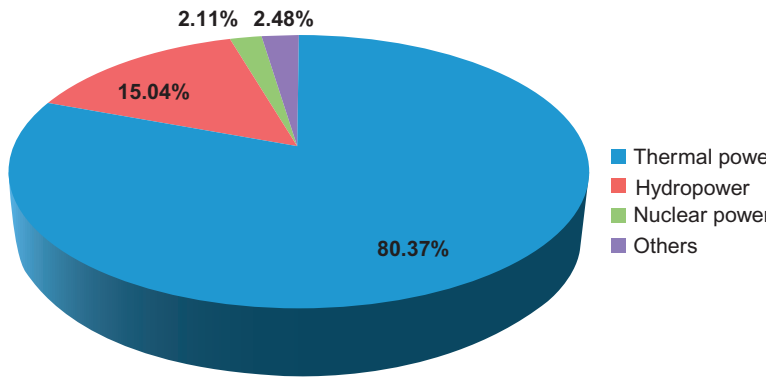

Figure 20.1 Distribution of total electricity production of China in 2013.

fuel management, the reasons why a closed fuel cycle strategy has been selected are the following:

- Full utilization of uranium resources and development of FBR.
- Disposal of radioactive wastes safely after separation of uranium and plutonium from spent fuel.

The middle-to-long-term plan to develop a closed fuel cycle has been considered, as shown in Figure 20.2. In the first stage, an experimental-scale manufacturing line for MOX fuel pellets was built near to the reprocessing pilot plant (RPP). Design of a MOX fuel assembly for CEFR, as well as the primary performance analysis, was carried out (Yu and Huang, 2013). Part of the reprocessed uranium will be used as fuel in a CANDU reactor. Up to now, the MOX pellet fabrication facility to provide MOX fuel for CEFR is under construction with the capability to process 500 kg/y (heavy metal). Spent fuel reprocessing is also a vital link in implementing the closed fuel cycle, especially for the advanced thermal reactor-fast reactor-based fuel cycle (International Atomic Energy Agency, 2011). In China, the first power reactor spent fuel reprocessing pilot plant (RPP) based on the conventional PUREX process has been taken through active commissioning in 2010, which indicates that China has obtained independent capability in reprocessing technology for PWR spent fuel (Zhang et al., 2011).

In the second stage, CDFR will be constructed based on the experience of CEFR. Furthermore, a new MOX fuel fabrication plant for CDFR will also be considered. Commercial reprocessing plants for PWR and fast reactor spent fuels, developed from

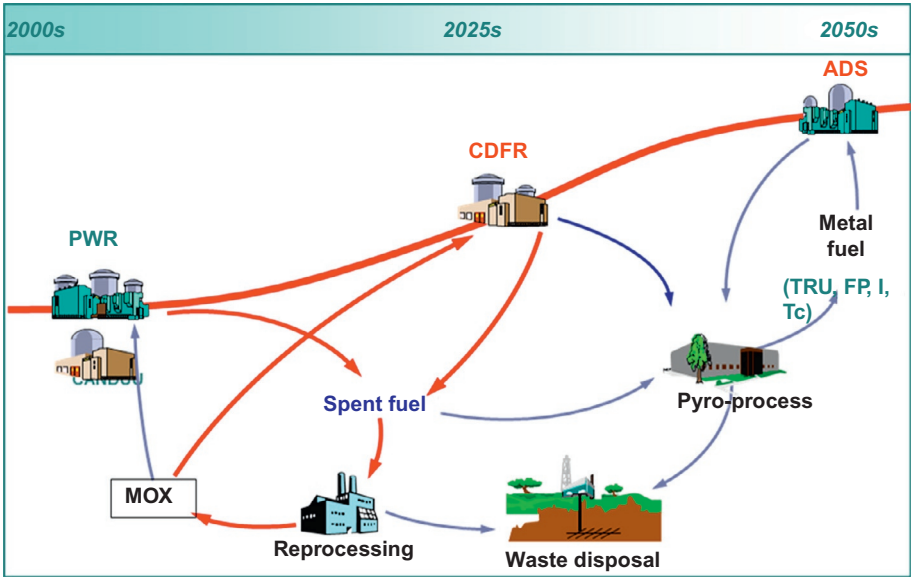

Figure 20.2 Middle-to-long-term plan to develop the closed fuel cycle in China.

the basis gained with the RPP, will need to be constructed in the near future. At the same time, metal fuel for future fast reactor and ADS technology are also under consideration.

The R&D of reprocessing technologies for PWR and fast reactor spent fuels are reviewed in greater detail in the ensuing section.

20.3 Development of reprocessing technology

In the PUREX process, uranium and plutonium are recovered through multiple extraction cycles based on differences between extraction behaviors of uranium, plutonium, other actinides, and fission products. The PUREX process was first developed in the United States in the 1950s and, thereafter, it was used to treat irradiated nuclear fuel from power plants in many countries including France, the United Kingdom, Russia, India, Japan, and China. It can be safely said that the PUREX process achieved worldwide acceptance as the premier fuel reprocessing scheme, still occupies that position today, and will possibly remain there in the foreseeable future.

20.3.1 Process of RPP

The main process in the RPP for spent LEU fuel reprocessing is based on a mechanical headend process followed by the PUREX-type process comprising two TBP extraction cycles and tail end processes (Zhang et al., 2011; Zheng and Ye, 2000). The functions of the RPP are as follows:

- Demonstrate the processes, equipment, and instrumentation under hot conditions.
- Experience accumulation in the design, construction, and operation.
- Train the operational personnel.
- Recover highly enriched uranium (HEU) from spent fuel from research and test reactors.
- Undertake R&D into reprocessing technology for MOX spent fuel in the future.

The designed and studied steps include the following: a shear-leach process, a clarification process including pulse filtration, porous stainless steel sintered tubes and centrifugation, a process for removal of radioiodine from the dissolution off-gas, a spent solvent treatment system using hydrazine carbonate, denitration of uranyl nitrate solution to UO_3, and others. Through 5%, 50%, and 100% active commissioning, a massive amount of data was accumulated for each process step. The recovery rates of uranium and plutonium, decontamination factors, and separation factors obtained satisfied the designed index. Qualified uranium trioxide and plutonium dioxide products were obtained. Recovered plutonium will be fabricated into MOX fuel for the fast reactor in a small-scale demonstration facility.

At present, some R&D studies are undertaken in institutes and universities, to ensure stable and safe operation of the RPP with a modified two-extraction cycle PUREX process. The aim is to optimize the process and minimize radioactive wastes, introducing the modified process after sufficient experience is obtained with RPP.

A lot of research is also being done to develop an advanced PUREX process for the future fuel cycle.

20.3.2 APOR process for PWR spent fuel reprocessing

Future reprocessing plants need to operate safely with minimum environmental impact and at a high level of safety. At the same time, higher requirements should be reached for the future spent fuel reprocessing due to the increase of the burn up of fuel. Research and development of salt-free technology is one of the important fields to meet these requirements.

20.3.2.1 Application of organic reagents

In present-day spent nuclear fuel reprocessing plants in the United Kingdom, France, and Japan, uranium and plutonium are separated by the reductive back-extraction of plutonium with hydrazine-stabilized tetravalent uranium (International Atomic Energy Agency, 2005). A serious obstacle to the success of this processing step is that the solutions to be processed contain technetium, which is among the few fission products extractable into tributyl phosphate together with uranium and plutonium. The significance of technetium is due to its catalytic action on the oxidation of uranium(IV) and hydrazine by nitric acid (nitrate anion). This results in increased plutonium accumulation on the extractor stages and, in some circumstances, in the complete failure of U/Pu separation (Taylor et al., 1987; Mashkin and Belyaev, 2006).

Therefore, reductants play an important role in the PUREX process. One important trend in the development of a future solvent-extraction process for reprocessing is the usage of salt-free, highly efficient reductants in U/Pu separation (Koltunov and Marchenko, 1998; Ye, 2004; Koltunov et al., 2000), such as butyraldehyde and isobutyraldehyde (Uchiyama et al., 1993; Wu et al., 1998) and, especially, hydrazine and hydroxylamine as well as their derivatives (Koltunov and Baranov, 1993; Zhang et al., 1997, 2001; He et al., 2002). In China, a series of salt-free organic reagents have also been studied extensively, such as acetohydroxamic acid (AHA) (Zheng et al., 2001), hydroxyurea (HU) (Zhu et al., 2004), dihydroxyurea (DHU) (Yan et al., 2009, 2010), and hydroxyl-semicarbazide (HSC) (Xiao et al., 2009). Interactions of these reagents with Pu(IV), Np(VI) were systematically studied. Further potential applications to U/Pu and U/Np separation in the PUREX process were also studied.

N,*N*-dimethylhydroxylamine (DMHAN) is a type of derivative of hydroxylamine in which two hydrogen atoms are substituted by methyl groups. An advanced plutonium and uranium recovery process has been established based on two organic reductants: *N*,*N*-dimethylhydroxylamine (DMHAN) and methylhydrazine (MH) as U/Pu separation reagents. The proposed flow sheet of the APOR (advanced PUREX process based on organic reductants) process is indicated in Figure 20.3. The APOR process is composed of three cycles: a U,Pu codecontamination/separation cycle, the uranium purification cycle, and plutonium purification. With using DMHAN and MH in the U,Pu codecontamination/separation cycle and plutonium purification cycle as

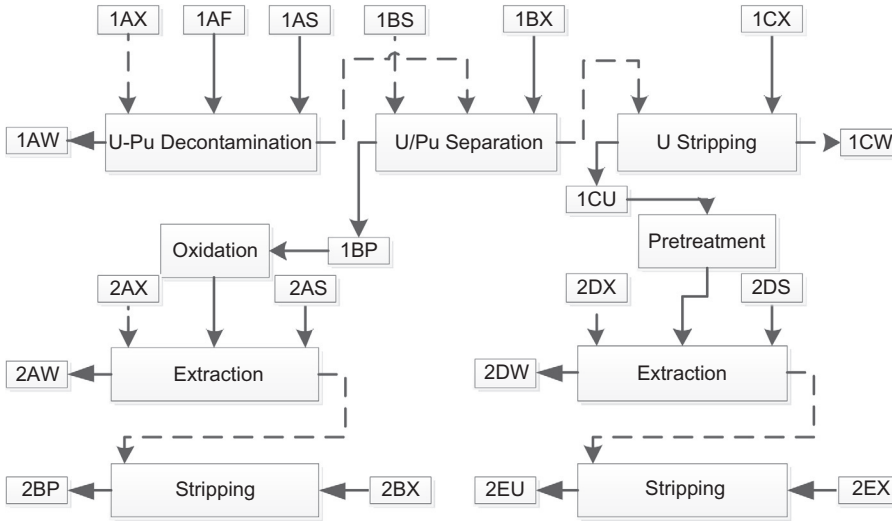

Figure 20.3 The proposed flow sheet of the APOR process.

plutonium stripping reagents, the APOR process exhibits high performance and can be characterized in general terms by

- high efficiency of U/Pu separation that can be achieved by DMHAN and MH in the first cycle;
- plutonium product solution of high concentration can be obtained in the plutonium purification cycle with a simple extraction-stripping operation instead of circumfluence extraction; and
- the process is simplified because of the elimination of the technetium scrubbing operation and the supplementary extraction operation.

U/Pu separation: In the U/Pu separation stage of the APOR process, DMHAN is used as a reducing agent for Pu(IV). Pu(IV) can be reduced by DMHAN quickly and completely. However, it is imperative to understand that Pu(III) is an unstable species at conditions of U/Pu separation and rapidly reoxidizes to Pu(IV) in the presence of nitrous acid. So MH is used as a nitrite scavenger to prevent the autocatalytic reoxidation of Pu(III). The experimental results showed that the recovery rate of plutonium is 99.98%, the separation factor of plutonium from uranium ($SF_{Pu/U}$) is about 2.5×10^4, and the separation factor of uranium from plutonium ($SF_{U/Pu}$) is about 6.11×10^4. High efficiency of U/Pu separation can be achieved even in the presence of technetium.

Technetium pathway: The behavior of technetium in the decontamination step is basically the same as in the decontamination step of the conventional PUREX process. Traditionally, technetium should be stripped from the solvent before the U/Pu separation step in order to avoid the effects of its autocatalytic reaction in U/Pu separation. In the APOR process, the extracted technetium enters completely into the U/Pu separation step. DMHAN has no obvious interactions with technetium, while

MH can reduce Tc(VII) to its inextractable low valence state (Wang et al., 2012).As a result, higher than 99.9% of technetium can be stripped into the aqueous stream with plutonium. In the plutonium purification cycle, technetium can be separated and routed into the aqueous raffinate waste stream.

Neptunium pathway/control: The separation of neptunium in the PUREX process is one of the main problems in spent fuel reprocessing because of the complexity in its chemical behavior (Taylor et al., 1997; Lin, 1995). The behavior of neptunium in the APOR decontamination step is similar to that in the decontamination step of the traditional PUREX process. Through increasing the acidity of feed and scrub solution, most of the neptunium would coextract into 30% TBP/kerosene with uranium and plutonium. In the U/Pu separation step, DMHAN and MH are used as reducing agents for Pu(IV). Experiments showed that the reduction of Np(VI) to Np(V) by DMHAN is quick, while further reduction of Np(V) to Np(IV) is so slow that no Np(IV) is observed in several hours at room temperature. The rig-scale test showed less than 1% of neptunium entered into the uranium stream and more than 99% of neptunium was stripped into the aqueous stream with the plutonium (labeled 1BP in Figure 20.3). In the plutonium purification cycle, about 98% of neptunium entered into the aqueous raffinate (2AW) and less than 2% of neptunium entered into the plutonium product stream. After the uranium purification cycle, the uranium product, meeting the specification, can be obtained by taking further technical measures.

20.3.2.2 Electrolytic partition of uranium and plutonium

Conventional solvent-extraction contactors, mixer-settlers or pulsed columns, have been used exclusively till now for the uranium and plutonium-partitioning step. The development of in situ electrolytic apparatus for the PUREX process is also mainly based on these two extraction contactors. Both apparatuses integrate electroreduction of tetravalent plutonium into liquid-liquid extractors. Researchers at Karlsruhe (Schmieder et al., 1974) have developed electrode-equipped mixer-settlers, in which the reduction occurred largely in the settled aqueous phase rather than in a heterogeneous mixture.

We designed a new type of electrolytic mixer-settler for uranium and plutonium separation (as shown in Figure 20.4) (Yuan et al., 2013); key features are an “E” shaped cathode and “U” shaped anode in the settling chamber. Because the cathodes of each stage are no longer connected, the current of one stage will not affect the current of the other stages. In the settling cell, both aqueous and organic phases have to flow through the channel that is formed by the electrodes. Therefore, the retention of the feed in the settling chamber is eliminated to a minor level. The experimental results show that this new type of mixer-settler has excellent separation performance. Flow ratio of feed solution (1BF) to the aqueous extraction stream (1BX) and to the organic wash stream (1BS) is 4:1:1. With the organic feed of 84 g/L uranium and 1.40-2.64 g/L plutonium, both the separation factors of plutonium from uranium and that of uranium from plutonium are apparently higher than 10^4.

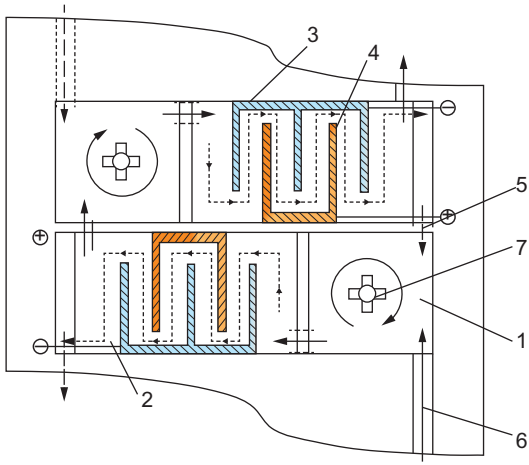

Figure 20.4 Schematic diagram of the new type electrolytic mixer-settler where 1 is the mixing chamber; 2, settling chamber; 3, "E" shape cathode; 4, "U" shape anode; 5, aqueous phase; 6, organic phase; 7, stirrer.

20.3.2.3 Plutonium valence adjustment with N_2O_4 (Zhang et al., 2002; Li et al., 2011)

The plutonium valence adjustment back to Pu(IV) in the PUREX process is a crucial problem. In the PUREX process, Pu(IV) is reduced to Pu(III) rapidly by a reductant at room temperature, and HNO_2 in the reaction system is cleared up rapidly by a holding reagent. The main purpose of the follow-up process is to oxidize Pu(III) back to Pu (IV) with salt-free oxidants. There have been several methods of oxidizing Pu(III) to Pu(IV). The N_2O_4 oxidation method is one of the class using salt-free reagents. The effects of the concentration of Pu(III), temperature, acidity, and so forth, on adjustment of plutonium in different 1BP and 2BP solutions by N_2O_4 have been studied. The experimental results show that quantitative oxidations of different systems [DMHAN-MMH-Pu(III), NH_2OH-N_2H_4-Pu(III), and U(IV)-N_2H_4-Pu(III)] can be achieved. Pu(III) oxidation is fast and complete. Further work on the scale-up of equipment and corresponding process parameters is in progress.

20.3.3 R&D for fast reactor MOX spent fuel reprocessing

Significant experience has been obtained in the reprocessing of thermal neutron reactor spent fuels using PUREX technology. It is proven that the PUREX process or its modified versions may be used for fast reactor oxide fuels as well. However, fast reactor fuel reprocessing differs from thermal reactor reprocessing in many respects (UKEA, 1980). The differences arise mainly from the following characteristics of spent fast reactor fuels:

- Higher specific activity and decay heat generation due to high fission products content.
- Higher plutonium content.
- Different assembly structure and presence of sodium on assemblies in the case of sodium-cooled reactors.

High fission products content due to the high burn up and short cooling time of FBR spent fuel increases the difficulties encountered in spent fuel dissolution and actinide products decontamination (when using aqueous recycling). More codecontamination cycles to achieve targeted decontamination factors from fission products may thus be required, which leads to an additional U,Pu costripping process between each codecontamination cycle. Associated with high plutonium content are problems relating to plutonium distribution, plutonium polymerization, third-phase formation, criticality, and so on. As a result, the objective of the U,Pu costripping process is to minimize the problem of plutonium polymerization during stripping while at the same time ensuring maximum plutonium recovery.

As an indispensable component of the FBR fuel cycle, the study of FBR spent fuel reprocessing in China was initiated in the 2000s. The schematic of the modified PUREX process flow sheet that is deployed for reprocessing MOX spent fuel is given in Figure 20.5. After chopping the fuel pins, the fuel pellets are dissolved in concentrated nitric acid. This dissolved solution is then subjected to solvent extraction with 30% TBP/kerosene for decontamination from fission products. Complete (or partial) separation of plutonium from uranium is performed by *in situ* electrolytic reduction. The R&D efforts carried out in various process steps are given in the following sections.

Countercurrent tests were carried out in mixer-settlers with simulated feed solutions, which contained uranium and plutonium under the condition that nitric acid concentration was adjusted to 4 mol/L, and 3 mol/L of HNO_3 was used as the scrubbing solution. The concentration of plutonium in the extraction-scrubbing bank at the organic phase was below 20 g/L, which reduced the possibility of third-phase formation. In the costripping bank, the possibility of plutonium polymerization is reduced by

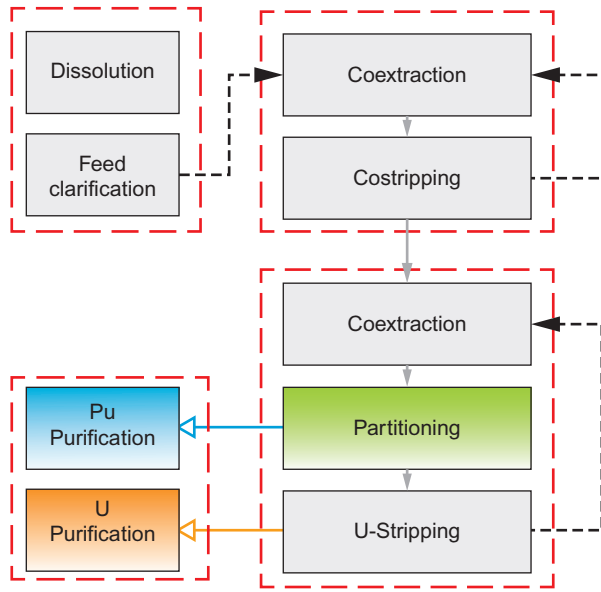

Figure 20.5 The schematic flow sheet for fast reactor MOX spent fuel reprocessing.

using a dual strip and maintaining a sufficient acid concentration that is commensurate with plutonium concentration. The results showed that the recovery rates for uranium and plutonium were 99.998% and 99.991%, respectively. In the costripping step, the recovery rates for uranium and plutonium were 99.94% and 99.994%, respectively (Zuo et al., 2013).

20.4 Separation of minor actinides

For the purpose of sustainable development of nuclear energy, uranium and plutonium in spent nuclear fuel will be recovered via reprocessing, which generates high-level liquid waste (HLLW). The main remaining long-term radiotoxicity in HLLW comes from the minor actinides (MAs). Partitioning and transmutation of minor actinides is one important option for high-level waste disposal. Therefore, the separation of MA from HLLW and separation of An from Ln is of importance. Up to now, several flow sheets for MA separation have been developed or even demonstrated at the laboratory scale, using simulated or genuine nuclear fuel solutions, such as TRUEX (Nash and Lumetta, 2011b), TRPO (Song and Zhu, 1994), DIDPA (Morita et al., 1996), DIAMEX (DIAMide EXtraction) (Serrano et al., 2005) processes, and others. The following section will give a brief introduction into R&D related to separation of HLLW in China.

20.4.1 TRPO process

The TRPO process for the removal of TRU elements has been developed since the 1980s by Tsinghua University (Song and Zhu, 1994). This is based on the use of trialkylphosphine oxide extractants (typically, Cyanex 923) to achieve a total actinide recovery from nitric acid-based HLLW. A schematic diagram of the TRPO process is shown in Figure 20.6. TRPO has good physicochemical properties and irradiation stability as well as excellent extraction selectivity to tri-, tetra-, and hexavalent

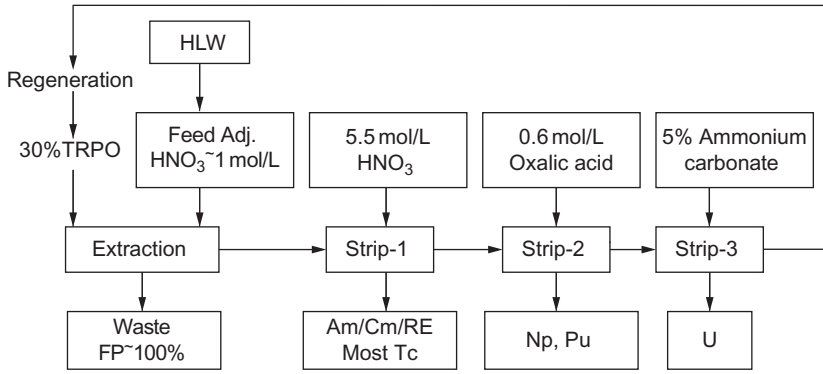

Figure 20.6 Schematic diagram of the TRPO process.

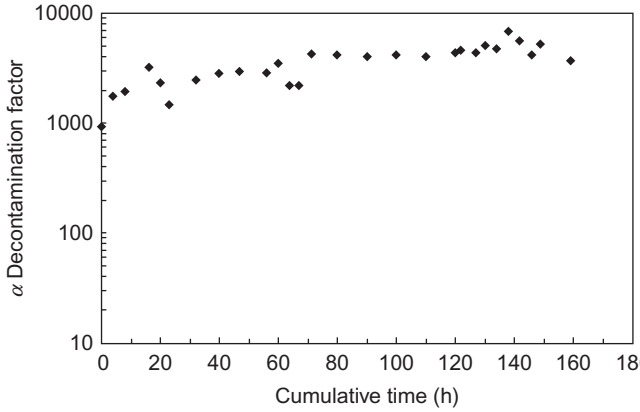

Figure 20.7 α-Decontamination factor obtained in the hot test treating defence HLLW by the TRPO process.

actinides. Hence, it was found that extraction percentages higher than 99% for U(VI), Np(IV,VI), and Pu(VI), from 1 mol/L HNO_3, were achieved using TRPO (with alkyl chains from C6 to C8) dissolved in kerosene (Song et al., 1992). In addition, Pu(III) and Am(III) can also be efficiently separated if the extraction conditions are adequately adjusted, whereas strontium, caesium, and ruthenium are only extracted at a remarkably low level. Several hot tests have been carried out by using the defence HLLW (Chen and Wang, 2011). The α-decontamination factor in the hot test is shown in Figure 20.7 and the results show that the average α-decontamination factor is higher than 3×10^3. No decrease of decontamination factor is found when using directly recycled TRPO. The average α-decontamination factors for ^{241}Am, ^{239}Pu, and uranium are higher than 4×10^3, 1.7×10^3, and 3×10^3, respectively.

20.4.2 TODGA-DHOA process

In recent years, diamide ligands have also been studied in China for their extraction ability toward minor actinides (Ye et al., 2000a,b; Chen et al., 1998). Some of these compounds exhibit excellent performance for minor actinides separation. *N*,*N*,*N*′,*N*′-tetraoctyldiglycolamide (TODGA) is one of the promising reagents for applications in the partitioning of trivalent actinides and lanthanides from HLLW solutions. Previous studies on TODGA focused on the distribution behaviors of metal ions in nitric acid solutions and design of new separation process (Sasaki et al., 2001, 2005). Unlike other reagents used for actinide partitioning, such as CMPO, DIDPA, and TRPO, which do not extract Sr(II), TODGA is reported to extract Sr(II) to a significant extent. This can possibly lead to the contamination of the product and may require additional decontamination steps. Furthermore, a third phase will form under higher concentrations of nitric acid. Some phase modifier must be added to the solvent-extraction system. Sasaki (Tachimori et al., 2002) found that DHOA added to TODGA/*n*-dodecane can increase the loading capacity of the extractant and thus suppress the formation of

the third phase. DHOA is composed of C, H, O, N atoms, which can be completely incinerated. Based on the previous studies of TODGA and DHOA, a new process for separation and recovery of actinides and lanthanides, and including the separation and recovery of strontium from HLLW was designed (Ye et al., 2013; Zhu et al., 2012, 2014), as shown in Figure 20.8. It uses the tridentate diglycolamide TODGA ligand and the monoamide DHOA and is termed the *TODGA process*.

Investigations on partitioning of HLLW for MAs have been conducted at CIAE, and the main results showed that (1) by adding DHOA, the third phase diminished while the distribution ratio of strontium decreased, thus separation of strontium should be realized using TODGA alone; (2) uranium and minor neptunium and plutonium could be back-extracted together using acetohydroxamic acid (AHA) as a complexing reagent; and (3) more than 95% americium was back-extracted with the rare earth elements (RE).

With regard to trivalent actinide separation from lanthanides, a conceptual process was proposed, and has been examined with simulated HLLW in multiple-stage centrifugal extractors. From the experiments, promising results were obtained.

20.4.3 An/Ln separation

A key challenge with the separation of minor actinides relates to the separation of trivalent actinides from the lanthanides because of their similar oxidation states, chemical properties, and ionic radii. The problem of selective extraction of actinides has been an extensively pursued area of research for over several decades in China. One type of promising extractant is Cyanex. The extraction behavior of bis(2,4,4-trimethylpentyl)dithiophosphinic acid (HBTMPDTP), purified from Cyanex 301, was first studied for extracting Am^{3+} and Ln (Zhu, 1995). Further countercurrent hot testing showed that An/Ln could be separated efficiently with high separation factors (Chen et al., 2002).

BTPs (1,2,4-triazin-3-yl bipyridines) and derivatives have been identified as excellent extractants for separation of actinides(III) from lanthanides(III) in nitric acid media. These BTP molecules can bind as tridentate ligands to metal cations.

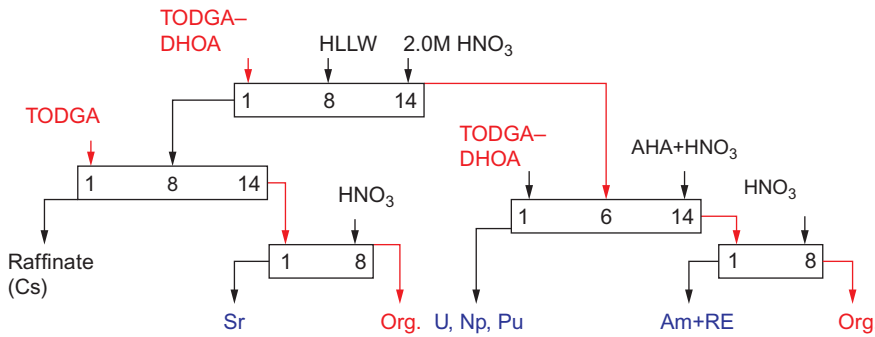

Figure 20.8 Schematic diagram of the TODGA process.

The separation efficiency of An/Ln was systemically studied using DPTP (2,6-bis(5,6-di-n-propyl-1,2,4-triazin-3-yl)-pyridine) (Tang et al., 2008), iPr-BTP (2,6-bis(5,6-di-isopropyl-1,2,4-triazin-3-yl)-pyridine) (Cheng et al., 2007), and C2-BTBP (6,6′-bis(5,6-diethyl-1,2,4-triazin-3-yl)-2,2′-bipyridine) (Hong et al., 2012). Though these extractants showed good selectivity for An/Ln separation, the degradation of BTPs by hydrolysis and radiolysis is a problem that needs to be solved before any engineering application.

20.5 Development of pyrochemical reprocessing

With the development of fast reactors (FRs) in China, accelerator-driven systems (ADS) and molten salt reactors (MSR), pyrometallurgy (dry reprocessing) is to be considered for the main route of spent fuel reprocessing and wastes partitioning, because of the high burn up (>100 GWd/te), high radiation, high heat release rate, high plutonium content, and high FP content. Based on the ambitious program to develop FR nuclear power, R&D on pyrochemical processing has been restarted in China.

Our recent work on pyrochemical studies mainly focuses on the measurement of basic parameters, including (1) electrochemical studies of uranium and rare earths both in molten chloride salts (LiCl-KCl) and molten fluoride salts (LiF-CaF_2 or lithium type cryolite); (2) dissolution of simulated fuel in molten salts; (3) purification and recycle of molten salts; and (4) some physical and chemical properties of the molten salts. Besides, development of equipment and techniques for process monitoring and control, precise measurement and control of temperature in molten salts has also received much attention.

Directions for improving the processes appear to be

- Minimization of TRU losses in wastes and increase of the purities of the separated actinide products.
- Routes to actinide products obtained through the combined use of several separations.
- Waste management, which is mostly corrosion-related owing to the aggressive nature of the salts.
- Characterization of the media and the high process temperatures need to be precisely estimated.

20.6 Conclusions

China is considering expanding its civil nuclear power programs to meet its growing energy needs. The closed nuclear fuel cycle is the strategic line of sustainable nuclear power development in China. This will ensure more efficient use of natural nuclear fuel and artificial fissile materials produced by reactors (e.g., plutonium) and will minimize radioactive waste by applying the partitioning and transmutation method. At present, the first power reactor spent fuel reprocessing pilot plant (RPP) based on

the conventional PUREX process has been completed with active commissioning in 2010. A lot of research is also being undertaken to develop an advanced PUREX process for future fuel reprocessing. An advanced plutonium and uranium recovery process has been established based on two organic reductants: dimethyhydroxylamine and methyl hydrazine. Considering the needs of further nuclear power development toward the fast reactor-based fuel cycle, recent research and development of FR spent nuclear fuel reprocessing is in progress following both advanced PUREX and pyrochemical options. Some innovative processes for the group separation of actinides from HLLW are also being developed in China.

References

Chen, J., Wang, J.C., 2011. Overview of 30 years research on TRPO process for actinides partitioning from high level liquid waste. Progr. Chem. 23, 1366–1371.

Chen, W.J., Zhu, L., Ding, S.D., Liu, Z.Q., Chen, S.J., Jin, Y.D., 1998. Influence of structure of diamides on the extractive properties of Eu(III) and Am(III). Chem. Res. Chin. Univ. 19 (11), 1724–1726.

Chen, J., Tian, G., Jiao, R., Zhu, Y., 2002. A hot test by purified Cyanex301 extraction in centrifugal contactors. J. Nucl. Sci. Technol. S3, 325–327.

Cheng, Q., Ye, G., Tang, H., 2007. Extraction of Am and Eu with iPr-BTP. J. Nucl. Radiochem. 29 (1), 23–26.

China Committee of Nuclear Power Operators, 2014. Nuclear power operation of China in 2013, 2014-02. Available from: http://www.china-nea.cn/html/2014-02/28745.html.

He, H., Hu, J., Zhang, X., Wang, F., 2002. The separation of U/Pu in multistages contactor with *N*,*N*-dimethylhydroxylamine and the simulation program. Atom. Energy Sci. Technol. 36 (2), 101–106.

Hong, Z., Ye, G., Tang, H., He, H., 2012. Separation of Am from Ln by C2-BTBP. J. Nucl. Radiochem. 35 (4), 211–215.

International Atomic Energy Agency, 2005. Status and Trends in Spent Fuel Reprocessing, Vienna, IAEA-TECDOC-1467.

International Atomic Energy Agency, 2011. Status of developments in the back end of the fast reactor fuel cycle, Vienna.

International Atomic Energy Agency, 2013. Nuclear Fuel Cycle Objectives. Vienna, NO, 1622.

Koltunov, V.S., Baranov, S.M., 1993. Organic derivatives of hydrazine and hydroxylamine in future technology of spent nuclear fuel reprocessing. Radiokhimiya 35, 11–19.

Koltunov, V.S., Marchenko, V.I., 1998. Stabilization of Pu and Np valences in PUREX process: problems and outlook. In: The French Nuclear Society and the European Nuclear Society. The 5th International Nuclear Conference on Recycling, Conditioning and Disposal. Nice, France, pp. 425–431.

Koltunov, V.S., Taylor, R.J., Baranov, S.M., et al., 2000. Acetaldoxime—a prompsing reducing agent for Pu and Np ions in the PUREX process. In: The French Nuclear Society.Proceedings of ATALANTE, France, 2000, O1-06.

Li, G., He, H., Zhen, W., et al., 2011. Study on valence adjustment of Pu in 1BP solution of CIAE-APOR process with N_2O_4. J. Radioanal. Nucl. Chem. 288 (1), 279–284.

Lin, Z., 1995. The behavior and control of neptunium in PUREX process. Chin. J. Nucl. Sci. Eng. 15, 72–76.

Mashkin, A.N., Belyaev, E.M., 2006. Instabilities of the reductive separation of uranium and plutonium in the PUREX process applied to spent nuclear fuel VVER-440 processing at the RT-1 plant. In: Materialy 5th Ross.konf.poradiokhimii "Radiokhimiya-2006". Proc. 5 Russian Conf. on Radiochemistry, Dubna, Moscow oblast, 2006, p. 198.

Morita, Y., Glatz, J.P., Kubota, M., 1996. Actinide partitioning from HLW in a continuous DIDPA extraction process by means of centrifugal extractors. Solvent Extr. Ion Exch. 14, 385–400.

Nash, K.L., Lumetta, G.J., 2011a. Advanced Separation Techniques for Nuclear Fuel Reprocessing and Radioactive Waste Treatment. Elsevier Science and Technology, Amsterdam.

Nash, K.L., Lumetta, G.J., 2011b. Advanced separation techniques for nuclear fuel reprocessing and radioactive waste treatment, Woodhead Publishing Series in Energy: Number 2. Woodhead, Cambridge.

National Development and Reform Commission, 2007. The medium and long-term nuclear power development planning (2005-2020). Available from: http://www.ndrc.gov.cn/gzdt/200711/W020071102332040700553.pdf.

National Energy Administration, 2013. The medium and long-term power generating capacity and electricity demand forecast. Available from: http://www.nea.gov.cn/2013-02/22/c_132185515.htm.

OECD/Nuclear Energy Agency, 2013. The Sodium Cooled Fast Reactor (SFR) Features a Fast-spectrum, Sodium Cooled Reactor and a Closed Fuel Cycle for Efficient Management of Actinides and Conversion of Fertile Uranium, Gen-IV. GENERATION IV International Forum, Paris, France.

Polyakov, A.S., Zakharkin, B.S., Smelov, V.S., 2000. Status and prospects for spent fuel reprocessing technology. Atom. Energy 89, 804–811.

Sasaki, Y., Sugo, Y., Suzuki, S., 2001. The novel extractants, diglycolamides, for the extraction of lanthanides and actinides in HNO_3-n-dodecane system. Solvent Extr. Ion Exch. 19, 91.

Sasaki, Y., Zhu, Z.X., Sugo, Y., 2005. Novel compounds, diglycolamides (DGA), for extraction of various metal ions from nitric acid to n-dodecane. In: Proceedings of GLOBAL. Tsukuba, Japan. Oct. 9-13, p. 344.

Schmieder, H., Baumgaertner, F., Goldacker, H., Hausberger, H., 1974. Electrolytic methods in the PUREX process. KFK-2082.

Serrano, P.D., Baron, P., Christiansen, B., 2005. Recovery of minor actinides from HLLW using DIAMEX process, Radiochim. Acta 93, 351–355.

Song, C.L., Zhu, Y.J., 1994. Partitioning of TRU elements from Chinese HLLW. In: China Nuclear Science and Technology Report, CNIC-00834. Atomic Energy Press, Beijing.

Song, C., Zhu, Y., Yang, D., He, R., Xu, J., 1992. The removal of actinide elements from high-level radioactive waste by trialkyl-phosphine oxide (TRPO). Cascade extraction verification with synthetic HAW solution. Chin. J. Nucl. Sci. Eng. 12, 225–234.

Tachimori, S., Sasaki, Y., Suzuk, S., 2002. Modification of TODGA-n-dodecane solvent with a monoamide for high loading of lanthanides(III) and actinides(III). Solvent Extr. Ion Exch. 20, 687–699.

Tang, H., Ye, G., Cheng, Q., 2008. Separation of Am from Ln in HNO_3 medium by DPTP in octanol-dodecane. J. Nucl. Radiochem. 42 (5), 390–395.

Taylor, R.J., Hudson, P.I., Phillips, C., 1987. Development of oxide fuel reprocessing at Sellafield. In: Back End of the Nuclear Fuel Cycle: Strategies and Options.Proc. YuntenSymp., Vienna, 1987, p. 399.

Taylor, R.J., Denniss, I.S., Wallwork, A.L., 1997. Neptunium control in an advanced PUREX process. Nucl. Energy 36, 39–46.

Uchiyama, G., Fujine, S., Hotoku, S., 1993. New separation process for neptunium, plutonium, and uranium using butyraldehydes as reductants in reprocessing. Nucl. Technol. 102, 341.
UKEA, 1980. Fast reactor fuel reprocessing. In: Proc. Symp. 1979. London, Dounreay Nuclear Power Development Establishment, Society of Chemical Industry.
Wang, H., Wei, Y., Liu, F., Jia, Y., Liu, Z., 2012. Distribution of technetium in 1B tank of APOR process. J. Nucl. Radiochem. 34 (2), 109–113.
Wigeland, R.A., Bauer, T.H., Fanning, T.H., Morris, E.E., 2006. Separations and transmutation criteria to improve utilization of a geological repository. Nucl. Technol. 154, 95–106.
Wu, Y., Lin, Z., Chen, Y., 1998. Studies on reaction kinetic of nitrous acid with n-butylaldehyde and Np(VI). J. Nucl. Radiochem. 17 (4), 216–222.
Xiao, S., Ye, G., Liu, X., Luo, F., Li, H., Li, F., 2009. Kinetics of reaction between hydroxysemicarbazide and HNO_2 in perchloric acid solution. Atom. Energy Sci. Technol. 45 (4), 402–406.
Xu, M., 2008. The status and prospects of fast reactor development in China. Eng. Sci. (1), 70–76.
Yan, T., Zheng, W., Ye, G.A., Zhang, Y., Xian, L., Di, Y., Bian, X., 2009. Synthesis of dihydroxyurea and its application to the U/Pu split in the PUREX process. J. Radioanal. Nucl. Chem. 279 (1), 293–299.
Yan, T., Zheng, W., Zuo, C., Xian, L., Zhang, Y., Bian, X., Li, R., Di, Y., 2010. The reduction of Np(VI) and Np(V) by dihydroxyurea and its application to the U/Np separation in the PUREX process. Radiochim. Acta 98 (1), 35–38.
Ye, G., 2004. Review on the study and application of organic salt-free reagent in PUREX process. Atom. Energy Sci. Technol. 38, 152.
Ye, G., 2011. R&D activities on nuclear fuel cycle in China. In: The 1st China-Japan Academic Symposium on Nuclear Fuel Cycle. Shanghai, China, Dec. 2011.
Ye, G.A., He, J.Y., Jiang, Y.Q., 2000a. Study on the extraction of Am(III) and Eu(III) with Amidopodand I: study on extraction mechanism. J. Nucl. Radiochem. 22 (2), 65–72.
Ye, G.A., He, J.Y., Luo, F.X., 2000b. Study on the extraction of Am(III) and Eu(III) with Amidopodand II: extraction thermodynamic and absorption spectrum. J. Nucl. Radiochem. 22 (3), 136–143.
Ye, G., Zhu, W., Li, F., Lin, R., Li, H., 2013. Study on separation of minor actinides from HLLW with new extractant of TODGA-DHOA/Kerosene. In: Global 2013, p. 7502.
Yu, H., Huang, C., 2013. Fast reactor development strategy in China. In: 2nd Sino-French Seminar on Back-end of fuel cycle. Beijing, China. Sep., 2013.
Yuan, Z., Yan, T., Zheng, W., 2013. Electrolytic partitioning of uranium and plutonium based on a new type of electrolytic mixer-settler. Radiochim. Acta 101 (9), 547–552.
Zhang, D., 2013. Fast reactor development strategy in China. In: The International Conference on Fast Reactors and Related Fuel Cycles: Safe Technologies and Sustainable Scenarios—FR13, Paris, France, 4-7 March 2013.
Zhang, X., Ye, G., Xiao, S., Yin, D., Hu, J., 1997. Reduction of Np(VI) with monomethylhydrazine II: studies on partition of U-Np in Purex process. Atom. Energy Sci. Technol. 31 (4), 130–137.
Zhang, A., Hu, J., Zhang, X., et al., 2001. Hydroxylamine derivative in Purex process—VI. Study on the partition of uranium/neptunium and uranium/plutonium with *N,N*-diethylhydroxylamine in the purification cycle of uranium contactor. Solvent Extr. Ion. Exch. 19 (6), 965–979.
Zhang, S., Wei, X., Ye, G., Zhuang, W., Liu, S., Zhang, X., Fu, L., 2002. Study on adjustment of Pu valent state by N_2O_4 in PUREX process. Atom. Energy Sci. Technol. 27 (2), 130–137.

Zhang, T., Wang, J., Wu, T., Chen, G., Diwu, Y., Ru, F., 2011. The active commissioning process for a power reactor spent fuel reprocessing pilot plant in China. Chin. Sci. Bull. 56, 2411–2415.

Zheng, H., Ye, G., 2000. The status and prospect of nuclear fuel cycle back-end in China. In: Atalante 2000 Conference.

Zheng, W., Zhang, Z., Lin, Z., Chang, Z., Zhu, J., Zhu, Z., 2001. Study on separation of Np from U by acetohydroxamic acid in Purex process. Chin. J. Nucl. Sci. Eng. 21 (4), 369–374.

Zhu, Y., 1995. The separation of Americium from light lanthanides by Cyanex301 extraction. Radiochim. Acta 68 (2), 95–98.

Zhu, Z., He, J., Zhang, Z., 2004. Uranium/plutonium and uranium/neptunium separation by the Purex process using hydroxyurea. J. Radioanal. Nucl. Chem. 262 (3), 707–711.

Zhu, W., Ye, G., Li, F., 2012. Extraction of metal ions from aqueous nitric acid solutions with TODGA and DHOA I: extraction of Np(IV, V, VI) ions. J. Nucl. Radiochem. 34 (5), 262–268.

Zhu, W., Ye, G., Li, F., 2014. Extraction of metal ions from aqueous nitric acid solutions with TODGA and DHOA III: extraction of Am(III) and trivalent lanthanides ions. J. Nucl. Radiochem. 36 (1), 24–33.

Zuo, C., Li, C., Yan, T., 2013. U, Pu Co-recovery process: cascade experiments. J. Nucl. Radiochem. 35 (4), 211–215.

Development of closed nuclear fuel cycles in Korea

21

Yeong-il Kim, Hansoo Lee
Korea Atomic Energy Research Institute, Daejeon, South Korea

Acronyms

ACPF	advanced spent fuel conditioning process facility
ADHRS	active decay heat removal systems
AHX	air heat exchanger
ANL	Argonne National Laboratory
APR1400	Advanced Power Reactor 1400
CR	conversion ratio
DFDF	DUPIC fuel development facility
DHRS	decay heat removal system
DHX	decay heat exchanger
DUPIC	direct use of spent pressurized water reactor fuel in the Canadian deuterium uranium reactors
FHX	finned-tube sodium-to-air heat exchanger
FDHX	forced-draft sodium-to-air heat exchanger
IHTS	intermediate heat transport system
IHX	intermediate heat exchanger
IVTM	in-vessel fuel transfer machine
KAEC	Korea Atomic Energy Commission
KAEPC	Korea Atomic Energy Promotion Commission
KAERI	Korea Atomic Energy Research Institute
KORAD	Korea Radioactive Waste Agency
LCC	liquid cadmium cathode
OPR1000	Optimized Power Reactor 1000
PDHRS	passive decay heat removal systems
PGSFR	Prototype Gen IV SFR
PHTS	primary heat transport system
PHWR	pressurized heavy water reactor
PRIDE	pyroprocessing integrated inactive demonstration
PUMA	performance of uranium metal fuel rod analysis (code)
PWR	pressurized water reactor
REE	rare earth elements
SCIEL	supercritical carbon dioxide integral experiment loop
SFR	sodium-cooled fast reactor
STELLA	sodium integral effect test loop for safety simulation and assessment
TMI	Three Mile Island
TRU	transuranic

Reprocessing and Recycling of Spent Nuclear Fuel. http://dx.doi.org/10.1016/B978-1-78242-212-9.00021-6

21.1 Introduction

Since the first nuclear power plant was introduced in Korea in 1978, nuclear power has played an important role in achieving energy self-reliance and stabilizing electricity prices. There are now 19 PWRs (pressurized water reactors) and 4 PHWRs (pressurized heavy water reactors) in operation as of December 2012. According to The Fifth Basic Plan for Long-term Electricity Supply and Demand (Ministry of Knowledge Economy, 2010), one OPR1000 (Optimized Power Reactor 1000) (Cheong et al., 2007) and four APR1400 (Advanced Power Reactor) units (Cheong et al., 2007) are currently under construction, and six additional APRs will be constructed by 2024.

For the time being, it is certain that PWRs will remain the major source of nuclear power in Korea. However, as about 700 metric tons of spent fuel is annually discharged from the present nuclear fleet, the management of the spent fuels produced from those PWRs is an impending challenge. The spent fuels are temporarily stored on-site in the spent fuel storage facilities, whose limit will be reached from 2016. Therefore, a decision-making process for spent fuel management is necessary.

The first discussions on spent fuel issues were started in the 249th KAEC (Korea Atomic Energy Commission), which is the top policy making body in Korea, in 1998. In the 253rd meeting of the KAEC in 2004, the following policy statements were made:

- Spent fuel is stored at reactor sites by 2016.
- National policy will be established based on open discussion and public consensus.

In 2008, the National Assembly passed the Radioactive Waste Management law. According to this law, the KORAD (Korea Radioactive Waste Agency), with responsibility for interim storage of spent fuel and final disposal of high-level waste, was established in January 2009, and radioactive waste management funds were established under the administration of the KORAD. A low- and intermediate-level waste disposal facility is under construction, with a plan to operate the first-phase facility in 2014.

The KAEPC (Korea Atomic Energy Promotion Commission), which used to be the KAEC, set out the basic plan for the public and stakeholder engagement program for spent fuel management in November 2012. The basic plan included organization of an independent committee for developing a public consensus on spent fuel management, which was launched in October 2013. The committee will propose the direction of spent fuel management and interim storage, including seeking public and stakeholder participation.

There are various options for spent fuel management: long-term storage; direct disposal; international management; treatment in a closed fuel cycle, which is the combination of pyroprocessing with a SFR (sodium-cooled fast reactor); and others. The benefits of closed fuel cycles are well-known (Till and Chang, 2011; Glatz et al., 2013; Shadrin et al., 2013). The group separation of usable elements from spent fuel followed by transmutation in a fast reactor leads to reduction of waste volume by recovery of uranium, which comprises about 93% of spent fuel; downsizing repository

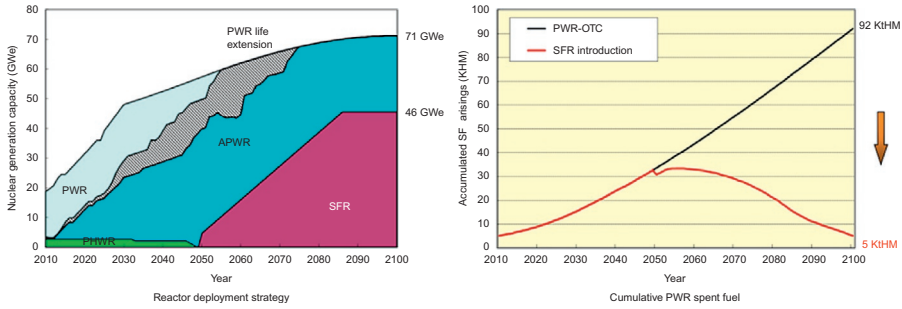

Figure 21.1 Reactor transition scenario and spent fuel inventories.

footprint by recovering long-lived high heat-emitting nuclides; and reduction of radiotoxicity, again by recovering long-lived highly radioactive nuclides.

In this closed fuel cycle, plutonium remains with other actinides throughout the process, which reduces the risk of nuclear proliferation. The radiation emitted by the TRU elements requires that the final product be confined in a hot cell and this self-protection also makes it far less open to misuse.

Introduction of the closed fuel cycle influences the strategy of reactor deployment. A favorable neutron balance is a feature of a fast reactor design and this makes waste management strategies flexible by introducing fast reactors with an appropriate CR (conversion ratio). Figure 21.1 is an example in which SFRs are introduced beginning in 2050 in the existing PWR-dominated fleet in Korea. The deployment of SFRs for TRU burning (CR $\sim$ 0.6) ensures a PWR spent fuel reduction of $\sim$95% and uranium savings of $\sim$31% by around 2100. The SFR mix ratio in the nuclear fleet near the year 2100 is estimated to be approximately 65%.

21.2 Future nuclear fuel cycle development requirements in Korea

To provide a consistent direction to long-term R&D activities, KAEC approved a long-term development plan in December 2008 for future nuclear reactor systems that included an SFR and pyroprocessing of spent fuel. Then the long-term plan was modified in November 2011, reflecting nuclear environment changes due to limited budget conditions and the agreement of the ROK-U.S. collaboration on pyroprocessing development.

According to the plan established in 2008, a pilot facility was supposed to be constructed to demonstrate pyroprocessing technology by 2016. The ROK and U.S. governments recognized this activity could be carried out in a U.S. facility, so in 2011 both sides agreed to launch the Joint Fuel Cycle Study. The purposes of this study are evaluation of technical feasibility, economic viability, and nonproliferation acceptability of pyroprocessing. This project will continue until 2020. In parallel with

the R&D activities conducted in the United States, the R&D activities using the PRIDE (pyroprocessing integrated inactive demonstration) facility in the ROK will support overall R&D objectives in terms of evaluation of scaled-up pyrotechnology.

Based on the modified long-term plan for the SFR and pyroprocess-coupled system, a roadmap for the development of a PGSFR (prototype Gen IV SFR) was established. The roadmap requires PGSFR design development by 2017, and its design approval and construction by 2020 and 2028, respectively, as shown in Figure 21.2. According to the roadmap, the KAERI (Korea Atomic Energy Research Institute) is currently developing a design for the PGSFR. The roles of the PGSFR are to test and demonstrate the performance of TRU-bearing metal fuel required for a commercial SFR and to demonstrate the TRU transmutation capability of a burner reactor as a part of an advanced fuel cycle.

21.3 Overview of the Korean R&D program and recent key highlights

21.3.1 Current status

In 2012, the PRIDE facility was constructed. Employing all major unit processes within an argon-inerted cell, the PRIDE functions to evaluate the performance of units with large capacity, interconnectivity between units, remote operability, monitoring systems, material tracking, process losses, cell control system, and feasibility of safeguards application. There are five unit processes: headend, oxide reduction,

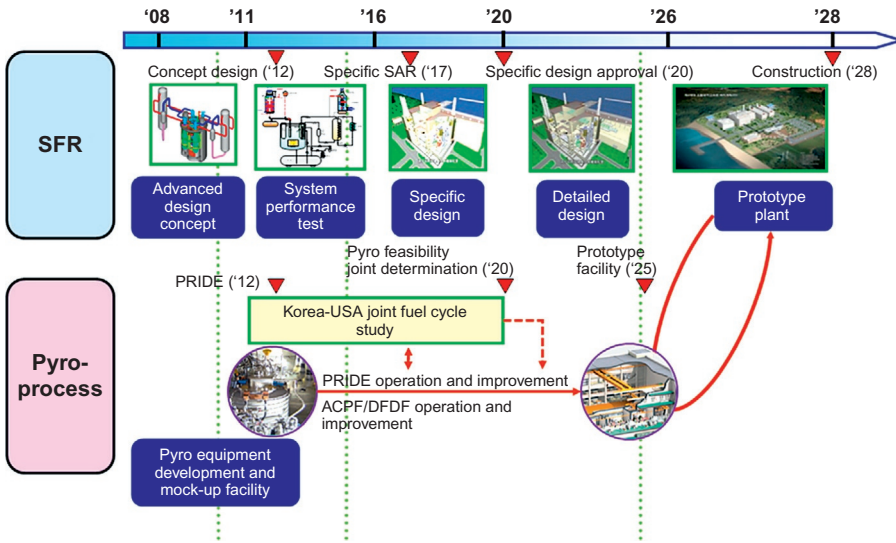

Figure 21.2 Long-term plan for SFR and pyroprocess development.

electrorefining, electrowinning, and salt waste treatment (Lee et al., 2013). Each unit process comprises various equipment items. An integral test that starts from the head-end process and ends at the electrowinning process with once-through material tracking is planned. It is easy to remove the rigs if they are not working properly in PRIDE, as the rigs are contaminated only with uranium. If it is tested in the hot cell with real spent fuel, then contamination by radionuclides will make it a more complex issue to adjust or repair the rigs. In this context, a newly designed apparatus with innovative concepts can be easily tested by switching the rigs. Valuable experience on the remote operation will be gained through the operation of PRIDE. The information from running PRIDE will be very important and instructive for plant and process design, process monitoring, and implementing process safeguards for the plant.

DFDF and ACPF are the hot cell facilities for the headend and oxide reduction processes with spent fuel. DFDF used to be a facility for the DUPIC program. The voloxidation and fuel fabrication for oxide reduction in ACPF will be carried out in DFDF. In ACPF, a 1 kg-scale oxide-reduction process will be conducted. As ACPF is under an air environment, an argon compartment including oxide reduction reactor will be introduced.

SFRs have been developed since the 1950s with an accumulated operational experience of about 400 reactor-years around the world. The SFR is one of the most developed and viable options among the six types of nuclear power plant systems of Generation IV, which are expected to be commercialized after 2030.

Commercial light water reactors currently in operation usually use water as the coolant and the moderator as well, and fissions are caused by low-energy thermal neutrons. The coolant water needs to be contained at high pressure, because it should remain in a liquid phase at the operating temperature to provide effective moderation and cooling. In contrast, sodium-cooled fast reactors use liquid sodium as the coolant at atmospheric pressure, and fissions are caused by high-energy fast neutrons. Sodium has excellent heat transfer and neutronic capabilities and a boiling temperature high enough to permit the primary system to operate at about atmospheric pressure. The high heat transfer performance is required as the reactor core is quite compact to minimize neutron and neutron energy losses resulting in a high power density.

More neutrons are emitted from fissions by fast neutrons than from those by thermal neutrons. This converts more U-238 in the fuel into the fissile isotope Pu-239 and, thus, can improve uranium utilization dramatically through the recycle of spent fuels. Plutonium and minor actinide isotopes usually have very long half-lives and high radiotoxicities and this is a challenge for spent fuel disposal; but with a fast reactor they can be fissioned efficiently by fast neutrons, which enables these waste management issues to be resolved through transmutation.

The purpose of the SFR development in the past was the efficient use of uranium resources for sustainability. The economics of the SFR was the primary concern in those times until the TMI and Chernobyl accidents occurred. After these accidents, many R&D efforts were devoted to secure inherent safety.

In order for the commercialization of the SFRs, the economics and safety need to be proven. Below are the areas where important SFR technology gaps exist (US DOE, 2002):

- Ensuring passively safe response to all design basis initiators, including anticipated transients without scram (a major advantage for these systems).
- Capital cost reduction.
- Proof by test of the ability of the reactor to accommodate bounding events.
- Scale-up and demonstration of high minor actinide recovery.
- Development of oxide fuel fabrication technology with remote operation and maintenance.

21.3.2 R&D activities

21.3.2.1 Pyroprocessing

There are three subtracks for pyroprocessing R&D activity: fundamental research, engineering work, and facility-related activities. Fundamental research covers electrochemistry related to evaluation of the rate determining step, electrode design and configuration, and electrode material alternatives and chemical analysis. For research on process fundamentals, impurities such as REE (rare earth elements) performance, distillation process, metal ingot casting, and modeling and simulation are investigated. Engineering studies are evaluating scale-up performance, design improvement, and application of remote operability. Facility-related activities involve integrating all unit processes, online/offline monitoring, process control, and safeguards.

The purposes of R&D are to increase throughput and to provide the data for scale-up. The hurdles to industrialization are caused by immaturity of technology. Simpler and smaller process units with high throughput are the direction of design improvements.

The headend process starts with decladding of spent fuel. Applying voloxidation pulverizes the oxidized pellet into powder, releasing volatile components such as iodine and cesium. The powder is pelletized for fuel loading into the oxide-reduction process. In the oxide-reduction process, the oxide pellet is reduced to metal. In the meantime, strontium and residual cesium are dissolved in the LiCl molten salt, for downstream treatment in the salt waste treatment system. Reduced metal is conveyed to the electrorefining process where mostly pure uranium is recovered. The residual uranium, TRU, and REE are dissolved in the LiCl-KCl eutectic salt, and are moved to the electrowinning process. A LCC (liquid cadmium cathode) recovers all elements dissolved in the LiCl-KCl salt. Parts of the REE are redissolved into the salt by $CdCl_2$ injection into liquid cadmium containing all elements. The flowchart of pyroprocessing is shown in Figure 21.3.

Equipment automation will be needed for larger-scale facilities. The surveillance and containment concept will need to be accepted for higher proliferation resistance. Enhanced safeguards technology is also needed to increase transparency and material control.

21.3.2.2 SFR

In 2012, the SFR program phase changed from key technology development to an overall system design development, which includes a prototype SFR system design and related R&D activities to support the design.

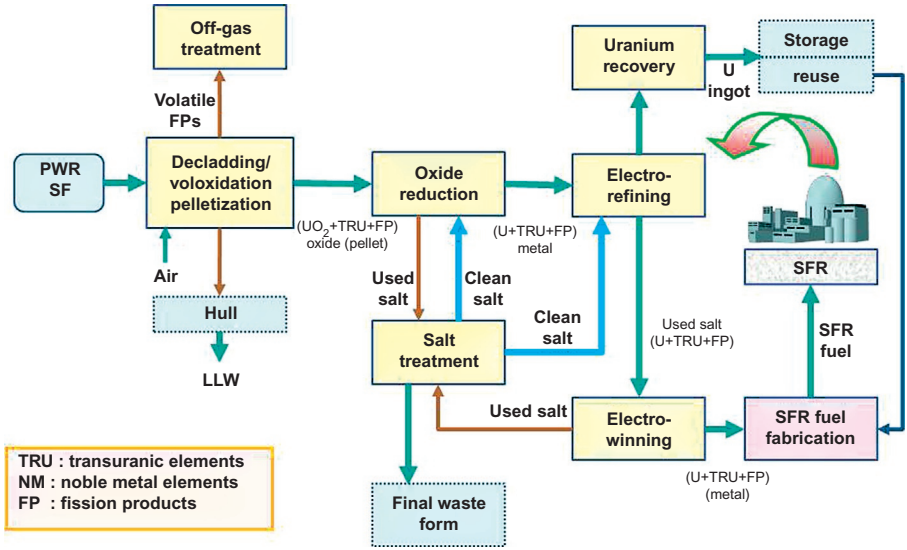

Figure 21.3 Flow diagram of pyroprocessing.

The top-tier design requirements of the prototype SFR are categorized by three criteria: general design requirements, safety and investment protection, and plant performance and economy. A summary of these design requirements is listed in Table 21.1. These requirements reflect the design policies, especially emphasizing proliferation resistance, safety assurance, and metal fuel performance.

Table 21.2 shows the key design parameters of the prototype SFR being developed at KAERI. The decay heat removal system, one of the safety design features, is composed of two passive decay heat removal systems and two active decay heat removal systems. The core is loaded with uranium fuels in the early stage of the operation due to an insufficient irradiation database for the TRU metal fuel. The core will move to a TRU core gradually after accumulating the TRU fuel database.

Figure 21.4 and Table 21.3 show the interim layout and key design parameters of the uranium core. The single enrichment fuels of 19.5% U-235 are loaded in the inner and outer cores. There are four batches in the inner core and five batches in the outer core, respectively.

The fluid system consists of a PHTS (primary heat transport system), an IHTS (intermediate heat transport system), a power conversion system, and a safety design feature such as a DHRS (decay heat removal system), as shown in Figure 21.5. The DHRS is composed of two PDHRS (passive decay heat removal systems) and two ADHRS (active decay heat removal systems). The DHRS is a safety-grade system and is designed to have sufficient capacity to remove the decay heat in all design basis events by incorporating the principles of redundancy and independency. Each PDHRS is comprised of a DHX (decay heat exchanger) immersed in the reactor cold pool and a natural-draft sodium-to-air AHX (air heat exchanger) located over the reactor

Table 21.1 Summary of top-tier design requirements of a prototype SFR

General design	• Reactor type: pool • Plant size: 400 MWt • Plant design lifetime: 60 years • Design basis earthquake: SSE 0.3 g • Initial core: U-Zr metal fuel • Reload core: U-TRU-Zr metal fuel
Safety and investment protection	• Design simplification • Negative power reactivity coefficient • Core damage frequency: $<10^{-6}$/reactor-yr • No fuel-cladding liquid phase propagation during DBEs • Diversified core shutdown mechanism • Reliable and diversified decay heat removal • Accommodating unprotected ATWS events without any operator action • Large radioactivity release frequency: $<10^{-7}$/reactor-yr • Minimum grace time without any operator action for DBEs and BDBEs: 3 days
Performance and economy	• Net plant thermal efficiency: >38% • Plant availability: $\geq$70% • Refueling interval: U-Zr initial core $\geq$6 months, TRU burner core $\geq$11 months • Spent fuel storage capacity in RV: $\geq$1.5 cycle discharge • 100% off-site load rejection without a plant trip • Safety grade diesel generator

building. Each ADHRS consists of a DHX, a FDHX (forced-draft sodium-to-air heat exchanger), an electromagnetic pump, and an FDHX blower. The electromagnetic pump and FDHX blower drive the sodium circulation in the loop and the air flow in the shell side of the FDHX, respectively. ADHRS can be also operated in a natural convection mode.

Improved mechanical design of the structures, systems, and components is needed to build the economic competitiveness of an SFR compared to the pressurized water reactor, without compromising the reactor safety level. The reactor vessel has a uniform thickness of 5 cm, and there are no penetrations or attachments on the reactor vessel. The reactor island adopts a horizontal seismic isolation design. The material of the IHX (intermediate heat exchanger), DHX, IHTS piping, and steam generator is a Mod.9Cr-1Mo-V steel, which can shorten the piping length. The material of the other sections such as the reactor vessel, reactor internal structures, and reactor head is 316 stainless steel.

Table 21.2 Key design parameters of a prototype SFR (current draft)

Overall	
Reactor	Pool type
Core power (MWt)	400
Gross plant efficiency (%)	41.9
Net plant efficiency (%)	38.2
Number of IHTS loops	2
Safety decay heat removal	Passive and active DHRS
Seismic design	Seismic isolation bearing
Core	
Fuel form	U-10%Zr (initial) U-TRU-10%Zr (reference)
Primary heat transport system	
Reactor core I/O temperature (°C)	390/545
Total PHTS flow rate (kg/s)	1991.8
Primary pump type	Centrifugal
Number of primary pumps	4
Intermediate heat transport system	
IHX I/O temperature (°C)	324/527
IHTS total flow rate (kg/s)	1515.9
IHTS pump type	Centrifugal
Total number of IHXs	4
Steam generation system	
Steam flow rate (kg/s)	170.7
Steam temperature (°C)	503.0
Steam pressure (MPa)	16.5
Number of SGs	2

Figure 21.6 shows the PHTS arrangement. The main design features of the prototype SFR are double vessels (a reactor vessel and a guard vessel), integral internal structures and a single rotating plug with a pantograph type IVTM (in-vessel fuel transfer machine), IHXs and primary pumps encompassed by a baffle plate. Within the upper internal structures, thermocouples are installed to cover all fuel assemblies. The advanced concepts of the in-service inspection, repair and replacement, installations, and fuel transfer mechanism were considered in the early conceptual design stage.

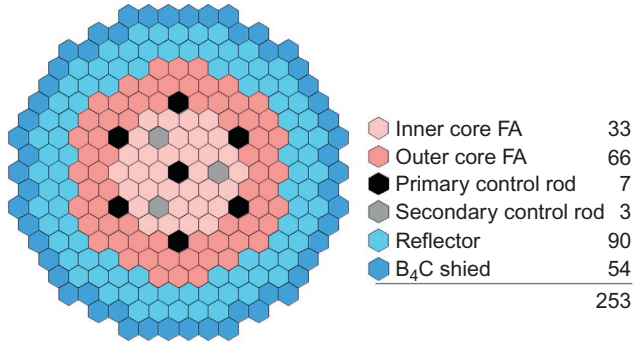

Figure 21.4 Layout of uranium core.

Table 21.3 Key design parameters (current draft)

Parameter	Value
Number of batches (inner core/outer core)	4/5
Active core height (cm)	90
Enrichment (IC/OC) (wt.%)	19.5/19.5
Upper plenum length (cm)	125
Lower reflector length (cm)	45
Lower/upper B_4C shield length (cm)	20.0/20.0
Fuel pin diameter (cm)	0.74
Pitch to diameter ratio	1.14
Effective full power days (EFPD)	290
Burnup reactivity swing (pcm)	2235
Discharge burnup (Avg./Peak) (MWD/kg)	66.5/104
Peak fast neutron fluence ($\times 10^{23}$ n/cm^2)	2.88
Linear power density (Avg./Peak) (W/cm)	163/324
Avg. power density (W/cm^3)	218

Various R&D activities are being performed to support the prototype SFR design. These activities include component tests in sodium loops, development of a metal fuel fabrication technology, development of an under-sodium viewing technology, a reactor physics experiment, thermal-hydraulic tests, development of computer codes, and experiments for a supercritical carbon dioxide (S-CO_2) Brayton cycle power conversion system.

The sodium component test loop STELLA-1 has been constructed to test thermal-hydraulic performances of major components for decay heat removal, such as heat exchangers and mechanical sodium pumps. STELLA-1 consists of a main test loop, a sodium purification system, and a gas supply and related auxiliary systems.

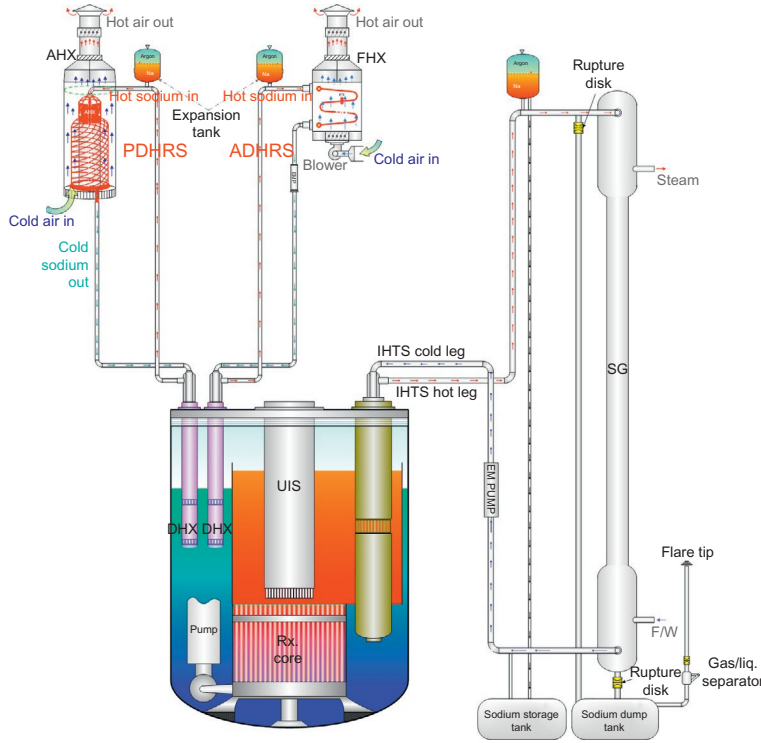

Figure 21.5 Configuration of the fluid system.

The main components of this facility are a sodium-to-sodium heat exchanger, a sodium-to-air heat exchanger, a mechanical sodium pump, loop heaters, a cold trap, a plugging meter, electromagnetic pumps, flow meters, and a sodium storage tank. The general arrangement of the STELLA-1 facility is shown in Figure 21.7.

An advanced fuel casting system to control transport of volatile elements during melting of a fuel alloy with minor actinides has been developed. The casting system employs a low-pressure gravity induction casting system in which the melt in a crucible is cast into the mold underneath through a distributer by the force of gravity, as shown in Figure 21.8 (Lee et al., 2009). Other innovative fuel fabrication methods such as continuous casting and powder metallurgy are also under investigation.

A cladding tube fabrication process is being developed in cooperation with a domestic steel company. After fabricating a medium-sized 1.0 ton HT9 ingot, followed by the multiple processes of hot and cold working, HT9 seamless cladding tubes were fabricated.

A new metal fuel performance analysis code PUMA (performance of uranium metal fuel rod analysis code) is being developed. Temperature and deformation modules have been prepared by using a 1-D finite element method. Code verification and validation are under way by comparison of calculation results with the predictions from other codes and fuel performance test data.

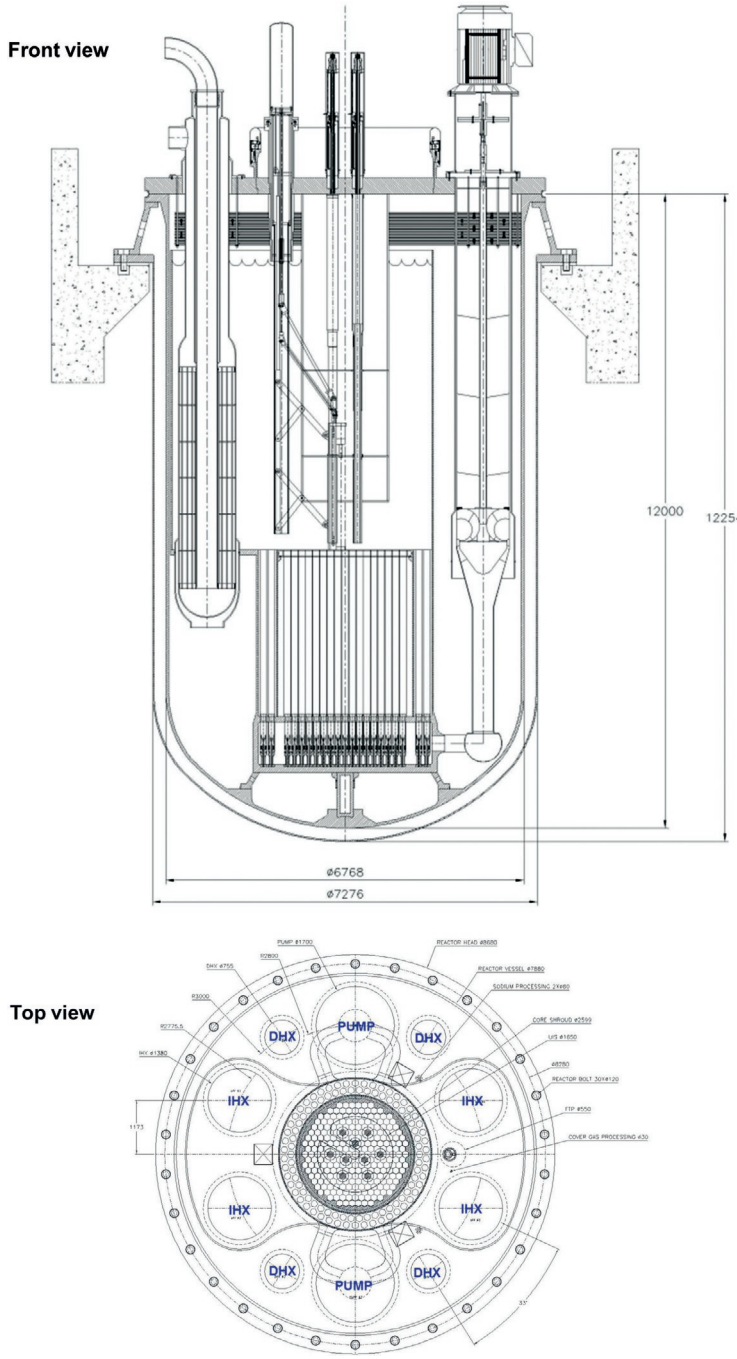

Figure 21.6 PHTS arrangement.

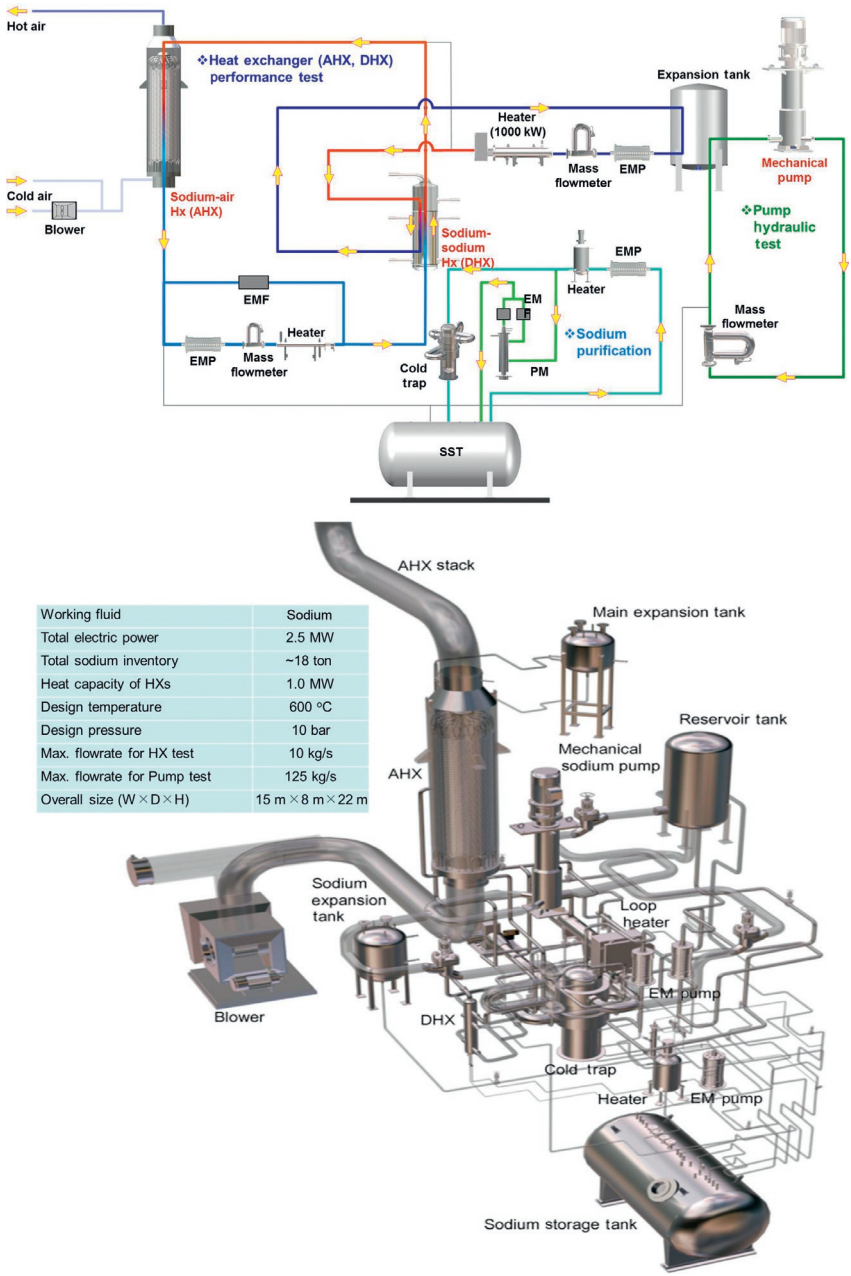

Working fluid	Sodium
Total electric power	2.5 MW
Total sodium inventory	~18 ton
Heat capacity of HXs	1.0 MW
Design temperature	600 °C
Design pressure	10 bar
Max. flowrate for HX test	10 kg/s
Max. flowrate for Pump test	125 kg/s
Overall size (W × D × H)	15 m × 8 m × 22 m

Figure 21.7 General arrangement of STELLA-1 facility.

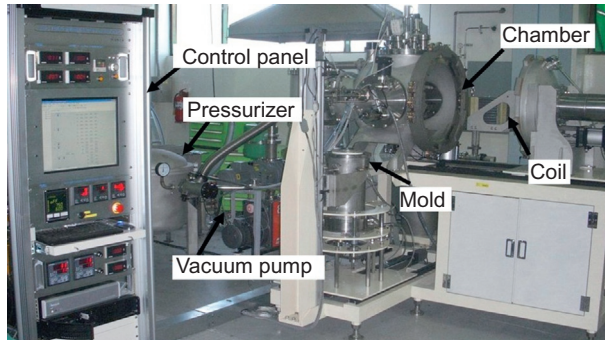

Figure 21.8 Low-pressure gravity casting system.

An irradiation test of U-Zr-(Ce) metal fuel in the research reactor HANARO was conducted from 2010 to 2012 (Kim et al., 2010). Postirradiation examination of the irradiated capsule and fuels has been carried out in the hot cell since 2012. Gamma scan analyses were carried out with 12 rodlets. Based on these measurements, irradiation growths were calculated for 12 rodlets. Irradiation growths of U-Zr fuel slug were calculated to be 10-12%.

The observation technique in liquid sodium using a plate-type ultrasonic waveguide sensor is being developed for the visual inspection of a reactor core and in-vessel structures in opaque liquid sodium. A well-developed beam profile could be obtained in sodium due to the beryllium coating layer and the sodium wetting was greatly enhanced due to the micropolished-nickel coating layer. The feasibility of a 10-m-long under-sodium ultrasonic waveguide sensor has been successfully demonstrated in sodium. A signal-to-noise ratio of 10 dB was achieved and a "SFR" character engraved with 2 mm slits was successfully recognized in sodium by the under-sodium waveguide sensor (Figure 21.9).

For the validation of the neutronic characteristics of the prototype SFR, currently being developed, the experiment "BFS-109-2A" started in 2012 through the collaboration with the Institute for Physics and Power Engineering in Russia. The core was constructed with high-enriched uranium (90 wt.%), depleted uranium, and zirconium metal to simulate the uranium metal fuel (U-10Zr) used in the prototype SFR.

A number of computer codes for SFR thermal-hydraulic design are being developed at KAERI. Validation tests for these codes are to be conducted in water or sodium. The following three test activities are to be performed: (1) the validation tests of reactor core thermal-hydraulic characteristics, (2) performance tests of the FHX (finned-tube sodium-to-air heat exchanger), and (3) V&V of steam generator design code.

SCIEL (supercritical carbon dioxide integral experiment loop) is being constructed to develop and verify the characteristics of the S-CO_2 recompression cycle. The expected operating condition of SCIEL is 550 °C for turbine inlet temperature and 20 MPa for compressor outlet pressure. The first step of the SCIEL experiment is to design a compressor test loop. The CO_2 mass flow rate of this loop was chosen

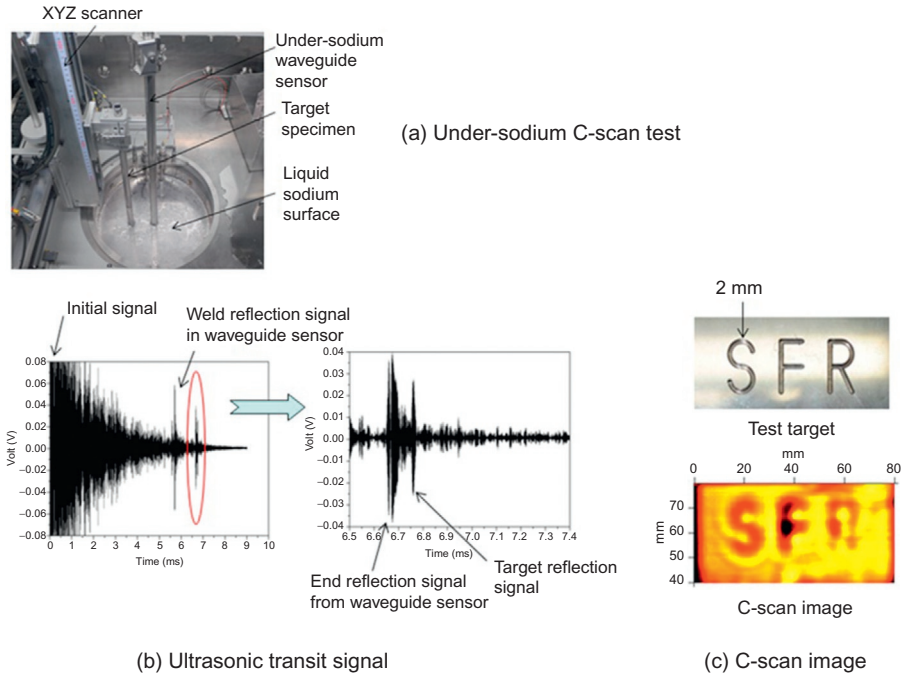

Figure 21.9 Feasibility tests of 10 m-long under-sodium ultrasonic waveguide sensor in liquid sodium.

to be that of the final recompression cycle so that the same compressor will be used for the final SCIEL. The main purpose of the compressor loop is to accumulate operating experience that can be applied to the integral test loop design.

The second step is to upgrade the compressor test loop to become the simple cycle test loop. The turbine and heater are added and the break-even performance will be tested. The third step is the simple recuperated cycle test with a recuperator added to the second step. The turbine inlet temperature will be increased to the design value and the operational strategy and equipment for control will be established and tested. For the final step, by adding another recuperator and an auxiliary compressor, the whole recompression cycle will be accomplished. In this phase the recompression ratio must be carefully controlled to improve the cycle efficiency and stability.

21.4 Future trends

Korea is now facing up to the spent fuel management issues due to the saturation of storage pools at reactor sites, which will become a problem in the next two years or so. The committee for implementation of the program of engagement of public and stakeholders was launched to discuss spent fuel management. To date, the Korean policy for spent fuel management may be described as “wait and see.” Although there are

many options for spent fuel management, it is obvious that the closed fuel cycle has crucial benefits when compared to the other options; in particular, under Korean conditions of small land area and high population. This emphasizes the need for R&D on closed fuel cycles and, consequently, such R&D will provide a technically feasible option for the committee to consider when addressing spent fuel issues.

Based on the long-term R&D program, Korea will continue the technology development aimed at closing the fuel cycle. As shown in the plan, pyroprocessing R&D will develop scaled-up technology using PRIDE/DFDF/ACPF. The Joint Fuel Cycle Study collaboration between the ROK and the United States will continue up to 2020 to evaluate the feasibility of pyroprocessing. The combination of these synergistic tracks will accelerate pyroprocessing technology development.

The PGSFR design development will continue to meet the goal of design approval by 2020. To achieve this, a preliminary safety review by a regulatory body is needed before the submission of the PGSFR safety analysis report for licensing application in 2017. The underlying key technology for the PGSFR is based on the fast reactor technologies developed at ANL (Argonne National Laboratory) in the 1980s and 1990s. The current joint design program between KAERI and ANL will play an important role in successful PGSFR design development.

These two tracks will provide Korea with a potential solution for closing the fuel cycle and dealing with the domestic issues around spent fuel management in the time frame of ~2030-2040.

References

Cheong, J., Kim, I., Kim, D., 2007. Nuclear reactor development in Korea: it's history and status. In: ICENES 2007.

Glatz, J.-P., Malmbeck, R., Ougier, M., Soucek, P., Murakami, T., Sukada, T.T., Koyama, T., 2013. Grouped actinide separation in advanced nuclear fuel cycles. In: Proceedings of Global2013, September 29-October 3, 2013, Salt Lake City.

Kim, B., Sohn, J., Choo, K., 2010. Development status of irradiation devices and instrumentation for material and nuclear fuel irradiation tests in HANARO. Nucl. Eng. Technol. 42 (2), 203–210.

Lee, C., Oh, S., Ryu, H., Kim, K., Lee, Y., Kim, S., Jang, S., Woo, Y., Ko, Y., Lee, C., 2009. Casting technology development for SFR metallic fuel. In: Global 2009.

Lee, H., Park, G.I., Lee, J.W., Kang, K.H., Hur, J.M., Kim, J.K., Paek, S., Kim, I.T., Cho, I.J., 2013. Current status of pyroprocessing development at KAERI. Sci. Technol. Nucl. Ins. 2013, 1–11.

Ministry of Knowledge Economy, 2010. The Fifth Basic Plan for Long-term Electricity Supply and Demand. Republic of Korea.

Shadrin, A., Dvoeglazov, K., Ivanov, V., 2013. Closing nuclear fuel cycle with fast reactors: problems and prospects. In: Proceedings of Global 2013, September 29-October 3, 2013, Salt Lake City.

Till, C.E., Chang, Y.I., 2011. Plentiful Energy—the Story of the Integral Fast Reactor, ISBN 978-1466384606.

US DOE and Generation IV International Forum (GIF), 2002. A Technology Roadmap for Generation IV Nuclear Energy Systems.

Development of closed nuclear fuel cycles in Japan

22

K. Minato
Japan Atomic Energy Agency, Tokai-mura, Ibaraki-ken, Japan

Acronyms

ADS	accelerator-driven systems
CMPO	octyl(phenyl)-*N*,*N*-diisobutylcarbamoylmethylphosphine oxide
CRIEPI	Central Research Institute of Electric Power Industry
DF	decontamination factor
DGA	diglycolamide
FaCT	Fast Reactor Cycle System Technology Development Project
FR	fast reactor
HDEHP	bis(2-ethylhexyl)hydrogen phosphate
HEDTA	hydroxylethylethylenediaminetriacetic acid
i-Hex-BTP	2,6-bis(5,6-dihexyl-1,2,4-triazine-3-yl)pyridine
JAEA	Japan Atomic Energy Agency
JAEC	Japan Atomic Energy Commission
JAERI	Japan Atomic Energy Research Institute
JNC	Japan Nuclear Cycle Development Institute
JRC-ITU	Joint Research Center, Institute for Transuranium Elements
LWR	light water reactors
MA	minor actinides
METI	Ministry of Economy, Trade, and Industry
MEXT	Ministry of Education, Culture, Sports, Science, and Technology
MOX	mixed oxide
NEXT	New Extraction System for TRU Recovery
NRA	Nuclear Regulation Authority
OMEGA	options making extra gains from actinides and fission products
PUREX	plutonium uranium reduction extraction
RRP	Rokkasho reprocessing plant
TBP	tri-*n*-butyl phosphate
TDdDGA	*N*,*N*,*N*′,*N*′-tetradodecyl-diglycolamide
TDDGA	*N*,*N*,*N*′,*N*′-tetradecyl-diglycolamide
TEPCO	Tokyo Electric Power Company
TODGA	*N*,*N*,*N*′,*N*′-tetraoctyl-3-oxapentane-1,5-diamide
TOPEN	*N*,*N*,*N*′,*N*′-tetrakis((5-octyloxypyridin-2-yl)methyl)ethylenediamine
TRP	Tokai reprocessing plant
UNH	uranium nitrate hexahydrate

Reprocessing and Recycling of Spent Nuclear Fuel. http://dx.doi.org/10.1016/B978-1-78242-212-9.00022-8

22.1 Introduction

Reprocessing and recycling technologies for spent nuclear fuels of light water reactors (LWR) have been developed in Japan. The Tokai reprocessing plant (TRP), whose capacity is 0.7 t-HM/day, came into operation in 1981 and about 1140 t-HM of the arising spent fuels were reprocessed at TRP. The Rokkasho reprocessing plant (RRP), whose capacity is 800 t-HM/year, was constructed and the final confirmation test of the plant, called the active test, has been almost finished (Sugiyama et al., 2009). Both the plants are based on the plutonium uranium reduction extraction (PUREX) process. The mixed oxide (MOX) fuel fabrication plant is under construction and is scheduled to be completed in October 2017; this being where the uranium-plutonium MOX fuels for LWR will be fabricated.

For the fast reactor (FR) cycle systems, the Feasibility Study on Commercialized Fast Reactor Cycle Systems was created in 1999-2006 to evaluate a wide range of advanced technologies related to reprocessing and fuel fabrication for the FR fuel cycle systems. The feasibility study came to the conclusion that the most promising concept was the combination of the sodium-cooled FR with oxide fuel, with advanced aqueous reprocessing and the simplified pelletizing fuel fabrication, and that the alternative was the pyrochemical reprocessing system with metal fuel (Sagayama, 2005). Following the feasibility study, the Fast Reactor Cycle System Technology Development Project (FaCT) was started in 2006, where the advanced aqueous reprocessing system with MOX fuel, together with the reactor system and the fuel fabrication technology, have been developed by the Japan Atomic Energy Agency (JAEA) (Ieda et al., 2011). The pyrochemical reprocessing system with metal fuel has been developed mainly by the Central Research Institute of Electric Power Industry (CRIEPI).

Besides the development for the FR fuel cycle system, basic and fundamental research and development of innovative partitioning technologies have been made. Part of the research and development of this kind has been made by JAEA within the framework of *Research and Development of Partitioning and Transmutation Technology in Japan*, aiming at the reduction of the amount and the potential hazard of the high-level radioactive waste to ease the burden of geological disposal of the radioactive waste (Oigawa, 2011).

On 11 March 2011, however, the Great East Japan Earthquake, followed by tsunamis, occurred, which triggered the severe accident at Tokyo Electric Power Company's (TEPCO's) Fukushima Daiichi Nuclear Power Station. The impact of the accident was so strong that a new nuclear safety regulatory system was established and the Basic Energy Plan was revised by the government of Japan.

22.2 Impact of severe accident at Fukushima

Apart from the establishment of the new nuclear safety regulatory system and the revision of the Basic Energy Plan due to the impact of the severe accident at TEPCO's Fukushima Daiichi Nuclear Power Station, which are described below, almost all

the activities of the research and development of the advanced nuclear fuel cycle technologies have been stopped since the accident. The reason is not only the uncertainty about the future nuclear fuel cycle policy but also the shortage of researchers and engineers for advanced nuclear fuel cycle technologies. This is because those who are now actively contributing to the research and development toward decommissioning of TEPCO's Fukushima Daiichi Nuclear Power Station are the same researchers and engineers who were involved in the development of the advanced nuclear fuel cycle technologies before the accident. Even if the Basic Energy Plan is decided, the activities devoted to the research and development of the advanced nuclear fuel cycle technologies would necessarily be smaller than before.

Many important lessons have been learned on nuclear safety issues from the severe accident at TEPCO's Fukushima Daiichi Nuclear Power Station. The government of Japan stated the need to strengthen its nuclear safety regulatory structures and to ensure effective independence of national regulatory bodies (NERH, 2011). The Nuclear Regulation Authority (NRA) was established on 19 September 2012, as a new independent regulatory authority that is fully separated from the nuclear promotional authorities.

The NRA carried out a complete review of safety guidelines and regulatory requirements aiming at formulating a set of new regulations to protect people and the environment. The New Regulatory Requirements for Commercial Nuclear Power Reactors came into force on 8 July 2013, and the New Regulatory Requirements for Nuclear Fuel Facilities, Research Reactors, and Nuclear Waste Storage/Disposal Facilities on 18 December 2013 (NRA, 2013). Seventeen power reactors at 10 power stations as well as the RRP, and other facilities, are under screening by the NRA as of April 2014.

The government of Japan created a new Basic Energy Plan on 11 April 2014 (METI, 2014), which sets the direction of Japan's medium to long-term energy policy. The government is required legally to check the Basic Energy Plan at least every 3 years and, if necessary, to revise it. This plan was the first revision since the accident at TEPCO's Fukushima Daiichi Nuclear Power Station, following the plans decided in 2003, 2007, and 2010.

The plan describes nuclear power as an important base-load electricity source, but the share of nuclear power is not mentioned. According to the plan, the restart of the nuclear power reactors, all 48 of which have been shut down since the accident at Fukushima, would be promoted when they passed the new regulatory requirements set by the NRA. The previous Basic Energy Plan decided before the accident at Fukushima, when the share of nuclear power was about 30%, called for increasing it to more than 50% by 2030.

The plan clearly states the need to pursue the nuclear fuel recycling program, where the reprocessing of the spent fuel and the use of recovered plutonium are promoted. To attain this goal of nuclear fuel recycling, completion of the RRP should be pursued and construction of the MOX Fuel Fabrication Plant and the Recyclable Fuel Storage Center should be promoted (METI, 2014).

The final disposal of the high-level radioactive waste is one of the major concerns among the public after the accident at TEPCO's Fukushima Daiichi Nuclear Power

Station. The plan describes that the government will take the initiative to resolve the stalled process of finding a final disposal site for the high-level radioactive waste. The plan also states that technology for reducing the amount and toxicity of the high-level radioactive waste could be the main measures in the future to mitigate the difficulties associated with the final disposal of the waste and, therefore, the research and development of this technology should be promoted to contribute to decisions regarding appropriate conditioning and disposal of wastes and to reduce long-term risks. The plan describes that the technology for transmutation of long-lived nuclides by FR and by accelerator-driven systems (ADS) will be developed through an international network. In this context, Monju, a prototype fast breeder reactor with MOX fuel, should serve as an international research center for the development of the technology for reducing the amount and toxicity of the high-level radioactive waste (METI, 2014).

22.3 Future nuclear fuel cycle development requirements in Japan

As the new Basic Energy Plan pointed out, technology for reducing the amount and toxicity of the high-level radioactive waste, which provides a wide range of options in radioactive waste management, is required for the future nuclear fuel cycle development. Research and development activities of this kind were started in 1988 under the long-term program for research and development on nuclide partitioning and transmutation technology, called the OMEGA (options making extra gains from actinides and fission products) program, and these activities have now been promoted for about 25 years in Japan. To achieve reduction of the amount and toxicity of the high-level radioactive waste, two types of partitioning and transmutation schemes were proposed and relevant technologies have been developed; that is, using a commercialized FR fuel cycle and using ADS in a dedicated transmutation cycle in the double-strata fuel cycle, as shown in Figure 22.1. In the scheme using a commercialized FR fuel cycle, a technology of minor actinide (MA)-bearing MOX fuel with aqueous reprocessing has been developed by the former Japan Nuclear Cycle Development Institute (JNC) and the succeeding JAEA, while technology for MA-bearing metal fuel with pyrochemical reprocessing has been developed by CRIEPI. In the scheme using ADS, MA-bearing nitride fuel technology with pyrochemical reprocessing has been studied by the former Japan Atomic Energy Research Institute (JAERI) and the succeeding JAEA. These research and development activities were reviewed by the Japan Atomic Energy Commission (JAEC) in 2000 (JAEC, 2000) and in 2009 (JAEC, 2009).

Prior to the decision of the Basic Energy Plan, two reports concerning partitioning and transmutation technology were published by working groups of the Ministry of Education, Culture, Sports, Science, and Technology (MEXT) in 2013. One is the Evaluation of Partitioning and Transmutation Technology (MEXT, 2013a), in which the present state and the future plan for partitioning and transmutation technology in Japan, which is aimed at reducing the amount and toxicity of the high level radioactive waste based on ADS, was discussed and evaluated. The other is the Monju Research

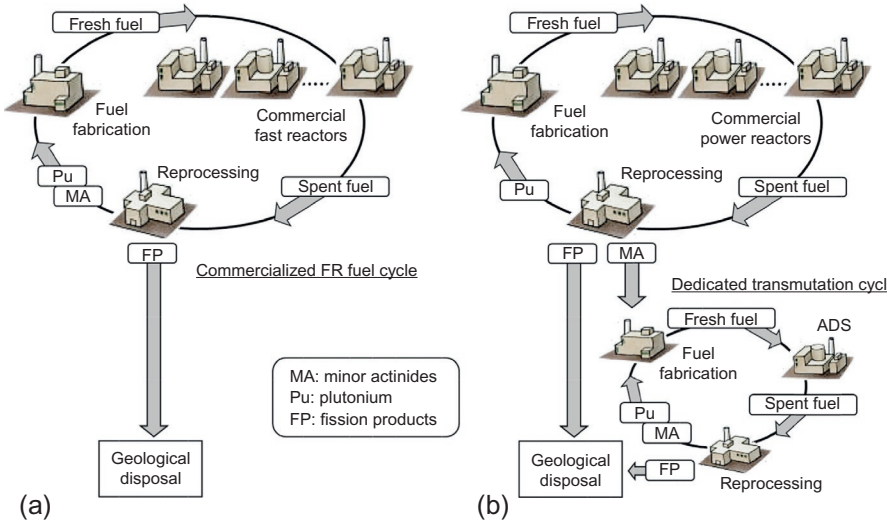

Figure 22.1 Two types of partitioning and transmutation schemes; (a) using a commercialized FR fuel cycle and (b) using a dedicated transmutation cycle with ADS.

Plan (MEXT, 2013b), in which the research plan using Monju for development of the FR technologies, including that for reducing the amount and toxicity of the high-level radioactive waste, was discussed and proposed.

To reduce the amount and toxicity of the high-level radioactive waste, the long-lived nuclides of MAs of neptunium, americium, and curium and the heat-generating fission products, cesium and strontium, should be separated from the waste. The report, the Evaluation of Partitioning and Transmutation Technology, describes that the present state of the development of the technology for partitioning of these nuclides from the spent fuel of commercial power reactors in the first stratum was still at a laboratory scale using simulated solution with tracer-level americium and that, although the actual high-level liquid waste was used in some cases, more experimental data should be obtained with high-level liquid wastes to compile flow sheets. After that, engineering-scale partitioning technology development should be made using high-level liquid waste to demonstrate the flow sheet (MEXT, 2013a).

According to the partitioning and transmutation concept explained above, high-concentrated MA-bearing nitride fuel would be used for transmutation of MA in ADS and the spent nitride fuel would be treated by a pyrochemical process. The report states that irradiation tests of the MA-bearing nitride fuel is needed to evaluate irradiation performance and that the pyrochemical process for nitride fuel, which is based on the process for metal fuel, should be developed using national and international cooperation (MEXT, 2013a).

The Monju Research Plan describes that Monju is one of a few experimental and prototype fast breeder reactors in the world and could offer the irradiation field for demonstration of the transmutation technology, these conditions being suitable for an

international research center for the development of the technology. The transmutation technology based on FRs requires the development of the technology for partitioning of MA, which is principally common to that needed for transmutation by ADS. The development should, therefore, be made in cooperation with each other (MEXT, 2013a).

22.4 Role of R&D, overview of R&D program, and recent key highlights

Since the accident at TEPCO's Fukushima Daiichi Nuclear Power Station, the majority of the research and development efforts related to advanced nuclear fuel cycle technologies have been suspended. The following sections provide an overview and highlights of the research and development made before the accident.

22.4.1 Advanced aqueous reprocessing

The advanced aqueous reprocessing system, the New Extraction System for TRU Recovery (NEXT) process, has been developed for recycling spent fuel from FR in the FaCT project (Takeda, 2011). The NEXT process consists of dissolution of the spent fuel into nitric acid (HNO_3), partial recovery of uranium by crystallization of uranium nitrate hexahydrate (UNH) from dissolver solution, co-recovery of U-Pu-Np by solvent extraction with a single cycle flow sheet using tri-*n*-butyl phosphate (TBP) and recovery of americium and curium by extraction chromatography, as shown in Figure 22.2.

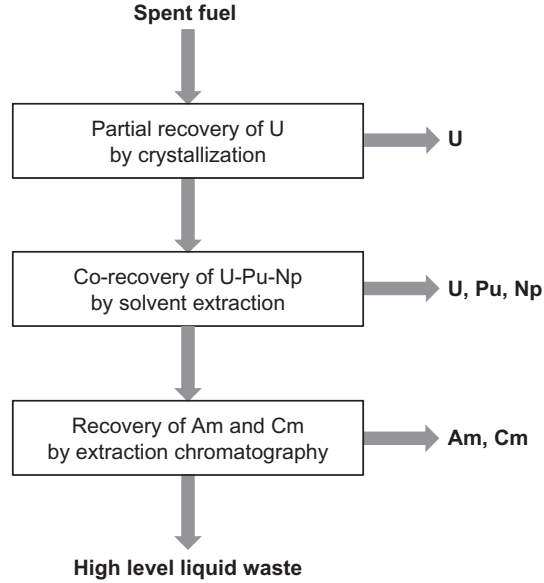

Figure 22.2 Simplified flow diagram of the NEXT process.

The crystallization of UNH to partially recover uranium is the first treatment for the spent fuel dissolver solution in the NEXT process. The recovery of more than 70% of uranium in the dissolver solution is targeted. This process reduces the amount of uranium to be treated in the following U-Pu-Np corecovery process and increases the Pu/U ratio in the solution equivalent to the composition of the fuel, based on the temperature dependence of the solubility of UNH crystals into HNO_3. Beaker-scale experiments with a dissolver solution of FR MOX spent fuel, where the valence of plutonium was adjusted to Pu(IV) to avoid cocrystallization of Pu(VI) with U(VI), showed that Pu(IV) forms a crystalline precipitate of $Cs_2Pu(NO_3)_6$ depending on the concentrations of Pu(IV), cesium, and NO_3^- (Sano et al., 2007). The refinement of the UNH crystal was studied to improve the decontamination factor (DF) for cesium and other fission products. The refinement consists of the removal of the liquid impurity (mother solution) contained inside the crystal by sweating and the separation of solid $Cs_2Pu(NO_3)_6$ impurity by filtration after melting the UNH crystal. Parallel to the beaker-scale experiments using FR MOX spent fuel, the engineering-scale crystallizer and solid-liquid separator were developed using uranium (Shibata et al., 2011).

The corecovery of U-Pu-Np by solvent extraction with a single cycle flow sheet using TBP, which eliminates the plutonium-partitioning section, follows the crystallization process. It is important to control the valence of neptunium for the effective coextraction of neptunium with uranium and plutonium in the extraction section. The feed solution from the crystallization process has high nitric acid concentration, that is quite favorable for the oxidation of neptunium to extractable Np(VI). Plutonium is costripped with uranium and neptunium by diluted HNO_3 solution without any reductants and complexants. In the stripping section, careful temperature control was needed to prevent the leakage of uranium and plutonium to the solvent and acidity adjustment was required to avoid plutonium polymer formation. The countercurrent experiments for U-Pu-Np corecovery were carried out with the dissolver solution of FR MOX spent fuel using centrifugal contactors. These experiments showed that corecovery of U-Np-Pu with sufficiently high DFs could be achieved under appropriate conditions (Sano et al., 2007).

Extraction chromatography has been developed for the recovery of americium and curium. This process uses no diluent in contrast with a solvent-extraction process, which allows a wide range of extractants to be examined. The extractants were loaded on porous silica particles. The adsorbents showed rapid adsorption-elution kinetics, high mechanical strength, small swelling and shrinking, and significantly low pressure loss in a packed column, compared with conventional polymer matrix resins (Koma et al., 2008).

The process developed for recovery of americium and curium consists of two cycles. In the first cycle, americium and curium are recovered with lanthanides from the highly acidic raffinate of the U-Np-Pu corecovery process. In the second cycle, americium and curium are separated from lanthanides. Octyl(phenyl)-*N*,*N*-diisobutylcarbamoylmethylphosphine oxide (CMPO) and *N*,*N*,*N*′,*N*′-tetraoctyl-3-oxapentane-1,5-diamide (TODGA) were tested as extractants in the first cycle, and bis(2-ethylhexyl)hydrogen phosphate (HDEHP), 2,6-bis(5,6-dihexyl-1,2,4-triazine-3-yl)pyridine (i-Hex-BTP), and *N*,*N*,*N*′,*N*′-tetrakis((5-octyloxypyridin-2-yl)methyl)

ethylenediamine (TOPEN) were tested in the second cycle. The column adsorption experiments with simulated solution revealed that the combination of TODGA and i-Hex-BTP was promising (Koma et al., 2012). To demonstrate the process with the TODGA and i-Hex-BTP system, experiments with high-level liquid waste were made using a column of 25.5 cm^3 bed volume (Watanabe et al., 2011). The results showed a lower recovery ratio of americium and curium than expected and further improvements are required.

22.4.2 Basic and fundamental research and development for aqueous reprocessing

Along with the development of the NEXT process in the FaCT project, basic and fundamental research and development of partitioning technologies, such as syntheses and process tests of new extractants that may support and improve the NEXT process and build alternative processes, have been made.

The new extractant, TODGA, has been developed for separation of americium and curium (Sasaki et al., 2001). TODGA is fully soluble in n-dodecane and has very high distribution ratios for americium, curium, and the rare earth elements at relatively high nitric acid concentration. As TODGA is one of the diamides, consisting of carbon, hydrogen, oxygen, and nitrogen (CHON principle), compounds of this kind can be easily synthesized and burnt without solid residue to reduce the waste from the separation process.

The study of the radiolytic stability of TODGA by gamma-ray irradiation revealed that the degradation rate of TODGA was faster than that of the malonamide. However, the extraction test for americium with degraded solvent irradiated to 400 kGy showed that the distribution ratio of americium was still lower than 1 at 0.1 M nitric acid. The radiolytic stability of TODGA, therefore, is acceptable for the separation of americium and curium from the high-level liquid waste in practical applications (Sugo et al., 2007).

The extraction capacity of 0.1 M TODGA in *n*-dodecane was evaluated by measuring the limits of metal concentration for neodymium and found to be lower than the stoichiometric value. Diglycolamide (DGA) compounds with longer alkyl groups, that is, *N*,*N*,*N*′,*N*′-tetradecyl-diglycolamide (TDDGA) and *N*,*N*,*N*′,*N*′-tetradodecyl-diglycolamide (TDdDGA) were examined to improve the extraction capacity, and TDdDGA was found to display the stoichiometric value, one-third of the extractant concentration (Sasaki et al., 2005).

To develop the separation process for americium and curium, a small-scale countercurrent continuous extraction test with 0.1 M TDdDGA in *n*-dodecane was carried out using simulated high-level liquid waste containing americium. In the test, very clear phase separation was observed without any crud formation and quantitative recovery of neodymium and americium was obtained. The recovery of americium was found to be more than 99.96%. The fission product elements, strontium, zirconium, and palladium, which have high distribution ratios at high nitric acid concentration, were separated from americium and neodymium by addition of

hydroxylethylethylenediaminetriacetic acid (HEDTA) and hydrogen peroxide and by proper control of nitric acid concentration. More experiments need to be conducted to clarify the separation performance for actinides against fission products and to obtain optimized process conditions (Morita et al., 2010).

Processes for separation of cesium and strontium have been developed. The purpose of the separation of cesium and strontium from high-level liquid waste is removal of heat sources of ^{137}Cs with a half-life of about 30 years and ^{90}Sr with a half-life of about 29 years from the waste to ease the burden of geological disposal of the radioactive waste.

Zeolite was used to study the adsorption of cesium and showed good adsorption performance even at an acid concentration of 0.5 M HNO_3. Titanic acid was used to study the adsorption of strontium and it was revealed that neutralization of the solution was needed for the adsorption. Separation processes were demonstrated in the four-group partitioning process with the concentrated high-level liquid waste, where the DFs for cesium and strontium at the adsorption steps were more than 10^6 and 10^4, respectively (Morita et al., 2000). As these inorganic materials for cesium and strontium adsorption can be converted to stable materials suitable for disposal, solidification of zeolite containing cesium was confirmed by the cold-pressing and calcination process and by the hot-pressing process, respectively (Tomiyama et al., 2012).

New innovative extractants of the class of phosphorus-free compounds have been developed for separation of cesium and strontium from acid solution. One of the advantages of the phosphorus-free compounds consisting of carbon, hydrogen, oxygen, and nitrogen is to reduce the waste from the separation processes because the compounds may be burnt without solid residue. The extractants of calix-crown derivatives for cesium and crown ether derivatives for strontium were studied by extraction chromatography using porous-silica-based material, where no diluent needs to be used. Calix-crown R14 (1,3-[(2,4-diethyl-heptylethoxy)oxy]-2,4-crown-6-calix[4]arene) for cesium and DtBuCH18C6 (di-t-butylcyclohexano-18-crown-6) for strontium were loaded on porous-silica particles and column adsorption experiments were performed using simulated solutions containing radioactive isotopes at nitric acid concentrations of 2-4 M, as well as using actual high-level liquid waste. The experiment confirmed the elemental behavior in the cesium and strontium adsorption processes (Morita and Kimura, 2012).

22.4.3 Pyrochemical reprocessing

The pyrochemical reprocessing technology for metal fuel has been developed, primarily by CRIEPI, for the sodium-cooled FR cycle system as the alternative option. The pyrochemical process has been developed taking account of the transition from LWR oxide to FR metal fuels; that is, not only for FR metal fuel but also for LWR MOX fuel and high-level liquid waste from LWR fuel reprocessing (Koyama et al., 2011). Besides the pyrochemical process development, waste treatment technology for the pyrochemical process has also been developed (Uozumi et al., 2011a). A detailed description of pyrochemical fuel cycle technology developments in Japan can be found in Chapter 18 of this book.

The pyrochemical process for metal fuel consists of electrorefining in LiCl-KCl eutectic melt at 773 K, where uranium is collected on a solid iron cathode and plutonium and MA with uranium are collected in a liquid cadmium cathode, and cathode processing at high temperature, where cadmium and salts are distilled to obtain the residue of actinide metal that is used to fabricate the fuel slug by injection casting. When oxide fuel is treated, an electroreduction process is added prior to the electrorefining, where the oxide is reduced to metal form to be suitable for the electrorefining (Koyama et al., 2011).

The pyrochemical process of electroreduction, electrorefining, and cathode processing was tested in sequential mode using unirradiated plutonium fuels in a joint study between CRIEPI and JAEA. The obtained mass balance for plutonium and americium was enough to demonstrate the feasibility of the process (Koyama et al., 2007). Electroreduction of LWR irradiated MOX fuel followed by electrorefining of the reduced fuel were performed in a joint study between CRIEPI and the Joint Research Center, Institute for Transuranium Elements (JRC-ITU). Uranium and Pu-MA-U were recovered by the electrorefining (Kato et al., 2011). Electrorefining experiments were also made using U-Pu-Zr fuel irradiated to a burn up of 7 at% in the Phenix reactor. Recovery of actinides was demonstrated with a reliable mass balance (Koyama et al., 2011).

The pyropartitioning process has been studied to recover MA from high-level liquid waste arising from LWR fuel reprocessing. The pyropartitioning process consists of denitration of high-level liquid waste to convert various elements in high-level liquid waste to oxides, chlorination of the denitration product to convert the oxides to chlorides, and reductive-extraction to separate actinides from fission products in the chlorination product and to recover them in a liquid cadmium phase. After the experiments on the pyropartitioning process using simulated high-level liquid waste-containing fission product elements and actinides, an experiment using 520 g of actual high-level liquid waste was made. Almost all uranium, plutonium, neptunium, americium, and curium in the high-level liquid waste were recovered in the liquid cadmium phase and the feasibility of the pyropartitioning process has thus been demonstrated (Uozumi et al., 2011b).

As the feasibility of pyrochemical reprocessing technology for metal fuel, including electroreduction technology, has been demonstrated in laboratory-scale experiments using unirradiated and irradiated fuels with accumulation of basic data, demonstration of industrialization feasibility is important for the next step. Engineering-scale tests using uranium and simulants with process equipment of 1 t-HM/year throughput have been started to develop an equipment design for long-term and hot cell operation with stable performance and to investigate the influence of impurities on the behavior of sensitive materials such as molten chlorides and active metals on material mass balance during repeated engineering-scale operations (Iizuka et al., 2013).

In the partitioning and transmutation scheme using ADS, the technology of MA-bearing nitride fuel with pyrochemical reprocessing has been developed. The pyrochemical processing has several advantages over the conventional aqueous process in the case of treating MA-bearing nitride fuel. The process consists of anodic dissolution of MA-bearing nitride fuel and recovery of MA and plutonium in a liquid cadmium cathode in LiCl-KCl molten salt and nitridation of MA and plutonium for recycling.

Anodic dissolution behaviors of actinide mononitrides (UN, NpN, PuN, (U, Pu)N, and AmN) and uranium-based burn up simulated nitrides containing molybdenum, palladium, or neodymium in LiCl-KCl molten salt were studied by electrochemical measurements, where evolution of nitrogen gas was also confirmed. Anodic dissolutions of the actinide nitrides and recovery of actinides in the liquid cadmium cathode as intermetallic compounds were demonstrated by potential-controlled electrolysis (Minato et al., 2009). Uranium was used as a surrogate in the first step of the experiments, even though uranium-free MA-bearing nitride fuel will be used in the ADS.

To recycle the recovered actinide, the nitridation-distillation combined method was developed using Pu-Cd, Am-Cd, and U-Pu-Cd alloys. Nitride actinides were obtained by heating the alloy in a nitrogen gas stream at 973 K, where nitridation of actinides and distillation of cadmium occurred simultaneously (Arai et al., 2008; Hayashi et al., 2009). Further, the pellet preparation was carried out successfully with recovered actinide nitride powder formed by the combined nitridation-distillation method (Arai et al., 2010).

These results suggested that pyrochemical reprocessing technology of MA-bearing nitride fuel is a feasible option for the dedicated transmutation cycle using an ADS. Becausee the pyrochemical process for MA-bearing nitride fuel has many similar technological backgrounds with that for metal fuel for FR, it is reasonable to utilize the progress of pyrochemical reprocessing technology for metal fuel for further development of that for nitride fuel (Minato et al., 2009).

22.5 Future trends

The Basic Energy Plan was decided in April 2014, and the research and development of advanced nuclear fuel cycle technologies will now be restarted gradually. The research and development plans will be made according to the guidelines in the Basic Energy Plan, which requires the development of the technology for reducing the amount and toxicity of high-level radioactive waste.

As the reports, the *Evaluation of Partitioning and Transmutation Technology* and the *Monju Research Plan*, pointed out, to fulfil the requirements a wide range of research and development, from basic and fundamental researches to engineering-scale development, should be made. The basic and fundamental researches include, for example, design and syntheses of new extractants for target elements with the help of computer simulation and incubation of new ideas. The engineering-scale development of equipment is needed to demonstrate flow sheets with high-level liquid waste. Laboratory-scale experiments will also be made to connect the basic and fundamental researches to engineering-scale development. Feedback of the results of research and development in other scales must be important and inevitable to improve the technology efficiently and effectively. From the viewpoint of nuclear fuel cycle technology, not only the reprocessing and partitioning processes but also the fuel refabrication process and the waste conditioning process should also be fully developed.

Along with research and development, training and education of students, graduate students, and young researchers and engineers must be made, as described in the

reports. Basic and fundamental research programs should also play an important role for this purpose. After the severe accident at TEPCO's Fukushima Daiichi Nuclear Power Station, new research and development areas emerged in decommissioning and waste treatment and these activities are not small. To compensate for the shortage of human resources for developing nuclear technologies, including the advanced nuclear fuel cycle technologies, every effort has to be made to secure human resources, especially students and graduate students, and to give them appropriate training and education.

References

Arai, Y., Iwai, T., Akabori, M., Minato, K., 2008. Synthesis of actinide nitrides in molten cadmium. Nucl. Technol. 162, 244–249.

Arai, Y., Akabori, M., Minato, K., Uno, M., 2010. Development of nitride fuel and pyrochemical process for transmutation of minor actinides. In: Proceedings of the 10th OECD/NEA Information Exchange Meeting on Actinide and Fission Product Partitioning & Transmutation, Mito, Japan, 6-10 October 2008. OECD/NEA, Paris, pp. 189–197.

Hayashi, H., Shibata, H., Akabori, M., Arai, Y., Minato, K., 2009. Electrolysis of AmN in LiCl-KCl eutectic melts and renitridation of Am recovered in liquid Cd cathode. Electrochemistry 77, 673–676.

Ieda, Y., Ono, K., Negishi, H., Shiotani, H., Nagaoki, Y., Namba, T., 2011. Overview of fast reactor cycle system technology development project (FaCT) phase 1 and future direction. In: Proceedings of GLOBAL 2011, Makuhari, Japan, 11–16 December 2011, Paper No. 451660.

Iizuka, M., Kinoshita, K., Sakamura, Y., Ogata, T., Koyama, T., 2013. Performance of pyroprocess equipment of semi-industrial design and material balance in repeated engineering-scale fuel cycle tests using simulated oxide/metal fuels. Nucl. Technol. 184, 107–120.

JAEC, 2000. Status and evaluation report on research and development of technologies for partitioning and transmutation of long-lived nuclide. In: Advisory Committee on Nuclear Fuel Cycle Back-end Policy, Japan Atomic Energy Commission, 31 March 2000.

JAEC, 2009. Current status and a way forward to promote the research and development of partitioning and transmutation technologies. In: Subcommittee on Partitioning and Transmutation Technology, Advisory Committee on Research and Development, Japan Atomic Energy Commission, 28 April 2009.

Kato, T., Murakami, T., Uozumi, K., Koyama, T., Ougier, M., Rodrigues, A., Winckel, S.V., Malmbeck, R., Glatz, J.-P., 2011. Actinides recovery from irradiated MOX fuel by pyrochemical reprocessing. In: Proceedings of GLOBAL 2011, Makuhari, Japan, 11-16 December 2011, Paper No. 391320.

Koma, Y., Watanabe, S., Sano, Y., Asakura, T., Morita, Y., 2008. Extraction chromatography for Am and Cm recovery in engineering scale. In: Proceedings of ATALANTE 2008, Montpellier, France, 19-22 May 2008, Paper No. O1_19.

Koma, Y., Sano, Y., Nomura, K., Watanabe, S., Matsumura, T., Morita, Y., 2012. Development of the extraction chromatography system for separation of americium and curium. In: Proceedings of the 11th OECD/NEA Information Exchange Meeting on Actinide and Fission Product Partitioning & Transmutation, San Francisco, USA, 1-5 November 2010, Poster presentation IV-4. Paper is available from http://www.oecd-nea.org/pt/iempt11/poster-sessions.html.

Koyama, T., Hijikata, T., Usami, T., Inoue, T., Kitawaki, S., Shinozaki, T., Fukushima, M., Myouchin, M., 2007. Integrated experiments of electrometallurgical pyroprocessing using plutonium oxide. J. Nucl. Sci. Technol. 44, 382–392.

Koyama, T., Ogata, T., Myochin, M., Arai, Y., 2011. Japanese programs in development of pyro-processing fuel cycle technology for sustainable energy supply with reduced burdens. In: Proceedings of GLOBAL 2011, Makuhari, Japan, 11-16 December 2011, Paper No. Pa-II-3.

METI, 2014. Basic energy plan. Ministry of Economy, Trade and Industry, April 2014.

MEXT, 2013a. Evaluation of partitioning and transmutation technology. Ministry of Education, Culture, Sports, Science and Technology, November 2013.

MEXT, 2013b. Monju research plan. Ministry of Education, Culture, Sports, Science and Technology, September 2013.

Minato, K., Morita, Y., Kimura, T., Oigawa, H., Arai, Y., Sasa, T., 2009. Recent research and development on partitioning and transmutation by "double-strata fuel cycle concept" in JAEA. In: Proceedings of Global 2009, Paris, France, 6-11 September 2009, Paper 9159.

Morita, Y., Kimura, T., 2012. Development of separation process for transuranium elements and some fission products using new extractants and adsorbents. In: Proceedings of the 11th OECD/NEA Information Exchange Meeting on Actinide and Fission Product Partitioning & Transmutation, San Francisco, USA, 1-5 November 2010. OECD/NEA, Paris, p. 235.

Morita, Y., Yamaguchi, I., Fujiwara, T., Koizumi, H., Tachimori, S., 2000. A demonstration test of 4-group partitioning process with real high-level liquid waste. In: Proceedings of International Conference ATALANTE 2000, Avignon, France, 24-26 October 2000, Paper No. P3-37. Available from: http://www.cea.fr/conferences/atalante2000/index.htm.

Morita, Y., Sasaki, Y., Asakura, T., Kitatsuji, Y., Sugo, Y., Kimura, T., 2010. Development of a new extractant and a new extraction process for minor actinide separation. IOP Conf. Ser. Mater. Sci. Eng. 9,012057.

NERH, 2011. Report of Japanese government to the IAEA ministerial conference on nuclear safety—the accident at TEPCO's Fukushima nuclear power stations. Nuclear Emergency Response Headquarters, the Government of Japan, June 2011.

NRA, 2013. Enforcement of the new regulatory requirements for commercial nuclear power reactors. Nuclear Regulation Authority, 8 July 2013.

Oigawa, H., 2011. Perspectives of partitioning and transmutation technology. In: Proceedings of GLOBAL 2011, Makuhari, Japan, 11-16 December 2011, Paper No. Pa-II-1.

Sagayama, Y., 2005. Feasibility study on commercialized fast reactor cycle systems. (1) Current status of the phase-II study. In: Proceedings of GLOBAL 2005, Tsukuba, Japan, 9-13 October 2005, Paper No. 380.

Sano, Y., Miura, S., Nakahara, M., Kamiya, M., Nomura, K., Komaki, J., 2007. Plutonium and other actinides behaviour in NEXT process. J. Alloys Compd. 444–445, 397–403.

Sasaki, Y., Sugo, Y., Suzuki, S., Tachimori, S., 2001. The novel extractants, diglycolamides, for the extraction of lanthanides and actinides in HNO_3-*n*-dodecane system. Solvent Extr. Ion Exch. 19, 91–103.

Sasaki, Y., Sugo, Y., Suzuki, S., Kimura, T., 2005. A method for the determination of extraction capacity and its application to *N*,*N*,*N*′,*N*′-tetraalkylderivatives of diglycolamide-monoamide/*n*-dodecane media. Anal. Chim. Acta. 543, 31–37.

Shibata, A., Yano, K., Sanbonmatsu, Y., Nakahara, M., Takeuchi, M., Washiya, T., Nagata, M., Chikazawa, T., 2011. FaCT phase I evaluation on the advanced aqueous reprocessing process (5)—research and development of uranium crystallization system. In: Proceedings of GLOBAL 2011, Makuhari, Japan, 11-16 December 2011, Paper No. 391745.

Sugiyama, H., Nago, T., Ishikawa, N., Suda, K., 2009. Summary of active test at Rokkasho reprocessing plant. In: Proceedings of GLOBAL 2009, Paris, France, 6-11 September 2009, Paper 9190.

Sugo, Y., Izumi, Y., Yoshida, Y., Nishijima, S., Sasaki, Y., Kimura, T., Sekine, T., Kudo, H., 2007. Influence of diluent on radiolysis of amides in organic solution. Radiat. Phys. Chem. 76, 794–800.

Takeda, S., 2011. Predominant achievements of fuel cycle technology development in the FaCT project. In: Proceedings of GLOBAL 2011, Makuhari, Japan, 11-16 December 2011, Paper No. 408617.

Tomiyama, S., Mimura, H., Niibori, Y., Yamagishi, I., Morita, Y., 2012. Immobilization of cesium by zeolites and characterization of ceramic solid forms. In: Proceedings of the 11th OECD/NEA Information Exchange Meeting on Actinide and Fission Product Partitioning & Transmutation, San Francisco, USA, 1-5 November 2010, Poster presentation II-7. Paper is available from http://www.oecd-nea.org/pt/iempt11/poster-sessions.html.

Uozumi, K., Kinoshita, K., Iizuka, M., Tsukada, T., Koyama, T., 2011a. Development of salt and metal waste treatment technology for pyroprocess in CRIEPI. In: Proceedings of GLOBAL 2011, Makuhari, Japan, 11-16 December 2011, Paper No. 387026.

Uozumi, K., Iizuka, M., Kurata, M., Inoue, T., Koyama, T., Ougier, M., Malmbeck, R., Glatz, J.-P., 2011b. Recovery of transuranium elements from real high-level liquid waste by pyro-partitioning process. J. Nucl. Sci. Technol. 48, 303–314.

Watanabe, S., Senzaki, T., Shibata, A., Nomura, K., Koma, Y., Nakajima, Y., 2011. MA recovery experiments from genuine HLLW by extraction chromatography. In: Proceedings of GLOBAL 2011, Makuhari, Japan, 11-16 December 2011, Paper No. 387433.

Proliferation resistance, used fuel and multinational approaches to the provision of fuel cycle services

23

Roger Cashmore[1], *Ben Koppelman*[2]
[1]UK Atomic Energy Authority, Oxfordshire, UK; [2]Science Policy Centre, The Royal Society, London, UK

Acronyms

ABACC	Brazilian-Argentine Agency for Accounting and Control of Nuclear Materials
COEX	coextraction of actinides (process)
ETC	Enrichment Technology Corporation
EURATOM	European Atomic Energy Community
EURODIF	European Gaseous Diffusion Uranium Enrichment
FBR	fast breeder reactor
GDF	geological disposal facility
HEU	highly enriched uranium
HLW	high-level waste
IAEA	International Atomic Energy Agency
IMF	inert matrix fuel
LEU	low-enriched uranium
LWRs	light water reactors
MOX	mixed oxide
MUF	material unaccounted for
NAS	U.S. National Academies of Science
NNWS	nonnuclear weapon states
NPT	Nuclear Non-Proliferation Treaty
NWS	nuclear weapon state
OECD	Organisation for Economic Cooperation and Development
PUREX	plutonium uranium extraction (process)
R&D	research and development
SMRs	small- and modular-sized reactors
UREX	uranium extraction (process)

23.1 Introduction

There is an ongoing debate about the relationship between civil nuclear power and proliferation threats, involving nation-states. More recently, debates have included the relationship between civil nuclear power and nuclear security threats, involving

Reprocessing and Recycling of Spent Nuclear Fuel. http://dx.doi.org/10.1016/B978-1-78242-212-9.00023-X

nonstate individuals or groups, such as criminal networks and terrorist organizations. These debates have renewed interest in the potential of both technical and nontechnical means to address the potential vulnerabilities posed by materials, technologies, and knowledge acquired through civil nuclear power programs.

The technical means refer to designing fuel cycles to reinforce "intrinsic barriers" to proliferation by altering the chemical, isotopic, physical, and radioactive properties of civil fissile materials and reducing their accessibility and attractiveness for use in nuclear weapons. Set up by the Australian and Japanese governments, the International Commission on Nuclear Non-Proliferation and Disarmament concluded that "proliferation resistance should be endorsed by governments and industry as an essential objective in the design and operation of nuclear facilities" (ICNND, 2009). At the first Nuclear Security Summit in 2010, participating states committed themselves to "encourage the use of low-enriched uranium and other proliferation resistant technologies and fuels in various commercial applications" (White House, 2010).

The nontechnical means refer to designing fuel cycles to facilitate the implementation of "extrinsic barriers," relating to the political decisions and institutional arrangements governing the fuel cycle. These include International Atomic Energy Agency (IAEA) safeguards; other bilateral, regional, or international verification measures, as well as import and export controls. In 2004, the IAEA established an Expert Group on Multilateral Approaches for the Nuclear Fuel Cycle. It concluded that "a scenario of a strong expansion of nuclear energy around the world calls for the development of nuclear fuel cycles with stronger multilateral arrangements and facilities—by region, by continent or by dedicated cooperation—and for a broader cooperation within the international community" (IAEA, 2005). The IAEA Expert Group was followed by over a dozen proposals from governments, industry, and international organizations. There has been limited uptake of these proposals; most focus on the supply of fresh fuel. Less recent attention has been paid to the international management of used fuel. This need was highlighted at the 2010 Nuclear Non-Proliferation Treaty (NPT) Review Conference when states committed themselves to explore "the development of multilateral approaches to the nuclear fuel cycle, including the possibilities to create mechanisms for assurance of nuclear fuel supply, as well as possible schemes dealing with the back end of the fuel cycle, without affecting rights under the Treaty and without prejudice to national fuel cycle policies, while tackling the technical, legal, and economic complexities surrounding these issues, including in this regard the requirement of IAEA full scope safeguards" (UN, 2010).

The Royal Society (the United Kingdom's national academy of science) recently published "*Fuel cycle stewardship in a nuclear renaissance*," an independent study that explored the potential of these technical and nontechnical means with a focus on the management of used fuel (Royal Society, 2011). This chapter draws on the Royal Society's analysis. The views expressed are those of the authors alone and do not necessarily represent the views of the Royal Society.

23.2 Basics of the nuclear fuel cycle and its regulation

23.2.1 Nuclear fuel cycle choices and the management of used fuel

Nuclear power reactors are refueled every 12-18 months. Only a quarter to a third of the total fuel is removed as used fuel. The remainder is moved back into the core at new positions appropriate for its reduced fissile content. The useful life of nuclear fuel in a thermal reactor is usually 3-7 years. By this time it is no longer an efficient energy producer. Its fissile content is either now too low or its content of neutron-absorbing fission products is too high. Used fuel is intensely hot and radioactive due to the natural decay processes of the fission products and minor actinides it contains. It is initially cooled under wet conditions in storage ponds located in the immediate proximity of the reactor. After 9-12 months, cooling requirements drop sufficiently for alternative management options to be considered. This depends on the choice of fuel cycle. Under the open fuel cycle, it is widely accepted that used fuel should be disposed of directly in a geological disposal facility (GDF). Under a closed fuel cycle, used fuel is reprocessed to separate uranium and plutonium that could be reused as new mixed oxide (MOX) fuel to generate more energy. Most current commercial nuclear reprocessing facilities use the plutonium uranium extraction (PUREX) process. Used fuel assemblies are chopped up and then dissolved in nitric acid. Plutonium and uranium nitrates are separately removed through solvent extraction and converted into plutonium oxide and uranium oxide products. Fission products and minor actinides that remain in the nitric acid solution are then immobilized as high-level waste (HLW) by chemically incorporating them into a robust matrix. This commonly involves vitrification into a glass waste form that is then poured into stainless steel containers for eventual geological disposal. Separated plutonium dioxide is recombined with depleted or reprocessed uranium dioxide to make MOX fuel.

Nuclear power reactors can be categorized by the neutrons responsible for fission reactions. Thermal reactors, such as light water reactors (LWRs), use ordinary water not just as a coolant but also as a moderator to slow down neutrons so that most of the fission is caused by those with relatively low energies, so-called thermal neutrons. Fast reactors do not include a moderator, so fission is caused by neutrons with higher energy, so-called fast neutrons. Fast reactors would enable fissile materials in used fuel to be reused, producing more than 60-70 times the energy per unit mass of original uranium than thermal reactors. Under the fast breeder reactor (FBR) concept, more fissile material is created than is consumed. Neutrons generated in the reactor core convert fertile U-238 in the core and the blanket of "breeder" fuel assemblies surrounding this core into fissile Pu-239 that can be reprocessed to make more fuel. The commercial trend has been to deploy large nuclear reactors with power outputs reaching 1000-1600 MWe. Small- and modular-sized reactors (SMRs) have also been developed that have power outputs of less than 300 MW.

Naturally occurring thorium consists almost entirely of fertile Th-232. It does not undergo fission itself, but on capturing a neutron it leads to fissile U-233. This is similar to natural uranium that consists mainly (approximately 99.3%) of fertile U-238 that is transmuted to fissile Pu-239 upon neutron capture. However, natural uranium contains fissile U-235 that is the essential component in current thermal reactors. As thorium does not have a naturally occurring fissile isotope, there is no analogue of U-235. Another fissile material, either U-235 or Pu-239, is needed to initiate the thorium fuel cycle or, alternatively, a thorium fuel cycle could be initiated by the neutrons generated by fast reactors or accelerator-driven systems.

23.2.2 Regulating the nuclear fuel cycle

Nonproliferation is generally regulated at an international level. It is not the industry per se, but the state in which the industry is based that is primarily the one being regulated. The negotiators of the NPT regarded proliferation as an event. Agreed in 1968 and coming into force in 1970, the NPT defines a nuclear weapon state (NWS) as one that has manufactured and exploded a nuclear weapon or other nuclear explosive device prior to January 1, 1967. This includes China, France, Russia, the United Kingdom, and the United States. Three other states have exploded a nuclear device, namely India, North Korea, and Pakistan, while Israel is also believed to possess nuclear weapons. Today, proliferation is increasingly being viewed as a process with at least three stages: a political decision to invest in a nuclear weapon capability; the acquisition or manufacture of the necessary nuclear and nonnuclear materials and physical components; and the weaponization of these materials and components.

Nonnuclear weapon states (NNWS) can gain access to nuclear materials and technologies in return for commitments to forsake acquiring or developing nuclear weapons. Under the NPT, all NNWS accept IAEA safeguards on their nuclear activities to verify these commitments are being implemented. NNWS are required to conclude a "comprehensive safeguards agreement" with the IAEA, involving declarations of the quantities and location of all nuclear material and facilities within their territories or under their jurisdictions. The IAEA verifies the correctness of these declarations through measures to verify the design and operation of nuclear facilities; nuclear material accountancy; and the containment and surveillance of materials and facilities through tags, seals, and cameras.

NWS are not obliged to do likewise. NWS have concluded "voluntary offer agreements," choosing to place certain facilities or nuclear material under IAEA safeguards. India, Israel, and Pakistan are not party to the NPT but have agreed to "item specific safeguards agreements" with the IAEA whereby they undertake not to use specified material, facilities, and some other items to further any military purpose. Despite its comprehensive safeguards agreement, Iraq had been conducting a clandestine nuclear weapons program prior to 1993 centered on the same nuclear site where the IAEA conducted routine inspections of declared nuclear material. This demonstrated that IAEA safeguards needed to be strengthened to include assurances of the absence of any clandestine activities at undeclared facilities. This required new legal authority, resulting in the adoption in 1997 of the Model Additional Protocol

to Agreement(s) between State(s) and the IAEA for the Application of Safeguards. This has equipped the IAEA with new tools to detect clandestine activities, including environmental sampling, satellite imagery, and other novel technologies, as well as nuclear trade analysis and open source information collection.

States provide independent assurances to other states, so nonproliferation is inspected by intergovernmental bodies, namely the IAEA, as well as the European Atomic Energy Community (EURATOM) in Europe and the Brazilian-Argentine Agency for Accounting and Control of Nuclear Materials (ABACC) in Argentina and Brazil. The IAEA has the power to refer noncompliance to the Security Council (and European Court of Justice in the case of EURATOM) that is the ultimate source of enforcing nonproliferation. National governments still have responsibilities for nonproliferation. It is in their interests to ensure legislation is in place so that industry provides all the support necessary to enable safeguards activities to be carried out effectively, and thereby avoid false accusations of proliferation.

In contrast, nuclear security is regulated at the national level (like nuclear safety). National governments are responsible for setting up a national regulator independent from the nuclear industry and government departments and agencies responsible for promoting nuclear power. By implementing a licensing, inspection, and enforcement system, regulators can provide national governments with independent assurance that the nuclear industry is operating securely as well as safely.

23.3 Major nuclear proliferation scenarios involving state-based threats

Nuclear power reactors and their operation alone are not the primary proliferation risk. It is the material that they use and produce. Technologies to enrich uranium to fuel reactors can also enrich uranium to higher levels suitable for nuclear weapons use. Also, the uranium transmuted into plutonium by nuclear power reactors could be used in nuclear weapons.

23.3.1 Diversion of used fuel from declared facilities

Used fuel could be removed from storage ponds and even replaced with dummy material, especially if it had been stored for a long time so that the heat load and radioactivity is reduced. This could make used fuel assemblies more accessible and easier to handle, although it would still be highly radioactive, heavy, and cumbersome to move.

Separated plutonium could be diverted at a declared reprocessing facility but this would be complicated. Operators could separate extra plutonium dioxide and then falsify the performance records of the facility, as well as the fuel history of a reactor. The facility's design could be modified to allow separated plutonium dioxide to be secretly removed, returning the facility back to its original configuration prior to the next IAEA inspection. This extra plutonium dioxide could be disguised as material unaccounted for (MUF). This is the standard accounting term for the difference between

the amount of material that is calculated to be present in a facility given its operating records and the amount that actually is present. MUF is inevitable in reprocessing and MOX fabrication facilities due to the uncertainties inherent in measurement systems, as well as accumulation in piping within the facility. Between IAEA inspection visits, the hot cells of a declared facility could be used to develop reprocessing activities to take place on a larger scale at an undeclared facility located elsewhere. Both Egypt and Iran admitted to past small-scale reprocessing of irradiated uranium targets, but reported this activity to the IAEA many years later.

Containers containing used fuel could be substituted at the surface of a GDF by dummy containers that contain nonfissile or nonnuclear material. Undeclared retrieval of containers containing used fuel from a GDF is also possible. A container could be opened underground and used fuel assemblies removed and transported to the surface or even reprocessed underground.

The historical record shows that IAEA safeguards have proven to be effective to make the diversion of nuclear materials from declared facilities unlikely. Given the likelihood of detection, other proliferation scenarios may be more likely (APS, 2005).

23.3.2 Clandestine activities at undeclared facilities

The size and complexity of an industrial-scale reprocessing plant needed to produce weapons-grade plutonium is too large to be easily hidden, although a smaller clandestine reprocessing plant could be built. A small research reactor could even be disguised within a nonnuclear industrial complex and use associated hot cell facilities to carry out small-scale reprocessing. Facilities could be constructed in advance of any reprocessing, providing a state with a potential breakout capability. The U.S. national laboratories have demonstrated the feasibility of "quick and dirty" clandestine reprocessing facilities specifically for separating plutonium for nuclear weapons use. Studies by Sandia National Laboratory in 1977 and 1996, respectively, have outlined designs that could possibly be built within six months and produce plutonium for nuclear weapons within a few extra months (GAO, 1978; DoE, 1996). There are some disagreements on the feasibility of these designs and ongoing debate about how technologically advanced a state would need to be to succeed in implementing them.

Clandestine tunnels could be excavated into a GDF or out from a GDF to the surface or to a nearby tunnel system. This would require a determined and sophisticated effort by the state. The drilling, mining, and processing involved would produce detectable signals and indicators of diversion.

23.3.3 Breakout from the NPT

The NPT allows a state to give three months' notice and then legally opt out of the treaty and renounce its safeguards obligations. This is of particular concern when a state has capabilities across the full civil fuel cycle, especially enrichment or reprocessing facilities. Timing would be crucial to maximize the amount of weapons-grade

plutonium that could be produced before experiencing the economic, political, and possible military consequences of breakout.

For example, North Korea embarked on a national nuclear research and reactor development program in the 1970s and 1980s. Its planned power reactors were to be graphite-moderated and gas-cooled, as they did not have access to enriched uranium fuel. Its fuel fabrication and reprocessing facilities were not declared or inspected by the IAEA because North Korea was not a state party to the NPT. In 1985, the USSR agreed to build LWRs in North Korea to meet its energy needs on condition that the USSR provided fresh fuel; North Korea repatriated the fuel once used; and that North Korea became party to the NPT. North Korea acceded to the NPT in 1985, but the arrangements for the USSR to supply North Korea with a LWR and their fuel collapsed after the dissolution of the USSR in 1991. Lengthy negotiations between North Korea and the IAEA secretariat over the wording of its safeguards agreement took place until 1992. This delayed the start of IAEA inspections. Verification of North Korea's initial declaration of plutonium uncovered accountancy discrepancies, with the consequence that safeguards could not be fully implemented. This standoff was terminated by the negotiation of an agreed framework with the United States in 1994. North Korea halted its national fuel fabrication and reprocessing activities in return for the funding and building by South Korea, Japan, and other states of two large LWRs. Building started on these and, in parallel, the IAEA monitored the cessation of operations of North Korea's prototype reactor and the building of additional power reactors. Following U.S. accusations in the early 2000s of clandestine uranium enrichment activities, North Korea declared in 2003 that it would withdraw from the NPT. IAEA inspectors were expelled and used fuel from North Korea's indigenous reactor was reprocessed. Nuclear tests of two plutonium-based devices were carried out in 2006 and 2009.

A multicountry breakout scenario is also possible whereby one country could produce used fuel that is then reprocessed in another country. This scenario should not be overlooked, given allegations of this type of collaboration between North Korea and Syria (IISS, 2008).

23.3.4 Managing dual use know-how

It is unclear whether personnel and knowledge gained from civil nuclear power programs have directly or indirectly assisted nuclear weapons programs in NNWS. In some cases, such as Libya, South Africa, and Syria, declared facilities may have helped to train personnel, who were then directed to work on weapons programs at undeclared facilities. The United States regarded Iranian attempts to rebuild and operate the civil reactor at Bushehr, after it was attacked by Iraqi air strikes during the Iran-Iraq war in the 1980s, as posing an unacceptable proliferation risk. This led to the United States' prolonged (and ultimately unsuccessful) diplomatic campaign to prevent this during the 1990s.

To ensure nuclear skills continue to be used responsibly, education and awareness raising courses on nuclear nonproliferation and nuclear security should be included in

relevant university and industrial training courses (Royal Society, 2011). As part of their induction, researchers at postgraduate level could be informed about the ethical and legal responsibilities relating to their work. This could be included in existing induction courses that deal with health, safety, and other general laboratory training. Outlining the implications for researchers of the NPT and other international treaties would be an integral part of this training. Education may also be needed for established researchers.

23.4 Major nuclear security scenarios involving non-state based threats

States without a suitable security infrastructure may not be able to protect nuclear facilities against attacks or sabotage. These states may not be able to prevent nuclear materials from being acquired by those who could use them in a dispersal device or even an unsophisticated and crudely designed nuclear weapon.

Responses to proliferation and nuclear security may overlap, drawing on similar measures, such as computer security and personnel vetting. Proliferation resistance should be restricted to measures responding to state-based threats, as in the IAEA's definition: "that characteristic of a nuclear system that impedes the diversion or undeclared production of nuclear material or misuse of technology by states in order to acquire nuclear weapons or other nuclear explosive devices" (IAEA, 2010)."Physical protection" should be used when responding to nonstate, nuclear security threats. Blurring this distinction could convey a misleading message about the potential benefits of a particular proliferation resistance measure. Measures to manage nonstate threats may have a low impact on managing state-level threats given the difference in their nature.

23.4.1 Theft of material during reuse

The likelihood that a sufficient amount of used fuel could be stolen for use in a radiological dispersal device is small (NAS, 2006). According to the U.S. National Academies of Science (NAS), the high radioactivity and sheer bulk of used fuel assemblies means "that the removal of a used fuel assembly from the pool or dry cask would prove extremely difficult under almost any terrorist attack scenario. Attempts by a knowledgeable insider to remove single rods and related debris from the pool might prove easier; but the amount of material that could be removed would be small" (NAS, 2006).

23.4.2 Use of separated civil plutonium in a dispersal device

The theft of separated plutonium is a major security concern at reprocessing and MOX fabrication facilities. As plutonium comprises predominantly alpha-emitting isotopes, separated plutonium could be relatively safely handled by those who access it

provided precautions are taken to limit exposure. If stolen, separated plutonium may be more easily used in a dispersal device. As a powder, separated plutonium could be toxic if ingested or inhaled.

23.4.3 Use of separated civil plutonium in an improvised nuclear weapon

There are debates about whether separated civil plutonium could be used in an unsophisticated and crudely designed nuclear weapon. If highly enriched uranium (HEU) is not easily accessible, then plutonium from civil nuclear power programs could be sought. This would pose a set of major technical challenges:

- Used fuel contains a number of intrinsic barriers to proliferation. Having been irradiated and removed from a reactor, the intense heat and radioactivity of used fuel makes the plutonium it contains highly inaccessible.
- Used fuel needs to be reprocessed to access the plutonium it contains, presupposing (access to) major industrial capabilities. Similar technologies are also necessary to separate plutonium from unirradiated MOX although shielded highly active cell facilities are not necessary.
- Plutonium dioxide needs to be converted into a plutonium metal to be used easily in a nuclear weapon. Various techniques to reduce plutonium dioxide to plutonium metal are already available in the public domain.
- The design of plutonium-based nuclear weapons is more technologically demanding than HEU-based, gun assembly designs. Sophisticated metallurgical and machining expertise is needed to manufacture plutonium metal into a suitable geometry with a highly uniform density and composition, and to shape the component parts. Advanced physics and engineering expertise is needed to ensure the assembly's components are accurately aligned, and that the functioning of the detonators is highly synchronised.
- Nuclear weapons capabilities range from highly advanced nuclear weapons capable of being carried by, and associated with, missile delivery systems of considerable range; through to simpler weapons with an associated delivery system of lesser military capability; and much cruder devices without highly predictable and reliable yields. Plutonium used in nuclear weapons has a high concentration of fissile Pu-239. Advanced nuclear weapons are likely to require the acquisition of this "weapons-grade" plutonium, especially if a reliable and predictable yield is sought.
- It should not be assumed that proliferators will necessarily seek the most advanced capabilities. A technologically advanced, proliferating state could use less sophisticated nuclear weapon designs to produce less reliable explosive yields, no greater than one or a few kilotons, the so-called fizzle yield. "Reactor-grade" plutonium in used civil fuel has a lower fraction of Pu-239. The isotopic quality of reactor-grade plutonium complicates its use in a nuclear weapon. Advanced nuclear weapon states may have the technical capability and knowledge of sophisticated nuclear weapon designs to use reactor-grade material to produce reliable explosive yields comparable to those made from weapons-grade plutonium. A less technologically advanced, proliferating state could possibly use reactor-grade plutonium in nuclear weapon designs, no more sophisticated than those used in first-generation nuclear weapons, to produce a fizzle yield. There are differences in expert opinion about whether nonstate groups could access the extensive scientific expertise and technical infrastructure required to overcome these challenges. Nonetheless, complacency must not be introduced into the management of plutonium.

23.5 The potential of technical means to increase the proliferation resistance of used fuel

23.5.1 Enhancing isotopic barriers

Weapons-grade plutonium is produced via very low burn up of uranium fuel; that is, when fuel is irradiated for a short time, even just for a few weeks. In civil nuclear power reactors, fuel is irradiated over several years to maximize its energy yield for electricity production. This significantly reduces the attractiveness of plutonium in used civil fuel for nuclear weapons use. The reactor-grade plutonium in used civil fuel has a lower fraction of Pu-239 due to the high levels of burn up in civil nuclear power reactors. It has a greater quantity of undesirable isotopes of plutonium that complicate the use of civil nuclear materials in nuclear weapons, decreasing the reliability of a nuclear explosion. Pu-238 decays relatively rapidly, generating significant amounts of heat. Pu-240 could set off the chain reaction prematurely, substantially reducing explosive yield as the weapon may blow itself apart and cut short the chain reaction. Pu-241 decays to Am-241 that absorbs neutrons and emits intense gamma radiation. These isotopes require careful management and extensive shielding to protect personnel when handling materials, and they could damage other components in a nuclear weapon. The additional irradiation of plutonium in MOX fuel further reduces the isotopic quality of plutonium in used MOX fuel.

There is no well-defined threshold for higher burn up above which plutonium becomes unusable for weapons, so the IAEA's working hypothesis is that all reactor grades of plutonium pose a proliferation risk. Adapting civil nuclear power reactors to lower burn ups would be difficult to conceal due to the safeguards arrangements in place, as well as the observable effects on national electricity generation.

23.5.2 Enhancing radiation barriers

Plutonium in used fuel produced by operating a LWR on an open fuel cycle is protected by the radiation from fission products in used fuel (at least in the near term). When operating on a closed fuel cycle, this radiation barrier decreases during reprocessing when a PUREX technique has traditionally been used to extract the fission products and then separate the plutonium from the uranium stream. There is ongoing international R&D to avoid the separation of pure plutonium, instead coprocessing plutonium with other materials. This R&D involves both aqueous techniques, such as coextraction of actinides (COEX), during which uranium and plutonium are extracted together, and uranium extraction (UREX), during which uranium is extracted and plutonium is left mixed with the minor actinides and fission products; as well as nonaqueous techniques, such as pyroprocessing. Many of these alternative-reprocessing techniques are not yet ready for more than laboratory testing. There are significant challenges relating to the reliability and availability of the proposed facilities and the generation of secondary wastes. PUREX remains cheaper, simpler, and is widely documented. With many years of industrial experience, it is likely

(at least in the near term) to be a more attractive choice for countries wanting to explore reprocessing.

Proliferation vulnerabilities could be more effectively addressed by optimizing the design of the wider system in which reprocessing takes place (Royal Society, 2011). Used fuel should be reprocessed only if there is a clear plan that minimizes the amount of time during which plutonium is in a separated form, and that converts it into MOX fuel as soon thereafter as is feasible. Reactors should be identified in advance that can irradiate MOX fuel, which, in turn, should be fabricated on timescales that match reactors' loading schedules. This would minimize any risks associated with the stockpiling of MOX fuel. A further advantage is the removal of the in-growth of americium. This complicates the handling of plutonium and MOX fuel and can affect the performance of the fuel in the reactor. Plutonium should be transported as MOX fuel rather than as separated plutonium. By colocating reprocessing and MOX fabrication facilities it may be possible to design a fully continuous process in which used fuel comes into the facility and new MOX fuel (plus wastes for disposal) leaves the facility. This may be difficult to achieve in practice. Industrial realities would require some interim storage of separated plutonium to serve as a buffer store so that MOX fuel could still be manufactured in the case of any unforeseen interruptions to the operation of the reprocessing plant. The size of this interim store should be minimized and the highest levels of physical protection should be implemented. If the reprocessing facility uses a COEX-type process, then there is no separated plutonium at any point in the process because plutonium is always diluted with uranium. More uranium can be added to dilute the material into MOX when ready. One disadvantage is that the volumes of plutonium-containing materials to be stored are greater due to the dilution factor.

Furthermore, fresh fuel could be spiked with small amounts of minor actinides, such as Np-237, to enhance the production of Pu-238 in used fuel, further complicating the use of civil plutonium in nuclear weapons. As Np-237 is itself fissionable, the use of separated neptunium would itself introduce new risks, and neptunium may need to be coprocessed with other minor actinides. Similarly, the degree of purification of the plutonium product could be relaxed or other radionuclides could be added to increase the radiation barrier of fresh fuel. It is unclear how new signatures could feasibly be introduced that did not degrade reactor operations.

The proliferation resistance of these reprocessing techniques may be limited. They do not eliminate the attractiveness of plutonium for nuclear weapons use. Some of the radioisotopes that plutonium is mixed with are fissile, resulting in a material that a technologically advanced state could use in a nuclear weapon. All fissile isotopes capable of being assembled into a critical mass are potentially usable weapons and are of proliferation concern.

23.5.3 Enhancing chemical barriers

The difficulty of extracting plutonium is affected by the manufacture of fresh fuel. MOX fuel is currently the most widely used and proven plutonium-bearing fuel. Alternatively, plutonium dioxide could be mixed with a nonfertile ceramic carrier

to produce an inert matrix fuel (IMF). While irradiating MOX fuel creates new plutonium, IMF offers the possibility of generating electricity from a plutonium-bearing fuel while producing no additional fissile material. The remaining plutonium is of even less-desirable quality for nuclear weapons use. Further irradiation is possible in fast reactors, which could also transmute the plutonium into isotopic forms that are even less attractive for weapons use. Matrix materials could be chosen that are optimized for different behavior, such as stability during long-term storage and disposal. IMF can be designed so that plutonium would be more difficult to extract compared to conventional MOX fuel. If used IMF is to be recycled, however, used IMF would need to be leachable, if possible under the same reprocessing conditions as used for uranium fuel. IMF is currently an unproven technology.

23.5.4 Using alternative nuclear fuels

Thorium has been advocated as an alternative to uranium or plutonium fuels because the thorium fuel cycle produces less plutonium in its used fuel. However, there is an emerging consensus that the thorium cycle may be no more proliferation resistant than uranium or plutonium-based fuel cycles. An open thorium fuel cycle will generally require U-235 or Pu-239 fuel to initiate it. Used thorium fuel that contains fissile U-233 can be reprocessed and the U-233 used to initiate the cycle instead. U-233 could be used in nuclear weapons.

23.5.5 The used fuel standard

The "used fuel standard" was specifically proposed in the context of disposing of weapons-grade plutonium from nuclear weapons by making it as inaccessible as used fuel. Some commentators propose that the used fuel standard should underpin the wider civil management of used fuel. There is an emerging consensus that this may not be a practical standard. It is ill-defined without any specification of the minimum radioactivity required to make plutonium inaccessible. It is also time-based because over a few hundred years the activity decreases to the point where it is not considered to be self-protecting.

23.6 The limitations of technical means to increase the proliferation resistance of used fuel

23.6.1 Technical feasibility

Many initiatives on proliferation resistance over the years have concluded that there is no technological "silver bullet" solution to proliferation, yet great promise was still placed in such solutions. There is an emerging consensus that some technical means to increase the intrinsic proliferation resistance of used fuel may have been oversold.

These measures cannot physically prevent a technologically advanced state from acquiring nuclear weapons if it decides that they are in its interests. These technical means should not be relied on in isolation but can complement other means, such as nuclear safeguards, that together provide a "defence in depth" approach to reducing and managing proliferation risks by involving a number of redundant, diverse, and independent controls.

23.6.2 Economic attractiveness

Governments would need to convince industry that existing technologies are not adequate to address the vulnerabilities of the fuel cycle. Some new measures may have adverse impacts on commercial aspects of fuel cycle performance, including operational efficiency and operating costs. Notwithstanding significantly increasing the costs, modifying fuel cycles to increase the radiological hazard of nuclear materials, for example, creates extra safety and environmental risks that pose extra regulatory burdens. As many of these measures are not mature, industry is likely to prefer using existing and less-expensive technologies where there is significant experience in deploying them at an industrial scale. In an era when nuclear power in some states is no longer heavily subsidized, governments would need to identify and provide the incentives necessary for industry to adopt such new measures.

23.6.3 Political acceptability

Even if deployed in less-technologically advanced states, the training of individuals to implement proliferation resistance measures could inadvertently lead to the spread of sensitive nuclear knowledge that could be misused to reverse engineer them. As the capabilities of these states continue to advance, their ability to overcome the barriers to proliferation are likely to increase. The effectiveness of any intrinsic proliferation resistance measure is likely to decrease with time.

Less-technologically advanced states could interpret the adoption of these measures as discriminatory and reinforcing a systemic division between haves and have-nots. To avoid these accusations, technologically advanced states would need to constrain their technology choices and adopt these measures, too. A system perceived to be discriminatory could foster resentment and undermine the enforcement process. The nonproliferation regime is affected not just by the ability of the international community to detect acts of proliferation, but also by its ability to respond once they have been detected.

23.6.4 Best practices for nonproliferation

In some NWS, the civil nuclear industry has matured to become solely a provider of electricity. France, the United Kingdom, and the United States have fully separated their nuclear weapons programs from their civil nuclear power programs. Only the

United Kingdom and France, by their own choice, are under specific obligations to place them under safeguards. The EURATOM Treaty requires France and the United Kingdom to place their entire civil nuclear power program under its safeguards system, including enrichment, reprocessing, and fuel fabrication facilities. Best practice for nonproliferation should require all states with nuclear weapons programs to separate them from their civil nuclear power programs, placing the latter under international safeguards to verify they do not provide materials for nuclear weapons (Royal Society, 2011).

The effectiveness of international safeguards depends on the extent of the IAEA's authority, which remains uneven from state to state. Safeguards agreements are in force in the majority of states party to the NPT. All NNWS with existing nuclear power programs or embarking on nuclear power for the first time should adopt and implement IAEA comprehensive safeguards and the Additional Protocol. IAEA comprehensive safeguards and the Additional Protocol should become the nonproliferation standard for a nuclear renaissance (Royal Society, 2011).

23.7 Multinational approaches to the provision of fuel cycle services

At the start of the Atomic Age and during the time of NPT negotiations, energy markets were generally directed by governmental monopolies and nuclear power programs were driven by national energy planning. This implied that each country needed to develop its own national industry. Recommendations for new international practices could be promoted by intergovernmental agreements, domestic legislation, and licensing arrangements, but commercial considerations complicated their implementation at the time. Today, globalization and the liberalization of energy markets provide an economic infrastructure that has facilitated the internationalization of the nuclear fuel cycle. Countries now look to the international market for the supply of fuel cycle services, including uranium enrichment, fuel fabrication, and reprocessing, although some fuel cycle services remain nationally focused, especially disposal.

The IAEA has identified three types of multinational arrangement (IAEA, 2005):

- Providing additional assurances for the supply of international fuel cycle services.
- Converting existing national fuel cycle facilities into multinationally owned and/or operated ones through partnerships between NWS and NNWS (add-on).
- Constructing new fuel cycle facilities to be owned and/or managed on a multinational or even regional basis from the outset (partnering).

Whereas a multinational approach involves a group of states or companies collaborating on some aspect of the nuclear fuel cycle, a multilateral approach involves an arrangement involving some form of intergovernmental oversight body, such as the IAEA. This is exemplified in agreements to set up an IAEA owned and managed low-enriched uranium (LEU) fuel bank. For example, the World Nuclear Association

proposed a "guarantee in depth" model to provide greater assurances in the supply of international enrichment services (WNA, 2006). It has a three-tiered structure:

- Customers look to the existing commercial market for the supply of enriched fuel.
- If a company cannot deliver on its contracts for political reasons unrelated to nonproliferation, then other companies guarantee to supply enriched fuel.
- Should this collective guarantee fail, then LEU is made available from a fuel bank under governmental or intergovernmental control.

In 2009, the IAEA approved a Russian initiative to establish a reserve of LEU for the IAEA to supply to its member states. In 2010, the IAEA Board of Governors authorized the IAEA Director General to set up an IAEA owned and managed LEU fuel bank. The IAEA would determine the legitimacy of the customer's claim in light of predefined criteria and the events leading up to the contract interruption. The IAEA would then notify the other enrichment companies to fulfill the obligations. International fuel fabrication services would still have to be assured for a fuel bank to be a credible assurance mechanism. An assured supply of nuclear material does not necessarily entail an assured supply of fabricated fuel.

23.8 International ownership and management of fuel cycle facilities

Due to concerns about the security of supply, further incentives may be necessary to rely on these multinational approaches to the provision of fuel cycle services. One incentive is to offer customers a direct stake in the ownership and/or management of the fuel cycle facilities providing these services (see the IAEA's add-on and partnering options above). This could make financing easier when it may be difficult to mobilize enough capital nationally. Risks could be shared, as well as financial losses, in case of technical or market failure. Such multinational arrangements could be considered alongside moves in many countries of national nuclear facilities moving from government-run enterprises to privately owned and operated, multinational companies. Globalization and the liberalization of energy markets have provided the conditions that support competition, leading to the merging of nuclear power companies. This reflects practices already well established in many other high-technology industries that are simply not sustainable at an individual national level given the high costs involved with development.

There is no single formula to satisfy all states' needs, whether service provider or customer. Different types of multinational arrangements may be necessary (Scheinman, 2004).

23.8.1 Eligibility for services

Commercial enrichment services are provided by the European Gaseous Diffusion Uranium Enrichment (EURODIF) company and URENCO. EURODIF was set up in 1973 by France, Belgium, Italy, Spain, and Sweden to provide enrichment services

to these countries. Sweden withdrew in 1974 and in 1975, its 10% share in the company was passed to Iran through the establishment of a joint French-Iranian enterprise. Today, EURODIF is a subsidiary of AREVA and operates an enrichment plant at the Tricastin nuclear site in France. URENCO was founded in 1971 by the Treaty of Almelo, signed by the governments of Germany, the Netherlands, and the United Kingdom. Whereas EURODIF provides enriched uranium to its members only, URENCO provides enrichment services for its members and others outside the company.

23.8.2 Different degrees of joint ownership

Joint ownership of fuel cycle facilities need not be proportionate. Shares in EURODIF correspond to the level of each member's investment. Initially, URENCO facilities were to be built with equal ownership and investment by the three partners, regardless of location. No single country would then have a majority of shares in the company, thus preventing any dominance in decision making.

23.8.3 Different degrees of joint operation

Joint ownership does not necessarily entail joint operation. A facility can be under multinational ownership yet nationally operated, as long as national decision making is subordinate to the decision of the group of owners. The operation (and regulation) of EURODIF's enrichment facilities remains a responsibility of the host state, France. The French Commissariat à l'Energie Atomique (CEA) proposed that the new Georges Besse II facility to replace EURODIF should be open to international partnerships.

23.8.4 Different degrees of access to technology

France provides and controls the sensitive technology used by EURODIF. Other nonsensitive technology is shared. After the revelations about A.Q. Kahn, URENCO placed stricter controls on its technology. In 2003, URENCO was divided organizationally into Enrichment Technology Corporation (ETC) and URENCO Enrichment Company Ltd (UEC). ETC is a joint venture between URENCO and the French company, AREVA. It provides enrichment technology to UEC, AREVA, and (soon) to the National Enrichment Facility currently being constructed in the United States. ETC develops centrifuge technology, designs centrifuge enrichment plants, and manufactures centrifuges. UEC owns and operates enrichment plants. Centrifuges are provided under a "black-box" arrangement whereby they are supplied, complete, and already assembled by ETC. The operator has no access to the centrifuges directly but only ever interacts with the outside of the black box. The black box remains the property of ETC and must be returned to ETC for repair or disposal when no longer needed. URENCO now operates its uranium enrichment activities under strict arrangements. In a breakout scenario, the facility operators could decide to misuse and modify the facility to produce HEU. While a team of ETC engineers may perhaps need approximately 3 months, other engineers without any experience with the technology within the black box would need 12 months or more to carry this out. This could provide extra

time for the international community to take action. It is unclear if a similar black-box arrangement can be applied to reprocessing, especially when the PUREX process is widely documented and accessible if a country wishes to explore reprocessing. An historic example is EUROCHEMIC, which provided direct access to reprocessing technology. Set up in 1957 by 13 OECD member governments, EUROCHEMIC acted as a training center to develop industrial experience with reprocessing. A pilot reprocessing plant in Belgium was commissioned in 1956, as well as facilities for nuclear chemistry research. It was not setup as an alternative to national reprocessing efforts. Due to competition from the latter, however, operations ceased in 1974 and EUROCHEMIC's installations were progressively taken over by the host country, Belgium, and the decision to close the plant was finally made in 1985.

23.9 Benefits of multinational approaches to the provision of fuel cycle services for nuclear non-proliferation

23.9.1 Increased transparency of national programs

Multinational companies owning and/or operating fuel cycle facilities could be less vulnerable to a state's desire to proliferate than a single state-owned and operated nuclear organization. Overt or covert diversion would be more difficult. A thoroughly interconnected global nuclear industry could allow earlier warning and whistle-blowing of suspicious activities. International professional networks could maintain greater awareness of colleagues' activities.

Multinational arrangements could serve as a confidence-building measure. If a country's desire to proliferate is due to concerns that another country may do so, too, then they could both voluntarily choose to participate in an arrangement that constrains their independent national capabilities to develop sensitive dual-use technologies (Smart, 1980). A country could participate in a similar arrangement to demonstrate its clear intentions not to proliferate, thereby gaining political legitimization to participate in certain fuel cycle activities. NWS may need to be willing to restrain their national capabilities to avoid accusation by NNWS that multinational arrangements are discriminatory.

23.9.2 Proactively assisting the IAEA

The IAEA's powers are constrained by its state-centric statute. The IAEA can only gain information through the voluntary support of member states. Multinational companies may have a greater awareness than national governments about the global circulation of materials, technologies, and personnel. They may be less constrained in proactively providing information directly to the IAEA, as well as informing the IAEA about technology relevant to safeguards being developed outside of member state support programs and national government laboratories.

23.9.3 Reinforcing safeguardability

Internationalization can help to reduce the number of facilities in need of safeguarding, allowing the IAEA to focus its resources more effectively. This is particularly important for the management of used fuel because this is one aspect of the fuel cycle that every nuclear country, however small, must address.

Many countries recognize the economic benefits of seeking international fuel cycle services rather than developing national fuel cycle facilities. Pilot research facilities may still be sought to maintain a national skills base in case the international market should fail. R&D activities can be prone to unauthorized or unreported experiments. Pilot research facilities still need to be fully safeguarded. Consideration should be given to offering some countries a direct stake in the ownership and/or management of research facilities elsewhere. Carrying out R&D on dual-use technology through an international framework increases transparency and maintains confidence that there are no clandestine nuclear weapons programs. However, knowledge could still be misused, as the case of A.Q. Khan demonstrates (IISS, 2007).

23.9.4 Increasing the costs of breakout

Even if certain arrangements do not limit the development of fuel cycle facilities, multinational ownership and/or management maintains the transparency of these activities. This does not eliminate proliferation risks. The host country could still expel multinational staff and breakout of the NPT, although the involvement of other countries in this multinational arrangement would significantly increase the economic and political costs of doing so.

23.9.5 Addressing country breakup

Internationalizing the management of nuclear materials could mitigate the consequences of any future breakup of countries or collapse of their political regimes. Thousands of scientists involved with nuclear weapons programs were left unemployed or underemployed following the dissolution of the USSR. At that time, there were concerns that they could be tempted to sell their expertise on the black market, leading to initiatives in the 1990s to redirect former weapons scientists into civil employment. A loss of control over nuclear materials also raised concerns about the illicit trafficking in these materials that could aid countries that are inclined toward possible nuclear proliferation.

23.9.6 Spreading best practice

The opportunity for technology transfer, or at least hands-on training may be an important attraction of multinational arrangements. While the scientific principles of enrichment and reprocessing may be well-known, the ability to operate a commercial enrichment or reprocessing facility successfully presupposes operational experience with the technology. Such arrangements could help to spread best practice,

especially from countries experienced with nuclear power to those embarking on nuclear power for the first time.

23.9.7 Wider benefits beyond nonproliferation

Internationalizing the management of nuclear materials would help countries that lack the national infrastructure to do so securely. This could help address security risks posed by the management of used fuel (see Section 23.4).

23.10 Internationalizing the management of used fuel

23.10.1 Cradle to grave fuel cycle services

International fuel cycle arrangements that couple the supply of fresh fuel with the management of used fuel could be a major attraction to countries embarking on nuclear power by allowing them to avoid some of the major uncertainties, costs, and complexities involved in developing a nuclear power program. These so-called cradle to grave fuel cycle services are not new. The former USSR leased fresh fuel to customer states for their nuclear power reactors, and used fuel was repatriated back to the USSR. The United States provided fuel for U.S.-built LWRs in other countries on 30-year contracts, specifying that used fuel was only to be reprocessed or exported to third parties with U.S. agreement. Contracts for U.K.-designed Magnox reactors in Japan and Italy provided for the fuel to be reprocessed in the United Kingdom and HLW to be repatriated. Conversely, Canada exported CANDU reactors fueled with natural uranium with no constraints on the management of used fuel, and used fuel from one of its reactors was reprocessed to provide the plutonium used in the Indian nuclear test in 1974. This event spurred governments to include constraints on the management of used fuel in fuel supply agreements through contractual obligations to consult before reprocessing and retransfer of used fuel.

A single company could provide commercial services across the fuel cycle from cradle to grave. This could involve fuel-leasing arrangements. Currently, an operator buys uranium from a mining company and then has it converted, enriched, and fabricated into fuel before irradiating it in its reactors. If a supplier of fresh fuel could retain ownership, it could manage the fuel once used. Only Russia is prepared to lease fuel and take it back once used. This has been exemplified by its arrangement with Iran for operating that country's reactor at Bushehr (albeit arrived at under considerable U. S. pressure). Russia may be negotiating with Vietnam to supply fuel and then take it back once used for reprocessing. Today, AREVA provides an "integrated offer" whereby it will construct nuclear reactors, provide the fuel for them, and reprocess the used fuel. Arguably, EDF provides a similar service by transmitting electricity generated by reactors in France across its borders to Germany, Italy, Spain, and the United Kingdom, while the used fuel remains and is managed in France.

Alternatively, several companies could provide fuel cycle services that between them cover the entire fuel cycle. Some companies could provide the same service,

which may be more attractive to potential customers by diversifying the supply of services. The grave need not be located in the same country as the cradle.

Cradle to grave services are being considered in the development of SMRs. Some SMR concepts are based on long-life cores so that the reactor does not need refueling. Fresh and used fuel management would be limited to the installation and replacement of the entire reactor unit. The storage, reprocessing, or disposal of used SMR fuel would be carried out elsewhere by a company or state with access to these fuel cycle facilities.

23.10.2 Options for international reuse

Not all countries will produce large enough volumes of used fuel to justify investing in their own reprocessing and MOX fabrication facilities. World capacity to reprocess used fuel is expected to exceed demand. Commercial reuse services are already provided internationally. Used fuel from Belgium, Germany, Italy, Japan, the Netherlands, Sweden, and Switzerland has been sent to France and the United Kingdom to be reprocessed. Plutonium has been returned as MOX fuel and irradiated in reactors in these countries.

Countries offering reuse services could be paid to burn MOX fuel in their own reactors so that only HLW is returned to customer countries. This option has been suggested in recent proposals to manage stockpiles of separated plutonium internationally (Suzuki et al., 2009). Utilities could declare some plutonium to be excess in exchange for an energy equivalent of LEU. Reactor operators would bid to irradiate this excess plutonium, having been fabricated into MOX fuel, as part of an international disposition program funded by the countries that own these stockpiles. The ownership of the resulting used MOX fuel and responsibilities for how and where it is managed in the longer term (including disposal) would still need to be clarified at the outset.

23.10.3 Next steps for internationalizing disposal

While options exist for international reuse, there is a lack of options for international storage and disposal. The U.S. Global Nuclear Energy Partnership and Russian Global Nuclear Power Initiative included provisions to lease fresh fuel and then reprocess it once used. Neither included provisions to dispose of HLW that would arise, except by returning it for disposal in the customer country. A comprehensive cradle to grave fuel cycle service that includes disposal could provide a key incentive for countries to decide not to construct enrichment or reprocessing facilities nationally.

Access to interim storage provided by third parties could be attractive to countries facing acute problems in storing their used fuel if national capacity is lacking. An international storage facility could be colocated with a reprocessing and MOX fabrication facility or a GDF. This may incentivize the country offering the storage service to ensure these final management options can be delivered when required. Alternatively, stored used fuel could be sent to a third party for reprocessing or disposal, although this would entail extra transport costs.

Transfer to an international storage facility may be difficult if a final management option is yet to be decided. Returning used fuel after a period of interim storage could reinstate the national problems that international storage was meant to address. International storage could be more politically acceptable if part of an international reuse or disposal arrangement. This is essentially what the United Kingdom has provided at Sellafield for storing then reprocessing used fuel from international partners.

Geological disposal is not yet offered internationally, although the large volumes of used fuel arising from a nuclear renaissance, especially if many countries opt for an open fuel cycle, could potentially create a commercial market for disposal services. No country has yet championed international disposal due to concerns that doing so could detract support for the country's own national disposal program. National programs must not be hindered because demonstrating progress in disposal is in everyone's interest. This does not mean that governments should reject international disposal outright as they need not commit themselves to implementing it at this stage. Rather, governments should be prepared to engage with it constructively so that even if they are not interested in international disposal themselves, it still remains open for other interested parties to explore.

23.11 Conclusions and the future

There is no proliferation-proof fuel cycle. Proliferation risks can be managed, not eliminated. A conclusion that a particular nuclear fuel cycle option has high proliferation resistance should not be interpreted to mean that it is proliferation proof. Even the term *proliferation resistant* can be misleading. Proliferation resistance is a relative concept used to compare different fuel cycle options.

No matter what fuel cycle technology is developed, it will still have to be placed under IAEA safeguards once deployed, irrespective of its intrinsic proliferation resistance. Proliferation resistance assessments could usefully focus on designing fuel cycles to increase their "safeguardability" so they can be more effectively and efficiently placed under international safeguards, as well as facilitating other extrinsic measures. In the short term, a robust safeguards research program may be the single most significant technological investment that can be made to improve the proliferation resistance of nuclear power. Technological investments would also be valuable to support international fuel cycle arrangements that may be more feasible in the longer term (APS, 2005).

Proliferation risk assessments should not assess the proliferation vulnerabilities of specific technologies in isolation. A particular technology may have proliferation vulnerabilities yet still improve net proliferation resistance when considered as part of a wider fuel cycle. The proliferation resistance of a given fuel cycle option should always be assessed from cradle to grave.

Technological assessments cannot, by themselves, identify a threshold below which a nuclear fuel cycle poses an acceptable level of proliferation risk. To establish such a threshold would ultimately require a political, not a technological, judgment to

be made. The proliferation resistance of a nuclear fuel cycle is directly related to the wider geopolitical system in which it is embedded. This, itself, is a dynamic system that can change over time. Technology may not even be the primary contributor to proliferation. A failure to appreciate fully the political dimension of nonproliferation makes the concept of proliferation resistance at best irrelevant and at worst counterproductive (Acton, 2009).

In many countries, the nuclear industry has moved from being purely state-run, national companies into multinational enterprises. This increases the transparency of civil nuclear power programs and this multinational practice should continue. A fully internationalized nuclear fuel cycle and thoroughly multinationalized global nuclear industry may be part of the solution to proliferation, rather than the problem.

There has been renewed interest in the potential of offering cradle to grave fuel cycle services that couple the supply of fresh fuel with the management of used fuel and radioactive wastes. Such a comprehensive offer could be attractive to some countries in preference to developing their own national fuel cycle capabilities, thereby providing a key nonproliferation incentive that also offers major nuclear security benefits. The sensitivities surrounding such arrangements should not be underestimated. This does not mean that governments should reject them. By supporting collaborative research to explore these options, governments can keep them open without needing to commit to their implementation at this stage.

A future in which nuclear power plays a major role in energy generation with manageable proliferation and security risks will require nation-states to support research on fuel cycles to keep policy options open; consider the commercial feasibility and political acceptability of fuel cycle arrangements; and establish regulatory systems globally that give confidence in whichever options are chosen.

References

Acton, J., 2009. The myth of proliferation resistant technology. Bull. At. Sci. 65 (6), 49–59. www.brc.gov/sites/default/files/meetings/presentations/james_m_acton-the_myth_of_proliferation-resistant_technology.pdf.

APS, 2005. Nuclear power and proliferation resistance: securing benefits, limiting risk. Nuclear Energy Study of the Panel on Public Affairs. American Physical Society, Maryland. www.aps.org/policy/reports/popa-reports/proliferation-resistance/upload/proliferation.pdf.

DoE, 1996. Proliferation vulnerability red team report. Sandia National Laboratories, SAND97-8203. Department of Energy, Washington, DC.

GAO, 1978. Quick and secret construction of plutonium reprocessing plants: a way to nuclear weapons proliferation? Oak Ridge Report. Government Accountability Office, Washington, DC. http://archive.gao.gov/f0902c/107377.pdf.

IAEA, 2005. Multilateral Approaches to the Nuclear Fuel Cycle. International Atomic Energy Agency, Vienna. http://www-pub.iaea.org/MTCD/publications/PDF/mna-2005_web.pdf.

IAEA, 2010. Technical features to enhance proliferation resistance of nuclear energy systems. In: IAEA Nuclear Energy Series NF-Y-T-4.5, International Atomic Energy Agency, Vienna. www-pub.iaea.org/MTCD/publications/PDF/Pub1464_web.pdf.

ICNND, 2009. Eliminating Nuclear Threats. International Commission on Nuclear Non-Proliferation and Disarmament, Canberra. www.icnnd.org/reference/reports/ent/pdf/ICNND_Report-EliminatingNuclearThreats.pdf.

IISS, 2007. Nuclear Black Markets: Pakistan, A.Q. Khan and the Rise of Proliferation Networks—A Net Assessment. International Institute for Strategic Studies, London. http://www.iiss.org/en/publications/strategic%20dossiers/issues/nuclear-black-markets–pakistan–a-q–khan-and-the-rise-of-proliferation-networks—a-net-assessmen-23e1.

IISS, 2008. Nuclear Programmes in the Middle East: in the Shadow of Iran. International Institute for Strategic Studies, London. www.iiss.org/en/publications/strategic%20dossiers/issues/nuclear-programmes-in-the-middle-east–in-the-shadow-of-iran-5993.

NAS, 2006. Safety and security of commercial spent nuclear fuel storage: public report. National Academies of Science, Washington, DC. www.nap.edu/openbook.php?record_id=11263&page=R1.

Royal Society, 2011. Responsible Stewardship of a Nuclear Renaissance. Royal Society, London. www.royalsociety.org/~/media/Royal_Society_Content/policy/projects/nuclear-non-proliferation/FuelCycleStewardshipNuclearRenaissance.pdf.

Scheinman, L., 2004. The nuclear fuel cycle: a challenge for non-proliferation. Disarmament Diplomacy (76). www.acronym.org.uk/dd/dd76/76ls.html.

Smart, I., 1980. Multinational arrangements for the nuclear fuel cycle. Energy Paper No. 43. Department of Energy, London.

Suzuki, T., et al., 2009. Japan's Initiative for Mutual Assured Dependence. Japan Cooperative Security Initiative, Center for Global Partnership of Japan Foundation, Toshiba International Foundation, Pugwash USA and Pugwash Japan, Washington DC, New York City. http://www.aec.go.jp/jicst/NC/about/kettei/100415.pdf.

UN, 2010. Review conference of the parties to the treaty on the non-proliferation of nuclear weapons: final document, vol. 1. United Nations, New York City. www.un.org/ga/search/view_doc.asp?symbol=NPT/CONF.2010/50.

White House, 2010. Work plan of the Washington nuclear security summit office of the press secretary. The White House, Washington, DC. http://www.whitehouse.gov/the-press-office/work-plan-washington-nuclear-security-summit.

WNA, 2006. Ensuring security of supply in the international nuclear fuel cycle. World Nuclear Association: London. http://www.world-nuclear.org/reference/pdf/security.pdf.

Developments in reprocessing of spent nuclear fuels for the thorium fuel cycle

24

Christian Ekberg
Chalmers University of Technology, Göteborg, Sweden

Acronyms

ATW	accelerator driven transmutation of wastes
BARC	Bhaba Atomic Research Centre
EAR	estimated additional reserves
HMTA	hexamethylenetetramine
HTGR/HTR	high-temperature (gas-cooled) reactor
IAEA	International Atomic Energy Agency
IGCAR	Indira Gandhi Centre for Atomic Research
IFR	integral fast reactor
LWR	light water reactor
MSBR	molten salts breeder reactor
NEA	Nuclear Energy Agency (of the OECD)
OECD	Organization for Economic Cooperation and Development
PUREX	plutonium uranium redox extraction
RAR	reasonably assured reserves
REE	rare earth elements
SX	solvent extraction
TBP	tributyl phosphate
USGS	U.S. Geological Survey

24.1 Introduction

In recent years there has been a revival of interest in thorium as a fuel for nuclear reactors. The history of the element thorium is rather short. In 1828, a strange new mineral was found by Hans Morten Thrane Esmark, who passed it to the well-known Swedish chemist Jöns Jakob Berzelius. He isolated the element and named it after the northern god of thunder, Torium (Tor in Swedish). The natural radioactivity of thorium was not discovered until 1898, independently by Marie Curie and Gerhard Carl Schmidt.

The by far most common naturally occurring nuclide of thorium is ^{232}Th, which is the mother of one of the four natural decay series (the 4n+ series). However, several other isotopes exist in nature as a result of other decay chains such as ^{234}Th and ^{230}Th from the ^{238}U decay chain. In water, thorium ions always are in the oxidation state +4

Reprocessing and Recycling of Spent Nuclear Fuel. http://dx.doi.org/10.1016/B978-1-78242-212-9.00024-1

and, thus, form strong complexes with hard electron donors such as oxygen making ThO_2 highly insoluble and also highly temperature resistant with a melting point of 3390 °C. This has advantages and disadvantages for the potential use of thorium oxide as a nuclear fuel.

In nature, thorium exists in several minerals such as thoranite ($ThO_2 + UO_2$), thorite ($ThSiO_4$), and allanite (which itself is not a thorium mineral but often contains thorium as an impurity). Even if these minerals are thorium-rich they are themselves not so common. The average content in the Earth's crust is about 10 g/ton and in water about 1 μg/ton. However, considerably richer common sources such as monazite sands are available and at present are one of the main sources of raw materials. In a possible future where thorium will be used as fuel for nuclear reactors, it will also be necessary to excavate from other mineral sources. The actual amount of thorium reserves, available at (or near) the current market price, has high uncertainties. Studies have been performed by the U.S. Geological Survey (USGS) and OECD/NEA yielding different results as seen in Table 24.1 (note that RAR means reasonably assured reserves and EAR means estimated additional reserves).

Tables of availability such as shown here are always difficult to make because figures vary as do the estimated costs. According to USGS the RAR <$80/kg for uranium are about 2.6 Million tons. This figure is rather close to that of today's price RAR for thorium. However, we should bear in mind that current nuclear reactors primarily use the fissile isotope ^{235}U, which is only 0.7% of the total uranium.

There have been several uses for thorium over the years. Due to its excellent thermal properties, one of the first real industrial uses was as lantern mantles but later high-temperature crucibles were also made. As a curiosity, it may be worth noting that it is also possible to make thorium-containing glass with a very high refractive index for use in very high-quality lenses. In science, thorium has often been used as an analogue for other tetravalent actinides such as plutonium and uranium as thorium has only one stable oxidation state in solution unlike the other early actinides. Therefore, experiments can be performed without any redox control. This use may, however, be questioned on the basis of the fact that although thorium is in the actinide series thorium (IV) does not possess any 5f electrons and is considerably larger than both plutonium (IV) and uranium (IV). Therefore, neither the covalency attributed by the 5f

Table 24.1 Estimates of the world thorium reserves by the U.S. Geological Survey and OECD/NEA

Country	RAR (USGS)	RAR (NEA) (kiloton)	EAR (NEA) (%)
India	963	519	21
USA	440	400	13
Australia	300	489	19
Brazil	16	302	10
Canada	100	44	2
Norway	170	132	4
World total	1913	2810	

electrons nor the ionic size effect could actually be considered to be analogous with the other tetravalent actinides; a better analogue could be zirconium (IV).

24.1.1 Nuclear fuel applications

Thorium is a fertile rather than a fissile nuclide with thermal neutrons. This means that it can be converted by nuclear reactions to fissile material that can then be fissioned by neutrons. Thus, the thermal behavior is in many cases similar to that of ^{238}U, where neutron irradiation is needed to produce the fissile material (e.g., ^{239}Pu). In the case of thorium fuel, the fissile material is mainly ^{232}U, ^{233}U, and ^{235}U (see Figure 24.1).

Another effect of the fact that thorium is not fissile is that there is need for the addition of a starter fissile material in the fuel (e.g., ^{239}Pu or ^{233}U). Once started, the reactor can facilitate breeding of fissile material during operation. Capture of neutrons in ^{233}U is not a serious drawback as a second capture (in ^{234}U) yields fissile ^{235}U, but reduces the breeding gain because two neutrons are consumed without a net increase in fissile material.

The radiotoxicity of some different nuclear fuel cycles has been discussed by Franken et al. (1995), where they presented radiotoxicity curves for both the once-through option (Figure 24.2) and some recycling options (see Figure 24.3).

It should be noted that in the case of the Th-Pu fuel presented in Figure 24.2, the fact that most of the plutonium is actually burnt during operation is not taken into account. Such considerations would require assumptions regarding power density used and other factors that were deemed unnecessary.

Similar calculations were made by the same authors for the case of recycling of the different fuels (see Figure 24.3). The contribution of the thorium itself to the

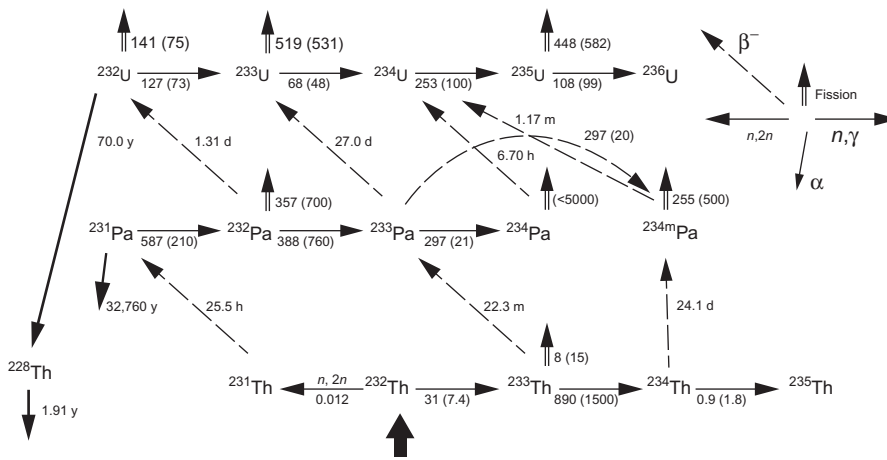

Figure 24.1 Nuclear reactions in irradiated thorium. Numbers are half-lives or effective reaction cross sections for an LWR. Thermal neutron data are given in parentheses. From Choppin et al. (2013).

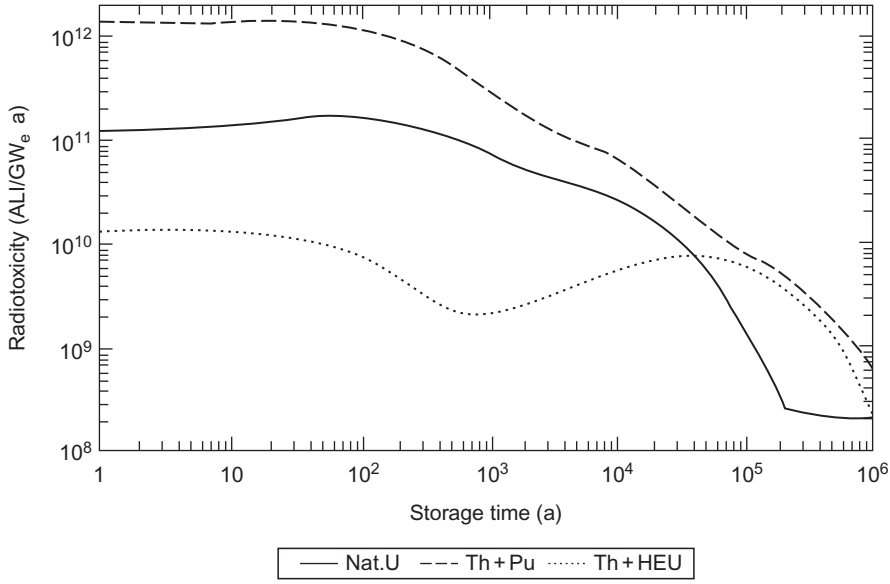

Figure 24.2 Radiotoxicity of different fuels in HWR once-through systems (Franken et al., 1995).

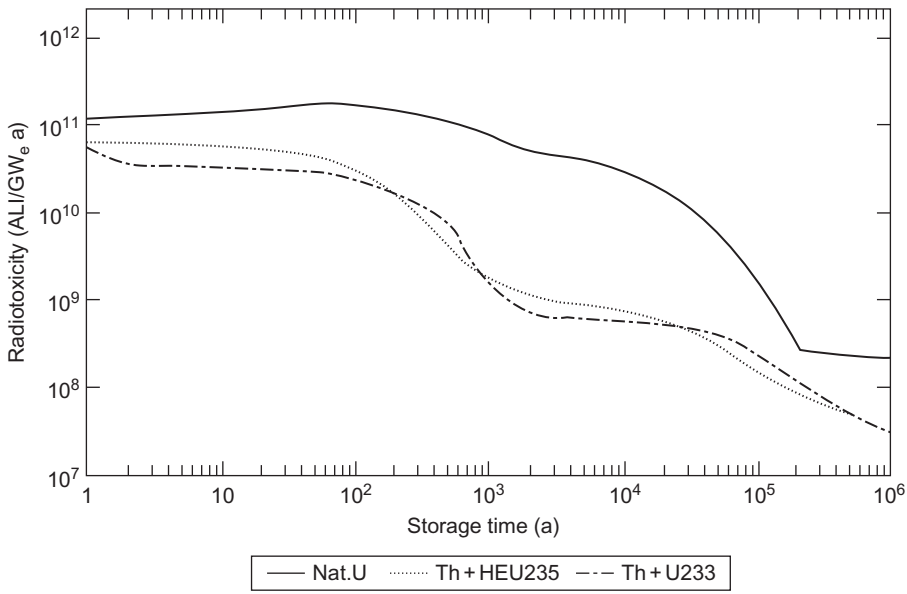

Figure 24.3 Radiotoxicity of different HWR cycles with U-recycling (Franken et al., 1995).

radiotoxicity is negligible, but the presence of uranium will lead to buildup of some smaller amounts of heavier isotopes and elements, mainly plutonium. This explains the relatively high radiotoxicity in the first centuries. If plutonium were to be recycled this early, radiotoxicity would naturally be reduced. Essentially, it would be possible to further reduce the long-term radiotoxicity by recycling the ^{231}Pa. This is generally unwanted because the protactinium and ^{232}U content in the newly fabricated fuel increases the gamma activity to levels that make fuel handling difficult. Another radiation hazard in thorium recycling is the ^{228}Th isotope. Like ^{232}U, which cannot be separated from the desirable ^{233}U, ^{228}Th cannot be separated from the natural ^{232}Th, thus increasing the gamma radiation dose from refabricated thorium fuel.

24.2 Virgin thorium production

Extractions of thorium from different ores have been done for many years now and, therefore, when considering recycling processes for thorium-based nuclear fuel there is a considerable amount of knowledge and experience in this field. Thus, as usual, a good knowledge of past experiences will be profitable in order to avoid making the same mistakes again but in a new context.

There was an increase in thorium production in the 1950s when the U.S. nuclear program started to consider thorium as a potential nuclear fuel and, thus, the purities had to be "nuclear standard." Then, new processes for increased purity were developed even if the starting processes were still unchanged. It should, however, be recognized that these high-purity methods, such as the IOWA process (using a tributyl phosphate (TBP)-based separation scheme), have not been used industrially to any great extent.

As pointed out earlier, in natural environments there are some dominating elements that could potentially be an issue in thorium production, including uranium and the lanthanides.

Regarding the possible use of thorium in nuclear applications, the lanthanide impurities must be kept to a very low amount due to their high cross-section for neutron absorption, which makes them act as neutron poisons in a reactor core, thus causing considerable neutron losses. In addition, there are also anionic species such as sulfates and phosphates that will disturb the solvent extraction-purification process.

It is worth mentioning here that some of the processes needed for handling thorium-rich deposits will not be needed for recycling of nuclear fuel because the material will be more homogeneous and the impurities rather well known. Therefore, a special section is dedicated to the recent developments in the reprocessing of spent thorium fuel (Section 24.4).

There are naturally several more or less similar ways to extract thorium from natural sources, of which the processes given here are examples. However, it should be noted that even if there are numerous suggestions in the literature, almost none of them have progressed to industrial maturity for one reason or another. Typically, the cost of the final product is the main reason followed by restrictions to process changes due to already existing equipment.

24.2.1 Starting material and treatment

As noted earlier, there are several different possible starting materials for thorium mining and they are usually divided into primary deposits or secondary deposits. In the first category we find rock types such as pegmatite, while the secondary deposits are typically different sands and clays (e.g., monazite sand). If we start with the primary deposits, the thorium concentration is rather low and, therefore, several enrichment processes are needed.

If we assume a starting material of a pegmatite containing thorium, a 63% concentrate can be obtained by crushing, fine grinding, and finally using a flotation process at slightly elevated temperature. Then the main constituents are thorium and the lanthanides, where the latter are typically present as carbonates. These carbonates are then leached by HCl, increasing the concentration by about 10% before the final thickening, filtration, and calcining, which will produce a concentrate of about 90% thorium and lanthanides content.

In the case of using a secondary deposit like monazite sand, there is still the need for rather complicated pretreatment. There are typically two sources for this starting material: either the sand is collected off the coast as a wet sludge, which is subjected to gravity separation in batteries of separators, or the sand from the beach is used and then the starting point is dry sorting following an initial removal of the coarse fraction.

After the initial refinement, the next step is separation by magnets of different strength, starting with the weakest. First, the minerals magnetite and ilmenite are removed and then in the next step garnet is removed. Due to the fact that lanthanides are paramagnetic, the next two strongest magnetic steps will recover the actual monazite as a fine and a coarse fraction, both of which now reach a purity of up to 97%. The final, nonmagnetic fraction is often used as a source for, for example, zircon, rutile, and gold, which will then be valuable by-products of the thorium production.

24.2.2 Mineral digestion and coarse separation

The fine-grained material from the pretreatment discussed above will have to be further purified and unwanted contaminants removed. Most of the starting materials are fairly inert; hence, rather harsh chemical methods are needed in order to reach a final solution suitable for the fine-separation processes, which are often performed by solvent extraction.

There are several issues concerning the digestion of the ore. The low solubility of the thorium fraction makes leaching a slow process. In addition, there are typically rather large concentrations of strong complexants like sulfate and phosphate, which makes the chemical composition and physical parameter window rather narrow and process control vital because of the potential for reprecipitation of thorium sulfate and phosphates. Essentially, there are two main methods of digestion: either the acidic route using hot, concentrated sulfuric acid or the alkaline route where hot sodium hydroxide solution is used. The latter method is more expensive but has the advantage that no phosphates are carried over into the final solvent-extraction-based purification step.

24.2.2.1 Acid digestion

The acid digestion route is the most common route of mineral digestion due to its lower cost. Usually the demand for high-purity product is not so important, which lessens concerns over any subsequent problems in the final purification step. The main steps of the acid digestion route are shown in Figure 24.4.

The process starts with the fine ground minerals/sand being contacted with about a 60% excess of sulfuric acid, which forms a slurry that thickens further to almost a solid product. This solid is then contacted with fuming sulfuric acid for about 5 h. It would, in principle, be possible to use a higher acid concentration to increase the reaction rate, but then the viscosity would increase and, thus, the overall reaction rate would be reduced. Also, the temperature is selected rather carefully. An increase by, for example, 70 °C, would increase the reaction rate but would also increase the risk of forming insoluble thorium compounds, while at lower temperatures the reaction rate becomes too slow for efficient processing. Typically, a ratio of acid to sand mass is about two, making sure that any possible precipitates formed will not hinder the contact between unreacted sand and acid. After the reaction is completed, the slurry is diluted with about 10 times its volume of water. The thorium and the lanthanides will then be in solution, while undissolved sand can be filtered off and entered into the process again. In the subsequent step of raising the pH, the base must be added very carefully to avoid local precipitation of insoluble material. This requires vigorous stirring of the mixture.

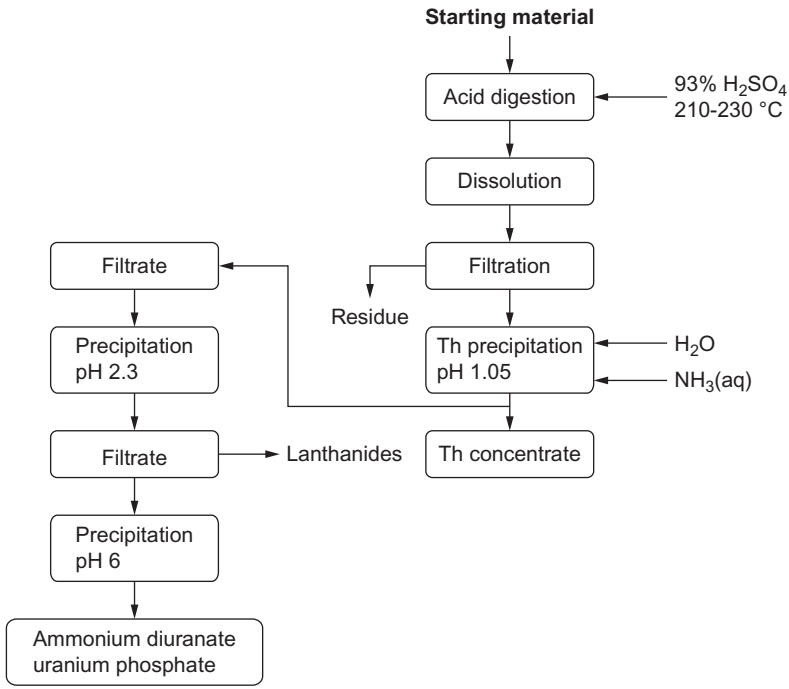

Figure 24.4 The acid digestion route (Habashi, 1997).

Thorium phosphate will precipitate at about pH 1, while the lanthanide phosphates will precipitate around pH 2. Finally, a thorium concentrate is obtained. This concentrate can be handled in different ways depending on subsequent fine purifications, but in principle it is redissolved in a suitable mineral acid such as HNO_3.

There are naturally several variations to the method described above, where the main objectives are to end up with either a mixture of thorium hydroxide and lanthanide hydroxide or a similar oxalate mixture. In the latter case, the pH of the leach solution is raised to about 1.5 while at the same time adding oxalate. However, regardless of chemical form, an enriched and partially purified solid is obtained. It is then redissolved and purified to a higher grade using solvent extraction.

24.2.2.2 *Alkaline digestion*

The alternative to acid digestion is to treat the ore material with sodium hydroxide. This is a more expensive process than acid digestion but the resulting solution is considerably purer, especially vis-à-vis the phosphate content, which is very low. A simplified scheme for an alkaline digestion process is shown in Figure 24.5.

There are some items worth mentioning in relation to the process outlined in Figure 24.5. The leaching conditions are rather mild, which means that in order to have a reasonably fast dissolution the input materials have to be as fine-grained as possible.

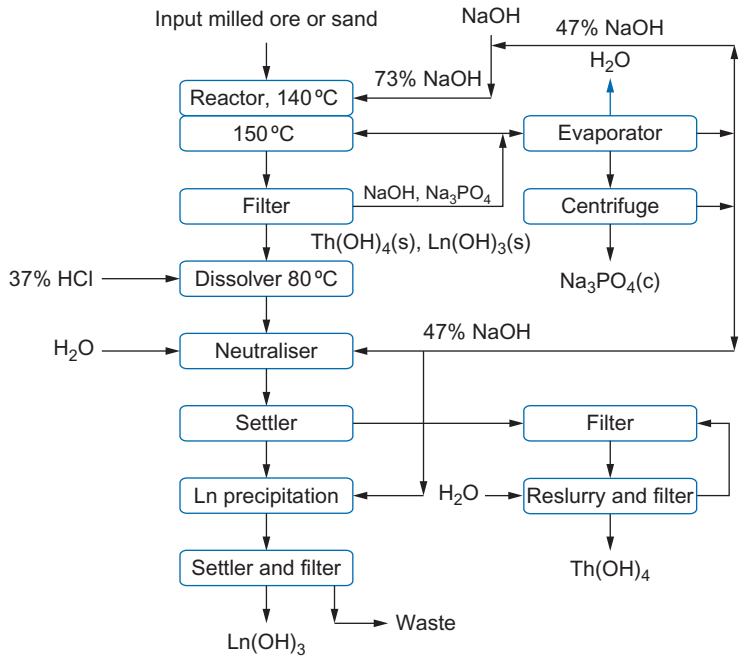

Figure 24.5 A caustic soda process, simplified from Habashi (1997).

The temperature in the process is another issue. If the temperature is too high, the precipitates/filtrates may be partially transformed into thorium oxide, which will not readily dissolve in the other parts of the process. Any uranium present will follow the trisodium phosphate as that precipitates when the temperature is lowered, thus ensuring that the product will be very low in phosphate, which allows for a simpler purification scheme in the solvent extraction stage. The amount of uranium initially dissolved will depend on the amount of dissolved SiO_2. In the neutralizer, the pH is selected so that thorium and any remaining uranium will precipitate but not the lanthanides. This is, however, not an efficient step for uranium separation as its solubility will depend heavily on the oxidation state. If it has been possible to keep the uranium in its tetravalent form it will follow the thorium, but if it has been oxidized to its hexavalent form it will follow the lanthanides. Thus, by adding some redox control it is possible to direct any remaining uranium to the desired end product.

From this process it is possible to proceed in different ways. If the purity from the digestion process is good enough, the thorium hydroxide may be heated up to produce thorium oxide directly. Alternatively, the thorium hydroxide may be dissolved in some acid, preferably nitric acid, and purified further using solvent extraction.

Despite some clear advantages, the alkaline digestion is not the preferred method by industry due to the higher costs and more complicated flows of solid materials and filtrates.

24.2.3 Fine purification using solvent extraction

Separating thorium from other cations using solvent extraction is in itself not a major problem because distinctions are usually made with respect to size, charge, shape (steric hindrance), and covalency of the interactions. Thorium is a stable tetravalent ion and, thus, can be separated from most other actinide ions by controlling the redox chemistry. It is also rather large, which distinguishes it from other tetravalent ions such as zirconium. Additionally, it has no 5f electrons and, thus, will not be prone to strong interactions with soft donor atoms.

Solvent extraction uses one (or a combination) of several possible mechanisms. Three basic mechanisms are typically given (which may be further subdivided): extraction by cation exchange, extraction by solvation, and extraction by anion exchange. Each of these mechanisms can be used for thorium extraction, but all have different advantages and disadvantages.

In the case of cation exchange, the main issue is that most cation exchangers use hydrogen as the exchanging atom and, thus, only work at relatively high pH where thorium will precipitate as the hydroxide (or, in the case of purification from mined ores, as phosphates). Thorium does not often form anionic complexes, but it is possible in the case of, for example, sulfate complexation where a tetra-sulfate anionic complex is formed. This complex can then be extracted by the use of an amine, for instance. It is, however, worth noting here that there is a distinct difference between primary and tertiary amines; the former are highly efficient for thorium extraction while the latter show very poor extraction of thorium (Amaral and Morais, 2010). The extraction mechanism most often used industrially is then extraction by solvation

where the metal is complexed by anions, typically nitrates, and then the remaining coordinating water molecules are replaced by the extracting agent.

In principle, the two last extraction mechanisms have been brought to either industrial scale or fairly large-scale pilot plant use. These are discussed further below with examples of processes that have been tested at least at the semipilot scale for thorium extraction from mineral leachates.

24.2.3.1 Anion exchange process

There are many possible anion exchangers to use in a process, but in the case of thorium extraction the amines are the most commonly used. One of the better-known thorium extraction processes using amines is the so-called AMEX process developed at Oak Ridge National Laboratory in the United States. The basis for the AMEX process is the extraction of a thorium sulfate complex by a primary amine into the organic phase where the diluent is typically 97% kerosene and 3% tridecanol. The extraction reaction is

$$4RNH_2H + HSO_4^-(org) + Th(SO_4)_4^{4-} \rightleftharpoons [RNH_2H]_4[Th(SO_4)_4](org) + 4HSO_4^-$$

Tests were conducted using different amines and the best extraction of thorium was found using either branched primary amines or secondary amines with the branching distant from the nitrogens (see Table 24.2).

Table 24.2 Extraction of some metals (about 1 g/L) from 1 M sulfate solution (pH 1) in contact with 0.1 M amine in kerosene with phase ratio 1/1

Amine type	Example amine	$D_{U(VI)}$	D_{Th}	D_{Ce}
Branched primary	Primene JM[a] or 1-(3-ethylpentyl)-4-ethyl-octylamine	5-30	>20,000	10-20
Secondary, alkyl branching distant from nitrogen	Di(tridecyl)amine	80	>500	<0.1
Secondary, alkyl branching on the first carbon	bis(1-isobutyl-3.5-dimethylhexyl)amine	80-120	5-15	<0.05
Tertiary with no branching or branching further than third carbon	alamine-336, triisooctylamine	140	<0.03	<0.01

[a]Trialkylmethylamine, homologous mixture, 18-24 carbons.
Crouse and Brown (1959).

When studying Table 24.2 it becomes evident that separation of thorium and uranium can be achieved by selecting different types of amines because thorium extraction is favored by the primary amines while uranium extraction is favored by the tertiary amines. In any case, some of the very high distribution ratios shown in Table 24.2 are not really relevant for industrial processes due to problems with stripping as well as imperfect phase separation. One additional complicating factor is that, as discussed before, the mineral leachate liquor will probably contain significant amounts of phosphate that will lower the distribution ratios and in addition, as in any chemical process, it is most profitable to perform the extraction at as high solvent loading as is practicable.

Stripping from the loaded organic phase can be done using several methods where contact with nitrate or chloride solutions are the most common. After stripping with nitrate, for example, the organic phase can be contacted with a base such as ammonium hydroxide and the nitrate can be recovered and the organic phase regenerated. When chloride is used for stripping, the hydroxide recovery of chloride is economically optional. There are also other stripping methods such as with hydroxide or carbonate. In the former case, the thorium is precipitated and separated, but the recovery of the often gelatinous hydroxide is difficult industrially. In the case of carbonate, it is important to have an excess of the anion to get a soluble thorium carbonate in the aqueous phase. If too little carbonate is used, a precipitate will be formed that will require special treatment to handle. It is sometimes suggested to run the solvent extraction process such that the organic phase is the continuous phase, whereupon the precipitate is more easily separated. However, avoiding a precipitate is always the better choice.

Using the knowledge described above, several test processes were developed using different stripping agents (see Figures 24.6 and 24.7).

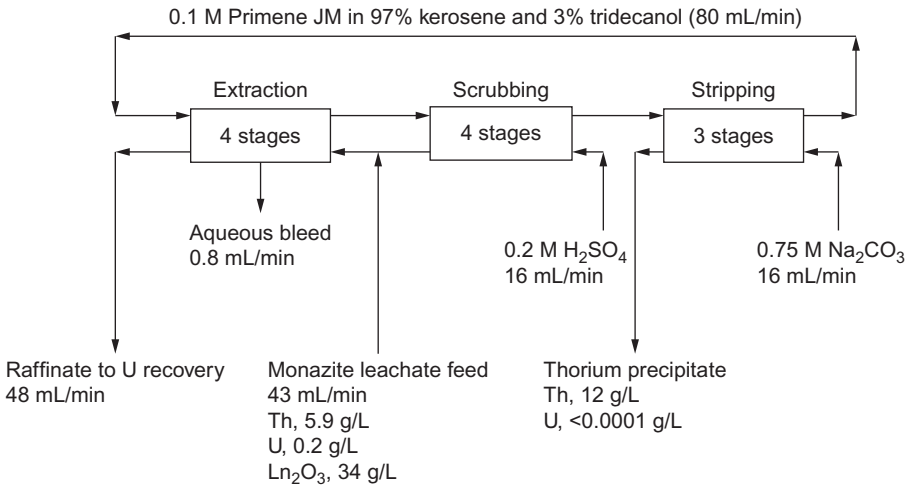

Figure 24.6 Separation process using carbonate as stripping agent. Thorium recovery >99.8%.

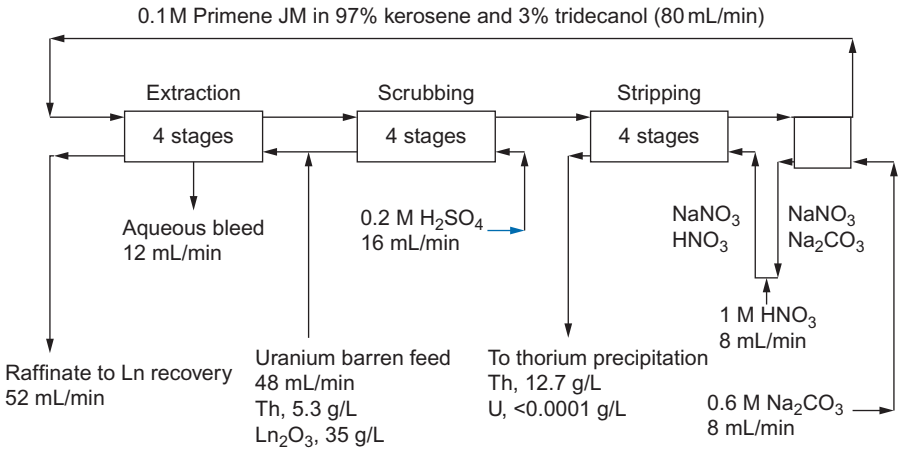

Figure 24.7 Thorium recovery using nitrate strip from uranium-barren liquor. The last stage is an amine regeneration step.

It is clear from the flow rates in Figures 24.6 and 24.7 that this is not an industrial process. Indeed, calculations for up-scaling were made, but it was considered too expensive at the time as the need for pure thorium was not that great.

Naturally, only recovering thorium from the mineral-rich leach liquor is not good enough for a profitable industrial process. Therefore, additional successful schemes were tested for the recovery of uranium and lanthanides from the raffinate solution resulting from the process described in Figure 24.6 (see Figures 24.8 and 24.9).

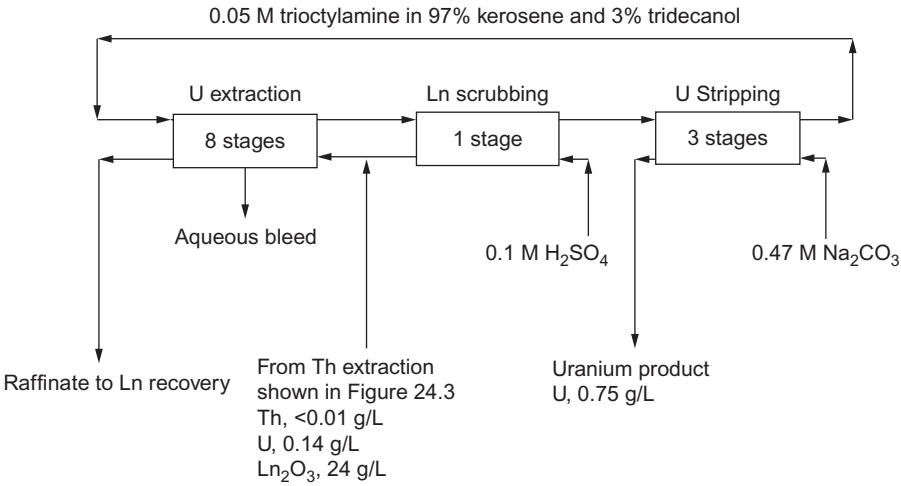

Figure 24.8 Uranium recovery part of the AMEX process.

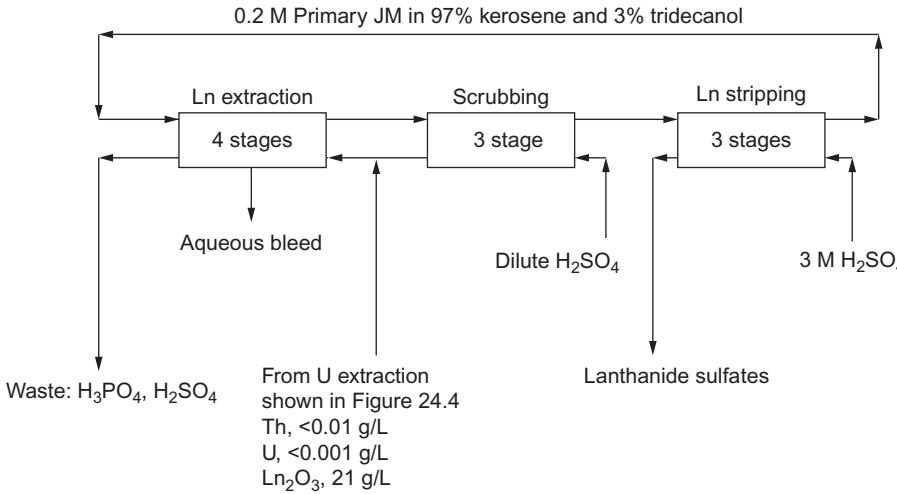

Figure 24.9 Lanthanide recovery part of the AMEX process.

As can be seen in Figures 24.8 and 24.9, the selectivity of the different amines is now used for the selective recovery of the valuable constituents from the original mineral source material. The purities obtained in this process are high, but the costs prevented an extension to use as an industrial process. However, the feasibility was clearly proven.

Because the content of both monazite sand and many other thorium-containing minerals face the same difficulties in separation, the pioneering work with the AMEX process was followed by several other similar processes as described below.

More recent studies of the amine extraction systems have been made by El-Yamani and Shabana (1985) where not only the extraction by different amines was studied but also the effect of several parameters such as temperature and different diluents. In addition, the extraction was further enhanced by using a synergic extraction with TBP (see Section 24.2.3.2). The optimal amine/TBP ratio was found to be close to three, and the effect of the diluents tested was practically negligible.

The development of these kinds of processes has continued; for example, the process suggested by Amaral and Morais (2010), where a combination of a primary amine and a tertiary amine (Alamine -336) was used. The flow sheet contained a regeneration stage similar to the one described in Figure 24.6. The flow sheet was optimized and the results were in reasonable agreement with the ones presented in the AMEX process; that is, a thorium recovery of >99.9%, a uranium recovery of 99.4%, and less than 0.001 g/L of these metals in the raffinate. The unwanted extraction of the lanthanides was less than 0.1%.

24.2.3.2 Solvation process

Solvation processes occur according to the following general reaction:

$$M^{\upsilon+} + \upsilon X^{-} + nL(org) \rightleftharpoons MX\upsilon Ln(org) \quad (24.1)$$

where M is the metal of interest, X is a neutralizing ligand, and L is the solvating molecule. Essentially, the ligand X can also be an organic extractant and then the extraction is called synergic because with the solvating molecule the extraction is more efficient.

One of the most well-used solvating ligands in the nuclear field is tributylphosphate (TBP). This molecule is used in the well-known PUREX process for separation of uranium and plutonium from dissolved used nuclear fuel. These previous experiences with TBP have led to the use of TBP to separate thorium from mineral leachates. However, in this case it is important that the phosphate concentration is kept low. This can be achieved in one of three ways: use of oxide or carbonate virgin thorium ore, removal of the phosphate prior to extraction, or by using the more expensive alkaline treatment method described above.

Because TBP is usually used to extract from nitrate solutions, the solid thorium hydroxide/oxide obtained in the alkaline treatment process is dissolved in nitric acid. Originally, this dissolution was not completely efficient due to the rather low solubility of the thorium oxide. However, a new method was shown to work in 1986 (Steinhauser, 1987). It was shown that by increasing the pressure to 10 bar and 230 °C, the thorium hydroxide was actually easily soluble.

The effect of the nitric acid concentration on the extraction of thorium, uranium, and lanthanides was investigated and an example is shown in Figure 24.10.

It is clear that by controlling the nitric acid concentration, a suitable separation scheme could be made. It was also shown that any traces of phosphate could be managed by additions of ferric ions (Ewing et al., 1952). Based on this work, a flow sheet was designed and tested with the performance well in accordance with requirements for thorium production (see Figure 24.11).

There are some interesting features in the process illustrated in Figure 24.11. Among these are the division of the organic phase into both the initial extraction and lanthanide scrub section and the following thorium product purification stages. Another is that even if the aqueous phase entering the thorium stripping stage is 0.1 M HNO_3, the thorium product is about 1 M HNO_3 as a result of the stripping of the acid from the loaded TBP phase. Thus, there is a loss of HNO_3 in the process, which is why there is the need for two extra stages loading the organic phase with acid again. This process results in less than 5 ppm lanthanides or uranium in the thorium product.

The process shown in Figure 24.11 is only an example. Several other similar and differently optimized processes were developed (e.g., Foley and Filbert, 1958) and Siddal (1959), but the main lines remained constant. However, even if TBP sometimes was exchanged by similar molecules, it was still industrially preferred to continue using the TBP extraction as an efficient and economical method for thorium recovery once the phosphate problem was solved.

The TBP-based process outlined above together with its improvement and lessons learned from the PUREX process gave rise to the THOREX process for the handling of thorium-based nuclear fuels, as discussed later in this chapter.

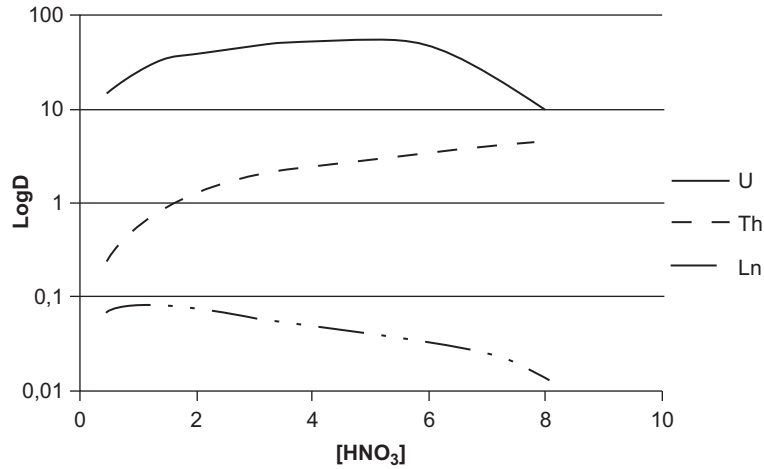

Figure 24.10 Extraction of some elements from varying nitric acid concentration into 40% TBP in kerosene (Ewing et al., 1952).

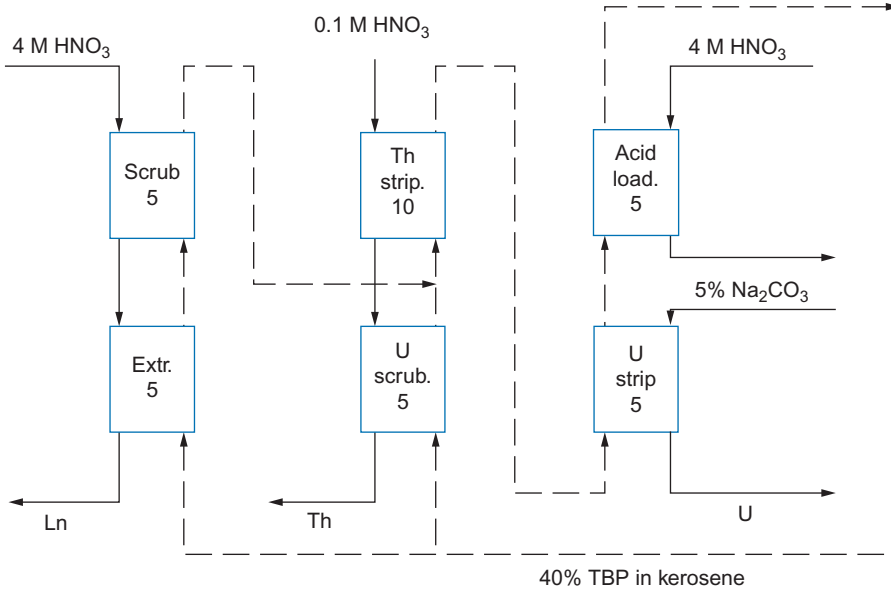

Figure 24.11 A TBP-based thorium purification scheme (Ewing et al., 1952). The numbers inside the boxes refer to the number of stages.

24.2.3.3 Combined methods

In addition to the pure solvent extraction techniques described above, there is also the possibility to use the very high selectivity of some cation exchangers once the main solubility issues are solved, and the pH could be changed during the extraction

procedure. In a recent report from IAEA (2005), such a method is described in brief (see Figure 24.12).

Clearly, the principles are the same as previous amine-based anion extraction processes with the exception of the second extraction using PC-88, which essentially is the acidic reagent 2-ethylhexyl hydrogen 2-ethylhexyl phosphonate. This is an extractant that has previously been used for successful lanthanide extraction from chloride solution (Gschneider, 1981). The extraction properties of thorium and uranium were investigated by Sarkar et al. (2000), who found that thorium was quantitatively extracted in the pH range 1-4 while uranium was extracted in the pH range 1-3.5.

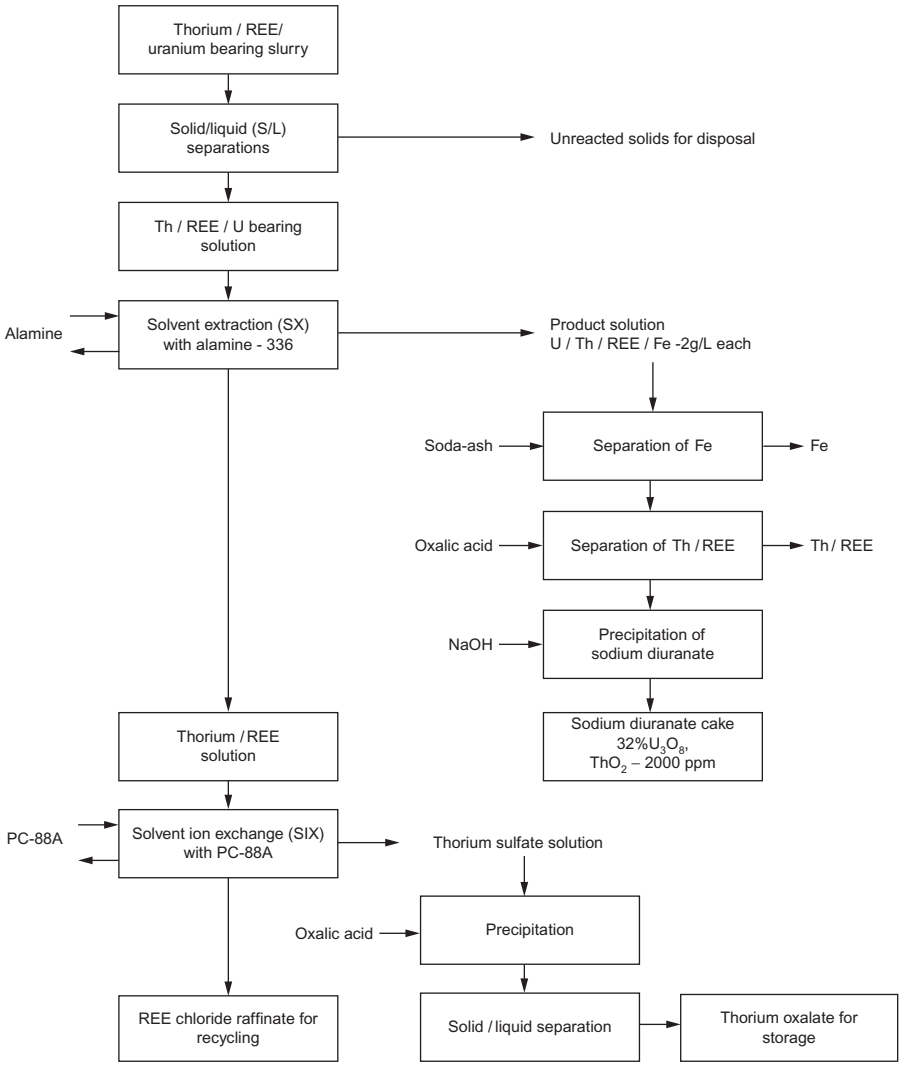

Figure 24.12 A monazite treatment process suggested by Mukherjee (2002).

At these quite high pH levels the thorium will, as described above, precipitate as the hydroxide unless complexed by a strong excess of sulfate. The precipitation is then obtained by addition of oxalate. In a more recent proposal for the manufacturing of nuclear-grade thorium material, it is actually sometimes preferred to have the oxalate as a starting material, which then fits well with some of the PUREX product streams.

24.3 Thorium fuel manufacturing

Thorium fuels have been fabricated for more than five decades now and several fuel types have been designed (see Table 24.3). It is clear that there are a wide variety of fuel types that have been proposed and sometimes tested. Essentially all thorium fuels are solid fuels in the form of tiny "ceramic fuel microspheres" (100-1000 μm), "ceramic fuel pellets," or "metallic alloy fuel rods." The only exception to this is the fuel for the molten salt breeder reactor, which uses mixed fluoride in liquid form as fuel and primary coolant.

These very different fuel types arise from relatively few manufacturing methods. In principle, they can be divided into dust-free solution methods and powder handling. These two methods each have advantages and disadvantages. These differences also make them more or less suitable to manufacturing fuel with different composition and origin; for example, virgin fuel or fuel from recycled material or, rather, material containing elements of high radiotoxicity or strongly gamma-emitting radionuclides. Essentially, one may make the distinction that fuel containing ^{235}U, ^{238}U, or ^{232}Th can be handled easily unless very fine powder is expected. Then, a well-ventilated closure is needed to handle any very fine airborne particles, preventing hazardous exposures to the operators. The other materials may need to be handled in sealed glove boxes due to alpha activity and, in the case where strong gamma emitters are included, there may also need to be remote handling behind radiation shielding.

Some of the major issues with producing thorium fuels are the very properties that made thorium oxide popular in the first place—its thermal properties. The melting point is very high, 3390 °C, which will affect the sintering temperature and the ability to form high-density material. This can be solved to some degree by adding metal ions of different valency. The addition of about 0.5 wt% of Ca^{2+} or Mg^{2+} or 0.25 wt% Nb^{5+} has been shown to reduce the sintering temperature from 1600-1700 °C down to 1150-1450 °C.

Although this chapter mainly deals with oxide fuels as they are still by far the most common, it is clear that some of the methods described (e.g., sol-gel) may be adopted to fabricate carbides or nitrides by the inclusion of some additional steps in the flow sheet. In addition, metallic fuel can be produced by burning thorium oxide in the presence of calcium (calciothermy process).

24.3.1 Powder methods

The production of ThO_2 fuel from powder material is similar to the one used extensively for UO_2 or MOX fuels. That is, conventionally, a green pellet is pressed at ambient temperature under high pressure and then sintered in a furnace at high

Table 24.3 Types of thorium-based fuels and fuel elements

Reactor type	Composition	Fuel shape	Fuel element
High-temperature gas-cooled reactors (HTGRs)	ThO_2, $(Th,U)O_2$, ThC_2, $(Th,U)C_2$: (^{235}U or ^{233}U)	Microspheres 200-800 coated with multiple layers of buffer and pyrolytic C and SiC	Mixed with graphite and pressed into tennis ball-size spheres for pebble bed reactors or fuel rods for HTGR with prismatic fuel elements
Light water reactors (LWRs)	ThO_2, $(Th,O)O_2$, $(Th,Pu)O_2$ (<5%Pu, ^{235}U, or ^{233}U)	High-density sintered pellets or high-density microspheres	Zircaloy clad pin cluster encapsulating pellet stack or zircaloy clad "vipac" pin cluster encapsulating fuel microspheres
Pressurized heavy water reactor (PHWR)	ThO_2 for neutron flux flattening of initial core		
Advanced heavy water reactor (AHWR)	$(Th,O)O_2$, $(Th,Pu)O_2$ (ca. 5%Pu, ^{235}U, or ^{233}U)	High-density sintered pellets	Zircaloy clad pin cluster encapsulating pellet stack
Fast reactors (FRs)	• ThO_2 blanket • $(Th,O)O_2$, $(Th,Pu)O_2$ (<5%Pu, ^{235}U, or ^{233}U) • Th metal blanket • Th-U-Zr or Th-U-Pu-Zr various such as nitrides or carbides	High-density sintered pellets or injection cast fuel rods	Stainless steel (SS) clad pin cluster encapsulating pellet stack. SS clad pin cluster encapsulating fuel rods
Molten salt reactor (MSR)	$LiF+BeF_2+ThF_4+UF_4$	Molten salt liquid form	Circulating molten salt acting as fuel and primary coolant

Adapted from IAEA (1987, 2005).

temperature. The pellet is then ground to the correct dimensions to meet agreed standards for use as a nuclear fuel. The starting material is often the thorium oxalate, which is obtained by adding oxalate to the final purification step as described in the previous section. Before the current method was established, there were also other routes tested; for example, direct ignition of the thorium nitrate and decomposition of the hydroxide

or carbonate. However, these methods resulted in rather large grain sizes, which were not well-suited to good sintering. One advantage with pure thorium oxide fuel is that thorium has only one stable oxidation state and, therefore, there is no need to control the atmosphere during the production of the fuel. Thus, the calcination of the thorium oxalate is performed in air at about 800-900 °C, producing a rather fine oxide powder. It has been shown that premilling of the oxalate will reduce the grain size and, thus, increase the possibility of obtaining higher pellet densities after sintering. Another route that has been shown to work is to control the temperature in the oxalate precipitation step. If this can be performed close to 0 °C, the powder will be finer and, thus, higher final densities can be obtained.

The density of the pellets seems to increase with the compaction pressure in the range of 40-280 MPa, but variations exist. The smallest scatter of data seems to be at pressures between 90 and 120 MPa (IAEA, 1987). Other methods such as precompaction followed by granulation and then pressing at even higher pressures in the range of 300 MPa have also been successfully tried.

In the case of mixed oxide fuel, there are several methods available depending on how the original material is obtained. One method is simply to mix the appropriately sized oxide powders before the pressing. Another is to keep the thorium nitrate solution from the purification step discussed above and add the correct amounts of uranium or plutonium nitrate solution. Because both uranium and plutonium have several stable oxidations states, it is now important to control the atmosphere and the redox potential in any solution used. If the conditions are correct, all of the actinides will be in the tetravalent state and oxalate can be added to obtain a solid solution precipitate. This can then be calcined under an Ar/H_2 atmosphere and pressed into a pellet as for the pure thorium fuel. It is worth noting here that if a mixed oxide is used there might be no need to add other elements to reduce the sintering temperature due to the inherently imperfect electron structure in the pellet due to the presence of oxidized uranium or plutonium. The higher the content of the other actinides, the lower the sintering temperature can be until it approaches that of pure uranium or plutonium fuels.

Even if the powder methods are typically used for producing fuel pellets, there is also a possibility to produce microspheres using the powder technology. A coated agglomerate pelletization process is being developed by Bhabha Atomic Research Centre (BARC) for the fabrication of ThO_2-UO_2 mixed oxide fuel pellets. By adding a binder/plasticiser material, microspheres are produced that are suitable for fabrication of HTR TRISO and sphere-pac fuels. The additive is added to the thorium powder at slightly elevated temperature and the mixture is then molded in an extruder and shaped into spheres in a "spheroidiser" (Kutty et al., 2009). If a coating of fissile material is desired this is then added in a second step.

24.3.2 Sol-gel methods

An alternative to the rather uncomplicated but dust-generating methods outlined above are the methods in which the active elements are handled in solution, thus reducing the contamination risks due to handling of fine powders. Unfortunately, this also reduces the robustness and increases the complexity of the process. However, in

addition to the reduced handling of radioactive powders, the solution methods also have the advantage that they can utilize solutions directly from the chemical separation process, thus making closure of the fuel cycles more proliferation-safe as no materials actually have to be handled separately from the dissolution of the used fuel until the final new fuel is produced. Many of these solution-based methods are often referred to as sol-gel methods where the main idea is to keep the actinides in solution and then transferring this solution directly to the final product, microspheres. These microspheres are typically in the size range of 50-1200 μm. If the spheres are not the desired state or fuel type, there is also the possibility to compact them and press them into pellets after a calcination. The pellets may then be sintered as described below. Also, in the sol-gel method it is possible to make other types of fuels such as nitrides or carbides by adding steps such as nitridation after the initial microspheres are made.

One of the drawbacks of these methods is that the chemistry of the solutions must be controlled rather carefully across the different process stages, which makes upscaling more difficult. In principle there are two main sol-gel processes: internal gelation and external gelation. A short description of the basics are given below and further information may be obtained from the literature (see, for example, Sood, 2011).

24.3.2.1 Internal gelation

The starting point of the internal gelation process is a nitric acid solution with the desired metal composition, which is kept cooled and then mixed with urea ($CO(NH_2)_2$) and hexamethylenetetramine (HMTA, $(CH_2)_6\,N_4$). This cold solution is then dripped into hot silicone oil. There are several possible methods to obtain the desired size of the droplets (e.g., varying the size of the nozzle used or using a vibrating nozzle). By changing the vibration frequency and/or the solution flow rate the sphere size will be changed.

The basic chemical reactions that occur in these steps are that the urea reacts with the actinides at low temperatures to form complexes that essentially prevent hydrolysis on the addition of HMTA. As the temperature is increased when the droplets hit the silicone oil (at 60-90 °C), several chemical reactions will occur. The metal urea complex weakens and the pH is increased due to the HMTA reactions, which occur in two steps.

$$(CH_2)_6N_4 + H^+ \rightleftharpoons \left((CH_2)_6N_4\right)H^+ \tag{24.2}$$

$$\left((CH_2)_6N_4\right)H^+ + 9H_2O \rightleftharpoons 6HCHO + NH_4{}^+ + 3NH_4OH \tag{24.3}$$

The ammonium hydroxide formed by Equation 24.3 will increase the pH and the metals present will start to hydrolyze in one or several steps (Equation 24.4). It should be noted that similar reactions will occur for any actinide present in the feed solution even if present in different oxidation states (e.g., uranium may be present as the hexavalent uranyl ion). These hydroxides may form different polymeric species (Equation 24.5).

$$Th^{4+} + xH_2O \rightleftharpoons Th(OH)_x^{(4-x)+} + xH^+ \tag{24.4}$$

$$n\left(\mathrm{Th(OH)}_x^{(4-x)+}\right) \rightleftharpoons \left(\mathrm{Th(OH)}_x\right)_n^{n(4-x)+} \tag{24.5}$$

The size and properties of the polymers formed will depend on factors such as HMTA/metal ratio and kinetics. Equation 24.2 is relatively fast while Equation 24.4 is slower, and both lower the pH. If the HMTA/metal ratio is too high, the reaction kinetics will be fast and there will not be enough time for proper polymerization, which is typically seen as a transparent or translucent gel.

When the microspheres are formed and gelled they are washed to remove remaining silicone oil and excess gelation agents. Typically, CCl_4 or tricholorethylene is used for the former washing step and NH_4OH solution for the latter. The microspheres are then dried and calcined up to 500 °C to remove remaining ammonium nitrate or organic matter. After this treatment, they may either be sintered as they are, coated, or be possibly pressed into pellets before sintering, depending on what kind of fuel is desired.

24.3.2.2 External gelation

External gelation is exactly as the name suggests. Instead of having the hydrolysis and subsequent gel formation of the heavy metals occurring by a base that is produced inside the droplets, this base is now added from the outside. Essentially, it should be possible to use pure nitrate solution in the initial droplet, but considerably better results will be achieved if an organic structure could also be used to provide a supporting "skeleton" and keep the hydroxide gel droplets rigid. Several combinations of organic additives have been used over time, but commonly used ones include a mixture of a polymer (e.g., polyvinylalcohol or hydroxypropyl methyl cellulose) and a modifier (e.g., formamide, urea, or tetrahydrofurfuryl alcohol).

The broth described above is then, as for the internal gelation, passed through a needle (or similar setup) to produce droplets of appropriate size. Typically, these droplets first fall through gaseous ammonia; whereupon the surface of the droplets quickly gels. Then these partially gelled droplets continue to solutions containing about 1% ammonia and 4 M NH_4NO_3 at a pH of about 8. This completes the gelation of the droplets. After complete gelation, the droplets are then washed to remove any excess organic additives and ammonium nitrate.

After drying, the treatment is similar to that of the internal gelation to produce dense microspheres that may either be compacted into pellets for fuel or used as is in sphere-pac-type fuels or coated for other types of fuels.

24.3.2.3 Sol dehydration

The dehydration method is basically the simplest sol-gel process. The starting material is typically a thorium solution to which ammonia is added. The thorium will then precipitate as thorium hydroxide. This hydroxide gel-like polynuclear complex is then mixed with some thorium nitrate ($Th(NO_3)_4$) and boiled. It has been shown (Haas et al., 1968) that an alternative is to start directly with a thorium nitrate solution and then remove some of the nitrate by solvent extraction before the pH is raised for the gel formation. These

polynuclear gels are then dehydrated by dripping droplets into a column containing 2-ethyl-1-hexanol. The final microspheres are collected at the bottom of the column and then dried in steam at 220 °C to remove any remaining hexanol. They are then calcined to remove any remaining nitrate. From this point, the spheres may either be sintered for use in nonpressed fuels or be pressed to a pellet before sintering.

This process has been developed and tested at the semi-industrial scale, but there are potential drawbacks. The making of thorium fuel is straightforward, but if other actinides are to be added to the fuel there is need for redox control in the original solution to ensure that a homogeneous hydroxide gel is formed. If the correct redox state cannot be ensured the higher oxidation states of, for example, uranium and plutonium, it will keep them in solution instead of in the formed hydroxide gel.

24.3.2.4 Total gelation

Fairly recently a method was developed in China where internal gelation was combined with external gelation (Fu et al., 2004). The starting metal nitrate solution is mixed with urea, polyvinylalcohol, and tetrahydrofurfuryl alcohol for external gelation. Then, HMTA is also added for the internal gelation. Thus, ammonia for the gelation was produced both from the inside by the HMTA reactions and from the outside by dipping in ammonia solution. The main advantage with this method is that better sphericity (large diameter/small diameter) was obtained and the molarity of the metal was increased. The mean sphericity was found to be 1.04, which is rather good. This makes these particles ideal for further coating and use in different nonpressed fuels.

24.4 Thorium fuel cycle back end

24.4.1 Introduction

A considerable amount of scientific interest has been invested in the thorium nuclear fuel cycle since the 1950s. Several arguments in favor of it, based on the abundance of thorium and the lack of plutonium in the waste, have been put forward. Furthermore, the inertness of the thorium oxide is good for direct disposal of the final waste but causes difficulties when it comes to recycling of the material. In this section we will look at the composition of the used thorium nuclear fuel and possible recycling options. The once-through cycle will not be discussed as the final repository is assumed to be similar to that of uranium-based fuel, which is handled extensively elsewhere in the literature; for example, a multitude of reports from the Swedish fuel and waste management company SKB.

24.4.2 Recycling

In principle, recycling of nuclear waste is either made using a wet process or a dry process. Today, only the wet processes have been used industrially, while promising results for dry processes have been shown in many cases. However, the step to

industrial maturity is rather large in this case. It is, however, important to continue focusing on the dry processes for future reactor systems that have a high content of plutonium where wet recycling can become troublesome due to criticality issues.

A wet recycling route typically consists of some basic steps. The first step is to remove any fuel cladding and separate it as much as possible from the actual fuel. Then the fuel is dissolved and the necessary separations of the elements are performed by solvent extraction or ion exchange. In the case of thorium, no large-scale reactor operation has been initiated and, thus, no larger-scale recycling process has been tested either. However, a process named THOREX was developed at Oak Ridge National Laboratory in the 1950s and early 1960s (Rainly et al., 1962). This process has up to now not really been matched, even if there have been optimizations and some changes of extractants. At this point it may be worth noting that there are several promising and possible processes to investigate if a thorough assessment of the virgin thorium separation processes development, as described in Section 24.2.3 and in the literature, is made.

Clearly, thorium recycling is not at all a new concept. Considerable efforts were given to this subject in the late 1950s though the 1960s, and from which most of the current knowledge base originates. It was, however, concluded in the beginning of the 1970s that thorium fuel recycling was not a viable option at that time. Some more recent assessments still basically concur with those conclusions (National Nuclear Laboratory, 2012). Therefore, the activities on the reprocessing in the last decades have been modest as will be clear from the description of the processes below. However, development of thorium fuel cycles has restarted again; mainly, perhaps, in India where thorium recycling is again considered as a serious alternative to the traditional uranium cycle. There is also a renewed interest in using thorium-based fuels in molten salt reactors with either fast or thermal spectra and on-line reprocessing (Delpech et al., 2009; Merle-Lucotte et al., 2013).

24.4.2.1 Decladding

The first step in a recycling process for used nuclear fuel is the mechanical or chemical preparation of the irradiated fuel elements prior to the chemical separation and purification processes. Typically, the first step is to separate the cladding material from the actual fuel to be recycled. As a minimum, the integrity of the cladding needs to be breached for the dissolution liquor to have access to the fuel. Several dissolution strategies may be possible, but the dominating one in industrial reprocessing is nitric acid leaching.

Essentially, there are two different ways to perform the decladding: mechanical or chemical. In the mechanical method, the fuel bundles or rods are simply sheared or crushed allowing for the dissolution liquor to access the fuel. This is described in some detail with respect to the PUREX process in Chapter 5 and will not be discussed here. For chemical methods, the cladding is selectively leached leaving the fuel to be dissolved in the second stage. Clearly, the efficient choice of chemical methods will be highly dependent on the type of cladding used. For the chemical treatment of thorium fuels there are essentially two different clad materials with industrial maturity that should be considered: stainless steel and zircaloy.

Stainless steel chemical decladding

For the chemical decladding of stainless steel there are essentially three different methods proposed in the literature: SULFLEX decladding, DAREX decladding, and dry fluorination.

SULFLEX decladding The SULFLEX process is well described in the literature, see Blanco et al. (1962) and Finney and Hannaford (1961). The main principle is to selectively dissolve the cladding in a threefold stoichiometric amount of 4-6 M H_2SO_4. The off-gas to be treated is hydrogen, which will be produced at a rate of about 1.1 moles per mole of steel dissolved (55 g). This hydrogen is collected separately and can be used for other purposes. The initial dissolution rate increases exponentially with the sulfuric acid concentration, but levels out rather quickly. Thus, a nominal value for dissolution could be that a 20-mm-thick clad will require 1.3 h for dissolution. Unfortunately, the solubility of stainless steel in sulfuric acid decreases with increasing hydrogen ion concentration from about 80 g/L at 5 M H^+ to 5 g/L at 15 M H^+.

A potential problem with this process could be passivation of the steel surface. It was shown that as little as 1 mM HNO_3 in the dissolvent can cause severe passivation. Therefore, traces of nitric acid are removed by reaction with formic acid. The passivation could also be broken by boiling in 12 M sulfuric acid, but this procedure is highly corrosive for the equipment and, if applied, the dilution to ~6 M sulfuric acid should be done rapidly afterward.

It has been shown (Blanco et al., 1962) that the unwanted dissolution of the actual fuel during the cladding dissolution was very small. Generally, less that 0.3 % of the uranium and less than 0.2 % of the thorium was lost during the process.

DAREX decladding The DAREX decladding method is more thoroughly described by Blanco et al. (1962) and Ferris and Kibbey (1960). The main principle involved is to dissolve the steel cladding in a boiling mixture of 5 M HNO_3 and 2 M HCl. The off-gasses in this case are somewhat more complex and include N_2O, NO, NO_2, NOCl, HCl, Cl_2, N_2, and H_2. There is no direct danger associated with the hydrogen content, but after the acidic components have been scrubbed in caustic soda a possibly explosive mixture of H_2, Cl_2, and N_2O has to be treated. Using the above composition, the dissolution of 20-mm-thick cladding took about 1 h of boiling, which is considerably faster than the SULFLEX process but, then, a more complicated off-gas treatment is needed.

The losses of fuel materials in this process were considerable. It was seen that uranium losses between 3% and 5% were not unusual depending on burn up (fragmentation) of the fuel. The thorium losses were, however, moderate at less than 0.4%. The lost uranium could be recovered by extraction with TBP, but this required that the chloride concentration of the solution was first decreased significantly.

High-temperature methods Several methods exist to manage decladding of various steel types by treatment with different gases at various temperatures. One method is based on exposure to hydrogen at about 250-300 °C (Adams and Glassner, 1964a,b). At this point the cladding (and partially the fuel) will be hydrated and simply break up into small fragments. An experiment was performed where a fuel pin clad in 4-mm-thick

TV-20 was exposed to 2 atm of hydrogen at 250-290°C for 20 h. It was observed that both the fuel and the cladding were hydrided and separated by selective dissolution.

Another example of high-temperature decladding is the use of hydrogen fluoride gas (Adams and Glassner, 1964a,b). It was shown that if a stainless steel-clad fuel pin was exposed to 43% HF in oxygen for 1 h at 550 °C and then for 2 more hours at 450 °C, the entire fuel pin was reduced to ferric oxide and uranium fluoride with no trace of the cladding remaining. This was then further treated to recover the fuel material (uranium in this case).

Zirconium-based cladding handling

Zirconium or zircaloy has been selected as the preferred cladding material for the BWR and PWR operating fleets using uranium and plutonium-based fuels today. There are several good reasons for this, including good neutronic behavior as well as very low solubility in most media. This has naturally led to the consequence that the decladding of these fuels is mainly mechanical. A drawback with zirconium-based cladding is the violent reaction with water at more than 850 °C, where a strongly exothermic hydrolysis of zirconium produces hydrogen that can be explosive. Nevertheless, some chemical processes have been developed and tested in the 1960s.

The ZIRFLEX process More information on the ZIRFLEX process can be found in Ferris (1960) and Swansson (1958). The main principle here is to dissolve the cladding material in a boiling mixture of either 6 M NH_4F or ammonium fluoride with 0.5 M NH_4NO_3. The main reason to add the nitrate solution is to minimize the evolution of hydrogen during the dissolution. The other gaseous compound released is ammonia according to,

$$Zr(s) + 6NH_4^+ + 6F^- \rightleftharpoons ZrF_6^{2-} + 2NH_4^+ + 4NH_3(g) + 2H_2(g)$$

Other alternative dissolution agents would be hydrofluoric acid or a mixture of hydrofluoric and nitric acids. However, these solutions will also dissolve any austenitic steel that is present. The dissolution rate of zircaloy-2 in the ZIRFLEX solution is about 100 mm/h, while the corresponding value for stainless steel is only 0.5 mm/month. It was found that increasing the concentration of the ammonium fluoride did not increase the rate of dissolution but rather the opposite. This was believed to be the result of formation of ammonium fluorzirconate passivating the surface against further dissolution. It was also noted that if the fluoride to zirconium ratio approached six, then the dissolution rate was significantly reduced. The reason for this is the very high stability of the corresponding zirconium fluoride complex, effectively reducing the amount of free fluoride in solution; the rate of dissolution being in principle first order with respect to the free fluoride concentration. Care has also to be taken for the concentration of the ammonium nitrate. At moderate concentrations, 0.5–1 M, the dissolution rate is increased and the hydrogen evolution is decreased. However, if the ammonium nitrate concentration is increased to 2 M, then the dissolution rate goes down. This is due to the same process described above passivating the surface.

Another problem is the formation of a protective oxide film on the zircaloy surface. This oxide layer is not at all dissolved by the selected liquor. The only way dissolution can then occur is through weaknesses in the oxide layer resulting in pitting dissolution. This will be very slow initially and then the rate will increase before finally decreasing again. A solution to this problem could be to initially break the oxide film in many places by mechanical methods.

Considering the losses of the core material it was calculated that about 1.5%/h of the uranium material was dissolved. Unfortunately, this then precipitated as sparingly soluble uranium fluorides. A similar behavior is expected for thorium. These losses could potentially, if separated, be dissolved in nitric acid and then entered into the separation process.

High-temperature methods There are, in addition to the solution methods described above, also techniques for selective dissolution of the cladding based on high-temperature reactions with different gases. One such method, the THERMOX process, as described by Tjälldin (1963, 1965) utilizes the previously described strongly exothermic reaction between zirconium and water to dissolve the cladding. The fuel rods are exposed to water vapor (steam) with about 40% to 90% nitrogen (as catalyst) and less than 30% oxygen at 800-825°C. This will oxidize the zirconium but leave the fuel intact. The fuel is then oxidized further by treatment with air and oxygen at 450-650°C. The all-oxide residue is then treated by normal dissolution methods. It needs to be noted here that this method is preferably used for uranium oxide fuels due to their better solubility in nitric acid. In the case of thorium fuels, the considerably harder dissolution procedure may result in rather high concentration of zirconium in the feed for the separation plant. As zirconium and thorium are both tetravalent ions, high levels of zirconium may cause problems in the separation process by being coextracted or precipitating or even causing third-phase formation.

24.4.2.2 Dissolution

When the cladding is removed by the selected method, normally mechanical means, and separated from the actual fuel, the next step in the headend treatment plant is the dissolution of the fuel matrix. This dissolution is naturally dependent on which type of fuel was used, and there are many alternatives such as oxides, carbides, metals, and so on. Of these, it is mainly the thorium oxides that pose special dissolution issues as thorium oxide is more insoluble than corresponding uranium or plutonium oxides. For this purpose, they are the focus of the current text. In the case of the other fuel types, they usually dissolve rather rapidly in the normal PUREX method using about 4-6 M nitric acid. Care has to be taken when dissolving carbides, though, due to the evolution of different organic materials and in particular gaseous organohalides such as methyl iodide. One remedy for this could be to preoxidize the carbide to oxide then dissolve in nitric acid. This is appealing in the case of uranium and plutonium fuels but the advantage is not as clear in the thorium case.

THOREX dissolution

Dissolution of the different actinide oxides showed that uranium oxide has faster dissolution kinetics than plutonium or thorium. During the development of the THOREX process and its predecessor, the Interim-23 process, several different dissolution protocols were developed. It was found that an optimal mixture for the dissolution of the thorium-uranium oxide fuel was 13 M HNO_3—0.04 M NaF—0.1 M $Al(NO_3)_3$. The exact composition may vary somewhat depending on fuel composition and burn up, but most kinetic investigations were conducted with the above composition of the dissolution liquor. The role of the fluoride ions is mainly to act as a catalyst in the dissolution. The addition of aluminum to the dissolution liquor is mainly for preventing unwanted corrosion by complexing with the excess fluoride ions. (Fluoride ions can also complex actinide ions, thus hindering solvent extraction.) After some time it was observed that the dissolved $Th(NO_3)_4$ had a similar anticorrosive effect. Moreover, this aluminum addition also has an adverse effect on the actual dissolution rate. It was shown that if the aluminum concentration increased from 0 to 0.2 M, the dissolution rate was decreased by 20%. Other additions such as neutron poisons (boron or cadmium) to the dissolution liquor to avoid criticality issues were also investigated. It was found that addition of, for example, 0.1 M H_3BO_3 or 0.75 M $Cd(NO_3)_3$ to the THOREX dissolution liquor did not affect the dissolution at all.

It was noted that in some cases there was a sort of secondary precipitation problem occurring after the initial solution cleared. This precipitate was shown to consist of molybdenum, platinum metal, and silver halogenides. In the latter case the iodides were not detected, which was considered to be due to the iodine having been distilled off in the earlier fuel dissolution step.

It is worth mentioning that the dissolution efficiency can be significantly affected by the decladding method selected. If, for example, the SULFEX process was used for the decladding it is important to remove any remains of sulfate. It was shown that if 0.1 M sulfate was present during the fuel dissolution, the rate was decreased by a factor of eight.

At the end of the dissolution step the solution will be made acid-deficient by boiling at 135 °C followed by column steam stripping. This procedure is shown in more detail in Figure 24.13, where the obtainable acid deficiencies are shown. After the deacidification, an addition of 0.02 M bisulfide ions can also be made in order to convert the ruthenium to nonextractable species.

In more recent years, the dissolution problem has been addressed by decreasing the fuel density to a lower value than normal for uranium-based fuels. It has also been found that addition of MgO significantly eases the dissolution and also decreases the sintering temperature. It seems that MgO additions of about 1.5% are optimal for fuel performance using the normal dissolution process; the dissolution time was decreased by almost one order of magnitude (Anantharaman et al., 2008).

Other dissolution techniques

Logically, there are a considerable number of possible dissolution process alternatives for thorium oxide-based fuels other than the one outlined above. However, even if they are feasible at the laboratory scale, the up-scaling and suitability with respect to the

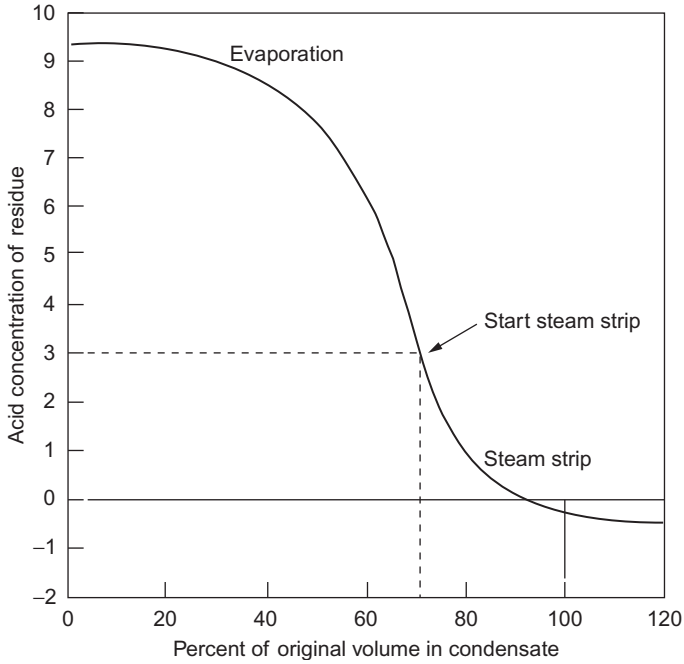

Figure 24.13 Feed adjustment by evaporation and steam stripping (Rainly and Moore, 1961).

downstream separation process may not be evident. Several examples were given above for the dissolution of monazite sands and, with modifications, they are possibly applicable to recycling spent thorium fuels, which will be more soluble then fresh sintered material.

There are also completely different dissolution methods that combine aqueous dissolution with thermal methods. One such method presented recently is the sulfurization of the oxide fuel material (Sato and Kirishima, 2010). This process is based on selective transformation of the fuel material to sulfides at different temperatures followed by dissolution of the nonoxide material, as described in Figure 24.14.

There are several additional options based on this technique. Although it is clear that selective sulfurization of the fission products occurs at lower temperatures than for the uranium or thorium, it was also shown that uranium and thorium could be separated by this method (Sato and Kirishima, 2011). The sulfurization of uranium can be well preformed at 500 °C. However, for a similar reaction to occur to completion for thorium, the temperature has to be 900 °C.

24.4.2.3 Separation

The treatment of the dissolved fuel materials will of course vary considerably depending on what is considered to be sufficiently valuable for recovery. In the early stages of the development and the use of U-Th fuel it was not considered worth the effort to

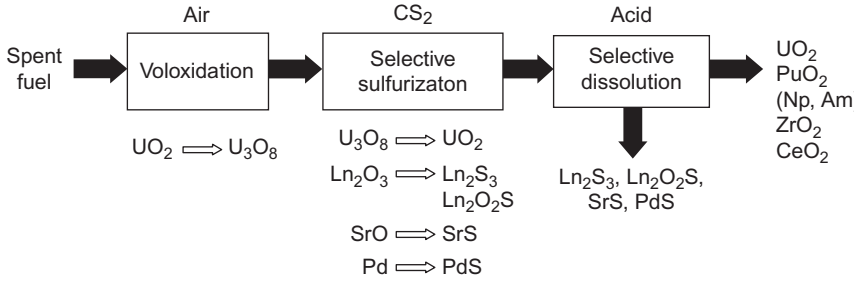

Figure 24.14 The sulfide process as described by Sato and Kirishima (2011).

actually recover the thorium but only the ^{233}U. Therefore, methods such as the Interim 23 process were developed. At a later stage it became interesting to develop processes that also recovered the thorium part of the fuel, which led to the development of the THPREC and acidic THOREX processes. In later years there have been improvements to these methods as well as some laboratory-scale attempts using different process ideas. However, none of these alternatives were tested at pilot plant scale.

The THOREX process

The only process successfully used for thorium and uranium recovery from used nuclear fuel was the generically named THOREX process. Several versions of this process were developed as will be shown below. At the Savannah River and Hanford sites in the United States, more than 850 tons of irradiated thorium fuel were treated yielding more than 1.4 tons of pure ^{233}U (using the THOREX-2 Process) (Orth, 1979; Jackson and Walser, 1977). In principle, the idea behind the THOREX process is very similar to that of the PUREX process. The main extraction is made by TBP in kerosene. However, there are some significant differences.

- As is clear from the PUREX name (plutonium uranium redox extraction), redox changes are used to separate uranium from plutonium. This is not the case in the separation of uranium and thorium because thorium is stable in the tetravalent oxidation state.
- The fissile material, that is, plutonium in PUERX and ^{233}U in THOREX, is present in different concentrations compared to the main recoverable material. In addition, the extractability of the major compound in THOREX is one order lower than that of uranium.
- The solubility of the extracted thorium complex is considerably lower in the hydrocarbon diluent than the corresponding uranium complex. Thus, the risk of organic phase splitting will require considerably lower loading and more organic volumes needed.
- The low loading also prevents the possibility to "squeeze out" unwanted coextraction of some fission products.

Otherwise, the processes are rather similar in approach when it comes to handling of fission and corrosion products.

A general problem in the THOREX process, as also partially in the PUREX process, is the protactinium. As discussed previously, there is a need to cool the fuel for at least 12 months for the ^{233}Pa to decay to uranium but there is still the issue of the ^{231}Pa.

This is an alpha emitting isotope with a relatively long half-life (3×10^4 a) that adds to the radiotoxicity. There have been attempts to extract the protactinium with the uranium and thorium in THOREX but this has not proven effective. However, recently there has been some success by adsorption of protactinium in Vycor glass before the actual separation process. The protactinium could then be eluted and a 98% protactinium separation has been reported (IAEA, 2005).

THOREX development and flow sheets Developments in the THOREX process have been gradual, with larger or smaller changes made over time to address different problems discovered during operation of the process. An early attempt called the Interim-23 process was developed for uranium extraction only (see Figure 24.15).

The first process called THOREX was the so-called THOREX-NO1-Process developed at Oak Ridge National Laboratory. Already then the protactinium issue was recognized because a preextraction using dibutylcarbitol was performed in the first extraction battery. In a second cycle, the uranium was extracted using 5% TBP and as a final stage the thorium was extracted using a 45% TBP solution (Gresky, 1953). This process was, however, never developed completely because it was considered to be too complicated and served mainly as a scientific starting point for the continued development. The main principle of first extracting the uranium and then the thorium was later abandoned in favor of selective stripping/scrubbing of these elements. The next stage in the development was the THOREX-2 process, as shown in Figure 24.16.

The same principal flow sheet was later used for the acid THOREX process. The main reason for this development was that it was recognized that the extra addition of $Al(NO_3)_3$ as a salting-out agent actually created a problem with secondary waste formation. Therefore, nitric acid was used as a salting-out agent instead. The main

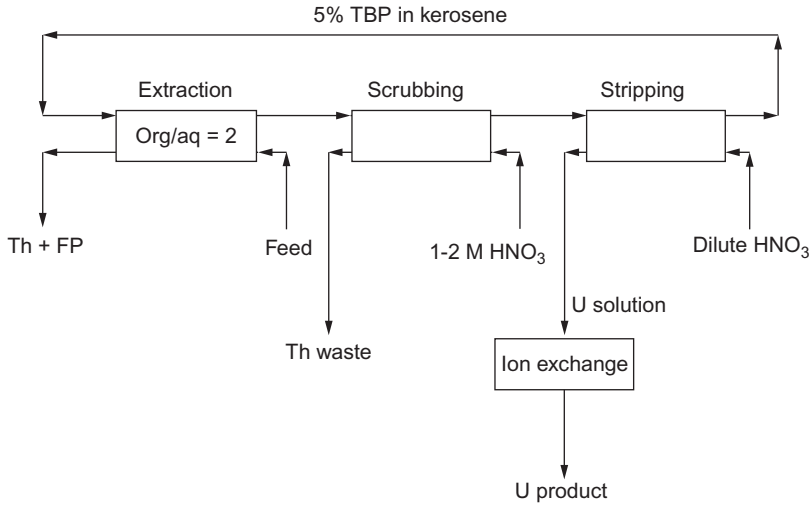

Figure 24.15 The Interim-23 process.

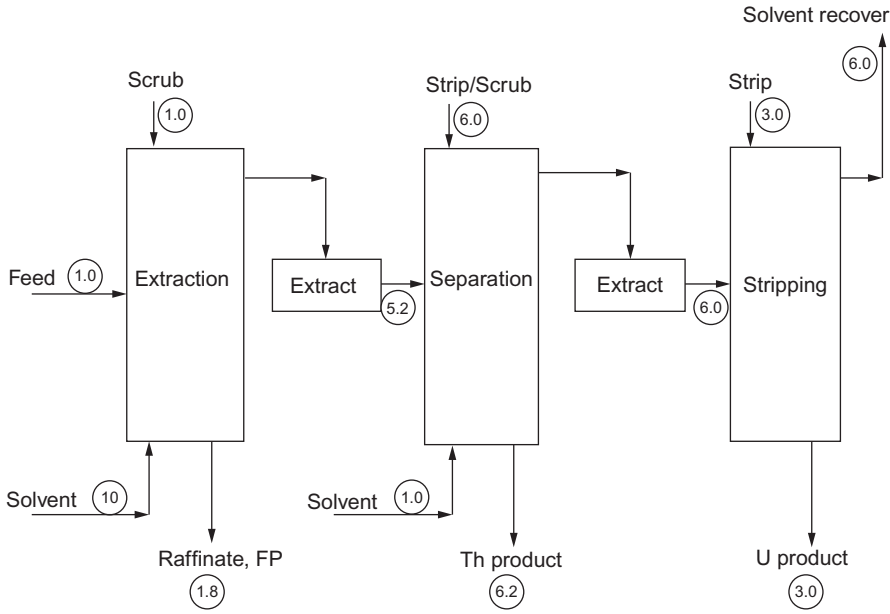

Figure 24.16 Flow sheet for the THOREX-2 and acid THOREX process. Relative flow in circles.
From Merz and Zimmer (1984).

solution composition for the THOREX and the acid THOREX process (Benedict, 1980) is given in Table 24.4.

The main changes are the decrease in TBP concentration in the extraction parts. The reason for this is higher selectivity in the uranium extraction stage. It is also clear that there is a lower acid content in the strip steps. One reason for this is that in the acid THOREX process there is a larger carryover of nitric acid from the extraction step, which will then in turn affect the strip stages in the process.

Table 24.4 Solution composition of the THOREX and acid THOREX process

	THOREX-2	Acid THOREX
Feed	1.5 M Th, 1.3 mM U, 0.5 M Al, 0.5 M HNO_3	1.5 M Th, 1.3 mM U, 1 M HNO_3
Solvent	40% TBP in kerosene	30% TBP in kerosene
Strip/scrub	0.2 M HNO_3, 40% TBP	0.2 M HNO_3, 30% TBP
Strip	0.02 M HNO_3	0.002 M HNO_3

Merz and Zimmer (1984).

Thorium has, in general, a rather poor extraction in the selected systems, which in turn means that a rather high flow ratio of the organic to aqueous phase is required. There is also an issue of the solubility and third-phase formation that limits the thorium concentration. This is coupled to the nitrate concentration; if it is too high, thorium nitrate will precipitate somewhere in the system. However, if the nitric acid concentration is too low, precipitation of thorium hydroxide may occur instead.

Another considerably more complicated process was also suggested by the Oak Ridge National Laboratory, the so-called acid deficient THOREX process. It may feel like being back at the beginning, but as seen in Figure 24.17 and Table 24.5 the flow sheet and the concentrations are significantly different from the previous processes in the stripping and scrubbing stages. Another development was the improved handling of ruthenium. It was shown that by digesting acid deficient THOREX feed with 0.04 M $NaHSO_3$ a majority of the ruthenium was converted to nonextractable species. This treatment can also be applied to the first and second cycle feeds to further reduce ruthenium decontamination.

A considerable amount of work was done on THOREX development at the research center Jülich in Germany, but this program was abandoned in 1985. Today, the main studies on reprocessing of thorium-based fuels are conducted in India. Several more or less novel flow sheets have been suggested, but the main consensus is to continue developing the THOREX process (Dey and Bansal, 2006). There are still considerable optimizations to be made to the whole process, including all the steps

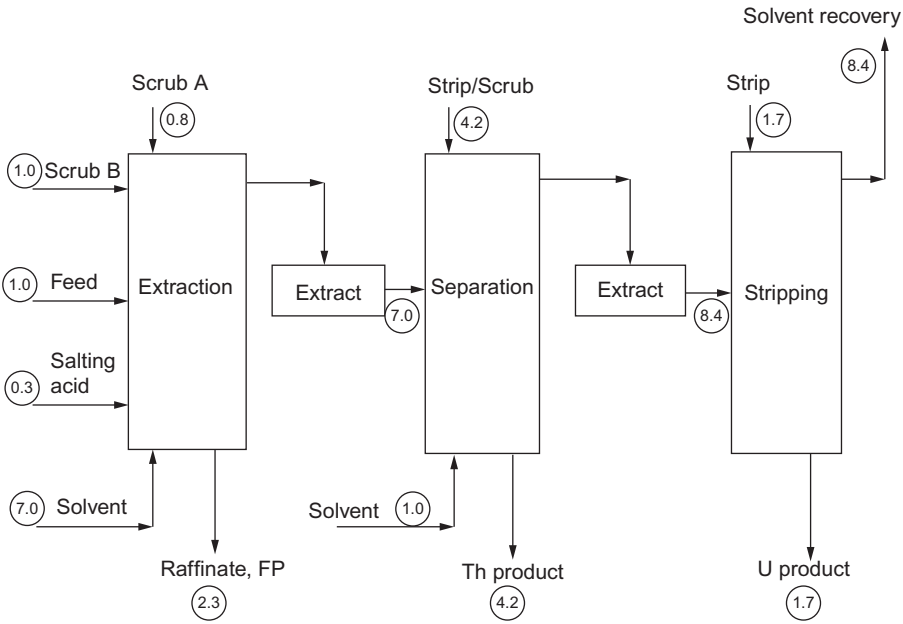

Figure 24.17 Flow sheet for the acid deficient THOREX process. Relative flows in circles. From Merz and Zimmer (1984).

Table 24.5 Solution composition of the acid deficient THOREX process

	Acid deficient THOREX
Feed	1.1 M Th, 63 mM U, 0.155 M Al, 0.15 M HNO_3
Solvent	30% TBP in kerosene
Scrub A	3 mM H_3PO_4
Scrub B	5.0 M HNO_3
Salting acid	13.0 M HNO_3
Strip/scrub	8 mM $Al(NO_3)_3$, 0.05 M HNO_3, 30% TBP
Strip	5 mM HNO_3

Merz and Zimmer (1984).

from dissolution to refabrication. A simplified flow sheet of a more modern THOREX process is given in Figure 24.18.

Several pilot plant tests have been made in India based on the THOREX principle, starting with one at BARC in the 1960s based on the 5% TBP design. A facility has also been constructed at Indira Gandhi Centre for Atomic Research (IGCAR), primarily for reprocessing fast reactor blanket fuel. In India, reprocessing of aluminum-clad thorium fuel has been carried out on fuel irradiated in the CIRUS reactor. The reprocessing of these rods, which had been irradiated to a level up to 1.2 kg of ^{233}U per ton of thorium, and cooled for more than two years, was made in a pilot-scale test facility at BARC and at the IGCAR (Anantharaman et al., 2008).

24.5 Non-aqueous techniques

During the work with uranium and plutonium-based fuels a significant effort has been invested in trying to develop non-aqueous based techniques for the treatment of the used fuel. There are some distinctive advantages with these methods:

1. Greater economic efficiency due to process simplification by compact design and fewer processes.
2. Lower radiolytic degradation of the chemicals used.
3. Simpler criticality control due to the absence of water, which is a good neutron moderator.
4. Simplified radioactive waste treatment in that the waste materials are produced directly in a solid or concentrated form.

All non-aqueous techniques are characterized by the absence of water as a reactant and the application of high temperatures. Considerably lower decontamination factors compared to aqueous techniques are another characteristic feature. Remote-controlled and radiation-shielded fuel element refabrication was thus originally planned. As time has passed more research and development have partially solved the decontamination efficiency issue, but it is still not on a par with aqueous techniques. Only two

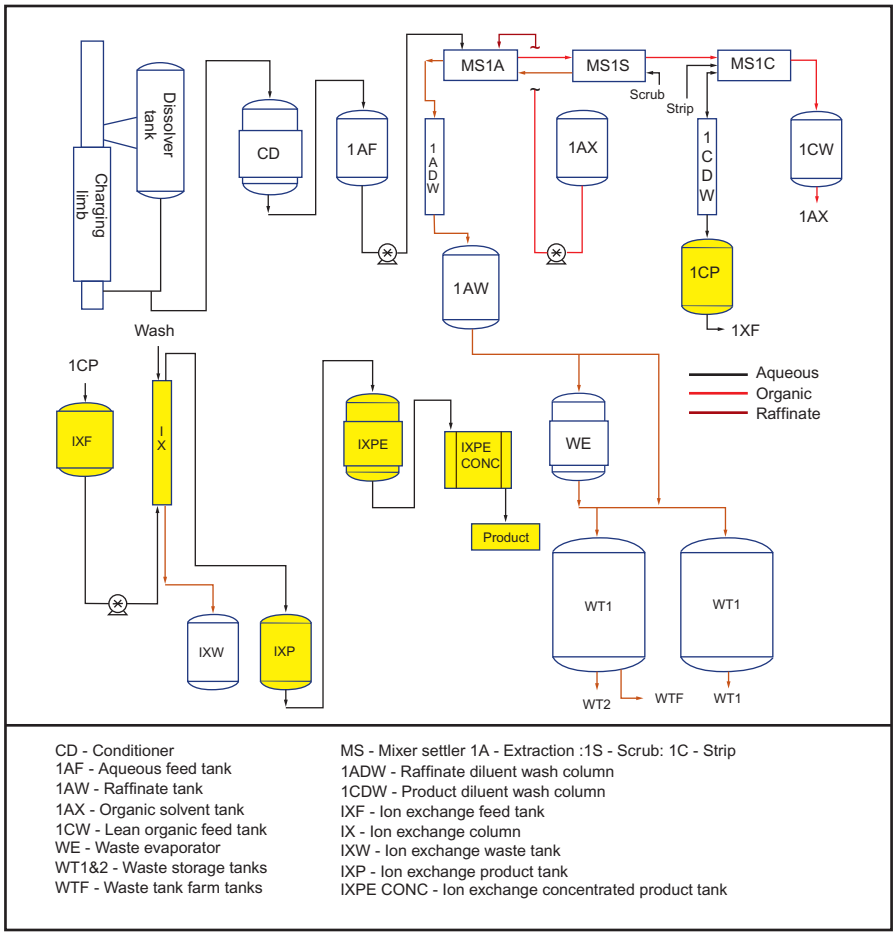

Figure 24.18 A complete THOREX flow sheet.
From Dey and Bansal (2006).

techniques from the large number of possibilities examined have been developed up to hot testing on a pilot scale: the fluoride volatility and the pyrochemical reprocessing methods.

24.5.1 Fluoride volatility

During the research on uranium-based fuel, it became evident that there was a distinct possibility to use the vapor pressure characteristics of UF_6 (sublimation at 56 °C). The main hope was to separate the uranium and plutonium from the rest of the used fuel by treatment with oxidative fluorine gas. However, it was proven that some fission

products like Mo, Sb, Ru, Tc, Nb, and Te also formed volatile fluorides at similar temperatures.

In the case of thorium, the fluorination process could potentially be used to separate out the uranium from the thorium. Unfortunately, the low vapor pressure of ThF_4 prevents quantitative uranium yields from a thorium matrix due to surface scaling. It was attempted to overcome this difficulty by the application of higher reaction temperatures up to approximately 700 °C or by molten salt fluorination. Nevertheless, the uranium yields remained unsatisfactory while material corrosion became intolerably high (Jonke, 1965). Process development for uranium partitioning from thorium-containing fuels concentrated primarily on graphite-containing Th/U elements from high-temperature reactors (Merz, 1968).

24.5.2 Pyrochemical reprocessing

These methods have so far mainly been concerned with the reprocessing of uranium-plutonium–based fuel. A considerably smaller interest has been devoted to thorium-based fuels; partially due to the rather high thermal stability of the thorium oxide. The main developments in pyrochemical processes were made in the 1960s, but recently there has been a revival. Some of these revived efforts relate to the development of the integral fast reactor fuel cycle and the concept for accelerator-driven transmutation of nuclear waste. The partitioning of transuranic elements from LWR spent fuels and from liquid high-level waste with the aid of pyrochemical techniques is also gaining some momentum. The most advanced and most popular method so far is the so-called EBR-II process for U/Pu-containing breeder elements (Burris et al., 1964).

The main characteristics of pyrochemical processes are the use of high to very high temperatures. The treatment typically leaves the recycled material either in metallic state or converted to oxides (in a dry atmosphere). In the first case, pyrometallurgical processes are involved and in the second pyrochemical processes. Reaction media are consequently molten metals, on the one hand, and molten salts, on the other. The proposed methods can be divided into two main groups:

1. Physical methods with fractionated distillation or sublimation and crystallization as well as methods of liquid-liquid extraction and distribution in immiscible molten metals and molten salts.
2. Chemical methods such as cyclic oxidation and reduction methods using chemical and electrochemical processes.

In all variants, all of the gaseous fission products and part of the highly volatile solid fission products are released into the off-gas due to the high process temperatures. The consequence is a rather difficult and expensive off-gas treatment. Recycling of the molten metal and molten salt used as the separation environment by fractionated distillation or sublimation was proposed in nearly all cases. Pyrochemical treatment methods for used nuclear fuels have been described in detail in earlier chapters of this book.

24.6 General considerations

Since the beginning of the nuclear era there has been discussion on which type of fuel to use and which fissile elements are the most advantageous. Historically, the selection was slightly enriched uranium dioxide for several reasons such as reasonably high melting point, low solubility under running conditions and in a repository, reasonable ease of dissolution in reprocessing conditions, and several more. However, even by the 1950s, thorium was considered a candidate fuel. This was later abandoned but has now gained a revival for several reasons. Among the ones most often mentioned are the higher abundance and the higher proliferation resistance. An overview of the issues concerning the thorium fuel cycle was recently made by Ashley (2012).

^{232}Th is several times more abundant than all isotopes of uranium taken together in the world, especially when considering the lower-cost category. When it comes to some other comparisons, the picture gets more complicated.

If we start looking at the reprocessing possibilities, it has been made rather clear in this chapter that developing a large-scale separation process for used thorium-based fuels is not straightforward. One of the main challenges lies in an efficient dissolution procedure that at the same time can be deployed at an industrial scale in normal equipment. For the subsequent separations processes there are considerable data available from the refining processes as well as past reprocessing studies to facilitate renewed research programs and, thus, rather quickly lead to potential designs for suitable processes, if desired.

For the nonproliferation issues, it gets more complicated. The main reason for claiming that the thorium cycle is more proliferation-resistant is the absence of plutonium in the cycle. This is true for a fully developed cycle and even if plutonium is used as a starter for the fission cycle its content will be relatively low anyway. Rather, the problem arises with the production of the fissile ^{233}U. This isotope is, in principle, as good as ^{235}U and ^{239}Pu as potential weapons material, lying between these isotopes in critical mass. Actually, ^{233}U is even somewhat better than plutonium as there are fewer spontaneous neutrons that could simplify weapons production.

It is argued that the above issue with weapons fabrication can be counteracted by the fact that in the thorium cycle the ^{233}U will be "contaminated" by ^{232}U, which, with its hard gamma radiation, will make fabrication and handling of both new fuels and weapons difficult as well as improving materials traceability. This can be solved by isotope separation, which already is used for fabrication of traditional uranium or plutonium weapons.

A more serious issue in relation to the nonproliferation argument of the thorium fuel cycle is the fact that if the reactors are equipped with online separation systems, which is often suggested for molten salt reactor concepts, it is possible to separate out ^{233}Pa. ^{233}Pa has a half-life of about 27 days, so if the separated protactinium is left to decay, the product will be isotopically pure ^{233}U. Thus, by performing this rather simple elemental separation there is no longer any need for a more complicated isotopic separation and rather good weapons-grade material can be obtained.

So, as a concluding remark one may state that we are essentially at the same position as in the 1950s, weighing advantages and disadvantages of different nuclear fuel cycles.

There will be an ongoing discussion about the pros and cons of this cycle or that cycle. However, presently in many countries around the world the main question seems to be whether nuclear power has a place in the current and future energy mix or not. The question of which fuel cycle to use will then be a later focus if the decisions are made to continue the nuclear era. Then the choice of cycle may well be decided by the consideration of those nations driving the development at that time. Given the growth of nuclear energy in Asia and the developing nations, coupled with the impacts of the Fukushima incident, it will probably not be the same nations that selected the uranium cycle we use today.

References

Adams, R.M., Glassner, A., 1964a. Reactor development program progress report, September, ANL-6944.

Adams, R.M., Glassner, A., 1964b. Reactor development program progress report, January, ANL-7003.

Amaral, J.C.B., Morais, C.A., 2010. Thorium uranium extraction from rare earth elements in monazite sulphuric acid liquor through solvent extraction. Miner. Eng. 23, 498–503.

Anantharaman, K., Shivakumar, V., Saha, D., 2008. Utilisation of thorium in reactors. J. Nucl. Mater. 383, 119–121.

Ashley, S.F., 2012. Thorium fuel has risks. Nature 492, 31–33.

Benedict, G., 1980. Improvements in thorium-uranium separation in the acid THOREX process. In: ACS Symposium Series, vol. 117, pp. 371–377 (Chapter 26).

Blanco, R.E., Ferris, L.M., Fergusson, D.E., 1962. ORNL-3219.

Burris, L., Dillon, I.G., Steunenberg, R.K., 1964. ANL-6818, 28.

Choppin, G.R., Rydberg, J., Liljenzin, J.-O., Ekberg, C., 2013. Radiochemistry and Nuclear Chemistry, fourth ed. Academic Press, New York.

Crouse, D.J., Brown, K.B., 1959. The Amex process for extracting thorium ores with alkyl amines. Ind. Eng. Chem. 51, 1461–1464.

Delpech, S., Merle-Lucotte, E., Heuer, D., Allibert, M., Ghetta, V., Le-Brun, C., Mathieu, L., Picard, G., 2009. Reactor physics and reprocessing scheme for innovative molten salt reactor system. J. Fluorine Chem. 130 (1), 11–17.

Dey, P.K., Bansal, N.K., 2006. Spent fuel reprocessing: a vital link in Indian nuclear power program. Nucl. Eng. Des. 236, 723–729.

El-Yamani, I.S., Shabana, E.I., 1985. Studies on extraction of Throium(IV) from sulphate media with mixtures of long-chained primary amines and tributylphosphate. J. Radioanal. Nucl. Chem. 88, 273–280.

Ewing, R.A., et al., 1952. Purification of thorium nitrate by solvent extraction with TBP. Fin Rep. USAEC-BMI, 946.

Ferris, L.M., 1960. Zirflex Process for PWR Blanket Fuel. II Revised Flowsheet, ORNL-2940.

Ferris, L.M., Kibbey, A.H., 1960. ORNL-2934.

Finney, B.C., Hannaford, B.A., 1961. ORNL-3072.

Foley, D.D., Filbert, R.B., 1958. Purifying thorium by solvent extraction. Ind. Eng. Chem. 50, 144.

Franken, W.M.P., Bultman, J.H., Konings, R.J.M., Wichers, V.A., 1995. Evaluation of thorium based nuclear fuel, extended summary. Technical Report ECN-R-95-006, Netherlands Energy Research Foundation (ECN), Petten, The Netherlands.

Fu, X., Liang, T., Tang, Y., Xu, Z., Tang, C., 2004. Preparation of UO2 kernel for HTR-10 fuel element. J. Nucl. Sci. Technol. 41, 943.

Gresky, A.T., 1953. Laboratory development of the THOREX process. Progress report, ORNL-1367.

Gschneider, K.A., 1981. Rare Earth Speciality Inorganic Chemicals. Rare Earth Information Centre and Department of Materials Science and Engineering, Iowa state University, AMES, IA, USA.

Haas, P.A., Haws, C.C., Kitts, F.G., Ryon, A.D., 1968. Engineering development of sol-gel processes at Oak Ridge National Laboratory, ORNL/TM-1978.

Habashi, F., 1997. In: Handbook of Extractive Metallurgy3, Wiley-VCH, pp. 1649–1684.

IAEA, 1987. Thorium based nuclear fuel: current status and perspectives, IAEA-TECDOC-412.

IAEA, 2005. Thorium fuel cycle – potential benefits and challenges, IAEA-TECDOC-1450.

Jackson, R.R., Walser, R.L., 1977. PUREX process operation and performance, 1970 thoria campaign. Report ARH-2127.

Jonke, A.A., 1965. At. Energy Rev. 3, 3–60.

Kutty, T.R.G., Somayajulu, P.S., Khan, K.B., Kumar, A., Kamath, H.S., 2009. Characterization of $(Th,U)O_2$ pellets made by advanced CAP process. J. Nucl. Mater. 384, 303–310.

Merle-Lucotte, E., Heuer, D., Allibert, M., Brovchenko, M., Ghetta, V., Rubiolo, P., Laureau, A., 2013. Recommandations for a demonstrator of molten salt fast reactor. In: Proceedings of the International Conference on Fast Reactors and Related Fuel Cycles: Safe Technologies and Sustainable Scenarios (FR13), Paris, France.

Merz, E., 1968. Atomwirtschaft 13, 417–421.

Merz, E., Zimmer, E., 1984. Aqueous chemical reprocessing of HTR fuel. Forschungszenter Julich report, JUL-1899,.

Mukherjee, T.K., 2002. Processing of Indian monazite for the recovery of thorium and uranium values. In: Ganguly, C. (Ed.), International Conference on Characterisation and Quality Control of Nuclear Fuels, Hyderabad, pp. 87–196.

National Nuclear Laboratory, 2012. Comparison of thorium and uranium fuel cycles. NNL 11(5), 11593.

Orth, D.A., 1979. Savannah river plant thorium processing experience. Nucl. Tech. 43, 63–74.

Rainly, R.H., Moore, J.G., 1961. Laboratory development of the acid THOREX process for recovery of thorium reactor fuel. Nucl. Sci. Eng. 10, 367–371.

RainlyR. H., Moore, J. G., 1962. Laboratory development of the acid THOREX process for recovery of consolidated Edison thorium reactor fuel, ORNL-3155, Oak Ridge National Laboratory, US.

Sato, N., Kirishima, A., 2010. Separation of thorium and uranium by sulfide method. Energy Procedia 7, 444–448.

Sato, N., Kirishima, A., 2011. Sulfurization behaviour of thorium dioxide with carbon disulphide. J. Nucl. Mat. 414, 324–327.

Sarkar, S.G., Bandekar, S.V., Dhadke, P.M., 2000. Solvent extraction separation of Th(IV) and U(UVI) with PC-88. J. Radioanal. Nucl. Chem. 243, 803–807.

Siddal, T.H., 1959. Trialkyl phosphates and dialkylphosphonates in uranium and thorium extraction. Ind. Eng. Chem. 51, 41–44.

Sood, D.D., 2011. The role of sol-gel process for nuclear fuels an overview. J. Sol-Gel Sci. Technol. 59, 404–416.

Steinhauser, M., 1987. Löslichkeitvon PuO_2 und ThO_2 in HNO_3. PhD thesis, Universität Munchen.

Swansson, L.J., 1958. The selective dissolution of zirconium or zircaloy cladding by the ZIRFLEX process. In: Proceedings of the Second United Nations International Conference on Peaceful Uses of Atomic Energy, vol. 17, p. 154.

Tjälldin, O., 1963. The Thermox Process. Aktiebolaget Atomenergi, AE-120, Stockholm, Sweden.

Tjälldin, O., 1965. British patent 997,355.

Index

Note: Page numbers followed by *f* indicate figures and *t* indicate tables.

B

G

H

O

P

T

V

W

X

Z